UAB
Universitat Autònoma de Barcelona

Permian and Triassic ecosystems of the Gymnesic Islands (western Mediterranean)

Rafel Matamales Andreu

ADVERTIMENT. L'accés als continguts d'aquesta tesi doctoral i la seva utilització ha de respectar els drets de la persona autora. Pot ser utilitzada per a consulta o estudi personal, així com en activitats o materials d'investigació i docència en els termes establerts a l'art. 32 del Text Refós de la Llei de Propietat Intel·lectual (RDL 1/1996). Per altres utilitzacions es requereix l'autorització prèvia i expressa de la persona autora. En qualsevol cas, en la utilització dels seus continguts caldrà indicar de forma clara el nom i cognoms de la persona autora i el títol de la tesi doctoral. No s'autoritza la seva reproducció o altres formes d'explotació efectuades amb finalitats de lucre ni la seva comunicació pública des d'un lloc aliè al servei TDX. Tampoc s'autoritza la presentació del seu contingut en una finestra o marc aliè a TDX (framing). Aquesta reserva de drets afecta tant als continguts de la tesi com als seus resums i índexs.

ADVERTENCIA. El acceso a los contenidos de esta tesis doctoral y su utilización debe respetar los derechos de la persona autora. Puede ser utilizada para consulta o estudio personal, así como en actividades o materiales de investigación y docencia en los términos establecidos en el art. 32 del Texto Refundido de la Ley de Propiedad Intelectual (RDL 1/1996). Para otros usos se requiere la autorización previa y expresa de la persona autora. En cualquier caso, en la utilización de sus contenidos se deberá indicar de forma clara el nombre y apellidos de la persona autora y el título de la tesis doctoral. No se autoriza su reproducción u otras formas de explotación efectuadas con fines lucrativos ni su comunicación pública desde un sitio ajeno al servicio TDR. Tampoco se autoriza la presentación de su contenido en una ventana o marco ajeno a TDR (framing). Esta reserva de derechos afecta tanto al contenido de la tesis como a sus resúmenes e índices.

WARNING. The access to the contents of this doctoral thesis and its use must respect the rights of the author. It can be used for reference or private study, as well as research and learning activities or materials in the terms established by the 32nd article of the Spanish Consolidated Copyright Act (RDL 1/1996). Express and previous authorization of the author is required for any other uses. In any case, when using its content, full name of the author and title of the thesis must be clearly indicated. Reproduction or other forms of for profit use or public communication from outside TDX service is not allowed. Presentation of its content in a window or frame external to TDX (framing) is not authorized either. These rights affect both the content of the thesis and its abstracts and indexes.

Permian and Triassic ecosystems of the Gymnesic Islands (western Mediterranean)

Rafel Matamales Andreu

Ph.D. dissertation

Supervisors: Dr. Àngel Galobart, Dr. Josep Fortuny

Academic tutor: Dr. Oriol Oms

Programa de doctorat en Geologia

Universitat Autònoma de Barcelona, departament de Geologia

Institut Català de Paleontologia Miquel Crusafont

2023

ICP Institut Català de Paleontologia Miquel Crusafont

UAB Universitat Autònoma de Barcelona

Als meus pares i padrins,

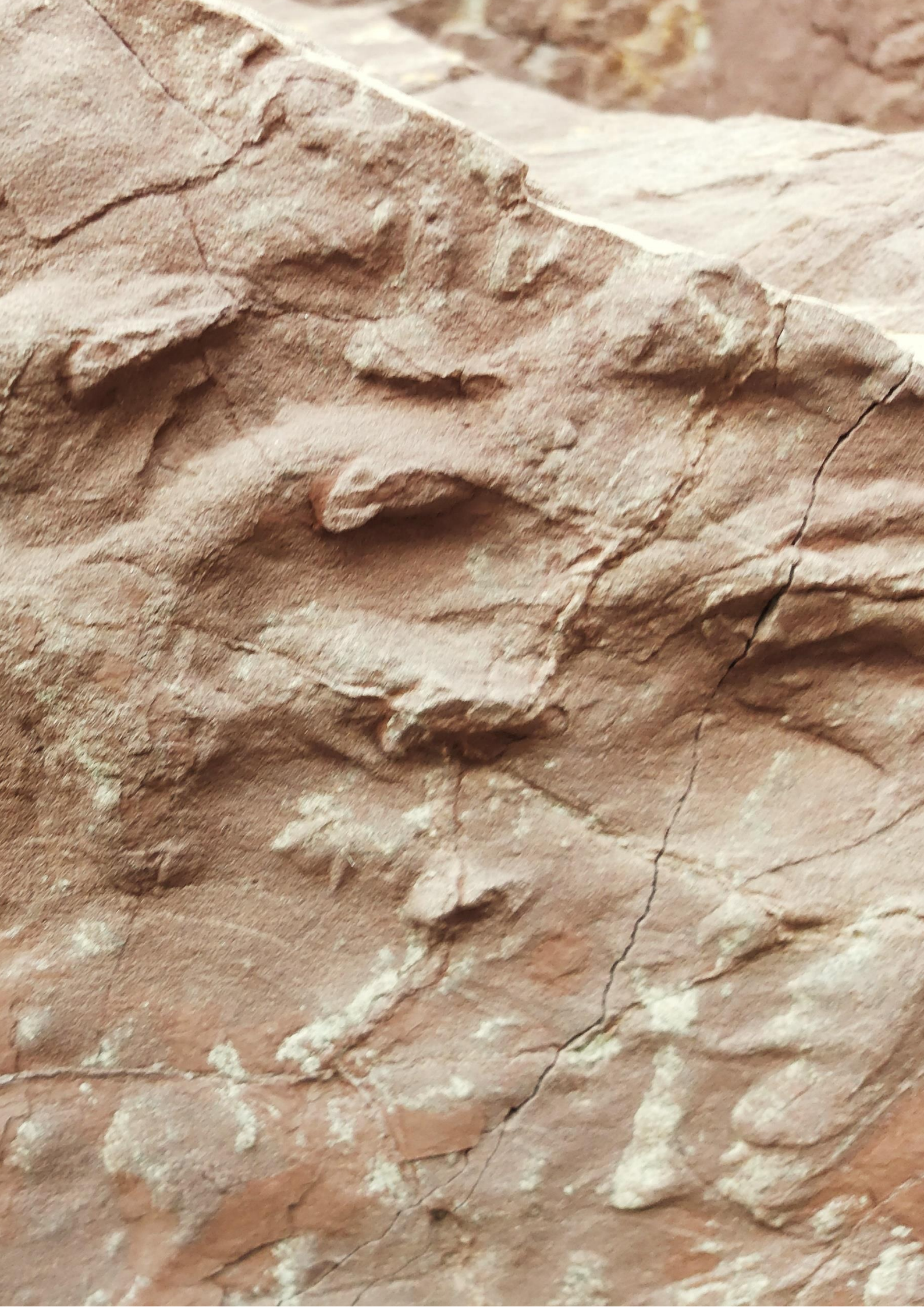

Table of contents

Abstract | Resum 16

Chapter 1 | Introduction, Objectives, Methods 21
Introduction 25
Permian and Triassic ecosystems 25
General context and previous works on the Permian and Triassic of the Gymnesic Islands 26
Permian 26
Lower–Middle Triassic (*Buntsandstein* facies) 34
Middle–Upper Triassic (*Muschelkalk* facies) 38
Upper Triassic–Lower Jurassic (*Keuper* facies and Felanitx formation) 41
Objectives of the present work 45
Material and methods 47
Stratigraphy and sedimentology 47
Fieldwork campaigns and permissions 54
Sampling methods for palaeomagnetism and palaeopalinology 54
Methods in vertebrate palaeoichnology 55
Methods in vertebrate palaeontology 58
References 61

Chapter 2 | The early–middle Permian of Mallorca 83
Abstract 87
Introduction 87
Geographical and geological context 88
Material and methods 88
Stratigraphy and sedimentology 88
Magnetostratigraphy 94
Palaeopalynology and palaeobotany 94
Tetrapod ichnites 95
Stratigraphy and sedimentology 95
Bec de s'Àguila Formation 95
Port des Canonge Formation 97
Pedra de s'Ase Formation 98
Magnetostratigraphy 98
Palaeobotany 99
Palynology 99
Macroplant remains 103
Sphenophyta indet. 103
?*Feysia* sp. 103
Hermitia sp. 103
Trace fossils 104
Invertebrate traces 104
Arenicolites isp. 105
Cochlichnus anguineus 105
Cruziana isp. 105
Palaeophycus tubularis 106
Planolites beverleyensis 106
Taenidium barretti 106
Ichnofacies 106
Tetrapod tracks 106
Hyloidichnus bifurcatus, large morphotype 106
Hyloidichnus bifurcatus, small morphotype 108
Dromopus isp. 108

cf. *Pachypes ollieri* 109
Dimetropus leisnerianus 109
cf. *Dimetropus* isp. 111
Characichnos isp. 111
Discussion 112
Age attribution 112
Magnetostratigraphy 112
Palynostratigraphy 113
Tetrapod track biostratigraphy 113
Sedimentary evolution and palaeoclimate 114
The early Permian tetrapod ichnoassemblages of Mallorca 116
The Permian–Triassic cycle in the Balearic Islands 119
Conclusions 121
References 122

Chapter 3 | The continental Early–Middle Triassic of Mallorca 127
Abstract 131
Introduction 131
Geographical and geological context 133
Material and methods 133
Stratigraphy and sedimentology 133
Tetrapod tracks 133
Fossil arthropods and fishes 135
Stratigraphy and sedimentology 135
Punta Roja Formation 135
Estellencs Formation 137
Pedra Alta Formation 139
Son Serralta Formation 140
Systematic palaeoichnology 140
Invertebrate ichnofossils 140
Gordia isp. 140
Skolithos isp. 141
Taenidium cf. *barretti* 141
Rusophycus isp. - *Cruziana* isp. - *Diplichnites* cf. *gouldi* 141
Tetrapod tracks 142
Rhynchosauroides isp. 1 142
Rhynchosauroides isp. 2 143
Prorotodactylus mesaxonichnus 143
Indeterminate morphotype 143
Systematic palaeontology 144
Clam shrimps ("conchostracans") 144
Hornestheria aff. *sollingensis* 144
Hornestheria? sp. 1 145
Hornestheria? sp. 2 145
"Conchostraca" indet. 145
Insects 145
Hammephemera cf. *pulchra* 145
Ephemerida indet., adult morphotype 1 146
Ephemerida indet., detritivore nymph type 146
Triassoephemera punctata 146
Triassonurus doliiformis 149
cf. *Voltziaephemera fossoria* 149
Blattodea indet. 149

Fishes 149
Osteichthyes indet. 149
Discussion 150
Palaeoenvironmental evolution and palaeogeography 150
Palaeoecosystems 153
Palaeobiogeography 155
Conclusions 155
References 156

Chapter 4 | The marine Middle–Late Triassic of Mallorca 161
Abstract 165
Introduction 165
Geographical and geological context 166
The *Muschelkalk* facies of Mallorca 166
The *Keuper* facies of Mallorca 167
Localities of provenance of the studied vertebrate fossils 167
Systematic palaeontology 168
Reptilia indet. 168
Nothosaurus sp. 169
Ichthyosauriformes indet. aff. Grippidia 170
Discussion 172
Conclusions 174
References 174

Chapter 5 | The middle–late Permian of Menorca 179
Abstract 183
Introduction 183
Geological and geographical context 184
Palaeoenvironment and climatic conditions 186
Material and methods 186
Collection number abbreviations 186
Stratigraphy and sedimentology 186
Provenance and three-dimensional (3D) modelling of tetrapod ichnofossils 186
Phylogenetic analysis 187
Systematic palaeoichnology 188
Hyloidichnus isp. 188
cf. *Erpetopus* isp. 188
Systematic palaeontology 189
Balearosaurus bombardensis 189
cf. *Balearosaurus bombardensis* 190
Moradisaurinae indet. 194
Discussion 196
Age attribution 196
Tetrapod fauna 196
Palaeobiogeography of moradisaurine captorhinid eureptiles 196
Phylogenetic relationships of moradisaurine captorhinid eureptiles 196
Conclusions 197
References 199

Chapter 6 | Discussion 205
Palaeoecosystems of the Permian and Triassic of Mallorca 209
Palaeoecosystems of the Permian of Menorca 215
Significance of the Gymnesic Islands Permian and Triassic tetrapod fossil record 217
References 222

Chapter 7 | Conclusions 233
Permian of Mallorca 237
Continental Triassic of Mallorca (*Buntsandstein* facies) 238
Marine Triassic of Mallorca (*Muschelkalk* and *Keuper* facies) 239
Permian of Menorca 240

Chapter 8 | Acknowledgements 241

Appendix 1 | Previous works on the Permian and Triassic of Mallorca 249
Resum / Abstract 251
Introducció 251
Unitats litostratigràfiques i paleoambients que representen 253
Registre fòssil 258
Plantes del permià 258
Traces d'invertebrats del permià 258
"Rèptils" del permià 258
Plantes del triàsic inferior(?)–mitjà 260
Crustacis, insectes i peixos del triàsic inferior(?)–mitjà 262
"Rèptils" del triàsic inferior(?)–mitjà 264
Datacions i edats 264
Permià 264
Triàsic 265
Discussió, síntesi i perspectives futures 266
Bibliografia 268

Appendix 2 | Supplementary Material, Permian of Mallorca 275
Previous works 278
Discussion on moradisaurine described by Liebrecht *et al.* (2017) 281
Supplementary Figures 282
Supplementary Table 1 286
Supplementary References 287
Supplementary Logs and Correlations 292
Racó de s'Algar 292
Torrent de na Nadala 307
Es Tamarell 327
Punta d'en Pere Mir 330
Pedra de s'Ase 333
Pedra de s'Ase - Summit 350
Volta des General 352
Platja de sa Pedrera 353
Port des Canonge 355
Sa Gratallosa 416
Pedrera de sa Cova 422
Marina de Valldemossa 430
Correlations 437
Supplementary Tables 2–5 440

Appendix 3 | Locomotion in cf. *Dimetropus*, Permian of Mallorca 451
Abstract 453
Introduction 453
Geographical and geological context 454
Material and methods 454
Systematic palaeoichnology 454
cf. *Dimetropus* isp. 454
Discussion 457

Comparison to other Permian ichnogenera 457
Comparison to other ichnospecies of *Dimetropus* 458
Trackmaker of cf. *Dimetropus* isp. from Mallorca 459
Locomotion of the trackmaker of cf. *Dimetropus* isp. from Mallorca 459
Notes on the evolution of synapsid locomotion 461
Conclusions 461
References 461

Appendix 4 | A new moradisaurine captorhinid and its locomotion 463
Abstract 465
Introduction 465
Geographical and geological setting 467
Material and methods 470
The studied skeleton 470
Phylogenetic analysis 470
Ichnology and track-trackmaker correlation 471
Systematic palaeontology 471
Tramuntanasaurus tiai 472
Discussion 484
Phylogeny 484
Comparison of *Tramuntanasaurus tiai* to other forms from the peri-Tethys 484
Correlation of *Tramuntanasaurus tiai* with ichnites from the same area 487
Conclusions 491
References 493
Supplementary Figure 500
Character matrix 501

Appendix 5 | First gorgonopsian therapsid from equatorial Pangaea 503
Abstract 505
Introduction 506
Results 507
Gorgonopsia indet. 507
Discussion 509
Conclusions 514
References 516
Supplementary Text 1: Materials and methods 521
Supplementary Text 2: Detailed description 522

Appendix 6 | Permian gorgonopsian tracks from Mallorca 537
Abstract 539
Introduction 540
Geographical and geological context 541
General context 541
Stratigraphy and sedimentology of the tracksite 541
Material and methods 543
Collected specimens 543
Three-dimensional models and silicon moulds 543
Ichnological study 544
Systematic palaeoichnology 544
Gorgonopsian tracks 544
Discussion 553
Ichnotaxonomical remarks 553
Track-trackmaker correlation 557
Locomotion 559

Conclusions 560
References 561

Appendix 7 | Supplementary Material, continental Triassic of Mallorca 565
Previous works 568
Supplementary Figures 571
Supplementary Tables 573
Supplementary References 575
Supplementary Logs 580
Pedra Alta 580
Punta Negra 582
Punta Roja 593
Tenassa de sa Tanca 606

Appendix 8 | Triassic clam shrimps from Mallorca 611
Abstract 613
Introduction 613
Geologic setting 614
Material and methods 615
Systematic palaeontology 617
Hornestheria aff. *sollingensis* 618
Hornestheria? sp. 1 621
Hornestheria? sp. 2 627
"Conchostraca" indet. 629
Discussion 629
Taxonomic remarks on the genus *Hornestheria* 629
Implications for biostratigraphy 631
Remarks on taphonomy 633
Summary 633
References 634

Appendix 9 | Triassic sedimentivorous mayfly nymphs from Mallorca 639
Abstract 641
Introduction 641
Geographical and geological context 642
Material and method 643
Results 644
Discussion 651
Cololite origin and composition 651
Detritivorous lifestyle of the mayfly nymphs 653
Early detritivory in insects of aquatic environments 654
Conclusion 655
References 656
Supplementary Figures 659

Appendix 10 | Triassic true flies from Mallorca 665
Abstract 667
Introduction 667
Geographical and geological context 668
Material and method 670
Systematic palaeontology 670
Protoanisolarva juarezi 671
Voltziapupa cf. *cornuta* 674
Nematocera indet. 674
Clavapartus latus 674

Discussion 677
Palaeobiological implications of the new anisopodid fossil larva 677
Palaeobiology of the aquatic insect community 678
Conclusion 680
References 681
Supplementary Figures 684

Appendix 11 | Triassic marine molluscs from Mallorca 689
Abstract 691
Introducción 691
Material y métodos 692
Resultados 692
Discusión y conclusiones 692
Referencias 693

Appendix 12 | Supplementary Material, Permian of Menorca 695
Supplementary Table 698
Supplementary Log: Cala del Pilar–Pla de Mar 699
Character matrix 731

Appendix 13 | Synthesis, Permian of Mallorca 733

Appendix 14 | Synthesis, continental Triassic of Mallorca 739

Appendix 15 | Synthesis, marine Triassic of Mallorca 745

Picture and figure credits 751

Abstract

The present Ph.D. dissertation provides an exhaustive account of the Permian and continental Triassic rock units and fossil record of Mallorca, as well as new data on the transitional/marine Triassic of Mallorca and the Permian of Menorca. Detailed stratigraphic and sedimentological analyses have made it possible to formally describe seven new lithostratigraphic formations that encompass the whole Permian–Triassic continental succession of Mallorca, from oldest to youngest: Bec de s'Àguila (alluvial fans and meandering rivers, ?Sakmarian–Artinskian), Port des Canonge (meandering rivers and floodplains, Artinskian–?Roadian), Pedra de s'Ase (meandering rivers and sheetfloods, Roadian–Wordian), Punta Roja (perennial shallow braided rivers, Olenekian–Anisian), Estellencs (meandering rivers and floodplains, Anisian), Pedra Alta (seasonal braided rivers and sheetfloods, Anisian), and Son Serralta (meandering rivers, floodplains and tidal mud flats, Anisian). Moreover, the magnetostratigraphic study has revealed that the three Permian formations of Mallorca are part of the Kiaman Reverse Superchron (late Carboniferous–middle Permian). Regarding the marine Triassic of Mallorca, the review of previous works has shown that it can be divided into five informal units, from oldest to youngest: M1 (carbonate platforms, Anisian), M2 (coastal lagoons, ?Anisian), M3 (carbonate platforms, Ladinian), *Keuper* (coastal lagoons, Carnian–Norian) and Felanitx formation (carbonate platforms, Norian–Hettangian). Finally, the three units of the Permian of Menorca, described by previous authors, have been reviewed, from oldest to youngest: P1 (alluvial fans, ?Cisuralian), P2 (floodplain lakes, ?Cisuralian–?Guadalupian), and P3 (meandering rivers, sheetfloods and floodplains, ?Guadalupian–Lopingian).

The study of the fossil record has revealed rich and diverse ecosystems, with representatives of several groups of plants, invertebrates and vertebrates. In the Permian of Mallorca, there was a rich plant community with elements indicative of semi-arid conditions that has dated the Pedra de s'Ase Formation in the lower part of the Guadalupian, abundant trace fossils that suggest a Cisuralian series for the Port des Canonge Formation, and tetrapod skeletons of different taxa. Among all those, a new species of medium-sized moradisaurine has been described. Moreover, of special relevance, there is a partial skeleton of an indeterminate gorgonopsian, potentially the oldest worldwide and the only one found in palaeoequatorial latitudes. In the continental Triassic of Mallorca, micro- and macroplant taxa, trace fossils and clam shrimps have dated the three upper formations in the Anisian. Among the exceptionally well-preserved fossils of insects and fishes, a new species of wood fly larva has been described, the oldest known true fly worldwide. The marine Triassic of Mallorca has produced remains of a basal ichthyosauriform and a nothosaur sauropterygian. Of note, the basal ichthyosauriform fills a biogeographical gap for the group, hitherto known from western North America and eastern Asia.

Finally, a new large moradisaurine has also been described from the Permian of Menorca, appearing together with small moradisaurine bones and tracks, and parareptile tracks.

All these new data build up a new and updated framework for the Permian and Triassic of the Gymnesic Islands, which in turn makes it possible to discuss it from a broader perspective. Specifically, it reveals that the ecosystems of equatorial Pangaea are key to understand the palaeobiogeography and evolution of Permian and Triassic organisms, with the oldest record of two important animal groups, such as dipterans (true flies) and therapsids ("proto-mammals"). Moreover, this record complements other sites, documenting the change of palaeoenvironments through time, possibly influenced in part by climate; the palaeobiogeographic distribution and patterns of dispersion of some animals, such as moradisaurines, therapsids and ichthyosauriforms; and new age constraints for the lithostratigraphic units, which will help in future inter-basinal correlations in the western peri-Tethys to determine the extent and timing of the Permian–Triassic rifting.

Resum

La present tesi doctoral proporciona una caracterització exhaustiva de les unitats de roca del Permià i el Triàsic continental de Mallorca i el seu registre fòssil, a més de noves dades sobre el Triàsic transicional/marí de Mallorca i el Permià de Menorca. Les anàlisis estratigràfiques i sedimentològiques detallades han permès de descriure formalment set noves formacions litostratigràfiques que comprenen tota la successió continental del Permià–Triàsic de Mallorca, de la més antiga a la més recent: Bec de s'Àguila (ventalls al·luvials i rius meandriformes, ?Sakmarià–Artinskià), Port des Canonge (rius meandriformes i planeres d'inundació, Artinskià–?Roadià), Pedra de s'Ase (rius meandriformes i inundacions laminars, Roadià–Wordià), Punta Roja (rius entrunyellats perennes i poc fondos, Oleniokià–Anisià), Estellencs (rius meandriformes i planeres d'inundació, Anisià), Pedra Alta (rius entrunyellats estacionals i inundacions laminars, Anisià), i Son Serralta (rius meandriformes, planeres d'inundació i planeres fangoses mareals, Anisià). A més, l'estudi magnetostratigràfic ha revelat que les tres formacions del Permià de Mallorca pertanyen al supercron invers de Kiaman (Carbonífer superior–Permià mitjà). Pel que fa al Triàsic marí de Mallorca, la revisió dels antecedents ha permès de dividir-lo en cinc unitats informals, de la més antiga a la més recent: M1 (plataformes carbonatades, Anisià), M2 (llacunes costaneres, ?Anisià), M3 (plataformes carbonatades, Ladinià), *Keuper* (llacunes costaneres, Carnià–Norià) i formació Felanitx (plataformes carbonatades i planeres mareals, Norià–Hettangià). Finalment, s'han revisat les tres unitats del Permià de Menorca, ja descrites per autors anteriors, de la més antiga a la més recent: P1 (ventalls al·luvials, ?Cisuralià), P2 (llacs de planera d'inundació, ?Cisuralià–?Guadalupià), i P3 (rius meandriformes, inundacions laminars i planeres d'inundació, ?Guadalupià–Lopingià).

L'estudi del registre fòssil ha revelat uns ecosistemes rics i diversos, amb representants de diferents grups de plantes, invertebrats i vertebrats. En el Permià de Mallorca hi havia una rica comunitat vegetal amb elements indicadors de condicions semi-àrides que han permès de datar la Formació Pedra de s'Ase en la part baixa del Guadalupià, abundants potades que suggereixen que la Formació Port des Canonge és cisuraliana, i esquelets de diferents tàxons de tetràpodes. Entre ells, s'ha descrit una nova espècie de moradisaurí de mida mitjancera. A més, i d'especial rellevància, també s'ha trobat un esquelet parcial d'un gorgonopsi indeterminat, el més antic del món i l'únic provinent de latituds paleoequatorials. Pel que fa al Triàsic continental de Mallorca, la micro- i macroflora, les potades i els "concostracis" han permès de datar les tres formacions superiors dins l'Anisià. S'ha descrit una nova espècie d'entre els fòssils d'insectes i peixos excepcionalment ben conservats, corresponent al mosquit veritable més antic conegut al món. El Triàsic marí de Mallorca ha lliurat restes d'un ictiosauriforme basal i un sauropterigi notosaure. És especialment interessant l'ictiosauriforme basal, per mor que umpl un buit biogeogràfic per al grup, fins ara sols conegut de l'oest de l'Amèrica del Nord i l'Àsia oriental.

Finalment, del Permià de Menorca s'ha descrit una nova espècie de moradisaurí de mida grossa, que apareix juntament amb ossos i potades d'un altre moradisaurí de mida petita i potades de pararrèptils.

Totes aquestes noves dades proporcionen una nova vasa per al Permià i Triàsic de les Gimnèsies, el que permet discutir-los des d'una perspectiva més àmplia. Concretament, revela que els ecosistemes de Pangea equatorial són clau per entendre la paleobiogeografia i l'evolució dels organismes del Permià i del Triàsic, amb el registre més antic de dos importants grups d'animals, com són els dípters i els teràpsids. A més, aquest registre complementa altres indrets, documentant el canvi dels paleoambients a través del temps, possiblement influenciat en part pel clima; la distribució paleobiogeogràfica i els patrons de dispersió d'alguns animals, com els moradisaurins, els teràpsids o els ictiosauriformes; i nova informació de les edats de les unitats litostratigràfiques, que ajudaran en futures correlacions entre conques en el peri-Tetis occidental i, al seu torn, la determinació de la extensió i la temporització de l'obriment de les conques de rift d'aquesta regió durant el Permià i el Triàsic.

Chapter 1

Introduction, Objectives and Methods

Chapter 1 was in part published as:

Matamales-Andreu, R.; Oms, O. & Fortuny, J. (2021). Paleoecosistemes del Permià i Triàsic continental de Mallorca (Illes Balears, Mediterrània occidental): síntesi i prespectives futures. *In*: Gómez-Pujol, L.; Roig-Munar, F.X.; Gelabert, B.; Martín, J.A. (Eds.). *De la terra a la mar i de la mar a la terra. Homenatge a Antonio Rodríguez-Perea. Monografies de la Societat d'Història Natural de Balears*, 34. Societat d'Història Natural de les Balears; Palma: 17–39. [in Catalan]

ISBN: 978-84-09-34554-0

DL: PM 00742-2021

Also, see Appendix 1: Matamales-Andreu *et al.* (2021), *Monografies de la Societat d'Història Natural de Balears*

Introduction

Permian and Triassic ecosystems

The Permian and Triassic (Figure 1.1) are two key geological periods to understand how life on Earth today was shaped. A great change of the climates caused the shift from the Carboniferous–early Permian icehouse conditions to the Triassic hothouse (Montañez *et al.*, 2007; Sun *et al.*, 2012; Montañez & Poulsen, 2013; MacLeod *et al.*, 2017) (Figure 1.2). This global warming started during the Artinskian (early Permian), probably as a consequence of the eruption of igneous provinces in present-day Asia (Marchetti *et al.*, 2022), and this trend towards more arid climates was sustained throughout the rest of the Permian (Michel *et al.*, 2015; Scotese *et al.*, 2021). Warm and dry conditions persisted during the Early and Middle Triassic (Sun *et al.*, 2012; Benton & Newell, 2014; Romano *et al.*, 2020), and it was not until the beginning of the Late Triassic that humid periods became longer and more frequent (Ruffell *et al.*, 2016; Ogg *et al.*, 2020; Scotese *et al.*, 2021). Among other factors, these environmental conditions affected the composition of the biological communities through time.

In terrestrial environments, these turnovers have been intensely studied in tetrapods. The earliest Permian faunas were reminiscent to those of the previous period, the Carboniferous, dominated by amphibians and "pelycosaur"-grade synapsids (Ruta & Benton, 2008; Brocklehurst *et al.*, 2013). Those groups co-occurred with basal amniotes, such as seymouriamorphs and diadectomorphs, and early reptiles, such as captorhinomorphs and diapsids. Recent studies show that reptiles may have been more abundant than once thought (Brocklehurst, 2021). From the middle Cisuralian on, reptiles started to become increasingly abundant while amphibian numbers dwindled (Marchetti *et al.*, 2019). Olson's extinction struck those communities in the latest Cisuralian–earliest Guadalupian, wiping out almost all the once-dominant "pelycosaurs", which were substituted by therapsid synapsids and several groups of parareptiles (Brocklehurst *et al.*, 2017; Brocklehurst, 2020; but see Lucas, 2017). During the Guadalupian, therapsids underwent an important radiation, but dinocephalians, the most diverse group, died out at the end of this epoch, in the end-Capitanian mass extinction (Lucas, 2009; Day *et al.*, 2015; Olroyd & Sidor, 2017; Day & Rubidge, 2021). The Lopingian faunas were characterised by the abundance of derived pareiasaurs and therapsids such as gorgonopsians, therocephalians and dicynodonts (Bernardi *et al.*, 2017; Lucas, 2017).

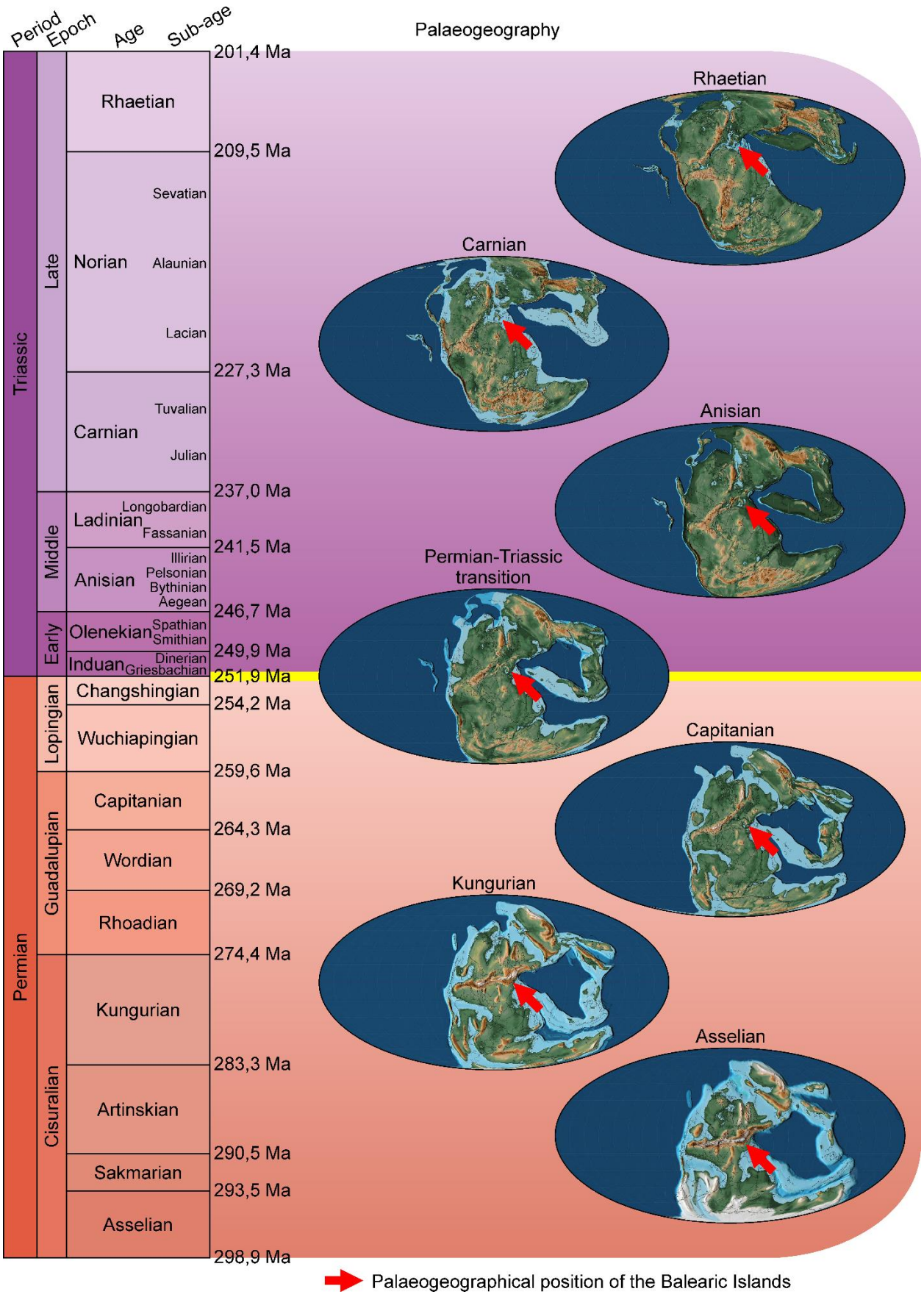
Period
Epoch
Age
Sub-age
Palaeogeography
Triassic
Permian
Late
Middle
Early
Lopingian
Guadalupian
Cisuralian
Rhaetian
Norian
Sevatian
Alaunian
Lacian
Carnian
Tuvalian
Julian
Ladinian
Longobardian
Fassanian
Anisian
Illirian
Pelsonian
Bythinian
Aegean
Olenekian
Spathian
Smithian
Induan
Dinerian
Griesbachian
Changshingian
Wuchiapingian
Capitanian
Wordian
Rhoadian
Kungurian
Artinskian
Sakmarian
Asselian
201,4 Ma
209,5 Ma
227,3 Ma
237,0 Ma
241,5 Ma
246,7 Ma
249,9 Ma
251,9 Ma
254,2 Ma
259,6 Ma
264,3 Ma
269,2 Ma
274,4 Ma
283,3 Ma
290,5 Ma
293,5 Ma
298,9 Ma
Rhaetian
Carnian
Anisian
Permian-Triassic transition
Capitanian
Kungurian
Asselian
Palaeogeographical position of the Balearic Islands

Figure 1.1. (previous page) Chronostratigraphic chart of the Permian and Triassic (based on Henderson et al., 2020, and Ogg et al., 2020), with the palaeogeographical world maps showing the position of the continents through those times (extracted from Scotese, 2014a, 2014b).

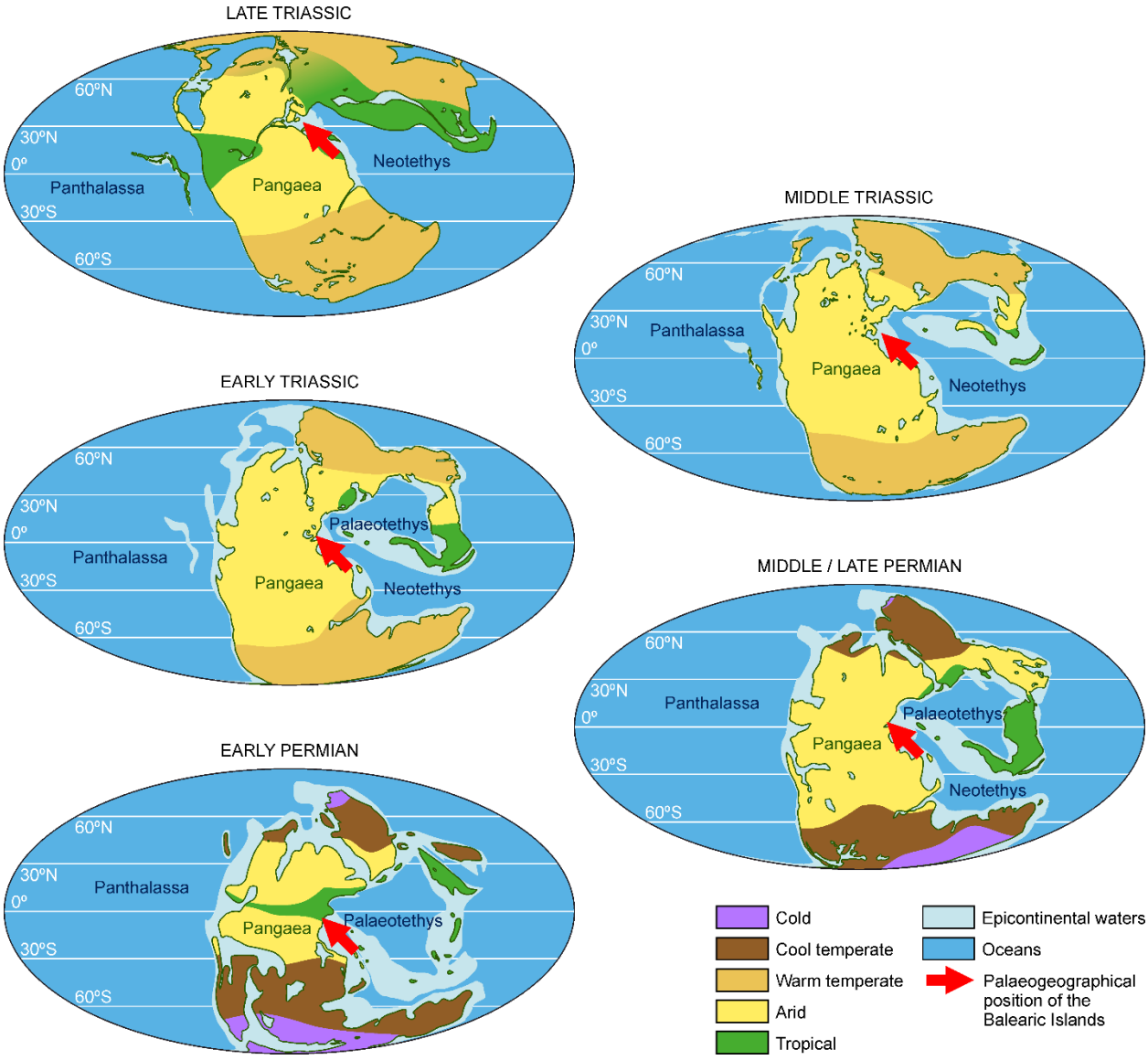

Figure 1.2. Palaeogeographical world maps with the distribution of climates during the Permian and Triassic (modified from Scotese, 2000, 2014a, 2014b).

The mass extinction event that occurred in the Permian–Triassic transition was the most dramatic biotic crisis in the Phanerozoic, wiping out many groups that had been dominant in

the Palaeozoic. It is thought that its main trigger was the eruption of the Siberian Traps, producing a cascade of effects that resulted in great perturbations of terrestrial and marine ecosystems, ultimately leading to the extinction of many taxa (Benton & Newell, 2014; Romano *et al.*, 2020 and references therein). Regarding the terrestrial tetrapods, many families of amphibians, reptiles and therapsids died out, including the last captorhinids, pareiasaurs, biarmosuchians and gorgonopsians (Retallack *et al.*, 2003; Botha & Smith, 2006; Benton & Newell, 2014; Lucas, 2017). Nevertheless, after the extinction, therapsids remained as the dominant component of the continental tetrapod faunas (Lucas, 2009).

The Triassic witnessed the rise of many modern tetrapod groups. The earliest Triassic terrestrial tetrapod communities were characterised by the great abundance of stereospondyl temnospondyls and dicynodont therapsids such as the genus *Lystrosaurus*, representing "disaster" taxa, clades that survived the extinction but would soon be replaced (Sahney & Benton, 2008; Benton & Newell, 2014; Lucas, 2017; Romano *et al.*, 2020 and references therein). By the Middle Triassic, archosauromorph diapsids and cynodont therapsids had become dominant components of the faunas (Chen & Benton, 2014). The former, which had first appeared (but were quite rare) during the Guadalupian–Lopingian, became increasingly abundant and ecologically diverse (Foth *et al.*, 2016; Ezcurra & Butler, 2018 and references therein). This was especially so during and after the Carnian Pluvial Episode (Late Triassic), a humid interval which appears to have prompted the rise of several well-known tetrapod clades, including dinosaurs, crocodylomorphs, phytosaurs, turtles and mammals (Benton *et al.*, 2014; Bernardi *et al.*, 2018; Dal Corso *et al.*, 2020). Those groups would become dominant during the rest of the Mesozoic (non-avian dinosaurs) and the Cenozoic (avian dinosaurs and mammals). The Triassic was also a time of diversification of several marine reptile groups, such as ichthyosauromorphs and sauropterygians (Neenan *et al.*, 2013; Motani *et al.*, 2017; Li & Liu, 2020).

The present Ph.D. dissertation studies the Permian and Triassic tetrapod fossil-bearing units of the Gymnesic Islands, the largest two islands of the Balearic Archipelago (western Mediterranean). They correspond to continental (Cisuralian–Middle Triassic) and marginal/marine (Middle–Upper Triassic) basins located at the eastern margin of Pangaea (Figure 1.1, 1.2), preserving rich fossil communities.

General context and previous works on the Permian and Triassic of the Gymnesic Islands

The Gymnesic Islands (Mallorca and Menorca) are the two largest islands of the Balearic Archipelago (western Mediterranean) and correspond to an emerged extension of the Betic Cordillera to the northeast (*e.g.*, Vera *et al.*, 2004). During the Permian and Triassic, the basins corresponding to the present-day Gymnesic Islands were part of the eastern margin of the supercontinent Pangaea, drifting from a latitude of 7° S in the Cisuralian (early Permian) to about 26° N in the Late Triassic (Scotese, 2014a, 2014b; Figure 1.1). Both islands show a similar sedimentary evolution (Figure 1.3), with several basal units of continental red-beds overlain by marine carbonates, then by gypsiferous marlstones and volcanic rocks, and finally by marine carbonates again (*e.g.*, Vera *et al.*, 2004). The present section reviews all the previous works for each of the two islands.

Permian

Mallorca

The hypothesis that Permian rocks cropped out on Mallorca was first put forward by Cuevas-López (1958a, 1958b). He recognised that a part of the units attributed to the Lower Triassic by previous authors (Hermite, 1879, 1888; Nolan, 1887, 1888; Darder, 1913, 1914a; Fallot, 1923) were in fact more similar to the *Rothliegend* units of the Central European Basin. There were two main units: a lower one made up of about 800 m of red sandstones and mudstones, and an upper one made up of 200 m of red sandstones and mudstones with interbedded cupriferous levels. Subsequent authors (Freeman & Obrador, 1974, 1979; Colom, 1975; Pomar-Gomà, 1979; Obrador, 1983; Martí *et al.*, 1985; Rodríguez-Perea *et al.*, 1987; Barnolas, 1991) accepted that the Permian could be present, but did not supply further data to individualise it from the Triassic.

During the late 1980s and early 1990s, several authors studied the Permian outcrops with more detail, confirming their age attribution. Ramos *et al.* (1985), Ramos & Doubinger (1989) and Ramos (1995) divided the Permian–Triassic continental sequence of Mallorca into three lithostratigraphic units: Port des Canonge unit, Asá [sic.] unit and Son Serralta unit. The study of palynomorphs revealed that the Asá unit was upper Permian and the Son Serralta unit

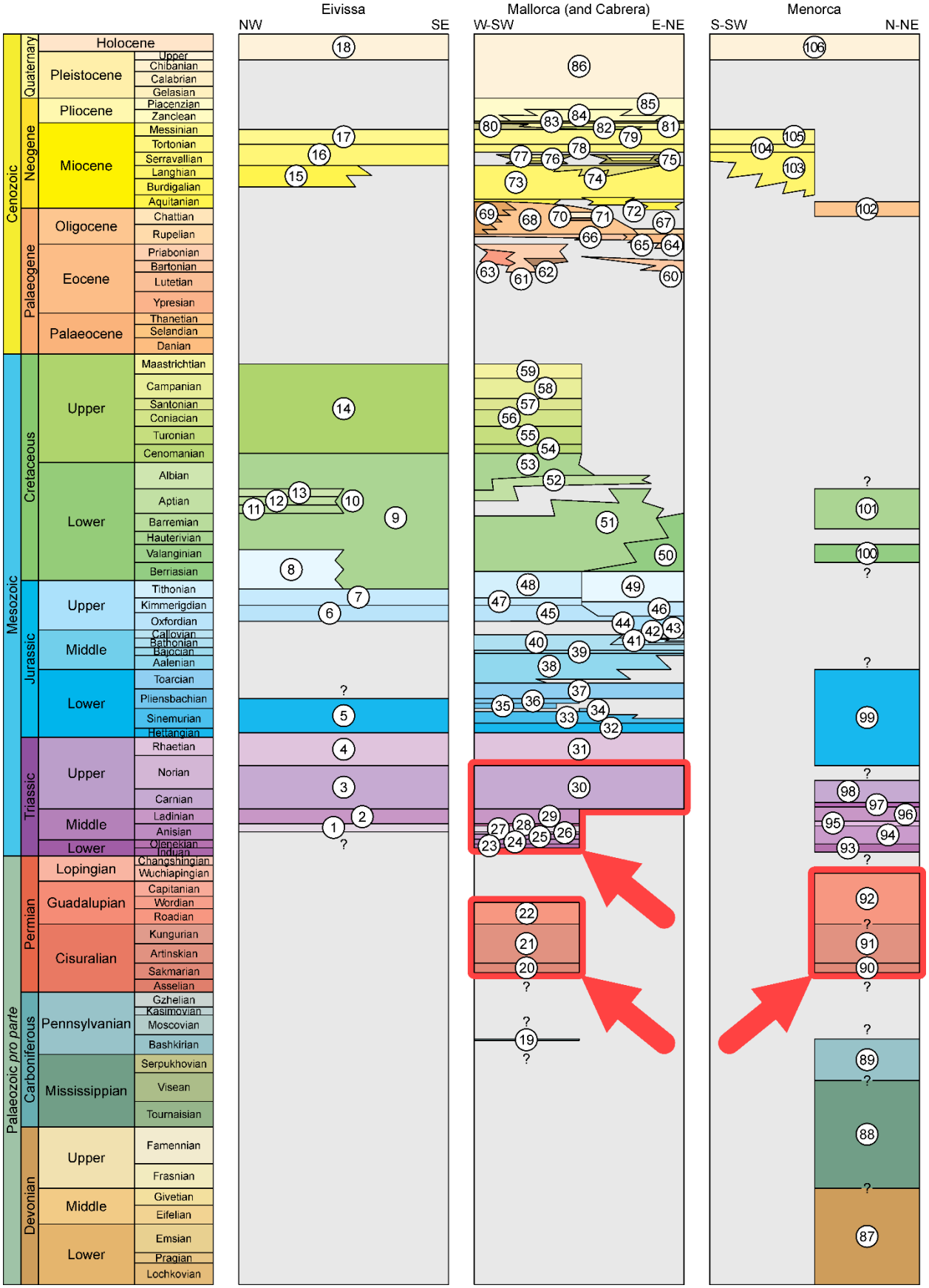
Eivissa
NW
SE
Mallorca (and Cabrera)
W-SW
E-NE
Menorca
S-SW
N-NE
Cenozoic
Quaternary
Neogene
Palaeogene
Mesozoic
Cretaceous
Jurassic
Triassic
Palaeozoic pro parte
Permian
Carboniferous
Devonian
Holocene
Upper
Pleistocene
Chibanian
Calabrian
Gelasian
Pliocene
Piacenzian
Zanclean
Miocene
Messinian
Tortonian
Serravallian
Langhian
Burdigalian
Aquitanian
Oligocene
Chattian
Rupelian
Eocene
Priabonian
Bartonian
Lutetian
Ypresian
Palaeocene
Thanetian
Selandian
Danian
Upper
Maastrichtian
Campanian
Santonian
Coniacian
Turonian
Cenomanian
Lower
Albian
Aptian
Barremian
Hauterivian
Valanginian
Berriasian
Upper
Tithonian
Kimmeridgian
Oxfordian
Middle
Callovian
Bathonian
Bajocian
Aalenian
Lower
Toarcian
Pliensbachian
Sinemurian
Hettangian
Upper
Rhaetian
Norian
Carnian
Middle
Ladinian
Anisian
Lower
Olenekian
Induan
Lopingian
Changshingian
Wuchiapingian
Guadalupian
Capitanian
Wordian
Roadian
Cisuralian
Kungurian
Artinskian
Sakmarian
Asselian
Pennsylvanian
Gzhelian
Kasimovian
Moscovian
Bashkirian
Mississippian
Serpukhovian
Visean
Tournaisian
Upper
Famennian
Frasnian
Middle
Givetian
Eifelian
Lower
Emsian
Pragian
Lochkovian

Figure 1.3. (previous page) Chronostratigraphic chart with all the formal and informal lithostratigraphic units defined for the Balearic Islands. Igneous intrusions and mio-plio-plestocenic cave breccias not represented. **1–18:** *Eivissa (Rangheard, 1971, 1984; Durand-Delga* et al., *1993; Díaz de Neira & Gil-Gil, 2009, 2014).* **1:** Muschelkalk *Dolostone unit,* **2:** Muschelkalk *Limestone unit,* **3:** Keuper *facies unit,* **4:** *Pedrera de Sant Miquel formation,* **5:** *Port de ses Caletes formation,* **6:** *Es Botafoc formation,* **7:** *Dalt Vila formation,* **8:** *Punta des Jondal Formation,* **9:** *Es Cubells Formation,* **10:** *Port de Sant Miquel Formation,* **11:** *Torre des Molar Member,* **12:** *Penyal de s'Àguila Member,* **13:** *Cala d'en Sardina Formation,* **14:** *Cala Llentrisca Formation,* **15:** *Cala d'Hort formation,* **16:** *Cap Jueu formation,* **17:** *Portinatx formation,* **18:** *Quaternary units.* **19–88:** *Mallorca (Álvaro* et al., *1982, 1984, 1989; Pomar* et al., *1983; Barnolas, 1984, 1991; Rodríguez-Perea, 1984; Rodríguez-Perea & Ramos, 1984; Rodríguez-Perea* et al., *1987; Ramos-Guerrero, 1988; Ramos-Guerrero* et al., *1989, 1994a, 1994b, 2000, 2001; Fornós* et al., *1991; Martin-Closas & Ramos, 2005; Arenas* et al., *2007; Mas, 2013, 2015; López-García* et al., *2014; Juárez-Ruiz & Matamales-Andreu, 2015, 2018; Moragues, 2015; Matamales-Andreu* et al., *2018; Mas & Fornós, 2020; Rosales* et al., *2021; Sevillano* et al., *2021; Juárez-Ruiz & Mas, 2022; the present work).* **19:** Culm *facies unit,* **20:** *Bec de s'Àguila Formation,* **21:** *Port des Canonge Formation,* **22:** *Pedra de s'Ase Formation,* **23:** *Punta Roja Formation,* **24:** *Estellencs Formation,* **25:** *Pedra Alta Formation,* **26:** *Son Serralta Formation,* **27:** *M1 unit,* **28:** *M2 unit,* **29:** *M3 unit,* **30:** Keuper *facies unit,* **31:** *Felanitx formation,* **32:** *Mal Pas Formation,* **33:** *Es Barracar Formation,* **34:** *Shallow Platform Limestone unit,* **35:** *Moleta Formation,* **36:** *Es Racó Formation,* **37:** *Cosconar Formation,* **38:** *Gorg Blau Formation,* **39:** *Cúber Formation,* **40:** *Puig d'Alpara Formation,* **41:** *Puig de Cutrí Formation,* **42:** *Sa Talaia Mudstone unit,* **43:** *Coves d'Artà Limestone unit,* **44:** *Puig de ses Fites Formation,* **45:** *Alfàbia Formation,* **46:** *Sa Carbonera Formation,* **47:** *Almadrà Formation,* **48:** *Son Torrella Formation,* **49:** *Puig d'en Borràs Formation,* **50:** *Cala Torta facies unit,* **51:** *Lower White Limestone unit,* **52:** *Grey Marlstone unit,* **53:** *Upper White Limestone unit,* **54:** *Lower White Silty Limestone unit,* **55:** *White Limestone with Silex Nodules unit,* **56:** *Lower Yellow-Pink Limestone unit,* **57:** *Upper Yellow-Pink Limestone unit,* **58:** *White-Pink Limestone unit,* **59:** *Upper White Silty Limestone unit,* **60:** *Puig de s'Envestida Formation,* **61:** *Peguera Formation,* **62:** *Binissalem Member,* **63:** *Platja des Morts Member,* **64:** *El Calvari Formation,* **65:** *Galdent Formation,* **66:** *Alaró Formation,* **67:** *Son Sastre Formation,* **68:** *Cala Blanca Formation,* **69:** *Puig d'en Tió Member,* **70:** *Sineu Member,* **71:** *Defla Member,* **72:** *Sant Elm Formation,* **73:** *Banyalbufar Formation,* **74:** *Randa*

unit, ***75:*** *Manacor unit,* ***76:*** *Sa Verdera unit,* ***77:*** *Pina unit,* ***78:*** *Calcisiltites with* Heterostegina *unit,* ***79:*** *Reefal unit,* ***80:*** *La Bonanova unit,* ***81:*** *Sant Jordi Gypsum unit,* ***82:*** *Santanyí unit,* ***83:*** *Ses Olles Formation,* ***84:*** *Son Mir unit,* ***85:*** *Sant Jordi unit,* ***86:*** *Palma unit.* ***87–105:*** *Menorca (Bourrouilh, 1983; Rosell* et al.*, 1989; Tiedt, 1994; Vera* et al.*, 2004; Martin-Closas & Ramos, 2005; Bercovici* et al.*, 2009; Linol* et al.*, 2009; Escudero-Mozo* et al.*, 2014; the present work).* ***87:*** *Low Energy Turbidite unit,* ***88:*** *Transition unit,* ***89:*** *Culm facies unit,* ***90:*** *P1 unit,* ***91:*** *P2 unit,* ***92:*** *P3 unit,* ***93:*** *B1 unit,* ***94:*** *B2 unit,* ***95:*** *El Toro formation,* ***96:*** *Arenal d'en Castell formation,* ***97:*** *Cala Fontanelles formation,* ***98:*** *Keuper facies unit,* ***99:*** *Dolostone and Limestone unit,* ***100:*** *Micritic Limestone unit,* ***101:*** *Limestone and Marlstone unit,* ***102:*** *Cala Blanca Formation,* ***103:*** *Basal Conglomerate unit,* ***104:*** *Lower Bar unit,* ***105:*** *Reefal unit,* ***106:*** *Quaternary units.*

was Middle Triassic. Logically, the underlying unit, namely, Port des Canonge, had to be Permian or older. Calafat (1986, 1987, 1988) showed that the units described by Ramos had been the result of a miscorrelation between outcrops, and defined five units for the Permian–Triassic rocks of continental origin: Bec de s'Àguila, Port des Canonge, Pedra de s'Ase (with the Punta Roja sub-unit), Estellencs and Son Serralta units. Gómez-Gras (1992, 1993) restudied most of the sections and proposed a division of the Permian of Mallorca into three main units, which he named Stretch 'a', 'b' and 'c'. All those units were interpreted as alluvial/fluvial deposits (Calafat, 1988; Gómez-Gras, 1993; Ramos, 1995) (Figure 1.4).

The fossil content of the Permian of Mallorca includes spores, pollen, tree logs, invertebrate traces, tetrapod tracks and tetrapod bones. A palynoassemblage with elements of the 'Thuringian' biofacies was reported by Ramos & Doubinger (1989), Diez (2000), Diez *et al.* (2005) and Juncal (2019) from the Asá/Pedra de s'Ase unit. In the same unit, Freeman & Obrador (1974, 1979), Calafat (1988), Ramos (1995) and Diez (2000) found and illustrated large carbonised tree logs. Regarding animal fossils, Ramos & García-Ramos (1992) and Ramos (1995) described several invertebrate bioturbation traces from the Port des Canonge and Asá units, and Calafat *et al.* (1986, 1986–1987) and Calafat (1988) reported four morphotypes of tetrapod tracks from the Racó de s'Algar unit. One of these was illustrated again in Sastre & Sastre (2002, 2005). Calafat *et al.* (1986, 1986–1987), Calafat (1988) and Liebrecht *et al.* (2017) also mentioned the presence of tetrapod bones in the Racó de s'Algar and Pedra de s'Ase units, but only one of them was described in detail as a maxilla of a moradisaurine captorhinid eureptile (Liebrecht *et al.*, 2017).

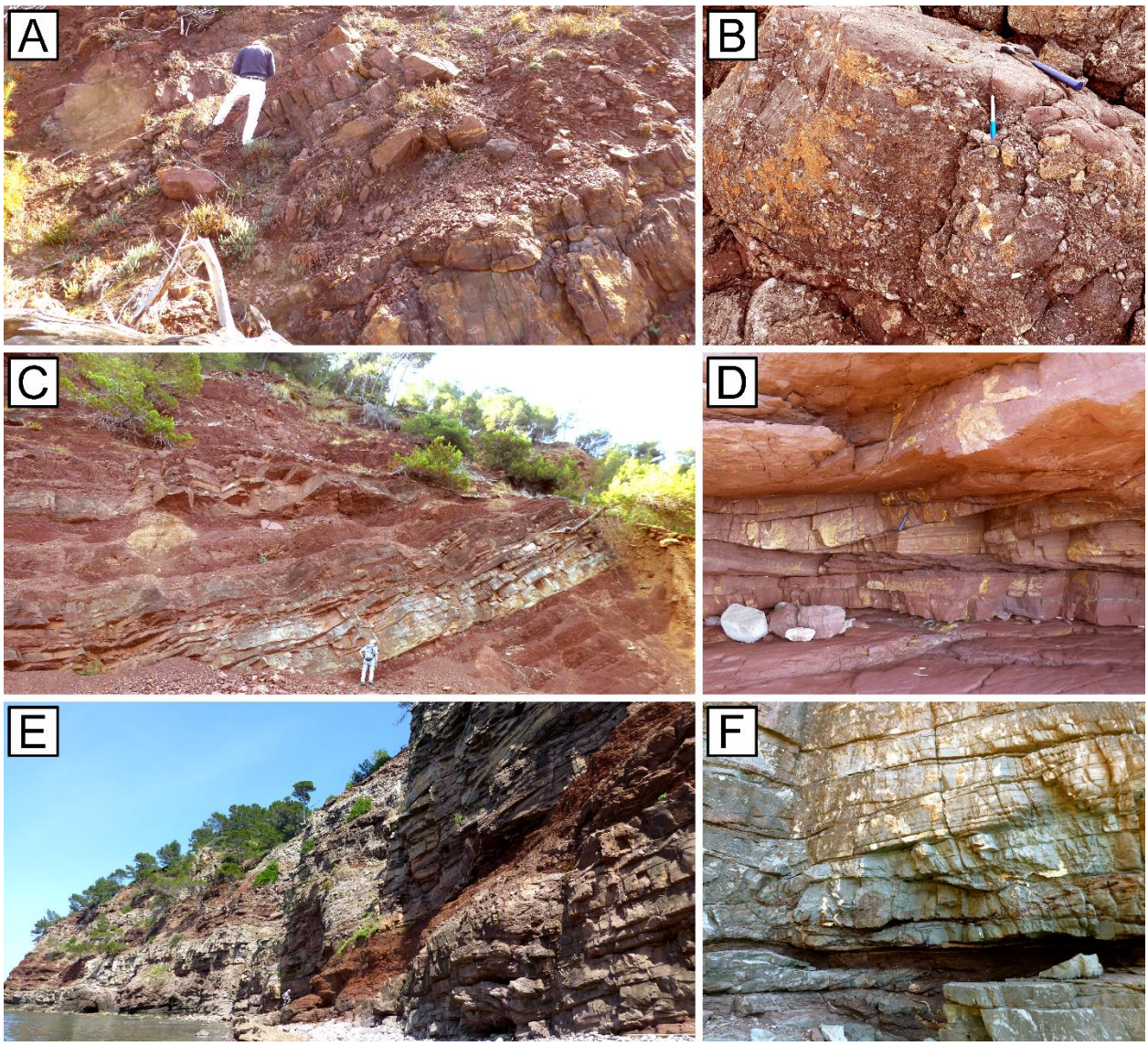

Figure 1.4. Units from the Permian of Mallorca. ***A–B:*** *Lower polygenic breccias and sandstones, outcrop view (Platja de sa Pedrera) and close-up (Sa Gratallosa), respectively.* ***C–D:*** *Middle red sandstones and lutites, outcrop view (Platjola des munt de Pedres) and close-up (near Torrent de cas Batliu), respectively.* ***E–F:*** *Upper white/blue/pink sandstones and scarce lutites, outcrop view (Platja d'en Sales) and close-up (Puig des Moro), respectively.*

Menorca

Permian rocks were first identified on Menorca by Bourrouilh (1973, 1983), distinguishing a basal unit of polymictic conglomerates, a middle one with abundant lutites and an upper one with lutites and sandstones. Until then, those units had been considered to be of Lower Triassic age because of its lithological similarity to the *Buntsandstein* facies (Hermite,

1879, 1888; Nolan, 1887, 1888). But from then on, all the authors acknowledged a Permian age for the lower red-beds of the island (Pomar-Gomà, 1979; Obrador, 1983; Martí *et al.*, 1985; Rodríguez-Perea *et al.*, 1987). Lithostratigraphic units, roughly corresponding to the ones described by Bourrouilh (1973, 1983), were informally defined by Gómez-Gras (1987, 1992, 1993) and Rosell *et al.* (1988, 1989), from lower to upper: P1, P2 and P3. Arribas *et al.* (1990) and Brandes & Tiedt (1991) studied the textural maturity and composition of some of the sandstones. All those units were interpreted as alluvial/fluvial deposits (Rosell *et al.*, 1988; Gómez-Gras & Alonso-Zarza, 2003; Linol *et al.*, 2009) (Figure 1.5).

Regarding its fossil content, Rosell *et al.* (1989), Broutin *et al.* (1992) and Bercovici *et al.* (2009) described rich palynoassemblages from several beds of the P3 unit, revealing a 'Thuringian' biofacies. Bercovici *et al.* (2009) also reported some plant remains, including conifer shoots and cones. Tetrapod bones were preliminarily described by Pretus & Obrador (1987) and Carmona (2004).

*Lower–Middle Triassic (*Buntsandstein *facies)*

Mallorca

Hermite (1879, 1888) and Lozano (1884) were the first to report the Triassic *Buntsandstein* facies on Mallorca based on the discovery of the horsetail *Equisetites* in the red-beds near Estellencs. Nolan (1887, 1888), Darder (1913, 1914a) and Fallot (1922) studied other similar outcrops, and also attributed them to the Lower Triassic *Buntsandstein* facies. Cuevas-López (1958a, 1958b) proposed that only a part of the red-beds were Triassic, and distinguished a lower, middle and upper *Buntsandstein* facies. This division was accepted by most of the subsequent works (Colom, 1975; Pomar-Gomà, 1979; Martí *et al.*, 1985; Rodríguez-Perea *et al.*, 1987; Barnolas, 1991).

Other studies provided more details regarding the stratigraphy and age of those rocks. A single Triassic lithostratigraphic unit was recognised in the works by Ramos *et al.* (1985), Ramos & Doubinger (1989) and Ramos (1995), which was dated in the Anisian using palynomorphs, and was called Son Serralta unit. Other works, such as those by Calafat (1986, 1987, 1988), split the succession into two: the Estellencs unit and the Son Serralta unit, both from the Anisian. Gómez-Gras (1992, 1993) provided yet another division, with two main units, the Stretch 'd' and the Stretch 'e', the latter of which was in turn divided into three.

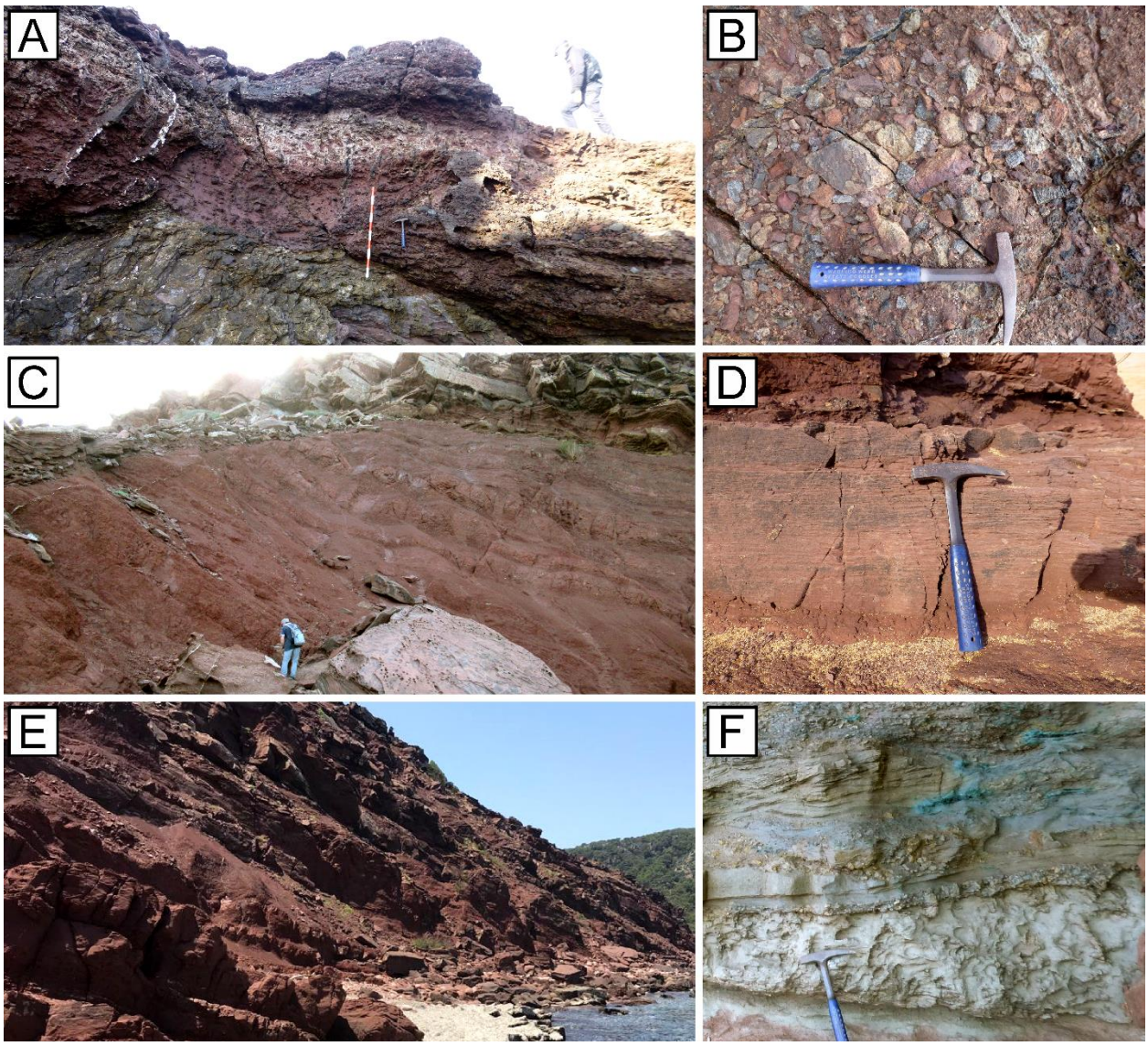

*Figure 1.5. Units from the Permian of Menorca. **A–B:** Lower polygenic breccias and sandstones, outcrop view and close-up, respectively (both from eastern Cala del Pilar). **C–D:** Middle lutites and sandstones, outcrop view and close-up, respectively (both from Punta des Carregador). **E–F:** Upper red sandstones and lutites, outcrop view (Sa Bombarda) and close-up of coal-bearing levels (coal mine near Pla de Mar), respectively.*

Regardless of the number of lithostratigraphic units distinguished, all the authors interpreted them as alluvial/fluvial environments, reworking aeolian sediments in the lower unit (Calafat, 1988; Clemmensen & Hansen, 2021) and with marine influence towards the top unit (Calafat, 1988; Ramos, 1995) (Figure 1.6).

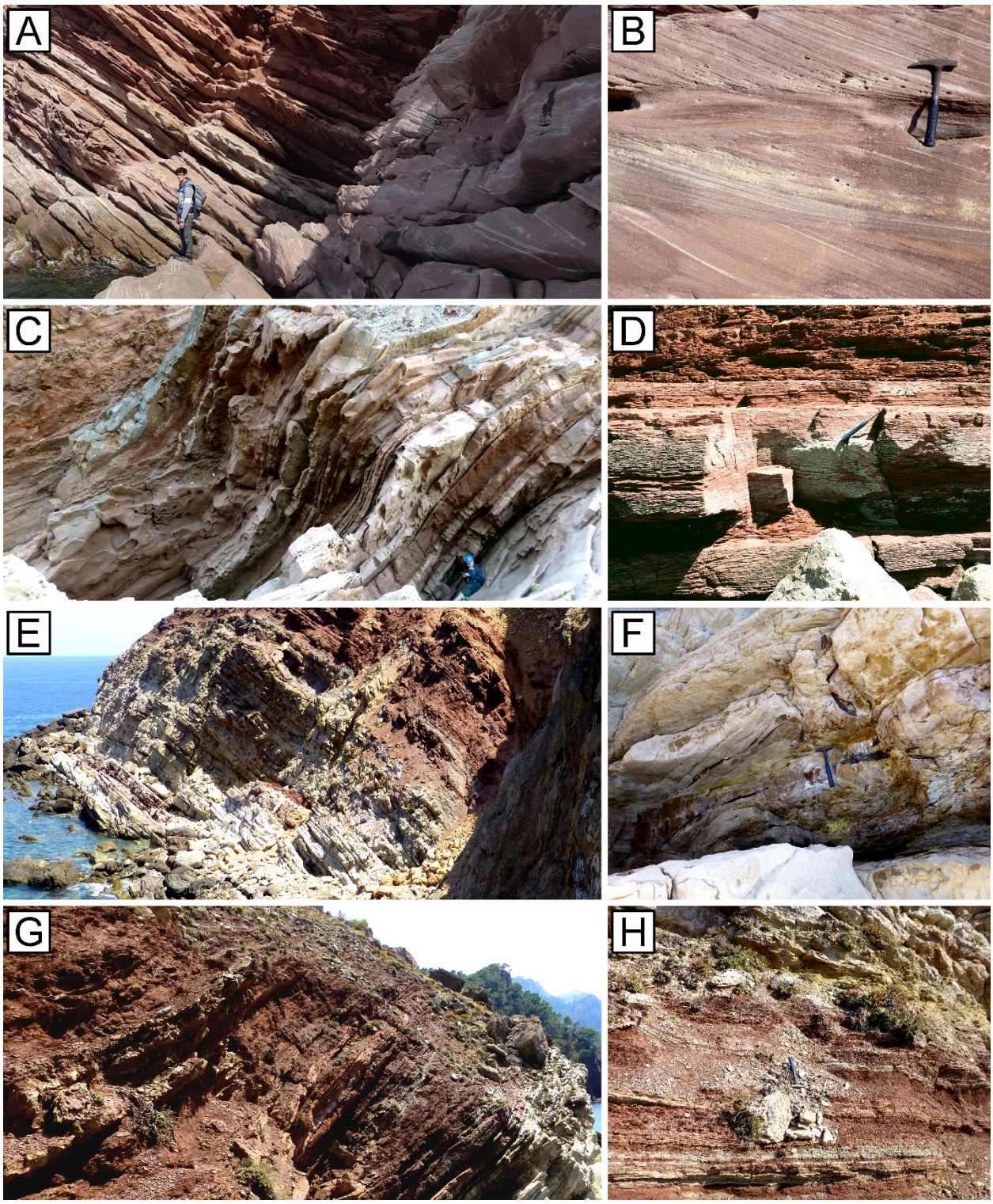

Figure 1.6. Units from the Lower–Middle Triassic Buntsandstein *facies of Mallorca. **A–B:** Basal cross-stratified sandstones, outcrop view and close-up, respectively (both from Punta Roja). **C–D:** Lower red sandstones and lutites, outcrop view (Punta Roja) and close-up (Punta Negra), respectively. **E–F:** Middle white/blue/pink sandstones, outcrop view and close-up, respectively (both from Tenassa de sa Tanca). **G–H:** Upper red lutites transitioning towards the* Muschelkalk *carbonates, outcrop view and close-up, respectively (both from Tenassa de sa Tanca).*

The continental Triassic of Mallorca contains fossils of spores, pollen, plant leaves and strobili, invertebrate traces, crustaceans, insects, tetrapod tracks and fishes. Palynoassemblages typical of the Anisian stage (Middle Triassic), and some specifically from the Aegean substage, were reported by Calafat (1988), Ramos & Doubinger (1989), Grauvogel-Stamm & Álvarez-Ramis (1994, 1996), Ramos (1995), Diez (2000) and Diez *et al.* (2005, 2010). Well-preserved fossils of horsetails, ferns and conifers were illustrated by Calafat (1988), Álvarez-Ramis *et al.* (1989, 1995), Grauvogel-Stamm & Álvarez-Ramis (1994, 1996) and Juárez-Ruiz & Wachtler (2015). Invertebrate ichnofossils were mentioned, but not studied, by Calafat (1988) and Zessin (2008b). Clam shrimps and several groups of insects were reported by Calafat & Sáez (1987), Calafat (1988), Gallemí *in* Gallemí *et al.* (1988) Martínez *in* Gallemí *et al.* (1988), Ansorge (1997), Zessin (2008a, 2008b), Aristov & Zessin (2009) and Juárez-Ruiz & Wachtler (2015). Tetrapod tracks were illustrated by Juárez-Ruiz & Wachtler (2015). Moreover, Calafat *et al.* (1987) and Calafat (1988) also reported the presence of large structures that could correspond to tracks. Finally, Calafat & Sáez (1987) and Calafat (1988) mentioned the presence of a small fish, and Zessin (2008b) claimed to have found a fish egg case.

Menorca

The *Buntsandstein* facies of Menorca were first reported and described by Hermite (1879, 1888) and Nolan (1887, 1888). Bourrouilh (1973, 1983) distinguished two main units in those facies: a lower one made up of red and grey sandstones, and an upper one consisting of red lutites and sandstones. Pomar-Gomà (1979), Martí *et al.* (1985) and Rodríguez-Perea *et al.* (1987) lumped together the Permian and the Triassic continental units, but they essentially distinguished the two main parts mentioned by previous authors. Gómez-Gras (1987) and Rosell *et al.* (1988, 1989) named them B1 and B2, respectively, and characterised the limit between Permian and Triassic units as an erosive surface overlain by quartz conglomerates. Arribas *et al.* (1990), Brandes & Tiedt (1991), Gómez-Gras (1992, 1993), Gómez-Gras & Alonso-Zarza (2003) and Linol *et al.* (2009) used this framework again, providing more data on the nature of the conglomerates of the B1 unit (with ventifacts), the carbonate palaeosols of the B2 unit, the textural maturity and composition of the sandstones, and the lateral variations of these units in different parts of the basin. Both units have been interpreted as fluvial/alluvial deposits with marine influence towards the top (Rosell *et al.*, 1988; Linol *et al.*, 2009).

The fossil record of the *Buntsandstein* facies of Menorca is extremely scarce. Bourrouilh (1973, 1983), Freeman & Obrador (1974, 1979), Gómez-Gras (1987), Gómez-Gras & Alonso-Zarza (2003) and Linol *et al.* (2009) mentioned the presence of rhizocretions, plant debris and tree logs in the lower sandstones, and Rosell *et al.* (1989) reported a palynoassemblage which could be dated in the Anisian, although they did not specify the bed or locality from where it came. Indeterminate animal trace fossils were mentioned by Gómez-Gras (1987).

Middle–Upper Triassic (Muschelkalk facies)

Mallorca

Hermite (1879, 1888) and Nolan (1887, 1888) were, again, the first authors to identify the Triassic *Muschelkalk* facies on Mallorca, attributing them to the Middle and Upper part of the period. Darder (1913, 1914a) and Fallot (1922) divided the sequence into two main units: a lower one from the Virglorian (Anisian), with dolomitic limestones, encrinites, limestones with burrows and massive limestones, and an upper one, from the Ladinian, with limestones containing the bivalve *Daonella* and burrows. This was further discussed by Schimdt (1935) and Virgili (1952), proposing that the fossiliferous limestones were Ladinian, and the marlstones with ammonoids were Longobardian (upper Ladinian). Cuevas-López (1958a, 1958b) was the first author to report a detrital interval made up of red lutites and sandstones, intercalated between the two carbonate units described by previous authors. Colom (1975) provided a synthesis of what was known until then. Pomar-Gomà (1979), Martí *et al.* (1985) and Rodríguez-Perea *et al.* (1987) coined the names M1, M2 and M3 for the three lithostratigraphic units, which were already in use for equivalent intervals in the Iberian Peninsula. They interpreted the succession as shallow-water carbonates with an interval of sub-aerial exposure (Rodríguez-Perea *et al.*, 1987) (Figure 1.7).

A few fossiliferous horizons have been reported from the *Muschelkalk* unit. In the M1 unit there is a level with disarticulated crinoid columnals (Darder, 1914a; Rodríguez-Perea *et al.*, 1987). On the other hand, in the M3 unit there are diverse assemblages with molluscs (bivalves, gastropods and cephalopods) (Nolan, 1887, 1888; Darder, 1913, 1914a; Fallot, 1922; Schmidt, 1935; Bauzá, 1945, 1946, 1971, 1981; Rotger, 1952; Virgili, 1952; Goy, 1995; Rein, 2008; Pérez-Valera & Goy, 2012; Pla & Enseñat, 2020), rare plants (Bauzá, 1946,

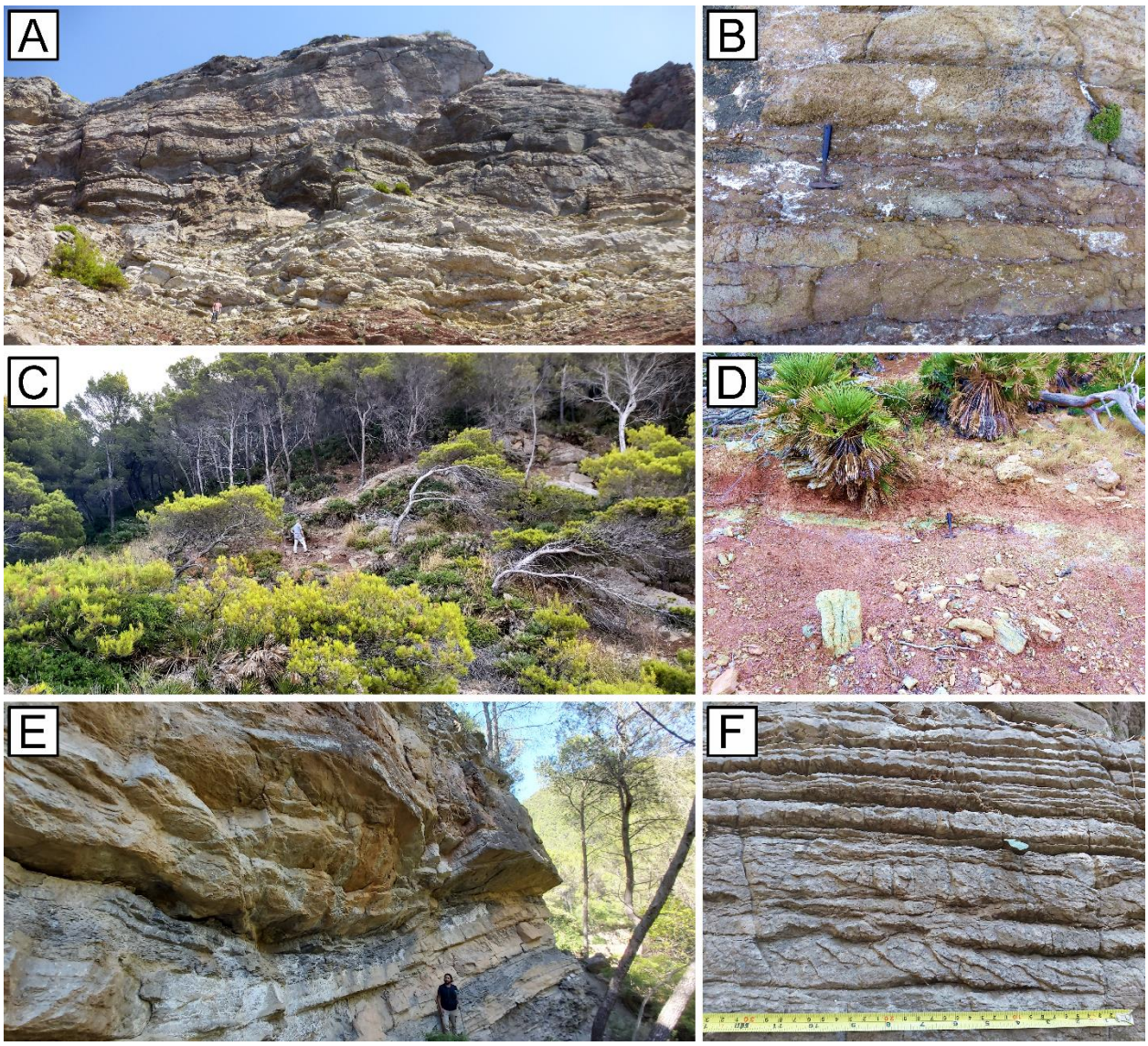

Figure 1.7. Units from the Middle–?Upper Triassic Muschelkalk *facies of Mallorca.* ***A–B:*** *Lower gray dolostones, outcrop view and close-up, respectively (both from Punta de son Serralta).* ***C–D:*** *Middle red lutites, outcrop view and close-up, respectively (both from Torrent de sa Tanca).* ***E–F:*** *Upper gray limestones and dolostones, outcrop view (Rotes des pinar de Canet) and close-up (Mola de na Costitxa), respectively.*

1971) and ophiuroids (Bauzá, 1981). Even though microfossils have not been extensively sampled in any of the outcrops, two forms of foraminifera (*Lingulina* and *Glomospira*) (Colom, 1975; Barnolas, 1991), two of testate amoebae (*Difflugia inesperata* and *Trigonopyxis keuperina*) (Colom, 1982), and two of conodonts (*Pseudofurnishius murcianus* and *Sephardiella mungoensis*) (Hirsch, 1972) have been reported. Regarding vertebrate fossils,

Bauzá (1955) figured a vertebra of a marine reptile, which was also mentioned by Bauzá (1971), Colom (1975, 1982) and Sanz (1980, 1983).

Menorca

Hermite (1979, 1988) and Nolan (1887, 1888, 1893, 1933) first reported and mentioned the *Muschelkalk* facies from Menorca, attributing them to the Middle and Upper Triassic. Subsequent works by Tornquist (1909), Wurm (1913) and Hollister (1934) reviewed the previous studies and provided new data, noting that the faunas, albeit in Germanic facies, showed Alpine influence. Bourrouilh (1973, 1983) studied those carbonate units with much more detail, integrating all the previous palaeontological studies. Pomar-Gomà (1979), Martí *et al.* (1985) and Rodríguez-Perea *et al.* (1987) provided some more general stratigraphic data. Llompart *et al.* (1987) carried out the first detailed biostratigraphic study of several sections of the island, recognising the lower Ladinian, the upper Ladinian and the lower Carnian, and dividing the *Muschelkalk* sequence of Menorca into three main carbonate stretches. Rosell *et al.* (1989) attributed those three stretches to the M3 unit, and doubtfully recognised the M1 dolostones and the M2 red-beds, which would result in a sequence very similar to those of Mallorca and the western Iberian Peninsula. However, they admitted that the purported M2 red-beds could be a tectonic repetition of the underlying *Buntsandstein* (B2 unit), and thus the M1 would in fact merely correspond to a dolostone bed of the M3. Those authors also supplied further micropalaeontological data, which allowed them to increase the precision of the age attributions within the M3. Escudero-Mozo *et al.* (2014) reviewed the stratigraphy, sedimentology and ammonoid taxonomy proposed by Llompart *et al.* (1987), and informally (they did not specify stratotypes) defined three lithostratigraphic formations: El Toro formation, Arenal d'en Castell formation and Cala Fontanelles formation. Those authors did not recognise the M1 and M2 units mentioned by Rosell *et al.* (1989); instead, they posited that the *Muschelkalk* of Menorca is entirely composed of carbonates. This whole succession has been interpreted as a shallow carbonate ramp evolving towards open sea conditions, with an abrupt sea level drop in the early Carnian followed by a brief period of deposition of shallow marine carbonates (Escudero-Mozo *et al.*, 2014).

The *Muschelkalk* facies are locally very fossiliferous on Menorca. Numerous brachiopod and mollusc assemblages have been reported (Hermite, 1879, 1888; Mojsisovics, 1882,

1887; Nolan, 1887, 1888, 1893, 1933; Tornquist, 1909; Fallot, 1922; Schmidt, 1929, 1930, 1931, 1935; Hollister, 1934; Llopis-Lladó, 1935; Bourrouilh, 1973, 1983; Hirsch, 1977; Llompart *et al.*, 1987; Rosell *et al.*, 1989; Goy, 1995; Escudero-Mozo *et al.*, 2014), being typical of the lower Ladinian, upper Ladinian and lower Carnian. Moreover, scarce remains of echinoids (Hermite, 1979, 1988) and even vertebrates such as fishes (Hermite, 1979, 1988) and reptiles (Manera, 1930, although from an indeterminate "Triassic") have also been found. Regarding microfossils, several authors mentioned palynomorphs, foraminifera, holothurian sclerites and conodonts (Hirsch, 1972, 1977; Bourrouilh, 1973, 1983; Rosell *et al.*, 1989; Vachard *et al.*, 1989; March, 1991; Vachard & Colin, 1994), generally indicative of the upper Ladinian–lower Carnian.

Upper Triassic–Lower Jurassic (Keuper facies and Felanitx formation)

Mallorca

Nolan (1887, 1888) considered that the variegated marlstones and dolostones overlying the *Muschelkalk* facies corresponded to the "Upper Triassic", which at that time was used interchangeably with the name "*Keuper*". Darder (1913, 1914a, 1914b) was the first author to recognise the quantitative importance of the *Keuper* marlstones and lutites in the mountain ranges of Mallorca. He also mentioned the "supra-Carnian limestone" over the *Keuper*. Fallot (1922) described new areas where these facies crop out, and Hollister (1934) mentioned again the sequences of marlostones and lutites overlain by dolostones and fenestral carbonates of uncertain age.

During the 1970s, 1980s and 1990s, several detailed studies were carried out. Bourrouilh (1973, 1988) characterised the *Keuper* in the Serres de Llevant, considering all dolostones to be from the Jurassic. Barnolas (1982) informally coined the term "Felanitx formation" to refer to the laminated, dark-coloured, lower dolostones overlaying the *Keuper* facies. Navidad & Álvaro (1985) studied the basalt and tuff deposits of Cala Tuent, characterising its stratigraphy and igneous petrology. They distinguished the "lower red stretch", corresponding to the upper *Keuper*, and the "upper carbonate stretch", corresponding to the Felanitx formation. Rodríguez-Perea *et al.* (1987) studied again the *Keuper* of Cala Tuent, together with that of Son Cabaspre, which was stated to be among the most complete *Keuper* sequences on the island, and the surroundings of Sóller, purportedly representing the transition

from the *Muschelkalk* to the *Keuper*. The sequences are mostly made up of variegated lutites and marls, with some interbedded levels of dolostones and fenestral carbonates. Intercalated volcanic rocks (basalts and pyroclasts) are very common in some sections and, towards the upper part of the unit, evaporite deposits (gypsum and anhydrite) become increasingly thicker. They did not mention the Felanitx formation. Barnolas (1991) mapped several outcrops throughout the island, and presented the log of Cala Tuent again, with a much more detailed description of the facies. Sanz *et al.* (2013) provided new information on some of the sequences and the igneous rocks. López-Gómez *et al.* (2017) described a new section near the town of Fornalutx, purportedly representing the *Muschelkalk–Keuper* transition and the lowermost part of the *Keuper* facies unit. Based on the sedimentary environments, they roughly correlated the section to the units K1 and K2 (Manuel Formation) of the Iberian Peninsula.

The *Keuper* facies correspond to continental deposits, coastal lagoons (sabkhat) and intertidal coastal environments (Rodríguez-Perea *et al.*, 1987), with subaerial and subaquatic volcanic activity (Sanz *et al.*, 2013). The Felanitx formation represents the carbonate sedimentation in sabkha and shallow, restricted platform environments (Barnolas, 1982) affected by occasional volcanic activity (Navidad & Álvaro, 1985) (**Figure 1.8**).

Fossils are very scarce in these two units. From the upper part of the *Keuper* facies, Colom (1982) reported a fragment of epiphysis of a limb bone of an indeterminate reptile (also see Colom, 1975). In the lower part of the Felanitx formation, Boutet *et al.* (1982) located a palynoassemblage indicative of the upper Norian, and Barnolas (1991) reported the ostracod "*Herpetocypris*" sp.

Igneous rocks appear in both units and have been studied by Adán de Yarza (1879), Fouqué & Michel-Lévy *in* Hermite (1879, 1888), Nolan (1887, 1888), Darder (1914a), San Miguel de la Cámara (1919, 1936), Fallot (1922), Colom (1975), Mataillet & Pechoux (1978), Álvaro *et al.* (1983), Martí *et al.* (1985), Navidad & Álvaro (1985), Enrique (1986, 1990, 2012), Enrique *et al.* (1987), Rodríguez-Perea *et al.* (1987), Lago *et al.* (1988, 1989, 1996), Pocoví *et al.* (1989), Barnolas (1991), Sanz *et al.* (2013) and López-Gómez *et al.* (2017). According to the aforementioned authors, in the *Keuper* facies there are synsedimentary lava flows, pyroclastic deposits and hypovolcanic sills, some of which show subaerial exposure, with development carbonate palaeosols in the finest sediments. Hypovolcanic and teschenite sills are also present, probably in the Felanitx formation.

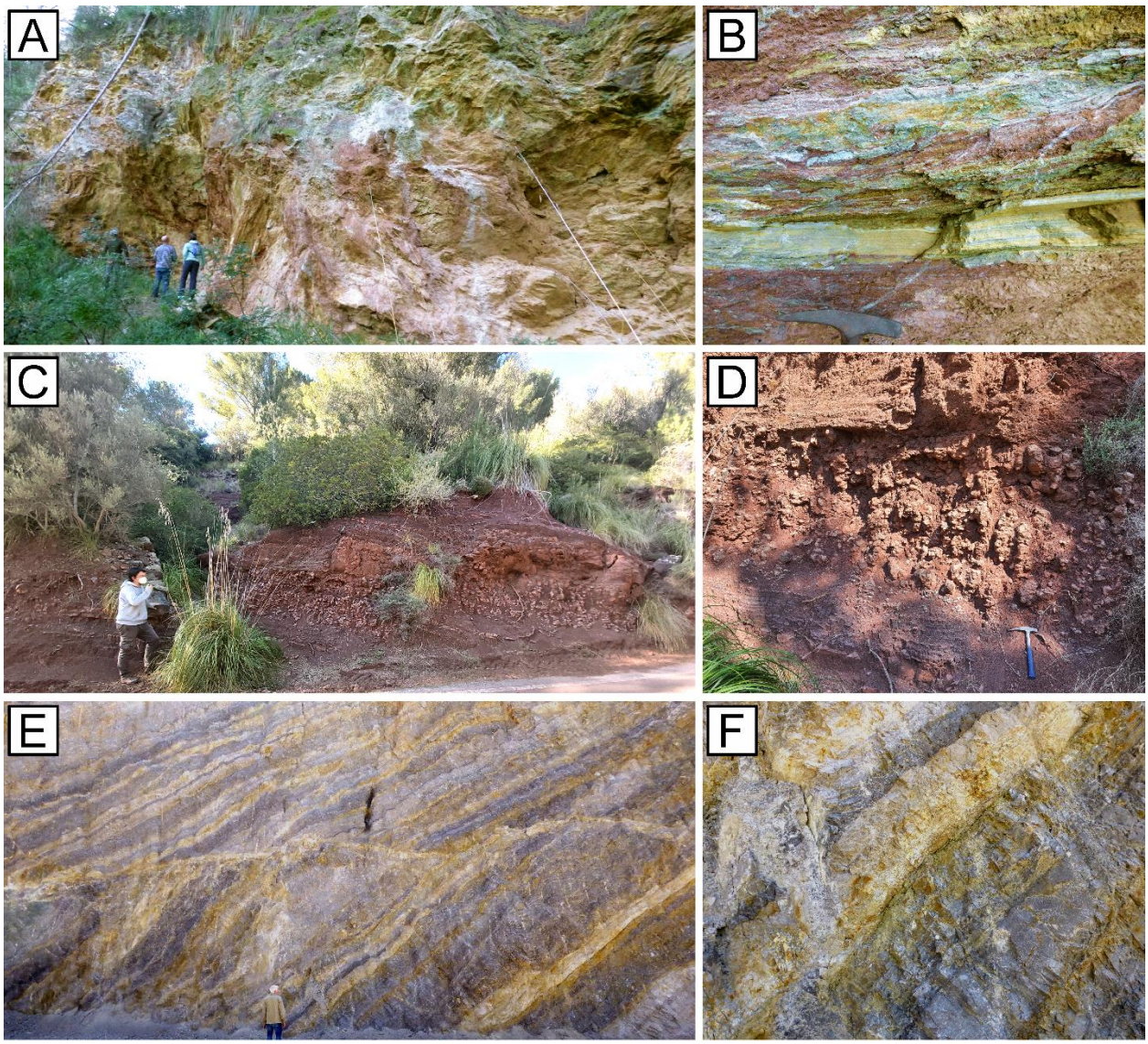

Figure 1.8. Units from the Upper Triassic Keuper *facies and the Upper Triassic–Lower Jurassic Felanitx Formation of Mallorca.* ***A–B:*** *Levels with evaporites and marlstones, outcrop view and close-up, respectively (both from Can Bleda).* ***C–D:*** *Levels with palaeosols formed on cinerites and basalts, outcrop view and close-up, respectively (both from Cala Tuent).* ***E–F:*** *Upper gray dolostones, outcrop view and close-up, respectively (both from Clots de sa grava de son Coletes).*

Menorca

Similarly to what happened on Mallorca, Nolan (1887, 1888) reported the "Upper Triassic" in Menorca, encompassing the limestones with *Daonella* and the overlying laminated dolostones. Tornquist (1909) was the first author to recognise the presence of typical *Keuper*

variegated marls, interbedded between dolostones and fenestral carbonates comparable to those of the Upper Triassic in other parts of Europe. Wurm (1913), Fallot (1922) and Hollister (1934) revised the previous works, reaching similar conclusions. Bourrouilh (1973, 1983) described three outcrops of dolostones and variegated marlstones, which were attributed to the *Keuper*. He considered that the dolostones overlaying the variegated marlstones were Jurassic. Rodríguez-Perea *et al.* (1987) briefly described those facies again. Rosell *et al.* (1989) is the most recent study considering the *Keuper* of Menorca, at Punta des Vernís and Punta de s'Aprés, recognising variegated marlstones overlaying a hard-ground over the brechified *Muschelkalk* dolostones. They also observed that in other areas, such as at Clot des Guix, the marlstones contain evaporites. The aforementioned authors considered that the dolostones overlaying the *Keuper* are not Triassic (as stated by classical authors and similar to the situation seen in Mallorca), but to the Jurassic, even though they contain no fossils. No palaeoenvironmental interpretations have been carried out for these facies.

The palaeontological content of the *Keuper* facies unit of Menorca is limited to a single palynoassemblage from Punta de s'Aprés, revealing a lower Carnian age (Rosell *et al.*, 1989). No fossils have been reported from the overlying dolostones, which could be either Triassic or Jurassic.

Objectives of the present work

The present Ph.D. dissertation has been conceived as a comprehensive characterisation of the ecosystems containing vertebrate fossils in the Gymnesic Islands (Mallorca and Menorca). Its main objectives can be summarised as follows:

- Part 1: Permian of Mallorca
  - Exhaustive review of the literature on the Permian of Mallorca.
  - Detailed stratigraphic and sedimentological characterisation of all the outcrops, in order to infer the palaeoenvironments and their evolution through time.
  - Correlation of sections among different outcrops, and definition of formal lithostratigraphic units (*i.e.*, Formations).
  - Taxonomical study of all the fossils found during the field trips (spores, pollen, macroplant remains, invertebrate trace fossils, tetrapod tracks and tetrapod body fossils), as well as those housed in museum or private collections.
  - Integration of palaeomagnetic and biostratigraphic data to provide age attributions for all the recognised units.
  - Reconstruction of the palaeoecosystems recorded in the different units.

- Part 2: Lower–Middle Triassic of Mallorca (*Buntsandstein* facies)
  - Exhaustive review of the literature on the *Buntsandstein* of Mallorca.
  - Detailed stratigraphic and sedimentological characterisation of all the outcrops, in order to infer the palaeoenvironments and their evolution through time.
  - Correlation of sections among different outcrops, and definition of formal lithostratigraphic units (*i.e.*, Formations).
  - Taxonomical study of all the fossils found during the field trips (invertebrate trace fossils, clam shrimps, insects, tetrapod tracks, fishes), as well as those housed in museum or private collections. Revision of previous works on macroplant remains.
  - Integration of biostratigraphic data to provide age attributions for all the recognised units.
  - Reconstruction of the palaeoecosystems recorded in the different units.

- Part 3: Middle–Upper Triassic of Mallorca (*Muschelkalk* and *Keuper* facies)
  - Exhaustive review of the literature on the *Muschelkalk* and *Keuper* of Mallorca.
  - Preliminary stratigraphic and sedimentological characterisation of the outcrops that have yielded tetrapod body fossils to infer the local palaeoenvironment.
  - Correlation of each interval to the general sequence of the Middle–Upper Triassic of Mallorca established by previous authors.
  - Taxonomical study of all the tetrapod body fossils housed in museum collections.

- Part 4: Permian of Menorca
  - Exhaustive review of the literature on the Permian of Menorca.
  - Detailed stratigraphic and sedimentological characterisation of the Cala del Pilar–Pla de Mar section, in order to infer the palaeoenvironments and their evolution through time.
  - Taxonomical study of all the tetrapod tracks found *in situ* and the tetrapod body fossils housed in museum collections.
  - Reconstruction of the palaeoecosystems recorded in the different units.

- Part 5: General objectives
  - Characterisation of the evolution of the ecosystems of the Gymnesic Islands through time.
  - Identification of global-scale patterns regarding palaeoenvironments, phylogeny and palaeobiogeography.

The level of detail in each of the parts was directly proportional to the abundance and relevance of the fossils found. Thus, more time and resources were invested on the Triassic *Buntsandstein* and, especially, the Permian of Mallorca. Although the Permian of Menorca also contains many vertebrate fossils, administrative setbacks prevented us from conducting a complete study there. Vertebrate remains are very scarce in the *Muschelkalk* and *Keuper* of Mallorca, so only local sections were logged. No vertebrate remains have been found in *Buntsandstein*, *Muschelkalk* and *Keuper* units of Menorca so far, and thus they were excluded from the present work.

Material and methods

Stratigraphy and sedimentology

A substantial part of the present Ph.D. dissertation has been devoted to providing an exhaustive characterisation of the outcrops of the Permian and Lower–Middle Triassic (*Buntsandstein* continental facies) of Mallorca. Such rocks only surface along the northwestern cliffs of the Serra de Tramuntana (Figure 1.9), in the form of small and almost vertical outcrops that are usually quite inaccessible. In order to determine the best profiles to log all representative sections, every single existing outcrop was thoroughly surveyed and mapped. It was established that, for the Permian, 12 sections had to be logged, whereas to fully characterise the Lower–Middle Triassic (*Buntsandstein* continental facies), four logs were needed. About 40 field days were used to survey the outcrops and log the sections. In the field, all strata were measured using a tape measure perpendicular to the stratification, down to a minimum thickness of 10 mm. Thicker intervals consisting of loose sediment or that were covered by vegetation or rock debris were measured using a Jacobs staff. Flooded passes were measured from within the water (Figure 1.10A) and the most vertical intervals were reached using climbing gear (Figure 1.10B–C). In all cases, apart from the thickness of the bed, other aspects such as grain size, colour, geometry, sedimentary structures and fossil content were also noted. Dip and strike were periodically measured on the best-exposed surfaces. This resulted in 279 pages of logs in 1:25 scale. Those were subsequently digitised in 1:40 scale, and were transformed in synthetic logs of scale 1:1160 to make visualisation and correlation more straightforward.

The 1,766 measured metres are distributed, from southwest to northeast, in the following sections. At the outcrops near Cala d'Estellencs, the logs were named "Pedra Alta" (PA, 18.5 m), "Punta Negra" (PN, 103.5 m), "Punta Roja" (PR, 126.5 m) and "Tenassa de sa Tanca" (TT, 47.5 m). At the outcrops between Punta de son Serralta and Port de sa pedra de s'Ase, the logs were named "Racó de s'Algar" (RA, 149.3 m), "Torrent de na Nadala" (NA, 192.5 m), "Es Tamarell" (TA, 27.8 m), "Punta d'en Pere Mir" (PM, 30.0 m), "Pedra de s'Ase" (PA, 167.3 m) and "Pedra de s'Ase - Summit" (PS, 11.0 m). At the outcrops between Bec de s'Àguila and Sa Gratallosa, the logs were named "Volta des General" (VG, 5.9 m), "Platja de sa Pedrera" (PP, 13.3 m), "Port des Canonge–Hort de sa Cova" (PC, 604.4 m), "Sa Gratallosa" (GR, 8.5 m) and "Pedrera de sa Cova" (CO, 190.0 m). Finally, at the outcrops

near Port de Valldemossa, the only log was named "Marina de Valldemossa" (MV, 70.0 m). The first four belong to the Early–Middle Triassic (*Buntsandstein* continental facies), whereas all the others are of Permian age, except for Pedrera de sa Cova, in which both periods might be represented.

The sedimentological study was then carried out, in order to provide an accurate characterisation of the palaeoenvironments represented in those outcrops. While logging the sections, a lithofacies code was assigned to each bed, mostly following the proposals of Miall (1977, 1985, 2006), with modifications and precisions from Postma (1990), Shanley *et al.* (1992), Mack *et al.* (1993), Gómez-Gras & Alonso-Zarza (2003), Bercovici *et al.* (2009), Linol *et al.* (2009) and Shiers *et al.* (2018). Recurrent lithofacies assemblages were identified as architectural elements (Miall, 1985, 2006), each of them representing a specific depositional process in a particular alluvial or fluvial palaeoenvironment. Additionally, all the synthetic logs were correlated, both in the same outcrop or general section and among different areas. The datums were chosen mainly based on lithological aspects, being the boundary between lithostratigraphic formations the main criterion to correlate the sections. Locally, lithological equivalence between series was used to correlate sections that were very close to each other. Unfortunately, the Permian sections cannot be confidently correlated with the Early–Middle Triassic sections, as the base of the Punta Roja Formation does not crop out at its type locality, and it has only been identified with doubts in the upper part of the Pedrera de sa Cova section.

The last step was to formally describe three lithostratigraphic formations for the Permian and four for the Early–Middle Triassic (*Buntsandstein* facies) of Mallorca. The stratotype sections were chosen based on (1) completeness of the series, (2) ease of access, (3) good exposition and (4) less possible number of faults distorting the succession. All the localities where each formation has been observed to crop out have been listed, together with a detailed description of its lithofacies, its architectural elements, its palaeoenvironment, its fossil content and its inferred age. In the case that the formation had been given an informal name by a previous author (*i.e.*, Ramos *et al.*, 1985; Calafat, 1986, 1987, 1988; Ramos & Doubinger, 1989; Ramos, 1995), it has been maintained to preserve priority and to avoid making its identification unnecessarily complicated. In the case that it had not been named so far, the toponyms presented by Homar (1985) and IDEIB (2022) were used, which were also the ones used in all the geological maps.

The general procedure in the case of the Permian of Menorca was somewhat similar to that of the Permian and the Early–Middle Triassic (*Buntsandstein* facies) of Mallorca, but it was focused on only one section (Cala del Pilar–Pla de Mar). There are two main reasons for it: (1) it is the only known site with Permian or Triassic vertebrate fossils on the island and (2) the lithostratigraphy of the Permian and Early–Middle Triassic (*Buntsandstein* facies) of Menorca is relatively well known since the works of Gómez-Gras (1987, 1992, 1993) and Rosell *et al.* (1988, 1989). Therefore, there was no need to repeat a detailed study on all the outcrops of the island, which are, moreover, larger and much more numerous than those of Mallorca. After mapping the study area and determining the most representative section including all the beds bearing fossil bones, it was logged under the name "Cala del Pilar–Pla de Mar" (CP, 315.2 m). Similarly to Mallorca, each stratum was measured using a tape measure perpendicular to the stratification, with a minimum resolution of 10 mm. Covered intervals, as well as those consisting of weathered lutites, were measured by means of a Jacobs staff. For each bed, the following information was noted: thickness, grain size, colour, geometry, sedimentary structures, lithofacies, fossil content and, in some cases, dip and strike. Lithofacies were mostly based on the same sources as in the case of Mallorca (Miall, 1977, 1985, 2006, with modifications and precisions of Postma, 1990; Mack *et al.*, 1993; Gómez-Gras & Alonso-Zarza, 2003; Bercovici *et al.*, 2009; Linol *et al.*, 2009). This resulted in 44 pages of this section in 1:25 scale, which were later digitised in 1:40 scale, and were finally transformed in a synthetic log in 1:1160 scale.

Regarding the Middle–Upper Triassic (*Muschelkalk* and *Keuper* facies) of Mallorca, the goal was not to be exhaustive but to specifically characterise the three localities that had yielded vertebrate fossils in the past. Since all those fossils are part of historical collections and the exact beds where they had been found are unknown, a preliminary survey was conducted in each of the sites in order to find the deposits better matching the descriptions of the original works (Bauzá, 1955, 1971; Colom, 1975, 1982; Moyà-Solà, pers. comm., 2019). Once they were found, short stratigraphic sections were logged to characterise the depositional palaeoenvironment of the area. Moreover, based on lithological similarity, each of the three sites was tentatively correlated with the general logs of Rodríguez-Perea *et al.* (1987), thus making it possible to infer an possible age for each of the studied fossils.

The general workflow in the case of the Permian of Menorca was somewhat similar to that of the Permian and the Early–Middle Triassic (*Buntsandstein* facies) of Mallorca, but it was

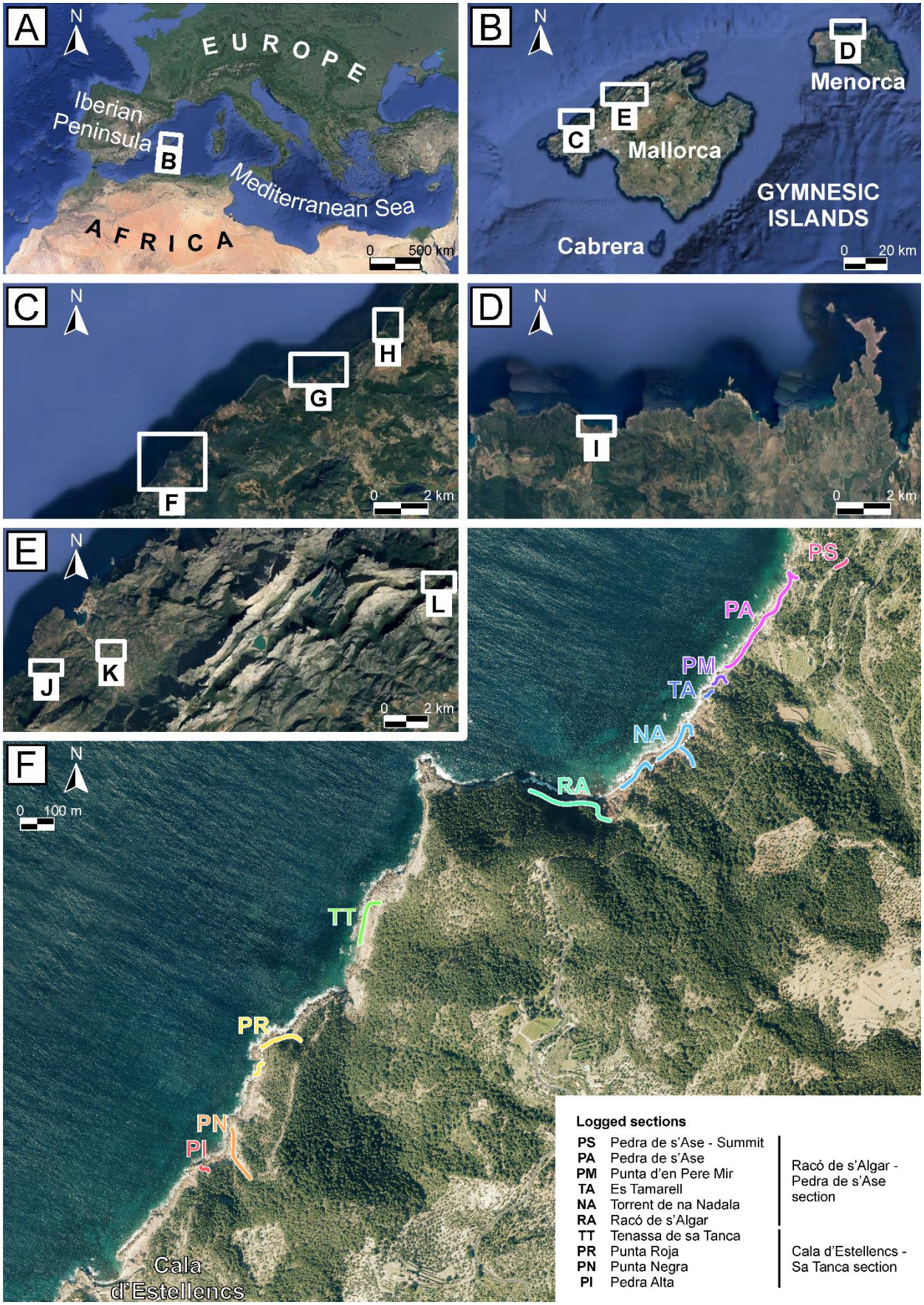

Logged sections

PS	Pedra de s'Ase - Summit	Racó de s'Algar - Pedra de s'Ase section
PA	Pedra de s'Ase	
PM	Punta d'en Pere Mir	
TA	Es Tamarell	
NA	Torrent de na Nadala	
RA	Racó de s'Algar	
TT	Tenassa de sa Tanca	Cala d'Estellencs - Sa Tanca section
PR	Punta Roja	
PN	Punta Negra	
PI	Pedra Alta	

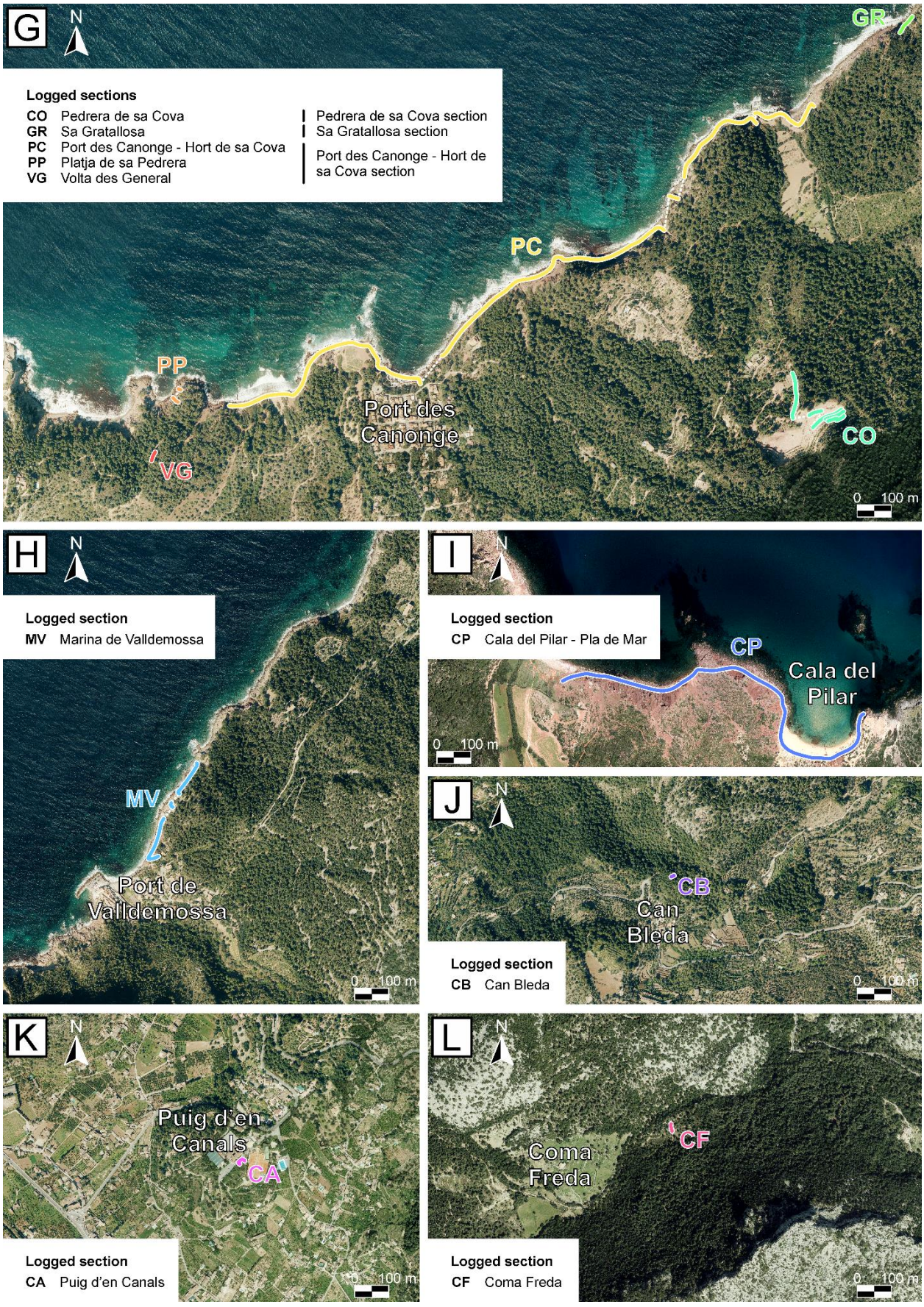
G
N
Logged sections
CO Pedrera de sa Cova
GR Sa Gratallosa
PC Port des Canonge - Hort de sa Cova
PP Platja de sa Pedrera
VG Volta des General
Pedrera de sa Cova section
Sa Gratallosa section
Port des Canonge - Hort de sa Cova section
GR
PC
PP
Port des Canonge
CO
VG
0 100 m
H
N
Logged section
MV Marina de Valldemossa
MV
Port de Valldemossa
0 100 m
I
N
Logged section
CP Cala del Pilar - Pla de Mar
CP
Cala del Pilar
0 100 m
J
N
CB
Can Bleda
Logged section
CB Can Bleda
0 100 m
K
N
Puig d'en Canals
CA
Logged section
CA Puig d'en Canals
0 100 m
L
N
CF
Coma Freda
Logged section
CF Coma Freda
0 100 m

Figure 1.9. (previous two pages) Orthophotographs of the studied localities (from IDEIB, 2022), with the position of the logged sections. A: Map of the Mediterranean Sea, showing the location of the Gymnesic Islands (subfigure B). B: Map of the Gymnesic Islands, with the position of the three main studied areas (subfigures C–E). C: Orthophotograph of the zone of Mallorca that contains the Permian and Lower–Middle Triassic continental deposits studied herein (subfigures F–H). D: Orthophotograph of the northern part of Menorca showing the studied area (subfigure I). E: Orthophotograph showing the deposits of Mallorca containing marine vertebrate remains from the Middle–Upper Triassic studied herein (subfigures J–L). F: Orthophotograph of the zone between Cala d'Estellencs and Port de sa pedra de s'Ase (Estellencs and Banyalbufar, Mallorca), marking the logged sections. G: Orthophotograph of the zone between Platja des Mabres and Sa Gratallosa (Valldemossa, Mallorca), marking the logged sections. H: Orthophotograph of the area near Port de Valldemossa (Valldemossa, Mallorca), marking the logged section. I: Orthophotograph of the zone between Cala del Pilar and Pla de Mar (Ciutadella, Menorca), marking the logged section. J: Orthophotograph of the area near Can Bleda (Sóller, Mallorca), marking the logged section. K: Orthophotograph of the area near Puig d'en Canals (Sóller, Mallorca), marking the logged section. L: Orthophotograph of the area near Coma Freda (Escorca, Mallorca), marking the logged section.

focused on only one section (Cala del Pilar–Pla de Mar). There are two main reasons for it: (1) it is the only known site with Permian or Triassic vertebrate fossils on the island and (2) the lithostratigraphy of the Permian and Early–Middle Triassic (*Buntsandstein* facies) of Menorca is relatively well known since the works of Gómez-Gras (1987, 1992, 1993) and Rosell *et al.* (1988, 1989). Therefore, there was no need to repeat a detailed study on all the outcrops of the island, which are, moreover, larger and much more numerous than those of Mallorca. After mapping the study area and determining the most representative section including all the beds bearing fossil bones, it was logged under the name "Cala del Pilar–Pla de Mar" (CP, 315.2 m). Similarly to Mallorca, each stratum was measured using a tape measure perpendicular to the stratification, with a minimum resolution of 10 mm. Covered intervals, as well as those consisting of weathered lutites, were measured by means of a Jacobs staff. For each bed, the following information was noted: thickness, grain size, colour, geometry, sedimentary structures, lithofacies, fossil content and, in some cases, dip and strike. Lithofacies were mostly based on the same sources as in the case of Mallorca (Miall, 1977, 1985, 2006, with

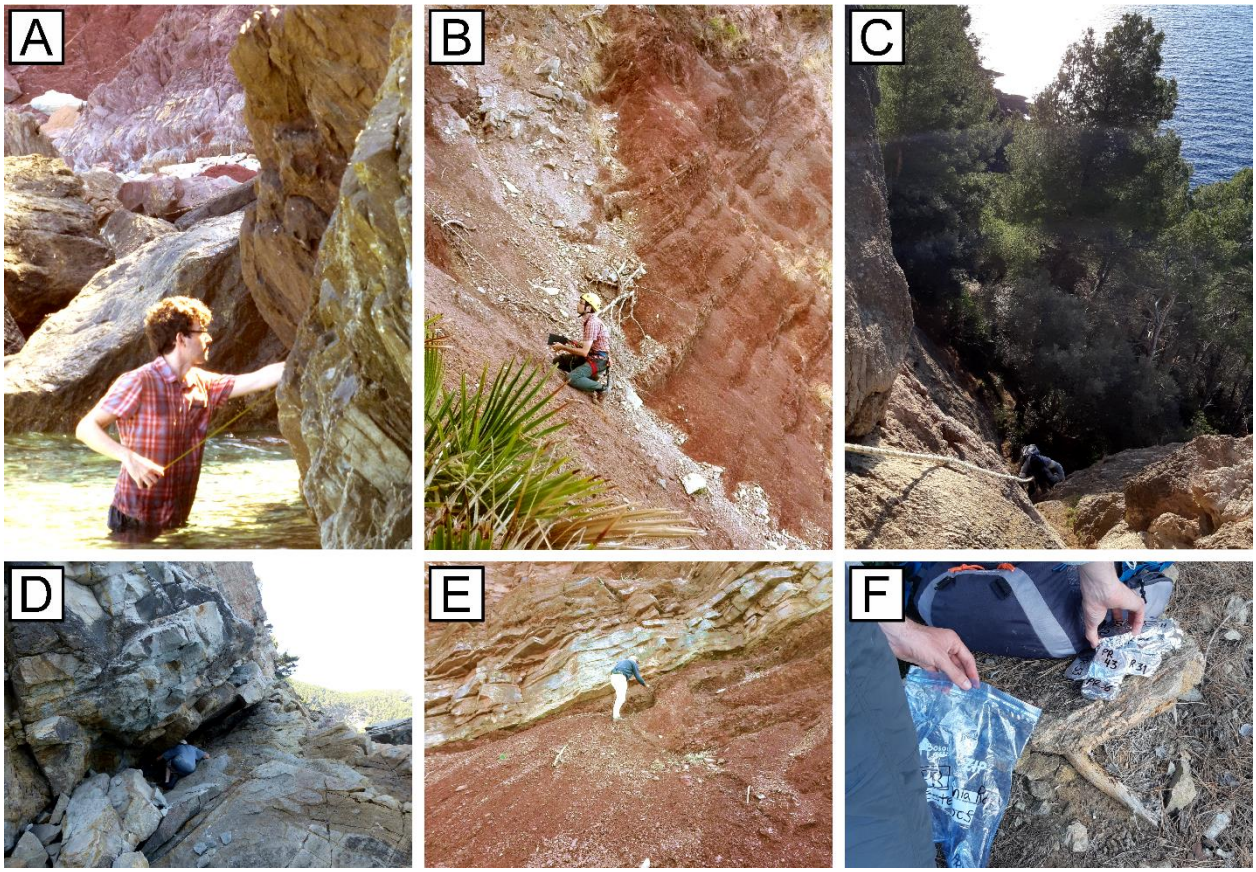

Figure 1.10. Different field methods used in the present work. ***A:*** *Logging sections from within the water.* ***B–C:*** *Logging sections and accessing outcrops using climbing gear.* ***D:*** *Collection of palynology samples.* ***E–F:*** *Collection of palaeomagnetism samples.*

modifications and precisions of Postma, 1990; Mack *et al.*, 1993; Gómez-Gras & Alonso-Zarza, 2003; Bercovici *et al.*, 2009; Linol *et al.*, 2009). This resulted in 44 pages of this section in 1:25 scale, which were later digitised in 1:40 scale, and were finally transformed in a synthetic log in 1:1160 scale.

Regarding the Middle–Upper Triassic (*Muschelkalk* and *Keuper* facies) of Mallorca, the goal was not to be exhaustive but to specifically characterise the three localities that had yielded vertebrate fossils in the past. Since all those fossils are part of historical collections and the exact beds where they had been found are unknown, a preliminary survey was conducted in each of the sites in order to find the deposits better matching the descriptions of the original works (Bauzá, 1955, 1971; Colom, 1975, 1982; Moyà-Solà, pers. comm., 2019). Once they were found, short stratigraphic sections were logged to characterise the depositional palaeoenvironment of the area. Moreover, based on lithological similarity, each of the three

sites was tentatively correlated with the general logs of Rodríguez-Perea *et al.* (1987), thus making it possible to infer an possible age for each of the studied fossils.

Fieldwork campaigns and permissions

Eight palaeontological interventions have been carried out in the course of the present Ph.D. dissertation. In the Balearic Islands, all the fossils are of public ownership, and cannot be collected without explicit permission granted by the 'Service of Historical Heritage' (*Servei de Patrimoni Històric*) of the council of the corresponding island, as per the 'Decree 14/2011, of the 25th of February, approving the Regulations for archaeological and palaeontological interventions in the Balearic Islands' (*Decret 14/2011, de 25 de febrer, pel qual s'aprova el Reglament d'intervencions arqueològiques i paleontològiques de les Illes Balears*). Prospection and excavation campaigns were conducted only on Mallorca, because it has been impossible to obtain the necessary permits on Menorca. A technical report was written to request each intervention, and yearly reports were submitted after each prospection or excavation, listing all the material collected. Table 1.1 lists all the palaeontological interventions that have been carried out.

Sampling methods for palaeomagnetism and palaeopalynology

For the present work, samples for analyses of palaeopalinology and palaeomagnetism were collected at several points in the studied sections. For the former analysis, 35 samples were taken from fine-grained, greyish/bluish beds, as the pollen is usually oxidised and destroyed in the red-beds. Between 300–500 g were collected from each of the suitable levels and stored in hermetic plastic bags (Figure 1.10D). For the palaeomagnetic analysis, 280 rock samples were taken at regular intervals (~1–2 m when possible) in all the sections, preferentially selecting the most fine-grained, red-coloured beds (Figure 1.10E). The maximum dip of the rock surface, which had to be as flat as possible, was drawn on the sample with a marker, and the dip and strike of that surface were measured, together with the dip and strike of the layer. All samples were numbered and wrapped in aluminium foil (Figure 1.10F), which was noted in the stratigraphic log. Relatively inaccessible areas or beds that were coarse-grained and not red were not sampled. The samples were sent to the *Naturmuseum Südtirol - Museo di Scienze*

Naturali dell'Alto Adige (Bolzano) and the *Istituto Nazionale di Geofisica e Vulcanologia* (Rome), respectively, where they were processed by Dr. Evelyn Kustatscher and Dr. Guido Roghi in the case of the palaeopalynological analysis and Dr. Jaume Dinarès-Turell (who also helped with the collection of the samples) in the case of the palaeomagnetism analysis.

Table 1.1. List of all the palaeontological interventions that have been conducted on Mallorca during the present work.

Reference code	Type	Site	Age	Date
128/2019	Prospection	All the outcrops	Permian and Middle Triassic	June 2019
305/2019	Excavation	Pedra Alta, Punta Negra and Punta Roja	Middle Triassic	August 2019
306/2019	Excavation	Torrent de na Nadala	Permian	October 2019
52/2021	Prospection	Port des Canonge to Hort de sa Cova	Permian	March 2021
52/2021	Prospection	Pedra Alta, Punta Negra and Punta Roja	Middle Triassic	March 2021
75/2021	Excavation	Torrent de na Nadala	Permian	May 2021
259/2022	Prospection	Torrent de na Nadala	Permian	April 2022
259/2022	Prospection	Port des Canonge to Hort de sa Cova	Permian	May 2022

Methods in vertebrate palaeoichnology: 3D models and casts

Photogrammetry is a technique extensively used in ichnological studies, because it makes it possible to collect and save information that would otherwise be inevitably lost to erosion in the case of big, unmovable rock surfaces. Moreover, it provides a cheap and swift alternative to the confection of artificial casts, which are sometimes hard to make in open environments or outcrops that are difficult to reach.

During the course of the present work, more than 50 photogrammetric 3D models have been made and subsequently processed, covering every single surface with ichnites found during fieldwork, regardless of its representativity or preservation state. Among those, the best

20 models (or parts of them) have been selected and studied. All of them have been made using the same methodology, mostly based on the procedures explained by Mujal *et al.* (2020), which are briefly explained as follows:

(1) Preparation: The surface of interest is cleaned with a brush, removing dust, rock fragments and plants that may cover any relevant part. A scale bar is placed somewhere on the surface near the ichnites, making sure it does not cover or cast a shadow on any of them. If the surface is overhanging (*i.e.*, it corresponds to the base of a stratum), the scale bar is stuck with tape or adhesive putty.

(2) Acquisition of images: Pictures are taken using a compact digital camera (Panasonic Lumix DMC-TZ27) (Figure 1.11A). The number of shots needed varies depending on the size of the surface and the complexity of the footprints. In general terms, about 40–50 pictures are taken for slabs of 20 × 20 cm or less (individual tracks or manus-pes sets), and about 150–250 pictures are taken in the case of surfaces of more than 100 × 100 cm (trackways or track assemblages). In all cases, each shot must overlap at least 2/3 with at least another one, so that homologous points can be recognised during processing. When taking the pictures, it is preferred for them to be approximately perpendicular to the slab surface, although a few oblique shots are also taken to include nooks and crannies not directly visible from above.

(3) Digital processing (making the mesh): Raw pictures are imported to the software Agisoft PhotoScan standard version 1.1.4. (www.agisoft.com), where the images are aligned (Figure 1.11B), and the dense point cloud, the mesh and the texture are produced (Figure 1.11C). In all cases, the models are made with the maximum quality permitted by the software.

(4) Digital processing (editing the mesh): Textured 3D meshes in .ply format are imported to the software MeshLab version 2016.12 (http://meshlab.sourceforge.net/). There, they are scaled, cropped and oriented so the flat surface of the slab is horizontal. The maximum and minimum height of the model is measured to obtain the information for the scale of the colour-coded height map.

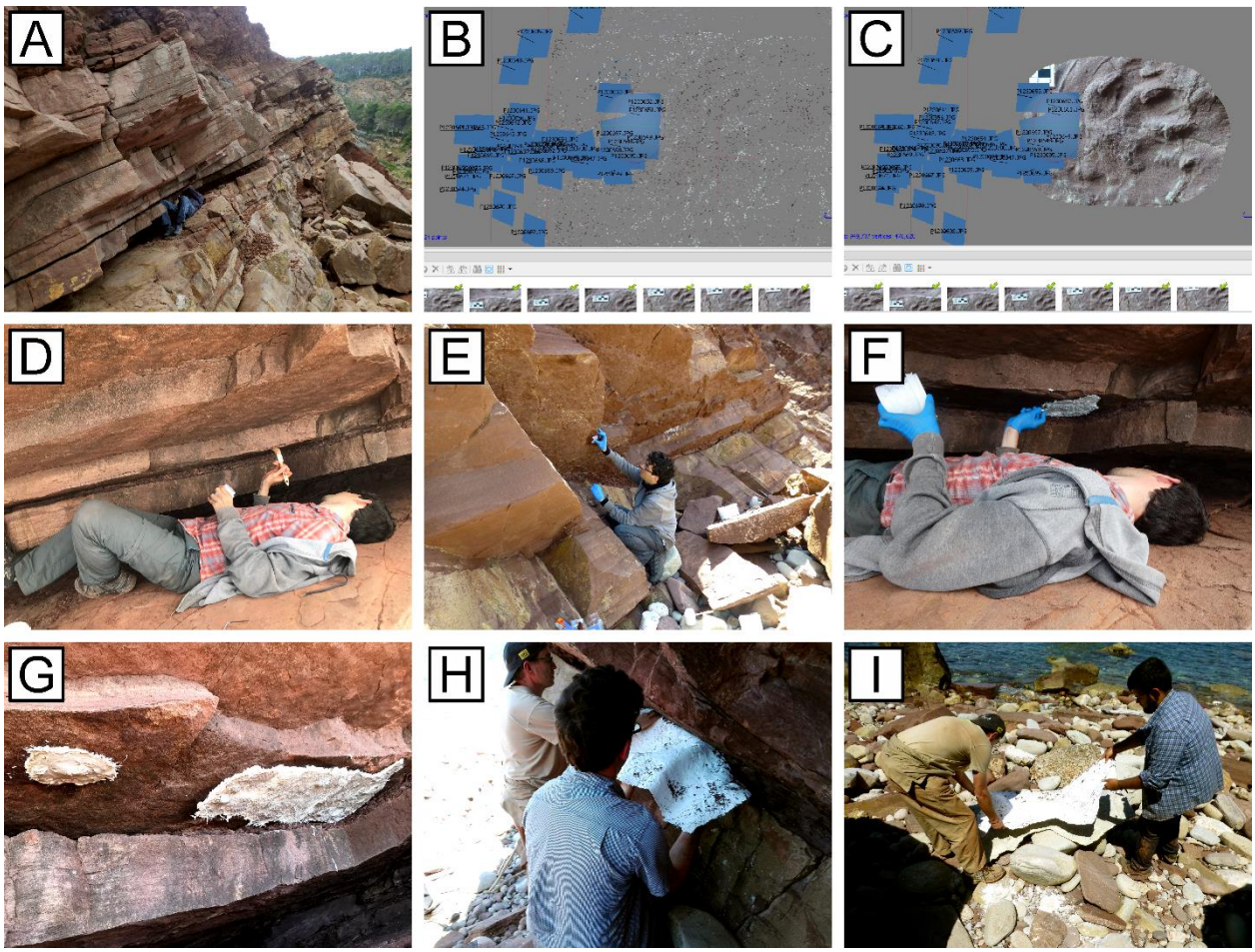

Figure 1.11. Methods to acquire the data of fossil tracks and trackways. ***A:*** *Obtaining pictures to make photogrammetry 3D models.* ***B:*** *Aligned pictures.* ***C:*** *Textured mesh of the same footprint in B.* ***D:*** *Application of petroleum jelly on the trackway surface.* ***E:*** *Application of ClayGum silicone over small tracks.* ***F:*** *Application of the silicone Silicast Tixo with a thixotroping agent on the same trackway surface as in E.* ***G:*** *Aspect of the silicone moulds of subfigure F after being covered with glass fibre.* ***H–I:*** *Silicone mould after being peeled off the surface.*

(5) Digital processing (false-colour height map): Edited, textured 3D meshes in .ply format are imported to the software ParaView version 4.1.0 64-bit (http://www.paraview.org). There, a false-colour height map is produced, using the "Rainbow desaturated" colour scale, with blue for the deepest areas and red for the highest areas. Then, contour lines are overprinted on the model; for small ones (*i.e.*, isolated ichnites or manus-pes sets), 50 regularly-spaced lines are added, whereas for large ones (*i.e.*, trackways or complete slabs), 100 regularly-spaced lines are added instead. The model is saved as high-quality, flat .tiff images to be used in the figures.

Interpretative drawings were then made, based on both the textured models (and pictures) and the false colour-coded 3D maps, using a vector-based graphic design software (Corel DRAW X8). By means of the software ImageJ v.1.52d (https://imagej.nih.gov/ij/), measurements were taken on the individual ichnites and the trackways (Figure 1.12), mostly following Leonardi (1987) and Hasiotis *et al.* (2007).

Moreover, a few artificial casts were made on the more relevant/representative ichnite-bearing surfaces. Two different procedures were used depending mainly on the area to be replicated. A first step for both was to cover the surface with petroleum jelly, in order to make it easier for the silicone cast to detach without damaging the fossils on the surface (Figure 1.11D). In the case of small surfaces (less than 10 × 10 cm), the polyaddition silicone paste ClayGum was applied (Figure 1.11E) and left it to dry for about 10 minutes. Then, the cast was carefully removed using a spatula. For larger surfaces, the silicone with a thixotroping agent Silicast Tixo was used instead (Figure 1.11F). A first layer of a thickness between 1–3 mm was applied on the rock and, when it had dried, a second layer of about 5 mm of thickness of either the same silicone, or Silicast 517 with an added thixotroping agent, was applied over the first layer. After drying for a whole night, a layer of Triaxial D-5 glass fibre and Plasticrete acrylic resin was applied on the silicone in order to create a hard surface that prevents the cast from bending (Figure 1.11G). After a few hours, when this last layer had become hard, it was removed and the silicone cast was peeled off the rock surface (Figure 1.11H–I). A counter-cast of some of the samples was later made using Acrylic One resin and painted.

Methods in vertebrate palaeontology: excavation, preparation, measurements, phylogeny

Before the present work, only a few studies had reported vertebrate fossils from the Permian and Triassic of the Balearic Islands (Bauzá, 1955, 1971; Colom, 1975, 1982; Calafat *et al.*, 1986, 1986–1987; Pretus & Obrador, 1987; Calafat, 1988; Carmona, 2004; Liebrecht *et al.*, 2017). Excavations have been, therefore, crucial to obtain a significant volume of new material, and they have also made it possible to collect detailed information regarding the precise stratigraphic position and taphonomical aspects (degree of articulation, orientation, degree of breaking, etc.) of the bones.

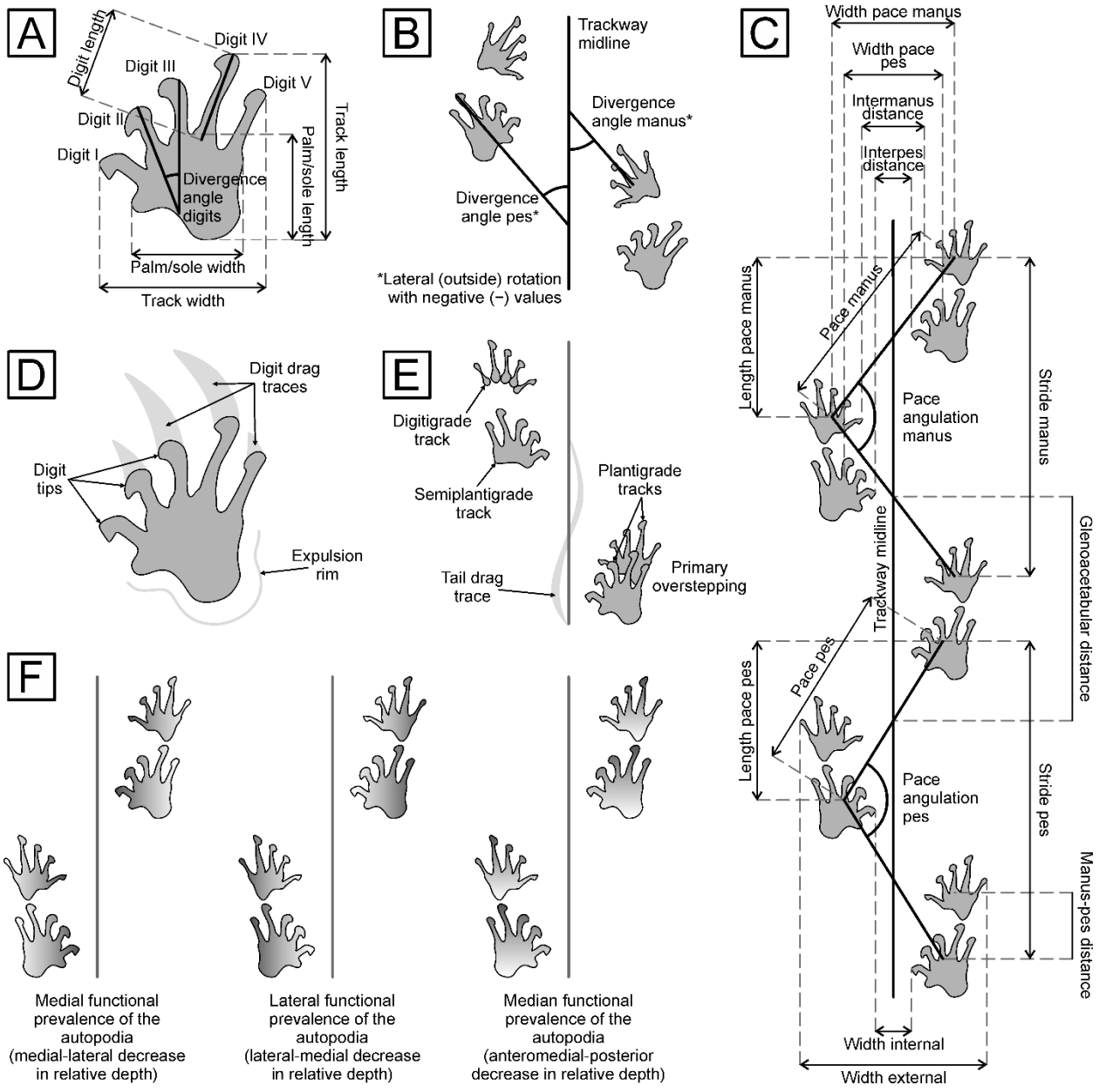

*Figure 1.12. Main parameters measured and described on the studied tetrapod tracks and trackways. **A:** Measurements and terminology of tracks. **B:** Divergence angles of tracks with respect to the trackway midline. **C:** Measurements and terminology of trackways. **D:** Other traits described on tracks. **E:** Terminology of tracks depending on the surface of the autopodia that contacts the ground. **F:** Types of functional prevalence of the autopodia. Based on Mujal (2017) and Mujal et al. (2020), tracks correspond to* Dimetropus leisnerianus *from the Central European Basin (Voigt, 2005).*

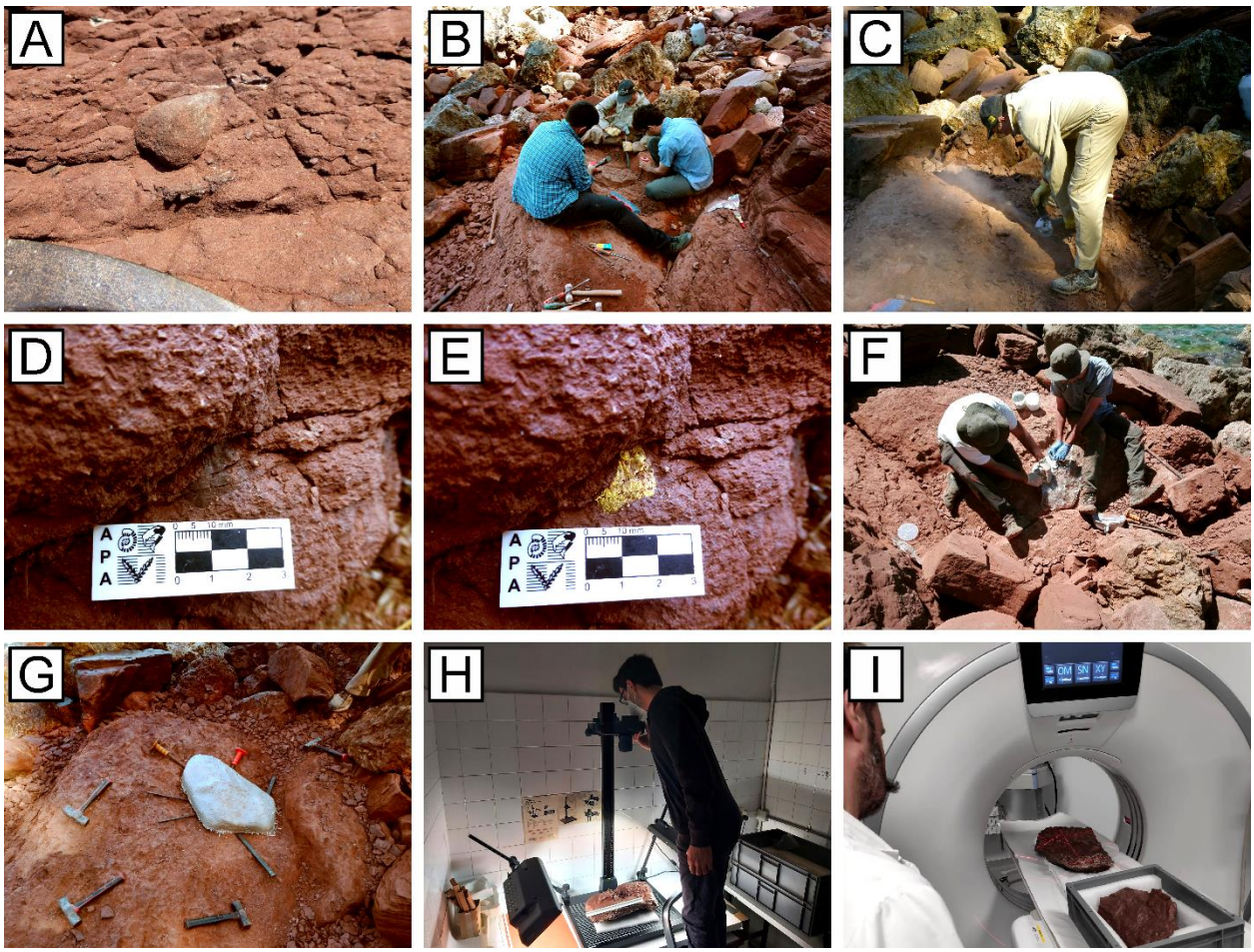

*Figure 1.13. Methods for vertebrate fossils. **A:** Bones preserved in situ on the outcrop surface. **B:** Excavation of blocks containing the specimens using hammers and chisels, screwdrivers and scalpels of different sizes. **C:** Extraction of bones using a battery-powered circular saw. **D:** Bone fragment under natural light. **E:** Same bone fragment as D, but under 365 nm ultraviolet light. **F:** Application of glass fibre and resins on the fossiliferous blocks to make a protective jacket for extraction and transport. **G:** Extraction of a block covered with a protective jacket. **H:** Photography of the specimens at the Palaeontology Unit (Geology Department) of the Universitat Autònoma de Barcelona (Cerdanyola del Vallès). **I:** Preliminary medical CT scan at the Hospital Universitari Mútua de Terrassa (Terrassa).*

The fossiliferous beds (Figure 1.13A) were excavated using hammers and chisels, screwdrivers and scalpels of different sizes (Figure 1.13B). Given their extreme fragility, bones were extracted in the rock matrix whenever possible, sometimes using a battery-powered circular saw (Figure 1.13C) to individualise large blocks of rock. Because carbonate nodules with singular shapes occur abundantly in the same horizons as the bones, a flashlight of

ultraviolet light Weslite® 365 nm was used to identify the bones, which usually, although not always, glow in a white–golden colour (Figure 1.13D–E). Brittle specimens were consolidated using Paraloid® B72 (5–10% in acetone) and the nitrocellulosic resin UHU® Hart. In some cases, sutures of glass fibre Silionne® T-24 g A/965 mm were applied on the cracks of the rock, in order to prevent them for opening further. In the case of relatively large blocks, protective jackets (Figure 1.13F–G), with either the epoxy paste Smooth-On® Free Form™ Air on plastic wrap, or D-5 triaxial glass fibre and Plasticrete acrylic resin on aluminium foil, were built around them to ensure their integrity during transportation.

The most relevant fossils were prepared at the Institut Català de Paleontologia Miquel Crusafont (Cerdanyola del Vallès) by Marina Rull, Ana Montemayor and Xènia Aymerich, using airscribes and micro-air abrasives. Once prepared, they were photographed at the Geology Department of the Universitat Autònoma de Barcelona (Cerdanyola del Vallès) (Figure 1.13H). Measurements were taken on the fossils themselves, using a digital calliper. A particular specimen was scanned using a medical CT at Hospital Universitari Mútua de Terrassa (Terrassa) (Figure 1.13I), and its skull was later scanned again using a μCT scan at the facilities of the Centro Nacional de Investigación sobre la Evolución Humana (Burgos).

Phylogenetic analysis have been run using PAUP* v.4.0 (Swofford, 2003) as a branch-and-bound search with parsimony as the optimality criterion, with unordered and unweighted characters. A strict consensus tree has subsequently been computed, and bootstrap support values have been calculated with 1000 repetitions, not showing values under 50.

References

Adán de Yarza, R. (1879). Examen microscópico de varias muestras de rocas eruptivas, recogidas por D. Luís Mariano Vidal en la isla de Mallorca. *Boletín de la Comisión del Mapa Geológico de España*, 6: 23–28.

Álvarez-Ramis, C.; Solé, N. & Calafat, F. (1989). Paleoflora del Triásico inferior de Mallorca. *In*: *Abstracts of the II European Paleobotanical Conference*. Madrid: p. 12.

Álvarez-Ramis, C.; Fernández-Marrón, T. & Calafat, F. (1995). Avance sobre la megaflora triásica, en facies germánica, de Estellencs (sector noroccidental de la sierra de

Tramontana, Mallorca). *Revista Española de Paleontología*, nº homenaje al Dr. Guillermo Colom: 55–58.

Álvaro, M.; Del Olmo, P. & Ramírez del Pozo, J. (1982). Baleares. *In:* García, A. (Ed.). *El Cretácico de España*. Universidad Complutense de Madrid; Madrid: 633–653.

Álvaro, M.; Del Olmo, P.; Ramírez, J. & Navidad, M. (1983). Facies vulcanosedimentarias en el Trías Superior de la Sierra Norte de Mallorca. *In*: Obrador, A. (Ed.). *Comunicaciones presentadas en el X Congreso Nacional de Sedimentología*. Grupo Español de Sedimentología, Universitat Autònoma de Barcelona; Bellaterra: 27–28.

Álvaro, M.; Barnolas, A.; Del Olmo, P.; Ramírez del Pozo, J. & Simó, A. (1984). El Neógeno de Mallorca: caracterización sedimentológica y bioestratigráfica. *Boletín Geológico y Minero*, 95(1): 3–25.

Álvaro, M.; Barnolas, A.; Cabra, P.; Comas-Rengifo, M.J.; Fernández-López, S.R.; Goy, A.; Del Olmo, P.; Ramírez del Pozo, J.; Simó, A. & Ureta, S. (1989). El Jurásico de Mallorca (Islas Baleares). *Cuadernos de Geología Ibérica*, 13: 67–120.

Ansorge, J. (1997). Insekten aus dem Buntsandstein (Untere Trias) von Mallorca (Spanien). *In*: *Abstracts für 4. Fachgespräch "Fossile Insekten"*. Clausthal-Zellerfeld: 1 pp.

Arenas, C.; Cabrera, L. & Ramos, E. (2007). Sedimentology of tufa facies and continental microbialites from the Paleogene of Mallorca Island (Spain). *Sedimentary Geology*, 197: 1–27.

Aristov, D. & Zessin, W. (2009). *Mallorcagryllus hispanicus* n. get. et sp. - eine neue Grylloblattide (Insecta: Grylloblattida: Blattogryllidae) aus dem Buntsadstein der Insel Mallorca, Spanien. *Virgo, Mitteilungsblatt des Entomologischen Vereins Mecklenburg*, 12(1): 30–34.

Arribas, J.; Gómez-Gras, D.; Rosell, J. & Tortosa, A. (1990). Estudio comparativo entre las areniscas paleozoicas y triásicas de la isla de Menorca: evidencias de procesos de reciclado. *Revista de la Sociedad Geológica de España*, 3: 105–116.

Barnolas, A. (1984) (Ed.). *Sedimentología del Jurásico de Mallorca*. Grupo Español del Mesozoico; Palma. 263 pp.

Barnolas, A. (1991) (Dir.). *Mapa Geológico de España, escala 1:50.000*. Instituto Tecnológico GeoMinero de España; Madrid. Sheets and memoirs: 643 (38-25) + 644 (39-25) Sa Calobra + Pollensa [1 map + 62 pp.]; 670 (38-26) Sóller [1 map + 62 pp.]; 671 (39-26) Inca [1 map + 68 pp.]; 672 (40-26) Artà [1 map + 53 pp.]; 697 (37-27) Andraitx [1 map + 56 pp.]; 698 (38-27) + 722B (37-28) + 723 (38-28) Palma + Illa del Toro + Cap de Cala Figuera [1 map + 64 pp.]; 699 (39-27) Porreres [1 map + 55 pp.]; 700 (40-27) Manacor [1 map + 59 pp.]; 724 (39-28) Lluchmayor [1 map + 49 pp.]; 725 (40-28) + 749 (40-29) Felanitx [1 map + 45 pp.].

Bauzá, J. (1945). Nueva contribución al conocimiento de la Paleontología de Mallorca. *Boletín de la Real Sociedad Española de Historia Natural*, 43(7–8): 397–401.

Bauzá, J. (1946). Nuevo yacimiento fosilífero en el Trias de la Sierra Norte de Mallorca. *Boletín de la Real Sociedad Española de Historia Natural*, 44: 335–338, pl. 21.

Bauzá, J. (1955). Notas paleontológicas de Mallorca: sobre el hallazgo del «*Nothosaurus*» en el Trias. *Boletín de la Sociedad de Historia Natural de Baleares*, 1: p. 87.

Bauzá, J. (1971). Ciento ochenta millones de años de la flora y fauna de Mallorca. *In*: Mascaró, J. (Coord.). *Historia de Mallorca*. Gráficas Miralles; Palma: 331–430.

Bauzá, J. (1981). Contribuciones a la paleontología de Mallorca. *Bolletí de la Societat d'Història Natural de Balears*, 25: 7–20.

Benton M.J. & Newell, A.J. (2014). Impacts of global warming on Permo-Triassic terrestrial ecosystems. *Gondwana Research*, 25: 1308–1337.

Benton, M.J.; Forth, J. & Langer, M.C. (2014). Models for the rise of the dinosaurs. *Current Biology*, 24: R87–R95.

Bercovici, A.; Diez, J.B.; Broutin, J.; Bourquin, S.; Linol, B.; Villanueva-Amadoz, U.; López-Gómez, J. & Durand, M. (2009). A palaeoenvirnomental analysis of Permian sediments in Minorca (Balearic Islands, Spain) with new palynological and megafloral data. *Review of Palaeobotany and Palynology*, 158: 14–28.

Bernardi, M.; Petti, F.M., Kustatscher, E.; Franz, M.; Hartkopf-Fröder, C.; Labandeira, C.C.; Wappler, T.; van Konijnenburg-van Cittert, J.H.A.; Peecook, B.R. & Angielczyk, K.D. (2017). Late Permian (Lopingian) terrestrial ecosystems: A global comparison with new data from the low-latitude Bletterbach Biota. *Earth-Science Reviews*, 175: 18–43.

Bernardi, M.; Gianolla, P.; Massimo Petti, F.; Mietto, P. & Benton, M.J. (2018). Dinosaur diversification linked with the Carnian Pluvial Episode. *Nature Communications*, 9: 1499.

Botha, J. & Smith, R.M.H. (2006). Rapid vertebrate recuperation in the Karoo Basin of South Africa following the End-Permian extinction. *Journal of African Earth Sciences*, 45: 502–514.

Bourrouilh, R. (1973). *Stratigraphie, sédimentologie et téctonique de l'île de Minorque et du Nord-Est de Majorque (Baléares). La terminaison nord-orientale des Cordilleres Bétiques en Méditerranée occidentale*. State Ph.D. dissertation. Université Pierre & Marie Curie, Paris VI; Paris. 1–516 [vol. 1] + 517–822 [vol. 2] + 6 maps and logs.

Bourrouilh, R. (1983). *Estratigrafía, sedimentología y tectónica de la isla de Menorca y del noreste de Mallorca*. Memorias del Instituto Geológico y Minero de España, 99. 672 pp. [vol. 1] + 99 pp. + 5 maps + 2 logs [vol. 2].

Boutet, C.; Rangheard, Y.; Rosenthal, P.; Visscher, H. & Durand-Delga, M. (1982). Découverte d'une microflore d'âge Norien dans la Sierra Norte de Majorque (Baléares, Espagne). *Comptes Rendus des séances de l'Académie des Sciences de Paris, Série 2*, 294: 1267–1270.

Brandes, C. & Tiedt, C. (1991). Petrographische Bestandsaufnahme der permotriassischen Sandsteine Menorcas (Balearen, westliches Mittelmeer). *Neues Jahrbuch für Geologie und Paläontologie, Monatshefte*, 1991: 233–242.

Brocklehurst, N. (2020). Olson's Gap or Olson's Extinction? A Bayesian tip-dating approach to resolving stratigraphic uncertainty. *Proceedings of the Royal Society B*, 287: 20200154.

Brocklehurst, N. (2021). The first age of reptiles? Comparing reptile and synapsid diversity, and the influence of Lagerstätten, during the Carboniferous and early Permian. *Frontiers in Ecology and Evolution*, 9: 669765.

Brocklehurst, N.; Kammerer, C.F. & Fröbisch, J. (2013). The early evolution of synapsids, and the influence of sampling on their fossil record. *Paleobiology*, 39: 470–490.

Brocklehurst, N.; Day, M.O.; Rubidge, B.S. & Fröbisch, J. (2017). Olson's Extinction and the latitudinal biodiversity gradient of tetrapods in the Permian. *Proceedings of the Royal Society B*, 284: 20170231.

Broutin, J.; Ferrer, J.; Gisbert, J. & Nmila, A. (1992). Première découverte d'une microflore thuringienne dans le faciès saxonien de l'île de Minorque (Baléares, Espagne). *Comptes Rendus de l'Académie des Sciences de Paris, Série 2*, 315: 117–122.

Calafat, F. (1986). Estratigrafía y sedimentología de la litofacies Buntsandstein de Mallorca. *In*: Cabrera, L. (Ed.). *Resúmenes del XI Congreso Español de Sedimentología*. Grupo Español de Sedimentología; Barcelona: p. 39.

Calafat, F. (1987). Paleoambients de les facies Buntsandstein de Mallorca. *In*: *Llibre de resums de les I Jornades del Medi Ambient de les Illes Balears*. Societat d'Història Natural de les Balears; Palma: 16–17.

Calafat, F. (1988). *Estratigrafía y sedimentología de la litofacies Buntsandstein de Mallorca*. Bachelor's Thesis. Universitat de Barcelona; Barcelona. 127 pp. + 31 annexed figs.

Calafat, F.; Fornós, J.J.; Marzo, M.; Ramos, E. & Rodríguez-Perea, A. (1986). Icnología de vertebrados de las facies Buntsandstein de Mallorca. *In*: Cabrera, L. (Ed.). *Resúmenes del XI Congreso Español de Sedimentología*. Grupo Español de Sedimentología; Barcelona: p. 40.

Calafat, F.; Fornós, J.J.; Marzo, M.; Ramos-Guerrero, E. & Rodríguez-Perea, A. (1986–1987). Icnología de vertebrados de las facies Buntsandstein de Mallorca. *Acta Geològica Hispànica*, 21–22: 515–520.

Carmona, R. (2004). *Estudi d'un seimuriamorfe (Amphibia: Batrachosauria) del Permià superior de Menorca*. Bachelor's Thesis. Universitat de Barcelona; Barcelona. 56 pp.

Chen, Z.-Q. & Benton, M.J. (2012). The timing and pattern of biotic recovery following the end-Permian mass extinction. *Nature Geoscience*, 5(6): 375–383.

Clemmensen, L.B. & Hansen, C.F. (2021). The Early-Middle Triassic of Arran (Scotland): a dryland terminal fluvial playa-lake system. *In*: Gómez-Pujol, L.; Roig-Munar, F.X.; Gelabert, B.; Martín, J.A. (Eds.). *De la terra a la mar i de la mar a la terra. Homenatge a Antonio Rodríguez-Perea*. Monografies de la Societat d'Història Natural de Balears, 34. Societat d'Història Natural de les Balears; Palma: 41–53.

Colom, G. (1975). *Geología de Mallorca*. Gráficas Miramar, Diputación Provincial de Baleares, Palma. 1–297 [vol. 1] + 301–522 [vol. 2].

Colom, G. (1982). Notas paleontológicas y estratigráficas (referentes a Mallorca e Ibiza). *Bolletí de la Societat d'Història Natural de Balears*, 26: 195–206.

Cuevas-López, F. (1958a). *Informe geológico y minero de los yacimientos de cobre de Banyalbufar y Estallenchs, Mallorca*. Barcelona. 37 pp. + 8 figs. Unpublished technical report.

Cuevas-López, F. (1958b). *Informe geológico y minero de los yacimientos de cobre de Banyalbufar y Valldemosa, Mallorca*. Barcelona. 23 pp. + 7 figs. Unpublished technical report.

Dal Corso, J.; Bernardi, M.; Sun, Y.; Song, H.; Seyfullah, L.J.; Preto, N.; Gianolla, P.; Ruffell, A.; Kustatscher, E.; Roghi, G.; Merico, A.; Hohn, S.; Schmidt, A.R.; Marzolli, A.; Newton, R.J.; Wignall, P.B. & Benton, M.J. (2020). Extinction and dawn of the modern world in the Carnian (Late Triassic). *Science Advances*, 6: eaba0099.

Darder, B. (1913). El Triásico de Mallorca. *Boletín de la Real Sociedad Española de Historia Natural*, 13: 476–484.

Darder, B. (1914a). El Triásico de Mallorca. *Trabajos del Museo Nacional de Ciencias Naturales, Serie Geológica*, 7: 1–85 + 1 map + 1 tab.

Darder, B. (1914b). Los yesos metamórficos de Mallorca. *Boletín de la Real Sociedad Española de Historia Natural*, 14: 179–185 + pl. 2.

Day, M.O.; Ramezani, J.; Bowring, S.A.; Sadler, P.M.; Erwin, D.H.; Abdala, F. & Rubidge, B.S. (2015). When and how did the terrestrial mid-Permian mass extinction occur? Evidence from the tetrapod record of the Karoo Basin, South Africa. *Proceedings of the Royal Society B*, 282: 20150834.

Day, M.O. & Rubidge, B.S. (2021). The late Capitanian mass extinction of terrestrial vertebrates in the Karoo Basin of South Africa. *Frontiers in Earth Science*, 9: 631198.

Díaz de Neira, J.A. & Gil, J. (2009). Unidades litoestratigráficas del Cretácico de Ibiza (Islas Baleares, España). *Boletín de la Real Sociedad Española de Historia Natural, Sección Geológica*, 103(1–4): 5–21.

Díaz de Neira, J.A. & Gil-Gil, J. (2014). Correlación litoestratigráfica entre las sucesiones mesozoicas de la isla de Ibiza y el prebético de Alicante. *Revista de la Sociedad Geológica de España*, 27(1): 91–109.

Diez, J.B. (2000). *Geología y Paleobotánica de la Facies Buntsandstein en la Rama Aragonesa de la Cordillera Ibérica. Implicaciones paleogeográficas en el Peritethys Occidental*. Ph.D. dissertation. Universidad de Zaragoza, Université Pierre & Marie Curie, Paris VI; Zaragoza, Paris. 424 pp.

Diez, J.B.; Broutin, J. & Ferrer, J. (2005). Difficulties encountered in defining the Permian–Triassic boundary in Buntsandstein facies of the western Peritethyan domain based on palynological data. *Palaeogeography, Palaeoclimatology, Palaeoecology*, 229: 40–53.

Diez, J.B.; Broutin, J.; Grauvogel-Stamm, L.; Bourquin, S.; Bercovici, A. & Ferrer, J. (2010). Anisian floras from the NE Iberian Peninsula and Balearic Islands: A synthesis. *Review of Palaeobotany and Palynology*, 162: 522–542.

Durand-Delga, M.; Freneix, S.; Magne, J.; Meon, H. & Rangheard, Y. (1993). La série saumâtre et continentale d'âge Miocène moyen et supérieur d'Eivissa (ex-Ibiza, Baléares). *Acta Geològica Hispànica*, 28(1): 33–46.

Enrique, P. (1986). Nota sobre les roques hipabissals de la serra de Tramuntana de Mallorca: algunes característiques petrogràfiques i geoquímiques. *Bolletí de la Societat d'Història Natural de les Balears*, 30: 19–50.

Enrique, P. (1990). Alkali basaltic intrusions of teschenitic affinity from north-western Mallorca. *In*: Sociedad Geológica de España (Ed.). *The Valencia Trough: geology and geophysics*. Blackwell Scientific Publications; Oxford, London, Edinburgh, Boston, Melbourne, Paris, Berlin, Vienna: 3–4.

Enrique, P. (2012). Rocas teschenítica en el Norte de Mallorca: aproximación a su clasificación. *Geogaceta*, 51: 11–14.

Enrique, P.; Lago, M.; Pocoví, A. & Vaquer, R. (1987). Aspectos petrológicos y geoquímicos del magmatismo alcalino, de edad triásica, en la sierra norte de Mallorca. *In*: Colegio de Geólogos (Ed.). *IIº Congreso de Geoquímica de España*. Colegio de Geólogos; Soria: 215–218.

Escudero-Mozo, M.J.; Martín-Chivelet, J.; Goy, A. & López-Gómez, J. (2014). Middle-Upper Triassic carbonate platforms in Minorca (Balearic islands): Implications for Western Tethys correlations. *Sedimentary Geology*, 310: 41–48.

Ezcurra, M.D. & Butler, R.J. (2018). The rise of the ruling reptiles and ecosystem recovery from the Permo-Triassic mass extinction. *Proceedings of the Royal Society B*, 285: 20180361.

Fallot, P. (1922). *Étude Géologique de la Sierra de Majorque*. Librairie Polytechnique Ch. Béranger; Paris, Liège. 16 pp. + 8 pls. + 476 pp. + 9 pls.

Fornós, J.; Marzo, M.; Pomar, L.; Ramos-Guerrero, E. & Rodríguez-Perea, A. (1991). *Evolución tectono-sedimentaria y análisis estratigráfico del Terciario de la isla de Mallorca. Libro-Guía Excursión nº2 del I Congreso del Grupo Español del Terciario*. Universitat de Barcelona; Vic. 145 pp.

Foth, C.; Ezcurra, M.D.; Sookias, R.B.; Brusatte, S.L. & Butler, R.J. (2016). Unappreciated diversification of stem archosaurs during the Middle Triassic predated the dominance of dinosaurs. *BMC Evolutionary Biology*, 16: 188.

Freeman, T. & Obrador, A. (1974). Paleosuelos y carbón en la zona distal del Buntsandstein español (Menorca, Mallorca, Islas Baleares). *In*: *Resúmenes del VII Congreso del Grupo Español de Sedimentología*. Grupo Español de Sedimentología; Bellaterra, Tremp: p. 56.

Freeman, T. & Obrador, A. (1979). Paleosoils and coal in the distal part of the Spanish Buntsandstein (Menorca and Mallorca, Balearic Islands). *Boletín de la Sociedad de Historia Natural de Baleares*, 23: 47–50.

Gallemí, J.; Riba, O.; Reguant, S.; Agustí, J.; Álvarez, G.; Calzada, S.; Caus, M.; López, C.; Martinell, J.; Martínez, R.; Martínez, X.; Porta, J. de; Sanz de Siria, A.; Solé, N.; Truyols, J.; Truyols, M. & Via, Ll. (1988). *Història Natural dels Països Catalans, 15: Registre Fòssil*. Enciclopèdia Catalana; Barcelona. 478 pp.

Gómez-Gras, D.M. (1987). *Estratigrafía física y petrología sedimentaria del Pérmico y Buntsandstein de la isla de Menorca*. Bachelor's Thesis. Universitat Autònoma de Barcelona; Barcelona. 117 pp.

Gómez-Gras, D.M. (1992). *El Permotrías de las Baleares, de la Cordillera Costero Catalana y de la vertiente mediterránea de la Cordillera Ibérica: Facies y Petrología Sedimentaria*.

Ph.D. dissertation. Universitat Autònoma de Barcelona; Barcelona. 242 pp. + 55 figs. + 7 tabs.

Gómez-Gras, D. (1993). El Permotrías de las Baleares y de la vertiente mediterránea de la Cordillera Ibérica y del Maestrat: Facies y Petrología Sedimentaria (Parte II). *Boletín Geológico y Minero*, 104: 467–515.

Gómez-Gras, D. & Alonso-Zarza, A.M. (2003). Reworked calcretes: their significance in the reconstruction of alluvial sequences (Permian and Triassic, Minorca, Balearic Islands, Spain). *Sedimentary Geology*, 158: 299–319.

Goy, A. (1995). Ammonoideos del Triásico Medio de España: Bioestratigrafía y correlaciones. *Cuadernos de Geología Ibérica*, 19: 21–60.

Grauvogel-Stamm, L. & Álvarez-Ramis, C. (1994). Macroflore et microflore in situ du Buntsandstein de l'île de Majorque (Baléares, Espagne). *In*: Arche, A. (Ed.). *Resúmenes del III Coloquio de Estratigrafía y Paleogeografía del Pérmico y Triásico de España*. Consejo Superior de Investigaciones Científicas, Universidad Complutense de Madrid; Cuenca: 51–53.

Grauvogel-Stamm, L. & Álvarez-Ramis, C. (1996). Conifères et pollen in situ du Buntsandstein de l'île de Majorque (Baléares, Espagne). *Cuadernos de Geología Ibérica*, 20: 229–243.

Hasiotis, S.T.; Platt, B.F.; Hembree, D.I. & Everhart, M.J. (2007). The trace-fossil record of vertebrates. *In*: William Miller, III (Ed.). *Trace Fossils: Concepts, Problems, Prospects*. Elsevier Science; Amsterdam, Oxford: 196–218.

Henderson, C.M.; Shen, S.Z.; Gradstein, F.M. & Agterberg, F.P. (2020). Chapter 24 - The Permian Period. *In*: Gradstein, F.M.; Ogg, J.G.; Schmitz, M.D. & Ogg, G.M. (Eds.). *Geologic Time Scale 2020*. Elsevier: 875–902.

Hermite, H. (1879). *Études géologiques sur les îles Baléares. Première partie: Majorque et Minorque*. Pichon et Savy; Paris. 362 pp. + 5 pls.

Hermite, H. (1888). Estudios Geológicos de las Islas Baleares. *Boletín de la Comisión del Mapa Geológico*, 15: 1–244 + 4 pl.

Hirsch, F. (1972). Middle Triassic conodonts from Israel, southern France and Spain. *Mitteilungen der Gesellschaft der Geologie- und Bergbaustudenten*, 21: 811–828.

Hirsch, F. (1977). Essai de correlation biostratigraphique des niveaux Meso et Neotriasiques de facies «Muschelkalk» du domaine sepharade. *Cuadernos de Geología Ibérica*, 4: 511–526.

Hollister, J.S. (1934). Die Stellung der Balearen im variscischen und alpinen Orogen. *Abhandlungen der Gesellschaft für Wissenschaft, Göttingen, Mathematische-Physikalische Klasse, III*, 10: 122–154 + pl. 1–5.

Homar, Ll. (1985). *Toponímia del litoral de la costa d'Estellencs, Banyalbufar i Valldemossa: de na Foradada a sa Foradada*. 7 aerial photographs. Unpublished data.

IDEIB (2022). *Infraestuctura de dades espacials de les Illes Balears*. Conselleria d'Agricultura, Medi Ambient i Territori, Govern de les Illes Balears. http://www.ideib.cat (last accessed on 22/02/2022).

Juárez-Ruiz, J. & Mas, G. (2022). Els dipòsits litorals atribuits històricament al Pliocè-Plistocè inferior de Mallorca (Illes Balears, Mediterrani occidental): revisió, biocronologia de mol·luscs i implicacions paleogeogràfiques. *Bolletí de la Societat d'Història Natural de les Balears*, 65: 237–257.

Juárez-Ruiz, J. & Matamales-Andreu, R. (2015). *Els ammonoïdeus (Phylloceratina, Lytoceratina, Protancyloceratina, Ancyloceratina) del Cretaci (Valanginià-Cenomanià) de Mallorca (Illes Balears, Espanya): catàleg raonat i consideracions taxonòmiques i evolutives*. 214 pp. + 26 pls. Unpublished manuscript.

Juárez-Ruiz, J. & Matamales-Andreu, R. (2018). Ammonoidea del intervalo Albiense terminal–Cenomaniense basal de Mallorca (Illes Balears). *In*: Almayuelas, E.; Bilbao-Lasa, P.; Bonilla, O.; del Val, M.; Errandonea-Martin, J.; Garate-Olave, I.; García-Sagastibelza, A.; Intxauspe-Zubiaurre, B.; Martinez-Braceras, N.; Perales-Gogenola, L.; Ponsoda-Carreres, M.; Portillo, H.; Serrano, H.; Silva-Casal, R.; Suárez-Bilbao, A. & Suarez-Hernando, O. (Eds.). *Life finds a way. Abstract book of the XVI Encuentro de Jóvenes Investigadores en Paleontología*. Aranzadi, Euskal Herriko Unibertsitatea; Gasteiz: 25–28.

Juárez-Ruiz, J. & Wachtler, M. (2015). *Early-Middle Triassic (Anisian) fossil flora from Majorca (Spain)*. Dolomythos Museum; Innichen: 49 pp.

Juncal, M.A. (2019). *Nuevas aportaciones a la palinoestratigrafía pérmica del dominio peritético occidental*. Ph.D. dissertation. Universidade de Vigo; Vigo. 361 pp.

Lago, M.; Zachmann, D.; Vaquer, R. & Pocoví, A. (1988). Geochemical behaviour of spilitization in alkaline magmatism, Trias–Lias, of the Iberian Chain and Mallorca (Spain). *Chemical Geology*, 70(1): p. 156.

Lago, M.; Vaquer, R.; Zachmann, D.; Pocoví, A.; Torres, J.A. & Enrique, P. (1989). Estudio geoquímico de procesos de espilitización afectando a basaltos alcalinos, Keuper terminal-Rhetiense, en la Cadena Ibérica, Cadenas Costeras Catalanas y Sierra Norte de Mallorca. *In*: *III Congreso de Geoquímica de España, vol. 1*. Consejo Superior de Colegios de Ingenieros de Minas; Madrid: 139–150.

Lago, M.; Pocoví, A.; Bastida, J.; Arranz, E.; Vaquer, R.; Dumitrescu, R.; Gil-Imaz, A. & Lapuente, M.P. (1996). El magmatismo alcalino, hettangiense, en el dominio nor-oriental de la Placa Ibérica. *Cuadernos de Geología Ibérica*, 20: 109–138.

Leonardi, G. (1987). *Glossary and Manual of Tetrapod Footprint Palaeoichnology*. Departamento Nacional de Produção Mineral; Brasília. 117 pp.

Li, Q. & Liu, J. (2020). An Early Triassic sauropterygian and associated fauna from South China provide insights into Triassic ecosystem health. *Communications Biology*, 3: 63.

Liebrecht, T.; Fortuny, J.; Galobart, A.; Müller, J. & Sander, P.M. (2017). A large, multiple-tooth-rowed captorhinid reptile (Amniota: Eureptilia) from the Upper Permian of Mallorca (Balearic Islands, Western Mediterranean). *Journal of Vertebrate Paleontology*, 37(1): e1251936.

Linol, B.; Bercovici, A.; Bourquin, S.; Diez, J.B.; López-Gómez, J.; Broutin, J.; Durand, M. & Villanueva-Amadoz, U. (2009). Late Permian to Middle Triassic correlations and palaeogeographical reconstructions in south-western European basins: New sedimentological data from Minorca (Balearic Islands, Spain). *Sedimentary Geology*, 220: 77–94.

Llompart, C.; Rosell, J.; Márquez-Aliaga, A. & Goy, A. (1987). El Muschelkalk de la isla de Menorca. *Cuadernos de Geología Ibérica*, 11: 323–335.

Llopis-Lladó, N. (1935). La microfauna de braquiópodos del Triásico de Monte Toro (Menorca). *Boletín de la Sociedad Española de Historia Natural*, 35: 217–226.

López-García, J.M.; Barnolas, A. & Sevillano, A. (2014). Caracterización litoestratigráfica del Jurásico medio y superior del Torrent de Sa Jonquera, sector noroccidental de la Sierra de Levante (Mallorca). *Geogaceta*, 55: 23–26.

López-Gómez, J.; Escudero-Mozo, M.J.; Martín-Chivelet, J.; Arche, A.; Lago, M. & Galé, C. (2017). Western Tethys continental-marine responses to the Carnian Humid Episode: Palaeoclimatic and palaeogeographic implications. *Global and Planetary Change*, 148: 79–95.

Lozano, R. (1884). *Anotaciones físicas y geológicas de la isla de Mallorca para las aplicaciones del mapa: dedicado á la Excma. Diputación Provincial de Baleares*. Imprenta de la Casa de la Misericordia; Palma. 68 pp.

Lucas, S.G. (2009). Timing and magnitude of tetrapod extinctions across the Permo–Triassic boundary. *Journal of Asian Earth Sciences*, 36: 491–502.

Lucas, S.G. (2017). Permian tetrapod extinction events. *Earth-Science Reviews*, 170: 31–60.

Mack, G.H.; James, W.C. & Monger, H.C. (1993). Classification of paleosols. *Geological Society of America Bulletin*, 105: 129–136.

MacLeod, K.G.; Quinton, P.C. & Bassett, D.J. (2017). Warming and increased aridity during the earliest Triassic in the Karoo Basin, South Africa. *Geology*, 45(6): 483–486.

Manera, J. (1930). Breve estudio geológico de la isla de Menorca. *Revista de Menorca*, 25: 40–53.

March, M. (1991). *Los conodontos del Triásico Medio (facies Muschelkalk) del Noreste de la Península Ibérica y de Menorca*. Ph.D. dissertation. Universitat de València; València. 395 pp.

Marchetti, L.; Voigt, S.; Lucas, S.G.; Francischini, H.; Dentzien-Dias, P.; Sacchi, R.; Mangiacotti, M.; Scali, S.; Gazzola, A.; Ronchi, A. & Millhouse, A. (2019). Tetrapod ichnotaxonomy in eolian paleoenvironments (Coconino and De Chelly formations, Arizona) and late Cisuralian (Permian) sauropsid radiation. *Earth-Science Reviews*, 190: 148–170.

Marchetti, L.; Forte, G.; Kustatscher, E.; DiMichele, W.A.; Lucas, S.G.; Roghi, G.; Juncal, M.A.; Hartkopf-Fröder, C.; Krainer, K.; Morelli, C. & Ronchi, A. (2022). The Artinskian Warming Event: an Euramerican change in climate and the terrestrial biota during the early Permian. *Earth-Science Reviews*, 226: 103922.

Martí, J.; Paniello, X.; Pomar, L.; Ramos, E. & Rodríguez-Perea, A. (1985). El Triásico de las Baleares. *In*: Mateu Ibars, F. & Marzo, M. (Eds.). *Resúmenes del II Coloquio de Estratigrafía y Paleogeografía del Pérmico y Triásico de España*. Institut d'Estudis Ilerdencs, Grupo Español del Mesozoico; La Seu d'Urgell: 84–85.

Martin-Closas, C. & Ramos, E. (2005). Palaeogene Charophytes of the Balearic Islands (Spain). *Geologica Acta*, 3(1): 39–58.

Mas, G. (2013). Definició i caracterització de la Formació ses Olles (*Lago Mare*, Messinià terminal) a l'Illa de Mallorca (Illes Balears, Mediterrània occidental). *Bolletí de la Societat d'Història Natural de Balears*, 56: 209–231.

Mas, G. (2015). *El registre estratigràfic del Messinià terminal i del Pliocè a l'illa de Mallorca. Relacions amb la crisi de salinitat de la Mediterrània*. Ph.D. dissertation. Universitat de les Illes Balears; Palma. 534 pp.

Mas, G. & Fornós, J.J. (2020). The Messinian Salinity Crisis in Mallorca: New insights for a Western Mediterranean stratigraphic scenario. *Marine and Petroleum Geology*, 122: 104656.

Mataillet, R. & Pechoux, J. (1978). *Étude géologique de l'extrémité occidentale de la Sierra Nord de Majorque (Baléares, Espagne)*. Ph.D. dissertation. Université de Franche-Comté; Besançon. 161 pp.

Matamales-Andreu, R.; Arnal, F.A.M. & Crespo, V.D. (2018). ¿Era Mallorca una isla durante el Paleógeno? *In*: Almayuelas, E.; Bilbao-Lasa, P.; Bonilla, O.; del Val, M.; Errandonea-Martin, J.; Garate-Olave, I.; García-Sagastibelza, A.; Intxauspe-Zubiaurre, B.; Martínez-Braceras, N.; Perales-Gogenola, L.; Ponsoda-Carreres, M.; Portillo, H.; Serrano, H.; Silva-Casal, R.; Suárez-Bilbao, A. & Suárez-Hernando, O. (Eds.). *Life finds a way. Abstract book of the XVI Encuentro de Jóvenes Investigadores en Paleontología*. Aranzadi, Euskal Herriko Unibertsitatea; Gasteiz: 191–194.

Miall, A.D. (1977). A review of the braided-river depositional environment. *Earth-Science Reviews*, 13: 1–62.

Miall, A.D. (1985). Architectural-Element Analysis: a new method of facies analysis applied to fluvial deposits. *Earth-Science Reviews*, 22: 261–308.

Miall, A.D. (2006). *The Geology of Fluvial Deposits: Sedimentary Facies, Basin Analysis, and Petroleum Geology*. 4th ed. Springer; Berlin, Heidelberg, New York. 582 pp.

Michel, L.A.; Tabor, N.J.; Montañez, I.P.; Schmitz, M.D. & Davydov, V.I. (2015). Chronostratigraphy and Paleoclimatology of the Lodève Basin, France: Evidence for a pan-tropical aridification event across the Carboniferous–Permian boundary. *Palaeogeography, Palaeoclimatology, Palaeoecology*, 430: 118–131.

Mojsisovics, E. (1882). Die Cephalopoden der mediterranen Triasprovinz. *Abhandlungen der Kaiserlich-Königlichen Geologischen Reichsanstalt*, 10: 1–322 + pl. 1–94.

Mojsisovics, E. (1887). Ueber ammoniten führende Kalke unternorischen Alters auf den balearischen Inseln. *Verhandlungen der Kaiserlich-Königlichen Geologischen Reichsanstalt*, 1887(17): 327–329.

Montañez, I.P. & Poulsen, C.J. (2013). The late Paleozoic ice age: an evolving paradigm. *Annual Review of Earth and Planetary Sciences*, 41: 629–656.

Montañez, I.P.; Tabor, N.J.; Niemeier, D.; DiMichele, W.A.; Frank, T.D.; Fielding, C.R.; Isbell, J.L.; Birgenheier, L.T. & Rygel, M. (2007). CO_2-forced climate and vegetation instability during Late Paleozoic glaciation. *Science*, 315: 87–91.

Moragues, Ll.G. (2015). *Aproximació a l'anàlisi geològic-estructural del sector nordoccidental de la península d'Artà*. Master's Thesis. Universitat de les Illes Balears; Palma. 85 pp.

Motani, R.; Jiang, D.-Y.; Tintori, A.; Ji, C. & Huang, J.-D. (2017). Pre- versus post-mass extinction divergence of Mesozoic marine reptiles dictated by time-scale dependence of evolutionary rates. *Proceedings of the Royal Society B*, 284: 20170241.

Mujal, E. (2017). *Registre sedimentari i icnològic del fini-Carbonífer, Permià i Triàsic continentals dels Pirineus catalans*. Ph.D. dissertation. Universitat Autònoma de Barcelona; Barcelona. 358 pp.

Mujal, E.; Marchetti, L.; Schoch, R.R. & Fortuny, J. (2020). Upper Paleozoic to lower Mesozoic tetrapod ichnology revisited: photogrammetry and relative depth pattern inferences on functional prevalence of autopodia. *Frontiers in Earth Science*, 8: 248.

Navidad, M. & Álvaro, M. (1985). El vulcanismo alcalino del Triásico Superior de Mallorca (Mediterráneo Occidental). *Boletín Geológico y Minero*, 96(1): 10–22.

Neenan, J.M.; Klein, N. & Scheyer, T.M. (2013). European origin of placodont marine reptiles and the evolution of crushing dentition in Placodontia. *Nature Communications*, 4: 1621.

Nolan, H. (1887). Note sur le Trias de Minorque et Majorque. *Bulletin de la Société Géologique de France*, 15: 592–599.

Nolan, H. (1888). El Trias de Mallorca y Menorca. *Boletín de la Comisión del Mapa Geológico*, 15: 234–241.

Nolan, H. (1893). Sur les terrains triasique et jurassique des îles Baléares. *Comptes Rendus des séances de l'Académie des Sciences*, 117: 821–823.

Nolan, H. (1933). Comparación entre el Pérmico y el Trias de los Alpes-Marítimos y del Archipiélago balear. *Revista de Menorca*, 28: 119–121.

Obrador, A. (1983). El Pérmico de las Baleares. *In*: Martínez-Díaz, C. (Ed.). *Carbonífero y Pérmico de España, X Congreso Internacional de Estratigrafía y Geología del Carbonífero*. Ministerio de Industria y Energía, Instituto Geológico y Minero de España; Madrid: 463–470.

Ogg, J.G.; Chen, Z.-Q.; Orchard, M.J. & Jiang, H.S. (2020): Chapter 25 - The Triassic Period. *In*: Gradstein, F.M.; Ogg, J.G.; Schmitz, M.D. & Ogg, G.M. (Eds.). *Geologic Time Scale 2020*. Elsevier: 903–953.

Olroyd, S.L. & Sidor, C.A. (2017). A review of the Guadalupian (middle Permian) global tetrapod fossil record. *Earth-Science Reviews*, 171: 583–597.

Pérez-Valera, J.A. & Goy, A. (2012) Amonoideos del Triásico Medio (Ladiniense) de la isla de Mallorca. *In*: Liao, J.-C.; Gámez Vintaned, J.A.; Valenzuela-Ríos, J.I. & García-Forner, A. (Eds.). *XXVIII Jornadas de la Sociedad Española de Paleontología y Simposios de los Proyectos n.º 587 y 596 del PICG. Valencia y Sóller, 1–6 de Octubre de 2012.*

Homenaje a Guillem Colom Casasnovas (1900–1993). Libro de Resúmenes. Universitat de València, Sociedad Española de Paleontología; València, Madrid: 179–182.

Pla, V. & Enseñat, J.J. (2020). El crui de ses Moletes (Puigpunyent, Mallorca). *Papers de la Societat Espeleològica Balear*, 3: 55–63.

Pocoví, A.; Lago, M.; Bastida, J.; Enrique, P.; Zachmann, D. & Vaquer, R. (1989). The Triassic-Liassic alkaline magmatism of the Iberian Chain, Tarragona and Majorca (Spain): petrological and geochemical features and setting conditions. *Terra Abstracts*, 1(1): p. 287.

Pomar-Gomà, L. (1979). *The Triassic of the Balearic Islands*. Geology Department, Palma de Mallorca University; Palma. 49 pp. + 7 petrologic logs. Unpublished technical report.

Pomar, L.; Obrador, A.; Fornós, J. & Rodríguez-Perea, A. (1983) (Eds.). *El Terciario de las Baleares (Mallorca - Menorca). Guía de las excursiones del X Congreso Nacional de Sedimentología, Menorca 1983*. Institut d'Estudis Baleàrics, Universidad de Palma de Mallorca; Palma. 255 pp.

Postma, G. (1990). Depositional architecture and facies of river and fan deltas: a synthesis. *In*: Colella, A. & David, B.P. (Eds.). *Coarse-grained deltas*. Special Publications of the International Association of Sedimentologists, 10. Blackwell Scientific Publications; Oxford, London, Edinburgh, Boston, Melbourne, Paris, Berlin, Vienna: 13–27.

Pretus, J.Ll. & Obrador, A. (1987). Presencia de restos óseos en el Pérmico de Menorca (nota previa). *Bolletí de la Societat d'Història Natural de Balears*, 31: 149–152.

Ramos, A. (1995). Transition from alluvial to coastal deposits (Permian–Triassic) on the Island of Mallorca, western Mediterranean. *Geological Magazine*, 132(4): 435–447.

Ramos, A. & Doubinger, J. (1989). Premières datations palynologiques dans le facies Buntsandstein de l'île de Majorque (Baléares, Espagne). *Comptes Rendus de l'Académie des Sciences de Paris, Série 2*, 309: 1089–1094.

Ramos, A. & García-Ramos, S. (1992). Niveles de bioturbación en las facies tipo Buntsandstein del Pérmico-Triásico de Mallorca. *In*: García-Ramos, J.C. (Ed.). *Reunión Monográfica sobre Biosedimentación*. Servicio de Publicaciones de la Universidad de Oviedo; Oviedo: 41–43.

Ramos, A.; Del Olmo, P. & Álvaro, M. (1985). El Buntsandstein de la isla de Mallorca. *In*: Mateu Ibars, F. & Marzo, M. (Eds.). *Resúmenes del II Coloquio de Estratigrafía y Paleogeografía del Pérmico y Triásico de España*. Institut d'Estudis Ilerdencs, Grupo Español del Mesozoico; La Seu d'Urgell: 103–104.

Ramos-Guerrero, E. (1988). *El Paleógeno de las Baleares, estratigrafía y sedimentología*. Ph.D. dissertation. Universitat de Barcelona; Barcelona. 219 pp. [vol. 1] + 104 figs. [vol. 2] + 150 pp. [vol. 3].

Ramos-Guerrero, E.; Cabrera, L. & Marzo, M. (1989). Sistemas lacustres paleógenos de Mallorca (Mediterráneo occidental). *Acta Geològica Hispànica*, 24(3–4): 185–203.

Ramos-Guerrero, E.; Cabrera, L. & Marzo, M. (1994a). The Eocene lacustrine–palustrine system of Peguera (Mallorca Island, western Mediterranean). *In*: Gierlowski-Kordesch, E.H. & Kelts, K.R. (Eds.). *Global Geological Record of Lake Basins. Volume 1*. Cambridge University Press; Cambridge, New York, Melbourne, Madrid, Cape Town, Singapore, São Paulo: 241–244.

Ramos-Guerrero, E.; Cabrera, L. & Marzo, M. (1994b). Oligocene lacustrine deposits in the Cala Blanca Formation (Mallorca Island, western Mediterranean). *In*: Gierlowski-Kordesch, E.H. & Kelts, K.R. (Eds.). *Global Geological Record of Lake Basins. Volume 1*. Cambridge University Press; Cambridge, New York, Melbourne, Madrid, Cape Town, Singapore, São Paulo: 285–288.

Ramos-Guerrero, E.; Berrio, I.; Fornós, J.J. & Moragues, Ll. (2000). The middle Miocene Son Verdera lacustrine-palustrine system (Santa Margalida Basin, Mallorca). *In*: Gierlowski-Kordesch, E.H. & Kelts, K.R. (Eds.). *Lake basins through space and time*. AAPG Studies in Geology, 46. American Association of Petroleum Geologists; Tulsa: 441–448.

Ramos-Guerrero, E.; Cabrera, L.; Hagemann, H.W.; Pickel, W. & Zamarreño, I. (2001). Palaeogene lacustrine record in Mallorca (NW Mediterranean, Spain): depositional, palaeogeographic and palaeoclimatic implications for the ancient southeastern Iberian margin. *Palaeogeography, Palaeoclimatology, Palaeoecology*, 172: 1–37.

Rangheard, Y. (1971). *Étude géologique des îles d'Ibiza et de Formentera (Baléares)*. Memorias del Instituto Geológico y Minero de España, 82. Instituto Geológico y Minero de España; Madrid. 340 pp. + 23 pl.

Rangheard, Y. (1984). The geological history of Eivissa and Formentera. *In*: Kuhbier, H.; Alcover, J.A. & Guerau d'Arellano Tur, C. (Eds.). *Biogeography and ecology of the Pityusic Islands*. Dr W. Junk Publishers; The Hague, Boston, Lancaster: 25–104.

Rein, S. (2008). *Ceratites atavus* auf Mallorca? – Die Muschelkalkammonoideen des Museu Balear Sciencies Naturals Sóller. *Vernate*, 27: 5–19.

Retallack, G.J.; Smith, R.M.H. & Ward, P.D. (2003). Vertebrate extinction across Permian-Triassic boundary in Karoo Basin, South Africa. *Geological Society of America Bulletin*, 115(9): 1133–1152.

Rodríguez-Perea, A. (1984). *El Mioceno de la Serra Nord de Mallorca (estratigrafía, sedimentología e implicaciones estructurales)*. Ph.D. dissertation. Universitat de Barcelona; Barcelona. 532 pp.

Rodríguez-Perea, A. & Ramos, E. (1984). Presencia de Paleozoico en la Sierra de Tramuntana (Mallorca). *Bolletí de la Societat d'Història Natural de Balears*, 28: 145–148.

Rodríguez-Perea, A.; Ramos-Guerrero, E.; Pomar, L.; Paniello, X.; Obrador, A. & Martí, J. (1987). El Triásico de las Baleares. *Cuadernos de Geología Ibérica*, 11: 295–321.

Romano, M.; Bernardi, M.; Petti, F.M.; Rubidge, B.; Hancox, J. & Benton, M.J. (2020). Early Triassic terrestrial tetrapod fauna: a review. *Earth-Science Reviews*, 210: 103331.

Rosales, I.; Barnolas, A.; López-García, J.M. & Sevillano, A. (2021). Strontium isotope stratigraphy (SIS) dating of the Bathonian regression in western Tethys (Mallorca island). *Journal of Iberian Geology*, 47: 171–188.

Rosell, J.; Arribas, J.; Elizaga, E. & Gómez, D. (1988). Caracterización sedimentológica y petrográfica de la serie roja permo–triásica de la isla de Menorca. *Boletín Geológico y Minero*, 99(1): 71–82.

Rosell, J.; Gómez-Gras, D. & Elízaga, E. (1989). *Mapa Geológico de España, escala 1:25.000. Isla de Menorca*. Instituto Tecnológico GeoMinero de España; Madrid. Sheets and memoirs: 617b (41-24) + 618 (40-24) Cap Menorca + Ciutadella [2 maps + 51 pp.]; 619 (43-24) Ses Coves Noves [1 map + 34 pp.]; 645B (40-25) + 646 (42-25) Cap Menorca + Cala en Brut y Alaior [3 maps + 38 pp.]; 647 (43-25) Maó [2 maps + 48 pp.]; 673 (43-26) Illa de l'Aire [1 map + 29 pp.].

Rotger, P. (1952). Hallazgo de un ammonites del tipo *Ceratites* en el Muschelkalk de Canet (Esporlas). *Boletín de la Sociedad de Historia Natural de Baleares*, January–February 1952: p. 6.

Ruffell, A.; Simms, M.J. & Wignall, P.B. (2016). The Carnian Humid Episode of the late Triassic: a review. *Geological Magazine*, 153(2): 271–284.

Ruta, M. & Benton, M.J. (2008). Calibrated diversity, tree topology and the mother of mass extinctions: the lesson of temnospondyls. *Palaeontology*, 51: 1261–1288.

Sahney, S. & Benton, M.J. (2008). Recovery from the most profound mass extinction of all time. *Proceedings of the Royal Society B*, 275: 759–765.

San Miguel de la Cámara, M. (1919). Nota petrográfica sobre algunas rocas eruptivas de Mallorca. *Memorias de la Real Academia de Ciencias y Artes de Barcelona*, 15(14): 1–19 + 8 pls.

San Miguel de la Cámara, M. (1936). Estudio de las rocas eruptivas de España. *Memorias de la Real Academia de Ciencias Exactas, Físicas y Naturales de Madrid*, 6: 1–659.

Sanz, J.L. (1980). *Los notosaurios españoles. Análisis filogenético y sistemático de los sauropterigios triásicos*. Ph.D. Thesis. Universidad Complutense de Madrid. 442 pp. + 44 pls.

Sanz, J.L. (1983). Los Nothosaurios (Reptilia, Sauropterygia) españoles. *Estudios Geológicos*, 39: 193–215.

Sanz, T.; Lago, M.; Galé, C.; Ubide, T.; Pocoví, A. & Gil, A. (2013). Las rocas magmáticas de la Sierra de Tramuntana (N de Mallorca, España): contexto estratigráfico. *Geogaceta*, 54: 39–42.

Sastre, J. & Sastre, V. (2002). *Mallorca vora mar: marines de Tramuntana I*. Edicions La Foradada; Palma. 304 pp.

Sastre, J. & Sastre, V. (2005). *El litoral de Mallorca: marinas de Tramuntana, de Sant Elm al Port de Sóller*. Diario de Mallorca; Palma. 304 pp.

Schmidt, M. (1929). Neue Funde in der Iberisch-Balearischen Trias. *Sitzungsberichten der Preusssischen Akademie der Wissenschaften, Physikalisch-Mathematische Klasse*, 25: 516-523.

Schmidt, M. (1930). Weitere Studien in der Iberisch-Balearischen Trias I. *Sitzungsberichten der Preusssischen Akademie der Wissenschaften, Physikalisch-Mathematische Klasse*, 26: 474–488.

Schmidt, M. (1931). Weitere Studien in der Iberisch-Balearischen Trias II. *Sitzungsberichten der Preusssischen Akademie der Wissenschaften, Physikalisch-Mathematische Klasse*, 27: 716–734.

Schmidt, M. (1935). Fossilien der spanischen Trias. *Abhandlungen der Heidelberger Akademie der Wissenschaften, Mathematisch-Naturwissenschaftliche Klasse*, 22: 1–140.

Scotese, C.R. (2000). Paleomap Project. http://www.scotese.com (last accessed on 22/02/2022).

Scotese, C.R. (2014a). *Atlas of Permo-Carboniferous Paleogeographic Maps, maps 53 – 64 from Volume 4 of the PALEOMAP Atlas for ArcGIS (Late Paleozoic), Mollweide Projection*. PALEOMAP Project; Evanston.

Scotese, C.R. (2014b). *Atlas of Middle & Late Permian and Triassic Paleogeographic Maps, maps 43 – 48 from Volume 3 of the PALEOMAP Atlas for ArcGIS (Jurassic and Triassic) and maps 49 – 52 from Volume 4 of the PALEOMAP Atlas for ArcGIS (Late Paleozoic), Mollweide Projection*. PALEOMAP Project; Evanston.

Scotese, C.R.; Song, H.; Mills, B.J.W. & van der Meer, D.G. (2021). Phanerozoic paleotemperatures: The earth's changing climate during the last 540 million years. *Earth Science Reviews*, 215: 103503.

Sevillano, A.; Rosales, I.; Barnolas, A.; Bádenas, B. & López-García, J.M. (2021). Revisión estratigráfica del Sinemuriense-Pliensbachiense inferior de Mallorca. *Estudios Geológicos*, 77(2): e142.

Shanley, K.W.; McCabe, P.J. & Hettinger, R.D. (1992). Tidal influence in Cretaceous fluvial strata from Utah, USA: a key to sequence stratigraphic interpretation. *Sedimentology*, 39: 905–930.

Shiers, M.N.; Mountney, N.P.; Hodgson, D.M. & Colombera, L. (2018). Controls on the depositional architecture of fluvial point-bar elements in a coastal-plain succession. In: Ghinassi, M.; Colombera, L.; Mountney, N.P.; Reesink, A.J.H. & Bateman, M. (Eds.). *Fluvial Meanders and Their Sedimentary Products in the Rock Record*. International

Association of Sedimentologists Special Publications, 48. Wiley Blackwell, International Association of Sedimentologists; Oxford: 15–46.

Sun, Y.; Joachimski, M.M.; Wignall, P.B.; Yan, C.; Chen, Y.; Jiang, H.; Wang, L. & Lai, X. (2012). Lethally hot temperatures during the Early Triassic greenhouse. *Science*, 338(6105): 366–370.

Swofford, D.L. (2003). *PAUP*: phylogenetic analysis using parsimony (*and other methods). Version 4*. Sinauer Associates; Sunderland.

Tiedt, C. (1994). *Die Oberdevonische bis Unterkarbonische Schichtfolge Menorcas (Balearen, Spanien). Stratigraphie - Geochemie - Tektonik*. Ph.D. dissertation. Universität Hannover; Hannover. 110 pp.

Tornquist, A.. (1909). Über die außeralpine Trias auf den Balearen und in Katalonien. *Sitzungsberichte der Königlich Preussischen Akademie der Wissenschaften*, 36: 902–918.

Vachard, D. & Colin, J.-P. (1994). Étude micropaléontologique et palynologique du "Muschelkalk" de Minorque (Trias, Iles Baléares, Espagne), et précisions sur la systématique des Involutinides (Foraminifères). *Revue de Paléobiologie*, 13(1): 235–257.

Vachard, D.; Colin, J.-P.; Rosell, J. & Hochuli, P. (1989). Incursions de microfaunes alpines dans le Trias des Iles Baléares et des Pyrénées espagnoles. *Comptes Rendus de l'Académie des Sciences de Paris, Série 2*, 308: 947–952.

Vera, J.-A.; Alonso-Chaves, F.M.; Andreo, B.; Arias, C.; Azañón, J.M.; Balanyá, J.C.; Barón, A.; Booth-Rea, G.; Castro, J.M.; Chacón, B.; Company, M.; Crespo-Blanc, A.; Delgado, F.; Díaz de Federico, A.; Esteras, M.; Estévez, A.; Fernández, J.; Fornós, J.J.; Galindo-Zaldívar, J.; García-Casco, A.; García-Dueñas, V.; García-Hernández, M.; Garrido, C.J..; Gea, G.A. de; Gelabert, B.; Gervilla, F.; González-Lodeiro, F.; Jabaloy, A.; López-Garrido, A.C.; Luján, M.; Martín-Algarra, A.; Martín-Chivelet, J.; Martín-Martín, M.; Molina, J.M.; Morata, D.; Nieto, J.M.; Obrador, A.; O'Dogherty, L.; Orozco, M.; Pérez-López, A.; Pomar, L.; Puga, E.; Ramos, E.; Rey, J.; Rivas, P.; Rodríguez-Cañero, R.; Ruiz-Cruz, M.D.; Ruiz-Ortiz, P.A.; Sàbat, F.; Sánchez-Gómez, M.; Sánchez-Navas, A.; Sandoval, J.; Sanz de Galdeano, C.; Soto, J.I.; Torres-Roldán,

R.L. & Villas, L. (2004). Capítulo 4. Cordillera Bética y Baleares. *In*: Vera, J.-A. (Ed.). *Geología de España*. Instituto Geológico y Minero de España; Madrid: 346–464.

Virgili, C. (1952). Hallazgo de nuevos *Ceratites* en el Triásico mallorquín. *Memorias y Comunicaciones del Instituto Geológico de la Diputación Provincial de Barcelona*, 9: 19–39.

Voigt, S. (2005). *Die Tetrapodenichnofauna des kontinentalen Oberkarbon und Perm im Thüringer Wald - Ichnotaxonomie, Paläoökologie und Biostratigraphie*. Cuvillier Verlag; Göttingen. 308 pp.

Wurm, A. (1913). Beiträge zur Kenntnis der iberisch-balearischen Triasprovinz. *Verhandlungen des Naturhistorisch-medizinischen Vereins zu Heidelberg, Neue Folge*, 12(4): 477–594 + pl. 19–20.

Zessin, W. (2008a). Einige neue Insekten aus der Unteren Trias (Buntsandstein) von Mallorca, Spanien (Blattaria, Coleoptera, Diptera, Heteroptera und Megaloptera). *Deutschen Gesellschaft für allgemeine und angewandte Entomologie – Nachrichten*, 22(1): 20–21.

Zessin, W. (2008b). Neue Insekten aus der Unteren Trias (Buntsadstein) von Mallorca, Spanien (Blattaria, Coleoptera, Diptera, Heteroptera, Orthopteroidea und Homoptera). *Virgo, Mitteilungsblatt des Entomologischen Vereins Mecklenburg*, 11(1): 99–101.

Chapter 2

The early–middle Permian of Mallorca

© Henry S. Sharpe

Chapter 2 was published as:

Matamales-Andreu, R.; Mujal, E.; Dinarès-Turell, J.; Kustatscher, E.; Roghi, G.; Oms, O.; Galobart, À. & Fortuny, J. (2022). Early–middle Permian ecosystems of equatorial Pangaea: Integrated multi-stratigraphic and palaeontological review of the Permian of Mallorca (Balearic Islands, western Mediterranean). *Earth-Science Reviews*, 228: 103948.

DOI: https://doi.org/10.1016/j.earscirev.2022.103948

In this work, R. Matamales-Andreu contributed in:

A. Literature review of the Permian of Mallorca.
B. Direct examination of all the collections containing fossils from the studied outcrops.
C. Geological cartography.
D. Logging of all the stratigraphic sections.
E. Co-direction of all fieldwork campaigns (prospections and excavations). Sampling of macroplant remains and tetrapod tracks.
F. Palaeopalinology sampling.
G. Collaboration in palaeomagnetism sampling.
H. 3D modelling and measurement of relevant parameters on tetrapod tracks and trackways.
I. Stratigraphic and sedimentological analysis and definition of new formal lithostratigraphic units.
J. Invertebrate and vertebrate palaeoichnology, including identification and description of all the morphotypes.
K. Interpretation and discussion of the results.
L. Writing of the original draft and supplementary materials, except for sections 3.2, 3.3, 5, 6, 8.1.1 and 8.1.2 of the main text (palaeomagnetism and palaeopalinology).
M. Preparation of tables 1–3, ST1 and ST5, figures 1–4, 7–15, 17 and SF3–4, and all the supplementary logs. Adaptation of figures 5–6 and SF1–2.
N. Collaboration in obtaining funding for fieldwork and fossil preparation.

Also, refer to:

Appendix 2: Supplementary Material for Matamales-Andreu *et al.* (2022)

Appendix 3: Matamales-Andreu *et al.* (2021), *Palaeogeography, Palaeoclimatology, Palaeoecology*, synapsid locomotion

Appendix 4: Matamales-Andreu *et al.* (under review), new moradisaurine captorhinid

Appendix 5: Matamales-Andreu *et al.* (in preparation), new gorgonopsian therapsid

Appendix 6: Matamales-Andreu *et al.* (in preparation), new gorgonopsian tracks

Earth-Science Reviews 228 (2022) 103948

Contents lists available at ScienceDirect

Earth-Science Reviews

journal homepage: www.elsevier.com/locate/earscirev

Early–middle Permian ecosystems of equatorial Pangaea: Integrated multi-stratigraphic and palaeontological review of the Permian of Mallorca (Balearic Islands, western Mediterranean)

Rafel Matamales-Andreu [a,b,*], Eudald Mujal [a,c], Jaume Dinarès-Turell [d], Evelyn Kustatscher [e,f], Guido Roghi [g], Oriol Oms [h], Àngel Galobart [a,i], Josep Fortuny [a]

[a] Institut Català de Paleontologia Miquel Crusafont, Universitat Autònoma de Barcelona, Edifici ICTA-ICP, c/ Columnes s/n, Campus de la UAB, 08193 Cerdanyola del Vallès, Barcelona, Spain
[b] Museu Balear de Ciències Naturals, carretera Palma–Port de Sóller Km. 30, 07100 Sóller, Mallorca, Spain
[c] Staatliches Museum für Naturkunde Stuttgart, Rosenstein 1, 70191 Stuttgart, Germany
[d] Istituto Nazionale di Geofisica e Vulcanologia, Via di Vigna Murata 605, 00143 Roma, Italy
[e] Department für Geo- und Umweltwissenschaften, Paläontologie und Geobiologie, Ludwig-Maximilians-Universität, Richard-Wagner-Straße 10, 80333 München, Germany
[f] Bayerische Staatssammlung für Paläontologie und Geobiologie, Richard-Wagner-Straße 10, 80333 München, Germany
[g] Istituto di Geoscienze e Georisorse - CNR, Via Gradenigo 6, 35131 Padova, Italy
[h] Departament de Geologia, Universitat Autònoma de Barcelona, av. de l'eix Central s/n, Campus de la UAB, 08193 Cerdanyola del Vallès, Barcelona, Spain
[i] Museu de la Conca Dellà, c/ del Museu 4, 25650 Isona i Conca Dellà, Lleida, Spain

ARTICLE INFO

Keywords:
Cisuralian
Guadalupian
Magnetostratigraphy
Palynology
Tetrapod tracks
Central Pangaea

ABSTRACT

The Cisuralian–Guadalupian (early–middle Permian) was a period of climate transition from the Carboniferous icehouse conditions to the latest Permian–Early Triassic hothouse. The landmasses had coalesced in the supercontinent Pangaea and the climate was progressively becoming more arid, especially in a belt over the palaeoequator. The deposits of present-day Mallorca (Balearic Islands, western Mediterranean) were located in those low palaeolatitudes, in the western margin of the Tethys Sea, and correspond to alluvial systems with meandering rivers. The present study divides the stratigraphic succession into three main units, formally described herein as the Bec de s'Àguila Formation, Port des Canonge Formation and Pedra de s'Ase Formation. Based on an exhaustive review of the literature and new magneto- and biostratigraphic data, the sequence has been dated between the early and middle Permian (Artinskian–Wordian). Moreover, the detailed study of the fossils has provided a complete account of the denizens of those ecosystems. Tetrapod tracks occur abundantly in the Port des Canonge Formation, with morphotypes attributed to moradisaurine captorhinid eureptiles, araeoscelidian diapsids/non-varanodontine varanopids, possible pareiasauromorph parareptiles, "pelycosaur"-grade synapsids and indeterminate synapsids. Spores and pollen grains from the Pedra de s'Ase Formation indicate an overall dominance of conifers, accompanied by sphenophytes, ferns and seed ferns. Overall, apart from providing the first detailed interpretation of the ecosystems of the Permian of Mallorca, these new data have made it possible to improve the characterisation of the Permian–Triassic tectonosedimentary cycle in the Balearic Islands, which contribute to the understanding of the evolution of the western peri-Tethys ecosystems.

1. Introduction

The Permian was a period of great climatic, environmental and biotic changes. The assembly of the supercontinent Pangaea during the Pennsylvanian (late Carboniferous) and throughout the Permian, together with the uplift of the Variscan mountains in the equatorial region, resulted in a profound alteration of the climates of the planet (*e.g.*, Tabor and Poulsen, 2008; Stampfli et al., 2013). There was a sustained aridification trend, from the Carboniferous icehouse conditions to the Triassic hothouse (Montañez et al., 2007; Sun et al., 2012; Montañez and

* Corresponding author at: Institut Català de Paleontologia Miquel Crusafont, Universitat Autònoma de Barcelona, Edifici ICTA-ICP, c/ Columnes s/n, Campus de la UAB, 08193 Cerdanyola del Vallès, Barcelona, Spain.
E-mail address: rafel.matamales@icp.cat (R. Matamales-Andreu).

https://doi.org/10.1016/j.earscirev.2022.103948
Received 19 October 2021; Received in revised form 17 January 2022; Accepted 24 January 2022
Available online 30 January 2022
0012-8252/© 2022 Elsevier B.V. All rights reserved.

Poulsen, 2013; MacLeod et al., 2017), which contributed to the settling of a megamonsoonal regime that affected the low latitudes of Pangaea, alternating arid seasons with episodes of heavy rainfalls (*e.g.*, Parrish, 1993). As a result, the ecosystems underwent extensive remodelling, which translated into several important events of biological turnover. The Cisuralian continental tetrapod faunas were reminiscent of those of the Carboniferous, with an abundance of amphibians and "pelycosaur"-grade synapsids (Ruta and Benton, 2008; Brocklehurst et al., 2013). However, a remarkable faunal turnover occurred by the Guadalupian when, in the aftermath of the so-called Olson's Extinction (Brocklehurst et al., 2017; Olroyd and Sidor, 2017; Brocklehurst, 2020; but see Lucas, 2017), several groups of parareptiles and therapsids first appeared and readily outnumbered the residual representatives of the once-dominant amphibian groups (Sahney and Benton, 2008; Benson and Upchurch, 2013). Another extinction event struck the tetrapod faunas just before the Lopingian (Retallack et al., 2006; Lucas, 2009; Day et al., 2015), which was dominated by a diverse array of derived therapsid groups (Bernardi et al., 2017; Lucas, 2017). The Permian period ended with the most dramatic extinction event in the Phanerozoic, which wiped out almost all life on earth (Erwin, 1994; Benton and Twitchett, 2003; Benton, 2008), leaving empty ecological niches for the succeeding Mesozoic communities to fill (Romano et al., 2020).

During the Permian, sedimentation in the western margins of the Tethys sea (including the present-day Balearic Islands, western Mediterranean) took place in many small, relatively isolated basins (*e.g.*, McCann et al., 2006), making lithostratigraphic comparison among basins, even close ones, difficult. Asselian–Sakmarian ('Autunian') deposits of the Iberian Peninsula, Massif Central, Provençe and Sardigna usually correspond to a continuation of the organic matter-rich facies of the underlying Carboniferous deposits, representing sedimentation of lakes and floodplains under humid conditions (Sopeña et al., 1977; Cassinis and Ronchi, 2002; Cassinis et al., 2003; Schneider et al., 2006; Durand, 2008; Lopez et al., 2008; Michel et al., 2015; Mujal et al., 2018; López-Gómez et al., 2019a, 2019b, 2021). Sakmarian–Kungurian ('Saxonian') deposits also appear in most of the basins mentioned above and in the Alps (Cassinis et al., 2012). They represent semi-arid settings, with playa lake and fluvial channel deposits, sometimes with lacustrine deposits near the top of the sequences (see references cited above). In the cases when both groups are present, they are usually, but not always, bound by an unconfomity corresponding to a sedimentary hiatus. Roadian–Wuchiapingian ('Thuringian') deposits are usually thicker and more widespread, and appear in Menorca, Iberian Peninsula, Massif Central, Provençe and Sardigna, representing semi-arid floodplains traversed by braided or meandering river systems (Cassinis et al., 2003; Gand and Durand, 2006; Schneider et al., 2006; Durand, 2008; Bercovici et al., 2009; Linol et al., 2009; De la Horra et al., 2012; Michel et al., 2015; Mujal et al., 2017a). In the Alps, the 'Thuringian' sequences, as defined originally, span from the Wuchiapingian to the Changshingian, and exhibit a marine influence towards the East (Cassinis et al., 2012; Bernardi et al., 2017). In most of the aforementioned sections, the sedimentary palaeoenvironments and even some palaeoclimatic signals seem to reflect local conditions (with a superimposed global aridification trend), which further complicates correlations. The majority of those units have absolute age attributions from volcanic rocks, which are altogether absent in the sequences of Mallorca studied here, and therefore the datings of the latter rely on constraints imposed by palaeomagnetism and fossils (magneto- and biostratigraphy).

The present work exhaustively reviews and integrates all the previous stratigraphic and palaeontological data on the Permian of Mallorca (Balearic Islands, western Mediterranean) with new pieces of evidence, including palaeomagnetic, palynological, palaeobotanical and ichnological data. The lithostratigraphic framework is revised, providing new stratigraphic sections, clearing previous misconceptions and describing three formal units with rank of formation. The palaeodepositional environments and their evolution through time are interpreted from the sedimentological study, and biotic communities are described by study of spores, pollen and macroplant remains, together with trace fossils produced by both invertebrates and vertebrates. These fossil remains provide relatively precise age attributions for the two upper formations, and the performed magnetostratigraphic analysis further constrains these datings. Finally, these data are considered in the context of equatorial Pangaea in order to identify patterns regarding climate and biogeography.

2. Geographical and geological context

The Balearic Islands are an archipelago located in the western Mediterranean (Fig. 1A), as a northeastern extension of the Betic fold and thrust belt, uplifted during the Alpine orogeny (Vera et al., 2004). Rocks of Permian age crop out only on the two largest islands, Mallorca and Menorca (Pomar-Gomà, 1979; Obrador, 1983; Rodríguez-Perea et al., 1987; Calafat, 1988; Rosell et al., 1988; Gómez-Gras, 1993), but their successions were probably deposited in separate basins along the eastern margin of the Iberian plate (Gómez-Gras, 1993; López-Gómez et al., 2019a). In fact, the upper Palaeozoic–lower Mesozoic basins of the Balearic Islands form part of the same structural system as the basins from the Iberian Peninsula, as a whole known as the Iberian area. The Permian basins of the Balearic Islands, similarly to those of the rest of the Iberian Peninsula, were opened during the latest Carboniferous–earliest Permian, when the Variscan orogen started to collapse (McCann et al., 2006; López-Gómez et al., 2019a). This resulted in a dominant transtensional and extensional tectonic regime acting on the region, which favoured the development of semi-grabens where the sediments accumulated (López-Gómez et al., 2019a). Those basins were palaeogeographically located in the western peri-Tethys (see Roscher and Schneider, 2006), drifting from a latitude of about 7 °S in the earliest Permian to about 4 °N during the latest Permian (Scotese, 2014a, 2014b). The climate is thought to have been tropical throughout (Roscher et al., 2008), under semi-arid, seasonal conditions (Gómez-Gras and Alonso-Zarza, 2003; Bercovici et al., 2009).

On Mallorca, rocks of Permian age intermittently crop out along the coastal cliffs of the northwestern side of the Serra de Tramuntana, between Racó de s'Algar (Banyalbufar) and Platja de sa font Figuera (Valldemossa) (Fig. 1). They extend inland only in the valley behind Port des Canonge, but there they are mostly covered by forests. The base of the Permian group of units remains unknown, as the boundary with the underlying Carboniferous *Culm* facies is on a geological fault (Rodríguez-Perea and Ramos, 1984; Ramos and Rodríguez-Perea, 1985; Calafat, 1988). The boundary with the overlying Lower Triassic *Buntsandstein* facies has tentatively been recognised as an unconformity at the Pedrera de sa Cova section for the first time in the present study. Previous authors divided the Permian series into two (Ramos et al., 1985; Ramos, 1995), three (Calafat, 1988) or four (Gómez-Gras, 1993) informal lithostratigraphic units (see Supplementary Text 1; Supplementary Table 1; Matamales-Andreu et al., 2021a), which were never properly collated. The present work provides a detailed study of all the relevant sections of the island (Fig. 1B–D) and formal definitions for each of the lithostratigraphic units to avoid ambiguity in future studies.

3. Material and methods

3.1. Stratigraphy and sedimentology

For the stratigraphic and sedimentological study, 12 stratigraphic sections have been logged at 1:25 scale (here presented at 1:40 scale in Supplementary Logs) by means of a Jacob's staff and a measuring tape, down to minimum resolution of 1 cm of bed thickness. Texture, thickness, sedimentary structures, colour, palaeontological content and lithofacies (Table 1) have been also considered. Part of some of the logs corresponds to flooded or vertical passes, which have been logged either from within the water or using climbing gear, respectively. The logs are named, from southwest to northeast (Fig. 1): 'Racó de s'Algar' (RA,

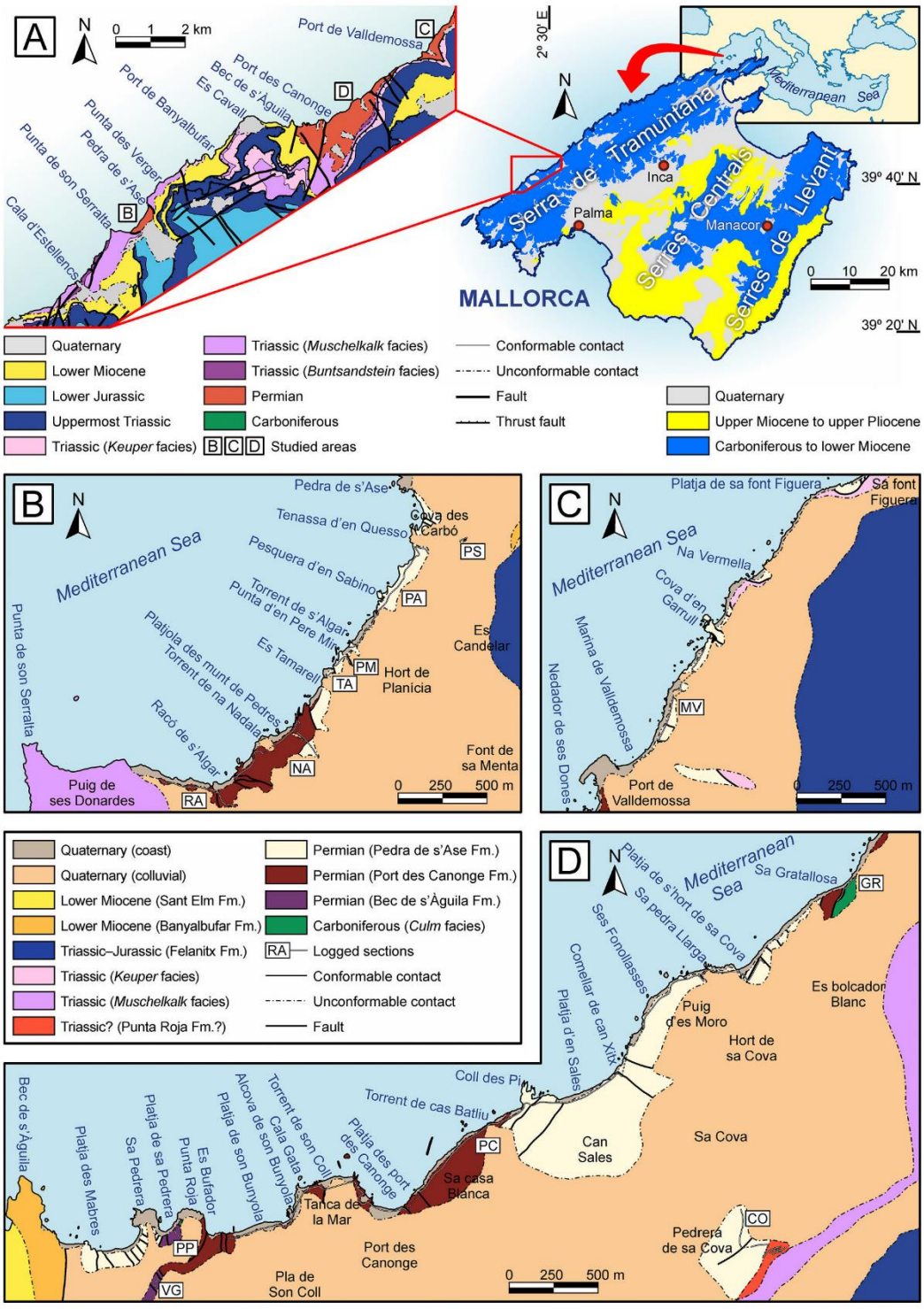

Fig. 1. A: Synthetic geological map of the island of Mallorca (Balearic Islands), with a close-up of the study zone, indicating the location of subfigures B, C and D. Simplified from Sevillano and Barnolas (2018). **B:** Detailed geological map of the outcrops between Punta de son Serralta and Pedra de s'Ase (Banyalbufar, Mallorca), with indication of the location of the six logged sections (RA: Racó de s'Algar; NA: Torrent de na Nadala; TA: Es Tamarell; PM: Punta d'en Pere Mir; PA: Pedra de s'Ase; PS: Pedra de s'Ase - Summit). **C:** Detailed geological map of the outcrops in the surroundings of Port de Valldemossa (Valldemossa, Mallorca), with indication of the location of the logged section (MV: Marina de Valldemossa). **D:** Detailed geological map of the outcrops between Bec de s'Àguila and Sa Gratallosa (Valldemossa, Mallorca), with indication of the location of the five logged sections (PP: Platja de sa Pedrera; VG: Volta des General; PC: Port des Canonge–Hort de sa Cova; GR: Sa Gratallosa; CO: Pedrera de sa Cova). Toponyms of all the maps after Homar (1985) and IDEIB (2019).

Table 1
Sedimentary lithofacies recognised in the outcrops of the Permian of Mallorca, mostly based on the table 1 of Matamales-Andreu et al. (2021b).

Code	Lithofacies	Sedimentary structures, processes and fossil content	Diagrams
Gt	Stratified, matrix to clast-supported, gravel to pebble-sized breccia of reworked mudstone, sandstone or calcrete (intraformational) clasts.	Distinct to crude trough-bedding. Positive grain sorting has rarely been observed in some beds. It corresponds to 3D megaripples that rework the floodplains, or scour fills of major channels (Miall, 1977; Gómez-Gras and Alonso-Zarza, 2003). In some cases, it contains tetrapod bones and bone fragments.	
Gm	Massive, matrix to clast-supported, gravel to pebble-sized breccia of reworked mudstone, sandstone or calcrete (intraformational) clasts.	Massive. It corresponds to 3D megaripples that rework the floodplains, or scour fills of major channels (Miall, 1977; Gómez-Gras and Alonso-Zarza, 2003). In some cases, it contains tetrapod bones and bone fragments.	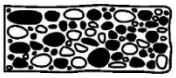
GmP	Massive, matrix to clast-supported, gravel to cobble-sized sub-rounded polygenic breccias and conglomerates of extraformational clasts.	Massive to very crude planar, irregular bedding. Positive or negative granoselection has been observed, although the clasts are usually randomly sorted. It corresponds to alluvial-fan debris flows and water-laid deposits, somewhat unconfined, similarly to the P1 unit of Menorca (Gómez-Gras and Alonso-Zarza, 2003). Large rhizocretions sometimes present.	
St	Stratified, very fine- to very coarse-grained sandstone.	Trough cross-bedding. It corresponds to sinuous or linguoid 3D megaripples of lower flow regime (Miall, 1985, 2006). In some cases, it contains rhizocretions.	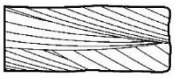
Sp	Stratified, very fine- to coarse-grained sandstone.	Planar cross-bedding. It corresponds to transverse or linguoid 2D bars of lower flow regime (Miall, 1977, 1985, 2006). In some cases, it contains rhizocretions.	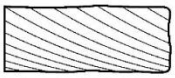
Sr	Stratified, very fine- to medium-grained sandstone.	Ripple-marks, mostly climbing ripples; current ripples and wave ripples are less frequent. Sometimes convolute lamination. It corresponds to low regime and waning flows, at the top of channel sequences or at crevasse splays (Miall, 1985). Rhizocretions or invertebrate traces sometimes present. Mud-cracks, tetrapod tracks and plant impressions may appear on the base.	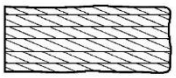
Sh	Stratified, very fine- to medium-grained sandstone.	Horizontal stratification and lamination, sometimes alternating finer-grained layers with coarser ones. It corresponds to planar bed flow of lower flow regime or traction carpets in upper flow regime (Miall, 1977, 1985, Postma, 1990).	
Sl	Stratified, very fine- to coarse-grained sandstone.	Low-angle cross-bedding. Sometimes convolute lamination. It corresponds to scour fills, crevasse splays, antidunes (Miall, 1985, 2006). Rhizocretions or invertebrate traces sometimes present. Mud-cracks, tetrapod tracks and leaf impressions may appear on the base.	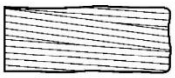
Ss	Stratified to massive, fine- to coarse-grained sandstone.	Clear to crude trough cross-bedding. Usually with soft pebbles. It corresponds to scour fills (Miall, 2006).	
Sm	Massive, very fine- to coarse-grained sandstone.	Massive (in macroscopic view). It corresponds to sediment gravity flows (Miall, 2006) or to beds with lamination obliterated by bioturbation. It may be affected by mud-cracks. Rarely, articulated to semi-articulated tetrapod skeletons may appear.	
Sb	Massive, very fine- to medium-grained sandstone.	Abundant invertebrate burrows and/or root traces. It corresponds to the biotic reworking of overbank deposits (Miall, 1985).	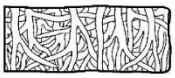
Fl	Laminated lutites.	Fine lamination, consisting of small ripples, low-angle cross lamination or horizontal lamination. It corresponds to overbank, abandoned channel (including oxbow lakes) or waning flood deposits (Miall, 2006).	
Fm	Massive lutites.	Massive. It corresponds to overbank, abandoned channel or drape deposits (Postma, 1990; Miall, 2006). Mud-cracks, leaf impressions and tetrapod tracks often present. Rarely, thin coal seams may appear.	
Fr	Lutites with roots.	Lamination usually obliterated by root bioturbation. Carbonate nodules sometimes present, indicating the formation of an incipient soil. It corresponds to the biotic (plant) reworking of other lutitic lithofacies.	
Fb	Lutites with burrows.	Lamination usually obliterated by horizontal and/or vertical burrows of invertebrates. Mud-cracks often present. It corresponds to the biotic reworking of other lutitic lithofacies.	
P	Lutites or sandstones with carbonate nodules and, generally, root traces.	Massive or crudely laminated because of the bioturbation (root traces or invertebrate burrows). Carbonate nodules are always very abundant, sometimes forming continuous crusts or even thick calcretes. Gleyed patches, sometimes surrounding coalified plant remains, are also common. It corresponds to either calcic Vertisols, vertic Calcisols or Calcisols (Mack et al., 1993).	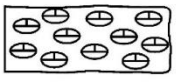

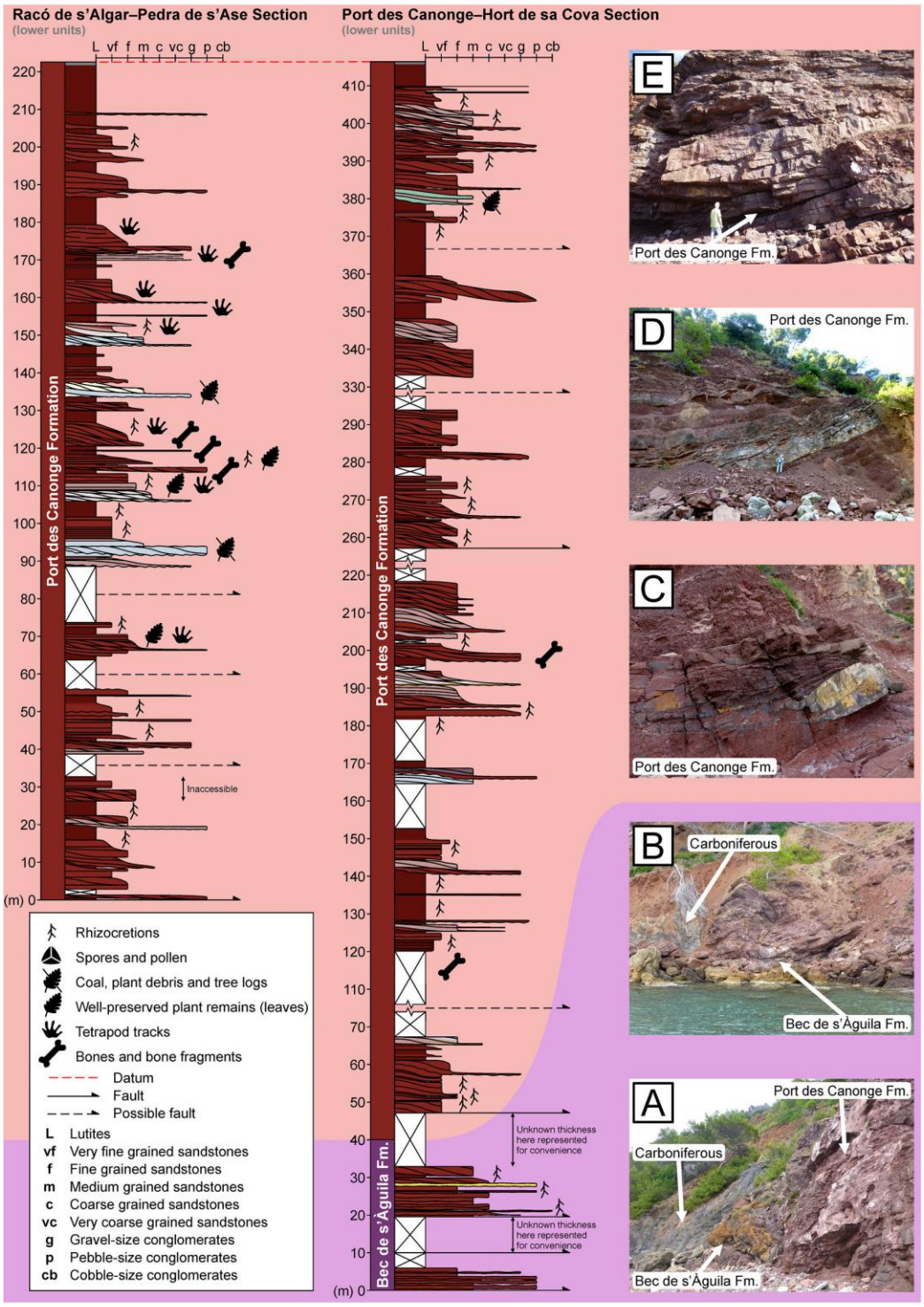

Fig. 2. Synthetic logs of the Bec de s'Àguila and Port des Canonge formations at the Racó de s'Algar–Pedra de s'Ase section and at the Port des Canonge–Hort de sa Cova section. See also Supplementary Logs and Supplementary Correlations. **A–E:** Field pictures of some representative points in those two logs. **A:** Faulted contact between the Carboniferous deposits, the Bec de s'Àguila Formation and the Port des Canonge Formation at Sa Gratallosa. **B:** Faulted contact between the Carboniferous deposits and the Bec de s'Àguila Formation at Platja de sa Pedrera. **C:** Infill deposits of a small channel with lateral accretion and associated crevasse splay and floodplain deposits, Port des Canonge Formation at Racó de s'Algar. **D:** General aspect of the Port des Canonge Formation at Platjola des munt de Pedres, note alternation of main channels (sandstones) and floodplain (lutites) deposits. **E:** General aspect of the Port des Canonge Formation near Torrent de cas Batliu, note the lateral accretion sets. Changes in background colour represent boundaries between formations.

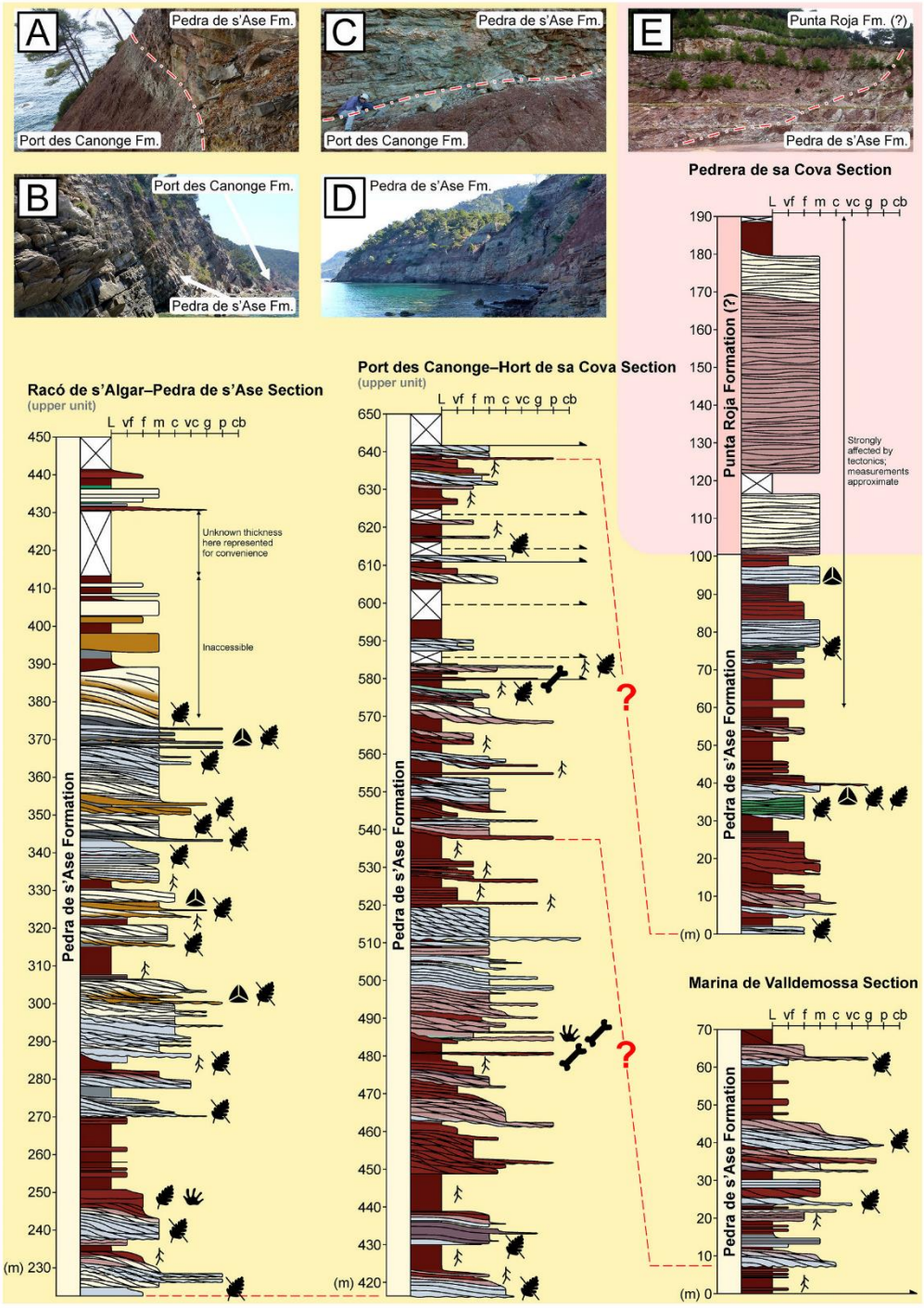

Fig. 3. Synthetic logs of the Pedra de s'Ase Formation and the Punta Roja Formation(?) at the Racó de s'Algar–Pedra de s'Ase section, at the Port des Canonge–Hort de sa Cova section, at the Pedrera de sa Cova section and at the Marina de Valldemossa section. Symbols of fossils, lithology and other structures as in Fig. 2. See also Supplementary Logs and Supplementary Correlations. **A–E:** Field pictures of some representative points in some of those logs. **A:** Boundary between the Port des Canonge Formation and the Pedra de s'Ase Formation at Platjola des munt de Pedres. **B:** General aspect of the Pedra de s'Ase Formation at Pedra de s'Ase, note the outcrops of the Port des Canonge Formation in the distance. **C:** Boundary between the Port des Canonge Formation and the Pedra de s'Ase Formation near Torrent de cas Batliu. **D:** General aspect of the Pedra de s'Ase Formation at Platja d'en Sales, note the higher abundance of interbedded red lutites compared to the type section. **E:** Boundary between the Pedra de s'Ase Formation and the Punta Roja Formation(?) at Pedrera de sa Cova (upper quarry). Changes in background colour represent boundaries between formations.

Table 2
Architectural elements recognised in the outcrops of the Permian of Mallorca, mostly based on table 2 of Matamales-Andreu et al. (2021b). Arrows (→) indicate the usual succession. Lithofacies in brackets are often missing in the "ideal" succession. Formations in brackets only present that architectural element rarely.

Code	Element	Principal lithofacies assemblages	Interpretation	Diagrams	Formation
GB + *SG*	Gravel bars and bedforms and Sediment gravity flows	*GmP→Sm*	Water-laid deposits by tractive currents and interbedded debris flows sedimented in alluvial fans (Colombo, 2010a, 2010b).	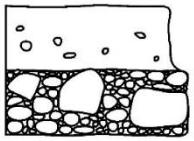	Bec de s'Àguila Formation
SB	Sandy bedforms	*(Gt/Gm)→Sp→(Sr)* *(Gt/Gm)→St→Sl→Sr*	Shallow channel-fill assemblages and channel-floor dune fields, respectively (both in the sense of Miall, 2006).	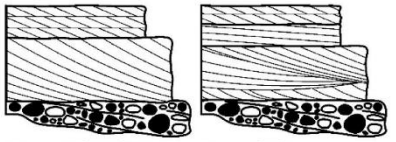	Pedra de s'Ase Formation
LA	Lateral accretion deposits	*Gt/Gm→St/Sl→Sr/Sl→(Fl)→Fm* *St→Fl*	Point bars of meandering rivers (Miall, 2006). Rarely, oxbow lakes with abundant plant remains.	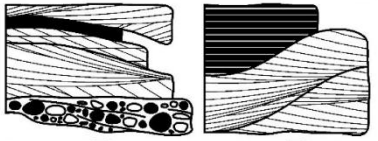	Pedra de s'Ase Formation Port des Canonge Formation Bec de s'Àguila Formation
LS	Laminated sand sheets	*Sh* *Sl*	Flash flood deposits under upper flow-regime plane bed conditions (Miall, 2006).	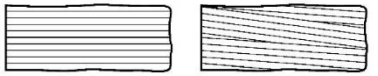	Pedra de s'Ase Formation
LV + *CR* + *CS*	Levees and Crevasse channels + and Crevasse splays	*(St)→Sl→Sr→(Sm/Sb/P)* *Gt/Gm/Ss→(Sl/Sr)→(Sm/Sb/P)*	Overbank flooding (Miall, 2006), including the sand wedges bordering the channels (levees), the crevasse channels and the sheetflood deposits of crevasse splays. May be affected by pedogenesis. Given the limited lateral extension of the studied deposits, it has usually not been possible to precisely differentiate the three architectural elements.	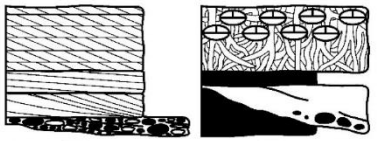	Pedra de s'Ase Formation Port des Canonge Formation
FF	Floodplain fines	*Fl→Fm→Fr/Fb→P*	Deposits of overbank low-energy flows or sedimentation in pools and playa-lakes (Miall, 2006). Carbonate or gleyed palaeosols usually appear towards the top of the sequences.	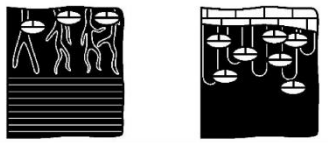	Pedra de s'Ase Formation Port des Canonge Formation (Bec de s'Àguila Formation)

149.3 m), 'Torrent de na Nadala' (NA, 192.5 m), 'Es Tamarell' (TA, 27.8 m), 'Punta d'en Pere Mir' (PM, 30.0 m), 'Pedra de s'Ase' (PA, 167.3 m), 'Pedra de s'Ase - Summit' (PS, 11.0 m), 'Volta des General' (VG, 5.9 m), 'Platja de sa Pedrera' (PP, 13.3 m), 'Port des Canonge–Hort de sa Cova' (PC, 604.4 m), 'Pedrera de sa Cova' (CO, 190.0 m), 'Sa Gratallosa' (GR, 8.6 m) and 'Marina de Valldemossa' (MV, 70.0 m). These logs have been synthesised (1:1160 scale) and correlated for each of the four main areas, in order to overcome the local distortion produced by faulting: 'Racó de s'Algar–Pedra de s'Ase section', 'Port des Canonge–Sa Gratallosa section', 'Pedrera de sa Cova section' and 'Marina de Valldemossa section' (see Supplementary Correlations). Finally, the synthetic logs of each of those sections have been correlated (see '4. Stratigraphy and sedimentology' below). The *datum* to correlate the two main synthetic sections, 'Racó de s'Algar–Pedra de s'Ase section' and 'Port des Canonge–Sa Gratallosa section', is the boundary between the Port des Canonge Formation and the Pedra de s'Ase Formation, that is, the change from dominant red lutites and fine-grained sandstones to pink/white/blue medium-grained sandstones (Fig. 2). The position of the 'Marina de Valldemossa section' within the Pedra de s'Ase Formation can only be tentatively assigned to its middle part based on the similarity of the sequences (Fig. 3). The boundary between Permian and Triassic units seems to be present at the 'Pedrera de sa Cova section' and thus it has been broadly assigned to the upper part of the Pedra de s'Ase Formation (Fig. 3). The sedimentary lithofacies and architectural elements were classified according to the nomenclature of Miall (1977, 1985, 2006) and Postma (1990), with modifications introduced by Linol et al. (2009) for the Permian sequence of the neighbouring island of Menorca (Table 1). The architectural elements have been classified according to Miall (1985, 2006) (Table 2).

3.2. Magnetostratigraphy

In order to characterise the geomagnetic polarity of rocks along the studied successions and erect a magnetostratigraphy, 234 oriented hand samples were taken from their corresponding stratigraphic levels, spanning about 835 m of strata. Sampling was focused on lithologies that were potentially most suitable for palaeomagnetism (*i.e.*, the red-coloured, finest-grained lithologies). A regular spacing between samples was usually maintained, although this was not possible in the intervals of medium-/coarse-grained sandstones and those that were not cropping out. Collected samples are distributed along several stratigraphic sections named, from southwest to northeast (Fig. 1): 'Racó de s'Algar' (RA1–RA4 sampling levels), 'Torrent de na Nadala' (NA1–NA46), 'Volta des General' (VG1–VG5), 'Platja de sa Pedrera' (PP1–PP3), 'Port des Canonge–Hort de sa Cova' (PC1–PC152), 'Pedrera de sa Cova' (CO1–CO24) (see Supplementary Logs for the precise location of all the collected samples). Disregarding major non-outcropped intervals, the overall sampling resolution is 2–4 m. The aforementioned sections have been correlated and integrated into three main synthesised stratigraphic logs, 'Racó de s'Algar–Pedra de s'Ase section', 'Port des Canonge–Hort de sa Cova section' and 'Pedrera de sa Cova section' (see '3.1. Stratigraphy and sedimentology' for details). Strata dip along those three sections is similar and moderate (strike/dip angles at about 090/30, 085/28, and 066/26 respectively, see Supplementary Table 2). The similar bedding attitude of the studied sections prevents a meaningful palaeomagnetic fold test.

Collected samples were subsequently cut in standard palaeomagnetic regular specimens for laboratory analysis. A total of 144 samples were fully demagnetised for the present study (about 62% of the collected samples, see Supplementary Table 2). Natural remanent magnetisation (NRM) and remanence through demagnetisation were measured on a 2G Enterprises DC SQUID high-resolution pass-through cryogenic magnetometer (manufacturer noise level of 10^{-12} Am^2) operated in a shielded room at the Istituto Nazionale di Geofisica e Vulcanologia in Rome, Italy. A Pyrox oven in the shielded room was used for thermal demagnetisations and alternating field (AF) demagnetisation was performed with three orthogonal coils installed inline with the cryogenic magnetometer. Progressive stepwise AF demagnetisation was routinely used and applied after a single heating step to 150 °C. AF demagnetisation included usually 14 steps (4, 8, 13, 17, 21, 25, 30, 35, 40, 45, 50, 60, 80, 100 mT). Subsequently, thermal demagnetisation resumed through variable temperature increments (20–100 °C) up to 690 °C. In the context of the studied redbeds, applying a first heating step followed by AF demagnetisation prior to full thermal demagnetisation makes it possible to both unblock eventual magnetisation carried by goethite (usually unblocking below 120 °C) and also magnetite-like low coercivity ferromagnetic phases. Consequently, magnetic phases even unblocking at relatively low temperatures during the final thermal protocol must be assigned to high coercivity phases (*i.e.*, hematite). Characteristic remanent magnetisations (ChRM) were calculated by Principal Component Analysis (Kirschvink, 1980) and by the great circle technique (McFadden and McElhinny, 1988) from orthogonal vector endpoint demagnetisation diagrams (Zijderveld, 2013) using the online open-source software Paleomagnetism.org (Koymans et al., 2016, 2020). The magnetic stratigraphy is based on virtual geomagnetic pole (VGP) latitudes.

In order to characterise ferromagnetic mineralogy, some rock-magnetic experiments were performed in selected samples. Thermomagnetic heating and cooling cycles where measured with an AGICO MFK1 susceptibility bridge with a CS3 furnace attachment with nominal sensitivity (5×10^{-7} SI) and open air into the tube. Hysteresis loops, isothermal remanent magnetization (IRM) acquisition and back-field IRM were measured at room temperature with a Princeton Measurements Corp. Model 3900 MicroMag^{TM} Vibrating Sample Magnetometer (VSM) (noise level 5×10^{-9} Am^2). IRM curve unmixing was performed with IRM MaxUnmix package (Maxbauer et al., 2016).

3.3. Palaeopalynology and palaeobotany

For the present study, 35 rock samples were collected from the studied stratigraphic sections in order to search fossil sporomorphs and palynomorphs (Supplementary Table 4). The beds chosen to be sampled were generally greyish-bluish lutites or very fine-grained sandstones. Specifically, there are three samples in the Port des Canonge Formation of log RA; one sample in the Port des Canonge Formation and three samples in the Pedra de s'Ase Formation of NA; 13 samples in the Pedra de s'Ase Formation of log PA; two samples in the Pedra de s'Ase Formation of log PS; one sample in the Port des Canonge Formation and three samples in the Pedra de s'Ase Formation of log PC; four samples in the Pedra de s'Ase Formation and one sample in the Punta Roja Formation(?) of log CO; and three samples in the Pedra de s'Ase Formation of log MV (see exact position of all the samples in Supplementary Logs).

To extract the sporomorphs and palynomorphs, rock samples were crushed and treated with HCl (37%) and HF (47%) to dissolve the non-organic material. After washing and sieving (15 μm nylon mesh), the residue was stored in water and then strew mounted onto microscope slides using Entellan glue as the mounting medium. The microscope slides were studied under a Leica DM750 light microscope, and the index species were photographed using a Leica ICC50 W digital camera. Slides are permanently housed in the Museu de Mallorca (Palma, Mallorca, Balearic Islands, Spain; see '3.5. Institutional abbreviations' below).

Among the different observed macroplant remains, some were not collected because of their very large size (*i.e.*, tree logs) or being included in very large and hard rock surfaces. Those were identified according to the following code: [stratigraphic log label]-[level]-[correlative number for each macroplant remain in that level]. Macroplant remains that were collected are permanently housed in the Museu de Mallorca (Palma, Mallorca, Balearic Islands, Spain; see '3.5. Institutional abbreviations' below).

3.4. Tetrapod ichnites

Digital 3D models of the surfaces with ichnites were made following the procedure explained by Mujal et al. (2020). Agisoft Photoscan standard v.1.1.4. (http://www.agisoft.com) was used to align the photographs and to create the dense point clouds, meshes and textures. MeshLab v.2016.12 (http://meshlab.sourceforge.net/) was used to scale, orient and crop the models. The false colour-coded height maps with contours were built using ParaView v.5.5.0-RC4 64-bit (http://www.paraview.org). ImageJ v.1.52d (https://imagej.nih.gov/ij/) was used to measure, whenever possible, the standard parameters of the ichnites recommended by Leonardi (1987) and Hasiotis et al. (2007). All measurements of the ichnites studied herein are listed in Supplementary Table 5.

The specific nature of the ichnological material, where one 'specimen' (=rock slab with footprints) may have several unrelated tracks, or some footprints forming a trackway, calls for a particular set of rules to accurately reference each ichnite. In the present work, the slabs are identified according to following code: [stratigraphic log label]-[level, "exs" if found *ex situ*]-[correlative number for each slab in that level]-[correlative number indicating the trackway][correlative letter indicating the ichnite] (see Supplementary Table 5). All the ichnites considered herein (both left in the field and collected) were consistently numbered using that code. Correspondence of that nomenclature with institutional catalogue numbers of the slabs that were collected from the field are in Supplementary Table 5. Slabs with ichnites that were collected are permanently housed in the Museu de Mallorca (Palma, Mallorca, Balearic Islands, Spain; see '3.5. Institutional abbreviations' below).

The tetrapod tracks studied herein show different states of preservation, depending on the layer and on the size of the ichnites. More than half of the ichnites have a type 3 preservation value (optimal) according to the scale of Marchetti et al. (2019a), and the rest are of types 2 (good), 1 (intermediate) and, very rarely, 0 (poor). To count the relative proportions of each ichnotaxon (see '8.1. Age attributions' below), the methodology of Marchetti et al. (2017a) was not used because most of the surfaces with ichnites were large (often 0.5–2 m^2) and profusely trampled. In this specific case, the "track/slab" method (Marchetti et al., 2017a) would severely underestimate the ichnotaxa with two or more trackways on the same surface, and their "weighting size" method (Marchetti et al., 2017a) would overestimate ichnotaxa with trackways (*i.e., Hyloidichnus, Dimetropus*) over those that appear as isolated ichnites (*i.e., Dromopus*). Therefore, in the present work each trackway, regardless of the number of ichnites imprinted, was counted as a single occurrence for that ichnotaxon in that layer. Isolated ichnites (or isolated manus-pes sets) that were not part of a trackway were also counted as a single occurrence. All ichnites have been revised and studied except for one morphotype, attributable to a synapsid trackmaker, which appears to be different from other coeval ichnogenera and is the object of a separate study. Regardless, it has been included in the counts of '8.1.3. Tetrapod track biostratigraphy' as "indeterminate synapsid tracks".

3.5. Institutional abbreviations

D/21: Museu de Mallorca, Palma, Mallorca, Balearic Islands, Spain.

MBCN: Museu Balear de Ciències Naturals, Sóller, Mallorca, Balearic Islands, Spain.

UIB: Universitat de les Illes Balears, Palma, Mallorca, Balearic Islands, Spain.

4. Stratigraphy and sedimentology

Formal lithostratigraphic units have hitherto never been defined for the Permian red-beds of Mallorca. Previous authors (Cuevas-López, 1958a, 1958b; Pomar-Gomà, 1979; Martí et al., 1985; Ramos et al., 1985; Calafat, 1986, 1987, 1988; Rodríguez-Perea et al., 1987; Barnolas, 1991a, 1991b; Gómez-Gras, 1992, 1993; Ramos, 1995) divided the Permian–Triassic continental sequence into several informal lithostratigraphic units (see Supplementary Text 1 and Supplementary Table 1). Subsequent reviews (Arche et al., 2002; López-Gómez et al., 2002, 2019a; Vera et al., 2004; Bourquin et al., 2007, 2011; Cassinis et al., 2012) upgraded some of those to the rank of formation, without proper description or characterisation. An additional complication is that most of the recent work is based on the stratigraphic framework proposed by Ramos et al. (1985) and Ramos (1995), which incorrectly correlated Permian and Triassic units from different outcrops (see Supplementary Text 1; Matamales-Andreu et al., 2021a,b). This section provides formal descriptions of all the Permian units of Mallorca, preserving the first name used for each of them. Descriptions and interpretations of all the lithofacies and architectural elements are here presented in Table 1 and Table 2.

4.1. Bec de s'Àguila Formation

This formation (Fig. 2) is identified by the presence of conglomerates with clasts of quartz or rocks from the Devonian/Carboniferous basement (in the other formations, the clasts are always soft pebbles and carbonate nodules). The clasts can also appear as isolated grains in the sandstone beds. Moreover, the red sandstone deposits are usually medium- or coarse-grained, in contrast to the overlying formations, in which red sandstones are very fine- or fine-grained. Beds of lutites are rare in this formation.

4.1.1. Location and boundaries

The only three outcrops of the Bec de s'Àguila Formation are small, mostly covered and heavily affected by tectonics. There are limited exposures at Volta des General and at Sa Gratallosa, and the tickest section has been measured at Platja de sa Pedrera (see Supplementary Logs). With 13.3 m of thickness, the section of Platja de sa Pedrera is hereby formally designed as the stratotype of this formation (Figs. 1D, 2; Supplementary Logs). Its lower boundary is always determined by faults, with Carboniferous *Culm* facies in the case of Sa Gratallosa (Rodríguez-Perea and Ramos, 1984; Ramos and Rodríguez-Perea, 1985) (Fig. 2A) and at Platja de sa Pedrera (Calafat, 1988) (Fig. 2B), and with the Port des Canonge Formation (by means of an inverse fault) in the case of Volta des General. Its upper boundary is a geological fault causing it to contact the Port des Canonge Formation in the case of the sections of Sa Gratallosa (Fig. 2A) and Volta des General. At Platja de sa Pedrera, this contact is covered (Fig. 2B).

4.1.2. Lithological features and palaeontological content

The lithofacies (Fig. 4, Table 1) and architectural elements (Table 2) present in this formation show a very particular arrangement, with abundance of conglomerates, that makes it possible to distinguish it from all other Permian formations of Mallorca. The conglomerate beds (lithofacies type *GmP*, Fig. 4B) are especially frequent in the lower part, and comprise a red or yellow matrix of medium- to very coarse-grained sandstones and clasts (of variable size) of quartz and lithic fragments of Carboniferous (or older) rocks, that are sub-rounded to very angular. No clear lamination can be seen in those beds, which are mostly horizontal with irregular tops and slightly erosive bases. The clasts are never imbricated and are usually unsorted, although some beds do present either positive or negative grain sorting. Traces of large roots similar to those described in the Permian P1 unit of Menorca (Gómez-Gras and Alonso-Zarza, 2003) can sometimes be observed. Medium to coarse-grained red sandstone beds are also frequent, and are mostly massive (lithofacies type *Sm*) or show crude trough cross-bedding (lithofacies type *St*). Sandstone deposits with basal scours (lithofacies type *Ss*), beds with planar cross-bedding (lithofacies type *Sp*), horizons with abundant rhizocretions (lithofacies type *Sb*) and even palaeosols (Calcisols, vertic Calcisols or Vertisols; lithofacies type *P*) may also appear. Finally, red lutite beds are very rare, being either massive (lithofacies type *Fm*) or

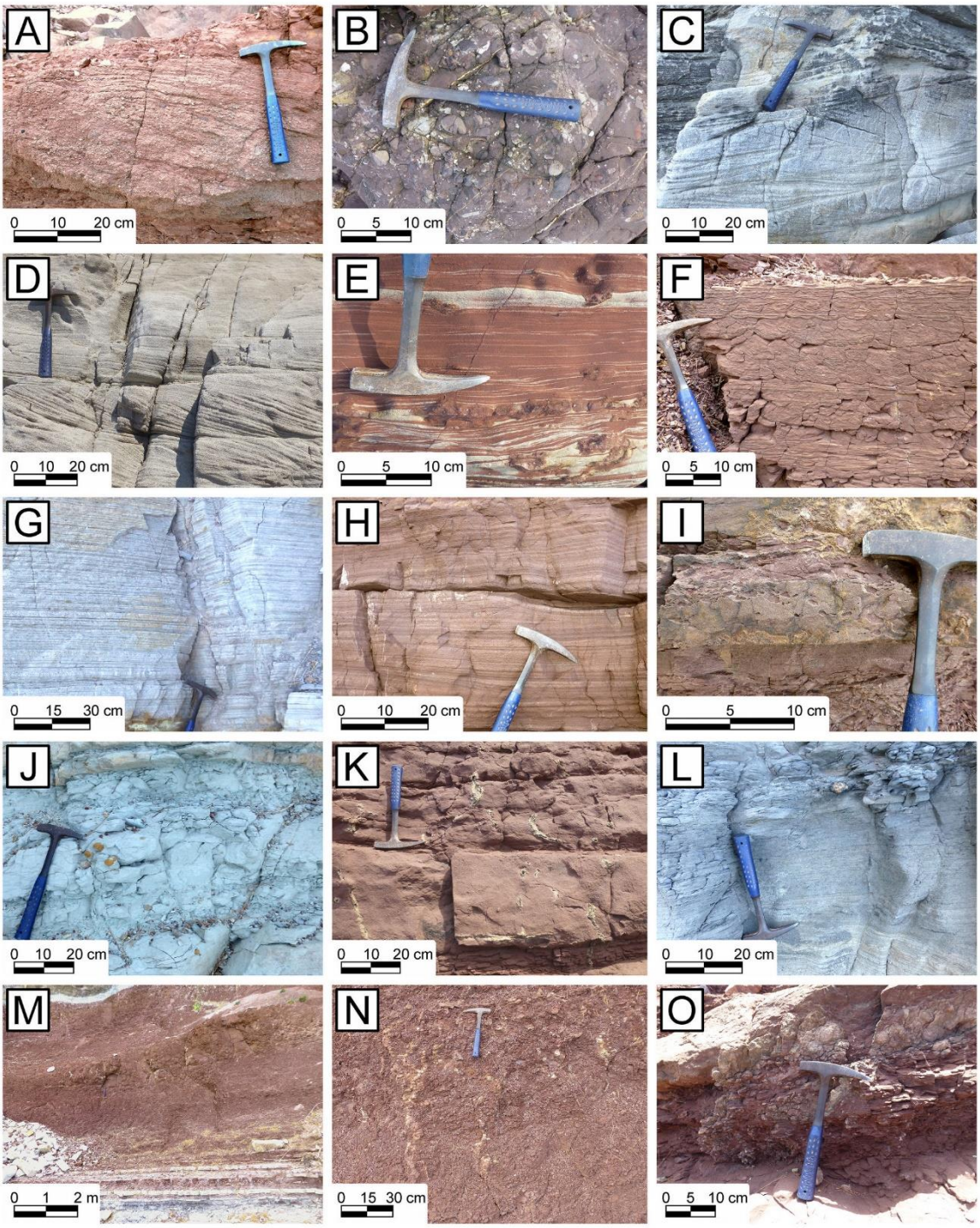

Fig. 4. Photographic examples of most of the lithofacies mentioned in the present work (see also Table 1). **A:** Intraformational breccias with trough cross-bedding (*Gt*), Port des Canonge Formation. **B:** Extraformational conglomerates (*GmP*), Bec de s'Àguila Formation. **C:** Sandstones with trough cross-bedding (*St*), Pedra de s'Ase Formation. **D:** Sandstones with planar cross-bedding (*Sp*), Pedra de s'Ase Formation. **E:** Sandstones with ripple lamination (*Sr*), Pedra de s'Ase Formation. **F:** Silty sandstones with ripple lamination, heavily affected by fluid-scape structures (*Sr?*), Port des Canonge Formation. **G:** Sandstones with horizontal bedding (*Sh*), Pedra de s'Ase Formation. **H:** Sandstones with low-angle cross-bedding (*Sl*), Port des Canonge Formation. **I:** Sandstones filling a scour, with soft pebbles and without visible bedding (*Ss*), Port des Canonge Formation. **J:** Massive sandstones (*Sm*) with nodules, Pedra de s'Ase Formation. **K:** Bioturbated sandstones (*Sb*) with rhizocretions, Port des Canonge Formation. **L:** Laminated lutites (*Fl*), in this case with horizontal lamination, Pedra de s'Ase Formation. **M:** Massive lutites (*Fm*), Pedra de s'Ase Formation. **N:** Lutites with rhizocretions (*Fr*), Port des Canonge Formation. **O:** Palaeosols (*P*), in this case a Calcisol, Port des Canonge Formation.

affected by root bioturbation (lithofacies type *Fr*). The dominant architectural elements in this formation are *GB/SG*. Secondarily, element *LA* appears in the upper part of the unit, with rare intercalations of element *FF*. The only fossils found so far in Bec de s'Àguila Formation are rhizocretions of diverse sizes.

4.1.3. Interpretation

In this formation, lithofacies type *GmP* represents the deposits of gravity and debris flows in a colluvial/alluvial-fan environment. Lithofacies type *Sm* also corresponds to deposition by dense flows. Other sandstone lithofacies, such as those of types *St* and *Sp*, have been interpreted to be deposited by fluvial currents during intervals of relatively lower flow regime, whereas type *Ss* corresponds to higher energy events with erosive capacity. Lithofacies of types *Sb* and *P* represent the alteration of other lithofacies types by biogenic activity. The presence of calcic Vertisols, vertic Calcisols and Calcisols point to a semi-arid climate with variations of the water table, possibly due to seasonality (Mack et al., 1993; Alonso-Zarza, 2003; Tabor and Poulsen, 2008). Lutite lithofacies of types *Fm* and *Fr* correspond to the fine sediments deposited in the floodplain, which can be bioturbated by plant roots. The architectural elements *GB/SG* record gravity flows in a colluvial/alluvial fan setting, the element *LA* corresponds to point bars of meandering channels, rarely interbedded with element *FF*, the floodplain fine deposits.

This formation represents colluvial and alluvial-fan debris-flow deposits and the transition towards the fine-grained meandering rivers of the Port des Canonge Formation (see '4.2. Port des Canonge Formation' below). Similar to the P1 unit of Menorca (Gómez-Gras and Alonso-Zarza, 2003; Matamales-Andreu et al., 2021c), the debris-flow conglomerates contain mostly extraformational clasts and may develop palaeosols (Calcisols) with large rhizocretions. The medium to coarse-grained sandstones that appear towards the upper part of the formation are usually massive and somewhat tabular but in some cases, such as at the Platja de sa Pedrera section, they present clear lateral accretion (Fig. 2), thus representing medium- to coarse-grained sinuous channels with almost no floodplain deposits. The few palaeocurrents measured in this formation (n = 2) point to a possible southeast direction (mean of 137.5°; see '8. Discussion' below).

4.2. Port des Canonge Formation

This formation (Fig. 2) can be identified in the field because of the great abundance of very fine-grained rocks compared to the other two Permian formations of Mallorca. Specifically, the typical sequence consists of intervals of very fine- to fine-grained red sandstones of about 2–4 metres-thick, with lateral accretion surfaces, overlain by about 2–5 metres of red lutites and very fine-grained red sandstones forming tabular beds.

4.2.1. Location and boundaries

The Port des Canonge Formation crops out extensively at the Racó de s'Algar–Pedra de s'Ase section (about 222.5 m thick, including covered intervals, Figs. 1B, 2C, 2D) and at the Port des Canonge–Hort de sa Cova section (about 368.8 m thick, including covered intervals, Fig. 1D). Smaller exposures also occur in the surroundings of Sa Gratallosa (Figs. 1D, 2A) and possibly at Nedador de ses Dones (Fig. 1C). The thickest and most easily accessible section is that of Port des Canonge–Hort de sa Cova, which is here formally designed as the stratotype for this formation (Fig. 2; Supplementary Logs). Its lower boundary is faulted in all cases, whereas its transitional upper boundary with the Pedra de s'Ase Formation is visible in both of the logged sections and is defined by a shift from very fine- to fine-grained red sandstone beds to medium- to coarse-grained pink/blue/white beds with blue lutites at their base (Fig. 3A, C; Supplementary Logs; Supplementary Correlations). There are large covered stretches in all the outcrops representing the lower half of this formation, probably concealing faults; for this reason, the thickness of this unit has been given in ranges. The minimum corresponds to the thickness of the part of the sequence that is certainly continuous and not faulted, whereas the maximum includes all the covered parts and faulted zones.

4.2.2. Lithological features and palaeontological content

The lithofacies (Fig. 4, Table 1) and architectural elements (Table 2) of this formation show a notable diversity accounting for different depositional palaeoenvironments. Breccia lithofacies of types *Gm* and *Gt* (Fig. 4A) constitute the base of sandstone packages or appear as isolated beds among lutites, may be massive or have crude bedding, and their clasts are always soft pebbles of lutite and sandstone, sometimes with carbonate nodules and fragments of rhizocretions. Sandstones account for about the 60% of all the rocks of the studied sections, and the most abundant lithofacies are those of types *St* and *Sl* (Fig. 4E). In some cases, lithofacies of types *Sp*, *Sm* and, rarely, *Sh* also appear. Lithofacies of types *Sr* and *Sl* become abundant towards the upper part of the sandstone intervals, and also occur in tabular beds intercalated between lutites. Lithofacies type *Ss* (Fig. 4I) appears rarely, in the form of sandstone beds with erosive bases, with crude bedding and usually containing soft pebbles. Lithofacies type *Sb* (Fig. 4C) corresponds to sandstones with abundant invertebrate bioturbation. Regarding lutite lithofacies, the most abundant type is certainly *Fm*, massive, followed by type *Fl*, with horizontal or ripple lamination. Lithofacies of types *Fr* and *Fb* (Fig. 4N) show bioturbation produced by plant roots and invertebrate burrows, respectively. Lithofacies type *P* (Fig. 4O), in the form of calcic Vertisols, vertic Calcisols and Calcisols, shows rhizocretions, carbonate nodules of about 1–3 cm of diameter (rarely, calcrete hardpans are present in the lower part of the unit) and/or gleyed patches. In terms of architectural elements, this formation is clearly dominated by the elements *LA*, with lateral accretion surfaces, *LV+CR+CS*, sandstones and lutites with tabular or locally erosive geometries, and *FF*, fine sediments. The element *SS* is also present very rarely. It is also interesting to note that at the type section (Port des Canonge–Hort de sa Cova), the element *LA* is overall more frequent than *LV+CR+CS* and *FF*, whereas at the Racó de s'Algar–Pedra de s'Ase section the three elements appear in a more balanced proportion. The Port des Canonge Formation is locally very rich in fossils, which include rhizocretions, macrofloral remains, invertebrate trace fossils, tetrapod tracks and tetrapod bones (including complete skeletons).

4.2.3. Interpretation

In this formation, breccia lithofacies of types *Gm* and *Gt* constitute the basal lag of lateral accretion bars and major channel deposits, or appear as isolated events interbedded between floodplain lutites. They can be interpreted as the reworking of the underlying sediments (usually floodplain lutites, sandstones or palaeosols) by meandering channels or unconfined flows of crevasse splays, respectively, exactly as in the Permian of Menorca as described in great detail by Gómez-Gras and Alonso-Zarza (2003). Sandstone lithofacies of types *St* and *Sl*, often *Sp* and *Sm* and, rarely, *Sh*, are the main constituents of the lateral accretion bars of major channels. Towards the top of the channel deposit sequences, lithofacies of types *Sr* and *Sl* become abundant, sepresenting the waning of the flow and overbank deposits over the floodplains. Lithofacies type *Ss* appears rarely in the floodplains, corresponding to confined flows, possibly from sporadic events of increased energy, forming scour deposits. Lithofacies type *Sb* can appear in any combination with the ones above, representing a halt of the sedimentation and the colonisation of those beds by burrower invertebrates and/or plants. Lutite lithofacies type *Fm* corresponds to settled sediments in the floodplains, although in some parts the slightly more energetic lithofacies type *Fl* can also appear. Lithofacies of types *Fr* and *Fb* represent the reworking of floodplain lutites by plant roots and invertebrate burrows, respectively, indicating periods of very little sedimentation or subaerial exposure. Finally, lithofacies type *P* culminates this biogenic occupation of the soils, with very abundant carbonate nodules and even

calcretes, with occasional gleyed patches, indicative of palaeosols formed under climatic conditions with low precipitation regimes (see Mack et al., 1993; Alonso-Zarza, 2003). Calcrete hardpans and large calcareous nodules appear only in the lower and middle parts of the Port des Canonge Formation, whereas in the upper part nodules are generally smaller. Architectural element *LA* represents point bar deposits, *LV+CR+CS* correspond to levée, crevasse channel and crevasse splay deposits, *SS* has been interpreted as sheetflood deposits, and *FF* as floodplain fine sediments (playas and playa lakes).

The fining-upwards sequences with thick lutitic packs corresponding to floodplain deposits, the abundance of lateral accretion surfaces in the vast majority of the sandstone channel deposits (Fig. 2D, E, F), and the fact that those surfaces dip mostly perpendicular to the main palaeocurrent trend (NE/SW *vs.* SE: Calafat, 1988), point to fine-grained sandy meandering river systems (Miall, 2006) as the main palaeoenvironment recorded in the Port des Canonge Formation. During the dry season, the swales and chute channels were ponded or even completely desiccated, as evidenced by the development of large mud cracks and palaeosols in the bar top lutites. Those ponds probably functioned as waterholes, and in some occasions they were intensely trampled by tetrapods (Matamales-Andreu et al., 2021d). The palaeocurrents measured in this formation (n = 50) show a wide dispersion but with a general trend towards the southeast (mean of 149.2°; see '8. Discussion' below).

4.3. Pedra de s'Ase Formation

This formation (Fig. 3) can be identified in the field because the sandstones form thick packages, they are usually medium-grained and their colour is usually yellowish, white, blue or pink (contrary to the red sandstones of the two other Permian formations of Mallorca). Lutites are comparatively less frequent, and they can either be red or blue in colour.

4.3.1. Location and boundaries

The two largest outcrops of the Pedra de s'Ase Formation are at the Racó de s'Algar–Pedra de s'Ase section (190.8–202.8 m, Figs. 1B, 3B) and at the Port des Canonge–Hort de sa Cova section (167.5–225.2 m, Figs. 1D, 3D). Other important sites are those including Pedrera de sa Cova (100.4 m, Figs. 1D, 3E) and Marina de Valldemossa (70 m, Fig. 1C) sections. There are smaller outcrops at Na Vermella (Fig. 1C), at Platja de sa font Figuera (Fig. 1C) and at Platja des Mabres (Fig. 1D), although they are heavily affected by tectonics and are in some cases mostly covered. The Racó de s'Algar–Pedra de s'Ase section is the thickest and the one least affected by tectonics and, although it is at some points quite inaccessible (flooded and vertical passes), it is here formally defined as the stratotype for this formation (Fig. 3). Its lower boundary has been described in '4.2. Port des Canonge Formation'. Its upper boundary probably crops out at Pedrera de sa Cova (Fig. 3E) in the form of an unconformable contact that gives way to the pink–white sandstones of the Triassic Punta Roja Formation (Matamales-Andreu et al., 2021b). Its minimum thickness is about 200 m and its total thickness is difficult to precisely establish because the section, including the top of the formation, cannot be reliably correlated with the rest.

4.3.2. Lithological features and palaeontological content

In this formation, all the lithofacies (Fig. 4, Table 1) broadly represent the same depositional processes and environments as those of the Port des Canonge Formation (see '4.2. Port des Canonge Formation' above), although their grain size is almost always coarser and the floodplain-related deposits are scarcer (Fig. 4D, F, G, J, K, M). Apart from that, the most remarkable difference is the appearance of blue or, very rarely, greenish lutites, horizontally laminated and rich in organic matter (lithofacies type *Fl*, Fig. 4L), that represent sedimentation in oxbow lakes. Lithofacies type *P* contains abundant invertebrate burrows, rhizocretions, carbonate nodules (diameter of 1–3 cm) and, occasionally, gleyed patches. The dominant architectural elements (Table 2) are *SS*, representing sheetflood deposits, and *LA*, corresponding to point bar deposits. Secondarily, elements *LV+CR+CS* and *FF* also appear as overbank deposits. In the Pedra de s'Ase Formation, sheetflood/channel sandstone deposits are dominant at the type section (Racó de s'Algar–Pedra de s'Ase), whereas at the Port des Canonge–Hort de sa Cova section the overbank deposits are almost as frequent as the sheetflood/channel deposits, contrary to the underlying formation. Plant fossils, usually in the form of unidentifiable debris, are very common in the Pedra de s'Ase Formation. Towards the middle part of the unit, some blue lutite beds have yielded palynomorphs. Rhizocretions and invertebrate trace fossils are abundant in the beds representing floodplain and crevasse splay deposits, which can also sporadically contain plant impressions and tetrapod tracks. Complete and fragmentary tetrapod bones rarely appear in the breccia beds.

4.3.3. Interpretation

The palaeoenvironments represented by this formation are also river systems with meandering channels, although their grain size is distinctly coarser than in the underlying Port des Canonge Formation. The common stacking of the channels, and the fact that floodplain deposits (red lutites and very fine to fine-grained sandstones) appear less frequently, point to a general prograding trend. This is perhaps related to a combined increase of both the subsidence rate of the basin and the sediment input (*e.g.*, Miall, 2006). The palaeocurrents measured in this formation (n = 50) show a rough trend towards the South (mean of 171.2°; see '8. Discussion' below). Floodplain settings had a rich biota, as indicated by the relative high abundance of rhizocretions and invertebrate traces, and sporadic occurrences of plant impressions, tetrapod tracks and bones. Fluvial channels probably transported large logs and other plant fragments, and oxbow lakes preserved a relatively rich record of microflora.

5. Magnetostratigraphy

The NRM intensity of the demagnetised specimens generally ranged from 10×10^{-4} to 88×10^{-4} A/m. Upon demagnetisation, NRM intensity decreases somewhat after the first heating step at 150 °C in most demagnetised specimens (Fig. 5A, C, D) but is noticeable in other samples (Fig. 5B) and may account for 30% NRM intensity loss. This may be an indication of goethite carrying a spurious secondary magnetisation. Then, stepwise AF demagnetisation up to 100 mT does not remove any remanence in some specimens (Fig. 5A, C), whereas in other specimens there is a slight decrease removing a relatively steep and downward component (Fig. 5B, D) denoting the presence of a minor magnetite-like phase. Finally, thermal demagnetisation defines a straight line toward the origin of the demagnetisation diagram, which is always southerly directed and shallowly upward in the 640–690 °C range that is ascribed to hematite, likely of detrital origin (Fig. 5A, C). This high temperature component conforms the ChRM direction. However, in many samples (74 out of the 144 demagnetised samples), remanence removal in the 300–640 °C range delineates a trajectory that does not trend towards the origin of the demagnetisation diagram and describes a great circle in stereographic projection. In such cases, further demagnetisation at higher temperature does not clearly define the ChRM (Fig. 5B, D), and thus the ChRM directions have been calculated using the McFadden and McElhinny (1988) great circle technique, implemented in the Paleomagnetism.org software. It is argued that the carrier of this medium temperature component, which has to be of high coercivity attending the demagnetisation protocol as discussed above, may be hematite of chemical origin that would carry an undefined secondary magnetisation.

Fig. 6 shows all ChRM computed directional data and derived VGP latitude plotted along corresponding lithological logs and in stereographic projections (see also Supplementary Table 2). The lack of sufficient bedding differences among the three sections precludes a fold test, and statistical parameters at specimen-level in geographic and

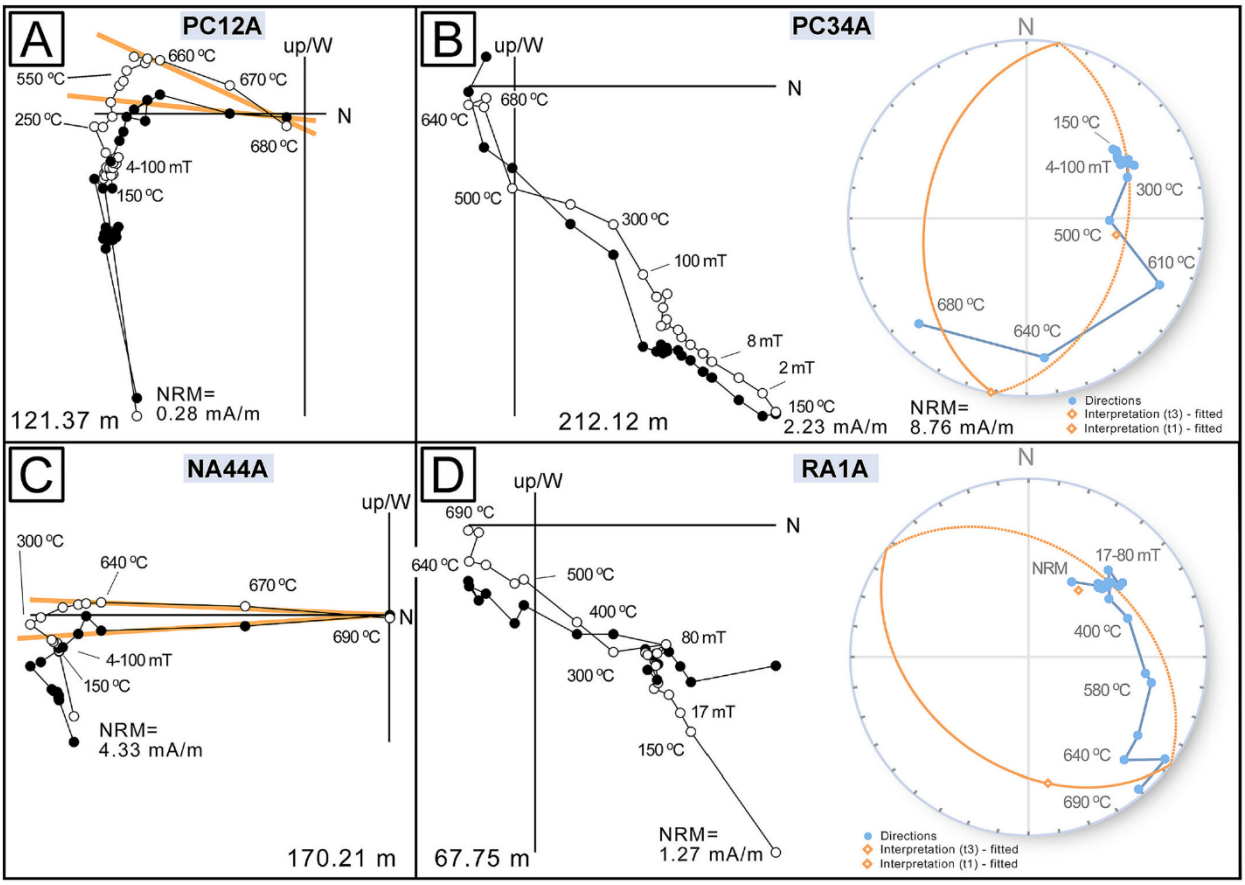

Fig. 5. A–D: Representative orthogonal demagnetisation diagrams with bedding corrected coordinates (tectonic). The natural remanent magnetisation (NRM) intensity, the stratigraphic position and some demagnetisation steps are indicated. Open and closed symbols represent inclination and declination, respectively. A coloured thick line shows the linear fitted reverse ChRM direction (samples PC12A and NA44A). For samples PC34A and RA1A, demagnetisation data are also plotted on respective equal-area stereogram showing a fitted great circle and interpreted directions.

tectonic coordinates are similar (Fig. 6B). Yet, the high temperature of the unblocked ChRM that suggests detrital hematite as the main magnetic carrier and its shallow inclination, which would be incompatible with an age older than Triassic, indicates that the ChRM directions are primary. All ChRM directions are reverse and conform to the Kiaman reverse polarity Superchron (see '8. Discussion' below). Note that the boundary of the Port des Canonge Formation and the Pedra de s'Ase Formation is included in both the Racó de s'Algar–Pedra de s'Ase and in the Port des Canonge–Hort de sa Cova sections. Consequently, the magnetostratigraphy from the first should overlap that from the latter section. In this scenario, the interval with no data due to lack of outcrops at the Port des Canonge–Hort de sa Cova section (290–235 m) is completed by the other section, assuming thickness of formations and intervals are comparable. Stereograms of ChRM directional data and VGPs from all analysed specimens divided for the three main sections are here presented in Supplementary Fig. 1. For full ChRM data and statistics see Supplementary Table 2 and Supplementary Table 3.

Some rockmagnetic experiments have been performed and are illustrated in Supplementary Fig. 2. Thermomagnetic heating curves (Supplementary Fig. 2A–B) appear blurred due to the low measured values close to the sensitivity of the instrument, and only a clear decrease below about 120 °C is seen. A subtle decrease above 640 °C as indication of hematite is doubtful. Heating curves are irreversible as cooling curves show increased values denoting the formation of new ferromagnetic phases upon heating. Two clear differentiated phases with Curie temperatures of about 580 °C and 420–450 °C are observed particularly for sample PC75A (Supplementary Fig. 2B). The presence of high coercivity phases is clearly illustrated by the acquisition of isothermal remanent magnetisation (IRM) curves and corresponding backfield IRMs (Supplementary Fig. 2B–C). IRM acquisition curves do not saturate at the maximum fields applied (1.2 T) and coercive force Hc values around 400–450 mT fall in the range of hematite (Özdemir and Dunlop, 2014). Unmixing of the magnetic coercivity distributions of the backfield IRM is best modelled by three components (Supplementary Fig. 2D–E). The predominant component (component_1) has coercivity log(B) values around 2.69 mT (B = 494 mT). Another two components have slightly higher and lower coercivity respectively (component_2, log (B)/(B) of 2.92 mT/870 mT, and component_3 log(B)/(B) of 2.23 mT/176 mT). These three relatively high coercivity components could correspond to different types of hematite or grain sizes.

6. Palaeobotany

6.1. Palynology

For the present work, only five out of 35 collected samples yielded palynomorphs (Fig. 7), as most of the sampled lithologies are too coarse-grained and oxidised to preserve any organic remains. In general, the

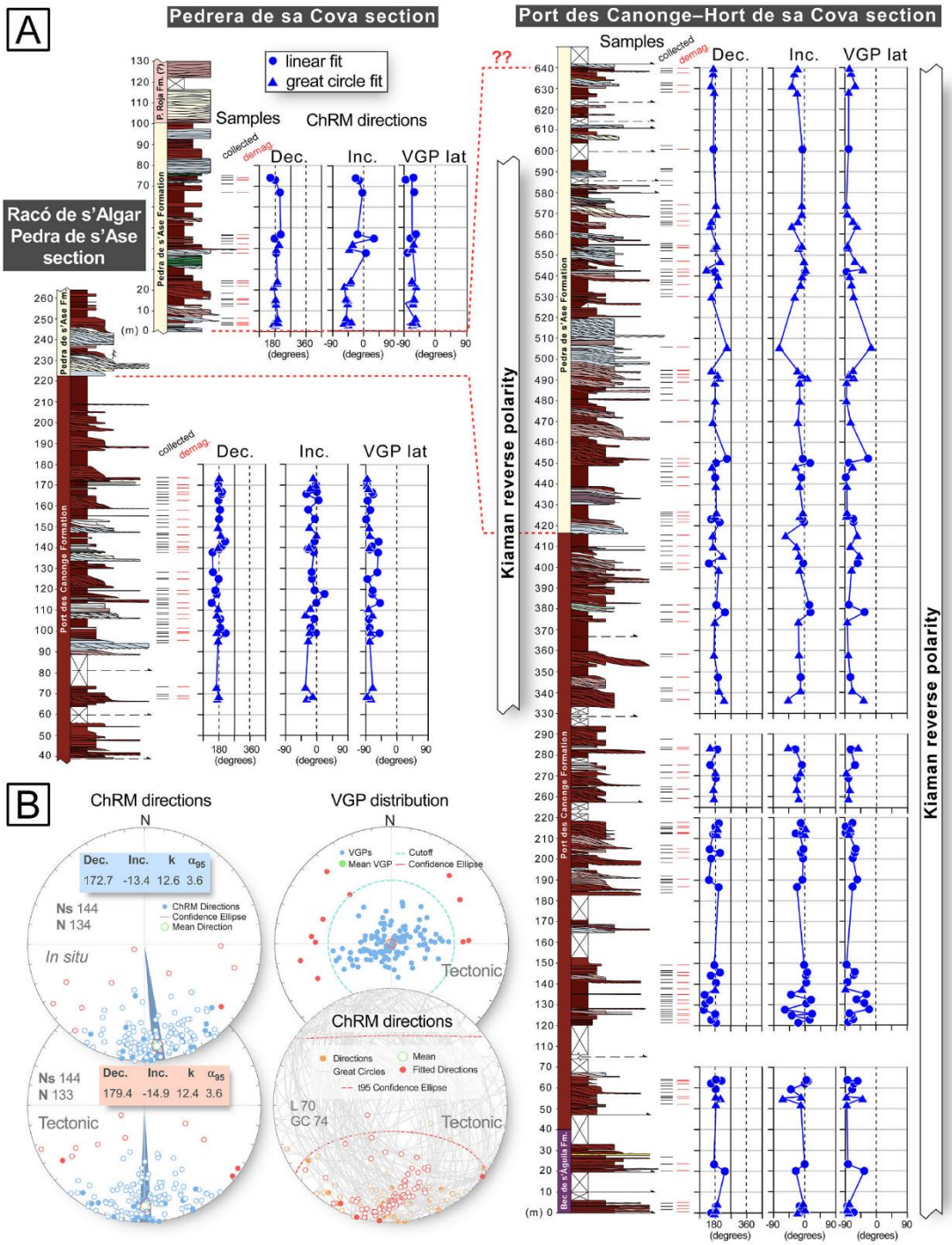

Fig. 6. **A:** ChRM directional data, VGP latitude and interpreted polarity of the analysed (demag., demagnetised) samples along synthetic logs of the Port des Canonge and Pedra de s'Ase formations at the Racó de s'Algar–Pedra de s'Ase section, at the Port des Canonge–Hort de sa Cova section and at the Pedrera de sa Cova section. Symbols of lithology as in Figs. 2, 3. See also Supplementary Logs for precise location of all the collected samples. **B:** Equal area projections of the geographic (*in situ*) and bedding corrected (tectonic) ChRM directions for all analysed samples. The confidence envelope (A95) and parachute are depicted. Statistical information is given (Ns, number of total samples; N, number of samples for the mean; Dec., declination; Inc., inclination; k, Fisher's precision parameter; α_{95}, radius of the 95% confidence cone). The upper-right stereogram is the VGP distribution in tectonic coordinates where red dots represent discarded directions after applying a 45° cut-off angle. The lower-right stereogram plots both all linear (L) fitted directions and the ones derived from great circles (GC). See Supplementary Tables 2 and 3 for all sample and mean directional data respectively.

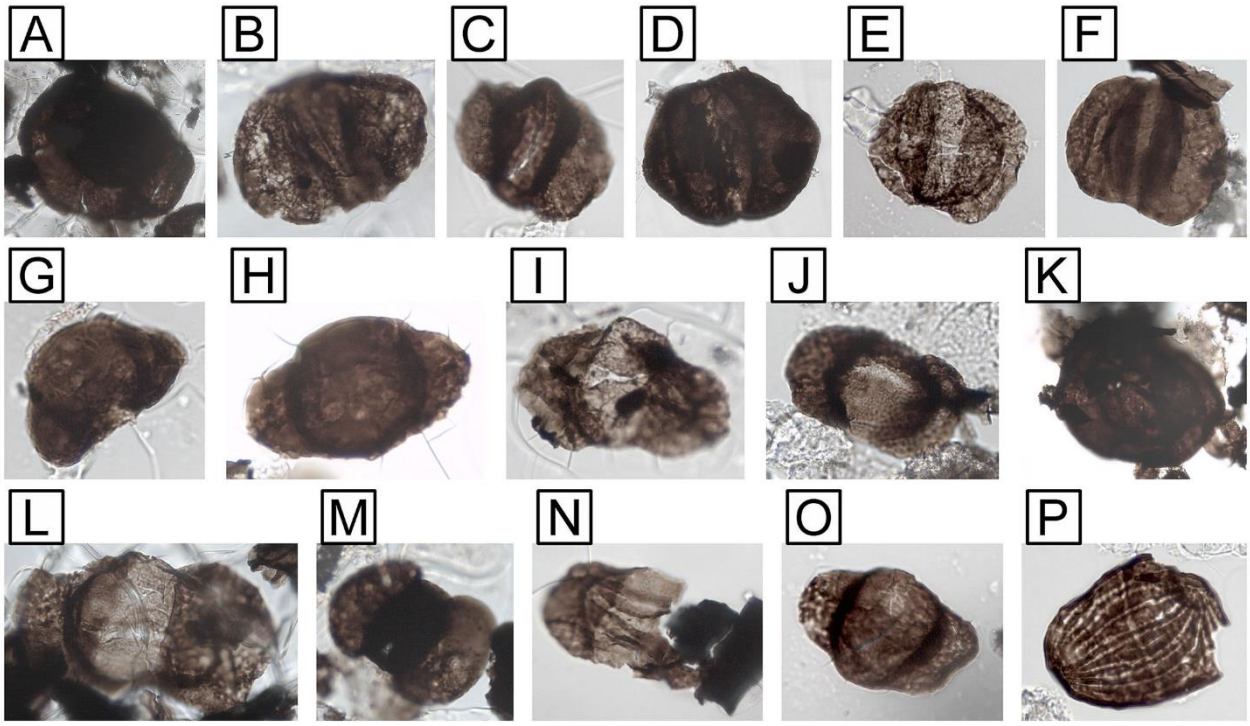

Fig. 7. Best-preserved spores and pollen from the Roadian–Wordian (middle Permian) middle part of the Pedra de s'Ase Formation of Mallorca. **A:** *Playfordiaspora cancellosa*, P-PA-05/IV, N16/4, diameter = 125 μm. **B:** *Alisporites splendens*, P-PA-05/III, J47/3, width = 73 μm. **C:** *Alisporites splendens*, P-PA-05/IV, N49/4, width = 60 μm. **D:** *Gigantosporites aletoides*, P-PA-05/III, C42/2, diameter = 125 μm. **E:** *Illinites* sp., P-PA-05/IV, R46/4, diameter = 50 μm. **F:** *Jugasporites delasaucei*, P-PA-12/II, U38/3, width = 64 μm. **G:** *Klausipollenites schaubergeri*, P-PA-05/II, K45, width = 43 μm, height = 31 μm. **H:** *Klausipollenites* sp., P-PA-05/I, H42, diameter = 80 μm. **I:** *Limitisporites rectus*, P-PA-05/IV, C39, width = 55 μm. **J:** *Lueckisporites virkkiae*, P-PA-09/I, E38, width = 52 μm, height = 32 μm. **K:** *Nuskoisporites dulhuntyi*, P-PA-05/III, Y52, diameter = 162 μm. **L:** *Strotersporites* sp., P-PA-05/III, Y30/3, width = 107 μm. **M:** *Platysaccus leschikii*, P-PA-05/III, C45, width = 56 μm. **N:** *Protohaploxypinus limpidus*, P-PA-05/IV, X47/2, width = 62 μm. **O:** ?*Triadispora* sp., P-PA-05/III, L47/1, width = 56 μm. **P:** *Vittatina* sp., P-PA-09/II, J37/4, width = 53 μm.

sporomorphs are severely damaged and altered, and the palynomorphs are heavily oxidised. The samples yielding palynomorphs from the Pedra de s'Ase log, P-PA-05, P-PA-09 and P-PA-12, are relatively well preserved, with up to 20 different taxa (Supplementary Table 4). The samples P-CO-03 and P-CO-04 from the Pedrera de sa Cova log are poorly preserved, but it has been possible to recognise at least some sporomorphs and identify them at genus and/or species level (Supplementary Table 4).

The palynological assemblages, with almost 30 genera and almost 40 taxa (Table 3), show how diverse the local and regional flora was, despite poor preservation of the macroremains (see '6.2. Macroplant remains' below). The palynological assemblages are dominated, both quantitatively and qualitatively, by pollen grains (see Supplementary Table 4), as was previously pointed out by Ramos and Doubinger (1989). Most of them are non-taeniate bisaccate pollen grains such as *Alisporites*, *Klausipollenites*, *Jugasporites*, *Gigantosporites* and *Minutosaccus*. Taeniate pollen grains are less abundant (but certainly more abundant than spores) and include, among others, the genera *Lueckisporites*, *Strotersporites* and *Protohaploxypinus*. Other bisaccate pollen grains such as *Limitisporites* and specimens assigned doubtfully to *Triadispora* are rare. Asaccate, costate pollen grains such as *Vittatina* or other genera such as *Marsupipollenites* are very rare. The spores are rare and poorly diverse; the only genera that could be identified are *Endosporites*, *Granulatisporites*, *Osmundacidites* and *Reticulatisporites*.

Among the samples from the Pedra de s'Ase log, P-PA-05 and P-PA-09 are the two with the most diverse palynological assemblages (20 and 19 taxa, respectively), whereas the sample P-PA-12 is less well preserved, with only 14 different identified taxa (Supplementary Table 4). The two samples from the Pedrera de sa Cova log (P-CO-03 and P-CO-04) are less diverse and yielded eight and four different taxa, respectively (Supplementary Table 4). Only *Lueckisporites virkkiae* is present in all samples yielding sporomorphs, and *Klausipollenites schaubergeri* and *Limitisporites* sp. are present at least in four of the five samples. Other taxa are present in only one of the samples, suggesting that they are rare in the palynological assemblages: among the spores, *Endosporites* sp., *Osmundacidites* sp. and *Reticulatisporites* sp., and among the pollen, *Falcisporites zapfei*, *Gardenasporites leonardii*, *Jugasporites delasaucei*, *Jugasporites* sp., *Limitisporites rectus*, *Lueckisporites globosus*, *Marsupipollenites* sp., *Minutosaccus* sp. 1, *Paravesicaspora* sp., *Platysaccus leschikii*, *Playfordiaspora cancellosa*, *Protohaploxypinus limpidus*, *Protohaploxypinus* sp., *Striatoabieites richteri*, *Strotersporites* sp., *Vitreisporites* sp., *Vittatina* sp., and doubtful assignements to the taxa *Cordaitina* sp. and *Triadispora* spp.

A comparison with previous papers of Permian rocks of Mallorca (Ramos and Doubinger, 1989; Diez, 2000; Juncal, 2019) (see Supplementary Table 4) shows that several taxa had already been mentioned before, such as the lycophyte genus *Endosporites*, whereas several fern genera such as *Granulatisporites* and *Osmundacidites* and putative bryophytes (*Reticulatisporites*) are reported here for the first time. On the other hand, some sphenophyte (*Calamospora*), lycophyte (*Kraeuselisporites*, *Lundbladispora*) and fern (*Deltoidospora*) spores, which were already known from the area, could not be identified in the samples studied for the present work. There is a close resemblance among the previous and the new assemblages, at least at a genus level. The genera ?*Bascanisporites*, *Crucisaccites*, *Crustaesporites*, *Maculatasporites*, *Platysaccus*, *Potonieisporites*, *Sahnisporites*, *Striatoabieites*, *Striatopodocarpites*, *Taeniaesporites* and *Tiwariasporis* were previously listed from the area (Diez, 2000; Juncal, 2019), whereas *Gigantosporites*, *Limitisporites*, *Marsupipollenites*, *Minutosaccus* and ?*Triadispora* have been identified here

Table 3
Botanical affinities of the various spores and pollen (see also Supplementary Table 4). The consideration of botanical affinities is based on in situ evidence from the Permian and closely related time periods. Several spore/pollen taxa have a higher putative botanical range than indicated here but for time periods outside the investigated time range and with plant groups that did not exist during the Permian.

Sporomorphs	Plant affinities	References
Alisporites	Seed ferns, Corystospermales (*Pteruchus*), Peltaspermales (*e.g., Amphorispermum, Autunia conferta*); Conifers, Voltziales, Ullmanniaceae (*Ullmannia*), Voltziales (*Willsiostrobus*)	Grauvogel-Stamm (1978), Balme (1995), Looy and Hotton (2014), Marchetti et al. (2015a)
Bascanisporites	Unknown affinity	-
Calamospora	Sphenophytes, Sphenophyllales, Equisetales, Calamitaceae	Balme (1995), Taylor et al. (2009), Looy and Hotton (2014)
Chordasporites	Conifers, unknown affinity	Kustatscher et al. (2010)
Cordaitina	Coniferales, Rufloriaceae, Vojnovskyaceae, Emporiaceae (*Kungurodendro*); Cordaitales	Meyen (1987), Balme (1995)
Crucisaccites	Unknown affinity	-
Crustaesporites	Seed ferns, Glossopteridales, perhaps aberrant forms	Lindström et al. (1997)
Deltoidospora	Ferns	Looy and Hotton (2014)
Densoisporites	Lycophytes, Selaginellales (*Bisporangiostrobus*)	Zavialova et al. (2010)
Endosporites	Lycophytes, Chalonieriaceae	Balme (1995), Bek et al. (2008), Marchetti et al. (2015a)
Falcisporites	Seed ferns, Corystospermales (*Nidiostrobus, Pteruchus*), Peltaspermales (*Cardiolepis, Permotheca*); Conifers, Ullmanniaceae, Voltziaceae	Potonié and Kremp (1956), Balme (1995), Looy and Hotton (2014), Marchetti et al. (2015a)
Gardenasporites	Unknown affinity	-
Gigantosporites	Conifers, Coniferales	Marchetti et al. (2015a)
Granulatisporites	Ferns, Botryopteridales, Lyginopteridales	Potonié (1962), Balme (1995), Looy and Hotton (2014)
Illinites	Conifers, Voltziales, *in situ* in *Willsiostrobus*	Grauvogel-Stamm (1978), Kustatscher et al. (2010), Looy and Hotton (2014)
Jugasporites	Conifers, Ullmanniaceae *in situ*, Voltziaceae	Balme (1995), Kustatscher et al. (2010)
Klausipollenites	Seed ferns, Peltaspermales or conifers	Raine et al. (2011), Mishra et al. (2017)
Kraeuselisporites	Lycophytes, Lycopodiales, Selaginellales	Kustatscher et al. (2010), Raine et al. (2011)
Leiotriletes	Seed ferns, Zygopteridales; Ferns, Botryopteridaceae	Good (1979), Balme (1995)
Limitisporites	Conifers, Ullmanniaceae	Balme (1995)
Lueckisporites	Conifers, Ullmanniaceae (*Majonica alpina*) but also associated with other conifers	Clement-Westerhof (1984, 1987), Meyen (1987)
Lunatisporites	Conifers	Clement-Westerhof (1974), Alvin et al. (1994), Balme (1995), Traverse (2007)
Lundbladispora	Lycophytes, Isoetales, Selaginellales	Balme (1995), Retallack (1997)
Lycospora	Lycophytes, Lepidodendrales (*Lepidostrobus binneyanus*)	Meyen (1987)
Maculatasporites	Algae	-
Marsupipollenites	Seed ferns, Glossopteridales (*Polytheca elongata*)	Pant and Nautiyal (1960), Balme (1995)
Minutosaccus	Conifers, Voltziales	Baranyi et al. (2019)
Nuskoisporites	Conifers, Voltziales (*Ortiseia*), Utrechtiaceae	Clement-Westerhof (1987), Balme (1995), Poort et al. (1997), Looy and Hotton (2014)
Osmundacidites	Ferns, Osmundales	Couper (1953), Litwin (1985), Balme (1995)
Palaeospongisporis	Unknown affinity	-
Paravesicaspora	Seed ferns, ?Callistophytaceae, ?Peltaspermaceae	Looy and Hotton (2014)
Platysaccus	Seed ferns, Peltaspermales	Mishra et al. (2017)
Playfordispora	Unknown affinity	-
Potonieisporites	Voltziales, Ullmanniaceae (*Otovicia hypnoides*), Rufloriaceae, Emporiaceae, Utrechtiaceae	Balme (1995), Hernández-Castillo et al. (2001), Rothwell et al. (2005)
Protohaploxypinus	Seed ferns, Glossopteridales (*Arberiella, Pterygospermum*), Peltaspermales (*Permotheca, Salpingocarpus, Tatarina*)	Gould and Delevoryas (1977), Balme (1995), Lindström et al. (1997), Traverse (2007), Looy and Hotton (2014), Marchetti et al. (2015a)
Reticulatisporites	Bryophytes	Balme (1995)
Sahnisporites	Conifers, Voltziales	Looy and Hotton (2014)
Striatoabieites	Unknown gymnosperms	-
Strotersporites	Seed ferns, Glossopteridales; Conifers	Mishra et al. (2017)
Taeniaesporites	Seed ferns, Corystospermales	Traverse (2007)
Tiwariasporis	Unknown affinity	-

(*continued on next page*)

Table 3 (*continued*)

Sporomorphs	Plant affinities	References
Triadispora	Conifers, Voltziales (*Darneya, Sertostrobus*)	Grauvogel-Stamm (1969, 1978), Schaarschmidt and Maubeuge (1969), Taylor and Taylor (1987)
Uvaesporites	Lycophytes, Selaginellales (*Selaginellites leonardii*)	Balme (1995), Kustatscher et al. (2019)
Verrucosisporites	Sphenophytes, Equisetales (*Bromsgrovia willsii*); Ferns, Marattiales (*Eoangiopteris goodii*); Seed ferns, Zygopteridales (*Corynepteris*)	Taylor et al. (2009), Seyfullah et al. (2013)
Vesicaspora	Seed ferns, Callistophytales (*Callospermarion, Idanothekion*), Peltaspermales	Kerp (1988), Balme (1995), Zavialova and Konijnenburg-van Cittert (2011), Looy and Hotton (2014)
Vitreisporites	Seed ferns, Corystospermales, Caytoniales	Meyen (1987), Traverse (2007)
Vittatina	Seed ferns, Peltaspermales	Balme (1995), Looy and Hotton (2014)

for the first time (Supplementary Table 4). With the exception of *Marsupipollenites* (Glossopteridales), these palynomorphs were all produced by primitive conifers (Table 3).

6.2. Macroplant remains

Well-preserved plant remains are very scarce in both the Port des Canonge and Pedra de s'Ase formations. In the former, Calafat (1988) mentioned unidentifiable carbonaceous debris, and from the latter, previous authors (Freeman and Obrador, 1979; Calafat, 1988; Ramos, 1995; Diez, 2000) mentioned and illustrated large carbonised tree logs from a specific bed near Cova des Carbó, which has been found again in the present work (Fig. 8A). This work is the first to report plant shoots preserved as impressions in very fine-grained sandstones, which are described below.

Sphenophyta indet.
Fig. 8B

Studied material: Several internal casts with surrounding organic material, preserved with random orientation in the sedimentary strata, left in the field. From the Pedra de s'Ase log (metre 81.0), middle part of the Pedra de s'Ase Formation, Roadian–Wordian.

Description: The stems are tens of decimetres long and few decimetres wide, the internal cast comprises yellowish to grey sandstone, surrounded by a few millimetres-thick organic film. No ornamentation is evident on the surface.

Remarks: Several of the stems probably belong to sphenophytes, although the surface is too badly preserved to show the casts of the vascular bundles. Although no clear distinction in nodes and internodes can be distinguished, this could be due to the broken surface that could also partly conceal them.

Genus *Hermitia* Kerp et Clement-Westerhof in Visscher et al., 1986
Hermitia sp.
Fig. 8C–D

Studied material: DA/21-15-05-01. From the Torrent de na Nadala log (metre 25.6), upper part of the Port des Canonge Formation, Artinskian–Kungurian. DA/21-15-05-03, DA/21-15-05-04 and DA/21-15-05-05. From the Torrent de na Nadala log (*ex situ* rock probably corresponding to metre 34.0), upper part of the Port des Canonge Formation, Artinskian–Kungurian.

Description: Three foliated penultimate shoot fragments of *Hermitia* sp. are preserved as coarse impressions in a reddish very fine-grained sandstone. The pinnately branched shoot fragments are up to 70 mm long with alternatively inserted two series of ultimate shoots up to 45 mm long, which arise at an angle of 45–60° from the axes. Leaves of ultimate shoots are needle-like, S-shaped and spirally arranged, 2–5 mm long and about 1 mm wide.

Remarks: The material is very fragmentary and badly preserved, with no organic material preserved. Nonetheless, the plant fossils show the typical pinnate architecture of the shoots and the narrow, needle-like leaves. The general morphological features mostly resemble *Ernestiodendron filiciformes* (Sternberg) Florin, 1934 emend. Clement-Westerhof, 1984. The fact that no epidermal features or reproductive structures are preserved, supports the assignment to the genus *Hermitia*, erected by Kerp & Clement-Westerhof (in Visscher et al., 1986) to accommodate remains previously assigned to the genus *Walchia*, which preserve no epidermal features and therefore can only be diagnosed in terms of leaf morphology (Visscher et al., 1986).

Genus *Feysia* Kerp et Clement-Westerhof in Visscher et al., 1986
?*Feysia* sp.
Fig. 8E–I

Studied material: DA21/15-03-01, DA21/15-03-02, DA21/15-03-03, DA21/15-03-04, DA21/15-03-05, DA21/15-03-06, DA21/15-03-07 and DA21/15-03-09. From the Racó de s'Algar log (metre 68.9), middle part of the Port des Canonge Formation, Artinskian–Kungurian. DA21/15-04-02. From the Racó de s'Algar area (*ex situ* rock), middle–upper part of the Port des Canonge Formation, Artinskian–Kungurian. DA21/15-05-06. From the Torrent de na Nadala log (*ex situ* rock probably corresponding to metre 34.0), upper part of the Port des Canonge Formation, Artinskian–Kungurian. DA21/15-08-05, DA21/15-08-06 and DA21/15-08-07. From the Platjola des munt de Pedres area (*ex situ* rock), upper part of the Port des Canonge Formation, Artinskian–Kungurian. DA21/15-15-01 and three other specimens left in the field. From Es Tamarell log (*ex situ* rock probably corresponding to metre 18.0), lower part of the Pedra de s'Ase Formation, Roadian–Wordian?

Description: Shoot fragments preserved as coarse impressions. The ultimate shoot fragments are 30–180 mm long with spirally arranged bifacial leaves, which arise with an angle of 40–65° and can turn, in the upper part, slightly toward the apex. Leaves are linear with a slightly smooth apex, 5–20 mm long and 0.5–1.5 mm wide. One specimen that is 72 mm long and 11 mm wide has spirally arranged lanceolate to triangular leaves with a slightly pointed apex, up to 6.5 mm long and 2 mm wide.

Remarks: The plant remains are very fragmentary and preserved only as impressions with no organic material. The shoot fragments show characteristic linear, long leaves that are spirally inserted. The most similar specimens were figured as *Pseudovoltzia* sp. by Bercovici et al. (2009) from the upper Permian of Menorca (Balearic Islands, western Mediterranean). However, the specimens of Bercovici et al. (2009) not only show the typical gross morphology of *Pseudovoltzia*, but are coalified and preserve a coaly film suggesting the presence of a cuticle, even if the latter is not figured nor described. The specimens of Mallorca studied here, on the other hand, do not permit the extraction of cuticle. *Pseudovoltzia liebeana* (Geinitz) Florin, 1927, from the upper Permian of Germany, closely resembles the impressions of Mallorca in the general shape of the leaves (slightly lanceolate to linear with a slightly pointed apex) and in the loose spiral of attachment of the leaves (see Schweitzer, 1962, for a detailed description). The specimens studied here, however, have much smaller and triangular leaves in the original conifer shoots (Broutin and Kerp, 1994). This rather supports an assignment to the

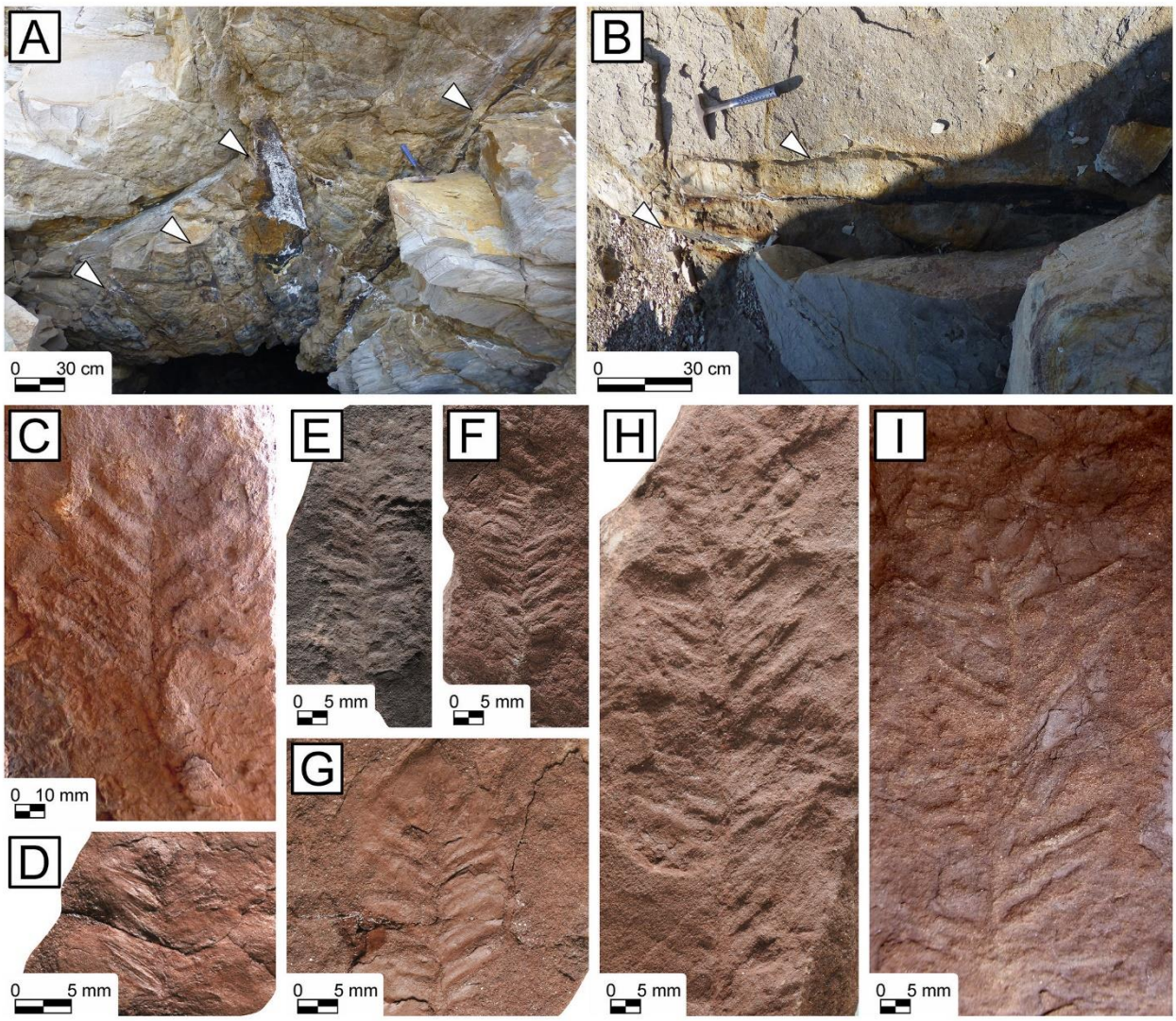

Fig. 8. Macroplant remains from the Permian of Mallorca. **A:** Large carbonised woody debris in the base of a fluvial channel deposit and oriented towards the main palaeocurrent trend, middle part of the Pedra de s'Ase Formation, Roadian–Wordian, Cova des Carbó. **B:** Sphenophyta indet., middle part of the Pedra de s'Ase Formation, Roadian–Wordian, between Tenassa d'en Quesso and Pesquera d'en Sabino. **C–D:** *Hermitia* sp.; **C:** DA/21-15-05-01, upper part of the Port des Canonge Formation, Artinskian–Kungurian, Racó de s'Algar; **D:** DA/21-15-05-05, from an *ex situ* rock in the upper part of the Port des Canonge Formation, Artinskian–Kungurian, Racó de s'Algar. **E–I:** ?*Feysia* sp.; **E:** DA/21-15-03-03, from the middle part of the Port des Canonge Formation, Artinskian–Kungurian, Racó de s'Algar; **F:** DA21/15-04-02, from an *ex situ* rock in the middle–upper part of the Port des Canonge Formation, Artinskian–Kungurian, Racó de s'Algar; **G:** DA/21-15-05-06, from an *ex situ* rock in the upper part of the Port des Canonge Formation, Artinskian–Kungurian, Racó de s'Algar. **H:** DA/21-15-08-07, from an *ex situ* rock in the upper part of the Port des Canonge Formation, Artinskian–Kungurian, Platjola des Munt de Pedres; **I:** Specimen not collected, from an *ex situ* rock in the lower part of the Pedra de s'Ase Formation, Roadian–Wordian?, Es Tamarell.

genus *Feysia*, since the latter was created for conifers with bifacial leaves that are spirally arranged and are broad triangular, oblong to obovate in shape with a constricted base. Most importantly, this genus includes those broad-leaved conifer shoots for which no cuticle is known. Macromorphologically very similar are the fragments of ultimate conifer shoots figured by Forte et al. (2018: fig. 10D) as *Quadrocladus* sp. from the Kungurian of the Southern Alps. Within the genus *Quadrocladus* Mädler, 1964, the most similar species is *Quadrocladus orobiformis* (Schlotheim) Schweitzer, 1962, typical of the upper Permian of the Central European Basin. Our specimens resemble *Quadrocladus orobiformis* in the loose spiral manner in which the leaves are attached and in the bifacial, linear shape of the leaves. The specimens from Mallorca and the Central European Basin differ, however, in the looser spiral with a wider angle (almost 90°), as well as in the more linear shape with a more rounded leaf apex of the latter. Unfortunately, similar to *Pseudovoltzia*, the genus *Quadrocladus* is a conifer with well-known cuticles and a general morphological similarity is not sufficient for a genus-level identification in Permian conifers.

7. Trace fossils

7.1. Invertebrate traces

In the sequences of the Port des Canonge Formation studied here, invertebrate bioturbation is abundant in most of the beds representing crevasse splay deposits and floodplain fine deposits, and even in the

upper part of some channel sequences. In the Pedra de s'Ase Formation, on the other hand, invertebrate burrows are less common and appear restricted to the red sandstone and lutite intervals between medium-grained whitish sandstone channel deposits. Ramos and García-Ramos (1992) reported the presence of the ichnogenera *Ancorichnus* Heinberg, 1974, *Palaeophycus* Hall, 1847, and *Planolites* Nicholson, 1873. Of these, only the latter two have been observed in the course of the present work, together with the four other ichnotaxa described here.

Ichnogenus *Arenicolites* Salter, 1857
Arenicolites isp.
Fig. 9A

Studied material: Numerous specimens, left in the field. From the Port des Canonge–Hort de sa Cova log (metre 494.2), among others, middle part of the Pedra de s'Ase Formation, Roadian–Wordian.

Description: Vertical, straight, unbranched, cylindrical burrows (diameter between 10–30 mm) filled with a sediment with a texture slightly different to that of the surrounding matrix (both very fine-grained sandstones), and almost always evident as paired circular openings on the bedding surface (similar to those illustrated by Díez-Canseco et al., 2016).

Remarks: The lack of complete specimens in lateral section has precluded ichnospecies-level identification. The tracemakers of this ichnogenus are considered to be suspension-feeding and deposit-feeding worms and crustaceans (Díez-Canseco et al., 2016 and references therein).

Ichnogenus *Cochlichnus* Hitchcock, 1858
Cochlichnus anguineus Hitchcock, 1858
Cochlichnus anguineus
Fig. 9B

Studied material: Six specimens, left in the field. From the Torrent de na Nadala log (metre 26.5), upper part of the Port des Canonge Formation, Artinskian–Kungurian.

Description: Convex hyporelief (natural cast) in the base of a medium-grained sandstone bed, corresponding to thin (about 1.2 mm wide), sinuous (wavelength 6.2–7.5 mm) grooves made on the sediment.

Remarks: This ichnotaxon occurs rarely and has only been observed on the base of one sandstone bed with climbing ripples corresponding to a point bar deposit, filling the surface of the underlying lutites. Laterally in the same bed, there are abundant tetrapod tracks and large mud-cracks. Nematodes and/or insect larvae are considered to be the most probable tracemakers of this trace (Uchman et al., 2004 and references therein).

Ichnogenus *Cruziana* d'Orbigny, 1842
Cruziana isp.
Fig. 9C

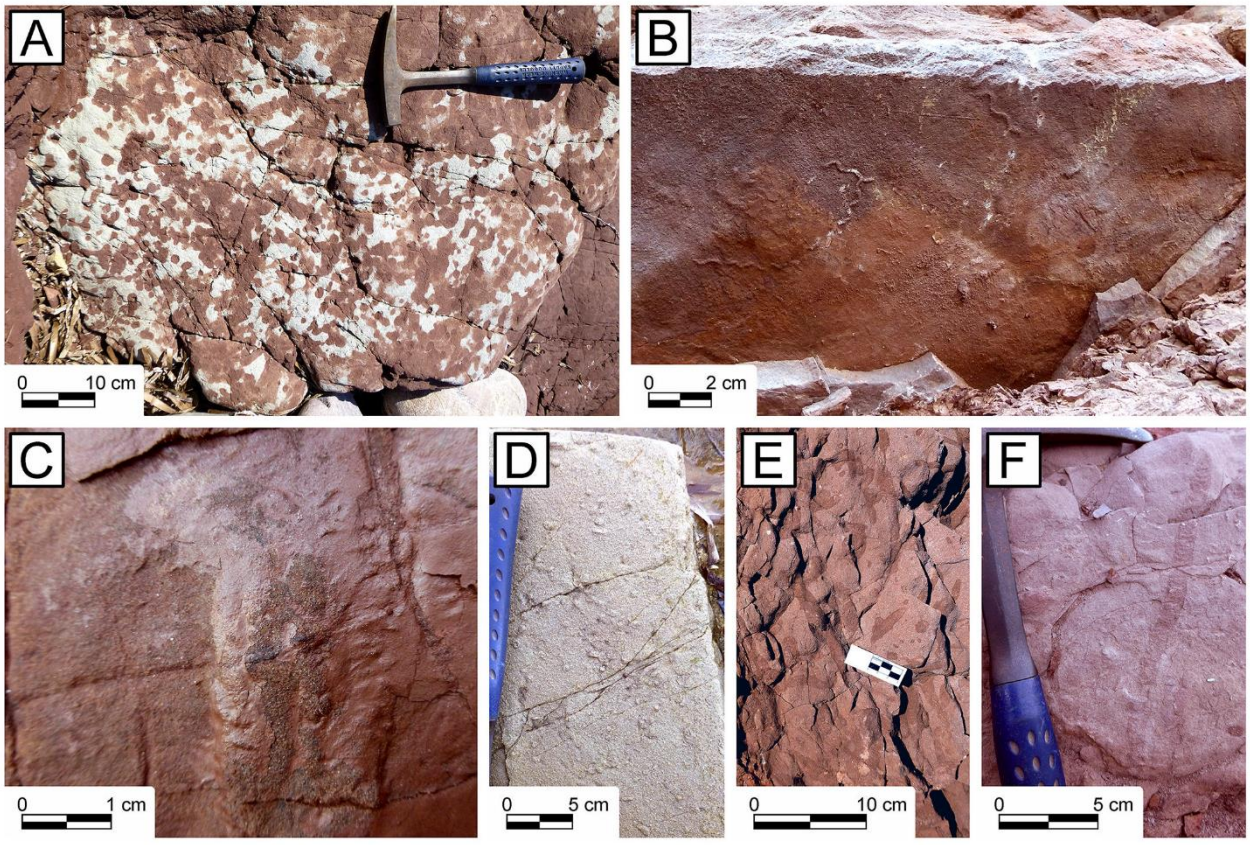

Fig. 9. Invertebrate trace fossils identified in the Permian sequences of Mallorca. **A:** *Arenicolites* isp., middle part of the Pedra de s'Ase Formation, Roadian–Wordian, Puig des Moro. **B:** *Cochlichnus anguineus*, upper part of the Port des Canonge Formation, Artinskian–Kungurian, Racó de s'Algar. **C:** *Cruziana* isp., lower part of the Port des Canonge Formation, Sakmarian–Kungurian?, Alcova de son Bunyola. **D:** *Palaeophycus tubularis*, upper part of the Pedra de s'Ase Formation, Roadian–Wordian, Platja de s'hort de sa Cova. **E:** *Planolites beverleyensis*, lower part of the Pedra de s'Ase Formation, Roadian–Wordian, Punta d'en Pere Mir. **F:** *Taenidium barretti*, middle part of the Pedra de s'Ase Formation, Roadian–Wordian, Pesquera d'en Sabino.

Studied material: One specimen, left in the field. From a recently fallen, *ex situ* block corresponding to the metres 95.0–97.0 of the Port des Canonge–Hort de sa Cova section, and thus in a channel deposit of the lower part of the Port des Canonge Formation, Sakmarian–Kungurian?

Description: Traceway preserved as a convex hyporelief on the base of a medium-grained sandstone bed. The observed morphotype corresponds to a bilobate trace about 20 mm wide, displaying a central longitudinal ridge with a furrow on each side. On each of the furrows, there are two rows of small impressions, anterolaterally enlongated, probably made by the tips of the appendices of the tracemaker.

Remarks: The only specimen studied here has not been identified to ichnospecies level because of its poor preservation. Given its size, this trace may have been produced by notostracan crustaceans, similar to those described from the Massif Central (Gand et al., 2008).

Ichnogenus *Palaeophycus* Hall, 1847
Palaeophycus tubularis Hall, 1847
Palaeophycus tubularis
Fig. 9D

Studied material: Numerous specimens, left in the field. From the Port des Canonge–Hort de sa Cova log (metre 570.0), among others, upper part of the Pedra de s'Ase Formation, Roadian–Wordian.

Description: Relatively small (diameter of 5–10 mm), cylindrical, linear to slightly sinuous burrows, which are sometimes branched, have smooth thin walls, are oblique or horizontal to stratification, and their filling is the same as the surrounding matrix (very fine- to medium-grained sandstone).

Remarks: The specimens observed in Mallorca correspond to the ichnospecies *Palaeophycus tubularis* because their walls are smooth and thin (see Pemberton and Frey, 1982). It has been observed sporadically in the sandstone deposits of the upper part of channel sequences, both in the Port des Canonge Formation and in the Pedra de s'Ase Formation. In continental settings, these traces have been interpreted as a dwelling structure, possibly made by orthopteran, hemipteran or coleopteran insects (Krapovickas et al., 2008 and references therein).

Ichnogenus *Planolites* Nicholson, 1873
Planolites beverleyensis (Billings, 1862)
Planolites beverleyensis
Fig. 9E

Studied material: Numerous specimens, left in the field. From the Pedra de s'Ase log (metre 3.0), among others, lower part of the Pedra de s'Ase Formation, Roadian–Wordian.

Description: Cylindrical, large (diameter between 5–15 mm), linear to slightly sinuous, usually umbranched, smooth, horizontal or oblique, unwalled burrows with a filling that is slightly different to that of the surrounding matrix (lutites, very fine- or fine-grained sandstones).

Remarks: Overall, this ichnospecies is dominant in the floodplain deposits of all studied sections, both in the Port des Canonge Formation and in the Pedra de s'Ase Formation. It corresponds to this ichnospecies because they are relatively large, straight to gently curved burrows (see Pemberton and Frey, 1982). This ichnogenus is thought to have been produced by deposit-feeder vermiform organisms (Díez-Canseco et al., 2016 and references therein).

Ichnogenus *Taenidium* Heer, 1877
Taenidium barretti (Bradshaw, 1981)
Taenidium barretti
Fig. 9F

Studied material: Several specimens, left in the field. From the Pedra de s'Ase log (metre 61.5), middle part of the Pedra de s'Ase Formation, Roadian–Wordian.

Description: Slightly sinuous to winding, unbranched, unwalled, horizontal burrows (width of about 10 mm) with a meniscate backfill (with short, arcuate and densely-packed menisci) filled with similar sediment to that of the surrounding matrix (medium-grained sandstones).

Remarks: This ichnospecies has been identified in a crevasse splay sandstone deposit in a floodplain interval of the middle part of the Pedra de s'Ase Formation. The specimens are similar to what Ramos (1995) figured as *Ancorichnus*, which is characterised by a thick wall (*e.g.*, Boyd and McIlroy, 2017) that is not observed in the ones studied here. In continental environments, *Taenidium* is thought to have been produced by coleopterans (Baucon et al., 2014) aestivating in moist sediment during dry periods (Minter et al., 2007).

7.2. Ichnofacies

The ichnofossils recognised in the present study can be attributed to different kinds of ichnofacies (Buatois and Mángano, 1998), making it possible to infer the palaeoenvironment in which they were formed. Among the recognised invertebrate trace fossils, *Arenicolites* isp. is a representative of the *Skolithos* ichnofacies, typical of high-energy environments (Buatois and Mángano, 1998), in this case crevasse splay lobes. *Cruziana* isp., *Taenidium barretti* and the tetrapod tracks (see '7.3. Tetrapod tracks' below) are indicative of the *Scoyenia* ichnofacies, representing areas with periodic flooding and desiccation (Buatois and Mángano, 1998). Finally, *Cochlichnus anguineus*, *Palaeophycus tubularis* and *Planolites beverleyensis* are indicative of the *Mermia* ichnofacies, typically developed in deposits with more persistent water bodies (Buatois and Mángano, 1998). Therefore, in the studied sequences, the *Skolithos* ichnofacies was probably established on freshly deposited crevasse splays, the *Scoyenia* ichnofacies corresponded to the margins of channels and playa lakes, and the *Mermia* ichnofacies developed in the deepest parts of the relatively shallow playa lakes and swales.

7.3. Tetrapod tracks

In the Permian deposits of Mallorca, ichnogenus-level identifiable tetrapod ichnites have so far only been found at the Racó de s'Algar–Pedra de s'Ase section. There, 15 beds with tracks have been located in the upper part of the Port des Canonge Formation, and two other beds have been observed in the lower part of the Pedra de s'Ase Formation. In almost all cases, they are preserved in convex hyporelief (natural casts) on the base of very fine- to fine-grained sandstone beds corresponding to crevasse splay deposits, which record the surface of underlying lutite beds where the tracks were originally imprinted. In only two cases, the ichnites are preserved as concave epireliefs on the surface of very fine-grained sandstones. Calafat et al. (1986, 1986–1987) and Calafat (1988) were the first to report some of the tracksites here studied, but they provided only preliminary identifications. In Supplementary Fig. 3 we present pictures taken by those authors in the 1980s. Most of those ichnites no longer exist.

Ichnogenus *Hyloidichnus* Gilmore, 1927
Hyloidichnus bifurcatus Gilmore, 1927
Hyloidichnus bifurcatus, large morphotype
Fig. 10A–C; Supplementary Table 5

Studied material: NA-25.6-01a, NA-25.6-01b, NA-25.6-01c, NA-25.6-01d, NA-25.6-01e, NA-25.6-01f (natural cast of a trackway with two left manus-pes sets, a right manus track and a right pes track). From the Torrent de na Nadala section (metre 25.6), upper part of the Port des Canonge Formation, Artinskian–Kungurian. NA-26.0-02c, NA-26.0-02d, NA-26.0-02e (natural cast of a partial trackway with a left manus-pes set and a right pes track). From the Torrent de na Nadala section (metre 26.0), upper part of the Port des Canonge Formation, Artinskian–Kungurian. NA-77.5-01a, NA-77.5-01b, NA-77.5-01c, NA-77.5-01d (natural cast of a partial trackway with two left manus-pes sets) and NA-77.5-01e (natural cast of a right pes track). From the Torrent de na Nadala section (metre 77.5), upper part of the Port des Canonge Formation, Artinskian–Kungurian. PM-15.7-01a, PM-15.7-01b (natural cast

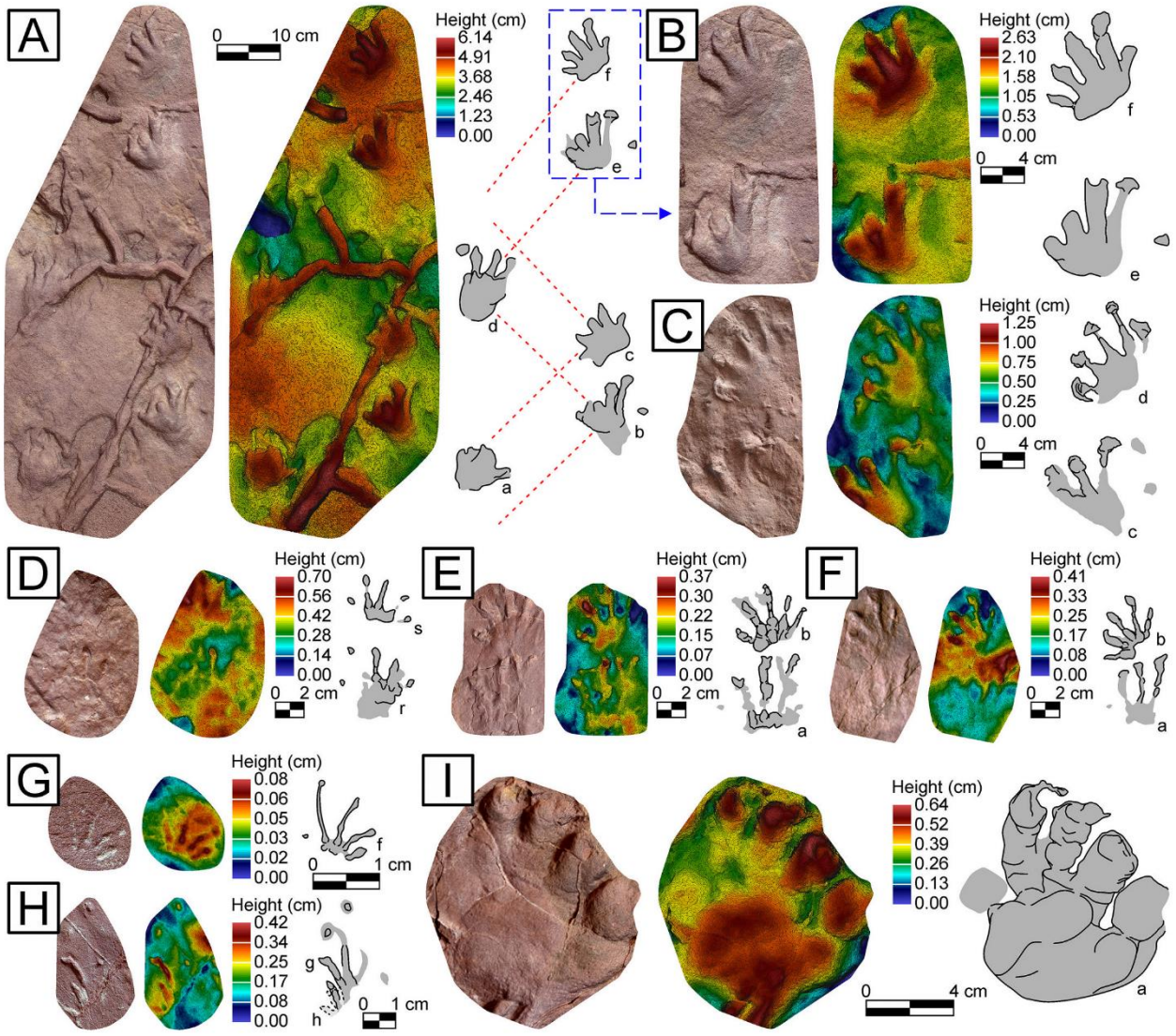

Fig. 10. Tetrapod ichnites attributed to eureptile and parareptile trackmakers studied herein, all as textured 3D models, false colour-coded 3D models and interpretative drawings. **A–C:** *Hyloidichnus bifurcatus*, large morphotype; **A–B:** NA-25.6-01; **C:** NA-26.0-02. **D–F:** *Hyloidichnus bifurcatus*, small morphotype; **D:** NA-26.0-09; **E:** NA-66.4-02; **F:** NA-66.4-04. **G–H:** *Dromopus* isp., NA-77.5-01. **I:** cf. *Pachypes ollieri*, NA-66.6-01. All from the Torrent de na Nadala section (Mallorca, Balearic Islands, western Mediterranean), Port des Canonge Formation, Artinskian–Kungurian, Permian.

of a right manus-pes set). From the Punta d'en Pere Mir section (metre 15.7), lower part of the Pedra de s'Ase Formation, Roadian–Wordian?

Description: Pes imprint semiplantigrade, pentadactyl, ectaxonic and slightly wider (ca. 10–12 cm) than long (ca. 7–10 cm). The digit imprints are relatively stout, straight and long, especially in the case of digits III and IV. The imprints of digits I and II are usually only preserved proximally, and that of digit V is either not present or preserved only as the tip. Their relative lengths are ordered as follows: I<V≈II<III<IV. There is a general decrease in depth from digit I to digit V, giving a more slender appearance to the imprints of digits III and, especially, IV. Moreover, those two often show expanded, "T"-shaped tip imprints. Digit imprints radiate from the sole with no superimposition, forming a wide digit I–V angle (ca. 135°). The oval sole imprint is anteroposteriorly short, much wider than it is long, and may be slightly concave posteriorly. The most deeply imprinted area is digit II, followed by the medial part of the sole and digits I and III, and then the tips of digits IV and V (medial functional prevalence of the autopodia).

Manus imprint semiplantigrade, pentadactyl, ectaxonic and wider (ca. 9–10 cm) than long (ca. 6.5–8.5 cm). The digit imprints are of variable stoutness (probably depending on the substrate), ranging from thin, straight, long digits with "T"-shaped expanded tip imprints to thick, straight, long digits with round tip imprints. Their relative lengths are ordered as follows: I<V<II<III<IV. All digits are equally well-imprinted except for the proximal part of digit V, which may be missing. Digit imprints radiate from the palm with no superimposition, forming a digit I–V angle of about 95°. The palm imprint is oval and very short anteroposteriorly, with a posterior margin than can be straight or slightly concave. The most deeply imprinted area is usually located around digit III, becoming shallower laterally (medial-median functional prevalence of the autopodia).

Trackway quadrupedal with semi-alternating manus-pes sets, and with pes imprints slightly larger than manus imprints. Pace angulations for both the pes and the manus imprints are around 90°. Pes impressions are essentially parallel to the midline (can be very slightly rotated

laterally or medially), whereas manus impressions are rotated ca. 30° medially and located anteromedially from the pes impressions. Pes and manus imprints are often well separated; however, in rare cases they are almost in contact, but never overstepping. No tail traces have been observed either.

Remarks: The specimens studied here agree with the ichnogenus *Hyloidichnus* based on the following combination of characters: (1) semiplantigrade ichnites, wider than long, ectaxonic, with relatively long, straight and radial digit imprints ended in expanded tips, (2) pes digit V impression short, (3) acute angle between manus digit IV–V imprints, (4) manus imprints slightly smaller than those of the pes, and (5) manus imprint rotated inwards and pes imprints parallel to the midline (Gand, 1988; Voigt, 2005; Marchetti, 2016; Marchetti et al., 2020). The Mallorcan material agrees with the only considered valid ichnospecies (see discussion in Marchetti et al., 2013), *Hyloidichnus bifurcatus*.

The ichnogenus *Hyloidichnus* is known from the Sakmarian (lower Permian) to the Wuchiapingian (upper Permian) of southern North America, South America, Lodève and Provençe, the Iberian Peninsula, the island of Menorca, the Alps, northern Africa, central Africa, and the Anatolian Peninsula (Schneider et al., 2020; Logghe et al., 2021; Matamales-Andreu et al., 2021c and references therein). It is generally agreed that the trackmakers of *Hyloidichnus* were captorhinomorph eureptiles (*e.g.*, Gand, 1988; Haubold, 2000; Gand and Durand, 2006; Voigt et al., 2010; Logghe et al., 2021). Interestingly, a fragment of maxilla with parts of the palate of an indeterminate moradisaurine captorhinid eureptile was recently reported from the Port des Canonge Formation at Platja de son Bunyola (Liebrecht et al., 2017; see also Matamales-Andreu et al., 2021c; Supplementary Text 2; Supplementary Logs: metre 69 of the Port des Canonge–Hort de sa Cova log presented herein). Although the scarcity of osteological remains makes it impossible to confirm it, these large *Hyloidichnus* tracks from the Racó de s'Algar site could correspond to footprints of a large moradisaurine such as the one recovered from Platja de son Bunyola.

Hyloidichnus bifurcatus, small morphotype

Fig. 10D–F; Supplementary Table 5

Studied material: NA-26.0-09r, NA-26.0-09s (natural cast of a right manus-pes set). From the Torrent de na Nadala section (metre 26.0), upper part of the Port des Canonge Formation, Artinskian–Kungurian. NA-66.4-02a, NA-66.4-02b (natural cast of a left manus-pes set) and NA-66.4-04a, NA-66.4-04b (natural cast of a left manus-pes set). From the Torrent de na Nadala section (metre 66.4), upper part of the Port des Canonge Formation, Artinskian–Kungurian.

Description: Pes imprint semiplantigrade, pentadactyl, ectaxonic and slightly wider (ca. 5–6 cm) than it is long (ca. 4–5.5 cm). The digit imprints are thin, straight and relatively long, often with expanded ("T"-shaped) tip imprints. Their relative lengths are ordered as follows: I<V≈II<III<IV. Digit imprints radiate from the sole with no superimposition, forming a wide digit I–V angle (ca. 122°). The oval sole is usually poorly imprinted, anteroposteriorly very short, much wider than it is long, and may be slightly concave posteriorly. The most deeply imprinted area is the tip of digit III, followed by the rest of the digit, digits II and IV and the sole (medial-median functional prevalence of the autopodia). Digits I and V are usually poorly imprinted, often only as the tip.

Manus imprint semiplantigrade, pentadactyl, ectaxonic and slightly wider (ca. 4.5–5 cm) than it is long (ca. 3–4.5 cm). The digit imprints are thin, straight and relatively long, with slightly expanded tips. Their relative lengths are ordered as follows: I<V<II<III<IV. There is a general decrease in depth from digit I to digit V, with digits IV and V being more weakly imprinted, especially their proximal parts. Digit imprints radiate from the palm with no superimposition, forming a digit I–V angle of about 113°. The palm imprint is very short anteroposteriorly, with a posterior margin than is somewhat concave. Metatarsophalangeal pads have been observed at the bases of digit I–V imprints. They are round and they diminish in size from digit I to V, but this is probably because the imprint is deepest in the medial part. The most deeply imprinted areas are the tips of digits II and III, followed by the rest of digits II, III, digits I and IV and the medial half of the palm (medial functional prevalence of the autopodia).

Trackway not clearly observed but certainly quadrupedal, with pes-manus sets showing that the manus imprints are slightly smaller than those of the pedes. The imprints of the manus are rotated medially and are located slightly medially (inwards) with respect to the pes imprints. No overstepping of pes and manus imprints has been observed.

Remarks: These ichnites are very similar to the larger *Hyloidichnus* described above, and can be attributed to the same ichnogenus and ichnospecies based on the features mentioned above. However, they have been individualised here because (1) the consistent separation in two size classes, which roughly correspond to the two different-sized moradisaurines of which bone fossils appear in the same formation (Liebrecht et al., 2017; Matamales-Andreu et al., 2021e), and (2) the slightly different relative depth pattern of both the pes and manus impressions. The functional prevalence of the autopodia of the large morphotype has been inferred to be medial for the pes and medial-median for the manus, whereas in the small morphotype it is medial-median and medial, respectively.

Ichnogenus *Dromopus* Marsh, 1894

Dromopus isp.

Fig. 10G–H; Supplementary Table 5

Studied material: NA-77.5-01f (natural cast of a right pes track) and NA-77.5-01g (natural cast of a right ichnite, possibly a pes track, partially overlapped with another ichnite, perhaps a manus track). From the Torrent de na Nadala section (metre 77.5), upper part of the Port des Canonge Formation, Artinskian–Kungurian.

Description: Pes imprint semiplantigrade–digitigrade, pentadactyl, ectaxonic and as long as it is wide (ca. 1 × 1 cm) (NA-77.5-01f), or clearly longer (2.6 cm) than it is wide (2 cm) (NA-77.5-01g). The digit imprints are long and slender, and have pointed tips. In NA-77.5-01f, they are very thin and knobby. Imprints of digits II, III and IV are distally curved medially (inwards) and have slightly expanded tips, corresponding to pointed to rounded claw traces. In NA-77.5-01f, digit I imprint is straight and digit V is only recorded by a triangular, pointed tip imprint. In NA-77.5-01g, only the proximal part and tip imprints of digits III and IV are preserved, and the imprint of digit V is present only as the tip. Their relative lengths are ordered as follows: I<V<II<III<IV. In the case of NA-77.5-01f, digit imprints radiate from the sole with no superimposition, whereas in NA-77.5-01g the imprints of digits I–IV are strongly directed anteriorly and their bases are slightly overlapped. Only the most anterior part of the sole is imprinted, in the form of the basal region of the digits I–IV. In the two studied ichnites, the angle between the imprint of digits II–IV ranges between 51–59°. In NA-77.5-01f, the most deeply imprinted area are the proximal parts of digits I–III, followed by its distal parts and the proximal part of digit IV (medial functional prevalence of the autopodia). In NA-77.5-01g, the most deeply imprinted area is the distal half of digit II, followed by digit I and the tips of digits III and IV (medial functional prevalence of the autopodia).

A possible manus imprint is overstepped by that of the pes in NA-77.5-01h. It is digitigrade, with three preserved digit imprints, which are much shorter than those of the pes. It has not been possible to measure most of the parameters, and it can only be said that it is located slightly medial–posterior with respect to the imprint of the pes.

Remarks: Ichnites of this morphotype are usually preserved in the form of a few isolated digits, hindering its description. The ichnites studied herein can be attributed to the ichnogenus *Dromopus* based on the following combination of characters: (1) long, slender digit imprints (especially those of III–IV), slightly curved medially and with pointed tips, (2) digit I imprint not curved posteriorly, and (3) pes imprint more deeply impressed than the manus imprint (see Gand, 1988; Voigt, 2005;

Marchetti et al., 2017b). However, it has been left in open nomenclature given the lack of complete manus imprint and trackway information.

Dromopus is a widespread ichnogenus of Europe, North America and North Africa, ranging from the Moscovian (upper Carboniferous) to the Changhsingian (upper Permian) (Voigt and Lucas, 2015; Meade et al., 2016 and references therein). Araeoscelidian diapsid reptiles and non-varanodontine varanopids are considered to be their most probable trackmakers (Gand, 1988; Haubold, 2000; Voigt, 2005; Gand and Durand, 2006; Marchetti et al., 2021a, 2022).

Ichnogenus *Pachypes* Leonardi, Conti, Leonardi, Mariotti et Nicosia, 1975

Pachypes ollieri (Ellenberger, 1983)

cf. *Pachypes ollieri*

Fig. 10I; Supplementary Table 5

Studied material: NA-66.6-01a (natural cast of a right pes track). From the Torrent de na Nadala section (metre 66.6), upper part of the Port des Canonge Formation, Artinskian–Kungurian.

Description: Pes imprint semiplantigrade–plantigrade, pentadactyl, ectaxonic and essentially as wide (9.49 cm) as it is long (9.52 cm). The digit imprints are stout, thick and relatively short, have round tips, and their relative lengths are ordered as follows: V<I<II<III<IV. The imprints of digits I and II are straight, whereas the tip imprints of digits III and IV are slightly curved medially, ending in sliding traces towards the medial part. There is a notable decrease in depth from digit I to digit IV, especially considering the proximal and middle parts of each of them. This gives a slenderer appearance to digit III and IV imprints, which are clearly shallower in their proximal and middle portions. Digit V imprint is the shortest, and is wide but faintly impressed. The imprints of digits II–IV are slightly convergent at their bases, whereas those of digits I and V are more separated. Possible skin impressions can be observed in the bases of the imprints of digits II–IV in the form of conspicuous creases. The sole imprint is wider than it is long, and its posterior margin is convex. There are two main depressed areas: the first one occupies the anterolateral region, from the base of the imprint of digit II to the base of the imprint of digit V (metatarsophalangeal pads of digits III–V); the second one, medial–posterior, goes from the base of the imprint of digit I (metatarsophalangeal pad of digit I) to the posterior margin of the sole impression. The most deeply imprinted areas are the tips of digits II–IV, followed by the medial part of the sole and the tip of digit I (medial functional prevalence of the autopodia).

Remarks: The ichnite studied here may be assigned to the ichnogenus *Pachypes* based on the following combination of characters: (1) pes imprint indicating a medial functional prevalence, almost as wide as long, (2) short and thick digit imprints that converge proximally and have round tips, and (3) well-impressed sole, slightly wider than it is long. Relatively similar, coeval ichnogenera with which it could be confused are *Limnopus* Marsh, 1894, *Amphisauropus* Haubold, 1970, *Ichniotherium* Pohlig, 1892 and *Hyloidichnus* Gilmore, 1927. It differs from *Limnopus* and *Amphisauropus* because the digit imprints of the Mallorcan track are relatively short, thick, stout, slightly curved medially (digits III and IV) and proximally superimposed (digits II–IV) (see Gand, 1988; Lucas et al., 2001; Voigt, 2005; Marchetti, 2016; Marchetti et al., 2017c). It differs from *Ichniotherium* because of the anteroposteriorly longer sole imprint lacking the distinct, mediolaterally extended ovate pad, in the lack of proximal superimposition of the digit imprints, and in the significantly shorter digit V imprint, well-separated from that of digit IV (see Voigt, 2005; Voigt et al., 2007; Romano et al., 2016; Buchwitz and Voigt, 2018; Marchetti et al., 2018; Mujal and Marchetti, 2020). It differs from *Hyloidichnus* in the anteroposteriorly long sole and in the digit imprints being very thick, stout, short, slightly curved medially and, in the case of imprints of digits II–IV, converging at their bases (see Gand, 1988; Voigt, 2005; Marchetti, 2016; Logghe et al., 2021). Nevertheless, the use of open nomenclature at ichnogenus level is here preferred, given that only one isolated ichnite is available for study.

The ichnogenus *Pachypes* currently includes three valid ichnospecies that differ essentially in their digit imprint thickness, superimposition and in the maximum size of the tracks (Marchetti et al., 2021b). Of those three, the only coeval ichnospecies is *Pachypes ollieri* (Ellenberger, 1983), which ranges from the Cisuralian to the Guadalupian of southern North America and southern Europe (Marchetti et al., 2021b and references therein). The Mallorcan specimen is quite large for that ichnospecies but falls in its range of sizes, being slightly smaller than the largest known specimen (see Marchetti et al., 2021b). Small specimens of *Pachypes dolomiticus* Leonardi, Conti, Leonardi, Mariotti et Nicosia, 1975, illustrated by Valentini et al. (2009: fig. 3A–B, G–H), are also similar to the track studied herein in terms of general proportions, but have thicker digit III–IV impressions and show a higher degree of proximal digit superimposition (see discussion in Marchetti et al., 2021b). Specimens of *Pachypes loxodactylus* (Dudgeon, 1878) have pes imprints with digits proportionally longer than the sole and less proximally superimposed (see Marchetti et al., 2019b, 2021b; Mujal et al., 2020). Taking all of the above into account, if the specimen on the slab NA-66.6-01 belonged to the ichnogenus *Pachypes*, it would agree with *Pachypes ollieri* in both age and general shape.

Ichnites of the ichnogenus *Pachypes* have been attributed to pareiasauromorph parareptiles (Valentini et al., 2009). Specifically, *Pachypes ollieri* was assigned to small nycteroletid non-pareiasaur pareiasauromorphs (Marchetti et al., 2021b).

Ichnogenus *Dimetropus* Romer et Price, 1940

Dimetropus leisnerianus (Geinitz, 1863)

Dimetropus leisnerianus

Fig. 11A–G; Supplementary Table 5

Studied material: NA-25.6-01g (natural cast of a left pes track), NA-25.6-01h (natural cast of a right pes track). From the Torrent de na Nadala section (metre 25.6), upper part of the Port des Canonge Formation, Artinskian–Kungurian. NA-26.0-02f, NA-26.0-02g (natural cast of a right manus-pes set), NA-26.0-03b, NA-26.0-03c, NA-26.0-03d, NA-26.0-03e, NA-26.0-03f, NA-26.0-03g, NA-26.0-03h, NA-26.0-03i, NA-26.0-03j, NA-26.0-03k (natural cast of a trackway with two right manus-pes sets and three left manus-pes sets) and NA-26.0-09g, NA-26.0-09h, NA-26.0-09i, NA-26.0-09j, NA-26.0-09k, NA-26.0-09l, NA-26.0-09m, NA-26.0-09n, NA-26.0-09o, NA-26.0-09p, NA-26.0-09q (natural cast of a trackway with three right manus-pes sets, two left manus-pes sets and a left manus track). From the Torrent de na Nadala section (metre 26.0), upper part of the Port des Canonge Formation, Artinskian–Kungurian.

Description: Pes imprint plantigrade, pentadactyl, ectaxonic and longer (ca. 4.0–6.2 cm) than wide (ca. 3.7–4.9 cm). The digit imprints are long, straight and thin; they are thinner proximally, because they are more weakly imprinted, whereas distally they are deeper and end in expanded, pointed claw traces with rounded to anteriorly elongated shape. The imprint of digit V is usually very shallow or only preserved as the tip. The relative lengths of the digit imprints are ordered as follows: V<I<II<III<IV. Digit imprints radiate from the sole with no superimposition, forming a variably wide digit I–V angle (ca. 54–118°). The imprints of the metatarsophalangeal pads in the bases of digits II–V are deep and round, and are especially conspicuous in digits II–IV. The sole imprint, slightly wider than it is long, is usually elongated posterolaterally, acquiring a crescent shape. The most deeply imprinted areas are the metatarsophalangeal pad imprints of digits III–IV and the median–lateral region of the sole, followed by the claw traces of digits I–IV and the rest of the sole (median–lateral functional prevalence of the autopodia).

Manus imprint semiplantigrade–plantigrade, pentadactyl, ectaxonic and slightly longer (ca. 4.0–4.9 cm) than wide (ca. 3.8–4.8 cm). The digit imprints are relatively long, thin and, in the case of digits II–IV, with their distal part slightly curved medially (inwards). They end in pointed claw traces that may be slightly curved medially. The relative lengths of the digit imprints are ordered as follows: I<V<II<III<IV. Digit imprints radiate from the palm with no superimposition, forming a wide I–V

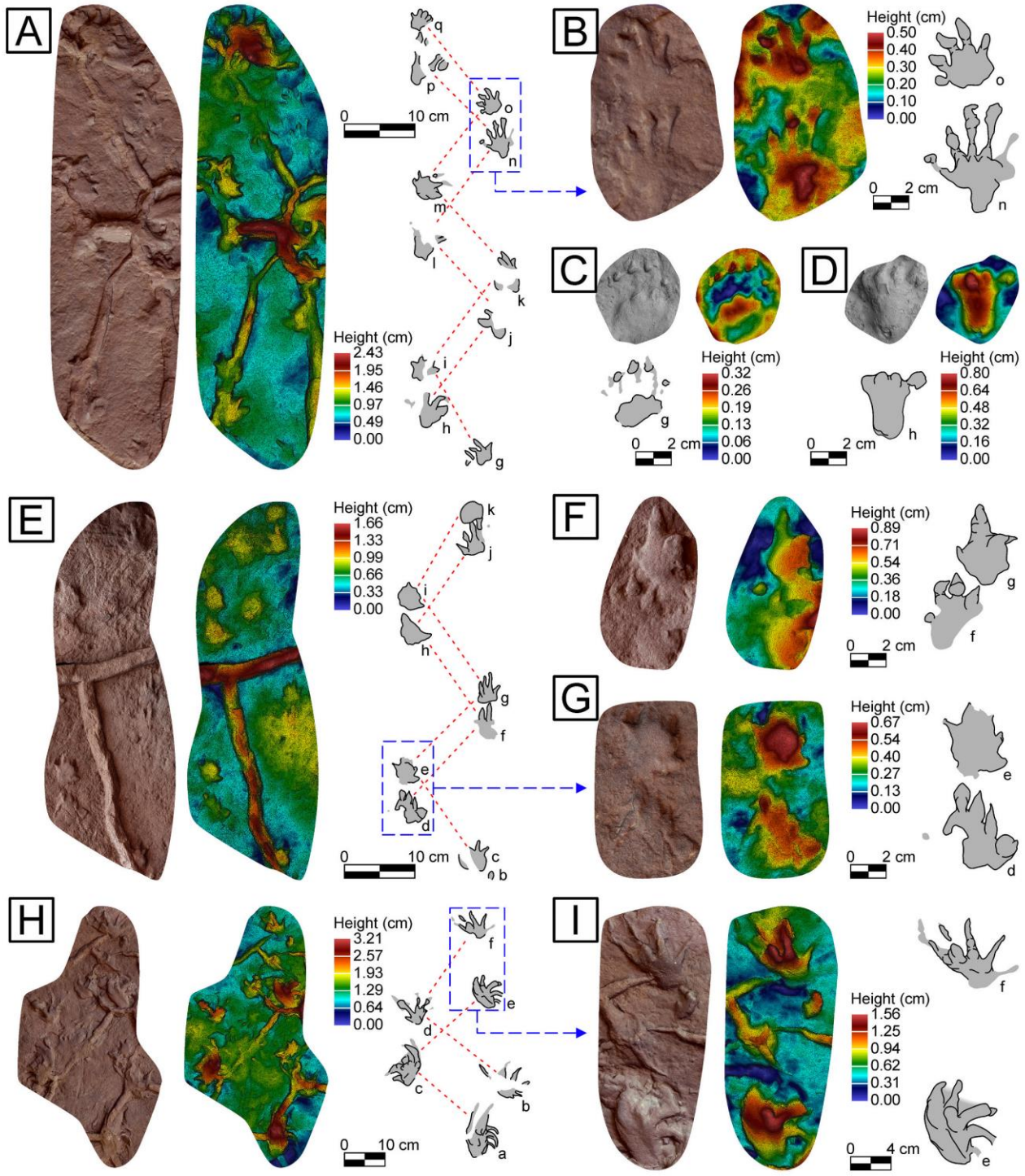

Fig. 11. Tetrapod ichnites attributed to "pelycosaur"-grade synapsid trackmakers studied herein, all as textured 3D models, false colour-coded 3D models and interpretative drawings. **A–H:** *Dimetropus leisnerianus*; **A–B:** NA-26.0-09; **C–D:** NA-25.6-01; **E, G:** NA-26.0-03; **F:** NA-26.0-02. **H–I:** cf. *Dimetropus* isp., NA-26.0-09 (taken from Matamales-Andreu et al., 2021d). All from the Torrent de na Nadala section (Mallorca, Balearic Islands, western Mediterranean), Port des Canonge Formation, Artinskian–Kungurian, Permian.

angle (ca. 83–144°). The imprints of the metacarpophalangeal pads are not always visible, but they are deep and round, and are especially conspicuous in the bases of the imprints of digits III–V. The palm imprint is wider than long, and is oval in shape, with a convex, curved posterior margin. The most deeply imprinted areas are the metacarpophalangeal pad imprints of digits III–V and the median–lateral region of the palm, followed by the claw traces of digits II–V and the rest of the palm (lateral functional prevalence of the autopodia).

Trackway quadrupedal with alternating manus-pes sets. Pes imprints slightly larger than manus imprints (weak heteropody). Pace angulations for manus imprints (99–113°) are slightly wider than those for the pes imprints (ca. 97–101°). Pes imprints usually slightly rotated medially (inwards), about 9–11°, whereas manus imprints are more strongly rotated medially, about 20–39°, and are located anteromedially from the pedes. Pes and manus imprints are usually close to each other (manus-pes distance = 4.6–7.8 cm), but they are usually not overstepping. The glenoacetabular distance ranges between 18.1 and 20.4 cm.

Remarks: The specimens studied here are attributed to the ichnogenus *Dimetropus* and, specifically, to the ichnospecies *Dimetropus leisnerianus*, based on the following combination of characters (see Gand, 1988; Voigt, 2005; Sacchi et al., 2014; Marchetti et al., 2019c; Matamales-Andreu et al., 2021d): (1) ectaxonic manus and pes imprints, (2) depth of the ichnites increasing towards the median–lateral part, (3) plantigrade pes imprint with posterolaterally elongated sole (somewhat "crescent-shaped"), and (4) digits II–IV weakly imprinted proximally, with the clawed tips being notably deeper. Preservation of all the digits is rare in the material studied herein (*e.g.*, Fig. 11B), and in most cases only the palm/sole imprint is preserved. When only the most proximal parts of the digit imprints are preserved, these ichnites are reminiscent of the ichnogenus *Gilmoreichnus* Haubold, 1971 (see Gand, 1988; Van Allen et al., 2005), which may in fact be a junior synonym of *Dimetropus leisnerianus*, but exploring this aspect is beyond the scope of the present work. Quite commonly, tracks of this ichnospecies can also have a "pseudo-tridactyl" mode of preservation, only with a well-imprinted digit IV, the proximal parts of digits III and V and the median–lateral part of the palm/sole (Fig. 11F).

Dimetropus leisnerianus has been reported from the upper Carboniferous to the lower Permian of Great Britain (Meade et al., 2016), central Europe (Voigt, 2005; Voigt et al., 2012), Lodève (Gand, 1988; Gand and Durand, 2006), the Iberian Peninsula (Mujal et al., 2016), and North America (*e.g.*, Lucas et al., 2016). The possible trackmakers for *Dimetropus leisnerianus* and other similar forms (*e.g.*, Gand, 1988; Voigt and Ganzelewski, 2010; Lagnaoui et al., 2018) are caseid, ophiacodontid, edaphosaurid and/or sphenacodontid "pelycosaur"-grade synapsids (Voigt and Ganzelewski, 2010 and references therein).

cf. *Dimetropus* isp.

Fig. 11H–I

Studied material: NA-26.0-02a, NA-26.0-02b (natural cast of a left manus-pes set), NA-26-03l (natural cast of a right pes imprint), NA-26.0-04a (natural cast of a right manus imprint), NA-26-05a (natural cast of a left manus imprint) and NA-26.0-09a, NA-26.0-09b, NA-26.0-09c, NA-26.0-09d, NA-26.0-09e, NA-26.0-09f (natural cast of a trackway with two left manus-pes sets and a right manus-pes set). From the Torrent de na Nadala section (metre 26.0), upper part of the Port des Canonge Formation, Artinskian–Kungurian.

Description: (adapted from Matamales-Andreu et al., 2021d) Pes track semiplantigrade, pentadactyl, almost as long as wide (*ca.* 7.3–8.3 cm). The digit imprints are slender, strongly curved laterally (outwards) and relatively long. Preservation is quite variable: in some cases, the distal parts of digits are not well imprinted (especially digits II and III), whereas in other cases digit I seems to be imprinted twice. No clear claw traces have been observed on any specimen. The relative length of the digit imprints is ordered as follows: V<I≈II≈IV≈III. The total divergence angle between digits I–V of pes tracks ranges from 77° to 95°. The digit imprints usually have sharp posterolateral margins, whereas their anteromedial margins have gentler slopes. The sole imprint is oval, with an almost straight to weakly convex posteromedial margin and a length of about 1/2 of the whole track. Metatarsophalangeal pads are well impressed, especially at the bases of digits I–III. The most deeply imprinted areas of the pes tracks are the metatarsophalangeal pads of digits I–III (medial functional prevalence of the autopodia).

Manus track plantigrade, pentadactyl, usually slightly wider (6.9–7.1 cm) than long (6.7–9.5 cm). Digit I–IV imprints are slender, relatively long and show clawed tips. The proximal parts of the digit imprints are directed medially, whereas the imprints of the tips are curved laterally, giving digit imprints a "hook-shaped" appearance, especially in digit III. They become thinner and gradually decrease in depth distally. Digit V imprint, which is the shortest, is almost as short as digit I, slender and usually straight, although its tip is often not well impressed. Some digit imprints, especially I and II, can have drag traces in front of their tips. The relative lengths of the digit imprints are ordered as follows: V≈I<II≈IV<III. Digits radiate from the palm, usually without significative overlapping, although the bases of digits I and II can be slightly superimposed. The total divergence angle between the imprints of digit I–V is wide, ranging between 115° and 150°. The palm imprint is posterolaterally elongated, with a concave medial margin ("lunate shape"). Metacarpophalangeal pads are rounded and well-impressed, especially at the bases of digits I–IV with slight overlap in I and II. The most deeply imprinted areas of the manus track are the metacarpophalangeal pads of digits II–III (medial-median functional prevalence of the autopodia), followed by those of digits I and IV.

Trackway produced by a quadrupedal animal, with pes tracks slightly larger than manus tracks (weak heteropody). The manus-pes sets are alternately arranged, with the manus tracks positioned at the height of the mid-proximal portion of the pes track of the next couple. The pace angulations of the pes and the manus imprints are of about 80° and 90°, respectively. With respect to the trackway midline, pes imprints are rotated laterally (outwards) by 20–30°, whereas manus imprints are rotated medially (inwards) by 9–26° and are located anteriorly from the pes imprints. Manus tracks can be positioned medially or laterally from the pes tracks. The glenoacetabular distance is of about 32.5 cm.

Remarks: Tracks attributable to this morphotype have been recently studied in depth by Matamales-Andreu et al. (2021d), and thus only the most relevant points will be addressed here. Tracks herein identified as cf. *Dimetropus* isp. (Fig. 11H) are consistently larger and have a different morphology than the *Dimetropus leisnerianus* tracks that appear on the same surface (Fig. 11A). Some particular traits of this morphotype are the mesaxonic manus tracks with distally tapering digit imprints, which have claw traces directed laterally. Its pes tracks are strongly rotated laterally, with digit imprints also curved laterally. The relative depth pattern of the tracks is also different to that of *Dimetropus leisnerianus*, as in the latter it becomes deeper laterally, whereas in the cf. *Dimetropus* isp. from Mallorca they are deeper laterally in their posterior part but medial-median in their anterior part. *Ennatosaurus*-like medium-sized caseid synapsids have been considered the possible trackmakers of this morphotype (Matamales-Andreu et al., 2021d).

Ichnogenus *Characichnos* Whyte et Romano, 2001

Characichnos isp.

Supplementary Fig. 4

Studied material: RA-exs-02a (natural cast). From the Racó de s'Algar section (*ex situ* rock), middle–upper part of the Port des Canonge Formation, Artinskian–Kungurian. NA-66.1-01 (natural casts). From the Torrent de na Nadala section (metre 66.1), upper part of the Port des Canonge Formation, Artinskian–Kungurian. NA-72.4-02a (natural cast). From the Torrent de na Nadala section (metre 72.4), upper part of the Port des Canonge Formation, Artinskian–Kungurian. PM-14.8-01a (natural cast). From the Punta d'en Pere Mir section (metre 14.8), lower part of the Pedra de s'Ase Formation, Roadian–Wordian.

Description: Elongate, parallel scratches of variable length (each of them generally between 2–11 cm long), which may be straight or

slightly curved. The ends of each scratch are usually pointed, but may also be round. Two to four dragged digit imprints are preserved.

Remarks: The ichnogenus *Characichnos* has been interpreted as a swimming trace of tetrapods attributed to a wide range of trackmakers (Whyte and Romano, 2001; Melchor and Sarjeant, 2004; Klein and Niedźwiedzki, 2012; Mujal et al., 2016, 2017b). The fact that *Characichnos* corresponds to a swimming trace does not exclude fully terrestrial forms as their possible trackmakers, as Smith et al. (2015) found swimming traces associated to *Hyloidichnus* tracks, and attributed them to the late Permian moradisaurine captorhinid eureptile *Moradisaurus* de Ricqlès et Taquet, 1982, which may have been able to swim in shallow ponds. In the case of the specimens from Mallorca, the identity of the producer(s) remains obscure.

8. Discussion

8.1. Age attributions

8.1.1. Magnetostratigraphy

Given that all ChRM directions display reverse polarity, the length of the studied sections and the biostratigraphic constraints (see '8.1.2. Palynostratigraphy' and '8.1.3. Tetrapod track biostratigraphy' below), the sampled succession is placed within the Kiaman Superchron. This long chron of reverse polarity extends from the middle Carboniferous to the middle Permian. It is set to end by the middle Wordian (middle Guadalupian), after which reverse and normal polarity intervals (the so-called Illawarra Series or Superchron) occur during the remainder of the Guadalupian and Lopingian (middle–upper Permian), extending into the Triassic (Steiner, 2006; Hounslow and Balabanov, 2018; Henderson et al., 2020) (Fig. 12A).

In a previous study (Banda et al., 1986) reported three palaeomagnetic sites sampled in red sandstones from northern Mallorca (MB03, Cala d'Estellencs, and MB01 and MB02, Port des Canonge) and assigned them to purported *Buntsandstein* facies (Triassic). They presented the mean directions plotted on a stereogram without detailed polarity and directional data, or site mean values. Later, Parés et al. (1989, 1992a, 1992b) reused the data from the three aforementioned sites and provided an overall mean for them (N = 3, Dec/Inc = 10.0/11.0, $a_{95} = 6.0$), still without information on polarity and/or individual site mean nor information at sample level. Nevertheless, the present work shows that the outcrops that Banda et al. (1986) sampled at Port des Canonge do not correspond to the *Bundsandstein* facies (Triassic) but rather to the Permian Port des Canonge Formation defined herein (specifically, the borings were found in metres 164–171 and 286–295 of the Port des Canonge log, see Supplementary Logs). It is difficult to compare datasets given the lack of detailed information, but our

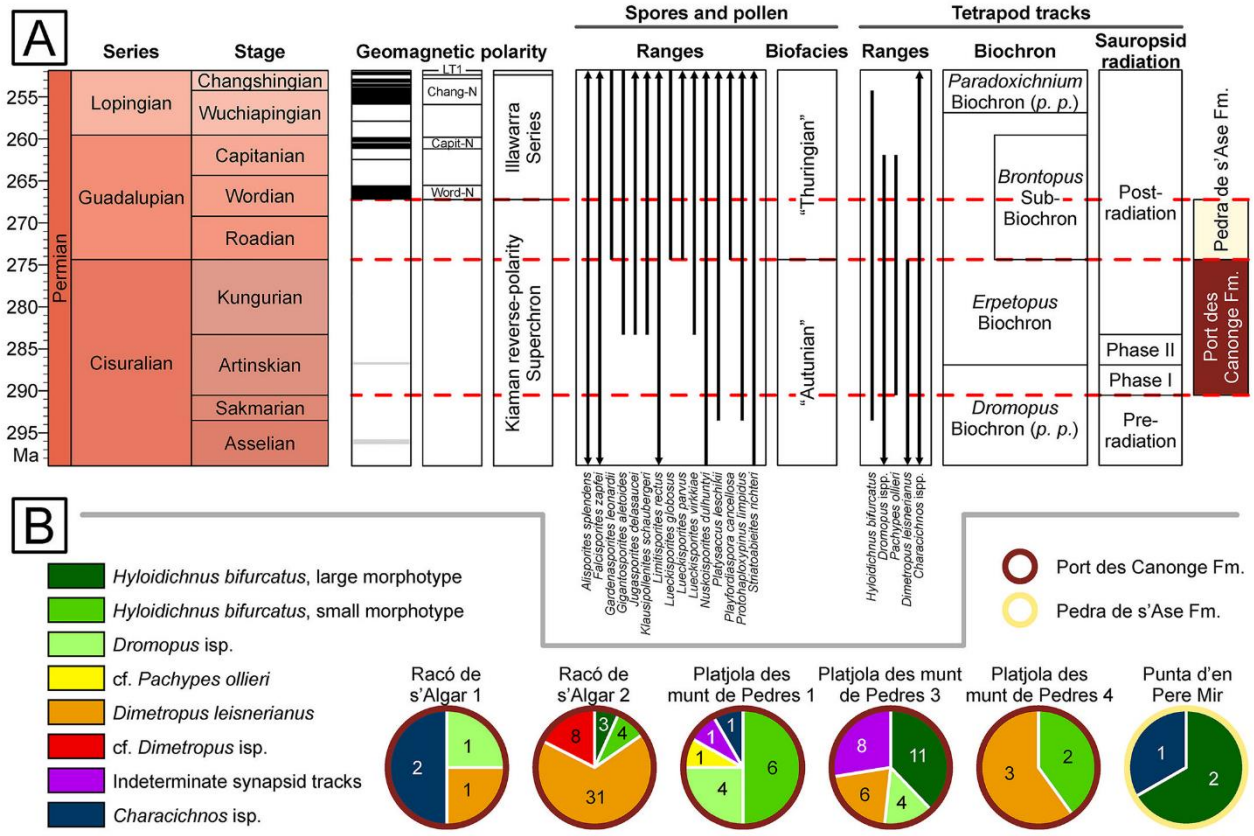

Fig. 12. A: Magneto- and biostratigraphic data of the Permian of Mallorca. The geomagnetic polarity reference scales are taken from Henderson et al. (2020) (the whole Permian sequence of Mallorca belongs to the Kiaman reverse-polarity Superchron). The biostratigraphic ranges of the spores and pollen found in the present work in the Pedra de s'Ase Formation are taken from Supplementary Table 4 and references therein. The biostratigraphic ranges of the ichnotaxa recognised in the Port des Canonge Formation are based on Schneider et al. (2020) and Marchetti et al. (2021b). **B:** Pie charts showing the relative proportions of the recognised ichnotaxa in the six main ichnite-bearing beds (Racó de s'Algar 1: lower part of log NA; Racó de s'Algar 2: m 25.6–26 of log NA; Platjola des munt de Pedres 1: m 66.5 of log NA; Platjola des munt de Pedres 2: m 72.5 of log NA; Platjola des munt de Pedres 3: m 77.5 of log NA; Platjola des munt de Pedres 4: m 90 of log NA; Punta d'en Pere Mir: m 15.7 of log PM). For the stratigraphic position of sites see Fig. 13.

bedding-corrected mean direction for the Port des Canonge–Hort de sa Cova section (N = 83, Dec/Inc = 179.41/−14.92, a_{95} = 3.63) clearly supersedes the previous data (see Supplementary Fig. 3).

It is well known that some sedimentary rocks, and particularly redbeds, are prone to the palaeomagnetic inclination shallowing effect, in which rocks block a magnetic remanence shallower than the expected direction for the site latitude at deposition time. Although there are methods to correct for this effect, the easiest one, which is the elongation/inclination (E–I) approach, requires a great number of directions (more than 100 are recommended) (Li and Kodama, 2016 and references therein). Considering that only 70 directions (out of the 144 computed ChRMs) are linear fits calculated with Principal Component Analysis, we refrain at this stage to attempt any correction for the shallowing effect or to provide a palaeopole from the studied strata.

8.1.2. Palynostratigraphy

Sporomorphs and palynomorphs have been found in the Pedra de s'Ase Formation, indicating a Guadalupian (middle Permian) age for at least its middle part (see Fig. 12A). It is peculiar that several species described from Mallorca were reported for the first time in upper Permian deposits of the Southern Alps (*e.g.*, Klaus, 1963) or Central Europe (*e.g.*, Visscher, 1967), but have lately also been identified in Kungurian deposits of Tregiovo (*e.g.*, *Gardenasporites*, *Gigantosporites*, *Limitisporites*) (Marchetti et al., 2015a; Forte et al., 2018). This mixed composition of the palynoflora, with "typical" early and late Permian elements, reflects its 'Thuringian' character (*e.g.*, Visscher, 1968; Juncal et al., 2018), corresponding to a "middle–late" Permian age. Originally, Visscher (1968) described those mixed floras as typical '*Zechstein*' assemblages, which today would correspond to part of the Wuchiapingian and the Changhsingian (*e.g.*, Legler and Schneider, 2013), but later the term was used more and more to describe a "middle Permian" flora (*e.g.*, Juncal et al., 2018). Generally speaking, it is possible to distinguish an 'Autunian' flora (early Permian flora), based on the presence of *Potonieisporites novicus* and *Vittatina costabilis*, among others, and a 'Thuringian' flora (middle–late Permian) characterised by *Lueckisporites virkkiae*, *Nuskoisporites dulhuntyi* and *Paravesicaspora splendens* (*e.g.*, Arche and López-Gómez, 2006; Juncal et al., 2020). In the deposits of Mallorca, these three typical 'Thuringian' taxa are well represented in the samples studied by Ramos and Doubinger (1989), Diez (2000) and Juncal (2019) (see Supplementary Table 4). However, the latter two authors also mentioned *Potonieisporites novicus* from the same bed, which is a typical 'Autunian' marker. Regarding the new samples yielding palynomorphs studied in the present work (Figs. 7, 12A; Supplementary Table 4), *Lueckisporites virkkiae* is present in all five, *Nuskoisporites dulhuntyi* has only been identified in P-PA-09 (Pedra de s'Ase log) and *Paravesicaspora splendens* has not been found in any of them. Moreover, the association of *Crucisaccites variosulcatus* (also present in all the samples reported by previous authors, see Supplementary Table 4) with pollen of the *Lueckisporites* complex is considered to be characteristic of the Roadian–Wordian in Western Europe (Vázquez and Césari, 2017).

Taking all the above into account, the samples studied by Ramos and Doubinger (1989), Diez (2000) and Juncal (2019) could be considered Roadian–Wordian, yet a slightly younger age cannot be completely excluded based on the palynomorphs alone. Indeed, Juncal (2019) proposed a Wordian–Capitanian stage, although all taxa described can also be present during the Roadian (see Supplementary Table 4), and the fact that this formation is still in the Kiaman Superchron excludes a Capitanian or younger stage (Fig. 12A, see also '8.1.1. Magnetostratigraphy' above). The age attributions for the samples collected in the present work are more uncertain. Only P-PA-12 (Pedra de s'Ase log), from the same bed as the samples studied by Diez (2000) and Juncal (2019), can be attributed to the same age. P-PA-05 and P-PA-09 (Pedra de s'Ase log), which are from below in the series, and P-CO-03 and P-CO-04 (Pedrera de sa Cova log), which are from above, show relatively similar assemblages suggesting a middle Permian age as well, given that they are still in the Kiaman Superchron (Fig. 12A).

Bercovici et al. (2009) assigned the upper part of the Cala del Pilar section (Menorca, Balearic Islands) to the middle–upper Permian ('Thuringian'). Their palynological samples and the conifer remains described from the stratigraphic succession of Cala del Pilar closely resemble those identified in the present paper, although the material described in Bercovici et al. (2009) is much more diverse. Most of the taxa described herein or listed by Ramos and Doubinger (1989), Diez (2000) and Juncal (2019) were also found by Bercovici et al. (2009) (see Supplementary Table 4). However, there are also some genera that have not been reported in Mallorca so far, such as *Densoisporites*, *Palaeospongisporis* and *Playfordispora* among the spores, and *Platysaccus*, *Striatoabieites*, *Taeniaesporites* and *Tiwariasporis* among the pollen. The presence of *Lueckisporites virkkiae*, and the absence of *Nuskoisporites dulhuntyi* and *Paravesicaspora splendens*, in combination with the younger taxa present in the section of Menorca, support a younger age for the upper part of the unit P3 in the Cala del Pilar section. Both the palynoflora and the macroflora of Menorca are definitively late Permian in age, whereas the samples from Mallorca are somewhat older.

8.1.3. Tetrapod track biostratigraphy

Tetrapod tracks indicate a Cisuralian (lower Permian) age for the Port des Canonge Formation (Fig. 12A). The present work has revised the ichnites studied by Matamales-Andreu et al. (2019), together with many new finds, which provide a thorough interpretation for the whole ichnoassemblage. The relative numbers of the identified ichnotaxa in each of the studied sites are presented in Fig. 12B. At the site located lowest in the stratigraphic section, Racó de s'Algar 1, swimming traces are dominant (50%) over reptile tracks (25%), "pelycosaur"-grade synapsid tracks (25%) and anamniote tracks (0%), although the sample is very small (n = 4). In the Racó de s'Algar 2 site, stratigraphically located slightly higher, the trackway sample is the most abundant of all the observed sites (n = 46), and there is a clear dominance of tracks attributed to "pelycosaur"-grade synapsid trackmakers (84.8%) over reptile tracks (15.2%) and anamniote tracks (0.0%). In the Platjola des munt de Pedres 1 site (n = 12), the proportions are reversed, with numerous reptile tracks (83.3%), few synapsid tracks (8.3%) and swimming traces (8.3%), and no anamniote tracks (0.0%). The site of Platjola des munt de Pedres 2 is not represented in the charts as the sample is very low (n = 2) and indeterminate. Stratigraphically higher, at the Platjola des munt de Pedres 3 site (n = 29), reptile (51.7%) and synapsid tracks (48.3%) show very similar proportions, whereas those of anamniotes are missing (0.0%). "Pelycosaur"-grade synapsid tracks are again more numerous (60.0%) than reptile tracks (40.0%) in the Platjola des munt de Pedres 4 site, but the small sample size (n = 5) could easily account for a skewed proportion. Finally, in the Punta d'en Pere Mir site, which is the only tracksite in the Pedra de s'Ase Formation, the ichnoassemblage comprises reptile tracks (66.7%) and swimming traces (33.3%) but again, the sample size is very low (n = 3).

From the foregoing data, it is clear that synapsid tracks are generally dominant in the Port des Canonge Formation, with only two sites (Platjola des munt de Pedres 1 and 3) in which reptile tracks are more numerous than synapsid tracks. In this sense, although the palaeoenvironment of all the ichnite-bearing beds is essentially the same, there could be slight differences affecting the local proportions of the different ichnotaxa. Because of this, the tetrapod ichnoassemblage has been considered as a whole for the relative proportions of tracks (n = 96) to minimise the impact of the local particularities. This way, synapsids account for slightly more than a half of the observations (59.4%), reptile tracks are less represented (37.5%), and swimming traces are the rarest (3.1%). Anamniote tracks are altogether absent.

Based on the stratigraphic range of the ichnotaxa identified in the present work (see '7.3. Tetrapod tracks' above), the Port des Canonge Formation can be dated in the Cisuralian (lower Permian); specifically, as Artinskian and/or Kungurian (Fig. 12A). One of the most relevant ichnotaxa to constrain the age of this formation is *Dimetropus*

leisnerianus, as it ranges from the upper Carboniferous to the lower Permian (upper Kungurian) (see Schneider et al., 2020). Other ichnotaxa provide additional information: *Hyloidichnus* ranges from the lower to the upper Permian (Sakmarian–Wuchiapingian) (see Schneider et al., 2020; Logghe et al., 2021; Matamales-Andreu et al., 2021c), *Dromopus* ranges from the upper Carboniferous to the middle Permian (middle Capitanian) (see Schneider et al., 2020), and *Pachypes ollieri* has been found from the lower to the middle Permian (Artinskian–middle Capitanian) (see Marchetti et al., 2021b). cf. *Dimetropus* isp. and *Characichnos* provide no additional information, as the former is so far only known from the Port des Canonge Formation (Matamales-Andreu et al., 2021d), and the latter is a long-ranging trace produced by a wide variety of tetrapods (*e.g.*, Whyte and Romano, 2001).

The relative proportions listed above make it possible to hypothesise a lower–middle Artinskian age for the Port des Canonge Formation (Fig. 12A). In the Cisuralian, two successive sauropsid radiation events occurred in the middle part of the Artinskian age, and are recognised by an increase of the proportions of reptile tracks in many sites worldwide (Marchetti et al., 2019d, 2022). Before the radiation, reptile tracks accounted for an average of 27% (0–40%) of the ichnoassemblages. Their numbers increased slightly during the first phase of the radiation, with an average of 37% (25–44%), and in the second phase, with an average of 47% (25–66%). In successions deposited after these two phases, reptile tracks become dominant, with an average of 68% (50–100%) (Marchetti et al., 2019d). Given the relative proportions of tracks in the Port des Canonge Formation, it could correspond to the first phase of the sauropsid radiation. Remarkably, the absence of the widespread ichnogenus *Erpetopus* Moodie, 1929, in the tracksites of Mallorca may point to a pre-*Erpetopus* biochron age (Schneider et al., 2020), and thus tentatively date the ichnite-bearing beds of the Port des Canonge Formation in the lower–middle Artinskian (Fig. 12A). However, this age attribution is based on a relatively small sample of tetrapod ichnites, the proportions of which could vary depending on the represented sedimentary setting. Therefore, for the present work, the Port des Canonge Formation is considered Artinskian–Kungurian (Fig. 12A), accepting the possibility that the lowermost part could also stretch into the Sakmarian.

8.2. Sedimentary evolution and palaeoclimate

Tectonics were the main factor shaping the environments in the Permian of Mallorca, which may secondarily have also been affected by changes in climate. During the Artinskian and the Kungurian, most rift basins of the western peri-Tethys, which had opened during the late Carboniferous, were reactivated (McCann et al., 2006; Cassinis et al., 2012; López-Gómez et al., 2019a). Of special interest for the present work are the tetrapod ichnite-bearing successions of the Sagra/Sotres Formation (western Pyrenees; see Gand et al., 1997; López-Gómez et al., 2019b), the Lower Red Unit/Peranera Formation (south-central Pyrenees; see Mujal et al., 2016, 2018) and the Rabejac Formation (Massif Central; see Gand and Durand, 2006; Michel et al., 2015), all dated as Artinskian and located relatively close to the study area. Those units share most of the tetrapod ichnotaxa reported here from the Port des Canonge Formation (see '7.2. Tetrapod tracks' above), such as *Hyloidichnus*, *Dromopus*, *Pachypes* and *Dimetropus* (although some are missing in certain sections) and correspond to fluvial palaeoenvironments and playa lake deposits (Gand and Durand, 2006; Mujal et al., 2016; López-Gómez et al., 2019b). Those units show a trend towards semi-arid conditions in the late Cisuralian and Guadalupian, as demonstrated by the study of palaeosols and geochemical proxies (Michel et al., 2015; compare Mujal et al., 2017a, and Mujal et al., 2018; López-Gómez et al., 2021). In fact, by the middle Permian, most basins of central Pangaea have evidence of arid climates (Schneider et al., 2006; Tabor and Poulsen, 2008; De la Horra et al., 2012; Michel et al., 2015). However, even though the succession of Mallorca spans part of the lower and middle Permian (see '8.1. Age attributions' above), no dramatic changes in river style or palaeosol types have been observed in the three described units.

The lowermost Permian unit of Mallorca, the Bec de s'Àguila Formation (Fig. 2), corresponds to alluvial fans developed near the footwall scarp during the first stages of rifting (Fig. 13). Similar conglomeratic units have been reported at the base of the Permian units of other western Tethyan basins (López-Gómez et al., 2019a), interpreted as systems that developed transversally to the main basin axis in response to the great erosion of the scarps in a period with high subsidence rates (*e.g.*, Speksnijder, 1985; Franzel et al., 2021; Matamales-Andreu et al., 2021c; see Miall, 2006 for a review of this kind of deposits). Towards the upper part of this formation, sinuous channels transporting coarse-grained sediments began to develop. The climate of the Bec de s'Àguila Formation was comparable to that interpreted for the Permian P1 unit of the neighbouring island of Menorca (Gómez-Gras and Alonso-Zarza, 2003; Matamales-Andreu et al., 2021c), that is, semi-arid conditions, which can be inferred because of the development of carbonate palaeosols and calcretes, typical of environments with low precipitation regimes (Mack et al., 1993; Alonso-Zarza, 2003; Tabor and Poulsen, 2008).

With the likely decrease of subsidence rate, the dominant depositional setting of the Port des Canonge Formation (Fig. 2) was a meandering river system flowing towards the southeast and following the main axis of the rift basin (Fig. 13). Generation of accommodation space was still significant, given the abundance of fine-grained deposits such as mudstones and very fine-grained sandstones. These sequences are typical of rift basins, which have an initial stage of alluvial sedimentation from the nearby scarps that is followed by the settling of a fluvial system longitudinal to the basin (Miall, 2006). The fine-grained meandering channels can readily be identified because of the abundant and conspicuous lateral accretion surfaces dipping roughly perpendicular to the main palaeocurrent trend. One of the main factors prompting the development of rivers of such style is the presence of abundant vegetation on the floodplains, stabilising the riverbanks and hampering the widening of the channel and the formation of bars (*e.g.*, Ebisemiju, 1994; Rowntree and Dollar, 1999; Huisink, 2000; Miall, 2006; Davies and Gibling, 2010; Borruel-Abadía et al., 2015). Evidence of such a plant cover lies in the abundant formation of soils on the floodplains, and the sporadic presence of vegetative plant organs and logs in some beds despite the unfavourable conditions for preservation of such remains in the heavily oxidised red-beds. Moreover, the presence of abundant carbonate palaeosols and calcretes (calcic Vertisols, vertic Calcisols and Calcisols) throughout the Port des Canonge Formation points to a seasonal climate with periods of very low precipitation (Mack et al., 1993; Alonso-Zarza, 2003; Gómez-Gras and Alonso-Zarza, 2003; Tabor and Poulsen, 2008), similar to the underlying formation. However, the presence of purported alfisols (metres 10 to 12.5 of the Torrent de na Nadala log), identical to those described by Bercovici et al. (2009) in Menorca, also suggests the presence of seasonally persistent water bodies on the floodplains. Accordingly, the climate for this formation may be inferred as the alternation of sub-humid and semi-arid conditions, probably as the effect of seasons. Since the palaeosols with the largest carbonate nodules and calcrete hardpans are in the lower and middle parts of the Port des Canonge Formation, the climate may have been slightly more arid during the deposition of those parts of the unit.

Energy conditions may have increased again during the time of deposition of the Pedra de s'Ase Formation (Figs. 3, 13), resulting in the increase of sand grain size and the amalgamation of meandering point bar deposits. The increase in grain size is abrupt, whereas the decrease in the amounts of lutites, very fine- and fine-grained sandstones is progressive (Fig. 3). In the upper part, there is again a progressive increase in the amount of lutites, very fine- and fine-grained sandstones (Fig. 3). Gómez-Gras (1993) suggested that in this unit, generation of new accommodation space by subsidence of the basin was decreasing, and the meandering channels kept migrating while reworking the floodplain and older channel deposits. This, however, could also be caused by an

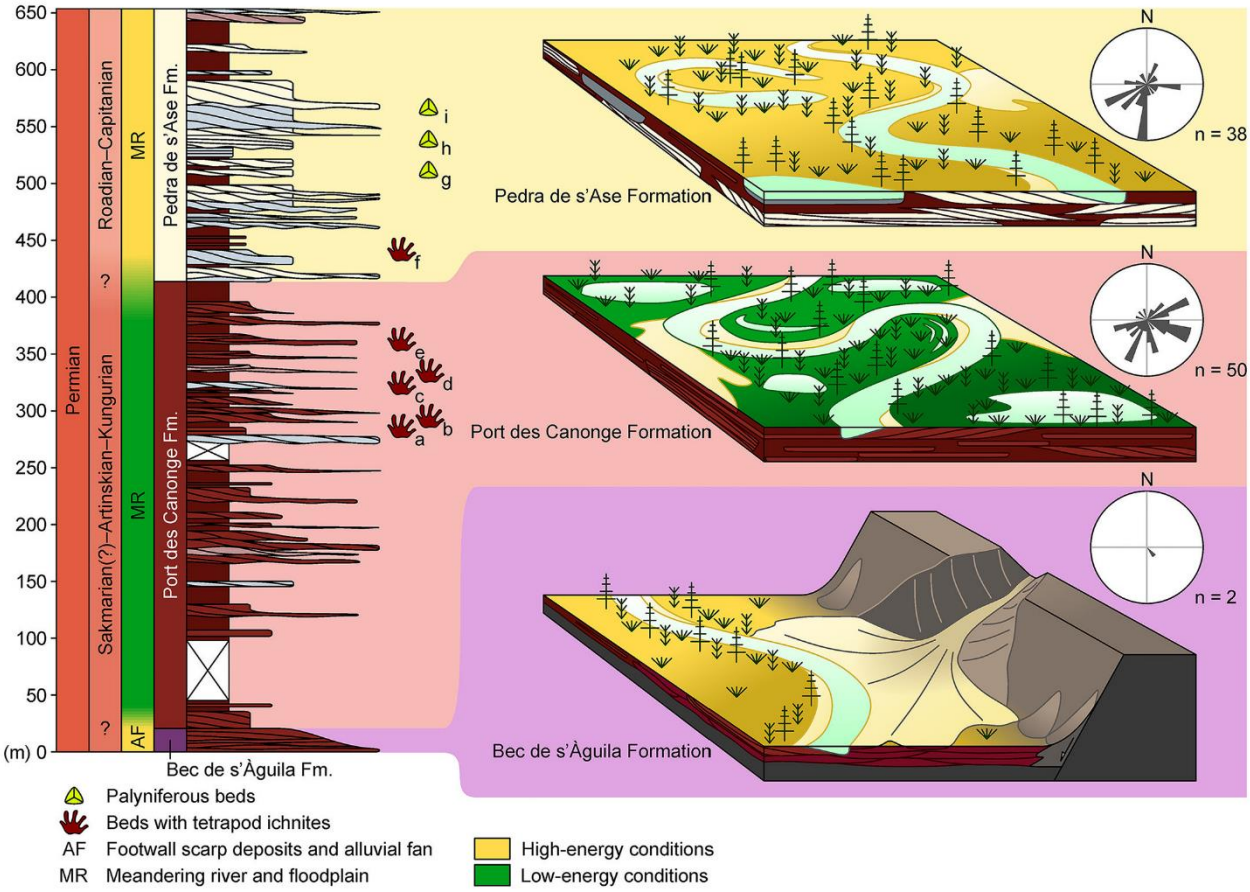

Fig. 13. Synthetic stratigraphic log for the three formations of the Permian of Mallorca defined here and their respective palaeoenvironmental interpretations, showing the beds that contain tetrapod tracks (some dated as lower Permian) and palynomorphs (some dated as middle Permian). Letters a–f correspond to tracksites, and letters g–i to palynological samples. a: Racó de s'Algar 1, b: Racó de s'Algar 2, c: Platjola des munt de Pedres 1, d: Platjola des munt de Pedres 3, e: Platjola des munt de Pedres 4, f: Punta d'en Pere Mir, g: sample P-PA-05, h: sample P-PA-09, i: sample P-PA-12 of the present work and sample "Pedra de s'Ase" of Diez (2000) and Juncal (2019). Uppermost part of the Pedra de s'Ase Formation (Pedrera de sa Cova section) not shown because correlations can only be made tentatively at present.

increase of water or sediment supply, or both. The former would be expected in a climate with a more regular precipitation regime, whereas the latter could be a consequence of higher subsidence rates (Speksnijder, 1985; Miall, 2006). The petrological study of sandstones performed by Gómez-Gras (1993) showed that the composition of the sand grains in the Port des Canonge and Pedra de s'Ase formations was very similar. This indicates that the source area of the sediments did not change significantly, thus pointing to tectonic stability. Therefore, the most probable cause of the sedimentological change between the two formations is increased water flow. Moreover, intercalated between point bar deposits, there are tabular sandstone deposits with structures of high-flow regime indicative of flashflood episodes, as also pointed out by Ramos (1995).

The accumulation of large woody debris in the margins or in the base of shallow channels of the Pedra de s'Ase Formation (Fig. 8A–B) may be either due to their being transported or even wrenched out during flashfloods, or by bank undercutting during lateral migration of the channels (*e.g.*, Baudrick and Grant, 2001; Gulbranson et al., 2020). The abundance of woody debris points to densely vegetated river margins, and the fact that it appears more frequently than in the underlying Port des Canonge Formation is probably because of the increased regularity of high-energy events that could transport more large woody debris and bury it faster. The development of the same dominant types of palaeosols (vertic Calcisols and Calcisols) in both the Port des Canonge Formation and the Pedra de s'Ase Formation (with calcareous nodules of roughly the same size: 1–3 cm) suggests that the climate did not change drastically from one unit to the other, and could conflict with the hypothesis of an increased water supply derived from a more humid climate. Nevertheless, the climate could be relatively more humid in the headwaters and similarly semi-arid in the basins here studied, which would increase the water flow, but the palaeosol types would remain the same (Miall, 2006). Added to this, the increased frequency of floods would also have played a part in the formation of high-energy deposits and the generally coarser grain size of the channel deposits. Therefore, during the deposition of the Pedra de s'Ase Formation, the climate seems to have been semi-arid but with more marked seasonality and a greater water input than in the Port des Canonge Formation. Because of increased flooding, high-energy events were relatively common and the sediments were coarser in an otherwise semi-arid climate.

In line with this hypothesis, the palynological assemblage of the Pedra de s'Ase Formation reflects a complex regional landscape with a variety of different habitats under a generally semi-arid regional climate. This is reflected by the dominance of bisaccate pollen, despite the macroplant fossil assemblage being mostly represented by horsetail

and/or putative conifer stems (Fig. 8A–B) and conifer shoot fragments (Fig. 8I). Spores of hygrophytic plants (*e.g.*, lycophytes, sphenophytes and ferns) are very rare. Those plants were probably restricted along the river banks, since most of the observed sporomorphs are bisaccates, and therefore they are well-adapted to travel over longer distances. Given that most sedimentary deposits are linked to water transport, the composition of the palynoflora is best explained by a semi-arid climate with occasional rainfall. Humid conditions in localised environments were, however, present at least occasionally, and were covered by vegetation. This is exemplified by spores of hygrophytic plants such as bryophytes (*Reticulatisporites*), lycophytes (*Endosporites*, *Kraeuselisporites*, *Lundbladispora*), sphenophytes (*Calamospora*), and ferns (*Granulatisporites*, *Osmundacidites*), which would have colonised the margins of rivers and ponds and/or the understorey of the humid lowland. The major component of the flora were voltzialean conifers, most of which belonging to the Utrechtiaceae and other primitive families such as the Rufloriaceae and Emporiaceae (*e.g.*, *Jugasporites*, *Limitisporites*, *Lueckisporites*, *Nuskoisporites*). Seed ferns such as Peltaspermales (*e.g.*, *Platysaccus*, *Vittatina*) were also very abundant. The botanical affinities of some palynomorphs would support the presence of Callistophytales (*e.g.*, *Vesicasporites*, *Paravesicaspora*), Zygopteridales (*Leiotriletes*), Corystospermales/Caytoniales (*e.g.*, *Vitreisporites*), and Glossopteridales (*Marsupipollenites*, *Protohaploxypinus*, *Crustaesporites*) (see Table 3). The presence of especially the latter two groups is, however, doubtful, since no macroremains of these groups have so far been found in the Permian of the Central European Basin. Therefore, it is possible that the botanical affinity of these taxa is too poorly known and that these palynomorphs belong to other gymnosperms that have not been identified so far. Nevertheless, it could also be possible that a few pollen grains were transported by the wind over a distance of some thousands of kilometres, from the nearest glossopteris floras in the Southern Hemisphere to the deposits of Mallorca.

8.3. The early Permian tetrapod ichnoassemblages of Mallorca in the context of equatorial Pangaea

The global record of Cisuralian tetrapod tracks is mainly concentrated in the palaeoequatorial latitudes of Pangaea (Fig. 14) (Marchetti et al., 2019c, 2022 and references therein). Most of the localities share a fairly constant set of ichnotaxa, although variations through time and space can also be observed. These tracks have been used to create a biostratigraphic framework, establishing biochrons and sub-biochrons of characteristic ichnogenera based on their presence (Lucas, 2019; Schneider et al., 2020). Track variation in time and space has made it possible to infer local (*i.e.*, depending on the sedimentary environment) (Hunt and Lucas, 2006; Marchetti et al., 2015b, 2015c; Mujal et al., 2016) or global (Marchetti et al., 2019b, 2020, 2021b, 2022; Francischini et al., 2020; Mujal and Marchetti, 2020; Matamales-Andreu et al., 2021d) patterns of distribution of the trackmakers.

8.3.1. Lack of tracks attributed to anamniotes in the Permian of Mallorca

Ichnogenera attributed to anamniote trackmakers, such as lepospondyls and/or temnospondyls (*Matthewichnus*, *Batrachichnus*, *Limnopus*) and "reptiliomorphs" (*Amphisauropus*, *Ichniotherium*) (see Lucas, 2019) appear to be absent in the deposits of Mallorca, which stands in sharp contrast with most other lower Permian localities worldwide (Marchetti et al., 2019d, 2022). Based on the recent reviews of Marchetti et al. (2019d, 2022), ichnites attributed to lepospondyl and/or temnospondyl trackmakers are present (decreasing in abundance towards the end of the lower Permian) in most fluvio-lacustrine units, which is consistent with their mode of life as aquatic animals, at least during the larval stage (*e.g.*, Schoch, 2014). In the upper Artinskian–upper Kungurian Coconino and De Chelly formations of southern North America, interpreted as erg palaeoenvironments with little water availability, tracks attributed to lepospondyl and/or temnospondyl trackmakers are missing (Marchetti et al., 2019d). Nevertheless, tracks attributed to seymouriamorph and diadectomorph "reptiliomorphs" have been reported from both formations (Marchetti et al., 2019d), indicating that those anamniotes may have been well adapted to thrive in such arid environments. Regarding the diadectomorphs, Francischini et al. (2020) hypothesised that this group may have developed directly without a larval stage, and that their reproduction and early ontogenetic development stages could have been relatively independent of water. In that context, however, the putative presence of co-ocurring seymouriamorphs is harder to explain, as they are known to have had aquatic larvae (*e.g.*, Klembara et al., 2007), and their reproduction and early stages of development may have been related to short-lived aquatic environments developed in those erg systems. In any case, the presence of tracks attributed to both seymouriamorphs and diadectomorphs suggests that, at least during their adult stages, those groups were already adapted to environments with very low water availability.

Even though the Port des Canonge Formation of Mallorca was

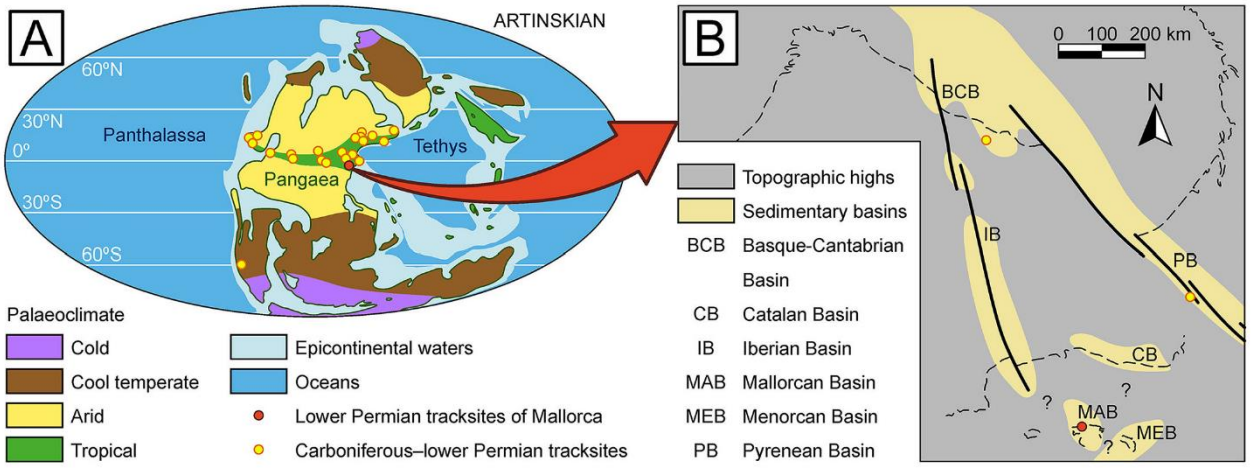

Fig. 14. Palaeogeographical position of the tracksites of Mallorca. **A:** Distribution of the known Carboniferous–Permian and lower Permian tracksites (data from Marchetti et al., 2019c and references therein). Note that almost all of them are in the equatorial latitudes and under tropical climates. Artinskian world map modified after Scotese (2014a), with palaeoclimate data after Tabor and Poulsen (2008). **B:** Detail of the Iberian area (dashed lines represent present-day coastline) with its main sedimentary basins and location of the known tracksites (Mujal et al., 2016; López-Gómez et al., 2021; the present work). Map based on Sopeña et al. (1977), Gretter et al. (2015) and López-Gómez et al. (2021).

deposited under a semi-arid climate (see '8.2. Sedimentary evolution and palaeoclimate' above), the lack of anamniote tracks and trackways amongst almost 100 occurrences is puzzling. This is especially remarkable in the case of "reptiliomorphs", because, as discussed above, species of those groups appear to have been able to endure seasonal drying of the water bodies. In the chronostratigraphically similar and palaeogeographically close Lower Red Unit/Peranera Formation of the Pyrenean Basin, Mujal et al. (2016) showed that the taxonomical composition of the ichnoassemblages hinged upon their proximity to the main water bodies (*i.e.*, meandering fluvial channels). Tracks and, in some cases, swimming traces (*Characichnos* isp.) attributable to lepospondyl/temnospondyl (*Batrachichnus*, *Limnopus*), diadectomorph (cf. *Ichniotherium*), parareptile (*Pachypes*, see Marchetti et al., 2021b) and araeoscelidian/bolosaurid (*Dromopus*) trackmakers were found in the

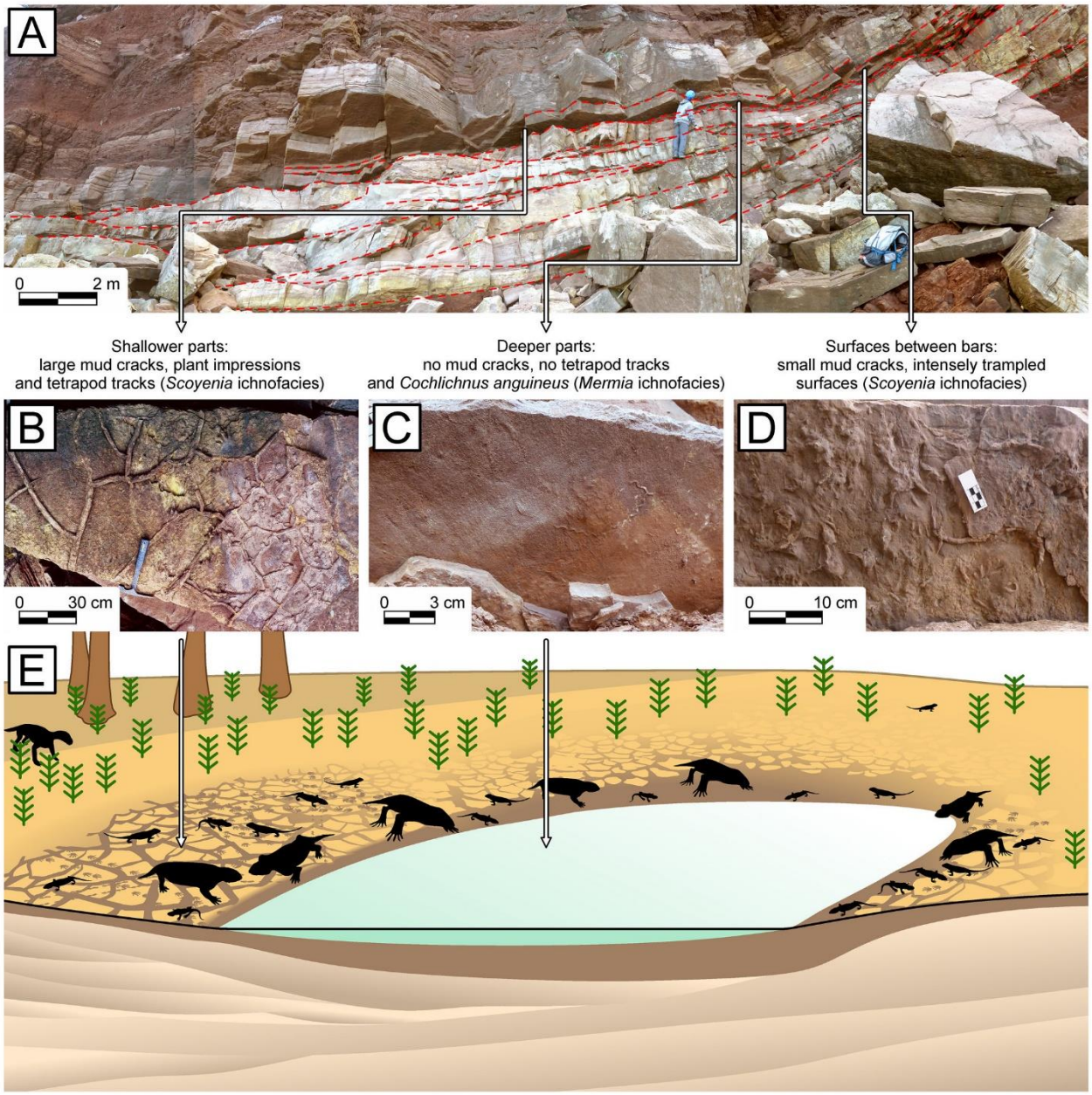

Fig. 15. Interpretation of the Racó de s'Algar 1 tracksite as a waterhole. **A:** Field view of the tracksite. **B:** Surface (UIB174620) with natural casts of large mud cracks and tetrapod ichnites (*Hyloidichnus*, *Dimetropus*), with a thin bed of lutites/very fine-grained sandstones below. Photograph courtesy of J.J. Fornós, taken in the 1980s. **C:** Surface without mud cracks and with natural casts of ichnofossils of the *Mermia* ichnofacies (*Cochlichnus anguineus*), with a thick bed of lutites/very fine-grained sandstones below. It is a lateral variation of the same surface depicted in B. **D:** Densely trampled (*Hyloidichnus*, *Dimetropus*) surface with natural casts of narrow mud cracks. It is located above a fine lutite drape between two sandstone bars. **E:** Schematic representation of the palaeoenvironment represented by the Racó de s'Algar 1 tracksite as a waterhole developed in a swale or an abandoned chute channel in the near-channel environment, indicating the inferred position for the sub-environments depicted in B and C. Plants and tetrapods represented only schematically.

lutite drapes of meandering river point bar deposits of non-functional channels (ponds or oxbow lakes). There, the swimming traces were located in the deeper parts of the channel (with traces being more abundant when it was still functioning), whereas the walking tracks had been imprinted near its margins (Mujal et al., 2016). Conversely, water runoff deposits representing palaeoenvironments with much less available water contained tracks attributable to captorhinomorph (*Hyloidichnus*), parareptile (cf. *Varanopus*) and "pelycosaur"-grade synapsid (*Dimetropus*) trackmakers (Mujal et al., 2016).

It is tempting to explain the lack of tracks attributed to anamniotes in Mallorca as a result of a similar bias produced by the local setting. However, both palaeoenvironments yielding tracks in the Pyrenean Basin are also represented in the sequences of the Port des Canonge Formation of Mallorca. Essentially all the tracksites of the latter correspond to waterhole deposits (Figs. 15, 16) developed in swales or abandoned chute channels in the near-channel environment, and in playa lakes in the floodplain environment (see description of similar environments by Smith, 1993). In both cases, the trampled mud was later covered by crevasse splay or low-energy channel sands. The sporadic presence of *Characichnos* (swimming traces) indicates that some of those water bodies were relatively deep, at least temporarily. The rest of the tracks were imprinted in the vicinity of those water bodies, without drastic changes in the main faunal components between near-channel environments and the floodplain. It is possible that those seasonal palaeoenvironments were more short-lived than those described in the Pyrenean Basin (Mujal et al., 2016, 2018), posing a challenge for the survival of aquatic taxa. Even though no evidence of their presence has been confirmed so far, it is likely that fish and amphibians did live in the major, active channels, where preservation of biotic traces or fossils was much more difficult given the generally coarser grain size, higher energy conditions and the mode of locomotion of the (aquatic) faunas, which may have not touched the substrate (Mujal and Schoch, 2020).

Therefore, compared to the ichnoassemblages of the lower Permian of the Pyrenean Basin, those from Mallorca show that tetrapods did not have a preferential distribution with respect to the main water bodies, as the ichnoassemblages of near-channel palaeoenvironments are essentially the same as those of the floodplain palaeoenvironments. It is unlikely that the apparent absence of anamniotes was because of the semi-arid climate, as even in the hyper-arid "wet desert" of the upper Permian Moradi Formation of central Africa, Smith et al. (2015 and references therein) reported fish coprolites and two endemic temnospondyl species: *Nigerpeton*, interpreted to have been aquatic, and *Saharastega*,

Fig. 16. Reconstruction of the palaeoecosystem of the Artinskian–Kungurian (Cisuralian, lower Permian) Port des Canonge Formation of Mallorca. In the foreground, there is a small captorhinid eureptile (Matamales-Andreu et al., 2021e, purported trackmaker of the small form of *Hyloidichnus bifurcatus*) walking on the mud, where desiccation cracks are starting to develop. Imprinted in it there are the ichnotaxa *Hyloidichnus bifurcatus* (small and large morphotypes), *Dromopus* isp. and *Dimetropus leisnerianus*. In the background, two indeterminate "pelycosaur"-grade synapsids (purported trackmakers of *Dimetropus leisnerianus*) approach a large moradisaurine captorhinid eureptile (Liebrecht et al., 2017; purported trackmaker of the large form of *Hyloidichnus bifurcatus*). On the water surface there are several ?*Feysia* conifer shoots, and a tree log uprooted in a previous flood. Created by Henry Sutherland Sharpe. © 2021 Henry Sutherland Sharpe. Used under license.

possibly more terrestrially adapted (Sidor et al., 2005; Steyer et al., 2006). All these animals probably lived in groundwater-fed perennial lakes. A situation similar to that of Mallorca probably occurs in the Artinskian deposits of northern Africa: in the Koudiat El Hamra - Haiane Basin, Zouicha et al. (2021) described an ichnoassemblage in which tracks attributable to anamniote trackmakers (cf. *Batrachichnus*) were scarce (<10%), whereas in the palaeogeographically close and probably coeval Tiddas Basin, Voigt et al. (2011) reported that tracks produced by anamniote trackmakers were very abundant (80%). This reflects the high variability in the distribution of these forms, and suggests that the lack of tracks attributed to anamniote trackmakers in Mallorca may be a consequence of the local palaeoenvironment rather than reflecting a true palaeobiogeographic pattern.

8.3.2. Distribution of the tetrapod tracks Hyloidichnus and Dimetropus

Hyloidichnus, attributed to captorhinomorph trackmakers (Logghe et al., 2021), and *Dimetropus*, attributed to "pelycosaur"-grade synapsids (Matamales-Andreu et al., 2021d), are two ichnogenera that appear in the Permian of Mallorca and that were common in the equatorial latitudes of central Pangaea (Marchetti et al., 2019d, 2022 and references therein; Matamales-Andreu et al., 2021c). However, despite the large number of samples collected from central Europe, *Hyloidichnus* seems to be missing (*e.g.*, Voigt, 2005). In a similar manner, *Dimetropus* appears to be extremely rare in the well-sampled sites of the Southern Alps (*e.g.*, Santi et al., 2020; Marchetti et al., 2022).

In both cases, those "gaps" in their distribution are probably caused by a biostratigraphic bias rather than by a true palaeobiogeographical effect. The oldest occurrence of *Hyloidichnus*, from the Abo Formation of Southern North America, has been dated as 'Coyotean', in this case corresponding to the Sakmarian (Lucas et al., 2013; Schneider et al., 2020). *Hyloidichnus* has yet to be reported from any other Sakmarian–lower Artinskian tetrapod-bearing units of the Massif Central and central Europe (Voigt, 2005; Gand and Durand, 2006; Marchetti et al., 2019d), perhaps reflecting low abundance or absence of trackmakers of *Hyloidichnus* there during the Sakmarian. It is only during the middle Artinskian and the Kungurian (after the sauropsid radiation *sensu* Marchetti et al., 2019d), that *Hyloidichnus* becomes abundant and almost ubiquitous (Marchetti et al., 2019d). The reason behind the rarity of *Dimetropus* in outcrops of the Southern Alps (Marchetti, 2016) is probably similar, as it is the youngest (*i.e.*, Kungurian) confirmed record of this ichnogenus worldwide (Marchetti et al., 2019d; Santi et al., 2020; but see Lucas et al., 1999, and Gand and Durand, 2006, for other putative records of this ichnogenus from the middle/upper Permian). Even though the presence of large "pelycosaur"-grade synapsids has been suggested in slightly younger deposits of the western peri-Tethys (Roadian of Sardigna: Romano et al., 2019), it is possible that by the late Kungurian they had become relatively rare (Marchetti et al., 2022). This is in contrast to the pre-Kungurian times, when pelycosaurs seem to have been abundant worldwide, at least based on their purported tracks (Marchetti et al., 2019d, 2022). Therefore, both *Hyloidichnus* and *Dimetropus* seem to have attained widespread distribution in central Pangaea, and their absence or paucity in some regions may reflect a bias caused by the chronology of the different units.

8.4. The Permian–Triassic cycle in the Balearic Islands

In the Balearic Islands, Permian and Lower–Middle Triassic rocks representing continental palaeoenvironments only crop out on Mallorca and Menorca, whereas Middle–Upper Triassic marine and lagoonal facies appear on Mallorca, Menorca, Eivissa and Cabrera. It is currently unknown if all the islands were part of the same basin or if sedimentation took place in separate, small basins, although the latter is currently the most accepted hypothesis (*e.g.*, López-Gómez et al., 2019a). Based on the review and update of all the age attributions kown so far, this section proposes a correlation scheme between the three major islands (Fig. 17).

The tripartite nature of the Permian series of Mallorca and Menorca could indicate they underwent a similar tectonic history with three main phases of activity, especially given their close geographical location. In Menorca, the Permian sequence consists of three units, named, from base to top, P1, P2 and P3 (Rosell et al., 1988) (Fig. 17). The P1 unit corresponds to transversal alluvial-fan conglomerates deposited in the first phases of rifting, the P2 unit comprises floodplain lutites with rare interbedded crevasse splay sandstones, and the P3 unit represents an alluvial plain with abundant sandstones corresponding to flashflood and meandering channel deposits (*e.g.*, Matamales-Andreu et al., 2021c). In Mallorca, the lower unit (Bec de s'Àguila Formation) is essentially equivalent to the P1 unit, although neither units have been precisely dated. Regarding the other units, a similar trend exists in that the upper ones (P3 unit and Pedra de s'Ase Formation) are coarser-grained and show evidence of high-energy episodes, which are very rare in the middle units (P2 unit and Port des Canonge Formation). The P2 unit has not been reliably dated (Matamales-Andreu et al., 2021c), whereas the upper part of the Port des Canonge Formation is here dated to the Artinskian–Kungurian (see '8.1.3. Tetrapod track biostratigraphy' above). The upper part of the P3 unit has been dated to the Wuchiapingian–Changshingian (Bercovici et al., 2009), whereas the middle part of the Pedra de s'Ase Formation is considered Roadian–Wordian (see '8.1.2. Palynostratigraphy' above). Following this scheme, the P2 unit is tentatively considered lower Permian, and deposition of the unit P3 and the Pedra de s'Ase Formation may also have been coeval, at least in their lower parts (Fig. 17).

The *Buntsandstein* facies (Lower–Middle Triassic) of Mallorca and Menorca also follow a similar upwards trend. On Menorca, the base of the B1 unit is represented by a conglomerate of rounded quartz pebbles and ventifacts (Rosell et al., 1988; Linol et al., 2009). Such beds were interpreted as the reworking of aeolian-dominated plains by braided rivers, and were tentatively dated as Lower Triassic upon correlation with similar units of the western peri-Tethys (Linol et al., 2009). The rest of the unit has been interpreted as a braided river system, with a marked paucity of fine-grained sediments (Rosell et al., 1988). This unit can be correlated to the Punta Roja Formation of Mallorca (Matamales-Andreu et al., 2021b), which is lithologically similar, but appears to lack the basal conglomerate (Fig. 17). This appears to be similar to the Triassic deposits of Provençe, where conglomerates only appeared in sections located near the depocentre of the basin ("Sanary type"), and towards the margins, the deposits are above a disconformity ("Gonfaron type") or an angular unconformity ("Vidauban type") (Durand, 2006). As indicated above, it is possible that the sequences of Mallorca and Menorca were deposited in two different basins; regardless, it appears that in the former, sedimentation took place near the margin of the basin (probably a "Vidauban type" boundary), whereas in the latter it occurred in the deepest parts ("Gonfaron type" boundary). The rest of the continental Triassic beds of Menorca are included in the unit B2, representing floodplain and meandering river deposits in its lower part, and coastal deposits transitional to the overlying *Muschelkalk* marine facies in the upper part (Gómez-Gras, 1987; Linol et al., 2009). On Mallorca, its lateral equivalents are the Estellencs Formation (Matamales-Andreu et al., 2021b) for the lower part and, possibly, the M2 unit for its upper part (Fig. 17). The braided river interval of the Pedra Alta Formation and the tidal mud-flats of the Son Serralta Formation (Matamales-Andreu et al., 2021b) have not been identified on Menorca (Fig. 17). The absence of the latter is because the M1 unit (see below) appears to be also missing on Menorca, and the Son Serralta Formation represents the coastal environments before the initial marine transgression during the Anisian (Matamales-Andreu et al., 2021b) (Fig. 17).

The *Muschelkalk* facies (Middle–Upper Triassic) crop out on the three major islands of the Balearic Archipelago, but each of them appears to have unique traits. On Mallorca, three main units have been described: M1, corresponding a first marine transgression, represented by dolostones, probably of middle–upper Anisian stage (Rodríguez-Perea et al., 1987; Matamales-Andreu et al., 2021f), M2, interpreted as mud-flats deposited during a brief regressive pulse (Matamales-Andreu et al.,

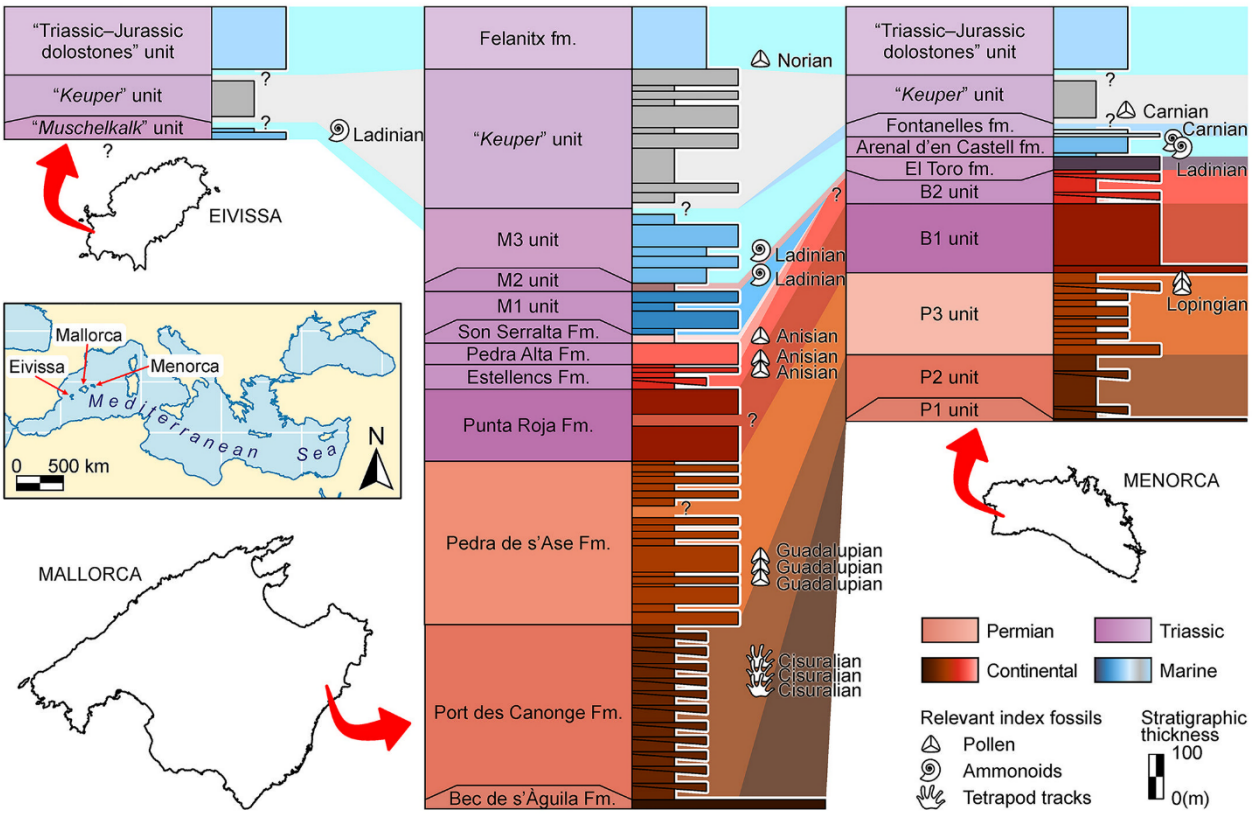

Fig. 17. Correlation proposal of the Permian and Triassic sequences of the Balearic Islands, with continental units represented by brown-red-pink colours, lagoonal units in grey and marine units in blue. Biostratigraphically relevant fossils are indicated, together with their age attribution. Changes in background colours represent boundaries between similar lithosomes, but do not imply isochrony. Thicknesses based on: Rangheard (1971) ["*Keuper*" and "Triassic–Jurassic dolostones" units of Eivissa, approximate]; Bourrouilh (1983) ["*Keuper*" and "Triassic–Jurassic dolostones" units of Menorca, approximate]; Gómez-Gras (1987) [B1 and B2 units]; Rodríguez-Perea et al. (1987) ["*Muschelkalk*" unit of Eivissa]; Barnolas (1991a, 1991b) [Felanitx fm., approximate]; Escudero-Mozo et al. (2014) [El Toro, Arenal d'en Castell and Fontanelles formations]; Matamales-Andreu et al. (2021b) [Estellencs Formation, Pedra Alta Formation, Son Serralta Formation and upper part of the Punta Roja Formation]; Matamales-Andreu et al. (2021c) [P1, P2 and P3 units]; Matamales-Andreu et al. (2021f) [M1, M2, M3 and "*Keuper*" units of Mallorca, approximate]; the present work [Bec de s'Àguila Formation, Port des Canonge Formation, Pedra de s'Ase Formation and lower part of the Punta Roja Formation]. Age attributions based on: Rangheard (1971) [upper Ladinian *Protrachyceras* sp. from Eivissa]; Boutet et al. (1982) [upper Norian spores/pollen from Mallorca]; Rosell et al. (1989) [lower Carnian spores/pollen from Menorca]; Bercovici et al. (2009) [Lopingian spores/pollen from Menorca]; Diez et al. (2010) [lower Anisian spores/pollen from Mallorca]; Escudero-Mozo et al. (2014) [lower Ladinian *Eoprotrachyceras vilanovai*, upper Ladinian *Protrachyceras* spp. and lower Carnian *Daxatina canadensis* from Menorca]; Matamales-Andreu et al. (2021f) [lower Ladinian *Gevanites* spp. and upper Ladinian *Protrachyceras* sp. from Mallorca]; the present work [Cisuralian *Dimetropus* ispp. and Guadalupian spores/pollen from Mallorca].

2021f), and M3, the second marine transgression, with a lower part comprising dolostones and an upper part of limestones (Rodríguez-Perea et al., 1987; Matamales-Andreu et al., 2021f). The ammonoids of the genus *Gevanites* reported by Virgili (1952) and Goy (1995) represent the lower Ladinian (Pérez-Valera et al., 2016), and ammonoids of the genus *Protrachyceras* found in the upper M3 limestones indicate an upper Ladinian stage for those (Matamales-Andreu et al., 2021f). On Eivissa, the Middle Triassic marine sequence has not yet been studied in detail. Rangheard (1971) distinguished two main units, a lower one made up of limestones and calcareous dolostones (not represented in Fig. 17 because of lack of more precise information), and an upper unit of limestones containing, among others, the ammonoid genus *Protrachyceras*, indicative of the upper Ladinian (Pérez-Valera, 2015). The lower unit might be correlatable to the lower M3 dolostones of Mallorca and El Toro formation of Menorca (note that the *Muschelkalk* formations of Menorca are not formally described, as stratotypes were not defined by Escudero-Mozo et al., 2014), and the upper unit is equivalent, at least in part, to the upper M3 limestones of Mallorca and the Arenal d'en Castell formation of Menorca (Fig. 17). On Menorca, it seems that the first Middle Triassic transgression event did not reach the area, as there is a single, continuous sequence (Escudero-Mozo et al., 2014). It probably rests upon a lateral equivalent of the M2 unit of Mallorca, which on Menorca is continuous with the underlying red-beds (Fig. 17), similar to the most proximal areas of Iberia (Arche et al., 2004; López-Gómez et al., 2019a). As implied above, El Toro formation, made up of dolostones, is probably equivalent to the lower part of the M3 dolostones of Mallorca and Eivissa (Fig. 17). The Arenal d'en Castell formation, with a lower part dated to the lower Ladinian because of the presence of the ammonoid *Eoprotrachyceras curionii*, a middle part dated as upper Ladinian based on the presence of the ammonoid *Protrachyceras hispanicum*, and an upper part dated as lower Carnian based on the presence of the ammonoid *Daxatina canadensis* (Escudero-Mozo et al., 2014), roughly agrees in age and lithology with the M3 of Mallorca and Eivissa (Fig. 17). The lower part of the M3 of Mallorca, however, also yielded the ammonoid genus *Gevanites* (*e.g.*, Goy, 1995) and is, therefore, of a different bioprovince than the deposits of Menorca (Sephardic faunas *vs.* northeastern Iberian Peninsula faunas: Pérez-Valera, 2015). This suggests that the units of Mallorca and Menorca were deposited in two different basins, at least until the lower part of the upper M3 limestones. The Fontanelles formation is dated as lower Carnian based on the

presence of the ammonoid species *Daxatina canadensis* in the upper part of the underlying Arenal d'en Castell formation, typical of the lower Carnian (Escudero-Mozo et al., 2014), and a lower Carnian palynoassemblage described from the base of the overlying *Keuper* facies (Rosell et al., 1989). An equivalent to the Fontanelles formation has not yet been found on the other islands, as it is probably coeval with the lower part of the *Keuper* facies elsewhere (Fig. 17).

Keuper facies (Upper Triassic) have been poorly studied on the three islands, as they are usually strongly deformed and relatively complete sequences have so far been described only on Mallorca (Rodríguez-Perea et al., 1987). On Menorca, the base of the *Keuper* contains a palynoassemblage that was dated to the lower Carnian (Rosell et al., 1989). Correlations among the *Keuper* units of each island are only tentative, given the lack of detailed stratigraphic and palaeontological studies (Fig. 17). The uppermost Triassic–lowermost Jurassic dolostones of the Balearic Islands (Felanitx formation on Mallorca, with a base dated to the upper Norian by Boutet et al., 1982) have not been described in detail either (Fig. 17).

Using this information, the following is a preliminary reconstruction of the tectonosedimentary evolution of the Permian–Triassic basins of the Balearic Islands. The basin of Mallorca experienced a higher subsidence rate, since in all cases, the sequences are thicker than those of Menorca. After an initial stage of colluvial/alluvial transverse sedimentation as a consequence of the opening of the basins (Bec de s'Àguila Formation and P1 unit), axial sedimentation took place through meandering river systems (Port des Canonge Formation and P2 unit). Towards the upper part of the sequences, flashflood events appear to have become more common (Pedra de s'Ase Formation and P3 unit). This was followed by a period of no sedimentation and erosion, probably during the uppermost Permian and lowermost Triassic. Deposition began again as a result of shallow braided river systems transporting quartz-rich sands (Punta Roja Formation and B1 unit). On Menorca, this unit is initiated with a basal conglomerate, probably indicating that the sequence corresponds to the deeper part of the basin, whereas in the case of Mallorca, the lack of basal conglomerate suggests that the sequences represent more marginal parts of the basin (see discussion above on unconformity types *sensu* Durand, 2006). Following this, floodplains and meandering rivers developed (Estellencs Formation and lower part of B2 unit). On Mallorca, this unit is overlain by braided river deposits (Pedra Alta Formation), tidal mud-flats (Son Serralta Formation) and the first shallow carbonate platform (M1 unit). This first marine unit is absent on Menorca, indicating that the Anisian Tethys transgression did not reach that basin, suggesting that it was at higher altitude and perhaps further inland. After that, there was a brief regressive event, in which mud-flats developed on Mallorca (M2 unit). This was followed by a more extensive transgression, developing tidal mud-flats on Menorca (upper part of the B2 unit) and completely flooding those basins ("*Muschelkalk*" unit of Eivissa, M3 unit, El Toro and Arenal d'en Castell formations). At least during the first stages of flooding, the basins of Mallorca and Menorca were not connected, as indicated by the different palaeobiogeographical affinities of the ammonoid faunas. An important regressive event took place at the early Carnian, indicated by a karstified interval on Menorca and probably the onset of sedimentation of the "*Keuper*" sabkha units on Eivissa and Mallorca. After that, a short-lived transgressive pulse again flooded the basin of Menorca (Fontanelles formation), which was followed by deposition of the "*Keuper*" unit. This transgression has not been recognised in neither Eivissa nor Mallorca, perhaps indicating a lower subsidence rate for the latter two during that time. Finally, another major transgressive event occurred in the late Norian (Felanitx formation and "Triassic–Jurassic dolostone" units of Menorca and Eivissa), which gave way to the Jurassic marine platforms.

9. Conclusions

The present work offers a comprehensive and interdisciplinary review of all the previous studies on the Permian deposits of Mallorca (Balearic Islands, western Mediterranean), together with new analyses, integrating data on lithostratigraphy, magnetostratigraphy, palaeobotany, palaeoichnology and biochronology. Three formal lithostratigraphic units have been described, from lower to upper these being: the Bec de s'Àguila Formation (colluvium, alluvial fans and meandering rivers), the Port des Canonge Formation (meandering rivers with abundant floodplain deposits) and the Pedra de s'Ase Formation (meandering rivers with scarce floodplain deposits). A detailed reconstruction of the palaeoecosystem has been provided for each of them, integrating the study of stratigraphy, sedimentology and fossils. The latter, together with the palaeomagnetic data, have also yielded chronostratigraphic information for all the units, dating the sequence between the lower and the middle Permian for the first time.

The floras and faunas are similar to those of other sites of the western peri-Tethys. The tetrapod ichnites of the Port des Canonge Formation reveal an ichnoassemblage with typical components of the palaeoequatorial early Permian, with tracks attributed to captorhinomorph eureptiles, araeoscelidian diapsids/non-varanodontine varanopids, pareiasauromorph parareptiles, "pelycosaur"-grade synapsids and other indeterminate synapsids. The lack of anamniote tracks probably points to a palaeoenvironmental bias, as the tracksites correspond to relatively short-lived waterhole margins in which water-dependent anamniotes may have struggled to survive. The pollen of the overlying Pedra Alta Formation, of 'Thuringian' character (middle–late Permian), shows a diverse plant community with abundance of conifers, where the paucity of horsetail/fern spores probably points to semi-arid climate conditions. The age of this formation has been further costrained by magnetostratigraphy, which revealed that the entire Permian sequence falls within the Kiaman reverse Superchron (middle Carboniferous–middle Permian). This detailed characterisation has made it possible to provide the timing of the different phases of the Permian–Triassic tectonosedimentary evolution of the Balearic Islands, which is similar to the situation in the rest of the western peri-Tethys.

The present work shows the diverse palaeoecosystems of the early–middle Permian of eastern equatorial Pangaea during a period of global sauropsid and synapsid diversification. It also manifests the fossiliferous potential of the deposits of the Iberian area, and the importance of comprehensive interdisciplinary studies to better correlate the sedimentary succesions from different basins and understand their evolution through time.

Declaration of Competing Interest

The authors declare that they have no known competing financial interests or personal relationships that could have appeared to influence the work reported in this paper.

Acknowledgements

We thank Sebastià Matamalas and Antoni Pasqual for assistance with fieldwork. To Feliu Calafat, Tomeu Sáez, Antoni Rodríguez Perea (UIB, Palma) and Joan Josep Fornós (UIB, Palma) for providing historical pictures of the outcrops and fossils. To David Gómez Gras (UAB, Cerdanyola del Vallès), Jocelyn Falconnet (MNHN, Paris) and Jean Broutin (UPMC, Paris) for providing literature. To Llorenç Homar (UIB, Palma) and Onofre Rullan (UIB, Palma) for offering an insight into local toponymy. To Judit Marigó (ICP, Cerdanyola del Vallès) for reviewing the English. To the three reviewers, two anonymous and Philip John Hancox (ESI, Johannesburg) for their insightful comments. To the editor, Christopher Fielding, for handling the manuscript. To the Comissió Insular de Patrimoni Històric (Consell Insular de Mallorca) for granting us the excavation permits (file number 75/2021). We acknowledge support from the CERCA program (Generalitat de Catalunya). R.M.A. was supported by the predoctoral grant FPU17/01922 (Ministerio de Ciencia, Innovación y Universidades) and the travel grant Synthesys+ DE-TAF-23 (European Commission). O.O. and À.G. are members of the

consolidated research group 2017 SGR 1666 GRC (Generalitat de Catalunya). J.F. is member of the consolidated research group 2017 SGR 086 GRC (Generalitat de Catalunya). J.F. acknowledges support of the grant PID2020-117118GB-I00 funded by MCIN/AEI/10.13039/501100011033. We acknowledge support from the project "Mallorca abans dels dinosaures: estudi dels ecosistemes continentals del Permià i Triàsic amb especial èmfasi en les restes de vertebrats" (ref. 15 - 619/2020), based at the Institut Català de Paleontologia Miquel Crusafont and funded by the Departament de Cultura, Patrimoni i Política Lingüística (Consell Insular de Mallorca).

Appendix A. Supplementary data

Supplementary data to this article can be found online at https://doi.org/10.1016/j.earscirev.2022.103948.

References

Alonso-Zarza, A.M., 2003. Palaeoenvironmental significance of palustrine carbonates and calcretes in the geological record. Earth Sci. Rev. 60, 261–298.
Alvin, K.L., Watson, J., Spicer, R.A., 1994. A new coniferous male cone from the English Wealden and a discussion of pollination in the Cheirolepidiaecae. Palaeontology 37 (1), 173–180.
Arche, A., López-Gómez, J., 2006. Late Permian to Early Triassic transition in central and NE Spain: biotic and sedimentary characteristics. Geol. Soc. Lond. Spec. Publ. 265, 261–280.
Arche, A., López-Gómez, J., Vargas, H., 2002. Propuesta de correlación entre los sedimentos Pérmicos y Triásicos de la Cordillera Ibérica Este y de las Islas Baleares. Geogaceta 32, 275–278.
Arche, A., López-Gómez, J., Marzo, M., Vargas, H., 2004. The siliciclastic Permian-Triassic deposits in Central and Northeastern Iberian Peninsula (Iberian, Ebro and Catalan Basins): a proposal for correlation. Geol. Acta 2 (4), 306–320.
Balme, B.E., 1995. Fossil in situ spores and pollen grains: an annotated catalogue. Rev. Palaeobot. Palynol. 87 (2–4), 81–323.
Banda, E., Parés, J.M., Freeman, R., 1986. La técnica del paleomagnetismo. Estudio piloto en los bordes de la cuenca balear. Estud. Geol. 42, 147–165.
Baranyi, V., Rostási, Á., Raucsik, B., Kürschner, W.M., 2019. Palynological and X-ray fluorescence (XRF) data of Carnian (Late Triassic) formations from western Hungary. Data in Brief 23, 103858.
Barnolas, A., 1991a. Mapa Geológico de España. Escala 1:50.000. Andraitx. Segunda serie, primera edición. Instituto Tecnológico GeoMinero de España, Madrid (56 pp. + 1 map + 5 stratigraphic logs).
Barnolas, A., 1991b. Mapa Geológico de España. Escala 1:50.000. Sóller. Segunda serie, primera edición. Instituto Tecnológico GeoMinero de España, Madrid (62 pp. + 1 map + 8 stratigraphic logs).
Baucon, A., Ronchi, A., Felletti, F., Neto de Carvalho, C., 2014. Evolution of Crustaceans at the edge of the end-Permian crisis: Ichnonetwork analysis of the fluvial succession of Nurra (Permian–Triassic, Sardinia, Italy). Palaeogeogr. Palaeoclimatol. Palaeoecol. 410, 74–103.
Baudrick, C.A., Grant, G.E., 2001. Transport and deposition of large woody debris in streams: a flume experiment. Geomorphology 41, 263–283.
Bek, J., Drábková, J., Dašková, J., Libertín, M., 2008. The sub-arborescent lycopsid genus Polysporia Newberry and its spores from the Pennsylvanian (Bolsovian–Stephanian B) continental basins of the Czech Republic. Rev. Palaeobot. Palynol. 152 (3–4), 176–199.
Benson, R.B., Upchurch, P., 2013. Diversity trends in the establishment of terrestrial vertebrate ecosystems: interactions between spatial and temporal sampling biases. Geology 41, 43–46.
Benton, M.J., 2008. When Life Nearly Died. The Greatest Mass Extinction of All Time. Thames & Hudson, London, p. 336.
Benton, M.J., Twitchett, R.J., 2003. How to kill (almost) all life: the end-Permian extinction event. Trends Ecol. Evol. 18 (7), 358–365.
Bercovici, A., Diez, J.B., Broutin, J., Bourquin, S., Linol, B., Villanueva-Amadoz, U., López-Gómez, J., Durand, M., 2009. A palaeoenvirnomental analysis of Permian sediments in Minorca (Balearic Islands, Spain) with new palynological and megafloral data. Rev. Palaeobot. Palynol. 158, 14–28.
Bernardi, M., Petti, F.M., Kustatscher, E., Franz, M., Hartkopf-Fröder, C., Labandeira, C. C., Wappler, T., van Konijnenburg-van Cittert, J.H.A., Peecook, B.R., Angielczyk, K. D., 2017. Late Permian (Lopingian) terrestrial ecosystems: a global comparison with new data from the low-latitude Bletterbach Biota. Earth Sci. Rev. 175, 18–43.
Billings, E., 1861–1865. Palaeozoic fossils. Volume I. Contaning descriptions and figures of new or little known species of organic remains from the Silurian rocks. In: Geological Survey of Canada. Dawson Brothers & Baillière, Montreal, London, New York, Paris, p. 426.
Borruel-Abadía, V., López-Gómez, J., De la Horra, R., Galán-Abellán, B., Barrenechea, J. F., Arche, A., Ronchi, A., Gretter, N., Marzo, M., 2015. Climate changes during the Early–Middle Triassic transition in the E. Iberian plate and their palaeogeographic significance in the western Tethys continental domain. Palaeogeogr. Palaeoclimatol. Palaeoecol. 440, 671–689.
Bourquin, S., Durand, M., Diez, J.B., Broutin, J., Fluteau, F., 2007. The Permian-Triassic boundary and Early Triassic sedimentation in Western European Basins: an overview. J. Iberian Geol. 33 (2), 221–236.
Bourquin, S., Bercovici, A., López-Gómez, J., Diez, J.B., Broutin, J., Ronchi, A., Durand, M., Arché, A., Linol, B., Amour, F., 2011. The Permian–Triassic transition and the onset of Mesozoic sedimentation at the northwestern peri-Tethyan domain scale: palaeogeographic maps and geodynamic implications. Palaeogeogr. Palaeoclimatol. Palaeoecol. 299, 265–280.
Bourrouilh, R., 1983. Estratigrafía, sedimentología y tectónica de la isla de Menorca y del noreste de Mallorca, 99. Memorias del Instituto Geológico y Minero de España (672 pp. + 95 pl. + 3 maps).
Boutet, C., Rangheard, Y., Rosenthal, P., Visscher, H., Durand-Delga, M., 1982. Découverte d'une microflore d'âge Norien dans la Sierra Norte de Majorque (Baléares, Espagne). Comp. Rend. Acad. Sci. Paris 2 (294), 1267–1270.
Boyd, C., McIlroy, D., 2017. Three-dimensional morphology of Beaconites capronus from northeast England. Ichnos 24 (4), 250–258.
Bradshaw, M.A., 1981. Paleoenvironmental interpretations and systematics of Devonian trace fossils from the Taylor Group (lower Beacon Supergroup), Antarctica. New Zeal. J. Geol. Geophys. 24, 615–652.
Brocklehurst, N., 2020. Olson's Gap or Olson's Extinction? A Bayesian tip-dating approach to resolving stratigraphic uncertainty. Proc. R. Soc. B 287, 20200154.
Brocklehurst, N., Kammerer, C.F., Fröbisch, J., 2013. The early evolution of synapsids, and the influence of sampling on their fossil record. Paleobiology 39, 470–490.
Brocklehurst, N., Day, M.O., Rubidge, B.S., Fröbisch, J., 2017. Olson's Extinction and the latitudinal biodiversity gradient of tetrapods in the Permian. Proc. R. Soc. B 284, 20170231.
Broutin, J., Kerp, H., 1994. Aspects of Permian palaeobotany and palynology. XIV. A new form-genus of broad-leaved late carboniferous and early Permian Northern hemisphere conifers. Rev. Palaeobot. Palynol. 83 (1–3), 241–251.
Buatois, L.A., Mángano, M.G., 1998. Trace fossil analysis of lacustrine facies and basins. Palaeogeogr. Palaeoclimatol. Palaeoecol. 140, 367–382.
Buchwitz, M., Voigt, S., 2018. On the morphological variability of Ichniotherium tracks and evolution of locomotion in the sistergroup of amniotes. PeerJ 6, e4346.
Calafat, F., 1986. Estratigrafía y sedimentología de la litofacies Buntsandstein de Mallorca. In: Cabrera, L. (Ed.), Resúmenes del XI Congreso Español de Sedimentología. Grupo Español de Sedimentología, Barcelona, p. 39.
Calafat, F., 1987. Paleoambients de les facies Buntsandstein de Mallorca. In: Llibre de resums de les I Jornades del Medi Ambient de les Illes Balears. Societat d'Història Natural de les Balears, Palma, pp. 16–17.
Calafat, F., 1988. Estratigrafía y sedimentología de la litofacies Buntsandstein de Mallorca. Bachelor's Thesis. Universitat de Barcelona, Barcelona (127 pp. + 31 annexed figs).
Calafat, F., Fornós, J.J., Marzo, M., Ramos, E., Rodríguez-Perea, A., 1986. Icnología de vertebrados de las facies Buntsandstein de Mallorca. In: Cabrera, L. (Ed.), Resúmenes del XI Congreso Español de Sedimentología. Grupo Español de Sedimentología, Barcelona, p. 40.
Calafat, F., Fornós, J.J., Marzo, M., Ramos-Guerrero, E., Rodríguez-Perea, A., 1986–1987. Icnología de vertebrados de las facies Buntsandstein de Mallorca. Acta Geol. Hispàn. 21–22, 515–520.
Cassinis, G., Ronchi, A., 2002. The (late-) Post-Variscan continental succession of Sardinia. Rend. Soc. Paleontol. Ital. 1, 77–92.
Cassinis, G., Durand, M., Ronchi, A., 2003. Permian-Triassic continental sequences of Northwest Sardinia and South Provence: stratigraphic correlations and palaeogeographical implications. Boll. Soc. Geol. Ital. 2, 119–129.
Cassinis, G., Perotti, C.R., Ronchi, A., 2012. Permian continental basins in the Southern Alps (Italy) and peri-mediterranean correlations. Int. J. Earth Sci. 101, 129–157.
Clement-Westerhof, J.A., 1974. *In situ* pollen from gymnospermous cones from the Upper Permian of Italian Alps – A preliminary account. Rev. Palaeobot. Palynol. 17, 63–73.
Clement-Westerhof, J.A., 1984. Aspects of Permian palaeobotany and palynology. IV. The conifer Ortiseia Florin from the Val Gardena Formation of the Dolomites and the Vicentinian Alps (Italy) with special reference to a revised concept of the Walchiaceae (Göppert) Schimper. Rev. Palaeobot. Palynol. 41 (1), 51–166.
Clement-Westerhof, J.A., 1987. Aspects of Permian palaeobotany and palynology. VII. The Majonicaceae, a new family of Late Permian conifers. Rev. Palaeobot. Palynol. 52 (4), 375–402.
Colombo, F., 2010a. Abanicos aluviales: procesos de transporte y acumulación de materiales detríticos. In: Arche, A. (Ed.), Sedimentología. Del proceso físico a la cuenca sedimentaria. Consejo Superior de Investigaciones Científicas, Madrid, pp. 85–130.
Colombo, F., 2010b. Abanicos aluviales: secuencias y modelos de sedimentación. In: Arche, A. (Ed.), Sedimentología. Del proceso físico a la cuenca sedimentaria. Consejo Superior de Investigaciones Científicas, Madrid, pp. 131–224.
Couper, R.A., 1953. Upper Mesozoic and Cainozoic spores and pollen grains from New Zealand. New Zeal. Geol. Surv. Paleontol. Bull. 22, 1–77.
Cuevas-López, F., 1958a. Informe geológico y minero de los yacimientos de cobre de Banyalbufar y Estallenchs, Mallorca (Barcelona. 37 pp. + 8 figs).
Cuevas-López, F., 1958b. Informe geológico y minero de los yacimientos de cobre de Banyalbufar y Valldemosa, Mallorca (Barcelona. 23 pp. + 7 figs).
d'Orbigny, A., 1842. Voyage dans l'Amérique méridionale (le Brésil, la République Orientale de l'Uruguay, la République Argentine, la Patagonie, la République du Chili, la République de Bolivia, la République du Perou) exécuté pendant les années 1826, 1827, 1828, 1829, 1830, 1831, 1832 et 1833. In: Pitois-Levrault, Paris, Levrault, Strasbourg, 3(4) ((Paléontologie). 188 pp.).
Davies, N.S., Gibling, M.R., 2010. Paleozoic vegetation and the Siluro-Devonian rise of fluvial lateral accretion sets. Geology 38 (1), 51–54.

Day, M.O., Ramezani, J., Bowring, S.A., Sadler, P.M., Erwin, D.H., Abdala, F., Rubidge, B. S., 2015. When and how did the terrestrial mid-Permian mass extinction occur? Evidence from the tetrapod record of the Karoo Basin, South Africa. Proc. R. Soc. B 282 (20150834).

De la Horra, R., Galán-Abellán, A.B., López-Gómez, J., Barrenechea, J.F., Luque, F.J., Arche, A., Benito, M.I., 2012. Paleoecological and paleoenvironmental changes during the continental Middle–Late Permian transition at the SE Iberian Ranges, Spain. Glob. Planet. Change 94–95, 46–61.

de Ricqlès, A., Taquet, P., 1982. La faune de vertébrés du Permien Supérieur du Niger. I. Le captorhinomorphe *Moradisaurus grandis* (Reptilia, Cotylosauria). Le crane. Annales de Paléontologie (Vert.-Invert.) 68, 33–106.

Diez, J.B., 2000. Geología y Paleobotánica de la Facies Buntsandstein en la Rama Aragonesa de la Cordillera Ibérica. Implicaciones paleogeográficas en el Peritethys Occidental. Ph.D. dissertation. Universidad de Zaragoza–Université Pierre & Marie Curie, Paris VI, Zaragoza, Paris (424 pp.).

Diez, J.B., Broutin, J., Grauvogel-Stamm, L., Bourquin, S., Bercovici, A., Ferrer, J., 2010. Anisian floras from the NE Iberian Peninsula and Balearic Islands: a synthesis. Rev. Palaeobot. Palynol. 162, 522–542.

Díez-Canseco, D., Buatois, L.A., Mángano, M.G., Díaz-Molina, M., Benito, M.I., 2016. Ichnofauna from coastal meandering channel systems (Upper Cretaceous Tremp Formation, South-Central Pyrenees, Spain): delineating the fluvial-tidal transition. J. Paleontol. 90 (2), 250–268.

Dudgeon, P., 1878. Note on a new fossil footprint from the Permian sandstone of Dumfriesshire. Proc. R. Soc. Edinburgh 9, 154–155.

Durand, M., 2006. The problem of the transition from the Permian to the Triassic Series in southeastern France: comparison with other Peritethyan regions. Geol. Soc. Lond. Spec. Publ. 265, 281–296.

Durand, M., 2008. Permian to Triassic continental successions in southern Provence (France): an overview. Boll. Soc. Geol. Ital. 127 (3), 697–716.

Ebisemiju, F.S., 1994. The sinuosity of alluvial river channels in the seasonally wet tropical environment: Case study of river Elemi, southwestern Nigeria. Catena 21, 13–25.

Ellenberger, P., 1983. Sur l'intérêt paléontologique de la dalle à pistes de la Lieude (commune de Mérifons, Hérault, France). Soc. Protect. Nat. Languedoc Roussillon 1, 11–20.

Erwin, D.H., 1994. The Permo–Triassic extinction. Nature 367, 231–236.

Escudero-Mozo, M.J., Martín-Chivelet, J., Goy, A., López-Gómez, J., 2014. Middle-Upper Triassic carbonate platforms in Minorca (Balearic islands): implications for Western Tethys correlations. Sediment. Geol. 310, 41–48.

Florin, R., 1927. Preliminary descriptions of some Palaeozoic genera of Coniferae. Arkiv För Botanik 21A (13), 1–7.

Florin, R., 1934. Notes on the nomenclature of Palaeozoic conifers. Svensk Botanisk Tidskrift 26 (4), 468–469.

Forte, G., Kustatscher, E., Roghi, G., Preto, N., 2018. The Permian (Kungurian, Cisuralian) palaeoenvironment and palaeoclimate of the Tregiovo Basin, Italy: palaeobotanical, palynological and geochemical investigations. Palaeogeogr. Palaeoclimatol. Palaeoecol. 495, 186–204.

Francischini, H., Lucas, S.G., Voigt, S., Marchetti, L., Santucci, V.L., Knight, C.L., Wood, J.R., Dentzien-Dias, P., Schultz, C.L., 2020. On the presence of Ichniotherium in the Coconino Sandstone (Cisuralian) of the Grand Canyon and remarks on the occupation of deserts by non-amniote tetrapods. Paläontologische Zeitschrift 94, 207–225.

Franzel, M., Jones, S.J., Meadows, N., Allen, M.B., McCaffrey, K., Morgan, T., 2021. Basin-scale fluvial correlation and response to the Tethyan marine transgression: an example from the Triassic of central Spain. Basin Res. 33 (1), 1–25.

Freeman, T., Obrador, A., 1979. Paleosoils and coal in the distal part of the Spanish Buntsandstein (Menorca and Mallorca, Balearic Islands). Bol. Soc. Histor. Nat. Baleares 23, 47–50.

Gand, G., 1988. Les traces de vertébrés tétrapodes du Permien français: paléontologie, stratigraphie, paléoenvironnements. Ph.D. dissertation. Université de Bourgogne, Dijon (368 pp.).

Gand, G., Durand, M., 2006. Tetrapod footprint ichno-associations from French Permian basins. Comparisons with other Euramerican ichnofaunas. Geol. Soc. Lond. Spec. Publ. 265, 157–177.

Gand, G., Kerp, H., Parsons, C., Martínez-García, E., 1997. Palaeoenvironmental and stratigraphic aspects of animal traces and plant remains in Spanish Permian red beds (Peña Sagra, Cantabrian Mountains, Spain). Geobios 30 (2), 295–318.

Gand, G., Garric, J., Schneider, J., Walter, H., Lapeyrie, J., Martin, C., Thiery, A., 2008. Notostraca trackways in Permian playa environments of the Lodève basin (France). J. Iberian Geol. 34 (1), 73–108.

Geinitz, H.B., 1863. Beiträge zur Kenntnis der organischen Überreste in der Dyas. Geol. Paläontol. 1863, 385–398.

Gilmore, C.W., 1927. Fossil footprints of the Grand Canyon: second contribution. Smithsonian Miscellaneous Collections 80 (3), 1–78. + 21 pls.

Gómez-Gras, D.M., 1987. Estratigrafía física y petrología sedimentaria del Pérmico y Buntsandstein de la isla de Menorca. Bachelor's Thesis. Universitat Autònoma de Barcelona, Barcelona (XIV + 117 pp.).

Gómez-Gras, D.M., 1992. El Permotrías de las Baleares, de la Cordillera Costero Catalana y de la vertiente mediterránea de la Cordillera Ibérica: Facies y Petrología Sedimentaria. Ph.D. dissertation. Universitat Autònoma de Barcelona, Barcelona. XIX + 242 pp. + 55 figs. + 7 tabs.

Gómez-Gras, D., 1993. El Permotrías de las Baleares y de la vertiente mediterránea de la Cordillera Ibérica y del Maestrat: Facies y Petrología Sedimentaria (Parte II). Bol. Geol. Minero 104, 467–515.

Gómez-Gras, D., Alonso-Zarza, A.M., 2003. Reworked calcretes: their significance in the reconstruction of alluvial sequences (Permian and Triassic, Minorca, Balearic Islands, Spain). Sediment. Geol. 158, 299–319.

Good, C.W., 1979. Botryopteris pinnules with abaxial sporangia. Am. J. Bot. 66 (1), 19.

Gould, R.E., Delevoryas, T., 1977. The biology of Glossopteris: evidence from petrified seed-bearing and pollen-bearing organs. Alcheringa 1 (4), 387–399.

Goy, A., 1995. Ammonoideos del Triásico Medio de España: Bioestratigrafía y correlaciones. Cuadernos Geol. Ibérica 19, 21–60.

Grauvogel-Stamm, L., 1969. Nouveaux types d'organes reproducteurs mâles de Conifères du Grès à Voltzia (Trias inférieur) des Vosges. Bulletin du Service de la carte géologique d'Alsace et de Lorraine 22 (2), 93–120.

Grauvogel-Stamm, L., 1978. La flore du Grès à Voltzia (Buntsandstein supérieur) des Vosges du Nord (France). Morphologie, anatomie, interpretations phylogénique et paléogéographique. Sci. Géol. 50, 1–225. + 54 pl.

Gretter, N., Ronchi, A., López-Gómez, J., Arche, A., De la Horra, R., Barrenechea, J., Lago, M., 2015. The Late Palaeozoic-Early Mesozoic from the Catalan Pyrenees (Spain): 60 Myr of environmental evolution in the frame of the western peri-Tethyan palaeogeography. Earth Sci. Rev. 150, 679–708.

Gulbranson, E.L., Cornamusini, G., Ryberg, P.E., Corti, V., 2020. When does large woody debris influence ancient rivers? Dendrochronology applications in the Permian and Triassic, Antarctica. Palaeogeogr. Palaeoclimatol. Palaeoecol. 541, 109544.

Hall, J., 1847. Palaeontology of New York. Volume I. Containing Descriptions of the Organic Remains of the Lower Division of the New York System (Equivalent to the Lower Silurian rocks of Europe). C. van Benthuysen, Albany, New York (338 pp.).

Hasiotis, S.T., Platt, B.F., Hembree, D.I., Everhart, M.J., 2007. The trace-fossil record of vertebrates. In: William Miller, I.I.I. (Ed.), Trace Fossils: Concepts, Problems, Prospects. Elsevier Science, Amsterdam, Oxford, pp. 196–218.

Haubold, H., 1970. Versuch der Revision der Amphibien-Fährten des Karbon und Perm. Freiberger Forschungshefte C 260, 83–117.

Haubold, H., 1971. Ichnia Amphibiourum et Reptiliorum fossilium. In: Kuhn, O. (Ed.), Handbuch der Paläoherpetologie. Gustav Fischer Verlag, Stuttgart (124 pp.).

Haubold, H., 2000. Tetrapodenfährten aus dem Perm – Kenntnisstand und Progress 2000. Hallesches Jahrbuch für Geowissenschaften B 22, 1–16.

Heer, O., 1876–1877. Flora fossilis Helvetiae. Die vorweltliche Flora der Schweiz. Verlag J. Wurster & Co, Zürich (182 pp. [Parts 1, 2 (1876):1–90; Parts 3, 4 (1877): 91–182]).

Heinberg, C., 1974. A dynamic model for the meniscus filled tunnel (Anchorichnus n. ichnogen) from the Jurassic Pecten Sandstone of Milne Land, East Greenland. Grønlands Geologiske Undersøgelse 62, 1–20.

Henderson, C.M., Shen, S.Z., Gradstein, F.M., Agterberg, F.P., 2020. Chapter 24 - the permian period. In: Gradstein, F.M., Ogg, J.G., Schmitz, M.D., Ogg, G.M. (Eds.), Geologic Time Scale 2020. Elsevier, pp. 875–902.

Hernández-Castillo, G.R., Rothwell, G.W., Mapes, G., 2001. Thucydiaceae Fam. Nov., with a review and reevaluation of Paleozoic walchian conifers. Int. J. Plant Sci. 162 (5), 1155–1185.

Hitchcock, E., 1858. Ichnology of New England. A Report on the Sandstone of the Connecticut Valley, Especially Its Fossil Footmarks. W. White, Boston (220 pp.).

Homar, Ll, 1985. Toponímia del litoral de la costa d'Estellencs, Banyalbufar i Valldemossa: de na Foradada a sa Foradada. 7 aerial photographs.

Hounslow, M.W., Balabanov, Y.P., 2018. A geomagnetic polarity timescale for the Permian, calibrated to stage boundaries. Geol. Soc. Lond. Spec. Publ. 450 (1), 61–103.

Huisink, M., 2000. Changing river styles in response to Weichselian climate changes in the Vecht valley, eastern Netherlands. Sediment. Geol. 133, 115–134.

Hunt, A.P., Lucas, S.G., 2006. Permian tetrapod ichnofacies. Geol. Soc. Lond. Spec. Publ. 265, 137–156.

IDEIB, 2019. Infraestuctura de dades espacials de les Illes Balears. Conselleria d'Agricultura, Medi Ambient i Territori. Govern de les Illes Balears. http://www.ideib.cat (last accessed on 26/07/2019).

Juncal, M.A., 2019. Nuevas aportaciones a la palinoestratigrafía pérmica del dominio peritético occidental. Ph.D. dissertation. Universidade de Vigo, Vigo (361 pp.).

Juncal, M.A., Bourquin, S., Beccaletto, L., Diez, J.B., 2018. New sedimentological and palynological data from the Permian and Triassic series of the Sancerre-Couy core, Paris Basin, France. Geobios 51, 517–535.

Juncal, M.A., Diez, J.B., Lloret, J., de la Horra, R., Gretter, N., Ronchi, A., Barrenechea, J. F., Borruel-Abadía, V., López-Gómez, J., 2020. Re-calibrating the Late Palaeozoic palynostratigraphy in the basins of the southern domain of the Variscan Belt (southwestern Europe). In: EGU General Assembly 2020, Online, 4–8 May 2020: EGU2020-19788.

Kerp, J.H.F., 1988. Aspects of Permian palaeobotany and palynology. X. The West- and Central European species of the genus Autunia Krasser emend. Kerp (Peltaspermaceae) and the form-genus Rhachiphyllum Kerp (Callipterid Foliage). Rev. Palaeobot. Palynol. 54 (3–4), 249–360.

Kirschvink, J.L., 1980. The least-squares line and plane and the analysis of palaeomagnetic data. Geophys. J. Int. 62 (3), 699–718.

Klaus, W., 1963. Sporen aus dem südalpinen Perm: Vergleichsstudie für die Gliederung nordalpiner Salzserien. Jahrbuch der Geologischen Bundesanstalt Wien 106, 229–363.

Klein, H., Niedźwiedzki, G., 2012. Revision of the Lower Triassic tetrapod ichnofauna from Wióry, Holy Cross Mountains, Poland. New Mexico Museum Nat. History Sci. Bull. 56, 1–62.

Klembara, J., Berman, D.S., Henrici, A.C., Čerňanský, A., Werneburg, R., Martens, T., 2007. First description of skull of lower Permian Seymouria sanjuanensis (Seymouriamorpha: Seymouriidae) at an early juvenile growth stage. Ann. Carnegie Museum 76 (1), 53–72.

Koymans, M.R., Langereis, C.G., Pastor-Galán, D., van Hinsbergen, D.J.J., 2016. Paleomagnetism.org: an online multi-platform open source environment for paleomagnetic data analysis. Comput. Geosci. 93, 127–137.
Koymans, M.R., van Hinsbergen, D.J.J., Pastor-Galán, D., Vaes, B., Langereis, C.G., 2020. Towards FAIR paleomagnetic data management through Paleomagnetism.org 2.0. Geochem. Geophys. Geosyst. 21 (2) (e2019GC008838).
Krapovickas, V., Mángano, M.G., Mancuso, A., Marsicano, C.A., Volkheimer, W., 2008. Icnofaunas triásicas en abanicos aluviales distales: evidencias de la Formación Cerro Puntudo, cuenca cuyana, Argentina. Ameghiniana 45 (2), 463–472.
Kustatscher, E., van Konijnenburg-van Cittert, J.H.A., Roghi, G., 2010. Macrofloras and palynomorphs as possible proxies for palaeoclimatic and palaeoecological studies: a case study from the Pelsonian (Middle Triassic) of Kühwiesenkopf/Monte Prà della Vacca (Olang Dolomites, N-Italy). Palaeogeogr. Palaeoclimatol. Palaeoecol. 290 (1–4), 71–80.
Kustatscher, E., Nowak, H., Forte, G., Roghi, G., 2019. Triassic macro- and microfloras of the Eastern Southern Alps. Geo.Alp 16, 5–43.
Lagnaoui, A., Voigt, S., Belahmira, A., Saber, H., Klein, H., Hminna, A., Schneider, J.W., 2018. Late Carboniferous Tetrapod Footprints from the Souss Basin, Western High Atlas Mountains, Morocco. Ichnos 25 (2–3), 81–93.
Legler, B., Schneider, J.W., 2013. High-frequency cyclicity preserved in nonmarine and marine deposits (Permian, Germany and North Sea). New Mexico Museum Nat. History Sci. Bull. 60, 200–211.
Leonardi, G., 1987. Glossary and Manual of Tetrapod Footprint Palaeoichnology. Departamento Nacional de Produção Mineral, Brasília (117 pp.).
Leonardi, P., Conti, M.A., Leonardi, G., Mariotti, N., Nicosia, U., 1975. Pachypes dolomiticus n. gen. n. sp.; Pareiasaur footprint from the "Arenaria di Val Gardena" (Middle Permian) in the Western Dolomites (N. Italy). In: Accademia Nazionale dei Lincei, Rendiconti, Classe Scienze matematiche fisiche e naturali, 8th series, 57 (3–4), pp. 221–232.
Li, Y.-X., Kodama, K.P., 2016. Detecting and correcting for paleomagnetic inclination shallowing of sedimentary rocks: a review. Front. Earth Sci. 4, 7.
Liebrecht, T., Fortuny, J., Galobart, A., Müller, J., Sander, P.M., 2017. A large, multiple-tooth-rowed captorhinid reptile (Amniota: Eureptilia) from the Upper Permian of Mallorca (Balearic Islands, Western Mediterranean). J. Vertebr. Paleontol. 37 (1), e1251936.
Lindström, S., McLoughlin, S., Drinnan, A.N., 1997. Intraspecific variation of taeniate bisaccate pollen within Permian glossopterid sporangia, from the Prince Charles Mountains, Antarctica. Int. J. Plant Sci. 158 (5), 673–684.
Linol, B., Bercovici, A., Bourquin, S., Diez, J.B., López-Gómez, J., Broutin, J., Durand, M., Villanueva-Amadoz, U., 2009. Late Permian to Middle Triassic correlations and palaeogeographical reconstructions in south-western European basins: New sedimentological data from Minorca (Balearic Islands, Spain). Sediment. Geol. 220, 77–94.
Litwin, R.J., 1985. Fertile organs and in situ spores of ferns from the late Triassic Chinle Formation of Arizona and New Mexico, with discussion of the associated dispersed spores. Rev. Palaeobot. Palynol. 44 (1), 101–146.
Logghe, A., Mujal, E., Marchetti, L., Nel, A., Pouillon, J.-M., Giner, S., Garrouste, R., Steyer, J.-S., 2021. Hyloidichnus trackways with digit and tail drag traces from the Permian of Gonfaron (Var, France): new insights on the locomotion of captorhinomorph eureptiles. Palaeogeogr. Palaeoclimatol. Palaeoecol. 573, 110436.
Looy, C.V., Hotton, C.L., 2014. Spatiotemporal relationships among Late Pennsylvanian plant assemblages: palynological evidence from the Markley Formation, West Texas, U.S.A. Rev. Palaeobot. Palynol. 211, 10–27.
Lopez, M., Gand, G., Körner, F., Schneider, J., 2008. The playa environments of the Lodève Permian basin (Languedoc-France). J. Iberian Geol. 34 (1), 29–56.
López-Gómez, J., Arche, A., Pérez-López, A., 2002. Permian and Triassic. In: Gibbons, W., Moreno, M.T. (Eds.), The Geology of Spain. Geological Society, London, pp. 185–212.
López-Gómez, J., Alonso-Azcárate, J., Arche, A., Arribas, J., Fernández-Barrenechea, J., Borruel-Abadía, V., Bourquin, S., Cadenas, P., Cuevas, J., De la Horra, R., Díez, J.B., Escudero-Mozo, M.J., Fernández-Viejo, G., Galán-Abellán, B., Galé, C., Gaspar-Escribano, J., Gisbert-Aguilar, J., Gómez-Gras, D., Goy, A., Gretter, N., Heredia-Carballo, N., Lago, M., Lloret, J., Luque, J., Márquez, L., Márquez-Aliaga, A., Martín-Algarra, A., Martín-Chivelet, J., Martín-González, F., Marzo, M., Mercedes-Martín, R., Ortí, F., Pérez-López, A., Pérez-Valera, F., Pérez-Valera, J.A., Plasencia, P., Ramos, E., Rodríguez-Méndez, L., Ronchi, A., Salas, R., Sánchez-Fernández, D., Sánchez-Moya, Y., Sopeña, A., Suárez-Rodríguez, Á., Tubía, J.M., Ubide, T., Valero-Garcés, B., Vargas, H., Viseras, C., 2019a. Permian-Triassic rifting stage. In: Vergés, J., Kullberg, J.C. (Eds.), The Geology of Iberia: A Geodynamic Approach. Volume 3: The Alpine Cycle. Springer, Cham, pp. 29–112.
López-Gómez, J., Martín-González, F., Heredia, N., De la Horra, R., Barrenechea, J.F., Cadenas, P., Juncal, M., Diez, J.B., Borruel-Abadía, V., Pedreira, D., García-Sansegundo, J., Farias, P., Galé, C., Lago, M., Ubide, T., Fernández-Viejo, G., Gand, G., 2019b. New lithostratigraphy for the Cantabrian Mountains: a common tectono-stratigraphic evolution for the onset of the Alpine cycle in the W Pyrenean realm, N Spain. Earth Sci. Rev. 188, 249–271.
López-Gómez, J., De la Horra, R., Barrenechea, J.F., Borruel-Abadía, V., Martín-Chivelet, J., Juncal, M., Martín-González, F., Heredia, N., Diez, B., Buatois, L.A., 2021. Early Permian during the Variscan orogen collapse in the equatorial realm: insights from the Cantabrian Mountains (N Iberia) into climatic and environmental changes. Int. J. Earth Sci. 110, 1355–1387.
Lucas, S.G., 2009. Timing and magnitude of tetrapod extinctions across the Permo–Triassic boundary. J. Asian Earth Sci. 36, 491–502.
Lucas, S.G., 2017. Permian tetrapod extinction events. Earth Sci. Rev. 170, 31–60.
Lucas, S.G., 2019. An ichnological perspective on some major events of Paleozoic tetrapod evolution. Boll. Soc. Paleontol. Ital. 58 (3), 223–266.
Lucas, S.G., Lozovsky, V.R., Shishkin, M.A., 1999. Tetrapod footprints from early Permian redbeds of the northern Caucasus, Russia. Ichnos 6 (4), 277–281.
Lucas, S.G., Lerner, A.J., Haubold, H., 2001. First record of Amphisauropus and Varanopus in the Lower Permian Abo Formation, central New Mexico. Hallesches Jahrbuch für Geowissenschaften B 23, 69–78.
Lucas, S.G., Krainer, K., Chaney, D.S., DiMichele, W.A., Voigt, S., Berman, D.S., Henrici, A.C., 2013. The Lower Permian Abo Formation in central New Mexico. New Mexico Museum Nat. History Sci. Bull. 59, 161–180.
Lucas, S.G., Kollar, A.D., Berman, D.S., Henrici, A.C., 2016. Pelycosaurian-grade (Amniota: Synapsida) footprints from the Lower Permian Dunkard Group of Pennsylvania and West Virginia. Ann. Carnegie Museum 83 (4), 287–294.
Mack, G.H., James, W.C., Monger, H.C., 1993. Classification of paleosols. Geol. Soc. Am. Bull. 105, 129–136.
MacLeod, K.G., Quinton, P.C., Bassett, D.J., 2017. Warming and increased aridity during the earliest Triassic in the Karoo Basin, South Africa. Geology 45 (6), 483–486.
Mädler, K., 1964. Die geologische Verbreitung von Sporen und Pollen - in der deutschen Trias. Beihefte zum Geologischen Jahrbuch 65, 1–145.
Marchetti, L., 2016. New occurrences of tetrapod ichnotaxa from the Permian Orobic Basin (Northern Italy) and critical discussion of the age of the ichnoassociation. Pap. Palaeontol. 2 (3), 363–386.
Marchetti, L., Avanzini, M., Conti, M.A., 2013. Hyloidichnus bifurcatus Gilmore, 1927 and Limnopus heterodactylus (King, 1845) from the Early Permian of Southern Alps (N Italy): a new equilibrium in the ichnofauna. Ichnos 20, 202–217.
Marchetti, L., Forte, G., Bernardi, M., Wappler, T., Hartkopf-Fröder, C., Krainer, K., Kustatscher, E., 2015a. Reconstruction of a Late Cisuralian (Early Permian) floodplain lake environment: Palaeontology and sedimentology of the Tregiovo Basin (Trentino-Alto Adige, Northern Italy). Palaeogeogr. Palaeoclimatol. Palaeoecol. 440, 180–200.
Marchetti, L., Ronchi, A., Santi, G., Schirolli, P., Conti, M.A., 2015b. Revision of a classic site for Permian tetrapod ichnology (Collio Formation, Trompia and Caffaro valleys, N. Italy), new evidences for the radiation of captorhinomorph footprints. Palaeogeogr. Palaeoclimatol. Palaeoecol. 433, 140–155.
Marchetti, L., Ronchi, A., Santi, G., Voigt, S., 2015c. The Gerola Valley site (Orobic Basin, Northern Italy): a key for understanding late Early Permian tetrapod ichnofaunas. Palaeogeogr. Palaeoclimatol. Palaeoecol. 439, 97–116.
Marchetti, L., Tessarollo, A., Felletti, F., Ronchi, A., 2017a. Tetrapod footprint palaeoecology: behavior, taphonomy and ichnofauna disentangled. A case study from the Lower Permian of the Southern Alps (Italy). Palaios 32, 506–527.
Marchetti, L., Voigt, S., Klein, H., 2017b. Revision of Late Permian tetrapod tracks from the Dolomites (Trentino–Alto Adige, Italy). Histor. Biol. 31 (6), 748–783, 2019.
Marchetti, L., Mujal, E., Bernardi, M., 2017c. An unusual Amphisauropus trackway and its implication for understanding seymouriamorph locomotion. Lethaia 50, 162–174.
Marchetti, L., Voigt, S., Santi, G., 2018. A rare occurrence of Permian tetrapod footprints: Ichniotherium cottae and Ichniotherium sphaerodactylum on the same stratigraphic surface. Ichnos 25 (2–3), 106–118.
Marchetti, L., Belvedere, M., Voigt, S., Klein, H., Castanera, D., Díaz-Martínez, I., Marty, D., Xing, L., Feola, S., Melchor, R.N., Farlow, J.O., 2019a. Defining the morphological quality of fossil footprints. Problems and principles of preservation in tetrapod ichnology with examples from the Palaeozoic to the present. Earth Sci. Rev. 193, 109–145.
Marchetti, L., Voigt, S., Lucas, S.G., 2019b. An anatomy-consistent study of the Lopingian eolian tracks of Germany and Scotland reveals the first evidence of the end-Guadalupian mass extinction at low paleolatitudes of Pangea. Gondwana Res. 73, 32–53.
Marchetti, L., Klein, H., Buchwitz, M., Ronchi, A., Smith, R.M.H., De Klerk, W.J., Sciscio, L., Groenewald, G.H., 2019c. Permian-Triassic vertebrate footprints from South Africa: ichnotaxonomy, producers and biostratigraphy through two major faunal crises. Gondwana Res. 72, 139–168.
Marchetti, L., Voigt, S., Lucas, S.G., Francischini, H., Dentzien-Dias, P., Sacchi, R., Mangiacotti, M., Scali, S., Gazzola, A., Ronchi, A., Millhouse, A., 2019d. Tetrapod ichnotaxonomy in eolian paleoenvironments (Coconino and De Chelly formations, Arizona) and late Cisuralian (Permian) sauropsid radiation. Earth Sci. Rev. 190, 148–170.
Marchetti, L., Voigt, S., Lucas, S.G., Stimson, M.R., King, O.A., Calder, J.H., 2020. Footprints of the earliest reptiles: Notalacerta missouriensis – Ichnotaxonomy, potential trackmakers, biostratigraphy, palaeobiogeography and palaeoecology. Ann. Soc. Geol. Poloniae 90, 271–290.
Marchetti, L., Voigt, S., Buchwitz, M., MacDougall, M.J., Lucas, S.G., Fillmore, D.L., Stimson, M.R., King, O.A., Calder, J.H., Fröbisch, J., 2021a. Tracking the origin and early evolution of reptiles. Front. Ecol. Evol. 9, 696511.
Marchetti, L., Voigt, S., Mujal, E., Lucas, S.G., Francischini, H., Fortuny, J., Santucci, V.L., 2021b. Extending the footprint record of Pareiasauromorpha to the Cisuralian: earlier appearance and wider palaeobiogeography of the group. Pap. Palaeontol. 7 (3), 1297–1319.
Marchetti, L., Forte, G., Kustatscher, E., DiMichele, W.A., Lucas, S.G., Roghi, G., Juncal, M.A., Hartkopf-Fröder, C., Krainer, K., Morelli, C., Ronchi, A., 2022. The Artinskian Warming Event: an Euramerican change in climate and the terrestrial biota during the early Permian. Earth Sci. Rev. (in press: 103922).
Marsh, O.C., 1894. Footprints of vertebrates in the Coal Measures of Kansas. Am. J. Sci. 48, 81–84.
Martí, J., Paniello, X., Pomar, L., Ramos, E., Rodríguez-Perea, A., 1985. El Triásico de las Baleares. In: Mateu Ibars, F., Marzo, M. (Eds.), Resúmenes del II Coloquio de Estratigrafía y Paleogeografía del Pérmico y Triásico de España. Institut d'Estudis Ilerdencs and Grupo Español del Mesozoico, La Seu d'Urgell, pp. 84–85.
Matamales-Andreu, R., Fortuny, J., Mujal, E., Galobart, À., 2019. Tetrapod tracks from the Permian of Mallorca (western Mediterranean): preliminary data, biostratigraphic

and biogeographic inferences. In: The Palaeontological Association, 63rd annual meeting, 15th–21st December 2019. The Palaeontological Association, València, p. 107.
Matamales-Andreu, R., Oms, O., Fortuny, J., 2021a. Paleoecosistemes del Permià i Triàsic continental de Mallorca (Illes Balears, Mediterrània occidental): síntesi i prespectives futures. In: Gómez-Pujol, L.L., Roig-Munar, F.X., Gelabert, B., Martín, J. A. (Eds.), De la terra a la mar i de la mar a la terra. Homenatge a Antonio Rodríguez-Perea. Monografies de la Societat d'Història Natural de Balears, 34. Societat d'Història Natural de les Balears, Palma, pp. 17–39.
Matamales-Andreu, R., Peñalver, E., Mujal, E., Oms, O., Scholze, F., Juárez, J., Galobart, À., Fortuny, J., 2021b. Early–Middle Triassic fluvial ecosystems of Mallorca (Balearic Islands): biotic communities and environmental evolution in the equatorial western peri-Tethys. Earth Sci. Rev. 222, 103783.
Matamales-Andreu, R., Roig-Munar, F.X., Oms, O., Galobart, À., Fortuny, J., 2021c. A captorhinid-dominated assemblage from the palaeoequatorial Permian of Menorca (Balearic Islands, western Mediterranean). Earth Environ. Sci. Trans. R. Soc. Edinburgh 112 (2), 125–145.
Matamales-Andreu, R., Mujal, E., Galobart, À., Fortuny, J., 2021d. Insights on the evolution of synapsid locomotion based on tetrapod tracks from the lower Permian of Mallorca (Balearic Islands, western Mediterranean). Palaeogeogr. Palaeoclimatol. Palaeoecol. 579, 110589.
Matamales-Andreu, R., Galobart, À., Fortuny, J., 2021e. New occurrences of small moradisaurine captorhinid eureptiles from the Permian of Mallorca (western Mediterranean). In: Belvedere, M., Díez Díaz, V., Mecozzi, B., Sardella, R. (Eds.), Abstract book of the XVIII annual conference of the European Association of Vertebrate Palaeontologists, online, 5th–9th July 2021. Palaeovertebrata, 44, p. 115.
Matamales-Andreu, R., Oms, O., Galobart, À., Fortuny, J., 2021f. Middle–Upper Triassic marine vertebrates of Mallorca (Balearic Islands, western Mediterranean). Histor. Biol. 33 (10), 2520–2533.
Maxbauer, D.P., Feinberg, J.M., Fox, D.L., 2016. MAX UnMix: a web application for unmixing magnetic coercivity distributions. Comput. Geosci. 95, 140–145.
McCann, T., Pascal, C., Timmerman, M.J., Krzywiec, P., López-Gómez, J., Wetzel, A., Krawczyk, C.M., Rieke, H., Lamarche, J., 2006. Post-Variscan (end Carboniferous–Early Permian) basin evolution in Western and Central Europe. Geol. Soc. Lond. Mem. 32, 355–388.
McFadden, P.L., McElhinny, M.W., 1988. The combined analysis of remagnetization circles and direct observations in palaeomagnetism. Earth Planet. Sci. Lett. 87 (1), 161–172.
Meade, L.E., Jones, A.S., Butler, R.J., 2016. A revision of tetrapod footprints from the late Carboniferous of the West Midlands, UK. PeerJ 4, e2718.
Melchor, R.N., Sarjeant, W.A.S., 2004. Small amphibian and reptile footprints from the Permian Carapacha Basin, Argentina. Ichnos 11, 57–78.
Meyen, S.V., 1987. Fundamentals of Palaeobotany. Chapman and Hall, London, p. 432.
Miall, A.D., 1977. A review of the braided-river depositional environment. Earth Sci. Rev. 13, 1–62.
Miall, A.D., 1985. Architectural-Element Analysis: a new method of facies analysis applied to fluvial deposits. Earth Sci. Rev. 22, 261–308.
Miall, A.D., 2006. The Geology of Fluvial Deposits: Sedimentary Facies, Basin Analysis, and Petroleum Geology, 4th ed. Springer, Berlin, Heidelberg, New York, p. 582.
Michel, L.A., Tabor, N.J., Montañez, I.P., Schmitz, M.D., Davydov, V.I., 2015. Chronostratigraphy and Paleoclimatology of the Lodève Basin, France: evidence for a pan-tropical aridification event across the Carboniferous–Permian boundary. Palaeogeogr. Palaeoclimatol. Palaeoecol. 430, 118–131.
Minter, N.J., Krainer, K., Lucas, S.G., Braddy, S.J., Hunt, A.P., 2007. Palaeoecology of an Early Permian playa lake trace fossil assemblage from Castle Peak, Texas, USA. Palaeogeogr. Palaeoclimatol. Palaeoecol. 246, 390–423.
Mishra, S., Jha, N., Gahalain, S.S., 2017. Taphonomic and palaeovegetational studies in lower Permian (Asselian-Sakmarian) deposits of Chintalapudi Area, Godavari Graben, South India. Rev. Micropaléontol. 60 (2), 193–211.
Montañez, I.P., Poulsen, C.J., 2013. The late Paleozoic ice age: an evolving paradigm. Ann. Rev. Earth Planet. Sci. 41, 629–656.
Montañez, I.P., Tabor, N.J., Niemeier, D., DiMichele, W.A., Frank, T.D., Fielding, C.R., Isbell, J.L., Birgenheier, L.T., Rygel, M., 2007. CO2-forced climate and vegetation instability during Late Paleozoic glaciation. Science 315, 87–91.
Moodie, R.L., 1929. Vertebrate footprints from the Red Beds of Texas. Am. J. Sci. 97, 352–368.
Mujal, E., Marchetti, L., 2020. Ichniotherium tracks from the Permian of France, and their implications for understanding the locomotion and palaeobiogeography of large diadectomorphs. Palaeogeogr. Palaeoclimatol. Palaeoecol. 547, 109698.
Mujal, E., Schoch, R.R., 2020. Middle Triassic (Ladinian) amphibian tracks from the Lower Keuper succession of southern Germany: implications for temnospondyl locomotion and track preservation. Palaeogeogr. Palaeoclimatol. Palaeoecol. 543, 109625.
Mujal, E., Fortuny, J., Oms, O., Bolet, A., Galobart, À., Anadón, P., 2016. Palaeoenvironmental reconstruction and early Permian ichnoassemblage from the NE Iberian Basin (Pyrenean Basin). Geol. Magazine 153 (4), 578–600.
Mujal, E., Fortuny, J., Pérez-Cano, J., Dinarès-Turell, J., Ibáñez-Insa, J., Oms, O., Vila, I., Bolet, A., Anadón, P., 2017a. Integrated multi-stratigraphic study of the Coll de Terrers late Permian–Early Triassic continental succession from the Catalan Pyrenees (NE Iberian Peninsula): a geologic reference record for equatorial Pangaea. Glob. Planet. Change 159, 46–60.
Mujal, E., Fortuny, J., Bolet, A., Oms, O., López, J.A., 2017b. An archosauromorph dominated ichnoassemblage in fluvial settings from the late Early Triassic of the Catalan Pyrenees (NE Iberian Peninsula). PLoS One 12 (4), e0174693.
Mujal, E., Fortuny, J., Marmi, J., Dinarès-Turell, J., Bolet, A., Oms, O., 2018. Aridification across the Carboniferous–Permian transition in central equatorial Pangea: the Catalan Pyrenean succession (NE Iberian Peninsula). Sediment. Geol. 363, 48–68.
Mujal, E., Marchetti, L., Schoch, R.R., Fortuny, J., 2020. Upper Paleozoic to lower Mesozoic tetrapod ichnology revisited: photogrammetry and relative depth pattern inferences on functional prevalence of autopodia. Front. Earth Sci. 8, 248.
Nicholson, H.A., 1873. Contributions to the study of the errant annelides of the older Palaeozoic rocks. Proc. R. Soc. Lond. 21, 288–290.
Obrador, A., 1983. El Pérmico de las Baleares. In: Martínez-Díaz, C. (Ed.), Carbonífero y Pérmico de España, X Congreso Internacional de Estratigrafía y Geología del Carbonífero. Ministerio de Industria y Energía, Instituto Geológico y Minero de España, Madrid, pp. 463–470.
Olroyd, S.L., Sidor, C.A., 2017. A review of the Guadalupian (middle Permian) global tetrapod fossil record. Earth Sci. Rev. 171, 583–597.
Özdemir, Ö., Dunlop, D.J., 2014. Hysteresis and coercivity of hematite. J. Geophys. Res. 119 (4), 2582–2594.
Pant, D.D., Nautiyal, D.D., 1960. Some seeds and sporangia of Glossopteris flora from Raniganj Coalfield, India. Palaeontogr. Abteilung B 107 (1–3), 41–64.
Parés, J.M., Freeman, R., Sàbat, F., 1989. Síntesis de los resultados paleomagnéticos de los bordes de la Cuenca Catalano-Balear. Cuadernos de Geología Ibérica 12, 59–74.
Parés, J.M., Freeman, R., Roca, E., 1992a. Neogene structural development in the Valencia trough margins from palaeomagnetic data. Tectonophysics 203, 111–124.
Parés, J.M., Roca, E., Freeman, R., 1992b. Datos paleomagnéticos de los márgenes del surco de Valencia. Papel de las rotaciones en la estructuración neógena. Física de la Tierra 4, 231–246.
Parrish, J.T., 1993. Climate of the supercontinent Pangea. J. Geol. 101, 215–233.
Pemberton, S.G., Frey, R.W., 1982. Trace fossil nomenclature and the Planolites-Palaeophycus dilemma. J. Paleontol. 56 (4), 843–881.
Pérez-Valera, J.A., 2015. Ammonoideos y bioestratigrafía del Triásico Medio (Ladiniense) del sector oriental de la Cordillera Bética. Ph.D. Dissertation. Universidad Complutense de Mardid, Madrid (489 pp.).
Pérez-Valera, J.A., Escudero-Mozo, M.J., Arche, A., Goy, A., López-Gómez, J., Pérez-López, A., Pérez-Valera, F., 2016. Los ammonoideos del Triásico Medio de España. Implicaciones bioestratigráficas y paleobiogeográficas. In: Meléndez, G., Núñez, A., Tomás, M. (Eds.), Actas de las XXXII Jornadas de la Sociedad Española de Paleontología, 20. Cuadernos del Museo Geominero, pp. 471–478.
Pohlig, H., 1892. Altpermische Saurierfährten, Fische und Medusen der Gegend von Friedrichroda i. Thüringen. In: Festschrift zum 70. Geburtstag von Rudolf Leuckardt. Engelmann, Leipzig, pp. 59–64.
Pomar-Gomà, L., 1979. The Triassic of the Balearic Islands. Geology Department, Palma de Mallorca University, Palma (49 pp. + 7 Petrologic Logs).
Poort, R.J., Clement-Westerhof, J.A., Looy, C.V., Visscher, H., 1997. Aspects of Permian palaeobotany and palynology. XVII. Conifer extinction in Europe at the Permian–Triassic junction: morphology, ultrastructure and geographic/stratigraphic distribution of Nuskoisporites dulhuntyi (prepollen of Ortiseia, Walchiaceae). Rev. Palaeobot. Palynol. 97 (1–2), 9–39.
Postma, G., 1990. Depositional architecture and facies of river and fan deltas: a synthesis. Spec. Publ. Int. Assoc. Sedimentol. 10, 13–27.
Potonié, R., 1962. Synopsis der Sporae in situ. Die Sporen der fossilen Fruktifikationen (thallophyta bis Gymnospermophyta) im natürlichen System und im Vergleich mit den Sporae dispersae, 52. Beihefte zum Geologischen Jahrbuch, Hannover, pp. 91–93.
Potonié, R., Kremp, G., 1956. Die Sporae Dispersae des Ruhrkarbons, ihre Morphographie und Stratigraphie mit Ausblicken auf Arten anderer Gebiete und Zeitabschnitte. Teil II. Palaeontogr. Abteilung B 99 (4–6), 85–191.
Raine, J.I., Mildenhall, D.C., Kennedy, E.M., 2011. New Zealand fossil spores and pollen: an illustrated catalogue. In: GNS Science Miscellaneous Series. GNS Science, Lower Hutt, New Zealand. https://www.gns.cri.nz/what/earthhist/fossils/spore_pollen/catalog/index.htm.
Ramos, A., 1995. Transition from alluvial to coastal deposits (Permian–Triassic) on the Island of Mallorca, western Mediterranean. Geol. Magazine 132 (4), 435–447.
Ramos, A., Doubinger, J., 1989. Premières datations palynologiques dans le facies Buntsandstein de l'île de Majorque (Baléares, Espagne). Comp. Rend. Acad. Sci. Paris 2 (309), 1089–1094.
Ramos, A., García-Ramos, S., 1992. Niveles de bioturbación en las facies tipo Buntsandstein del Pérmico-Triásico de Mallorca. In: García-Ramos, J.C. (Ed.), Reunión Monográfica sobre Biosedimentación. Servicio de Publicaciones de la Universidad de Oviedo, Oviedo, pp. 41–43.
Ramos, E., Rodríguez-Perea, A., 1985. Découverte d'un affleurement de terrains paléozoïques dans l'île de Majorque (Baléares, Espagne). Comp. Rend. Acad. Sci. Paris 2 (16), 1205–1207, 301.
Ramos, A., del Olmo, P., Alvaro, M., 1985. El Buntsandstein de la isla de Mallorca. In: Mateu Ibars, F., Marzo, M. (Eds.), Resúmenes del II Coloquio de Estratigrafía y Paleogeografía del Pérmico y Triásico de España. Institut d'Estudis Ilerdencs and Grupo Español del Mesozoico, La Seu d'Urgell, pp. 103–104.
Rangheard, Y., 1971. Étude géologique des îles d'Ibiza et de Formentera (Baléares), 82. Memorias del Instituto Geológico y Minero de España, pp. 2–340 (+ 23 pl).
Retallack, G.J., 1997. Earliest Triassic origin of Isoetes and quillwort evolutionary radiation. J. Paleontol. 71 (3), 500–521.
Retallack, G.J., Metzger, C.A., Greaver, T., Jahren, A.H., Smith, R.M.H., Sheldon, N.D., 2006. Middle-Late Permian mass extinction on land. GSA Bull. 118 (11/12), 1398–1411.
Rodríguez-Perea, A., Ramos, E., 1984. Presencia de Paleozoico en la Sierra de Tramuntana (Mallorca). Boll. Soc. Històr. Nat. Balears 28, 145–148.
Rodríguez-Perea, A., Ramos-Guerrero, E., Pomar, L., Paniello, X., Obrador, A., Martí, J., 1987. El Triásico de las Baleares. Cuadernos Geol. Ibérica 11, 295–321.

Romano, M., Citton, P., Nicosia, U., 2016. Corroborating trackmaker identification through footprint funcional analysis: the case study of Ichniotherium and Dimetropus. Lethaia 49, 102–116.

Romano, M., Citton, P., Maganuco, S., Sacchi, E., Caratelli, M., Ronchi, A., Nicosia, U., 2019. New basal synapsid discovery at the Permian outcrop of Torre del Porticciolo (Alghero, Italy). Geol. J. 54 (3), 1554–1566.

Romano, M., Bernardi, M., Petti, F.M., Rubidge, B., Hancox, J., Benton, M.J., 2020. Early Triassic terrestrial tetrapod fauna: a review. Earth Sci. Rev. 210, 103331.

Romer, A.S., Price, L.I., 1940. Review of the Pelycosauria. Geol. Soc. Am. Spec. Pap. 28, 1–538.

Roscher, M., Schneider, J.W., 2006. Permo-Carboniferous climate: early Pennsylvanian to Late Permian climate development of central Europe in a regional and global context. Geol. Soc. Lond. Spec. Publ. 265, 95–136.

Roscher, M., Berner, U., Schneider, J.W., 2008. A tool for the assessment of the paleo-distribution of source and reservoir rocks. In: Oil Gas European Magazine, 3, pp. 131–137.

Rosell, J., Arribas, J., Elizaga, E., Gómez, D., 1988. Caracterización sedimentológica y petrográfica de la serie roja permo–triásica de la isla de Menorca. Bol. Geol. Minero 99 (1), 71–82.

Rosell, J., Gómez-Gras, D., Elízaga, E., 1989. Mapa Geológico de España. Escala 1: 25.000. Isla de Menorca. Cap Menorca y Ciutadella. Segunda serie, primera edición. Instituto Tecnológico GeoMinero de España, Madrid (51 pp. + 3 maps).

Rothwell, G.W., Mapes, G., Hernández-Castillo, G.R., 2005. Hanskerpia gen. nov. and phylogenetic relationships among the most ancient conifers (Voltziales). Taxon 54 (3), 733–750.

Rowntree, K.M., Dollar, E.S.J., 1999. Vegetation controls on channel stability in the Bell River, Eastern Cape, South Africa. Earth Surf. Proc. Landforms 24, 127–134.

Ruta, M., Benton, M.J., 2008. Calibrated diversity, tree topology and the mother of mass extinctions: the lesson of temnospondyls. Palaeontology 51, 1261–1288.

Sacchi, E., Cifelli, R., Citton, P., Nicosia, U., Romano, M., 2014. Dimetropus osageorum n. isp. from the Early Permian of Oklahoma (USA): a trace and its trackmaker. Ichnos 21, 175–192.

Sahney, S., Benton, M.J., 2008. Recovery from the most profound mass extinction of all time. Proc. R. Soc. B 275, 759–765.

Salter, J.W., 1857. On annelide-burrows and surface-markings from the Cambrian rocks of the Longmynd. No. 2. Q. J. Geol. Soc. 13, 199–206.

Santi, G., Marchetti, L., Schirolli, P., Ronchi, A., 2020. The Cisuralian tetrapod ichnoassociation from Italy: from historical findings to a standard reference status. J. Mediterranean Earth Sci. 12, 39–59.

Schaarschmidt, F., Maubeuge, P.L., 1969. Eine männliche Gymnospermen–Fruktifikation aus dem Voltziensandstein (Untere Trias) der Vogesen. Senckenbergiana lethaea 50 (5–6), 377–397.

Schneider, J.W., Körner, F., Roscher, M., Kroner, U., 2006. Permian climate development in the northern peri-Tethys area — the Lodève basin, French Massif Central, compared in a European and global context. Palaeogeogr. Palaeoclimatol. Palaeoecol. 240, 161–183.

Schneider, J.W., Lucas, S.G., Scholze, F., Voigt, S., Marchetti, L., Klein, H., Opluštil, S., Werneburg, R., Golubevb, V.K., Barrick, J.E., Nemyrovska, Y., Ronchil, A., Day, M. O., Silantiev, V.V., Rößler, R., Saber, H., Linnemann, U., Zharinova, V., Shen, S.-Z., 2020. Late Paleozoic–early Mesozoic continental biostratigraphy — links to the Standard Global Chronostratigraphic Scale. Palaeoworld 29 (2), 186–238.

Schoch, R.R., 2014. Amphibian Evolution: The Life of Early Land Vertebrates. Wiley Blackwell (264 pp.).

Schweitzer, H.J., 1962. Die Makroflora des niederrheinischen Zechsteins. Fortschritte der Geologie des Rheinlande und Westfalen 6, 331–376.

Scotese, C.R., 2014a. Atlas of Permo-Carboniferous Paleogeographic Maps, Maps 53 – 64 from Volume 4 of the PALEOMAP Atlas for ArcGIS (Late Paleozoic), Mollweide Projection. PALEOMAP Project, Evanston, Illinois.

Scotese, C.R., 2014b. Atlas of Middle & Late Permian and Triassic Paleogeographic Maps, Maps 43 – 48 from Volume 3 of the PALEOMAP Atlas for ArcGIS (Jurassic and Triassic) and maps 49 – 52 from Volume 4 of the PALEOMAP Atlas for ArcGIS (Late Paleozoic), Mollweide Projection. PALEOMAP Project, Evanston, Illinois.

Sevillano, A., Barnolas, A., 2018. Mapa Geológico Digital Continuo E. 1:50.000, Zona Mallorca (Zona-2210). In: GEODE. Mapa Geológico Digital continuo de España. Available online at: http://info.igme.es/visorweb/ (last visited: 06/06/2018).

Seyfullah, L.J., Kustatscher, E., Taylor, W.A., 2013. The first discovery of in situ Verrucosisporites applanatus spores from the Middle Triassic flora from Bromsgrove (Worcestershire, UK). Rev. Palaeobot. Palynol. 197, 15–25.

Sidor, C.A., O'Keefe, F.R., Damiani, R., Steyer, J.S., Smith, R.M.H., Larsson, H.C.E., Sereno, P.C., Ide, O., Maga, A., 2005. Permian tetrapods from the Sahara show climate-controlled endemism in Pangaea. Nature 434, 886–889.

Smith, R.M.H., 1993. Vertebrate taphonomy of late Permian floodplain deposits in the southwestern Karoo Basin of South Africa. Palaios 8, 45–67.

Smith, R.M.H., Sidor, C.A., Tabor, N.J., Steyer, J.S., 2015. Sedimentology and vertebrate taphonomy of the Moradi Formation of northern Niger: a Permian wet desert in the tropics of Pangaea. Palaeogeogr. Palaeoclimatol. Palaeoecol. 440, 128–141.

Sopeña, A., Virgili, C., Hernando, S., Ramos, A., 1977. Pérmico continental en España. Cuadernos Geol. Ibérica 4, 11–34.

Speksnijder, A., 1985. Anatomy of a strike-slip fault controlled sedimentary basin, Permian of the southern Pyrenees, Spain. Sediment. Geol. 44, 179–223.

Stampfli, G.M., Hochard, C., Vérard, C., Wilhem, C., vonRaumer, J., 2013. The formation of Pangea. Tectonophysics 593, 1–19.

Steiner, M.B., 2006. The magnetic polarity time scale across the Permian-Triassic boundary. Geol. Soc. Lond. Spec. Publ. 265 (1), 15–38.

Steyer, J.S., Damiani, R., Sidor, C.A., O'Keefe, F.R., Larsson, H.C.E., Magal, A., Ide, O., 2006. The vertebrate fauna of the Upper Permian of Niger. IV. Nigerpeton ricqlesi (Temnospondyli: Cochleosauridae), and the edopoid colonization of Gondwana. J. Vertebr. Paleontol. 26 (1), 18–28.

Sun, Y., Joachimski, M.M., Wignall, P.B., Yan, C., Chen, Y., Jiang, H., Wang, L., Lai, X., 2012. Lethally hot temperatures during the Early Triassic greenhouse. Science 338 (6105), 366–370.

Tabor, N.J., Poulsen, C.J., 2008. Palaeoclimate across the Late Pennsylvanian–Early Permian tropical palaeolatitudes: a review of climate indicators, their distribution, and relation to palaeophysiographic climate factors. Palaeogeogr. Palaeoclimatol. Palaeoecol. 268, 293–310.

Taylor, T.N., Taylor, E.L., 1987. The ultrastructure of fossil gymnosperm pollen. Bull. Soc. Bot. France 134 (2), 121–140.

Taylor, T.N., Taylor, E.L., Krings, M., 2009. Paleobotany: The Biology and Evolution of Fossil Plants. Elsevier Academic Press, Amsterdam (1252 pp.).

Traverse, A.T., 2007. Paleopalynology. Topics Geobiol. 28, 1–832.

Uchman, A., Pika-Biolzi, M., Hochuli, P.A., 2004. Oligocene trace fossils from temporary fluvial plain ponds: an example from the Freshwater Molasse of Switzerland. Eclogae Geol. Helvet. 97, 133–148.

Valentini, M., Nicosia, U., Conti, M.A., 2009. A re-evaluation of Pachypes, a pareiasaurian track from the Late Permian. Geol. Paläontol. 251, 71–94.

Van Allen, H.E.K., Calder, J.H., Hunt, A.P., 2005. The trackway record of a tetrapod community in a walchian conifer forest from the Permo-Carboniferous of Nova Scotia. New Mexico Museum Nat. History Sci. Bull. 30, 322–332.

Vázquez, M.S., Césari, S.N., 2017. The Permian palynological Lueckisporites-Weylandites Biozone in the San Rafael Block and its correlation in Western Gondwana. J. South Am. Earth Sci. 76, 165–181.

Vera, J.-A., Alonso-Chaves, F.M., Andreo, B., Arias, C., Azañón, J.M., Balanyá, J.C., Barón, A., Booth-Rea, G., Castro, J.M., Chacón, B., Company, M., Crespo-Blanc, A., Delgado, F., Díaz de Federico, A., Esteras, M., Estévez, A., Fernández, J., Fornós, J.J., Galindo-Zaldívar, J., García-Casco, A., García-Dueñas, V., García-Hernández, M., Garrido, C.J., de Gea, G.A., Gelabert, B., Gervilla, F., González-Lodeiro, F., Jabaloy, A., López-Garrido, A.C., Luján, M., Martín-Algarra, A., Martín-Chivelet, J., Martín-Martín, M., Molina, J.M., Morata, D., Nieto, J.M., Obrador, A., O'Dogherty, L., Orozco, M., Pérez-López, A., Pomar, L., Puga, E., Ramos, E., Rey, J., Rivas, P., Rodríguez-Cañero, R., Ruiz-Cruz, M.D., Ruiz-Ortiz, P.A., Sàbat, F., Sánchez-Gómez, M., Sánchez-Navas, A., Sandoval, J., Sanz de Galdeano, C., Soto, J. I., Torres-Roldán, R.L., Villas, L., 2004. Capítulo 4. Cordillera Bética y Baleares. In: Vera, J.-A. (Ed.), Geología de España. Instituto Geológico y Minero de España, Madrid, pp. 346–464.

Virgili, C., 1952. Hallazgo de nuevos Ceratites en el Triásico mallorquín. In: Memorias y Comunicaciones del Instituto Geológico de la Diputación Provincial de Barcelona, 9, pp. 19–39.

Visscher, H., 1967. Permian and Triassic palynology and the concept of "Tethys twist". Palaeogeogr. Palaeoclimatol. Palaeoecol. 3, 151–166.

Visscher, H., 1968. On the Thuringian age of the upper Palaeozoic sedimentary and volcanic deposits of the Estérel (Southern France). Rev. Palaeobot. Palynol. 6, 71–83.

Visscher, H., Kerp, J.H.F., Clement-Westerhof, J.A., 1986. Aspects of Permian Palaeobotany and palynology. VI. Towards a flexible system of naming Paleozoic conifers. Acta Botanica Neerlandica 35, 87–100.

Voigt, S., 2005. Die Tetrapodenichnofauna des kontinentalen Oberkarbon und Perm im Thüringer Wald – Ichnotaxonomie, Paläoökologie und Biostratigraphie. Cuvillier Verlag, Göttingen (308 pp.).

Voigt, S., Ganzelewski, M., 2010. Toward the origin of amniotes: Diadectomorph and synapsid footprints from the early Late Carboniferous of Germany. Acta Palaeontol. Polonica 55 (1), 57–72.

Voigt, S., Lucas, S.G., 2015. Permian tetrapod ichnodiversity of the Prehistoric Trackways National Monument (south-central New Mexico, USA). New Mexico Museum Nat. History Sci. Bull. 65, 153–167.

Voigt, S., Berman, D.S., Henrici, A.C., 2007. First well-established track-trackmaker association of Paleozoic tetrapods based on Ichniotherium trackways and diadectid skeletons from the lower Permian of Germany. J. Vertebr. Paleontol. 27 (3), 553–570.

Voigt, S., Hminna, A., Saber, H., Schneider, J.W., Klein, H., 2010. Tetrapod footprints from the uppermost level of the Permian Ikakern Formation (Argana Basin, Western High Atlas, Morocco). J. Afr. Earth Sci. 57, 470–478.

Voigt, S., Lagnaoui, A., Hminna, A., Saber, H., Schneider, J.W., 2011. Revisional notes on the Permian tetrapod ichnofauna from the Tiddas Basin, central Morocco. Palaeogeogr. Palaeoclimatol. Palaeoecol. 302, 474–483.

Voigt, S., Niedźwiedzki, G., Raczyński, P., Mastalerz, K., Ptaszyński, T., 2012. Early Permian tetrapod ichnofauna from the Intra-Sudetic Basin, SW Poland. Palaeogeogr. Palaeoclimatol. Palaeoecol. 313–314, 173–180.

Whyte, M.A., Romano, M., 2001. A dinosaur ichnocoenosis from the Middle Jurassic of Yorkshire, UK. Ichnos 8, 223–234.

Zavialova, N., van Konijnenburg-van Cittert, J.H.A., 2011. Exine ultrastructure of in situ peltasperm pollen from the Rhaetian of Germany and its implications. Rev. Palaeobot. Palynol. 168 (1), 7–20.

Zavialova, N., Kustatscher, E., van Konijnenburg-van Cittert, J.H.A., 2010. Spore ultrastructure of Selaginellites leonardii and diversity of Selaginellalean spores. Geo. Alp 7, 1–17.

Zijderveld, J.D.A., 2013. A. C. demagnetization of rocks: analysis of results. Dev. Solid Earth Geophys. 3, 254–286.

Zouicha, A., Voigt, S., Saber, H., Marchetti, L., Hminna, A., El Attari, A., Ronchi, A., Schneider, J.W., 2021. First record of permian continental trace fossils in the jebilet massif, Morocco. J. Afr. Earth Sci. 173, 104015.

Chapter 3

The continental Early–Middle Triassic of Mallorca

© Henry S. Sharpe

Chapter 3 was published as:

Matamales-Andreu, R.; Peñalver, E.; Mujal, E.; Oms, O.; Scholze, F.; Juárez, J.; Galobart, À. & Fortuny, J. (2021). Early–Middle Triassic fluvial ecosystems of Mallorca (Balearic Islands): Biotic communities and environmental evolution in the equatorial western peri-Tethys. *Earth-Science Reviews*, 222: 103783.

DOI: https://doi.org/10.1016/j.earscirev.2021.103783

In this work, R. Matamales-Andreu contributed in:

A. Literature review of the Triassic of Mallorca in *Buntsandstein* facies.
B. Direct examination of most of the collections containing fossils from the studied outcrops.
C. Geological cartography.
D. Logging of all the stratigraphic sections.
E. Co-direction of all fieldwork campaigns (prospections and excavations). Sampling of clam shrimps and tetrapod tracks.
F. 3D modelling and measurement of relevant parameters on tetrapod tracks and trackways.
G. Stratigraphic and sedimentological analysis and definition of new formal lithostratigraphic units.
H. Invertebrate and vertebrate palaeoichnology, including identification and description of all the morphotypes.
I. Interpretation and discussion of the results.
J. Writing of the original draft and supplementary materials, except for sections 3.3 and 6 of the main text (invertebrate palaeontology).
K. Preparation of tables 1–2 and ST1–3, figures 1–5, 10–11 and SF1, and all the supplementary logs. Adaptation of figures 6–9 and SF2.
L. Collaboration in obtaining funding for fieldwork and fossil preparation.

Also, refer to:

Appendix 7: Supplementary Material for Matamales-Andreu *et al.* (2021)

Appendix 8: Scholze & Matamales-Andreu (2021), *Zootaxa*, clam shrimps

Appendix 9: Peñalver *et al.* (2023), *Papers in Palaeontology*, sedimentivory

Appendix 10: Peñalver *et al.* (2022), *Papers in Palaeontology*, dipterans

Earth-Science Reviews 222 (2021) 103783

Contents lists available at ScienceDirect

Earth-Science Reviews

journal homepage: www.elsevier.com/locate/earscirev

Early–Middle Triassic fluvial ecosystems of Mallorca (Balearic Islands): Biotic communities and environmental evolution in the equatorial western peri-Tethys

Rafel Matamales-Andreu [a,b,*], Enrique Peñalver [c], Eudald Mujal [a,d], Oriol Oms [e], Frank Scholze [f], Josep Juárez [b], Àngel Galobart [a,g], Josep Fortuny [a]

[a] Institut Català de Paleontologia Miquel Crusafont, Universitat Autònoma de Barcelona, Edifici ICTA-ICP, c/ Columnes s/n, Campus de la UAB, 08193 Cerdanyola del Vallès, Barcelona, Spain
[b] Museu Balear de Ciències Naturals, ctra. Palma-Port de Sóller km 30, 07100, Sóller, Mallorca, Illes Balears, Spain
[c] Instituto Geológico y Minero de España (Museo Geominero), CSIC, c/ Cirilo Amorós 42, 46004 València, València, Spain
[d] Staatliches Museum für Naturkunde Stuttgart, Rosenstein 1, 70191 Stuttgart, Germany
[e] Departament de Geologia, Universitat Autònoma de Barcelona, av. de l'Eix Central s/n, Campus de la UAB, 08193 Cerdanyola del Vallès, Barcelona, Spain
[f] Institut für Geowissenschaften, Friedrich-Schiller-Universität Jena, Burgweg 11, 07749 Jena, Germany
[g] Museu de la Conca Dellà, c/ del Museu 4, 25650 Isona i Conca Dellà, Lleida, Spain

ARTICLE INFO

Key-words:
Olenekian
Anisian
Clam shrimps
Insects
Tetrapod tracks
Central Pangaea

ABSTRACT

During the Early–Middle Triassic, the biosphere was recovering from the most severe mass extinction event of multicellular life, in the Permian–Triassic transition. Continental basins corresponding to present-day Mallorca (Balearic Islands, western Mediterranean) were located in the equatorial region of the supercontinent Pangaea, in the western peri-Tethys. Its recorded stratigraphic succession can be divided into four alluvial/fluvial formations, formally described here: Punta Roja Formation, Estellencs Formation, Pedra Alta Formation and Son Serralta Formation. Based on an exhaustive review of all available literature and new stratigraphic and palaeontological data, an upper Olenekian–lower Anisian interval is proposed for the whole succession. The richest fossil assemblage is that of Estellencs Formation, with abundant invertebrate and vertebrate trace fossils, and remains of plants, arthropods and rare fishes, which together represent a lotic/riverine ecosystem with a relatively complex food web. Plants and insects show strong biogeographical affinities with those of the Vosges, in central Europe; clam shrimps are similar to those of central Europe and Asia; and tetrapod tracks are also reminiscent to those of Eurasia and North America. Ultimately, integration of all these data provides a comprehensive and multidisciplinary characterisation of one of the oldest Triassic ecosystems of equatorial Pangaea, providing new insights to understand the evolution of palaeoenvironments of the Iberian Plate, an area that has historically suffered from severe undersampling.

1. Introduction

The Triassic is a key period in the history of life, as its ecosystems were recovering from the most critical mass extinction event in the Phanerozoic, in the Permian–Triassic transition (Erwin, 1994; Benton, 2008; Romano et al., 2020). Although the former complexity of the ecosystems was eventually restored, its floras and, especially, its faunas, had experienced profound turnovers (still not fully understood in the terrestrial realm), leading to more typically Mesozoic assemblages (Retallack et al., 1996; Labandeira, 2005; Benton and Newell, 2014; Romano et al., 2020). Those organisms lived and evolved under a megamonsoonal regime caused by the Pangaean supercontinental configuration, characterised by a marked seasonality, with alternating arid seasons and heavy rainfalls (Parrish, 1993; Zeng et al., 2019).

In the western peri-Tethys, initial Triassic sedimentation resulted in the *Buntsandstein* continental red-bed facies, usually overlaying a hiatus in the form of an unconformity, and representing semi-arid to arid climates (Durand, 2006; Bourquin et al., 2011; Mujal et al., 2016, 2017a,

* Corresponding author at: Institut Català de Paleontologia Miquel Crusafont, Universitat Autònoma de Barcelona, Edifici ICTA-ICP, c/ Columnes s/n, Campus de la UAB, 08193 Cerdanyola del Vallès, Barcelona, Spain.
E-mail address: rafel.matamales@icp.cat (R. Matamales-Andreu).

https://doi.org/10.1016/j.earscirev.2021.103783
Received 7 May 2021; Received in revised form 18 August 2021; Accepted 20 August 2021
Available online 25 August 2021
0012-8252/© 2021 Elsevier B.V. All rights reserved.

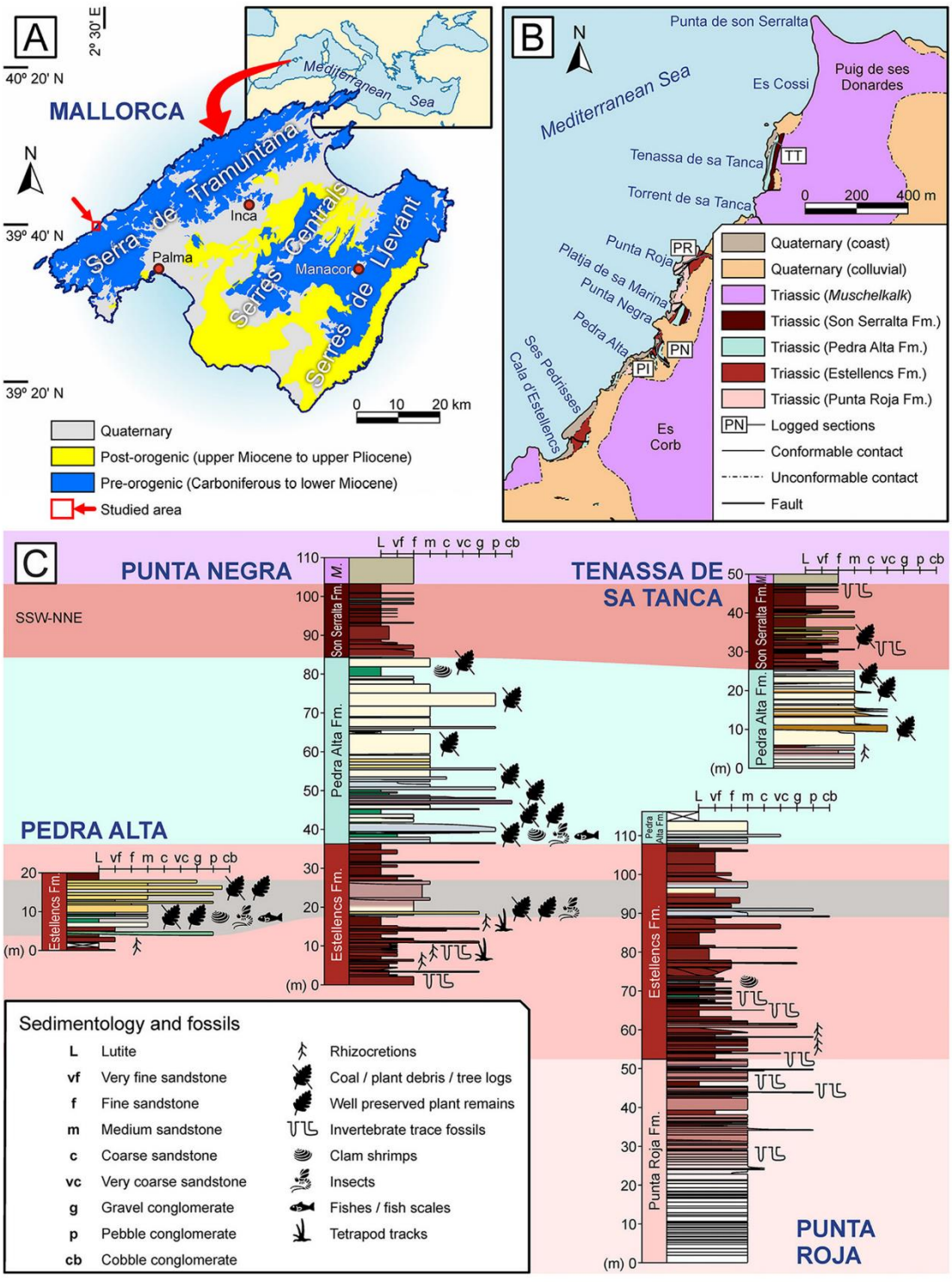

Fig. 1. A: Synthetic geological map of the island of Mallorca (Balearic Islands), with position of the study area (red rectangle and arrow). Simplified from Sevillano and Barnolas (2019). B: Detailed geological map of the outcrops between Cala d'Estellencs and Punta de son Serralta (Estellencs, Mallorca), with indication of the location of the four confected logs (PI: Pedra Alta; PN: Punta Negra; PR: Punta Roja; TT: Tenassa de sa Tanca). Toponyms after Homar (1985) and IDEIB (2019). C: Correlation of the four synthetic stratigraphic logs of the Lower–Middle Triassic red-beds of Mallorca (detailed stratigraphic logs are included in Appendix A. Supplementary data: Supplementary Logs). Changes of the background colour represent boundaries between formations or particular units, which have been used as datums to correlate the logs. (For interpretation of the references to colour in this figure legend, the reader is referred to the web version of this article).

2017b; López-Gómez et al., 2019a). In the case of Iberia, those sediments were deposited into half-graben basins that opened as a result of the relaxation of the Variscan orogen and subsequent fragmentation of the supercontinent (Bourquin et al., 2011; Frizon de Lamotte et al., 2015) in the intra-Pangaean dextral megashear zone (*e.g.*, Irving, 2004). During the Olenekian, semi-arid climates have been inferred in most of the sections because of the development of wadi and erg systems in the central part of Iberia (Marzo, 1986; Soria et al., 2011; López-Gómez et al., 2012, 2019a; Galán-Abellán et al., 2013a). Conversely, during the latest Olenekian and early Anisian, the ecosystems flourished under more humid climates, recognised because of the meandering style of the rivers and other geochemical and palaeopedological proxies (Borruel-Abadía et al., 2014, 2015), with a biotic diversity that evidences the richness of the ecosystems of palaeoequatorial Pangaea. Typical of this stage are plant assemblages composed of horsetails, ferns, conifers, spores and pollen (*e.g.*, Diez et al., 2005, 2010 and references therein). In some cases, arthropod fossils, including both traces (*e.g.*, Mujal et al., 2018a) and body fossils (Aristov and Zessin, 2009; Béthoux et al., 2009), are also locally abundant. Tetrapod fossils usually appear in the form of ichnites (*e.g.*, Fortuny et al., 2011a and references therein; Mujal et al., 2016, 2017b), but bone remains have been occasionally reported as well (Fortuny et al., 2011a, 2011b, 2014; Ezcurra et al., 2017).

The present work focuses on the Lower–Middle Triassic *Buntsandstein* facies of Mallorca, with outcrops located in a limited coastal area between Cala d'Estellencs and Punta de son Serralta (Estellencs, Mallorca, western Mediterranean). Its aim is to provide an accurate palaeoecological reconstruction integrating environmental, botanical, entomological and ichnological data. For that reason, the stratigraphy and sedimentology of all the outcrops are revised, formally defining lithostratigraphic units, namely, formations, in order to clear previous inaccuracies and misconceptions. This also makes it possible to infer the specific depositional palaeoenvironments represented in their rocks, as well as their evolution through time. Moreover, all the previous works on fossil plants and spores/pollen are reviewed, and the arthropod assemblages and invertebrate and vertebrate ichnoassemblages are studied in detail for the first time. These data are useful for the study of the palaeoenvironmental and palaeobiogeographical evolution of ecosystems recorded in the formations of Mallorca in the context of the western peri-Tethys, and, therefore, the importance of the present work lies not only in the improvement of the regional knowledge on the continental Triassic lithostratigraphic units and palaeoecosystems, but also in contextualising these data in a broader framework for equatorial Pangaea.

2. Geographical and geological context

Mallorca, the largest of the Balearic Islands (western Mediterranean) (Fig. 1A), is a northeast extension of the Betic orogen, tectonically structured in a series of grabens and horsts by northeast-southwest faults of late Miocene age (Vera et al., 2004). The oldest rocks that crop out on the island, as part of the lowermost unit of the Serra de Tramuntana, have been assigned to the Carboniferous marine *Culm* facies (Rodríguez-Perea and Ramos, 1984; Ramos and Rodríguez-Perea, 1985; Calafat, 1988). Above them and by means of a mechanical contact, Permian rocks appear, recording the sedimentation in continental environments such as alluvial fans, rivers and floodplains. Those palaeoenvironments persist in the Lower–Middle Triassic, with red-beds that appear in a group of very localised and precipitous outcrops along the northern coast of the island (Fig. 1A–B), which are the object of the present study.

In the Early–Middle Triassic, Mallorca was part of a continental basin located in the western Tethyan domain of central Pangaea (Scotese, 2014; Scotese and Schettino, 2017), where the Variscan belt, uplifted during the Palaeozoic (*e.g.*, Edel et al., 2018), still constituted a major geographical feature. The sediments resulting from its erosion ended up in the grabens of rifts that had started to open all over the western peri-Tethys (present-day western Europe and northern Africa), due to the extensional tectonic regime that prevailed until the late Mesozoic (Arche and López-Gómez, 1996; Hounslow and Ruffell, 2006; McCann et al., 2006; Stampfli and Hochard, 2009; Frizon de Lamotte et al., 2015). In the case of Iberia, which was right in the midst of the intra-Pangaean dextral megashear zone (*e.g.*, Irving, 2004), such basins followed a general northwest-southeast trend, and contained river systems flowing towards the southeast (Borruel-Abadía et al., 2015; López-Gómez et al., 2019a). The Basque-Cantabrian and Pyrenean basins were an exception, as there the rivers had variable palaeocurrent directions (Nagtegaal, 1969; Robles and Llompart, 1987; Borruel-Abadía et al., 2015; Gretter et al., 2015; López-Gómez et al., 2019b), probably pointing to the endorheic character of those basins. Six main basins (each with several sub-basins) were opened in the Iberian area: the Basque-Cantabrian Basin, the Pyrenean Basin, the Catalan Basin, the Iberian Basin (with the Castilian and Aragonese branches) and the basins of Mallorca and Menorca. Those of the present-day Balearic Islands record the most distal deposits of the Iberian area and, specifically on Mallorca, the successions are well exposed and are very rich in fossil plants and animals.

The inaccessibility of the sections of Mallorca had so far precluded their correct characterisation. Over time, several informal lithostratigraphic divisions had been proposed (Appendix A. Supplementary data: Supplementary Text 1, Supplementary Table 1), resulting in a plethora of disagreeing approaches that had never been properly collated. The present work provides a detailed study of all the sections of the island (Fig. 1C) and formal definitions for each of the lithostratigraphic units to avoid ambiguity in future studies.

3. Material and methods

3.1. Stratigraphy and sedimentology

For the stratigraphic and sedimentological study, four stratigraphic sections have been measured bed by bed to a minimum resolution of 1 cm of bed thickness. Covered and semi-covered intervals have been measured using a Jacobs staff. Most zones of complicate access due to the steepness of the outcrops have been reached using climbing gear. They all have been logged in detail (in 1:25 scale) (presented in Appendix A. Supplementary data: Supplementary Logs in 1:40 scale). Those have been named, from southwest to northeast: 'Pedra Alta' (18.5 m), 'Punta Negra' (103.5 m), 'Punta Roja' (126.5 m, including a repeated stretch of 14 m) and 'Tenassa de sa Tanca' (47.5 m) (Fig. 1B). The logs have been synthesised (1:1160 scale) and correlated in Fig. 1C. The datum to correlate Pedra Alta (PI) and Punta Negra (PN) logs is the top of the green/pink interval in the upper part of Estellencs Formation. The datum to correlate Punta Negra and Punta Roja (PR) logs is the boundary between Estellencs Formation and Pedra Alta Formation, that is, the change of colour from dominant red to dominant white/blue/green. The datum to correlate Punta Negra and Tenassa de sa Tanca (TT) logs is the boundary between Son Serralta Formation and the *Muschelkalk* marine facies. The recognised sedimentary lithofacies have been classified according to Miall (1977, 1985, 2006) and Postma (1990), with additional support of more specific works such as Shanley et al. (1992), Mack et al. (1993), Gómez-Gras and Alonso-Zarza (2003) and Shiers et al. (2018) (Table 1). Architectural elements have been classified according to Miall (1985, 2006) (Table 2).

3.2. Tetrapod tracks

The specimens of tetrapod tracks, which were left in the field, were assigned numbers depending on their position in the stratigraphic logs. The ones under the code PN-7.6?-[slab number]-[ichnite number] were found *ex situ* near the metre 7.6 of Punta Negra log and may belong to that bed. PN-7.6-[slab number]-[ichnite number] were the only ones found *in situ* there. PN-14.6-[slab number]-[ichnite number] and PN-14.7-[slab number]-[ichnite number] were found *in situ* in an unequivocal lateral equivalent of the metres 14.6 and 14.7, respectively, of

Table 1
Sedimentary lithofacies recognised in the outcrops of the Triassic red-beds of Mallorca.

Code	Lithofacies	Sedimentary structures, processes and fossil content	Geometry and structures
Gt	Stratified, matrix to clast-supported, gravel to pebble-sized breccia of reworked lutite, sandstone or calcrete (intraformational) clasts.	Crude trough cross-bedding. Positive granoselection has been observed in some beds. It corresponds to 3D megaripples that rework the floodplains, or scour fills of major channels (Miall, 1977; Gómez-Gras and Alonso-Zarza, 2003). Tree logs are common.	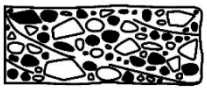
St	Stratified, very fine to very coarse-grained sandstone.	Trough cross-bedding. It corresponds to sinuous or linguoid 3D megaripples of lower flow regime (Miall, 1985, 2006). No fossils have been found.	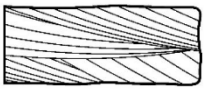
Sp	Stratified, very fine to fine-grained sandstone.	Planar cross-bedding. It corresponds to transverse or linguoid 2D bars of lower flow regime (Miall, 1977, 1985, 2006). No fossils have been found.	
Sr	Stratified, very fine to medium-grained sandstone.	Ripple-marks, mostly climbing and wave ripples. Sometimes convolute lamination. It corresponds to ripples formed during low regime and waning flows, at the top of channel sequences or at crevasse splays (Miall, 1985). Rarely with rhizocretions, burrows, invertebrate traces and/or tetrapod ichnites.	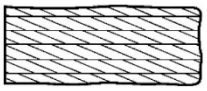
Sh	Stratified, very fine to fine-grained sandstone.	Horizontal stratification and lamination. It corresponds to deposition under planar bed flow of lower flow regime or traction carpets in upper flow regime (Miall, 1977, 1985, Postma, 1990). Plant remains appear frequently.	
Sl	Stratified, very fine to medium-grained sandstone.	Low-angle cross-bedding. Sometimes convolute lamination. It corresponds to deposition during low regime and waning flows, at the top of channel sequences or at crevasse splays (Miall, 2006). Rarely with rhizocretions, burrows, invertebrate traces and/or tetrapod ichnites.	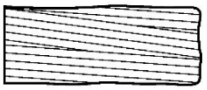
Ss	Stratified to massive, fine- to coarse-grained sandstone.	Clear to crude trough cross-bedding. Usually with soft pebbles. It corresponds to scour fills (Miall, 2006). No fossils have been found.	
Sm	Massive, very fine to medium-grained sandstone.	Massive (in macroscopic view). It corresponds to sediment gravity flows (Miall, 2006) or to beds with lamination obliterated by bioturbation.	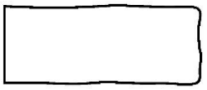
Sb	Massive, fine-grained sandstone.	Abundant invertebrate burrows and/or root traces. It corresponds to the biotic reworking of overbank deposits (Miall, 1985).	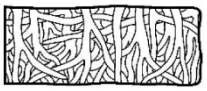
Si	Very fine to fine-grained sandstones interbedded with lutites.	Alternation of thin layers of sand and lutite, usually irregular or deformed, sometimes even brechified. Often with retraction cracks. It corresponds to sands deposited under upper flow regime and lutites deposited under low flow regime, probably because of tidal influence (Shanley et al., 1992; Shiers et al., 2018). No fossils have been found.	
Fl	Laminated lutites.	Fine lamination, mostly horizontal, but can also be low angle cross lamination or ripple lamination. It corresponds to abandoned channel or pool, overbank or waning flood deposits (Miall, 1977, 2006). Plant remains and arthropods are very abundant in some horizons.	
Fm	Massive lutites.	Massive, sometimes bioturbated with root traces and burrows. It corresponds to overbank, abandoned channel or drape deposits (Postma, 1990; Miall, 2006).	
P	Lutites or sandstones without clear lamination.	Massive to crudely laminated. Very abundant carbonate nodules; root traces and gleyed patches are common. It represents palaeosols, corresponding to either vertic Calcisols or to Calcisols (Mack et al., 1993).	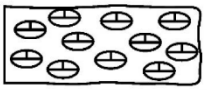

Punta Negra log but at Platja de sa Marina, where no log was confected. All studied tetrapod tracks are preserved as concave epireliefs. In some cases, the natural cast is also preserved as a convex hyporelief (providing the same information as the studied epireliefs), although it is usually eroded because it is proportionally finer-grained.

In order to study the tetrapod footprints, the layers of rock covering them were removed, and the exposed surface was recorded in a digital 3D model. Photogrammetry was made mostly following the procedure explained by Mujal et al. (2020), using Agisoft Photoscan standard version 1.1.4. (http://www.agisoft.com) to create the mesh and the texture, MeshLab version 2016.12 (http://meshlab.sourceforge.net) to align, scale and measure the mesh, and ParaView version 4.1.0 64-bit (http://www.paraview.org) to create the false colour-coded depth maps with contours. The main descriptive parameters of each footprint (Leonardi, 1987; Hasiotis et al., 2007) were measured on schematic diagrams, using the software ImageJ version 1.52d (https://imagej.nih.gov/ij), and are here presented in Appendix A. Supplementary data: Supplementary Table 2. No trackway measurements were taken given the fragmentary nature of all the specimens.

3.3. Fossil arthropods and fishes

The present research is based on three different collections. The most important one is the historical Tomeu Sáez private collection (Binissalem, Mallorca, Balearic Islands, Spain), which had been studied by Calafat and Sáez (1987) and Calafat (1988). It contains over 60 compression fossils of animals (30 insects, about 30 clam shrimps and a fish) in 10 slabs (A–J). All these specimens have been identified using the acronym TS-[slab letter]-[specimen number] and were obtained in the early 1980s from a single lutitic horizon rich in arthropods of Pedra Alta section (*ca.* metre 4.75 of the log presented in Appendix A. Supplementary data: Supplementary Logs; T. Sáez, pers. comm., 2020). Specimens of a same slab have been correlatively numbered.

The second collection is that of Museu Balear de Ciències Naturals (Sóller, Mallorca, Balearic Islands, Spain). It includes one insect specimen under the acronym MBCN[specimen number] from a lutitic horizon of Pedra Alta section (*ca.* metre 7.55 of the log presented in Appendix A. Supplementary data: Supplementary Logs).

The third collection of *ca.* 100 slabs with clam shrimps ("conchostracans") and insects has been sampled for the present work with permission of Consell de Mallorca (file numbers 305/2019 and 52/2021), and are deposited in Museu de Mallorca (Palma, Mallorca, Balearic Islands, Spain) with the acronym DA21/[campaign number]-[horizon number]-[specimen number]. Those were collected from four different stratigraphic levels: a few clam shrimps are from a lutitic horizon of Punta Roja section (metre 86.5 of Punta Roja log presented in Appendix A. Supplementary data: Supplementary Logs); all insects (n = 120) and most clam shrimps were sampled from a lutitic bed of Pedra Alta section (*ca.* metre 7.20–7.30 of Pedra Alta log presented in Appendix A. Supplementary data: Supplementary Logs); and several more clam shrimps were collected from lutitic horizons of Punta Negra section (metre 39.5 and 82.0 of Punta Negra log presented in Appendix A. Supplementary data: Supplementary Logs). Parts/counterparts are identified with a number "1"/"2" following the museum collection number. Different specimens on a same rock slab have been identified with correlative letters.

Photographs of clam shrimps were taken using a LEICA MZ12 stereomicroscope with a WILD drawing mirror tube, and a BRESSER MikroCamII digital camera. Insects from Tomeu Sáez collection were photographed using a single-lens reflex camera Canon EOS 40D and a digital camera Olympus SC30 attached to an Olympus SZ61-TR stereomicroscope; some of its specimens were wet with alcohol to be photographed enhancing the contrast of the carbonaceous parts. Specimens housed at Museu de Sóller and at Museu de Mallorca were photographed using a digital camera Olympus Camedia MODEL N.C5050 ZOOM attached to an Olympus SZX9 stereomicroscope.

Clam shrimp measurements and terminology follow Scholze and Schneider (2015). Mayfly morphological terminology follows that of Sinitshenkova et al. (2005) and Bashkuev et al. (2012); body lengths of the mayfly nymphs were measured up to the base of cerci and paracercus. Abbreviations for the wing venation are as follows: CuA: anterior cubitus, CuP: posterior cubitus, M: media, MA: media anterior, R: radius, Rs: radial sector, Sc: subcosta.

4. Stratigraphy and sedimentology

Formal units have hitherto never been defined for the Lower–Middle Triassic red-beds of Mallorca. Several works (Cuevas-López, 1958a, 1958b; Pomar-Gomà, 1979; Martí et al., 1985; Ramos et al., 1985; Calafat, 1986, 1987, 1988; Rodríguez-Perea et al., 1987; Barnolas, 1991a, 1991b; Gómez-Gras, 1992, 1993; Ramos, 1995) provided informal classifications of the different units (Appendix A. Supplementary data: Supplementary Table 1), and other reviews upgraded them to formations without any formal description (Arche et al., 2002; López-Gómez et al., 2002, 2019a; Vera et al., 2004; Bourquin et al., 2007, 2011; Cassinis et al., 2012). This situation, as well as some miscorrelations between units (see Appendix A. Supplementary data: Supplementary Text 1, Supplementary Table 1), required a formal description of the lithostratigraphic units of the *Buntsandstein* facies of Mallorca. Whenever possible, however, the first name used for each of the units has been preserved. Descriptions and interpretations of all the lithofacies and architectural elements are here presented in Table 1 and Table 2.

4.1. Punta Roja Formation

This formation (Fig. 2A) can be identified in the field because of the abundance of medium-grained sandstone beds, which are often tabular and show abundant planar cross-bedding. Those sandstones are white or pink in colour, and near the base of the unit they show a very distinct alternation of white and pink laminae. Red lutites are extremely rare in the lower part of the formation, and they become progressively more abundant towards the top.

4.1.1. Location and boundaries

A small part of Punta Roja Formation crops out at Cala d'Estellencs and southwest of Pedra Alta (Fig. 1B). The most complete outcrop is at Punta Roja and, although it lacks its base, up to 53 m have been measured until its boundary with Estellencs Formation. The Punta Roja outcrop (Fig. 1B) is herein formally designated as the stratotype of Punta Roja Formation. Its lower boundary cannot be observed, and its upper boundary with Estellencs Formation is transitional, characterised by the change of colour from pink to red, the presence of thick lutitic beds and a switch from dominant planar cross-bedding to dominant trough cross-bedding and ripple lamination.

4.1.2. Lithological features

The lithofacies (Fig. 3, Table 1) and architectural elements (Table 2) present in Punta Roja Formation are reduced to a few dominant types, the rest being quantitatively less important. Breccias (lithofacies type *Gt*) are rare, and are composed of intraformational clasts and carbonate nodules, appearing as isolated beds among sandstone deposits in the uppermost part of the formation, both in the base of sandstone packs and intercalated between lutites. Sandstones are clearly dominant, especially in the lower part. The lower half of the formation is essentially made up of medium-grained sandstones of lithofacies type *Sp*, whereas lithofacies type *St* (Fig. 3I) appears more frequently towards the top of the formation. Lithofacies of types *Sl* and *Sh* also appear abundantly in the upper part of the formation, together with lithofacies type *Sr*, *Ss*, *Sm* and *Sb*, which are rarer. Lutite lithofacies (types *Fl* and *Fm*) are more frequent towards the upper part of the formation and they are often associated with lithofacies type *P*, which displays abundant carbonate nodules (diameter between 0.5 and 3 cm) and rhizocretions. The dominant architectural element is *SB*, with sporadic intercalations of the elements *LS* and *FF* towards the upper part.

4.1.3. Interpretation

In this formation, lithofacies type *Gt* represents reworked floodplain deposits (as the clasts are always soft pebbles and carbonate nodules) in the basal lag of some channels and in the floodplain, similarly to the cases described by Gómez-Gras and Alonso-Zarza (2003). Regarding sandstone deposits, lithofacies type *Sp* corresponds to transverse fluvial bar deposits, *St* represents megaripple deposits formed under lower flow regime conditions, *Sl* and *Sh* correspond to events of sediment deposition under higher flow regimes, *Sr* was formed by waning flows, and *Ss* corresponds to the infill of scours. Moreover, lithofacies type *Sm* probably corresponds to events of rapid deposition or to beds reworked by bioturbation, similarly to *Sb*, which possesses abundant burrowing. Lutite lithofacies (types *Fl* and *Fm*) correspond to overbank and floodplain fine-grained deposition, and lithofacies type *P* can be interpreted as palaeosols, which in this case would correspond to Calcisols given the abundance of carbonate nodules and lack of gleyed patches (Mack et al.,

Table 2
Architectural elements recognised in the outcrops of the Triassic red-beds of Mallorca. Arrows (→) indicate the usual succession. Lithofacies in brackets are often missing in the "ideal" succession. Formations in brackets only present that architectural element rarely. Diagrams not to the same scale.

Code	Element	Principal lithofacies assemblages	Features and interpretation	Diagrams	Formation
SB	Sandy bedforms	*(Gt)→Sp→(Sr)* *(Gt)→(Sm)→Sl→Sl→Sr* *Sr→Fl→(Fm)*	Shallow channel-fill assemblages, channel-floor dune fields, and bar top assemblages, respectively (all in the sense of Miall, 2006). Metric thickness.		Pedra Alta Formation Punta Roja Formation
LA	Lateral accretion deposits	*St→(Sm)→Sr→Fm* *Sm*	Point bars of meandering rivers (Miall, 2006) or tidally influenced point bars (*e.g.*, Ghinassi et al., 2021). Metric and metric–centimetric thickness.		Son Serralta Formation Estellencs Formation
LS	Laminated sand sheets	*Sh* *Sl*	Upper flow-regime plane bed conditions (Miall, 2006). Metric–centimetric thickness.		Pedra Alta Formation (upper part of Punta Roja Formation)
LV+ CS	Levees and Crevasse splays	*(Gt)→(St)→(Sl)→Sr* *Ss* *Sb* *P*	Overbank flooding (Miall, 2006). May be affected by pedogenesis. Given the limited lateral extension of the studied deposits, it cannot be established whether the observed deposits belong to one architectural element or to the other. Centimetric thickness.		Son Serralta Formation Estellencs Formation
FF	Floodplain fines	*(Fl)→Fm→(P)* *Si*	Deposits of overbank low-energy flows or sedimentation in pools and playa-lakes (Miall, 2006). May be affected by pedogenesis. The lithofacies *Si* indicates deposits under probable tidal influence. Metric–centimetric thickness.		Son Serralta Formation Estellencs Formation (upper part of Punta Roja Formation)

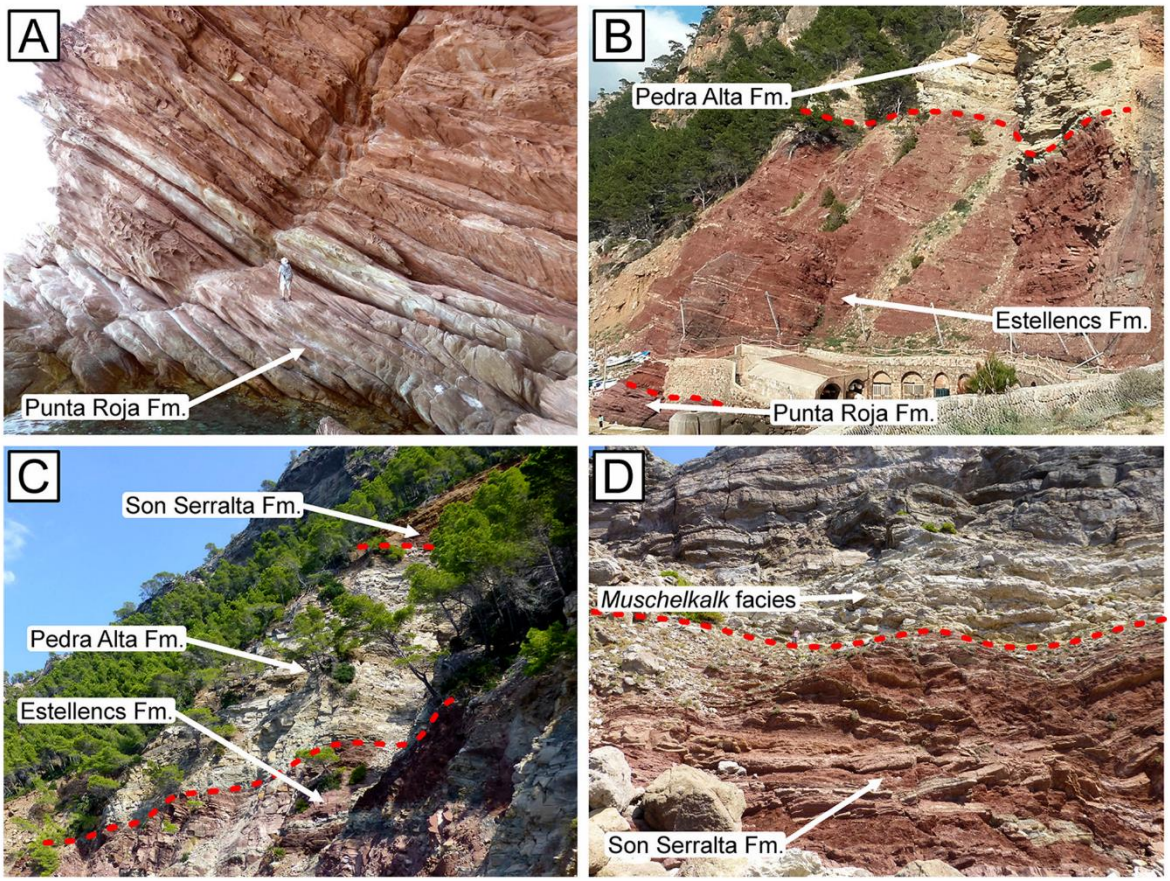

Fig. 2. Representative views of the studied formations and their boundaries. A: Panoramic view of Punta Roja, showing the typical facies assemblage of Punta Roja Formation. B: Panoramic view of Cala d'Estellencs, showing the upper and lower boundaries of Estellencs Formation. C: Panoramic view of the ravine between Pedra Alta and Punta Negra, showing the upper and lower boundaries of Pedra Alta Formation. D: Panoramic view of the cliffs at Tenassa de sa Tanca, showing the upper boundary of Son Serralta Formation. Dashed red lines mark the boundaries between formations. (For interpretation of the references to colour in this figure legend, the reader is referred to the web version of this article).

1993). Architectural element *SB* represents shallow channel-fill assemblages, whereas *LS* and *FF* correspond to sheetflood deposits and floodplain fines, respectively.

This formation represents a shallow perennial braided river in the sense of Miall (2006), because of the dominance of architectural element *SB*, made up of lithofacies type *Sp*, corresponding to transverse bar deposits. Calafat (1988) suggested an aeolian origin for this unit, because of the overall lack of fine sediments and the well-sorted sands. Indeed, in thin sections, those sandstones do have a relatively consistent grain size distribution (medium-grained sands), yet mica flakes are very abundant. In aeolian contexts, such minerals are usually blown away by the wind (*e.g.*, Glennie, 1970), thus making it more probable for Punta Roja Formation to be of mixed aeolian–fluvial origin. Specifically, it would correspond to river deposits that reworked aeolian dune fields, hence the well-sorted sand grains. The palaeocurrent direction, based on field measurements ($n = 20$), had a dominant direction towards the southwest, with little dispersion (see '7. Discussion'). Towards the top of the formation, the transition towards meandering rivers with associated floodplain deposits can be observed because of the overall increase of the relative abundance of lutites. This formation has not been confidently dated because of its lack of fossil content, however, here it is assumed to be of upper Olenekian (Spathian) age, based on the age of the overlying units and correlation with lithologically similar formations of Iberia (see '7. Discussion' and Appendix A. Supplementary data: Supplementary Table 3), altough a younger age, *i.e.*, lower Anisian (lowermost Aegean), cannot be completely ruled out for its upper part.

4.2. Estellencs Formation

This formation (Fig. 2B–C) can be identified in the field because of the abundance of very fine- and fine-grained sandstones with dominant trough cross-bedding and ripple lamination, interbedded with abundant lutites. Both the sandstones and the lutites are of a bright red colour. In the upper part of the formation, there is an intercalation of coarser deposits (breccias and medium-grained sandstones) that are pink, white or green.

4.2.1. Location and boundaries

Estellencs Formation crops out completely at Cala d'Estellencs and at Punta Roja. Smaller outcrops can be observed in a roadcut near Cala d'Estellencs, between Pedra Alta and Punta Negra and at Platja de sa Marina (Fig. 1B). At Punta Roja, where this formation is well accessible and crops out completely, 55 m have been measured. The Punta Roja outcrop is herein formally designated as the stratotype of Estellencs Formation. Its lower boundary is gradual and its upper boundary is sharp. Its upper boundary with Pedra Alta Formation is characterised by the change of dominant colour from red to green/blue/white, the almost complete absence of red lutites and the dominant planar cross-bedding.

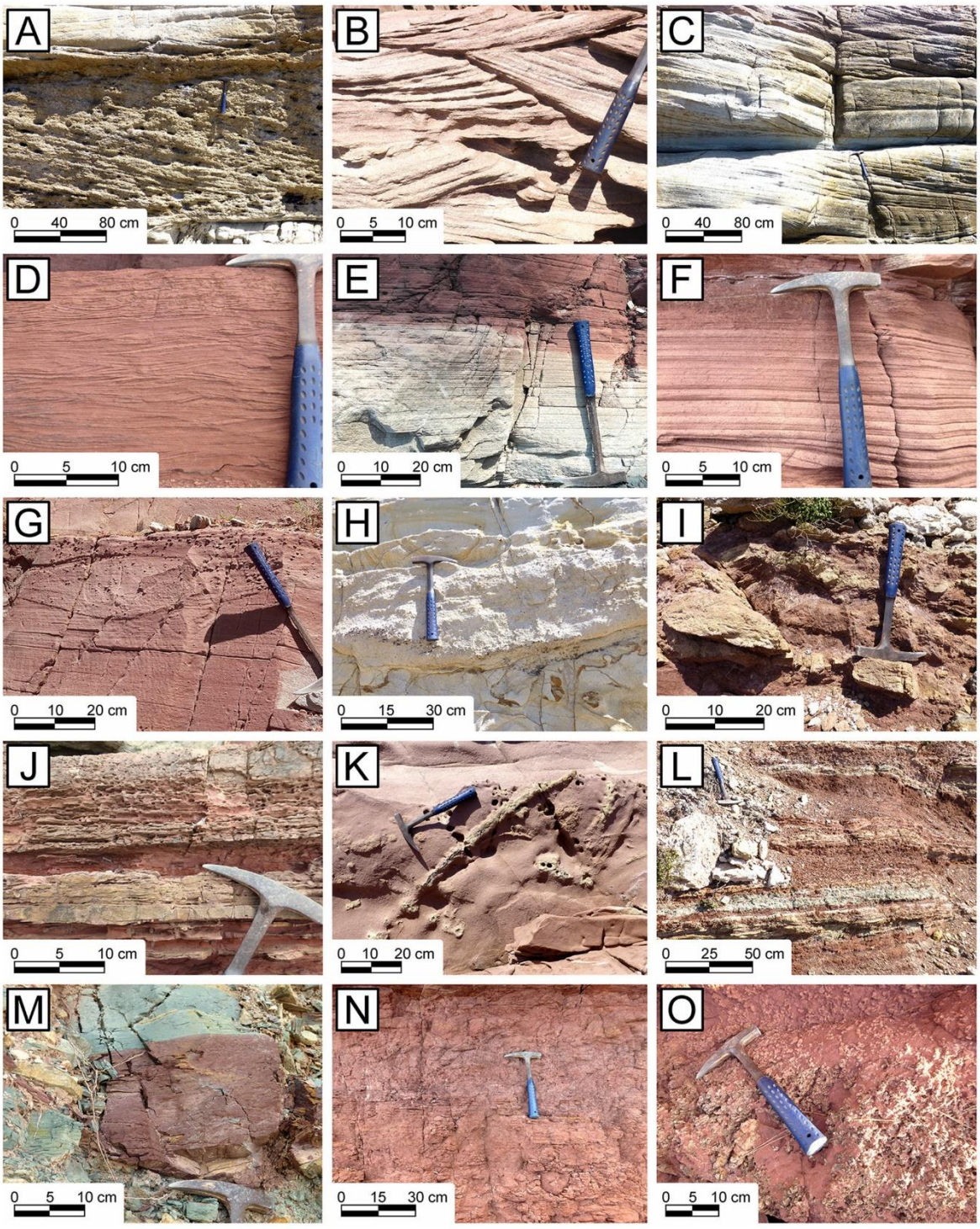

Fig. 3. Photographic examples of each of the recognised lithofacies. A: Breccias with trough cross-bedding (*Gt*), Pedra Alta Formation. B: Sandstone with trough cross-bedding (*St*), Punta Roja Formation. C: Sandstone with planar cross-bedding (*Sp*), Pedra Alta Formation. D: Sandstone with ripple cross-lamination (*Sr*), Estellencs Formation. E: Sandstone with horizontal bedding (*Sh*), Estellencs Formation. F: Sandstone with low angle cross-bedding (*Sl*), Pedra Alta Formation. G: Sandstone infilling a scour (*Ss*), Estellencs Formation. H: Massive sandstone (*Sm*), Pedra Alta Formation. I: Massive yellowish and irregular sandstone (*Sm*), Son Serralta Formation. J: Sandstone with burrows (*Sb*), Estellencs Formation. K: Sandstone with root traces (*Sb*), Pedra Alta Formation. L: Sandstones with interbedded lutites (*Si*), Son Serralta Formation. M: Laminated lutites (*Fl*), Estellencs Formation. N: Massive lutites (*Fm*), Estellencs Formation. O: Palaeosols (*P*), in this case a Calcisol, Estellencs Formation.

4.2.2. Lithological features

The lithofacies (Fig. 3, Table 1) and architectural elements (Table 2) present in this formation are quite varied, consisting mostly of lutite and sandstone types. Breccias (lithofacies type *Gt*) are not frequent, and they appear as isolated events scouring underlying lutites or sandstones, both in the base of sandstone packs or as isolated beds in the lutite intervals. They show crude trough lamination, and are composed of intraformational clasts (mudstones, sandstones) and reworked calcretes. The sandstone lithofacies of types *Sh*, *Sp*, *Ss*, *St* and *Sm* (Fig. 3D, H) are also rare except for the stretch between metres 18–27 of Punta Negra log and its lateral equivalent: Pedra Alta log (Fig. 1C). The sandstone lithofacies of types *Sl* and *Sr* (Fig. 3G) are by far the most abundant, usually in the form of thin, very fine- to fine-grained, tabular beds, although they can also be part of sequences showing clear lateral accretion, especially in the base of the formation. On the top of the beds, wrinkle structures (Porada and Bouougri, 2007) are sometimes well visible. Lithofacies type *Sb* is characterised by profuse burrowing and is usually found associated to lithofacies of types *Sl* and *Sr*. Lithofacies type *P* (Fig. 3O) contains abundant carbonate nodules (diameter between 0.5 and 3 cm) and often root traces and gleyed patches as well. Lutite lithofacies (types *Fl* and *Fm*, Fig. 3M, N) often appear over lithofacies of types *Sl/Sr* and form relatively thick packs. The dominant architectural elements are *LV/CS* and *FF*, and sporadically *LA* can also be observed.

4.2.3. Interpretation

In this formation, lithofacies type *Gt* represents high-energy deposits reworking floodplains, produced by occasional events of heavy rains or as the basal lags of channels, similarly to the case described in the Permian of Menorca (Gómez-Gras and Alonso-Zarza, 2003). Sandstone lithofacies of types *Sh*, *Sp*, *Ss*, *St* and *Sm* correspond to bedforms of major river channels under different flow regimes (see '4.3. Pedra Alta Formation'). Lithofacies of types *Sl* and *Sr* are interpreted as the result of the waning flows in major sheetfloods, as overbank deposits over the floodplains or as point bar deposits of meandering channels. The wrinkle structures that appear on the top of some beds of these lithofacies types were probably formed by microbial mats (Porada and Bouougri, 2007), which favour the preservation of small tetrapod ichnites (Carmona et al., 2011). Lithofacies of types *Sb* and *P* are nothing but the reworking of the other types mentioned above and, specifically, lithofacies type *P* can be interpreted to correspond to vertic Calcisols when small carbonate nodules and gleyed patches are present, whereas Calcisols can be inferred when there are only carbonate nodules, generally larger (Mack et al., 1993). Lithofacies of types *Fl* and *Fm* correspond to deposition of low-energetic to still waters in environments such as the uppermost part of crevasse splay deposits and playa lake deposits (in the sense of Briere, 2000). Architectural elements *LV/CS* and *FF* represent the floodplain palaeoenvironment, whereas *LA* corresponds to point bars of meandering channel deposits.

The lower half of this formation corresponds to meandering river channels with conspicuous lateral accretion. Towards the upper part, interbedded floodplain deposits, including crevasse splays, start to appear more frequently. However, the stretch between metres 18–27 of Punta Negra log, metres 103–112 of Punta Roja log and the whole Pedra Alta log represent a relatively higher energy pulse with sedimentary environments comparable to those of Pedra Alta Formation (see '4.3. Pedra Alta Formation'). The palaeocurrents measured in this formation ($n = 13$) show a wide dispersion but with a general trend towards the southeast (see '7. Discussion'). The palynoassemblages of this formation made it possible to date it as lower Anisian, probably lower Aegean, because the base of the overlying formation is of upper? Aegean age (see '4.3. Pedra Alta Formation', '7. Discussion' and Appendix A. Supplementary data: Supplementary Table 3).

4.3. Pedra Alta Formation

This formation (Fig. 2B–C) can be identified in the field because of the abundance of medium-grained sandstone beds, which are of a clear colour (white, yellowish, bluish, pink), intercalated with intervals of blue or green lutites. The dominant sedimentary structures in the sandstones are planar or trough cross-bedding, whereas the lutites frequently have planoparallel lamination.

4.3.1. Location and boundaries

Pedra Alta Formation crops out completely between Pedra Alta and Punta Negra, and at Platja de sa Marina. It can also partially be observed at a roadcut near Cala d'Estellencs, at Cala d'Estellencs and at Tenassa de sa Tanca (Fig. 1B). The outcrop located in the precipitous ravine between Pedra Alta and Punta Negra (Punta Negra log) is herein formally designated as the stratotype for Pedra Alta Formation, where 44 m have been measured. Both its lower and upper boundaries are sharp but apparently not erosive. Its upper boundary with Son Serralta Formation is characterised by the change of dominant colour from green/blue/white to red and the appearance of thick beds of red lutites.

4.3.2. Lithological features

The lithofacies (Fig. 3, Table 1) and architectural elements (Table 2) present in this formation are somewhat constant, with sequences with a lower part made up of sandstones (sometimes with basal breccias as well) and an upper part made by lutites. Breccias (lithofacies type *Gt*, Fig. 3A) are exclusively composed of intraformational clasts (sandstones and lutites, sometimes also with carbonised remains of large woody debris), and possess crude trough cross-bedding. The sandstone lithofacies of types *Sp* and *St* (Fig. 3F) are rather abundant and are usually constituted by medium-grained sandstones with planar or through cross-bedding, respectively. Over them, lithofacies of types *Sl* or *Sr* (Fig. 3E) appear, usually in very fine- to fine-grained sandstones grading to the lutite lithofacies. Very fine-grained sandstone lithofacies type *Sh* and horizontally laminated lithofacies type *Fl* with abundant remains of plants, arthropods and, rarely, fishes constitute the top of the sequences, sometimes with lithofacies type *Fm* as well. The dominant architectural element is *SB*, but *FF* also appears between the sandy bedforms.

4.3.3. Interpretation

In this formation, lithofacies type *Gt* represents the basal lags of major channel deposits. Lithofacies of types *Sp* and *St* correspond to linguoid and/or transverse bars and sand dunes migrating on the channel floor, and those of types *Sl/Sr* were deposited during waning currents in channel top sequences. Lithofacies of types *Sh* (very fine-grained) and *Fl* have been interpreted as fine sediments deposited during intervals of low energy flow, and lithofacies type *Fm* corresponds to deposition in periods of still waters in abandoned channels or backswamps. Architectural element *SB* represents channel-floor dune fields and top-bar assemblages, whereas element *FF* was formed by the deposition of fine sediments in abandoned channels or backswamps.

This formation represents several sequences of a sheetflood distal braided river (as defined by Miall, 2006), consisting in superimposed flood cycles with abundant bedforms without associated floodplain deposits (the element *FF* corresponds to the infill of the channels during low water stage). Linguoid and transverse bars amount to more than half of sandstone elements, deposited during flood stage. Over them and fining upwards, low angle cross-bedded and ripple-laminated beds appear, as a result of the waning of the flow after the main flood events. The sequences often end with greenish or red lutite deposits, either laminated or apparently massive. They represent pools with still to very low energetic flows (Coleman, 1969; Williams and Rust, 1969; Miall, 1977, 2006), isolated in abandoned channels among the remnants of megaripples (similar to those described in the Upper Cretaceous of the southern Pyrenees by Vila et al., 2013) or backswamps (similar to those described for the Lower Triassic of the Central European Basin by Kustatscher et al., 2014). The variety of colours of the lutites can result from pedogenetic alteration or water circulation during diagenetic processes, but in some specific beds it can also be explained by the height of the

water table in the time of sediment deposition, since the fossil content varies greatly from red lutites to green lutites, being by far more abundant in the latter. Thus, lutites that were sedimented in well-drained areas underwent oxidation and became red, whereas the green/grey/blue lutites were deposited below the water table. Similar environments were inferred for the clay levels of the Middle Triassic *Grès à Voltzia* of the Vosges (Gall, 1971) and the Solling Formation (Kustatscher et al., 2014), both in the Central European Basin. This accounts for the very high preservation potential of plant remains, clam shrimps, insects and, rarely, scales and very small fishes in the fossiliferous horizons of the studied sections. The palaeocurrents measured in this formation ($n = 23$) show a wide dispersion but with a general trend towards the southeast (see '7. Discussion'). This formation was dated as Aegean (lower Anisian), probably upper Aegean, by Diez (2000) and Diez et al. (2005, 2010) based on the study of spores and pollen (see '7. Discussion' and Appendix A. Supplementary data: Supplementary Table 3).

4.4. Son Serralta Formation

This formation (Fig. 2C–D) can be identified in the field because of the absolute dominance of fine sediments and lack of thick sandstone elements. The most abundant lithologies are red very fine- to fine-grained sandstones and red lutites. Sporadically and especially towards the top, intercalations of greenish lutites become progressively more abundant.

4.4.1. Location and boundaries

Son Serralta Formation crops out completely at Tenassa de sa Tanca, between Pedra Alta and Punta Negra, and at Platja de sa Marina (Fig. 1B). Of those three, the most accessible outcrop is at Tenassa de sa Tanca, which is herein formally designated as the stratotype of this formation, with a measured thickness of 22 m. Both its lower and upper boundaries are sharp. Its upper boundary is characterised by the onset of carbonate shallow marine sedimentation (M-1 unit of the *Muschelkalk* facies; *e.g.*, Matamales-Andreu et al., 2021).

4.4.2. Lithological features

The lithofacies (Fig. 3, Table 1) and architectural elements (Table 2) present in this formation are few and quite constant throughout, with very fine to fine-grained sandstone lithofacies representing about a half of the whole sequence. At its base, the most abundant lithofacies is type *Sr* that, together with type *Sl*, form tabular deposits of very fine- to fine-grained sandstones. The lithofacies of types *St* and *Sp* are also constituted by very fine- to fine-grained sandstones, are relatively less abundant and have usually less lateral continuity. The lutite lithofacies (types *Fl*, *Fm*) appear over the sandstone beds and form intervals that are thicker towards the top of the unit. Very typical of this formation are the yellowish massive sandstones (herein classified in lithofacies type *Sm*, Fig. 3I) that appear as channelled or irregular beds isolated among the lutites, and the presence of interlayered sand/mud bedding (lithofacies type *Si*, Fig. 3L), forming packs of up to 60 cm of thickness, which are usually deformed and affected by desiccation cracks. The dominant architectural elements are *LV/CS* and *FF*, whereas the element *LA* appears in the middle part of the formation.

4.4.3. Interpretation

In this formation, lithofacies of types *Sr* and *Sl* represent crevasse splay deposits, and lithofacies of types *St* and *Sp* correspond to small fluvial channel deposits. Lutite lithofacies such as type *Fl* and type *Fm* have been interpreted as the result of deposition of suspended fine sediments on the floodplain. Moreover, there are two types of lithofacies that are typical of this formation and common in tidal environments. In the middle part, there appear irregular or channelled beds of yellowish, massive sandstones isolated among the lutites (herein classified as a particular kind of lithofacies type *Sm*). Some of them show clear lateral accretion sets separated by lutite drapes (Fig. 3I), corresponding to inclined heterolithic point bars of tidal creeks (*e.g.*, Ghinassi et al., 2021). In the middle and upper part of the formation, sandstone beds are arranged in very thin layers alternating with lutites (lithofacies type *Si*), which is another typical (albeit not exclusive) trait of tidally-influenced environments, especially mixed-flats and mud-flats (*e.g.*, Nio and Yang, 1991; Davis Jr., 2012; Shiers et al., 2018). Architectural elements *LV/CS* and *FF* represent the floodplain palaeoenvironment, whereas element *LA* corresponds to small tidal creek deposits.

This formation represents the transition between the continental environments of the three underlying units to a marine environment such as the overlying *Muschelkalk* facies shallow platform carbonates (Calafat, 1988; Gómez-Gras, 1993; Ramos, 1995; Matamales-Andreu et al., 2021), and thus representing a local expression of the so-called *Röt* facies. The lower part of Son Serralta Formation still shows a great amount of fluvial influence, with relatively thin sandstone beds with ripples representing crevasse splay deposits over the lutitic floodplain, similarly to the lower and middle parts of Estellencs Formation (see '4.2. Estellencs Formation'). In the middle and upper parts of Son Serralta Formation, there appear inclined heterolithic point bars that conform tidal-influence criterion for red-bed successions (see Ghinassi et al., 2021). Some intervals of this portion of the formation also display interlayered sand/mud bedding, which is very typical (albeit not exclusive) of tidal environments (*e.g.*, Nio and Yang, 1991; Davis Jr., 2012; Shiers et al., 2018). Moreover, from this formation, Ramos (1995) reported the presence of tepee/pseudo-anticline structures, which are indicative of marine influence, appearing together with other structures such as wave ripples, flaser bedding and evaporite solution breccias, which are also common in such settings. The few palaeocurrents measured ($n = 2$) have not been considered representative, and therefore no palaeocurrent data are available, although the same trend towards the southeast is probably followed, similarly to the underlying units. This formation was dated as Anisian by Calafat (1988), just 12 m below the boundary with the *Muschelkalk* facies, which was confirmed by subsequent works such as Diez (2000) and Diez et al. (2005, 2010) (see Appendix A. Supplementary data: Supplementary Table 3). Given that the base of the underlying Pedra Alta Formation is of upper? Aegean age (see '4.3. Pedra Alta Formation'), this formation could belong to either the uppermost Aegean (lower Anisian) or even the Bithynian (lower part of the middle Anisian) (see '7. Discussion' and Appendix A. Supplementary data: Supplementary Table 3).

5. Systematic palaeoichnology

5.1. Invertebrate ichnofossils

Ichnogenus *Gordia* Emmons, 1844

Gordia isp.

Fig. 4A

Studied material: One specimen, left in the field. From Punta Negra section (metre 9.00), middle part of Estellencs Formation, Aegean.

Description: Horizontal trace preserved in convex hyporelief, consisting in a loosely winding, unbranched burrow, thin and with a somewhat irregular wall. The preserved trace appears to make a loop that would cross over itself. The fill is the same as the surrounding matrix (very fine-grained sandstone).

Remarks: The studied ichnofossil differs from similar unspecialised freshwater grazing traces of the *Mermia* ichnofacies (Buatois and Mángano, 1998) such as *Cochlichnus*, *Helminthoidichnites*, *Helminthopsis* or *Mermia*, because of its irregular winding course and the fact that the trace crosses over itself (Hofmann and Patel, 1989; Han and Pickerill, 1995; Gaigalas and Uchman, 2004; Uchman et al., 2009; Getty et al., 2017). The ichnogenus *Gordia* occurs in marine and continental facies from the Precambrian to the Holocene (Pickerill and Peel, 1991), and, in the case of freshwater environments, the probable trackmakers were insect larvae (Gaigalas and Uchman, 2004; Minter et al., 2007).

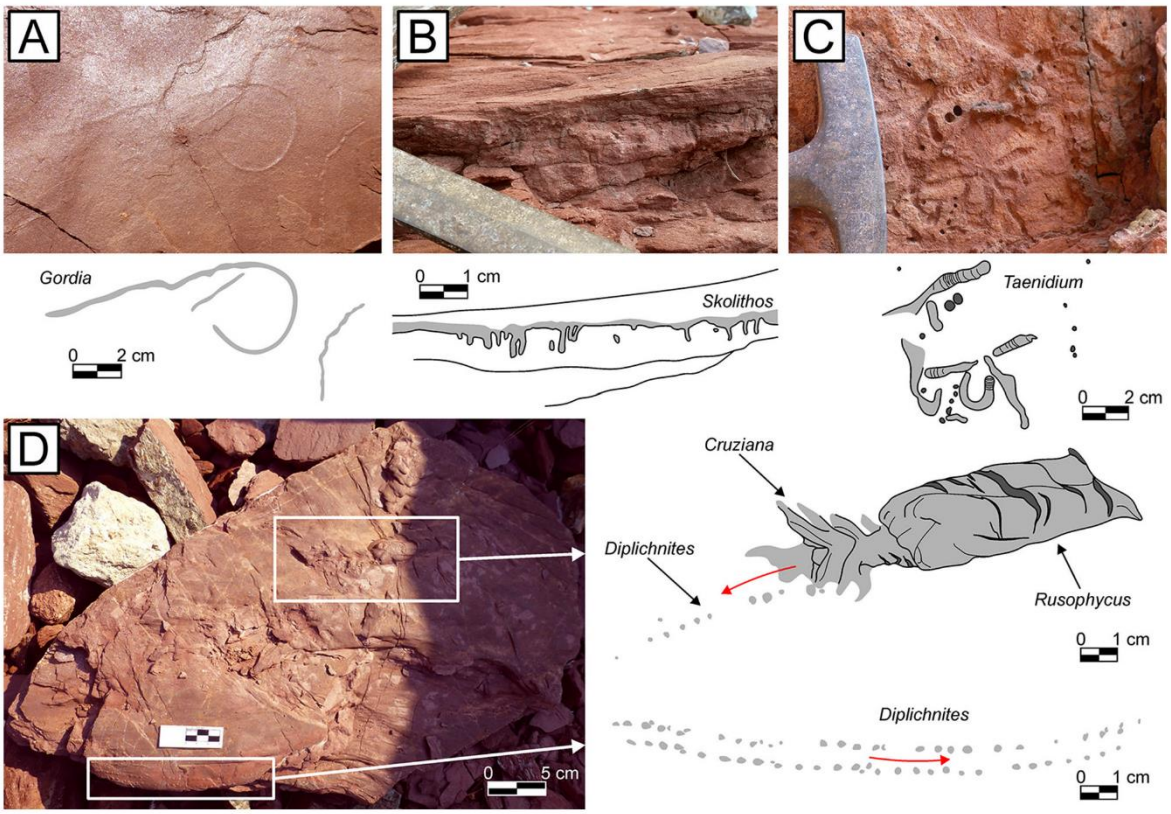

Fig. 4. Field photographs and schematic drawings of the studied invertebrate trace fossils from Punta Negra and Punta Roja sections, middle part of Estellencs Formation, Aegean. A: *Gordia* isp., Punta Negra. B: *Skolithos* isp., Punta Negra. C: *Taenidium* isp. cf. *T. barretti*, Punta Roja. D: *Rusophycus* isp. - *Cruziana* isp. - *Diplichnites* isp. cf. *D. gouldi*, Punta Negra. Red arrows in D represent direction of movement. (For interpretation of the references to colour in this figure legend, the reader is referred to the web version of this article).

Ichnogenus *Skolithos* Haldeman, 1840

Skolithos isp.

Fig. 4B

Studied material: Many specimens, left in the field. From Punta Negra (metre 8.00) and Punta Roja (metre 81.00) sections, among others, middle part of Estellencs Formation, Aegean.

Description: Subvertical, straight to slightly curved, unbranched burrows of circular section. The fill is massive; it usually corresponds to the sediment of the overlying bed (very fine-grained sandstone).

Remarks: The ichnogenus *Skolithos* occurs in marine and continental facies from the Precambrian to the Holocene (Fillion and Pickerill, 1990), and, in the case of freshwater environments, the probable trackmakers were insect larvae (Bromley and Asgaard, 1979; Ratcliffe and Fagerstrom, 1980; Fitzgerald and Barrett, 1986). In continental deposits, it usually appears in the *Scoyenia* ichnofacies (Buatois and Mángano, 1998).

Ichnogenus *Taenidium* Heer, 1877

Taenidium barretti (Bradshaw, 1981)

Taenidium isp. cf. *T. barretti*

Fig. 4C

Studied material: Many specimens, left in the field. From Punta Roja section (metre 81.00), among others, middle part of Estellencs Formation, Aegean.

Description: Variably oriented (usually horizontal but vertical sections also observed), unwalled, sinuous to winding, unbranched burrows of circular section. They have a meniscate backfill with a similar sediment to that of the surrounding matrix (fine-grained sandstone). Menisci are short, arcuate and closely spaced.

Remarks: Ichnotaxonomy of meinscate backfilled traces is somewhat contentious (*e.g.*, Minter et al., 2007; Smith et al., 2008; Díez-Canseco et al., 2016) and it is beyond the scope of the present work to provide a systematic review of such ichnotaxa. The specimens studied herein are comparable to those illustrated by Minter et al. (2007) under the identification of *T. barretti*. Those traces have been interpreted to be produced by arthropods, probably coleopterans (Baucon et al., 2014), which would aestivate in the moist sediment during the dry season (Minter et al., 2007). In continental deposits, this ichnogenus usually appears in the *Scoyenia* ichnofacies (Buatois and Mángano, 1998).

Ichnogenera *Rusophycus* Hall, 1852, *Cruziana* d'Orbigny, 1842, and *Diplichnites* Dawson, 1873

Diplichnites gouldi (Gevers *in* Gevers, Frakes, Edwards et Marzolf, 1971)

Rusophycus isp. - *Cruziana* isp. - *Diplichnites* isp. cf. *D. gouldi*

Fig. 4D

Studied material: Two specimens, left in the field. From Punta Negra section (on an *ex situ* block, probably from metre 6.00), middle part of Estellencs Formation, Aegean.

Description: Positive hyporelief of a compound trace with three different ichnotaxa in fine-grained sandstone. The part corresponding to *Rusophycus* is a weakly bilobate mound, with a longitudinal, very smoothed ridge. The part corresponding to *Cruziana* originates from the central part of the anterior margin of the *Rusophycus*, and corresponds to a chevronate (V-shaped) trace with more or less symmetric lobes on each side of its longitudinal axis. Finally, *Diplichnites* isp. cf. *D. gouldi* appears

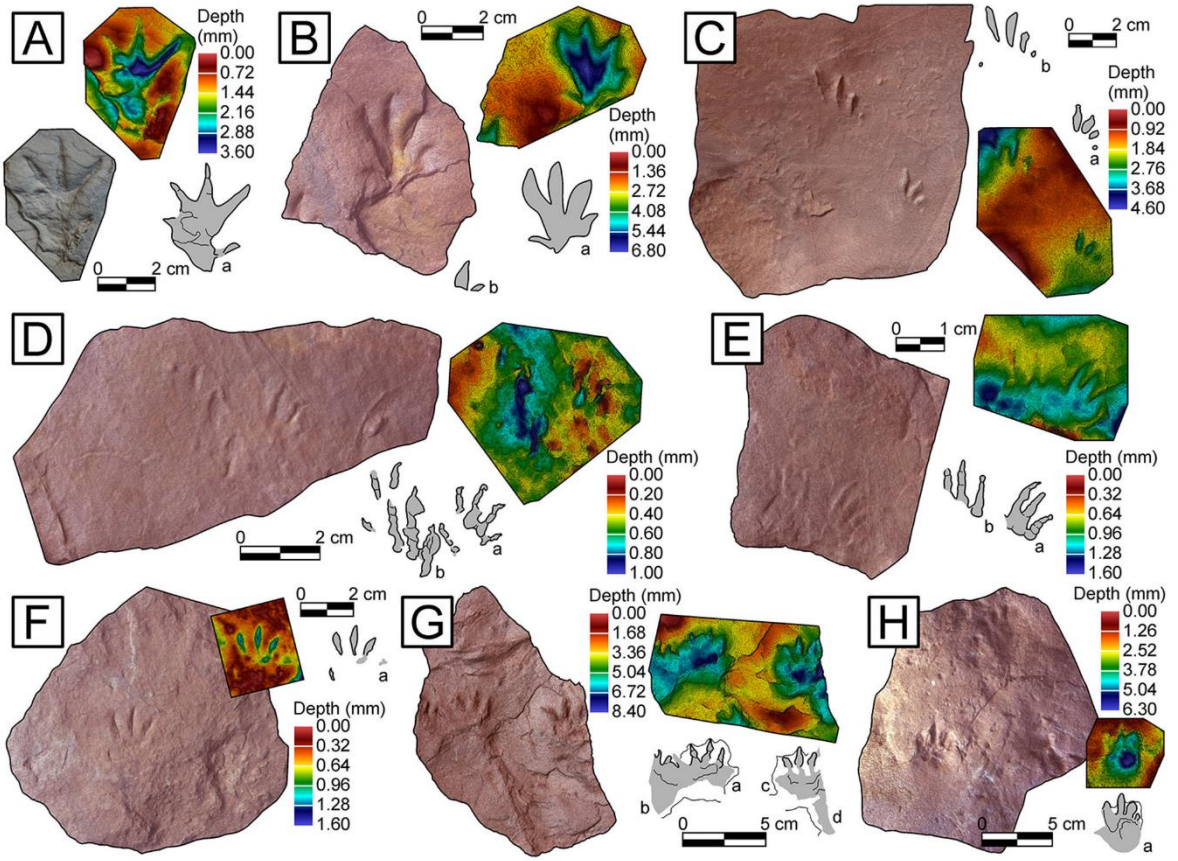

Fig. 5. Textured 3D models, false colour-coded depth maps and schematic drawings of the studied ichnites from Punta Negra section and its lateral equivalent at Platja de sa Marina, middle part of Estellencs Formation, Aegean. A: *Rhynchosauroides* isp. 1, PN-7.6?-01, Punta Negra. B: *Rhynchosauroides* isp. 1, PN-14.7-01, Platja de sa Marina. C: *Rhynchosauroides* isp. 2, PN-7.6?-03, Punta Negra. D: *Prorotodactylus mesaxonichnus*, PN-14.6-02, Platja de sa Marina. E: cf. *Prorotodactylus mesaxonichnus*, PN-14.6-03, Platja de sa Marina. F: cf. *Prorotodactylus mesaxonichnus*, PN-14.6-01, Platja de sa Marina. G: Indeterminate morphotype, PN-7.6-01, Punta Negra. H: Indeterminate morphotype, PN-7.6?-02, Punta Negra. See Appendix A. Supplementary data: Supplementary Table 2 for measurements. (For interpretation of the references to colour in this figure legend, the reader is referred to the web version of this article).

connected to the open part of the V of the chevrons. The parts corresponding to *Diplichnites* isp. cf. *D. gouldi* consist of two parallel trace series of circular to tear-shaped, regularly spaced impressions. In the more completely preserved areas, the impressions form a V shape with two smaller imprints located outwards and anteriorly, and two larger imprints located inwards and posteriorly.

Remarks: The studied specimens represent the traces left by three different behaviours of a same organism, recording its movement from a resting position in the sediment (*Rusophycus*), to crawling to get out of it (*Cruziana*), to walking over it (*Diplichnites* isp. cf. *D. gouldi*). Such behaviour, expressed in the same ichnotaxa, is well known from Palaeozoic trilobites (*e.g.*, Crimes, 1970), but it has also been reported in younger deposits (*e.g.*, Bromley and Asgaard, 1979; Minter et al., 2007; Hminna et al., 2020), meaning that the potential producers of these ichnofossil are disparate (see Hammersburg et al., 2018, for a review of the possible producers of these three ichnogenera). In the case of the traces studied here, the most likely producer was a notostracan crustacean, similarly to the cases described by Bromley and Asgaard (1979), Minter et al. (2007) and Gand et al. (2008). In continental deposits, these traces usually appear in the *Scoyenia* ichnofacies (Buatois and Mángano, 1998).

5.2. Tetrapod tracks

Ichnogenus *Rhynchosauroides* Maidwell, 1911

Rhynchosauroides isp. 1

Fig. 5A–B; Appendix A. Supplementary data: Supplementary Table 2

Studied material: PN-7.6?-01 (gypsum cast made in the 1980s of a right manus undertrack). PN-14.7-01 (left manus undertrack and a partially preserved probable left pes undertrack, left in the field). From Punta Negra section and its lateral equivalent at Platja de sa Marina, middle part of Estellencs Formation, Aegean.

Description: Manus track semiplantigrade to plantigrade, pentadactyl, with the base of the digits III–IV being the deepest imprinted zone. The imprints of the digits I–IV end in pointed tips and can be slightly curved inwards. The imprint of digit V also possesses a pointed tip and is slightly curved outwards. The length of the digit impressions can be ordered as follows: I < V < II < III ≈ IV. Pes track located behind and exteriorly to the manus in the case of PN-14.7-01. The palm impression is anteroposteriorly short, with a concave distal outline.

Remarks: This morphotype is preserved in very fine-grained sandstones and agrees with the ichnogenus *Rhynchosauroides*, for which a revision is much needed (Klein and Niedźwiedzki, 2012; Mujal et al., 2018b). Regardless, the specimens here described show strong similarities in terms of size, shape and digit divergence with *Rhynchosauroides brevidigitatus*, *Rhynchosauroides peabodyi*, *Rhynchosauroides rdzaneki*,

Rhynchosauroides schochardti and *Rhynchosauroides tirolicus* (Haubold, 1971; Avanzini and Renesto, 2002; Klein and Lucas, 2010a; Klein and Niedźwiedzki, 2012). Most of the diagnostic features of the aforementioned ichnospecies are in the pes imprint and in the trackway pattern, which are unavailable in the case of the specimens from Mallorca. Therefore, we prefer to use open nomenclature.

In Triassic beds, this ichnogenus has been reported from Europe, north Africa, south and north America and Asia (*e.g.*, Haubold, 1971; Melchor and De Valais, 2006; Gand et al., 2007; Klein and Lucas, 2010a; Lucas et al., 2010; Avanzini et al., 2011; Klein et al., 2011; Klein and Niedźwiedzki, 2012; Mujal et al., 2016, 2017a, 2018b; De Jaime-Soguero et al., 2021; Xing and Klein, 2021). Distantly related clades have been suggested as possible *Rhynchosauroides* trackmackers, from archosauromorphs (Avanzini and Renesto, 2002; Mujal et al., 2017a, 2018b) to non-archosaurian neodiapsids (Lucas, 2019).

Rhynchosauroides isp. 2

Fig. 5C; Appendix A. Supplementary data: Supplementary Table 2

Studied material: PN-7.6?-03 (left manus-pes set (undertracks), left in the field). From Punta Negra section, middle part of Estellencs Formation, Aegean.

Description: Manus track digitigrade, probably pentadactyl, with deeply imprinted straight digits II–IV ending in pointed tips. Of digit I, only the tip is impressed. The length of the digit impressions can be ordered as follows: I < II < III < IV. Pes track digitigrade, pentadactyl, with deeply imprinted straight digits II–IV and tips of digits I and V. The distal portion of the digits III and IV are the deepest imprinted parts. The length of the digit impressions can be ordered as follows: I < V < II < III < IV. Although no clear track midline can be established, it can be said that the manus is smaller than the pes and is located internally and behind it, denoting a complete anterolateral overstepping. The manus track is slightly rotated inwards with respect to the pes track.

Remarks: The fact that the only studied specimen (preserved in very fine-grained sandstone) is an isolated manus-pes set and that only some digits are partially imprinted makes ichnospecies-level identification difficult. The traits that make it possible to distinguish PN-7.6?-03 from the other specimens from Mallorca are that the manus digit IV imprint is clearly longer than the digit III imprint, that the manus track is located clearly behind the pes track and that the manus and pes are distinctly digitigrade/unguligrade, with digit V impression present only in the case of the pes. However, all these traits are common in several ichnospecies of *Rhynchosauroides* (*e.g.*, Haubold, 1971) and might in part respond to extramorphological variability. Therefore, the specimen studied here is left in open nomenclature.

Ichnogenus *Prorotodactylus* Ptaszyński, 2000

Prorotodactylus mesaxonichnus Mujal, Fortuny, Bolet, Oms et López, 2017

Prorotodactylus mesaxonichnus

Fig. 5D–F; Appendix A. Supplementary data: Supplementary Table 2

Studied material: PN-14.6-03 (left manus-pes set (undertracks), left in the field) and perhaps PN-14.6-01 (left manus undertrack, left in the field) and PN-14.6-02 (left manus-pes set (undertracks), left in the field). From the lateral equivalent of Punta Negra section at Platja de sa Marina, middle part of Estellencs Formation, Aegean.

Description: Manus track digitigrade, pentadactyl, with digits II–III being the deepest imprinted zones, especially in their basal phalangeal impressions. The digit I–IV imprints are thin, straight to slightly curved inwards, and end in distinctly pointed claw traces. The imprint of digit I is shallower than those of digits II and III. The basal phalangeal impressions of digits II and III are oval-shaped (anteriorly elongated) and somewhat connected. The proximal parts of digits IV and V are not very deeply imprinted, and only its distal portion may appear. Although the length cannot be confidently measured on all the digit imprints, they seem to be ordered as: V ≈ I < II ≈ IV < III.

Pes track digitigrade, pentadactyl, with digits I–II being the deepest imprinted zones. The digits I–IV are straight to very slightly curved inwards, and end in pointed tips corresponding to claw traces. Digits I and II have expanded distal portions, which correspond to deformation of the sediment during the kick-off phase. Digit III is weakly imprinted proximally, whereas the clawed tip is deeper. The imprint of digit IV is only very shallowly preserved in its distal part, but the tip is not well defined. Digit V is not very well defined either, and only the tip can be observed. Although the length cannot be confidently measured on all the digit imprints, they seem to be ordered as: V < I < II < IV < III. The divergence angles between digits I, II, III and IV are very low, always smaller than 10°.

Trackway pattern not visible in any of the studied specimens. However, from the manus/pes sets, it can be said that the manus imprints are located approximately at the same height than those of the pedes, and the pes tracks are slightly rotated outwards and laterally positioned regarding those of the manus.

Remarks: The tracks here considered (preserved in very fine-grained sandstone) have a somewhat 'lacertoid' morphology, but a combination of characters such as that the manus digit III is longer than IV and that the divergence angle between digits IV–V is very low makes it possible to exclude the ichnogenus *Rhynchosauroides*. The specimens from Mallorca are also different from *Gwyneddichnium* (see Lucas et al., 2014) because, in the latter, the digit III is not much longer than IV, and digit IV is longer than II. All these traits listed above, together with a relatively short digit V and the pes imprints rotated outwards with respect to the manus, agree with the ichnospecies *P. mesaxonichnus* described by Mujal et al. (2017a) from the upper Lower Triassic–lower Middle Triassic of the Pyrenean Basin (Mujal et al., 2016, 2017a), and thus of a very similar age and palaeogeographic position than the material from Mallorca. Their potential trackmakers are non-archosaurian archosauromorphs (Mujal et al., 2017a).

Indeterminate morphotype

Fig. 5G–H; Appendix A. Supplementary data: Supplementary Table 2

Studied material: PN-7.6?-02 (left ?manus and right ichnite (undertracks) of the same trackway, left in the field), PN-7.6-01 (partial left and right manus-pes sets (undertracks) of the same trackway, and traces of other ichnites (undertracks), left in the field). From Punta Negra section, middle part of Estellencs Formation, Aegean.

Description: Manus imprint plantigrade to semiplantigrade, pentadactyl, with the palm being the most deeply impressed region, followed by the distal region of the digits II–IV (excluding the claw impressions). The length of the digits of the manus imprint can be ordered as follows: V < I < II < III < IV. They are relatively straight and end in pointed tips, corresponding to claw impressions. The palm has a somewhat diffuse proximal end and a more weakly impressed zone in the union with the digits. Pes imprint apparently plantigrade, probably pentadactyl, with the sole and the digit tips being the deepest impressed parts. The digits are not clearly impressed in any of the studied specimens and measurement is complicated, but it can be said that the digit impressions of the pedes are somewhat straight and with pointed to somewhat rounded tips. Even though no clear midline has been established, the manus imprints are rotated slightly inwards (lines drawn following the angle of digit III impressions of both manus end up converging), and are located slightly in front of and internal to the pes imprints. The pes imprints slightly overstep the manus imprints and the pace length is very short, with the manus-pes sets almost at the same height in the trackway, in the case of PN-7.6-01.

Remarks: The paucity of material and the fact that almost all the studied specimens correspond to manus undertracks (preserved in very fine-grained sandstones) has hindered its ichnogenus-level identification. Small manus tracks that are almost as long as wide and with a relatively short palm, median functional prevalence, with short and stout digits ended in pointed tips (claw impressions) and with digit III longer than IV, point to archosauromorph trackmakers, or more generally diapsid reptiles (*e.g.*, Haubold, 1971; Mujal et al., 2020).

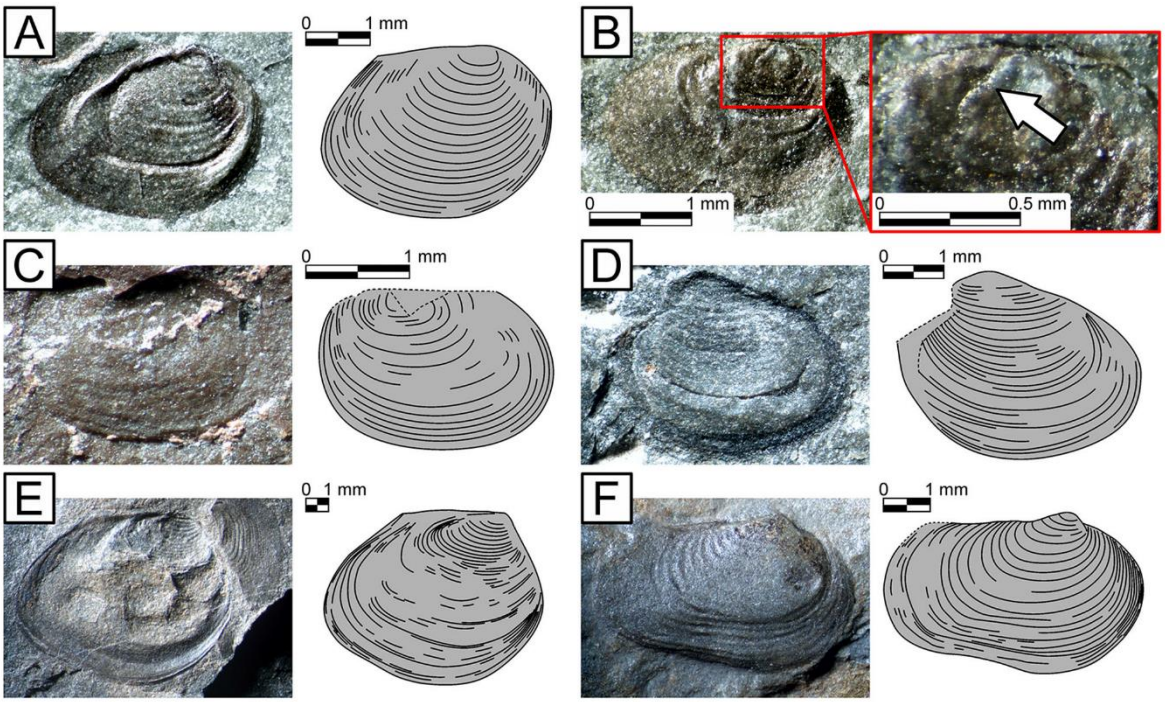

Fig. 6. Photographs and schematic drawings of the different forms of studied clam shrimp ("conchostracan") carapace valves. A: *Hornestheria* sp. aff. *Ho. sollingensis*, DA21/03-02-58, Aegean, Pedra Alta. B: *Hornestheria* sp. aff. *Ho. sollingensis*, DA21/03-02-81, Aegean, Pedra Alta. C: "Conchostraca" indet., DA21/03-01-01a, Aegean, Punta Roja. D: "Conchostraca" indet., DA21/03-03-02, Aegean, ravine between Pedra Alta and Punta Negra. E: *Hornestheria*? sp. indet. morphotype 1, DA21/03-04-11, lower–middle? Anisian, ravine between Pedra Alta and Punta Negra. F: *Hornestheria*? sp. indet. morphotype 2, DA21/03-04-07-1b, lower–middle? Anisian, ravine between Pedra Alta and Punta Negra. White arrow in B indicates sculpture on the larval carapace valve.

Chirotheriids, however, may be excluded because their manus tracks possess a very weakly imprinted palm and there is no manus-pes overstepping (Haubold, 1971; Klein and Haubold, 2007; Klein and Lucas, 2010b; Reolid et al., 2020). Other ichnogenera attributed to archosauromorphs, such as *Gwyneddichnium*, *Prorotodactylus* and *Rhynchosauroides* (as already mentioned above) show slightly different digit proportions and divarication angles, the digits are not as stout as in the specimens from Mallorca, and the manus is slightly less wide (Klein and Niedźwiedzki, 2012; Niedźwiedzki et al., 2013; Lucas et al., 2014; Mujal et al., 2017a). Some tracks included in 'Morphotype A' by Mujal et al. (2016) are similar to those studied here, with relatively stout and short manus digit imprints and the divarication angle between digits II–III being greater than that of digits III–IV (Appendix A. Supplementary data: Supplementary Table 2). However, the lack of trackway data and the small number of specimens available for study make it impossible to confidently identify them, thus leaving them under 'Indeterminate morphotype', waiting for future specimens that may shed light on their ichnospecies-level identification.

Additionally, from the middle part of Pedra Alta Formation, Calafat et al. (1986, 1986–1987) and Calafat (1988) reported the presence of several circular, concave structures of 30–40 cm of diameter, which were thought to correspond to very large tetrapod ichnites (Appendix A. Supplementary data: Supplementary Text 1, Supplementary Fig. 1A). However, after examining them *in situ* for the present work (Appendix A. Supplementary data: Supplementary Fig. 1B), it has been concluded that they are not ichnites, given their very large size and the lack of expulsion rims, any distinct pes or manus-like shape and trackway arrangement.

Almost all the ichnofossils mentioned above (*Skolithos*, *Taenidium*, *Rusophycus-Cruziana-Diplichnites* and tetrapod tracks) are typical of the *Scoyenia* ichnofacies, corresponding to areas with recurrent flooding and desiccation (Buatois and Mángano, 1998). This is consistent with the inferred palaeoenvironment from the middle part of Estellencs Formation, that is, a floodplain setting with sporadic overbank flows that produced crevasse splays. Nevertheless, the ichnogenus *Gordia* is typical of the *Mermia* ichnofacies, corresponding to relatively more stable water bodies (Buatois and Mángano, 1998). Indeed, the presence of symmetrical wave ripples in some beds also suggests the development of seasonal playa lakes (in the sense of Briere, 2000). Although the specimens of *Gordia* do not appear in the exact same bed as the wave ripples, both structures are separate pieces of evidence for the presence of stable bodies of water, at least seasonally.

6. Systematic palaeontology

6.1. *Clam shrimps ("conchostracans")*

Diplostraca Gerstaecker, 1866
Superfamily Lioestheriacea Raymond, 1946
Family Xiangxiellidae Shen (*in* Chang, Chen et Shen, 1976)
Genus *Hornestheria* Kozur et Lepper (*in* Kozur et Weems, 2010)
Hornestheria sollingensis Kozur et Lepper (*in* Kozur et Weems, 2010)
Hornestheria sp. aff. *Ho. sollingensis*
Fig. 6A–B

Studied material: Eight specimens, DA21/03-02-58, DA21/03-02-68, DA21/03-02-72, DA21/03-02-75, DA21/03-02-77, DA21/03-02-78, DA21/03-02-80, DA21/03-02-81. From Pedra Alta section (metre 7.2–7.3), upper part of Estellencs Formation, Aegean.

Description: Carapace valves of medium to large size (carapace valve length between 2.5 and 3.9 mm), oval to elongated oval in shape (carapace valve height/length ratio values between 0.57 and 0.70). Its dorsal margin is straight, of a length between 1.8 and 2.3 mm. The

height of the larval carapace valve varies between 0.1 and 0.5 mm. The umbo is in submedially and marginal to inframarginal position. The points of maximum curvature along the anterior and posterior margins are located in the median-dorsal to median-ventral region, and along the ventral margin they are located in the median to median-posterior region. On the external side of the shells, the studied specimens show either indistinct or finely reticulated ornamentation.

Remarks: The specimens from Pedra Alta section differ from *Hornestheria sollingensis* because of its very small larval carapace valve and the fact that the characteristic radial element on it is not clearly recognisable in most of the specimens from Mallorca (except for the specimen illustrated in Fig. 6B), due to a variable degree of deformation in the umbonal area. Therefore, an affinity-based, open nomenclature is preferred. Occurrences of the genus *Hornestheria* are known to range biostratigraphically from the uppermost Olenekian (uppermost Spathian) to the Anisian (Kozur and Weems, 2010; Scholze and Matamales-Andreu, 2021).

Hornestheria? sp. indet. morphotype 1

Fig. 6E

Studied material: Nine specimens, DA21/03-04-01, DA21/03-04-02, DA21/03-04-07-1a, DA21/03-04-07-2a (counterpart), DA21/03-04-07-1c, DA21/03-04-07-2c (counterpart), DA21/03-04-07-1d, DA21/03-04-10, DA21/03-04-11, DA21/03-04-12-1, DA21/03-04-12-2 (counterpart), DA21/03-04-13a, DA21/03-04-13b (counterpart). From Punta Negra section (metre 82), upper part of Pedra Alta Formation, Aegean.

Description: Carapace valves very large (carapace valve length between 4.9 and 7.8 mm) and round in shape (carapace valve height/length ratio values between 0.76 and 0.87). The dorsal margin is straight, of a length between 2.7 and 4.6 mm. The height of the larval carapace valve ranges between 0.3 and 0.9 mm. The umbo is in anterior to slightly submedial and inframarginal to slightly marginal position. The points of maximum curvature along the anterior margin are located median-dorsal to median-ventral, in the posterior margin they are located median-ventral, and in the ventral margin they are located median-anterior. The ventral margin is often indented in its median-posterior area.

Remarks: Instead of using formal genus and species names, an open nomenclature is applied here due to both a limited number of studied individuals and the generally needed taxonomic revision of clam shrimp records of the uppermost *Buntsandstein* deposits of Europe (*i.e.*, "*Euestheria albertii albertii*" in the sense of Kozur et al., 1993; Kozur and Weems, 2010). Carapace valves of *Hornestheria*? sp. indet. morphotype 1 show irregular remnants of brownish shell substance, whereas neither radial sculptures on the larval carapace valve nor microstructures (ornamentation) are preserved. In comparison, similarly sized carapace valves of *Dictyonatella* have been described from the upper *Buntsandstein* central European deposits of the Vosges (*e.g.*, Kozur, 1982) and from the Holy Cross Mountains (Żyła et al., 2013), but they differ from *Hornestheria*? sp. indet. morphotype 1 either because of their larger-sized reticulated ornamentation or by a concavely recurved posterior margin directly below the dorsal margin (Scholze and Matamales-Andreu, 2021).

Hornestheria? sp. indet. morphotype 2

Fig. 6F

Studied material: Five specimens, DA21/03-04-04a, DA21/03-04-06, DA21/03-04-07-1b, DA21/03-04-07-2b (counterpart), DA21/03-04-08, DA21/03-04-09. From Punta Negra section (metre 82), upper part of Pedra Alta Formation, Aegean.

Description: Carapace valves very large (carapace valve length between 3.2 and 4.9 mm) and oval to very elongated-oval in shape (carapace valve height/length ratio values between 0.57 and 0.71). Dorsal margin slightly to moderately curved, with a length ranging between 3.0 and 4.0 mm. The larval carapace valve height is between 0.2 and 0.9 mm. The umbo is located in submedial and marginal to supramarginal position. The points of maximum curvature are located median or slightly median-dorsal in the anterior and posterior margins, and in the ventral margin they are located median-anterior. The ventral margin is often concavely indented in the median-posterior area of the carapace valve.

Remarks: *Hornestheria*? sp. indet. morphotype 2 occurs in the same stratigraphic level than *Hornestheria*? sp. indet. morphotype 1, and can be differenced because the former has a smaller total carapace valve size and a more oval shape than the latter. Both morphotypes might reflect a stout and a slender form of a same species; however, this cannot be confirmed with the present material. *Hornestheria*? sp. indet. morphotype 2 is also very similar to the specimens here considered as *Hornestheria* sp. aff. *Ho. sollingensis*, but the latter are usually smaller and their umbo is less intensely curved (Scholze and Matamales-Andreu, 2021).

"Conchostraca" indet.

Fig. 6C–D

Studied material: Three specimens, DA21/03-01-01a, DA21/03-01-01b, DA21/03-01-02. From Punta Roja section (metre 86.5), middle part of Estellencs Formation, Aegean. Two specimens, DA21/03-03-01, DA21/03-03-02. From Punta Negra section (metre 39.5), lower part of Pedra Alta Formation, Aegean.

Description: Individuals are either fragmented or deformed (*i.e.*, diagenetically compacted); their total carapace valve length is up to 3.5 mm, and their height is up to 2.6 mm.

Remarks: Based on preliminary observations, the most completely preserved specimen (Fig. 6D) from Punta Negra section is morphologically reminiscent of *Hornestheria* sp. aff. *Ho. sollingensis* (Fig. 6A) from Pedra Alta section (Scholze and Matamales-Andreu, 2021). The study of further material seems necessary in order to fully understand both their intraspecific and preservational variability.

6.2. Insects

Ephemeroptera Hyatt et Arms, 1891

Family Sharephemeridae Sinitshenkova, 2002

Genus *Hammephemera* Sinitshenkova (*in* Bashkuev, Sell, Aristov, Ponomarenko, Sinitshenkova et Mahler, 2012)

Hammephemera pulchra Sinitshenkova (*in* Bashkuev, Sell, Aristov, Ponomarenko, Sinitshenkova et Mahler, 2012)

Hammephemera sp. cf. *Ha. pulchra*

Fig. 7A–E, N

Studied material: Four specimens, TS-A-1, TS-A-2, TS-D-1, TS-F-1. From Pedra Alta section (metre 4.75), upper part of Estellencs Formation, Aegean. One specimen, DA21/03-02-88. From Pedra Alta section (metre 7.20–7.30), upper part of Estellencs Formation, Aegean. The specimen TS-D-1 (see Fig. 7B) is virtually complete and with a well-exposed forewing venation (the description below is mainly from this specimen, which Calafat (1988) figured as a lepidopteran in his photo 22).

Description: Body length *ca.* 7.5 mm. Forewing length 7.25 mm, maximum width *ca.* 3.00 mm. Forewing two times as long as wide (but slight deformation in some of the specimens), with base broad and with anal area narrowed, and cubital area narrow. Anterior margin of the forewing slightly convex and its top rounded. Tornus in a distal position, close to the middle of wing. Rs with seven longitudinal veins. Forks of MA and CuA relatively short. Long CuA fork with intercalary vein, CuP long and simple, anal veins simple and long.

Remarks: The extinct family Sharephemeridae contains two genera based on isolated forewings, *Sharephemera* and *Hammephemera*, from the Upper Jurassic of Mongolia and Middle Triassic (lower Anisian) of Germany (Bashkuev et al., 2012), respectively. The new specimens from Mallorca are the first articulate, but details of the body remain obscure. General forewing venation and the forewing size are coincident with the German species. Despite the five articulated adult specimens from the same level with well-exposed forewing venations, the slight deformation

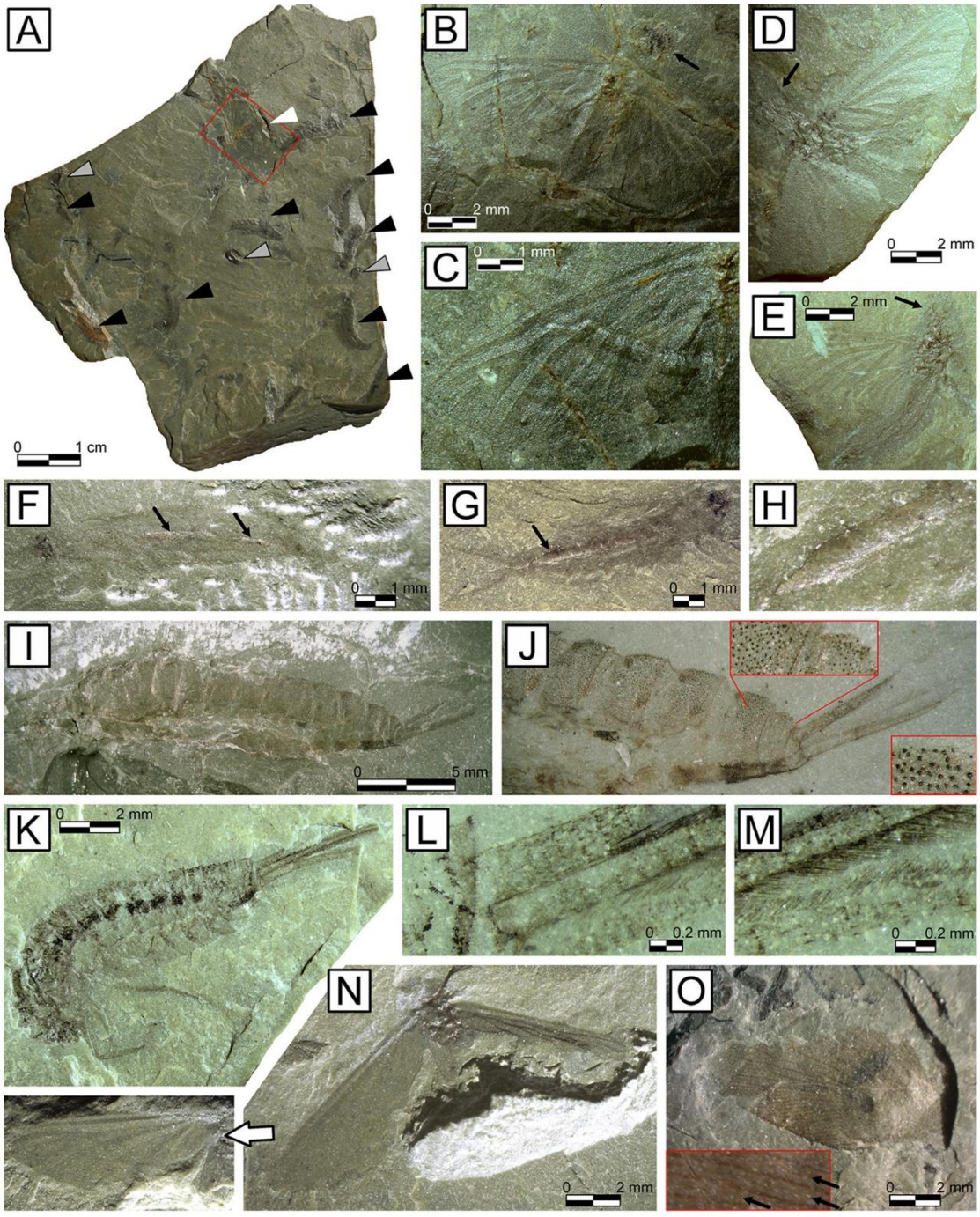

Fig. 7. Insects from Pedra Alta section, upper part of Estellencs Formation, Aegean. A: Slab TS-D, showing mayflies (white arrowhead indicates an adult specimen, and black arrowheads indicate nymphs) and clam shrimps (some of them marked with grey arrowheads). B–C: *Hammephemera* sp. cf. *Ha. pulchra* (Sharephemeridae), TS-D-1, complete adult mayfly (white arrowhead and red square in A), and detail of its left forewing. D–E: *Hammephemera* sp. cf. *Ha. pulchra*, TS-A-1 and TS-F-1 respectively, adult specimens. F–H: Detritivore mayfly nymph type, DA21/03-02-87a and DA21/03-02-90a respectively, very abundant form that appears in the same slabs having *Hammephemera* adults, and that commonly show 3D cololites (arrows in F and G, and H detail of cololite in G). I–J: *Triassoephemera punctata* (Triassoephemeridae), MBCN23697a, nymph specimen (insets in J are details of its cuticle punctuations). K–M: *Triassonurus doliiformis* (Siphlonuridae), TS-C-1, nymph specimen (details of chaetotaxy in cerci and paracercus; L base of the cerci and paracercus). N: *Hammephemera* sp. cf. *Ha. pulchra*, DA21/03-02-88, adult specimen (photograph on the right with forewing showing venation). O: Blattodea indet., DA21/03-02-85, forewing of an indeterminate cockroach, possibly of the species *Voltziablatta intercalata* (note the intercalary veins marked by the arrows in the inset). Photographs J and L–M taken with the specimens wet with alcohol. (For interpretation of the references to colour in this figure legend, the reader is referred to the web version of this article).

of the wings and some not well-resolved venation details prevent an accurate comparison with the exceptionally preserved holotype of *Hammephemera pulchra*. Therefore, we consider the specimens from Mallorca as *Hammephemera* sp. cf. *Ha. pulchra*. This taxon is relatively abundant in Pedra Alta section (two additional specimens could correspond to this form: TS-E-2 and TS-H-1), so more specimens will probably be discovered and will inform if it corresponds to this previously described species or to a new one. An enigmatic adult specimen (TS-B-1; Appendix A. Supplementary data: Supplementary Fig. 2A–B), only showing a few anatomical details and apparently without head due to disarticulation, was figured by Calafat (1988) as an indeterminate winged form. That specimen was later suggested to be an indeterminate dipteran by Shcherbakov et al. (1995), based on the not very detailed photograph in the study by Calafat (1988), in which the habitus strongly suggests a dipteran. However, it actually corresponds to a mayfly that may have died during emersion from the nymphal stage, because the aspect of its wings is similar to unexpanded wings (note that the length of thorax plus abdomen is 5.5 mm in this specimen, being 5.9 mm in the best *Hammephemera* sp. cf. *Ha. pulchra* specimen, and thus their sizes are very similar).

Family indet.

Adult morphotype 1

Appendix A. Supplementary data: Supplementary Fig. 2C–G

Studied material: Two specimens, TS-G-1a, TS-G-1b (counterpart), TS-G-2, the slab with the part is 5 × 3.5 cm. From Pedra Alta section (metre 4.75), upper part of Estellencs Formation, Aegean.

Description: Body length *ca.* 3 mm. Only a few features of the forewings can be described, as most of the anatomical details are not preserved. Distal margins of the four studied forewings are not preserved or are obscure, and therefore a suitable measure of the forewing length is not available. Longitudinal veins in the costal margin and some of other longitudinal veins (Rs and MA) are well preserved, but this only indicates that these adult specimens are mayflies.

Remarks: These two adult mayfly specimens preserved one next to the other exhibit a very few anatomical details due to their poor preservation, but they are clearly conspecific. It is not possible to classify them at family level, and they certainly correspond to a morphotype different from the other adults reported in the present work, based on their different size compared to the *Hammephemera* sp. cf. *Ha. pulchra* specimens (*ca.* 3.0 mm *vs. ca.* 7.5 mm of body length). They occur in the same slab surface together with a clam shrimp (TS-G-7) and four mayfly nymphs (TS-G-3, TS-G-4, TS-G5 and TS-G-6; three of them virtually complete), notably much larger (Appendix A. Supplementary data: Supplementary Fig. 2C), and thus not conspecific; the counterside contains two clam shrimps (TS-G-9 and TS-G-10) and a small mayfly nymph (TS-G-8).

Family indet.

Detritivore nymph type

Fig. 7F–H

Studied material: Over 50 specimens in the two collections studied. From Pedra Alta section (metres 4.75 and 7.20–7.30), upper part of Estellencs Formation, Aegean.

Description: This group of forms is very abundant in Pedra Alta section but only a few specimens are virtually complete and well preserved. There are diverse stages of development, from specimens of 3–4 mm of body length (specimens DA21/03-02-05 and DA21/03-02-30) to more developed specimens, with body lengths of *ca.* 6.6–7.0 mm. Body flattened or not clearly cylindrical (only a few specimens preserved in lateral position). Wing pads not conspicuous. Legs simple, short and slender. Tergaliae large, rounded, slightly fringed on the borders, slightly overlapped, present in the abdominal segments I–VII. Except for a few specimens that show the digestive preserved as a carbonaceous tube, these nymphs exhibit 3D cololites (see Fig. 7F–H). Cerci and paracercus (= terminal filament) not very long (*ca.* 3/5 of the abdominal length in a specimen without 3D cololite) and covered with hairs.

Remarks: The digestive contents in these nymphs did not collapse during stratigraphic compression, as revealed by their 3D cololites, indicating that they contained detritic particles, apparently including abundant fine sediment grains. This indicates that this group of mayflies was detritivore during aquatic, preimaginal stages, most likely obtaining organic particles present in the fine sediment of the pools. Taphonomy of the outcrop suggests that this extremely abundant group of detritivore nymphs could be conspecific with the adults identified as *Hammephemera* sp. cf. *Ha. pulchra*. The taphonomic observations are: (1) the abundant mayfly nymph record is virtually constituted by this type; (2) there are different stages of development; (3) all these specimens are articulated (in all the cases in which this circumstance could be observed); (4) adults of *Hammephemera* sp. cf. *Ha. pulchra* are abundant in the deposit of Mallorca, considering that the family Sharephemeridae was known previously by only two isolated forewings; (5) all these adults are articulated; (6) these adults occur together with this nymph type in the slabs (for example, slab D, 7 × 5.5 cm in size, see Fig. 7A, contains the adult TS-D-1 and remains of 10 nymphs); and (7) the largest detritivore nymphs have sizes that could match with the adult body sizes. However, in the studied fossil assemblage there are also two small-sized mayfly adults (adult morphotype 1; see above), and therefore some of the small detritivorous nymphs may be conspecific with these adults. Further research and new specimens with exceptional preservation could elucidate this topic and complete the description herein provided.

Family Triassoephemeridae Sinitshenkova et Papier (*in* Sinitshenkova, Marchal-Papier, Grauvogel-Stamm et Gall, 2005)

Genus *Triassoephemera* Sinitshenkova et Papier (*in* Sinitshenkova, Marchal-Papier, Grauvogel-Stamm et Gall, 2005)

Triassoephemera punctata Sinitshenkova et Papier (*in* Sinitshenkova, Marchal-Papier, Grauvogel-Stamm et Gall, 2005)

Triassoephemera punctata

Fig. 7I–J

Studied material: A single, articulate specimen, MBCN23697a, MBCN23697b (counterpart). From Pedra Alta section (metre 7.55), upper part of Estellencs Formation, Aegean. One clam shrimp is close the thorax in ventral position.

Description: Large nymph. Head not preserved (likely not due disaticulation, but preservational) and thorax partially preserved (wing pads not observed). Body length is *ca.* 18 mm as preserved (estimated 20 mm), and the greater width of the abdomen is 4 mm. Legs not preserved, and therefore claw features unknown. Body not flattened (clearly cylindrical), and abdomen with short segments and without side protrusions. All the 10 abdominal segments preserved. Gills in latero-ventral position at least in the abdominal segments I–V, as plates rounded in shape, densely fringed on the borders. Dense punctuated ornamentation of the abdominal tergal cuticle (Fig. 7J). Absence of a 3D cololite preserved. Base of cerci and paracercus preserved.

Remarks: This genus and species were described based on 9 specimens from the Vosges (Sinitshenkova et al., 2005), with body lengths of 15, 20 and 30 mm depending on the nymphal stages represented (the preserved body portion of the specimen from Mallorca is *ca.* 18 mm, with an estimated body length of about 20 mm). The deposit of Mallorca is the second with the presence of this Anisian species, implying a faunal similitude with the Vosges at species level. In the Vosges, *Te. punctata* is rare, as it only represents the 2.5% of the mayflies (Sinitshenkova et al., 2005), but it is even rarer in the deposit of Mallorca (0.7%). The absence of a 3D cololite in the specimen studied herein (and not described in the Vosges specimens), suggests that this mayfly species was not detritivore, contrarily to the "detritivore nymph type" described above.

Family Siphlonuridae Ulmer, 1920 (*sensu lato*)

Genus *Triassonurus* Sinitshenkova et Papier (*in* Sinitshenkova, Marchal-Papier, Grauvogel-Stamm et Gall, 2005)

Triassonurus doliiformis Sinitshenkova et Papier (*in* Sinitshenkova,

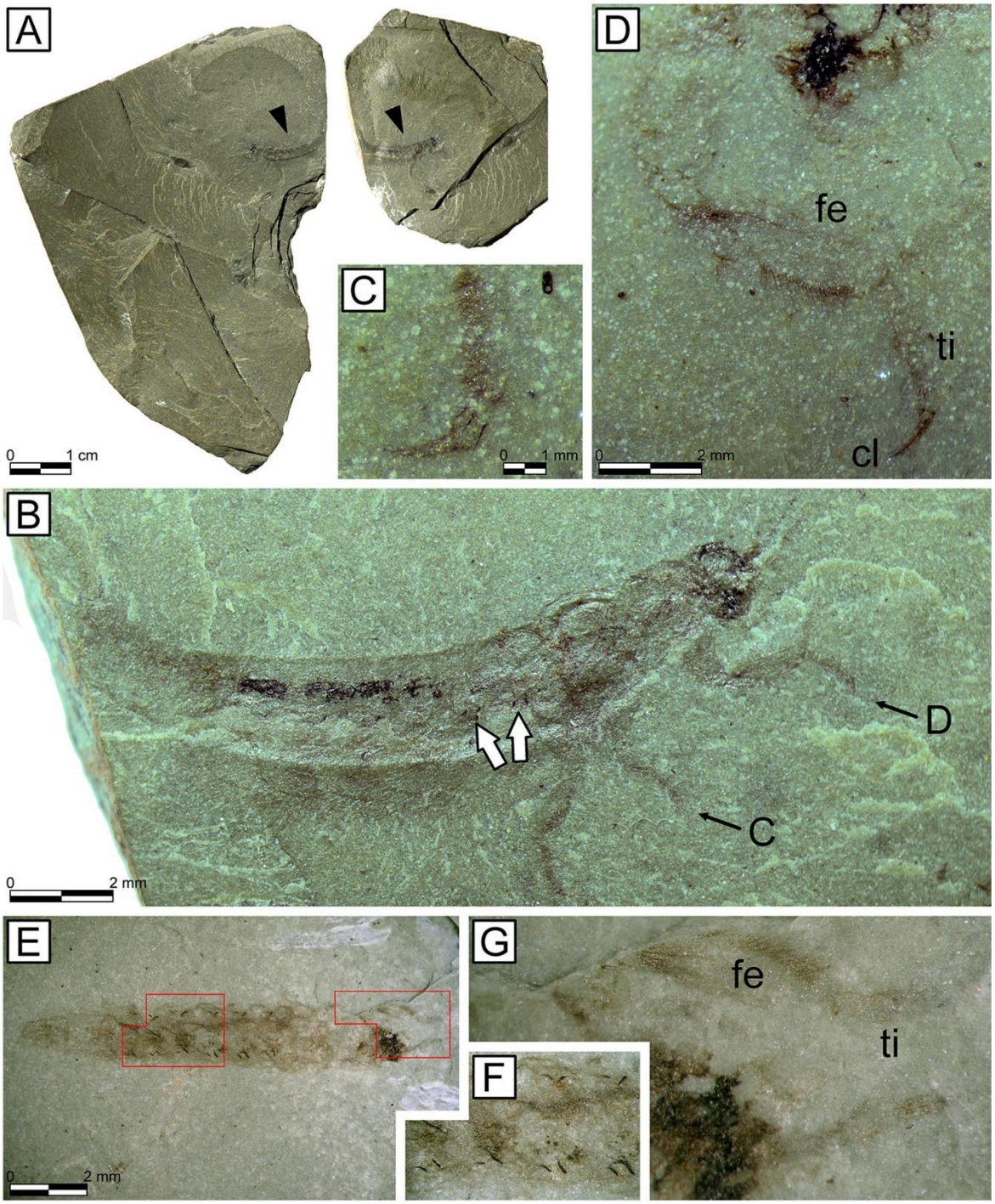

Fig. 8. cf. *Voltziaephemera fossoria* (Voltziaephemeridae) from Pedra Alta section, upper part of Estellencs Formation, Aegean. A: Counterpart (left) and part (right) of the slab TS-J having the virtually complete nymph figured by Calafat (1988) (black arrowheads indicate the nymph). B: TS-J-1a, habitus of specimen (white arrows indicate some of the abdominal "black-coloured comma-shaped sclerified structures" *sensu* Sinitshenkova et al., 2005). C–D: Detail of the distal mid leg showing distal setae in the tibia (C) and detail of the fore leg of burrowing type (D), both showing a simple claw each. E–G: DA/21-03-02-38a, exuvium and details of its abdominal "black-coloured comma-shaped sclerified structures" in F, and fore leg of burrowing type and head in G. Photographs C–D and E–G taken with the specimens wet with alcohol. Scale of F and G referred to graphic scale in E. Abbreviations: cl = claw, fe = femur, ti = tibia.

Marchal-Papier, Grauvogel-Stamm et Gall, 2005)

Triassonurus doliiformis

Fig. 7K–M

Studied material: A single, articulate specimen, TS-C-1. From Pedra Alta section (metre 4.75), upper part of Estellencs Formation, Aegean. Four clam shrimps are present in the same surface having the nymph.

Description: Large nymph exceptionally preserved. Body length is *ca.* 11 mm, and the greater width of the abdomen in lateral position excluding tergaliae is *ca.* 2 mm. Body cylindrical (not flattened). Head triangular, wider than long, narrowing towards the anterior margin; it is longer than the prothorax, which is short. Mesothorax large. Wing pads apparently not preserved. Legs simple, short and slender; femora shorter than tibiae and tarsi slightly shorter than tibiae. Abdominal segments short, 2.5 times wider than long, with short denticles in their posterior margins. Tergaliae very large, rounded, with thickened anterior margin, and overlapped between them forming a close surface (their dimensions in respect to the abdominal segments as described for this species by Sinitshenkova et al., 2005). Cerci and paracercus incomplete, but based on their preserved basal portions they were long; they are segmented and densely covered with hairs (the posterior margin of the segments show a line of small, short spines). Absence of a 3D cololite preserved, but the digestive is strongly marked as a carbonaceous tube.

Remarks: This specimen shows an excellent preservation and is virtually complete. It was figured in Calafat (1988) and Martínez *in* Gallemí et al. (1988) as an indeterminate mayfly nymph. The specimen matches all the features described for *Tn. doliiformis*, but the forewing pads, which are large in this species, are apparently not preserved in the specimen from Mallorca. Its body length (*ca.* 11 mm) is close to the estimated for the holotype of *Tn. doliiformis* (ca. 12 mm; see Sinitshenkova et al., 2005). The deposit of Mallorca is the second with the presence of this Anisian species, implying a second faunal similitude with the Vosges at species level. The fossils of this genus are the oldest of the family Siphlonuridae (Sinitshenkova et al., 2005). In the Vosges, *Tn. doliiformis* is relatively abundant (13% of the Grauvogel and Gall collection, as indicated in Sinitshenkova et al., 2005), but it is very rare in the deposit studied here (0.7%). This species was not detritivore, similarly to *Te. punctata* described above and unlike the "detritivore nymph type".

Family Voltziaephemeridae Sinitshenkova et Papier (*in* Sinitshenkova, Marchal-Papier, Grauvogel-Stamm et Gall, 2005)

Genus *Voltziaephemera* Sinitshenkova et Papier (*in* Sinitshenkova, Marchal-Papier, Grauvogel-Stamm et Gall, 2005)

Voltziaephemera fossoria Sinitshenkova et Papier (*in* Sinitshenkova, Marchal-Papier, Grauvogel-Stamm et Gall, 2005)

cf. *Voltziaephemera fossoria*

Fig. 8

Studied material: A single, virtually complete nymph, TS-J-1a, TS-J-1b (counterpart). From Pedra Alta section (metre 4.75), upper part of Estellencs Formation, Aegean. One specimen corresponding to an incomplete exuvium, DA21/03-02-38. From Pedra Alta section (metre 7.20–7.30), upper part of Estellencs Formation, Aegean.

Description: Nymph in lateral position (Fig. 8A–D). Estimated body length of 14.5 mm. Head details not clear, but antennae preserved. Head with anterior rounded protrusion (observed in lateral habitus; character not conspicuous). Large eyes, elongate in lateral view. Prothorax longer than the head. Wing pads not well discernible in this specimen. Legs well developed, with abundant hairs and with a terminal single claw, thus of burrowing type (see Sinitshenkova et al., 2005). Fore and hind legs about a quarter of estimated body length. Fore legs not shorter than hind legs, but slightly longer; tibiae lacking a conspicuous protrusion. Fore and hind femora swollen; mid femur not well discernible. First seven abdominal segments with tergaliae marginally with long and slender fringes. The abdominal segments present "small black-coloured comma-shaped sclerified structures" (peculiar structures as described by Sinitshenkova et al., 2005) on their lateral parts. No cololite, but digestive as a carbonaceous tube. Cerci and paracercus not preserved by slab margin.

Remarks: Sinitshenkova (2000) considered this nymph from Mallorca, figured in photo 24 of Calafat (1988), as a burrowing form. The specimen shares all its important preserved characters with the species *Voltziaephemera fossoria* from the Vosges. For example, the fore legs are identical to those of this fossil burrowing species (Sinitshenkova et al., 2005; fig. 6B, D, E in p. 386). That species was described based on specimens preserved in dorso-ventral position, not lateral. The specimen from Mallorca apparently lacks convergent tusks in its head and protruding anterior eye margins, but surely this is due to preservation and/or lateral position (these features were only observed in a few specimens from the Vosges and, in fact, the head features of the specimen from Mallorca are similar to those of the specimen paratype 9229 in Sinitshenkova et al., 2005). The relative leg lengths of the specimen from Mallorca are not identical to the Vosges specimens, but its body length has been based on an estimation, and the legs of the Vosges specimens apparently are not well preserved to allow accurate descriptions. Unfortunately, the wing pads of the specimen from Mallorca are not well discernible and its cerci and paracercus cannot be compared as they are not preserved. Most likely, this new specimen belongs to *Voltziaephemera fossoria*, but new material will be necessary to confirm that identification. Another specimen from Mallorca, corresponding to an incomplete exuvium (Fig. 8E–G), is from a younger stage and only shows a few structures, but it can be considered conspecific with the other specimen found in this locality because it has the same abdominal "small black-coloured comma-shaped sclerified structures" and same fore leg of burrowing type.

Blattodea Brunner von Wattenwyl, 1882

Blattodea indet.

Fig. 7O

Studied material: One isolated tegmina (= forewing), DA21/03-02-85. From Pedra Alta section (metre 7.20), upper part of Estellencs Formation, Aegean. One isolated tegmina, DA21/14-02-03a, DA21/14-02-03b (counterpart). From Pedra Alta section (metre 7.55), upper part of the Estellencs Formation, Aegean.

Description: Specimen DA21/14-02-03 shows few details. Specimen DA21/03-02-85 is partial but exceptionally preserved as a carbonaceous film lacking slight relief. The incomplete wing (proximal portion) shows a well-marked venation (but its intricate, dichotomous venation has not been completely resolved), with slightly marked intercalary veins in R, M, CuA systems, and possibly in Sc as well.

Remarks: Ansorge (1997) cited three wings of cockroaches from this deposit, but without description. Wings of cockroaches are difficult to interpret, and they show vein variation even in the same individual. The partial wing DA21/03-02-85 has been compared to other known Mesozoic species with intercalary veins, but identification has been unsuccessful. Nevertheless, that portion is similar to the wings of the species *Voltziablatta intercalata* from the Anisian of the Vosges (Papier and Grauvogel-Stamm, 1995), a deposit that yielded over 5000 specimens, the 40% of the individuals being cockroaches. Cockroaches are very polyphagous, mainly saprophagous, and thus not very informative for the reconstruction of the palaeoecosystem.

6.3. Fishes

Osteichthyes Huxley, 1880

Osteichthyes indet.

Fig. 9

Studied material: One specimen, virtually complete, TS-E-1. From Pedra Alta section (metre 4.75), upper part of Estellencs Formation, Aegean. The same slab surface contains a mayfly adult (TS-E-2) at a distance of 2.5 cm from the fish.

Description: The specimen is preserved in a dorso-ventral position, except for the posterior third of the body, which is in lateral position. Its estimated length is 16 mm (the preserved portion is 13 mm long). The

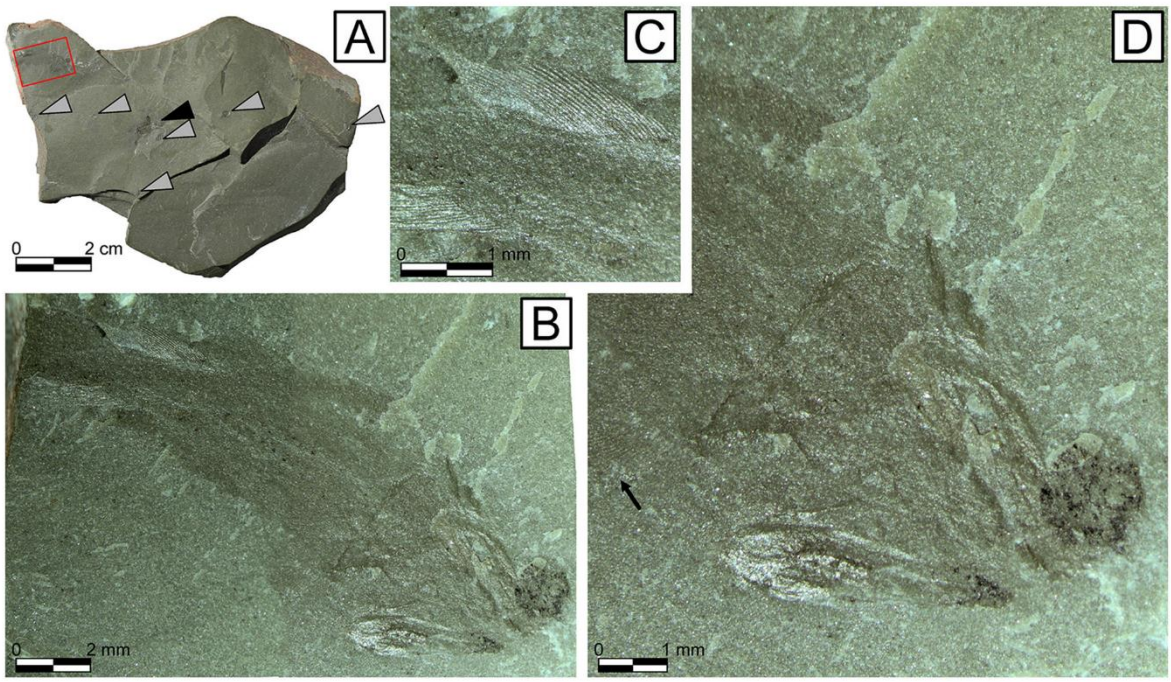

Fig. 9. Indeterminate juvenile osteichthyan. From Pedra Alta section, upper part of Estellencs Formation, Aegean. A: Complete view of the slab TS-E, black arrowhead indicates the remain of a mayfly adult (TS-E-2), grey arrowheads indicate clam shrimp specimens (TS-E-3 to TS-E-8) and the red rectangle indicates the area corresponding to picture B. B: Complete view of the fish (TS-E-1). C: Detail of the anal fin (upper in the photograph) and dorsal fin (possible second dorsal fin); note that the fin radii are well marked in this compression fossil. D: Detail of the head (arrow indicates the right pectoral fin). (For interpretation of the references to colour in this figure legend, the reader is referred to the web version of this article).

right pectoral, the dorsal (perhaps a second dorsal fin as well) and the anal fins are preserved, all with well-marked radii. The caudal fin is distally missing due to its being on the edge of the slab. No remains of the vertebral column or ribs are preserved, neither as carbonaceous films nor as their impressions.

Remarks: The poor preservation of this specimen has precluded any precise identification. It had been figured by Calafat (1988), who identified it as an indeterminate fish, and here it is identified as an osteichthyan based on the presence of opercles and fins with radii. Its very small size and lack of ossification makes it possible to consider it as a juvenile specimen.

The aquatic palaeocommunity described above (clam shrimps, mayfly nymphs and fishes) developed in ponds near the channels or among sand bars. Some horizons lacking bioturbation show abundant specimens of mayfly nymphs in complete articulation, without a preferred orientation and sharing the same or a very similar stage of development (slab TS-A, 5.0 × 3.5 cm in size, contains 4 nymphs; slab TS-D, 7.0 × 5.5 cm, contains 10 nymphs; and slab DA21/14-02-01, 6.5 × 6.0 cm, contains 14 nymphs, but in this case they are not in a clear, single surface). These records do not indicate accumulations caused by currents, but high mortality in a short time, in a population with individuals of very similar age. These features are indicative of mass mortality, implying the presence of many carcasses covering an anoxic bottom, most likely due to a low transport in the water column before their final sinking. Such evidences suggest sudden variations of the environmental conditions, probably related with desiccation and/or depletion of oxygen in those water bodies.

Other terrestrial insect material from unspecified beds of Estellencs Formation and/or Pedra Alta Formation was reported by Zessin (2008a, 2008b), who illustrated some of the specimens and preliminarily identified remains of the orders "Blattaria", Coleoptera, Diptera, Heteroptera, (?)Megaloptera, Homoptera and (?)Orthopteroidea. From the same beds, Aristov and Zessin (2009) described a new grylloblattid species: *Mallorcagryllus hispanicus*. Despite the intensive fieldwork campaigns carried out during the present work, beds bearing such a rich terrestrial palaeoassemblage have not been found again.

7. Discussion

7.1. Palaeoenvironmental evolution and palaeogeography

The sedimentary palaeoenvironments in the Iberian area during the Triassic were likely strongly influenced by the climate (Borruel-Abadía et al., 2015). Previous works have shown that subsidence rates were irregular among the different sub-basins of each of the main basins, and yet similar sedimentary successions were recorded, varying mostly in the thickness of each of the lithostratigraphic units (*e.g.*, Arche and López-Gómez, 1996; Borruel-Abadía et al., 2015; Mujal et al., 2017a, 2017b; López-Gómez et al., 2019a). In the case of Mallorca, even though the Triassic continental succession echoes those of the southeastern Iberian Basin (located in the central-eastern zone of the Iberian area; see below) in the succession of the different palaeoenvironments through time, the lack of detailed studies on palaeoclimate indicators (clay mineralogy, palaeosols, *etc.*) in the former prevents extrapolating the climatic conditions inferred for each of the units of the latter. Therefore, in this section, the changes in palaeoenvironments are not attributed directly to climate but, more broadly, to shifts in the energy conditions, which may be caused by the climate but also by tectonics and geomorphology (*e.g.*, Miall, 2006).

The lowermost lithostratigraphic unit of the Triassic of Mallorca, Punta Roja Formation (Fig. 10), is here considered a distal equivalent to the southeast of the fluvial units reworking aeolian sediments recognised in the central part of southwestern Europe (eastern Iberia,

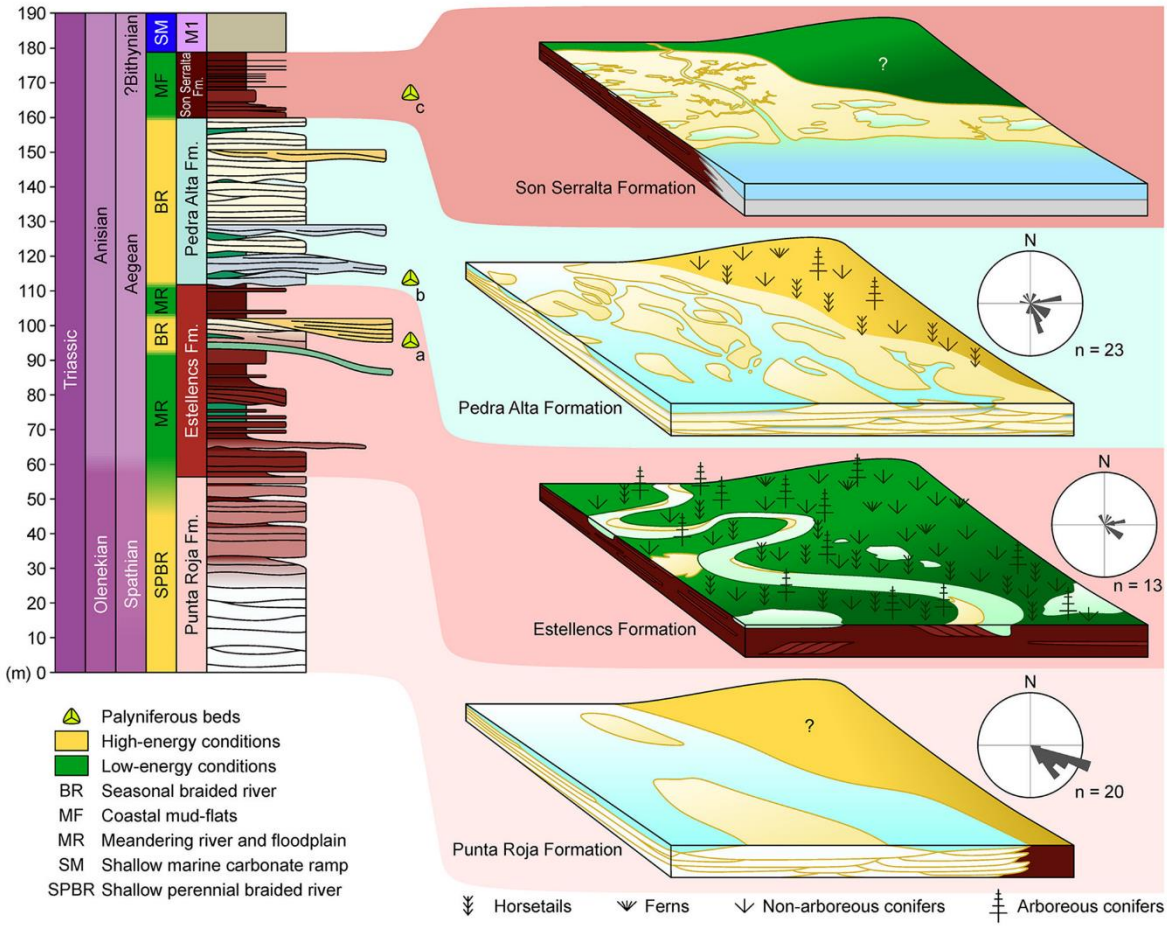

Fig. 10. Synthetic stratigraphic log for the four formations of the Triassic *Buntsandstein* facies of Mallorca defined herein and their respective palaeoenvironmental interpretation, with indication of the three beds that have been dated with spores and pollen: [a, sample 4481 of Calafat, 1988 and conifer cones of Grauvogel-Stamm and Álvarez-Ramis, 1996], dated as indeterminate lower Anisian (Grauvogel-Stamm and Álvarez-Ramis, 1996; Diez et al., 2010), here inferred as lower? Aegean (Appendix A. Supplementary data: Supplementary Table 3); [b, samples ME0 to ME7 of Diez, 2000], dated as upper? Aegean (Diez, 2000; Diez et al., 2010; Appendix A. Supplementary data: Supplementary Table 3); [c, sample 4389 of Calafat, 1988], dated as indeterminate lower Anisian (Diez et al., 2010), here inferred as uppermost Aegean, perhaps even stretching into the Bithynian (Appendix A. Supplementary data: Supplementary Table 3).

Menorca, Sardigna and Provençe). There, wind-transported sediments have been identified in several areas, recognising fluvial systems with aeolian reworking in the Catalan Basin (Marzo, 1986; Galán-Abellán et al., 2013a), in the Castilian branch of the Iberian Basin (López-Gómez et al., 2012), and an erg system in the Aragonese branch of the Iberian Basin (Soria et al., 2011). The aforementioned units have been dated, usually by inference, as Spathian (upper Olenekian) to Aegean (lower Anisian) (reviews in Durand, 2006; López-Gómez et al., 2019a), coinciding with the late part of an arid period recognised in central Europe (Péron et al., 2005; Durand, 2006; Bourquin et al., 2011; Sun et al., 2012; Borruel-Abadía et al., 2015; Trotter et al., 2015). However, towards the northern and southern margins of eastern Iberia, Menorca, Sardigna and Provençe, those aeolian sediments were often reworked by rivers, appearing in the form of well-sorted fluvial deposits, sometimes with ventifacts (Cassinis et al., 2003; Durand, 2006; Linol et al., 2009; López-Gómez et al., 2012; Galán-Abellán et al., 2013a). As posited in '4. Stratigraphy and sedimentology', Punta Roja Formation also corresponds to a perennial shallow braided river that reworked aeolian sediments, with an increase of sinuosity towards the top, probably near the Olenekian–Anisian transition (Fig. 10).

With the decrease of the energy of the systems, the depositional environment gradually shifted to sand-bed meandering rivers that traversed lutitic floodplains, corresponding to Estellencs Formation (Fig. 10). Abundant growth of vegetation under more favourable conditions may have contributed to the stabilisation of the river banks (plant roots make them more cohesive and thus more difficult to erode) and led to the development of sinuous channels, a process that has been observed in both modern and ancient systems (Ebisemiju, 1994; Rowntree and Dollar, 1999; Huisink, 2000; Michaelsen, 2002; Miall, 2006; Davies and Gibling, 2010; López-Gómez et al., 2012; Borruel-Abadía et al., 2015). Evidence of such a plant cover lies in the presence in this unit of sporadic hygrophytic plant remains such as *Equisetites* (found in living position, see Juárez-Ruiz and Wachtler, 2015) and well-developed palaeosols. The latter always present abundant small-sized carbonate concretions, thus corresponding to Calcisols, which are indicative of climates with low precipitation regimes (semi-arid conditions), at least during part of the year (Mack et al., 1993; Alonso-Zarza, 2003; Tabor and Poulsen, 2008). Moreover, almost all the ichnofossils, including the tetrapod footprints, belong to the *Scoyenia* ichnofacies (Buatois and Mángano, 1998), typical of aquatic non-marine palaeoenvironments with recurring desiccation events, such as river margins (Buatois and Mángano, 1998; Minter et al., 2007; Hminna et al., 2020). The *Mermia*

ichnofacies, on the other hand, was developed in playa lakes (see Buatois and Mángano, 1998). All these pieces of evidence suggest the alternation of semi-arid seasons (characterised by desiccation of playa lakes) and more humid seasons (characterised by inundation and plant sprouting). Calcification of palaeosols could have taken place in either season (Alonso-Zarza, 2003). This parallels with the probably coeval lower units of the Eslida Formation of the Iberian Basin (Borruel-Abadía et al., 2015; Juncal et al., 2017), which also correspond to meandering rivers deposited under similar conditions.

In the upper part of Estellencs Formation (metres 18–27 of Punta Negra log, metres 103–112 of Punta Roja log and the whole Pedra Alta log: Fig. 1C; Appendix A. Supplementary data: Supplementary Logs), there is an interval characterised by high-regime flow structures, channel migration and the formation of bars (Fig. 10). The fossil content is much more abundant in this interval than in the rest of the formation (see '7.2. Palaeoecosystem'), but this is probably because (1) the low preservation potential that any remains would have had in the underlying heavily oxidised red-beds and (2) the fact that the floods that deposited the sediments of this interval swept hinterland conifer forests, carrying and rapidly burying large fragments of plant material, including branches with leaves and strobyles with *in situ* pollen (Calafat, 1988; Álvarez-Ramis et al., 1989, 1995; Grauvogel-Stamm and Álvarez-Ramis, 1994, 1996; Juárez-Ruiz and Wachtler, 2015). Mayfly nymphs develop well in this kind of environment of still, limpid, well-oxygenated freshwater but, similarly to the palaeoassemblages of *Grès à Voltzia* of the Central European Basin, the mayflies from Mallorca show evidence of mass mortality in some horizons, most likely due to sudden changes in the environmental aquatic conditions. In fact, recent mayfly nymphs are very sensitive to oxygen concentration, salinity variation and water turbidity (Sinitshenkova et al., 2005).

The uppermost part of Estellencs Formation records a very similar palaeoenvironment to that of the lower 35 m of the formation, as evidenced by the presence of lutitic floodplains with small, sinuous channels and crevasse splay deposits (Fig. 10). Therefore, it may have been deposited under similar energy conditions of the system.

After this interval, the higher-energy conditions were restored again, but this time it was for a thicker interval, represented by Pedra Alta Formation (Fig. 10). The sand-bed braided rivers expanded over the floodplains during seasonal heavy rains, and created new ephemeral aquatic niches in which arthropods and fish thrived. This formation has been confidently dated as Aegean (Diez, 2000; Diez et al., 2005, 2010), and does not have any recognisable equivalent in the series of the southeastern Iberian Basin. It is somewhat reminiscent of the unit Ems-5 of the most distal part of the Eslida Formation, which consists of a

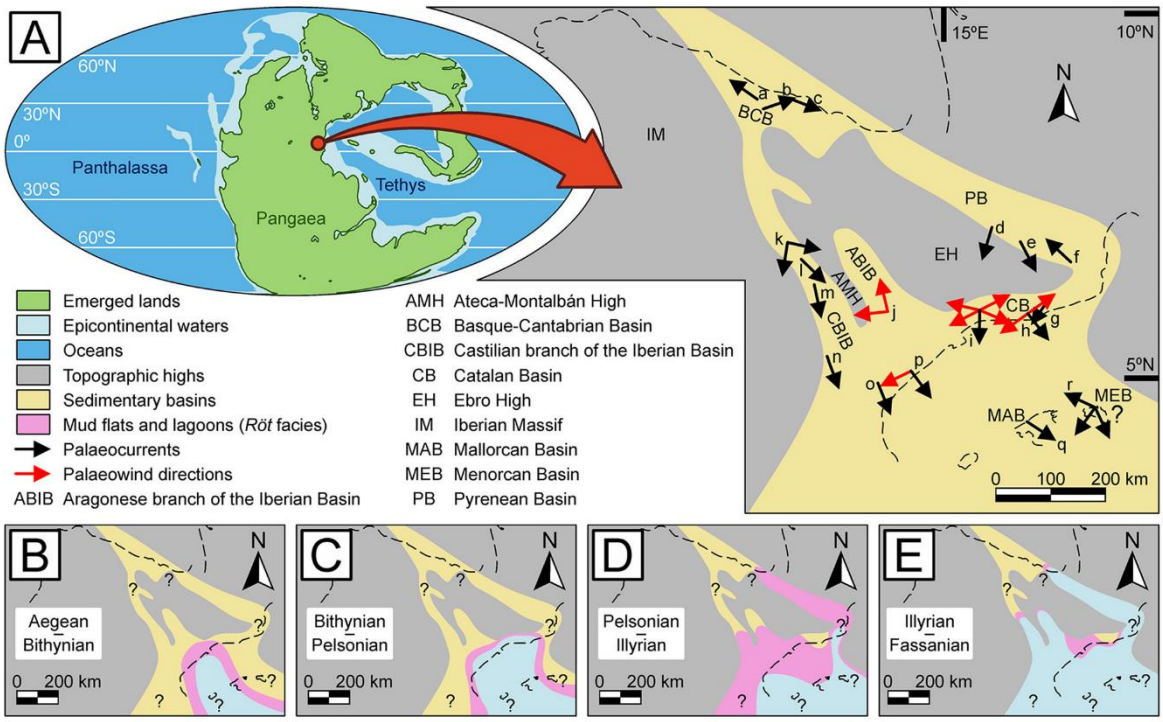

Fig. 11. Palaeogeographical evolution of the western peri-Tethys during the Anisian. Dashed lines correspond to present-day coastline. A: Map of the Iberian area during the Anisian, with indication of the main basins and palaeocurrent directions. Base map modified from Edel et al. (2018), basin margins modified from Lago et al. (2012) and palaeocurrent/palaeowind direction data from the following works: [a, Cicera] [b, Peña Sagra–Cohilla] [c, Riocorvo] from López-Gómez et al. (2019b); [d, Peranera] from Nagtegaal (1969); [e, Segre] from Robles and Llompart (1987); [f, Castellar de n'Hug] from Borruel-Abadía et al. (2015); [g, carretera Figueró–Montmany] from Marzo (1980); [h, Eramprunyà] from Marzo (1986); [i, Sant Gregori–l'Albiol] from Galán-Abellán et al. (2013a); [j, Peñarroyas–Torre de las Arcas] from Soria et al. (2011); [k, Ayllón–Castro] from Matesanz-Yagüe (1987); [l, Riba de Santiuste] from Franzel et al. (2021); [m, Rillo de Gallo] from Ramos (1979); [n, Landete] from López-Gómez (1985); [o, Gàtova] from Borruel-Abadía et al. (2015); [p, Benicàssim] from López-Gómez et al. (2012); [q, Mallorca] from the present work; [r, Menorca] from Linol et al. (2009). Palaeocurrents and palaeowind directions have been corrected for both the counterclockwise rotation of Iberia in the Alpine orogeny and for the clockwise rotation of the Balearic Islands due to the opening of the València trough during the Miocene (Parés et al., 1992; Roca, 1992). B: Extension of the carbonate ramps in the upper Aegean–lower Bithynian (mostly based on biostratigraphic data of Diez et al., 2010). C: Extension of the carbonate ramps in the Bithynian–Pelsonian (mostly based on biostratigraphic data of Diez et al., 2010 and Ortí et al., 2020). D: Extension of the carbonate ramps in the Pelsonian–Illyrian (mostly based on biostratigraphic data of Diez et al., 2010 and Ortí et al., 2018, 2020). E: Extension of the carbonate ramps in the Illyrian–Fassanian (mostly based on biostratigraphic data of Diez et al., 2010 and Ortí et al., 2018, 2020). Note that Mallorca, together with the southwestern Catalan Basin and the southeastern Iberian Basin, were the first areas to be reached by the sea.

braided interval that has been recognised in all the sections in south-eastern Iberia (Borruel-Abadía et al., 2014, 2015). That unit appears a few metres below the *Röt* facies, and has been interpreted as a semi-arid interval based on the local presence of aeolian sediments, xerophytic flora and the unconfinement of the fluvial systems (Borruel-Abadía et al., 2014, 2015). The age of the Iberian unit, however, has been inferred to be upper Bithynian (Borruel-Abadía et al., 2015), whereas this formation in Mallorca is well dated as Aegean (Diez, 2000; Diez et al., 2005, 2010; Appendix A. Supplementary data: Supplementary Table 3). Therefore, they are not lateral equivalents of a same unit, but two different units deposited under comparable local conditions.

Son Serralta Formation is generally equivalent to the *Röt* facies described elsewhere in Iberia (López-Gómez and Arche, 1992; Ramos, 1995; López-Gómez et al., 2019a), representing the transition from fluvial deposits to the shallow marine carbonate ramps of the *Muschelkalk* facies (Fig. 10). The mud-flats were established in response to the rise of the base level during the *Muschelkalk* transgression (Franzel et al., 2021), a phenomenon also reported in other basins of different age (*e.g.*, Miall, 2006).

As previously stated, this fluvial succession and its evolution through time is in part parallel to that of the southeastern Iberian Basin, providing clues on the possible distribution of palaeoenvironments in the most distal part of Iberia, that is, the Balearic basins, during the Early–Middle Triassic. Several works have attempted to propose a location for the Balearic Islands in the western Tethys in the early Mesozoic, leading to disparate hypotheses (*e.g.*, Lonergan and White, 1997; Diez et al., 2005; Linol et al., 2009; Bourquin et al., 2011; Fortuny et al., 2011a; Gretter et al., 2015; Edel et al., 2018; Borruel-Abadía et al., 2019). In the present work, the palaeogeographic position of Mallorca is reconstructed using the work of Roca (1992), who studied the tectonic history of the opening of the modern Catalan-Balearic Basin in detail, and Parés et al. (1992), who, by means of palaeomagnetism, observed a 10° clockwise rotation in Mallorca during the opening of the València Trough (Fig. 11), separating Mallorca from continental Iberia. The resulting position of Mallorca is somewhat aligned with the Iberian Basin (Fig. 11) and, although this does not necessarily imply that the sediments of Mallorca were deposited in a lateral extension of that basin (a claim which is impossible to back up with surface data), it supports the idea of a similar palaeoenvironmental evolution of both regions. The palaeogeographical location of Menorca is still contentious (Sàbat et al., 2018), but here it has been included in the map of Fig. 11 in its modern position relative to Mallorca in order to show its palaeocurrent directions during the Early–Middle Triassic.

Consequently, from a regional point of view, the fluvial series from the Lower–Middle Triassic of Mallorca were deposited in the most distal areas of the systems traversing Iberia towards the southeast (Fig. 11A). In addition, the fact that the succession is in part comparable to that of the Iberian Basin makes it possible to infer that high-energy conditions with river systems reworking aeolian sediments were widespread in Iberia until the late Olenekian–earliest Aegean (Punta Roja Formation) and that the energy of the systems dwindled in the early? Aegean (Estellencs Formation). In the late? Aegean, however, there was a local interval with slightly higher energy conditions (Pedra Alta Formation) followed by the reestablishment of lower energy conditions, probably at some point during the latest Aegean–Bithynian (Son Serralta Formation).

This proves the hypothesis that the first *Muschelkalk* transgression occurred on Mallorca, as the most distal region of Iberia towards the Tethys, approximately at the same time as in the most distal basins of the Iberian Peninsula. In the other Balearic Islands, the age of the base of the Triassic marine carbonate ramps is unknown, and previous inferences as Illyrian by means of lithological correlation with Iberia (Arche et al., 2002; Escudero-Mozo et al., 2014) are here considered unfounded because lateral facies variations were not taken into account. Diez et al. (2010) reviewed all the palynological data of the Anisian of the Iberian Peninsula known until then, concluding that in Mont-roig del Camp, in the southwest Catalan Basin, the *Röt* facies, equivalent to the Son Serralta Formation of Mallorca, were also of Aegean age (Fig. 11B). However, in other deposits of the Catalan Basin located further North, equivalent *Röt* facies were dated as Bithynian, both in Els Hostalets de Balenyà and in L'Espluga de Francolí (Diez et al., 2010 and references therein) (Fig. 11C). The upper *Buntsandstein* lutites were dated as lower? Pelsonian in the Pyrenean Basin (in Igüerri and Sant Sebastià de Buseu) (Diez et al., 2010 and references therein) (Fig. 11D), whereas in the Basque-Cantabrian Basin (in Amaiur), similar units were dated as Bithynian–Pelsonian (Diez et al., 2010 and references therein) (Fig. 11D). In the Castilian branch of the Iberian Basin (in Almarja), the lower part of the *Muschelkalk* succession was also dated as Bithynian–Pelsonian (Ortí et al., 2020) (Fig. 11C).

After this first transgression, during the highstand phase, a system of mud-flats, coastal lagoons and, in some cases, alluvial sediments, developed in the margins of the Ebro High (Ortí et al., 2018, 2020). These units have been dated between the Pelsonian and the Illyrian (Diez et al., 2010 and references therein; Ortí et al., 2020), and reached Mallorca in the form of a brief interval of red fine-grained sediments, evaporites and dolostones (Cuevas-López, 1958a, 1958b; Rodríguez-Perea et al., 1987; Matamales-Andreu et al., 2021) (Fig. 11D). The upper part of these systems was affected by a second transgressive event, generating *Röt* facies similar to those of the uppermost part of the *Buntsandstein*. In the Iberian Basin, both in the Aragonese branch (in Fombuena) and in the Castilian branch (in Andilla, El Paraíso and Montant), those facies were considered as Pelsonian–Illyrian (Diez et al., 2010 and references therein; Ortí et al., 2020) (Fig. 11D), and Franzel et al. (2021) determined that the *Muschelkalk* sea reached the north-western, most proximal margins of the Castilian branch of the Iberian Basin (in Riba de Santiuste), in the middle Ladinian (Fig. 11E). All these data agree with studies on other peri-Tethyan basins that suggested a progressive rise of the sea level during the Early–Middle Triassic (*e.g.*, Rüffer and Zühlke, 1994; Narkiewicz and Szulc, 2004), in this case in two main pulses, and show how the first areas to be drowned under the sea were Mallorca, the southern Catalan Basin and the southeastern Iberian Basin, followed by the northern Catalan Basin and then by the Basque-Cantabrian and Pyrenean basins. The last areas to be flooded by the sea were both branches of the Iberian Basin, and especially the Castilian branch, which was the one opening deeper inland (Arche et al., 2004; López-Gómez et al., 2019a; Fig. 11E).

7.2. Palaeoecosystems

After the Permian–Triassic mass extinction event, palaeoequatorial continental environments remained quite inhospitable because of the very high temperatures and fast climate changes that affected them (Sun et al., 2012; Trotter et al., 2015; MacLeod et al., 2017; Bernardi et al., 2018). This situation became more stable towards the Middle Triassic, when those continental ecosystems started to regain their lost complexity (Chen and Benton, 2012; Benton and Newell, 2014; Romano et al., 2020). In the western peri-Tethys, it has been suggested that high acidity levels delayed the recovery of its ecosystems until the Middle Triassic (Galán-Abellán et al., 2013b, 2013c; Borruel-Abadía et al., 2016, 2019), which coincides with the rise in abundance of palaeosols and trace fossils (Borruel-Abadía et al., 2019).

In the case of Punta Roja Formation of Mallorca, biotic activity has been recorded in the form of carbonate palaeosols (vertic Calcisols or Calcisols) and invertebrate burrows only in the upper part of the unit. In its lower part, this formation is composed of transverse sand bars, in which the oxidation of the sediments and the general paucity of fine-grained beds most probably caused a preservation bias, as it is very unlikely for biogenic traces to be preserved in the medium-grained sands of an active river channel (bars of braided rivers are usually colonised only during intervals of interruption or waning of the flow: *e.g.*, Stanley and Fagerstrom, 1974). The first trace fossils appear in Punta Roja Formation once the grain size decreases and the first floodplain deposits

appear. López-Gómez et al. (2012) suggested that such a lack of fossils in equivalent strata of the Iberian formations was indicative of ecosystems that had not still recovered from the Permian–Triassic extinction. This, however, cannot be applied to Mallorca, because biogenic structures (palaeosols and burrows) appear as soon as the fossilisation conditions became better (finer and waterlogged sediment) towards the upper part of Punta Roja Formation. This is similar to what happens in the Pyrenean sections, where the first biotic traces appear abundantly just above the basal Triassic conglomerates (Mujal et al., 2018a).

The palaeoecosystem represented in Estellencs Formation is certainly the richest of the ones of the continental Lower–Middle Triassic of Mallorca, with at least three recognisable trophic levels. In general terms, the heavily oxidised red-beds only preserve palaeosols, large plant fragments such as stems and logs and bioturbation traces produced by both invertebrates and vertebrates (Figs. 4–5). In addition, some fine-grained beds deposited under reducing conditions enclose very well-preserved plant remains (leaves, branches, spores and pollen), clam shrimps, insects and, rarely, fishes and fish scales (Figs. 6–9).

The plant remains found in Estellencs Formation suggest the presence of a hygrophytic local flora (Fig. 12) and fragments from the hinterland conifer forests dragged and rapidly buried by sheetfloods. The species mentioned below are based on the review of the figures of Álvarez-Ramis et al. (1995) and Juárez-Ruiz and Wachtler (2015) (E. Kustatscher, pers. comm., 2021). Horsetails are represented by *Equisetites mougeotii* (*e.g.*, Álvarez-Ramis et al., 1995: pl. 1, fig. 1), *Neocalamites merianii* (*e.g.*, Juárez-Ruiz and Wachtler, 2015: p. 31, fig. 6) and *Schizoneura paradoxa* (*e.g.*, Álvarez-Ramis et al., 1995: pl. 1, fig. 3). Among the ferns, there are *Anomopteris mougeotii* (*e.g.*, Juárez-Ruiz and Wachtler, 2015: p. 34, fig. 1) and *Chiropteris digitata* (*e.g.*, Álvarez-Ramis et al., 1995: pl. 1, fig. 8). In the case of non-arboreous conifers, *Aethophyllum stipulare* (*e.g.*, Juárez-Ruiz and Wachtler, 2015: p. 17, fig. 1), *Albertia latifolia* (*e.g.*, Juárez-Ruiz and Wachtler, 2015: p. 9, figs. 2–3) and *Pelourdea vogesiaca* (*e.g.*, Juárez-Ruiz and Wachtler, 2015: p. 34, fig. 2) have been identified. Arboreous conifers are represented by *Voltzia heterophylla* (*e.g.*, Juárez-Ruiz and Wachtler, 2015: p. 25, fig. 1) and *Voltzia walchiaeformis* (*e.g.*, (Álvarez-Ramis et al., 1995): pl. 2, fig. 4). Finally, among the different types of reproductive organs, there is one specimen assignable putatively to *Cycadocarpidium* sp. (*e.g.*, Álvarez-Ramis et al., 1995: pl. 2, fig. 3) and numerous conifer cones of the species *Willsiostrobus acuminatus* (*e.g.*, Álvarez-Ramis et al., 1995: pl. 2, fig. 1), *Willsiostrobus hexasacciphorus* (*e.g.*, Álvarez-Ramis et al., 1995: pl. 2, fig. 7) and *Willsiostrobus rhomboidalis* (*e.g.*, Álvarez-Ramis et al., 1995: pl. 2, fig. 8). These plant fossils are found in two different assemblages, also noted by Juárez-Ruiz and Wachtler (2015): green sandstones with *Equisetites mougeotii*, *Schizoneura paradoxa*, *Chiropteris digitata*, *Aethophyllum stipulare*, *Pelourdea vogesiaca*, *Voltzia* spp., *Willsiostrobus acuminatus* and *Willsiostrobus hexasacciphorus*, and white sandstones with abundant *Albertia latifolia*, accompanied by *Anomopteris mougeotii*, *Pelourdea vogesiaca*, *Voltzia* spp., *Willsiostrobus rhomboidalis* and, rarely, *Neocalamites merianii*. Although both are located in the upper part of Estellencs Formation, the former assemblage probably corresponds to a relatively autochtonous, hygrophytic plant community developed on the river banks, whereas the latter were probably dragged by sheetfloods from further inland. Similar assemblages have been

Fig. 12. Reconstruction of the palaeoecosystem of the Aegean (Anisian, Middle Triassic) Estellencs Formation of Mallorca. In the foreground, bottom left-hand corner, a specimen of the mayfly nymph *Triassoephemera punctata* emerging from the water on a stem of the horsetail plant *Equisetites mougeotii*. In the water, several specimens of the clam shrimp *Hornestheria* sp. aff. *Ho. sollingensis*. Behind, three "detritivore type" mayfly nymphs resting on the base of a stem of *Equisetites mougeotii*. Outside the water, several *Hammephemera* sp. cf. *Ha. pulchra* adult mayflies fluttering around. In the background, there are some more stems of *Equisetites mougeotii* and different species of conifers: on the left, specimens of the conifer *Aethophyllum stipulare*; in the centre, arboreal conifers of the genus *Voltzia*; and on the right, the conifer *Pelourdea vogesiaca*. Among the vegetation, there is a diapsid reptile (*Macrocnemus*-like, one of the possible producers of tracks here identified as *Rhynchosauroides* ispp.) that has catched a small osteichthyan fish, and several more *Hammephemera* sp. cf. *Ha. pulchra* specimens. Created by Henry Sutherland Sharpe. © 2021 Henry Sutherland Sharpe. Used under license.

recognised in other European basins of a similar age (*e.g.*, Gall, 1971; Grauvogel-Stamm, 1978; Grauvogel-Stamm and Grauvogel, 1980; Kustatscher et al., 2014; Borruel-Abadía et al., 2015).

Decaying plant fragments that had fallen into the water bodies, together with algae, were probably consumed by the various arthropods found in Estellencs Formation. Modern clam shrimps are usually filter feeders, consuming plankton and organic detritus suspended in the water (*e.g.*, Dodson and Frey, 2001). Larger crustaceans, such as the notostracans, which probably produced the *Rusophycus-Cruziana-Diplichnites* traces, are nowadays grazers, detritivores, scavengers, and can also hunt small prey such as other arthropods and small vertebrates (*e.g.*, Dodson and Frey, 2001). Other bioturbation traces such as *Gordia* and *Skolithos* were made by indeterminate insect larvae, and thus will not be considered further in this discussion. Mayfly nymphs, recorded as body fossils in Estellencs Formation (Fig. 12), can be assigned to different feeding guilds in aquatic environments such as detritivores, grazers and filter-feeders (Sinitshenkova et al., 2005). Their abundance indicates that they were important components of the aquatic trophic net together with clam shrimps, similarly to the palaeoassemblages of the Triassic of the Vosges (Sinitshenkova et al., 2005). Representatives of the terrestrial insect community, such as coleopterans (which are the purported producers of *Taenidium*) and cockroaches are either herbivorous or omnivorous. Other entomological remains found in this palaeoenvironment (Ansorge, 1997; Zessin, 2008a, 2008b; Aristov and Zessin, 2009) suggest a richer terrestrial insect community, but since no more specimens have been found for the present study and previous authors have generally offered only preliminary determinations, those will not be further assessed here.

In the aquatic environments, osteichthyan fishes were probably the main predators on invertebrates, although they could also feed on the terrestrial insects that reached the water surface, since the few terrestrial specimens (most likely para-autochthonous) are represented in the studied deposit by isolated wings. On land, small-sized diapsid reptiles (Fig. 12), such as the ones that made the tracks studied herein, possibly preyed on the adult insects and other small animals. The trackmakers of *Rhynchosauroides* and *Prorotodactylus mesaxonichnus* are thought to have been small archosauromorphs such as tanystropheids or euparkeriids (Avanzini and Renesto, 2002; Mujal et al., 2017b, 2018b), and some coeval body fossil genera such as *Macrocnemus* and *Euparkeria* have been inferred to have an insectivorous diet based on anatomical features (*e.g.*, Sookias and Butler, 2013; Rieppel, 2019), supporting our hypothesis. Triassic ichnoassemblages dominated by small ichnites, such as the one studied herein, have been correlated to coastal settings and/or areas with presence of microbial mats (De Jaime-Soguero et al., 2021). No structures diagnostic of marine influence have been recognised in Estellencs Formation, but wrinkle structures are indeed very common in the tetrapod footprint horizons, thus pointing to the presence of microbial mat development in the floodplain (Porada and Bouougri, 2007; Carmona et al., 2011). It has been considered that under these conditions, larger tetrapods were at disadvantage when walking, as their feet would penetrate too deep in the substrate hindering their movement, and thus small footprints of lighter tetrapods are usually dominant (Mujal et al., 2018b; De Jaime-Soguero et al., 2021).

The palaeoecosystem recorded in Pedra Alta Formation is somewhat similar to that of the underlying Estellencs Formation, although fossil remains are much scarcer. Plant remains are usually preserved in the form of unidentifiable debris or large tree logs, although well-preserved *Neocalamites* stems were found *ex situ* (Juárez-Ruiz and Wachtler, 2015). Arthropods are represented by clam shrimps and scarce ephemeropterans, appearing together with rare fish scales. No macrofossils have been reported from Son Serralta Formation.

7.3. Palaeobiogeography

The rich palaeoecosystems preserved in the Lower–Middle Triassic formations of Mallorca show strong similarities with those of southern and central Europe, and secondarily also with North America and Asia, in the "*Voltzia* and *Pleuromeia* floras" of Dobruskina (1994) and the "N-American–Eurasian Fauna" of Romano et al. (2020). Plant fossils of Estellencs Formation, although comparatively poorly sampled, have the main components of fossil floras of similar age found in Iberia (*e.g.*, Diez et al., 2010; Borruel-Abadía et al., 2014), the Alpine region (*e.g.*, Dobruskina, 1994; Kustatscher et al., 2004, 2007; Kustatscher and van Konijnenburg-van Cittert, 2005; Van Konijnenburg-van Cittert et al., 2006), the Vosges (*e.g.*, Gall, 1971; Grauvogel-Stamm, 1978; Dobruskina, 1994), and central Europe (*e.g.*, Dobruskina, 1994; Kustatscher et al., 2014).

Clam shrimp assemblages of Estellencs and Pedra Alta formations, of carapace valve morphologies similar to *Hornestheria*, suggest a correlation to upper Olenekian–Anisian occurrences of this genus in central Europe and Asia (Kozur and Weems, 2010) and are different from those of the Vosges, dated as Bithynian (Gall, 1971; Kozur and Weems, 2010). Insect assemblages of Estellencs Formation are the second in importance based on mayfly abundance, just after those of the Vosges (Sinitshenkova et al., 2005), with which they share at least two species of mayfly nymphs, *Triassoephemera punctata* and *Triassonurus doliiformis*.

Tetrapod ichnites, although scarce, are similar to those found in southern and central Europe and in southern North America, belonging to the N-American–Eurasian faunas of Romano et al. (2020). The ichnospecies *Prorotodactylus mesaxonichnus* had so far only been reported from the upper Olenekian–lower Anisian of the Pyrenean Basin (Mujal et al., 2017b), but the morphologically similar ichnogenus *Gwynnedichnium* is known from the Anisian of central Europe and the Anisian–Rhaetian of southern North America (Lucas et al., 2014; Klein and Lucas, 2018), and other ichnospecies of *Prorotodactylus* are known from the Olenekian of the Central European Basin (Niedźwiedzki et al., 2013; Klein and Lucas, 2021). Conversely, the ichnogenus *Rhynchosauroides* has little palaeobiogeographic value because of its sub-cosmopolitan distribution (De Jaime-Soguero et al., 2021 and references therein). These data are consistent with the abundance of archosauromorphs and lepidosauromorphs in the palaeoequatorial latitudes of Pangaea during the Early Triassic (Mujal et al., 2017b; Romano et al., 2020).

In summary, these facts indicate that, during the Early–Middle Triassic, the Iberian area was biogeographically well connected to the Central European Basin, and therefore they suggest that there were no important barriers or strong climatic gradients between the two areas, especially in the distribution of floras and invertebrates. This implies that the Variscan orogen had little impact in the distribution of species or that there were corridors that made migration possible, and that Iberia (including Mallorca) and central Europe were under similar semi-arid climatic conditions, as suggested by Romano et al. (2020).

8. Conclusions

The present work provides, for the first time, a comprehensive and interdisciplinary characterisation of the palaeoecosystems of the Lower–Middle Triassic of Mallorca (Balearic Islands, western Mediterranean). Four lithostratigraphic units have been formally described, and are named, from lower to upper: Punta Roja Formation (shallow perennial braided rivers), Estellencs Formation (meandering rivers with a braided interval in the upper part), Pedra Alta Formation (braided rivers) and Son Serralta Formation (mud-flats with tidal influence). For all of them and based on a review of all the previous literature and new data, detailed stratigraphic, sedimentological and palaeontological interpretations have been provided in order to reconstruct their ecosystems and their evolution over time.

The Lower–Middle Triassic sequence of Mallorca is reminiscent of those of eastern Iberian Peninsula, which represent more proximal deposits of the river systems that developed in the different basins, and that flowed from the Iberian Massif (and Ebro High) towards the Tethys. The macroflora is comparable to those of other Anisian localities of the western peri-Tethys, and a review of the palynofloras makes it possible

to date Estellencs and Pedra Alta formations in the Aegean (lower Anisian). The clam shrimp fauna from Estellencs Formation can be dated in the upper Olenekian–Anisian, and is biogeographically similar to other Eurasian palaeoassemblages. The insect fauna shows a diverse aquatic community, very similar to that of the Vosges, which is slightly younger (Bithynian) but palaeogeographically close (central Europe). Tetrapod ichnofaunas are also comparable to coeval assemblages of North America and Eurasia, and are especially similar to those of the Pyrenees and central Europe. Nevertheless, both the insect and vertebrate faunas seem to be not very diverse compared to other sites of similar age. In fact, the insect assemblage shows an overrepresentation of mayflies, both in number of specimens and different forms, and a notable paucity of terrestrial forms. In the case of tetrapod footprints, there is clear dominance of small-sized tracks, but more data is needed to elucidate whether it is just a product of sampling bias or is actually related to the palaeoenvironment.

In any case, the results of the present work indicate that ecosystems of palaeoequatorial Pangaea, such as Mallorca, showed strong signs of recovery from the Permian–Triassic mass extinction by the earliest Middle Triassic, presenting diverse and complex aquatic and terrestrial communities. Moreover, this work also suggests that although the biota of the continental Triassic of Mallorca was quite similar to that of nearby basins of similar age, the stratigraphic succession does not appear to reflect global patterns, but local particularities instead. This stresses the need for caution when interpreting global trends from regional successions, as the imprint of more geographically-limited causes may mask that of more widespread changes.

Declaration of Competing Interest

The authors declare that they have no known competing financial interests or personal relationships that could have appeared to influence the work reported in this paper.

Acknowledgements

To Tomeu Sáez, Feliu Calafat, David Gómez-Gras and Antoni Rodríguez-Perea for their valuable insights and data on the outcrops they discovered and studied, and for providing bibliographic references. To Bernadí Gelabert for information and literature on the possible palaeogeographic position of Mallorca during the Triassic. To Sebastià Matamalas, Francesc Baiget, Eduardo Barrón, Ana Rodrigo and Enric Pedrón for aid in fieldwork. To Pedro Agustín Robledo, Ana Sevillano and José María López García, who facilitated the field and laboratory palaeontological research on Mallorca, and to Tomeu Sáez, who kindly travelled to Palma with his collection to allow that research. To Evelyn Kustatscher for the revision of the identifications of plant fossils figured by previous authors. To Fran Poyato for comments on the indeterminate osteichthyan. To Llorenç Homar and Onofre Rullan for offering an insight into local toponymy. To Hendrik Klein and an anonymous reviewer for their insightful comments that considerably improved the initial version of the manuscript, and to Christopher Fielding, editor, for handling the manuscript. To the Comissió Insular de Patrimoni Històric (Consell Insular de Mallorca, Spain) for granting us the excavation permits (file numbers 305/2019 and 52/2021). We acknowledge support from the CERCA program (Generalitat de Catalunya, Spain). R.M.A. was supported by the predoctoral grant FPU17/01922 (Ministerio de Ciencia, Innovación y Universidades, Spain). O.O. and À.G. are members of the consolidated research group 2017 SGR 1666 GRC (Generalitat de Catalunya, Spain). J.F. was supported by the Agencia Estatal de Investigación (Spain) and the European Regional Development Fund AEI/FEDER EU, project CGL2017–82654-P (European Union). J.F. is member of the consolidated research group 2017 SGR 086 GRC (Generalitat de Catalunya, Spain). We acknowledge support from the project "Mallorca abans dels dinosaures: estudi dels ecosistemes continentals del Permià i Triàsic amb especial èmfasi en les restes de vertebrats" (ref. 15 - 619/2020), based at the Institut Català de Paleontologia Miquel Crusafont and funded by the Departament de Cultura, Patrimoni i Política Lingüística (Consell Insular de Mallorca, Spain).

Appendix A. Supplementary data

Supplementary data to this article can be found online at https://doi.org/10.1016/j.earscirev.2021.103783.

References

Alonso-Zarza, A.M., 2003. Palaeoenvironmental significance of palustrine carbonates and calcretes in the geological record. Earth Sci. Rev. 60, 261–298.
Álvarez-Ramis, C., Fernández-Marrón, T., Calafat, F., 1995. Avance sobre la megaflora triásica, en facies germánica, de Estellencs (sector noroccidental de la sierra de Tramontana, Mallorca). Revista Española de Paleontología nº homenaje al Dr. Guillermo Colom, 55–58.
Álvarez-Ramis, C., Solé, N., Calafat, F., 1989. Paleoflora del Triásico inferior de Mallorca. In: Abstracts of the II European Paleobotanical Conference. Madrid, p. 12.
Ansorge, J., 1997. Insekten aus dem Buntsandstein (Untere Trias) von Mallorca (Spanien). In: Abstracts für 4. Fachgespräch "Fossile Insekten". Clausthal-Zellerfeld (1 pp.).
Arche, A., López-Gómez, J., 1996. Origin of the Permian-Triassic Iberian Basin, central-eastern Spain. Tectonophysics 266, 443–464.
Arche, A., López-Gómez, J., Vargas, H., 2002. Propuesta de correlación entre los sedimentos Pérmicos y Triásicos de la Cordillera Ibérica Este y de las Islas Baleares. Geogaceta 32, 275–278.
Arche, A., López-Gómez, J., Marzo, M., Vargas, H., 2004. The siliciclastic Permian-Triassic deposits in Central and Northeastern Iberian Peninsula (Iberian, Ebro and Catalan Basins): a proposal for correlation. Geol. Acta 2 (4), 306–320.
Aristov, D., Zessin, W., 2009. *Mallorcagryllus hispanicus* n. get. et sp. - eine neue Grylloblattide (Insecta: Grylloblattida: Blattogryllidae) aus dem Buntsadstein der Insel Mallorca, Spanien. Virgo, Mitteilungsblatt des Entomologischen Vereins Mecklenburg 12 (1), 30–34.
Avanzini, M., Renesto, S., 2002. A review of *Rhynchosauroides tirolicus* Abel, 1926 ichnospecies (Middle Triassic: Anisian-Ladinian) and some inference on *Rhynchosauroides* trackmaker. Riv. Ital. Paleontol. Stratigr. 108 (1), 51–66.
Avanzini, M., Bernardi, M., Nicosia, U., 2011. The Permo-Triassic tetrapod faunal diversity in the Italian southern Alps. In: Ahmad Dar, I. (Ed.), Earth and Environmental Sciences, pp. 591–608.
Barnolas, A., 1991a. Mapa Geológico de España. Escala 1:50.000. Andraitx. Segunda serie, primera edición. Instituto Tecnológico GeoMinero de España, Madrid (56 pp. + 1 map + 5 stratigraphic logs).
Barnolas, A., 1991b. Mapa Geológico de España. Escala 1:50.000. Sóller. Segunda serie, primera edición. Instituto Tecnológico GeoMinero de España, Madrid (62 pp. + 1 map + 8 stratigraphic logs).
Bashkuev, A., Sell, J., Aristov, D., Ponomarenko, A., Sinitshenkova, N., Mahler, H., 2012. Insects from Buntsandstein of Lower Franconia and Thuringia. Paläontol. Z. 86, 175–185.
Baucon, A., Ronchi, A., Felletti, F., Neto de Carvalho, C., 2014. Evolution of Crustaceans at the edge of the end-Permian crisis: Ichnonetwork analysis of the fluvial succession of Nurra (Permian–Triassic, Sardinia, Italy). Palaeogeogr. Palaeoclimatol. Palaeoecol. 410, 74–103.
Benton, M.J., 2008. When Life Nearly Died. The Greatest Mass Extinction of all Time. Thames & Hudson, London (336 pp.).
Benton, M.J., Newell, A.J., 2014. Impacts of global warming on Permo-Triassic terrestrial ecosystems. Gondwana Res. 25, 1308–1337.
Bernardi, M., Petti, F.M., Benton, M.J., 2018. Tetrapod distribution and temperature rise during the Permian–Triassic mass extinction. Proc. R. Soc. B 285, 20172331.
Béthoux, O., De la Horra, R., Benito, M.I., Barrenechea, J.F., Galán, A.B., López-Gómez, J., 2009. A new triadotypomorphan insect from the Anisian (Middle Triassic), Buntsandstein facies, Spain. J. Iber. Geol. 35 (2), 179–184.
Borruel-Abadía, V., Galán-Abellán, A.B., Kustatscher, E., Diéguez, C., López-Gómez, J., De la Horra, R., Barrenechea, J.F., Arche, A., 2014. Palaeoenvironmental reconstruction of the early Anisian from sedimentology and plant remains in the SE Iberian Range (E Spain). Palaeogeogr. Palaeoclimatol. Palaeoecol. 414, 352–369.
Borruel-Abadía, V., López-Gómez, J., De la Horra, R., Galán-Abellán, B., Barrenechea, J. F., Arche, A., Ronchi, A., Gretter, N., Marzo, M., 2015. Climate changes during the Early–Middle Triassic transition in the E. Iberian plate and their palaeogeographic significance in the western Tethys continental domain. Palaeogeogr. Palaeoclimatol. Palaeoecol. 440, 671–689.
Borruel-Abadía, V., Barrenechea, J.F., Galán-Abellán, A.B., Alonso-Azcárate, J., De la Horra, R., Luque, F.J., López-Gómez, J., 2016. Quantifying aluminium phosphate–sulphate minerals as markers of acidic conditions during the Permian–Triassic transition in the Iberian Ranges, E Spain. Chem. Geol. 429, 10–20.
Borruel-Abadía, V., Barrenechea, J.F., Galán-Abellán, A.B., De la Horra, R., López-Gómez, J., Ronchi, A., Luque, F.J., Alonso-Azcárate, J., Marzo, M., 2019. Could acidity be the reason behind the Early Triassic biotic crisis on land? Chem. Geol. 515, 77–86.
Bourquin, S., Durand, M., Diez, J.B., Broutin, J., Fluteau, F., 2007. The Permian-Triassic boundary and Early Triassic sedimentation in Western European Basins: an overview. J. Iber. Geol. 33 (2), 221–236.

Bourquin, S., Bercovici, A., López-Gómez, J., Diez, J.B., Broutin, J., Ronchi, A., Durand, M., Arche, A., Linol, B., Amour, F., 2011. The Permian–Triassic transition and the onset of Mesozoic sedimentation at the northwestern peri-Tethyan domain scale: Palaeogeographic maps and geodynamic implications. Palaeogeogr. Palaeoclimatol. Palaeoecol. 299, 265–280.

Bradshaw, M.A., 1981. Paleoenvironmental interpretations and systematics of Devonian trace fossils from the Taylor Group (lower Beacon Supergroup), Antarctica. N. Z. J. Geol. Geophys. 24, 615–652.

Briere, P.R., 2000. Playa, playa lake, sabkha: proposed definitions for old terms. J. Arid Environ. 45, 1–7.

Bromley, R., Asgaard, U., 1979. Triassic freshwater ichnocoenoses from Carlsberg Fjord, East Greenland. Palaeogeogr. Palaeoclimatol. Palaeoecol. 28, 39–80.

Brunner von Wattenwyl, K., 1882. Prodromus der europäischen Orthopteren. Engelmann, Leipzig (XX + 488 pp.).

Buatois, L.A., Mángano, M.G., 1998. Trace fossil analysis of lacustrine facies and basins. Palaeogeogr. Palaeoclimatol. Palaeoecol. 140, 367–382.

Calafat, F., 1986. Estratigrafía y sedimentología de la litofacies Buntsandstein de Mallorca. In: Cabrera, L. (Ed.), Resúmenes de Comunicaciones del IX Congreso Español de Sedimentología. Grupo Español de Sedimentología, Barcelona, p. 39.

Calafat, F., 1987. Paleoambients de les facies Buntsandstein de Mallorca. In: Llibre de resums de les I Jornades del Medi Ambient de les Illes Balears. Societat d'Història Natural de les Balears, Palma, pp. 16–17.

Calafat, F., 1988. Estratigrafía y sedimentología de la litofacies Buntsandstein de Mallorca. Bachelor's thesis. Universitat de Barcelona, Barcelona (127 pp. + 31 annexed fig).

Calafat, F., Sáez, B., 1987. Paleofauna lacustre del Triàsic Inferior de Mallorca. In: Llibre de resums de les I Jornades del Medi Ambient de les Illes Balears. Societat d'Història Natural de les Balears, Palma, pp. 18–19.

Calafat, F., Fornós, J.J., Marzo, M., Ramos, E., Rodríguez-Perea, A., 1986. Icnología de vertebrados de las facies Buntsandstein de Mallorca. In: Cabrera, L. (Ed.), Resúmenes de Comunicaciones del IX Congreso Español de Sedimentología. Grupo Español de Sedimentología, Barcelona, p. 40.

Calafat, F., Fornós, J.J., Marzo, M., Ramos-Guerrero, E., Rodríguez-Perea, A., 1986–1987. Icnología de vertebrados de las facies Buntsandstein de Mallorca. Acta Geol. Hispàn. 21–22, 515–520.

Carmona, N., Bournod, C., Ponce, J.J., Cuadrado, D., 2011. The role of microbial mats in the preservation of bird footprints: a case study from the mesotidal Bahía Blanca estuary (Argentina). Soc. Sediment. Geol. Spec. Publ. 101, 37–45.

Cassinis, G., Durand, M., Ronchi, A., 2003. Permian-Triassic continental sequences of northwest Sardinia and south Provence: stratigraphic correlations and palaeogeographical implications. Boll. Soc. Geol. Ital. 2, 119–129.

Cassinis, G., Perotti, C.R., Ronchi, A., 2012. Permian continental basins in the Southern Alps (Italy) and peri-mediterranean correlations. Int. J. Earth Sci. 101, 129–157.

Chang, W.-T., Chen, P.-J., Shen, Y.-B., 1976. Fossil Conchostraca of China. Science Press, Beijing (325 pp. + 138 pls).

Chen, Z.-Q., Benton, M.J., 2012. The timing and pattern of biotic recovery following the end-Permian mass extinction. Nat. Geosci. 5 (6), 375–383.

Coleman, J.M., 1969. Brahmaputra river: channel processes and sedimentation. Sediment. Geol. 3 (2), 129–239.

Crimes, T.P., 1970. Trilobite tracks and other trace fossils from the Upper Cambrian of North Wales. Geol. J. 7 (1), 47–68.

Cuevas-López, F., 1958a. Informe geológico y minero de los yacimientos de cobre de Banyalbufar y Estallenchs, Mallorca. Barcelona (37 pp. + 8 fig).

Cuevas-López, F., 1958b. Informe geológico y minero de los yacimientos de cobre de Banyalbufar y Valldemosa, Mallorca. Barcelona (23 pp. + 7 fig).

d'Orbigny, A., 1842. Voyage dans l'Amérique méridionale (le Brésil, la République Orientale de l'Uruguay, la République Argentine, la Patagonie, la République du Chili, la République de Bolivia, la République du Perou) exécuté pendant les années 1826, 1827, 1828, 1829, 1830, 1831, 1832 et 1833. Pitois-Levrault, Paris, Levrault, Strasbourg, 3(4) (Paléontologie) (188 pp.).

Davies, N.S., Gibling, M.R., 2010. Paleozoic vegetation and the Siluro-Devonian rise of fluvial lateral accretion sets. Geology 38 (1), 51–54.

Davis Jr., R.A., 2012. Tidal signatures and their preservation potential in stratigraphic sequences. In: Davis Jr., R.A., Dalrymple, R.W. (Eds.), Principles of Tidal Sedimentology. Springer, Dordrecht, Heidelberg, London, New York, pp. 35–55.

Dawson, S.J.W., 1873. Impressions and footprints of aquatic animals and imitative markings on Carboniferous rocks. Am. J. Sci., 3rd series 5, 16–24.

De Jaime-Soguero, Ch., Mujal, E., Dinarès-Turell, J., Oms, O., Bolet, A., Orlandi-Oliveras, G., Fortuny, J., 2021. Palaeoecology of Middle Triassic tetrapod ichnoassociations (middle Muschelkalk, NE Iberian Peninsula) and their implications for palaeobiogeography in the western Tethys region. Palaeogeogr. Palaeoclimatol. Palaeoecol. 565, 110204.

Diez, J.B., 2000. Geología y Paleobotánica de la Facies Buntsandstein en la Rama Aragonesa de la Cordillera Ibérica. Implicaciones paleogeográficas en el Peritethys Occidental. Ph.D. dissertation. Universidad de Zaragoza–Université Pierre & Marie Curie, Paris VI, Zaragoza, Paris (424 pp.).

Diez, J.B., Broutin, J., Ferrer, J., 2005. Difficulties encountered in defining the Permian–Triassic boundary in Buntsandstein facies of the western Peritethyan domain based on palynological data. Palaeogeogr. Palaeoclimatol. Palaeoecol. 229, 40–53.

Diez, J.B., Broutin, J., Grauvogel-Stamm, L., Bourquin, S., Bercovici, A., Ferrer, J., 2010. Anisian floras from the NE Iberian Peninsula and Balearic Islands: a synthesis. Rev. Palaeobot. Palynol. 162, 522–542.

Díez-Canseco, D., Buatois, L.A., Mángano, M.G., Díaz-Molina, M., Benito, M.I., 2016. Ichnofauna from coastal meandering channel systems (Upper Cretaceous Tremp Formation, South-Central Pyrenees, Spain): delineating the fluvial-tidal transition. J. Paleontol. 90 (2), 250–268.

Dobruskina, I.A., 1994. Triassic floras of Eurasia. In: Zapfe, H. (Ed.), Osterreichische Akademie der Wissenschaften Schriftenreihe der Erdwissenschaftlichen Kommissionen, 10. Springer-Verlag, New York (422 pp.).

Dodson, S.I., Frey, D.G., 2001. Cladocera and other branchiopoda. In: Thorp, J.H., Covich, A.P. (Eds.), Ecology and Classification of North American Freshwater Invertebrates. Academic Press, California, pp. 849–913.

Durand, M., 2006. The problem of the transition from the Permian to the Triassic Series in southeastern France: comparison with other Peritethyan regions. Geol. Soc. Lond., Spec. Publ. 265, 281–296.

Ebisemiju, F.S., 1994. The sinuosity of alluvial river channels in the seasonally wet tropical environment: Case study of river Elemi, southwestern Nigeria. Catena 21, 13–25.

Edel, J.B., Schulmann, K., Lexa, O., Lardeaux, J.M., 2018. Late Palaeozoic palaeomagnetic and tectonic constraints for amalgamation of Pangea supercontinent in the European Variscan belt. Earth Sci. Rev. 177, 589–612.

Emmons, E., 1844. The Taconic System: Based on Observations in New York, Massachusetts, Maine, Vermont, and Rhode Island. Caroll and Cook, Albany (68 pp.).

Erwin, D.H., 1994. The Permo–Triassic extinction. Nature 367, 231–236.

Escudero-Mozo, M.J., Martín-Chivelet, J., Goy, A., López-Gómez, J., 2014. Middle-Upper Triassic carbonate platforms in Minorca (Balearic islands): implications for Western Tethys correlations. Sediment. Geol. 310, 41–58.

Ezcurra, M.D., Fortuny, J., Mujal, E., Bolet, A., 2017. First direct archosauromorph remains from the Early-Middle Triassic transition of the Iberian Peninsula. Palaeontol. Electron. 20.3.62A, 1–10.

Fillion, D., Pickerill, R.K., 1990. Ichnology of the upper Cambrian? to Lower Ordovician Bell Island and Wabana groups of eastern Newfoundland, Canada. Palaeontogr. Can. 7, 1–119.

Fitzgerald, P.G., Barrett, P.J., 1986. Skolithos in a Permian braided river deposit, southern Victoria Land, Antarctica. Palaeogeogr. Palaeoclimatol. Palaeoecol. 52 (3–4), 237–247.

Fortuny, J., Bolet, A., Sellés, A.G., Cartanyà, J., Galobart, À., 2011a. New insights on the Permian and Triassic vertebrates from the Iberian Peninsula with emphasis on the Pyrenean and Catalonian basins. J. Iber. Geol. 37 (1), 65–86.

Fortuny, J., Galobart, À., De Santiesteban, C., 2011b. A new capitosaur from the Middle Triassic of Spain and the relationships within the Capitosauria. Acta Palaeontol. Pol. 56 (3), 553–566.

Fortuny, J., Bolet, A., Sellés, A.G., Galobart, À., 2014. A potential record of a procolophonid parareptile from the Triassic of the Iberian Peninsula. Geol. Acta 12 (2), 121–126.

Franzel, M., Jones, S.J., Meadows, N., Allen, M.B., McCaffrey, K., Morgan, T., 2021. Basin-scale fluvial correlation and response to the Tethyan marine transgression: an example from the Triassic of Central Spain. Basin Res. 33 (1), 1–25.

Frizon de Lamotte, D., Fourdan, B., Leleu, S., Leparmentier, F., de Clarens, P., 2015. Style of rifting and stages of Pangea breakup. Tectonics 34, 1009–1029.

Gaigalas, A., Uchman, A., 2004. Trace fossils from Upper Pleistocene varved clays S of Kaunas, Lithuania. Geologija 45, 16–26.

Galán-Abellán, B., López-Gómez, J., Barrenechea, J.F., Marzo, M., De la Horra, R., Arche, A., 2013a. The beginning of the Buntsandstein cycle (Early–Middle Triassic) in the Catalan Ranges, NE Spain: sedimentary and palaeogeographic implications. Sediment. Geol. 296, 86–102.

Galán-Abellán, A.B., Barrenechea, J.F., Benito, M.I., De la Horra, R., Luque, F.J., Alonso-Azcárate, J., Arche, A., López-Gómez, J., Lago, M., 2013b. Palaeoenvironmental implications of aluminium phosphate-sulphate minerals in Early–Middle Triassic continental sediments, SE Iberian Range (Spain). Sediment. Geol. 289, 169–181.

Galán-Abellán, A.B., Alonso-Azcárate, J., Newton, R.J., Bottrell, S.H., Barrenechea, J.F., Benito, M.I., De la Horra, R., López-Gómez, J., Luque, J., 2013c. Sources of Sr and S in aluminum-phosphate–sulfate minerals in Early–Middle Triassic sandstones (Iberian Ranges, Spain) and paleoenvironmental implications for the West Tethys. J. Sediment. Res. 83, 406–426.

Gall, J.-C., 1971. Faunes et paysages du Grès à Voltzia du nord des Vosges. Essai paléoécologique sur le Buntsandstein supérieur. Service de la Carte Géologique d'Alsace et de Lorraine 34, 1–318.

Gallemí, J., Riba, O., Reguant, S., Agustí, J., Álvarez, G., Calzada, S., Caus, M., López, C., Martinell, J., Martínez, R., Martínez, X., Porta, J. de, Sanz de Siria, A., Solé, N., Truyols, J., Truyols, M., Via, Ll., 1988. Història Natural dels Països Catalans, 15: Registre Fòssil. Enciclopèdia Catalana, Barcelona (478 pp.).

Gand, G., Demathieu, G., Montenat, C., 2007. Les traces de pas d'amphibiens, de dinosaures et autres reptiles du Mesozoïque français: inventaire et interpretations. Palaeovertebrata 2007 (1–4), 1–149.

Gand, G., Garric, J., Schneider, J., Walter, H., Lapeyrie, J., Martin, C., Thiery, A., 2008. Notostraca trackways in Permian playa environments of the Lodève basin (France). J. Iber. Geol. 34 (1), 73–108.

Gerstaecker, A., 1866–1879. Die Klassen und Ordnungen der Arthropoden wissenschaftlich dargestellt in Wort und Bild. Erste Abtheilung Crustacea (Erste Hälfte). In: Bronn, H.G. (Ed.), Die Klassen und Ordnungen des Thier-Reichs wissenschaftlich dargestellt in Wort und Bild. Fünfter Band Gliederfüssler (Arthropoda). C.F. Winter, Leipzig, Heidelberg (1320 pp.).

Getty, P.R., Sproule, R., Stimson, M.R., Lyons, P.C., 2017. Invertebrate trace fossils from the Pennsylvanian Rhode Island Formation of Massachusetts, USA. Atl. Geol. 53, 185–206.

Gevers, T.W., Frakes, L.A., Edwards, L.N., Marzolf, J.E., 1971. Trace fossils in the lower Beacon sediments (Devonian), Darwin Mountains, southern Victoria Land, Antarctica. J. Paleontol. 45 (1), 81–94.

Ghinassi, M., Oms, O., Cosma, M., Finotello, A., Munari, G., 2021. Reading tidal processes where their signature is cryptic: the Maastrichtian meandering channel deposits of the Tremp Formation (Southern Pyrenees, Spain). Sedimentology 68 (5), 2009–2042.
Glennie, K.W., 1970. Desert sedimentary environments. In: Developments in Sedimentology, 14. Elsevier, Amsterdam, London, New York (222 pp. + 4 maps).
Gómez-Gras, D.M., 1992. El Permotrías de las Baleares, de la Cordillera Costero Catalana y de la vertiente mediterránea de la Cordillera Ibérica: facies y petrología sedimentaria. Ph.D. dissertation. Universitat Autònoma de Barcelona, Barcelona (XIX + 242 pp. + 55 fig. + 7 tab).
Gómez-Gras, D., 1993. El Permotrías de las Baleares y de la vertiente mediterránea de la Cordillera Ibérica y del Maestrat: Facies y Petrología Sedimentaria (Parte II). Bol. Geol. Min. 104, 467–515.
Gómez-Gras, D., Alonso-Zarza, A.M., 2003. Reworked calcretes: their significance in the reconstruction of alluvial sequences (Permian and Triassic, Minorca, Balearic Islands, Spain). Sediment. Geol. 158, 299–319.
Grauvogel-Stamm, L., 1978. La flore du Grès à Voltzia (Buntsandstein supérieur) des Vosges du Nord (France). Morphologie, anatomie, interpretations phylogénique et paléogéographique. Sci. Géol. Bull. Mém. 50, 1–225 (+ 54 pl).
Grauvogel-Stamm, L., Álvarez-Ramis, C., 1994. Macroflore et microflore in situ du Buntsandstein de l'île de Majorque (Baléares, Espagne). In: Arche, A. (Ed.), Resúmenes del III Coloquio de Estratigrafía y Paleogeografía del Pérmico y Triásico de España. Consejo Superior de Investigaciones Científicas, Universidad Complutense de Madrid, Cuenca, pp. 51–53.
Grauvogel-Stamm, L., Álvarez-Ramis, C., 1996. Conifères et pollen in situ du Buntsandstein de l'île de Majorque (Baléares, Espagne). Cuadernos Geol. Ibérica 20, 229–243.
Grauvogel-Stamm, L., Grauvogel, L., 1980. Morphologie et anatomie d'*Anomopteris mougeotii* Brongniart (synonyme: *Pecopteris sulziana* Brongniart), une fougère du Buntsandstein supérieur des Vosges (France). Sci. Géol. Bull. 33 (1), 56–66.
Gretter, N., Ronchi, A., López-Gómez, J., Arche, A., De la Horra, R., Barrenechea, J., Lago, M., 2015. The Late Palaeozoic-Early Mesozoic from the Catalan Pyrenees (Spain): 60 Myr of environmental evolution in the frame of the western peri-Tethyan palaeogeography. Earth Sci. Rev. 150, 679–708.
Haldeman, S.S., 1840. Supplement to Number one of "A Monograph of the *Limniades*, or Freshwater Unicarapace Valve Shells of North America," Containing Descriptions of Apparently New Animals in Different Classes, and the Names and Characters of the Subgenera in *Paludina* and *Anculosa*. J. Dobson, Philadelphia (3 pp.).
Hall, J., 1852. Palaeontology of New York. Volume II. Containing Descriptions of the Organic Remains of the Lower Middle Division of the New York System, (Equivalent in Part to the Middle Silurian Rocks of Europe). C. van Benthuysen, Albany, New York (362 pp.).
Hammersburg, S.R., Hasiotis, S.T., Robison, R.A., 2018. Ichnotaxonomy of the Cambrian Spence Shale Member of the Langston Formation, Wellsville Mountains, Northern Utah, USA. Paleontol. Contrib. 20, 1–66.
Han, Y., Pickerill, R.K., 1995. Taxonomic review of the ichnogenus *Helminthopsis* Heer 1877 with a statistical analysis of selected ichnospecies. Ichnos 4, 83–118.
Hasiotis, S.T., Platt, B.F., Hembree, D.I., Everhart, M.J., 2007. The trace-fossil record of vertebrates. In: William Miller, I.I.I. (Ed.), Trace Fossils: Concepts, Problems, Prospects. Elsevier, pp. 196–218.
Haubold, H., 1971. Die Tetrapodenfährten des Buntsandsteins in der Deutschen Demokratische Republik und in Westdeutschland und ihre Äquivalente in der gesamten Trias. Paläontol. Abhandlungen Abteilung A 4 (3), 395–660.
Heer, O., 1876–1877. Flora fossilis Helvetiae. Die vorweltliche Flora der Schweiz. Verlag J. Wurster & Co, Zürich (182 pp. [Parts 1, 2 (1876):1–90; Parts 3, 4 (1877): 91–182]).
Hminna, A., Lagnaoui, A., Zouheir, T., Saber, H., Schneider, J.W., 2020. Late Triassic ichnoassemblage from a playa-lake system of the Coastal Meseta, Morocco: Palaeoenvironmental and palaeoecological implications. J. Afr. Earth Sci. 172, 103995.
Hofmann, H.J., Patel, I.M., 1989. Trace fossils from the type "Etchemnian Series" (Lower Cambrian Ratcliffe Brook Formation), Saint John area, New Brunswick, Canada. Geol. Mag. 126, 139–157.
Homar, Ll., 1985. Toponímia del litoral de la costa d'Estellencs, Banyalbufar i Valldemossa: de na Foradada a sa Foradada. 7 Aerial Photographs.
Hounslow, M.W., Ruffell, A.H., 2006. Triassic: seasonal rivers, dusty deserts and saline lakes. In: Brenchley, P.J., Rawson, P.F. (Eds.), The Geology of England and Wales. Geological Society of London, London, pp. 295–324.
Huisink, M., 2000. Changing river styles in response to Weichselian climate changes in the Vecht valley, eastern Netherlands. Sediment. Geol. 133, 115–134.
Huxley, T.H., 1880. On the application of the laws of evolution to the arrangement of the Vertebrata, and more particularly of the Mammalia. Proc. Zool. Soc. Lond. 649–662.
Hyatt, A., Arms, J.M., 1891. A novel diagrammatic representation of the orders of insects. Psyche 6 (177), 11–13.
IDEIB, 2019. Infraestuctura de dades espacials de les Illes Balears. Conselleria d'Agricultura, Medi Ambient i Territori. Govern de les Illes Balears. http://www.ideib.cat (last accessed on 26/07/2019).
Irving, E., 2004. The case for Pangea B, and the intra-Pangean megashear. Geophys. Monogr. 145, 13–27.
Juárez Ruiz, J., Wachtler, M., 2015. Early–middle Triassic (Anisian) fossil flora from Majorca (Spain). Dolomythos 2015, 1–49.
Juncal, M., Diez, J.B., De la Horra, R., Galán-Abellán, B., Borruel-Abadía, V., Barrenechea, J.F., Arche, A., López-Gómez, J., 2017. Palynostratigraphy of the Middle Triassic (Anisian) Eslida Formation, SE Iberian Ranges, Spain. Palynology 42 (2), 149–157.
Klein, H., Haubold, H., 2007. Archosaur footprints – potential for biochronology of Triassic continental sequences. New Mexico Museum Nat. History Sci. Bull. 41, 120–130.
Klein, H., Lucas, S.G., 2010a. Review of the tetrapod ichnofauna of the Moenkopi Formation/Group (Early-Middle Triassic) of the American Southwest. New Mexico Museum Nat. History Sci. Bull. 50, 1–67.
Klein, H., Lucas, S.G., 2010b. Tetrapod footprints – their use in biostratigraphy and biochronology of the Triassic. Geol. Soc. Lond., Spec. Publ. 334, 419–446.
Klein, H., Lucas, S.G., 2018. Diverse Middle Triassic tetrapod footprints assemblage from the Muschelkalk of Germany. Ichnos 25, 162–176.
Klein, H., Lucas, S.G., 2021. The Triassic tetrapod footprint record. New Mexico Museum Nat. History Sci. Bull. 83, 1–194.
Klein, H., Niedźwiedzki, G., 2012. Revision of the Lower Triassic tetrapod ichnofauna from Wióry, Holy Cross Mountains, Poland. New Mexico Museum Nat. History Sci. Bull. 56, 1–62.
Klein, H., Voigt, S., Saber, H., Schneider, J.W., Hminna, A., Fischer, J., Lagnaoui, A., Brosig, A., 2011. First occurrence of a Middle Triassic tetrapod ichnofauna from the Argana Basin (Western High Atlas, Morocco). Palaeogeogr. Palaeoclimatol. Palaeoecol. 307, 218–231.
Kozur, H., 1982. Beiträge zur Taxonomie und stratigraphischen Auswertung der untertriassischen Conchostracen. Geol. Paläontol. Mitteil. Innsbruck 11 (11), 355–398.
Kozur, H.W., Weems, R.E., 2010. The biostratigraphic importance of conchostracans in the continental Triassic of the northern hemisphere. Geol. Soc. Lond. Spec. Publ. 334, 315–417.
Kozur, H.W., Mahler, H., Sell, J., 1993. Stratigraphic and paleobiologic importance of the latest Olenekian and Early Anisian conchostracans of Middle Europe. New Mexico Museum Nat. History Sci. Bull. 3, 255–259.
Kustatscher, E., van Konijnenburg-van Cittert, J.H.A., 2005. The Ladinian flora (Middle Triassic) of the Dolomites: palaeoenvironmental reconstructions and palaeoclimatic considerations. Geo. Alp 2, 31–51.
Kustatscher, E., Wachtler, M., van Konijnenburg-van Cittert, J.H.A., 2004. A number of additional and revised taxa from the Ladinian flora of the Dolomites, northern Italy. Geo. Alp 1, 57–69.
Kustatscher, E., Wachtler, M., van Konijnenburg-van Cittert, J.H.A., 2007. Horsetails and seed ferns from the Middle Triassic (Anisian) locality Kühwiesenkopf (Monte Prà della Vacca), Dolomites, northern Italy. Palaeontology 50 (5), 1277–1298.
Kustatscher, E., Franz, M., Heunisch, C., Reich, M., Wappler, T., 2014. Floodplain habitats of braided river systems: depositional environment, flora and fauna of the Solling Formation (Buntsandstein, Lower Triassic) from Bremke and Fürstenberg (Germany). Palaeodivers. Palaeoenviron. 94 (2), 237–270.
Labandeira, C.C., 2005. The fossil record of insect extinction: new approaches and future directions. Am. Entomol. 51 (1), 14–29.
Lago, M., De la Horra, R., Ubide, T., Galé, C., Galán-Abellán, B., Barrenechea, J.F., López-Gómez, J., Benito, M.I., Arche, A., Alonso-Azcárate, J., Luque, F.J., Timmerman, M. J., 2012. First report of a Middle-Upper Permian magmatism in the SE Iberian Ranges: characterisation and comparison with coeval magmatisms in the western Tethys. J. Iber. Geol. 38 (2), 331–348.
Leonardi, G., 1987. Glossary and Manual of Tetrapod Footprint Palaeoichnology. Departamento Nacional de Produção Mineral, Brasília (117 pp.).
Linol, B., Bercovici, A., Bourquin, S., Diez, J.B., López-Gómez, J., Broutin, J., Durand, M., Villanueva-Amadoz, U., 2009. Late Permian to Middle Triassic correlations and palaeogeographical reconstructions in south-western European basins: New sedimentological data from Minorca (Balearic Islands, Spain). Sediment. Geol. 220, 77–94.
Lonergan, L., White, N., 1997. Origin of the Betic-Rif mountain belt. Tectonics 16 (3), 504–522.
López-Gómez, J., 1985. Sedimentología y estratigrafía de los materiales pérmicos y triásicos del sector SE. de la rama castellana de la cordillera Ibérica entre cueva de Hierro y Chelva (provincias de Cuenca y Valencia). Seminarios de Estratigrafía, 11. Universidad Complutense de Madrid & Consejo Superior de Investigaciones Científicas, Madrid (344 pp.).
López-Gómez, J., Arche, A., 1992. Paleogeographical significance of the Röt (Anisian, Triassic) Facies (Marines clays, muds and marls Fm.) in the Iberian ranges, eastern Spain. Palaeogeogr. Palaeoclimatol. Palaeoecol. 91, 347–361.
López-Gómez, J., Arche, A., Pérez-López, A., 2002. Permian and Triassic. In: Gibbons, W., Moreno, M.T. (Eds.), The Geology of Spain. Geological Society, London, pp. 185–212.
López-Gómez, J., Galán-Abellán, B., De la Horra, R., Barrenechea, J.F., Arche, A., Bourquin, S., Marzo, M., Durand, M., 2012. Sedimentary evolution of the continental Early–Middle Triassic Cañizar Formation (Central Spain): implications for life recovery after the Permian–Triassic crisis. Sediment. Geol. 249–250, 26–44.
López-Gómez, J., Alonso-Azcárate, J., Arche, A., Arribas, J., Fernández-Barrenechea, J., Borruel-Abadía, V., Bourquin, S., Cadenas, P., Cuevas, J., De la Horra, R., Díez, J.B., Escudero-Mozo, M.J., Fernández-Viejo, G., Galán-Abellán, B., Galé, C., Gaspar-Escribano, J., Gisbert-Aguilar, J., Gómez-Gras, D., Goy, A., Gretter, N., Heredia-Carballo, N., Lago, M., Lloret, J., Luque, J., Márquez, L., Márquez-Aliaga, A., Martín-Algarra, A., Martín-Chivelet, J., Martín-González, F., Marzo, M., Mercedes-Martín, R., Ortí, F., Pérez-López, A., Pérez-Valera, F., Pérez-Valera, J.A., Plasencia, P., Ramos, E., Rodríguez-Méndez, L., Ronchi, A., Salas, R., Sánchez-Fernández, D., Sánchez-Moya, Y., Sopeña, A., Suárez-Rodríguez, Á., Tubía, J.M., Ubide, T., Valero-Garcés, B., Vargas, H., Viseras, C., 2019a. Permian-Triassic rifting stage. In: Vergés, J., Kullberg, J.C. (Eds.), The Geology of Iberia: A Geodynamic Approach. Volume 3: The Alpine Cycle. Springer, Cham, pp. 29–112.
López-Gómez, J., Martín-González, F., Heredia, N., De la Horra, R., Barrenechea, J.F., Cadenas, P., Juncal, M., Diez, J.B., Borruel-Abadía, V., Pedreira, D., García-

Sansegundo, J., Farias, P., Galé, C., Lago, M., Ubide, T., Fernández-Viejo, G., Gand, G., 2019b. New lithostratigraphy for the Cantabrian Mountains: a common tectono-stratigraphic evolution for the onset of the Alpine cycle in the W Pyrenean realm, N Spain. Earth Sci. Rev. 188, 249–271.
Lucas, S.G., 2019. An ichnological perspective on some major events of Paleozoic tetrapod evolution. Boll. Soc. Paleontol. Ital. 58 (3), 223–266.
Lucas, S.G., Spielmann, J.A., Klein, H., Lerner, A.J., 2010. Ichnology of the Upper Triassic (Apachean) Redonda Formation, east-central New Mexico. New Mexico Museum Nat. History Sci. Bull. 47, 3–75.
Lucas, S.G., Szajna, M.J., Lockley, M.G., Fillmore, D.L., Simpson, E.L., Klein, H., Boyland, J., Hartline, B.W., 2014. The Middle-Late Triassic tetrapod footprint ichnogenus Gwyneddichnium. New Mexico Museum Nat. History Sci. Bull. 62, 135–156.
Mack, G.H., James, W.C., Monger, H.C., 1993. Classification of paleosols. Geol. Soc. Am. Bull. 105, 129–136.
MacLeod, K.G., Quinton, P.C., Bassett, D.J., 2017. Warming and increased aridity during the earliest Triassic in the Karoo Basin, South Africa. Geology 45 (6), 483–486.
Maidwell, F.T., 1911. Notes on footprints from the Keuper of Runcorn Hill. Proceedings of the Liverpool Geological Society 11, 140–152.
Martí, J., Paniello, X., Pomar, L., Ramos, E., Rodríguez-Perea, A., 1985. El Triásico de las Baleares. In: Mateu Ibars, F., Marzo, M. (Eds.), Resúmenes del II Coloquio de Estratigrafía y Paleogeografía del Pérmico y Triásico de España. Institut d'Estudis Ilerdencs, Grupo Español del Mesozoico, La Seu d'Urgell, pp. 84–85.
Marzo, M., 1980. El Buntsandstein de los Catalánides: estratigrafía y procesos de sedimentación. Ph.D. dissertation. Universitat de Barcelona, Barcelona (317 pp. + 12 pls).
Marzo, M., 1986. Secuencias fluvio-eólicas en el Buntsandstein del macizo del Garraf (provincia de Barcelona). Cuadernos Geol. Ibérica 10, 207–233.
Matamales-Andreu, R., Oms, O., Galobart, À., Fortuny, J., 2021. Middle–Upper Triassic marine vertebrates of Mallorca (Balearic Islands, western Mediterranean). Hist. Biol. https://doi.org/10.1080/08912963.2020.1810682 (in press).
Matesanz-Yagüe, J., 1987. Estudio sedimentológico de las facies Buntsandstein en el extremo NW. de la rama castellana de la cordillera Ibérica (prov. de Soria). Estud. Geol. 43, 79–94.
McCann, T., Pascal, C., Timmerman, M.J., Krzywiec, P., López-Gómez, J., Wetzel, A., Krawczyk, C.M., Rieke, H., Lamarche, J., 2006. Post-Variscan (end Carboniferous–Early Permian) basin evolution in Western and Central Europe. Geol. Soc. Lond. Mem. 32, 355–388.
Melchor, R.N., De Valais, S., 2006. A review of Triassic tetrapod track assemblages from Argentina. Palaeontology 49 (2), 355–379.
Miall, A.D., 1977. A review of the braided-river depositional environment. Earth Sci. Rev. 13, 1–62.
Miall, A.D., 1985. Architectural-Element Analysis: a new method of facies analysis applied to fluvial deposits. Earth Sci. Rev. 22, 261–308.
Miall, A.D., 2006. The Geology of Fluvial Deposits: Sedimentary Facies, Basin Analysis, and Petroleum Geology, 4th ed. Springer, Berlin, Heidelberg, New York. (582 pp.).
Michaelsen, P., 2002. Mass extinction of peat-forming plants and the effect on fuvial styles across the Permian–Triassic boundary, northern Bowen Basin, Australia. Palaeogeogr. Palaeoclimatol. Palaeoecol. 179, 173–188.
Minter, N.J., Krainer, K., Lucas, S.G., Braddy, S.J., Hunt, A.P., 2007. Palaeoecology of an Early Permian playa lake trace fossil assemblage from Castle Peak, Texas, USA. Palaeogeogr. Palaeoclimatol. Palaeoecol. 246, 390–423.
Mujal, E., Gretter, N., Ronchi, A., López-Gómez, J., Falconnet, J., Diez, J.B., De la Horra, R., Bolet, A., Oms, O., Arche, A., Barrenechea, J.F., Steyer, J.-S., Fortuny, J., 2016. Constraining the Permian/Triassic transition in continental environments: stratigraphic and palaeontological record from the Catalan Pyrenees (NE Iberian Peninsula). Palaeogeogr. Palaeoclimatol. Palaeoecol. 445, 18–37.
Mujal, E., Fortuny, J., Bolet, A., Oms, O., López, J.A., 2017a. An archosauromorph dominated ichnoassemblage in fluvial settings from the late Early Triassic of the Catalan Pyrenees (NE Iberian Peninsula). PLoS One 12 (4), e0174693.
Mujal, E., Fortuny, J., Pérez-Cano, J., Dinarès-Turell, J., Ibáñez-Insa, J., Oms, O., vola, I., Bolet, A., Anadón, P., 2017b. Integrated multi-stratigraphic study of the Coll de Terrers late Permian–Early Triassic continental succession from the Catalan Pyrenees (NE Iberian Peninsula): a geologic reference record for equatorial Pangaea. Glob. Planet. Chang. 159, 46–60.
Mujal, E., Belaústegui, Z., Fortuny, J., Bolet, A., Oms, O., López, J.A., 2018a. Ichnological evidence of a horseshoe crab hot-spot in the Early Triassic Buntsandstein continental deposits from the Catalan Pyrenees (NE Iberian Peninsula). J. Iber. Geol. 44, 139–153.
Mujal, E., Iglesias, G., Oms, O., Fortuny, J., Bolet, A., Méndez, J.M., 2018b. *Rhynchosauroides* footprint variability in a Muschelkalk detrital interval (late Anisian–middle Ladinian) from the Catalan Basin (NE Iberian Peninsula). Ichnos 25 (2–3), 150–161.
Mujal, E., Marchetti, L., Schoch, R.R., Fortuny, J., 2020. Upper Paleozoic to lower Mesozoic tetrapod ichnology revisited: photogrammetry and relative depth pattern inferences on functional prevalence of autopodia. Front. Earth Sci. 8, 248.
Nagtegaal, P.J.C., 1969. Sedimentology, paleoclimatology, and diagenesis of post-Hercynian continental deposits in the south-central Pyrenees, Spain. Leidse. Geol. Meded. 42, 143–238.
Narkiewicz, K., Szulc, J., 2004. Controls on migration of conodont fauna in peripheral oceanic areas. An example from the Middle Triassic of the Northern Peri-Tethys. Geobios 37, 425–436.
Niedźwiedzki, G., Brusatte, S.L., Butler, R.J., 2013. *Prorotodactylus* and *Rotodactylus* tracks: an ichnological record of dinosauromorphs from the Early–Middle Triassic of Poland. Geol. Soc. Lond. Spec. Publ. 379, 319–351.
Nio, S.-D., Yang, C.-S., 1991. Diagnostic attributes of clastic tidal deposits: a review. Can. Soc. Petrol. Geol. 16, 3–28.
Ortí, F., Salvany, J.M., Rosell, L., Castelltort, X., Inglès, M., Playà, E., 2018. Middle Triassic evaporite sedimentation in the Catalan basin: Implications for the paleogeographic evolution in the NE Iberian platform. Sediment. Geol. 374, 158–178.
Ortí, F., Guimerà, J., Götz, A.E., 2020. Middle-Upper Triassic stratigraphy and structure of the Alt Palància (eastern Iberian Chain): a multidisciplinary approach. Geol. Acta 18 (4), 1–25.
Papier, F., Grauvogel-Stamm, L., 1995. Les Blattodea du Trias: le genre *Voltziablatta* n. gen. du Buntsandstein supérieur des Vosges (France). Palaeontographica A 235 (4/6), 141–162.
Parés, J.M., Freeman, R., Roca, E., 1992. Neogene structural development in the Valencia trough margins from palaeomagnetic data. Tectonophysics 203, 111–124.
Parrish, J.T., 1993. Climate of the supercontinent Pangea. J. Geol. 101, 215–233.
Péron, S., Bourquin, S., Fluteau, F., Guillocheau, F., 2005. Paleoenvironment reconstructions and climate simulations of the Early Triassic: impact of the water and sediment supply on the preservation of fluvial systems. Geodin. Acta 18 (6), 431–446.
Pickerill, R.K., Peel, J.S., 1991. *Gordia nodosa* isp. nov. and other traces from the Cass Fjord Formation (Cambrian) of North Greenland. Rapp. Grønl. Geol. Unders. 150, 15–28.
Pomar-Gomà, L., 1979. The Triassic of the Balearic Islands. Geology Department, Palma de Mallorca University, Palma (49 pp. + 7 Petrologic Logs).
Porada, H., Bouougri, E.H., 2007. Wrinkle structures—a critical review. Earth Sci. Rev. 81 (3–4), 199–215.
Postma, G., 1990. Depositional architecture and facies of river and fan deltas: a synthesis. Spec. Publ. Int. Assoc. Sedimentol. 10, 13–27.
Ptaszyński, T., 2000. Lower Triassic vertebrate footprints from Wióry, Holy Cross Mountains, Poland. Acta Palaeontol. Pol. 45 (2), 151–194.
Ramos, A., 1979. Estratigrafía y paleogeografía del Pérmico y Triásico al Oeste de Molina de Aragón (prov. de Guadalajara). Seminarios de Estratigrafía, 6. Universidad Complutense de Madrid & Consejo Superior de Investigaciones Científicas, Madrid (313 pp.).
Ramos, A., 1995. Transition from alluvial to coastal deposits (Permian–Triassic) on the Island of Mallorca, western Mediterranean. Geol. Mag. 132 (4), 435–447.
Ramos, E., Rodríguez-Perea, A., 1985. Découverte d'un affleurement de terrains paléozoïques dans l'île de Majorque (Baléares, Espagne). Comp. Rend. Acad. Sci. Paris, 2nd series 16 (301), 1205–1207.
Ramos, A., del Olmo, P., Alvaro, M., 1985. El Buntsandstein de la isla de Mallorca. In: Mateu Ibars, F., Marzo, M. (Eds.), Resúmenes del II Coloquio de Estratigrafía y Paleogeografía del Pérmico y Triásico de España. Institut d'Estudis Ilerdencs, Grupo Español del Mesozoico, La Seu d'Urgell, pp. 103–104.
Ratcliffe, B.C., Fagerstrom, J.A., 1980. Invertebrate lebensspuren of Holocene floodplains: their morphology, origin and paleoecological significance. J. Paleontol. 54 (3), 614–630.
Raymond, P.E., 1946. The genera of fossil Conchostraca – an order of bivalved crustaceans. Bull. Museum Comp. Zool. 96, 217–370.
Reolid, J., Cardenal, F.J., Reolid, M., Mata, E., 2020. 3D imaging of the southernmost Triassic footprints from Europe (southern Spain). J. Iber. Geol. 46, 145–161.
Retallack, G.J., Veevers, J.J., Morante, R., 1996. Global coal gap between Permian–Triassic extinction and Middle Triassic recovery of peat-forming plants. Bull. Geol. Soc. Am. 108, 195–207.
Rieppel, O., 2019. Mesozoic Sea Dragons: Triassic Marine Life From the Ancient Tropical Lagoon of Monte San Giorgio. Indiana University Press, Indiana (256 pp.).
Robles, S., Llompart, C., 1987. Análisis paleogeográfico y consideraciones paleoicnológicas del Pérmico superior y Triásico Inferior en la transversal del río Segre (Alt Urgell, pirineo de Lérida). Cuadernos Geol. Ibérica 11, 115–130.
Roca, E., 1992. L'estructura de la conca Catalano-Balear: paper de la compressió i de la distensió en la seva gènesi. Ph.D. dissertation. Universitat de Barcelona, Barcelona (564 pp. [Volume 1: 1–330; Volume 2: 206 figs. + 5 seismic profiles]).
Rodríguez-Perea, A., Ramos, E., 1984. Presencia de Paleozoico en la Sierra de Tramuntana (Mallorca). Boll. Soc. Hist. Nat. Balears 28, 145–148.
Rodríguez-Perea, A., Ramos-Guerrero, E., Pomar, L., Paniello, X., Obrador, A., Martí, J., 1987. El Triásico de las Baleares. Cuadernos Geol Ibérica 11, 295–321.
Romano, M., Bernardi, M., Petti, F.M., Rubidge, B., Hancox, J., Benton, M.J., 2020. Early Triassic terrestrial tetrapod fauna: a review. Earth Sci. Rev. 210, 103331.
Rowntree, K.M., Dollar, E.S.J., 1999. Vegetation controls on channel stability in the Bell River, Eastern Cape, South Africa. Earth Surf. Process. Landf. 24, 127–134.
Rüffer, T., Zühlke, R., 1994. Sequence stratigraphy and sea-level changes in the Early to Middle Triassic of the Alps: a global comparison. In: Haq, B.U. (Ed.), Sequence Stratigraphy and Depositional Response to Eustatic, Tectonic and Climatic Forcing. Springer, pp. 161–207.
Sàbat, F., Gelabert, B., Rodríguez-Perea, A., 2018. Minorca, an exotic Balearic island (western Mediterranean). Geol. Acta 16 (4), 411–426.
Scholze, F., Matamales-Andreu, R., 2021. Triassic clam shrimps ("Conchostraca"; Branchiopoda: Diplostraca) from Mallorca: taxonomic description and interregional comparisons. Zootaxa 4964 (3), 471–496.
Scholze, F., Schneider, J.W., 2015. Improved methodology of 'conchostracan' (Crustacea: Branchiopoda) classification for biostratigraphy. Newsl. Stratigr. 48, 287–298.
Scotese, C.R., 2014. Atlas of Middle & Late Permian and Triassic Paleogeographic Maps, Maps 43–48 From Volume 3 of the PALEOMAP Atlas for ArcGIS (Jurassic and Triassic) and Maps 49–52 From Volume 4 of the PALEOMAP Atlas for ArcGIS (Late Paleozoic), Mollweide Projection, PALEOMAP Project, Evanston, IL.

Scotese, C.R., Schettino, A., 2017. Late Permian-Early Jurassic paleogeography of western Tethys and the world. In: Soto, J.I., Flinch, J.F., Tari, G. (Eds.), Permo-Triassic Salt Provinces of Europe, North Africa and the Atlantic Margins. Tectonics and Hydrocarbon Potential. Elsevier, Amsterdam, Oxford, Cambridge, pp. 57–95.
Sevillano, A., Barnolas, A., 2019. Mapa Geológico Digital Continuo E. 1:50.000, Zona Mallorca (Zona-2210). In: GEODE. Mapa Geológico Digital continuo de España. Available online at: http://info.igme.es/visorweb/ (last accessed on 26/07/2019).
Shanley, K.W., McCabe, P.J., Hettinger, R.D., 1992. Tidal influence in Cretaceous fluvial strata from Utah, USA: a key to sequence stratigraphic interpretation. Sedimentology 39, 905–930.
Shcherbakov, D.E., Lukashevich, E.D., Blagoderov, V.A., 1995. Triassic Diptera and initial radiation of the order. J. Dipterol. Res. 6 (2), 75–115.
Shiers, M.N., Mountney, N.P., Hodgson, D.M., Colombera, L., 2018. Controls on the depositional architecture of fluvial point-bar elements in a coastal-plain succesion. Int. Assoc. Sedimentol. Spec. Publ. 48, 15–46.
Sinitshenkova, N.D., 2000. A review of Triassic mayflies, with the description of new species from Western Siberia and Ukraine (Ephemerida = Ephemeroptera). Paleontol. J. 34 (3), S275–S283.
Sinitshenkova, N.D., 2002. New Late Mesozoic mayflies from the Shar-Teeg Locality, Mongolia (Insecta, Ephemerida=Ephemeroptera). Paleontol. J. 36 (3), 270–276.
Sinitshenkova, N.D., Marchal-Papier, F., Grauvogel-Stamm, L., Gall, J.-C., 2005. The Ephemeridea (Insecta) from the Grès à Voltzia (early Middle Triassic) of the Vosges (NE France). Paläontol. Z. 79 (3), 377–397.
Smith, J.J., Hasiotis, S.T., Kraus, M.J., Woody, D.T., 2008. *Naktodemasis bowni*: new ichnogenus and ichnospecies for adhesive meniscate burrows (AMB), and paleoenvironmental implications, Paleogene Willwood Formation, Bighorn Basin, Wyoming. J. Paleontol. 82 (2), 267–278.
Sookias, R.B., Butler, R.J., 2013. Euparkeriidae. Geol. Soc. Lond., Spec. Publ. 379, 35–48.
Soria, A.R., Liesa, C.L., Rodríguez-López, J.P., Meléndez, N., de Boer, P.L., Meléndez, A., 2011. An Early Triassic evolving erg system (Iberian Chain, NE Spain): palaeoclimate implications. Terra Nova 23, 76–84.
Stampfli, G.M., Hochard, C., 2009. Plate tectonics of the Alpine realm. Geol. Soc. Lond., Spec. Publ. 327, 89–111.
Stanley, K.O., Fagerstrom, J.A., 1974. Miocene invertebrate trace fossils from a braided river environment, western Nebraska, U.S.A. Palaeogeogr. Palaeoclimatol. Palaeoecol. 15 (1), 63–82.
Sun, Y., Joachimski, M.M., Wignall, P.B., Yan, C., Chen, Y., Jiang, H., Wang, L., Lai, X., 2012. Lethally hot temperatures during the Early Triassic greenhouse. Science 338 (6105), 366–370.
Tabor, N.J., Poulsen, C.J., 2008. Palaeoclimate across the Late Pennsylvanian–Early Permian tropical palaeolatitudes: a review of climate indicators, their distribution, and relation to palaeophysiographic climate factors. Palaeogeogr. Palaeoclimatol. Palaeoecol. 268, 293–310.
Trotter, J.A., Williams, I.S., Nicora, A., Mazza, M., Rigo, M., 2015. Long-term cycles of Triassic climate change: a new $\delta^{18}O$ record from conodont apatite. Earth Planet. Sci. Lett. 415, 165–174.
Uchman, A., Kazakauskas, V., Gaigalas, A., 2009. Trace fossils from Late Pleistocene varved lacustrine sediments in eastern Lithuania. Palaeogeogr. Palaeoclimatol. Palaeoecol. 272, 199–211.
Ulmer, G., 1920. Übersicht über die Gattungen der Ephemeropteren, nebst Bemerkungen über einzelne Arten. Stettiner Entomologische Zeitung 81 (1–2), 97–144.
Van Konijnenburg-van Cittert, J.H.A., Kustatscher, E., Wachtler, M., 2006. Middle Triassic (Anisian) ferns from Kühwiesenkopf (Monte Prá Della Vacca), Dolomites, Northern Italy. Palaeontology 49 (5), 943–968.
Vera, J.-A., Alonso-Chaves, F.M., Andreo, B., Arias, C., Azañón, J.M., Balanyá, J.C., Barón, A., Booth-Rea, G., Castro, J.M., Chacón, B., Company, M., Crespo-Blanc, A., Delgado, F., Díaz de Federico, A., Esteras, M., Estévez, A., Fernández, J., Fornós, J.J., Galindo-Zaldívar, J., García-Casco, A., García-Dueñas, V., García-Hernández, M., Garrido, C.J., de Gea, G.A., Gelabert, B., Gervilla, F., González-Lodeiro, F., Jabaloy, A., López-Garrido, A.C., Luján, M., Martín-Algarra, A., Martín-Chivelet, J., Martín-Martín, M., Molina, J.M., Morata, D., Nieto, J.M., Obrador, A., O'Dogherty, L., Orozco, M., Pérez-López, A., Pomar, L., Puga, E., Ramos, E., Rey, J., Rivas, P., Rodríguez-Cañero, R., Ruiz-Cruz, M.D., Ruiz-Ortiz, P.A., Sàbat, F., Sánchez-Gómez, M., Sánchez-Navas, A., Sandoval, J., Sanz de Galdeano, C., Soto, J. I., Torres-Roldán, R.L., Villas, L., 2004. Cordillera Bética y Baleares. In: Vera, J.-A. (Ed.), Geología de España. Instituto Geológico y Minero de España, Madrid, pp. 346–464.
Vila, B., Oms, O., Fondevilla, V., Gaete, R., Galobart, À., Riera, V., Canudo, J.I., 2013. The latest succession of dinosaur tracksites in Europe: hadrosaur ichnology, track production and palaeoenvironments. PLoS One 8 (9), e72579.
Williams, P.F., Rust, B.R., 1969. The sedimentology of a braided river. J. Sediment. Petrol. 39 (2), 649–670.
Xing, L., Klein, H., 2021. *Chirotherium* and first Asian *Rhynchosauroides* tetrapod trackways from the Middle Triassic of Yunnan, China. Hist. Biol. 33 (6), 791–801.
Zeng, Z., Zhu, H., Yang, X., Zeng, H., Hu, X., Xia, C., 2019. The Pangaea megamonsoon records: evidence from the Triassic Mungaroo Formation, northwest shelf of Australia. Gondwana Res. 69, 1–24.
Zessin, W., 2008a. Einige neue Insekten aus der Unteren Trias (Buntsandstein) von Mallorca, Spanien (Blattaria, Coleoptera, Diptera, Heteroptera und Megaloptera). Deutschen Gesellschaft für allgemeine und angewandte Entomologie – Nachrichten 22 (1), 20–21.
Zessin, W., 2008b. Neue Insekten aus der Unteren Trias (Buntsadstein) von Mallorca, Spanien (Blattaria, Coleoptera, Diptera, Heteroptera, Orthopteroidea und Homoptera). Virgo, Mitteilungsblatt des Entomologischen Vereins Mecklenburg 11 (1), 99–101.
Żyła, D., Wegierek, P., Krzysztof, O., Niedźwiedzki, G., 2013. Insects and crustaceans from the latest Early–early Middle Triassic of Poland. Palaeogeogr. Palaeoclimatol. Palaeoecol. 371, 136–144.

Chapter 4

The marine Middle–Late Triassic of Mallorca

Henry S. Sharpe

© Henry S. Sharpe

Chapter 4 was published as:

Matamales-Andreu, R.; Oms, O.; Galobart, À. & Fortuny, J. (2021). Middle–Upper Triassic marine vertebrates of Mallorca (Balearic Islands, western Mediterranean). *Historical Biology*, 33(10): 2520–2533.

DOI: https://doi.org/10.1080/08912963.2020.1810682

In this work, R. Matamales-Andreu contributed in:

A. Literature review of the Triassic of Mallorca in *Muschelkalk* and *Keuper* facies.
B. Direct examination of all the collections containing vertebrate fossils from the studied rock units.
C. Logging of all the local stratigraphic sections.
D. Stratigraphic and sedimentological analysis of the logs.
E. Vertebrate palaeontology, including identification and description of all the bone remains.
F. Interpretation and discussion of the results.
G. Writing of the original draft.
H. Preparation of all the figures (1–6).
I. Collaboration in obtaining funding for fossil preparation.

Also, refer to:

Appendix 11: Juárez-Ruiz & Matamales-Andreu (2021), *Ciências da Terra Procedia*, molluscs *Muschelkalk*

HISTORICAL BIOLOGY
2021, VOL. 33, NO. 10, 2520–2533
https://doi.org/10.1080/08912963.2020.1810682

Taylor & Francis
Taylor & Francis Group

ARTICLE

Check for updates

Middle–Upper Triassic marine vertebrates of Mallorca (Balearic Islands, western Mediterranean)

Rafel Matamales-Andreu [a,b], Oriol Oms [c], Àngel Galobart [a,d] and Josep Fortuny [a]

[a]Institut Català de Paleontologia Miquel Crusafont, Catalunya, Spain; [b]Museu Balear de Ciències Naturals, Illes Balears, Spain; [c]Departament de Geologia, Universitat Autònoma de Barcelona, Catalunya, Spain; [d]Museu de la Conca Dellà, Catalunya, Spain

ABSTRACT

During the Triassic, many groups of predatory marine reptiles appeared and diversified. On Mallorca, fossils of marine reptiles have been found in *Muschelkalk* (Anisian–Ladinian) and *Keuper* (Carnian–Norian) facies. Here we describe an anterior caudal vertebra of a basal ichthyosauriform similar to Grippidia (Reptilia: Ichthyosauriformes) from the Ladinian carbonate ramps of the *Muschelkalk* of Mallorca, which fills a biogeographic gap for the group, hitherto only known from the eastern and western margins of Panthalassa. The most plausible hypothesis to explain the fact that the Mallorcan specimen is younger than all the other related species described so far is supported by a rather isolated condition of the carbonate ramps surrounding eastern Iberia during the Anisian, which might point to a relict character of the Mallorcan species, representing the youngest record of basal ichthyosauriforms to date. Moreover, an epiphysis of an indeterminate reptile and four vertebrae assigned to *Nothosaurus* sp. (Reptilia: Eosauropterygia) from the *Keuper* sabkhat provide a new record of the latter genus on Mallorca, which falls within its known distribution area. Therefore, the present work provides an exhaustive review of all the marine vertebrate fossils found so far in the Middle–Upper Triassic of Mallorca, some of them with remarkable palaeobiogeographical implications.

ARTICLE HISTORY
Received 15 July 2020
Accepted 12 August 2020

KEYWORDS
Muschelkalk; *Keuper*; Balearic Islands; Eosauropterygia; Ichthyosauriformes

Introduction

During the Middle–Late Triassic, the Iberian area was located in subtropical palaeolatitudes under warm and arid climates (López-Gómez et al. 2017; Ortí et al. 2017). From the middle–late Anisian, a generalised but slightly diachronous marine transgression affected the eastern margin of the Iberian Massif, including what are now the Balearic Islands, drowning the fluvial, continental red-beds of *Buntsandstein* facies (Escudero-Mozo et al. 2015; López-Gómez et al. 2019). The record of extensive carbonate ramps, usually of a very coastal character, is what defines the *Muschelkalk* facies, which were well-developed from the Anisian to the Ladinian (López-Gómez et al. 2019), stretching in some cases into the Carnian in the most distal areas, such as Menorca (Escudero-Mozo et al. 2014). A subsequent regressive event, also slightly diachronous (early–middle Carnian) ended up in the formation of a system of coastal lagoons and sabkhat where great amounts of evaporitic rocks were locally deposited (Ortí et al. 2017; López-Gómez et al. 2019). These are known as *Keuper* facies, and generally span from the Carnian to the Norian (López-Gómez et al. 2017, 2019; Ortí et al. 2017).

During the Triassic, many groups of marine reptiles appeared and experienced important events of radiation. The sauropterygians, which are first recorded in the latest Early Triassic (*e.g.*, Rieppel 2000a; Li and Liu 2020), achieved great morphological disparity during the Middle and Upper Triassic, from heavily armoured, durophagous placodonts to piscivorous swift swimmers such as nothosaurs and pachypleurosaurs (Rieppel 2000a; Stubbs and Benton 2016). The ichthyosauromorphs probably originated in the warm seas of present-day south China (Motani et al. 2015), and acquired progressively more streamlined bodies, becoming widespread worldwide by the Middle Triassic (Sander 2000; McGowan and Motani 2003; Maisch 2010; Rieppel 2019).

Numerous reports of Triassic marine reptiles from the Iberian Peninsula have been published over the years (Fortuny et al. 2011; de Miguel Chaves et al. 2015, 2018a, 2018b, 2020 and references therein). Eosauropterygian remains have been collected in several localities, recognising the genera *Nothosaurus* Münster, 1834, *Hispaniasaurus* Márquez-Aliaga et al., 2019, *Lariosaurus* Curioni, 1847 (and its probable synonym, *Ceresiosaurus* Peyer, 1931b), *Simosaurus* Meyer, 1842, *Paludidraco* de Miguel Chaves et al., 2018a and indeterminate nothosaurs, pachypleurosaurs and pistosauroids (reviews in Fortuny et al. 2011; de Miguel Chaves et al. 2015; Berrocal-Casero et al. 2018). Placodonts have also been represented in many sites by the genera *Paraplacodus* Peyer, 1931a, *Psephosauriscus* Rieppel, 2002, *Parahenodus* de Miguel Chaves et al. 2018b and indeterminate cyamodontoids and placochelyids (reviews in de Miguel Chaves et al., 2018b, 2020). Ichthyosaurs have only been reported from two localities: Collbató, with a tooth and a vertebra that were attributed to an omphalosaurid (Fortuny et al. 2011), and La Manzanera, with two isolated partial vertebral centra of unknown affinities (de Miguel Chaves et al. 2015). Thalattosaurs have been reported from Mont-ral–Alcover based on a caudal vertebrae string (Rieppel and Hagdorn 1998).

On the Balearic Islands, however, the record of marine Middle–Upper Triassic vertebrate body fossils is very scarce. Only two remains had been found so far: Bauzá (1955, 1971) reported a vertebra, herein revised, that he thought to belong to the sauropterygian genus *Nothosaurus*. The fossil was found in the beds with *Entolium discites* (Schlotheim, 1820) of the locality of Puig d'en Canals (Sóller, Mallorca), in *Muschelkalk* facies (Bauzá 1955).

CONTACT Rafel Matamales-Andreu rafel.matamales@icp.cat Institut Català de Paleontologia Miquel Crusafont. Carrer de les Columnes s/n, Edifici Z (ICTA-ICP), Campus de la Universitat Autònoma de Barcelona, Catalunya, Spain

© 2020 Informa UK Limited, trading as Taylor & Francis Group

Published online 13 Sep 2020

Later, however, Colom (1982) assigned that outcrop to *Keuper* facies and, in the same work, Colom (1982) also illustrated for the first time a fragment of epiphysis, which had already been mentioned in Colom (1975, p. 51), collected from the *Keuper* gypsiferous beds of Can Bleda (Sóller, Mallorca), which is also considered herein. The only other report of Mesozoic reptile fossils from the Balearic Islands is the 'reptile jaw', nowadays lost, reported by Manera (1930) from an undetermined 'Triassic' of Menorca (which at that time also included the Permian red-beds present on the island).

The aim of the present work is to revise the re-prepared Middle–Late Triassic tetrapod fossils from Mallorca already reported by Bauzá (1955, 1971) and Colom (1975, 1982), together with previously unpublished specimens. By inferring the age and palaeoenvironment of each specimen, this work offers an updated account on the taxa that roamed the shores and shallow seas of Mallorca during the Middle–Late Triassic, based on all the vertebrate fossils found so far.

Institutional acronyms and anatomical abbreviations

IPS: Institut Català de Paleontologia Miquel Crusafont (formerly Institut de Paleontologia de Sabadell), Sabadell, Barcelona, Catalunya, Spain; **MBCN**: Museu Balear de Ciències Naturals, Sóller, Mallorca, Illes Balears, Spain.

asl: anterospinal lamina; **azg**: prezygapophysis; **cr**: cortical rim; **haf**: haemal arch facet; **hk**: haemal keel; **nc**: neural canal; **ncc**: notochordal canal; **ncs**: neurocentral suture; **ns**: neural spine; **pd**: neural arch pedicel; **psf**: postspinal fossa; **psl**: posterospinal lamina; **pzg**: postzygapophysis; **tp**: transverse process; **zgp**: zygosphene; **zgt**: zygantrum.

Geographical and geological context

Mallorca is the largest island of the Balearic Archipelago (western Mediterranean) and is structured in two main ranges uplifted during the Alpine orogeny. The Serra de Tramuntana, at the NW, is built up of materials ranging from the Carboniferous to the lower Miocene, whereas the Serres de Llevant, at the SE, contain rocks from the Upper Triassic to the lower Miocene. The margins of the mountain ranges, as well as part of the central area, were filled with sediments from the upper Miocene to the Quaternary (Vera et al. 2004). The Triassic rocks have traditionally been divided into the three Germanic facies: *Buntsandstein* continental red-beds, *Muschelkalk* carbonate marine ramps and *Keuper* variegated lagoonar claystones. The last two, of interest to this work, are mostly found in the Serra de Tramuntana, although some *Keuper* outcrops marginally appear on the rest of the island (Barnolas 1991).

The Muschelkalk *facies of Mallorca*

The *Muschelkalk* facies have only been reported in the Serra de Tramuntana, with a minimum thickness of 253 m in the most complete series measured so far: Punta de son Serralta–Sa Talaia (Pomar-Gomà 1979; Rodríguez-Perea et al. 1987; Barnolas 1991; Figure 1(a)). It has been divided into three main units, named M-1 (about 85–100 m-thick), M-2 (18 m-thick) and M-3 (about 150 m-thick) (Rodríguez-Perea et al. 1987):

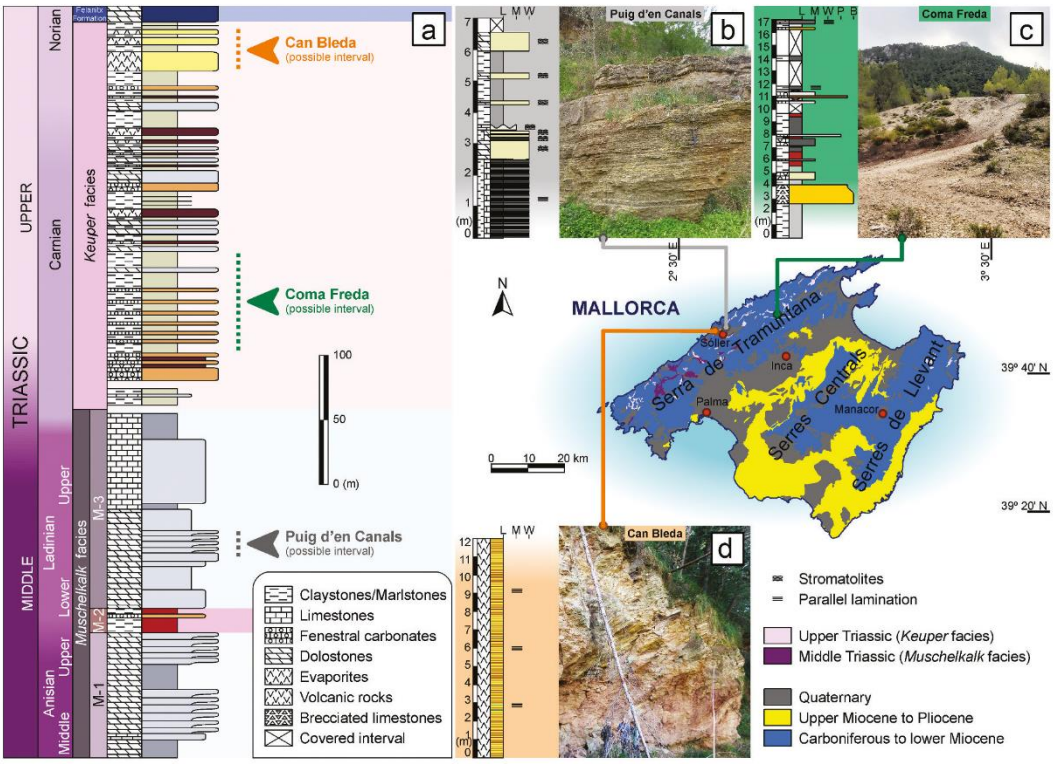

Figure 1. (a) Synthetic stratigraphic log of the *Muschelkalk* and *Keuper* facies of Mallorca, modified from Rodríguez-Perea et al. (1987), with indication of the inferred position of the fossiliferous localities. (b) Stratigraphic log and photography of Puig d'en Canals. (c) Stratigraphic log and photography of Coma Freda. (d) Stratigraphic log and photography of Can Bleda. L: Claystones/marlstones, M: Mudstones, W: Wackestones, P: Packstones, B: Brecciated limestones.

- The M-1 represents a shallow carbonate ramp, transitional from the underlying continental red-beds of *Buntsandstein* facies dated as lower Anisian by means of palynomorphs collected just 12 m below the boundary (Calafat 1988; Diez et al. 2010). The age attribution of the M-1 is uncertain, but it probably comprises part of the middle and upper Anisian and perhaps even the lowermost Ladinian.
- The M-2 represents a brief, regressive event in which detrital sediments, mainly red claystones and gypsum, were deposited (Colom 1975; Rodríguez-Perea et al. 1987). Its lower boundary is transitional, and its age is also uncertain, although it probably spans part of the upper Anisian or the lowermost Ladinian. This unit appears to be missing in most of the sections (Colom 1975).
- The M-3 represents the settlement of a second carbonate ramp, slightly deeper than the previous M-1, but still with a marked coastal character (Rodríguez-Perea et al. 1987). Its lower boundary is sharp, and it spans, at least, from the lower Ladinian (Curionii Zone) to the upper Ladinian (Hispanicum Zone), dated by means of ammonoids (see below).

The only fossils reported in the M-1 have been stromatolites and disarticulated crinoids (Darder 1914; Rodríguez-Perea et al. 1987; Calafat 1988). No fossils have been reported from the M-2 so far. The M-3 possesses the most abundant fossil record of the three units, although most of them were reported without stratigraphic control. Darder (1914), Fallot (1922), Schmidt (1936), Bauzá (1945, 1946, 1971, 1981), Rotger (1952), Virgili (1952), Goy (1995), Pérez-Valera (2005), Rein (2008), Pérez-Valera and Goy (2012), Pérez-Valera et al. (2016) and Juárez-Ruiz and Matamales-Andreu (2020a, 2020b) reported very rich assemblages containing stromatolites, land plants, brachiopods, bivalves, gastropods, nautiloids, ammonoids and ophiuroids. The ammonoid *Gevanites virgiliae* Goy, 1986 allowed to recognise the lower Ladinian (Awadi Subzone, Curionii Zone) (Pérez-Valera 2005; Pérez-Valera et al. 2016), whereas the ammonoid *Protrachyceras hispanicum* (Mojsisovics, 1881) allowed to recognise the upper Ladinian (Hispanicum Subzone, Hispanicum Zone) (Juárez-Ruiz and Matamales-Andreu 2020a, 2020b).

The Keuper facies of Mallorca

The *Keuper* facies have been extensively reported from the Serra de Tramuntana, although they also crop out in the Serres de Llevant and in the Serres Centrals (Bourrouilh 1973; Colom 1975; Rodríguez-Perea et al. 1987; Barnolas, 1991). The minimum thickness of the whole unit in the Serra de Tramuntana amounts to about 300 m (Rodríguez-Perea et al. 1987; Figure 1(a)). It mostly records sabkha palaeoenvironments (in the sense of Briere 2000), constituted by variegated claystones and marlstones with intercalations of dolostones and cargneules (fenestral carbonates, in this case also dolostones). Limestones are very rare, appearing only near the base and the top of the unit. Locally, thick packs of subaquatic and subaerial alkaline volcanic rocks are also interbedded (Navidad and Álvaro 1985; Enrique-Gisbert 1986; Enrique-Gisbert et al. 1987; Rodríguez-Perea et al. 1987; Barnolas 1991; Sanz et al. 2013; López-Gómez et al. 2017). Towards the top of the *Keuper* unit, there is an interval of variable thickness (0–100 m) of evaporitic rocks, mainly anhydrite and gypsum (Rodríguez-Perea et al. 1987). Based on lithostratigraphic correlation with Iberia, it has been suggested that the base of the *Keuper* facies is of Carnian age on Mallorca (López-Gómez et al. 2017). Its top probably is of upper Norian age based on the palynomorphs reported from the base of the overlying unit (Boutet et al. 1982), the Felanitx Formation, which stretches into the Hettangian (Barnolas-Cortinas 1984; Barnolas 1991).

Localities of provenance of the studied vertebrate fossils

Puig d'en Canals

The Puig d'en Canals is a hill of M-3 carbonates located in the town of Sóller (Mallorca) (Figure 1(b)). Bauzá (1955) claimed to have found MBCN155 in a marlstone bed with the bivalve *Entolium discites*. For the present study, an extensive field survey of the zone has been carried out, but no outcrop matching the one described by Bauzá has been found. During the twentieth century, there was a small cement quarry in one of the slopes of the hill, recently reconverted into tennis courts. In fact, the examination of aerial photographs from 1945/1946 has revealed that it was the only significant outcrop in the area. Bauzá might have been given the vertebra by the quarry workers, and thus nowadays the original locality is mostly inaccessible. Nevertheless, a small stratigraphic section has been logged at an old quarry front at the top of the hill in order to infer the recorded depositional palaeoenvironment of the area (Figure 1(b)). It represents an inner or mid-ramp palaeoenvironment with alternation of stromatolitic carbonates and marlstones. The Puig d'en Canals outcrop most probably belongs to the interval with abundance of stromatolites in the lower third of the M-3 as described by Rodríguez-Perea et al. (1987), and therefore it can be dated between the uppermost part of the lower Ladinian and the lower part of the upper Ladinian. No new fossils have been located.

Coma Freda

Coma Freda is a valley between the mountains of the Puig Caragoler and Sa Moleta (Mallorca) (Figure 1(c)). Three of the fossil vertebrae herein studied (IPS103319, IPS103320 and IPS103321) were fortuitously discovered by hikers in the early 1970s. They were collected *ex situ*, found scattered on the surface of a mountain trail. Some days later, IPS103318 was found in the same place, also *ex situ* (S. Moyà-Solà, pers. comm. to R.M.A. 2020). A limited stratigraphic section of 17 m of thickness (Figure 1(c)) has now been logged; it cannot be expanded because of the strong tectonic deformation that affects *Keuper* beds there. Nevertheless, it can be asserted that the dominant lithology of the outcrop are grey/blackish marlstones, with intercalations of red claystones, white/yellow/brownish fenestral carbonates and brecciated carbonates. Thus, the palaeoenvironment can be interpreted as periodically flooded mud-flats on a coastal setting. The typical *Keuper* facies of this outcrop, and the fact that the site is located in the base of a sequence of more than 200 m of thickness, allow to situate it in the lower–middle part of the *Keuper* unit, and thus relatively date it in the Carnian. No new fossils have been located.

Can Bleda

Can Bleda is a hill near the town of Sóller (Mallorca) (Figure 1(d)), with several abandoned quarries that were exploited until the XX century. In the only gypsum quarry, where Colom (1982)'s bone fragment (MBCN2513) probably came from, a sequence of about 15 m of evaporites alternating with variegated (red, blue, grey, black) claystones and marlstones is preserved in the quarry front (Figure 1(d)). The recorded environment corresponds to a sabkha. This outcrop belongs to the uppermost interval in the *Keuper* facies characterised by the abundance of evaporitic deposits, and thus can be tentatively dated as lower Norian. No new fossils have been located.

Systematic palaeontology

Tetrapoda Jaekel, 1909
Reptilia Laurenti, 1768
Reptilia indet.
Figure 2(a)–(f), 3(a)–(f)

Studied material

MBCN2513, a fragmentary epiphysis of a limb or girdle bone found by Colom (1982) in the *Keuper* facies of Can Bleda (Sóller, Mallorca), herein tentatively dated as lower Norian.

Description

Fragment of bone of 26.5 mm of maximum proximal–distal length, 36.5 mm of maximum dorsoventral width and 26.7 mm of maximum anteroposterior width. In proximal aspect, its outline is somewhat triangular, with a flat posterior side and a clearly convex anterior side with several elongated nutritive foramina on its surface. Towards the ventral part, the bone is expanded forming a thick lamina. The articular surface of the epiphysis is somewhat eroded, revealing the underlying trabecular bone. Towards the diaphysis, diameter of the bone decreases, reaching the broken surface on the distal side.

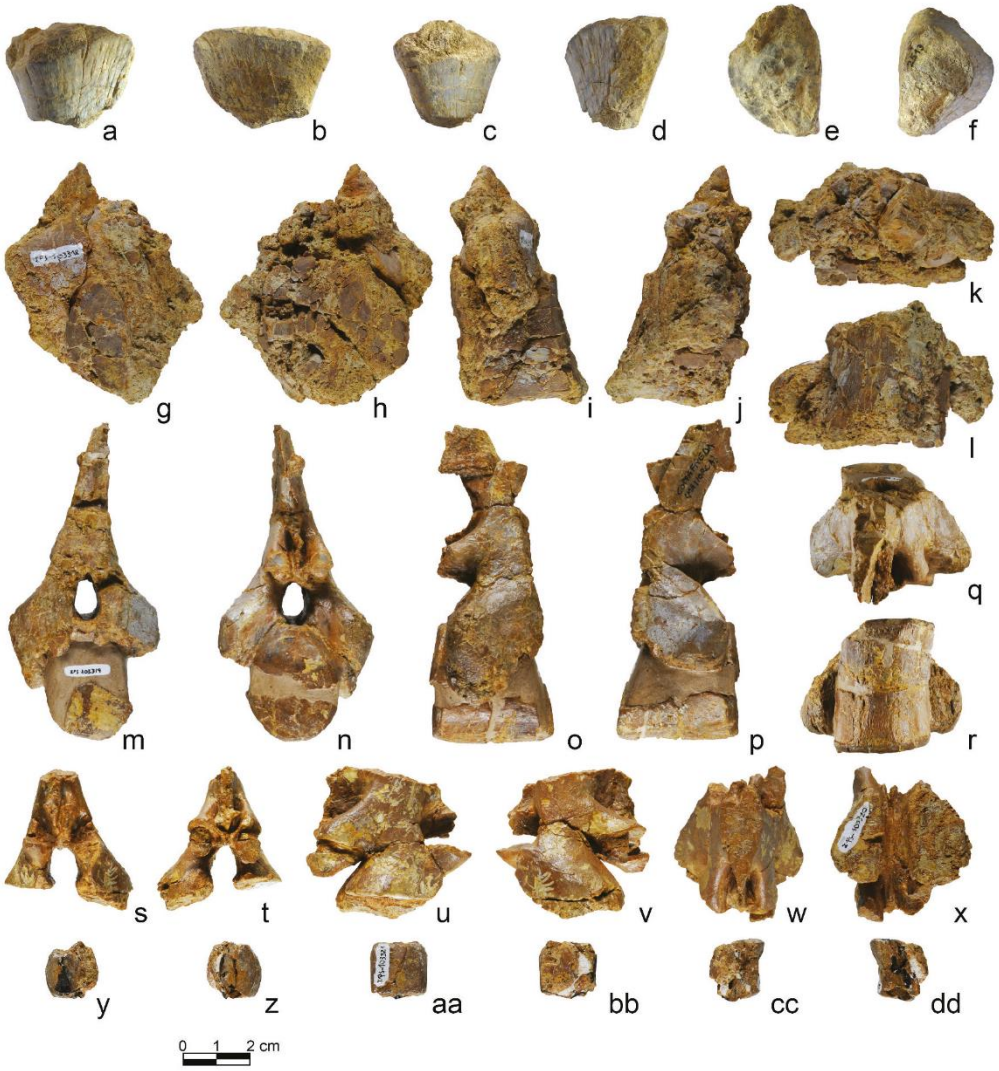

Figure 2. (a)–(f): Reptilia indet., MBCN2513, fragmentary epiphysis of a limb or girdle bone, Can Bleda, lower Norian. (a) anterior view (proximal up), (b) posterior view (proximal up), (c) dorsal view (proximal up), (d) ventral view (proximal up), (e) proximal view (dorsal up), (f) distal view (dorsal up). (g)–(dd): *Nothosaurus* sp., Coma Freda, Carnian. (g)–(l): IPS103318, partial pectoral vertebra. (g) anterior view, (h) posterior view, (i) right lateral view, (j) left lateral view, (k) dorsal view (anterior up), (l) ventral view (anterior up). (m)–(r): IPS103319, fairly complete pectoral vertebra. (m) anterior view, (n) posterior view, (o) right lateral view, (p) left lateral view, (q) dorsal view (anterior up), (r) ventral view (anterior up). (s)–(x): IPS103320, posterior cervical (?) neural arch. (s) anterior view, (t) posterior view, (u) right lateral view, (v) left lateral view, (w) dorsal view (anterior up), (x) ventral view (anterior up). (y)–(dd): IPS103321, posterior caudal centrum. (y) anterior view, (z) posterior view, (aa) right lateral view, (bb) left lateral view, (cc) dorsal view (anterior up), (dd) ventral view (anterior up).

Remarks

This specimen is poorly informative, and its fragmentary state precludes any confident determination. Its triangular section is comparable to right femoral proximal epiphyses of some Triassic marine reptiles such as sauropterygians (see Rieppel 1994, 2000a; Diedrich 2012; Krahl et al. 2013; de Miguel Chaves et al. 2017), thalattosaurs (see Müller 2005) and icthyosauriforms (see McGowan and Motani 2003; Maxwell et al. 2012; Massare and Lomax 2018), among others. Conversely, in coeval terrestrial reptiles, such as the case of archosauromorphs, humeri, femora and girdle elements are normally more laterally compressed and their epiphyses show higher complexity (*e.g.*, Nesbitt et al. 2013; Klein et al. 2017). Due to the palaeoenvironmental context, it is likely for this bone to belong to an eosauropterygian, but the lack of morphological diagnostic traits precludes any identification.

Diapsida Osborn, 1903
Sauropterygia Owen, 1860
Eosauropterygia Rieppel, 1994
Eusauropterygia Tschanz, 1989
Nothosauroidea Baur, 1889
Nothosauria Baur, 1889
Family Nothosauridae Baur, 1889
Genus *Nothosaurus* Münster, 1834
Nothosaurus sp.
Figure 2(g)–(dd), 3(g)–(dd)

Studied material

Four vertebral remains: IPS103318, a partial pectoral vertebra; IPS103319, a fairly complete pectoral vertebra; IPS103320,

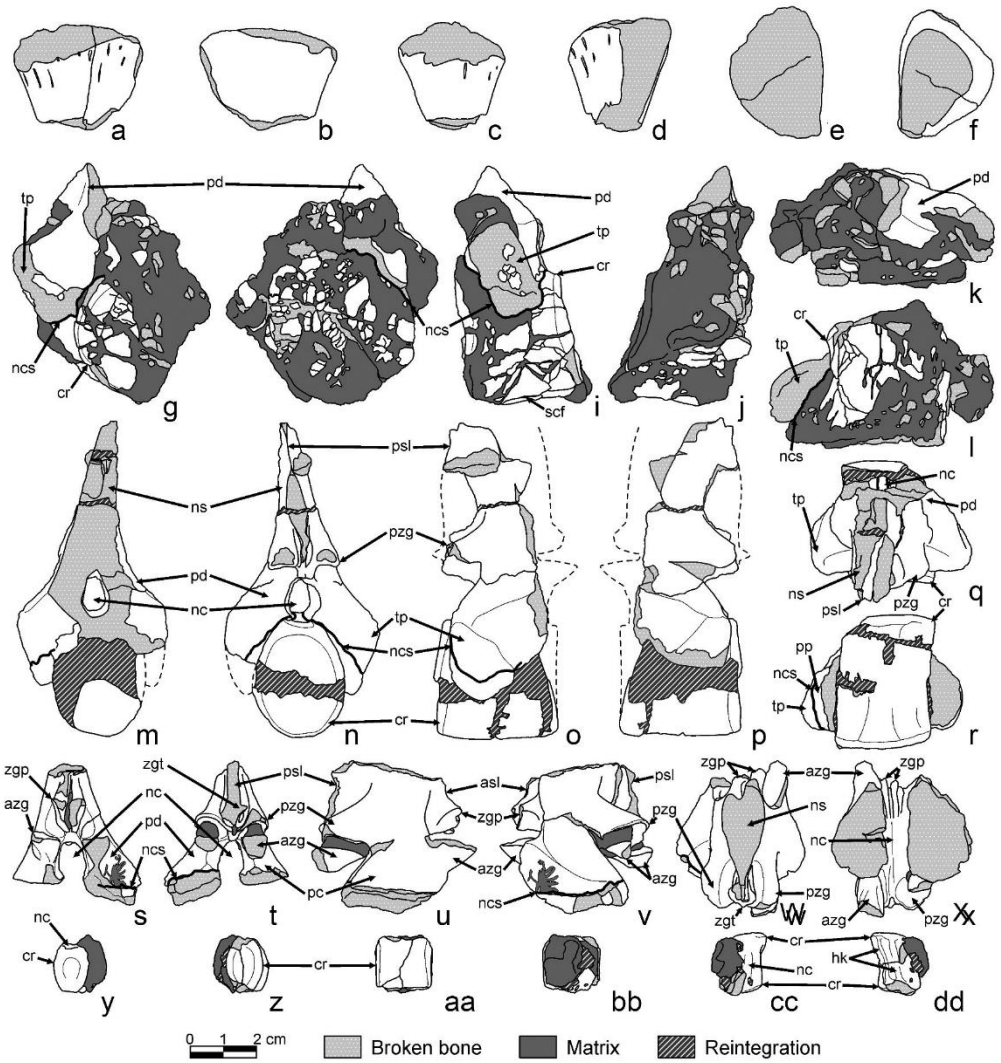

Figure 3. (a)–(f): Reptilia indet., MBCN2513, fragmentary epiphysis of a limb or girdle bone, Can Bleda, lower Norian, interpretative drawings. (a) anterior view (proximal up), (b) posterior view (proximal up), (c) dorsal view (proximal up), (d) ventral view (proximal up), (e) proximal view (dorsal up), (f) distal view (dorsal up). (g)–(dd): *Nothosaurus* sp., Coma Freda, Carnian, interpretative drawings. (g)–(l): IPS103318, partial pectoral vertebra. (g) anterior view, (h) posterior view, (i) right lateral view, (j) left lateral view, (k) dorsal view (anterior up), (l) ventral view (anterior up). (m)–(r): IPS103319, fairly complete pectoral vertebra. (m) anterior view, (n) posterior view, (o) right lateral view, (p) left lateral view, (q) dorsal view (anterior up), (r) ventral view (anterior up). (s)–(x): IPS103320, posterior cervical (?) neural arch. (s) anterior view, (t) posterior view, (u) right lateral view, (v) left lateral view, (w) dorsal view (anterior up), (x) ventral view (anterior up). (y)–(dd): IPS103321, posterior caudal centrum. (y) anterior view, (z) posterior view, (aa) right lateral view, (bb) left lateral view, (cc) dorsal view (anterior up), (dd) ventral view (anterior up).

a partial posterior cervical (?) neural arch with attached prezygapophyses of another vertebra; and IPS103321, a posterior caudal centrum. All of them were collected *ex situ* but very close to each other, so it is possible they belonged to only one animal. From the *Keuper* facies of Coma Freda (Escorca, Mallorca), herein tentatively dated as indeterminate Carnian.

Description

IPS103318, IPS103319, IPS103320, pectoral/posterior cervical (?) vertebrae: vertebrae of 94.91 mm of height, 46.92 mm of width and 36.06 mm of length (IPS103319). Laterally compressed, platycoelous centra of 34.82 mm of height, 26.77 mm of width and 36.06 mm of length (IPS103319). In anteroposterior view, their outline is oval, and their cortical rim is only slightly (IPS103318) or not flared at all (IPS103319). In the case of IPS103319, the transverse processes are attached to the dorsolateral edges of the centrum, protruding from both the centrum and the base of the neural arch, and are divided in two by the neurocentral suture. In ventral aspect, the centrum is not constricted and its surface appears to be smooth. The neural canal has a somewhat tear-shaped contour in anterior aspect (15.27 mm of height x 7.30 mm of width) and an oval contour in posterior aspect (12.41 mm of height x 9.00 mm of width), with a flat floor. The neurocentral suture is conspicuous in IPS103319, descending from the edges of the neural canal, straddling the centrum and dividing the transverse processes. The neural arch is tilted about 5° posteriorly. The pedicels extend from the bulky diapophyses and surround the lower half of the neural canal. In anterior aspect, IPS103320 shows that the prezygapophyses originate at about half the height of the neural canal, and are relatively narrow and strongly pointing anteriorly. Its articular surface is flat and slightly tilted inwards (15°). Just above the prezygapophyses, there are two shallow depressions, and above them there is a prominent zygosphene divided in two by a deep furrow. The articular surfaces of the zygosphene are strongly tilted outwards (68°). In posterior aspect, both IPS103319 and IPS103320 show that the postzygapophyses are located above the neural canal, being relatively narrow and strongly pointed posteriorly. In IPS103319, the articular surfaces of the postzygapophyses are almost flat and horizontal (6° inwards), whereas in IPS103320 they are concave and tilted outwards (35°). Just above the postzygapophyses there is a fossa divided in two by a thin posterospinal lamina. In its lower part, in IPS103320, the zygantrum articular surfaces can be observed, being strongly tilted outwards (39°). The neural spine is not well-preserved in any of the studied specimens, and it only can be said that it appears to get progressively thinner dorsally.

IPS103321, posterior caudal centrum: slightly amphicoelous centrum of 14.00 mm of height, 10.28 mm of width and 15.58 mm of length. In anteroposterior view, the centrum possesses a laterally compressed oval outline, the dorsal edge being slightly wider than the ventral. Two haemal keels traverse the centrum longitudinally in ventral aspect. In dorsal aspect, two other longitudinal ridges are also visible, corresponding to the facets for the bases of the neural arch pedicels and the borders of the most lateroventral edges of the neural canal.

Remarks

The platycoelous centra, the conspicuous neurocentral suture and the zygosphene-zygantrum articulation allow to attribute these vertebrae to the Eosauropterygia (Rieppel 1994, 2000a; Rieppel and Wild 1996). Their large size and the fact that they possess tall neural spines and do not present pachyostotic zygapophyses allow to dismiss pachypleurosaurs (Rieppel 2000a). Cymatosaurids have relatively short and anteroposteriorly broad neural spines (Storrs 1991; Sander et al. 2013), so they are also at odds with our material. The absence of peg-like structures under the neural arch pedicels (IPS103320) and the lack of subcentral foramina (IPS103318 and IPS103319) in the Mallorcan material makes it possible to exclude pistosaurids and similar forms as well (Sues 1987; Rieppel 1994, 2000a; Dalla Vecchia 2006; Sato et al. 2010). Simosaurid vertebrae have infraprezygapophyses and infrapostzygapophyses (Rieppel 1994, 2000a; de Miguel Chaves et al. 2018a), absent in our material. Finally, within nothosaurids (sensu de Miguel Chaves et al. 2018a), *Germanosaurus* Nopcsa, 1928 is known from cranial material only (Rieppel 2000a), and *Lariosaurus* vertebrae possess zygapophyseal pachyostosis (Rieppel 2000a), unlike the Mallorcan material. IPS103318–103321 possess strong affinities with some species of the genus *Nothosaurus*, including tall and slender neural spines, well-developed zygosphene-zygantrum articulation, non-pachyostotic zygapophyses, lack of infrazygapophyses, amphicoelous centrum and lack of subcentral foramina. Recent works have suggested that the genus *Nothosaurus* is probably paraphyletic (Klein et al. 2016; Lin et al. 2017; Li and Liu 2020), and therefore here we use this determination in broad sense, although this aspect is beyond the scope of the present study. Moreover, given the fragmentary nature of our material, no specific determination can be reached.

It is also important to note that these fossils show clear signs of having been reworked, since conspicuous bioerosion traces (*Maeandropolydora* Voigt, 1965) can be observed, especially on IPS103320. Given that that specimen preserves the prezygapophyses of another vertebra still in connection, it seems unlikely that the bioeroders settled on the freshly exposed bones on the seafloor a short time after the death of the animal. This is because if the bones had been exposed for a long time, currents or other animals would have eventually detached them. In fact, it is more plausible that bioerosion occurred once the remains had undergone part of the diagenetic process only to become exposed again. *Maeandropolydora* is only known from hard, massive substrates such as rocks, seashells and tusks (Bromley and D'Alessandro 1983; Domènech et al. 2008; Santos et al. 2008; Antonelli et al. 2019), but it has yet to be found, to our knowledge, in unaltered bone. Therefore, it is probable that the *Nothosaurus* vertebrae studied here are somewhat older than the deposit containing them, but it is impossible to settle this matter with the present data.

Ichthyosauromorpha Motani et al., 2015
Ichthyosauriformes Motani et al., 2015
? Grippidia Wiman, 1929
Ichthyosauriformes indet. aff. Grippidia
Figure 4(a)–(l)

Studied material

MBCN155, a mostly complete anterior caudal vertebra found by Bauzá (1955) in the *Muschelkalk* facies of Puig d'en Canals (Sóller, Mallorca), herein tentatively dated as uppermost part of the lower Ladinan–lower part of the upper Ladinian.

Description

Vertebra of 68.88 mm of height, 35.05 mm of maximum width, and 44.65 mm of length. Amphicoelous notochordal centrum of 30.50 mm of height and 35.05 mm of width in anteroposterior view. It possesses a sub-hexagonal outline with a dorsal edge that is wider than the ventral edge. The cortical rim is flared outwards laterally and ventrally, giving a constricted appearance to the centrum in lateral view. Its maximum length (lateral view) is 28.79 mm. In ventral aspect there are two haemal keels connecting the anterior and posterior cortical rims, and on one of them there seems to be

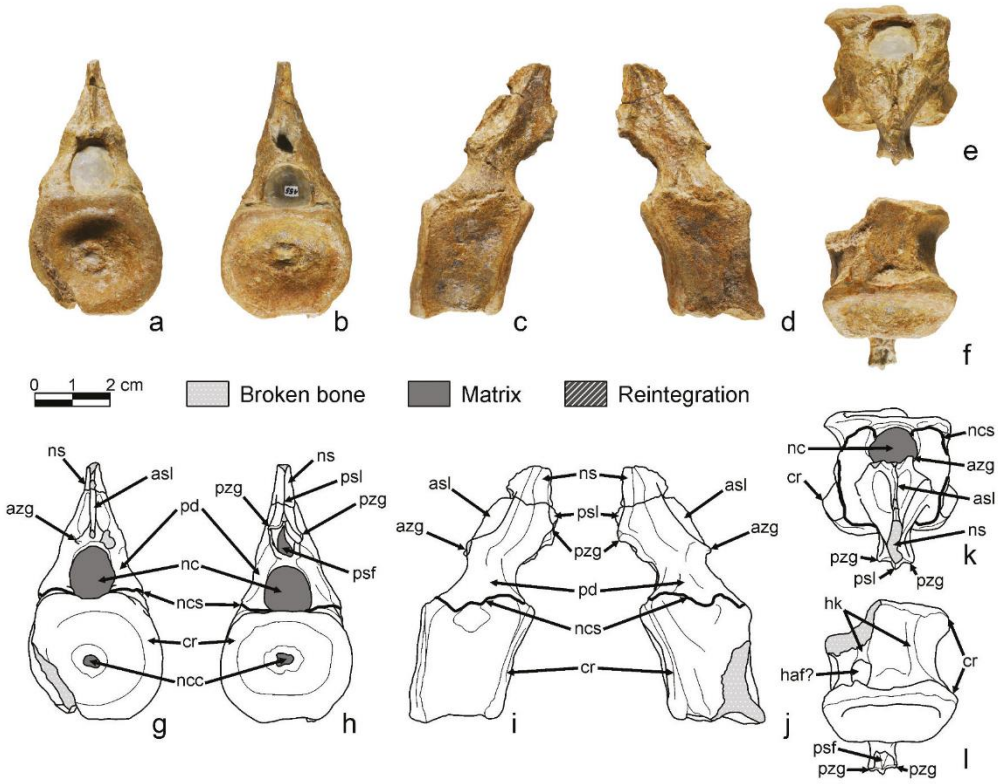

Figure 4. Ichthyosauriformes indet. aff. Grippidia, Puig d'en Canals, Ladinian. (a)–(f): MBCN155, anterior caudal vertebra. (a) anterior view, (b) posterior view, (c) right lateral view, (d) left lateral view, (e) dorsal view (anterior up), (f) ventral view (anterior up). (g)–(l): MBCN155, interpretative drawings. (g) anterior view, (h) posterior view, (i) right lateral view, (j) left lateral view, (k) dorsal view (anterior up), (l) ventral view (anterior up).

a facet for articulation of the haemal arch in posterior right position, although given its asymmetry it could also correspond to a pathology or to a teratology. The neural canal has an oval contour in anterior aspect (18.40 mm of height x 12.04 mm of width), and a sub-trapezoidal contour in posterior aspect (11.86 mm of height x 12.51 mm of width). The neurocentral suture is well visible and horizontally located just above the centrum. The neural arch stands above, tilted 25° posteriorly. Its pedicels are broad and somewhat swollen in their bases, and become thinner dorsally. In anterior aspect, just above the neural canal there is a pair of small, conical bulges, corresponding to atrophied paired prezygapophyses. Above them, the neural spine rises from another somewhat swollen base and gets progressively thinner until the tip, which is not preserved in MBCN155. The spine possesses a shallow depression divided in two by a thin anterospinal lamina, resulting in two elongated, tear-shaped fossae. In posterior aspect, above the neural canal, there is a deep, triangle-shaped postspinal fossa with two small protuberances on the lateral margins, corresponding to the atrophied paired postzygapophyses. In lateral aspect, the neural arch has a shallow groove from the posterior opening of the neural canal to the tip of the neural spine.

Remarks

Although this specimen was originally referred as a nothosaur (Bauzá 1955, 1971; Colom 1975, 1982), Sanz (1980, 1983) stated that, at face value, several anatomical characters were at odds with the typical nothosaurian vertebrae. Based on the examination of pictures of the specimen, he pointed out that the centrum was deeply excavated posteriorly, that the vertebra lacked the neurocentral suture and that the articulation of the haemal arch was anteroventrally located. Indeed, the centrum is clearly amphicoelous, whereas all coeval eosauropterygians have platycoelous or only slightly amphicoelous vertebral centra (Rieppel 2000a). However, the vertebra does possess a conspicuous neurocentral suture, and the chevron facets seem to actually be located posteroventrally. The former points to postcranial skeletal paedomorphosis, typical of some aquatic groups (Rieppel 2000a), and the latter is a very variable character even within a same individual depending on the position in the column, and therefore it bears little taxonomic value by itself. In any case, all eosauropterygians (including pistosaurs and derived clades) can be ruled out because of the following combination of characters: reduction of zygapophyses, lack of zygantrum-zygosphene articulation, posterior slanting of the neural arch pedicels, lack of rib articulation in this position in the column, and lack of any kind of subcentral/nutritive foramina on the ventral region of the centrum (Sues 1987; Rieppel 1994, 2000a; Rieppel and Wild 1996, 1996; Rieppel et al. 1999; Dalla Vecchia 2006; Sander et al. 2013).

Placodontian affinity of MBCN155 can be also dismissed because of the following reasons: (1) In most placodonts, the neurocentral suture is located on slightly elevated ridges protruding from the dorsal side of the centrum (Rieppel 2000a), although in *Paraplacodus* this suture is right on the centrum (Rieppel 2000b), much like in eosauropterygians and in MBCN155. (2) The neural arch pedicels are anteriorly directed in sauropterygians (see examples in Rieppel 2000a, 2000b; Diedrich 2010, 2013), whereas in

MBCN155 they are posteriorly slanted. (3) The zygapophyses are reduced to very small, conical bulges in MBCN155, whereas they retain their shape and function in sauropterygians (see examples in Rieppel 2000a, 2000b; Diedrich 2010, 2013). (4) MBCN155 lacks the hypantrum-hyposphene articulation, present in the placodontoids (Rieppel 2000a, 2000b). Saurosphargids also possess anteriorly slanted neural arch pedicels with well-developed zygapophyses in the caudal region (Li et al. 2013), so they can be ruled out as well.

Helveticosaurus Peyer, 1955 possesses caudal vertebrae with centra of similar proportions as MBCN155, but its neural arches are less tilted posteriorly and the zygapophyses are not reduced (Rieppel 2019). *Eusaurosphargis* Nosotti and Rieppel, 2003 differs from MBCN155 because of its caudal vertebrae with low, stocky neural arches (Nosotti and Rieppel 2003; Scheyer et al. 2017).

Thalattosaurs possess caudal vertebrae that are somewhat reminiscent in some aspects to MBCN155. However, within the askeptosauroids, the caudal vertebrae centra are always longer than they are high, and the zygapophyses remain prominent throughout (Liu and Rieppel 2005; Müller 2005; Müller et al. 2005; Rieppel et al. 2006; Wu et al. 2009; Zhao et al. 2010), contrarily to the vertebra herein studied. Some species of thalattosauroids are very incompletely known, but the best preserved specimens possess caudal vertebrae with centra that are slightly higher than they are long, similarly to MBCN155. Their zygapophyses, however, retain its shape over all the column, and their neural arches are very thin and straight (Rieppel 1987; Nicholls and Brinkman 1993b; Liu 2013; Liu et al. 2013; Maisch 2014; Li et al. 2016). The scarce vertebral material known from the purported thalattosaur *Blezingeria* Fraas, 1896 possesses pentagonal centra in anteroposterior view and well-developed zygapophyses (Fraas 1896; Diedrich 2015), contrary to MBCN155, although they certainly do correspond to different parts of the column.

Basal ichthyosauromorphs such as hupehsuchians present very broad neural spines segmented in two parts (Chen et al. 2014a, 2014b, 2014c, 2015; Wu et al. 2015), which are completely different from those of MBCN155. The slightly more derived nasorostrans (sensu Huang et al. 2019) possess very short and broad neural arches (Motani et al. 2015; Jiang et al. 2016).

Ichthyosauriform anterior caudal vertebrae are the ones that best match MBCN155. Centra with semi-hexagonal outline in anteroposterior view are typical of the caudal region of ichthyosauriforms, and reduction or even elimination of zygapophyses, especially towards the posterior region of the column, is also very characteristic of this group (McGowan and Motani 2003). The centrum of MBCN155 is almost as high as it is long (height/length ratio = 0.94), and thus points to basal forms from the Early–Middle Triassic. The species of the genus *Chaohusaurus* Young and Dong, 1972 have anterior caudal vertebrae centra with similar height/length proportions than those of MBCN155, and the neural arches also look quite alike but are more slanted posteriorly (see examples in Chen et al. 2013; Motani et al. 2014, 2018; Huang et al. 2019). The clade Grippidia Wiman, 1929 (sensu Huang et al. 2019) includes four genera: *Utatsusaurus* Shikama et al., 1978, *Grippia* Wiman, 1929, *Gulosaurus* Cuthbertson et al., 2013 and *Parvinatator* Nicholls and Brinkman, 1995, but the anterior caudal region is not well-preserved in any specimen (Shikama et al. 1978; Mazin 1981; Brinkman et al. 1992; Nicholls and Brinkman 1995; Cuthbertson et al. 2013). In any case, the height/length ratios of the centra of the posterior dorsal vertebrae in those genera are also remarkably similar to the one of MBCN155. Therefore, although a generic determination for MBCN155 is impossible with the present material, it shows strong morphological affinities with the genus *Chaohusaurus* and the clade Grippidia (sensu Huang et al. 2019).

The other genera of Triassic ichthyopterygians known so far belong to the Ichthyosauria De Blainville, 1835 (sensu Huang et al. 2019) and either possess anterior caudal vertebral centra with a more derived morphology, that is, significantly higher height/length proportions, laterally compressed centra and/or proportionally smaller neural arches than MBCN155 (Merriam 1908; Tichy 1995; Dal Sasso and Pinna 1996; Sander 1997, 2000; Lucas 2002; Maisch and Matzke 2002; Nicholls et al. 2002; McGowan and Motani 2003; Nicholls and Manabe 2004; Schmitz et al. 2004; Jiang et al. 2006b, 2008; Shang and Li 2009; Maisch 2010; Sander et al. 2011; Ji et al. 2013), or the anterior caudal vertebrae are not sufficiently well known (Mazin et al. 1991; McGowan 1995, 1996; Maisch and Matzke 1997, 1998, 2003; Motani 1999; Motani et al. 1999; Maisch 2000, 2010; McGowan and Motani 2003; Dalla Vecchia 2004) but are assumed to not vary greatly from their close relatives.

Discussion

Marine vertebrate fossils from the Middle–Upper Triassic of Mallorca, although scarce, provide additional clues on the palaeobiogeography of those taxa in the western Tethys. Sauropterygian remains are well known from the Triassic of the Iberian Peninsula, including the genus *Nothosaurus* (Sanz 1980, 1983; de Miguel Chaves et al. 2015, 2016, 2017), which occurs frequently in the *Muschelkalk* and *Keuper* of Europe, north Africa, Middle East and southern Asia (Assmann 1937; Sanz 1980, 1983; Rieppel and Wild 1996; Rieppel et al. 1997, 1999; Rieppel 2000a; Dalla Vecchia and Avanzini 2002; Li and Rieppel 2004; Shang 2006; Jiang et al. 2006a; Kear et al. 2010; Ősi et al. 2013; Ji et al. 2014; Liu et al. 2015; Klein et al. 2015; de Miguel Chaves et al. 2016). Therefore, finding it in coeval deposits of Mallorca is not surprising, as it falls within the already known distribution area for this genus (Figure 5).

On the other hand, the finding of a purported non-nasorostran basal ichthyosauriform (sensu Huang et al. 2019) such as MBCN155 is indeed more unanticipated. The genus *Chaohusaurus* currently includes four species and is restricted to the Spathian (upper Olenekian, Lower Triassic) of China (Sander 2000; Chen et al. 2013; Motani et al. 2014, 2018; Huang et al. 2019). Within Grippidia, *Utatsusaurus* has been found in the Spathian of Japan, the British Columbia and perhaps Nevada (Shikama et al. 1978; Nicholls and Brinkman 1993a; Motani et al. 1998; Cuthbertson et al. 2014; Kelley et al. 2016), *Grippia* has been reported from the Spathian of Spitsbergen (Mazin 1981), and *Gulosaurus* comes from the Spathian of the British Columbia (Cuthbertson et al. 2013). Finally, the age of *Parvinatator* from the British Columbia is contentious, ranging from the Olenekian (Lower Triassic) to the Ladinian (Middle Triassic) (Motani 1999). These data immediately raise a red flag: MBCN155 was found on Mallorca, corresponding to the westernmost edge of the Tethys sea during the Ladinian (Middle Triassic), whereas all other similar well-dated ichthyosauriforms have been reported around the western and eastern margins of Panthalassa during the Spathian (upper Olenekian, Lower Triassic) (Cuthbertson et al. 2013; Kelley et al. 2016) (Figure 6).

Motani et al. (1996, 1998) posited that basal ichthyosauriforms had a somewhat anguilliform style of swimming, although tail propulsion was starting to gain importance as well (Sander 2000). Thus, they were inferred to live in shallow, epicontinental seas as ambush predators (Massare and Callaway 1990; Cuthbertson et al. 2013). Given the remarkable fact that basal ichthyosauriforms have been found in both margins of the Panthalassa ocean, Cuthbertson et al. (2013) hypothesised four possible dispersal routes during the latest Permian: the first two

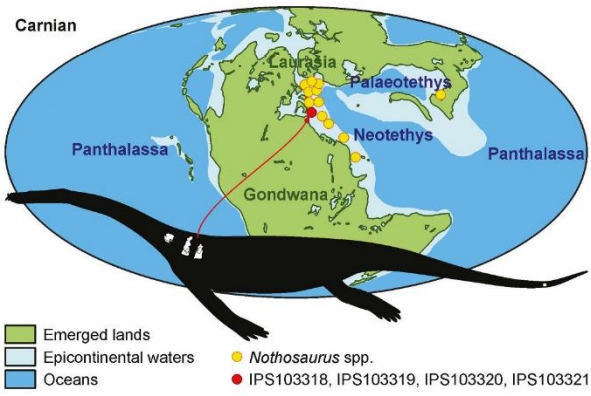

Figure 5. Palaeogeographic map of the Carnian indicating the sites that have yielded *Nothosaurus* fossils (of any age, referenced in the text) (yellow circles) and the Coma Freda site (red circle). Map modified from Scotese (2014), silhouette modified from Araújo and Correia (2015), indicating the inferred anatomical position of IPS103318, IPS103319, IPS103320 and IPS103321.

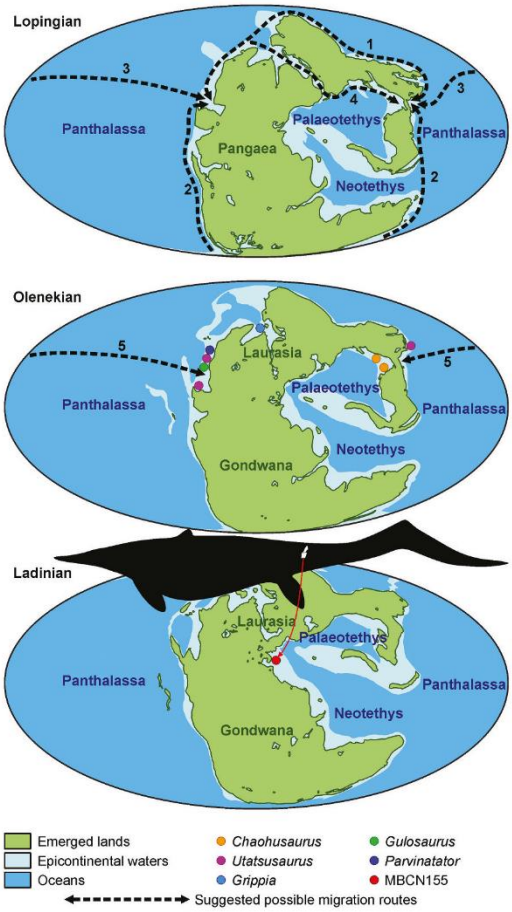

Figure 6. Palaeogeographic maps of the Lopingian, Olenekian and Ladinian indicating the possible dispersal routes of non-nasorostran basal ichthyosauriforms (1, 2, 3, 4: hypotheses 1, 2, 3 and 4 of Cuthbertson et al. 2013; 5: hypothesis of Kelley et al. 2016). Coloured circles represent occurrences of *Chaohusaurus* and Grippidia (references in the text), and the red circle represents the Puig d'en Canals site. Maps modified from Scotese (2014), silhouette modified from the one of *Utatsusaurus* by McGowan and Motani (2003), indicating the inferred anatomical position of MBCN155.

implied that these species would have had to circumnavigate Laurasia or Gondwana around the northern and southern margins, respectively, overcoming the latitudinal climatic gradients (Figure 6). The third one, also suggested by Kelley et al. (2016), was that some of these species would have managed to cross the Panthalassa ocean (Figure 6), and the fourth option hinged upon their migrating through an epicontinental seaway traversing Laurasia during the latest Permian (Cuthbertson et al. 2013) (Figure 6). The first two options were dismissed due to the large diversity of environments that the basal ichthyosauriforms would have had to endure to reach the other side of the continents (Cuthbertson et al. 2013). Cuthbertson et al. (2013) also cast doubts on the third option, since these species, that seem to be best fit for nearshore environments, would have had to cross an enormous oceanic distance. Conversely, Kelley et al. (2016) advocated that migration route based on coeval dispersal events of ammonoids (Brayard et al. 2009). Ammonoids, however, possess planktic larvae with notably high capacities of dispersal, especially by oceanic currents (*e.g.*, De Baets et al. 2015 and references therein), which could easily explain that migration event, but it would certainly be not so easy for the one involving basal ichthyosauriforms. Finally, the fourth option was the most plausible according to Cuthbertson et al. (2013), because the climatic variations were not very prominent and the whole dispersal route would be in shallow seas, even though it implied that basal ichthyosauriforms already existed during the latest Permian and used the Tethys as a corridor.

MBCN155 would fill that biogeographic gap, but it is of course much younger that all other known basal ichthyosauriforms (late Olenekian vs. Ladinian) (Figure 6). It is not in the scope of the present work to discuss whether the third or the fourth dispersal hypotheses put forward by Cuthbertson et al. (2013) is the one more probable, because they both have the same implication: an eventual colonisation of the western Tethys shallow seas by basal ichthyosauriforms. Given the age attribution to MBCN155, three main scenarios can be hypothesised:

(1) The Mallorcan specimen might actually not be related to *Chaohusaurus* and Grippidia, and in fact, it may belong to a younger lineage that retained plesiomorphic characters such as similar height/length vertebral centrum proportions and relatively tall and bulky neural arches. However, this hypothesis is not very solid, as all other coeval ichthyosauriforms known so far are within the clade Ichthyosauria (sensu Huang et al. 2019), characterised by discoidal vertebral centra and generally slender neural arches (see references in the 'Remarks' section of MBCN155). Shastasaurids and related taxa do possess stout neural arches that are notably thickened distally, but the centra of their proximal caudal vertebrae are clearly discoidal like all other derived ichthyosaurs (*e.g.*, Merriam 1908; Fischer et al. 2014).

(2) MBCN155 might correspond to the *Chaohusaurus*-Grippidia group, and the Mallorcan species might have reached the western Tethys in the c. 10 million years between the last recorded basal ichthyosauriforms in Asia and North America (upper Olenekian) and the deposits of Mallorca (Ladinian) (Figure 6). This scenario seems to be more plausible than the previous one, but if ichthyosauriforms had expanded throughout the epicontinental shallow seas of the Tethys during the Anisian and Ladinian, one would expect to find members of such group in the well-known and sampled European localities of Germany, Switzerland and Italy. However, such reports do not exist so far, most probably pointing to a more restricted palaeobiogeographical distribution of those ichthyosauriforms during the Middle Triassic.

(3) The lineage including *Chaohusaurus* and Grippidia may have persisted until the Ladinian as an endemism in the epicontinental seas near the coasts of Iberia (Figure 6), when all other basal ichthyosauriforms had virtually disappeared elsewhere. The stratigraphic record of the Lower and part of the Middle Triassic in the western Tethys is either absent or represented by continental deposits (López-Gómez et al. 2019), and therefore it is impossible to know when basal ichthyosauriforms reached this region. Later, during the middle Anisian, eastern Iberia was flooded by the *Muschelkalk* transgression, but those epicontinental seas remained relatively isolated from the rest of the Tethys (Escudero-Mozo et al. 2015; Manzanares et al. 2020), which may explain the relict character of some of its denizens, such as MBCN155. Other ichthyosaurs recorded in Tethyan deposits of similar age, such as omphalosaurids, mixosaurids, cymbospondylids and besanosaurids (*e.g.*, Maisch 2010; Renesto et al. 2020), have more streamlined bodies and laterally compressed caudal vertebrae that surely improved their swimming aptitude in open waters, reflected by the sub-cosmopolitan distribution of most of those families (Massare and Callaway 1990; Sander 2000; Schmitz et al. 2004; Maisch 2010; Renesto et al. 2020). Thus, here we consider that the geographical and stratigraphical difference of MBCN155 from other basal ichthyosauriforms can be reasonably explained if the Mallorcan taxon represents a relic species of a primitive group of ichthyosauriforms that became restricted to the western Tethys during the Anisian–Ladinian.

Conclusions

The study of all the vertebrate fossils from the Middle and Upper Triassic of Mallorca (Balearic Islands, western Mediterranean) found so far has allowed the identification of three taxa: an epiphysis belonging to an indeterminate reptile, from the lower Norian; four vertebrae (an anterior cervical (?) neural arch, two pectoral vertebrae and a posterior caudal centrum) of *Nothosaurus* sp., from the Carnian; and an anterior caudal vertebra of an indeterminate ichthyosauriform similar to the clade Grippidia, from the Ladinian. The distribution area of the genus *Nothosaurus* encompassed the area occupied by Mallorca, and thus the discovery of the four vertebrae studied herein is not particularly surprising. On the other hand, the first report of a non-nasorostran basal ichthyosauriform from the western Tethys is certainly remarkable because it fills a palaeobiogeographic gap of the group, known from the eastern and western margins of Panthalassa but hitherto absent in the most probably corridor between these two regions: the western Tethyan margin. The age of the Mallorcan specimen is, however, at odds with the other known non-nasorostran basal ichthyosauriforms, which are about 10 million years older (late Olenekian: Spathian vs. Ladinian). This has allowed us to put forward several hypotheses to explain that seemingly incongruous distribution, and the one that has been deemed most probable is that the coasts of Iberia may have served as a refuge for the last members of this group, supported by the results of other works that infer a notable degree of isolation of those shallow carbonate ramps during the Anisian.

Acknowledgments

We thank Ryosuke Motani (University of California, Davis) and P. Martin Sander (Rheinische Friedrich-Wilhelms-Universität Bonn) for discussion and most valuable insight on MBCN155. To Joan Arbona (MBCN) for aid in fieldwork and for leading R.M.A. to the sites of Puig d'en Canals and Can Bleda, and for providing insight on local geology. To Salvador Moyà-Solà (ICP) for showing to R.M.A. the Coma Freda site, and for sharing the story of how the *Nothosaurus* vertebrae were found and collected in the 1970s. To Carol Constantino (MBCN) for access to the fossils of the historical collections of J. Bauzá and G. Colom. To Sebastià Matamalas and Josep Juárez for aid in fieldwork. To Marina Rull and Xènia Aymerich (both ICP) for preparation of the specimens. To Enric Vicens (Universitat Autònoma de Barcelona) for letting R.M.A. use the photographic equipment of the department. To Daniela Schwarz (Museum für Naturkunde Berlin), Rainer Schoch (Staatliches Museum für Naturkunde Stuttgart) and Ingmar Werneburg (Eberhard Karls Universität Tübingen) for access to comparison material in their respective institutions. To Gareth Dyke, editor-in-chief of the journal, Jiandong Huang, editor, and Valentin Fischer (Université de Liège) and an anonymous reviewer for their constructive comments and remarks that improved the initial manuscript. We acknowledge support from the CERCA program (Generalitat de Catalunya, Spain). R.M.A. was supported by the predoctoral grant FPU17/01922 (Ministerio de Ciencia, Innovación y Universidades, Spain) and the grant Synthesys+ DE-TAF-23 (European Commission). J.F. was supported by the Agencia Estatal de Investigación (Spain) and the European Regional Development Fund AEI/FEDER EU, project CGL2017-82654-P (European Union). J.F. is member of the consolidated research group 2017 SGR 086 GRC (Generalitat de Catalunya, Spain). O.O. is member of the consolidated research group 2017 SGR 11666 GRC (Generalitat de Catalunya, Spain).

Disclosure statement

No potential conflict of interest was reported by the authors.

Funding

This work was supported by the European Commission [Synthesys+ DE-TAF -23]; Generalitat de Catalunya [2017 SGR 086 GRC,2017 SGR 11666 GRC]; Ministerio de Ciencia, Innovación y Universidades [FPU17/01922]; Agencia Estatal de Investigación (Spain) and European Regional Development Fund AEI/FEDER EU [CGL2017-82654-P].

ORCID

Rafel Matamales-Andreu http://orcid.org/0000-0001-9914-0510
Oriol Oms http://orcid.org/0000-0001-8355-847X
Àngel Galobart http://orcid.org/0000-0003-1508-4561
Josep Fortuny http://orcid.org/0000-0003-4282-1619

References

Antonelli F, Ricci S, Petriaggi BD, Buendía Ortuño M. 2019. Study of the bioerosion of Phoenician elephant tusks from the shipwreck of Bajo de la Campana: lots of hypotheses, few certainties. Facies. 65(2):10. doi:10.1007/s10347-019-0553-8.

Araújo R, Correia F. 2015. Soft-tissue of the Plesiosaur pectoral girdle inferred from basal Eosauropterygia taxa and the extant phylogenetic bracket. Palaeontol Electron. 18.1.8A:1–32.

Assmann P. 1937. Revision der Fauna der Wirbellosen der oberschlesischen Trias [Revision of the invertebrate fauna of the Upper Silesian Triassic]. Abh Der Preuss Geol Landesanst. 170:1–126. German.

Barnolas A, director. 1991. Mapa Geológico de España, escala 1:50.000 [Geological Map of Spain, scale 1:50.000]. Sheets and memoirs: 643 (38-25) + 644 (39-25) Sa Calobra + Pollensa [1 map + 62 pp.]; 670 (38-26) Sóller [1 map + 62 pp.]; 671 (39-26) Inca [1 map + 68 pp.]; 672 (40-26) Artà [1 map + 53 pp.]; 697 (37-27) Andraitx [1 map + 56 pp.]; 698 (38-27) + 722B (37-28) + 723 (38-28) Palma + Illa del Toro + Cap de Cala Figuera [1 map + 64 pp.]; 699 (39-27) Porreres [1 map + 55 pp.]; 700 (40-27) Manacor [1 map + 59 pp.]; 724 (39-28) Lluchmayor [1 map + 49 pp.]; 725 (40-28) + 749 (40-29) Felanitx [1 map + 45 pp.]. Madrid: Instituto Tecnológico GeoMinero de España. Spanish.

Barnolas-Cortinas A, editor. 1984. Sedimentología del Jurásico de Mallorca [Sedimentology of the Jurassic of Mallorca]. Palma: Grupo Español del Mesozoico. Spanish.

Baur G. 1889. Nothosauridae. In: Zittel KA, editor. Handbuch der Paläontologie. I. Abth. Paläozoologie. III. Band. Vertebrata (Pisces, Amphibia, Reptilia, Aves) [Handbook of Palaeontology. I. Section Palaeozoology. III. Volume. Vertebrata (Pisces, Amphibia, Reptilia, Aves)]. Munich: R. Oldenbourg; p. 478. German.

Bauzá J. 1945. Nueva contribución al conocimiento de la Paleontología de Mallorca [A new contribution to the knowledge of the Palaeontology of Mallorca]. Bol R Soc Esp Hist Nat. 43(7–8):397–401. Spanish.

Bauzá J. 1946. Nuevo yacimiento fosilífero en el Trias de la Sierra Norte de Mallorca [A new fossiliferous deposit in the Triassic of the Northern Ranges of Mallorca]. Bol R Soc Esp Hist Nat. 44:335–338. pl. 21. Spanish.

Bauzá J. 1955. Notas paleontológicas de Mallorca: sobre el hallazgo del «*Nothosaurus*» en el Trias [Palaeontological notes of Mallorca: about the finding of the "*Nothosaurus*" in the Triassic]. Bol Soc Hist Nat Baleares. 1:87. Spanish.

Bauzá J. 1971. Ciento ochenta millones de años de la flora y fauna de Mallorca [One-hundred and eighty million years of the flora and fauna of Mallorca]. In: Mascaró J, editor. Historia de Mallorca [History of Mallorca]. Palma: Gráficas Miralles; p. 331–430. Spanish.

Bauzá J. 1981. Contribuciones a la paleontología de Mallorca [Contributions to the palaeontology of Mallorca]. Boll. Soc. Hist. Nat. Balears. 25:7–20. Spanish.

Berrocal-Casero M, Audije-Gil J, Castanhinha RA, Pérez-Valera JA, Dos Santos VF, Segura M. 2018. New discoveries of vertebrate remains from the Triassic of Riba de Santiuste, Guadalajara (Spain). Proc Geol Assoc. 129 (4):526–541. doi:10.1016/j.pgeola.2018.04.009.

Bourrouilh R. 1973. Stratigraphie, sédimentologie et téctonique de l'île de Minorque et du Nord-Est de Majorque (Baléares). La terminaison nord-orientale des Cordilleres Bétiques en Méditerranée occidentale [Stratigraphy, sedimentology and tectonics of the island of Menorca and of the North-East of Mallorca (Balearic Islands). The north-western termination of the Betic Cordillera in the western Mediterranean] [dissertation] (2 volumes). Paris: Université Pierre and Marie Curie, Paris VI. French.

Boutet C, Rangheard Y, Rosenthal P, Visscher H, Durand-Delga M. 1982. Découverte d'une microflore d'âge Norien dans la Sierra Norte de Majorque (Baléares, Espagne) [Discovery of a microflora of Norian age in the Northern Ranges of Mallorca (Balearic Islands, Spain)]. C R Acad Sci Paris. 294(Série 2):1267–1270. French.

Brayard A, Escarguel G, Bucher H, Brühwiler T. 2009. Smithian and Spathian (Early Triassic) ammonoid assemblages from terranes: paleoceanographic and paleogeographic implications. J Asian Earth Sci. 36(6):420–433. doi:10.1016/j.jseaes.2008.05.004.

Briere PR. 2000. Playa, playa lake, sabkha: proposed definitions for old terms. J Arid Environ. 45(1):1–7. doi:10.1006/jare.2000.0633.

Brinkman D, Xijin Z, Nicholls EL. 1992. A primitive ichthyosaur from the Lower Triassic of British Columbia, Canada. Palaeontology. 35(2):465–474.

Bromley R, D'Alessandro A. 1983. Bioerosion in the Pleistocene of southern Italy: ichnogenera *Caulostrepsis* and *Maeandropolydora*. Riv It Paleontol Strat. 89:283–309.

Calafat F. 1988. Estratigrafía y sedimentología de la litofacies Buntsandstein de Mallorca [Stratigraphy and sedimentology of the Buntsandstein lithofacies of Mallorca] [bachelor's thesis]. Barcelona: Universitat de Barcelona. Spanish.

Chen X-H, Motani R, Cheng L, Jiang D-Y, Rieppel O. 2014a. A carapace-like bony 'body tube' in an Early Triassic marine reptile and the onset of marine tetrapod predation. PLoS ONE. 9(4):e94396. doi:10.1371/journal.pone.0094396.

Chen X-H, Motani R, Cheng L, Jiang D-Y, Rieppel O. 2014b. The enigmatic marine reptile *Nanchangosaurus* from the Lower Triassic of Hubei, China and the phylogenetic affinities of Hupehsuchia. PLoS ONE. 9(7):e102361. doi:10.1371/journal.pone.0102361.

Chen X-H, Motani R, Cheng L, Jiang D-Y, Rieppel O. 2014c. A small short-necked hupehsuchian from the Lower Triassic of Hubei Province, China. PLoS ONE. 9(12):e115244. doi:10.1371/journal.pone.0115244.

Chen X-H, Motani R, Cheng L, Jiang D-Y, Rieppel O. 2015. A new specimen of Carroll's mystery hupehsuchian from the Lower Triassic of China. PLoS ONE. 10(5):e0126024. doi:10.1371/journal.pone.0126024.

Chen X-H, Sander PM, Cheng L, Wang X-F. 2013. A new Triassic primitive ichthyosaur from Yuanan, South China. Acta Geol Sinica Engl Ed. 87 (3):672–677. doi:10.1111/1755-6724.12078.

Colom G. 1975. Geología de Mallorca [Geology of Mallorca] (2 volumes). Palma: Gráficas Miramar, Diputación Provincial de Baleares. Spanish.

Colom G. 1982. Notas paleontológicas y estratigráficas (referentes a Mallorca e Ibiza) [Palaeontological and stratigraphical notes (referring to Mallorca and Eivissa)]. Boll. Soc. Hist. Nat. Balears. 26:195–206. Spanish.

Curioni G. 1847. Cenni sopra un nuovo saurio fossile dei monti di Perledo sul Lario e sul terreno che lo racchiude [Notes on a new fossil saurian from the Perledo mountain in Lario and on the rocks that enclose it]. G J.R Inst Lomb Sci Let Art. 16:159–170.

Cuthbertson RS, Russell A, Anderson J. 2014. The first substantive evidence of *Utatsusaurus* (Ichthyopterygia) from the Sulphur Mountain Formation (Lower–Middle Triassic) of British Columbia, Canada: a skull roof description with comparison to other early taxa. Can J Earth Sci. 51(2):180–185. doi:10.1139/cjes-2013-0185.

Cuthbertson RS, Russell AP, Anderson JS. 2013. Cranial morphology and relationships of a new grippidian (Ichthyopterygia) from the Vega-Phroso siltstone member (Lower Triassic) of British Columbia, Canada. J Vert Paleontol. 33(4):831–847. doi:10.1080/02724634.2013.755989.

Dal Sasso C, Pinna G. 1996. *Besanosaurus leptorhynchus* n. gen. n. sp., a new shastasaurid ichthyosaur from the Middle Triassic of Besano (Lombardy, N. Italy). Paleo Lomb. n.s. 4: 3–23.

Dalla Vecchia FM. 2004. First record of the rare marine reptile *Tholodus schmidi* from the Middle Triassic of the Southern Alps. Riv It Paleontol Strat. 110 (2):479–492.

Dalla Vecchia FM. 2006. A new sauropterygian reptile with plesiosaurian affinity from the Late Triassic of Italy. Riv It Paleontol Strat. 112(2):207–225.

Dalla Vecchia FM, Avanzini M. 2002. New findings of isolated remains of Triassic reptiles from Northeastern Italy. Boll Soc Paleo It. 42(2–3):215–235.

Darder B. 1914. El Triásico de Mallorca [The Triassic of Mallorca]. Trab Mus Nac Cienc Nat. Geol. 7:1–85. Spanish.

De Baets K, Landman NH, Tanabe K. 2015. Ammonoid embryonic development. In: Klug C, Korn D, De Baets K, Kruta I, Mapes RH, editors. Ammonoid Paleobiology: from anatomy to ecology. Topics in Geobiology, 43; p. 113–205. Springer.

De Blainville HMD. 1835. Description de quelques espèces de reptiles de la Californie, précédée de l'analyse d'une système générale d'Erpetologie et d'Amphibiologie [Description of some species of reptiles from California, preceded by a analysis of a general system of erpetology and amphibiology]. Nouv Ann Mus Hist Nat Paris. 4:233–296. French.

de Miguel Chaves C, García-Gil S, Ortega F, Sanz JL, Pérez-García A. 2016. First Triassic tetrapod (Sauropterygia, Nothosauridae) from Castilla y León: evidence of an unknown taxon for the Spanish record. J Iber Geol. 42(1):29–38. doi:10.5209/rev_JIGE.2016.v42.n1.51210.

de Miguel Chaves C, Ortega F, Pérez-García A. 2017. The eosauropterygian fossils from the Middle Triassic of Canales de Molina (Guadalajara, Spain). J Iber Geol. 43(2):129–138. doi:10.1007/s41513-017-0011-9.

de Miguel Chaves C, Ortega F, Pérez-García A. 2018a. New highly pachyostotic nothosauroid interpreted as a filter-feeding Triassic marine reptile. Biol Lett. 14(8):20180130. doi:10.1098/rsbl.2018.0130.

de Miguel Chaves C, Ortega F, Pérez-García A. 2018b. A new placodont from the Upper Triassic of Spain provides new insights on the acquisition of the specialized skull of Henodontidae. Pap Palaeontol. 4(4):567–576. doi:10.1002/spp2.1218.

de Miguel Chaves C, Pérez-García A, Cobos A, Royo-Torres R, Ortega F, Alcalá L. 2015. A diverse Late Triassic tetrapod fauna from Manzanera (Teruel, Spain). Geobios. 48(6):479–490. doi:10.1016/j.geobios.2015.09.002.

de Miguel Chaves C, Scheyer TM, Ortega F, Pérez-García A. 2020. The placodonts (Sauropterygia) from the Middle Triassic of Canales de Molina (Central Spain), and an update on the knowledge about this clade in the Iberian record. Hist Biol. 32(1):34–48. doi:10.1080/08912963.2018.1462805.

Diedrich CJ. 2010. Palaeoecology of *Placodus gigas* (Reptilia) and other placodontids — middle Triassic macroalgae feeders in the Germanic Basin of central Europe — and evidence for convergent evolution with Sirenia. Palaeogeogr Palaeoclimat Palaeoecol. 285(3–4):287–306. doi:10.1016/j.palaeo.2009.11.021.

Diedrich CJ. 2012. The Middle Triassic marine reptile biodiversity in the Germanic Basin, in the centre of the Pangaean world. Open Geosci. 4 (1):9–46. doi:10.2478/s13533-011-0060-0.

Diedrich CJ. 2013. Review of the Middle Triassic "sea cow" *Placodus gigas* (Reptilia) in Pangea's shallow marine macroalgae meadows of Europe. New Mexico Mus Nat Hist Sci Bull. 61:104–131.

Diedrich CJ. 2015. The vertebrates from the Lower Ladinian (Middle Triassic) bonebed of Lamerden (Germany) as palaeoenvironment indicators in the Germanic Basin. Open Geosci. 7(7):1–28. doi:10.1515/geo-2015-0062.

Diez JB, Broutin J, Grauvogel-Stamm L, Bourquin S, Bercovici A, Ferrer J. 2010. Anisian floras from the NE Iberian Peninsula and Balearic Islands: A synthesis. Rev Palaeobot Palynol. 162(3):522–542. doi:10.1016/j.revpalbo.2010.09.003.

Domènech R, Martinell J, de Porta J. 2008. Bioerosión por poliquetos espiónidos (Polychaeta, Spionidae) en moluscos marinos del cuaternario caribeño de Colombia [Bioerosion by spionid polychaetes (Polychaeta, Spionidae) in molluscs from the Caribbean Quaternary of Colombia]. Rev Acad Colomb Cienc Exactas Fis Nat. 32(124):411–419. Spanish.

Enrique-Gisbert P. 1986. Nota sobre les roques hipabissals de la serra de Tramuntana de Mallorca: algunes característiques petrogràfiques i geoquímiques [Note on the hipabissal rocks of the Tramuntana Ranges of Mallorca: some petrographical and geochemical characteristics]. Boll. Soc. Hist. Nat. Balears. 30:19–50. Catalan.

Enrique-Gisbert P, Lago-San José M, Pocoví-Juan A, Vaquer-Navarro R. 1987. Aspectos petrológicos y geoquímicos del magmatismo alcalino, de edad triásica, en la sierra norte de Mallorca [Petrological and geochemical aspects of the alkaline magmatism, of Triassic age, in the northern ranges of Mallorca]. In: Colegio de Geólogos, editor. IIº Congreso de Geoquímica de España. Soria: Colegio de Geólogos; p. 215–218. Spanish.

Escudero-Mozo MJ, Márquez-Aliaga A, Goy A, Martín-Chivelet J, López-Gómez J, Márquez L, Arche A, Plasencia P, Pla C, Marzo M, et al. 2015. Middle Triassic carbonate platforms in eastern Iberia: evolution of their fauna and palaeogeographic significance in the western Tethys. Palaeogeogr Palaeoclimat Palaeoecol. 417:236–260. doi:10.1016/j.palaeo.2014.10.041.

Escudero-Mozo MJ, Martín-Chivelet J, Goy A, López-Gómez J. 2014. Middle-Upper Triassic carbonate platforms in Minorca (Balearic islands): implications for Western Tethys correlations. Sediment Geol. 310:41–48. doi:10.1016/j.sedgeo.2014.06.002.

Fallot P. 1922. Étude Géologique de la Sierra de Majorque [Geological study of the mountain range of Mallorca]. Paris and Liège: Librairie Polytechnique Ch. Béranger. French.

Fischer V, Cappetta H, Vincent P, Garcia G, Gooalerts S, Martin JE, Roggero D, Valentin X. 2014. Ichthyosaurs from the French Rhaetian indicate a severe turnover across the Triassic–Jurassic boundary. Naturwissenschaften. 101 (12):1027–1040. doi:10.1007/s00114-014-1242-7.

Fortuny J, Bolet A, Sellés AG, Cartanyà J, Galobart À. 2011. New insights on the Permian and Triassic vertebrates from the Iberian Peninsula with emphasis on the Pyrenean and Catalonian basins. J Iber Geol. 37(1):65–86.

Fraas E. 1896. Die Schwäbischen Trias-Saurier nach dem Material der Kgl. Naturalien-Sammlung in Stuttgart zusammengestellt. Festgabe des Königlichen Naturalien-Cabinets in Stuttgart zur 42. Versammlung der Deutschen geologischen Gesellschaft in Stuttgart [The Swabian Triassic saurians compiled from the material from the Royal Natural Collection in Stuttgart. Specification of the Royal Natural Cabinet in Stuttgart for the 42nd Assembly of the German Geological Society in Stuttgart]. Stuttgart: E. Schweizerbart'sche Verlagshandlung (E. Koch). German.

Goy A 1986. Ammonoideos del Triásico de España [Triassic ammonoids of Spain] [cathedra thesis]. Madrid: Universidad Complutense de Madrid. Spanish.

Goy A. 1995. Ammonoideos del Triásico Medio de España: bioestratigrafía y correlaciones [Middle Triassic ammonoids of Spain: biostratigraphy and correlations]. Cuad Geol Ibér. 19:21–60. Spanish.

Huang JD, Motani R, Jiang D-Y, Tintori A, Rieppel O, Zhou M, Ren X-X, Zhang R. 2019. The new ichthyosauriform *Chaohusaurus brevifemoralis* (Reptilia, Ichthyosauromorpha) from Majiashan, Chaohu, Anhui Province, China. PeerJ. 7:e7561. doi:10.7717/peerj.7561.

Jaekel O. 1909. Über die Klassen der Tetrapoden [On the classes of tetrapods]. Zool Anz. 34:193–212. German.

Ji C, Jiang D-Y, Motani R, Hao W-C, Sun Z-Y, Cai T. 2013. A new juvenile specimen of *Guanlingsaurus* (Ichthyosauria, Shastasauridae) from the Upper Triassic of southwestern China. J Vert Paleontol. 33(2):340–348. doi:10.1080/02724634.2013.723082.

Ji C, Jiang D-Y, Rieppel O, Motani R, Tintori A, Sun Z-Y. 2014. A new specimen of *Nothosaurus youngi* from the Middle Triassic of Guizhou, China. J Vert Paleontol. 34(2):465–470. doi:10.1080/02724634.2013.808204.

Jiang D-Y, Maisch MW, Hao W-C, Sun Y-L, Sun Z-Y. 2006a. *Nothosaurus yangjuanensis* n. sp. (Reptilia, Sauropterygia, Nothosauridae) from the middle Anisian (Middle Triassic) of Guizhou, southwestern China. Neues Jahrb Geol Paläont Monatsh. 5(5):257–276. doi:10.1127/njgpm/2006/2006/257.

Jiang D-Y, Motani R, Hao W, Schmitz L, Rieppel O, Sun Y, Sun Z. 2008. New primitive ichthyosaurian (Reptilia, Diapsida) from the Middle Triassic of Panxian, Guizhou, southwestern China and its position in the Triassic biotic recovery. Progr Nat Sci. 18(10):1315–1319. doi:10.1016/j.pnsc.2008.01.039.

Jiang D-Y, Motani R, Huang J-D, Tintori A, Hu Y-C, Rieppel O, Fraser NC, Ji C, Kelley NP, Fu W-L, et al. 2016. A large aberrant stem ichthyosauriform indicating early rise and demise of ichthyosauromorphs in the wake of the end-Permian extinction. Sci Rep. 6(1):26232. doi:10.1038/srep26232.

Jiang D-Y, Schmitz L, Hao W-C, Sun Y-L. 2006b. A new mixosaurid ichthyosaur from the Middle Triassic of China. J Vert Paleontol. 26(1):60–69. doi:10.1671/0272-4634(2006)26[60:ANMIFT]2.0.CO;2.

Juárez-Ruiz J, Matamales-Andreu R. 2020a. Mollusca (Ammonoidea, Gastropoda, Bivalvia) from the Upper Ladinian (Middle Triassic) of the island of Mallorca (Balearic Islands, western Mediterranean): preliminary data. In: Gilabert V, Medrano E, García Á, Ferratges FA, Laita E, Pérez M, Moya R, Alonso A, Galán J, Núñez C, editors. Novelties in Iberian Palaeontology. Abstract book of the XVII Encuentro de Jóvenes Investigadores en Paleontología. Andorra. p. 19.

Juárez-Ruiz J, Matamales-Andreu R. Forthcoming 2020b. Mollusca (Ammonoidea, Gastropoda, Bivalvia) del Ladiniense superior (Triásico Medio) de la isla de Mallorca (Islas Baleares, Mediterráneo occidental): datos preliminares [Mollusca (Ammonoidea, Gastropoda, Bivalvia) from the upper Ladinian (Middle Triassic) of the island of Mallorca (Balearic Islands, western Mediterranean): preliminary data]. Ciênc. Terra. Spanish.

Kear BP, Rich TH, Vickers-Rich P, Ali MA, Al-Mufarrih YA, Matari AD, Al-Masary AM, Halawani MA. 2010. A review of aquatic vertebrate remains from the Middle-Upper Triassic Jilh Formation of Saudi Arabia. Proc R Soc Vic. 122(1):1–8. doi:10.1071/RS10001.

Kelley NP, Motani R, Embree P, Orchard MJ. 2016. A new Lower Triassic ichthyopterygian assemblage from Fossil Hill, Nevada. PeerJ. 4:e1626. doi:10.7717/peerj.1626.

Klein N, Foth C, Schoch RR. 2017. Preliminary observations on the bone histology of the Middle Triassic pseudosuchian archosaur *Batrachotomus kupferzellensis* reveal fast growth with laminar fibrolamellar bone tissue. J Vert Paleontol. 37(4):e1333121. doi:10.1080/02724634.2017.1333121.

Klein N, Voeten DFAE, Haarhuis A, Bleeker R. 2016. The earliest record of the genus *Lariosaurus* from the early middle Anisian (Middle Triassic) of the Germanic Basin. J Vert Paleontol. 36(4):e1163712. doi:10.1080/02724634.2016.1163712.

Klein N, Voeten DFAE, Lankamp J, Bleeker R, Sichelschmidt OJ, Liebrand M, Nieweg DC, Sander PM. 2015. Postcranial material of *Nothosaurus marchicus* from the Lower Muschelkalk (Anisian) of Winterswijk, The Netherlands, with remarks on swimming styles and taphonomy. Paläontol Z. 89 (4):961–981. doi:10.1007/s12542-015-0273-5.

Krahl A, Klein N, Sander PM. 2013. Evolutionary implications of the divergent long bone histologies of *Nothosaurus* and *Pistosaurus* (Sauropterygia, Triassic). BMC Evol Biol. 13(1):123. doi:10.1186/1471-2148-13-123.

Laurenti JN. 1768. Specimen Medicum, Exhibens Synopsin Reptilium Emendatam cum Experimentis Circa Venena et Antidota Reptilium Austriacorum. Vienna: Typis Joannis Thomae Nobilis de Trattnern. Latin.

Li C, Jiang D-Y, Cheng L, Wu X-C, Rieppel O. 2013. A new species of *Largocephalosaurus* (Diapsida: Saurosphargidae), with implications for the morphological diversity and phylogeny of the group. Geol Mag. 151 (1):100–120. doi:10.1017/S001675681300023X.

Li J, Rieppel O. 2004. A new nothosaur from Middle Triassic of Guizhou, China. Vert PalAs. 42(1):1–12.

Li Q, Liu J. 2020. An Early Triassic sauropterygian and associated fauna from South China provide insights into Triassic ecosystem health. Commun Biol. 3:63. doi:10.1038/s42003-020-0778-7.

Li Z-G, Jiang D-Y, Rieppel O, Motani R, Tintori A, Sun Z-Y, Ji C. 2016. A new species of *Xinpusaurus* (Reptilia, Thalattosauria) from the Ladinian (Middle Triassic) of Xingyi, Guizhou, southwestern China. J Vert Paleontol. 36(6): e1218340. doi:10.1080/02724634.2016.1218340.

Lin W-B, Jiang D-Y, Rieppel O, Motani R, Ji C, Tintori A, Sun Z-Y, Zhou M. 2017. A new specimen of *Lariosaurus xingyiensis* (Reptilia, Sauropterygia) from the Ladinian (Middle Triassic) Zhuganpo Member, Falang Formation, Guizhou, China. J Vert Paleontol. 37(2):e1278703. doi:10.1080/02724634.2017.1278703.

Liu J. 2013. On the taxonomy of *Xinpusaurus* (Reptilia: Thalattosauria). Vert PalAs. 51(1):17–23.

Liu J, Hu S-X, Rieppel O, Jiang D-Y, Benton MJ, Kelley NP, Aitchison JC, Zhou C-Y, Wen W, Huang J-Y, et al. 2015. A gigantic nothosaur (Reptilia: Sauropterygia) from the Middle Triassic of SW China and its implication for the Triassic biotic recovery. Sci Rep. 4(1):7142. doi:10.1038/srep07142.

Liu J, Rieppel O. 2005. Restudy of *Anshunsaurus huangguoshuensis* (Reptilia: Thalattosauria) from the Middle Triassic of Guizhou, China. Am Mus Novit. 3488:1–34. doi:10.1206/0003-0082(2005)488[0001:ROAHRT]2.0.CO;2.

Liu J, Zhao L-J, Li C, He T. 2013. Osteology of *Concavispina biseridens* (Reptilia, Thalattosauria) from the Xiaowa Formation (Carnian), Guanling, Guizhou, China. J Paleontol. 87(2):341–350. doi:10.1666/12-059R1.1.

López-Gómez J, Alonso-Azcárate J, Arche A, Arribas J, Fernández-Barrenechea J, Borruel-Abadía V, Bourquin S, Cadenas P, Cuevas J, De la Horra R, et al. 2019. Permian-Triassic rifting stage. In: Vergés J, Kullberg JC, editors. The Geology of Iberia: a geodynamic approach. Volume 3: the alpine cycle. Cham: Springer; p. 29–112.

López-Gómez J, Escudero-Mozo MJ, Martín-Chivelet J, Arche A, Lago M, Galé C. 2017. Western Tethys continental-marine responses to the Carnian Humid Episode: palaeoclimatic and palaeogeographic implications. Glob Planet Change. 148:79–95. doi:10.1016/j.gloplacha.2016.11.016.

Lucas SG. 2002. *Toretocnemus*, a Late Triassic ichthyosaur from California, U.S.A. and Sonora, Mexico. New Mexico Mus Nat Hist Sci Bull. 21:275–278.

Maisch MW. 2000. The mixosaurid ichthyosaur *Contectopalatus* from the Middle Triassic of the German Basin. Lethaia. 33(2):71–74. doi:10.1080/00241160050150186.

Maisch MW. 2010. Phylogeny, systematics, and origin of the Ichthyosauria – the state of the art. Palaeodiversity. 3:151–214.

Maisch MW. 2014. On the morphology and taxonomic status of *Xinpusaurus kohi* Jiang et al. 2004 (Diapsida: Thalattosauria) from the Upper Triassic of China. Palaeodiversity. 7:47–59.

Maisch MW, Matzke AT. 1997. *Mikadocephalus gracilirostris* n. gen., n. sp., a new ichthyosaur from the Grenzbitumenzone (Anisian-Ladinian) of Monte San Giorgio (Switzerland). Paläontol Z. 71(3/4):267–289. doi:10.1007/BF02988496.

Maisch MW, Matzke AT. 1998. Observations on Triassic ichthyosaurs. Part II: A new ichthyosaur with palatal teeth from Monte San Giorgio. Neues Jahrb Geol Paläont Monatsh. 1(1):26–41. doi:10.1127/njgpm/1998/1998/26.

Maisch MW, Matzke AT. 2002. Observations on Triassic ichthyosaurs. Part IX. The first associated skeletal remains of *Merriamosaurus* n. g. (Ichthyosauria, Lower Triassic) and their bearing on the systematic position of the Omphalosauria. Neues Jahrb Geol Paläont Abh. 226(1):59–94.

Maisch MW, Matzke AT. 2003. Observations on Triassic ichthyosaurs. Part XII. A new Early Triassic ichthyosaur genus from Spitzbergen. Neues Jahrb Geol Paläont Abh. 229(3):317–338. doi:10.1127/njgpa/229/2003/317.

Manera J. 1930. Breve estudio geológico de la isla de Menorca [Brief geological study of the island of Menorca]. Rev Menorca. 25:40–53. Spanish.

Manzanares E, Escudero-Mozo MJ, Ferrón H, Martínez-Pérez C, Botella H. 2020. Middle Triassic sharks from the Catalan Coastal ranges (NE Spain) and faunal colonization patterns during the westward transgression of Tethys. Palaeogeogr Palaeoclimat Palaeoecol. 539:109489. doi:10.1016/j.palaeo.2019.109489.

Márquez-Aliaga A, Klein N, Reolid M, Plasencia P, Villena JA, Martínez-Pérez C. 2019. An enigmatic marine reptile, *Hispaniasaurus cranioelongatus* (gen. et sp. nov.) with nothosauroid affinities from the Ladinian of the Iberian Range (Spain). Hist Biol. 31(2):223–233. doi:10.1080/08912963.2017.1359264.

Massare JA, Callaway JM. 1990. The affinities and ecology of Triassic ichthyosaurs. Geol Soc Am Bull. 102(4):409–416. doi:10.1130/0016-7606(1990)102<0409:TAAEOT>2.3.CO;2.

Massare JA, Lomax DR. 2018. Hindfins of Ichthyosaurus: effects of large sample size on 'distinct' morphological characters. Geol Mag. 156(4):725–744. doi:10.1017/S0016756818000146.

Maxwell EE, Zammit M, Druckenmiller PS. 2012. Morphology and orientation of the ichthyosaurian femur. J Vert Paleontol. 32(5):1207–1211. doi:10.1080/02724634.2012.682834.

Mazin J-M. 1981. *Grippia longirostris* Wiman, 1929, un Ichthyopterygia primitif du Trias inférieur du Spitsberg [*Grippia longirostris* Wiman, 1929, a primitive ichthyopterigian of the Lower Triassic of Spitsberg]. Bull Mus Natl Hist Nat. 4:317–340. French.

Mazin J-M, Suteethorn V, Buffetaut E, Jaeger JJ, Elmcke-Ingavat R. 1991. Preliminary description of *Thaisaurus chonglakmanii* n. g., n. sp., a new ichthyopterygian (Reptilia) from the Early Triassic of Thailand. C R Acad Sci. 313:1207–1212.

McGowan C. 1995. A remarkable small ichthyosaur from the Upper Triassic of British Columbia, representing a new genus and species. Can J Earth Sci. 32(3):292–303. doi:10.1139/e95-024.

McGowan C. 1996. A new and typically Jurassic ichthyosaur from the Upper Triassic of British Columbia. Can J Earth Sci. 33(1):24–32. doi:10.1139/e96-003.

McGowan C, Motani R. 2003. Part 8: Ichthyopterygia. In: Sues H-D, editor. Handbook of Paleoherpetology. München: Verlaf Dr. Friederich Pfeil.

Merriam JC. 1908. Triassic Ichthyosauria with special reference to the American forms. Mem Univ California. 1:1–154.

Meyer HV. 1842. *Simosaurus*, die Stumpfschnauze, ein Saurier aus dem Muschelkalke von Luneville [*Simosaurus*, the stump snout, a saurian from the Muschelkalk of Luneville]. Neues Jahrb Mineral Geog Geol Petref. 1842:184–197. German.

Mojsisovics E. 1881. Über die Cephalopoden fauna der Triasschichten von Mora de Ebro in Spanien [On the cephalopod fauna of the Triassic layers of Móra d'Ebre in Spain]. Jb K-K Geol Reichsanst Wien. 1881:105–107.

Motani R. 1999. Phylogeny of the Ichthyopterygia. J Vert Paleontol. 19(3):473–496. doi:10.1080/02724634.1999.10011160.

Motani R, Huang J-D, Jiang D-Y, Tintori A, Rieppel O, You H, Hu Y-C, Zhang R. 2018. Separating sexual dimorphism from other morphological variation in a specimen complex of fossil marine reptiles (Reptilia, Ichthyosauriformes, *Chaohusaurus*). Sci Rep. 8(1):14978. doi:10.1038/s41598-018-33302-4.

Motani R, Jiang D-Y, Chen G-B, Tintori A, Rieppel O, Ji C, Huang J-D. 2015. A basal ichthyosauriform with a short snout from the Lower Triassic of China. Nature. 517(7535):485–488. doi:10.1038/nature13866.

Motani R, Jiang D-Y, Tintori A, Rieppel O, Chen G-B. 2014. Terrestrial origin of viviparity in Mesozoic marine reptiles indicated by Early Triassic embryonic fossils. PLoS ONE. 9(2):e88640. doi:10.1371/journal.pone.0088640.

Motani R, Manabe M, Dong Z-M. 1999. The status of *Himalayasaurus tibetensis* (Ichthyopterygia). Paludicola. 2(2):174–181.

Motani R, Minoura N, Ando T. 1998. Ichthyosaurian relationships illuminated by new primitive skeletons from Japan. Nature. 393(6682):255–257. doi:10.1038/30473.

Motani R, You H-L, McGowan C. 1996. Eel-like swimming in the earliest ichthyosaurs. Nature. 382(6589):347–348. doi:10.1038/382347a0.

Müller J. 2005. The anatomy of *Askeptosaurus italicus* from the Middle Triassic of Monte San Giorgio and the interrelationships of thalattosaurs (Reptilia, Diapsida). Can J Earth Sci. 42(7):1347–1367. doi:10.1139/e05-030.

Müller J, Renesto S, Evans SE. 2005. The marine diapsid reptile *Endennasaurus* from the Upper Triassic of Italy. Palaeontology. 48(1):15–30. doi:10.1111/j.1475-4983.2004.00434.x.

Münster G. 1834. Vorläufige Nachricht über einige neue Reptilien im Muschelkalke von Baiern [Preliminary news about some new reptiles in the Muschelkalk of Baiern]. Neues Jahrb Mineral Geog Geol Petref. 1834:521–527. German.

Navidad M, Álvaro M. 1985. El vulcanismo alcalino del Triásico Superior de Mallorca (Mediterráneo Occidental) [The alkaline volcanism of the Upper Triassic of Mallorca (western Mediterranean)]. Bol Geol Minero. 96(1):10–22. Spanish.

Nesbitt SJ, Desojo JB, Irmis RB. 2013. Anatomy, phylogeny and palaeobiology of early archosaurs and their kin. London: Geological Society, London, Special Publications.

Nicholls EL, Brinkman D. 1993a. A new specimen of *Utatsusaurus* (Reptilia: Ichthyosauria) from the Lower Triassic Sulphur Mountain Formation of British Columbia. Can J Earth Sci. 30(3):486–490. doi:10.1139/e93-037.

Nicholls EL, Brinkman D. 1993b. New thalattosaurs (Reptilia: Diapsida) from the Triassic Sulphur Mountain Formation of Wapiti Lake, British Columbia. J Paleontol. 67(2):263–278. doi:10.1017/S0022336000032194.

Nicholls EL, Brinkman D. 1995. A new ichthyosaur from the Triassic Sulphur Mountain formation of British Columbia. In: Sarjeant WAS, editor. Vertebrate fossils and the evolution of scientific concepts. London: Gordon and Breach; p. 521–535.

Nicholls EL, Manabe M. 2004. Giant ichthyosaurs of the Triassic—a new species of *Shonisaurus* from the Pardonet Formation (Norian: Late Triassic) of British Columbia. J Vert Paleontol. 24(4):838–849. doi:10.1671/0272-4634-(2004)024[0838:GIOTTN]2.0.CO;2.

Nicholls EL, Wei C, Manabe M. 2002. New material of *Qianichthyosaurus* Li, 1999 (Reptilia, Ichthyosauria) from the Late Triassic of southern China, and implications for the distribution of Triassic ichthyosaurs. J Vert Paleontol. 22(4):759–765. doi:10.1671/0272-4634(2002)022[0759:NMOQLR]2.0.CO;2.

Nopcsa F. 1928. Palaeontological notes on reptiles. Geol Hung S Palaeontol. 1:3–84.

Nosotti S, Rieppel O. 2003. *Eusaurosphargis dalsassoi* n. gen. n. sp., a new, unusual diapsid reptile from the Middle Triassic of Besano (Lombardy, N Italy). Mem Soc Ital Sci Nat Mus Civ Stor Nat Milano. 31(3):1–33.

Ortí F, Pérez-López A, Salvany JM. 2017. Triassic evaporites of Iberia: sedimentological and palaeogeographical implications for the western Neotethys evolution during the Middle Triassic–Earliest Jurassic. Palaeogeogr Palaeoclimat Palaeoecol. 471:157–180. doi:10.1016/j.palaeo.2017.01.025.

Osborn HF. 1903. The reptilian subclass Diapsida and Synapsida and the early history of the Diaptosauria. Mem Am Mus Nat Hist. 1:449–507.

Ősi A, Botfalvai G, Prondvai E, Hajdu Z, Czirják G, Szentesi Z, Pozsgai E, Götz AE, Makádi L, Csengdi D, et al. 2013. First report of Triassic vertebrate assemblages from the Villány Hills (southern Hungary). Cent Euro Geol. 56:297–335.

Owen R. 1860. Palaeontology; or, a systematic summary of extinct animals and their geologic remains. Edinburgh: Adam and Charles Black.

Pérez-Valera JA. 2005. Ammonoideos y bioestratigrafía del Triásico Medio (Anisiense superior-Ladiniense) en la sección de Calasparra (sector oriental de la Cordillera Bética, Murcia, España) [Ammonoids and biostratigraphy of the Middle Triassic (upper Anisian–Ladinian) in the Calasparra section (eastern sector of the Betic Cordillera, Murcia, Spain)]. Coloq Paleontol. 55:125–161. Spanish.

Pérez-Valera JA, Escudero-Mozo MJ, Arche A, Goy A, López-Gómez J, Pérez-López A, Pérez-Valera F. 2016. Los ammonoideos del Triásico Medio de España. Implicaciones bioestratigráficas y paleobiogeográficas [Middle Triassic ammonoids of Spain: biostratigraphic and palaeobiogeographic implications]. In: Meléndez G, Núñez A, Tomás M, editors. Actas de las XXXII Jornadas de la Sociedad Española de Paleontología. Cuad Mus Geomin. 20:471–478. Spanish.

Pérez-Valera JA, Goy A. 2012. Amonoideos del Triásico Medio (Ladiniense) de la isla de Mallorca [Middle Triassic (Ladinian) ammonoids of the island of Mallorca]. In: Liao J-C, Gámez Vintaned JA, Valenzuela-Ríos JI, García-Forner A, editors. XXVIII Jornadas de la Sociedad Española de Paleontología y Simposios de los Proyectos n.º 587 y 596 del PICG. Valencia y Sóller, 1–6 de Octubre de 2012. Homenaje a Guillem Colom Casasnovas (1900–1993). Libro de Resúmenes. Valencia and Madrid: Universitat de València and Sociedad Española de Paleontología; p. 179–182. Spanish.

Peyer B. 1931a. *Paraplacodus broilii* nov. gen. nov. sp., ein neuer Placodontier aus der Tessiner Trias: vorläufige Mitteilung [*Paraplacodus broilii* nov. gen. nov. sp., a new placodont from the Triassic of Ticino: preliminary communication]. Centralbl Mineral Geol Paläontol B. 1931:570–573. German.

Peyer B. 1931b. Die Triasfauna der Tessiner Kalkalpen. IV. *Ceresiosaurus calcagnii* nov. gen. nov. spec. [The fauna from the Triassic of the Ticino calcareous Alps. IV. *Ceresiosaurus calcagnii* nov. gen. nov. spec.]. Abh Schweiz Paläontol Ges. 51:1–68. German.

Peyer B. 1955. Die Triasfauna der Tessiner Kalkalpen. XVIII. *Helveticosaurus zollingeri*, n.g. n.sp. [The fauna from the Triassic of the Ticino calcareous Alps. XVIII. *Helveticosaurus zollingeri*, n.g. n.sp.]. Schweiz Paläontol Abh. 72:3–50. German.

Pomar-Gomà L. 1979. The Triassic of the Balearic Islands. Palma: Geology Department, Palma de Mallorca University.

Rein S. 2008. *Ceratites atavus* auf Mallorca? – die Muschelkalkammonoideen des Museu Balear Sciencies Naturals Sóller [*Ceratites atavus* in Mallorca? – the Muschelkalk ammonoids of the Museu Balear de Ciències Naturals of Sóller]. Vernate. 27:5–19. German.

Renesto S, Dal Sasso C, Fogliazza F, Ragni C. 2020. New findings reveal that the Middle Triassic ichthyosaur *Mixosaurus cornalianus* is the oldest amniote with a dorsal fin. Acta Palaeontol Pol. doi:10.4202/app.00731.2020

Rieppel O. 1987. *Clarazia* and *Hescheleria*: a re-investigation of two problematical reptiles from the Middle Triassic of Monte San Giorgio (Switzerland). Palaeontogr Ab A. 195(4–6):101–129.

Rieppel O. 1994. Osteology of *Simosaurus gaillardoti* and the relationships of stem-group Sauropterygia. Fieldiana Geol. 28:1–85.

Rieppel O. 2000a. Part 12A: Sauropterygia I: Placodontia, Pachypleurosauroidea, Nothosauroidea, Pistosauroidea. In: Wellnhofer P, editor. Handbuch der Paläoherpetologie/Encyclopedia of Paleoherpetology. München: Verlaf Dr. Friederich Pfeil.

Rieppel O. 2000b. *Paraplacodus* and the phylogeny of the Placodontia (Reptilia: Sauropterygia). Zool J Linn Soc. 130(4):635–659. doi:10.1111/j.1096-3642.2000.tb02204.x.

Rieppel O. 2002. The dermal armor of the cyamodontoid placodonts (Reptilia, Sauropterygia): morphology and systematic value. Fieldiana Geol. 46:1–41.

Rieppel O. 2019. Mesozoic sea dragons: Triassic marine life from the ancient tropical lagoon of Monte San Giorgio. Indiana: Indiana University Press.

Rieppel O, Hagdorn H. 1998. Fossil reptiles from the Spanish Muschelkalk (Mont-ral and Alcover, Province Tarragona). Hist Biol. 13(1):77–97. doi:10.1080/08912969809386575.

Rieppel O, Liu J, Li C. 2006. A new species of the thalattosaur genus *Anshunsaurus* (Reptilia: Thalattosauria) from the Middle Triassic of Guizhou Province, southwestern China. Vert PalAs. 40(2):114–126.

Rieppel O, Mazin JM, Tchernov E. 1997. Speciation along rifting continental margins: A new nothosaur from the Negev (Israel). Earth Planet Sci. 325:991–997.

Rieppel O, Mazin J-M, Tchernov E. 1999. Sauropterygia from the Middle Triassic of Makhtesh Ramon, Negev, Israel. Fieldiana Geol. 40:1–85.

Rieppel O, Wild R. 1996. A revision of the genus *Nothosaurus* (Reptilia: Sauropterygia) from the Germanic Triassic, with comments on the status of *Conchiosaurus clavatus*. Fieldiana Geol. 34:1–82.

Rodríguez-Perea A, Ramos-Guerrero E, Pomar L, Paniello X, Obrador A, Martí J. 1987. El Triásico de las Baleares [The Triassic of the Balearic Islands]. Cuad Geol Ibér. 11:295–321. Spanish.

Rotger P. 1952. Hallazgo de un ammonites del tipo *Ceratites* en el Muschelkalk de Canet (Esporlas) [Discovery of a *Ceratites*-like ammonite in the Muschelkalk of Canet (Esporles)]. Bol Soc Hist Nat Baleares. 1952(1):6. Spanish.

Sander PM. 1997. The paleobiogeography of *Shastasaurus*. In: Callaway JM, Nicholls EL, editors. Ancient marine reptiles. London and New York: Academic Press; p. 17–43.

Sander PM. 2000. Ichthyosauria: their diversity, distribution, and phylogeny. Paläontol Z. 74(1/2):1–35. doi:10.1007/BF02987949.

Sander PM, Chen X, Cheng L, Wang X. 2011. Short-snouted toothless ichthyosaur from China suggests Late Triassic diversification of suction feeding ichthyosaurs. PLoS ONE. 6(5):e19480. doi:10.1371/journal.pone.0019480.

Sander PM, Klein N, Albers PCH, Bickelmann C, Winkelhorst H. 2013. Postcranial morphology of a basal Pistosauroidea (Sauropterygia) from the Lower Muschelkalk of Winterswijk, The Netherlands. Paläontol Z. 88 (1):55–71. doi:10.1007/s12542-013-0181-5.

Santos A, Mayoral E, da Silva CM, Cachão M, Domènech R, Martinell J. 2008. Trace fossil assemblages on Miocene rocky shores of southern Iberia. In: Wisshak M, Tapanila L, editors. Current Developments in Bioerosion. Berlin and Heidelberg: Springer-Verlag; p. 431–450.

Sanz JL. 1980. Los notosaurios españoles. Análisis filogenético y sistemático de los sauropterigios triásicos [The Spanish nothosaurs. Phylogenetic and systematic analysis of the Triassic sauropterygians] [dissertation]. Madrid: Universidad Complutense de Madrid. Spanish.

Sanz JL. 1983. Los Nothosaurios (Reptilia, Sauropterygia) españoles [The Spanish nothosaurs (Reptilia, Sauropterygia)]. Estudios Geol. 39:193–215. Spanish.

Sanz T, Lago M, Galé C, Ubide T, Pocoví A, Gil A. 2013. Las rocas magmáticas de la Sierra de Tramuntana (N de Mallorca, España): contexto estratigráfico [The magmatic rocks of the Tramuntana Ranges (N of Mallorca, Spain): stratigraphic context]. Geogaceta. 54:39–42. Spanish.

Sato T, Cheng Y-N, Wu X-C, Li C. 2010. Osteology of *Yunguisaurus* Cheng et al. 2006 (Reptilia; Sauropterygia), a Triassic Pistosauroid from China. Paleontol Res. 14(3):179–195. doi:10.2517/1342-8144-14.3.179.

Scheyer TM, Neenan JM, Bodogan T, Furrer H, Obrist C, Plamondon M. 2017. A new, exceptionally preserved juvenile specimen of *Eusaurosphargis dalsassoi* (Diapsida) and implications for Mesozoic marine diapsid phylogeny. Sci Rep. 7(1):4406. doi:10.1038/s41598-017-04514-x.

Schlotheim EFV. 1820. Die Petrefactenkunde auf ihrem jetzigen Standpunkte durch die Beshreibung seiner Sammlung versteinerter und fossiler Überreste des Thier- und Pflanzernreichs der Vorwelt erläutert [The Petrefactenkunde explained at its current point of view by describing its collection of petrified and fossil remains of the animal and plant kingdom of the previous world]. Gotha: Becker. German.

Schmidt M. 1936. Fossilien der spanischen Trias [Fossils from the Spanish Triassic]. Sitzungsber Heidelb Akad Wiss Math Naturwiss Kl. 22:1–140. German.

Schmitz L, Sander PM, Storrs GW, Rieppel O. 2004. New Mixosauridae (Ichthyosauria) from the Middle Triassic of the Augusta Mountains (Nevada, USA) and their implications for mixosaur taxonomy. Palaeontogr Abt A. 270:133–162.

Scotese CR. 2014. Atlas of Middle and Late Permian and Triassic Paleogeographic Maps, maps 43 – 48 from Volume 3 of the PALEOMAP Atlas for ArcGIS (Jurassic and Triassic) and maps 49 – 52 from Volume 4 of the PALEOMAP Atlas for ArcGIS (Late Paleozoic). Evanston (IL): Mollweide Projection, PALEOMAP Project.

Shang Q-H. 2006. A new species of *Nothosaurus* from the early Middle Triassic of Guizhou, China. Vert PalAs. 4(3):237–249.

Shang Q-H, Li C. 2009. On the occurrence of the ichthyosaur *Shastasaurus* in the Guanling Biota (Late Triassic), Guizhou, China. Vert PalAs. 47(3):178–193.

Shikama T, Kamei T, Murata M. 1978. Early Triassic Ichthyosaurus, *Utatsusaurus hataii* Gen. et Sp. Nov., from the Kitakami Massif, Northeast Japan. Sci Rep Tohoku Univ 2s (Geol). 48(1–2):77–97.

Storrs GW. 1991. Anatomy and relationships of *Corosaurus alcovensis* (Diapsida: Sauropterygia) and the Triassic Alcova Limestone of Wyoming. Bull Peabody Mus Nat Hist. 44:1–151.

Stubbs TL, Benton MJ. 2016. Ecomorphological diversifications of Mesozoic marine reptiles: the roles of ecological opportunity and extinction. Paleobiology. 42(4):547–573. doi:10.1017/pab.2016.15.

Sues H-D. 1987. Postcranial skeleton of *Pistosaurus* and interrelationships of the Sauropterygia (Diapsida). Zool J Linn Soc. 90(2):109–131. doi:10.1111/j.1096-3642.1987.tb01351.x.

Tichy G. 1995. Ein früher, durophager Ichthyosaurier (Omphalosauridae) aus der Mitteltrias der Alpen [An early, durophagous ichthyosaur (Omphalosauridae) from the Middle Triassic of the Alps]. Geol-Paläontol Mitt Innsbr. 20:349–369. German.

Tschanz K. 1989. *Lariosaurus buzzii* n. sp. from the Middle Triassic of Monte San Giorgio (Switzerland), with comments on the classification of nothosaurs. Palaeontogr Abt A. 208:153–179.

Vera J-A, Alonso-Chaves FM, Andreo B, Arias C, Azañón JM, Balanyá JC, Barón A, Booth-Rea G, Castro JM, Chacón B, et al. 2004. Capítulo 4. Cordillera Bética y Baleares [Chapter 4: Betic Cordillera and Balearic Islands]. In: Vera J-A, editor. Geología de España [Geology of Spain]. Madrid: IGME; p. 346–464. Spanish.

Virgili C. 1952. Hallazgo de nuevos *Ceratites* en el Triásico mallorquín [Discovery of new *Ceratites* in the Mallorcan Triassic]. Mem Com Inst Geol Diput Prov Barc. 9:19–39. Spanish.

Voigt E. 1965. Über parasitische Polychaeten in Kreide-Austern sowie einige andere in Muschelschalen bohrende Würmer [About parasitic polychaetes in Cretaceous oysters as well as some other worms burrowing bivalve shells]. Paläontol Z. 39(3–4):193–211. German. doi:10.1007/BF02990164.

Wiman C. 1929. Eine neue Reptilien-Ordnung aus der Trias Spitzbergens [A new reptile order from the Triassic of Spitzbergen]. Bull Geol Inst Univ Upsala. 22:183–196. German.

Wu X-C, Cheng Y-N, Sato T, Shan H-Y. 2009. *Miodentosaurus brevis* Cheng et al. 2007 (Diapsida: Thalattosauria): its postcranial skeleton and phylogenetic relationships. Vert PalAs. 47(1):1–20.

Wu X-C, Zhao L-J, Sato T, Gu S-X, Jin X-S. 2015. A new specimen of *Hupehsuchus nanchangensis* Young, 1972 (Diapsida, Hupehsuchia) from the Triassic of Hubei, China. Hist Biol. 28(1–2):43–52. doi:10.1080/08912963.2015.1013953.

Young C-C, Dong Z-M. 1972. *Chaohusaurus geishanensis* from Anhui Province. Mem Inst Vert Paleontol Paleoanthrop Acad Sinica A. 9:11–14.

Zhao L-J, Sato T, Liu J, Li C, Wu X-C. 2010. A new skeleton of *Miodentosaurus brevis* (Diapsida: Thalattosauria) with a further study of the taxon. Vert PalAs. 48(1):1–10.

Chapter 5

The middle–late Permian of Menorca

© Henry S. Sharpe

Chapter 5 was published as:

Matamales-Andreu, R.; Roig-Munar, F.X.; Oms, O.; Galobart, À. & Fortuny, J. (2021). A captorhinid-dominated assemblage from the palaeoequatorial Permian of Menorca (Balearic Islands, western Mediterranean). *Earth and Environmental Science Transactions of the Royal Society of Edinburgh*, 112(2): 125–145.

DOI: https://doi.org/10.1017/S1755691021000268

In this work, R. Matamales-Andreu contributed in:

A. Literature review of the Permian of Menorca.
B. Direct examination of all the collections containing fossils from the studied outcrop.
C. Geological cartography.
D. Logging of the stratigraphic section.
E. 3D modelling and measurement of relevant parameters on tetrapod tracks.
F. Stratigraphic and sedimentological analysis.
G. Vertebrate palaeoichnology and palaeontology, including identification and description of all the morphotypes.
H. Coding the character matrix and running the phylogenetic analysis.
I. Formal description of the new species *Balearosaurus bombardensis*.
J. Interpretation and discussion of the results.
K. Writing of the original draft and supplementary materials.
L. Preparation of tables 1 and ST1, figures 1–7 and 9, and all the supplementary logs.
M. Collaboration in obtaining funding for palaeoillustration.

Also, refer to:

Appendix 12: Supplementary Material for Matamales-Andreu *et al.* (2021)

Earth and Environmental Science Transactions of the Royal Society of Edinburgh, **112**, 125–145, 2021

Article

A captorhinid-dominated assemblage from the palaeoequatorial Permian of Menorca (Balearic Islands, western Mediterranean)

Rafel MATAMALES-ANDREU[1,2*], Francesc X. ROIG-MUNAR[3], Oriol OMS[4], Àngel GALOBART[1,5] and Josep FORTUNY[1]

[1] Institut Català de Paleontologia Miquel Crusafont, Universitat Autònoma de Barcelona, Edifici ICTA-ICP, c/ Columnes s/n, Campus de la UAB, 08193 Cerdanyola del Vallès, Barcelona, Spain. Email: rafel.matamales@icp.cat
[2] Museu Balear de Ciències Naturals, ctra. Palma-Port de Sóller km 30, 07100 Sóller, Mallorca, Illes Balears, Spain.
[3] Freelance researcher, C/ Carritxaret 18-6, 07749 es Migjorn Gran, Menorca, Illes Balears, Spain.
[4] Departament de Geologia, Universitat Autònoma de Barcelona, avda. de l'Eix Central s/n, Campus de la UAB, 08193 Cerdanyola del Vallès, Barcelona, Spain.
[5] Museu de la Conca Dellà, c/ del Museu 4, 25650 Isona i Conca Dellà, Lleida, Spain.
*Corresponding author. Email: rafel.matamales@icp.cat

ABSTRACT: Moradisaurine captorhinid eureptiles were a successful group of high-fibre herbivores that lived in the arid low latitudes of Pangaea during the Permian. Here we describe a palaeoassemblage from the Permian of Menorca (Balearic Islands, western Mediterranean), consisting of ichnites of small captorhinomorph eureptiles, probably moradisaurines (*Hyloidichnus*), and parareptiles (cf. *Erpetopus*), and bones of two different taxa of moradisaurines. The smallest of the two is not diagnostic beyond Moradisaurinae *incertae sedis*. The largest one, on the other hand, shows characters that are not present in any other known species of moradisaurine (densely ornamented maxillar teeth), and it is therefore described as *Balearosaurus bombardensis* gen. et sp. nov. Other remains found in the same outcrop are identified as cf. *Balearosaurus bombardensis* gen. et sp. nov., as they could also belong to the newly described taxon. This species is sister to the moradisaurine from the lower Permian of the neighbouring island of Mallorca, and is also closely related to the North American genus *Rothianiscus*. This makes it possible to suggest the hypothesis that the Variscan mountains, which separated North America from southern Europe during the Permian, were not a very important palaeobiogeographical barrier to the dispersion of moradisaurines. In fact, mapping all moradisaurine occurrences known so far, it is shown that their distribution area encompassed both sides of the Variscan mountains, essentially being restricted to the arid belt of palaeoequatorial Pangaea, where they probably outcompeted other herbivorous clades until they died out in the late Permian.

KEY WORDS: captorhinidae, central Pangaea, *Hyloidichnus*, moradisaurinae, palaeobiogeography.

Captorhinids were a clade of small to medium-sized early eureptiles that became widespread on Laurasia and Gondwana during the Permian. The earliest known member of the group, of small size and with a single-rowed dentition well suited for insectivory, lived in North America during the late Carboniferous (Müller & Reisz 2005; Reisz *et al.* 2016). Captorhinids radiated during the early Permian, maintaining small forms with a single row of teeth that likely fed on insects or even on smaller tetrapods (e.g., Brocklehurst 2017; Modesto *et al.* 2018 and references therein), which coexisted with other small to medium-sized forms that developed other food processing styles. Some of those species were omnivorous, with teeth arranged in a single row or with several rows of teeth oblique to the jaw margins (Modesto *et al.* 2007; LeBlanc & Reisz 2015; Brocklehurst 2017; Reisz *et al.* 2020), whereas others were high-fibre herbivores, always with multiple rows of teeth arranged more or less parallel to the jaw margins (Dodick & Modesto 1995; Reisz & Sues 2000; Modesto *et al.* 2014, 2019; LeBlanc *et al.* 2015; Brocklehurst 2017). This last group has been classified in a subfamily of their own, the Moradisaurinae de Ricqlès et Taquet, 1982.

Moradisaurines showed a wide range of sizes, from very small species with a skull length of about 25 mm (Olson 1970), to medium-sized species with a skull length of about 450 mm (de Ricqlès & Taquet 1982; Modesto *et al.* 2019). All of them possessed tooth plates with several tooth rows on the dentary and on the maxilla, well suited for high-fibre herbivory (e.g., Dodick & Modesto 1995; Reisz & Sues 2000; LeBlanc *et al.* 2015). In fact, some representatives of both small and medium-sized forms have been inferred to be able to produce a propalinal motion of the lower jaw during food processing (Dodick & Modesto 1995; Modesto *et al.* 2007, 2014, 2019), which enabled them to efficiently grind and shred the plant material on which they fed. The number of rows and teeth per row were variable among the different species and throughout ontogeny (e.g., LeBlanc & Reisz 2015; Jung & Sumida 2017; Modesto *et al.* 2019). In the largest forms, the limb bones became distinctly

©The Author(s), 2021. Published by Cambridge University Press on behalf of The Royal Society of Edinburgh. doi:10.1017/S1755691021000268

more robust (e.g., Modesto *et al.* 2019), but not as much as theoretically expected (Romano & Rubidge 2019). In order to reduce the mechanical stress on the limb bones during locomotion, those herbivorous large forms probably moved more slowly (Romano & Rubidge 2019), which did not compromise their ability to obtain plant food, contrarily to smaller captorhinids, which needed to catch their prey.

Ichnites attributed to captorhinomorphs that could be produced by moradisaurines, corresponding to the ichnogenus *Hyloidichnus* Gilmore, 1927, first appear in Sakmarian rocks (lower Permian) of North America (Lucas *et al.* 2013; Schneider et al. 2020), slightly earlier than the oldest known moradisaurines, which belong to the genus *Captorhinikos* Olson, 1954, reported from the Artinskian to the middle Kungurian (lower Permian) of North and South America (Cisneros *et al.* 2020a and references therein). The genus *Captorhinikos* is currently considered the most basal member and the first high-fibre herbivore of the clade (Brocklehurst 2017; Modesto *et al.* 2019). Larger herbivorous species started to appear shortly after, represented by the genera *Labidosaurikos* Stovall, 1950 (Kungurian, early Permian: Dodick & Modesto 1995), *Kahneria* Olson, 1962a (Kungurian/Roadian?, early/middle Permian: Olson 1962a) and *Rothianiscus* Kuhn, 1961 (Kungurian/Roadian?, early/middle Permian: Olson 1962a), together with other undetermined specimens from southern North America (Kungurian, early Permian: Modesto *et al.* 2016) and Mallorca (Artinskian–Kungurian?, early Permian: Liebrecht *et al.* 2017; Matamales-Andreu *et al.* 2019). This also coincided with an increase in morphological disparity (Brocklehurst 2017), which may have played a part in the ecological success of the group, contributing to the shift to eureptile dominance in the post-Artinskian ichnoassemblages of both Europe and North America (Marchetti *et al.* 2015b, 2019c). There, the ichnogenus *Hyloidichnus* becomes abundant, and in rare cases, it is accompanied by another ichnogenus purportedly produced by large moradisaurines, *Merifontichnus* Gand, Garric, Demathieu et Ellenberger, 2000 (Gand & Durand 2006; Marchetti 2016; Citton *et al.* 2019; Santi *et al.* 2020). In the middle–upper Permian, moradisaurines appear represented by small-sized species in eastern Europe (*Gecatogomphius* Vjushkov et Chudinov, 1957, middle Permian: Ivakhnenko 2008), central-east Asia (*Gansurhinus* Reisz, Liu, Li et Müller, 2011, middle–late Permian: Reisz *et al.* 2011) and North Africa (*Acrodenta* Dutuit, 1976, and other unidentified moradisaurines, late? Permian: Jalil & Dutuit 1996; Hmich *et al.* 2006), and the largest known species, in central Africa (*Moradisaurus* Taquet, 1969, middle–late? Permian: Olroyd & Sidor 2017; Modesto *et al.* 2019). The most recent ichnites attributed to moradisaurines belong to the ichnogenus *Hyloidichnus* and were found in upper Permian rocks of North Africa (Voigt *et al.* 2010).

As evidenced by some of the works cited above, the record of body fossils of moradisaurine captorhinid eureptiles in southern Europe was hitherto restricted to the island of Mallorca (Balearic Islands, western Mediterranean). Liebrecht *et al.* (2017) described a fragment of maxilla and parts of the palate of a large moradisaurine, which confirmed the presence of this clade on the island, previously inferred from tracks (Calafat *et al.* 1986, 1986–1987; Calafat 1988; Gand *et al.* 2010; Matamales-Andreu *et al.* 2019). Both the bones and the tracks were found in Port des Canonge unit, the age of which is at present unclear and under study, preliminarily dated as lower Permian (Artinskian or Kungurian) (Matamales-Andreu *et al.* 2019). Nevertheless, from the Permian beds of the neighbouring island of Menorca, some authors (Pretus & Obrador 1987; Carmona 2004) had also reported large bones of unidentified tetrapods, which had not been studied in detail so far.

The first report of vertebrate remains on Menorca was published by Pretus & Obrador (1987), illustrating a large scapula found *ex situ*. That and other bones, herein revised, were the object of the preliminary work of Carmona (2004), who suggested that two of the fossil vertebrae belonged to a large and a small species of indeterminate seymouriamorphs. However, it is worth noting that Carmona (2004) did not consider all the bones that had been collected until then, because some of them had yet to be prepared.

The present work resumes the study of tetrapod bone remains from the Permian of Cala del Pilar–Pla de Mar section (Menorca, Balearic Islands, western Mediterranean), re-assigning all of them to moradisaurine captorhinid eureptiles. This includes the detailed description of all the material present in old collections except for the scapula figured by Pretus & Obrador (1987), which is currently housed in a private collection and preparation required to properly study it has not been possible. Moreover, new ichnological material found at the outcrop is also studied. Unfortunately, new prospection/excavation campaigns have not been carried out due to administrative setbacks. Nevertheless, this study aims to shed light on the hitherto poorly described tetrapod fossils of this site, characterising a new locality of Permian palaeoequatorial faunas.

1. Geological and geographical context

Menorca is the northeasternmost island of the Balearic Archipelago, located in the western Mediterranean. Even as an extension towards the NE of the Betic Orogen, Menorca is quite different from the rest of the Balearic Islands in structural and stratigraphic terms (Bourrouilh 1973; Vera *et al.* 2004; Sàbat *et al.* 2018). Geologically, the island is neatly divided into two main regions: Migjorn, at the S, where a post-orogenic upper Miocene cover is largely dominant; and Tramuntana, at the N, with older materials that broadly span from the Lochkovian (Lower Devonian) to the Rupelian (lower Oligocene) (Bourrouilh 1973, 1983; Vera *et al.* 2004; Martin-Closas & Ramos 2005) (Fig. 1a). The Permian red-beds studied in the present paper, framed between two erosive surfaces, lay within the latter structural unit. They are unconformably disposed over the underlying Devonian or Carboniferous rocks, and the top of their sequence is eroded and overlain by the Lower–Middle Triassic *Buntsandstein* facies (Gómez-Gras 1987, 1992, 1993; Rosell *et al.* 1988, 1989a, b; Bercovici *et al.* 2009; Linol *et al.* 2009). Those beds were first attributed to the upper Permian by Bourrouilh (1973, 1983) and were subsequently studied by Pomar-Gomà (1979), Obrador (1983), Martí *et al.* (1985), Rodríguez-Perea *et al.* (1987), Gómez-Gras (1987, 1992, 1993), Rosell *et al.* (1988, 1989a, b), Arribas *et al.* (1990), Brandes & Tiedt (1991), Broutin *et al.* (1992), Gómez-Gras & Alonso-Zarza (2003), Bercovici *et al.* (2009), Linol *et al.* (2009) and Borruel-Abadía *et al.* (2019).

Despite all these detailed works, the precise palaeogeographic position of Menorca before the Alpine orogeny is still a matter of discussion. During the late Carboniferous–early Permian, the extensional collapse of the Variscan orogen in Iberia and neighbouring regions opened many rift basins, which were filled with continental sediments until the Middle Triassic (López-Gómez *et al.* 2019a). Some authors (Gómez-Gras 1992, 1993; Sàbat *et al.* 2018) have argued that the sections of Menorca have a sedimentary evolution that is somewhat reminiscent to that of the basins of the SW of the Catalan Coastal Ranges, in the eastern margin of the Iberian Peninsula. However, the palaeocurrent directions of the Permian and Triassic of Menorca point generally towards the SW (Linol *et al.* 2009), whereas in the Iberian Peninsula the trend is towards the SE (López-Gómez & Arche 1987, 1992; Arche & López-Gómez 1992), and, therefore, it is unlikely that they were part of a same fluvial system or (sub) basin. The most probable scenario with the data available

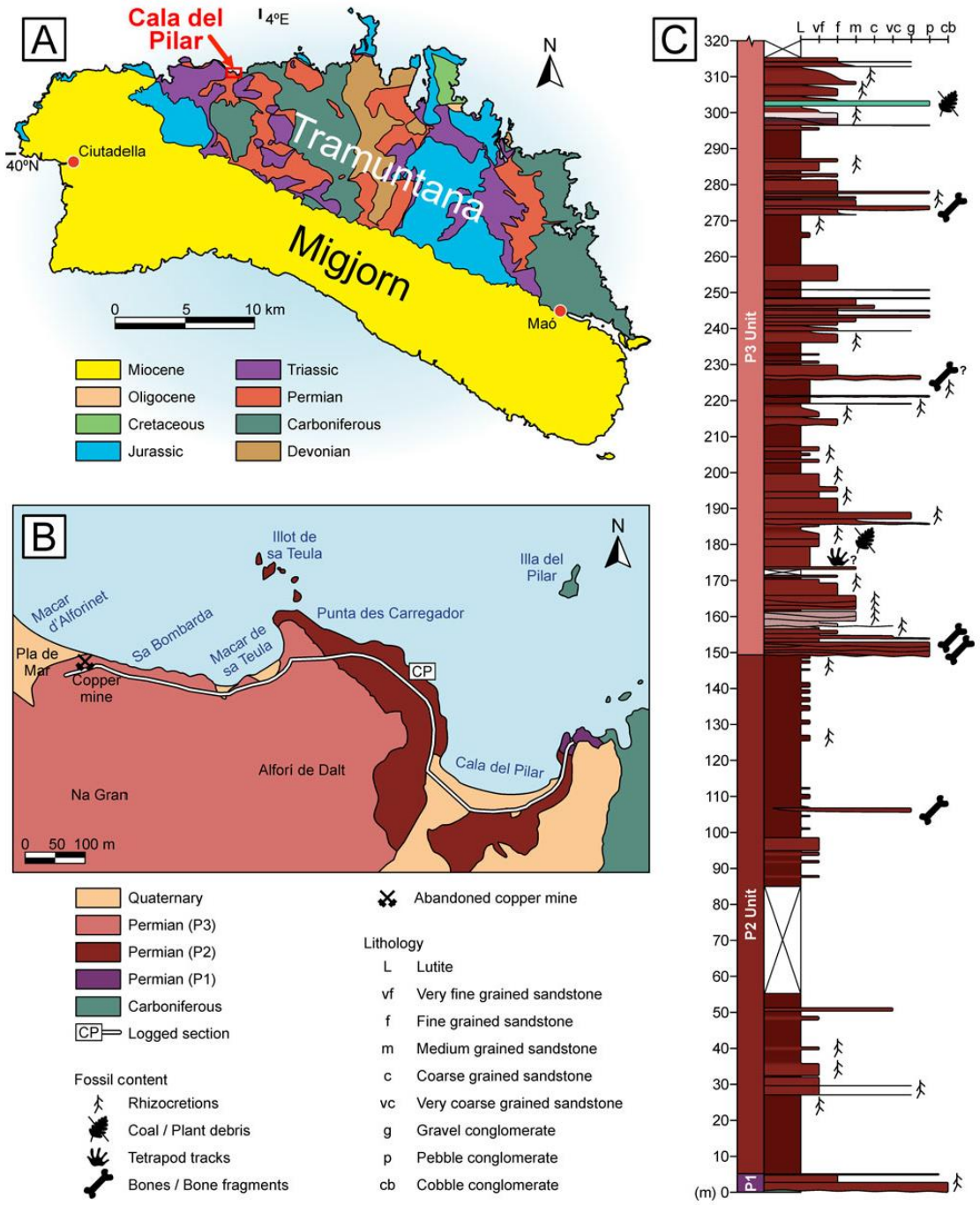

Figure 1 (A) Geological map of Menorca (modified after Rosell *et al.* 1989a), indicating the location of Cala del Pilar. (B) Detailed geological map of the study zone, indicating where the section was logged (toponyms after Buenaventura 2004). (C) Synthetic stratigraphic log of Cala del Pilar–Pla de Mar section, indicating the fossiliferous horizons. Those with a question mark were found *ex situ* and attributed to that bed based on lithological equivalence.

today is that the Menorcan basin was relatively independent from the other basins of Iberia, including that of the neighbouring island of Mallorca. In any case, the Menorcan basin was probably located very close to the equator throughout the Permian, approximately in a latitude of 4° N (Scotese 2014), in the western margin of the Palaeotethys ocean (Bercovici *et al.* 2009; Linol *et al.* 2009). The climate was tropical, alternating arid and hot seasons with rainy seasons (Gómez-Gras & Alonso-Zarza 2003; Bercovici *et al.* 2009; Roscher *et al.* 2011).

Gómez-Gras (1987) described three lithostratigraphic units for the Permian of Menorca (informally named P1, P2 and P3), which were revised by Rosell *et al.* (1988, 1989a, b), Gómez-Gras (1992, 1993), Bercovici *et al.* (2009) and Linol *et al.* (2009). For the present paper, one stratigraphic section has been logged

in detail at the cliffs between Cala del Pilar and Pla de Mar (Fig. 1b, c; Supplementary Material 1 available at https://doi.org/10.1017/S1755691021000268), encompassing the three lithostratigraphic units.

1.1. Palaeoenvironment and climatic conditions

The palaeoenvironments of the Permian recorded in Cala del Pilar–Pla de Mar section changed through time, responding to the evolution of the basin and its climatic conditions. A review of the three main lithostratigraphic units, based on the works of Gómez-Gras (1987, 1992, 1993), Rosell *et al.* (1988, 1989a, b), Gómez-Gras & Alonso-Zarza (2003), Bercovici *et al.* (2009), Linol *et al.* (2009) and new data collected for the present study, is offered here.

In the studied section, the P1 unit consists of 4–6 m of crudely bedded, coarse breccias with intercalated sandstones, overlaying the angular, erosive boundary with the Carboniferous *Culm* facies. In the first stages of rifting, when the subsidence rates are high, alluvial/colluvial fans transverse to the main axis of the basin usually develop near the footwall scarp (e.g., Speksnijder 1985; Miall 2006; Franzel *et al.* 2021 and references therein). The P1 unit is here interpreted as one of such deposits, and the formation of calcareous mature palaeosols on top of each of the breccia beds (Gómez-Gras & Alonso-Zarza 2003; Bercovici *et al.* 2009) attests that the depositional events that formed this unit were multiple, separated in time and under a climate with periods of very low precipitation (Gómez-Gras & Alonso-Zarza 2003). Apart from rhizocretions, no fossils have been reported from the P1 unit so far.

In the studied section, the P2 unit consists of about 150 m of massive lutites with sporadic intercalations of sandstones with climbing ripples and, rarely, microbreccias of reworked pedogenic calcretes. This unit represents a playa lake palaeoenvironment (as defined by Briere 2000) in which lutites from overbank flows were deposited (Bercovici *et al.* 2009). Throughout the sequence, there is an alternation of 1–12 m-thick lutitic packs with 0.25–1.5 m-thick intervals that are more resistant to the erosion, with immature palaeosols and/or mud cracks. The former correspond to the deposition of fine sediments during high water table periods, whereas the latter reflect intervals of desiccation of the playa lakes and subsequent formation of mud cracks and incipient palaeosols. Appearing between those, there are sandstone and microbreccia beds with geometries ranging from lenticular (channelled flow) to tabular (unconfined flow), representing crevasse splays and sheetfloods that reworked the floodplains in sporadic heavy rain events (Gómez-Gras & Alonso-Zarza 2003). The fossil content of this unit consists of rhizocretions developed in different types of palaeosols (Bercovici *et al.* 2009), and bones and bone fragments that have been observed in a bed of reworked pedogenic calcrete fragments.

The studied section also comprises the lower 170 m of the P3 unit, consisting of sandstones intercalated with lutites. The bases of the sandstone elements are usually erosive, with a lag of abundant reworked pedogenic calcretes from the floodplains (Gómez-Gras & Alonso-Zarza 2003). Sandstones are organised in two main sequence types: the first, with lateral accreting surfaces and a general upwards decrease of grain size, representing meandering channels, and the second, consisting mostly of tabular beds with horizontal, low-angle cross-bedding or climbing ripple lamination, representing sheetflood deposits. Lutites are mostly massive and with a pervasive development of calcareous palaeosols (Bercovici *et al.* 2009). This unit represents a floodplain (playa, as per Briere 2000) with abundant vegetation under a seasonal climate. It was traversed by meandering rivers and, during the rainy seasons, unconfined sheetfloods covered the floodplain. One of the meandering channels, observed at m 301.5–303.5 of the studied section, corresponds to sandstone and breccia beds with abundant lignite lenses and plant debris. This channel was probably abandoned as an oxbow lake, where local reducing conditions favoured precipitation of copper minerals (Crespí & Merino 1998; Llull & Perelló 2013). Other areas of the floodplain were swamped or with a high water table for long time intervals, developing alfisols (Bercovici *et al.* 2009), which have been recognised in several beds of this unit. The most abundant fossils of the P3 unit are rhizocretions (Bercovici *et al.* 2009) and ichnofossils of the *Scoyenia* ichnofacies, including tetrapod tracks. Bones and bone fragments are also locally abundant as part of reworked pedogenic calcrete breccias.

The uppermost part of the P3 unit, cropping out NW of Pla de Mar at Penyals d'Alforinet, has not been considered in the present study because it is separated from the lower part by a very thick covered interval, probably faulted and, moreover, no tetrapod fossils have been found there so far. It was studied in great detail by Bercovici *et al.* (2009) and Linol *et al.* (2009), and the palaeoenvironments recorded there are similar to those of the rest of the P3 unit.

2. Material and methods

2.1. Collection number abbreviations

FMNH = Field Museum of Natural History, Chicago, Illinois, USA; IPS = Institut Català de Paleontologia Miquel Crusafont (formerly Institut de Paleontologia de Sabadell), Sabadell, Barcelona, Spain; MBCN = Museu Balear de Ciències Naturals, Sóller, Mallorca, Balearic Islands, Spain; MNHN = Muséum National d'Histoire Naturelle, Paris, France; MT = Macar de sa Teula, field code for the rock with the ichnites, which was left in the field: GPS coordinates [40°3′9″N, 3°58′24″E].

2.2. ZooBank registration of new names

New taxon names have been registered in ZooBank (http://zoobank.org) in order to comply with the rules of the International Code of Zoological Nomenclature for electronic publications (article 8.5.3). The LSID for this publication is: urn:lsid:zoobank.org:pub:8153E0E1-9B66-4C55-89B9-A246195DCD02.

2.3. Stratigraphy and sedimentology

For the stratigraphic and sedimentological study, one section has been logged *in situ*, bed by bed, to a minimum resolution of 1 cm of bed thickness (in 1:25 scale), using a tape measure in well-exposed outcrops and a Jacobs staff for lutite, semi-covered and covered intervals. This section, named Cala del Pilar–Pla de Mar, is presented here in Supplementary Material 1 (in 1:40 scale), and a synthetic version is in Figure 1c (in 1:1160 scale). The recognised sedimentary lithofacies have been classified according to Miall (1985, 2006), Postma (1990), Mack *et al.* (1993), Gómez-Gras & Alonso-Zarza (2003), Bercovici *et al.* (2009) and Linol *et al.* (2009) (Supplementary Material 1).

2.4. Provenance and three-dimensional (3D) modelling of tetrapod ichnofossils

The tetrapod ichnites studied in the present work (MT01) were all preserved as natural casts on the surface of an *ex situ* rock found on the beach of Macar de sa Teula. The rock seemed freshly detached from its original bed, which was determined on the outcrop that had to be the one from m 174.0–179.5 (Fig. 1c), because both the bed and the *ex situ* rock had approximately the same thickness and consisted in very fine sandstones (somewhat silty) with abundant invertebrate burrows and common gleyed patches, unlike other nearby beds. Therefore, its position has been indicated in Figure 1c with a question mark. A photogrammetric 3D model of the ichnites was created (see '3.

Table 1 Set of measurements taken on selected footprints of MT01. Although all the ichnites have been numbered, only the best preserved ones have been measured. Columns without data correspond to poorly-preserved ichnites that have been used for trackway measurements, such as MT01-3, or to well-preserved ichnites without trackway information, such as MT01-10 and MT01-13.

Track parameters						
Footprint number	MT01-1 (right pes)	MT01-2 (right manus)	MT01-3 (left pes)	MT01-4 (right pes)	MT01-10 (left ?pes)	MT01-13 (right ?manus)
Identification	*Hyloidichnus* isp.					cf. *Erpetopus* isp.
Length (mm)	26.4				22.8	10.9
Width (mm)						11.5
Length sole (mm)	13.0	9.0		13.9	9.5	4.7
Width sole (mm)		15.0		12.6	12.5	5.5
Length I (mm)	6.7				7.3	4.3
Length II (mm)	10.0				8.8	6.4
Length III (mm)	11.4				11.3	7.6
Length IV (mm)	15.0	12.8			15.0	7.8
Length V (mm)		7.8				2.9
Divergence angle I II (°)	15.4				16.7	44.3
Divergence angle II III (°)	4.3				27.9	21.6
Divergence angle III IV (°)	21.7				18.7	
Divergence angle IV V (°)		21.4				95.3
Divergence angle I V (°)						161.5

Trackway parameters (in brackets, footprints taken into consideration for that measurement)			
Footprint numbers of each trackway	MT01-1, MT01-2, MT01-3, MT01-4 (right manus pes set, left pes and right pes)	MT01-10 (left ?pes)	MT01-13 (right ?pes)
Pace angulation pes (°)	71.9 (1 3 4)		
Pace angulation manus (°)			
Divarication pes midline (°)	5.0 (1)		
Divarication manus midline (°)	44.6 (2)		
Stride pes (mm)	78.7 (1 4)		
Stride manus (mm)			
Pace pes (mm)	67.0 (mean of 1 3: 69.4, 3 4: 64.6)		
Pace manus (mm)			
Length pace pes (mm)	39.4 (mean of 1 3: 43.3, 3 4: 35.4)		
Length pace manus (mm)			
Width pace pes (mm)	54.0 (mean of 1 3: 54.0, 3 4: 54.0)		
Width pace manus (mm)			
Interpes distance (mm)	39.9 (1 3)		
Intermanus distance (mm)			
Manus pes distance (mm)	12.9 (1 2)		
Width external (mm)			
Width internal (mm)			
Glenoacetabular distance (mm)			

Systematic palaeoichnology') and then the rock was left in the outcrop.

Photogrammetry is a technique that has recently become widespread in ichnological studies (e.g., Falkingham 2012; Mujal *et al.* 2016, 2020), making it possible to collect and save information that would otherwise be lost to erosion in the case of big, unmovable rock surfaces. Moreover, it provides an alternative to the confection of artificial casts, which are sometimes hard to make in open environments that are difficult to reach. The present study has broadly followed the same methodology as Mujal *et al.* (2016, 2020 and references therein), using the open-source software MeshLab v2016.12 (http://meshlab.sourceforge.net/) and ParaView 5.5.0-RC4 64-bit (http://www.paraview.org) to process the meshes. However, to create the mesh, the licensed software Agisoft Photoscan standard v1.1.4. (www.agisoft.com) has been used instead. In order to produce the 3D model, 89 pictures of the surface of MT01 were taken from different angles and distances using a digital camera (Panasonic Lumix DMC-TZ27). Then, they were aligned, and the dense point cloud and the mesh were created. After that, a false-colour height map and contour lines were superimposed on the 3D model, and finally it was drawn on a vector-based graphics design software and measured using the open-source software ImageJ 1.52d (https://imagej.nih.gov/ij/), following the criteria of Leonardi (1987) and Hasiotis *et al.* (2007) (Table 1). The ichnites selected for study correspond to the category '1' of footprint preservation scale by Marchetti *et al.* (2019a) – that is, relatively poorly preserved ichnites missing some diagnostic structures (i.e., some digits). The other ichnites present on the slab scored a '0', that is, their preservation was very poor (Marchetti *et al.* 2019a), so they could not be studied.

The 3D models studied herein are archived and freely available in MorphoSource (https://www.morphosource.org/) with the following DOI: MT01-1 and MT01-2 (https://doi.org/10.17602/M2/M367858), MT01-10 (https://doi.org/10.17602/M2/M367864) and MT01-13 (https://doi.org/10.17602/M2/M367870).

2.5. Phylogenetic analysis

The phylogenetic analysis was performed using a modified version (Supplementary Material 2) of the matrix of Cisneros *et al.* (2020a), mainly with changes introduced by Modesto *et al.* (2019) and Brocklehurst (2020). All character state changes for *Captorhinikos chozaensis* were applied following Modesto *et al.* (2019), except for their character '72' (here, character

'73') as there was no state 2 (see character list in Modesto *et al.* 2019). Character states for *Moradisaurus* were also recoded following Modesto *et al.* (2019). The rest of character state changes listed by Modesto *et al.* (2019) had already been applied in the matrix of Cisneros *et al.* (2020a). MBCN15730 (the moradisaurine from Mallorca) and *Kahneria* were added to the matrix with the character state codes of Brocklehurst (2020), modifying the following: character '10' of the matrix used by Brocklehurst (2020) was redefined into two characters by Cisneros *et al.* (2020a), so they are now in both cases character '10' with state 1 and character '11' with state 1. Character '42' of MBCN15730 (character '41' in Brocklehurst 2020) was changed from 1 to ?, as the ventral side of the palatine is not visible on the specimen. *Balearosaurus bombardensis* gen. et sp. nov. and the other indeterminate small moradisaurine from Menorca studied in the present work have been coded first-hand. For the final analysis, both the indeterminate small moradisaurine from Menorca and MAP PV664 (Moradisaurinae indet.) from Brazil (Cisneros *et al.* 2020a) were removed because of their large amount of missing data, which caused significant polytomies in the Moradisaurinae. Phylogenetic analysis was run using PAUP* v.4.0 (Swofford 2003) as a branch-and-bound search with parsimony as the optimality criterion, unordered and unweighted characters and with branches collapsing when their maximum length was zero. Then, a strict consensus tree was computed, and bootstrap support values were calculated with 1000 repetitions, not showing values under 50.

3. Systematic palaeoichnology

Ichnogenus *Hyloidichnus* Gilmore, 1927

***Hyloidichnus* isp.**

(Fig. 2a–d; Table 1)

Studied material. MT01-1, MT01-2, MT01-3, MT01-4, natural cast of a partial trackway with a right manus pes set, a left pes imprint and a right pes imprint. MT01-5, natural cast of an isolated left manus imprint. MT01-10, natural cast of a left ?pes imprint. Most of the other footprints of the same surface (MT01-6, MT01-7, MT01-8, MT01-9, MT01-11, MT01-12) may also belong to this ichnogenus given their similar size and general shape but their preservation is too incomplete. All of them were found on an *ex situ* boulder at Macar de sa Teula, attributable to m 174–179.5 of Cala del Pilar–Pla de Mar section, P3 unit, indeterminate Permian, Menorca, Balearic Islands, western Mediterranean.

Description. Pes imprints semiplantigrade, pentadactyl, probably slightly longer (26.4 mm) than wide. The most deeply imprinted parts are digits I and II (medial functional prevalence of the autopodia). The digit imprints radiate from the sole and are relatively slender and straight, with some tips ending in pointed claw traces. The relative length of the preserved digit imprints can be ordered as follows (MT01-1): I < II < III < IV (digit V imprint is not preserved). The sole is anteroposteriorly short, with a well-marked posterior margin that is slightly concave. Manus imprint slightly smaller than pes imprint, semiplantigrade, pentadactyl, wider than long. The most deeply imprinted part is the distal region of digit IV, but digits I–III are not preserved so it is not possible to evaluate the functional prevalence of the autopodia. The digit imprints radiate from the palm and are straight and rather short, with tips ending in pointed claw traces. Given the faint imprints of the two available manus (MT01-2 and MT01-5), the relative length of the preserved digit imprints cannot be established, although digit IV appears to be the longest. Acute divergence angle between digit IV and V imprints (21.4 °). Palm anteroposteriorly short, with a well-marked posterior margin that is very slightly concave. The imprints of the basal parts of all the digits are well defined, and are the deepest imprinted areas of the sole. Trackway of a quadrupedal animal with a simple alternating pattern, with a pace angulation of 71.86 ° for the pedes. The pes imprints are almost parallel to the midline (divarication of 5 °), whereas the manus imprints are strongly rotated inwards (divarication of 44.6 °) and seem to be slightly smaller than those of the pes. The pace of the pes ranges between 64.6 and 69.4 mm, the length of the pace of the pes ranges between 35.4 and 43.3 mm, and the width of its pace is 54.0 mm. The interpes distance is 39.9 mm, and the manus–pes distance is 12.9 mm.

Remarks. The following combination of characters makes it possible to assign these footprints to *Hyloidichnus* (see Gand 1987; Voigt 2005; Voigt *et al.* 2010; Marchetti 2016; Marchetti *et al.* 2020a; Logghe *et al.* 2021): (1) manus imprints slightly smaller than those of the pedes; (2) orientation of pes imprints parallel to the midline; (3) manus imprints rotated inwards; (4) manus imprint located internally to the pes imprint; (5) acute angle between manus digit IV and V imprints; (6) digit imprints with clawed tips; (7) straight and radiating digits in both the pes and the manus imprints; (8) short sole/palm imprints; (9) ectaxonic tracks; and (10) medial–lateral decrease in relief of the track imprints. However, the incomplete preservation of the manus imprints and the trackway precludes any ichnospecies-level assignation. Captorhinomorph eureptiles, and more specifically captorhinids and moradisaurine captorhinids, have been deemed as its most probable trackmakers (e.g., Gand 1987; Haubold 2000; Gand & Durand 2006; Voigt *et al.* 2010; Logghe *et al.* 2021), and this ichnogenus has been found from the Sakmarian (lower Permian) to the Wuchiapingian (upper Permian) (e.g., Lucas 2019; Schneider *et al.* 2020; Logghe *et al.* 2021).

Ichnogenus *Erpetopus* Moodie, 1929

cf. *Erpetopus* isp.

(Fig. 2a, b, e; Table 1)

Studied material. MT01-13, a natural cast of an isolated right ichnite, possibly a manus imprint. Found on an *ex situ* boulder at Macar de sa Teula, attributable to m 174–179.5 of Cala del Pilar–Pla de Mar section, P3 unit, indeterminate Permian, Menorca, Balearic Islands, western Mediterranean.

Description. Semiplantigrade, pentadactyl ichnite, slightly wider (11.5 mm) than long (10.9 mm). The most deeply imprinted parts are the bases of the digit imprints, and, especially, those of digits II and V. The digit imprints are thin and those of digits II–IV are distinctly curved inwards distally, whereas the imprints of digits I and V are somewhat straight. Although some of the digit tip imprints undoubtedly have drag traces (I and V), others show a slightly expanded tip that may have corresponded to claw traces (II–IV). The relative length of the digit imprints can be ordered as follows: V < I < II < III < IV. The divergence angles of digit IV–V imprints is high (95.3 °), and that of the digit I–V imprints forms a clearly obtuse angle (161.5 °). The sole is anteroposteriorly short, concave and well imprinted posteriorly.

Remarks. MT01-13 can be assigned to *Erpetopus* because of the following combination of characters (Marchetti *et al.* 2014): (1) pes slightly wider than long; (2) slender, curved digit imprints with clawed tips; (3) digit imprints with overlapping digit bases, typical of parareptiles (Marchetti *et al.* 2020b); (4) short digit V imprint; (5) high IV–V divergence; (6) high I–V divergence; and (7) small size, less than 20 mm. The most probable trackmakers for *Erpetopus* are acleistorhinid and nyctiphruretid parareptiles, and this ichnogenus has been found from the middle Artinskian (lower Permian) to the Wuchiapingian (upper Permian), being the reference ichnotaxon for the *Erpetopus* footprint biochron (e.g., Lucas 2019; Schneider *et al.* 2020; Cisneros *et al.* 2020b).

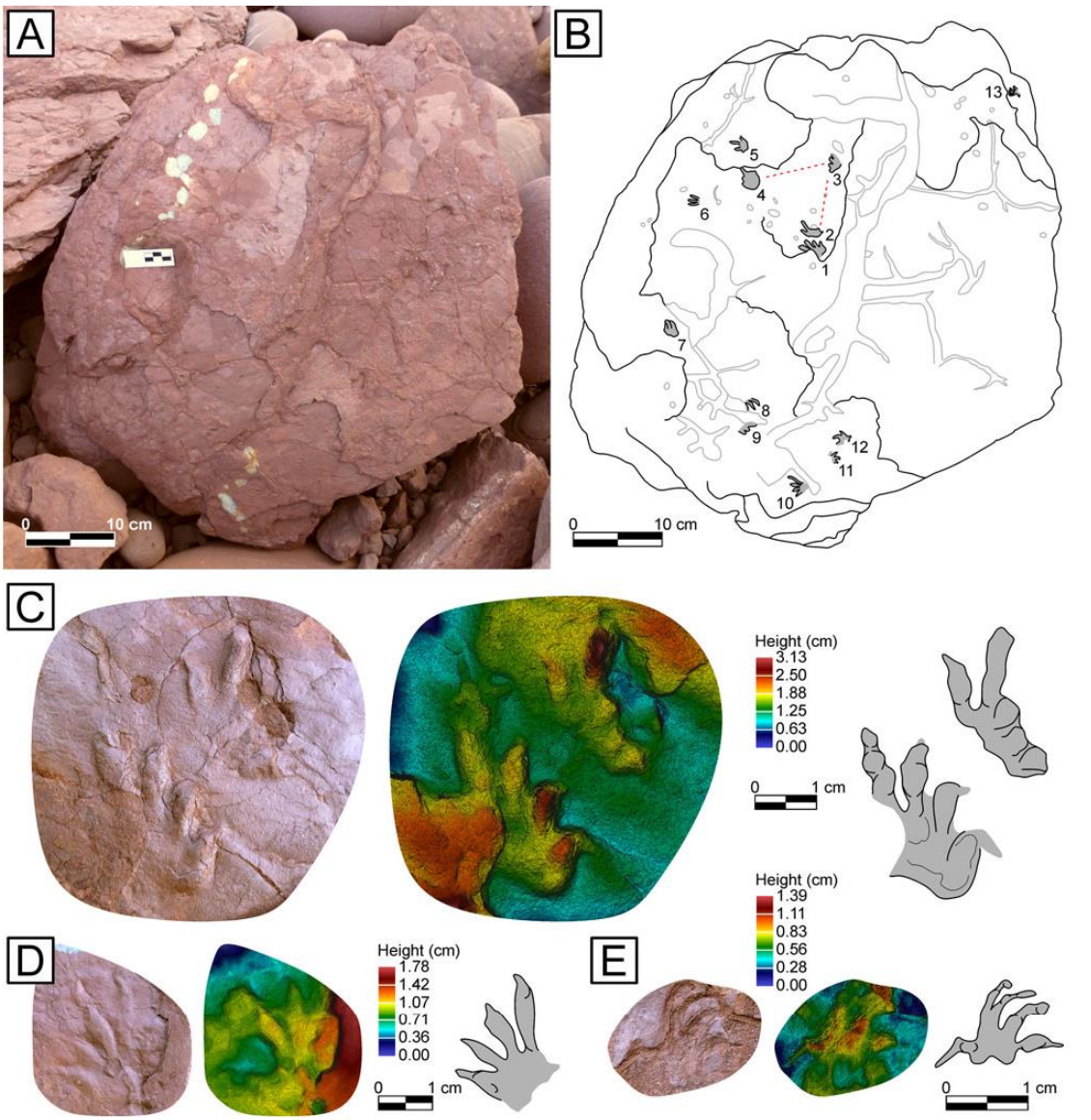

Figure 2 Ichnites of the boulder herein named MT01 from an indeterminate Permian of Cala del Pilar Pla de Mar section (Menorca), with height models and interpretative drawings. (A) Picture of MT01 as it was found. (B) Interpretative drawing of MT01, with each number referring to a specific ichnite under the nomenclature MT01-[number]. (C) Picture, false colour-coded height model and interpretative drawing of MT01-1 and MT01-2 (*Hyloidichnus* isp.). (D) Picture, false colour-coded height model and interpretative drawing of MT01-10 (*Hyloidichnus* isp.). (E) Picture, false colour-coded height model and interpretative drawing of MT01-13 (cf. *Erpetopus* isp.).

4. Systematic vertebrate palaeontology

Reptilia Laurenti, 1768

Eureptilia Olson, 1947

Family Captorhinidae Case, 1911

Subfamily Moradisaurinae de Ricqlès et Taquet, 1982

Genus *Balearosaurus* gen. nov

Type and only included species. *Balearosaurus bombardensis* gen. et sp. nov.

Origin of the name. Combination of *Balearo-*, as it was found in the Balearic Islands, and *-saurus*, Latin for 'lizard'.

Diagnosis. As for the type species.

***Balearosaurus bombardensis* gen. et sp. nov.**

(Fig. 3a–f)

Type specimen. Holotype IPS35597 (fragment of right maxilla and palatine), Cala del Pilar–Pla de Mar section, P3 unit, indeterminate Permian, Menorca, Balearic Islands, western Mediterranean.

Origin of the name. Because most of the fossils here considered to belong to this species were found in the coastal zone called Sa Bombarda (Menorca, Balearic Islands, western Mediterranean).

Studied material. IPS35597 (fragment of right maxilla and palatine), from an *ex situ* rock at Punta des Carregador,

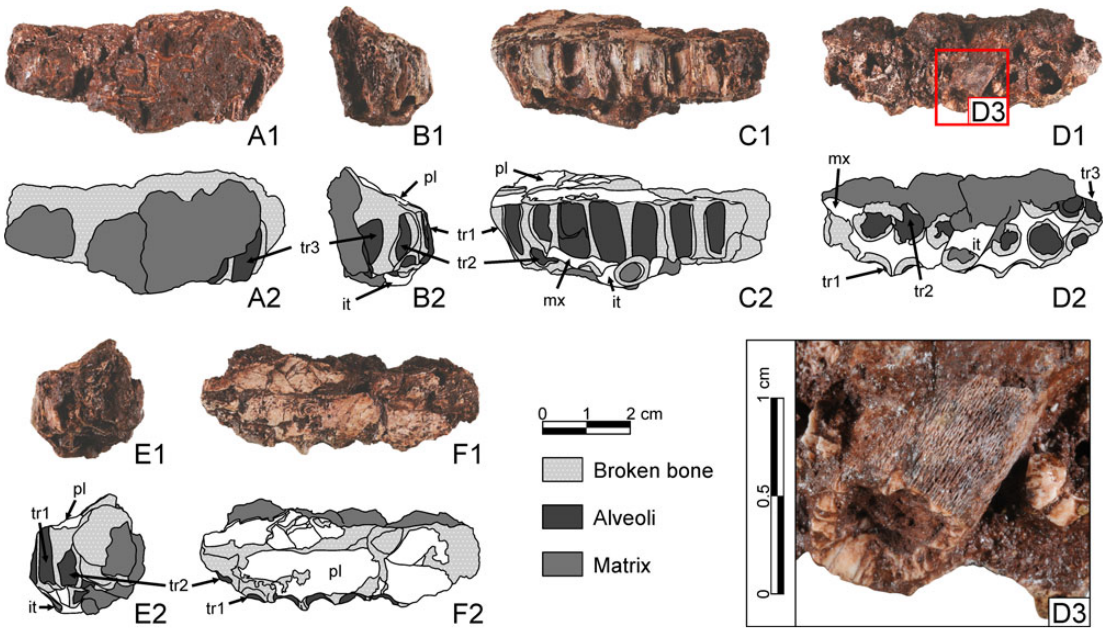

Figure 3 Holotype specimen of *Balearosaurus bombardensis* gen. et sp. nov. (IPS35597, right maxillar and palatine), from an indeterminate Permian of Cala del Pilar Pla de Mar section (Menorca): (A) labial view; (B) anterior view; (C) lingual view; (D) occlusal view; (E) posterior view; (F) dorsal view. Abbreviations: it = isolated tooth; mx = maxillar; pl = palatine; tr1 3 = teeth row 1 3. All specimens in the same scale except for D3.

attributable to m 149.5 of Cala del Pilar–Pla de Mar section, P3 unit, indeterminate Permian, Menorca, Balearic Islands, western Mediterranean.

Diagnosis. Large moradisaurine captorhinid eureptile with a maxilla with at least three rows of cylindrical teeth that possess an external ornamentation based on longitudinal thin ridges and furrows.

Description. Fragment of right maxilla and palatine measuring 67.0 mm in maximum anteroposterior length, with a maximum labiolingual width of 25.6 mm and a maximum dorsoventral height of 27.1 mm. No sutures are visible. Three rows of alveoli can be observed: the one in the lingual side shows traces of six alveoli, all of them sectioned. Some still have remains of thecodont teeth attached. The middle row has also six partially covered alveoli. The labial row has five preserved alveoli, three of which are also sectioned and two that are covered by matrix. All of them have a similar size (maximum diameter 6.4–7.4 mm), and are arranged diagonally to each other. Horizontally on the occlusal side of the maxilla there is a partial isolated cylindrical tooth. Its diameter (7.8 mm) agrees with that of the surrounding alveoli, and its outer surface is covered by an ornamentation consisting of numerous and very thin longitudinal furrows and ridges (Fig. 3d3). On the dorsal side of the maxilla there is a flat surface corresponding to the palatine, tilted 27.3 ° towards the medial part of the cranium.

Remarks. The maxilla clearly agrees with those of large moradisaurine captorhinid eureptiles. IPS35597 shows at least three parallel rows of teeth; the presence of several longitudinal rows of teeth, organised approximately parallel to the jaw margins, is a diagnostic character of Moradisaurinae (Vjushkov & Chudinov 1957; Olson 1962a, b, 1965; de Ricqlès & Taquet 1982; de Ricqlès & Bolt 1983; Jalil & Dutuit 1996; Ivakhnenko 2008; Reisz *et al.* 2011; Modesto *et al.* 2014, 2016, 2019; LeBlanc *et al.* 2015; LeBlanc & Reisz 2015; Jung & Sumida 2017). The maxillary teeth are of a similar diameter than that of the largest members of the subfamily, such as *Labidosaurikos* (see Dodick & Modesto 1995), *Moradisaurus* (see de Ricqlès & Taquet 1982; Modesto *et al.* 2019), *Rothianiscus* (see Olson 1962a, 1965), and the unidentified tooth plates from the 'KB' locality of Texas (Modesto *et al.* 2016) and Mallorca (Liebrecht *et al.* 2017). However, the teeth of all the species in those genera have a smooth surface, devoid of any kind of ornamentation (Olson 1962a, 1965; de Ricqlès & Taquet 1982; Dodick & Modesto 1995; Modesto *et al.* 2016, 2019; Liebrecht *et al.* 2017), contrarily to what can be observed on the isolated tooth on the surface of the maxilla in IPS35597, which is traversed by numerous longitudinal furrows and ridges. Only the *Captorhinikos* sp. described by Cisneros *et al.* (2020a, fig. 2) has small furrows and ridges on some teeth, but they seem to be restricted on the base of the crown, contrarily to the isolated tooth of IPS35597, which has a much denser ornamentation that completely covers the preserved surface of the tooth.

The phylogenetic analysis (Fig. 4) places *Balearosaurus bombardensis* as a derived species within the moradisaurine captorhinids, sister to the undetermined moradisaurine of the neighbouring island of Mallorca, based mostly on the low number of tooth rows. Those two, in turn, are a sister clade of the North American *Rothianiscus*, a genus of large forms with also relatively few rows of teeth, similarly to the Balearic species.

cf. *Balearosaurus bombardensis* gen. et sp. nov.

(Figs 5, 6)

Studied material. IPS35588 (chevron?), IPS35590 (middle caudal vertebra), IPS35592 (anterior dorsal vertebra), IPS35598 (distal fragment of left jaw), IPS120163 (right ilium), IPS120164 (left pubis) and IPS120165 (proximal epiphysis of left tibia), all found in close association in an *ex situ* rock at Sa Bombarda, attributable to m 226–227 of Cala del Pilar–Pla de Mar section, P3 unit, indeterminate Permian, Menorca, Balearic Islands, western Mediterranean.

Description. IPS35598 (Fig. 5a–f): distal fragment of left jaw measuring 66.5 mm in maximum anteroposterior length,

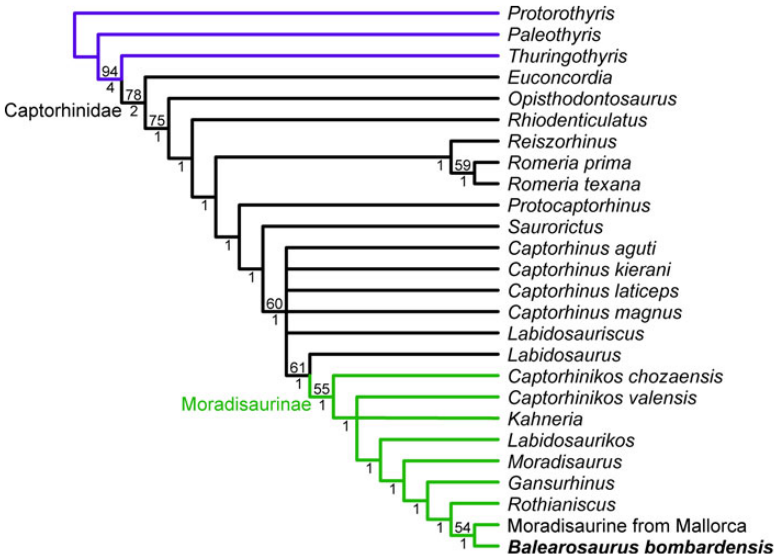

Figure 4 Strict consensus of the best 36 trees recovered (tree length = 251 steps) of the Captorhinomorpha, including the large moradisaurines of the Balearic Islands, using a branch-and-bound search. Consistency index (CI) = 0.553; retention index (RI) = 0.756. Double-digit numbers on the branches represent the bootstrap support values (n = 1000, values under 50 not shown), and single digits below represent the Bremer decay support value of that node.

maximum labiolingual width of 30.9 mm and maximum dorsoventral height of 35.4 mm. No sutures are visible. The anterior and posterior ends are broken off, and the occlusal region and part of the lingual and ventral sides are strongly abraded. Although the teeth are missing, one row of five alveoli, which are hemiellipsoidal in shape, can be observed. The first two alveoli are tilted anteriorly, whereas the other three point dorsally. All the alveoli are relatively small (maximum diameter 5.7–6.1 mm) except for the fourth, which is clearly the largest (diameter 15.2 mm), and must certainly have born a large caniniform. Given the symmetrical shape of the alveoli, the mode of attachment of the teeth was thecodont. In dorsal aspect, the jaw is narrowest in its anterior end, and its lingual side expands considerably near the largest alveolus. In labial aspect, the surface is rather flat, and it is traversed by several shallow grooves. In ventral aspect, it possesses a longitudinal groove.

IPS35592 (Fig. 5g–l): anterior dorsal vertebra measuring 92.0 mm in height, with a maximum width of 93.8 mm and a maximum length of 53.0 mm. Anteroposteriorly compressed, amphicoelous pleurocentrum that measures 36.2 mm in height, with a width of 42.0 mm and length of 26.8 mm, its axis slanting 24 ° anteriorly with respect to the horizontal. The outline of the pleurocentrum is circular in anteroposterior view and spool-shaped in lateral view, because the cortical rim is slightly flared outwards laterally and ventrally. In ventral aspect, the pleurocentrum is slightly flattened, and no evidence of a ridge or keel can be observed. The neural canal has a somewhat pentagonal contour, being more rounded in anterior view (10.5 mm high × 14.7 mm wide) than in posterior view (8.4 mm high × 13.9 mm wide), flattening the dorsal edge of the pleurocentrum. The pedicels are attached dorsolaterally to the pleurocentrum, anteriorly developing a rather shallow, small fossa just above the cortical rim. From the anterior lateroventral sides of the neural canal, two rounded centroprezygapophyseal processes extend laterally on the pedicels, and possess associated infraprezygapophyseal fossae dorsally, just below the edge of the articular surfaces of the prezygapophyses. The neural arch that stands above is notably expanded and swollen, extending out as much as the width of the pleurocentrum. The prezygapophyses extend laterally from the pedicels (each apophysis corresponding to 1/3 of the total width of the vertebra) and are connected to the transverse processes (diapophysis + parapophysis) posterolaterally. The articular surfaces of the prezygapophyses are slightly tilted inwards from the horizontal plane (10 °), and possess a faintly convex obovate contour, which is twice as wide laterally than it is anteroposteriorly. From the medial edges of the prezygapophyses, two carinae extend dorsally, converging at the base of the neural spine. The transverse processes are located between the pre- and postzygapophyses, and are tilted 27 ° from the vertical axis in anteroposterior aspect. The diapophysis is slightly (15 %) thicker than the parapophysis, and they are both connected by an osseous lamina with an angle of 13 ° from the vertical axis in lateral view. Whereas the diapophysis is dorsolaterally detached forming a small process, the parapophysis fuses at mid-length of the posterior region of the prezygapophysis, being reduced to a small bulge. The postzygapophyses are located just behind the diapophyses in anterior view, separated by a rather deep emargination. A small, laterally elongated suprapostzygapophyseal fossa is present anteriorly on the emarginated side. The postzygapophyseal articular facets are slightly tilted inwards (6.5 °) from the horizontal plane, and possess a flat surface. The margins of these surfaces are slightly flared outwards, extending as ridges towards the roof of the neural channel, delimiting the postspinal fossa, which possesses a distinct triangular shape. The hypothetical two edges of the base of that triangle appear on the laminae framing it as two small, dorsolaterally elongated centropostzygapophyseal processes. The dorsal outline of the neural arch in anteroposterior aspect is rather flat, only with small undulations corresponding to the two postzygapophyses and the base of the neural spine. The neural spine is very low (10 % of the total height in anterior view) and thin (6 % of the total width).

IPS35590 (Fig. 5m–r): middle caudal vertebra measuring 44.3 mm in preserved height, with a maximum width of 24.8 mm and a maximum length of 39.8 mm. Cylindrical, amphicoelous pleurocentrum that measures 28.3 mm in height, with a width of 24.8 mm and a length of 26.7 mm, its axis slanting 13.5 ° anteriorly with respect to the horizontal. The cortical rim is slightly flared outwards, and it bears a conspicuous

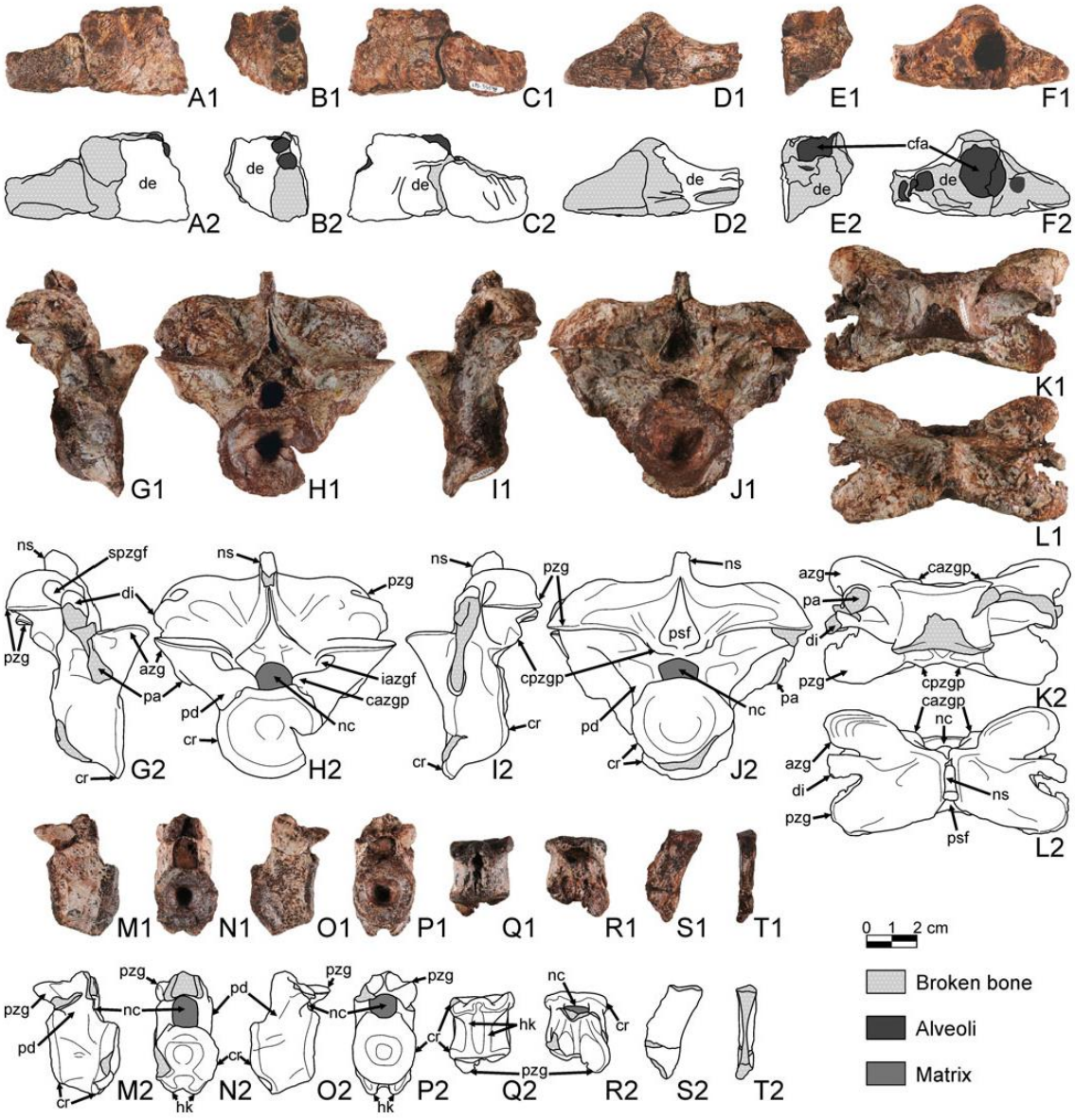

Figure 5 Pictures and interpretative drawings of cranial and axial elements of cf. *Balearosaurus bombardensis* gen. et sp. nov. from an indeterminate Permian of Cala del Pilar Pla de Mar section (Menorca). (A–F) IPS35598, distal fragment of left jaw: (A) lingual view; (B) anterior view; (C) labial view; (D) ventral view; (E) posterior view; (F) occlusal view. (G–L) IPS35592, anterior dorsal vertebra: (G) right lateral view; (H) anterior view; (I) left lateral view; (J) posterior view; (K) ventral view; (L) dorsal view. (M–R) IPS35590, middle caudal vertebra: (M) right lateral view; (N) anterior view; (O) left lateral view; (P) posterior view; (Q) ventral view; (R) dorsal view. (S, T) IPS35588, possible fragment of haemal arch: (S) right lateral view; (T) anterior view. Abbreviations: azg = prezygapophysis; cazgp = centroprezygapophyseal process; cfa = alveolus of caniniform; cpzgp = centropostzygapophyseal process; cr = cortical rim; de = dentary; di = diapophysis; hk = haemal keel; iazgf = infraprezygapophyseal fossa; nc = neural canal; ns = neural spine; pa = parapophysis; pd = pedicel; pl = palatine; psf = postspinal fossa; pzg = postzygapophysis; spzgf = suprapostzygapophyseal fossa.

bulge on the ventral part of the anterior side, located dorsally just between the haemal keels. In ventral aspect, two haemal keels traverse the pleurocentrum, being more prominent on the anterior cortical rim, and decreasing in height towards the posterior end. No clear facets for the haemal arch have been observed. The neural canal has a rectangular contour in anterior view (12.8 mm high × 9.7 mm wide) and is narrower and almost circular in posterior view (8.8 mm high × 10.3 mm wide). In anterior aspect, the neural arch is broken just above the neural canal. Conversely, in posterior aspect, the postzygapophyses can be observed, the right one being complete. It is strongly directed posteriorly, and the articular surface is flat and slightly tilted inwards (24.5 °). The neural spine is not preserved.

IPS35588 (Fig. 5s, t): possible fragment of haemal arch (chevron) measuring 37.5 mm in maximum dorsoventral height, with a lateral width of 7.9 mm and an anteroposterior length of 14.7 mm. Laterally compressed, dorsoventrally elongated fragment, with a rounded anterior margin that becomes thinner posteriorly. Its distal region is broken; its proximal region, corresponding to the articular surface, is not completely ossified and somewhat irregular, forming an angle of about 65.3 ° with respect to the main axis of the bone.

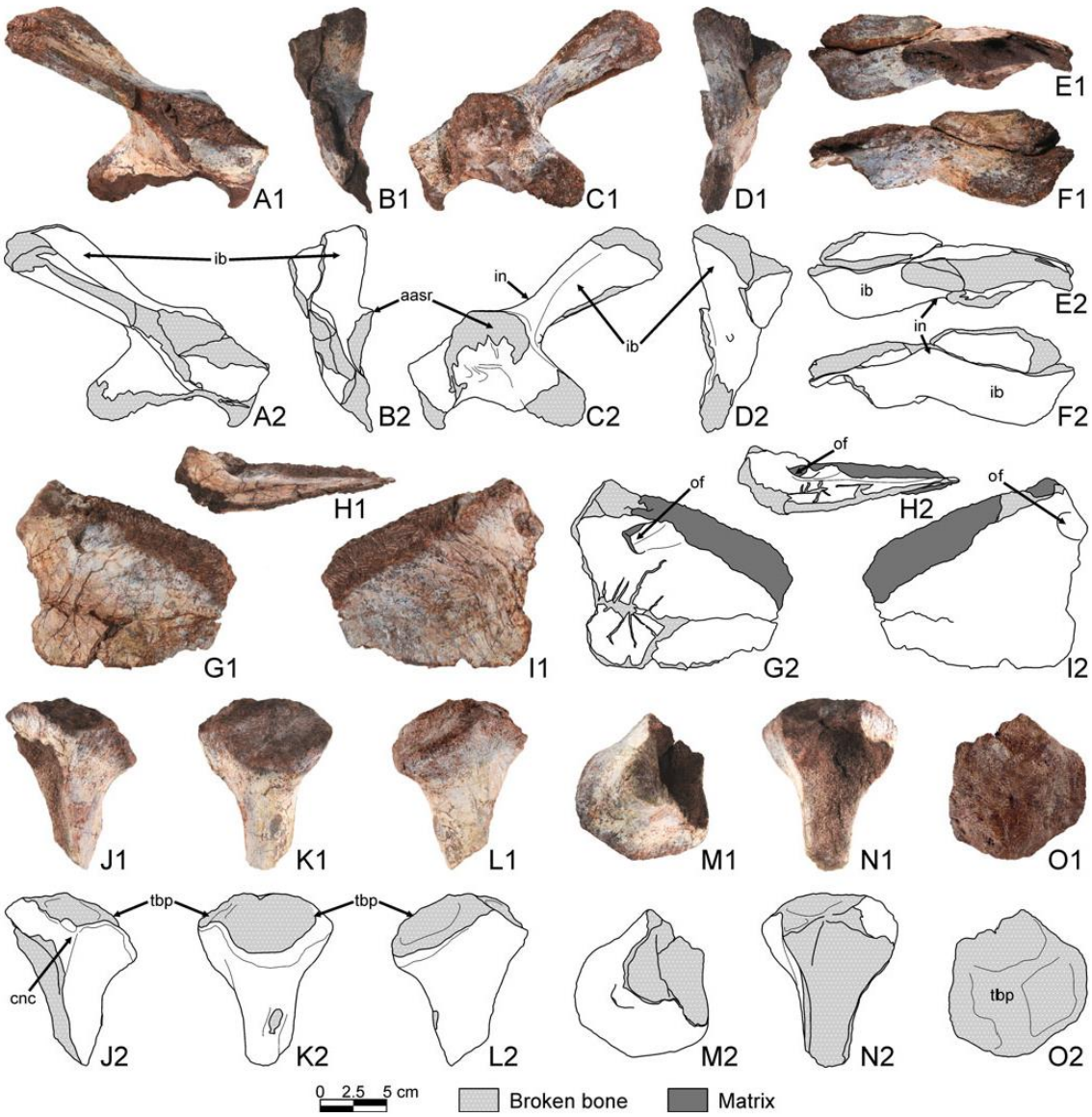

Figure 6 Pictures and interpretative drawings of girdle and limb elements of cf. *Balearosaurus bombardensis* gen. et sp. nov. from an indeterminate Permian of Cala del Pilar Pla de Mar section (Menorca). (A F) IPS120163, right ilium: (A) lateral view; (B) anterior view; (C) medial view; (D) posterior view; (E) ventral view; (F) dorsal view. (G I) IPS120164, left pubis: (G) medial view; (H) ventral view; (I) lateral view. (J O) IPS120165, fragment of the proximal epiphysis of a left tibia: (J) extensor view; (K) lateral view; (L) flexor view; (M) distal view; (N) medial view; (O) proximal view. Abbreviations: aasr = area of attachment of sacral ribs; cnc = cnemial crest; ib = iliac blade; in = iliac neck; of = obturator foramen; tbp = tibial plateau.

IPS120163 (Fig. 6a–f): right ilium, with a lateral surface that appears to be smooth and with no trace of the acetabulum. Anteriorly, the bone ends abruptly in a flat, unfinished surface, corresponding to the suture with the pubis. Ventrally and posteriorly, the bone is eroded, as it was the exposed part when it was found, thus missing the sutural surfaces to the ischium and part of that to the pubis. On its medial surface, there is a somewhat oval area of attachment of the sacral ribs, measuring 66.6–77.1 mm in diameter. It is located anteriorly to the iliac neck; its dorsal margin is slightly protruding, its anterior margin is somewhat depressed, and its posterior margin is flat and continuous with the rest of the bone. The iliac blade (length 123.1 mm, maximum width of 72.6 mm and height of 47.6 mm) forms an angle of about 63.4 ° with the posterior part of the bone. Its neck has a semicircular section, dorsally flattened and with a rounded ventral part, and the blade is elongated, dorsoventrally compressed and expanded distally, with a flattened triangular section. Its posterior end has an unfinished, irregular surface.

IPS120164 (Fig. 6g–i): left pubis consisting of a thin, relatively flat, triangular plate (maximum anteroposterior length of 148.1 mm and maximum height of 142.8 mm), which is slightly curved ventromedially. The maximum lateral width is around its posterior–dorsal edge, reaching 32.3 mm. The anterior, dorsal and posterior margins of the plate are either unfinished or broken, whereas the ventral margin becomes progressively thinner and sharp-edged. The obturator foramen has a subtriangular to oval contour (13.5–20.1 mm in height × 12.3–13·3 mm in width), and obliquely pierces the bone from an anterior–dorsal

position in the medial side to a posterior–ventral position on the lateral side.

IPS120165 (Fig. 6j–o): fragment of the proximal epiphysis of a left tibia, measuring 131.8 mm in maximum proximal–distal length, with an articular surface of 108.5 mm in anteroposterior width and a mediolateral width of 96.4 mm. Most of the medial part of the shaft has been eroded, as it was exposed on the surface when the fossil was found. Articular surfaces can be distinguished on the tibial plateau with some degree of confidence, even though there the bone is slightly eroded (or was not completely ossified). In the lateral half of the plateau, there is a somewhat semicircular depression to accommodate the lateral condyle of the femur. Additionally, another (less clear) elongated or lunate depression can be observed on the medial–extensor edges of the plateau, corresponding to the articulation surface for the medial condyle of the femur. In extensor view, the most proximal part of the cnemial crest can be observed, and although it has been mostly eroded, it appears to bear a fairly inconspicuous knob. Moreover, in lateral view, there is a conspicuous ridge about 44.5 mm below the edge of the tibial plateau.

Remarks. All of the bone remains considered here were found in close association, albeit not articulated, and so, given their consistent size and lack of duplicate elements, they can all be considered to belong to the same individual. IPS35597, the holotype specimen of *Balearosaurus bombardensis* gen. et. sp. nov., was collected from a lower stratigraphic position, and given its consistent size and taxonomical attribution it could be considered to be conspecific with the remains herein identified as cf. *Balearosaurus bombardensis* gen. et. sp. nov. However, there is no decisive proof that this specimen (mostly represented by postcranial elements) belongs to the same species as the holotype maxilla of *Balearosaurus bombardensis* gen. et. sp. nov., and, therefore, it is treated here separately under open nomenclature.

Cranial remains clearly agree with those of large moradisaurine captorhinid eureptiles. IPS35598 is conspicuously heterodont, differentiating a caniniform from other smaller teeth, a condition that is not known to occur in the other Permian tetrapods with swollen vertebral neural arches such as seymouriamorphs and diadectomorphs (see below), which have teeth of similar size in the anterior region of the jaws (e.g., Case 1911; Case & Williston 1912; White 1939; Olson 1947; Carroll *et al.* 1972; Berman *et al.* 1987, 1998; Berman & Sumida 1995; Kissel 2010). Conversely, the dentition of moradisaurines does differ in being relatively small, bullet-shaped teeth and having larger caniniforms (Vjushkov & Chudinov 1957; Olson 1962a, 1965; de Ricqlès & Taquet 1982; Dodick & Modesto 1995; Ivakhnenko 2008; LeBlanc *et al.* 2015; Modesto *et al.* 2019). However, the fact that IPS35598 is broken and abraded precludes detailed comparison with other species; regardless, it can be stated that the alveolus for the caniniform is approximately as large as that of the largest known captorhinid, *Moradisaurus grandis* Taquet, 1969 (see de Ricqlès & Taquet 1982).

Elements of the axial skeleton, especially IPS35592, are also diagnostic of moradisaurines. Swollen vertebral neural arches are found in seymouriamorphs, diadectomorphs, moradisaurine captorhinomorphs and parareptiles (e.g., Olson & Beerbower 1953; Olson & Barghusen 1962; Olson 1962a, b, 1979; Kuhn 1969; Sullivan & Reisz 1999; Modesto *et al.* 2014). Contrarily to the Menorcan material, seymouriamorph anterior dorsal vertebrae show distinct diapophyses that laterally extend past the zygapophyses (White 1939; Sumida 1990). Moreover, in seymouriamorphs, the parapophyses are located on the intercentra (White 1939; Sumida 1990), whereas in IPS35592 they are on the lateral sides of the neural arches, connected to the diapophyses by a thin lamina, a condition that is seen in captorhinomorphs (e.g., Olson & Barghusen 1962; Olson 1962a, b; Sumida 1990; Reisz *et al.* 2011). Dorsal vertebrae of diadectomorphs and parareptiles are also reminiscent of IPS35592; however, they always possess a thickened and dorsally elongated neural spine, and additional articulation facets in the form of the hypantrum–hyposphene complex (von Meyer 1860; Stappenbeck 1905; Case 1911; Kuhn 1969; Carroll *et al.* 1972; Sumida 1990; Berman *et al.* 1998; Nyakatura *et al.* 2015). The vertebra studied herein does possess what seem to be paired, small additional articulation facets, but in the form of the centrozygapophyseal processes and fossae, which are by no means comparable to the stout and conspicuous hypantrum–hyposphene of diadectomorphs and parareptiles. Illustration of isolated vertebral remains of moradisaurines is scarce in the literature, but IPS35592 is remarkably similar to the *Rothianiscus* vertebra (FMNH UR 829) illustrated by Olson & Barghusen (1962) (R.M.A., pers. obs.) and to a purported juvenile *Moradisaurus* vertebra, uncatalogued, in the collections of the MNHN (J.F. & R.M.A., pers. obs.).

The elements of the pelvic girdle are slightly different from those of other moradisaurines of which the pelvis is known, such as *Captorhinikos* (see Olson 1962b) and *Rothianiscus* (see Olson & Barghusen 1962), in that the iliac blade is dorsoventrally flatter and more posteriorly directed in IPS120163. Some smaller captorhinids, such as *Captorhinus* Cope, 1896, do have iliac blades strongly directed posteriorly (see Holmes 2003), but, apart from in its size, they differ from IPS120163 in that the blade is dorsoventrally flattened in the latter.

Moradisaurinae indet.

(Fig. 7)

Studied material. IPS35593 (middle/posterior dorsal vertebra), found in an *ex situ* rock attributable to m 226–227 of Cala del Pilar–Pla de Mar section (the same as the specimens IPS35588, IPS35590, IPS35592, IPS35598, IPS120163, IPS120164 and IPS120165 mentioned above). IPS120166 (proximal fragment of left jaw), collected *in situ* from the bed at m 273–274 of Cala del Pilar–Pla de Mar section, P3 unit, indeterminate Permian, Menorca, Balearic Islands, western Mediterranean.

Description. IPS120166 (Fig. 7a–f): proximal fragment of left jaw measuring 42.6 mm in maximum anteroposterior length, with a maximum labiolingual width of 13.6 mm and a maximum dorsoventral height of 26.6 mm. Five bones are partially represented in the studied fragment, although only sutures between two pairs of them are visible (prearticular–splenial and angular–prearticular). Three rows of teeth can be observed on a platform on the dentary, overhanging in the lingual side (maximum labiolingual width of 11.9 mm and maximum dorsoventral height of 7.6 mm). Four small (maximum diameter of 2.0 mm), bullet-shaped teeth are preserved in the labial row. Detailed preparation has not been possible due to its small size and the potential risk of damaging the fossil, but they seem to be conical and somewhat pointed. Four teeth can be distinguished in the middle row, the most posterior of which is clearly larger (maximum diameter of 5.0 mm). Two other small teeth have been counted in the lingual row. All of them are arranged diagonally to each other. In labial view, the dentary is rather flat and tilted laterally (38.3 °), and its lower two-thirds are ornamented with irregular grooves. Posterior to the teeth plate rises the coronoid process (tilted 48.3 ° posteriorly), although the suture between the dentary and the coronoid is not visible, and part of the mandibular ramus. In lingual view, just below the tooth plate there is a flat and smooth surface corresponding to the prearticular. In its posterior part, and although it is covered by matrix, there is an area that corresponds to the articular facet of the hemimandible. The ventral edge of the prearticular is connected to the angular below with a distinct suture and a conspicuous angulation of the

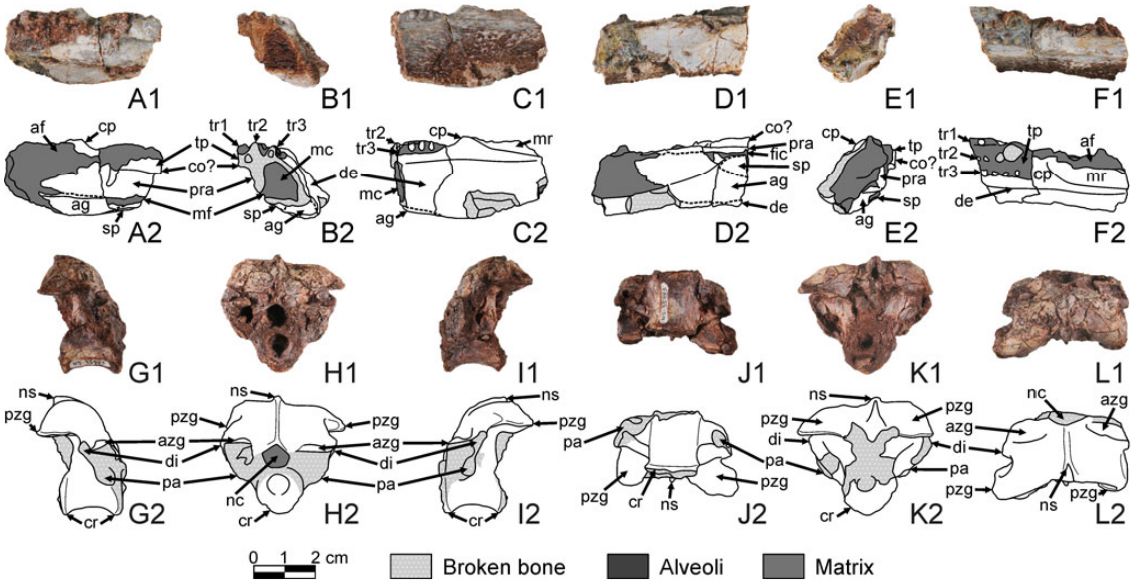

Figure 7 Pictures and interpretative drawings of cranial and axial elements of Moradisaurinae indet. from an indeterminate Permian of Cala del Pilar Pla de Mar section (Menorca). (A–F) IPS120166, proximal fragment of left jaw: (A) lingual view; (B) anterior view; (C) labial view; (D) ventral view; (E) posterior view; (F) occlusal view. (G–L) IPS35588, middle/posterior dorsal vertebra: (G) right lateral view; (H) anterior view; (I) left lateral view; (J) posterior view; (K) ventral view; (L) dorsal view. Abbreviations: af = adductor fossa; ag = angular; azg = prezygapophysis; co = coronoid; cp = coronoid process; cr = cortical rim; de = dentary; di = diapophysis; mc = mandibular canal; mf = Meckelian foramen; mr = mandibular ramus; nc = neural canal; ns = neural spine; pa = parapophysis; pd = pedicel; pra = prearticular; pzg = postzygapophysis; sp = splenial; tp = teeth plate; tr1–3 = teeth row 1–3.

surface, which becomes almost horizontal. In the most anterior preserved part of the connexion between the prearticular and the angular there is an anteroposteriorly stretched foramen (Meckelian foramen) that connects to the mandibular canal visible in anterior aspect. Just below this foramen there is a small portion of the splenial, connecting posteriorly and ventrally with the angular by means of a conspicuous suture.

IPS35588 (Fig. 7g–l): middle/posterior dorsal vertebra measuring 33.9 mm in height, with a maximum width of 38.0 mm and a maximum length of 26.9 mm. Cylindrical, amphicoelous pleurocentrum measuring 14.5 mm in height, with a width of 14.6 mm and a length of 17.2 mm, its axis being almost horizontal. The outline of the pleurocentrum is circular in anteroposterior view and spool-shaped in lateral view, because the cortical rim is slightly flared outwards laterally and ventrally. In ventral aspect, there is no evidence of a ridge or keel. The neural canal has a somewhat pentagonal contour in anterior view (7.1 mm in height × 7.9 mm in width) and is covered by matrix in posterior view. The pedicels are attached dorsolaterally to the pleurocentrum supporting the neural arch, which is notably expanded and swollen, extending out as much as the width of the pleurocentrum. The prezygapophyses extend laterally from the pedicels and are connected to the transverse processes posterolaterally. The articular surfaces of the prezygapophyses are essentially horizontal, and are approximately twice as wide laterally than they are wide anteroposteriorly. Transverse processes are located between the pre- and postzygapophyses, and are tilted 23.1° from the vertical axis in anteroposterior aspect. The diapophysis appears to be half as thick as the parapophysis, and they are both connected by an osseous lamina with an angle of 31° from the vertical axis in lateral view. Whereas the diapophysis is dorsolaterally detached forming a small process, the parapophysis fuses at mid-length of the posterior region of the prezygapophysis. The postzygapophyses are located just behind the diapophyses in anterior view, separated by a rather deep emargination. A small, laterally elongated suprapostzygapophyseal fossa is present anteriorly on the emarginated side. The postzygapophyseal articular facets essentially horizontal, possess a flat surface and their margins are slightly flared outwards. The neural spine is very low (8% of the total height in anterior view) and thin (7% of the total width). In anterior aspect, it continues ventrally as a faint lamina that fades halfway to the neural canal; in posterior aspect, the spine bifurcates ventrally in two thin laminae that delimit the postspinal fossa, which possesses a distinct triangular shape.

Remarks. The fossils considered here come from two beds separated by a thickness of about 50 m. Therefore, they certainly do not belong to the same specimen (the vertebra would belong to a slightly larger animal), but they have been grouped here because they agree in general size and purported taxonomical attribution. The vertebra (IPS35588) shows typical moradisaurine traits and it is essentially a smaller version of IPS35592, very similar to the vertebrae illustrated by Reisz *et al.* (2011). However, it does not belong to a juvenile specimen of *Balearosaurus bombardensis* but, rather, to an adult of a distinct, smaller species, as it is completely ossified and there remain no traces of the neurocentral suture. The jaw (IPS120166) is also small, and broadly comparable to that of some genera of small moradisaurines such as *Captorhinikos* (see Olson 1962b; LeBlanc *et al.* 2015; Cisneros *et al.* 2020a), *Kahneria* (see Olson 1962a), *Gecatogomphius* (see Ivakhnenko 2008), *Acrodenta* (see Jalil & Dutuit 1996) and the unidentified tooth plate from the Argana Basin (Jalil & Dutuit 1996). It differs from most of those genera in that IPS120166 only has three rows of teeth in the most proximal part of the jaw, whereas the others have four or more with a comparable or smaller jaw size. *Acrodenta* does have three rows of teeth, and differs from all other moradisaurine captorhinids in the acrodont mode of implantation of its teeth, which are thin and sharply pointed (Jalil & Dutuit 1996). Teeth in IPS120166 are not as thin and pointed as in *Acrodenta*, as they are more similar to the bullet-shaped teeth of *Captorhinikos* or *Kahneria*, and their mode of implantation cannot be observed in the present material. Therefore, it has been identified in open nomenclature.

5. Discussion

5.1. Age attribution

The precise age attribution for each of the Permian units of Menorca remains mostly unresolved. Bourrouilh (1973, 1983) was the first author to carry out a palynological study on those units with a sample collected at 16.9 km along the road from Es Mercadal to Alaior, which pointed to an upper Permian age (Bourrouilh 1973, 1983). That outcrop was assigned to the lower half of the P3 unit by Rosell *et al.* (1989a, b), who also provided another palynological analysis from an unspecified locality that revealed a 'Thuringian' biofacies (middle–upper Permian). A few years later, Broutin *et al.* (1992) reported yet another palynoassemblage from Pla de Mar, found in the copper mine beds (in m 301.5–303.5 of the log presented here, and, thus, in the middle part of the P3 unit), and also considered it to belong to the 'Thuringian' biofacies. That palyniferous horizon could not be relocated by Bercovici *et al.* (2009), but they did find more layers that yielded palynomorphs in the uppermost beds of the P3 unit at Penyals d'Alforinet (not considered herein; see '1.1. Palaeoenvironment and climatic conditions'), arguing a Wordian–Changhsingian stage (middle–uppermost Permian) interval for them. More recent works, such as Bourquin *et al.* (2011) or Borruel-Abadía *et al.* (2019), considered that palynoassemblage to be of lower Wuchiapingian stage (Lopingian, upper Permian) without providing further proof. Then, they inferred that the lower–middle P3 unit was of upper Capitanian stage (Guadalupian, middle Permian), the P2 unit was of Wordian–lower Capitanian stage (Guadalupian, middle Permian) and the P1 unit was of lower Wordian stage (Guadalupian, middle Permian), without presenting specific data or any compelling argument on how these conclusions were reached.

From a review of the literature, it becomes clear that the only interval of the Permian of Menorca that has been confidently dated, albeit in a notably wide range of time, is the middle–upper part of the P3 unit as Wordian–Changhsingian (middle–uppermost Permian) (Bourrouilh 1973, 1983; Rosell *et al.* 1989a, b; Broutin *et al.* 1992; Bercovici *et al.* 2009). Additionally, the ichnological study of the present work has dated the lower part of the P3 unit as middle Artinskian–Wuchiapingian. All other age inferences, especially those for the lower units, are here considered unfounded, as with the present data it is only possible to attribute the P3 unit to an undetermined interval between the middle Artinskian and the Changhsingian (lower–uppermost Permian), lacking any data for units P1 and P2.

5.2. Tetrapod fauna

All the body fossils from the Permian P3 unit of Cala del Pilar–Pla de Mar section have been identified to belong to the captorhinid eureptile subfamily Moradisaurinae, similarly to most of the ichnological material, which was produced by captorinomorphs, perhaps moradisaurines as well (*Hyloidichnus* isp.) (Fig. 8). The lack of precise age constraints in the case of the Menorcan units limits the possibility of making detailed palaeobiogeographical inferences. Still, this section will explore the possible relationships with all the other similar species.

5.2.1. Palaeobiogeography of moradisaurine captorhinid eureptiles. The distribution of all known moradisaurine fossils (bones and putative ichnites) throughout the Permian was essentially restricted to low palaeolatitudes between 30 °N and 30 °S (Fig. 9) (the only exception being the *Hyloidichnus* reported from Argentina by Melchor & Sarjeant 2004). Modesto *et al.* (2016) suggested that moradisaurines and caseids replaced diadectids and edaphosaurids as the dominant high-fibre herbivores in the late part of the early Permian because they may have been better suited to thrive in more arid climates. Indeed, from the early Permian to the middle–late Permian, the low-latitude belt of Pangaea shifted from a tropical climate to an arid climate (Tabor & Poulsen 2008). With moradisaurines restricted to intertropical latitudes, the niches as dominant herbivores in temperate and high latitudes were filled, during the middle and late Permian, by taxa of other groups such as dicynodonts, pareiasaurs and some dinocephalians (e.g., Day *et al.* 2015; Viglietti *et al.* 2016; Bernardi *et al.* 2017; Olroyd & Sidor 2017; Sennikov & Golubev 2017; Marchetti *et al.* 2019b). Such latitudinal provincialism was supported by the analysis of Bernardi *et al.* (2017), who showed that the late Permian faunal palaeoassemblages of low latitudes clustered in what were named 'tropical faunas', which were clearly distinct from the palaeoassemblages of higher latitudes. This had also been argued by Sidor *et al.* (2005) regarding the singular middle/upper? Permian assemblage of the Moradi Formation of Niger, with relict representatives of Carboniferous temnospondyl clades that were little related to other coeval taxa. The present work adds to that evidence, as the distribution of moradisaurines, from the early Permian to the late Permian (Fig. 9), supports the hypothesis of a strong latitudinal provincialism, especially isolating the faunas of the most arid, intertropical regions of Pangaea.

Therefore, if central Pangaea was an area that hindered faunal exchanges between temperate latitudes of both hemispheres, the alternative corridors that explain the great similarities between northern and southern temperate faunas should be sought either in the coastal environments, with less harsh climates (Sidor *et al.* 2005), or in the Cathaysian Bridge, which preserved more humid conditions throughout the Permian (Tabor & Poulsen 2008). Brocklehurst *et al.* (2018) argued that, in all cases, the Permian assemblages of Gondwana were more similar to the ones of eastern Laurasia, whereas it seemed that dispersion had been low between Gondwana and western Laurasia (which includes most of the moradisaurine localities). Thus, the most probable explanation was that the Cathaysian Bridge operated as the main dispersal route at least until the Guadalupian (middle Permian), and that the most important dispersal barrier between western Gondwana and western Laurasia were the high mountains of the Variscan orogen (Brocklehurst *et al.* 2018). Among the different clades included in the analysis, eureptiles seemed to be the group least affected by this barrier, as their dispersal and vicariance rates remained relatively stable throughout the period of uplifting of the mountains (Brocklehurst *et al.* 2018). This agrees with the pattern observed in Figure 9 herein, which shows that moradisaurines were present and radiated in both the northern and southern sides of the Variscan mountains from the very beginning of their evolutionary history. Therefore, even though it appears that the arid climatic belt in central Pangaea or the Variscan mountains could have served as a strong obstacle for dispersion of certain tetrapod groups such as amphibians, parareptiles and synapsids (Brocklehurst *et al.* 2018), they provided comfortable environments for a specialised clade such as moradisaurines.

5.2.2. Phylogenetic relationships of moradisaurine captorhinid eureptiles. The phylogenetic tree of the Captorhinomorpha obtained in the present work (Fig. 4) differs in some aspects from those recently published; specifically, it recovers one polytomy in all the species of *Captorhinus*, the genus *Labidosauriscus* and the clade (*Labidosaurus* + Moradisaurinae), and another polytomy including *Captorhinikos valensis*, *Kahneria* and all the other moradisaurines except for *Captorhinikos chozaensis*. The first polytomy is probably the result of merging the character matrix of Modesto *et al.* (2019), resulting in a polytomy between *Captorhinus aguti*, *Captorhinus laticeps* and *Captorhinus magnus*, and the character matrix provided by Cisneros *et al.* (2020a), which obtains a polytomy between *Captorhinus kierani*, *Labidosauriscus* and (*Labidosaurus* + Moradisaurinae). In the former, the polytomy is caused by coding changes in *C. chozaensis*,

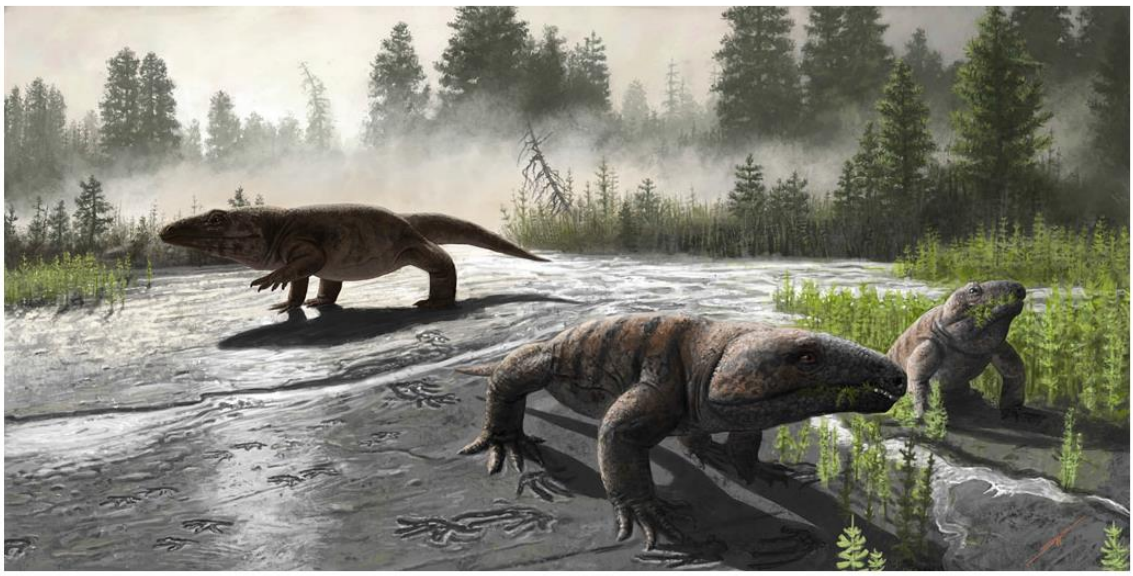

Figure 8 Reconstruction of the palaeoassemblage of the Permian P3 unit of Menorca, representing one specimen of *Balearosaurus bombardensis* gen. et sp. nov. (background) and two specimens of the smaller Moradisaurinae indet. (foreground), wandering on a crevasse splay lobe and leaving their tracks (*Hyloidichnus*) near other cf. *Erpetopus* tracks. Created by Henry Sutherland Sharpe. © 2021 Henry Sutherland Sharpe. Used under license.

which have been verified again in the present work; in the latter, it is caused by the addition of the two recently described taxa *C. kierani* and *Labidosauriscus richardi*. The second polytomy is obtained as a result of adding *Kahneria* to the matrix; nevertheless, it does not affect the clade (Balearic species + *Rothianiscus*), which is recovered regardless of *Kahneria* being included in the data matrix or not.

A significative topological difference between the trees of Modesto *et al.* (2019) and Cisneros *et al.* (2020a) is in the position of the single tooth-rowed genus *Labidosaurus*. It is recovered outside all the multiple tooth-rowed Moradisaurinae in the former, whereas in the latter it appears between *C. chozaensis* and the rest of multiple tooth-rowed moradisaurines. The tree presented in Figure 4 concurs with the tree recovered by Modesto *et al.* (2019). This aspect has important implications for the phylogeny of the Moradisaurinae, making it a clade restricted to the species with several rows of teeth parallel to the jaw margin, implying that high-fibre herbivory evolved only once within the Captorhinomorpha. In any case, the topology within derived moradisaurines remains the same in the three trees, with the lower–middle Permian North American genus *Rothianiscus*, with one species with three rows of teeth in the major part of its tooth plates (Olson 1962a) as sister to the two large species from Mallorca (Liebrecht *et al.* 2017) and Menorca (Fig. 4).

The large moradisaurine from the island of Mallorca was described by Liebrecht *et al.* (2017), based on a fragment of right maxilla and parts of the palate that belonged to an unknown, large species with three rows of teeth. It was initially assumed (Liebrecht *et al.* 2017) to be of upper Permian age based on the work of Ramos & Doubinger (1989), which dated the palynoassemblages of the upper lithostratigraphic unit of the Permian of the island (Pedra de s'Ase unit) as 'Thuringian', and thus as middle–upper Permian. However, the moradisaurine fossil was collected in the lower unit (Port des Canonge unit) (Liebrecht *et al.* 2017), which did not have any reliable age attribution. That unit is now currently under study, and has been preliminarily dated as lower Permian (Artinskian–Kungurian) based on its tetrapod ichnological assemblage (Matamales-Andreu *et al.* 2019). Therefore, the unidentified moradisaurine from Mallorca (Liebrecht *et al.* 2017) should be considered of lower Permian age awaiting further available paleontological and geological data.

As stated above, the phylogenetic analysis offered in the present work (Fig. 4) places this taxon as sister to the large captorhinid from the neighbouring island of Menorca described herein, *Balearosaurus bombardensis* gen. et sp. nov. They belong, however, to clearly distinct species, and possibly genera, which can be set apart mostly based on dental characters, as the Mallorcan moradisaurine has smooth, bulbous teeth (Liebrecht *et al.* 2017), whereas in the Menorcan species the teeth are more cylindrical and ornamented with numerous ridges and furrows (Fig. 3). Despite its great palaeogeographical proximity, it is important to stress that the Permian units of eastern Iberia (including what are now the Balearic Islands) were deposited in small, semi-isolated half-graben basins (e.g., Gómez-Gras 1992, 1993), which probably operated as biogeographical islands for local speciation of some groups such as moradisaurines.

The close relationship of *Rothianiscus* with the two large moradisaurines of the Balearic Islands further supports the hypothesis put forward in '5.2.1. Palaeobiogeography of moradisaurine captorhinid eureptiles', since the former genus has been found in southern North America, which was on the northwestern side of the Variscan mountains, whereas the Balearic Islands were on its southeastern side (Fig. 9). Therefore, the general case made for all Moradisaurinae is repeated here on a smaller scale, with closely related taxa separated by the Variscan mountains, suggesting that they were not a strong barrier to dispersal of eureptiles.

Regarding the small moradisaurine of Menorca described in the present work, which was impossible to determine with the present material, its relationships within the Moradisaurinae are less clear, and will not be discussed here awaiting the discovery of more complete specimens in the future.

6. Conclusions

The present work has characterised, by means of ichnological and osteological data, a palaeoassemblage from an indeterminate Permian of Cala del Pilar–Pla de Mar section (Menorca,

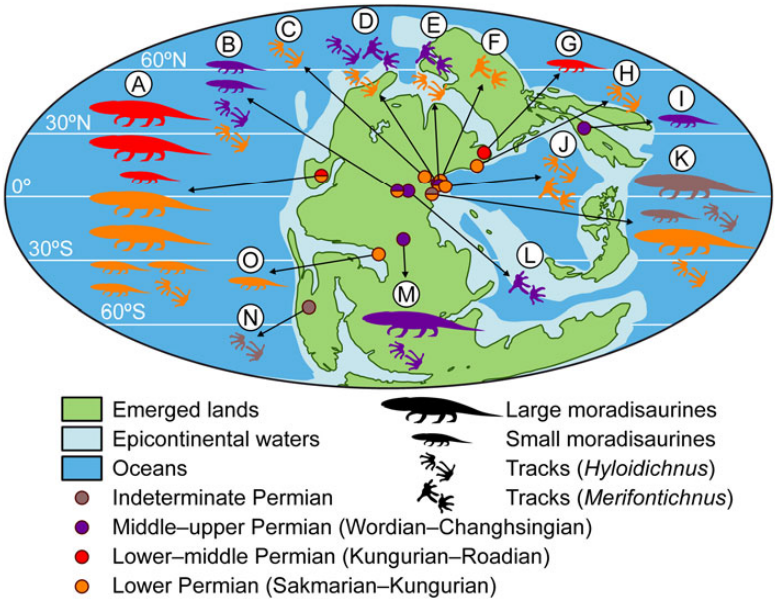

Figure 9 World map during the Permian (modified from Scotese 2014) with the localities that have yielded bones and tracks of possible moradisaurine captorhinid eureptiles. (A) *Captorhinikos chozaensis, Captorhinikos parvus, Captorhinikos valensis, Labidosaurikos meachami*, a tooth plate from an indeterminate species and *Hyloidichnus* isp. from the lower Permian (Gilmore 1927; Stovall 1950; Olson 1954, 1962b, 1970; Haubold *et al.* 1995; Lucas *et al.* 2013; Modesto *et al.* 2014, 2016; LeBlanc *et al.* 2015; Voigt & Lucas 2015, 2017; Schneider *et al.* 2020), and *Kahneria seltina, Rothianiscus multidonta* and *Rothianiscus robusta* from the lower middle Permian of southern North America (Olson & Beerbower 1953; Olson & Barghusen 1962; Olson 1962a; 1965). (B) *Hyloidichnus* isp. from the lower Permian (Voigt *et al.* 2011; Zouicha *et al.* 2021), and *Acrodenta irerhi*, an indeterminate moradisaurine and *Hyloidichnus* isp. from the middle upper Permian of northeastern Africa (Jalil & Dutuit 1996; Hmich *et al.* 2006; Voigt *et al.* 2010; Hminna *et al.* 2012; Moreau *et al.* 2020). (C) *Hyloidichus* isp. from the lower Permian of northern Iberian Peninsula (Gand *et al.* 1997; López-Gómez *et al.* 2019b). (D) *Hyloidichnus* isp. from the lower Permian, and *Hyloidichnus* isp. and *Merifontichnus* isp. from the middle Permian of southern Massif Central and Provence (Heyler & Lessertisseur 1963; Gand 1987, 1993; Gand *et al.* 2000; Gand & Durand 2006; Michel *et al.* 2015; Logghe *et al.* 2021). (E) *Hyloidichnus* isp. from the lower Permian (Voigt & Haubold 2015; Mujal *et al.* 2016) and possible *Merifontichnus* isp. from the middle Permian of the Pyrenees (Mujal *et al.* 2017). (F) *Merifontichnus* isp. from the lower Permian of Sardinia (Citton *et al.* 2019; Santi *et al.* 2020). (G) *Gecatogomphius kavejevi* from the middle Permian of eastern Europe (Vjushkov & Chudinov 1957; Olson 1962a; Ivakhnenko 2008). (H) *Hyloidichnus* isp. from the lower Permian of northern Anatolia (Gand *et al.* 2011). (I) *Gansurhinus qingtoushanensis* from the middle upper Permian of central-east Asia (Reisz *et al.* 2011). (J) *Hyloidichnus* isp. and *Merifontichnus* isp. from the lower Permian of the Alps (Marchetti *et al.* 2013, 2015a, b, c; Marchetti 2016; Santi *et al.* 2020). (K) Indeterminate moradisaurine and *Hyloidichus* isp. from the lower Permian of Mallorca (Calafat *et al.* 1986, 1986 1987; Calafat 1988; Gand *et al.* 2010; Liebrecht *et al.* 2017; Matamales-Andreu *et al.* 2019), and *Balearosaurus bombardensis* gen. et sp. nov., an indeterminate moradisaurine and *Hyloidichnus* isp. from an indeterminate Permian of Menorca (the present work). (L) possible *Merifontichnus* isp. from the middle upper Permian of north-central Africa (Contessi *et al.* 2018). (M) *Hyloidichnus* isp. and *Moradisaurus grandis* from the middle upper? Permian of central Africa (de Ricqlès & Taquet 1982; O'Keefe *et al.* 2005; Smith *et al.* 2015; Olroyd & Sidor 2017; Modesto *et al.* 2019). (N) *Hyloidichnus* isp. from an indeterminate Permian of southern South America (Melchor & Sarjeant 2004; Marchetti *et al.* 2020a). (O) *Captorhinikos* sp. from the lower Permian of northern South America (Cisneros *et al.* 2020a).

Balearic Islands, western Mediterranean) dominated by moradisaurine captorhinid eureptiles. The field study has allowed us to locate and characterise the palaeoenvironments of the bone-bearing beds from which some fossils were extracted and preliminarily studied in the 1980s. This, together with an exhaustive review of the literature, has shown that most of the previous age assignations to those deposits were unfounded, as only the uppermost part of the section had been confidently dated as middle/upper Permian. Additionally, from the middle part of the section, ichnites have been discovered and described for the first time in the Permian of Menorca, recognising the ichnogenera *Hyloidichnus*, purportedly produced by captorhinomorph eureptiles, in this case probably moradisaurine captorhinids, and possibly *Erpetopus*, of acleistorhinid or nyctiphruretid parareptile trackmakers. Two taxa of moradisaurines have also been identified by means of the study of all the fossil bones from the middle part of the Cala del Pilar–Pla de Mar section present in historical collections, which has been the main focus of the present work. The smallest of the two has been identified as an indeterminate moradisaurine based on two bones collected from different beds: a fragment of jaw with three rows of teeth, and an isolated dorsal vertebra with typical characters of the group. The largest of the two taxa has been described as *Balearosaurus bombardensis* gen. et sp. nov. based on a fragment of maxilla with at least three rows of bullet-shaped teeth ornamented with ridges and furrows. Another relatively incomplete specimen consisting of cranial, axial and appendicular bones has also been tentatively assigned to the same species. *Balearosaurus bombardensis* gen. et sp. nov. was closely related to the large moradisaurine reported from the neighbouring island of Mallorca, and those two were, in turn, phylogenetically related to *Rothianiscus*, a genus of large moradisaurines from the lower–middle Permian of southern North America. This, together with the distribution of all other known moradisaurines, has allowed us to put forward the hypothesis that the Variscan mountains were not an important barrier to the biogeographical dispersion of moradisaurines, because species of this clade occurred on both sides of the mountains since the earliest members of the group. Moreover, all known moradisaurines lived in palaeolatitudes between 30 °N and 30 °S, in regions where other herbivorous groups more typical of temperate palaeolatitudes have rarely been reported. This suggests that moradisaurines, together with caseids, may have been among the herbivores best suited to thrive in the arid climates of the low latitudes of Pangaea, outcompeting

the other herbivorous groups until their demise in the late Permian.

7. Supplementary material

Supplementary material is available online at https://doi.org/10.1017/S1755691021000268

8. Acknowledgements

We thank Antoni Obrador, Miquel Fernàndez, Enric Vicens and Joan Lluís Pretus for the information about the original discovery of the tetrapod bone remains studied herein. Our thanks to David Gómez-Gras, Antoni Rodríguez-Perea, Eudald Mujal and Raül Carmona for the bibliography provided and discussion on some aspects; to Miquel Fernàndez and Sebastià Matamalas for their aid in the fieldwork; to Marina Rull and Xènia Aymerich for repreparation of the specimens; to Enric Vicens for letting R.M.A. use the photographic equipment of the Palaeontology Unit of the Universitat Autònoma de Barcelona; to William F. Simpson and Kenneth D. Angielczyk for the pictures of vertebral material of moradisaurines housed in the Field Museum (Chicago); to Daniela Schwarz, Florian Witzmann, Igmar Werneburg and Tom Hübner for access to the materials of the collections of Museum für Naturkunde (Berlin), Eberhard Karls Universität Tübingen (Tübingen) and Museum der Natur (Gotha), used here for comparison; to John A. Nyakatura for giving R.M.A. the raw computed tomography scans of *Orobates* for comparison; to Henry S. Sharpe for the illustration in Figure 8, funded with the grant 2112-2020-000001 of the Consell Insular de Menorca granted to R.M.A., À.G. and J.F.; to Neil Brocklehurst and Lorenzo Marchetti, reviewers of this paper, for their thoughtful and constructive comments that improved the original manuscript; and to the head editor Stig Walsh. We acknowledge support from the CERCA program (Generalitat de Catalunya, Spain). R.M.A. was supported by the predoctoral grant FPU17/01922 (Ministerio de Ciencia, Innovación y Universidades, Spain) and the grant Synthesys+ DE-TAF-23 (European Commission). J.F. was supported by the Agencia Estatal de Investigación (Spain) and the European Regional Development Fund AEI/FEDER EU, project CGL2017-82654-P (European Union). J.F. is member of the consolidated research group 2017 SGR 086 GRC (Generalitat de Catalunya, Spain). O.O. and À.G. are members of the consolidated research group 2017 SGR 1666 GRC (Generalitat de Catalunya, Spain).

9. References

Arche, A. & López-Gómez, J. 1992. Una nueva hipótesis sobre las primeras etapas de la evolución tectonosedimentaria de la cuenca pérmico-triásica del SE de la Cordillera Ibérica. *Cuadernos de Geología Ibérica* **16**, 115–43.

Arribas, J., Gómez-Gras, D., Rosell, J. & Tortosa, A. 1990. Estudio comparativo entre las areniscas paleozoicas y triásicas de la isla de Menorca: evidencias de procesos de reciclado. *Revista de la Sociedad Geológica de España* **3**, 105–116.

Bercovici, A., Diez, J. B., Broutin, J., Bourquin, S., Linol, B., Villanueva-Amadoz, U., López-Gómez, J. & Durand, M. 2009. A palaeoenvironmental analysis of Permian sediments in Minorca (Balearic Islands, Spain) with new palynological and megafloral data. *Review of Palaeobotany and Palynology* **158**, 14–28.

Berman, D. S., Reisz, R. R. & Eberth, D. A. 1987. *Seymouria sanjuanensis* (Amphibia, Batrachosauria) from the Lower Permian Cutler Formation of north-central New Mexico and the occurrence of sexual dimorphism in that genus questioned. *Canadian Journal of Earth Sciences* **24**, 1769–84.

Berman, D. S., Sumida, S. S. & Martens, T. 1998. *Diadectes* (Diadectomorpha: Diadectidae) from the early Permian of Central Germany, with description of a new species. *Annals of Carnegie Museum* **67**, 53–93.

Berman, D. S. & Sumida, S. S. 1995. New cranial material of the rare diadectid *Desmatodon hesperis* (Diadectomorpha) from the late Pennsylvanian of central Colorado. *Annals of Carnegie Museum* **64**, 315–36.

Bernardi, M., Petti, F. M., Kustatscher, E., Franz, M., Hartkopf-Fröder, C., Labandeira, C. C., Wappler, T., van Konijnenburg-van Cittert, J. H. A., Peecook, B. R. & Angielczyk, K. D. 2017. Late Permian (Lopingian) terrestrial ecosystems: a global comparison with new data from the low-latitude Bletterbach Biota. *Earth-Science Reviews* **175**, 18–43.

Borruel-Abadía, V., Barrenechea, J. F., Galán-Abellán, A. B., De la Horra, R., López-Gómez, J., Ronchi, A., Luque, F. J., Alonso-Azcárate, J. & Marzo, M. 2019. Could acidity be the reason behind the Early Triassic biotic crisis on land? *Chemical Geology* **515**, 77–86.

Bourquin, S., Bercovici, A., López-Gómez, J., Diez, J. B., Broutin, J., Ronchi, A., Durand, M., Arché, A., Linol, B. & Amour, F. 2011. The Permian–Triassic transition and the onset of Mesozoic sedimentation at the northwestern peri-Tethyan domain scale: palaeogeographic maps and geodynamic implications. *Palaeogeography, Palaeoclimatology, Palaeoecology* **299**, 265–80.

Bourrouilh, R. 1973. *Stratigraphie, sédimentologie et téctonique de l'île de Minorque et du Nord-Est de Majorque (Baléares). La terminaison nord-orientale des Cordilleres Bétiques en Méditerranée occidentale.* State PhD Dissertation, Université Pierre & Marie Curie, Paris VI, Paris.

Bourrouilh, R. 1983. Estratigrafía, sedimentología y tectónica de la isla de Menorca y del noreste de Mallorca. *Memorias del Instituto Geológico y Minero de España* **99**, 1–672 + 95 pl. + 3 maps.

Brandes, C. & Tiedt, C. 1991. Petrographische Bestandsaufnahme der permotriassischen Sandsteine (Balearen, westliches Mittelmeer). *Neues Jahrbuch für Geologie und Paläontologie, Monatshefte* **1991**, 233–42.

Briere, P. R. 2000. Playa, playa lake, sabkha: proposed definitions for old terms. *Journal of Arid Environments* **45**, 1–7.

Brocklehurst, N. 2017. Rates of morphological evolution in Captorhinidae: an adaptive radiation of Permian herbivores. *PeerJ* **5**, e3200.

Brocklehurst, N. 2020. Olson's Gap or Olson's Extinction? A Bayesian tip-dating approach to resolving stratigraphic uncertainty. *Proceedings of the Royal Society B* **287**, 20200154.

Brocklehurst, N., Dunne, E. M., Cashmore, D. D. & Fröbisch, J. 2018. Physical and environmental drivers of Paleozoic tetrapod dispersal across Pangaea. *Nature Communications* **9**, 5216.

Broutin, J., Ferrer, J., Gisbert, J. & Nmila, A. 1992. Permière découverte d'une microflore thuringienne dans le faciès saxonien de l'île de Minorque (Baléares, Espagne). *Comptes Rendus de l'Académie des Sciences de Paris, s.2* **315**, 117–22.

Buenaventura, A. 2004. *Menorca, Atlas Náutico*. Maó: Editorial Menorca S.A.

Calafat, F. 1988. *Estratigrafía y sedimentología de la litofacies Buntsandstein de Mallorca*. Bachelor's Thesis, Universitat de Barcelona, Barcelona.

Calafat, F., Fornós, J. J., Marzo, M., Ramos, E. & Rodríguez-Perea, A. 1986. Icnología de vertebrados de las facies Buntsandstein de Mallorca. *In* Cabrera, L. (ed.) *XI Congreso Español de Sedimentología. Libro de Resúmenes*, 40. Barcelona: Universitat de Barcelona.

Calafat, F., Fornós, J. J., Marzo, M., Ramos-Guerrero, E. & Rodríguez-Perea, A. 1986 1987. Icnología de vertebrados de las facies Buntsandstein de Mallorca. *Acta Geològica Hispànica* **21–22**, 515–20.

Carmona, R. 2004. *Estudi d'un seimuriamorfe (Amphibia: Batrachosauria) del Permià superior de Menorca*. Bachelor's Thesis, Universitat de Barcelona, Barcelona.

Carroll, R. L., Kuhn, O. & Tatarinov, L. P. 1972. *Handbuch der Paläoherpetologie/Encyclopedia of Paleoherpetology. Teil 5B/Part 5B: Batrachosauria (Anthracosauria) Gephyrostegida Chroniosuchida*. Stuttgart and Portland: Gustav Fischer Verlag.

Case, E. C. 1911. A revision of the Cotylosauria of North America. *Carnegie Institution of Washington Publication* **145**, 1–121.

Case, E. C. & Williston, S. W. 1912. A description of the skills of *Diadectes lentus* and *Animasaurus carinatus*. *American Journal of Science, s. 4* **33**, 339–48.

Cisneros, J. C., Angielczyk, K., Kammerer, C. F., Smith, R. M. H., Fröbisch, J., Marsicano, C. A. & Richter, M. 2020a. Captorhinid reptiles from the lower Permian Pedra de Fogo Formation, Piauí, Brazil: the earliest herbivorous tetrapods in Gondwana. *PeerJ* **8**, e8719.

Cisneros, J. C., Kammerer, C. F., Angielczyk, K. D., Fröbisch, J., Marsicano, C., Smith, R. M. & Richter, M. 2020b. A new reptile from the lower Permian of Brazil (*Karutia fortunata* gen. et sp. nov.) and the interrelationships of Parareptilia. *Journal of Systematic Palaeontology* **18**, 1939–59.

Citton, P., Ronchi, A., Maganuco, S., Caratelli, M., Nicosia, U., Sacci, E. & Romano, M. 2019. First tetrapod footprints from the Permian of

Sardinia and their palaeontological and stratigraphical significance. *Geological Journal* **54**, 2084 98.
Contessi, M., Voigt, S. & Bibonne, R. 2018. Permian tetrapod footprints from Tunisia. *Ichnos* **25**, 119 27.
Cope, E. D. 1896. The reptilian order Cotylosauria. *Proceedings of the American Philosophical Society* **34**, 436 57.
Crespí, D. & Merino, A. 1998. Contribució al coneixement de les mines de coure situades en el Permo-Trias de Menorca. *Endins* **22**, 119 23.
Day, M. O., Ramezani, J., Bowring, S. A., Sadler, P. M., Erwin, D. H., Abdala, F. & Rubidge, B. S. 2015. When and how did the terrestrial mid-Permian mass extinction occur? Evidence from the tetrapod record of the Karoo Basin, South Africa. *Proceedings of the Royal Society B* **282**, 20150834.
de Ricqlès, A. & Bolt, J. R. 1983. Jaw growth and tooth replacement in *Captorhinus aguti* (Reptilia: Captorhinomorpha): a morphological and histological analysis. *Journal of Vertebrate Paleontology* **3**, 7 24.
de Ricqlès, A. & Taquet, P. 1982. La faune de vertébrés du Permien Supérieur du Niger. I. Le captorhinomorphe *Moradisaurus grandis* (Reptilia, Cotylosauria). Le crane. *Annales de Paléontologie (Vert.-Invert.)* **68**, 33 106.
Dodick, J. T. & Modesto, S. P. 1995. The cranial anatomy of the captorhinid reptile *Labidosaurikos meachami* from the lower Permian of Oklahoma. *Palaeontology* **38**, 687 711.
Dutuit, J. M. 1976. Il est probable que les Rhynchocéphales sont représentés dans la faune du Trias marocain. *Compte-Rendus de l'Académie des Sciences, Paris* **238**, 483 86.
Falkingham, P. L. 2012. Acquisition of high resolution three-dimensional models using free, open-source, photogrammetric software. *Palaeontologia Electronica* **15**, 1T:15p.
Franzel, M., Jones, S. J., Meadows, N., Allen, M. B., McCaffrey, K. & Morgan, T. 2021. Basin-scale fluvial correlation and response to the Tethyan marine transgression: an example from the Triassic of central Spain. *Basin Research* **33**, 1 25.
Gand, G. 1987. *Les traces de vertébrés tétrapodes du Permien français: paléontologie, stratigraphie, paléoenvironnements.* State PhD Dissertation, Université de Bourgogne, Dijon.
Gand, G. 1993. La palichnofaune de vertébrés tétrapodes du basin permien de Saint-Affrique (Aveyron): comparaisons et conséquences stratigraphiques. *Géologie de la France* **1**, 41 56.
Gand, G., Kerp, H., Parsons, C. & Martínez-García, E. 1997. Palaeoenvironmental and stratigraphic aspects of animal traces and plant remains in Spanish Permian red beds (Peña Sagra, Cantabrian Mountains, Spain). *Geobios* **30**, 295 318.
Gand, G., Garric, J., Demathieu, G. & Ellenberger, P. 2000. La palichnofaune de vertébrés tétrapodes du Permien supériéur du bassin de Lodève (Languedoc-France). *Palaeovertebrata* **29**, 1 82.
Gand, G., De La Horra, R., Galán-Abellán, B., López-Gómez, J., Barrenechea, J. F., Arche, A. & Benito, M. I. 2010. New ichnites from the Middle Triassic of the Iberian Ranges (Spain): palaeoenvironmental and paleogeographical implications. *Historical Biology* **22**, 40 56.
Gand, G., Tüysüz, O., Steyer, J. S., Allain, R., Sakınç, M., Sanchez, S., Şengör, A. M. C. & Sen, S. 2011. New Permian tetrapod footprints and macroflora from Turkey (Çakraz Formation, northwestern Anatolia): biostratigraphic and palaeoenvironmental implications. *Comptes Rendus Palevol* **10**, 617 25.
Gand, G. & Durand, M. 2006. Tetrapod footprint ichno-associations from French Permian basins. Comparisons with other Euramerican ichnofaunas. *Geological Society, London, Special Publications* **265**, 157 77.
Gilmore, C. W. 1927. Fossil footprints of the Grand Canyon: second contribution. *Smithsonian Miscellaneous Collections* **80**, 1 78 + 21 pls.
Gómez-Gras, D. M. 1987. *Estratigrafía física y petrología sedimentaria del Pérmico y Buntsandstein de la isla de Menorca.* Bachelor's Thesis, Universitat Autònoma de Barcelona, Barcelona.
Gómez-Gras, D. M. 1992. *El Permotrías de las Baleares, de la Cordillera Costero Catalana y de la vertiente mediterránea de la Cordillera Ibérica: Facies y Petrología Sedimentaria.* PhD Dissertation, Universitat Autònoma de Barcelona, Barcelona.
Gómez-Gras, D. 1993. El Permotrías de las Baleares y de la vertiente mediterránea de la Cordillera Ibérica y del Maestrat: Facies y Petrología Sedimentaria (Parte II). *Boletín Geológico y Minero* **104**, 467 515.
Gómez-Gras, D. & Alonso-Zarza, A. M. 2003. Reworked calcretes: their significance in the reconstruction of alluvial sequences (Permian and Triassic, Minorca, Balearic Islands, Spain). *Sedimentary Geology* **158**, 299 319.
Hasiotis, S. T., Platt, B. F., Hembree, D. I. & Everhart, M. J. 2007. The trace-fossil record of vertebrates. *In* William, M. III (ed.) *Trace fossils: concepts, problems, prospects*, 196 218. Amsterdam & Oxford: Elsevier Science.
Haubold, H. 2000. Tetrapodenfährten aus dem Perm Kenntnisstand und Progress 2000. *Hallesches Jahrbuch für Geowissenschaften, B* **22**, 1 16.
Haubold, H., Hunt, A. P., Lucas, S. G. & Lockley, M. G. 1995. Wolfcampian (Early Permian) vertebrate tracks from Arizona and New Mexico. *New Mexico Museum of Natural History and Science Bulletin* **6**, 135 65.
Heyler, D. & Lessertisseur, J. 1963. Pistes de tétrapodes Permiens dans la région de Lodève (Hérault). *Muséum National d'Histoire Naturelle, C* **11**, 1 100.
Hmich, D., Schneider, J. W., Saber, H., Voigt, S. & El Wartiti, M. 2006. New continental Carboniferous and Permian faunas of Morocco: implications for biostratigraphy, palaeobiogeography and palaeoclimate. *Geological Society, London, Special Publications* **265**, 297 324.
Hminna, A., Voight, A., Saber, H., Schneider, J. W. & Hmich, D. 2012. On a moderately diverse continental ichnofauna from the Permian Ikakern Formation (Argana Basin, Western High Atlas, Morocco). *Journal of African Earth Sciences* **68**, 15 23.
Holmes, R. B. 2003. The hind limb of *Captorhinus aguti* and the step cycle of basal amniotes. *Canadian Journal of Earth Sciences* **40**, 515 26.
Ivakhnenko, M. F. 2008. Podklass Captorhinomorpha [Subclass Captorhinomorpha]. *In* Ivakhnenko, M. F. & Kurotchkin, E. N. (eds) *Iskopaemye pozvonotchnye Rossii i sopredel'nykh stran: Iskopaemye reptilii i ptitsy, Tchast' 1* [*Fossil vertebrates of Russia and adjacent countries: Fossil reptiles and birds, Part 1*], 86 94. Moskva: GEOS.
Jalil, N. E. & Dutuit, J. M. 1996. Permian captorhinid reptiles from the Argana Formation, Morocco. *Palaeontology* **39**, 907 18.
Jung, J. P. & Sumida, S. S. 2017. A juvenile of the multiple-tooth-rowed reptile *Labidosaurikos* (Eureptilia, Captorhinidae, Moradisaurinae) from the Lower Permian of north-central Texas. *PaleoBios* **34**, 1 5.
Kissel, R. 2010. *Morphology, phylogeny, and evolution of Diadectidae (Cotylosauria: Diadectomorpha).* PhD Dissertation, University of Toronto, Toronto.
Kuhn, O. 1961. *Fossilium Catalogus. I: Animalia. Pars 99. Reptilia (Supplementum 1(2)).* The Hague, Netherlands: Uitgeverij Dr. W. Junk.
Kuhn, O. 1969. *Handbuch der Paläoherpetologie/Encyclopedia of Paleoherpetology. Teil 6/Part 6: Cotylosauria.* Stuttgart and Portland: Gustav Fischer Verlag.
Laurenti, J. N. 1768. *Specimen Medicum, Exhibens Synopsin Reptilium Emendatam cum Experimentis Circa Venena et Antidota Reptilium Austriacorum.* Vienna: Typis Joannis Thomae Nobilis de Trattnern.
LeBlanc, A. R. H., Brar, A. K., May, W. & Reisz, R. R. 2015. Multiple tooth-rowed captorhinids from the early Permian fissure fills of the Bally Mountain Locality of Oklahoma. *Vertebrate Anatomy Morphology Palaeontology* **1**, 35 49.
LeBlanc, A. R. H. & Reisz, R. R. 2015. Patterns of tooth development and replacement in captorhinid reptiles: a comparative approach for understanding the origin of multiple tooth rows. *Journal of Vertebrate Paleontology* **35**, e919928.
Leonardi, G. 1987. *Glossary and manual of tetrapod footprint palaeoichnology.* Brasília: Departamento Nacional de Produção Mineral.
Liebrecht, T., Fortuny, J., Galobart, À, Müller, J. & Sander, P. M. 2017. A large, multiple-tooth-rowed captorhinid reptile (Amniota: Eureptilia) from the Upper Permian of Mallorca (Balearic Islands, Western Mediterranean). *Journal of Vertebrate Paleontology* **37**, e1251936.
Linol, B., Bercovici, A., Bourquin, S., Diez, J. B., López-Gómez, J., Broutin, J., Durand, M. & Villanueva-Amadoz, U. 2009. Late Permian to Middle Triassic correlations and palaeogeographical reconstructions in south-western European basins: new sedimentological data from Minorca (Balearic Islands, Spain). *Sedimentary Geology* **220**, 77 94.
Llull, B. & Perelló, L. 2013. La mineria de coure a Menorca. De la prehistòria a l'actualitat. *Bolletí de la Societat Arqueològica Lul·liana. Revista d'Estudis Històrics* **69**, 75 93.
Logghe, A., Mujal, E., Marchetti, L., Nel, A., Pouillon, J.-M., Giner, S., Garrouste, R. & Steyer, J.-S. 2021. *Hyloidichnus* trackways with digit and tail drag traces from the Permian of Gonfaron (Var, France): new insights on the locomotion of captorhinomorph eureptiles. *Palaeogeography, Palaeoclimatology, Palaeoecology* **573**, 110436.
López-Gómez, J., Alonso-Azcárate, J., Arche, A., Arribas, J., Fernández-Barrenechea, J., Borruel-Abadía, V., Bourquin, S., Cadenas, P., Cuevas, J., De la Horra, R., Díez, J. B., Escudero-Mozo, M. J., Fernández-Viejo, G., Galán-Abellán, B., Galé, C., Gaspar-Escribano, J., Gisbert-Aguilar, J., Gómez-Gras, D., Goy, A., Gretter, N., Heredia-Carballo, N., Lago, M., Lloret, J., Luque, J., Márquez, L., Márquez-Aliaga, A., Martín-Algarra, A., Martín-Chivelet, J., Martín-González, F., Marzo, M., Mercedes-Martín, R., Ortí, F., Pérez-López, A., Pérez-Valera, F., Pérez-Valera, J. A., Plasencia, P., Ramos, E., Rodríguez-Méndez, L., Ronchi, A.,

Salas, R., Sánchez-Fernández, D., Sánchez-Moya, Y., Sopeña, A., Suárez-Rodríguez, Á., Tubía, J. M., Ubide, T., Valero-Garcés, B., Vargas, H. & Viseras, C. 2019a. Permian-Triassic rifting stage. *In* Vergés, J. & Kullberg, J. C. (coords) *The geology of Iberia: a geodynamic approach. Volume 3: the alpine cycle*, 29 112. Cham: Springer.

López-Gómez, J., Martín-González, F., Heredia, N., De la Horra, R., Barrenechea, J. F., Cadenas, P., Juncal, M., Diez, J. B., Borruel-Abadía, V., Pedreira, D., García-Sansegundo, J., Farias, P., Galé, C., Lago, M., Ubide, T., Fernández-Viejo, G. & Gand, G. 2019b. New lithostratigraphy for the Cantabrian Mountains: a common tectono-stratigraphic evolution for the onset of the Alpine cycle in the W Pyrenean realm, N Spain. *Earth-Science Reviews* **188**, 249 71.

López-Gómez, J. & Arche, A. 1987. Evolución sedimentológica de la Unidad «Limos y areniscas de Alcotas». Tramo medio de la Facies Buntsandstein del sector SE de la Rama Castellana de la Cordillera Ibérica (Provincias de Cuenca y Valencia). *Acta Geològica Hispànica* **21–22**, 9 18.

López-Gómez, J. & Arche, A. 1992. Las unidades litoestratigráficas del Pérmico y Triásico Inferior y Medio en el sector SE de la Cordillera Ibérica. *Estudios Geológicos* **48**, 123 43.

Lucas, S. G. 2019. An ichnological perspective on some major events of Paleozoic tetrapod evolution. *Bollettino della Società Paleontologica Italiana* **58**, 223 66.

Lucas, S. G., Krainer, K., Chaney, D. S., DiMichele, W. A., Voigt, S., Berman, D. S. & Henrici, A. C. 2013. The Lower Permian Abo Formation in central New Mexico. *New Mexico Museum of Natural History and Science Bulletin* **59**, 161 80.

Mack, G. H., James, W. C. & Monger, H. C. 1993. Classification of paleosols. *Geological Society of America Bulletin* **105**, 129 36.

Marchetti, L. 2016. New occurrences of tetrapod ichnotaxa from the Permian Orobic Basin (Northern Italy) and critical discussion of the age of the ichnoassociation. *Papers in Palaeontology* **2**, 363 86.

Marchetti, L., Avanzini, M. & Conti, M. A. 2013. *Hyloidichnus bifurcatus* Gilmore, 1927 and *Limnopus heterodactylus* (King, 1845) from the Early Permian of Southern Alps (N Italy): a new equilibrium in the ichnofauna. *Ichnos* **20**, 202 17.

Marchetti, L., Santi, G. & Avanzini, M. 2014. The problem of small footprints in paleoichnology: remarks on the early Permian ichnotaxon *Erpetopus cassinsi*, a local species from southern Alps (northern Italy). *Rivista Italiana di Paleontologia e Stratigrafia* **120**, 129 43.

Marchetti, L., Forte, G., Bernardi, M., Wappler, T., Hartkopf-Fröder, C., Krainer, K. & Kustatscher, E. 2015a. Reconstruction of a Late Cisuralian (Early Permian) floodplain lake environment: palaeontology and sedimentology of the Tregiovo Basin (Trentino Alto Adige, Northern Italy). *Palaeogeography, Palaeoclimatology, Palaeoecology* **440**, 180 220.

Marchetti, L., Ronchi, A., Santi, G., Schirolli, P. & Conti, M. A. 2015b. Revision of a classic site for Permian tetrapod ichnology (Collio Formation, Trompia and Caffaro valleys, N. Italy), new evidences for the radiation of captorhinomorph footprints. *Palaeogeography, Palaeoclimatology, Palaeoecology* **433**, 140 55.

Marchetti, L., Ronchi, A., Santi, G. & Voigt, S. 2015c. The Gerola Valley site (Orobic Basin, Northern Italy): a key for understanding late Early Permian tetrapod ichnofaunas. *Palaeogeography, Palaeoclimatology, Palaeoecology* **439**, 97 116.

Marchetti, L., Belvedere, M., Voigt, S., Klein, H., Castanera, D., Díaz-Martínez, I., Marty, D., Xing, L., Feola, S., Melchor, R. N. & Farlow, J. O. 2019a. Defining the morphological quality of fossil footprints. Problems and principles of preservation in tetrapod ichnology with examples from the Palaeozoic to the present. *Earth-Science Reviews* **193**, 109 45.

Marchetti, L., Klein, H., Buchwitz, M., Ronchi, A., Smith, R. M. H., De Klerk, W. J., Sciscio, L. & Groenewald, G. H. 2019b. Permian-Triassic vertebrate footprints from South Africa: ichnotaxonomy, producers and biostratigraphy through two major faunal crises. *Gondwana Research* **72**, 139 68.

Marchetti, L., Voigt, S., Lucas, S. G., Francischini, H., Dentzien-Dias, P., Sacchi, R., Mangiacotti, M., Scali, S., Gazzola, A., Ronchi, A. & Millhouse, A. 2019c. Tetrapod ichnotaxonomy in Eolian paleoenvironments (Coconino and De Chelly formations, Arizona) and late Cisuralian (Permian) sauropsid radiation. *Earth-Science Reviews* **190**, 148 70.

Marchetti, L., Voigt, S., Lucas, S. G., Stimson, M. R., King, O. A. & Calder, J. H. 2020a. Footprints of the earliest reptiles: *Notalacerta missouriensis* ichnotaxonomy, potential trackmakers, biostratigraphy, palaeobiogeography and palaeoecology. *Annales Societatis Geologorum Poloniae* **90**, 271 90.

Marchetti, L., Voigt, S., Mujal, E., Lucas, S. G., Francischini, H., Fortuny, J. & Santucci, V. L. 2020b. Extending the footprint record of Pareiasauromorpha to the Cisuralian: earlier appearance and wider palaeobiogeography of the group. *Papers in Palaeontology* **2020**, 1 23.

Martí, J., Paniello, X., Pomar, L., Ramos, E. & Rodríguez-Perea, A. 1985. El Triásico de las Baleares. *In* Mateu Ibars, F. & Marzo, M. (eds) *II Coloquio de Estratigrafía y Paleogeografía del Pérmico y Triásico de España*, 84 85. La Seu d'Urgell: Institut d'Estudis Ilerdencs and Grupo Español del Mesozoico.

Martin-Closas, C. & Ramos, E. 2005. Palaeogene Charophytes of the Balearic Islands (Spain). *Geologica Acta* **3**, 39 58.

Matamales-Andreu, R., Fortuny, J., Mujal, E. & Galobart, À. 2019. Tetrapod tracks from the Permian of Mallorca (western Mediterranean): preliminary data, biostratigraphic and biogeographic inferences. *In* The Palaeontological Association, 63rd annual meeting, 15th 21st December 2019, 107. València: The Palaeontological Association.

Melchor, R. N. & Sarjeant, W. A. S. 2004. Small amphibian and reptile footprints from the Permian Carapacha Basin, Argentina. *Ichnos* **11**, 57 78.

Miall, A. D. 1985. Architectural-element analysis: a new method of facies analysis applied to fluvial deposits. *Earth-Science Reviews* **22**, 261 308.

Miall, A. D. 2006. *The geology of fluvial deposits: sedimentary facies, basin analysis, and petroleum geology*. 4th edn. Berlin, Heidelberg, New York: Springer.

Michel, L. A., Tabor, N. J., Montañez, I. P., Schmitz, M. D. & Davydov, V. I. 2015. Chronostratigraphy and Paleoclimatology of the Lodève Basin, France: evidence for a pan-tropical aridification event across the Carboniferous Permian boundary. *Palaeogeography, Palaeoclimatology, Palaeoecology* **430**, 118 31.

Modesto, S. P., Scott, D. M., Berman, D. S., Müller, J. & Reisz, R. R. 2007. The skull and the palaeoecological significance of *Labidosaurus hamatus*, a captorhinid reptile from the Lower Permian of Texas. *Zoological Journal of the Linnean Society* **149**, 237 62.

Modesto, S. P., Lamb, A. J. & Reisz, R. R. 2014. The captorhinid reptile *Captorhinikos valensis* from the lower Permian Vale Formation of Texas, and the evolution of herbivory in eureptiles. *Journal of Vertebrate Paleontology* **34**, 291 302.

Modesto, S. P., Fear, V. J., Danley, M. M. & Reisz, R. R. 2016. A large moradisaurine tooth plate from the lower Permian of Texas and its biostratigraphic implications. *Journal of Vertebrate Paleontology* **36**, e1221832.

Modesto, S. P., Scott, D. & Reisz, R. R. 2018. A new small captorhinid reptile from the lower Permian of Oklahoma and resource partitioning among small captorhinids in the Richards Spur fauna. *Papers in Palaeontology* **4**, 293 307.

Modesto, S. P., Richards, C. D., Ide, O. & Sidor, C. A. 2019. The vertebrate fauna of the upper Permian of Niger X. The mandible of the captorhinid reptile *Moradisaurus grandis*. *Journal of Vertebrate Paleontology* **38**, e1531877.

Moodie, R. L. 1929. Vertebrate footprints from the Red Beds of Texas. *American Journal of Science* **97**, 352 68.

Moreau, J.-D., Benaouiss, N., Tourani, A., Steyer, J.-S., Laurin, M., Peyer, K., Béthoux, O., Aouda, A. & Jalil, N.-E. 2020. A new ichnofauna from the Permian of the Zat Valley in the Marrakech High Atlas of Morocco. *Journal of African Earth Sciences* **172**, 103973.

Mujal, E., Fortuny, J., Oms, O., Bolet, A., Galobart, À & Anadón, P. 2016. Palaeoenvironmental reconstruction and early Permian ichnoassemblage from the NE Iberian Basin (Pyrenean Basin). *Geological Magazine* **153**, 578 600.

Mujal, E., Fortuny, J., Pérez-Cano, J., Dinarès-Turell, J., Ibáñez-Insa, J., Oms, O., Vila, I., Bolet, A. & Anadón, P. 2017. Integrated multistratigraphic study of the Coll de Terrers late Permian Early Triassic continental succession from the Catalan Pyrenees (NE Iberian Peninsula): a geologic reference record for equatorial Pangaea. *Global and Planetary Change* **159**, 46 60.

Mujal, E., Marchetti, L., Schoch, R. R. & Fortuny, J. 2020. Upper Paleozoic to lower Mesozoic tetrapod ichnology revisited: photogrammetry and relative depth pattern inferences on functional prevalence of autopodia. *Frontiers in Earth Science* **8**, 1 23.

Müller, J. & Reisz, R. R. 2005. An early captorhinid reptile (Amniota, Eureptilia) from the Upper Carboniferous of Hamilton, Kansas. *Journal of Vertebrate Paleontology* **25**, 561 68.

Nyakatura, J. A., Allen, V. R., Lauströer, J., Andikfar, A., Danczak, M., Ullrich, H.-J., Hufenbach, W., Martens, T. & Fischer, M. S. 2015. A three-dimensional skeletal reconstruction of the stem amniote *Orobates pabsti* (Diadectidae): analyses of body mass, centre of mass position, and joint mobility. *PLoS ONE* **10**, e0137284.

O'Keefe, F. R., Sidor, C. A., Larsson, H. C., Maga, A. & Ide, O. 2005. The vertebrate fauna of the upper Permian of Niger III, Morphology and ontogeny of the hindlimb of *Moradisaurus grandis* (Reptilia, Captorhinidae). *Journal of Vertebrate Paleontology* **25**, 309 19.

Obrador, A. 1983. El Pérmico de las Baleares. *In* Martínez-Díaz, C. (ed.). *Carbonífero y Pérmico de España, X Congreso Internacional de Estratigrafía y Geología del Carbonífero*, 463 470. Madrid: Ministerio de Industria y Energía, Instituto Geológico y Minero de España.

Olroyd, S. L. & Sidor, C. A. 2017. A review of the Guadalupian (middle Permian) global tetrapod fossil record. *Earth-Science Reviews* **171**, 583 97.

Olson, E. C. 1947. The family Diadectidae and its bearing on the classification of reptiles. *Fieldiana: Geology* **11**, 1 53.

Olson, E. C. 1954. Fauna of the Vale and Choza: 9. Captorhinomorpha. *Fieldiana: Geology* **10**, 211 18.

Olson, E. C. 1962a. Late Permian terrestrial vertebrates, U.S.A. and U.S.S.R. *Transactions of the American Philosophical Society* **52**, 1 224.

Olson, E. C. 1962b. Permian vertebrates from Oklahoma and Texas. Part II. The osteology of *Captorhinikos chozaensis* Olson. *Oklahoma Geological Survey Circular* **59**, 49 68.

Olson, E. C. 1965. New Permian vertebrates from the Chickasha Formation in Oklahoma. *Oklahoma Geological Survey Circular* **70**, 1 70.

Olson, E. C. 1970. New and little known genera and species of vertebrates from the Lower Permian of Oklahoma. *Fieldiana: Geology* **18**, 359 434.

Olson, E. C. 1979. *Seymouria grandis* n. sp. (Batrachosauria: Amphibia) from the middle Clear Fork (Permian) of Oklahoma and Texas. *Journal of Paleontology* **53**, 720 28.

Olson, E. C. & Barghusen, H. 1962. Permian vertebrates from Oklahoma and Texas. Part I. Vertebrates from the Flowerpot Formation, Permian of Oklahoma. *Oklahoma Geological Survey Circular* **59**, 4 48.

Olson, E. C. & Beerbower, J. R. 1953. The San Angelo Formation, Permian of Texas, and its vertebrates. *The Journal of Geology* **61**, 389 423.

Pomar-Gomà, L. 1979. *The Triassic of the Balearic Islands*. Palma: Geology Department, Palma de Mallorca University.

Postma, G. 1990. Depositional architecture and facies of river and fan deltas: a synthesis. *Special publications of the international association of sedimentologists* **10**, 13 27.

Pretus, J. L. & Obrador, A. 1987. Presencia de restos óseos en el Pérmico de Menorca (nota previa). *Bolletí de la Societat d'Història Natural de Balears* **31**, 149 52.

Ramos, A. & Doubinger, J. 1989. Premières datations palynologiques dans le facies Buntsandstein de l'île de Majorque (Baléares, Espagne). *Comptes Rendus de l'Académie des Sciences de Paris, s. 2* **309**, 1089 94.

Reisz, R. R., Liu, J., Li, J.-L. & Müller, J. 2011. A new captorhinid reptile, *Gansurhinus qingtoushanensis*, gen. et sp. nov., from the Permian of China. *Naturwissenschaften* **98**, 435 41.

Reisz, R. R., Haridy, Y. & Müller, J. 2016. *Euconcordia* nom. nov., a replacement name for the captorhinid eureptile *Concordia* Müller and Reisz, 2005 (non Kingsley, 1880), with new data on its dentition. *Vertebrate Anatomy Morphology Palaeontology* **3**, 1 6.

Reisz, R. R., MacDougall, M. J., LeBlanc, A. R. H., Scott, D. & Nagesan, R. S. 2020. Lateralized feeding behaviour in a Paleozoic reptile. *Current Biology* **30**, 2374 78.

Reisz, R. R. & Sues, H.-D. 2000. Herbivory in late Paleozoic and Triassic terrestrial vertebrates. *In* Sues, H.-D. (ed) *Evolution of herbivory in terrestrial vertebrates*, 9 41. Cambridge, New York, Melbourne, Madrid, Cape Town, Singapore, São Paulo: Cambridge University Press.

Rodríguez-Perea, A., Ramos-Guerrero, E., Pomar, L., Paniello, X., Obrador, A. & Martí, J. 1987. El Triásico de las Baleares. *Cuadernos de Geología Ibérica* **11**, 295 321.

Romano, M. & Rubidge, B. 2019. Long bone scaling in Captorhinidae: do limb bones scale according to elastic similarity in sprawling basal amniotes? *Lethaia* **52**, 389 402.

Roscher, M., Stordal, F. & Svensen, H. 2011. The effect of global warming and global cooling on the distribution of the latest Permian climate zones. *Palaeogeography, Palaeoclimatology, Palaeoecology* **309**, 186 200.

Rosell, J., Arribas, J., Elízaga, E. & Gómez-Gras, D. 1988. Caracterización sedimentológica y petrográfica de la serie roja permo triásica de la isla de Menorca. *Boletín Geológico y Minero* **99**, 71 82.

Rosell, J., Gómez-Gras, D. & Elízaga, E. 1989a. *Mapa Geológico de España. Escala 1:25.000. Isla de Menorca. Cap Menorca y Ciutadella. Segunda serie, primera edición*. Madrid: Instituto Tecnológico GeoMinero de España.

Rosell, J., Gómez-Gras, D. & Elízaga, E. 1989b. *Mapa Geológico de España. Escala 1:25.000. Isla de Menorca. Cala en Brut i Alaior. Segunda serie, primera edición*. Madrid: Instituto Tecnológico GeoMinero de España.

Sàbat, F., Gelabert, B. & Rodríguez-Perea, A. 2018. Minorca, an exotic Balearic island (western Mediterranean). *Geologica Acta* **16**, 411 26.

Santi, G., Marchetti, L., Schirolli, P. & Ronchi, A. 2020. The Cisuralian tetrapod ichnoassociation from Italy: from historical findings to a standard reference status. *Journal of Mediterranean Earth Sciences* **12**, 39 59.

Schneider, J. W., Lucas, S. G., Scholze, F., Voigt, S., Marchetti, L., Klein, H., Opluštil, S., Werneburg, R., Golubevb, V. K., Barrick, J. E., Nemyrovska, Y., Ronchil, A., Day, M. O., Silantiev, V. V., Rößler, R., Saber, H., Linnemann, U., Zharinova, V. & Shen, S.-Z. 2020. Late Paleozoic early Mesozoic continental biostratigraphy links to the Standard Global Chronostratigraphic Scale. *Palaeoworld* **29**, 186 238.

Scotese, C. R. 2014. Atlas of Middle & Late Permian and Triassic Paleogeographic Maps, maps 43 48 from Volume 3 of the PALEOMAP Atlas for ArcGIS (Jurassic and Triassic) and maps 49 52 from Volume 4 of the PALEOMAP Atlas for ArcGIS (Late Paleozoic), Mollweide Projection, PALEOMAP Project: Evanston, Illinois, USA.

Sennikov, A. G. & Golubev, V. K. 2017. Sequence of Permian tetrapod faunas of Eastern Europe and the Permian Triassic ecological crisis. *Paleontological Journal* **51**, 600 11.

Sidor, C. A., O'Keefe, F. R., Damiani, R., Steyer, J. S., Smith, R. M. H., Larsson, H. C. E., Sereno, P. C., Ide, O. & Maga, A. 2005. Permian tetrapods from the Sahara show climate-controlled endemism in Pangaea. *Nature* **434**, 886 89.

Smith, R. M., Sidor, C. A., Tabor, N. J. & Steyer, J.-S. 2015. Sedimentology and vertebrate taphonomy of the Moradi Formation of northern Niger: a Permian wet desert in the tropics of Pangaea. *Palaeogeography, Palaeoclimatology, Palaeoecology* **440**, 128 41.

Speksnijder, A. 1985. Anatomy of a strike-slip fault controlled sedimentary basin, Permian of the southern Pyrenees, Spain. *Sedimentary Geology* **44**, 179 223.

Stappenbeck, R. 1905. Über *Stephanospondylus* n. g. und *Phanerosaurus* H. v. Meyer. *Zeitschrift der Deutschen Geologischen Gesellschaft* **57**, 380 437.

Stovall, J. W. 1950. A new cotylosaur from North Central Oklahoma. *American Journal of Science* **248**, 46 54.

Sullivan, C. & Reisz, R. R. 1999. First record of *Seymouria* (Vertebrata: Seymouriamorpha) from Early Permian fissure fills at Richards Spur, Oklahoma. *Canadian Journal of Earth Sciences* **36**, 1257 66.

Sumida, S. S. 1990. Vertebral morphology, alternation of neural spine height, and structure in Permo-Carboniferous tetrapods, and a reappraisal of primitive modes of terrestrial locomotion. *University of California Publications in Zoology* **122**, 1 129 + 3 pls.

Swofford, D. L. 2003. *PAUP*. phylogenetic analysis using parsimony (*and other methods). Version 4*. Sunderland, Massachusetts: Sinauer Associates.

Tabor, N. J. & Poulsen, C. J. 2008. Palaeoclimate across the Late Pennsylvanian Early Permian tropical palaeolatitudes: a review of climate indicators, their distribution, and relation to palaeophysiographic climate factors. *Palaeogeography, Palaeoclimatology, Palaeoecology* **268**, 293 310.

Taquet, P. 1969. Première découverte en Afrique d'un reptile captorhinomorphe (cotylosaurien). *Comptes Rendus Hebdomadaires des Séances de l'Academie des Sciences Paris, s. D* **268**, 779 81.

Vera, J.-A., Alonso-Chaves, F. M., Andreo, B., Arias, C., Azañón, J. M., Balanyá, J. C., Barón, A., Booth-Rea, G., Castro, J. M., Chacón, B., Company, M., Crespo-Blanc, A., Delgado, F., Díaz de Federico, A., Esteras, M., Estévez, A., Fernández, J., Fornós, J. J., Galindo-Zaldívar, J., García-Casco, A., García-Dueñas, V., García-Hernández, M., Garrido, C. J., de Gea, G. A., Gelabert, B., Gervilla, F., González-Lodeiro, F., Jabaloy, A., López-Garrido, A. C., Luján, M., Martín-Algarra, A., Martín-Chivelet, J., Martín-Martín, M., Molina, J. M., Morata, D., Nieto, J. M., Obrador, A., O'Dogherty, L., Orozco, M., Pérez-López, A., Pomar, L., Puga, E., Ramos, E., Rey, J., Rivas, P., Rodríguez-Cañero, R., Ruiz-Cruz, M. D., Ruiz-Ortiz, P. A., Sàbat, F., Sánchez-Gómez, M., Sánchez-Navas, A., Sandoval, J., Sanz de Galdeano, C., Soto, J. I., Torres-Roldán, R. L. & Villas, L. 2004. Capítulo 4. Cordillera Bética y Baleares. *In* Vera, J.-A. (ed.) *Geología de España*, 345 464. Madrid: Instituto Tecnológico GeoMinero de España.

Viglietti, P. A., Smith, R. M., Angielczyk, K. D., Kammerer, C. F., Fröbisch, J. & Rubidge, B. S. 2016. The *Daptocephalus* Assemblage Zone (Lopingian), South Africa: a proposed biostratigraphy based on a new compilation of stratigraphic ranges. *Journal of African Earth Sciences* **113**, 153 64.

Vjushkov, B. P. & Chudinov, P. K. 1957. Otkrytie Kaptorinid v verkhnnej Permi SSSR [Discovery of a captorhinid in the upper Permian of the USSR]. *Doklady Akademii Nauk SSSR* **112**, 523 36.

Voigt, S. 2005. *Die Tetrapodenichnofauna des kontinentalen Oberkarbon und Perm im Thüringer Wald - Ichnotaxonomie, Paläoökologie und Biostratigraphie*. Göttingen: Cuvillier Verlag.

Voigt, S., Hminna, A., Saber, H., Schneider, J. W. & Klein, H. 2010. Tetrapod footprints from the uppermost level of the Permian Ikakern Formation (Argana Basin, Western High Atlas, Morocco). *Journal of African Earth Sciences* **57**, 470 78.

Voigt, S., Lagnaoui, A., Hminna, A., Saber, H. & Schneider, J. W. 2011. Revisional notes on the Permian tetrapod ichnofauna from the Tiddas Basin, central Morocco. *Palaeogeography, Palaeoclimatology, Palaeoecology* **302**, 474 83.

Voigt, S. & Haubold, H. 2015. Permian tetrapod footprints from the Spanish Pyrenees. *Palaeogeography, Palaeoclimatology, Palaeoecology* **417**, 112 20.

Voigt, S. & Lucas, S. G. 2015. Permian tetrapod ichnodiversity of the Prehistoric Trackways National Monument (south-central New Mexico, USA). *New Mexico Museum of Natural History and Science Bulletin* **65**, 153 67.

Voigt, S. & Lucas, S. G. 2017. Early Permian tetrapod footprints from central New Mexico. *New Mexico Museum of Natural History and Science Bulletin* **77**, 333 52.

von Meyer, H. 1860. *Phanerosaurus Naumanni* ans dem Sandstein des Rothliegenden in Deutschland. *Paleontographica* **7**, 248 52 + pl. 27.

White, T. E. 1939. Osteology of *Seymouria baylorensis* Broili. *Bulletin of the Museum of Comparative Zoölogy* **85**, 323 409 + 3 pls.

Zouicha, A., Voigt, S., Saber, H., Marchetti, L., Hminna, A., El Attari, A., Ronchi, A. & Schneider, J. W. 2021. First record of Permian continental trace fossils in the Jebilet Massif, Morocco. *Journal of African Earth Sciences* **173**, 104015.

MS received 8 February 2021. Accepted for publication 21 June 2021. First published online 22 July 2021

Chapter 6

Discussion

Chapter 6 was in part published as:

Matamales-Andreu, R. (2022). Rèptils i avantpassats dels mamífers: registre fòssil del Permià de Mallorca. *In*: Pons, G.X.; del Valle, L.; McMinn, M.; Pinya, S. & Vicens, D. (Eds.). *Llibre de ponències i comunicacions de les VIII Jornades de Medi Ambient de les Illes Balears*. Societat d'Història Natural de les Balears, Universitat de les Illes Balears; Palma: 83–86. [in Catalan]

Matamales-Andreu, R. (2022). Rèptils i primers mosquits: registre fòssil del Triàsic continental de Mallorca. *In*: Pons, G.X.; del Valle, L.; McMinn, M.; Pinya, S. & Vicens, D. (Eds.). *Llibre de ponències i comunicacions de les VIII Jornades de Medi Ambient de les Illes Balears*. Societat d'Història Natural de les Balears, Universitat de les Illes Balears; Palma: 87–90. [in Catalan]

Matamales-Andreu, R. (2022). Mol·luscs, notosaures i ictiosaures: registre fòssil del Triàsic marí de Mallorca. *In*: Pons, G.X.; del Valle, L.; McMinn, M.; Pinya, S. & Vicens, D. (Eds.). *Llibre de ponències i comunicacions de les VIII Jornades de Medi Ambient de les Illes Balears*. Societat d'Història Natural de les Balears, Universitat de les Illes Balears; Palma: 91–94. [in Catalan]

ISBN: 978-84-09-45184-5

DL: PM 00851-2022

Also, see Appendix 13: Matamales-Andreu (2022a), *Jornades de Medi Ambient de les Balears*

Appendix 14: Matamales-Andreu (2022b), *Jornades de Medi Ambient de les Balears*

Appendix 15: Matamales-Andreu (2022c), *Jornades de Medi Ambient de les Balears*

Discussion

Palaeoecosystems of the Permian and Triassic of Mallorca

As detailed in Chapters 2–4 and Appendices 1–11, 13–15 (and references therein), the palaeoenvironments and biotic communities of Mallorca changed throughout the Permian and the Triassic, in response to both global and local events and conditions. By integrating all this information, a general chronostratigraphic panel can be assembled (Figure 6.1). It shows an initial interval of continental sedimentation from the early/middle Permian to the Middle Triassic, followed by a period of marine conditions, from the Middle to the Upper Triassic, with at least three conspicuous transgressive-regressive cycles.

The Permian group corresponds to the oldest continental rocks of Mallorca and records the development of a continental rift basin. It started with colluvial and alluvial fan sedimentation, typical of the first opening stages (Bec de s'Àguila Formation). Over time, meandering rivers and associated floodplains started to gain importance, as a result of the development of an axial fluvial system flowing towards the southwest. Initially, the load of those rivers was relatively coarse (medium-grained sands), as they reworked the alluvial fan sediments (Bec de s'Àguila Formation). This stage was followed by an interval of finer sedimentation (very fine-grained sands and mud) when the system became relatively stable in terms of tectonics and eustatism (Port des Canonge Formation), and later by another coarser interval (medium-grained sands) with higher-flow structures, perhaps reflecting an increased water supply (Pedra de s'Ase Formation). The main facies assemblages of the aforementioned formations reflect environmental conditions of alternating dry and wet periods, similar to other coeval basins of the western peri-Tethys.

The Permian units have yielded rich fossil assemblages that, together with magnetostratigraphy, have shed light on the age of the different formations (Chapter 2). Regarding fossils, there is representation of several groups of algae, plants (bryophytes, horsetails, lycophytes, ferns, seed ferns and conifers), invertebrates (worms, notostracans and insect larvae) and terrestrial vertebrates (sauropsids and synapsids) (Figure 6.2). Palynoassemblages suggest a Guadalupian–Lopingian series for the Pedra de s'Ase Formation, which is further constrained by the palaeomagnetic data. Since the whole Permian sequence of Mallorca falls in the Kiaman Reverse Superchron, the Pedra de s'Ase Formation can be, at

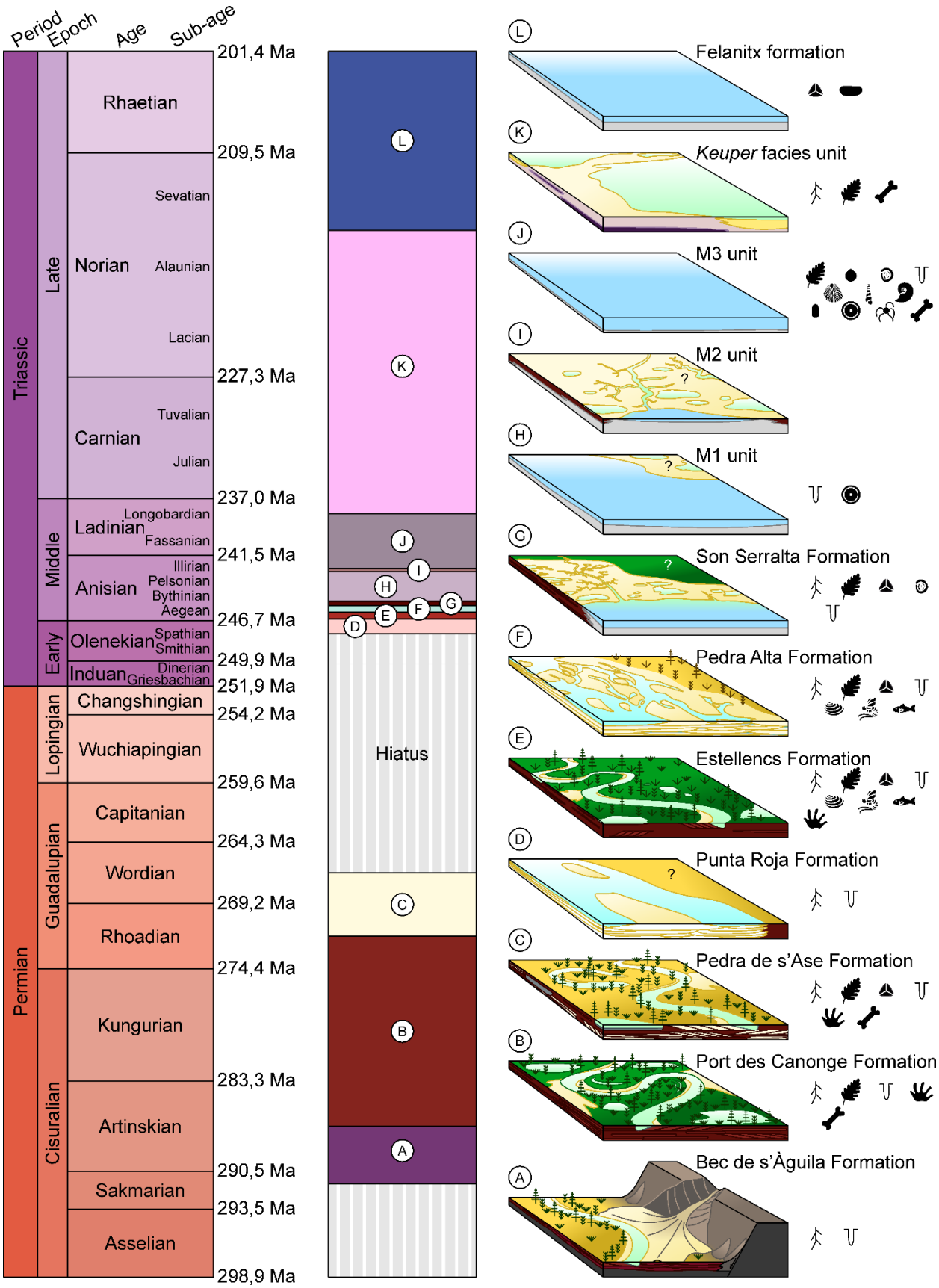
Period
Epoch
Age
Sub-age
Triassic
Permian
Late
Middle
Early
Lopingian
Guadalupian
Cisuralian
Rhaetian
Norian
Sevatian
Alaunian
Lacian
Carnian
Tuvalian
Julian
Ladinian
Longobardian
Fassanian
Anisian
Illirian
Pelsonian
Bythinian
Aegean
Olenekian
Spathian
Smithian
Induan
Dinerian
Griesbachian
Changshingian
Wuchiapingian
Capitanian
Wordian
Rhoadian
Kungurian
Artinskian
Sakmarian
Asselian
201,4 Ma
209,5 Ma
227,3 Ma
237,0 Ma
241,5 Ma
246,7 Ma
249,9 Ma
251,9 Ma
254,2 Ma
259,6 Ma
264,3 Ma
269,2 Ma
274,4 Ma
283,3 Ma
290,5 Ma
293,5 Ma
298,9 Ma
Hiatus
L
K
J
I
H
G
F
E
D
C
B
A
Felanitx formation
Keuper facies unit
M3 unit
M2 unit
M1 unit
Son Serralta Formation
Pedra Alta Formation
Estellencs Formation
Punta Roja Formation
Pedra de s'Ase Formation
Port des Canonge Formation
Bec de s'Àguila Formation

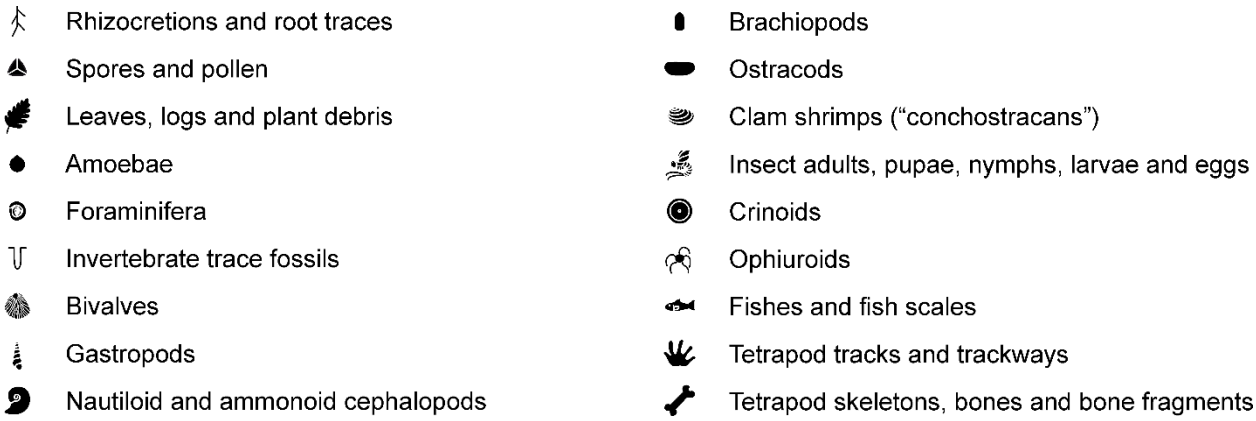

Figure 6.1. (previous page) Permian–Triassic palaeoenvironmental evolution in Mallorca, and fossil record of each lithostratigraphic unit. Age ranges are an estimation based on current data but some of them, especially the lower and upper boundaries of A and B, are uncertain. ***A:*** *Bec de s'Àguila Formation,* ***B:*** *Port des Canonge Formation,* ***C:*** *Pedra de s'Ase Formation,* ***D:*** *Punta Roja Formation,* ***E:*** *Estellencs Formation,* ***F:*** *Pedra Alta Formation,* ***G:*** *Son Serralta Formation,* ***H:*** *M1 unit,* ***I:*** *M2 unit,* ***J:*** *M3 unit,* ***K:*** Keuper *facies unit,* ***L:*** *Felanitx formation.*

most, middle Guadalupian. Tetrapod tracks of the underlying Port des Canonge Formation suggest a middle–upper Cisuralian series for it, although presence of therapsids could point to a lowermost Guadalupian.

After deposition of the Permian units, there was a period of no sedimentation (and/or erosion) that spanned from the middle Guadalupian to the late Early Triassic. This diachronic gap has been recognised in most basins of the western peri-Tethys (Cassinis *et al.*, 2003, 2012; Bourquin *et al.*, 2006; Schenider *et al.*, 2006; Durand, 2008; Linol *et al.*, 2009; Mujal *et al.*, 2017a; López-Gómez *et al.*, 2019), although there are instances in which it could be very reduced or even absent (Mujal *et al.*, 2017a). In any case, this means that the Permian–Triassic transition was not recorded in Mallorca.

The continental Triassic group represents the so-called Buntsandstein facies. Deposition started with shallow braided rivers that flowed towards the southeast, reworking aeolian sediments (well-sorted medium-grained sands) and following the main axis of the basin (Punta Roja Formation). Fine-grained (very fine-sand and mud) low-energy meandering rivers settled in progressively, with pervasive development of floodplains and playa lakes (Estellencs

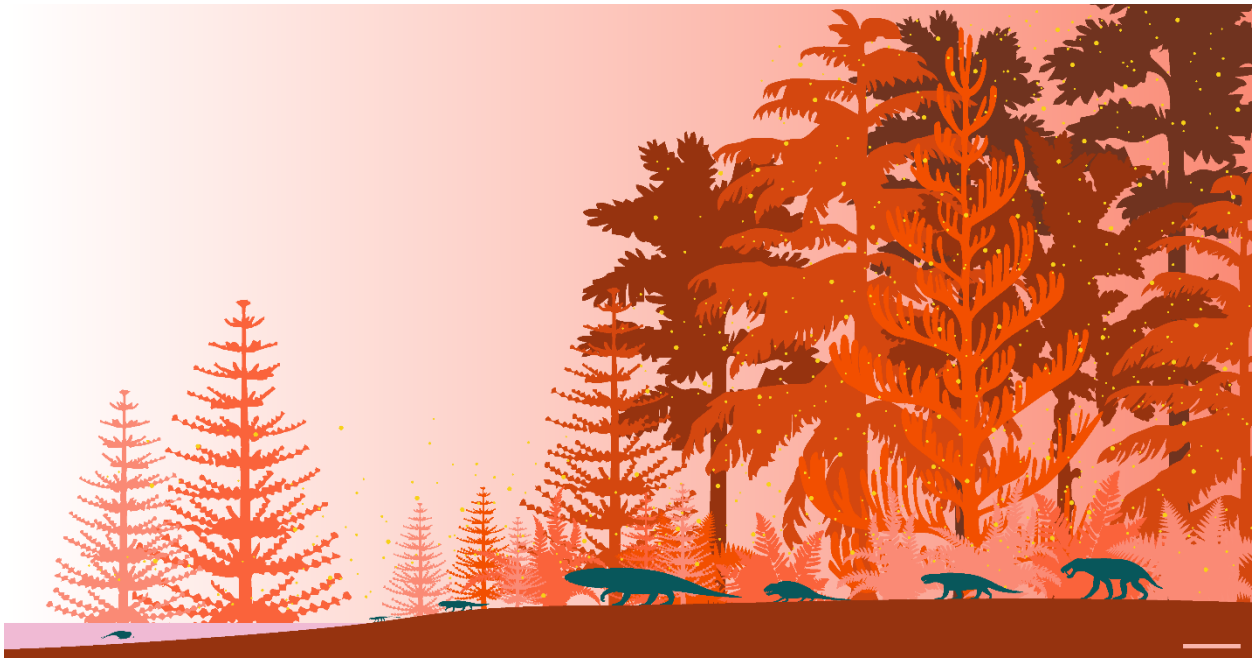

Figure 6.2. Schematic representation of the fauna and flora of the Cisuralian–Guadalupian (early–middle Permian) of Mallorca, with some plants (horsetails, ferns, seed ferns and conifers), invertebrates (notostracans) and vertebrates (araeoscelidians, moradisaurine captorhinids, "pelycosaur"-grade synapsids and gorgonopsian therapsids). Some of the taxa have been inferred based on spores, pollen or trace fossils. Scale bar: 50 cm.

Formation). Such conditions charged again due to an increase of the system energy, developing braided rivers with coarser loads (medium-grained sands), associated to backswamps (Pedra Alta Formation). Finally, transition to coastal environments was marked by the settling of mud flats with typical tidal traits (Son Serralta Formation). In general terms, the facies assemblages reveal that deposition occurred under arid climates alternating dry and wet periods.

The continental Triassic units abound in fossils (exceptionally well preserved locally), yielding fairly accurate age attributions for some of the formations (Chapter 3). Specifically, there is record of acritarchs, algae, plants (horsetails, lycophytes, ferns, seed ferns, cicadophytes, ginkgophytes and conifers), invertebrates (worms, clam shrimps, notostracans, mayflies, grylloblattids, beetles, true bugs, cockroaches and true flies) and vertebrates (fish and sauropsids) (Figure 6.3). Palynoassemblages, clam shrimps and, to a lesser extent, tetrapod tracks, situate the Estellencs Formation and the Pedra Alta Formation in the lowermost Middle Triassic.

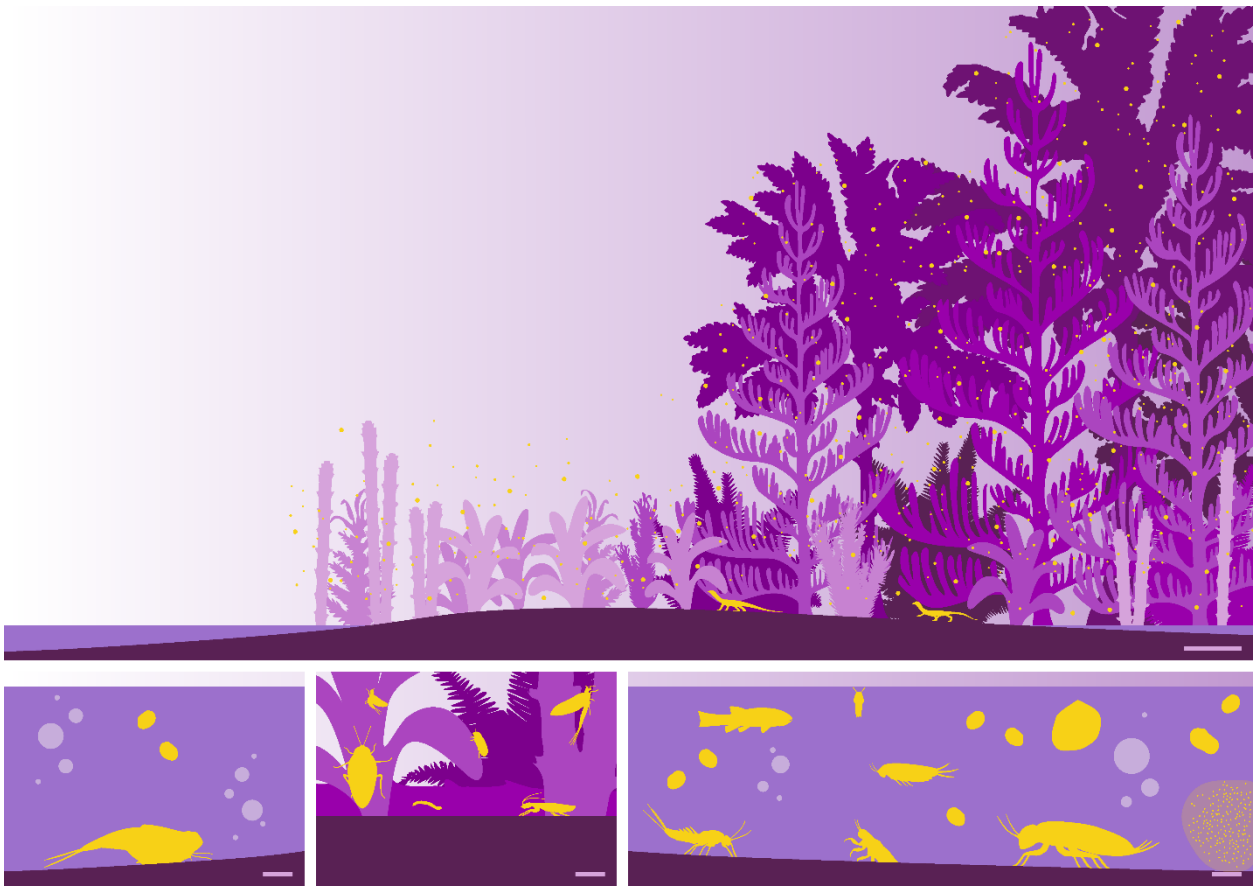

Figure 6.3. Schematic representation of the fauna and flora of the continental Early–Middle Triassic of Mallorca, with some plants (horsetails, ferns, seed ferns and conifers), invertebrates (clam shrimps, notostracans, mayfly larvae and adults, true fly eggs, larvae and pupae, true beetles, cockroaches and grylloblattids) and vertebrates (fishes and archosauromorphs). Some of the taxa have been inferred based on spores, pollen or trace fossils. Scale bar in upper picture: 50 cm. Scale bars in the three lower, zoomed-in pictures: 0.5 cm.

Continental Triassic alluvial plains were subsequently drowned by the shallow seas that originated the *Muschelkalk* facies. There was a slight deepening of the depositional setting during the first transgressive event (M1 unit), although the environments usually represent intertidal conditions. Later, a regressive episode resulted in the establishment of sabkha conditions, with evaporitic mud flats (M2 unit), which would be overlain by marine carbonates again in a more extensive transgressive event (M3 unit). The latter records an intertidal–subtidal setting, with tidal bundles and algal mats and, in some instances, platform sand bars.

Figure 6.4. Schematic representation of the fauna of the marine Middle Triassic of Mallorca, with some invertebrates (nautiloids, ammonoids, crinoids) and vertebrates (basal ichthyosauriforms). Scale bar: 50 cm.

These marine Triassic units contain many invertebrate fossils; vertebrates, although extremely rare, have also been found (Chapter 4). Among invertebrates, the most abundant ones are molluscs (bivalves, gastropods and cephalopods, both nautiloids and ammonoids), although there are also records of brachiopods, crinoids, echinoids and ophiuroids. Plants (horsetails), foraminifera, amoebae and conodonts have also been reported. Finally, vertebrates (sauropsids) were represented by basal ichthyosauriforms (*sensu* Huang *et al.*, 2019) (Figure 6.4). Ammonoid and conodont assemblages show that the M3 unit ranges, at least, from the lower to the upper Ladinian (upper Middle Triassic).

Marine carbonate platforms emerged again in another, more generalised regression, originating sabkha environments corresponding to the *Keuper* marlstone facies. Such lagoons were highly variable laterally, which greatly complicates the establishment of a common framework for these facies on the island. In some instances, the lagoons were more restricted (with evaporites), in others, they were relatively open (with dolostones), and in others, there was an important supply of pyroclastic materials and lava flows. Over time, the subtidal carbonate platform conditions became widespread again, corresponding to the Felanitx formation.

Figure 6.5. Schematic representation of the fauna and flora of the lagoonal Late Triassic of Mallorca, with some plants (conifers) and vertebrates (sauropterygians). Plant taxa have been inferred based on pollen. Scale bar: 50 cm.

Fossils are extremely rare in the *Keuper* facies and in the Felanitx formation (Chapter 4), probably due to the extreme conditions most of the environments of the former (evaporite lagoons located near volcanoes), and the fact that in the latter is heavily dolomitised, erasing all traces of fossils. Only vertebrates (sauropsids), represented by nothosaurs, have been recognised in the *Keuper* facies, whereas in the Felanitx formation plants (lycophytes and conifers) and invertebrates (ostracods) have been reported (Figure 6.5). The palynoassemblage suggests that the lowermost Felanitx formation can be attributed to the middle–upper part of the Upper Triassic.

Palaeoecosystems of the Permian of Menorca

The Permian of Menorca has been briefly treated in Chapter 5 and in Appendix 12 (and references therein), with palaeoenvironments that changed following a similar trend to the Permian units of Mallorca. Deposition started in the form of alluvial fan conglomerates (P1 unit), typical of transverse sedimentation in opening rift basins. Fine-grained (very fine-grained

Figure 6.6. Schematic representation of the fauna and flora of the Guadalupian–Lopingian (middle–late Permian) of Menorca, with some plants (horsetails, ferns, seed ferns and conifers) and vertebrates (parareptiles and moradisaurine captorhinids). Some of the taxa have been inferred based on spores, pollen or trace fossils. Scale bar: 50 cm.

sand and mud) floodplains with playa lakes developed once the subsidence waived, and were traversed by meandering river channels (P2 unit). This fluvial style persisted, with less mud and with higher-flow structures, until the end of the period (P3 unit). In general terms, facies assemblages and palaeosols indicate that deposition occurred under a tropical climate alternating arid and more humid periods.

Fossils are locally abundant in the P3 unit of Menorca (Chapter 5). The record contains algae, plants (horsetails, lycophytes, seed ferns and conifers), invertebrates (worms and insect larvae) and terrestrial vertebrates (sauropsids) (Figure 6.6). The palynoassemblage points to a Lopingian series for the upper part of the P3 unit, whereas tetrapod tracks provide a broad Permian age for the lower part of the P3 unit.

Significance of the Gymnesic Islands Permian and Triassic tetrapod fossil record

Tetrapod fossils, especially tracks and trackways, have been reported from many Permian (*e.g.*, Voigt, 2005; Gand & Durand, 2006; Mujal *et al.*, 2016a; Bernardi *et al.*, 2017; Olroyd & Sidor, 2017; Martens, 2018; Marchetti *et al.*, 2020; Santi *et al.*, 2020), continental Triassic (*e.g.*, Romano *et al.*, 2020; De Jaime-Soguero *et al.*, 2021) and marine Triassic (*e.g.*, Diedrich, 2012; Rieppel, 2019; de Miguel Chaves *et al.*, 2020) units of the western peri-Tethys. Chapters 2–5 and Appendices 1–12 of the present Ph.D. dissertation have provided many new data on the richness and diversity of tetrapod fossils from the Permian and Triassic rock formations of the Gymnesic Islands, contributing to the increase of the overall knowledge on these periods in palaeoequatorial latitudes (Figure 5.7).

Many Cisuralian tetrapod fossil assemblages are known from the western peri-Tethys. However, the vast majority of them correspond to tracks and trackways, with remarkable examples such as the Central European Basin (*e.g.*, Voigt, 2005; Voigt *et al.*, 2012), the Massif Central and Provençe (*e.g.*, Gand & Durand, 2006), the southern Alps (*e.g.*, Santi *et al.*, 2020), the Iberian Peninsula (Gand *et al.*, 1997; Voigt & Haubold, 2015; Mujal *et al.*, 2016a), northern Africa (Voigt *et al.*, 2011; Zouicha *et al.*, 2021) and Anatolia (Gand *et al.*, 2011). Conversely, sites with bone remains are much scarcer: the Central European Basin and the Massif Central are the most fossiliferous areas in which tetrapod remains have been found (*e.g.*, Werneburg *et al.*, 2007a; Reisz *et al.*, 2011; Spindler, 2015, 2016; Spindler *et al.*, 2016, 2018, 2019a, 2019b; Martens, 2018; Berman *et al.*, 2020). The ichnoassemblage of the Port des Canonge Formation of Mallorca contains the main elements of middle/upper Cisuralian deposits elsewhere, especially in the Iberian Peninsula, the Massif Central, the Southern Alps and northern Africa, with abundant sauropsid (*Dromopus*, *Hyloidichnus*) and synapsid (*Dimetropus*) tracks. Nevertheless, the ichnoassemblage from Mallorca is singular because of two facts: (1) lack of tracks produced by lepospondyl, temnospondyl and reptiliomorph trackmakers (*Matthewichnus*, *Batrachichnus*, *Limnopus*, *Amphisauropus*, *Ichniotherium*) despite its being in an alluvial/fluvial setting, and (2) presence of tracks attributed to therapsid (gorgonopsian) trackmakers, a clade that is only known from Guadalupian and Lopingian deposits elsewhere. The latter could imply that the bone-bearing deposits of the Port des Canonge Formation, also containing gorgonopsian body fossils, are younger than initially thought; nevertheless, even though the attribution to the Cisuralian is not incontestable, the five

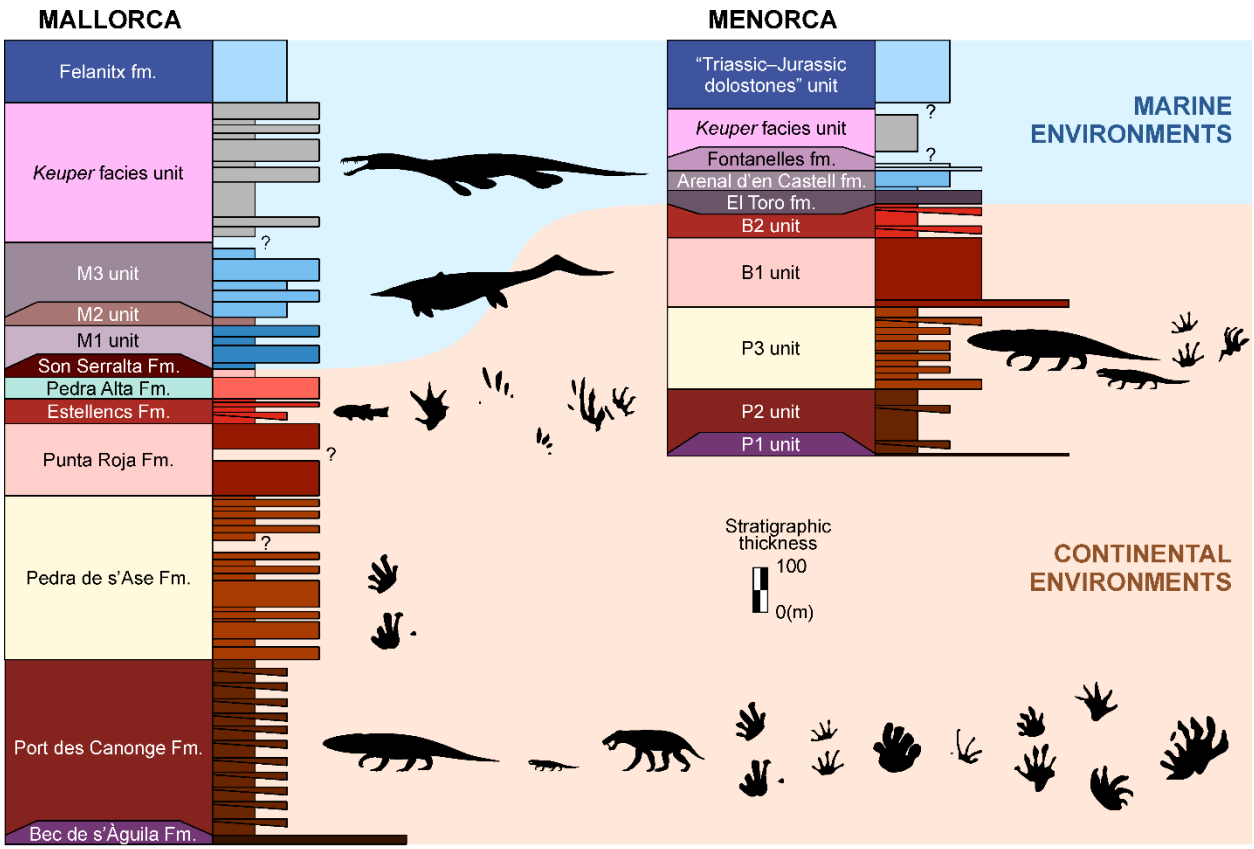
MALLORCA
MENORCA
Felanitx fm.
Keuper facies unit
M3 unit
M2 unit
M1 unit
Son Serralta Fm.
Pedra Alta Fm.
Estellencs Fm.
Punta Roja Fm.
Pedra de s'Ase Fm.
Port des Canonge Fm.
Bec de s'Àguila Fm.
"Triassic–Jurassic dolostones" unit
Keuper facies unit
Fontanelles fm.
Arenal d'en Castell fm.
El Toro fm.
B2 unit
B1 unit
P3 unit
P2 unit
P1 unit
MARINE ENVIRONMENTS
CONTINENTAL ENVIRONMENTS
Stratigraphic thickness
100
0(m)

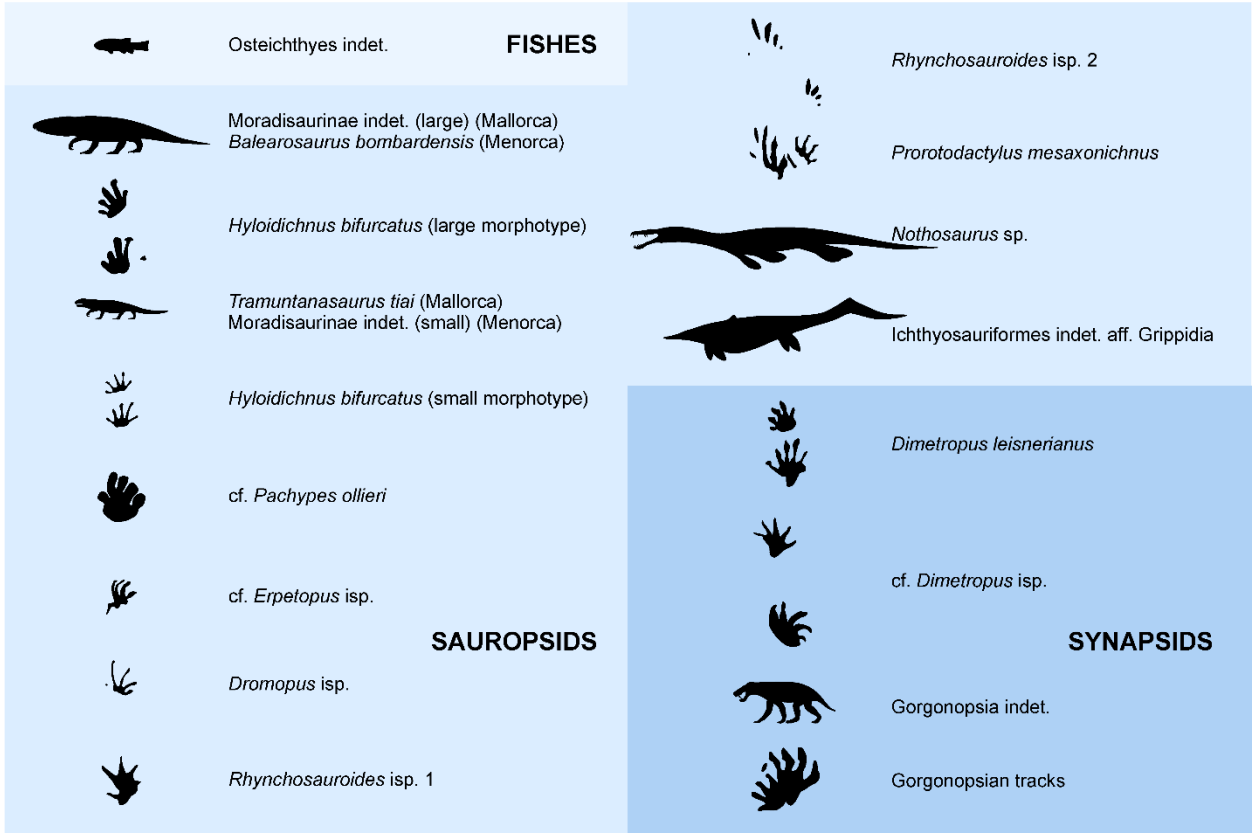
Osteichthyes indet.
FISHES
Moradisaurinae indet. (large) (Mallorca)
Balearosaurus bombardensis (Menorca)
Hyloidichnus bifurcatus (large morphotype)
Tramuntanasaurus tiai (Mallorca)
Moradisaurinae indet. (small) (Menorca)
Hyloidichnus bifurcatus (small morphotype)
cf. Pachypes ollieri
cf. Erpetopus isp.
SAUROPSIDS
Dromopus isp.
Rhynchosauroides isp. 1
Rhynchosauroides isp. 2
Prorotodactylus mesaxonichnus
Nothosaurus sp.
Ichthyosauriformes indet. aff. Grippidia
Dimetropus leisnerianus
cf. Dimetropus isp.
SYNAPSIDS
Gorgonopsia indet.
Gorgonopsian tracks

Figure 6.7. (previous page) Tetrapod fossil record in each of the Permian–Triassic continental and marine formations of the Gymnesic Islands (Mallorca and Menorca). Tetrapod silhouettes all in the same scale; tracks and fish not to scale to tetrapod silhouettes nor to each other. Question marks in the synthetic logs indicate unknown stretches, meaning that the thickness of those units could be greater than what is represented here.

main lines of evidence point towards that direction (presence of *Dimetropus*, lack of *Erpetopus*, relative abundance of sauropsid compared to synapsid tracks, and palynological and magnetostratigraphic data pointing to a middle Wordian stage, at most, in a level 250 m stratigraphically above the beds with Cisuralian-like ichnoassemblages). Tetrapod bones show that moradisaurine captorhinid eureptiles were quite abundant, perhaps being the dominant herbivores of the ecosystem. Outside of Mallorca, Cisuralian moradisaurines had so far only been reported from North and South America, substituting caseids and diadectomorphs as the dominant high-fibre herbivores during the late part of this epoch (Modesto *et al.*, 2016). The present work has shown that the situation was probably similar in the western peri-Tethys, as diadectomorphs, abundant in the slightly older Tambach Formation (Central European Basin) both in the form of tracks and body fossils (Berman *et al.*, 1998, 2004; Voigt, 2005; Voigt *et al.*, 2007), are absent on Mallorca. The bones found in the Port des Canonge Formation also record the presence of a small gorgonopsian therapsid. Gorgonopsians are an iconic clade of the Guadalupian and Lopingian epochs, becoming the top predators in the Lopingian (late Permian) terrestrial ecosystems (Sigogneau-Russell, 1989; Kammerer, 2016; Kammerer & Rubidge, 2022). Until now, gorgonopsians were known from the Cis-Urals, southern and eastern Africa, western Asia, central Africa and perhaps the Indian subcontinent and eastern Asia (Bernardi *et al.*, 2017; Olroyd & Sidor, 2017; Liu & Yang, 2022). All these records correspond to the Guadalupian and Lopingian; the oldest of them, albeit probably not the most basal (Kammerer & Masyutin, 2018), being an indeterminate, fragmentary specimen from the Wordian of southern Africa (Kammerer & Rubidge, 2022). Regardless of the exact age of the specimen of Mallorca (Cisuralian/?Guadalupian), it is almost certainly the oldest gorgonopsian known, and fills a biogeographical gap, being the first of its clade found essentially in the equator of Pangaea. Even though desert belts extended over the tropics of Pangaea, the gorgonopsian from Mallorca suggests that dispersion did occur. This confirms that

gorgonopsians had essentially a cosmopolitan distribution not limited to temperate palaeolatitudes, similar to well-known other Permian groups such as captorhinids, pareiasaurs, dinocephalians and therocephalians (the latter two recognised in the palaeoequator because of their ichnites; Gand & Durand, 2006; Marchetti *et al.*, 2019, 2020, 2022).

Guadalupian/Lopingian sites yielding tetrapod body fossils concentrate in areas representing the temperate palaeolatitudes of Pangaea (Bernardi *et al.*, 2017 and references therein; Olroyd & Sidor, 2017 and references therein), whereas in the palaeoequator, body fossils are scarcer (Jalil & Dutuit, 1996; Jalil & Janvier, 2005; Werneburg *et al.*, 2007b, 2022; Steyer & Jalil, 2009; Germain, 2010; Romano & Nicosia, 2014; Mujal *et al.*, 2016b; Romano *et al.*, 2019; Laurin & Hook, 2022) and usually much of the information is inferred from the abundant track record (Gand & Durand, 2006; Voigt *et al.*, 2010; Hminna *et al.*, 2012; Mujal *et al.*, 2017a; Contessi *et al.*, 2018; Citton *et al.*, 2019; Marchetti *et al.*, 2020, 2022). The assemblage from the P3 unit of Menorca has not been studied in great detail yet, but the preliminary account provided in the present Ph.D. dissertation suggests that it was a moradisaurine captorhinid eureptile-dominated palaeoenvironment, with at least two different species: a large one, *Balearosaurus bombardensis*, and a smaller (unnamed) one. Moreover, there are ichnites that can be attributed to the smaller moradisaurine form (*Hyloidichnus*) and to small parareptiles (cf. *Erpetopus*). There is also a large scapula (Pretus & Obrador, 1987) that cannot be attributed to a moradisaurine, and may have belonged to a large synapsid. Guadalupian and Lopingian (middle and upper Permian) assemblages with abundant moradisaurines can be found in central Africa (de Ricqlès & Taquet, 1982; Smith *et al.*, 2015; Modesto *et al.*, 2019; Sidor *et al.*, 2022), northern Africa (Jalil & Dutuit, 1996; Voigt *et al.*, 2010; Hminna *et al.*, 2012) and the Massif Central and Provençe (Gand & Durand, 2006; Logghe *et al.*, 2021; Marchetti *et al.*, 2022), all of them in the lower palaeolatitudes of Pangaea, just like Menorca. Therefore, it appears that moradisaurines remained as key components of the intertropical palaeoecosystems of Pangaea even when other high-fibre herbivores were present, such as caseid "pelycosaur"-grade synapsids (Romano & Nicosia, 2014; Werneburg *et al.*, 2022), tapinocephalian dinocephalian therapsids (Gand & Durand, 2006; Marchetti *et al.*, 2019) and pareiasaur parareptiles (Jalil & Janvier, 2005; Valentini *et al.*, 2009; Voigt *et al.*, 2010; Marchetti *et al.*, 2021). Conversely, moradisaurines may have not been well-suited for cooler climates, as the main herbivores in temperate palaeolatitudes

were pareiasaurs, dicynodont therapsids and tapinocephalians (Bernardi *et al.*, 2017; Olroyd & Sidor, 2017).

The Lower/Middle Triassic continental sites of Europe have yielded an abundant record of land vertebrates (Romano *et al.*, 2020 and references therein; De Jaime-Soguero *et al.*, 2021 and references therein). Compared to those, the assemblage of the Estellencs Formation is rather poor, with no body fossils and only four ichnomorphotypes found, all produced by small diapsid eureptiles. Among them, the most interesting one might be *"Prorotodactylus" mesaxonichnus*, a form that has been found in the Pyrenees (Mujal *et al.*, 2017b) but, apparently, nowhere else (even though a detailed comparison to *Gwyneddichnium* ispp. from the Upper Triassic of North America and central Europe is needed). *"Prorotodactylus" mesaxonichnus* could have been produced by a tetrapod species endemic to the western Tethys, and thus have a palaeobiogeographical interest apart from its biostratigraphic value. This ichnospecies is indicative of the uppermost Lower Triassic–lowermost Middle Triassic (Mujal *et al.*, 2016b, 2017b; the present Ph.D. dissertation).

The Middle/Upper Triassic marine deposits of the western peri-Tethys have produced, over the years, an extraordinarily rich amount of tetrapod fossils, especially in the Central European Basin (*e.g.*, Diedrich, 2012). On Mallorca, these deposits are usually barren, with even invertebrate fossils being remarkably scarce. Regardless, one of them, *i.e.*, the basal ichthyosauriform (*sensu* Huang *et al.*, 2019) proximal caudal vertebra from the M3 unit, provides important new data on the palaeobiogeographical distribution of its group. Other similar taxa, such as the Lower Triassic *Baisesaurus*, *Chaohusaurus*, *Grippia*, *Gulosaurus* and *Utatsusaurus*, have been found in the western and eastern coasts of Pangaea, in present-day western North America and eastern Asia (Shikama *et al.*, 1978; Nicholls & Brinkman, 1993; Motani *et al.*, 1998, 2014, 2018; Sander, 2000; Chen *et al.*, 2013; Cuthbertson *et al.*, 2013, 2014; Kelley *et al.*, 2016; Huang *et al.*, 2019; Ren *et al.*, 2022). The specimen from Mallorca, from the Middle Triassic, occupies a position central to the two main distribution areas. It is therefore possible that basal ichthyosauriforms had migrated through Laurasia in the late Lopingian (latest Permian), obtaining the apparent disjunct distribution of the Early Triassic. The nothosaur from the *Keuper* facies unit, on the other hand, belongs to a very well-known form found in all the surrounding areas with coeval rocks, and thus it does not provide any new information other than the first record of the genus on Mallorca.

References

Berman, D.S.; Sumida, S.S. & Martens, T. (1998). *Diadectes* (Diadectomorpha: Diadectidae) from the early Permian of Central Germany, with description of a new species. *Annals of Carnegie Museum*, 67(1): 53–93.

Berman, D.S.; Henrici, A.C.; Kissel, R.A.; Sumida, S.S. & Martens, T. (2004). A new diadectid (Diadectomorpha), *Orobates pabsti*, from the Early Permian of Central Germany. *Bulletin of Carnegie Museum of Natural History*, 35: 1–36.

Berman, D.S.; Maddin, H.C.; Henrici, A.C.; Sumida, S.S.; Scott, D. & Reisz, R.R. (2020). New primitive caseid (Synapsida, Caseasauria) from the early Permian of Germany. *Annals of Carnegie Museum*, 86(1): 43–75.

Bernardi, M.; Petti, F.M., Kustatscher, E.; Franz, M.; Hartkopf-Fröder, C.; Labandeira, C.C.; Wappler, T.; van Konijnenburg-van Cittert, J.H.A.; Peecook, B.R. & Angielczyk, K.D. (2017). Late Permian (Lopingian) terrestrial ecosystems: A global comparison with new data from the low-latitude Bletterbach Biota. *Earth-Science Reviews*, 175: 18–43.

Bourquin, S.; Péron, S. & Durand, M. (2006). Lower Triassic sequence stratigraphy of the western part of the Germanic Basin (west of Black Forest): fluvial system evolution through time and space. *Sedimentary Geology*, 186: 187–211.

Cassinis, G.; Durand, M. & Ronchi, A. (2003). Permian-Triassic continental sequences of Northwest Sardinia and South Provence: stratigraphic correlations and palaeogeographical implications. *Bollettino della Società Geologica Italiana*, volume speciale 2: 119–129.

Cassinis, G.; Perotti, C.R. & Ronchi, A. (2012). Permian continental basins in the Southern Alps (Italy) and peri-mediterranean correlations. *International Journal of Earth Sciences/GR Geologische Rundschau*, 101: 129–157.

Chen, X.-H.; Sander, P.M.; Cheng, L. & Wang, X.-F. (2013). A new Triassic primitive ichthyosaur from Yuanan, South China. *Acta Geologica Sinica English Edition*, 87(3): 672–677.

Citton, P.; Ronchi, A.; Maganuco, S.; Caratelli, M.; Nicosia, U.; Sacci, E. & Romano, M. (2019). First tetrapod footprints from the Permian of Sardinia and their palaeontological and stratigraphical significance. *Geological Journal*, 54(4): 2084–2098.

Contessi, M.; Voigt, S. & Bibonne, R. (2018). Permian tetrapod footprints from Tunisia. *Ichnos*, 25: 119–127.

Cuthbertson, R.S.; Russell, A.P. & Anderson, J.S. (2013). Cranial morphology and relationships of a new grippidian (Ichthyopterygia) from the Vega-Phroso siltstone member (Lower Triassic) of British Columbia, Canada. *Journal of Vertebrate Paleontology*, 33(4): 831–847.

Cuthbertson, R.S.; Russell, A. & Anderson, J. (2014). The first substantive evidence of *Utatsusaurus* (Ichthyopterygia) from the Sulphur Mountain Formation (Lower–Middle Triassic) of British Columbia, Canada: a skull roof description with comparison to other early taxa. *Canadian Journal of Earth Sciences*, 51(2): 180–185.

De Jaime-Soguero, Ch.; Mujal, E.; Dinarès-Turell, J.; Oms, O.; Bolet, A.; Orlandi-Oliveras, G. & Fortuny, J. (2021). Palaeoecology of Middle Triassic tetrapod ichnoassociations (middle Muschelkalk, NE Iberian Peninsula) and their implications for palaeobiogeography in the western Tethys region. *Palaeogeography, Palaeoclimatology, Palaeoecology*, 565: 110204.

de Miguel Chaves, C.; Ortega, F. & Pérez-García, A. (2020). The Iberian Triassic fossil record of Sauropterygia: an update. *Journal of Iberian Geology*, 46: 445–464.

de Ricqlès, A. & Taquet, P. (1982). La faune de vertébrés du Permien Supérieur du Niger. I. Le captorhinomorphe *Moradisaurus grandis* (Reptilia, Cotylosauria). Le crane. *Annales de Paléontologie (Vert.-Invert.)*, 68: 33–106.

Diedrich, C.J. (2012). The Middle Triassic marine reptile biodiversity in the Germanic Basin, in the centre of the Pangaean world. *Open Geosciences*, 4(1): 9–46.

Durand, M. (2008). Permian to Triassic continental successions in southern Provence (France): an overview. *Bollettino della Società Geologica Italiana*, 127(3): 697–716.

Gand, G. & Durand, M. (2006). Tetrapod footprint ichno-associations from French Permian basins. Comparisons with other Euramerican ichnofaunas. *Geological Society, London, Special Publications*, 265: 157–177.

Gand, G.; Kerp, H.; Parsons, C. & Martínez-García, E. (1997). Palaeoenvironmental and stratigraphic aspects of animal traces and plant remains in Spanish Permian red beds (Peña Sagra, Cantabrian Mountains, Spain). *Geobios*, 30(2): 295–318.

Gand, G.; Tüysüz, O.; Steyer, J.-S.; Allain, R.; Sakınç, M.; Sanchez, S.; Şengör, A.M.C. & Sen, S. (2011). New Permian tetrapod footprints and macroflora from Turkey (Çakraz Formation, northwestern Anatolia): Biostratigraphic and palaeoenvironmental implications. *Comptes Rendus Palevol*, 10: 617–625.

Germain, D. (2010). The Moroccan diplocaulid: the last lepospondyl, the single one on Gondwana. *Historical Biology*, 22(1–3): 4–39.

Hminna, A.; Voight, A.; Saber, H.; Schneider, J.W. & Hmich, D. (2012). On a moderately diverse continental ichnofauna from the Permian Ikakern Formation (Argana Basin, Western High Atlas, Morocco). *Journal of African Earth Sciences*, 68: 15–23.

Huang, J.D.; Motani, R.; Jiang, D.-Y.; Tintori, A.; Rieppel, O.; Zhou, M.; Ren, X.-X. & Zhang, R. (2019). The new ichthyosauriform *Chaohusaurus brevifemoralis* (Reptilia, Ichthyosauromorpha) from Majiashan, Chaohu, Anhui Province, China. *PeerJ*, 7: e7561.

Jalil, N.-E. & Dutuit, J.M. (1996). Permian captorhinid reptiles from the Argana Formation, Morocco. *Palaeontology*, 39: 907–918.

Jalil, N.-E. & Janvier, P. (2005). Les pareiasaures (Amniota, Parareptilia) du Permien supérieur du Bassin d'Argana, Maroc. *Geodiversitas*, 27(1) : 35–132.

Kammerer, C.F. (2016). Systematics of the Rubidgeinae (Therapsida: Gorgonopsia). *PeerJ*, 4: e1608.

Kammerer, C.F. & Masyutin, V. (2018). Gorgonopsian therapsids (*Nochnitsa* gen. nov. and *Viatkogorgon*) from the Permian Kotelnich locality of Russia. *PeerJ*, 6: e4954.

Kammerer, C.F. & Rubidge, B.S. (2022). The earliest gorgonopsians from the Karoo Basin of South Africa. *Journal of African Earth Sciences*, 194: 104631.

Kelley, N.P.; Motani, R.; Embree, P. & Orchard, M.J. (2016). A new Lower Triassic ichthyopterygian assemblage from Fossil Hill, Nevada. *PeerJ*, 4: e1626.

Laurin, M. & Hook, R.W. (2022). The age of North America's youngest Paleozoic continental vertebrates: a review of data from the Middle Permian Pease River (Texas) and El Reno (Oklahoma) Groups. *BSGF - Earth Sciences Bulletin*, 193: 10.

Linol, B.; Bercovici, A.; Bourquin, S.; Diez, J.B.; López-Gómez, J.; Broutin, J.; Durand, M. & Villanueva-Amadoz, U. (2009). Late Permian to Middle Triassic correlations and palaeogeographical reconstructions in south-western European basins: New sedimentological data from Minorca (Balearic Islands, Spain). *Sedimentary Geology*, 220: 77–94.

Liu, J. & Yang, W. (2022). A gorgonopsian from the Wutonggou Formation (Changhsingian, Permian) of Turpan Basin, Xinjiang, China. *Palaeoworld*, 31: 383–388.

Logghe, A.; Mujal, E.; Marchetti, L.; Nel, A.; Pouillon, J.-M.; Giner, S.; Garrouste, R. & Steyer, J.-S. (2021). *Hyloidichnus* trackways with digit and tail drag traces from the Permian of Gonfaron (Var, France): New insights on the locomotion of captorhinomorph eureptiles. *Palaeogeography, Palaeoclimatology, Palaeoecology*, 573: 110436.

López-Gómez, J.; Alonso-Azcárate, J.; Arche, A.; Arribas, J.; Fernández-Barrenechea, J.; Borruel-Abadía, V.; Bourquin, S.; Cadenas, P.; Cuevas, J.; De la Horra, R.; Díez, J.B.; Escudero-Mozo, M.J.; Fernández-Viejo, G.; Galán-Abellán, B.; Galé, C.; Gaspar-Escribano, J.; Gisbert-Aguilar, J.; Gómez-Gras, D.; Goy, A.; Gretter, N.; Heredia-Carballo, N.; Lago, M.; Lloret, J.; Luque, J.; Márquez, L.; Márquez-Aliaga, A.; Martín-Algarra, A.; Martín-Chivelet, J.; Martín-González, F.; Marzo, M.; Mercedes-Martín, R.; Ortí, F.; Pérez-López, A.; Pérez-Valera, F.; Pérez-Valera, J.A.; Plasencia, P.; Ramos, E.; Rodríguez-Méndez, L.; Ronchi, A.; Salas, R.; Sánchez-Fernández, D.; Sánchez-Moya, Y.; Sopeña, A.; Suárez-Rodríguez, Á.; Tubía, J.M.; Ubide, T.; Valero-Garcés, B.; Vargas, H. & Viseras, C. (2019). Permian-Triassic rifting stage. *In*: Vergés, J. & Kullberg, J.C. (Coord.). *The Geology of Iberia: A Geodynamic Approach. Volume 3: The Alpine Cycle*. Springer; Cham: 29–112.

Martens, T. (2018). *Scientific importance of the Fossillagerstätte Bromacker (Germany, Tambach Formation, Lower Permian) - vertebrate fossils / Wissenschaftliche Bedeutung der Fossillagerstätte Bromacker (Deutschland, Tambach-Formation, Unteres Perm) - Wirbeltierfossilien*. Curvillier Verlag; Göttingen. 47 pp.

Marchetti, L.; Klein, H.; Buchwitz, M.; Ronchi, A.; Smith, R.M.H.; De Klerk, W.J.; Sciscio, L. & Groenewald, G.H. (2019). Permian-Triassic vertebrate footprints from South Africa: Ichnotaxonomy, producers and biostratigraphy through two major faunal crises. *Gondwana Research*, 72: 139–168.

Marchetti, L.; Ceoloni, P.; Leonardi, G.; Massari, F.; Mietto, P.; Sacchi, E. & Valentini, M. (2020). The Lopingian tetrapod ichnoassociation from Italy, a key for the understanding of low-latitude faunas before the end-Permian crisis. *Journal of Mediterranean Earth Sciences*, 12: 61–81.

Marchetti, L.; Voigt, S.; Mujal, E.; Lucas, S.G.; Francischini, H.; Fortuny, J. & Santucci, V.L. (2021). Extending the footprint record of Pareiasauromorpha to the Cisuralian: earlier appearance and wider palaeobiogeography of the group. *Papers in Palaeontology*, 7(3): 1297–1319.

Marchetti, L.; Logghe, A.; Mujal, E.; Barrier, P.; Montenat, C.; Nel, A.; Pouillon, J.M.; Garrouste, R. & Steyer, J.-S. (2022). Vertebrate tracks from the Permian of Gonfaron (Provence, Southern France) and their implications for the late Capitanian extinction event. *Palaeogeography, Palaeoclimatology, Palaeoecology*, 599: 111043.

Modesto, S.P.; Flear, V.J.; Dilney, M.M. & Reisz, R.R. (2016). A large moradisaurine tooth plate from the lower Permian of Texas and its biostratigraphic implications. *Journal of Vertebrate Paleontology*, 36(6): e1221832.

Modesto, S.P.; Richards, C.D.; Ide, O. & Sidor, C.A. (2019). The vertebrate fauna of the upper Permian of Niger — X. The mandible of the captorhinid reptile *Moradisaurus grandis*. *Journal of Vertebrate Paleontology*, 38(6): e1531877.

Motani, R.; Minoura, N. & Ando, T. (1998). Ichthyosaurian relationships illuminated by new primitive skeletons from Japan. *Nature*, 393: 255–257.

Motani, R.; Jiang, D.-Y.; Tintori, A.; Rieppel, O. & Chen, G.-B. (2014). Terrestrial origin of viviparity in Mesozoic marine reptiles indicated by Early Triassic embryonic fossils. *PLoS ONE*, 9(2): e88640.

Motani, R.; Huang, J.; Jiang, D.-Y.; Tintori, A.; Rieppel, O.; You, H.; Hu, Y.-C. & Zhang, R. (2018). Separating sexual dimorphism from other morphological variation in a specimen complex of fossil marine reptiles (Reptilia, Ichthyosauriformes, *Chaohusaurus*). *Scientific Reports*, 8: 14978.

Mujal, E.; Fortuny, J.; Oms, O.; Bolet, A.; Galobart, À. & Anadón, P. (2016a). Palaeoenvironmental reconstruction and early Permian ichnoassemblage from the NE Iberian Basin (Pyrenean Basin). *Geological Magazine*, 153(4): 578–600.

Mujal, E.; Gretter, N.; Ronchi, A.; López-Gómez, J.; Falconnet, J.; Diez, J.B.; De la Horra, R.; Bolet, A.; Oms, O.; Arche, A.; Barrenechea, J.F.; Steyer, J.-S. & Fortuny, J. (2016b). Constraining the Permian/Triassic transition in continental environments: Stratigraphic and palaeontological record from the Catalan Pyrenees (NE Iberian Peninsula). *Palaeogeography, Palaeoclimatology, Palaeoecology*, 445: 18–37.

Mujal, E.; Fortuny, J.; Pérez-Cano, J.; Dinarès-Turell, J. Ibáñez-Insa, J.; Oms, O.; Vila, I.; Bolet, A. & Anadón, P. (2017a). Integrated multi-stratigraphic study of the Coll de Terrers late Permian–Early Triassic continental succession from the Catalan Pyrenees (NE Iberian Peninsula): A geologic reference record for equatorial Pangaea. *Global and Planetary Change*, 159: 46–60.

Mujal, E.; Fortuny, J.; Bolet, A.; Oms, O. & López, J.A. (2017b). An archosauromorph dominated ichnoassemblage in fluvial settings from the late Early Triassic of the Catalan Pyrenees (NE Iberian Peninsula). *PLoS ONE*, 12(4): e0174693.

Nicholls, E.L. & Brinkman, D. (1993). A new specimen of *Utatsusaurus* (Reptilia: Ichthyosauria) from the Lower Triassic Sulphur Mountain Formation of British Columbia. *Canadian Journal of Earth Sciences*, 30(3): 486–490.

Olroyd, S.L. & Sidor, C.A. (2017). A review of the Guadalupian (middle Permian) global tetrapod fossil record. *Earth-Science Reviews*, 171: 583–597.

Reisz, R.R.; Maddin, H.C.; Fröbisch, J. & Falconnet, J. (2011). A new large caseid (Synapsida, Caseasauria) from the Permian of Rodez (France), including a reappraisal of *"Casea" rutena* Sigogneau-Russell & Russell, 1974. *Geodiversitas*, 33(2): 227–246.

Ren, J.; Jiang, H.; Xiang, K.; Sullivan, C.; He, Y.; Cheng, L. & Han, F. (2022). A new basal ichthyosauromorph from the Lower Triassic (Olenekian) of Zhebao, Guangxi Autonomous Region, South China. *PeerJ*, 10: e13209

Rieppel, O. (2019). *Mesozoic sea dragons: Triassic marine life from the ancient tropical lagoon of Monte San Giorgio*. Indiana University Press; Indiana. 256 pp.

Romano, M. & Nicosia, U. (2014). *Alierasaurus ronchii*, gen. et sp. nov., a caseid from the Permian of Sardinia, Italy. *Journal of Vertebrate Paleontology*, 34(4): 900–913.

Romano, M.; Citton, P.; Maganuco, S.; Sacchi, E.; Caratelli, M.; Ronchi, A. & Nicosia, U. (2019). New basal synapsid discovery at the Permian outcrop of Torre del Porticciolo (Alghero, Italy). *Geological Journal*, 54(3): 1554–1566.

Romano, M.; Bernardi, M.; Petti, F.M.; Rubidge, B.; Hancox, J. & Benton, M.J. (2020). Early Triassic terrestrial tetrapod fauna: a review. *Earth-Science Reviews*, 210: 103331.

Sander, P.M. (2000). Ichthyosauria: their diversity, distribution, and phylogeny. *Paläontologische Zeitschrift*, 74(1/2): 1–35.

Santi, G.; Marchetti, L.; Schirolli, P. & Ronchi, A. (2020). The Cisuralian tetrapod ichnoassociation from Italy: from historical findings to a standard reference status. *Journal of Mediterranean Earth Sciences*, 12: 39–59.

Schneider, J.W.; Kömer, F.; Roscher, M. & Kroner, U. (2006). Permian climate development in the northern peri-Tethys area — The Lodève basin, French Massif Central, compared in a European and global context. *Palaeogeography, Palaeoclimatology, Palaeoecology*, 240: 161–183.

Shikama, T.; Kamei, T. & Murata, M. (1978). Early Triassic Ichthyosaurus, *Utatsusaurus hataii* Gen. et Sp. Nov., from the Kitakami Massif, Northeast Japan. *Science Reports of the Tohoku University, Second Series (Geology)*, 48(1–2): 77–97.

Sidor, C.A.; Ide, O.; Larsson, H.C.; O'Keefe, F.R.; Smith, R.M.H.; Steyer, J.-S. & Modesto, S.P. (2022). The vertebrate fauna of the upper Permian of Niger—XI. Cranial material of a juvenile *Moradisaurus grandis* (Reptilia: Captorhinidae). *Journal of Vertebrate Paleontology*, 41(5): e2030345.

Sigogneau-Russell, D. (1989). *Handbuch der Paläoherpetologie / Encyclopedia of Paleoherpetology. Teil 17 B/I / Part 17 B/I: Theriodontia I. Phthinosuchia, Biarmosuchia, Eotitanosuchia, Gorgonopsia*. Gustav Fischer Verlag; Stuttgart, New York. 127 pp.

Smith, R.M.H.; Sidor, C.A.; Tabor, N.J. & Steyer, J.S. (2015). Sedimentology and vertebrate taphonomy of the Moradi Formation of northern Niger: A Permian wet desert in the tropics of Pangaea. *Palaeogeography, Palaeoclimatology, Palaeoecology*, 440: 128–141.

Spindler, F. (2015). *The basal Sphenacodontia – systematic revision and evolutionary implications*. Ph.D. dissertation. Technischen Universität Bergakademie Freiberg; Freiberg. 385 pp.

Spindler, F. (2016). Morphological description and taxonomic status of *Palaeohatteria* and *Pantelosaurus* (Synapsida: Sphenacodontia). *Freiberger Forschungshefte C*, 550(23): 1–57.

Spindler, F.; Falconnet, J. & Fröbisch, J. (2016). *Callibrachion* and *Datheosaurus*, two historical and previously mistaken basal caseasaurian synapsids from Europe. *Acta Palaeontologica Polonica*, 61(3): 597–616.

Spindler, F.; Werneburg, R.; Schneider, J.W.; Luthardt, L.; Annacker, V. & Rößler, R. (2018). First arboreal 'pelycosaurs' (Synapsida: Varanopidae) from the early Permian Chemnitz Fossil Lagerstätte, SE Germany, with a review of varanopid phylogeny. *Paläontologische Zeitschrift*, 92: 315–364.

Spindler, F.; Werneburg, R. & Schneider, J.W. (2019a). A new mesenosaurine from the lower Permian of Germany and the postcrania of *Mesenosaurus*: implications for early amniote comparative osteology. *Paläontologische Zeitschrift*, 93: 303–344.

Spindler, F.; Voigt, S. & Fischer, J. (2019b). Edaphosauridae (Synapsida, Eupelycosauria) from Europe and their relationship to North American representatives. *Paläontologische Zeitschrift*, 94: 125–153.

Steyer, J.S. & Jalil, N.-E. (2009). First evidence of a temnospondyl in the late Permian of the Argana Basin, Morocco. *Special Papers in Palaeontology*, 81: 155–160.

Valentini, M.; Nicosia, U. & Conti, M.A. (2009). A re-evaluation of *Pachypes*, a pareiasaurian track from the Late Permian. *Neues Jahrbuch für Geologie und Paläontologie*, 251: 71–94.

Voigt, S. (2005). *Die Tetrapodenichnofauna des kontinentalen Oberkarbon und Perm im Thüringer Wald - Ichnotaxonomie, Paläoökologie und Biostratigraphie*. Cuvillier Verlag; Göttingen. 308 pp.

Voigt, S. & Haubold, H. (2015). Permian tetrapod footprints from the Spanish Pyrenees. *Palaeogeography, Palaeoclimatology, Palaeoecology*, 417: 112–120.

Voigt, S.; Berman, D.S. & Henrici, A.C. (2007). First well-established track-trackmaker association of paleozoic tetrapods based on *Ichniotherium* trackways and diadectid skeletons from the Lower Permian of Germany. *Journal of Vertebrate Paleontology*, 27(3): 553–570.

Voigt, S.; Hminna, A.; Saber, H.; Schneider, J.W. & Klein, H. (2010). Tetrapod footprints from the uppermost level of the Permian Ikakern Formation (Argana Basin, Western High Atlas, Morocco). *Journal of African Earth Sciences*, 57: 470–478.

Voigt, S.; Lagnaoui, A.; Hminna, A.; Saber, H. & Schneider, J.W. (2011). Revisional notes on the Permian tetrapod ichnofauna from the Tiddas Basin, central Morocco. *Palaeogeography, Palaeoclimatology, Palaeoecology*, 302: 474–483.

Voigt, S.; Niedźwiedzki, G.; Raczyński, P.; Mastalerz, K & Ptaszyński, T. (2012). Early Permian tetrapod ichnofauna from the Intra-Sudetic Basin, SW Poland. *Palaeogeography, Palaeoclimatology, Palaeoecology*, 313–314: 173–180.

Werneburg, R.; Ronchi, A. & Schneider, J.W. (2007a). The early Permian branchiosaurids (Amphibia) of Sardinia (Italy): Systematic palaeontology, palaeoecology, biostratigraphy

and palaeobiogeographic problems. *Palaeogeography, Palaeoclimatology, Palaeoecology*, 252: 383–404.

Werneburg, R.; Steyer, J.S.; Sommer, G.; Gand, G.; Schneider, J.W. & Vianey-Liaud, M. (2007b). The earliest tupilakosaurid amphibian with diplospondylus vertebrae from the late Permian of Southern France. *Journal of Vertebrate Paleontology*, 27(1): 26–30.

Werneburg, R.; Spindler, F.; Falconnet, J.; Steyer, J.-S.; Vianey-Liaud, M. & Schneider, J.W. (2022). A new caseid synapsid from the Permian (Guadalupian) of the Lodève basin (Occitanie, France). *Palaeovertebrata*, 45(2): e2.

Zouicha, A.; Voigt, S.; Saber, H.; Marchetti, L.; Hminna, A.; El Attari, A.; Ronchi, A. & Schneider, J.W. (2021). First record of Permian continental trace fossils in the Jebilet Massif, Morocco. *Journal of African Earth Sciences*, 173: 104015.

Chapter 7

Conclusions

Conclusions

A) Permian of Mallorca

a. The detailed stratigraphic, sedimentological and magnetostratigraphic studies have made it possible to describe three new formal lithostratigraphic units with the rank of Formation, to interpret the sedimentary palaeoenvironment they represent, and to constrain their age attributions.

   i. The Bec de s'Àguila Formation (probably lower–middle Cisuralian) represents conglomerate and meandering river deposits near the footwall scarp, included in the Kiaman Reverse Superchron.

   ii. The Port des Canonge Formation (upper Cisuralian – ?lower Guadalupian) corresponds to very fine-grained meandering river and floodplain deposits, part of the Kiaman Reverse Superchron.

   iii. The Pedra de s'Ase Formation (lower Guadalupian) has been interpreted as medium-grained meandering river and sheetflood deposits, also in the Kiaman Reverse Superchron.

b. The description of the palyno- and ichnoassemblages has further constrained the age attributions, and has revealed the plant and animal diversity of those ecosystems.

   i. Spores and pollen of the Pedra de s'Ase Formation have been assigned to algae, bryophytes, horsetails, ferns, lycophytes, seed ferns and conifers, with components typical of the Guadalupian ("Thuringian" biofacies).

   ii. Macroplant remains have been identified as horsetails and conifers.

   iii. Invertebrate trace fossils have revealed the presence of worms, insect larvae, beetles and notostracans.

   iv. Tetrapod tracks and trackways contain morphotypes attributed to moradisaurine captorhinid eureptiles (small and large species), possible pareiasauromorph parareptiles, araeoscelidian diapsids or non-varanodontine varanopids, "pelycosaur"-grade synapsids (two forms), gorgonopsian therapsids and indeterminate tetrapod swimming traces. The ichnoassemblage suggests an upper Cisuralian series for the Port des Canonge Formation, although the gorgonopsian tracks might point to the lower Guadalupian.

c. The osteological study of the tetrapod skeletons found in the Port des Canonge Formation has resulted in the report of two different animals.

i. A semi-complete skeleton of a new small moradisaurine captorhinid eureptile species (*Tramuntanasaurus tiai*), similar in size and shape to other taxa in the same family.

ii. A partial skeleton of an indeterminate gorgonopsian, the oldest of this clade known worldwide and also the first to be reported from palaeoequatorial Pangaea (almost all gorgonopsians are known from temperate palaeolatitudes in present-day southern and eastern Africa and eastern Europe).

B) Continental Triassic of Mallorca (*Buntsandstein* facies)

a. Detailed studies on the stratigraphy and sedimentology have resulted in the description of four formal lithostratigraphic units with the rank of Formation, and the interpretation of the sedimentary palaeoenvironments in which the sediments were deposited.

   i. The Punta Roja Formation (upper Olenekian) represents shallow perennial braided river deposits, reworking aeolian sediments.

   ii. The Estellencs Formation (upper Olenekian–lower Anisian) has been interpreted as meandering river and floodplain deposits, with a braided interval in the upper part.

   iii. The Pedra Alta Formation (lower Anisian) corresponds to seasonal braided rivers.

   iv. The Son Serralta Formation (lower–?middle Anisian) has a lower part with meandering river and floodplain deposits, grading upwards to tidal flat deposits contacting the overlying marine *Muschelkalk* facies.

b. The palaeobotanical review and the study of the ichnoassemblages has shed new light on the floras and the faunas of the region.

   i. From the review of previous studies, it has been concluded that the pollen and spores of the three upper formations can be assigned to acritarchs, algae, bryophytes, horsetails, ferns, lycophytes, seed ferns, cicadophytes, ginkgophytes and conifers. Altogether, they suggest a lower Anisian stage.

   ii. Macroplant remains have been identified as horsetails (three species), ferns (two species), cicadophytes (one cone species), and conifers (five species and three cone species).

   iii. Invertebrate trace fossils contain evidence of worms, insect larvae, beetles and notostracans.

   iv. Tetrapod tracks appear in the form of four different morphotypes, all of them attributed to small diapsid reptiles, probably archosauromorphs.

c. Some levels of the Estellencs and Pedra Alta formations show exceptionally well-preserved invertebrate and vertebrate fossils, which have been studied in much detail.

   i. Clam shrimps ("conchostracans") are represented with three forms (although two of them could be conspecific sexual dimorphs) and suggest an uppermost Olenekian–lowermost Anisian stage.

   ii. Aquatic insects are locally abundant, in the form of mayfly nymphs (four species) and true fly eggs and pupae (one species each). One morphotype of mayfly nymph preserves in situ cololites, which has made is possible to infer a sedimentivore feeding style, unknown in the fossil record and only present in one present-day genus of mayflies.

   iii. Terrestrial insects are rare, at least in the sampled levels, with mayfly adults (two species), cockroaches (one species), grylloblattids (one species, described by previous authors), and a newly-described wood fly larva (*Protoanisolarva juarezi*), the oldest true fly worldwide.

   iv. A single fish has also appeared, identified as an indeterminate juvenile osteichthyan.

C) Marine Triassic of Mallorca (*Muschelkalk* and *Keuper* facies)

a. The revision of fossil reptile bones housed in museum collections and the preliminary description of the outcrops in which they were found has provided new information on the Upper Triassic marine vertebrates of Mallorca.

   i. One bone fragment from the *Keuper* gypsums of Can Bleda has been identified as Reptilia indet. Its fragmentary state has precluded a more specific identification.

   ii. Four vertebrae from the *Keuper* of Coma Freda correspond to the genus *Nothosaurus*, a sauropterygian known from many other sites in the western peri-Tethys.

   iii. A caudal vertebrae from the *Muschelkalk* of the Puig d'en Canals has been attributed to an indeterminate basal ichthyosauriform (Ichthyosauriformes indet. aff. Grippidia). Similar species were so far only known from western North America and eastern Asia, in opposite margins of the palaeoocean Panthalassa during the Triassic. The Mallorcan specimen suggests that connection between these populations might have taken place through the Tehys, which was halfway palaeogeographically.

D) Permian of Menorca

a. The stratigraphic and sedimentological study of the Cala del Pilar–Pla de Mar section has provided context for the tetrapod fossils historically found there.

   i. The Permian of Menorca can be divided into three informal lithostratigraphic units, described by previous authors but revised herein: the P1 unit (interpreted as the conglomerate and channel deposits near the footwall scarp), the P2 unit (corresponding to a large floodplain with scarce channels), and the P3 unit (with meandering river and floodplain deposits).

   ii. The P1 and P2 units are of indeterminate stages within the Permian, probably in the Cisuralian and Guadalupian. The P3 unit, which contains most of the bone remains, can be broadly dated as Guadalupian–Lopingian ("Thuringian" biofacies recognised by previous authors).

b. The study of the tetrapod tracks and bones has provided new information on the faunas of the region.

   i. There are two different morphotypes of tetrapod tracks found near the base of the P3 unit, corresponding to moradisaurine captorhinid eureptiles and small parareptiles. Broadly, they range between the upper Cisuralian and the Lopingian.

   ii. Two different species of moradisaurine captorhinid eureptiles have been recognised based on the bone remains, a newly-described larger one (*Balearosaurus bombardensis*), and an indeterminate, smaller one.

Chapter 8

Acknowledgements

Acknowledgements

First off, I would like to express my deepest appreciation to my thesis supervisors, Dr. Josep Fortuny (Computational Palaeobiology Research Group, Institut Català de Paleontologia Miquel Crusafont) and Dr. Àngel Galobart (Dinosaur Ecosystems Research Group, Institut Català de Paleontologia Miquel Crusafont), who helped me in every step of the process: coordinating fieldwork and preparation, helping with the obtention of funding, and insightfully reviewing the manuscripts. I would also like to extend my sincere thanks to Dr. Eudald Mujal (Staatliches Museum für Naturkunde Stuttgart), who helped a lot in most of the manuscripts, especially in the topics of stratigraphy, sedimentology and tetrapod ichnology. To Dr. Oriol Oms (Departament de Geologia, Universitat Autònoma de Barcelona), my academic tutor, for the long discussions on sedimentary geology that certainly improved those parts of the papers.

Apart from Drs. Josep Fortuny, Àngel Galobart and Eudald Mujal, other people helped a lot during the fieldwork campaigns. This endeavour would not have been possible without the help of Sebastià Matamalas, who accompanied me in the more than 50 days of fieldwork to log all the stratigraphic sections and participated as a volunteer in some of the excavations. Other people that participated in the fieldwork on Mallorca were Dr. Jaume Dinarès (Istituto Nazionale di Geofisica e Vulcanologia), Chabier De Jaime (Computational Palaeobiology Research Group, Institut Català de Paleontologia Miquel Crusafont), Josep Juárez, Francesc Baiget, Dr. Salvador Moyà (Paleoprimatology and Paleoanthropology Research Group, Institut Català de Paleontologia Miquel Crusafont), Joan Arbona (Museu Balear de Ciències Naturals), Marc Riccetto and Antoni Pasqual. On Menorca, Dr. Francesc Xavier Roig and Miquel Fernàndez showed me the sites and helped with fieldwork. In Catalunya, I also shared fieldtrips with Dr. Arnau Bolet (Paleoprimatology and Paleoanthropology Research Group, Institut Català de Paleontologia Miquel Crusafont), Dr. Ramon Mercedes (Departament de Geologia, Universitat Autònoma de Barcelona), Manel Méndez (Institut Català de Paleontologia Miquel Crusafont) and Rubén Garcia (Universitat de Barcelona).

The fieldwork and preparation projects were authorised by the Comissió Insular de Patrimoni Històric (Consell Insular de Mallorca). Specifically, the campaigns with file numbers 128/2019, 305/2019, 306/2019, 52/2021, 52/2021, 75/2021, 259/2022 and 259/2022, and the preparation projects with file numbers 374/2020, 393/2020, 295/2021 and 288/2022. I acknowledge Helena Inglada and Jaume Cardell for their willingness to clear any doubts on how to request and proceed with those.

I would also like to extend my sincere thanks to the people that helped during the first stages of this work, such as Dr. Emilio Ramos (Departament d'Estratigrafia, Paleontologia i Geociències Marines,

Universitat de Barcelona), who, by giving me a copy of the Bachelor's Thesis of Feliu Calafat, triggered this whole project. Moreover, to Feliu Calafat, Tomeu Sáez and Dr. Antoni Rodríguez (Departament de Geografia, Universitat de les Illes Balears), who provided more literature and directions to some of the fossil sites of Mallorca they had discovered and studied, and to Miquel Fernández, Raül Carmona, Dr. Antoni Obrador (Departament de Geologia, Universitat Autònoma de Barcelona), Dr. Josep Lluís Pretus (Departament d'Ecologia, Universitat de Barcelona), Dr. Enric Vicens (Departament de Geologia, Universitat Autònoma de Barcelona) and Dr. David Gómez (Departament de Geologia, Universitat Autònoma de Barcelona) in the case of Menorca.

I would also like to thank the other fellow predoctoral researchers at the Institut Català de Paleontologia Miquel Crusafont, with whom I shared many lunchtimes (at 13:30, as it should be) and NOT talking about work: Dr. Guillem Orlandi, Guillem Pons, Chabi De Jaime, Dr. Alessandro Urciuoli, Dr. Sílvia Jovells, Dr. Teresa Calderón, Florian Bouchet, Leonardo Sorbelli, Maria Prat, Oriol Monclús and Sharrah Mckenzie, who were also grad students at the time. Other staff of the ICP, Enric Menéndez, Mònica Vincent, Dr. Jordi Galindo, Dr. Josep Robles, Josep Torres and Dr. Albert G. Sellés helped me navigate through red tape or shared experience and knowledge. I want to especially thank Marina Rull, Xènia Aymerich and Ana Montemayor, who skilfully prepared most of the specimens studied in the present work, and Dr. Alex Serrano, who processed the μCT. During the years I gave classes at the Universitat Autònoma de Barcelona, Dr. Enric Vicens, Dr. Carme Boix, Dr. Marc Furió, Dr. Judit Marigó, Dr. Bernat Vila and Dr. Joan Madurell helped me prepare the course materials and exams.

I also appreciate the work put on all the manuscripts by the co-authors: Dr. Àngel Galobart (Dinosaur Ecosystems Research Group, Institut Català de Paleontologia Miquel Crusafont), Dr. Jaume Dinarès (Istituto Nazionale di Geofisica e Vulcanologia), Dr. Josep Fortuny (Computational Palaeobiology Research Group, Institut Català de Paleontologia Miquel Crusafont), Josep Juárez, Dr. Enrique Peñalver (Instituto Geológico y Minero de España), Dr. Eudald Mujal (Staatliches Museum für Naturkunde Stuttgart), Dr. Evelyn Kustatscher (Department für Geo- und Umweltwissenschaften, Paläontologie und Geobiologie, Ludwig-Maximilians-Universität), Dr. Francesc Xavier Roig, Dr. Frank Scholze (Institut für Geowissenschaften, Friedrich-Schiller-Universität Jena), Dr. Guido Roghi (Istituto di Geoscienze e Georisorse - CNR), and Dr. Oriol Oms (Departament de Geologia, Universitat Autònoma de Barcelona). I would also like to acknowledge the work of Henry S. Sharpe (University of Alberta), who made several outstanding pieces of artwork to illustrate the papers, and all the reviewers and editors that provided valuable insight on the original manuscripts, improving their quality.

Regarding the material for comparison, I want to thank Dr. Daniela Schwarz (Museum für Naturkunde Berlin), Florian Witzmann (Museum für Naturkunde Berlin), Igmar Werneburg (Eberhard Karls Universität Tübingen), Tom Hübner (Museum der Natur Gotha), Rainer Schoch (Staatliches

Museum für Naturkunde Stuttgart) and Carolina Constantino (Museu Balear de Ciències Naturals) for access to the collections under their care; to Dr. John A. Nyakatura (Humboldt-Universität Berlin) for providing the µCT raw data of *Orobates pabsti* for comparison; to Dr. William F. Simpson (Field Museum of Natural History) and Dr. Kenneth D. Angielczyk (Field Museum of Natural History) for the pictures of *Rothianiscus* and some of Olson's putative early therapsids from the USA; and to Dr. Ryosuke Motani (University of California) and Dr. P. Martin Sander (Rheinische Friedrich-Wilhelms-Universität Bonn) for discussion on the ichthyosauriform vertebra. Some of the manuscripts also benefitted from the discussion with Dr. Bernadí Gelabert (Departament de Biologia, Universitat de les Illes Balears), Dr. Onofre Rullan (Departament de Geografia, Universitat de les Illes Balears) and Llorenç Homar.

Lastly, I want to acknowledge the support of friends and family throughout the years of working on this project. Especially to my parents, Sebastiana M. Andreu, who helped me code some of the character data matrices by dictating the character states aloud, and Sebastià Matamalas, who accompanied me in most field days and excavations.

The present Ph.D. dissertation was supported by the following funding sources:

- Ph.D. grant 2018 FI_B 00060 (Generalitat de Catalunya) awarded to R. Matamales Andreu, from April to August 2018.
- Ph.D. grant FPU17/01922 (Ministerio de Ciencia, Innovación y Universidades) awarded to R. Matamales Andreu, from September 2018 to October 2021.
- Travel grant Synthesys+ DE-TAF-23 (European Commission) awarded to R. Matamales Andreu, for 10 days of November 2019 in Berlin and Stuttgart.
- Publication grant 2112-2020-000001 (Consell Insular de Menorca), awarded to R. Matamales Andreu, Dr. À. Galobart and Dr. J. Fortuny.
- Preparation grant with file number 25 - 393/2020 (Consell Insular de Mallorca), awarded to R. Matamales Andreu.
- Preparation grant with file number 26 - 374/2020 (Consell Insular de Mallorca), awarded to R. Matamales Andreu.
- Preparation grant with file number 2 - 295/2021 (Consell Insular de Mallorca), awarded to R. Matamales Andreu.
- Preparation grant with file number 2 - 288/2022 (Consell Insular de Mallorca), awarded to R. Matamales Andreu.
- Research project grant with file number 15 - 619/2021 (Consell Insular de Mallorca) for the three-year project entitled *"Mallorca abans dels dinosaures: estudi dels ecosistemes continentals del Permià i Triàsic amb especial èmfasi en les restes de vertebrats"*, awarded to Dr. J. Fortuny, Dr. À. Galobart and R. Matamales Andreu.

Appendix 1

Previous works on the Permian and Triassic of Mallorca

Appendix 1 was published as:

Matamales-Andreu, R.; Oms, O. & Fortuny, J. (2021). Paleoecosistemes del Permià i Triàsic continental de Mallorca (Illes Balears, Mediterrània occidental): síntesi i prespectives futures. *In*: Gómez-Pujol, L.; Roig-Munar, F.X.; Gelabert, B.; Martín, J.A. (Eds.). *De la terra a la mar i de la mar a la terra. Homenatge a Antonio Rodríguez-Perea. Monografies de la Societat d'Història Natural de Balears*, 34. Societat d'Història Natural de les Balears; Palma: 17–39. [in Catalan]

ISBN: 978-84-09-34554-0

DL: PM 00742-2021

In this work, R. Matamales-Andreu contributed in:

A. Literature review of the Permian and Triassic of Mallorca.
B. Integration and discussion of the previous data.
C. Writing of the original draft.
D. Preparation of all the tables (1–4), and figures (1–7).

PALEOECOSISTEMES DEL PERMIÀ I EL TRIÀSIC CONTINENTAL DE MALLORCA (ILLES BALEARS, MEDITERRÀNIA OCCIDENTAL): SÍNTESI I PERSPECTIVES FUTURES

Rafel Matamales-Andreu [1,2], Oriol Oms [3] i Josep Fortuny [1]

[1] Institut Català de Paleontologia Miquel Crusafont, Universitat Autònoma de Barcelona, Edifici ICTA-ICP, Carrer de les Columnes s/n, Campus de la UAB, 08193 Cerdanyola del Vallès (Catalunya)

[2] Museu Balear de Ciències Naturals, Carretera Palma-Port de Sóller Km. 30, 07100, Sóller (Illes Balears)

[3] Departament de Geologia, Universitat Autònoma de Barcelona, Avinguda de l'eix Central s/n, Campus de la UAB, 08193 Cerdanyola del Vallès (Catalunya)

Resum: El present article ofereix una revisió exhaustiva de tots els antecedents bibliogràfics sobre el permià i el triàsic de Mallorca en fàcies continentals, sintetitzant les dades més importants pel que fa a la geologia, paleontologia i datacions. Així, es destrien tres unitats litostratigràfiques del permià inferior–mitjà i quatre del triàsic inferior(?)–mitjà, amb un abundant registre fòssil que representa uns rics ecosistemes a la vorera de grans rius, situats a una paleolatitud equatorial amb un clima tropical. Aquesta publicació pretén servir de base per a futurs estudis sobre aquest tema, ressaltant la potencial gran importància del registre mallorquí en l'àmbit mundial per entendre com era la Terra fa més de 240 milions d'anys.

Paraules clau: *permià, triàsic, estratigrafia, paleontologia, Mallorca.*

Abstract: The present paper offers an exhaustive review of all the previous works on the continental Permian and Triassic of Mallorca, synthesising all the relevant data regarding their geology, palaeontology and age attributions. This makes it possible to recognise three lithostratigraphic units for the lower–middle Permian and four for the Lower(?)–Middle Triassic, with an abundant fossil record representing rich ecosystems on the banks of large rivers, located in an equatorial palaeolatitude and under a tropical climate. This work aims to serve as a basis for future studies to be built on, highlighting the potentially great international importance of the Mallorcan record to understand how the Earth looked like more than 240 million years ago.

Keywords: *Permian, Triassic, stratigraphy, palaeontology, Mallorca.*

Introducció

El permià i el triàsic (Fig. 1) són dos períodes geològics clau en la història de la vida a la Terra, separats per l'extinció massiva més grossa que hi ha haguda mai (fa 251,902 ± 0,024 milions d'anys), que va fer desaparèixer més del 90% de les espècies marines i terrestres del món (ROMANO *et al.*, 2020, i referències que s'hi esmenten). En aquell temps, quasi tots els continents estaven confegits en una única massa de terra anomenada Pangea, que tenia un gran golf en el seu marge oriental ocupat per l'oceà de Tetis (Fig. 1). Durant el permià, els ecosistemes tenien una complexitat comparable a l'actual, i hi ha autors que el consideren la "primera edat dels mamífers", per mor que els sinàpsids eren els vertebrats dominants a la majoria de regions del món (*e.g.*, BENTON, 2008). Després del gran cataclisme, els ecosistemes es torbaren molts de milions d'anys a recuperar-se, i quan ho feren, en el triàsic mitjà, les faunes de vertebrats terrestres dominants ja havien estat substituïdes per representants del grup dels "rèptils", amb llinatges que evolucionarien cap als dinosaures (*e.g.*, BENTON, 2008; ROMANO *et al.*, 2020).

A la península Ibèrica, excloent les conques pirinenques, les seqüències continentals del permià i del triàsic corresponen als dipòsits de grans rius que fluïen cap al sud–est, dins conques de *semirift* que s'obriren en la mateixa direcció (LÓPEZ-GÓMEZ *et al.*, 2019). Aquestes conques s'enfonsaren com a resultat del relaxament de l'orogen varisc a partir del carbonífer superior, sumat a una diferència de rotació de les dues meitats de Pangea que va provocar una zona de megacisalla a la regió occidental del

MATAMALES, R., OMS, O. i FORTUNY, J. (2021): Paleoecosistemes del permià i el triàsic continental de Mallorca (Illes Balears, Mediterrània occidental): síntesi i perspectives futures. In: *De la terra a la mar i de la mar a la terra. Homenatge a Antonio Rodríguez-Perea*. Mon. Soc. Hist. Nat. Balears, 34: 17-39. ISBN: 978-84-09-34554-0.

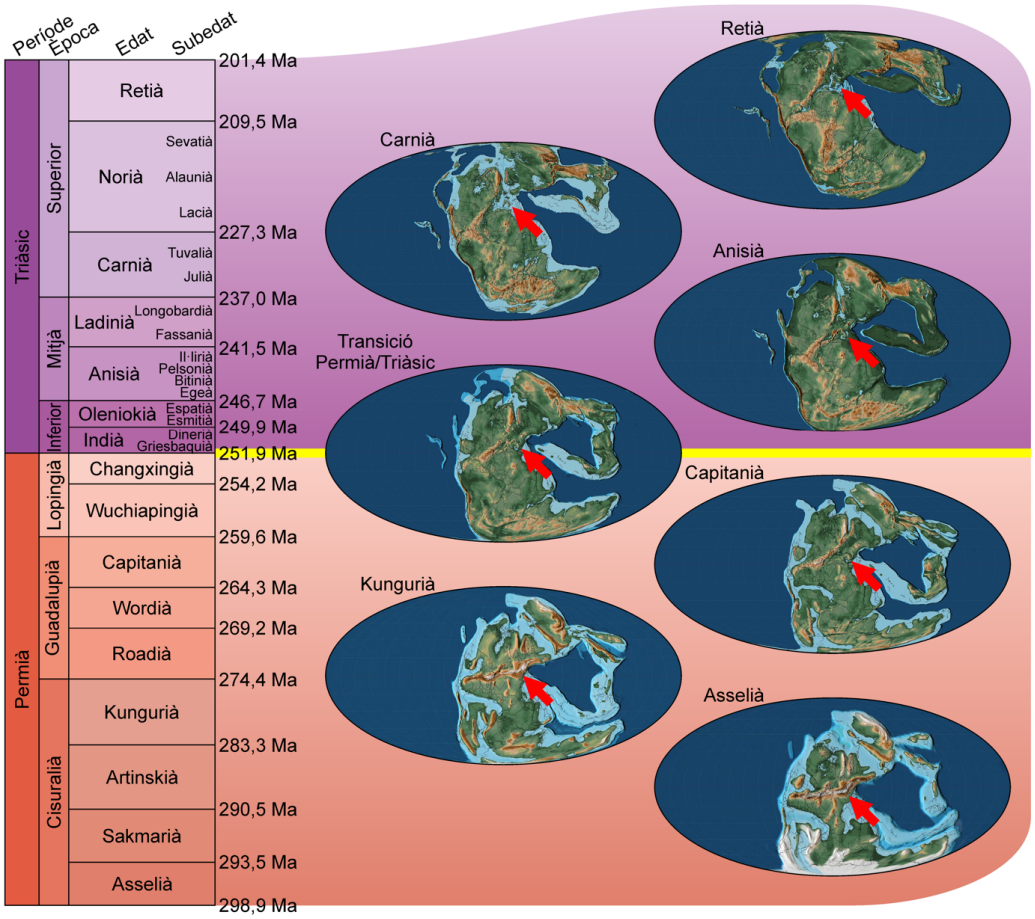

Fig. 1. Taula cronostratigràfica del permià i del triàsic (modificada de COHEN *et al.*, 2013, amb datacions actualitzades a partir de HENDERSON *et al.*, 2020, i OGG *et al.*, 2020) amb la nomenclatura que s'emprarà en aquest article, i mapes paleogeogràfics (extrets de SCOTESE, 2014a, 2014b, amb permís de l'autor) amb fletxes vermelles que indiquen la paleoposició aproximada de Mallorca. Ma = milions d'anys.

peri-Tetis (McCANN *et al.*, 2006; LÓPEZ-GÓMEZ *et al.*, 2019). A la majoria de conques ibèriques s'hi han reconegut entre dos i tres intervals principals de sedimentació continental, que coincideixen amb moments de reactivació tectònica devers el permià inferior, el permià superior i el triàsic inferior–mitjà (LÓPEZ-GÓMEZ *et al.*, 2019). Durant tot aquest temps, la zona d'Ibèria era pràcticament a l'equador de Pangea (Fig. 1) i el seu clima era tropical, més o manco àrid (*e.g.*, ROSCHER *et al.*, 2011). Correlacionant les seqüències de diferents afloraments del triàsic i observant-hi tendències comunes, BORRUEL-ABADÍA *et al.* (2015) varen concloure que el clima era un dels factors principals que determinava el paleoambient deposicional. Mentre que les unitats més inferiors eren dominades per sediments eòlics, indicadors d'un clima molt àrid, les unitats més superiors tenien associacions típicament fluvials, que juntament amb un registre fòssil més ric (i altres criteris) indicaven uns climes més humits (BORRUEL-ABADÍA *et al.*, 2015).

Per paga, les correlacions tornen més males de fer quan hom vol considerar l'extrem més distal d'aquells sistemes, és a dir, les Balears. Tan sols es poden trobar roques del permià i triàsic continental a les Gimnèsies, i a on afloren més extensament és al sector de Tramuntana de Menorca. Allà s'hi reconegueren tres unitats del permià i tres més del triàsic inferior–mitjà (GÓMEZ-GRAS, 1987, 1992, 1993; ROSELL *et al.*, 1988, 1989a, 1989b; LINOL *et al.*, 2009) amb un contingut fòssil molt escàs, que no

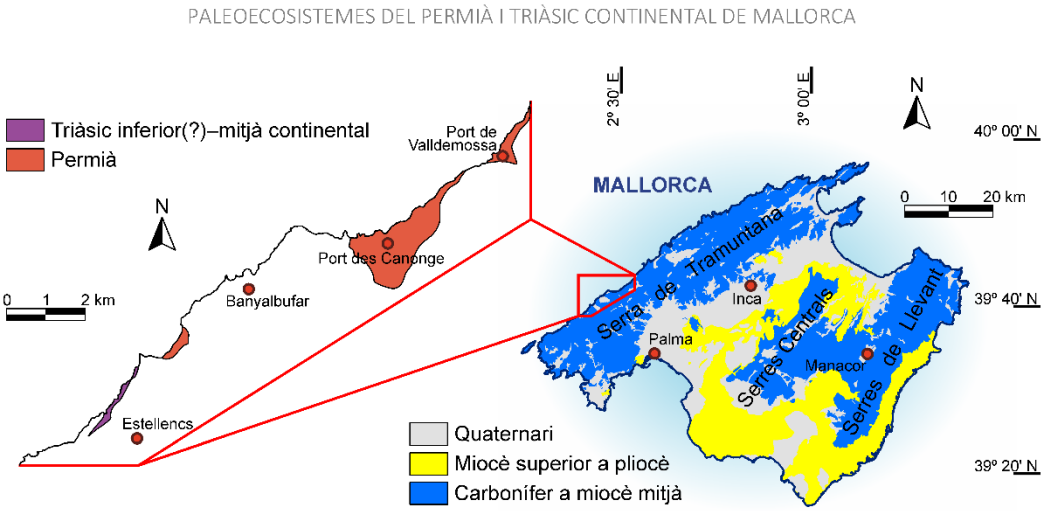

Fig. 2. Mapa geològic simplificat de Mallorca amb una ampliació de la zona del vessant nord-occidental de la serra de Tramuntana on hi aflora el permià i el triàsic inferior(?)–mitjà continental.

va permetre datar la majoria d'unitats amb seguretat. Tan sols es va datar la unitat més superior del permià ('P3'), mitjançant esporomorfs i palinomorfs, dins l'interval wordià–changxingià (permià mitjà–superior) (BERCOVICI *et al.*, 2009). D'aquesta unitat en destaquen també les restes vegetals relativament ben conservades (BERCOVICI *et al.*, 2009) i els ossos de vertebrats, qualcuns de mida molt grossa (PRETUS & OBRADOR, 1987; CARMONA, 2004), que recentment s'han estudiat en detall (MATAMALES-ANDREU *et al.*, 2021d).

D'altra banda, a l'illa de Mallorca, els afloraments del permià i del triàsic inferior(?)–mitjà que representen paleoambients continentals es troben restringits a una partida de localitats a vorera de mar en el vessant nord–oest de la serra de Tramuntana, en els municipis d'Estellencs, Banyalbufar i Valldemossa (Fig. 2). No obstant això, moltes d'elles són de difícil accés, per mor que tan sols s'hi pot arribar per la mar o fent servir cordes. Històricament, això ha fet que els estudis detallats fossin escassos i de vegades pobrament contextualitzats, afegint confusió tant a l'hora d'aclarir la seqüència estratigràfica general com a les datacions de les diferents unitats i fòssils. La present contribució pretén oferir una revisió crítica de tots els antecedents del permià i triàsic continental de Mallorca, endegant i sintetitzant el coneixement sobre aquestes edats que es té actualment.

Unitats litostratigràfiques i paleoambients que representen

A final del segle XIX i durant la primera meitat del segle XX es varen publicar els primers estudis sobre la geologia del permià i triàsic continental de Mallorca. HERMITE (1879, 1888) va ser el primer autor que va reconèixer la presència de roques del triàsic prop de la cala d'Estellencs, i les va correlacionar amb la fàcies *Buntsandstein* (='gresos bigarrats') d'Europa central, proposant-los una edat triàsic inferior. Els autors posteriors, com NOLAN (1887, 1888), DARDER (1914) i FALLOT (1922), varen documentar unitats litològicament equivalents de gresos bigarrats i lutites a la costa sud-occidental de Banyalbufar, per devora el Port des Canonge i al Port de Valldemossa, emperò no varen proporcionar noves dades que aclarissin la seva estratigrafia o edat. No va esser fins més de tres dècades més tard, que CUEVAS-LÓPEZ (1958a, 1958b) va suggerir que per ventura sols una part dels gresos bigarrats eren del triàsic, essent la majoria d'ells del permià, correlacionant-los amb les fàcies *Rothliegende* (='vermell infrajacent'), *Zechstein* (='roca forta') i *Kupferschiefer* (='lutites amb coure') d'Europa central (Taula 1A– i B).

Taula 1A. Noms i equivalències entre les unitats del permià i triàsic continental de Mallorca.

<table>
<tr><th>CUEVAS-LÓPEZ (1958a, 1958b)</th><th>POMAR-GOMÀ (1979)</th><th>MARTÍ et al. (1985)</th><th>RAMOS et al. (1985), RAMOS & DOUBINGER (1989)</th><th>CALVET & MARZO in SANTANACH (1986)</th><th>CALAFAT (1986), CALAFAT et al. (1986–1987)</th><th colspan="2">CALAFAT (1987)</th></tr>
<tr><td colspan="8">Fàcies Muschelkalk del triàsic mitjà</td></tr>
<tr><td>Nivell V, sostre (100 m)</td><td rowspan="4">(no es va estudiar)</td><td rowspan="4">(no es va estudiar)</td><td>Lutites i Gresos de Son Serralta (65 m)</td><td rowspan="3">(no es va estudiar)</td><td>Unitat de trànsit (25 m)</td><td colspan="2">“Formació” Lutites de Son Serralta (27 m)</td></tr>
<tr><td>Nivell IV (40 m)</td><td rowspan="3">Gresos de “Asá” [sic.] (140 m)</td><td>Unitat superior (100 m)</td><td colspan="2">“Formació” Gresos i Lutites d’Estellencs (124 m)</td></tr>
<tr><td>Nivell III (50–60 m)</td><td rowspan="2">Unitat intermèdia (100 m)</td><td rowspan="2">“Formació” Gresos de la Pedra de s’Ase (150 m)</td><td>“Membre” Gresos de la Punta Roja (25 m)</td></tr>
<tr><td>Nivell V, base (30–40 m)</td><td rowspan="2">Darrera secció lutítica (≈80 m)</td><td rowspan="2">Lutites i Gresos de Son Serralta (120 m)</td><td rowspan="2">“Membre” Gresos de la Pedra de s’Ase (125 m)</td></tr>
<tr><td>Nivell III (50–60 m)</td></tr>
<tr><td>Nivell II (200 m)</td><td>Gresos de colors clar (127 m)</td><td>Tram gresós</td><td>Gresos de la Pedra de s’Ase (100 m)</td><td colspan="3"></td></tr>
<tr><td rowspan="2">Nivell I (800 m)</td><td rowspan="2">Secció lutítica inferior (213 m)</td><td>Tram inferior pelític</td><td rowspan="2">Gresos i Lutites del Port des Canonge (176 m)</td><td rowspan="2">Gresos i Lutites del Port d’es Canonge (260 m)</td><td>Unitat inferior (150–250 m)</td><td colspan="2">“Formació” Gresos i Lutites del Racó de s’Algar (144 m)</td></tr>
<tr><td>Bretxa poligènica</td><td>Unitat basal (10 m)</td><td colspan="2">“Formació” Gresos i Conglomerats del Bec de s’Àguila (25 m)</td></tr>
<tr><td colspan="8">Fàcies Culm del carbonífer</td></tr>
</table>

La proposta de CUEVAS-LÓPEZ (1958a, 1958b) la varen seguir, en part, estudis posteriors com COLOM (1975), POMAR-GOMÀ (1979), OBRADOR (1983), MARTÍ *et al.* (1985), CALVET & MARZO *in* SANTANACH *et al.* (1986), RODRÍGUEZ-PEREA *et al.* (1987) i BARNOLAS (1991a, 1991b), acceptant que les unitats més inferiors podien pertànyer al permià, tot i que sense aportar noves dades pel que fa a la seva datació. No obstant això, qualcuns d’ells sí que varen presentar noves divisions preliminars en unitats litostratigràfiques (Taula 1A–B), però basades tan sols en la secció entre el racó de s’Algar i el port de sa pedra de s’Ase (Banyalbufar), on la seqüència que hi aflora no és completa. Paral·lelament, RAMOS *et al.* (1985) també varen intentar delimitar unitats litostratigràfiques (Taula 1A–B), però la gran consemblança litològica entre les unitats del permià i del triàsic va resultar en la correlació de litosomes d’edats diferents, limitant la utilitat de la proposta. BANDA *et al.* (1986) varen fer un estudi paleomagnètic preliminar, analitzant mostres de la cala d’Estellencs i del Port des Canonge, i varen concloure que les direccions de la magnetització romanent característica s’assemblaven a les de la fàcies *Buntsandstein* de Menorca i les serralades costaneres Catalanes. PARÉS *et al.* (1989, 1992a, 1992b) varen discutir aquests resultats amb una mica més de detall.

CALAFAT (1986, 1987, 1988) va dur a terme el primer estudi exhaustiu de l’estratigrafia i la sedimentologia d’aquestes unitats, distingint-n’hi cinc (Taula 1A–B). Segons aquest autor, la unitat més inferior, els ‘Gresos i Conglomerats del Bec de s’Àguila’, corresponia a dipòsits de rius entrunyellats (també coneguts com a ‘trenats’ o *‘braided’*) efímers que s’estenien damunt la fàcies *Culm* (=‘carbó’) del carbonífer infrajacent (Fig. 3A–B). Segons Calafat (1988), la segona unitat, els ‘Gresos i Lutites del Racó de s’Algar’, havia estat dipositada per rius amb una morfologia intermèdia entre entrunyellat i meandriforme, que solcaven grans planes d’inundació (Fig. 3C–D). Tot seguit apareixia la tercera unitat, els ‘Gresos de la Pedra de s’Ase’, que es podia atribuir a la sedimentació en rius entrunyellats (Fig. 3E–

Taula 1B. Noms i equivalències entre les unitats del permià i triàsic continental de Mallorca (continuació).

<table>
<tr><th>RODRÍGUEZ-PEREA et al. (1987)</th><th colspan="3">CALAFAT (1988), ÁLVAREZ-RAMIS et al. (1995), GRAUVOGEL-STAMM & ÁLVAREZ-RAMIS (1996), DIEZ (2000), JUÁREZ-RUIZ & WACHTLER (2015)</th><th colspan="2">BARNOLAS (1991a, 1991b)</th><th colspan="2">GÓMEZ-GRAS (1992, 1993)</th><th>RAMOS (1995), ARCHE et al. (2002), LÓPEZ-GÓMEZ et al. (2002, 2019), VERA et al. (2004), BOURQUIN et al. (2007, 2011), CASSINIS et al. (2012), JUNCAL (2019)</th><th>Nomenclatura del present treball</th></tr>
<tr><td colspan="8">Fàcies Muschelkalk del triàsic mitjà</td></tr>
<tr><td rowspan="3">(no es va estudiar)</td><td colspan="3">Unitat Lutites de Son Serralta (27 m)</td><td rowspan="3">(no es va estudiar)</td><td rowspan="3">Tram e) (160 m)</td><td>Pelites i gresos superiors</td><td rowspan="3">Lutites i Gresos de Son Serralta (65 m)</td><td>Unitat G</td></tr>
<tr><td colspan="3" rowspan="2">Unitat Gresos i Lutites d'Estellencs (124 m)</td><td>Gresos intermedis</td><td>Unitat F</td></tr>
<tr><td rowspan="4">Gresos de "Asá" [sic.] (110 m)</td><td>Pelites i gresos inferiors</td><td>Unitat E</td></tr>
<tr><td rowspan="3">Unitat Gresos de la Pedra de s'Ase (150 m)</td><td rowspan="2">Sub-unitat Gresos de la Punta Roja (25 m)</td><td colspan="3">Tram d) (58 m)</td><td>Unitat D</td></tr>
<tr><td rowspan="2">Tram pelític–gresós superior (≈80 m)</td><td rowspan="2">Lutites vermelles i verdes (>20 m)</td><td rowspan="2">Tram c) (135 m)</td><td rowspan="2">Unitat C</td></tr>
<tr><td rowspan="2">Sub-unitat Gresos de la Pedra de s'Ase (125 m)</td></tr>
<tr><td>Tram intermedi de gresos (127 m)</td><td>Gresos blancs i vermells (120 m)</td><td colspan="2">Tram b) (110 m)</td></tr>
<tr><td>Tram gresós–pelític inferior (213 m)</td><td colspan="2">Unitat Gresos i Lutites del Racó de s'Algar (144 m)</td><td>Lutites vermelles (>100 m)</td><td rowspan="2">Tram a) (403 m)</td><td rowspan="2">Gresos i Lutites del Port des Canonge (160 m)</td><td>Unitat B</td></tr>
<tr><td>Tram basal conglomeràtic–gresós (<20 m)</td><td colspan="2">Unitat Gresos i Conglomerats del Bec de s'Àguila (25 m)</td><td>(no es va estudiar)</td><td>Unitat A</td></tr>
<tr><td colspan="8">Fàcies Culm del carbonífer</td></tr>
</table>

F), i la seva subunitat superior, els 'Gresos de la Punta Roja', de rius entrunyellats que remobilitzaven sediments eòlics (Fig. 4A–B). Per damunt hi havia la quarta unitat, els 'Gresos i Lutites d'Estellencs', que presentaven un terme inferior corresponent a planes d'inundació i un de superior de dipòsits de rius entrunyellats (Fig. 4C–F). Finalment, la unitat més superior, les 'Lutites de Son Serralta', va esser interpretada com una plana d'inundació vora la mar (Fig. 4G–H).

Poc temps després d'aquests estudis, GÓMEZ-GRAS (1992, 1993) va publicar una nova investigació que incloïa la reinterpretació de la geologia del permià i el triàsic continental de Mallorca, distingint-hi també cinc unitats litostratigràfiques informals (Taula 1A–B), considerant una partida d'afloraments que CALAFAT (1988) no havia estudiat per mor de la seva mala accessibilitat. Específicament, el seu 'Tram A' corresponia a les dues unitats més inferiors de CALAFAT (1988), que foren reinterpretades com a dipòsits de rius meandriformes (Fig. 3A–D). Els trams B, C i D equivalien a la tercera unitat de CALAFAT (1988): el 'Tram B' presentava una interpretació difícil, amb possibles trets mareals (Fig. 3E–F); el 'Tram C' corresponia a dipòsits de canals meandriformes o anastomosats, també amb influència mareal (Fig. 3E–F); i el 'Tram D' (subunitat 'Punta Roja' de CALAFAT, 1988) representava rius entrunyellats que funcionaven durant una fase tectònicament activa (Fig. 4A–B). El 'Tram E', el més superior, es dividia en tres subtrams: els dos més inferiors equivalien a la quarta unitat de CALAFAT (1988) i es varen interpretar com dipòsits de rius meandriformes durant períodes de major i menor subsidència, respectivament (Fig. 4C–F), mentre que el subtram més superior corresponia a la cinquena unitat de CALAFAT (1988), dipositat a una plana mareal mixta (Fig. 4G–H). Mitjançant l'estudi petrològic dels gresos de cadascun dels trams, GÓMEZ-GRAS (1992, 1993) va concloure que el 'Tram A', el 'Tram B' i el 'Tram C' s'assemblaven notablement entre ells, mentre que el 'Tram D' era el que tenia la maduresa composicional i textural més elevada, possiblement perquè remobilitzava dipòsits anteriors. Finalment,

el 'Tram E' era clarament diferent dels anteriors pel que fa a la seva composició. Això, juntament amb les datacions que s'havien fetes fins a aquell moment, li va permetre suggerir que el 'Tram A', el 'Tram B' i el 'Tram C' podrien esser del permià i el 'Tram D' i el 'Tram E' del triàsic. Basant-se en la consemblança de les sèries mallorquines amb les d'altres localitats de la península Ibèrica, aquest autor va proposar que la conca on es varen dipositar aquests materials era la mateixa que aflora a les serralades Ibèriques.

El darrer estudi detallat que es va publicar sobre l'estratigrafia i la sedimentologia dels afloraments del permià i el triàsic continental de Mallorca va ser el de RAMOS (1995), desenvolupant la proposta preliminar de RAMOS *et al.* (1985). Per paga, no va desfer l'errada de correlació de l'estudi original, i per tant les tres unitats litostratigràfiques que va descriure (Taula 1A–B) tenen utilitat limitada. La seva unitat de 'Gresos i Lutites del Port des Canonge', interpretada com a dipòsits de rius meandriformes,

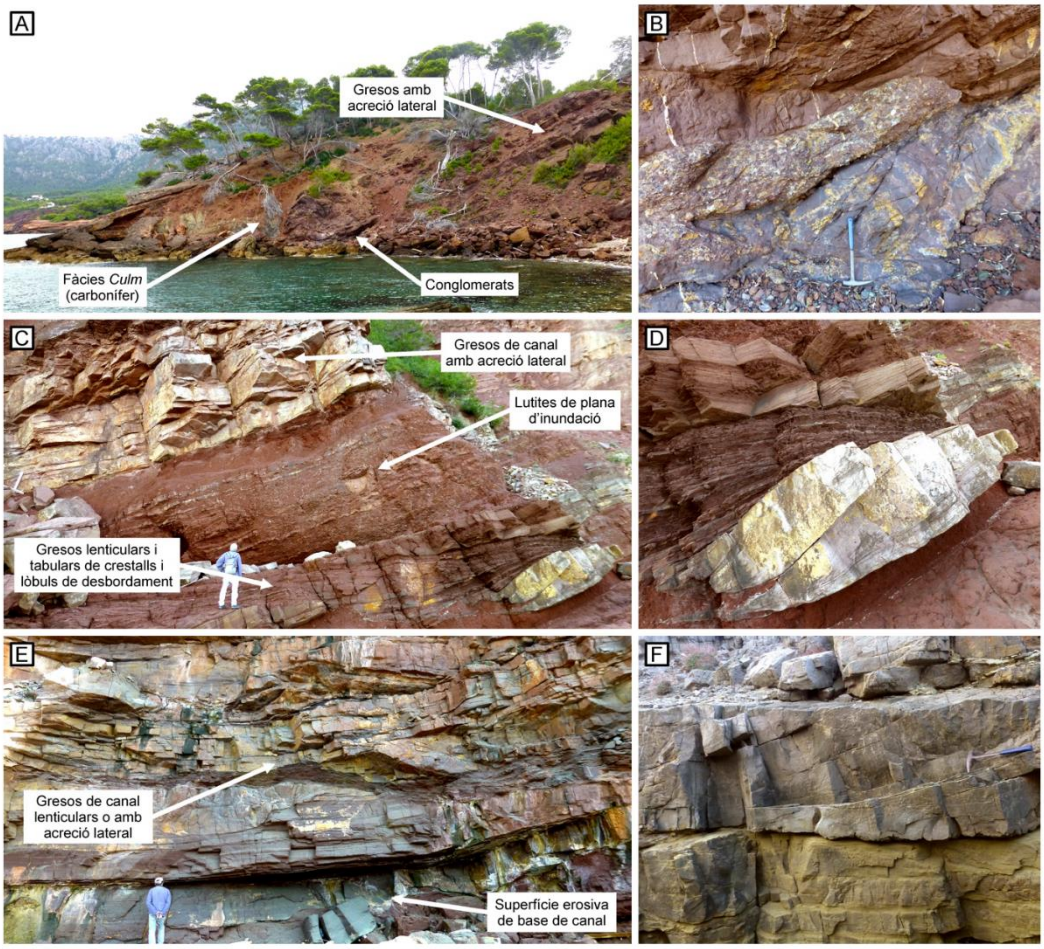

Fig. 3. Unitats del permià de Mallorca. **A–B:** Unitat A; **A:** vista general d'una sèrie típica, amb conglomerats i gresos amb acreció lateral (canals) damunt el carbonífer, de la platja de sa Pedrera; **B:** detall dels nivells de conglomerats, de la platja de sa Pedrera. **C–D:** Unitat B; **C:** vista general d'una seqüència d'intercalació de gresos amb acreció lateral (canals) i lutites i gresos fins (plana d'inundació), del racó de s'Algar; **D:** detall dels dipòsits de barra de meandre d'un canal petit, del racó de s'Algar. **E–F:** Unitat C; **E:** vista general dels gresos clars de gra mitjà amb poques lutites intercalades, que poden tenir acreció lateral (canals) o ser lenticulars (dipòsits de torrentades), del comellar de can Xitx; **F:** detall d'un nivell de gres corresponent a una barra de meandre, de la platja de sa Pedrera.

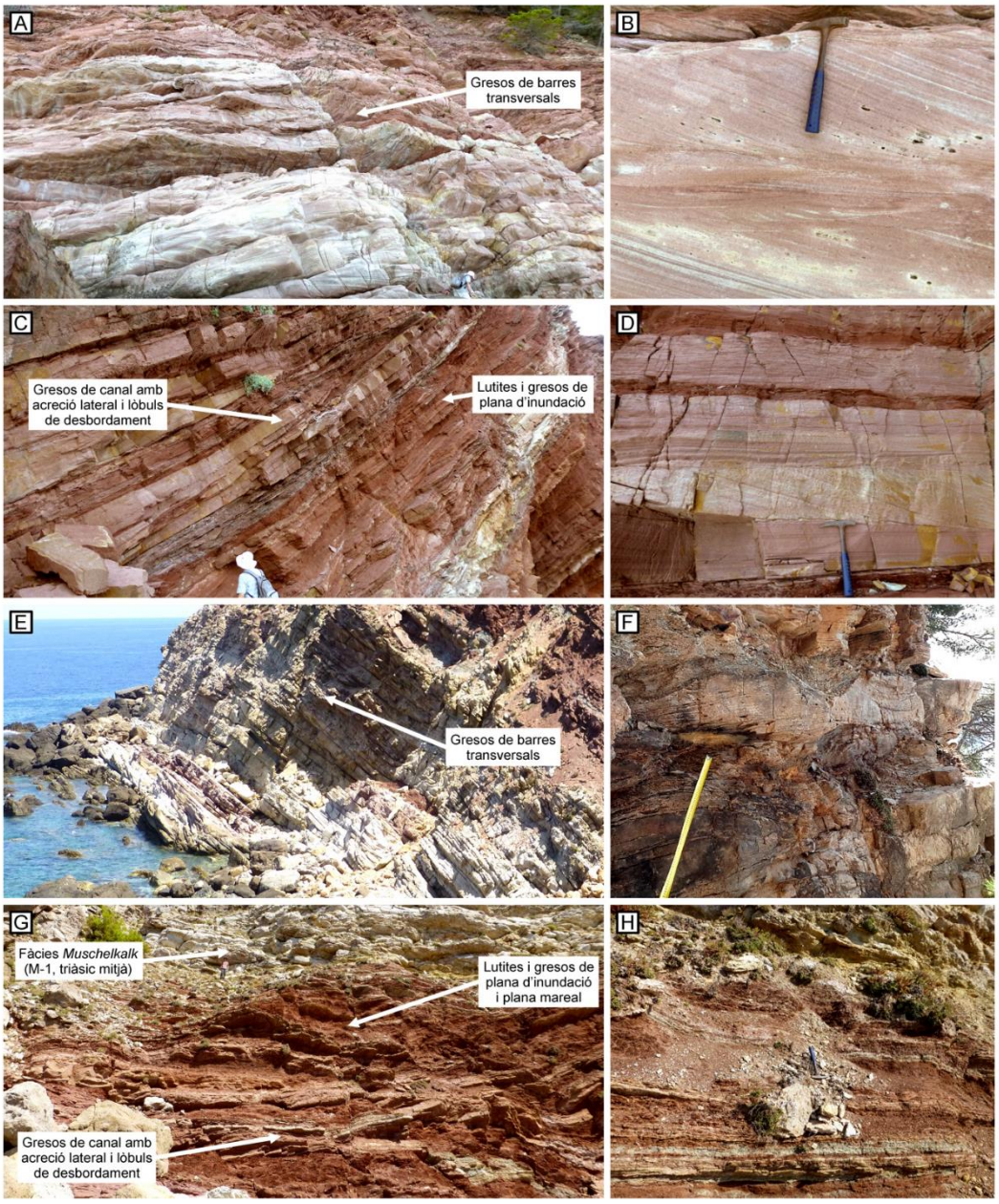

Fig. 4. Unitats del triàsic continental de Mallorca. **A–B:** Unitat D; **A:** vista general d'una seqüència de superposició de capes tabulars de gres, de punta Roja; **B:** detall dels dipòsits de barres fluvials transversals, de punta Roja. **C–D:** Unitat E; **C:** vista general dels gresos fins tabulars (lòbuls de desbordament) o amb acreció lateral (canals) i lutites (plana d'inundació), de punta Roja; **D:** detall d'uns gresos de canal amb els dipòsits de dunes submergides, de punta Roja. **E–F:** Unitat F; **E:** vista general d'una seqüència típica de superposició de capes lenticulars de gres (barres fluvials transversals) i escasses lutites, de la tenassa de sa Tanca; **F:** detall d'uns gresos corresponents a dunes submergides tapades de lutites blavoses de quan es va abandonar el canal, de la pedra Alta. **G–H:** Unitat G; **G:** vista general d'aquesta unitat de gresos i lutites i el seu contacte superior amb els carbonats de la fàcies *Muschelkalk* (triàsic mitjà), de la tenassa de sa Tanca; **H:** detall dels nivells de plana mareal lutítica i el contacte *Buntsandstein–Muschelkalk*, de la tenassa de sa Tanca.

correspon a parts de les unitats 'Bec de s'Àguila', 'Racó de s'Algar' i la part inferior de la unitat 'Estellencs' de CALAFAT (1988). La unitat de 'Gresos de Asá' [sic.] és una mescla de les unitats 'Pedra de s'Ase' (incloent-hi 'Punta Roja') i la part mitjana de la unitat 'Estellencs' de CALAFAT (1988). Aquesta unitat es va interpretar com a dipòsits de rius meandriformes amb episodis puntuals de pluges torrencials amb fluxos d'alt règim que generaven estructures tractives. Finalment, la unitat de 'Lutites i Gresos de Son Serralta', corresponent a la part superior de la unitat 'Estellencs' i tota la unitat 'Son Serralta' de CALAFAT (1988), va ser interpretada com una plana entrunyellada distal que evolucionava cap a una plana mareal. Dissortadament, totes les publicacions de síntesi posteriors (ARCHE *et al.*, 2002; LÓPEZ-GÓMEZ *et al.*, 2002, 2019; VERA *et al.*, 2004; BOURQUIN *et al.*, 2007, 2011; CASSINIS *et al.*, 2012; JUNCAL, 2019) s'han basat en aquesta concepció errònia per interpretar el registre d'aquests períodes geològics a Mallorca (Taula 1A–B).

En resum, la divisió més fina que es pot fer de la sèrie del permià i triàsic continental de Mallorca consisteix en set unitats litostratigràfiques diferents. Per simplificar-ho, en el present article, a partir d'aquest apartat, s'anomenaran amb les lletres consecutives A–G de més inferior a més superior (Taula 1A–B; Figs. 3–4).

Registre fòssil

Plantes del permià

En el permià de Mallorca, les macrorestes vegetals normalment compareixen en forma de bocins impossibles d'identificar. No obstant això, FREEMAN & OBRADOR (1974, 1979), CALAFAT (1988), RAMOS (1995) i DIEZ (2000) varen esmentar i il·lustrar grans troncs carbonitzats a la base de canals fluvials a la part alta de la Unitat C (Fig. 5A). A més a més, a totes les unitats també hi abunden els nòduls carbonatats i les restes de rels (rizocrecions) corresponents a paleosòls que es varen formar a les planes d'inundació en un clima àrid (CALAFAT, 1988; GÓMEZ-GRAS, 1992, 1993; RAMOS, 1995) (Fig. 5B).

La microflora és abundant en segons quins nivells de la Unitat C en forma de diferents castes d'esporomorfs i de palinomorfs, descrits per RAMOS i DOUBINGER (1989), DIEZ (2000), DIEZ *et al.* (2005) i JUNCAL (2019), que aquí es llisten a la Taula 2.

Traces d'invertebrats del permià

Baldament les traces fòssils d'invertebrats són molt habituals en les seqüències del permià (i del triàsic) de Mallorca (*e.g.*, CALAFAT, 1988) (Fig. 5C), hi ha hagut molt poques investigacions que les hagin estudiades en detall. Tan sols hi ha dues publicacions, RAMOS i GARCÍA-RAMOS (1992) i RAMOS (1995), que identificaren aquests icnofòssils, emperò de manera molt general. Concretament, esmentaren la presència dels icnogèneres *Planolites* i *Palaeophycus* a les unitats B i C (també podria incloure la Unitat E, vegeu l'apartat 'Unitats litostratigràfiques i paleoambients que representen'), i destacaren l'icnogènere *Ancorichnus* a la Unitat C. Argumentaren que aquestes traces, fetes per cucs o artròpodes, eren indicadores d'ambients esporàdicament amarats que estarien eixuts durant una bona part de l'any.

"Rèptils" del permià

Els sediments fins de les planes d'inundació de la Unitat B són els més adients per conservar les potades dels animals que hi capllevaven. Les impressions en el fang quedaven tapades per l'arena dipositada pels lòbuls de desbordament dels rius, fent que les potades es conservassin com a motlles naturals a les bases de les capes de gres (Fig. 5D). A més, els dipòsits dels crestalls dels rius (també coneguts com a 'dics naturals' o *'levées'*) també eren un ambient propici per la conservació d'ossos de vertebrats, que normalment solen desaparèixer (BEHRENSMEYER, 1982). Així, en aquesta unitat s'estrevé la situació poc freqüent que s'hi poden trobar potades quasi associades amb els ossos de les

Taula 2. Esporomorfs i palinomorfs del permià de Mallorca esmentats en els diferents estudis. **A:** RAMOS & DOUBINGER (1989), **B:** mostra "MA-1" de DIEZ (2000), **C1:** mostra "Mallorca" de DIEZ *et al.* (2005), **C2:** mostra "Racó de s'Algar – Sa pedra de s'Ase" de DIEZ *et al.* (2005), **D:** mostra "MA-1" de JUNCAL (2019). Les cel·les omplides de negre indiquen la presència del tàxon a la localitat.

Espècie	A	B	C		D
			C1	C2	
Alisporites opii		■		■	■
Alisporites splendens		■		■	■
Alisporites sp.		■		■	■
Bascanisporites sp.					■
cf. *Bascanisporites* sp.		■			
Calamospora sp.	■	■	■	■	■
Chordasporites sp.		■		■	■
Cordaitina sp.		■		■	■
Crucisaccites variosulcatus	■	■	■	■	■
Crustaesporites sp.	■		■		
Densiosporites sp.					■
Endosporites cf. *velatus*	■				
Endosporites sp.		■	■	■	■
Falcisporites zapfei	■	■		■	■
Falcisporites sp.					■
Gardenasporites heisseli					■
Gardenasporites sp.		■		■	■
Jugasporites delasaucei	■	■	■		
Klausipollenites schaubergeri	■	■		■	■
Klausipollenites sp.		■		■	■
Kraeuselisporites cf. *spinosus*		■			■
Leiotriletes sp.		■		■	■
Limitisporites sp.	■		■		
Lueckisporites globosus					■
Lueckisporites cf. *hyalinus*		■			
Lueckisporites singhii	■		■		■
Lueckisporites virkkiae	■	■	■	■	■
Lueckisporites sp.		■		■	■
Lunatisporites albertae					■

Espècie	A	B	C		D
			C1	C2	
Lunatisporites noviaulensis		■		■	■
Lunatisporites pellucidus					■
Lunatisporites variesectus					■
Lunatisporites sp.		■		■	
Lundbladispora sp.		■		■	
Maculatasporites amplus		■		■	
Maculatasporites sp.	■		■		
Nuskoisporites dulhuntyi	■	■	■	■	■
Nuskoisporites klausi					■
Nuskoisporites cf. *klausi*		■			
Nuskoisporites sp.		■		■	
Paravesicaspora splendens	■		■		
Paravesicaspora cf. *splendens*		■			■
Paravesicaspora sp.				■	
Platysaccus papilionis		■		■	■
Playfordiaspora sp.	■		■		
Potonieisporites novicus		■		■	■
Potonieisporites sp.					■
Protohaploxypinus microcorpus	■	■			■
Protohaploxypinus sp.	■	■	■	■	
Sahnisporites saarensis		■		■	■
Sahnisporites cf. *saarensis*		■		■	
Striatoporocarpidites sp.					■
Uvaesporites sp.					■
Verrucosisporites sp.					■
Vesicaspora wilsoni	■		■		
Espores indeterminades		■			
Bisacats indeterminats		■			
Monosacats indeterminats		■			

espècies productores, la qual cosa proporciona informació no només anatòmica, sinó també de l'ecologia d'aquests animals.

CALAFAT *et al.* (1986, 1986–1987) i CALAFAT (1988) foren els primers autors que esmentaren fòssils de vertebrats del permià de Mallorca, tant icnites (potades) com restes òssies. CALAFAT *et al.* (1986) distingiren una casta d'icnita pentadàctila de mida grossa, bastant freqüent, unes altres de més petites i amb els dits prims, i un tercer tipus que formava un carrerany de traces mal definides. Els tres tipus eren a la Unitat B. A més, varen esmentar un possible fragment ossi provinent de la base de la Unitat C (il·lustrat aquí a la Fig. 5E). CALAFAT *et al.* (1986–1987) aprofundiren en l'estudi de les icnites, i varen distingir les de 'Tipus A' (equivalents a les del primer tipus de CALAFAT *et al.*, 1986), les de 'Tipus B' (equivalents a les del tercer tipus de CALAFAT *et al.*, 1986), les del 'Tipus Ca', pentadàctiles i de mida petita, i la del 'Tipus Cb', una icnita aïllada, pentadàctila i de mida molt grossa que mai no es va figurar. Totes aquestes icnites provenien de la Unitat B, juntament amb "abundants restes òssies (vèrtebres, etc.)", que no es varen arribar a estudiar mai. CALAFAT (1988) bàsicament reproduí allò que s'havia dit a la publicació anterior, distingint el 'Tipus A', el 'Tipus B', el 'Tipus C' (equivalent al 'Tipus Ca' de CALAFAT *et al.*, 1986–1987) i el 'Tipus D' (equivalent al 'Tipus Cb' de CALAFAT *et al.*, 1986–1987). També va esmentar les vèrtebres i el fragment ossi provinents de la Unitat B i de la base de la Unitat C, respectivament, que havia anomenat en les publicacions anteriors. CALAFAT *et al.* (1986–1987) i CALAFAT (1988) identificaren les icnites del 'Tipus A' (il·lustrades aquí a la Fig. 5D) com a *Cheirotherium* [sic.], típicament triàsic, emperò GAND *et al.* (2010) les redeterminà dins l'icnogènere *Hyloidichnus*, feta per rèptils captorinomorfs, possiblement captorínids moradisaurins, del permià.

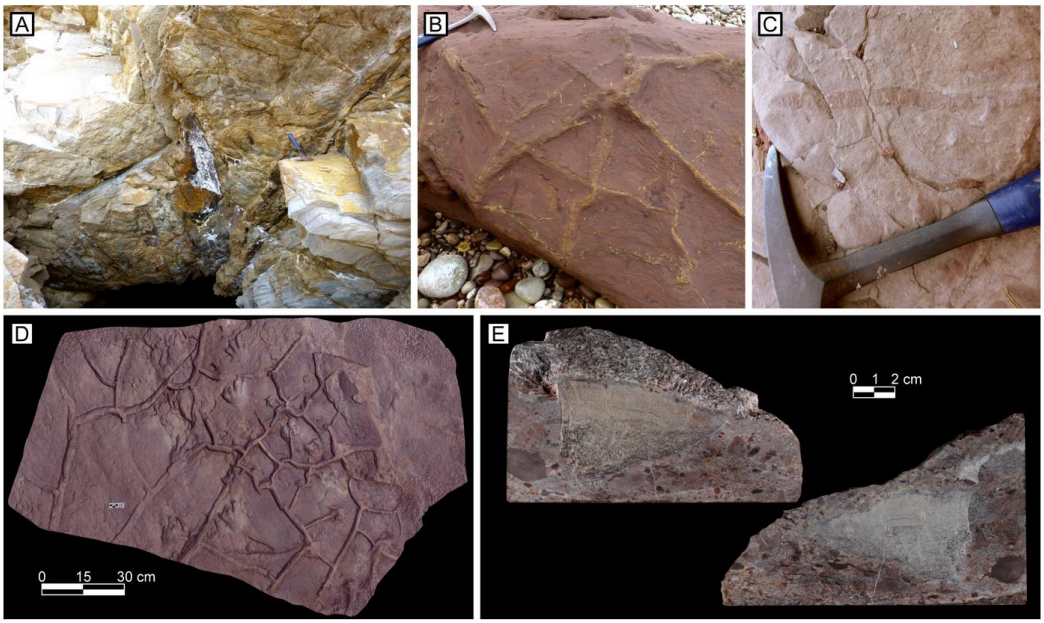

Fig. 5. Exemples de fòssils del permià de Mallorca. **A:** troncs carbonitzats a la base d'un canal orientats segons el paleocorrent, de la cova des Carbó. **B:** rizocrecions, de la platja de son Bunyola. **C:** traces fòssils d'invertebrats, de la pesquera d'en Sabino. **D:** icnites de tetràpodes (UIB174620), del racó de s'Algar. **E:** fragment d'os indeterminable (MBCN21305a i MBCN21305b), del comellar de can Xitx.

Recentment, LIEBRECHT *et al.* (2017) varen descriure un fragment de maxil·la i parts del paladar atribuïble a un rèptil captorínid moradisaurí, que per mida podria correspondre a les potades esmentades anteriorment. El varen datar dins el permià superior basant-se en les datacions de RAMOS i DOUBINGER (1989) per la Unitat C, emperò el fòssil en realitat provenia de la unitat infrajacent, la Unitat B, que en aquell moment encara mai no s'havia datada.

Finalment, MATAMALES-ANDREU *et al.* (2019) varen presentar unes identificacions preliminars de tot el material de potades de tetràpodes del permià de Mallorca, considerant tot allò que havia figurat CALAFAT *et al.* (1986–1987), les fotografies que mai no s'havien publicades i noves troballes als jaciments. De manera provisional, es varen reconèixer els icnogèneres *Dimetropus*, *Hyloidichnus* i, tot i que més dubtosos, *Amphisauropus*, cf. *Ichniotherium*, *Varanopus* i *Dromopus*. Aquests corresponen, respectivament, a sinàpsids esfenacodòntids, rèptils captorinomorfs (possiblement captorínids moradisaurins), possibles seimuriamorfs, diadectomorfs, rèptils captorinomorfs i rèptils areoscelidis (*e.g.*, LUCAS, 2019). MATAMALES-ANDREU *et al.* (2021a) varen estudiar en detall una morfologia identificada com a cf. *Dimetropus* isp., i varen proposar que corresponia a potades fetes per sinàpsids del grup dels caseids.

Plantes del triàsic inferior(?)–mitjà

En el triàsic continental de Mallorca les macrorestes vegetals són més abundants que no a les roques del permià, tot i que també hi solen sortir en forma de bocins indeterminables (Fig. 6A–B). No obstant això, hi ha nivells concrets de les unitats E i F, tant de lutites verdes com de gresos blancs, on les restes vegetals que hi compareixen tenen un estat de conservació bo o molt bo.

Els primers autors que varen esmentar plantes del triàsic mallorquí foren HERMITE (1879, 1888) i LOZANO (1884), a partir d'uns fòssils trobats prop de la cala d'Estellencs, que varen determinar com a *Equisetum arenaceum*. Un segle després, BAUZÁ (1971, 1981) va publicar noves restes paleobotàniques d'aquesta localitat, amb la mateixa identificació que la dels autors anteriors.

CALAFAT (1988) va il·lustrar, per primera vegada, fòssils ben conservats provinents de la Unitat E, que es varen publicar en uns estudis preliminars d'ÁLVAREZ-RAMIS *et al.* (1989, 1995). Aquests autors hi varen reconèixer espècies dels grups de les coes de cavall (*Equisetites mougeotii*, *Equisetites* spp. i *Schizoneura-Echinostachys paradoxa*), les falgueres (*Anomopteris mougeotii*, *Neuropteridium* aff. *intermedium*, *Neuropteridium* sp. i aff. *Pecopteris* sp.), les cícades (restes indeterminades), els ginkgòfits (*Ginkgophyllum* sp.?), les coníferes (*Aetophyllum stipulare*, *Yuccites* cf. *vogesiacus*, *Albertia* sp., *Voltzia heterophylla*, *Voltzia walchiaeformis* i *Endolepis* sp.) i òrgans reproductors de coníferes (*Willsiostrobus hexasacciphorus*, *Willsiostrobus* sp.). Probablement, allò que anomenaren *Equisetites mougeotii* correspon a l'*Equisetum arenaceum* dels autors clàssics, que és una espècie normalment més moderna. A més a més, GRAUVOGEL-STAMM i ÁLVAREZ-RAMIS (1994, 1996) varen dar a conèixer exemplars de *Willsiostrobus rhomboidalis* i *Willsiostrobus hexasacciphorus* (que varen descriure com una espècie nova) amb el pol·len encara *in situ*, corresponent a les espècies de palinomorfs *Voltziaceaesporites heteromorpha* per la primera i *Stellapollenites thiergartii* i *Hexasaccites muelleri* (actualment considerades sinònimes) en el cas de la segona.

JUÁREZ-RUIZ i WACHTLER (2015) és l'estudi més recent d'aquesta associació paleobotànica, on es consideraren tant una part dels exemplars de les col·leccions clàssiques com nous fòssils trobats a les unitats E i F, revisant la majoria d'atribucions taxonòmiques i descrivint nous gèneres i espècies. De coes de cavall n'esmentaren tan sols una espècie, *Equisetites mougeotii*, i de falgueres també una, *Anomopteris mougeotii*, ja conegudes d'aquests jaciments. De "falgueres amb llavor" (pteridospermatòfits) en varen descriure una espècie nova, *Sagenopteris nadalii*, corresponent a allò que ÁLVAREZ-RAMIS *et al.* (1995) havien considerat restes de ginkgòfits. Pel que fa a les coníferes no arborescents, es va reconèixer *Aethophyllum stipulare* (descrita dins la nova *balearica*) amb els seus estròbils masculins anomenats *Willsiostrobus acuminatus*; *Pelourdea vogesiaca*, amb estròbils masculins anomenats *Willsiostrobus rhomboidalis*; i *Estellencsia saezii*, que va esser el nom triat per al nou gènere i espècie de conífera que ÁLVAREZ-RAMIS *et al.* (1995) havien inclòs dins el gènere *Albertia*. Una nova espècie de conífera arborescent va ser *Ortiseia collii*, que corresponia a allò que ÁLVAREZ-RAMIS *et al.* (1995) havien determinat com a diferents espècies del gènere *Voltzia*, que compareixia juntament amb el seu estròbil masculí *Willsiostrobus hexasacciphorus*. Amb aquestes dades, JUÁREZ-RUIZ i WACHTLER (2015) varen distingir dues fitoassociacions principals: una de dominada per *Equisetites*, *Sagenopteris*, *Aethophyllum*, *Pelourdea* i *Ortiseia*, i una altra amb *Anomopteris*, *Pelourdea* i *Estellencsia*, que possiblement representaven dues paleocomunitats diferents, una de més higrofítica i una altra de més xerofítica, respectivament.

La microflora (esporomorfs i palinomorfs) és abundant a una partida de nivells de les unitats E, F i G, i va ser estudiada per primer pic per SOLÉ DE PORTA *in* CALAFAT (1988). No obstant això, posteriorment hi ha hagut diverses publicacions que han revisat les determinacions conegudes i han afegit mostres de nous nivells, com és el cas de RAMOS i DOUBINGER (1989), DIEZ (2000) i DIEZ *et al.* (2005, 2010), que es resumeixen a la Taula 3A–B. A més a més, CALAFAT (1988) va esmentar també la presència de micro-

Fig. 6. Exemples de fòssils del triàsic continental de Mallorca. **A–B:** restes vegetals, de la platja de sa Marina i la tenassa de sa Tanca. **C:** icnita de tetràpode, de la platja de sa Marina.

Taula 3A. Esporomorfs i palinomorfs del triàsic continental de Mallorca esmentats en els diferents estudis. **A1:** mostra "4481" de CALAFAT (1988), **A2:** mostra "4389" de CALAFAT (1988), **B:** RAMOS i DOUBINGER (1989), **C:** GRAUVOGEL-STAMM i ÁLVAREZ-RAMIS (1994, 1996), **D1–D8:** mostres "ME0" a "ME7" de DIEZ (2000), **E1:** mostra "Sa pedra Alta" de DIEZ *et al.* (2005), **E2:** mostra "Punta de son Serralta" de DIEZ *et al.* (2005), **E3:** mostra "Moll d'Estellencs" de DIEZ *et al.* (2005), **E4:** mostra "Mallorca" de DIEZ *et al.* (2005), **F1:** mostra "Mallorca" de DIEZ *et al.* (2010), **F2:** mostra "Sa pedra Alta" de DIEZ *et al.* (2010), **F3:** mostra "Punta de son Serralta" de DIEZ *et al.* (2010), **F4:** mostra "Moll d'Estellencs" de DIEZ *et al.* (2010). Les cel·les omplides de negre indiquen la presència del tàxon a la localitat.

Espècie	A		B	C	D								E				F			
	1	2			1	2	3	4	5	6	7	8	1	2	3	4	1	2	3	4
Aequitriradites sp.			■													■	■			
Alisporites cacheutensis					■										■					■
Alisporites grauvogeli		■	■		■		■	■	■					■	■	■			■	■
Alisporites magnus			■													■	■			
Alisporites opii					■			■	■						■					■
Alisporites toralis			■													■	■			
Alisporites townrovii						■									■					■
Alisporites sp.		■								■				■	■		■		■	■
Angustisulcites cf. *klausii*	■																	■		
Angustisulcites sp.													■		■					■
Baltisphaeridium sp.								■							■					■
Brachysaccus ovalis															■					■
Brachysaccus cf. *ovalis*			■									■					■			
Brachysaccus sp.									■							■				■
Calamospora tener					■		■	■	■	■	■				■					■
Calamospora sp.		■	■					■						■	■	■	■		■	■
Camarozonosporites sp.							■								■					■
Cannanoropollis sp.								■	■						■					■
Chordasporites singulichorda							■				■				■					■
Chordasporites sp.					■					■	■				■					■
Convolutispora sp.								■	■						■					■
Cuneatisporites sp.						■				■					■					■
cf. *Cuneatisporites* sp.									■											
Cycadopites acerrimus		■												■					■	
Cycadopites subgranulosus	■												■					■		
Cycadopites sp.			■				■	■								■				■
Densoisporites sp.									■		■				■					
Dictyotidium reticulatum								■							■					
Endosporites papillatus					■										■					
Falcisporites snopkovae							■								■					■
Falcisporites sp.										■					■					■
cf. *Falcisporites* sp.											■									
Fuldaesporites sp.			■													■	■			
Heliosaccus dimorphus								■							■					■
cf. *Heliosaccus* sp.					■															
Hexasaccites muelleri			■	■	■			■	■	■	■	■	■	■	■	■	■	■	■	■
Illinites kosankei	■							■	■		■		■		■			■		■
Illinites sp.		■					■							■	■				■	■
Klausipollenites sp.											■				■					■
Limitisporites sp.							■								■					■

foraminífers a un nivell amb esporomorfs i palinomorfs de la Unitat G, que mai no varen esser estudiats en detall.

Crustacis, insectes i peixos del triàsic inferior(?)–mitjà

Les unitats E i F presenten esporàdicament nivells d'origen lacunar consistents en lutites molt fines i de colors verdosos i blavosos, indicadores d'un medi reductor. Dins aquestes lutites s'hi troba una fauna de petits animals excepcionalment ben preservats (*Konservat-Lagerstätte* ='jaciment de preservació excepcional'), que conserven restes de les parts blanes i fins i tot el contingut de les butzes.

Taula 3B. Esporomorfs i palinomorfs del triàsic continental de Mallorca esmentats en els diferents estudis (continuació). **A1:** mostra "4481" de CALAFAT (1988), **A2:** mostra "4389" de CALAFAT (1988), **B:** RAMOS i DOUBINGER (1989), **C:** GRAUVOGEL-STAMM i ÁLVAREZ-RAMIS (1994, 1996), **D1–D8:** mostres "ME0" a "ME7" de DIEZ (2000), **E1:** mostra "Sa pedra Alta" de DIEZ *et al.* (2005), **E2:** mostra "Punta de son Serralta" de DIEZ *et al.* (2005), **E3:** mostra "Moll d'Estellencs" de DIEZ *et al.* (2005), **E4:** mostra "Mallorca" de DIEZ *et al.* (2005), **F1:** mostra "Mallorca" de DIEZ *et al.* (2010), **F2:** mostra "Sa pedra Alta" de DIEZ *et al.* (2010), **F3:** mostra "Punta de son Serralta" de DIEZ *et al.* (2010), **F4:** mostra "Moll d'Estellencs" de DIEZ *et al.* (2010). Les cel·les omplides de negre indiquen la presència del tàxon a la localitat.

Espècie	A		B	C	D								E				F			
	1	2			1	2	3	4	5	6	7	8	1	2	3	4	1	2	3	4
Lunatisporites acutus							■								■					■
Lunatisporites noviaulensis							■								■					■
Lunatisporites puntii									■						■					■
Lunatisporites sp.		■								■				■	■				■	■
Maculatasporites indicus						■		■			■				■					■
Microcachryidites sittleri										■					■					■
Microcachryidites sp.											■				■					■
Palaeospongisporis europaeus									■		■				■					■
Paravesicaspora sp.											■				■					■
Platysaccus leschikii							■								■					■
Platysaccus papilionis							■								■					■
Platysaccus cf. *papilionis*							■													■
Platysaccus sp.								■							■					■
Porcellispora longdonensis			■													■	■			
cf. *Porcellispora longdonensis*							■													
Protodiploxypinus sp.															■					
Protohaploxypinus microcorpus					■										■					■
Protohaploxypinus cf. *microcorpus*					■															■
Punctatisporites fungosus							■	■		■					■					■
Punctatisporites triassicus									■	■		■			■					■
Punctatisporites sp.												■			■					■
Retusotriletes sp.								■							■					■
*Stellapollenites thiergartii**		■		■																
cf. *Stellapollenites thiergartii**	■																			
Striatoabieites aytugii		■					■	■						■	■				■	■
Striatopodocarpites cf. *pantii*												■								■
Sulcosaccispora minuta			■													■				■
Triadispora crassa	■	■											■	■				■	■	
Triadispora epigona								■							■					■
Triadispora plicata					■	■		■				■			■					■
Triadispora staplini			■													■	■			
Triadispora suspecta						■					■				■					■
Triadispora sp.	■	■	■							■			■	■	■	■	■	■	■	■
Verrucosisporites remyanus									■											■
Verrucosisporites thuringiacus			■													■	■			
Verrucosisporites sp.							■								■					■
Voltziaceaesporites heteromorpha			■	■		■	■	■	■	■	■	■					■			■
Voltziaceaesporites cf. *heteromorpha*					■	■									■					■
cf. *Voltziaceaesporites heteromorpha*	■															■				
Espores triletes indeterminades	■	■																		
Bialats indeterminats		■																		

*Actualment, *Stellapollenites thiergartii* és considerat sinònim menor d'*Hexasaccites muelleri*.

CALAFAT i SÁEZ (1987) i CALAFAT (1988) varen dur a terme l'estudi preliminar d'aquesta fauna, esmentant la presència molt abundant de crustacis "concostracis" (nom informal d'un grup actualment parafilètic) de mida petita que varen identificar preliminarment dins el gènere *Estheria* (T. SÁEZ, com. pers., 2020). Més esporàdicament també hi compareixien fòssils de nimfes i adults d'insectes, que varen determinar com a escarabats (coleòpters), papallones (lepidòpters), moscards d'aigua (efemeròpters) i altres formes no identificades (CALAFAT, 1988). No obstant això, SHCHERBAKOV *et al.* (1995) varen considerar que un dels exemplars no identificats podria ser un mosquit (díptera), PEÑALVER *et al.* (1999) suggeriren que el possible lepidòpter podria ser un efemeròpter adult, i SINITSHENKOVA (2000) va dir

que hi havia al manco dues espècies de nimfes d'efemeròpters, i que una d'elles feia llorigueres. A més dels artròpodes, CALAFAT i SÁEZ (1987) i CALAFAT (1988) també varen esmentar la presència d'un peix molt menut, que es va identificar preliminarment dins el grup dels paleoniscoides (T. SÁEZ, com. pers., 2020). GALLEMÍ *in* GALLEMÍ *et al.* (1988), MARTÍNEZ *in* GALLEMÍ *et al.* (1988) i JUÁREZ-RUIZ i WACHTLER (2015) varen refigurar qualcuns d'aquests espècimens, emperò sense aportar-ne informació nova.

Els nivells fossilífers foren remostrejats per ANSORGE (1997), qui va esmentar la presència de tres ales de cuques molles (blataris), que mai no va estudiar en detall ni figurar. Una dècada després, ZESSIN (2008a, 2008b) hi va agafar més fòssils, entre els que, preliminarment, hi va identificar crustacis "concostracis" (*Euestheria*), insectes dels grups de les cuques molles (blataris), escarabats (coleòpters), mosquits (dípters), xinxes (hemípters), cigales (homòpters), (?)megalòpters i (?)ortopteroïdeus, traces fòssils indeterminades d'insectes i càpsules d'ous de taurons hibodòntids d'aigua dolça (*Palaeoxyris*). Dels mateixos nivells, ARISTOV i ZESSIN (2009) també varen descriure una espècie nova d'insecte gril·loblàtid: *Mallorcagryllus hispanicus*. Recentment, SCHOLZE i MATAMALES-ANDREU (2021) esmentaren una partida de morfotips de valves de "concostracis" provinents de quatre nivells diferents: *Hornestheria* aff. *sollingensis* (que corresponia a allò que els autors anteriors havien anomenat *Estheria* o *Euestheria*) dels nivells de la Unitat E amb insectes (CALAFAT, 1988); *Hornestheria*? morfotip 1 i *Hornestheria*? morfotip 2 d'un mateix nivell al sostre de la Unitat F; i dos morfotips indeterminats provinents de la part mitjana de la Unitat E i de la base de la Unitat F, respectivament. Aquests darrers també podrien esser *Hornestheria* aff. *sollingensis* perquè s'hi avenen per mida i forma general, emperò estan massa mal conservats per poder-ho saber cert.

"Rèptils" del triàsic inferior(?)–mitjà

Els ambients de plana d'inundació de la Unitat E oferien unes condicions òptimes per la preservació de les icnites (potades) de rèptils. A diferència de la Unitat B del permià, però, aquí les icnites compareixen enmig dels nivells de gres, conservant tant la impressió original com el seu motlle natural (Fig. 6C).

L'únic estudi que ha figurat aquestes icnites ha estat JUÁREZ-RUIZ i WACHTLER (2015), il·lustrant una parella de mà i peu atribuïble a l'icnogènere *Rhynchosauroides*. El productor d'aquesta casta de traces era un petit rèptil diàpsid (*e.g.*, AVANZINI i RENESTO, 2002). Les altres icnites que surten retratades, suposadament pertanyents a l'icnogènere *Rodotactylus*, no ho són, per mor que provenen de la Unitat B (T. SÁEZ, com. pers., 2020) i corresponen a l'icnogènere *Dimetropus* esmentat per MATAMALES-ANDREU *et al.* (2019, 2021a) per al permià.

CALAFAT *et al.* (1986, 1986–1987) trobaren unes suposades icnites de la Unitat F, que anomenaren 'Tipus D'. CALAFAT (1988) en torna a parlar, anomenant-les 'Tipus E' i figurant-les per primera vegada, descrivint-les com a una partida de clots circulars d'un diàmetre molt gros (30–40 cm) que no formaven cap carrerany clar. Després d'haver-les examinades en directe (R.M.A., obs. pers., 2019), s'ha pogut concloure que són qualque casta d'estructura sedimentària, que també és present a les unitats del permià, per mor que tenen una mida molt més grossa que cap altra icnita coetània coneguda, no s'organitzen en cap patró (rastre) i no s'hi reconeix cap estructura anatòmica (dits, call/sola, etc.).

Datacions i edats

Permià

El primer estudi que va demostrar inqüestionablement la presència de roques d'edat permiana a Mallorca va ser el de RAMOS i DOUBINGER (1989), que varen analitzar els esporomorfs i palinomorfs de dues mostres de la Unitat C (Taula 2), emperò de posició exacta desconeguda. Varen considerar que la majoria d'espècies eren característiques de les palinoassociacions del "turingià" dels Alps i del Nord d'Europa, que en aquell temps se'ls atribuïa una edat de permià superior (lopingià) (Taula 4). Aquesta

Taula 4. Datacions de les diferents unitats del permià i triàsic continental de Mallorca.

Posició estratigràfica	PERMIÀ			TRIÀSIC			
	Part alta Unitat B	Part mitjana/alta Unitat C (?)	Part alta Unitat C	Part alta Unitat E	Base Unitat F	Part baixa Unitat G (?)	Part mitjana Unitat G
Fòssils índex	Icnites de tetràpodes	Esporomorfs i palinomorfs	Esporomorfs i palinomorfs	Esporomorfs i palinomorfs	Esporomorfs i palinomorfs	Esporomorfs i palinomorfs	Esporomorfs i palinomorfs
CALAFAT (1988)				Anisià			Anisià
RAMOS & DOUBINGER (1989)		"Turingià"*				Anisià mitjà–superior**	
GRAUVOGEL-STAMM & ÁLVAREZ-RAMIS (1996)				Anisià (anisià inferior**?)			
DIEZ (2000)		"Turingià"*	"Turingià"*	Egeà–pelsonià	Egeà (egeà superior?)	Egeà–pelsonià	Egeà–pelsonià
DIEZ *et al.* (2005)		"Turingià"*	"Turingià"*	Anisià	Egeà	Egeà–pelsonià	Anisià
DIEZ *et al.* (2010)				Anisià inferior**	Egeà	Egeà–pelsonià	Anisià
JUNCAL (2019)			Guadalupià (wordià–capitanià)				
MATAMALES-ANDREU *et al.* (2019)	Cisuralià (artinskià–kungurià)						

*El "turingià" és una palinoassociació (biofàcies) sense gaire valor cronostratigràfic que es creu que pot variar d'edat entre el permià mitjà (guadalupià) i el permià superior (lopingià) (JUNCAL 2019).
**L'anisià inferior correspon al subestatge egeà, el mitjà correspon al bitinià i pelsonià i el superior correspon a l'il·lirià (vegeu OGG *et al.*, 2020).

palinoassociació va ser revisada per DIEZ (2000) i DIEZ *et al.* (2005), que varen estar d'acord en el fet que pertanyia al "turingià", i aquest al permià superior.

DIEZ (2000) va estudiar una altra mostra paleopalinològica (MA-1) agafada de la part alta de la Unitat C, molt més rica que l'anterior (Taula 2), però que també era clarament atribuïble al "turingià" (Taula 4), que va considerar com a permià superior. DIEZ *et al.* (2005) varen tornar a revisar aquesta mostra, confirmant l'assignació anterior i, baldament encara afirmaven que el "turingià" equivalia al permià superior, admeteren que la correlació entre conques diferents és impossible de fer, i que podria ser una biofàcies diacrònica. JUNCAL (2019) tornà a estudiar la mostra MA-1 de DIEZ (2000) i afirmà que pertany al permià mitjà (guadalupià), amb afinitat al wordià–capitanià, per mor de la presència de les espècies *Crucisaccites variosulcatus* i *Potonieisporites novicus* i l'absència de *Vittatina costabilis*. Per tant, per primer pic es datà aquesta palinoassociació del "turingià" fora del permià superior.

D'altra banda, MATAMALES-ANDREU *et al.* (2019) varen presentar una comunicació preliminar on s'estudiaven les icnites (potades) de vertebrats de la Unitat B, reconeixent-hi diferents icnogèneres. Aquesta icnoassociació va permetre proposar, per primera vegada, una datació de permià inferior (cisuralià) per aquesta unitat causa la presència de l'icnogènere *Dimetropus*, i concretament es podria correspondre a l'artinskià o al kungurià per mor de l'abundància d'icnites de rèptils (*Hyloidichnus*) i l'absència d'icnites d'anamniotes.

Triàsic

SOLÉ DE PORTA *in* CALAFAT (1988) va donar les primeres determinacions d'esporomorfs i palinomorfs de les unitats E i G (Taula 3A–B), i en els dos casos va afirmar que pertanyien al triàsic mitjà (anisià) (Taula 4). Tot seguit, RAMOS i DOUBINGER (1989) varen estudiar la palinoassociació d'un altre nivell, possiblement de la part baixa de la Unitat G (la posició exacta és desconeguda i fins i tot podria esser de la Unitat F) (Taula 3A–B), i hi varen determinar formes característicament anisianes,

concretament de l'anisià mitjà–superior o fins i tot del ladinià inferior (triàsic mitjà) (Taula 4). GRAUVOGEL-STAMM i ÁLVAREZ-RAMIS (1994, 1996), en el seu estudi dels grans de pol·len de dins els estròbils de conífera de la Unitat E, varen argumentar que l'associació de Mallorca es podia comparar amb la del *Grès à Voltzia* (='gres amb *Voltzia*') dels Vosges (França), proposant una datació d'anisià inferior per als jaciments mallorquins.

DIEZ (2000) va agafar vuit mostres noves de la base de la Unitat F (Taula 3A–B) i les va considerar conjuntament per afirmar que, per superposició de biozones de les diferents espècies d'esporomorfs i palinomorfs, aquells nivells eren de l'egeà (anisià inferior). A més a més, va afegir que la presència de *Triadispora suspecta*, que normalment sol comparèixer a partir del pelsonià (anisià mitjà), podria indicar que les mostres estudiades per ventura eren de la part alta de l'egeà (Taula 4). DIEZ *et al.* (2005) revisaren tots els estudis anteriors, i assignaren les mostres de CALAFAT (1988) a un anisià indeterminat, la de RAMOS i DOUBINGER (1989) a un egeà–pelsonià (anisià inferior–mitjà) i les de DIEZ (2000) a l'egeà (Taula 4). Finalment, DIEZ *et al.* (2010) tornaren a revisar-les totes, i en el cas de les de CALAFAT (1988) mantengueren la datació d'anisià indeterminat per la mostra de la Unitat G, mentre que la de la Unitat E la pogueren datar temptativament com a anisià inferior (=egeà) per mor de la presència d'*Illinites kosankei* (Taula 4). En el cas de la mostra de RAMOS i DOUBINGER (1989), es mantengué l'assignació d'egeà–pelsonià, i es confirmà la datació d'egeà per les mostres de DIEZ (2000) (Taula 4).

Discussió, síntesi i perspectives futures

Les roques del permià i del triàsic continental de Mallorca es poden dividir en set unitats litostratigràfiques principals, que aquí s'han anomenat amb lletres consecutives de la A a la G (Figs. 3–4). Cadascuna d'aquestes té uns trets sedimentològics propis, que permeten inferir-ne el paleoambient deposicional on es varen formar. Aquest, juntament amb la informació que es pot extreure de les restes fòssils, fa possible reconstruir l'ecosistema i, en segons quins casos, proporciona informació de la seva edat.

La Unitat A (Fig. 3A–B) consisteix en gresos i conglomerats extraformacionals disposats en làmines irregulars o en unitats amb acreció lateral que corresponen als primers estadis de rebliment de la conca amb sistemes predominantment al·luvials/col·luvials. Just s'hi han trobat fòssils de rels de mida grossa, que indiquen que s'hi varen formar sòls. No se sap l'edat d'aquesta unitat, però possiblement es trobi entre el carbonífer superior i la part baixa del permià inferior, que és quan moltes de conques del peri-Tetis es varen començar a obrir (*e.g.*, McCANN *et al.*, 2006).

La Unitat B (Fig. 3C–D) és formada per intervals de gresos amb superfícies d'acreció lateral i lutites amb intercalacions de gresos tabulars, i es pot interpretar com a dipòsits de grans rius d'alta sinuositat (meandriformes) que solcaven una plana d'inundació periòdicament negada. Per devora els rius hi creixien plantes de manera abundant, que han quedat enregistrades en forma de paleosòls i restes de rels (rizocrecions) carbonatats, el que indica un clima àrid. Entremig d'aquesta vegetació hi havia una important comunitat de vertebrats, que es coneixen tant pel seu abundant registre icnològic (potades) com per qualque os. En destaquen els rèptils captorínids moradisaurins, dels que se n'han trobat tant les potades com els ossos. Els seus depredadors possiblement eren del grup dels sinàpsids (avantpassats dels mamífers), dels que també se n'hi han trobat potades. L'estudi biostratigràfic de les potades ha permès de proposar preliminarment que aquesta unitat és de la part alta del permià inferior.

La Unitat C (Fig. 3E–F) és representada per paquets potents de gresos de colors clars, organitzats internament en unitats d'acreció lateral amb capes tabulars intercalades. Entremig dels gresos, adesiara hi compareixen intervals predominantment lutítics. Aquesta associació de fàcies correspon a grans rius sinuosos (meandriformes) amb una remobilització constant de les planes d'inundació, que durant les estacions més plogueres quedaven tapats per dipòsits tabulars (desconfinats) d'arena arrossegada per torrentades. Devora aquests rius hi creixia una vegetació de coes de cavall, falgueres i coníferes, reconegudes a partir de les seves espores, pol·len, troncs fòssils i restes de carbó. També hi havia

vertebrats, dels que se n'ha trobat un bocí d'os. L'estudi dels esporomorfs i dels palinomorfs de la part alta de la unitat ha revelat una edat dins la part superior del permià mitjà.

La Unitat D (Fig. 4A–B) es caracteritza pels nivells de gresos tabulars amb molt pocs intervals lutítics, que representen els dipòsits de grans rius entrunyellats. No s'hi coneix registre fòssil, i per això no s'ha pogut datar. Per correlació amb altres unitats litostratigràfiques de la península Ibèrica més o manco equivalents, podria pertànyer a la part alta del triàsic inferior.

La Unitat E (Fig. 4C–D) té nivells de gres amb acreció lateral o de forma tabular, intercalats amb paquets de lutites, que corresponen a rius amb canals sinuosos, lòbuls de desbordament i planes d'inundació. Aquesta unitat és la que presenta un registre fòssil més divers, amb una comunitat de plantes de ribera amb coes de cavall, falgueres, coníferes no arborescents i qualque conífera arborescent. Dins l'aigua hi vivien crustacis del grup parafilètic dels "concostracis", larves d'insectes i peixos, i per la vorera dels rius hi havia insectes de diferents grups i petits rèptils diàpsids que hi varen deixar impreses les seves potades. Un poc més enfora, es desenvolupaven brolles de coníferes i falgueres. De les plantes d'aquesta unitat també se n'han trobat les espores i el pol·len, que han permès datar-la dins la base del triàsic mitjà.

La Unitat F (Fig. 4E–F) consisteix en gresos organitzats en estrats tabulars o lenticulars, amb molt poques lutites intercalades. Representa els dipòsits de grans rius entrunyellats i els bassiots dins els canals abandonats. La comunitat biològica s'assemblava a la de la unitat infrajacent, amb diverses castes de plantes, crustacis, insectes i peixos. L'estudi de les espores i del pol·len ha revelat una edat dins la base del triàsic mitjà.

La Unitat G (Fig. 4G–H), la més superior de totes, és formada per lutites amb qualque intercalació de gres. En general, correspon a planes mareals fangoses i mixtes, que la mar negava periòdicament, fins que al sostre donen pas a les rampes carbonatades marines poc fondes de la fàcies *Muschelkalk* (='calcària amb copinyes'). Dins nivells lutítics d'aquesta unitat s'hi han trobat foraminífers marins, i esporomorfs i palinomorfs que han permès datar-la com a triàsic mitjà indeterminat.

En resum, la seqüència del permià i triàsic continental de Mallorca conté un grup inferior de tres unitats fluvio-al·luvials del permià i un grup superior de quatre unitats fluvio-al·luvials del triàsic inferior(?) i mitjà, probablement separades per un hiatus que comprèn part del permià superior i del

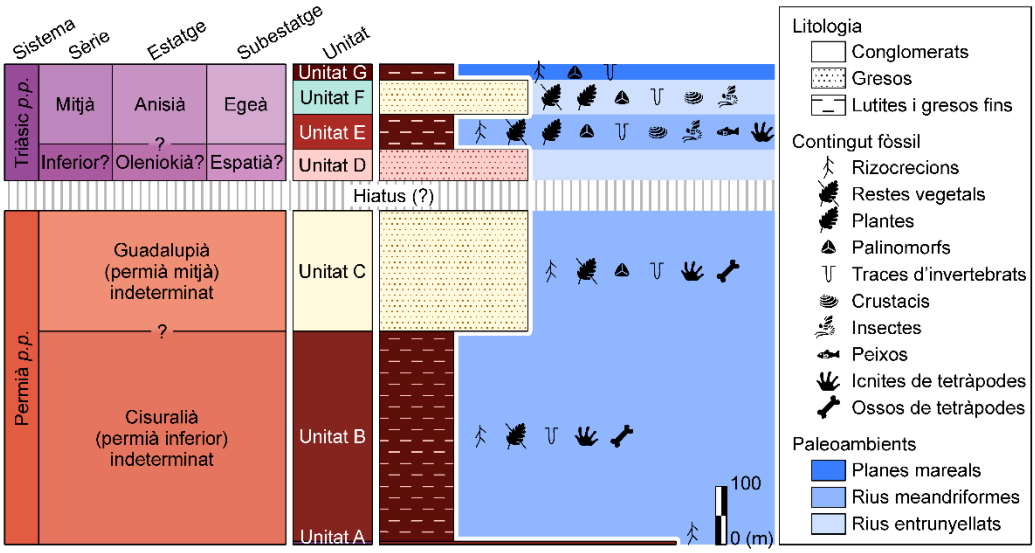

Figura 7. Columna estratigràfica sintètica del permià i el triàsic inferior(?)–mitjà continental de Mallorca, simplificada i modificada de GÓMEZ-GRAS (1993) amb dades de paleontologia de CALAFAT (1988), DIEZ (2000), ZESSIN (2008b) i JUÁREZ-RUIZ i WACHTLER (2015).

triàsic inferior (Fig. 7), com a la resta del peri-Tetis occidental (*e.g.*, BOURQUIN *et al.*, 2011). El seu registre fòssil és molt ric, consistint en esporomorfs, palinomorfs, restes vegetals, potades i ossos de vertebrats en el permià, i esporomorfs, palinomorfs, plantes, artròpodes i potades de vertebrats en el triàsic (Fig. 7). Aquesta gran diversitat fa que els jaciments de Mallorca siguin dels més rics de tota la zona paleoequatorial de Pangea, essent de gran rellevància en l'àmbit mundial.

En els darrers anys, la feina per a la tesi doctoral d'un dels autors del present article (R.M.A.) ha permès revisar tota l'estratigrafia i la sedimentologia d'aquests períodes. També s'han trobat nous jaciments fossilífers, que s'han pogut prospectar i excavar en una partida de campanyes de camp, obtenint una gran quantitat de material fòssil que ara es troba en estudi. Amb tot això, es preveu que en els anys que vénen es podrà donar a conèixer una visió molt més completa dels ecosistemes del permià i triàsic de Mallorca, des del refinament de la caracterització geològica, fins a datacions més precises i noves dades sobre la flora i fauna que hi capllevava (MATAMALES-ANDREU *et al.*, 2021a, 2021b, 2021c, en preparació).

Agraïments

Els autors del present article agraïm l'ajuda de Sebastià Matamalas, Àngel Galobart, Josep Juárez Antoni Pasqual i Francesc Baiget en la feina de camp. A Antonio Rodríguez-Perea, Feliu Calafat, David Gómez-Gras i Tomeu Sáez per proporcionar-nos bibliografia i entresenyes de qualque localitat. A Eudald Mujal per la discussió de l'estratigrafia, sedimentologia i icnologia. A Carol Constantino per l'accés als fòssils de les col·leccions del Museu Balear de Ciències Naturals. A Lluís Gómez-Pujol, editor, i a dos revisors anònims pels comentaris sobre el manuscrit. Al Consell de Mallorca pels permisos de prospecció i excavació. Agraïm també el suport del programa CERCA (Generalitat de Catalunya). R.M.A. compta amb el contracte predoctoral FPU17/01922 (Ministerio de Ciencia, Innovación y Universidades). O.O. és membre del grup de recerca consolidat 2017 SGR 1666 GRC (Generalitat de Catalunya). J.F. és membre del grup de recerca consolidat 2017 SGR 086 GRC (Generalitat de Catalunya) i també reconeix el suport de l'Agencia Estatal de Investigación i l'European Regional Development Fund AEI/FEDER EU, projecte CGL2017-82654-P (Unió Europea). Aquest estudi s'emmarca en el projecte "Mallorca abans dels dinosaures: estudi dels ecosistemes continentals del Permià i Triàsic amb especial èmfasi en les restes de vertebrats" (ref. 15 - 619/2020), amb base a l'ICP i finançat pel Departament de Cultura, Patrimoni i Política Lingüística (Consell Insular de Mallorca).

Bibliografia

ÁLVAREZ-RAMIS, C., SOLÉ, N. i CALAFAT, F. (1989): Paleoflora del Triásico inferior de Mallorca. In: *Abstracts of the II European Paleobotanical Conference*: p. 12. Madrid.

ÁLVAREZ-RAMIS, C., FERNÁNDEZ-MARRÓN, T. i CALAFAT, F. (1995): Avance sobre la megaflora triásica, en facies germánica, de Estellencs (sector noroccidental de la sierra de Tramontana, Mallorca). *Revista Española de Paleontología*, nº homenaje al Dr. Guillermo Colom: 55-58.

ANSORGE, J. (1997): Insekten aus dem Buntsandstein (Untere Trias) von Mallorca (Spanien). In: *Abstracts für 4. Fachgespräch, "Fossile Insekten"*: 1 pp. Clausthal-Zellerfeld.

ARCHE, A., LÓPEZ-GÓMEZ, J. i VARGAS, H. (2002): Propuesta de correlación entre los sedimentos Pérmicos y Triásicos de la Cordillera Ibérica Este y de las Islas Baleares. *Geogaceta*, 32: 275-278.

ARISTOV, D. i ZESSIN, W. (2009): *Mallorcagryllus hispanicus* n. get. et sp. - eine neue Grylloblattide (Insecta: Grylloblattida: Blattogryllidae) aus dem Buntsadstein der Insel Mallorca, Spanien. *Virgo, Mitteilungsblatt des Entomologischen Vereins Mecklenburg*, 12(1): 30-34.

AVANZINI, M. i RENESTO, S. (2002): A review of *Rhynchosauroides tirolicus* Abel, 1926 ichnospecies (Middle Triassic: Anisian-Ladinian) and some inference on *Rhynchosauroides* trackmaker. *Rivista Italiana di Paleontologia e Stratigrafia*, 108(1): 51-66.

BANDA, E., PARÉS, J.M. i FREEMAN, R. (1986): La técnica del paleomagnetismo. Estudio piloto en los bordes de la cuenca balear. *Estudios Geológicos*, 42: 147-165.

BARNOLAS, A. (1991a): *Mapa Geológico de España. Escala 1:50.000. Andraitx*. Segona sèrie, primera edició. Instituto Tecnológico GeoMinero de España, Madrid. 56 pp. + 1 mapa + 5 columnes estratigràfiques.

BARNOLAS, A. (1991b): *Mapa Geológico de España. Escala 1:50.000. Sóller.* Segona sèrie, primera edició. Instituto Tecnológico GeoMinero de España, Madrid. 62 pp. + 1 mapa + 8 columnes estratigràfiques.

BAUZÁ, J. (1971): Ciento ochenta millones de años de la flora y fauna de Mallorca. In: MASCARÓ, J. (coord.), *Historia de Mallorca*: 331-430. Gráficas Miralles, Palma.

BAUZÁ, J. (1981): Contribuciones a la paleontología de Mallorca. *Bolletí de la Societat d'Història Natural de Balears*, 25: 7-20.

BEHRENSMEYER, A.K. (1982): Time resolution in fluvial vertebrate assemblages. *Paleobiology*, 8(3): 211-227.

BENTON, M.J. (2008): *When life nearly died. The greatest mass extinction of all time*. Thames & Hudson, Londres. 336 pp.

BERCOVICI, A., DIEZ, J.B., BROUTIN, J., BOURQUIN, S., LINOL, B., VILLANUEVA-AMADOZ, U., LÓPEZ-GÓMEZ, J. i DURAND, M. (2009): A palaeoenvirnomental analysis of Permian sediments in Minorca (Balearic Islands, Spain) with new palynological and megafloral data. *Review of Palaeobotany and Palynology*, 158: 14-28.

BORRUEL-ABADÍA, V., LÓPEZ-GÓMEZ, J., DE LA HORRA, R., GALÁN-ABELLÁN, B., BARRENECHEA, J.F., ARCHE, A., RONCHI, A., GRETTER, N. i MARZO, M. (2015): Climate changes during the Early–Middle Triassic transition in the E. Iberian plate and their palaeogeographic significance in the western Tethys continental domain. *Palaeogeography, Palaeoclimatology, Palaeoecology*, 440: 671-689.

BOURQUIN, S., DURAND, M., DIEZ, J.B., BROUTIN, J. i FLUTEAU, F. (2007): The Permian-Triassic boundary and Early Triassic sedimentation in Western European Basins: an overview. *Journal of Iberian Geology*, 33(2): 221-236.

BOURQUIN, S., BERCOVICI, A., LÓPEZ-GÓMEZ, J., DIEZ, J.B., BROUTIN, J., RONCHI, A., DURAND, M., ARCHE, A., LINOL, B. i AMOUR, F. (2011): The Permian–Triassic transition and the onset of Mesozoic sedimentation at the northwestern peri-Tethyan domain scale: Palaeogeographic maps and geodynamic implications. *Palaeogeography, Palaeoclimatology, Palaeoecology*, 299: 265-280.

CALAFAT, F. (1986): Estratigrafía y sedimentología de la litofacies Buntsandstein de Mallorca. In: CABRERA, L. (ed.), *Libro de Resúmenes del XI Congreso Español de Sedimentología*: p. 39. Grupo Español de Sedimentología, Barcelona.

CALAFAT, F. (1987): Paleoambients de les facies Buntsandstein de Mallorca. In: *Llibre de Resums de les I Jornades del Medi Ambient de les Illes Balears*: 16-17. Societat d'Història Natural de les Balears, Palma.

CALAFAT, F. (1988): *Estratigrafía y sedimentología de la litofacies Buntsandstein de Mallorca*. Tesina de Llicenciatura. Universitat de Barcelona, Barcelona. 127 pp. + 31 columnes estratigràfiques annexes. Inèdita.

CALAFAT, F. i SÁEZ, B. (1987): Paleofauna lacustre del Triàsic Inferior de Mallorca. In: *Llibre de Resums de les I Jornades del Medi Ambient de les Illes Balears*: 18-19. Societat d'Història Natural de les Balears, Palma.

CALAFAT, F., FORNÓS, J.J., MARZO, M., RAMOS, E. i RODRÍGUEZ-PEREA, A. (1986): Icnología de vertebrados de las facies Buntsandstein de Mallorca. *Libro de Resúmenes del XI Congreso Español de Sedimentología*: p. 40. Grupo Español de Sedimentología, Barcelona.

CALAFAT, F., FORNÓS, J.J., MARZO, M., RAMOS-GUERRERO, E. i RODRÍGUEZ-PEREA, A. (1986–1987): Icnología de vertebrados de las facies Buntsandstein de Mallorca. *Acta Geològica Hispànica*, 21-22: 515-520.

CARMONA, R. (2004): *Estudi d'un seimuriamorfe (Amphibia: Batrachosauria) del Permià superior de Menorca*. Tesina de Llicenciatura. Universitat de Barcelona, Barcelona. 56 pp. Inèdita.

CASSINIS, G., PEROTTI, C.R. i RONCHI, A. (2012): Permian continental basins in the Southern Alps (Italy) and peri-mediterranean correlations. *International Journal of Earth Sciences/GR Geologische Rundschau*, 101: 129-157.

COHEN, K.M., FINNEY, S.C., GIBBARD, P.L. & FAN, J.-X. (2013; actualitzada): The ICS International Chronostratigraphic Chart. *Episodes*, 36: 199-204.

COLOM, G. (1975): *Geología de Mallorca*. Gráficas Miramar, Diputación Provincial de Baleares, Palma. 2 vols., 552 pp.

CUEVAS-LÓPEZ, F. (1958a): *Informe geológico y minero de los yacimientos de cobre de Banyalbufar y Estallenchs, Mallorca*. Barcelona. 37 pp. + 8 figs. Inèdit.

CUEVAS-LÓPEZ, F. (1958b): *Informe geológico y minero de los yacimientos de cobre de Banyalbufar y Valldemosa, Mallorca*. Barcelona. 23 pp. + 7 figs. Inèdit.

DARDER, B. (1914): El Triásico de Mallorca. *Trabajos del Museo Nacional de Ciencias Naturales, Serie Geológica*, 7: 85 pp. + 1 mapa + 1 taula.

DIEZ, J.B. (2000): *Geología y Paleobotánica de la Facies Buntsandstein en la Rama Aragonesa de la Cordillera Ibérica. Implicaciones paleogeográficas en el Peritethys Occidental*. Tesi doctoral. Universidad de Zaragoza–Université Pierre & Marie Curie, Paris VI, Saragossa i París. 424 pp.

DIEZ, J.B., BROUTIN, J. i FERRER, J. (2005): Difficulties encountered in defining the Permian–Triassic boundary in Buntsandstein facies of the western Peritethyan domain based on palynological data. *Palaeogeography, Palaeoclimatology, Palaeoecology*, 229: 40-53.

DIEZ, J.B., BROUTIN, J., GRAUVOGEL-STAMM, L., BOURQUIN, S., BERCOVICI, A. i FERRER, J. (2010): Anisian floras from the NE Iberian Peninsula and Balearic Islands: A synthesis. *Review of Palaeobotany and Palynology*, 162: 522-542.

FALLOT, P. (1922): *Étude Géologique de la Sierra de Majorque*. Librairie Polytechnique Ch. Béranger, París i Lieja. 16 pp. + 8 làms. + 476 pp. + 9 làms.

FREEMAN, T. i OBRADOR, A. (1974): Paleosuelos y carbón en la zona distal del Buntsandstein español (Menorca, Mallorca, Islas Baleares). In: *Resúmenes del VII Congreso del Grupo Español de Sedimentología*: p. 56. Grupo Español de sedimentología, Bellaterra-Tremp.

FREEMAN, T. i OBRADOR, A. (1979): Paleosoils and coal in the distal part of the Spanish Buntsandstein (Menorca and Mallorca, Balearic Islands). *Boletín de la Sociedad de Historia Natural de Baleares*, 23: 47-50.

GALLEMÍ, J., RIBA, O., REGUANT, S., AGUSTÍ, J., ÁLVAREZ, G., CALZADA, S., CAUS, M., LÓPEZ, C., MARTINELL, J., MARTÍNEZ, R., MARTÍNEZ, X., PORTA, J. de; SANZ DE SIRIA, A., SOLÉ, N., TRUYOLS, J., TRUYOLS, M. i VIA, Ll. (eds.) (1988): *Història Natural dels Països Catalans, 15: Registre Fòssil.* Enciclopèdia Catalana, Barcelona. 478 pp.

GAND, G., DE LA HORRA, R., GALÁN-ABELLÁN, B., LÓPEZ-GÓMEZ, J., BARRENECHEA, J.F., ARCHE, A. i BENITO, M.I. (2010): New ichnites from the Middle Triassic of the Iberian Ranges (Spain): paleoenvironmental and paleogeographical implications. *Historical Biology*, 22(1-3): 40-56.

GÓMEZ-GRAS, D.M. (1987): *Estratigrafía física y petrología sedimentaria del Pérmico y Buntsandstein de la isla de Menorca*. Tesina de Llicenciatura. Universitat Autònoma de Barcelona, Barcelona. XIV + 117 pp. Inèdita.

GÓMEZ-GRAS, D.M. (1992): *El Permotrías de las Baleares, de la Cordillera Costero Catalana y de la vertiente mediterránea de la Cordillera Ibérica: Facies y Petrología Sedimentaria*. Tesi doctoral. Universitat Autònoma de Barcelona, Barcelona. XIX + 242 pp. + 55 figs. + 7 taules.

GÓMEZ-GRAS, D. (1993): El Permotrías de las Baleares y de la vertiente mediterránea de la Cordillera Ibérica y del Maestrat: Facies y Petrología Sedimentaria (Parte II). *Boletín Geológico y Minero*, 104: 467-515.

GRAUVOGEL-STAMM, L. i ÁLVAREZ-RAMIS, C. (1994): Macroflore et microflore in situ du Buntsandstein de l'île de Majorque (Baléares, Espagne). In: *Resúmenes del III Coloquio de Estratigrafía y Paleogeografía del Pérmico y Triásico de España:* 51-53. Consejo Superior de Investigaciones Científicas, Universidad Complutense de Madrid, Madrid.

GRAUVOGEL-STAMM, L. i ÁLVAREZ-RAMIS, C. (1996): Conifères et pollen in situ du Buntsandstein de l'île de Majorque (Baléares, Espagne). *Cuadernos de Geología Ibérica*, 20: 229-243.

HENDERSON, C.M., SHEN, S.Z., GRADSTEIN, F.M. i AGTERBERG, F.P. (2020): *Chapter 24 - The Permian Period*. In: GRADSTEIN, F.M., OGG, J.G., SCHMITZ, M.D. i OGG, G.M. (eds.), *Geologic Time Scale 2020*: 875-902. Elsevier.

HERMITE, H. (1879): *Études géologiques sur les îles Baléares. Première partie: Majorque et Minorque*. Pichon et Savy, París. 362 pp. + 5 làms.

HERMITE, H. (1888): Estudios Geológicos de las Islas Baleares. *Boletín de la Comisión del Mapa Geológico*, 15: 1-244 + 4 làms.

JUÁREZ-RUIZ, J. i WACHTLER, M. (2015): Early–middle Triassic (Anisian) fossil flora from Majorca (Spain). *Dolomythos*, 2015: 1-49.

JUNCAL, M. (2019): *Nuevas aportaciones a la palinoestratigrafía pérmica del dominio peritético occidental*. Tesi doctoral. Universidade de Vigo, Vigo. 361 pp. Inèdita.

LIEBRECHT, T., FORTUNY, J., GALOBART, A., MÜLLER, J. i SANDER, P.M. (2017): A large, multiple-tooth-rowed captorhinid reptile (Amniota: Eureptilia) from the Upper Permian of Mallorca (Balearic Islands, Western Mediterranean). *Journal of Vertebrate Paleontology*, 37(1): e1251936, 1-6.

LINOL, B., BERCOVICI, A., BOURQUIN, S., DIEZ, J.B., LÓPEZ-GÓMEZ, J., BROUTIN, J., DURAND, M. i VILLANUEVA-AMADOZ, U. (2009): Late Permian to Middle Triassic correlations and palaeogeographical reconstructions in south-western European basins: New sedimentological data from Minorca (Balearic Islands, Spain). *Sedimentary Geology*, 220: 77-94.

LÓPEZ-GÓMEZ, J., ARCHE, A. i PÉREZ-LÓPEZ, A. (2002): Permian and Triassic. In: GIBBONS, W. & MORENO, M.T. (eds.), *The Geology of Spain*: 185-212. Geological Society, Londres.

LÓPEZ-GÓMEZ, J., ALONSO-AZCÁRATE, J., ARCHE, A., ARRIBAS, J., FERNÁNDEZ-BARRENECHEA, J., BORRUEL-ABADÍA, V., BOURQUIN, S., CADENAS, P., CUEVAS, J., DE LA HORRA, R., DIEZ, J.B., ESCUDERO-MOZO, M.J., FERNÁNDEZ-VIEJO, G., GALÁN-ABELLÁN, B., GALÉ, C., GASPAR-ESCRIBANO, J., GISBERT-AGUILAR, J., GÓMEZ-GRAS, D., GOY, A., GRETTER, N., HEREDIA-CARBALLO, N., LAGO, M., LLORET, J., LUQUE, J., MÁRQUEZ, L.,

MÁRQUEZ-ALIAGA, A., MARTÍN-ALGARRA, A., MARTÍN-CHIVELET, J., MARTÍN-GONZÁLEZ, F., MARZO, M., MERCEDES-MARTÍN, R., ORTÍ, F., PÉREZ-LÓPEZ, A., PÉREZ-VALERA, F., PÉREZ-VALERA, J.A., PLASENCIA, P., RAMOS, E., RODRÍGUEZ-MÉNDEZ, L., RONCHI, A., SALAS, R., SÁNCHEZ-FERNÁNDEZ, D., SÁNCHEZ-MOYA, Y., SOPEÑA, A., SUÁREZ-RODRÍGUEZ, Á., TUBÍA, J.M., UBIDE, T., VALERO-GARCÉS, B., VARGAS, H. i VISERAS, C. (2019): Permian-Triassic rifting stage. In: VERGÉS, J. i KULLBERG, J.C. (coord.), *The Geology of Iberia: A Geodynamic Approach. Volume 3: The Alpine Cycle*: 29–112. Springer, Cham.

LOZANO, R. (1884): *Anotaciones físicas y geológicas de la isla de Mallorca para las aplicaciones del mapa: dedicado á la Excma. Diputación Provincial de Baleares*. Imprenta de la Casa de la Misericordia, Palma. 68 pp.

LUCAS, S.G. (2019): An ichnological perspective on some major events of Paleozoic tetrapod evolution. *Bollettino della Società Paleontologica Italiana*, 58(3): 223-266.

MARTÍ, J., PANIELLO, X., POMAR, L., RAMOS, E. i RODRÍGUEZ-PEREA, A. (1985): El Triásico de las Baleares. In: MATEU IBARS, F. i MARZO, M. (eds.), *Resúmenes del II Coloquio de Estratigrafía y Paleogeografía del Pérmico y Triásico de España*: 84-85. Institut d'Estudis Ilerdencs i Grupo Español del Mesozoico, La Seu d'Urgell.

MATAMALES-ANDREU, R., FORTUNY, J., MUJAL, E. i GALOBART, À. (2019): Tetrapod tracks from the Permian of Mallorca (western Mediterranean): preliminary data, biostratigraphic and biogeographic inferences. In: *The Palaeontological Association, 63rd annual meeting, 15th–21st December 2019*: p. 107. The Palaeontological Association, València.

MATAMALES-ANDREU, R., MUJAL, E., DINARÈS-TURELL, J., KUSTATSCHER, E., ROGHI, G., OMS, O., GALOBART, À. i FORTUNY, J. (en preparació): Early–middle Permian ecosystems of equatorial Pangaea: integrated multi-stratigraphic and palaeontological review of the Permian of Mallorca (Balearic Islands, Western Mediterranean).

MATAMALES-ANDREU, R., MUJAL, R., GALOBART, À. i FORTUNY, J. (2021a): Insights on the evolution of synapsid locomotion based on tetrapod tracks from the lower Permian of Mallorca (Balearic Islands, western Mediterranean). *Palaeogeography, Palaeoclimatology, Palaeoecology*, 579: 110589.

MATAMALES-ANDREU, R., OMS, O., GALOBART, À. i FORTUNY, J. (2021b): Middle–Upper Triassic marine vertebrates of Mallorca (Balearic Islands, western Mediterranean). *Historical Biology*, 33(10): 2520-2533.

MATAMALES-ANDREU, R., PEÑALVER, E., MUJAL, E., OMS, O., SCHOLZE, F., JUÁREZ, J., GALOBART, À. i FORTUNY, J. (2021c). Early–Middle Triassic fluvial ecosystems of Mallorca (Balearic Islands): Biotic communities and environmental evolution in the equatorial western peri-Tethys. *Earth-Science Reviews*, 222: 103783.

MATAMALES-ANDREU, R., ROIG-MUNAR, F.X., OMS, O., GALOBART, À. i FORTUNY, J. (2021d): A captorhinid-dominated assemblage from the palaeoequatorial Permian of Menorca (Balearic Islands, western Mediterranean). *Earth and Environmental Science Transactions of the Royal Society of Edinburgh*, 112(2): 125-145.

McCANN, T., PASCAL, C., TIMMERMAN, M.J., KRZYWIEC, P., LÓPEZ-GÓMEZ, J., WETZEL, A., KRAWCZYK, C.M., RIEKE, H. i LAMARCHE, J. (2006): Post-Variscan (end Carboniferous–Early Permian) basin evolution in Western and Central Europe. *Geological Society, London, Memoirs*, 32: 355-388.

NOLAN, H. (1887): Note sur le Trias de Minorque et Majorque. *Bulletin de la Société géologique de France*, 15: 592-599.

NOLAN, H. (1888): El Trias de Mallorca y Menorca. *Boletín de la Comisión del Mapa Geológico*, 15: 234-241.

OBRADOR, A. (1983): El Pérmico de las Baleares. In: MARTÍNEZ-DÍAZ, C. (ed.), *Carbonífero y Pérmico de España, X Congreso Internacional de Estratigrafía y Geología del Carbonífero*: 463-470. Ministerio de Industria y Energía i Instituto Geológico Minero de España, Madrid.

OGG, J.G., CHEN, Z.-Q., ORCHARD, M.J. i JIANG, H.S. (2020): Chapter 25 - The Triassic Period. In: GRADSTEIN, F.M., OGG, J.G., SCHMITZ, M.D. i OGG, G.M. (eds.), *Geologic Time Scale 2020*: 903-953. Elsevier.

PARÉS, J.M., FREEMAN, R. i SÀBAT, F. (1989): Síntesis de los resultados paleomagnéticos de los bordes de la Cuenca Catalano-Balear. *Cuadernos de Geología Ibérica*, 12: 59-74.

PARÉS, J.M., FREEMAN, R. i ROCA, E. (1992a): Neogene structural development in the Valencia trough margins from palaeomagnetic data. *Tectonophysics*, 203: 111-124.

PARÉS, J.M., ROCA, E. i FREEMAN, R. (1992b): Datos paleomagnéticos de los márgenes del surco de Valencia. Papel de las rotaciones en la estructuración neógena. *Física de la Tierra*, 4: 231-246.

PEÑALVER, E., MARTÍNEZ-DELCLÒS, X. i ARILLO, A. (1999): Yacimientos con insectos fósiles en España. *Revista Española de Paleontología*, 14(2): 231-245.

POMAR-GOMÀ, L. (1979): *The Triassic of the Balearic Islands*. Geology Department, Palma de Mallorca University, Palma. 49 pp. + 7 columnes estratigràfiques. Inèdit.

PRETUS, J.Ll. i OBRADOR, A. (1987): Presencia de restos óseos en el Pérmico de Menorca (nota previa). *Bolletí de la Societat d'Història Natural de Balears*, 31: 149-152.

RAMOS, A. (1995): Transition from alluvial to coastal deposits (Permian–Triassic) on the Island of Mallorca, western Mediterranean. *Geological Magazine*, 132(4): 435-447.

RAMOS, A. i DOUBINGER, J. (1989): Premières datations palynologiques dans le facies Buntsandstein de l'île de Majorque (Baléares, Espagne). *Comptes Rendus de l'Académie des Sciences de Paris*, segona sèrie, 309: 1089-1094.

RAMOS, A. i GARCÍA-RAMOS, S. (1992): Niveles de bioturbación en las facies tipo Buntsandstein del Pérmico-Triásico de Mallorca. In: GARCÍA-RAMOS, J.C. (ed.), *Reunión Monográfica sobre Biosedimentación*: 41-43.

RAMOS, A., OLMO, P. del i ALVARO, M. (1985): El Buntsandstein de la isla de Mallorca. In: MATEU IBARS, F. & MARZO, M. (eds.), *II Coloquio de Estratigrafía y Paleogeografía del Pérmico y Triásico de España*: 103-104.

RODRÍGUEZ-PEREA, A., RAMOS-GUERRERO, E., POMAR, L., PANIELLO, X., OBRADOR, A. i MARTÍ, J. (1987): El Triásico de las Baleares. *Cuadernos de Geología Ibérica*, 11: 295-321.

ROMANO, M., BERNARDI, M., PETTI, F.M., RUBIDGE, B., HANCOX, J. i BENTON, M.J. (2020; *en premsa*): Early Triassic terrestrial tetrapod fauna: a review. *Earth-Science Reviews*, 210: 103331.

ROSCHER, M., STORDAL, F. i SVENSEN, H. (2011): The effect of global warming and global cooling on the distribution of the latest Permian climate zones. *Palaeogeography, Palaeoclimatology, Palaeoecology*, 309: 186-200.

ROSELL, J., ARRIBAS, J., ELÍZAGA, E. i GÓMEZ-GRAS, D. (1988): Caracterización sedimentológica y petrográfica de la serie roja permo–triásica de la isla de Menorca. *Boletín Geológico y Minero*, 99(1): 71-82.

ROSELL, J., GÓMEZ-GRAS, D. i ELÍZAGA, E. (1989a): *Mapa Geológico de España. Escala 1:25.000. Isla de Menorca. Cap Menorca y Ciutadella.* Segona sèrie, primera edició. Instituto Tecnológico GeoMinero de España, Madrid. 51 pp. + 3 mapes.

ROSELL, J., GÓMEZ-GRAS, D. i ELÍZAGA, E. (1989b): *Mapa Geológico de España. Escala 1:25.000. Isla de Menorca. Cala en Brut i Alaior.* Segona sèrie, primera edició. Instituto Tecnológico GeoMinero de España, Madrid. 38 pp. + 3 mapes.

SANTANACH, P., BANDA, E., CALVET, F., CARRERAS, J., CASAS, J.M., FONTBOTÉ, J.M., FORNÓS, J., GISBERT, J., JULIVERT, M., MARZO, M., RODRÍGUEZ-PEREA, A., SALAS, R. i SOUQUET, P. (eds.) (1986): *Història Natural dels Països Catalans, 1: Geologia (I).* Enciclopèdia Catalana, Barcelona. 439 pp.

SCOTESE, C.R. (2014a): Atlas of Permo-Carboniferous Paleogeographic Maps, maps 53 – 64 from Volume 4 of the PALEOMAP Atlas for ArcGIS (Late Paleozoic), Mollweide Projection, PALEOMAP Project, Evanston, Illinois.

SCOTESE, C.R. (2014b): Atlas of Middle & Late Permian and Triassic Paleogeographic Maps, maps 43 – 48 from Volume 3 of the PALEOMAP Atlas for ArcGIS (Jurassic and Triassic) and maps 49 – 52 from Volume 4 of the PALEOMAP Atlas for ArcGIS (Late Paleozoic), Mollweide Projection, PALEOMAP Project, Evanston, Illinois.

SHCHERBAKOV, D.E., LUKASHEVICH, E.D. i BLAGODEROV, V.A. (1995): Triassic Diptera and initial radiation of the order. *Journal of Dipterological Research*, 6(2): 75-115.

SCHOLZE, F. i MATAMALES-ANDREU, R. (2021). Triassic clam shrimps ("Conchostraca"; Branchiopoda: Diplostraca) from Mallorca: Taxonomic description and interregional comparisons. *Zootaxa*, 4964(3): 471-496.

SINITSHENKOVA, N.D. (2000): A review of Triassic mayflies, with the description of new species from Western Siberia and Ukraine (Ephemerida = Ephemeroptera). *Paleontological Journal*, 34 (3): S275-S283.

VERA, J.-A., ALONSO-CHAVES, F.M., ANDREO, B., ARIAS, C., AZAÑÓN, J.M., BALANYÁ, J.C., BARÓN, A., BOOTH-REA, G., CASTRO, J.M., CHACÓN, B., COMPANY, M., CRESPO-BLANC, A., DELGADO, F., DÍAZ DE FEDERICO, A., ESTERAS, M., ESTÉVEZ, A., FERNÁNDEZ, J., FORNÓS, J.J., GALINDO-ZALDÍVAR, J., GARCÍA-CASCO, A., GARCÍA-DUEÑAS, V., GARCÍA-HERNÁNDEZ, M., GARRIDO, C.J., GEA, G.A. de; GELABERT, B., GERVILLA, F., GONZÁLEZ-LODEIRO, F., JABALOY, A., LÓPEZ-GARRIDO, A.C., LUJÁN, M., MARTÍN-ALGARRA, A., MARTÍN-CHIVELET, J., MARTÍN-MARTÍN, M., MOLINA, J.M., MORATA, D., NIETO, J.M., OBRADOR, A., O'DOGHERTY, L., OROZCO, M., PÉREZ-LÓPEZ, A., POMAR, L., PUGA, E., RAMOS, E., REY, J., RIVAS, P., RODRÍGUEZ-CAÑERO, R., RUIZ-CRUZ, M.D., RUIZ-ORTIZ, P.A., SÀBAT, F., SÁNCHEZ-GÓMEZ, M., SÁNCHEZ-NAVAS, A., SANDOVAL, J., SANZ DE GALDEANO, C., SOTO, J.I., TORRES-ROLDÁN, R.L. i VILLAS, L. (2004): Cordillera Bética y Baleares. In: VERA, J.-A. (ed.), *Geología de España*: 346-464. Instituto Geológico y Minero de España, Madrid.

ZESSIN, W. (2008a): Einige neue Insekten aus der Unteren Trias (Buntsandstein) von Mallorca, Spanien (Blattaria, Coleoptera, Diptera, Heteroptera und Megaloptera). *Deutschen Gesellschaft für allgemeine und angewandte Entomologie – Nachrichten*, 22(1): 20-21.

ZESSIN, W. (2008b): Neue Insekten aus der Unteren Trias (Buntsadstein) von Mallorca, Spanien (Blattaria, Coleoptera, Diptera, Heteroptera, Orthopteroidea und Homoptera). *Virgo, Mitteilungsblatt des Entomologischen Vereins Mecklenburg*, 11(1): 99-101.

PALEOECOSISTEMES DEL PERMIÀ I TRIÀSIC CONTINENTAL DE MALLORCA

Nota: Els autors volen fer constar que per indicació dels editors –els quals s'acullen als criteris de l'Institut d'Estudis Catalans i allò que recomanen els manuals d'estil a l'ús (cf. Optimot), de més a més de mantenir la unitat d'estil de tota la monografia– i en contra de l'opinió dels autors, la terminologia cronoestratigràfica i geocronològica s'ha posat sempre en minúscula.

Data recepció: 30.03.21
Data revisió: 08.06.21
Revisió acceptada: 26.06.21

Appendix 2

Supplementary Material, Permian of Mallorca

Appendix 2 was published as the supplementary material of:

Matamales-Andreu, R.; Mujal, E.; Dinarès-Turell, J.; Kustatscher, E.; Roghi, G.; Oms, O.; Galobart, À. & Fortuny, J. (2022). Early–middle Permian ecosystems of equatorial Pangaea: Integrated multi-stratigraphic and palaeontological review of the Permian of Mallorca (Balearic Islands, western Mediterranean). *Earth-Science Reviews*, 228: 103948.

DOI: https://doi.org/10.1016/j.earscirev.2022.103948

Also, refer to:

Chapter 2: Matamales-Andreu *et al.* (2022), *Earth-Science Reviews*

APPENDIX A. SUPPLEMENTARY TEXTS, FIGURES, TABLES, LOGS AND CORRELATIONS

Early–middle Permian ecosystems of equatorial Pangaea: integrated multi-stratigraphic and palaeontological review of the Permian of Mallorca (Balearic Islands, western Mediterranean)

Rafel Matamales-Andreu[a,b]*, Eudald Mujal[a,c], Jaume Dinarès-Turell[d], Evelyn Kustatscher[e,f], Guido Roghi[g], Oriol Oms[h], Àngel Galobart[a,i] & Josep Fortuny[a]

[a] Institut Català de Paleontologia Miquel Crusafont, Universitat Autònoma de Barcelona, Edifici ICTA-ICP, c/ Columnes s/n, Campus de la UAB, 08193 Cerdanyola del Vallès, Barcelona, Spain.

[b] Museu Balear de Ciències Naturals, carretera Palma–Port de Sóller Km. 30, 07100 Sóller, Mallorca, Spain.

[c] Staatliches Museum für Naturkunde Stuttgart, Rosenstein 1, 70191 Stuttgart, Germany.

[d] Istituto Nazionale di Geofisica e Vulcanologia, Via di Vigna Murata 605, 00143 Roma, Italy.

[e] Department für Geo- und Umweltwissenschaften, Paläontologie und Geobiologie, Ludwig-Maximilians-Universität, Richard-Wagner-Straße 10, 80333 München, Germany.

[f] Bayerische Staatssammlung für Paläontologie und Geobiologie, Richard-Wagner-Straße 10, 80333 München, Germany.

[g] Istituto di Geoscienze e Georisorse - CNR, Dipartimento di Geoscienze, Università di Padova, Via Gradenigo 6, 35131 Padova, Italy.

[h] Departament de Geologia, Universitat Autònoma de Barcelona, av. de l'eix Central s/n, Campus de la UAB, 08193 Cerdanyola del Vallès, Barcelona, Spain.

[i] Museu de la Conca Dellà, c/ del Museu 4, 25650 Isona i Conca Dellà, Lleida, Spain.

*Corresponding author: rafel.matamales@icp.cat

Supplementary Text 1. Previous works

The first authors that studied the pre-Jurassic red-beds of Mallorca considered them to homogeneously represent Lower–Middle Triassic *Buntsandstein* facies (Nolan, 1887, 1888; Darder, 1914; Fallot, 1922). However, their source, Hermite (1879, 1888), had only dated the beds cropping out near the Cala d'Estellencs, but not those in the rest of areas where red-beds were present. Several decades later, Cuevas-López (1958a, 1958b) cast doubt on this previous conception when he noted that there existed a lower stretch similar to the Germanic *Rothliegende*, *Zechstein* and *Kupferscheifer* facies, and thus of purported Permian age, and an upper stretch comparable to the Germanic *Buntsandstein* facies, and thus of purported Triassic age (Supplementary Table 1). Subsequent works (Freeman & Obrador, 1974, 1979; Colom, 1975; Obrador, 1983) broadly acknowledged the proposal of Cuevas-López (1958a, 1958b), but did not provide further detailed stratigraphic analyses to confirm it. Barón (1970, 1976) found deposits of marls and gypsum below the *Muschelkalk* facies, and hypothesised that the *Buntsandstein* facies (including Permian red-beds) changed laterally towards the East to such deposits. Moreover, Barón (1976) mentioned that below the red-beds near Port de Valldemossa there were "about 70 metres of solid dolostones with fissures injected with gypsum, massive gypsum and layers of ashes or volcanic rocks"[1], which could correspond to the *Keuper* facies, and thus the whole Permian sequence near Port de Valldemossa would be allochtonous. Pomar-Gomà (1979), Martí *et al.* (1985), Rodríguez-Perea *et al.* (1987) and Barnolas (1991a, 1991b) attempted to establish a comprehensive lithostratigraphic division of the different units of the Permian–Triassic deposits of Mallorca, but based their interpretations only on the Racó de s'Algar–Pedra de s'Ase section, where the series is not complete, lacking all the Triassic (Figures 2, 3 of the main text, Supplementary Table 1; Supplementary Logs; Supplementary Correlations). Similarly, Ramos *et al.* (1985) and Ramos (1995) miscorrelated similar Permian and Triassic lithosomes among outcrops, thus only considering part of the total sequence (Supplementary Table 1; see Matamales-Andreu *et al.*, 2021a).

Calafat (1986, 1987, 1988) retrieved the approach of Cuevas-López (1958a, 1958b), providing an exhaustive and detailed study of the Permian–Triassic red-beds of Mallorca and defining five informal lithostratigraphic units (Supplementary Table 1). A basal stretch, named Bec de s'Àguila Sandstone and Conglomerate Unit, corresponding to ephemeral braided river deposits developed over the Carboniferous basement, was overlain by the Racó de s'Algar Sandstone and Lutite Unit, interpreted as deposits of rivers of an intermediate style between meandering and braided. Above it, the Pedra de s'Ase Unit, representing braided river deposits, appeared

[1] *"Por otra parte un sodeo perforado en Cala Valldemosa encontró bajo las areniscas rojas unos 70 m. de dolomias* [sic] *sólidas con las fisuras inyectadas de yesos, yesos masivos y capas de cenizas o roca volcánica; Virgili Capina (1974, comunicación verbal) que podría tratarse de Permico* [sic]. *La comparación con ciertas facies del Keuper de la Isla puede inducir a atribuirlo a este piso"* (Barón, 1976: p. 3).

after an unconformity. One year later, Ramos & Doubinger (1989) provided the first accurate palaeopalynological analysis of two beds of the Pedra de s'Ase Unit, confirming a Permian age ("Thuringian") for it. This age attribution was further supported with additional data by Diez (2000), Diez *et al.* (2005) and Juncal (2019). The uppermost two lithostratigraphic units defined by Calafat (1988) have been dated in the Triassic, and will not be discussed here (see Matamales-Andreu *et al.*, 2021a).

Integrating all the previous data with new fieldwork observations, Gómez-Gras (1992, 1993) provided a new lithostratigraphic division, very similar to the one of Calafat (1988), only with higher resolution (Supplementary Table 1). It is important to note, however, that all the review papers to date (Calvet & Marzo *in* Santanach *et al.*, 1986; Arche *et al.*, 2002; López-Gómez *et al.*, 2002, 2019; Vera *et al.*, 2004; Bourquin *et al.*, 2007, 2011; Cassinis *et al.*, 2012) were based on the division in informal units posited by Ramos *et al.* (1985) and Ramos (1995), which failed to carry out successful correlations between outcrops with similar lithosomes (also argued by Matamales-Andreu *et al.*, 2021a, for the case of the overlaying *Buntsandstein* facies). Virgili *et al.* (2006) and Virgili (2008) considered that all the Permian sediments of the Balearic Islands constituted a single unit that could be attributed to an upper Permian "Thuringian" biofacies.

Regarding the fossil content of the Permian units of Mallorca, Freeman & Obrador (1979), Calafat (1988), Ramos (1995) and Diez (2000) illustrated large tree logs in the base of some channel deposits of the Pedra de s'Ase Unit, oriented towards the main palaeocurrent trend. Invertebrate trace fossils were also mentioned from many beds by Calafat (1988), but they were never studied in detail until Ramos & García-Ramos (1992) and Ramos (1995), who reported the ichnogenera *Planolites*, *Palaeophycus* and *Ancorichnus*.

Calafat *et al.* (1986) were the first authors to report tetrapod ichnites from the Racó de d'Algar Unit, with three morphotypes: the first and most abundant type were medium-sized (c. 15 cm) footprints, which appeared either isolated or forming trackways (Supplementary Figure 3A, C, D, E and perhaps 3J–K); the second type were smaller (c. 2–3 cm) ichnites with very thin digits (perhaps referring to those here illustrated in Supplementary Figure 3L), always found isolated; and the third type formed a trackway of poorly detailed ichnites (each of c. 6 cm) (Supplementary Figure 3F). Calafat *et al.* (1986–1987) went a step further and described four morphotypes of tetrapod ichnites: 'type A' (='first type' of Calafat *et al.*, 1986), pentadactyl footprints identified as *Cheirotherium* [sic] isp.; 'type B' (='third type' in Calafat *et al.*, 1986), ovoid, probably unidentifiable ichnites; 'type Ca' (not described by Calafat *et al.*, 1986), pentadactyl ichnites, smaller than those of 'type A' (c. 4 cm) (Supplementary Figure 3H–I); and 'type Cb' (not described by Calafat *et al.*, 1986), an isolated, large (c. 25 cm) pentadactyl ichnite. Calafat (1988) mostly reproduced the information given by Calafat *et al.* (1986–1987),

adding data on the locality and stratigraphic position of the ichnites. 'Type A' (='type A' in Calafat *et al.*, 1986–1987) were again thought to belong to *Cheirotherium* [sic], and were found at the base of the lower bed with mud-cracks of the metre 25.6 of the NA log of the present work (Figure 2 of the main text; Supplementary Logs) (crosschecked with the log 'E' of Calafat, 1988), as well as on an *ex situ* boulder thought to belong to the same bed (UIB174620). 'Type B' ('type B' in Calafat *et al.*, 1986–1987) were on an *ex situ* slab assignable to the beds of the 25.6 of the NA log (Figure 2 of the main text; Supplementary Logs), but they are nowadays eroded (Supplementary Figure 3G). 'Type C' ('type Ca' in Calafat *et al.*, 1986–1987) were also found *ex situ* near the ichnite-bearing beds of the 25.6 of the NA log. Finally, 'type D' ('type Cb' in Calafat *et al.*, 1986–1987) was found in the lower unit of the Mallorcan Permian, although the precise bed or locality was never specified. Sastre & Sastre (2005) illustrated again the 'type B' ichnites. Some years later, Gand *et al.* (2010) revised the figures of 'type A' ichnites of Calafat *et al.* (1986–1987), tentatively determining them as *Hyloidichnus* isp., and thus suggesting an upper Permian age for them.

Another slab from the Permian Racó de s'Algar site, recovered in the early 1980s, was figured by Juárez-Ruiz & Wachtler (2015), who misidentified the cf. *Dimetropus* isp. (Matamales-Andreu *et al.*, 2021b) on the slab as Triassic *Rotodactylus*. Recently, Matamales-Andreu *et al.* (2019) presented a preliminarily study on the ichnoassemblage of the Permian of Mallorca, recognising the ichnogenera *Hyloidichnus* and *Dimetropus* and, more doubtfully, *Amphisauropus*, *Varanopus*, *Dromopus* and cf. *Ichniotherium*. The abundance of captorhinomorph tracks (*Hyloidichnus*), together with the absence of temnospondyl amphibian tracks, made it possible to suggest that the ichnite-bearing beds could belong to the lower Permian (Artinskian–Kungurian?).

Calafat *et al.* (1986–1987) and Calafat (1988) also reported "abundant bone remains (vertebrae, etc.)"[2] from the Racó de s'Algar Unit, although they were finally never illustrated or studied in detail. From the base of the Pedra de s'Ase Unit, Calafat *et al.* (1986) and Calafat (1988) mentioned the discovery of a bone fragment as well. Liebrecht *et al.* (2017) were the first ones to provide a taxonomic assignation for a bone fragment from the Permian of Mallorca (Port des Canonge Unit), identifying it as a maxilla (with parts of the palate) of a large moradisaurine captorhinid eureptile (see Supplementary Text 2).

[2] *"Es muy interesante resaltar la presencia en estos yacimientos, formando parte de los clastos, de abundantes restos óseos (vértebras, etc.) en relativo buen estado de consevación, pero que no han sido, sin embargo, objeto de estudio en el presente trabajo"* (Calafat *et al.*, 1986–1987: p. 515).

Supplementary Text 2. Discussion on the provenance and age of the moradisaurine captorhinid eureptile maxilla described by Liebrecht *et al.* (2017)

Liebrecht *et al.* (2017) were the first authors to provide a detailed taxonomical study of a bone remain (maxilla with parts of the palate) from the Permian beds of Mallorca, identifying it as a moradisaurine captorhinid eureptile. They claimed that the fossil had been found *ex situ* among the cobbles of the Cala Gata beach, near an outcrop of the Port des Canonge lithostratigraphic unit in the sense of Ramos (1995). Liebrecht *et al.* (2017) dated the fossil as upper Permian based on the work of Ramos & Doubinger (1989), who recognised the "Thuringian" biofacies in the overlaying "Asá" [sic.] unit of Mallorca, based on the analysis of palynomorphs.

However, Matamales-Andreu *et al.* (2021c) recently argued that both the locality name and the age attribution of that fossil were different from what was originally thought. Liebrecht *et al.* (2017) said that the maxilla was found on a beach named Cala Gata. However, the map they provided (Liebrecht *et al.*, 2017: figure S3) clearly shows that the specimen actually came from another nearby beach called Platja de son Bunyola. During the present study, another unidentifiable bone fragment (DA21/14-09-01) has also been found *ex situ* on Platja de son Bunyola, further confirming the presence of vertebrate fossils there. In the surroundings of Platja de son Bunyola, the only lithostratigraphic formation that crops out is the Port des Canonge Formation as described herein (= Port des Canonge unit of Ramos *et al.*, 1985; Ramos & Doubinger, 1989; Ramos, 1995; = Racó de s'Algar unit of Calafat, 1988; = Stretch a of Gómez-Gras, 1993; see Supplementary Table 1 herein). This formation was recently considered as lower Permian and, more specifically, in the Artinskian or Kungurian (Matamales-Andreu *et al.*, 2019), a claim which is further supported in the present work (see '8.1.3. Tetrapod track biostratigraphy' in the main text).

Supplementary Figures

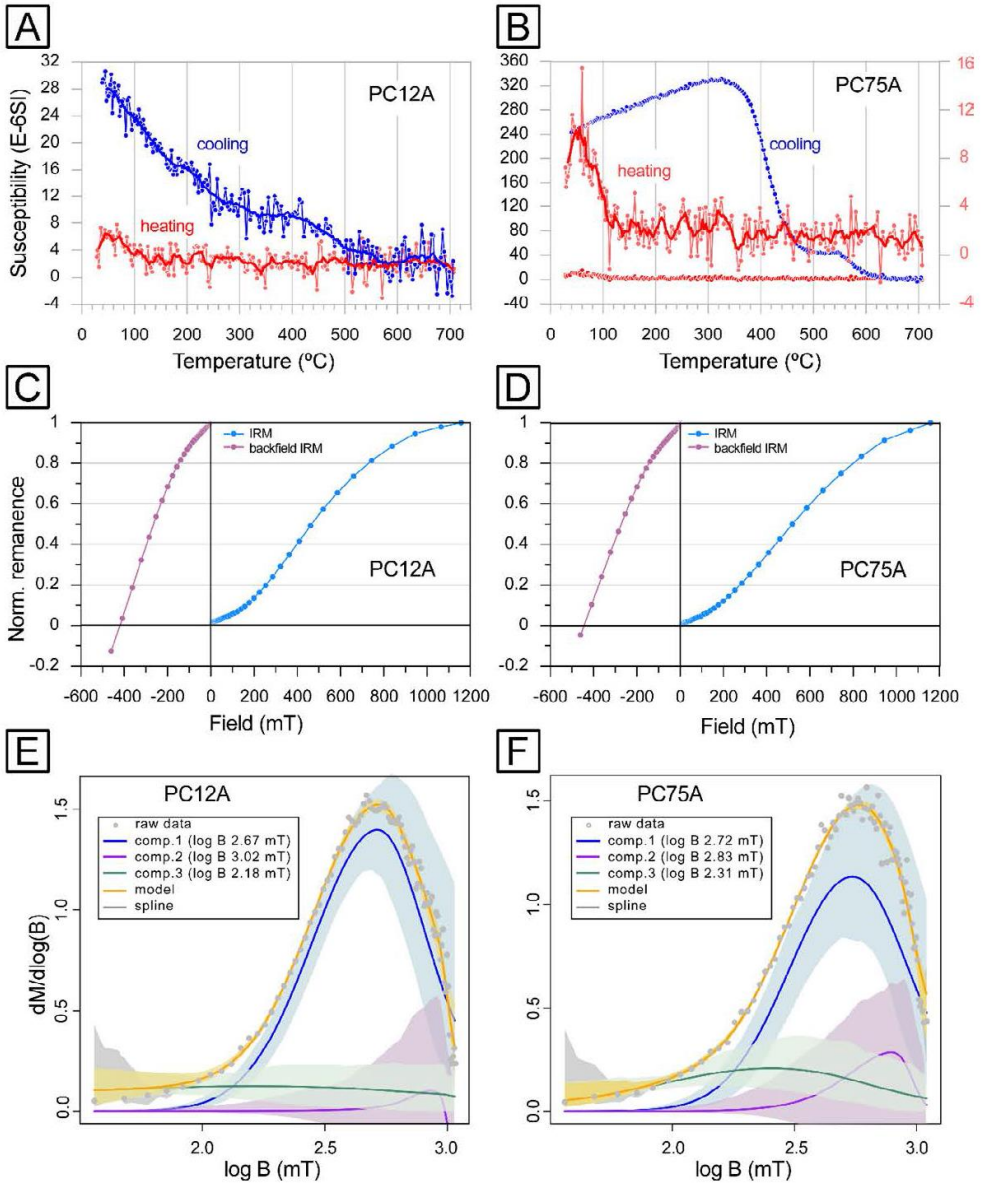

Supplementary Figure 1. A–B: Thermomagnetic curves from representative samples. 5-point running average fit is shown for the heating cycle in A. **B–C**: IRM acquisition curves and back-field IRM of the same samples. **D–E**: Model fit examples to unmix coercivity distributions (Maxbauer *et al.*, 2016) derived from back-field IRM acquisition data for the same samples. Shaded area represents error envelopes of 95% confidence intervals.

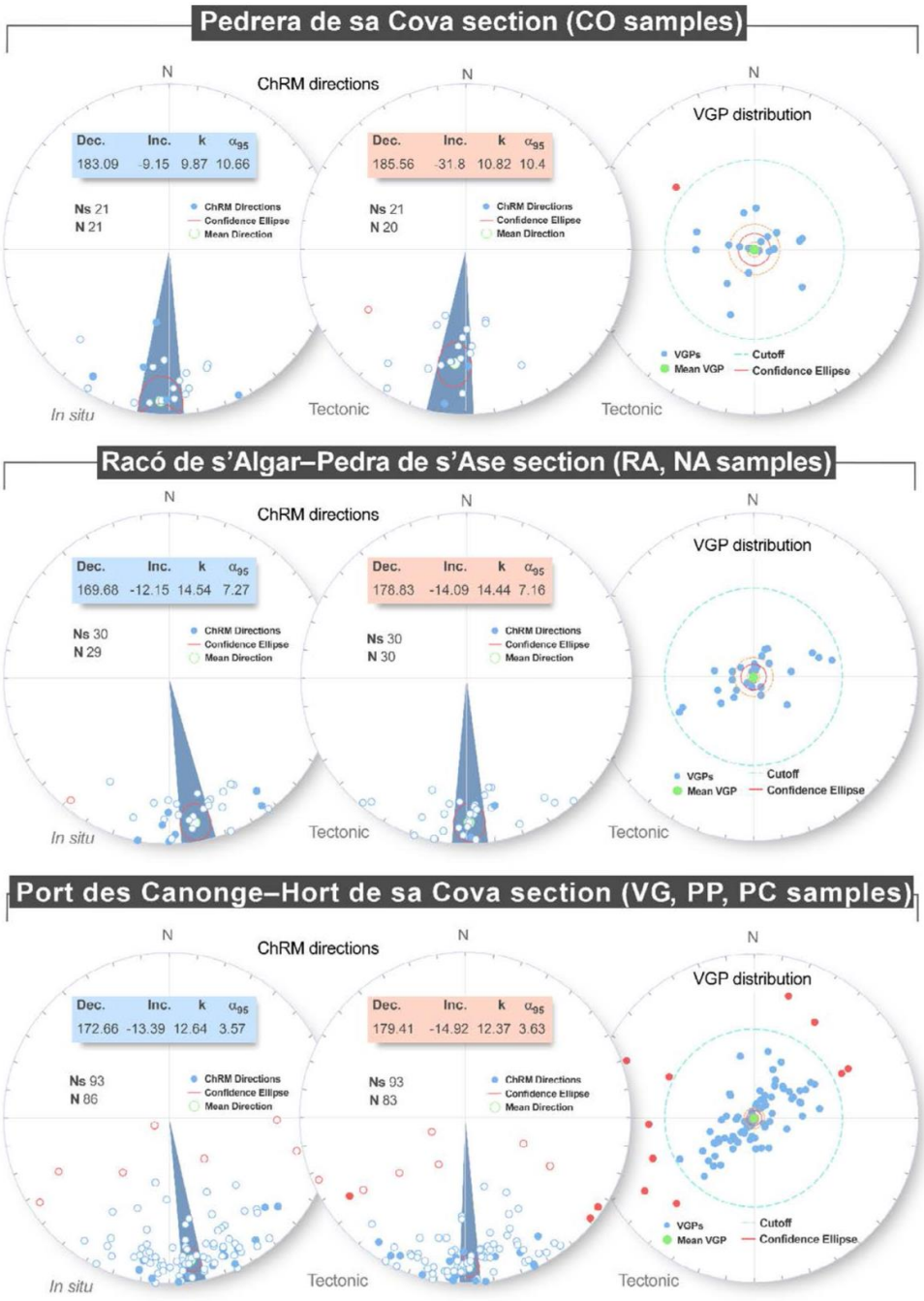

Supplementary Figure 2. ChRM directional and VGP results in geographic (*in situ*) and bedding-corrected (tectonic) coordinates for the three studied sections. The confidence envelope (A95) and parachute are depicted. Red dots are those that fall outside of the 45° cut-off. For full directional and statistical data see Supplementary Table 2 and Supplementary Table 3.

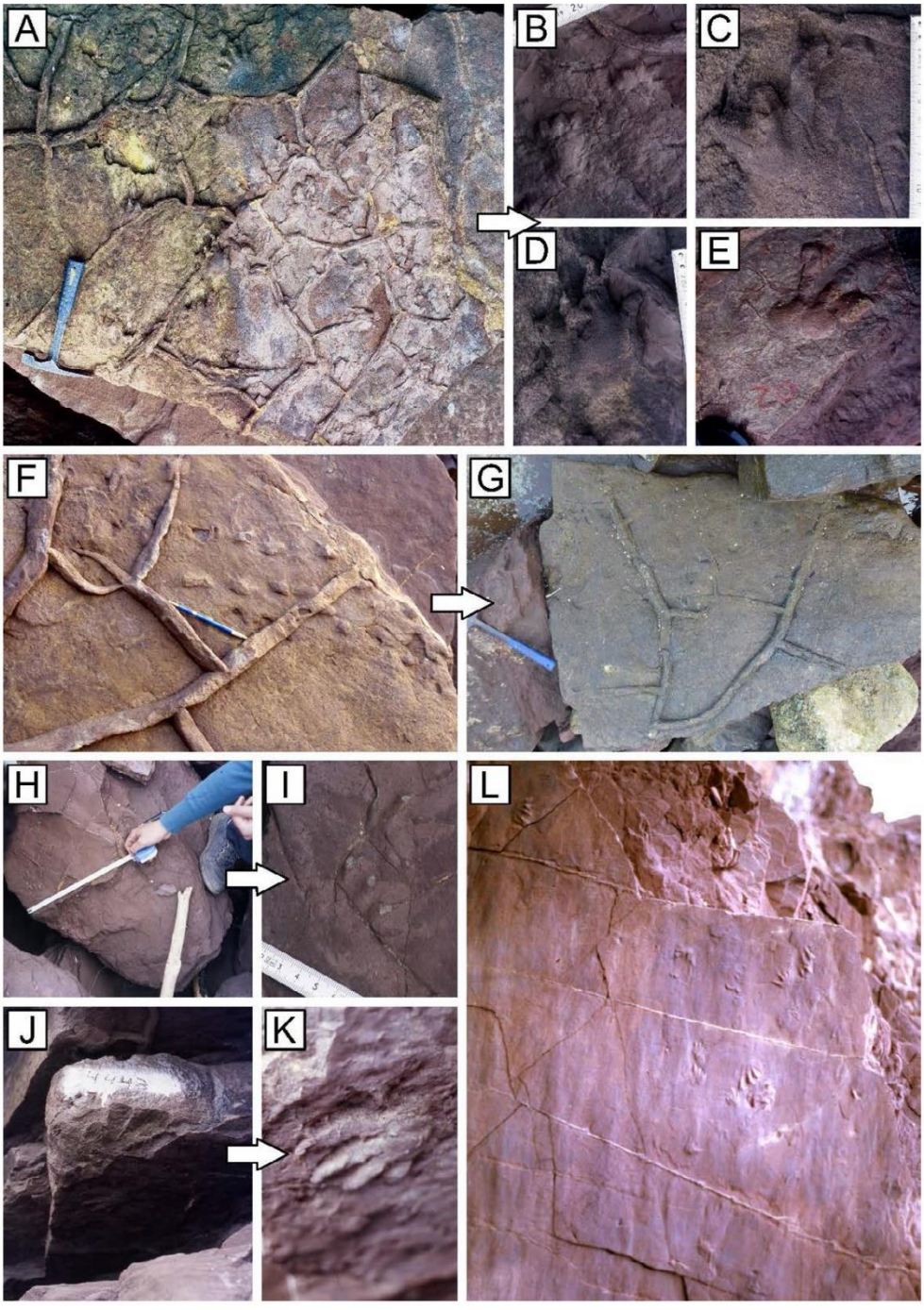
A
B
C
D
E
F
G
H
I
L
J
K

Supplementary Figure 3. (previous page) **A:** General view of the specimen UIB174620, collected in the 1980s and here partially refigurated as NA-25.6-01 (Figures 10A–B, 11C–D of the main text). **B:** Detail of a right manus-pes set of *Dimetropus leisnerianus* on slab UIB174620. **C:** Detail of a left pes track of the large morphotype of *Hyloidichnus bifurcatus* on slab UIB174620 (originally identified as *Cheirotherium* [sic.] by Calafat *et al.*, 1986–1987). **D:** Detail of a left manus track of the large morphotype of *Hyloidichnus bifurcatus* on slab UIB174620 (originally identified as 'Type A' ichnites, *Cheirotherium* [sic.], by Calafat *et al.*, 1986–1987). **E:** Right pes track of the large morphotype of *Hyloidichnus bifurcatus*, on a slab that was never collected. **F–G:** Trackway, perhaps of very poorly defined *Dimetropus leisnerianus* (originally identified as 'Type B' ichnites by Calafat *et al.*, 1986–1987), on a slab that was never collected, and current aspect of the surface with all the ichnites eroded away. **H–I:** General view and detail of a right manus-pes set of the small morphotype of *Hyloidichnus bifurcatus* (originally identified as 'Type Ca' ichnites by Calafat *et al.*, 1986–1987), on a slab that was never collected. **J–K:** General view and detail of a possible left manus track of cf. *Dimetropus* sp., on a slab that was never collected. **L:** Several tracks and trackways of *Dimetropus leisnerianus* and the small morphotype of *Hyloidichnus bifurcatus*, on a slab that was never collected. All are from the upper part of the Port des Canonge Formation, Racó de s'Algar–Pedra de s'Ase section; A–K were found in the Racó de s'Algar 1 tracksite, whereas L was probably located in the NE corner of Platjola des munt de Pedres. All pictures except G, courtesy of Antoni Rodríguez Perea, Feliu Calafat and Joan Josep Fornós.

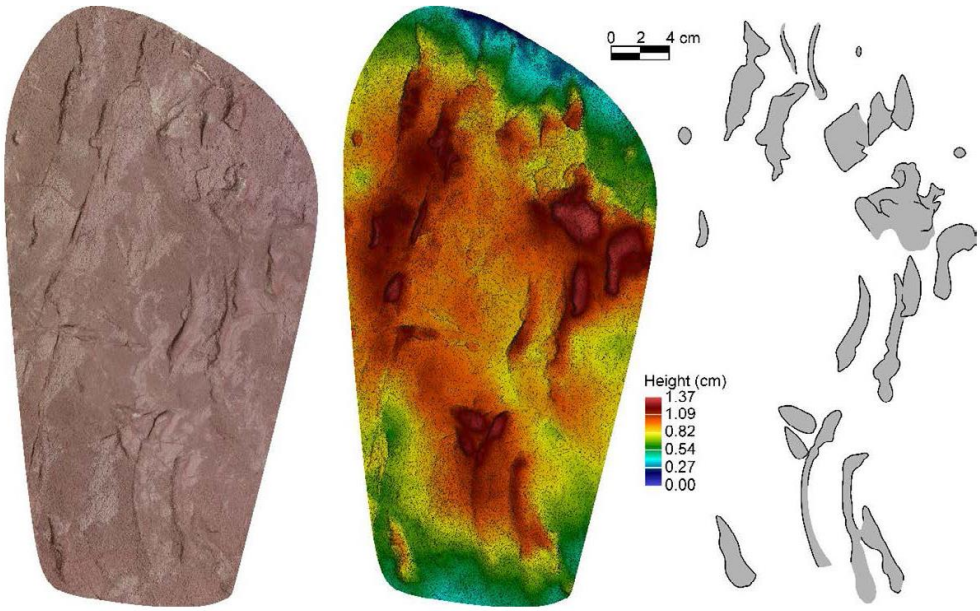

Supplementary Figure 4. Tetrapod ichnites herein studied attributed to *Characichnos* isp. (RA-exs-02) as textured 3D models, false colour-coded 3D models and interpretative drawings. From the Racó de s'Algar section (Mallorca, Balearic Islands, western Mediterranean), Artinskian/Kungurian, Permian.

Supplementary Table 1. Usage and equivalences of the different names for the Permian and Middle Triassic *p.p.* (*Buntsandstein* facies) units of Mallorca. Thickness in brackets, in some cases given in ranges.

<table>
<tr><th>Cuevas-López (1958a, 1958b)</th><th>Pomar-Gomà (1979)</th><th>Martí et al. (1985)</th><th>Ramos et al. (1985), Ramos & Doubinger (1989)</th><th>Calvet & Marzo in Santanach et al. (1986)</th><th>Calafat (1986), Calafat et al. (1987)</th><th colspan="2">Calafat (1987)</th><th>Rodríguez-Perea et al. (1987)</th><th colspan="2">Calafat (1988), Álvarez-Ramis et al. (1995), Gauvogel-Stamm & Álvarez-Ramis (1996), Diez (2000), Juárez-Ruiz & Wachtler (2015)</th><th>Barnolas (1991a, 1991b)</th><th colspan="2">Gómez-Gras (1992, 1993)</th><th>Ramos (1995), Arche et al. (2002), López-Gómez et al. (2002, 2019a), Vera et al. (2004), Bourquin et al. (2007, 2011), Cassinis et al. (2012)</th><th>The present work</th><th></th></tr>
<tr><td colspan="14">Middle Triassic Muschelkalk facies</td></tr>
<tr><td>Level V, top (100 m)</td><td rowspan="3">(not studied)</td><td rowspan="4">(not studied)</td><td>Son Serralta Lutites and Sandstones (65 m)</td><td>Son Serralta Lutites and Sandstones (120 m)</td><td>Transit unit (25 m)</td><td colspan="2">Son Serralta Lutite formation (27 m)</td><td rowspan="3">(not studied)</td><td colspan="2">Son Serralta Lutite Unit (27 m)</td><td rowspan="3">(not studied)</td><td rowspan="2">Stretch e) (160 m)</td><td>Upper Pelites and Sandstones</td><td>Son Serralta Lutites and Sandstones (65 m)</td><td>Son Serralta Formation (22 m)</td><td rowspan="5">TRIASSIC (Matamales-Andreu et al., 2021a)</td></tr>
<tr><td>Level IV (40 m)</td><td rowspan="3">Pedra de s'Ase Sandstones (100 m)</td><td rowspan="2">Upper unit (100 m)</td><td colspan="2" rowspan="2">Estellencs Sandstone and Lutite formation (124 m)</td><td colspan="2" rowspan="2">Estellencs Sandstone and Lutite Unit (124 m)</td><td>Middle Sandstones</td><td rowspan="3">Asá Sandstones (110 m)</td><td>Pedra Alta Formation (48 m)</td></tr>
<tr><td>Level III (50–60 m)</td><td>Lower Pelites and Sandstones</td><td>Estellencs Formation (55 m)</td></tr>
<tr><td>Level V, base (30–40 m)</td><td rowspan="2">Asá Sandstones (140 m)</td><td rowspan="3">Middle unit (100 m)</td><td rowspan="3">Pedra de s'Ase Sandstone formation (150 m)</td><td>Punta Roja Sandstone member (25 m)</td><td rowspan="3">Pedra de s'Ase Sandstone Unit (150 m)</td><td>Punta Roja Sandstone Sub-Unit (25 m)</td><td colspan="2">Stretch d) (58 m)</td><td>Punta Roja Formation (>67 m)</td></tr>
<tr><td>Level III (50–60 m)</td><td>Last Lutitic Stretch (≈80 m)</td><td rowspan="2">Pedra de s'Ase Sandstone member (125 m)</td><td>Upper Pelite-Sandstone Stretch (≈80 m)</td><td>Red and green lutites (>20 m)</td><td colspan="2">Stretch c) (135 m)</td><td rowspan="3">Pedra de s'Ase Formation (191–326 m)</td><td rowspan="3">PERMIAN</td></tr>
<tr><td>Level II (200 m)</td><td>Light-coloured Sandstone Stretch (127 m)</td><td>Sandstone Stretch</td><td>Middle Light-Coloured Sandstones (127 m)</td><td>White and red sandstones (120 m)</td><td colspan="2">Stretch b) (110 m)</td></tr>
<tr><td rowspan="2">Level I (800 m)</td><td rowspan="2">Lower Lutitic Stretch (213 m)</td><td>Lower Pelitic Stretch</td><td rowspan="2">Port des Canonge Sandstones and Lutites (176 m)</td><td rowspan="2">Port d'es Canonge Sandstones and Lutites (260 m)</td><td>Lower unit (150–250 m)</td><td colspan="2">Racó de s'Algar Sandstone and Lutite formation (144 m)</td><td>Lower Sandstone-Pelitic Stretch (213 m)</td><td colspan="2">Racó de s'Algar Sandstone and Lutite Unit (144 m)</td><td>Red lutites (>100 m)</td><td colspan="2" rowspan="2">Stretch a) (403 m)</td><td rowspan="2">Port des Canonge Sandstones and Lutites (160 m)</td><td>Port des Canonge Formation (134–369 m)</td></tr>
<tr><td>Polygenic Breccia</td><td>Basal unit (10 m)</td><td colspan="2">Bec de s'Àguila Sandstone and Conglomerate formation (25 m)</td><td>Basal Conglo-merate-Sand-stone Stretch (<20 m)</td><td colspan="2">Bec de s'Àguila Sandstone and Conglomerate Unit (25 m)</td><td>(not studied)</td><td>Bec de s'Àguila Formation (13–19m)</td></tr>
<tr><td colspan="14">Carboniferous Culm facies</td></tr>
</table>

Supplementary References (except for Supplementary Table 2)

Álvarez-Ramis, C.; Fernández-Marrón, T. & Calafat, F. (1995). Avance sobre la megaflora triásica, en facies germánica, de Estellencs (sector noroccidental de la sierra de Tramontana, Mallorca). *Revista Española de Paleontología*, nº homenaje al Dr. Guillermo Colom: 55–58.

Arche, A.; López-Gómez, J. & Vargas, H. (2002). Propuesta de correlación entre los sedimentos Pérmicos y Triásicos de la Cordillera Ibérica Este y de las Islas Baleares. *Geogaceta*, 32: 275–278.

Barnolas, A. (1991a). *Mapa Geológico de España. Escala 1:50.000. Andraitx.* Segunda serie, primera edición. Instituto Tecnológico GeoMinero de España, Madrid. 56 pp. + 1 map + 5 stratigraphic logs.

Barnolas, A. (1991b). *Mapa Geológico de España. Escala 1:50.000. Sóller.* Segunda serie, primera edición. Instituto Tecnológico GeoMinero de España, Madrid. 62 pp. + 1 map + 8 stratigraphic logs.

Barón, A. (1970). *Estudio estructural del borde meridional de la Sierra Norte de Mallorca (entre Esporlas y Pollensa)*. Bachelor's Thesis. Universitat de Barcelona, Barcelona. 63 pp. + 6 annexed figs.

Barón, A. (1976). *Estudio geológico del Mioceno medio y superior postorogénico, de la isla de Mallorca.* Premio Ciudad de Palma de Investigación 1974, Palma. 183 pp.

Bourquin, S.; Durand, M.; Diez, J.B.; Broutin, J. & Fluteau, F. (2007). The Permian-Triassic boundary and Early Triassic sedimentation in Western European Basins: an overview. *Journal of Iberian Geology*, 33(2): 221–236.

Bourquin, S.; Bercovici, A.; López-Gómez, J.; Diez, J.B.; Broutin, J.; Ronchi, A.; Durand, M.; Arché, A.; Linol, B. & Amour, F. (2011). The Permian–Triassic transition and the onset of Mesozoic sedimentation at the northwestern peri-Tethyan domain scale: Palaeogeographic maps and geodynamic implications. *Palaeogeography, Palaeoclimatology, Palaeoecology*, 299: 265–280.

Calafat, F. (1986). Estratigrafía y sedimentología de la litofacies Buntsandstein de Mallorca. *In*: Cabrera, L. (Ed.). *Resúmenes del XI Congreso Español de Sedimentología.* Grupo Español de Sedimentología, Barcelona: p. 39.

Calafat, F. (1987). Paleoambients de les facies Buntsandstein de Mallorca. *In*: *Llibre de resums de les I Jornades del Medi Ambient de les Illes Balears.*Societat d'Història Natural de les Balears, Palma: 16–17.

Calafat, F. (1988). *Estratigrafía y sedimentología de la litofacies Buntsandstein de Mallorca.* Bachelor's Thesis. Universitat de Barcelona, Barcelona. 127 pp. + 31 annexed figs.

Calafat, F.; Fornós, J.J.; Marzo, M.; Ramos, E. & Rodríguez-Perea, A. (1986). Icnología de vertebrados de las facies Buntsandstein de Mallorca. *In*: Cabrera, L. (Ed.). *Resúmenes del XI Congreso Español de Sedimentología.* Grupo Español de Sedimentología, Barcelona: p. 40.

Calafat, F.; Fornós, J.J.; Marzo, M.; Ramos-Guerrero, E. & Rodríguez-Perea, A. (1986–1987). Icnología de vertebrados de las facies Buntsandstein de Mallorca. *Acta Geològica Hispànica*, 21–22: 515–520.

Cassinis, G.; Perotti, C.R. & Ronchi, A. (2012). Permian continental basins in the Southern Alps (Italy) and peri-mediterranean correlations. *International Journal of Earth Sciences/GR Geologische Rundschau*, 101: 129–157.

Colom, G. (1975). *Geología de Mallorca*. Gráficas Miramar, Diputación Provincial de Baleares, Palma. 2 vol., 552 pp.

Cuevas-López, F. (1958a). *Informe geológico y minero de los yacimientos de cobre de Banyalbufar y Estallenchs, Mallorca*. Barcelona. 37 pp. + 8 figs.

Cuevas-López, F. (1958b). *Informe geológico y minero de los yacimientos de cobre de Banyalbufar y Valldemosa, Mallorca*. Barcelona. 23 pp. + 7 figs.

Darder, B. (1914). El Triásico de Mallorca. *Trabajos del Museo Nacional de Ciencias Naturales, Serie Geológica*, 7: 85 pp. + 1 map + 1 tab.

Diez, J.B. (2000). *Geología y Paleobotánica de la Facies Buntsandstein en la Rama Aragonesa de la Cordillera Ibérica. Implicaciones paleogeográficas en el Peritethys Occidental.* Ph.D. dissertation. Universidad de Zaragoza–Université Pierre & Marie Curie, Paris VI, Zaragoza, Paris. 424 pp.

Diez, J.B.; Broutin, J. & Ferrer, J. (2005). Difficulties encountered in defining the Permian–Triassic boundary in Buntsandstein facies of the western Peritethyan domain based on palynological data. *Palaeogeography, Palaeoclimatology, Palaeoecology*, 229: 40–53.

Fallot, P. (1922). *Étude Géologique de la Sierra de Majorque*. Librairie Polytechnique Ch. Béranger, Paris, Liège. 16 pp. + 8 pls. + 476 pp. + 9 pls.

Freeman, T. & Obrador, A. (1974). Paleosuelos y carbón en la zona distal del Buntsandstein español (Menorca, Mallorca, Islas Baleares). *In*: *Resúmenes del VII Congreso del Grupo Español de Sedimentología*. Grupo Español de Sedimentología, Bellaterra–Tremp: p. 56.

Freeman, T. & Obrador, A. (1979). Paleosoils and coal in the distal part of the Spanish Buntsandstein (Menorca and Mallorca, Balearic Islands). *Boletín de la Sociedad de Historia Natural de Baleares*, 23: 47–50.

Gand, G.; De La Horra, R.; Galán-Abellán, B.; López-Gómez, J.; Barrenechea, J.F.; Arche, A. & Benito, M.I. (2010). New ichnites from the Middle Triassic of the Iberian Ranges

(Spain): palaeoenvironmental and paleogeographical implications. *Historical Biology*, 22(1–3): 40–56.

Gómez-Gras, D.M. (1992). *El Permotrías de las Baleares, de la Cordillera Costero Catalana y de la vertiente mediterránea de la Cordillera Ibérica: Facies y Petrología Sedimentaria*. Ph.D. dissertation. Universitat Autònoma de Barcelona, Barcelona. XIX + 242 pp. + 55 figs. + 7 tabs.

Gómez-Gras, D. (1993). El Permotrías de las Baleares y de la vertiente mediterránea de la Cordillera Ibérica y del Maestrat: Facies y Petrología Sedimentaria (Parte II). *Boletín Geológico y Minero*, 104: 467–515.

Grauvogel-Stamm, L. & Álvarez-Ramis, C. (1996). Conifères et pollen in situ du Buntsandstein de l'île de Majorque (Baléares, Espagne). *Cuadernos de Geología Ibérica*, 20: 229–243.

Hermite, H. (1879). *Études géologiques sur les îles Baléares. Première partie: Majorque et Minorque*. Pichon et Savy, Paris. 362 pp. + 5 pls.

Hermite, H. (1888). Estudios Geológicos de las Islas Baleares. *Boletín de la Comisión del Mapa Geológico*, 15: 1–244 + 4 pl.

Juárez-Ruiz, J. & Wachtler, M. (2015). Early–middle Triassic (Anisian) fossil flora from Majorca (Spain). *Dolomythos*, 2015: 1–49.

Juncal, M.A. (2019). *Nuevas aportaciones a la palinoestratigrafía pérmica del dominio peritético occidental*. Ph.D. dissertation. Universidade de Vigo, Vigo. 361 pp.

Liebrecht, T.; Fortuny, J.; Galobart, A.; Müller, J. & Sander, P.M. (2017). A large, multiple-tooth-rowed captorhinid reptile (Amniota: Eureptilia) from the Upper Permian of Mallorca (Balearic Islands, Western Mediterranean). *Journal of Vertebrate Paleontology*, 37(1): e1251936.

López-Gómez, J.; Arche, A. & Pérez-López, A. (2002). Permian and Triassic. *In*: Gibbons, W. & Moreno, M.T. (Eds.). *The Geology of Spain*. Geological Society, London: 185–212.

López-Gómez, J.; Alonso-Azcárate, J.; Arche, A.; Arribas, J.; Fernández-Barrenechea, J.; Borruel-Abadía, V.; Bourquin, S.; Cadenas, P.; Cuevas, J.; De la Horra, R.; Díez, J.B.; Escudero-Mozo, M.J.; Fernández-Viejo, G.; Galán-Abellán, B.; Galé, C.; Gaspar-Escribano, J.; Gisbert-Aguilar, J.; Gómez-Gras, D.; Goy, A.; Gretter, N.; Heredia-Carballo, N.; Lago, M.; Lloret, J.; Luque, J.; Márquez, L.; Márquez-Aliaga, A.; Martín-Algarra, A.; Martín-Chivelet, J.; Martín-González, F.; Marzo, M.; Mercedes-Martín, R.; Ortí, F.; Pérez-López, A.; Pérez-Valera, F.; Pérez-Valera, J.A.; Plasencia, P.; Ramos, E.; Rodríguez-Méndez, L.; Ronchi, A.; Salas, R.; Sánchez-Fernández, D.; Sánchez-Moya, Y.; Sopeña, A.; Suárez-Rodríguez, Á.; Tubía, J.M.; Ubide, T.; Valero-Garcés, B.; Vargas, H. & Viseras, C. (2019). Permian-Triassic rifting stage. *In*: Vergés, J. & Kullberg, J.C. (Coord.). *The Geology of Iberia: A Geodynamic Approach. Volume 3: The Alpine Cycle*. Springer, Cham: 29–112.

Matamales-Andreu, R.; Fortuny, J.; Mujal, E. & Galobart, À. (2019). Tetrapod tracks from the Permian of Mallorca (western Mediterranean): preliminary data, biostratigraphic and biogeographic inferences. *In*: *The Palaeontological Association, 63rd annual meeting, 15th–21st December 2019*. The Palaeontological Association, València: p. 107.

Matamales-Andreu, R.; Peñalver, E.; Mujal, E.; Oms, O.; Scholze, F.; Juárez, J.; Galobart, À. & Fortuny, J. (2021a). Early–Middle Triassic fluvial ecosystems of Mallorca (Balearic Islands): biotic communities and environmental evolution in the equatorial western peri-Tethys. *Earth-Science Reviews*, 222: 103783.

Matamales-Andreu, R.; Mujal, E.; Galobart, À. & Fortuny, J. (2021b). Insights on the evolution of synapsid locomotion based on tetrapod tracks from the lower Permian of Mallorca (Balearic Islands, western Mediterranean). *Palaeogeography, Palaeoclimatology, Palaeoecology*, 579: 110589.

Matamales-Andreu, R.; Roig-Munar, F.X.; Oms, O.; Galobart, À. & Fortuny, J. (2021c). A captorhinid-dominated assemblage from the palaeoequatorial Permian of Menorca (Balearic Islands, western Mediterranean). *Earth and Environmental Science Transactions of the Royal Society of Edinburgh*, 112(2): 125–145.

Martí, J.; Paniello, X.; Pomar, L.; Ramos, E. & Rodríguez-Perea, A. (1985). El Triásico de las Baleares. *In*: Mateu Ibars, F. & Marzo, M. (Eds.). *Resúmenes del II Coloquio de Estratigrafía y Paleogeografía del Pérmico y Triásico de España*. Institut d'Estudis Ilerdencs and Grupo Español del Mesozoico, La Seu d'Urgell: 84–85.

Maxbauer, D.P.; Feinberg, J.M. & Fox, D.L. (2016). MAX UnMix: A web application for unmixing magnetic coercivity distributions. *Computers & Geosciences*, 95: 140–145.

Nolan, H. (1887). Note sur le Trias de Minorque et Majorque. *Bulletin de la Société géologique de France*, 15: 592–599.

Nolan, H. (1888). El Trias de Mallorca y Menorca. *Boletín de la Comisión del Mapa Geológico*, 15: 234–241.

Obrador, A. (1983). El Pérmico de las Baleares. *In*: Martínez-Díaz, C. (Ed.). *Carbonífero y Pérmico de España, X Congreso Internacional de Estratigrafía y Geología del Carbonífero*. Ministerio de Industria y Energía, Instituto Geológico y Minero de España, Madrid: 463–470.

Pomar-Gomà, L. (1979). *The Triassic of the Balearic Islands*. Geology Department, Palma de Mallorca University, Palma. 49 pp. + 7 Petrologic Logs.

Ramos, A. (1995). Transition from alluvial to coastal deposits (Permian–Triassic) on the Island of Mallorca, western Mediterranean. *Geological Magazine*, 132(4): 435–447.

Ramos, A. & Doubinger, J. (1989). Premières datations palynologiques dans le facies Buntsandstein de l'île de Majorque (Baléares, Espagne). *Comptes Rendus de l'Académie des Sciences de Paris, Série 2*, 309: 1089–1094.

Ramos, A. & García-Ramos, S. (1992). Niveles de bioturbación en las facies tipo Buntsandstein del Pérmico-Triásico de Mallorca. *In*: García-Ramos, J.C. (Ed.). *Reunión Monográfica sobre Biosedimentación*, Servicio de Publicaciones de la Universidad de Oviedo, Oviedo: 41–43.

Ramos, A.; Olmo, P. del & Alvaro, M. (1985). El Buntsandstein de la isla de Mallorca. *In*: Mateu Ibars, F. & Marzo, M. (Eds.). *Resúmenes del II Coloquio de Estratigrafía y Paleogeografía del Pérmico y Triásico de España.* Institut d'Estudis Ilerdencs and Grupo Español del Mesozoico, La Seu d'Urgell: 103–104.

Rodríguez-Perea, A.; Ramos-Guerrero, E.; Pomar, L.; Paniello, X.; Obrador, A. & Martí, J. (1987). El Triásico de las Baleares. *Cuadernos de Geología Ibérica*, 11: 295–321.

Santanach, P.; Banda, E.; Calvet, F.; Carreras, J.; Casas, J.M.; Fontboté, J.M.; Fornós, J.; Gisbert, J.; Julivert, M.; Marzo, M.; Rodríguez-Perea, A.; Salas, R. & Souquet, P. (Eds.) (1986). *Història Natural dels Països Catalans, 1: Geologia (I).* Enciclopèdia Catalana, Barcelona. 439 pp.

Sastre, J. & Sastre, V. (2005). *El litoral de Mallorca: marinas de Tramuntana, de Sant Elm al Port de Sóller*. Diario de Mallorca, Palma. 304 pp.

Vera, J.-A.; Alonso-Chaves, F.M.; Andreo, B.; Arias, C.; Azañón, J.M.; Balanyá, J.C.; Barón, A.; Booth-Rea, G.; Castro, J.M.; Chacón, B.; Company, M.; Crespo-Blanc, A.; Delgado, F.; Díaz de Federico, A.; Esteras, M.; Estévez, A.; Fernández, J.; Fornós, J.J.; Galindo-Zaldívar, J.; García-Casco, A.; García-Dueñas, V.; García-Hernández, M.; Garrido, C.J..; Gea, G.A. de; Gelabert, B.; Gervilla, F.; González-Lodeiro, F.; Jabaloy, A.; López-Garrido, A.C.; Luján, M.; Martín-Algarra, A.; Martín-Chivelet, J.; Martín-Martín, M.; Molina, J.M.; Morata, D.; Nieto, J.M.; Obrador, A.; O'Dogherty, L.; Orozco, M.; Pérez-López, A.; Pomar, L.; Puga, E.; Ramos, E.; Rey, J.; Rivas, P.; Rodríguez-Cañero, R.; Ruiz-Cruz, M.D.; Ruiz-Ortiz, P.A.; Sàbat, F.; Sánchez-Gómez, M.; Sánchez-Navas, A.; Sandoval, J.; Sanz de Galdeano, C.; Soto, J.I.; Torres-Roldán, R.L. & Villas, L. (2004). Capítulo 4. Cordillera Bética y Baleares. *In*: Vera, J.-A. (Ed.). *Geología de España.* Instituto Geológico y Minero de España, Madrid: 346–464.

Virgili, C. (2008). The Permian-Triassic transition: Historical review of the most important ecological crises with special emphasis on the Iberian Peninsula and Western-Central Europe. *Journal of Iberian Geology*, 34(1): 123–158.

Virgili, C.; Cassinis, G. & Broutin, J. (2006). Permian to Triassic sequences from selected continental areas of southwestern Europe. *Geological Society, London, Special Publications*, 265: 231–259.

Supplementary Logs and Supplementary Correlations

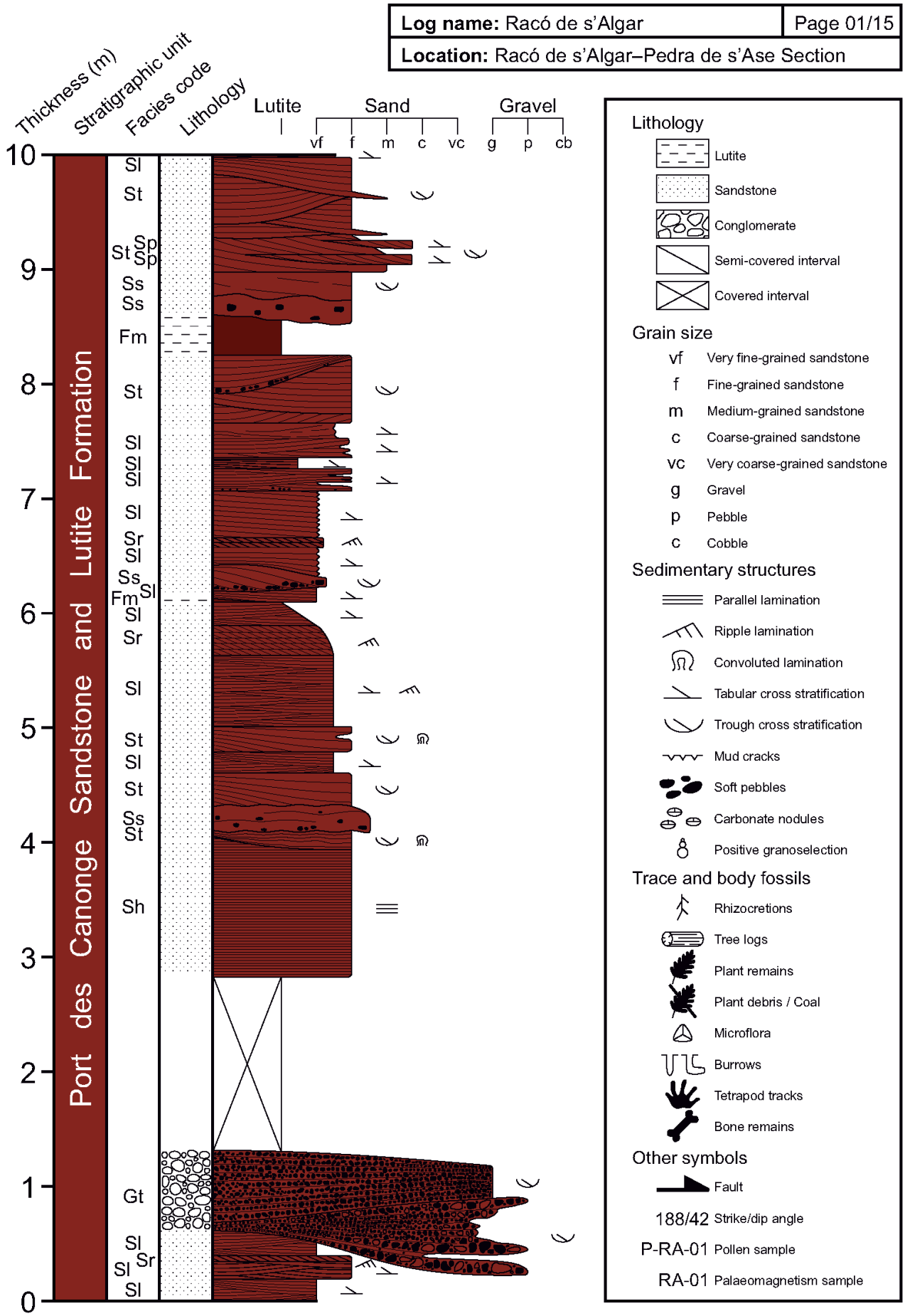
Log name: Racó de s'Algar
Page 01/15
Location: Racó de s'Algar–Pedra de s'Ase Section
Thickness (m)
Stratigraphic unit
Facies code
Lithology
Lutite
Sand
Gravel
vf f m c vc g p cb
Port des Canonge Sandstone and Lutite Formation
Sl St Sp Ss Fm Sr Gt
Lithology
Lutite
Sandstone
Conglomerate
Semi-covered interval
Covered interval
Grain size
vf Very fine-grained sandstone
f Fine-grained sandstone
m Medium-grained sandstone
c Coarse-grained sandstone
vc Very coarse-grained sandstone
g Gravel
p Pebble
c Cobble
Sedimentary structures
Parallel lamination
Ripple lamination
Convoluted lamination
Tabular cross stratification
Trough cross stratification
Mud cracks
Soft pebbles
Carbonate nodules
Positive granoselection
Trace and body fossils
Rhizocretions
Tree logs
Plant remains
Plant debris / Coal
Microflora
Burrows
Tetrapod tracks
Bone remains
Other symbols
Fault
188/42 Strike/dip angle
P-RA-01 Pollen sample
RA-01 Palaeomagnetism sample

Log name: Racó de s'Algar	Page 02/15
Location: Racó de s'Algar–Pedra de s'Ase Section	

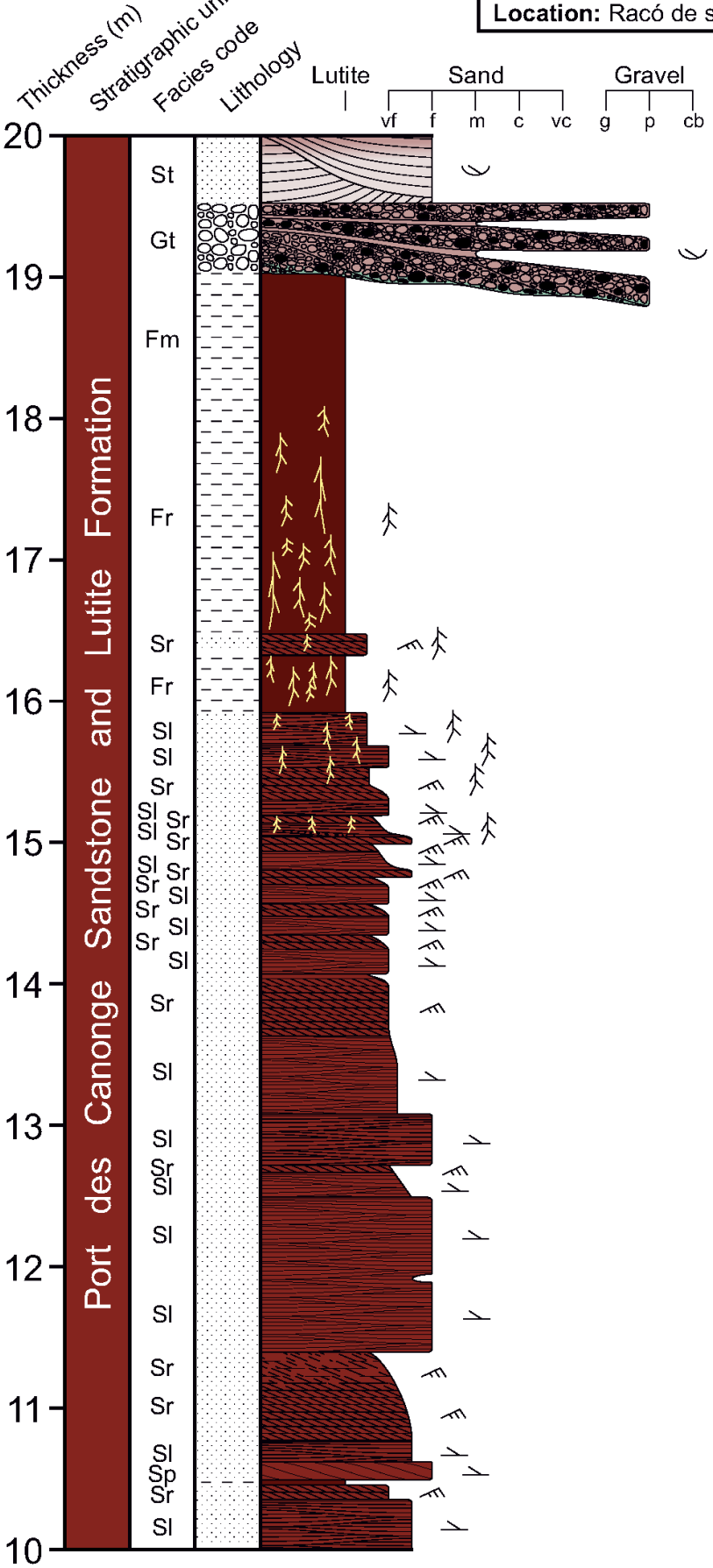

Lithology
- Lutite
- Sandstone
- Conglomerate
- Semi-covered interval
- Covered interval

Grain size
- vf Very fine-grained sandstone
- f Fine-grained sandstone
- m Medium-grained sandstone
- c Coarse-grained sandstone
- vc Very coarse-grained sandstone
- g Gravel
- p Pebble
- c Cobble

Sedimentary structures
- Parallel lamination
- Ripple lamination
- Convoluted lamination
- Tabular cross stratification
- Trough cross stratification
- Mud cracks
- Soft pebbles
- Carbonate nodules
- Positive granoselection

Trace and body fossils
- Rhizocretions
- Tree logs
- Plant remains
- Plant debris / Coal
- Microflora
- Burrows
- Tetrapod tracks
- Bone remains

Other symbols
- Fault
- 188/42 Strike/dip angle
- P-RA-01 Pollen sample
- RA-01 Palaeomagnetism sample

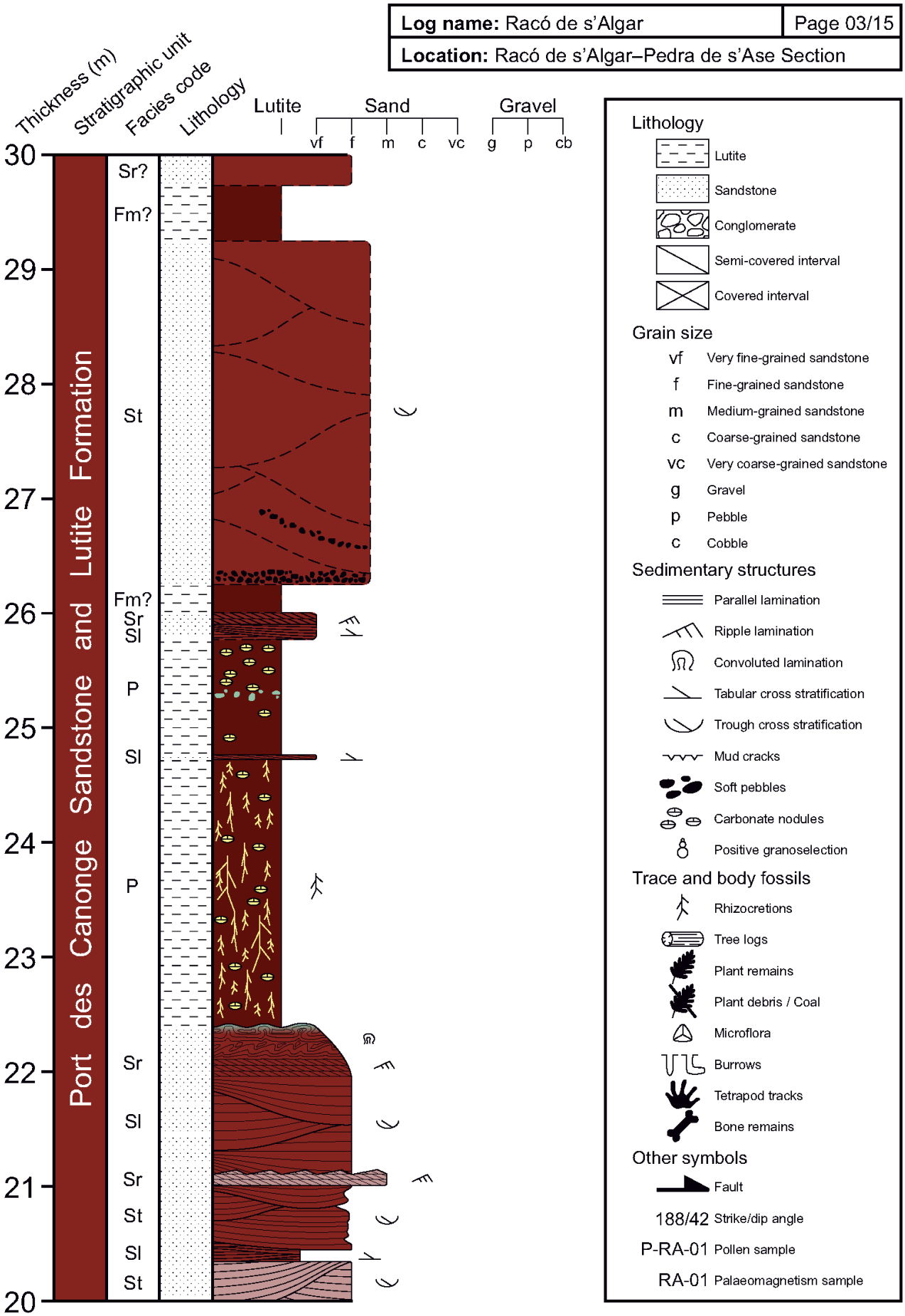
Log name: Racó de s'Algar
Page 03/15
Location: Racó de s'Algar–Pedra de s'Ase Section
Thickness (m)
Stratigraphic unit
Facies code
Lithology
Lutite
Sand
Gravel
vf f m c vc g p cb
Port des Canonge Sandstone and Lutite Formation
30
29
28
27
26
25
24
23
22
21
20
Sr?
Fm?
St
Fm?
Sr
Sl
P
Sl
P
Sr
Sl
Sr
St
Sl
St
Lithology
Lutite
Sandstone
Conglomerate
Semi-covered interval
Covered interval
Grain size
vf Very fine-grained sandstone
f Fine-grained sandstone
m Medium-grained sandstone
c Coarse-grained sandstone
vc Very coarse-grained sandstone
g Gravel
p Pebble
c Cobble
Sedimentary structures
Parallel lamination
Ripple lamination
Convoluted lamination
Tabular cross stratification
Trough cross stratification
Mud cracks
Soft pebbles
Carbonate nodules
Positive granoselection
Trace and body fossils
Rhizocretions
Tree logs
Plant remains
Plant debris / Coal
Microflora
Burrows
Tetrapod tracks
Bone remains
Other symbols
Fault
188/42 Strike/dip angle
P-RA-01 Pollen sample
RA-01 Palaeomagnetism sample

Log name: Racó de s'Algar	Page 04/15
Location: Racó de s'Algar–Pedra de s'Ase Section	

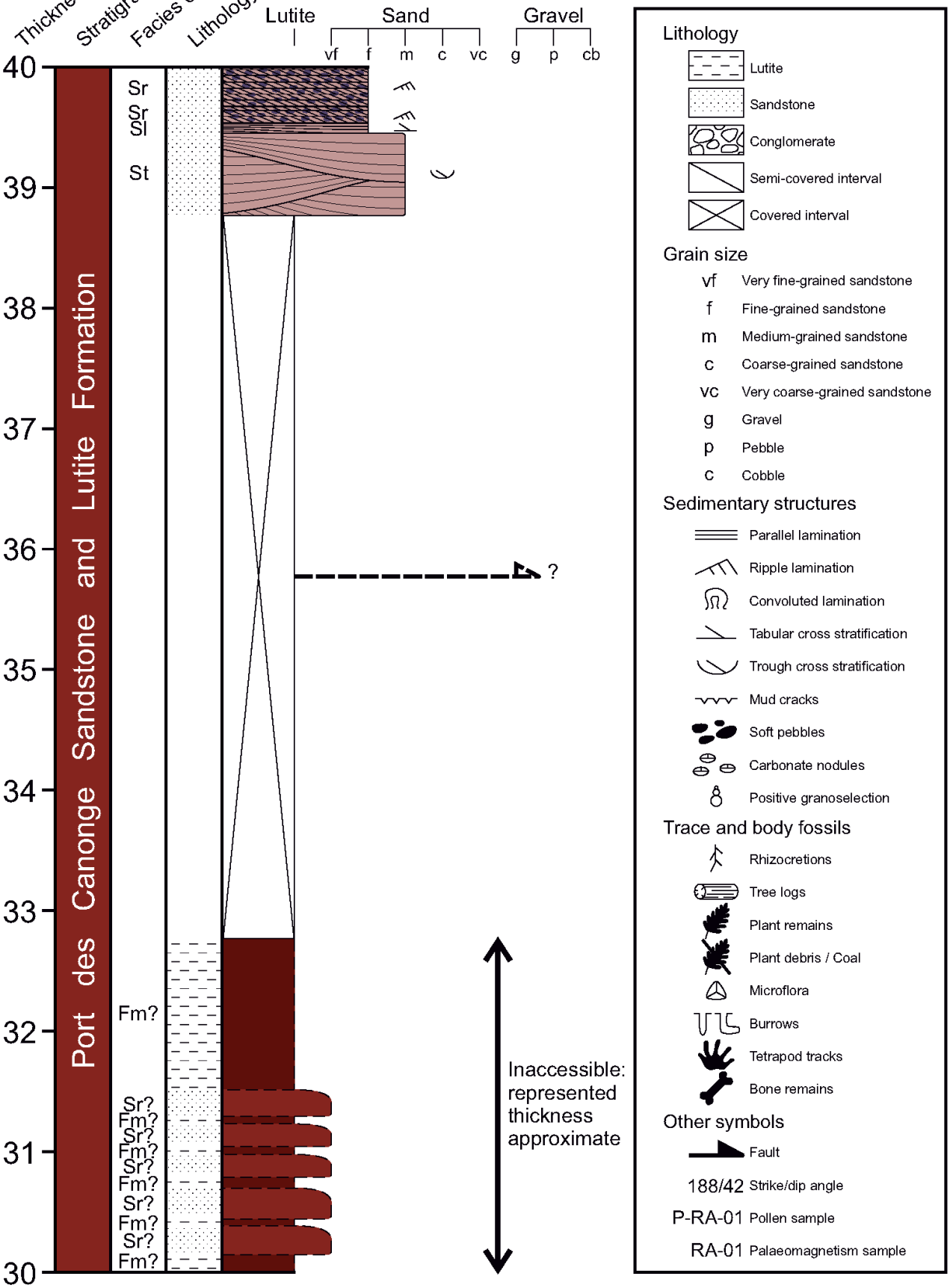

Log name: Racó de s'Algar	Page 05/15
Location: Racó de s'Algar–Pedra de s'Ase Section	

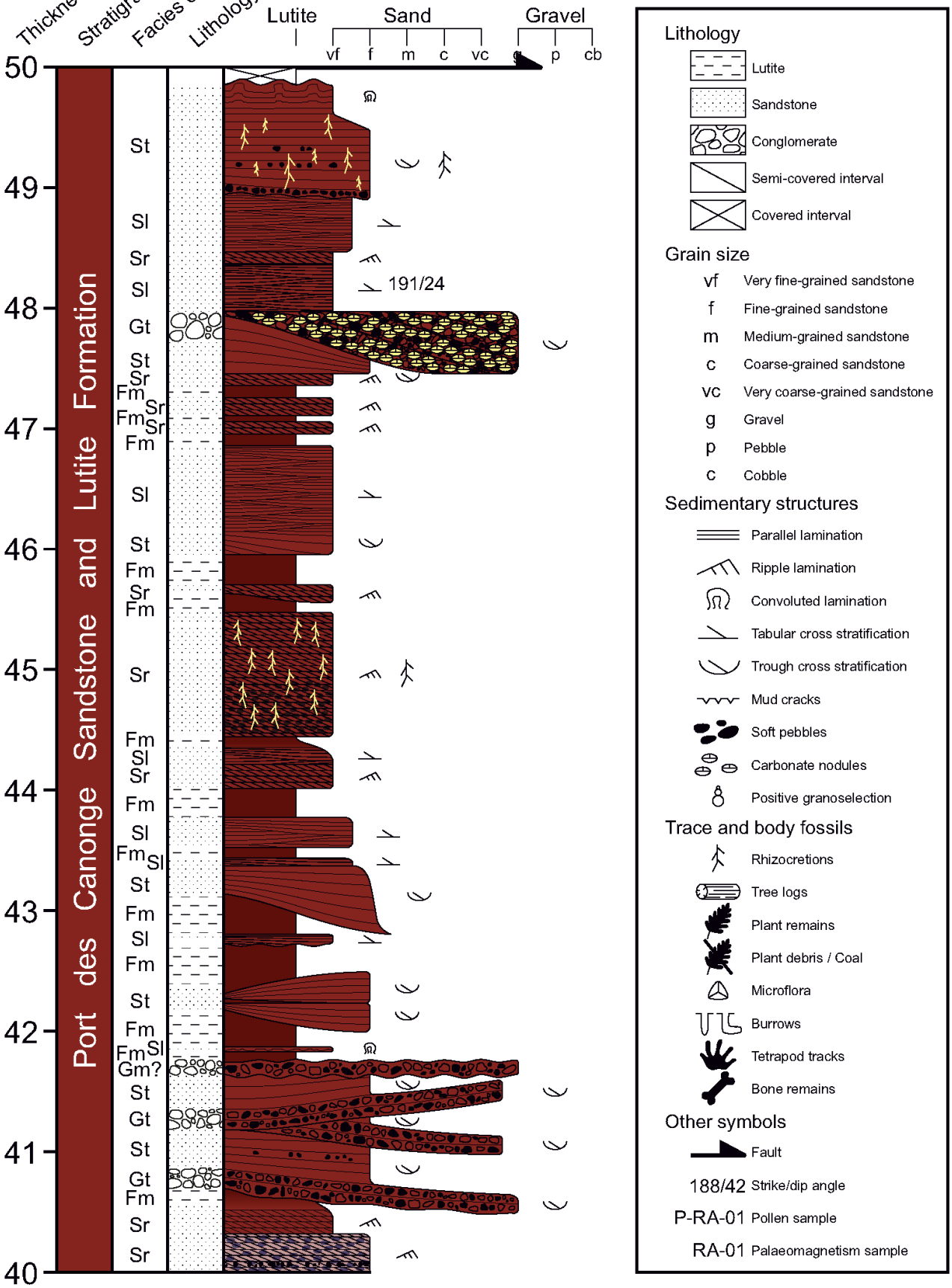

Log name: Racó de s'Algar	Page 06/15
Location: Racó de s'Algar–Pedra de s'Ase Section	

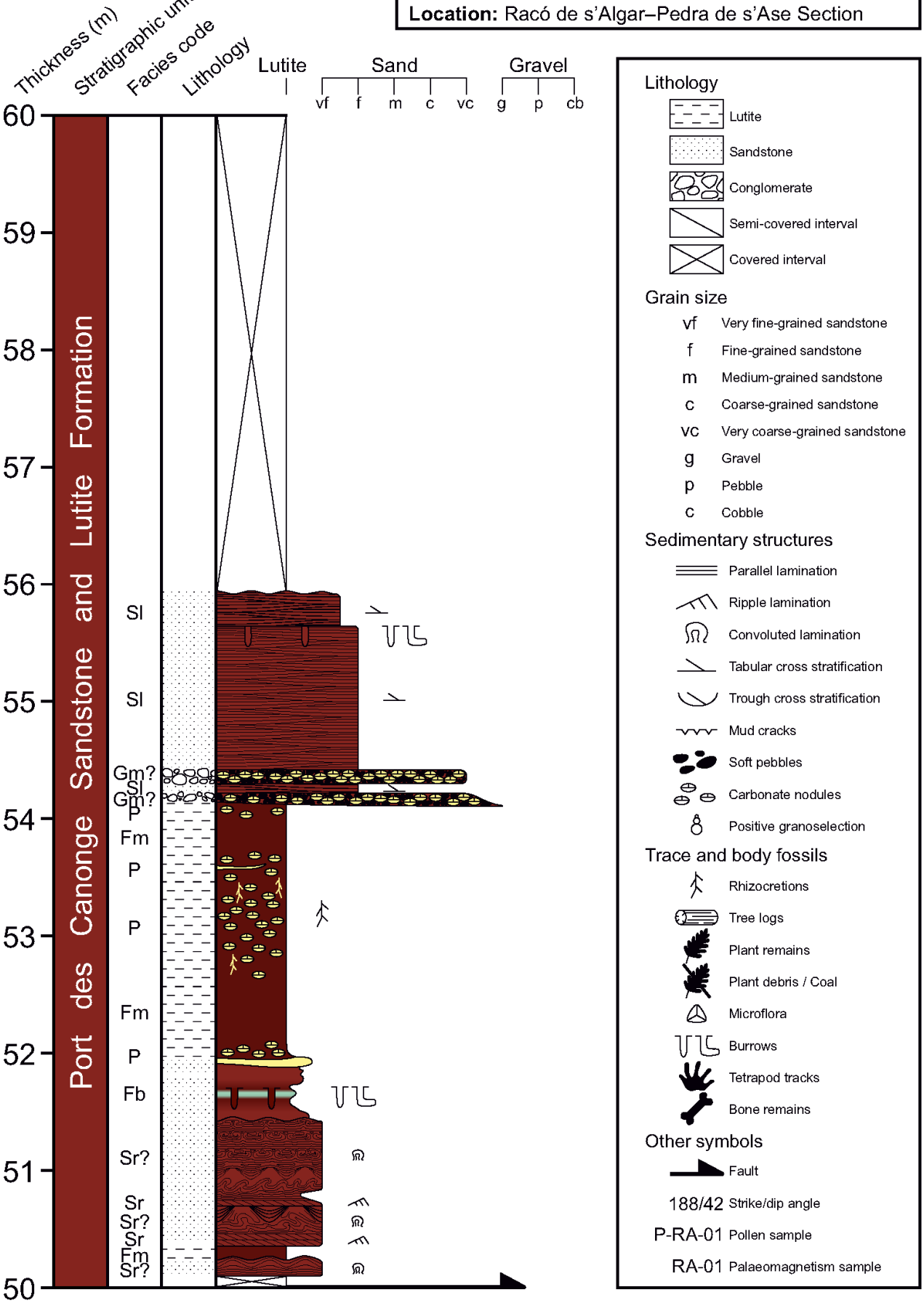

Log name: Racó de s'Algar	Page 07/15
Location: Racó de s'Algar–Pedra de s'Ase Section	

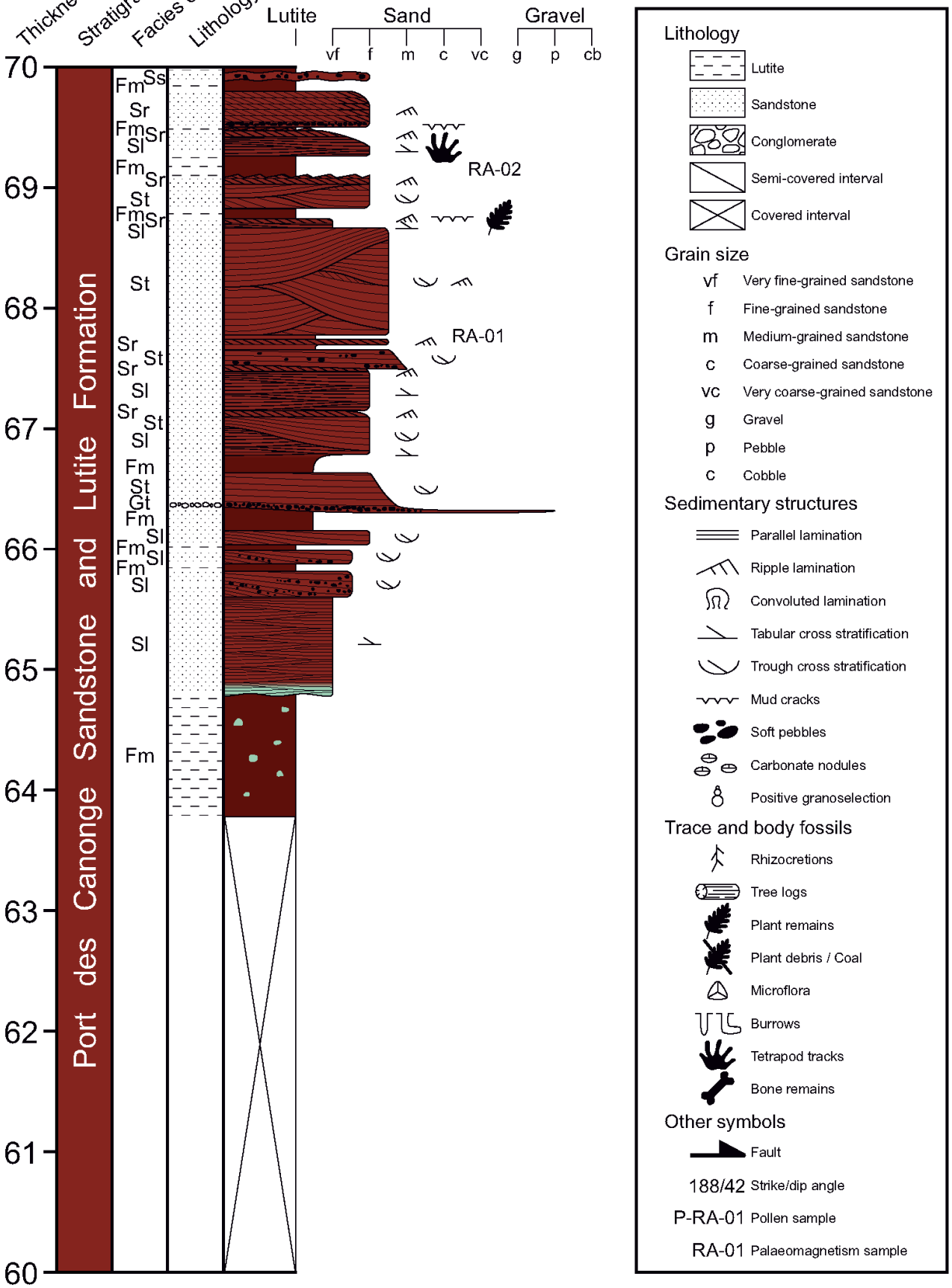

Log name: Racó de s'Algar	Page 08/15
Location: Racó de s'Algar–Pedra de s'Ase Section	

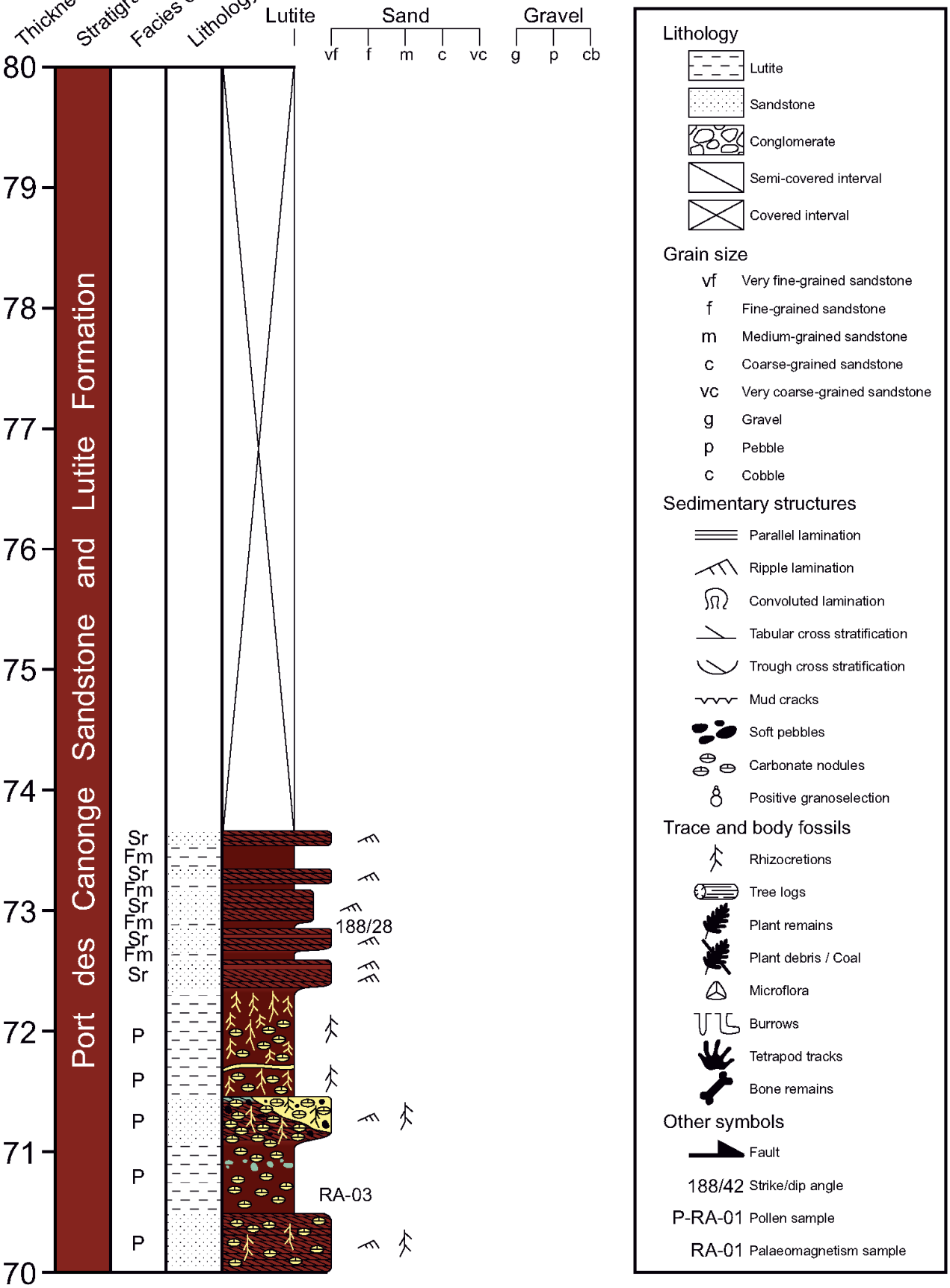

Log name: Racó de s'Algar	Page 09/15
Location: Racó de s'Algar–Pedra de s'Ase Section	

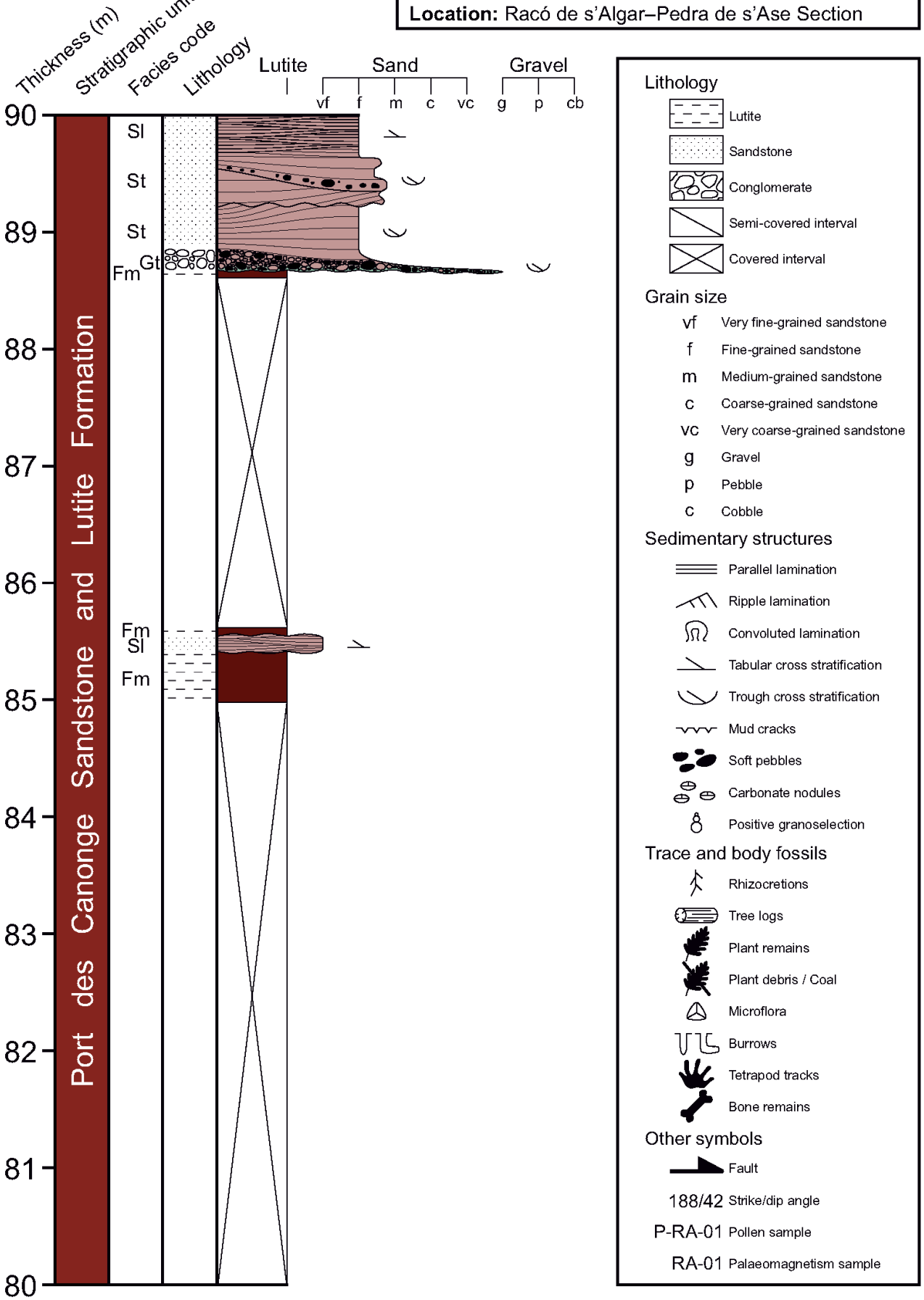

Lithology
- Lutite
- Sandstone
- Conglomerate
- Semi-covered interval
- Covered interval

Grain size
- vf Very fine-grained sandstone
- f Fine-grained sandstone
- m Medium-grained sandstone
- c Coarse-grained sandstone
- vc Very coarse-grained sandstone
- g Gravel
- p Pebble
- c Cobble

Sedimentary structures
- Parallel lamination
- Ripple lamination
- Convoluted lamination
- Tabular cross stratification
- Trough cross stratification
- Mud cracks
- Soft pebbles
- Carbonate nodules
- Positive granoselection

Trace and body fossils
- Rhizocretions
- Tree logs
- Plant remains
- Plant debris / Coal
- Microflora
- Burrows
- Tetrapod tracks
- Bone remains

Other symbols
- Fault
- 188/42 Strike/dip angle
- P-RA-01 Pollen sample
- RA-01 Palaeomagnetism sample

Log name: Racó de s'Algar	Page 10/15
Location: Racó de s'Algar–Pedra de s'Ase Section	

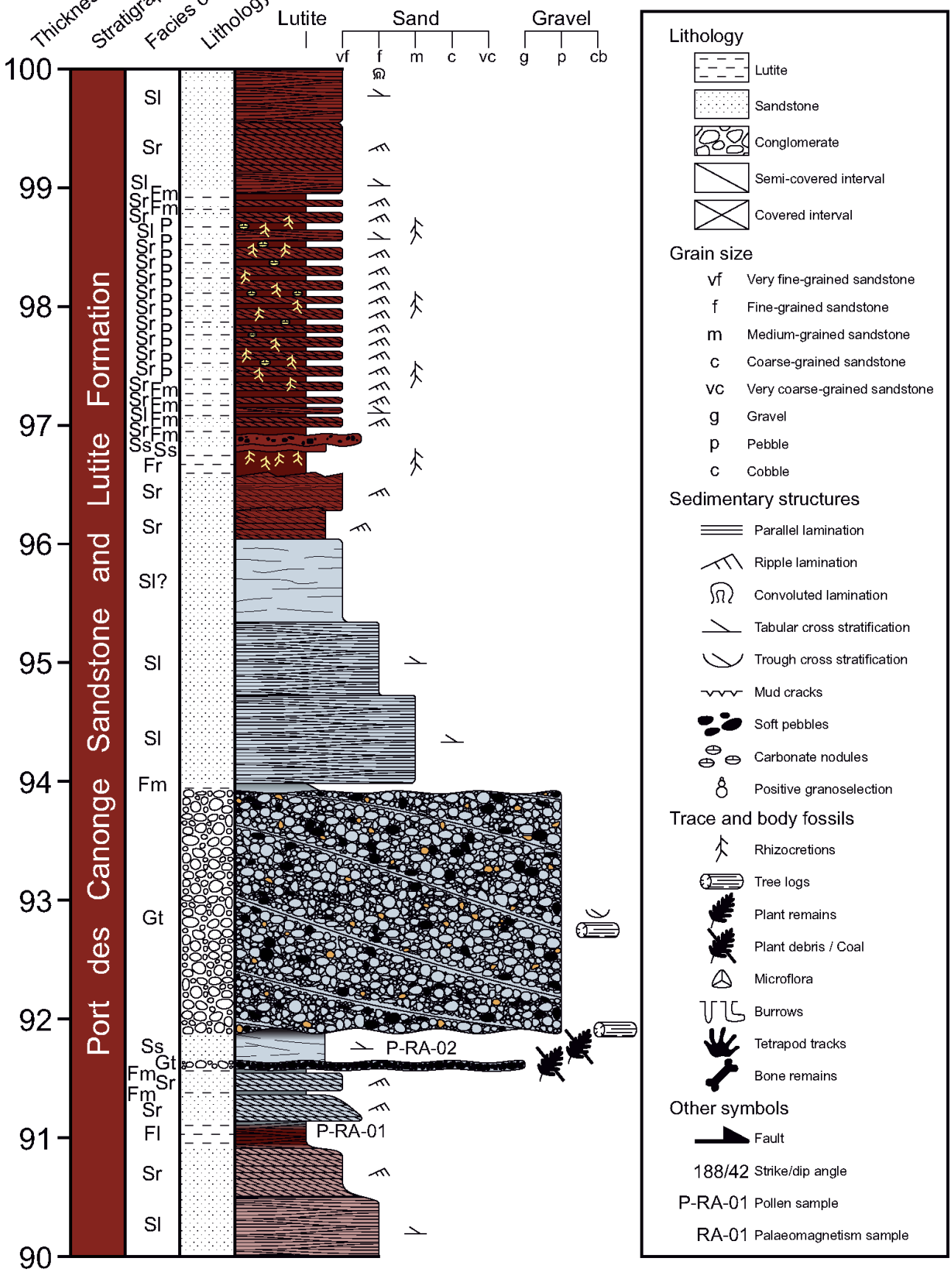

Log name: Racó de s'Algar | Page 11/15

Location: Racó de s'Algar–Pedra de s'Ase Section

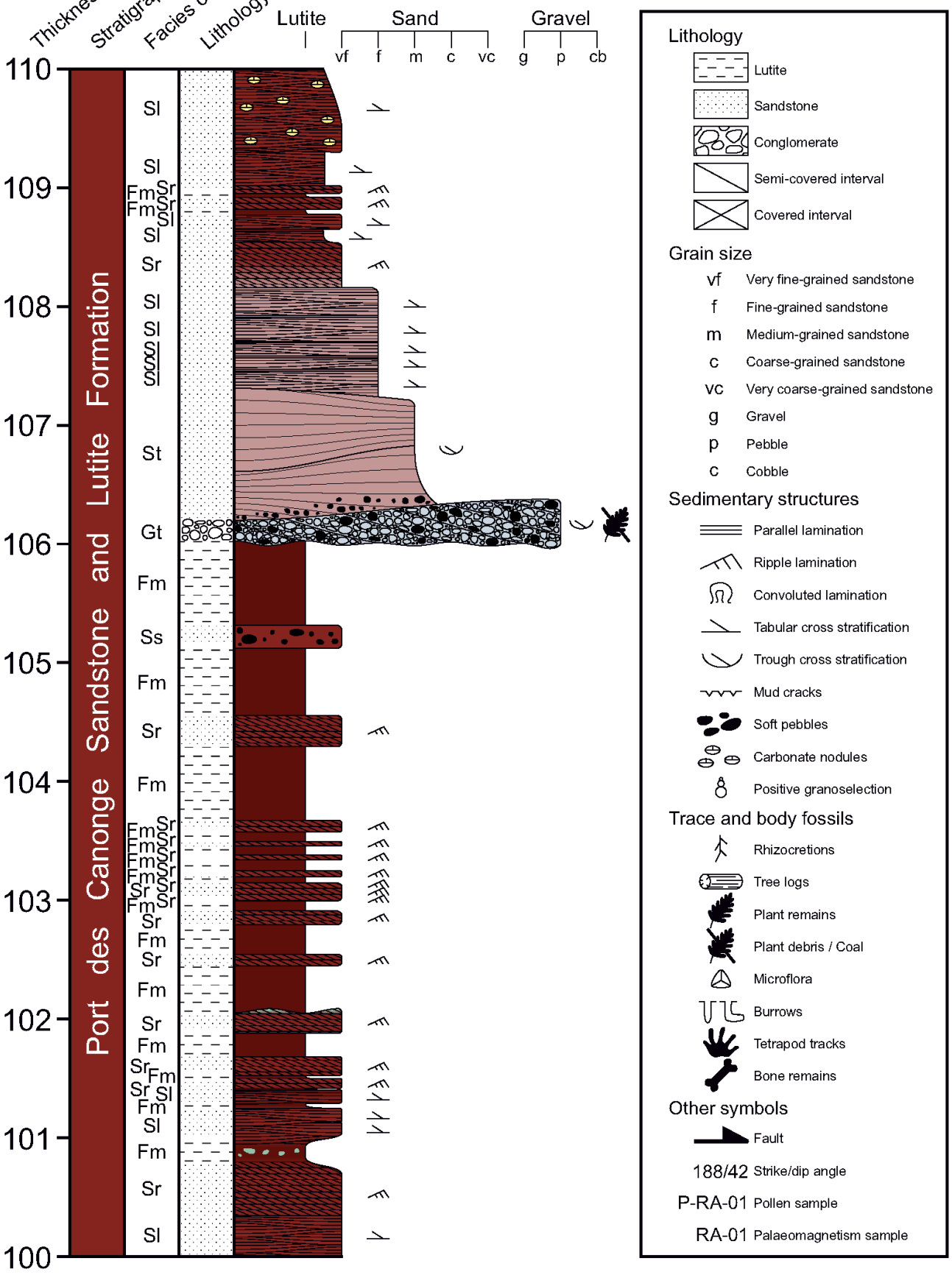

Log name: Racó de s'Algar	Page 12/15
Location: Racó de s'Algar–Pedra de s'Ase Section	

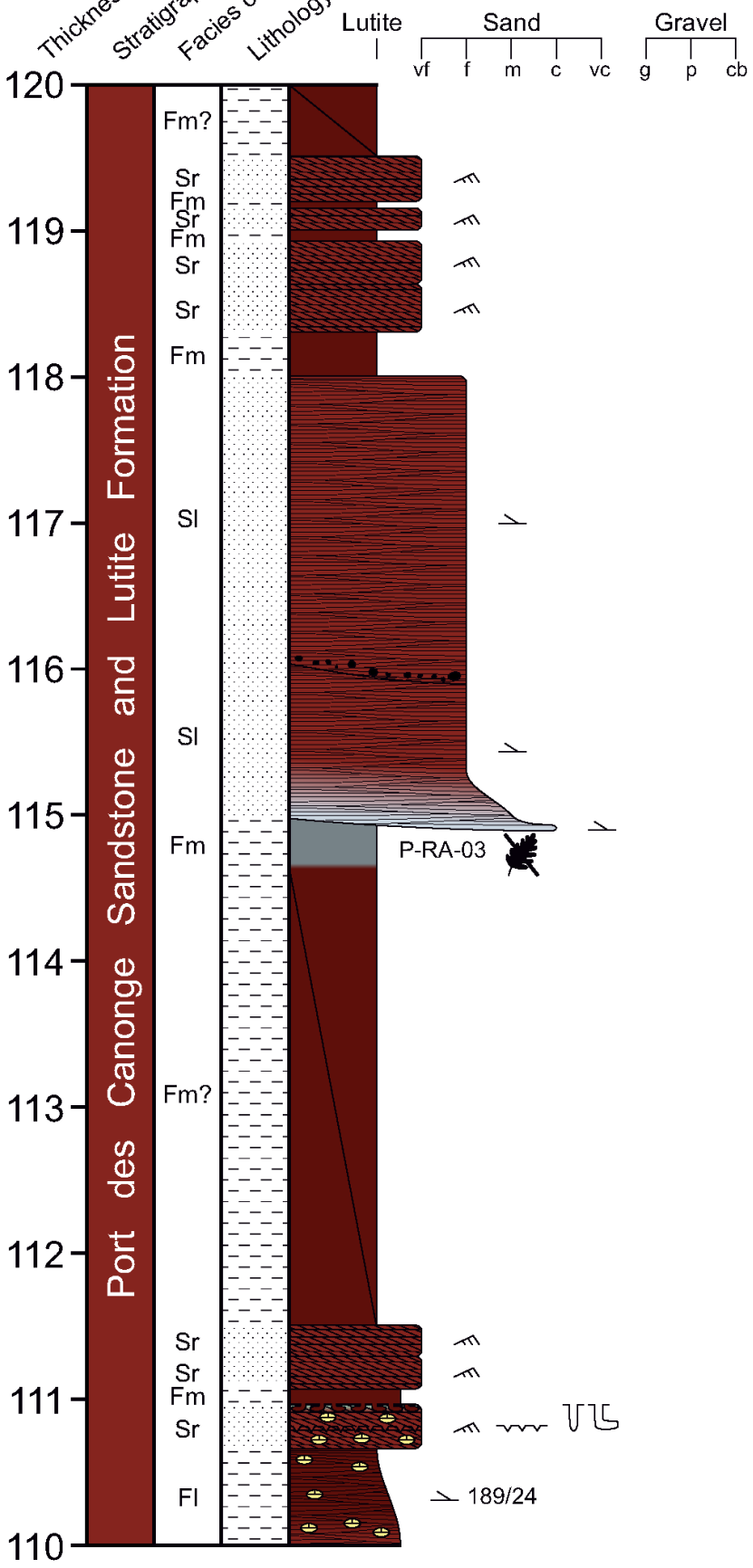

Lithology
- Lutite
- Sandstone
- Conglomerate
- Semi-covered interval
- Covered interval

Grain size
- vf Very fine-grained sandstone
- f Fine-grained sandstone
- m Medium-grained sandstone
- c Coarse-grained sandstone
- vc Very coarse-grained sandstone
- g Gravel
- p Pebble
- c Cobble

Sedimentary structures
- Parallel lamination
- Ripple lamination
- Convoluted lamination
- Tabular cross stratification
- Trough cross stratification
- Mud cracks
- Soft pebbles
- Carbonate nodules
- Positive granoselection

Trace and body fossils
- Rhizocretions
- Tree logs
- Plant remains
- Plant debris / Coal
- Microflora
- Burrows
- Tetrapod tracks
- Bone remains

Other symbols
- Fault
- 188/42 Strike/dip angle
- P-RA-01 Pollen sample
- RA-01 Palaeomagnetism sample

Log name: Racó de s'Algar	Page 13/15
Location: Racó de s'Algar–Pedra de s'Ase Section	

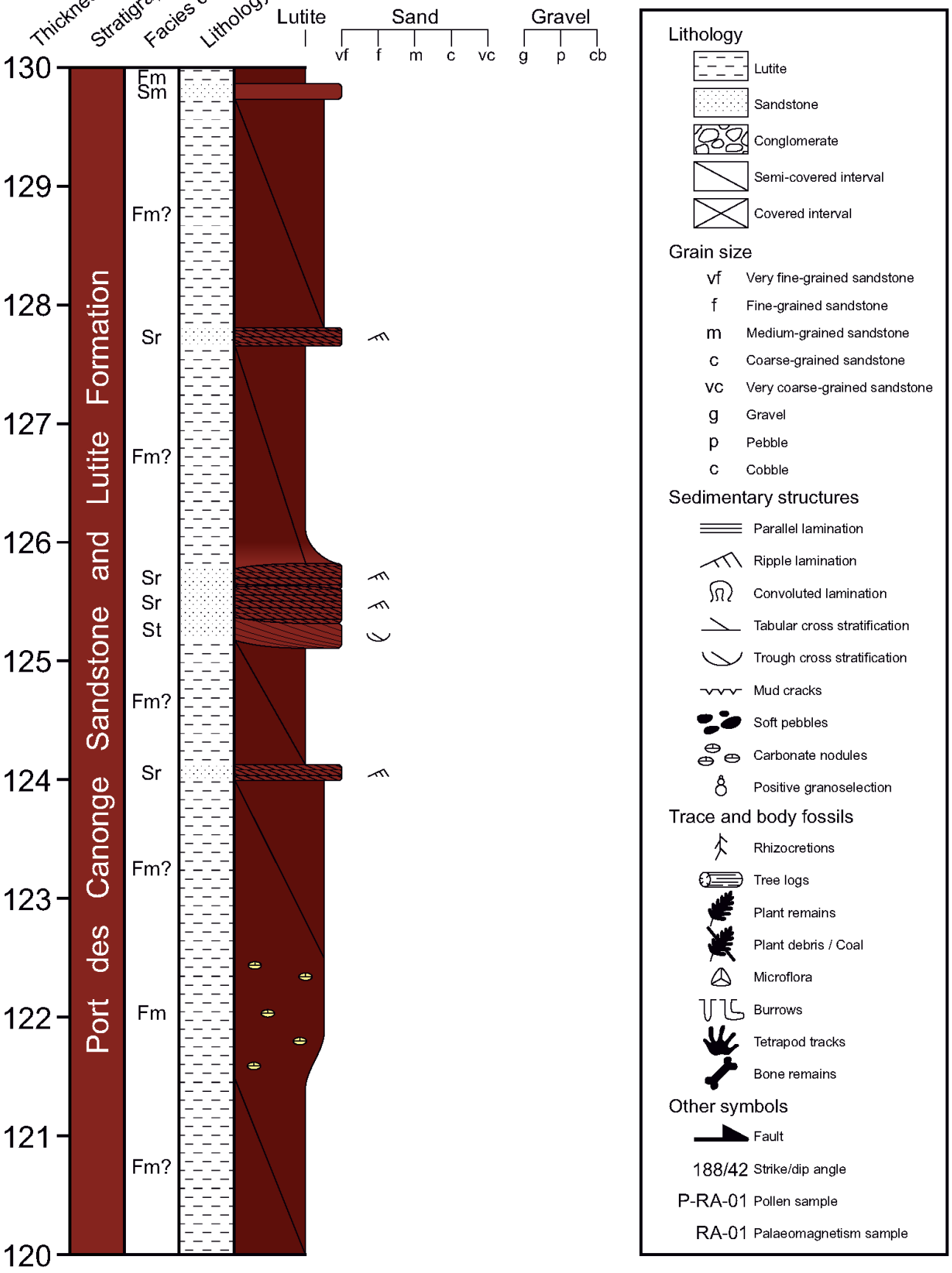

Log name: Racó de s'Algar	Page 14/15
Location: Racó de s'Algar–Pedra de s'Ase Section	

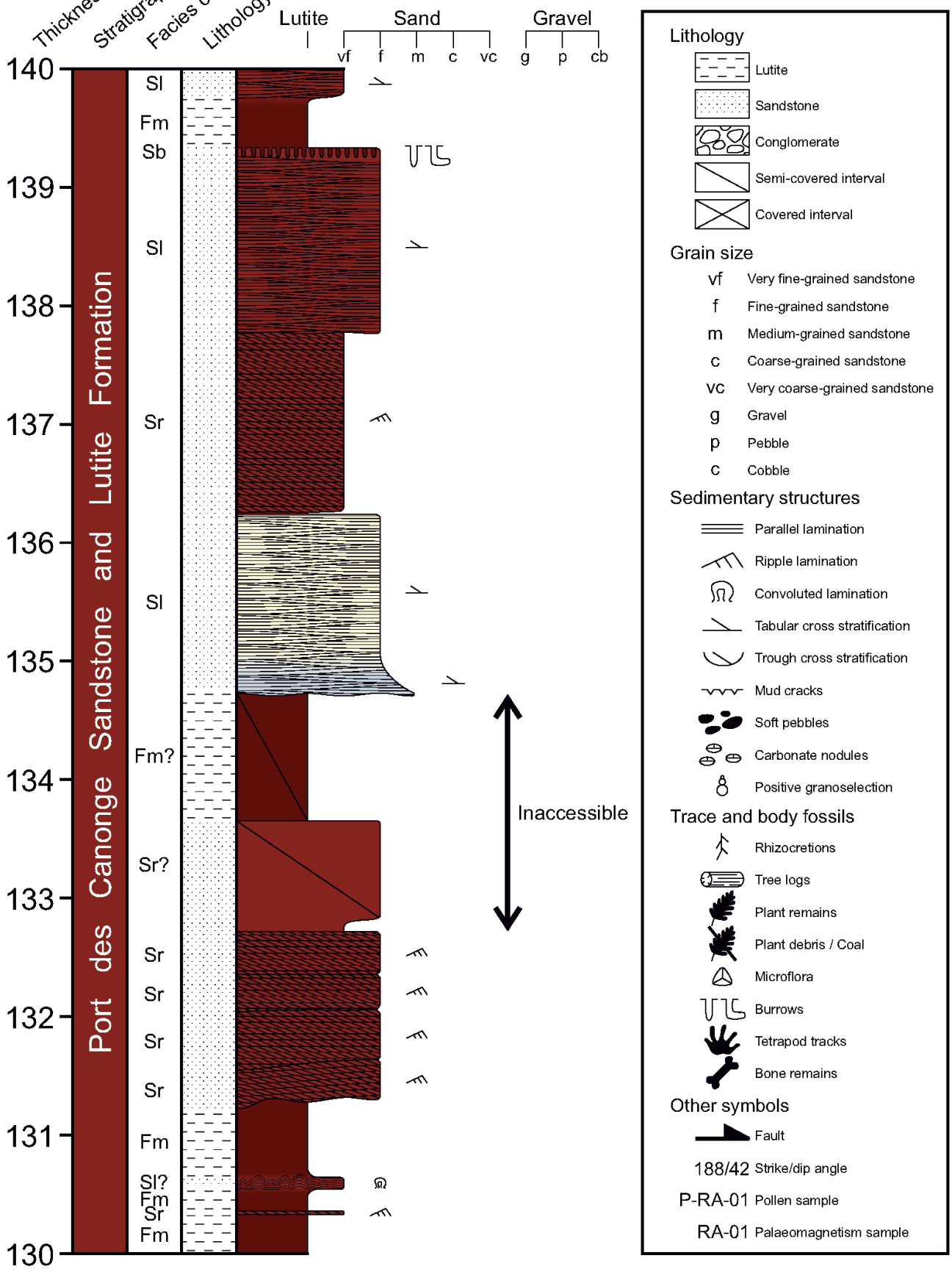

Log name: Racó de s'Algar	Page 15/15
Location: Racó de s'Algar–Pedra de s'Ase Section	

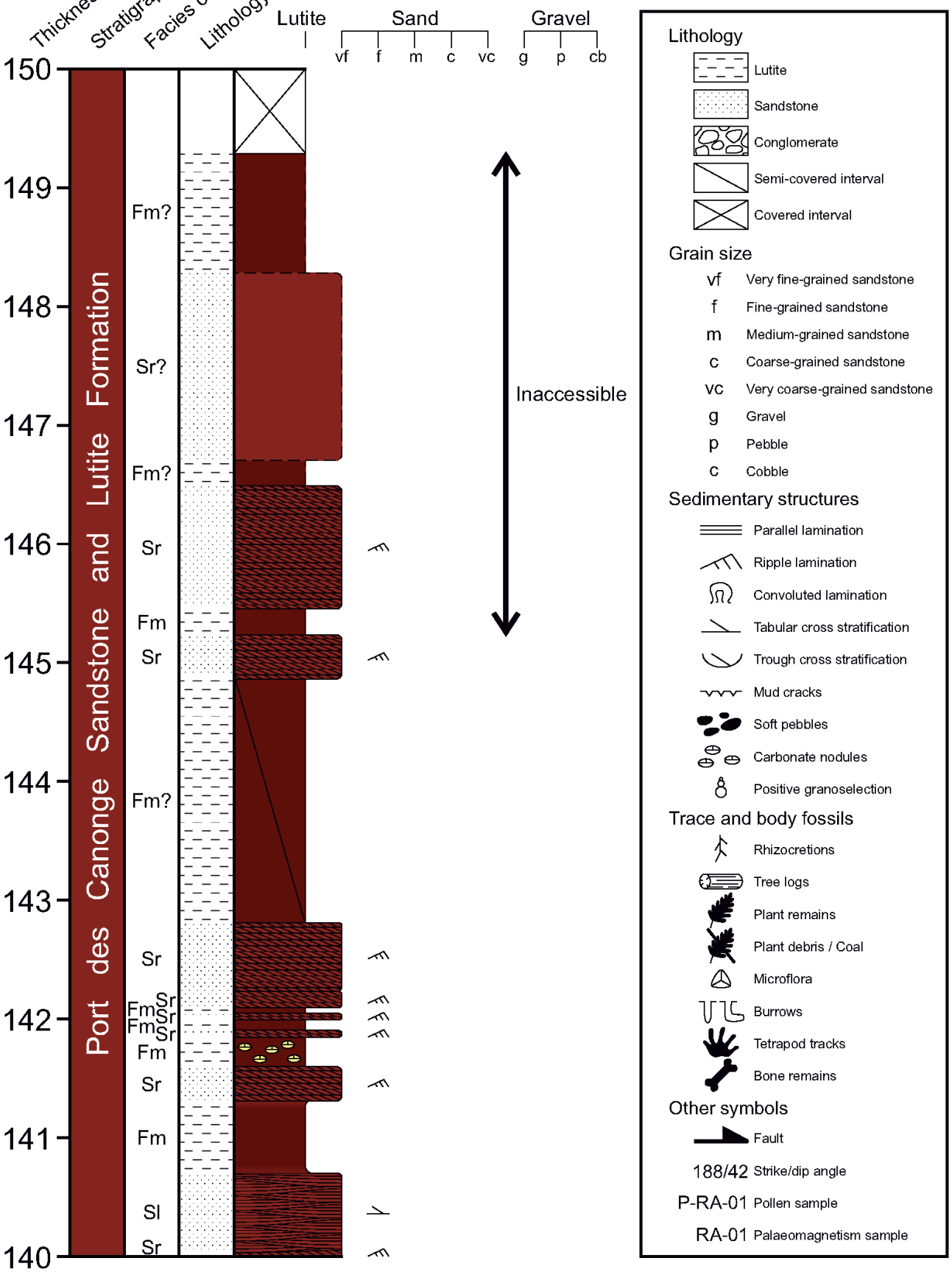

Log name: Torrent de na Nadala	Page 01/20
Location: Racó de s'Algar–Pedra de s'Ase Section	

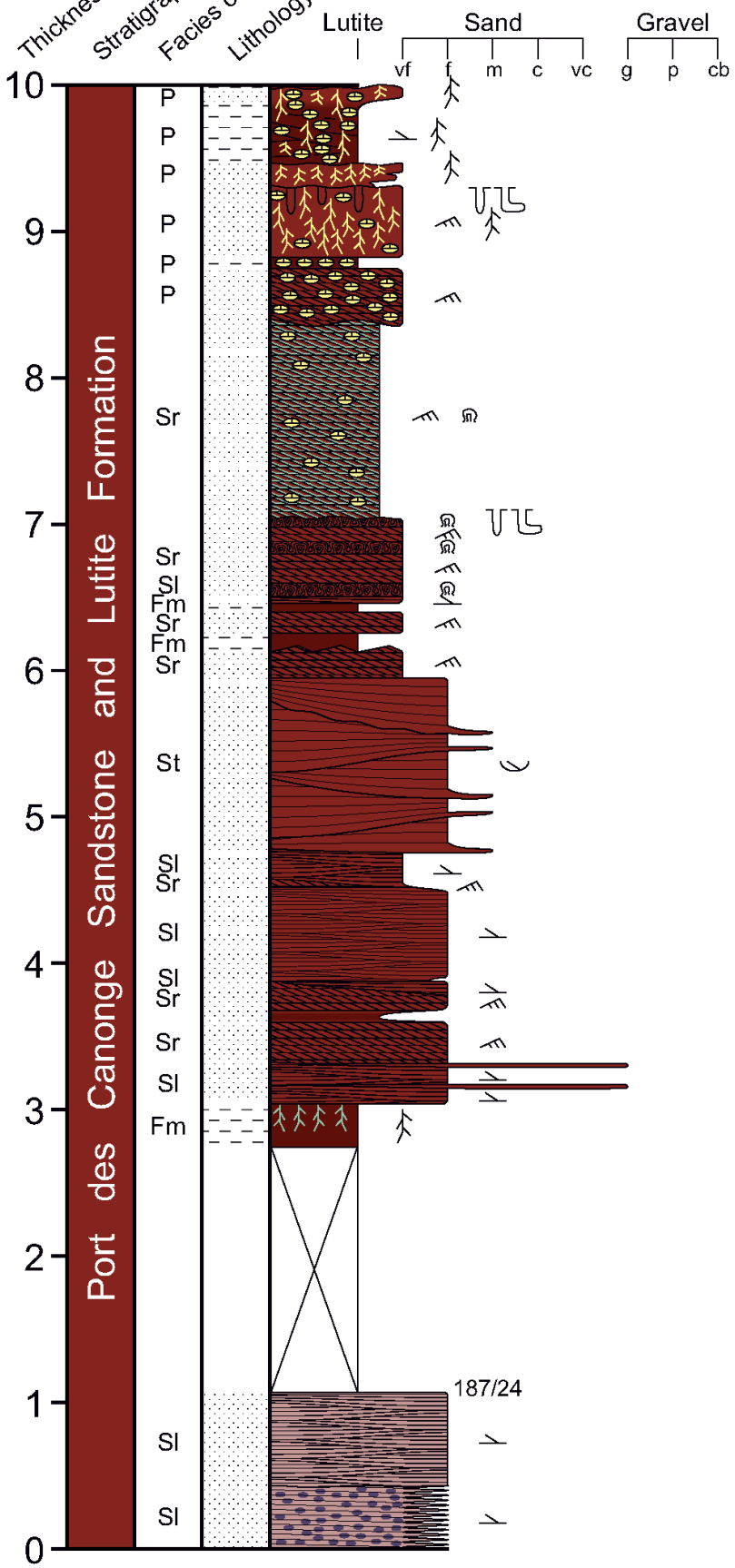

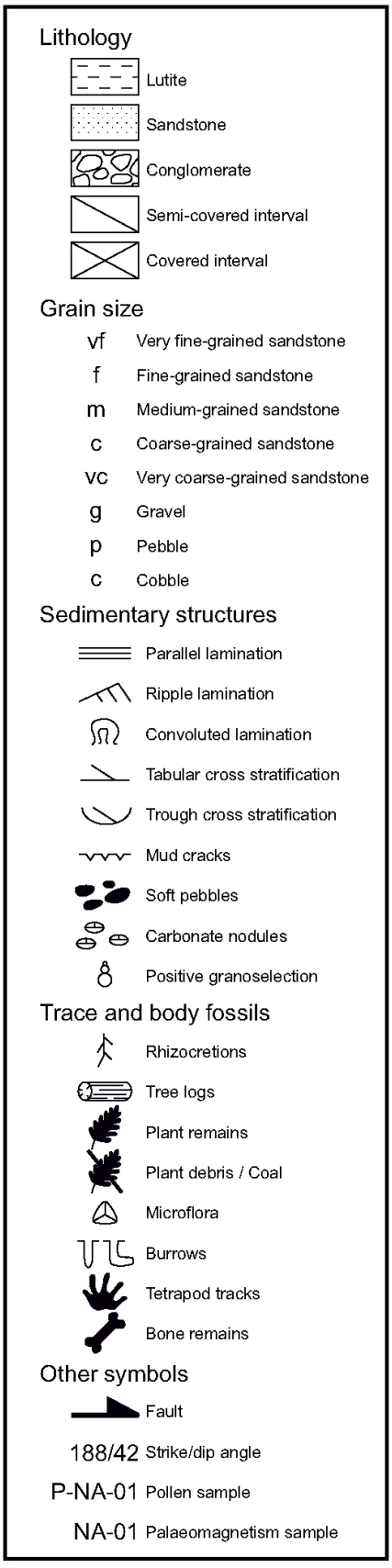

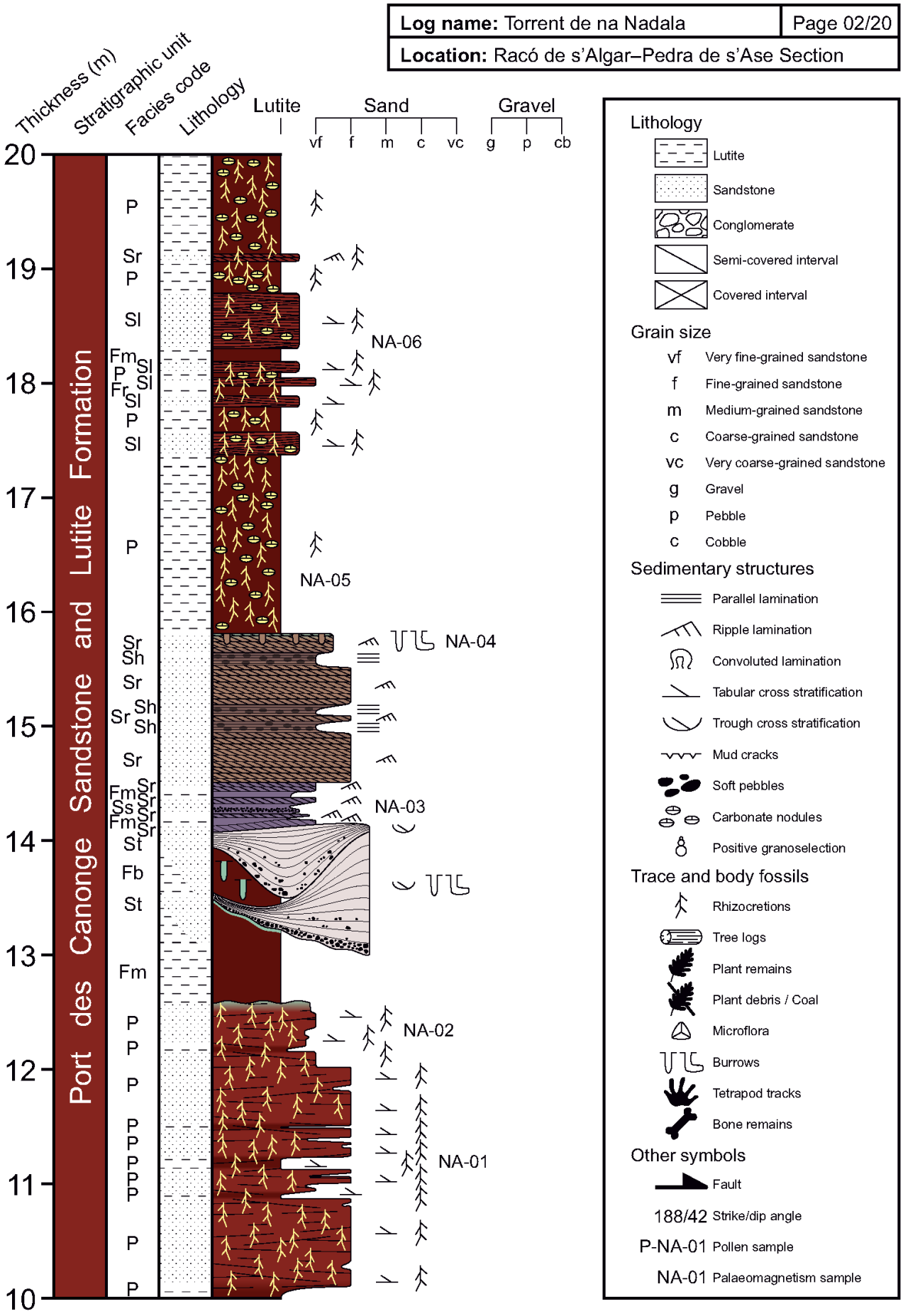
Log name: Torrent de na Nadala
Page 02/20
Location: Racó de s'Algar–Pedra de s'Ase Section
Thickness (m)
Stratigraphic unit
Facies code
Lithology
Lutite
Sand
Gravel
vf f m c vc g p cb
Port des Canonge Sandstone and Lutite Formation
NA-06
NA-05
NA-04
NA-03
NA-02
NA-01
Lithology
Lutite
Sandstone
Conglomerate
Semi-covered interval
Covered interval
Grain size
vf Very fine-grained sandstone
f Fine-grained sandstone
m Medium-grained sandstone
c Coarse-grained sandstone
vc Very coarse-grained sandstone
g Gravel
p Pebble
c Cobble
Sedimentary structures
Parallel lamination
Ripple lamination
Convoluted lamination
Tabular cross stratification
Trough cross stratification
Mud cracks
Soft pebbles
Carbonate nodules
Positive granoselection
Trace and body fossils
Rhizocretions
Tree logs
Plant remains
Plant debris / Coal
Microflora
Burrows
Tetrapod tracks
Bone remains
Other symbols
Fault
188/42 Strike/dip angle
P-NA-01 Pollen sample
NA-01 Palaeomagnetism sample

Log name: Torrent de na Nadala	Page 03/20
Location: Racó de s'Algar–Pedra de s'Ase Section	

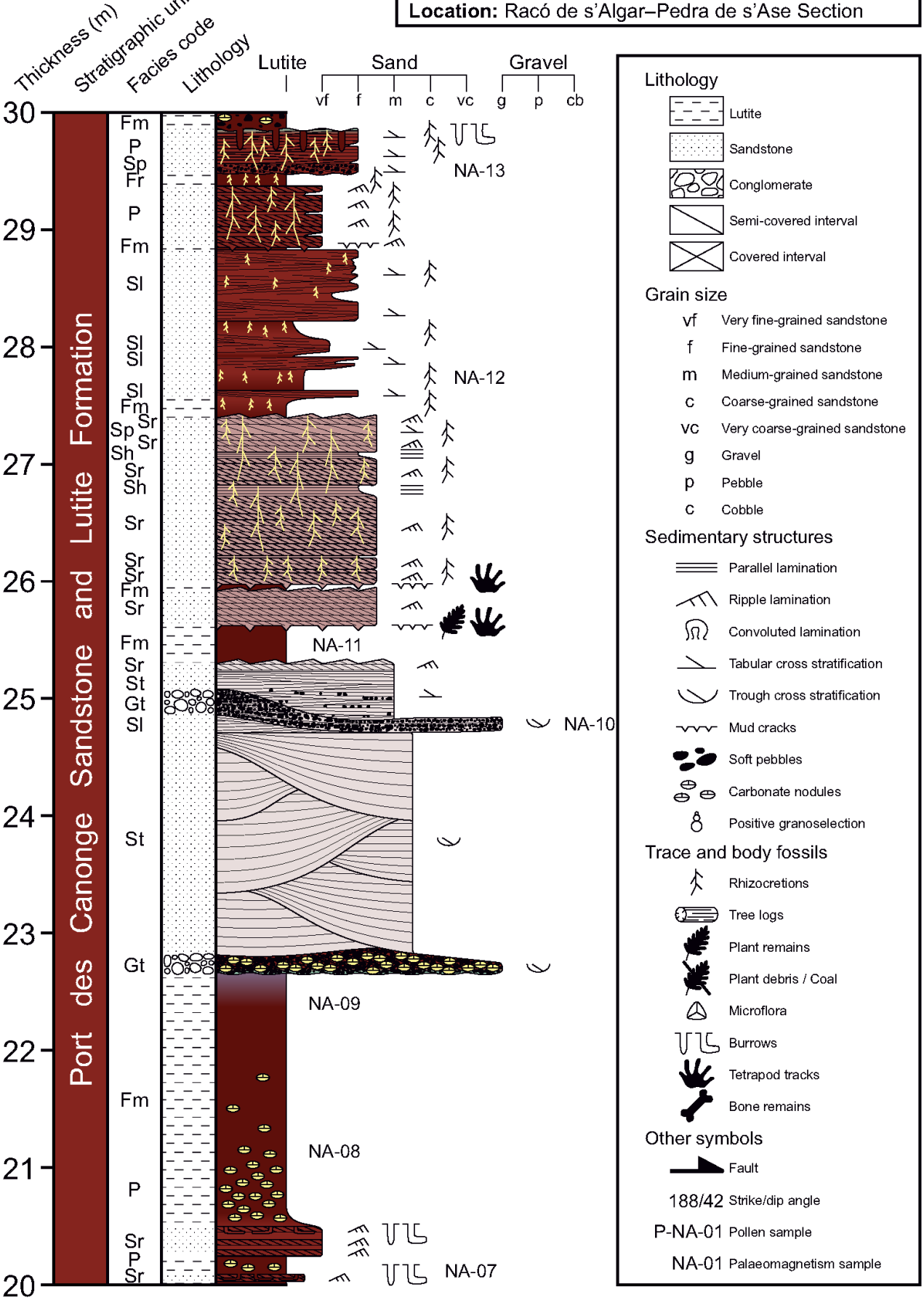

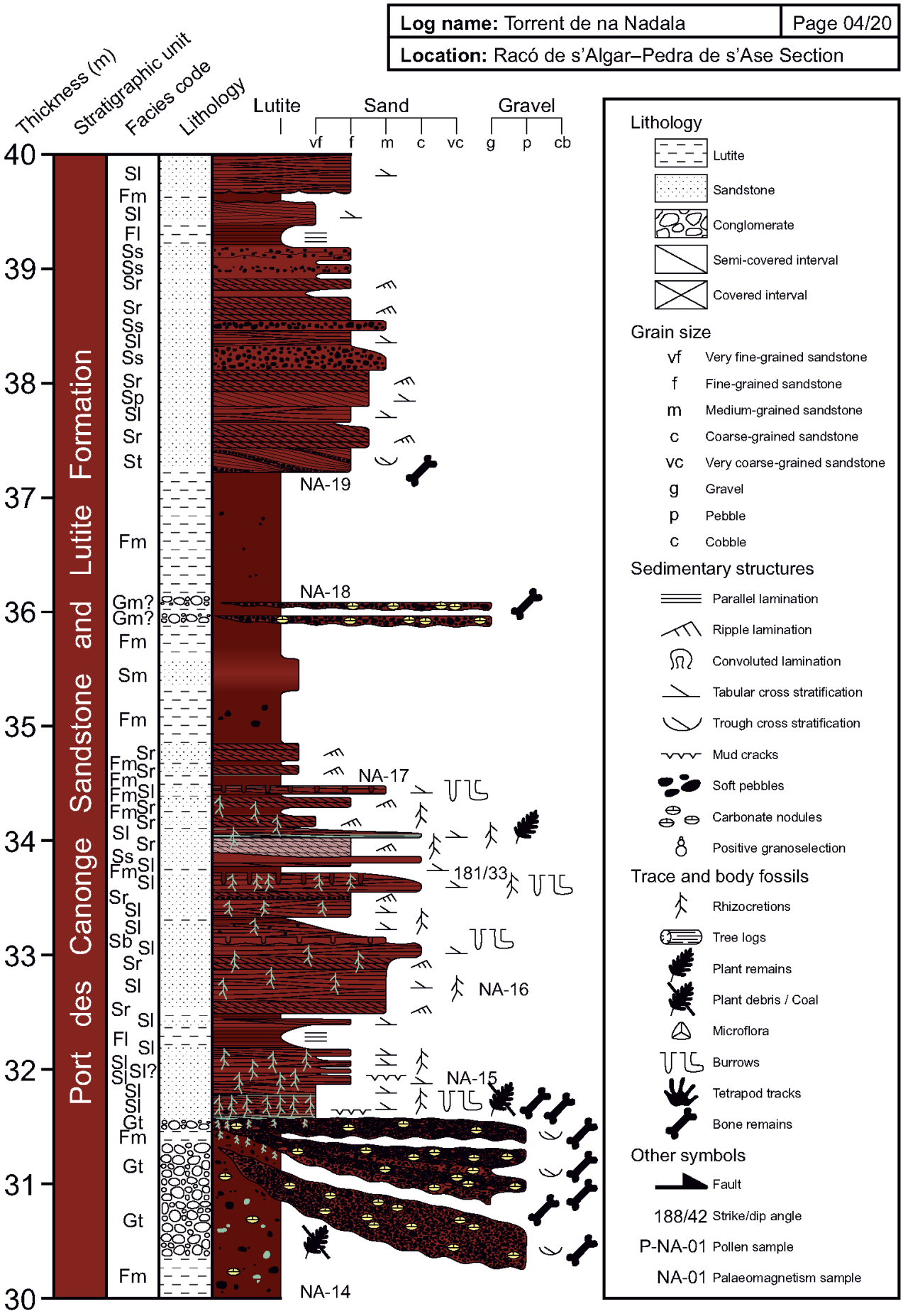
Log name: Torrent de na Nadala
Page 04/20
Location: Racó de s'Algar–Pedra de s'Ase Section
Thickness (m)
Stratigraphic unit
Facies code
Lithology
Lutite
Sand
Gravel
vf f m c vc g p cb
Port des Canonge Sandstone and Lutite Formation
NA-19
NA-18
NA-17
181/33
NA-16
NA-15
NA-14
Lithology
Lutite
Sandstone
Conglomerate
Semi-covered interval
Covered interval
Grain size
vf Very fine-grained sandstone
f Fine-grained sandstone
m Medium-grained sandstone
c Coarse-grained sandstone
vc Very coarse-grained sandstone
g Gravel
p Pebble
c Cobble
Sedimentary structures
Parallel lamination
Ripple lamination
Convoluted lamination
Tabular cross stratification
Trough cross stratification
Mud cracks
Soft pebbles
Carbonate nodules
Positive granoselection
Trace and body fossils
Rhizocretions
Tree logs
Plant remains
Plant debris / Coal
Microflora
Burrows
Tetrapod tracks
Bone remains
Other symbols
Fault
188/42 Strike/dip angle
P-NA-01 Pollen sample
NA-01 Palaeomagnetism sample

Log name: Torrent de na Nadala	Page 05/20
Location: Racó de s'Algar–Pedra de s'Ase Section	

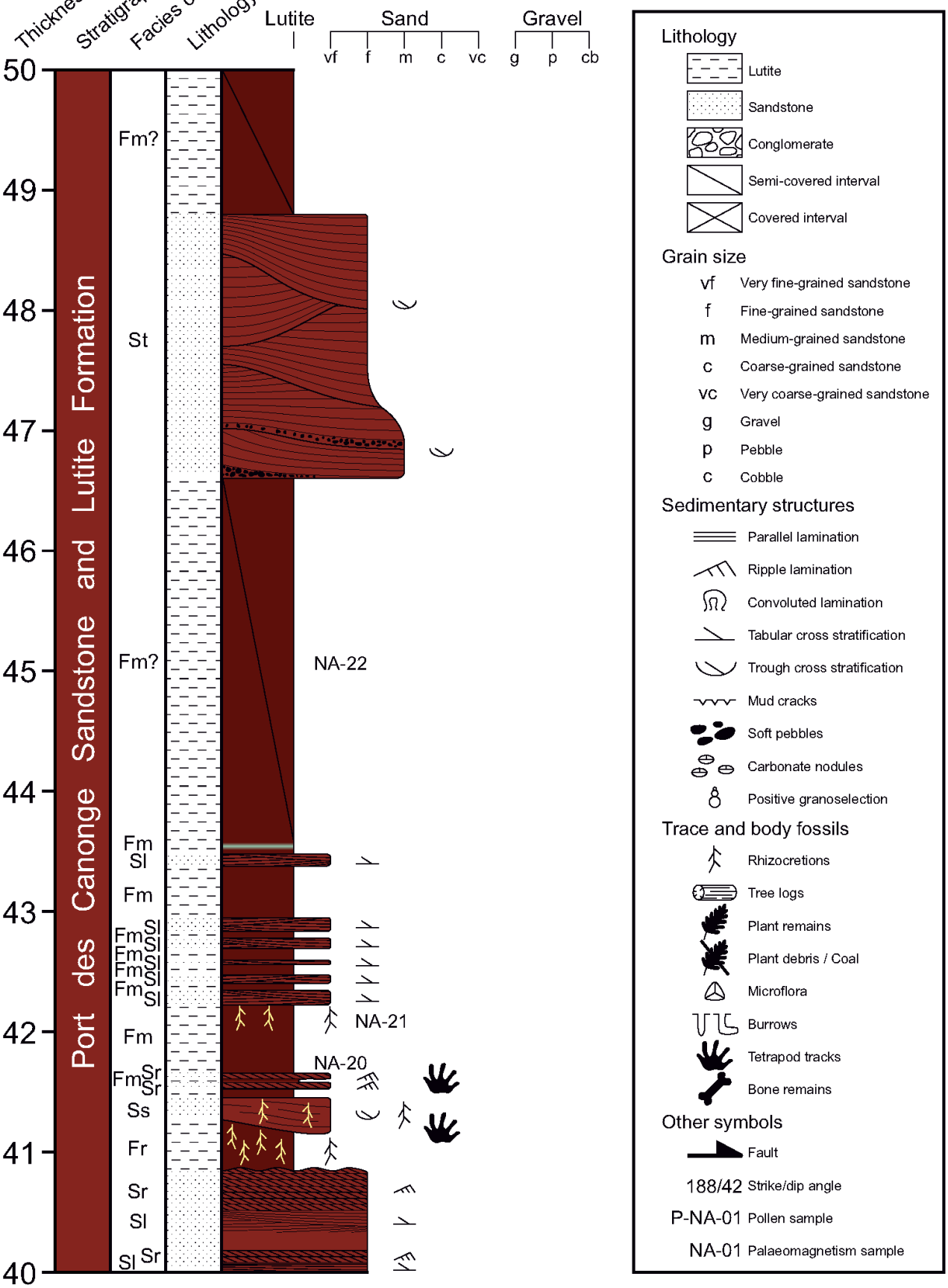

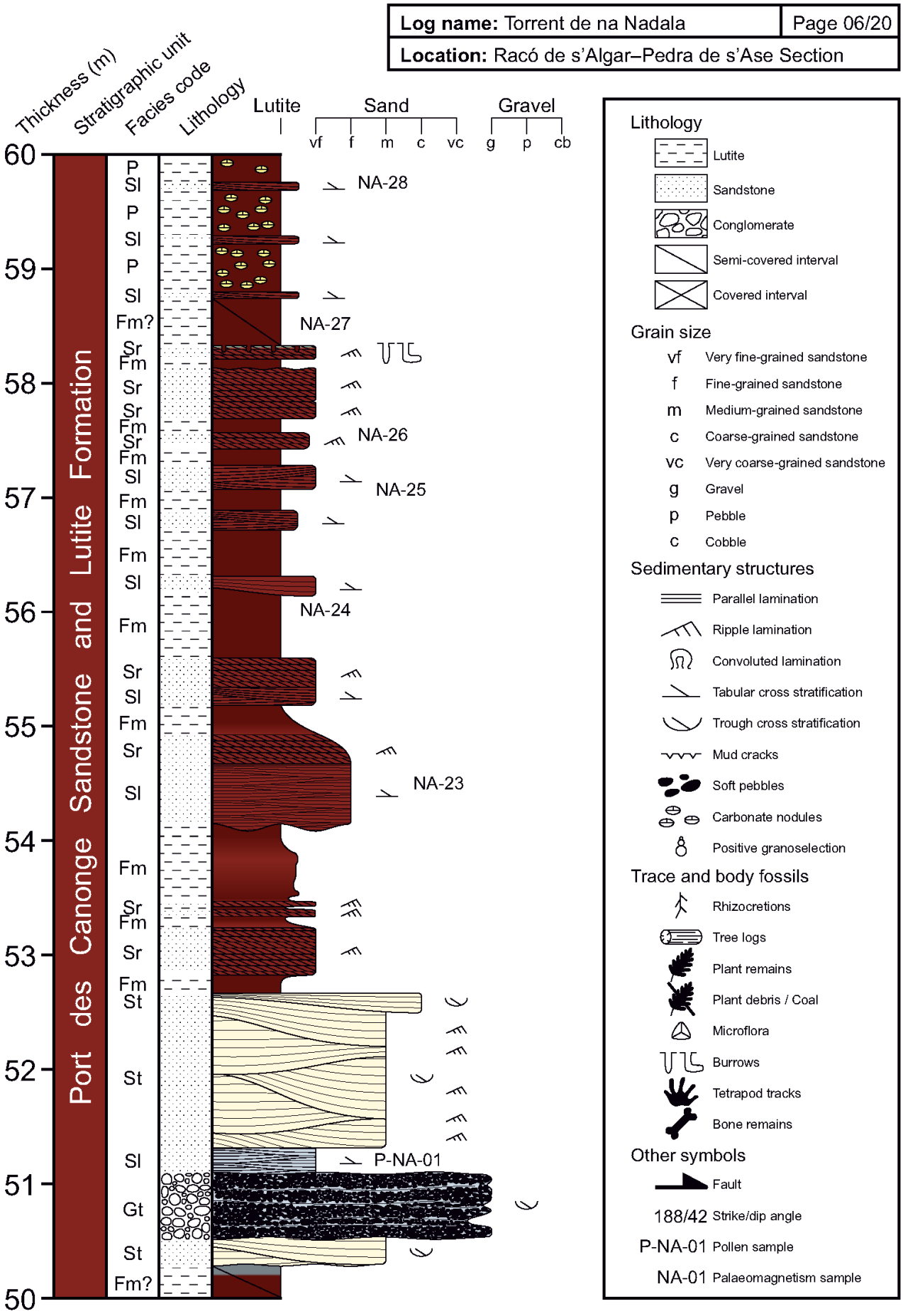
Log name: Torrent de na Nadala
Page 06/20
Location: Racó de s'Algar–Pedra de s'Ase Section
Thickness (m)
Stratigraphic unit
Facies code
Lithology
Lutite
Sand
Gravel
vf f m c vc g p cb
Port des Canonge Sandstone and Lutite Formation
NA-28
NA-27
NA-26
NA-25
NA-24
NA-23
P-NA-01
Lithology
Lutite
Sandstone
Conglomerate
Semi-covered interval
Covered interval
Grain size
vf Very fine-grained sandstone
f Fine-grained sandstone
m Medium-grained sandstone
c Coarse-grained sandstone
vc Very coarse-grained sandstone
g Gravel
p Pebble
c Cobble
Sedimentary structures
Parallel lamination
Ripple lamination
Convoluted lamination
Tabular cross stratification
Trough cross stratification
Mud cracks
Soft pebbles
Carbonate nodules
Positive granoselection
Trace and body fossils
Rhizocretions
Tree logs
Plant remains
Plant debris / Coal
Microflora
Burrows
Tetrapod tracks
Bone remains
Other symbols
Fault
188/42 Strike/dip angle
P-NA-01 Pollen sample
NA-01 Palaeomagnetism sample

Log name: Torrent de na Nadala	Page 07/20
Location: Racó de s'Algar–Pedra de s'Ase Section	

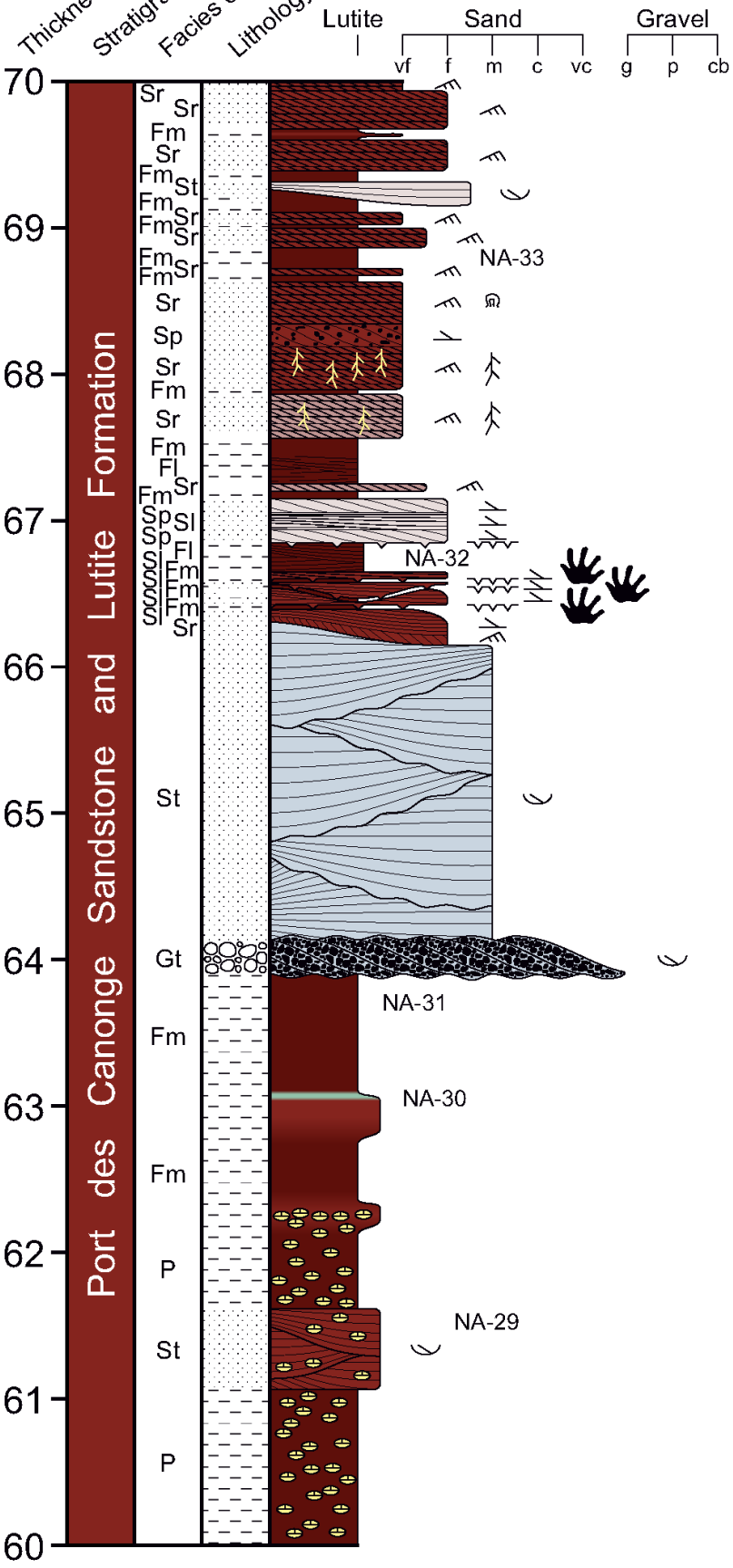

Lithology
- Lutite
- Sandstone
- Conglomerate
- Semi-covered interval
- Covered interval

Grain size
- vf Very fine-grained sandstone
- f Fine-grained sandstone
- m Medium-grained sandstone
- c Coarse-grained sandstone
- vc Very coarse-grained sandstone
- g Gravel
- p Pebble
- c Cobble

Sedimentary structures
- Parallel lamination
- Ripple lamination
- Convoluted lamination
- Tabular cross stratification
- Trough cross stratification
- Mud cracks
- Soft pebbles
- Carbonate nodules
- Positive granoselection

Trace and body fossils
- Rhizocretions
- Tree logs
- Plant remains
- Plant debris / Coal
- Microflora
- Burrows
- Tetrapod tracks
- Bone remains

Other symbols
- Fault
- 188/42 Strike/dip angle
- P-NA-01 Pollen sample
- NA-01 Palaeomagnetism sample

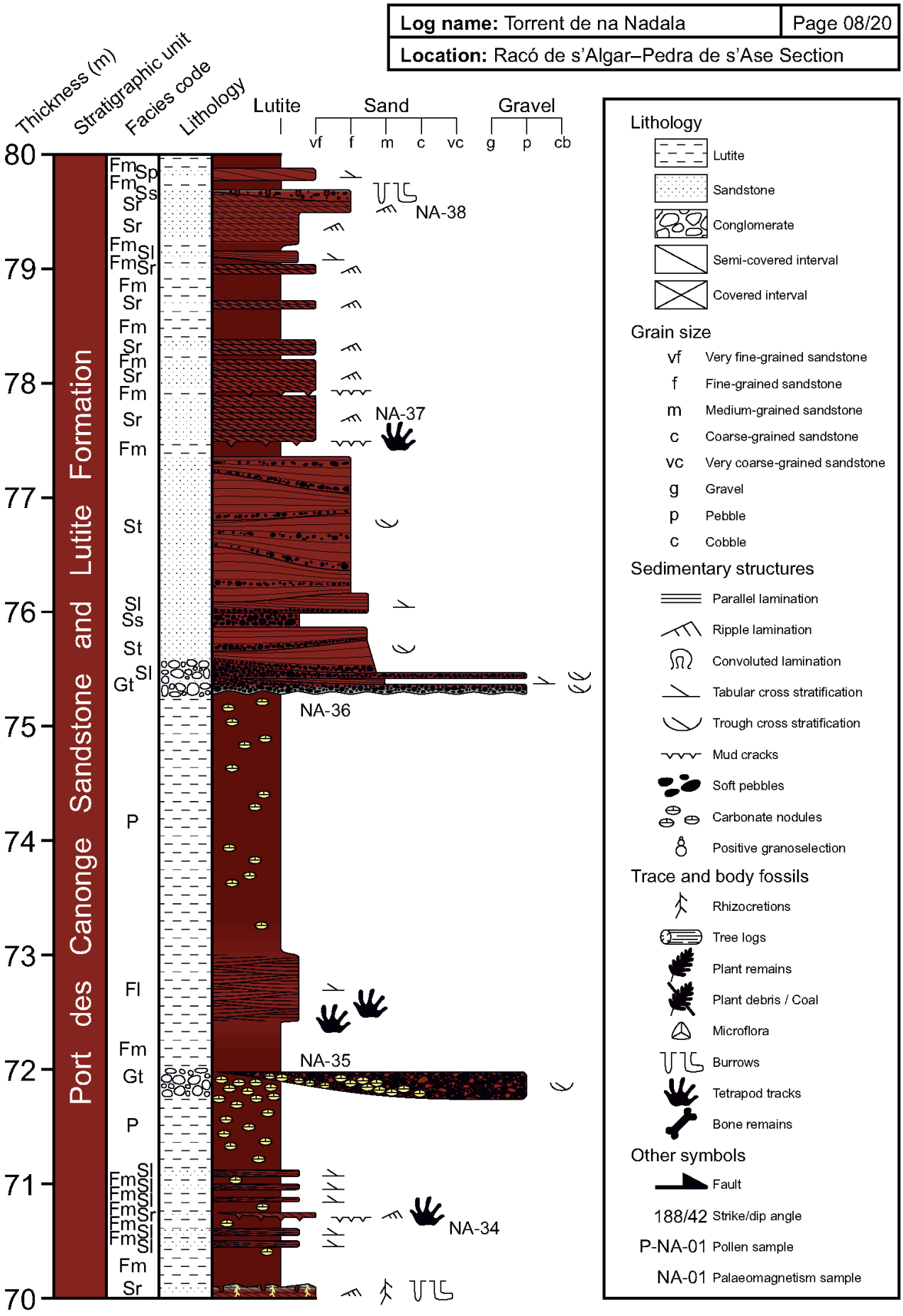
Log name: Torrent de na Nadala
Page 08/20
Location: Racó de s'Algar–Pedra de s'Ase Section
Thickness (m)
Stratigraphic unit
Facies code
Lithology
Lutite
Sand
Gravel
vf f m c vc g p cb
Port des Canonge Sandstone and Lutite Formation
NA-38
NA-37
NA-36
NA-35
NA-34
Lithology
Lutite
Sandstone
Conglomerate
Semi-covered interval
Covered interval
Grain size
vf Very fine-grained sandstone
f Fine-grained sandstone
m Medium-grained sandstone
c Coarse-grained sandstone
vc Very coarse-grained sandstone
g Gravel
p Pebble
c Cobble
Sedimentary structures
Parallel lamination
Ripple lamination
Convoluted lamination
Tabular cross stratification
Trough cross stratification
Mud cracks
Soft pebbles
Carbonate nodules
Positive granoselection
Trace and body fossils
Rhizocretions
Tree logs
Plant remains
Plant debris / Coal
Microflora
Burrows
Tetrapod tracks
Bone remains
Other symbols
Fault
188/42 Strike/dip angle
P-NA-01 Pollen sample
NA-01 Palaeomagnetism sample

Log name: Torrent de na Nadala	Page 09/20
Location: Racó de s'Algar–Pedra de s'Ase Section	

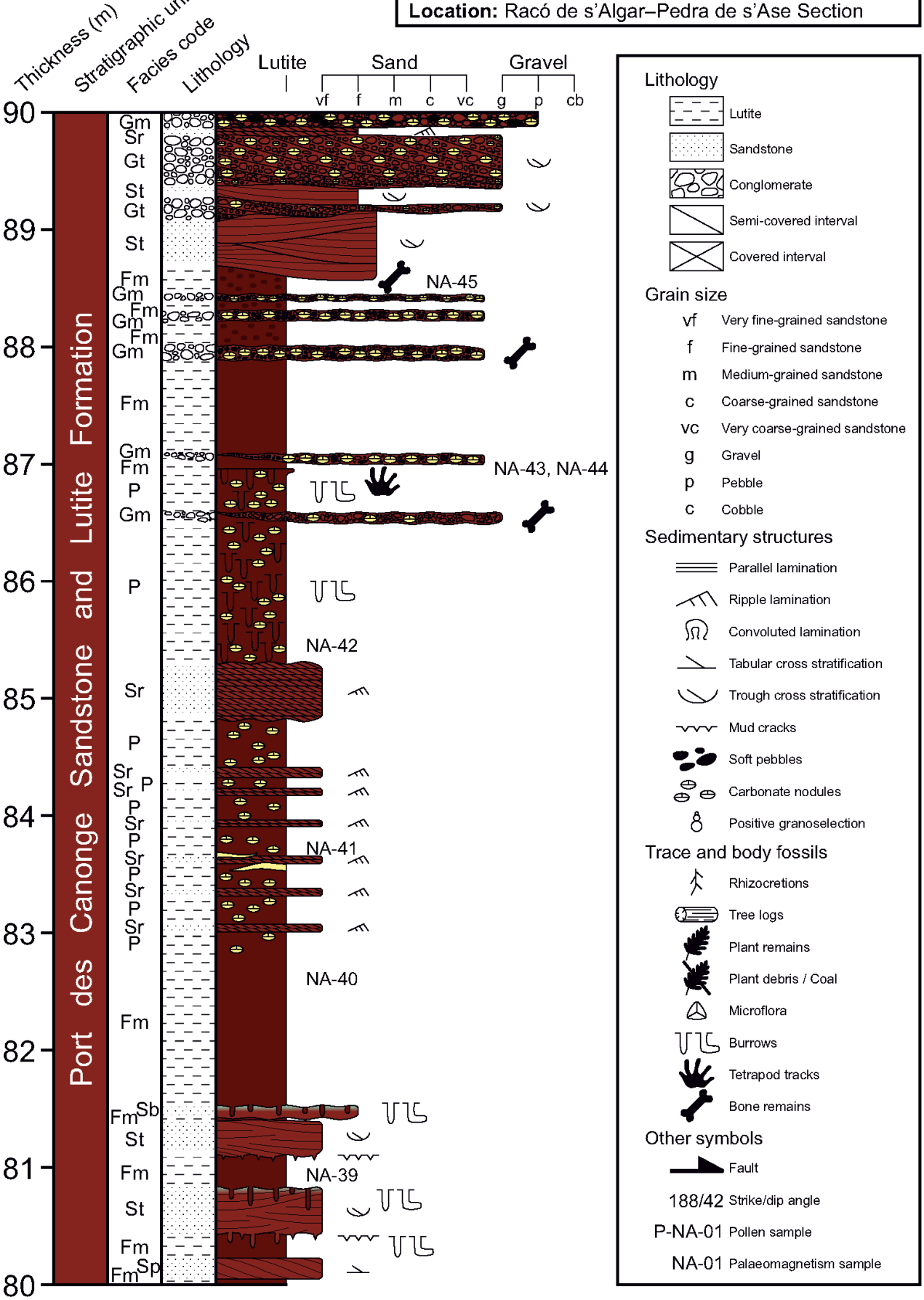

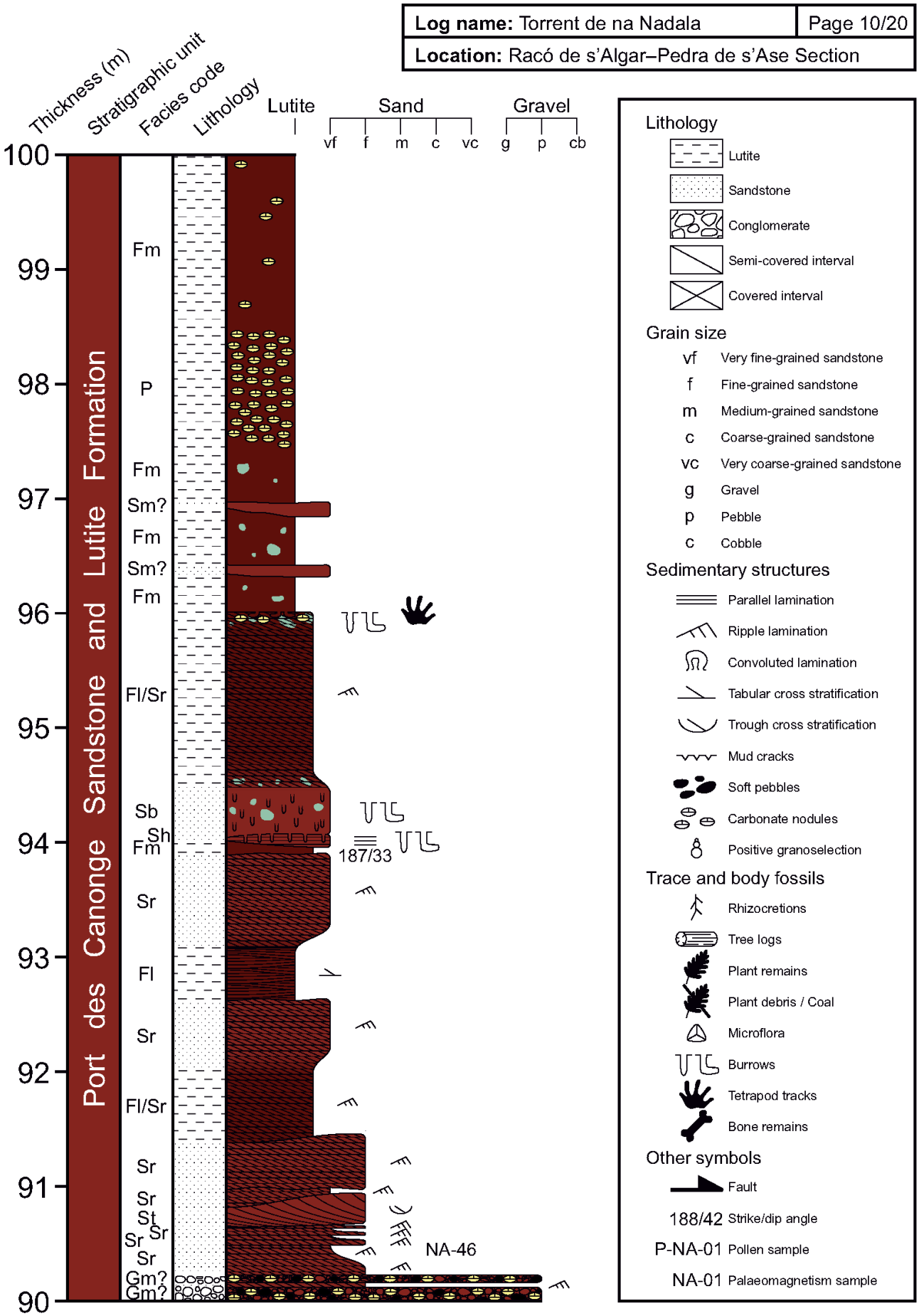
Log name: Torrent de na Nadala
Page 10/20
Location: Racó de s'Algar–Pedra de s'Ase Section
Thickness (m)
Stratigraphic unit
Facies code
Lithology
Lutite
Sand
Gravel
vf f m c vc g p cb
100
99
98
97
96
95
94
93
92
91
90
Port des Canonge Sandstone and Lutite Formation
Fm
P
Fm
Sm?
Fm
Sm?
Fm
Fl/Sr
Sb
Sh
Fm
Sr
Fl
Sr
Fl/Sr
Sr
Sr
St
Sr
Sr
Sr
Gm?
Gm?
187/33
NA-46
Lithology
Lutite
Sandstone
Conglomerate
Semi-covered interval
Covered interval
Grain size
vf Very fine-grained sandstone
f Fine-grained sandstone
m Medium-grained sandstone
c Coarse-grained sandstone
vc Very coarse-grained sandstone
g Gravel
p Pebble
c Cobble
Sedimentary structures
Parallel lamination
Ripple lamination
Convoluted lamination
Tabular cross stratification
Trough cross stratification
Mud cracks
Soft pebbles
Carbonate nodules
Positive granoselection
Trace and body fossils
Rhizocretions
Tree logs
Plant remains
Plant debris / Coal
Microflora
Burrows
Tetrapod tracks
Bone remains
Other symbols
Fault
188/42 Strike/dip angle
P-NA-01 Pollen sample
NA-01 Palaeomagnetism sample

Log name: Torrent de na Nadala	Page 11/20
Location: Racó de s'Algar–Pedra de s'Ase Section	

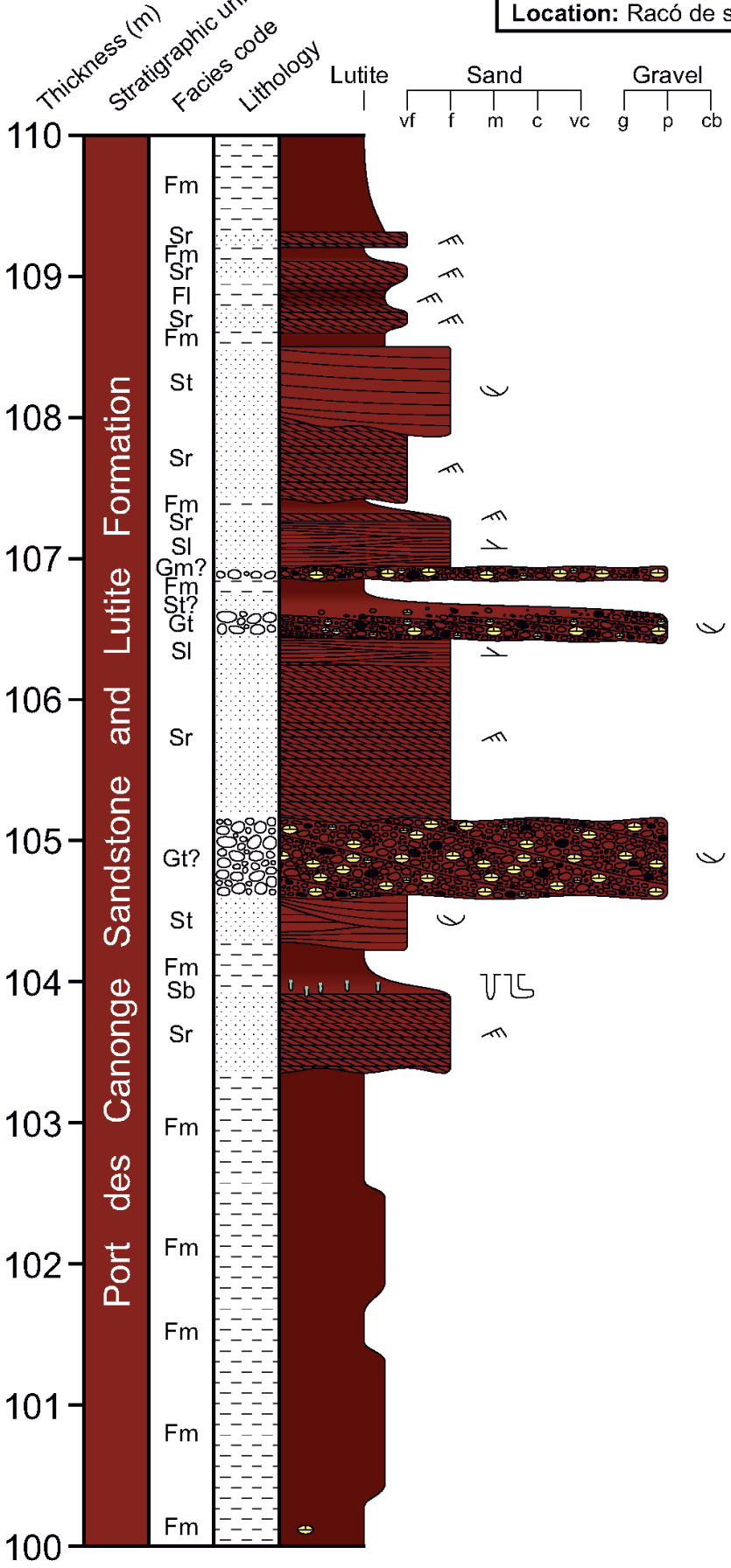

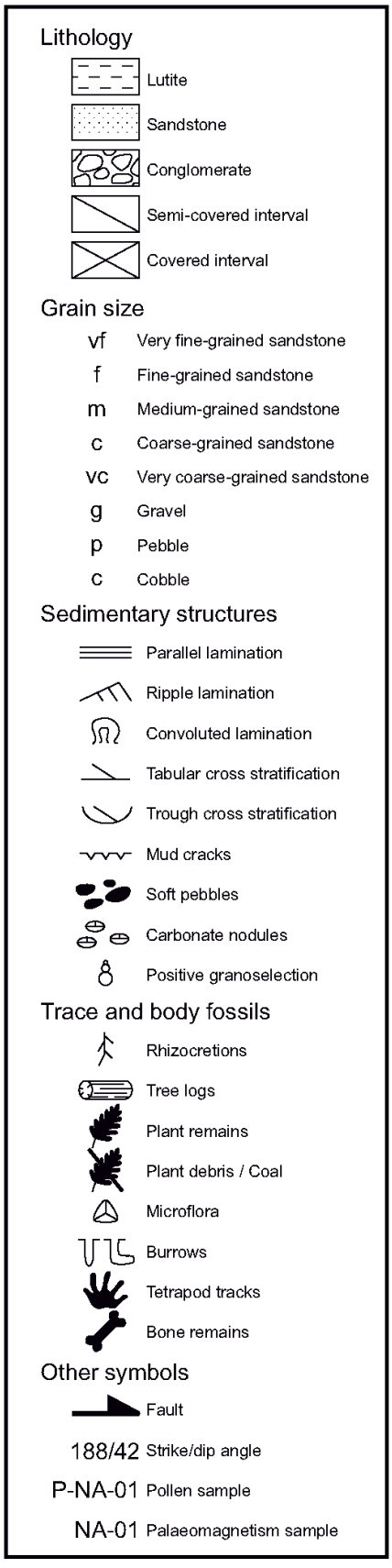

Log name: Torrent de na Nadala | Page 12/20

Location: Racó de s'Algar–Pedra de s'Ase Section

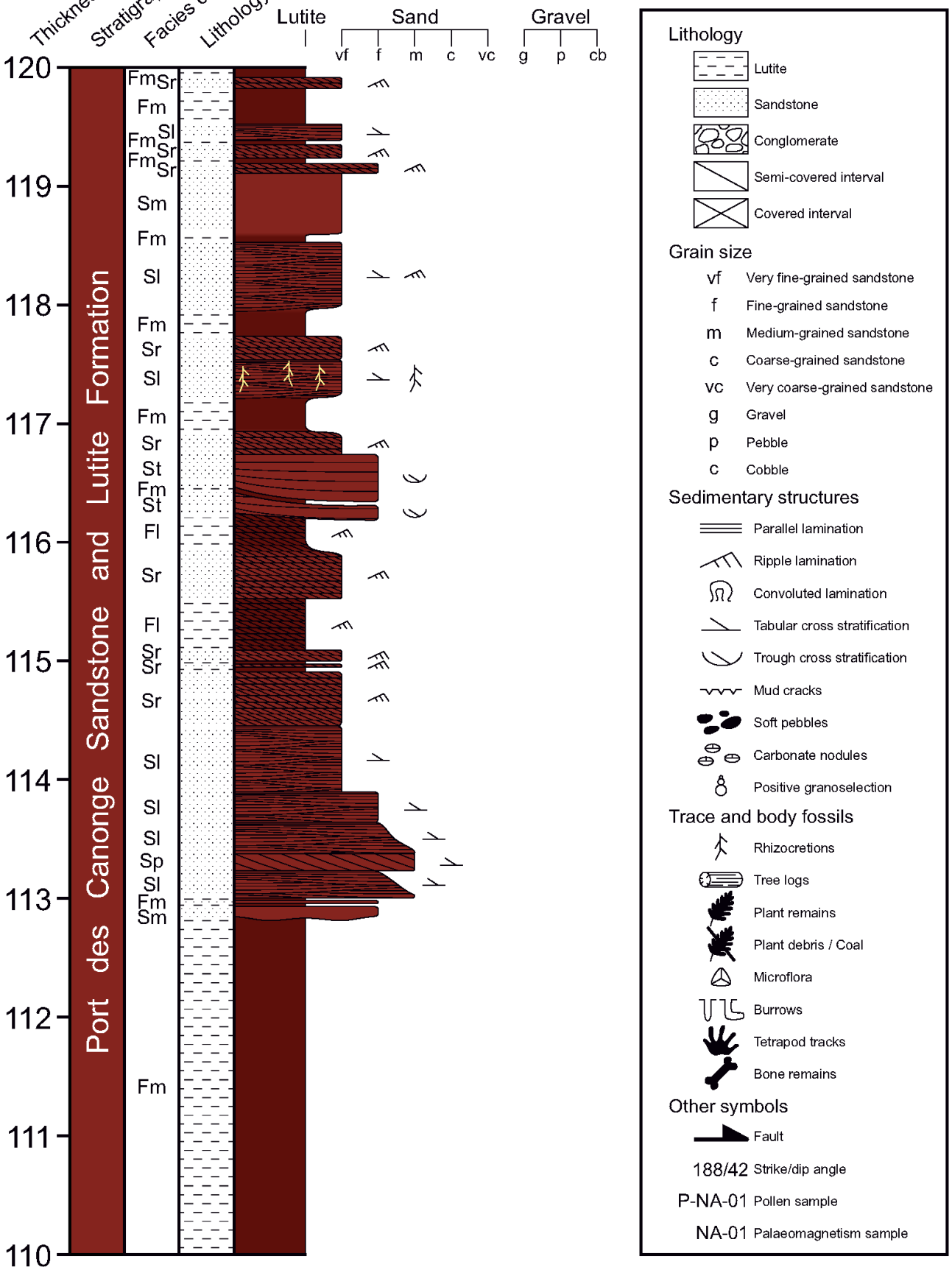

Log name: Torrent de na Nadala	Page 13/20
Location: Racó de s'Algar–Pedra de s'Ase Section	

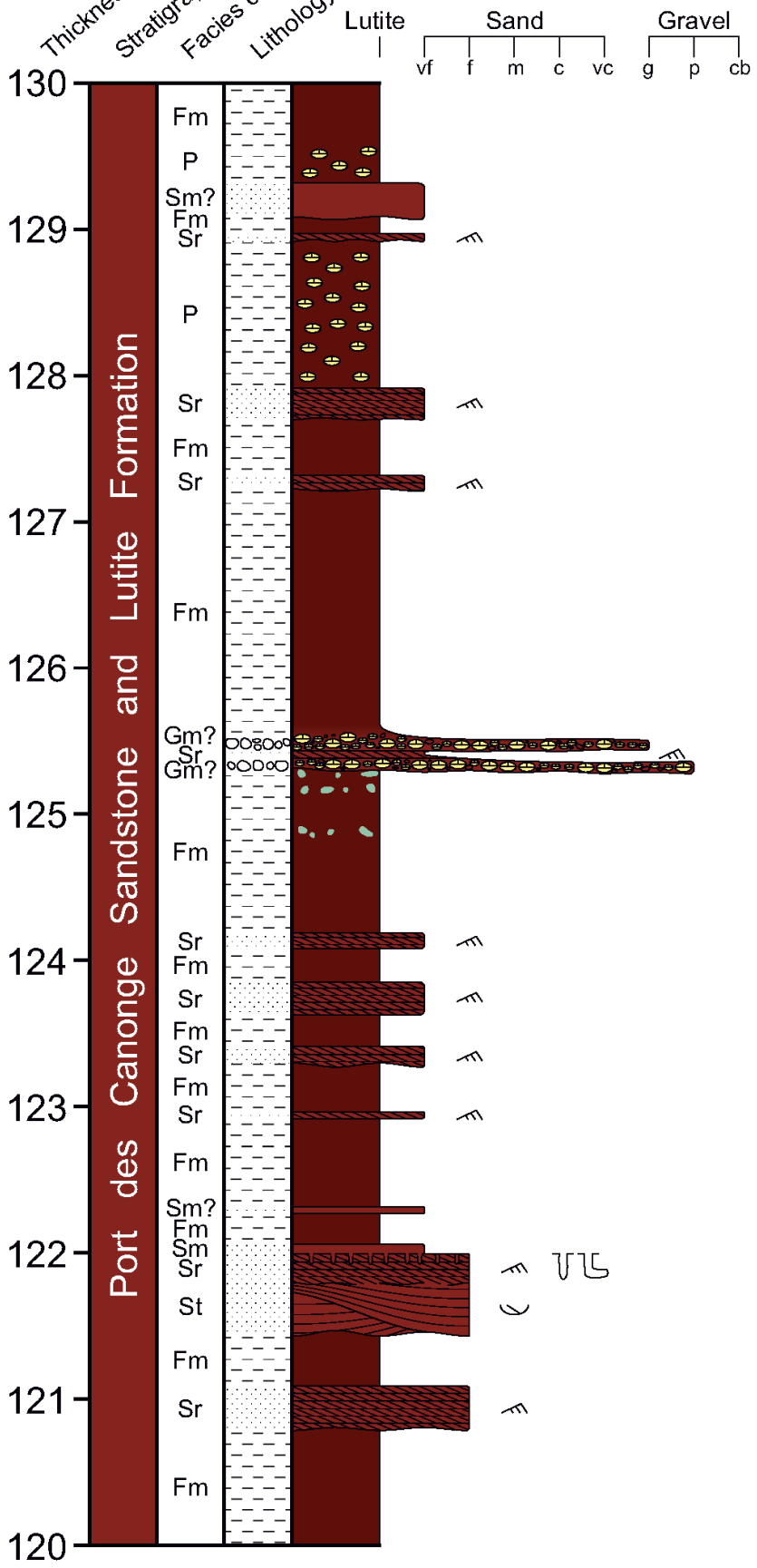

Lithology
- Lutite
- Sandstone
- Conglomerate
- Semi-covered interval
- Covered interval

Grain size
- vf Very fine-grained sandstone
- f Fine-grained sandstone
- m Medium-grained sandstone
- c Coarse-grained sandstone
- vc Very coarse-grained sandstone
- g Gravel
- p Pebble
- c Cobble

Sedimentary structures
- Parallel lamination
- Ripple lamination
- Convoluted lamination
- Tabular cross stratification
- Trough cross stratification
- Mud cracks
- Soft pebbles
- Carbonate nodules
- Positive granoselection

Trace and body fossils
- Rhizocretions
- Tree logs
- Plant remains
- Plant debris / Coal
- Microflora
- Burrows
- Tetrapod tracks
- Bone remains

Other symbols
- Fault
- 188/42 Strike/dip angle
- P-NA-01 Pollen sample
- NA-01 Palaeomagnetism sample

Log name: Torrent de na Nadala	Page 14/20
Location: Racó de s'Algar–Pedra de s'Ase Section	

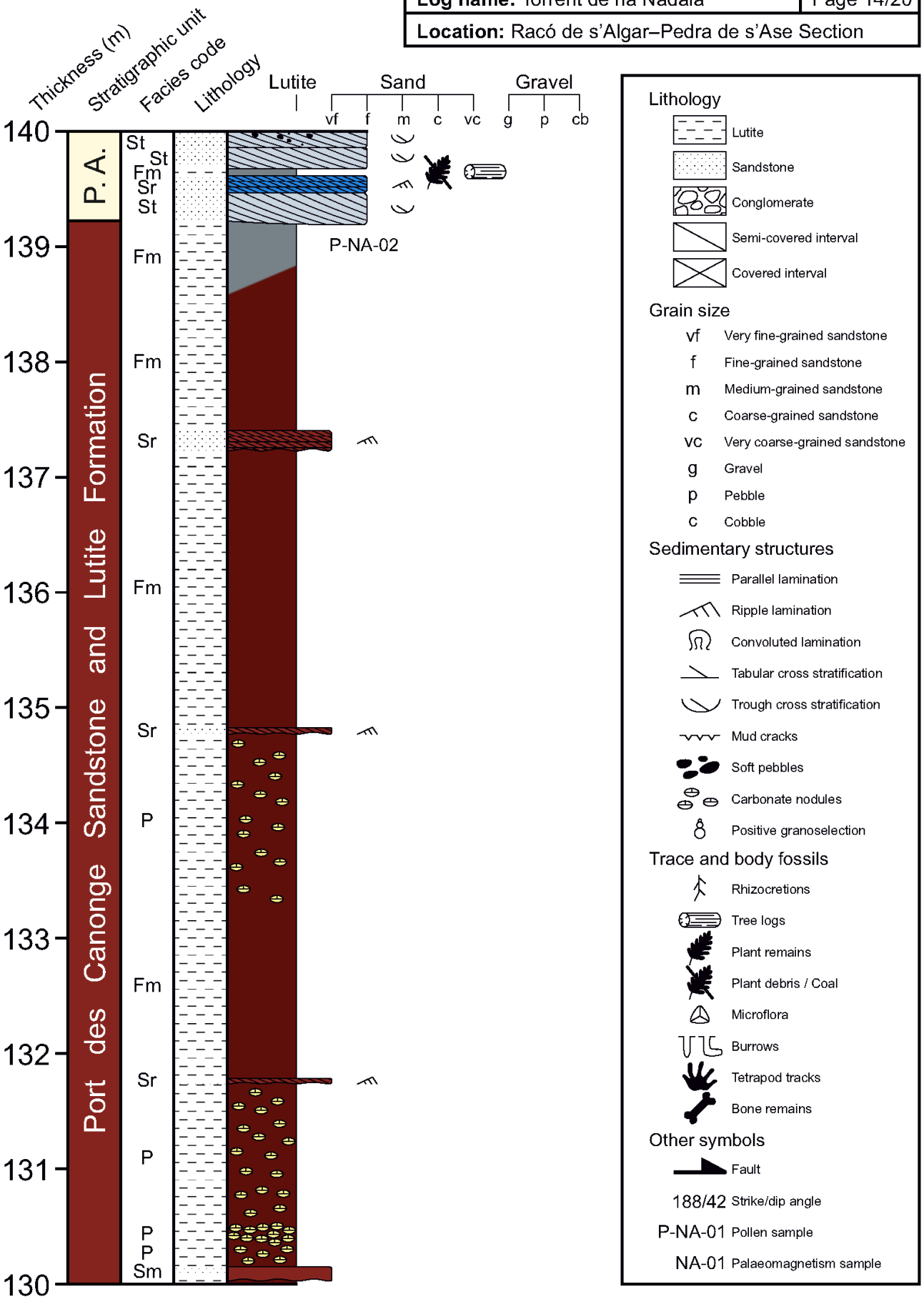

Log name: Torrent de na Nadala	Page 15/20
Location: Racó de s'Algar–Pedra de s'Ase Section	

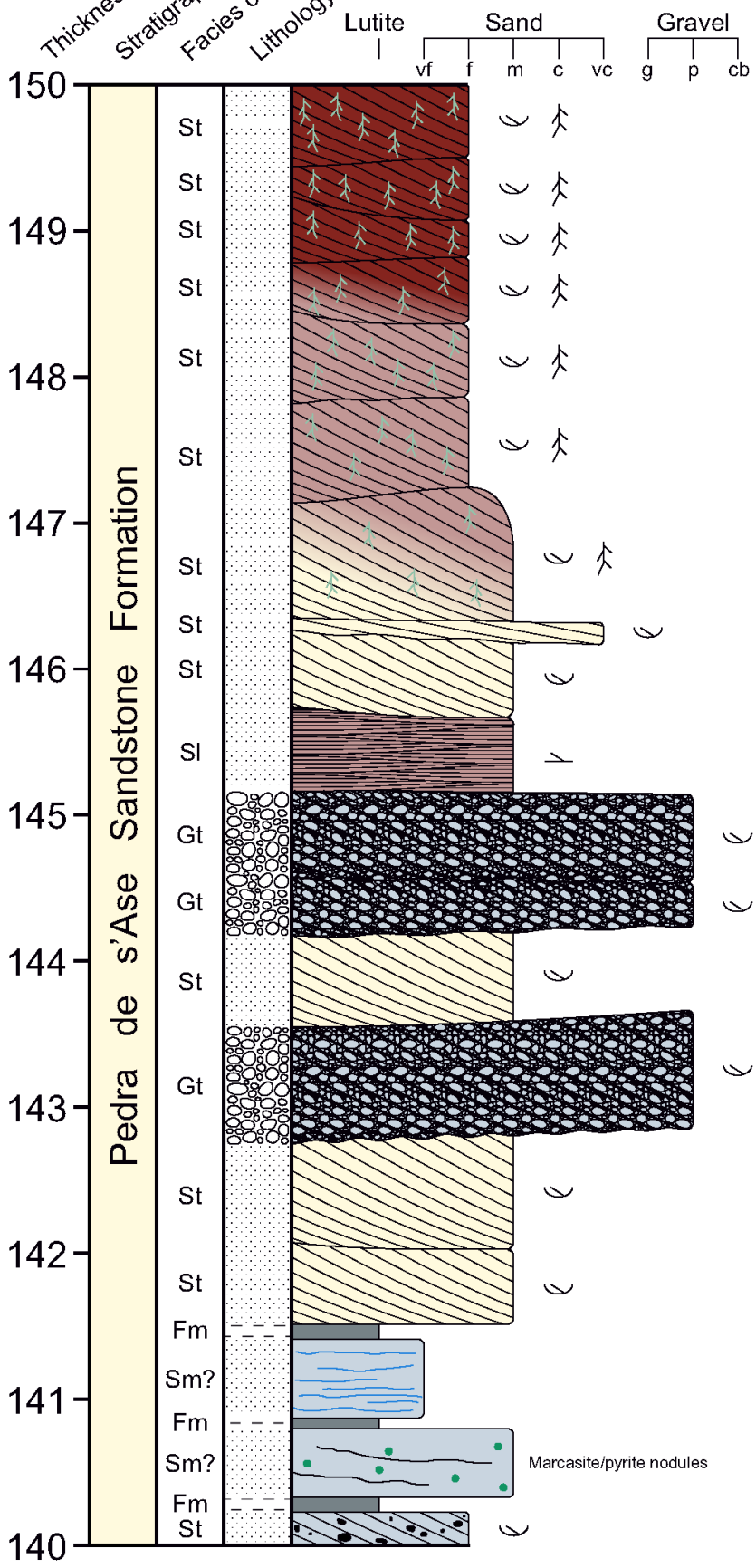

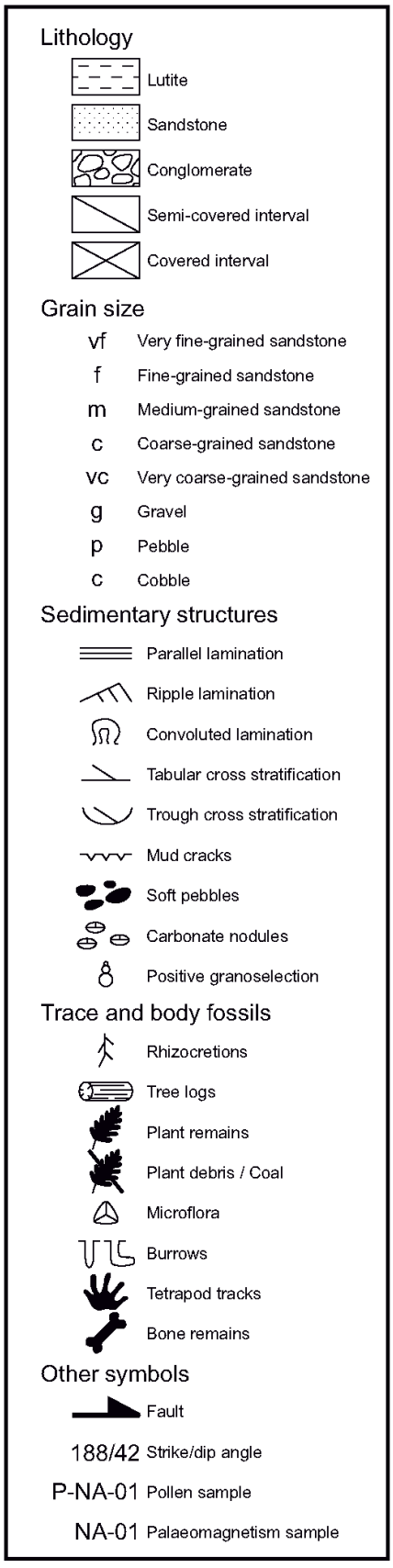

Log name: Torrent de na Nadala	Page 16/20
Location: Racó de s'Algar–Pedra de s'Ase Section	

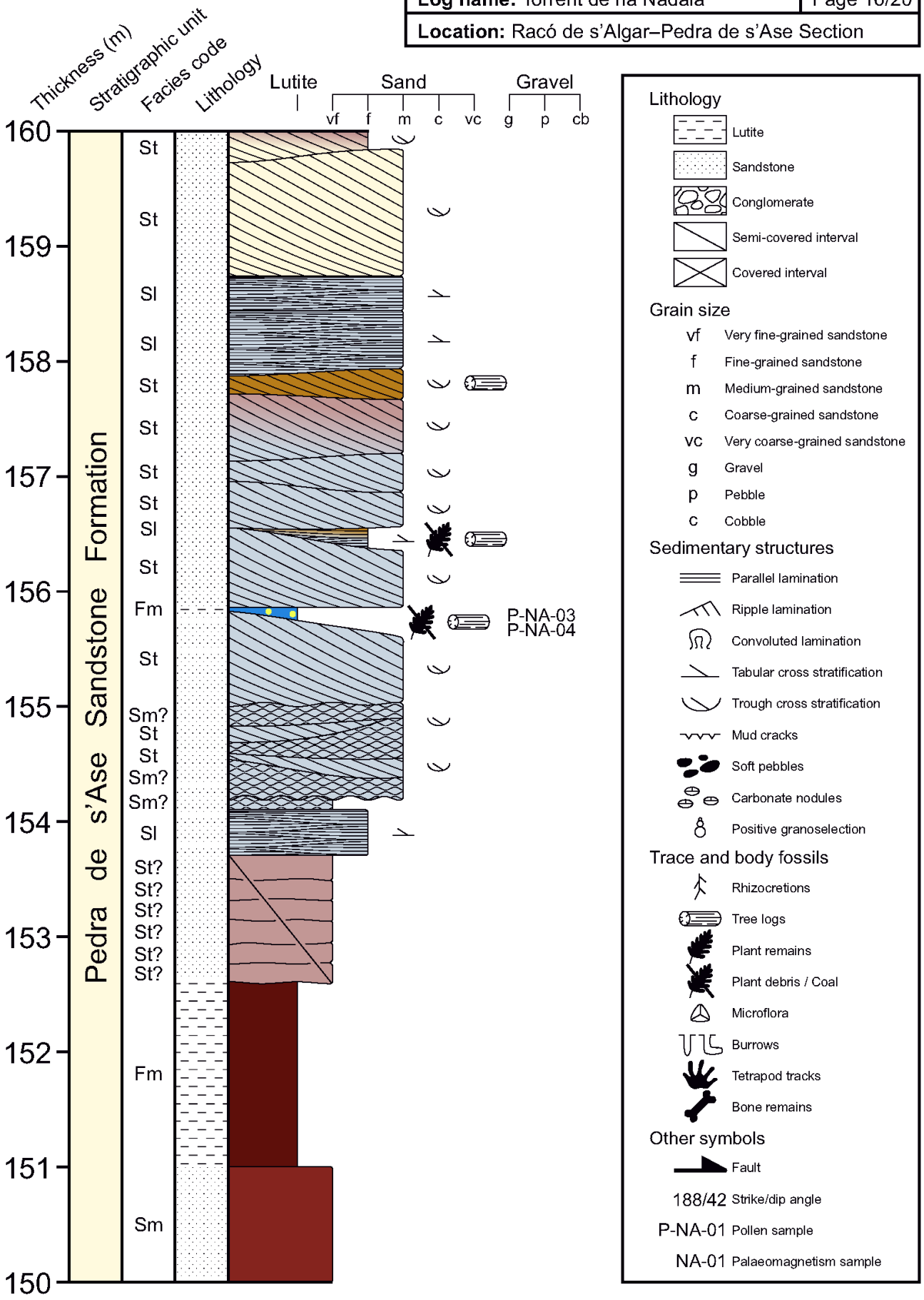

Log name: Torrent de na Nadala	Page 17/20
Location: Racó de s'Algar–Pedra de s'Ase Section	

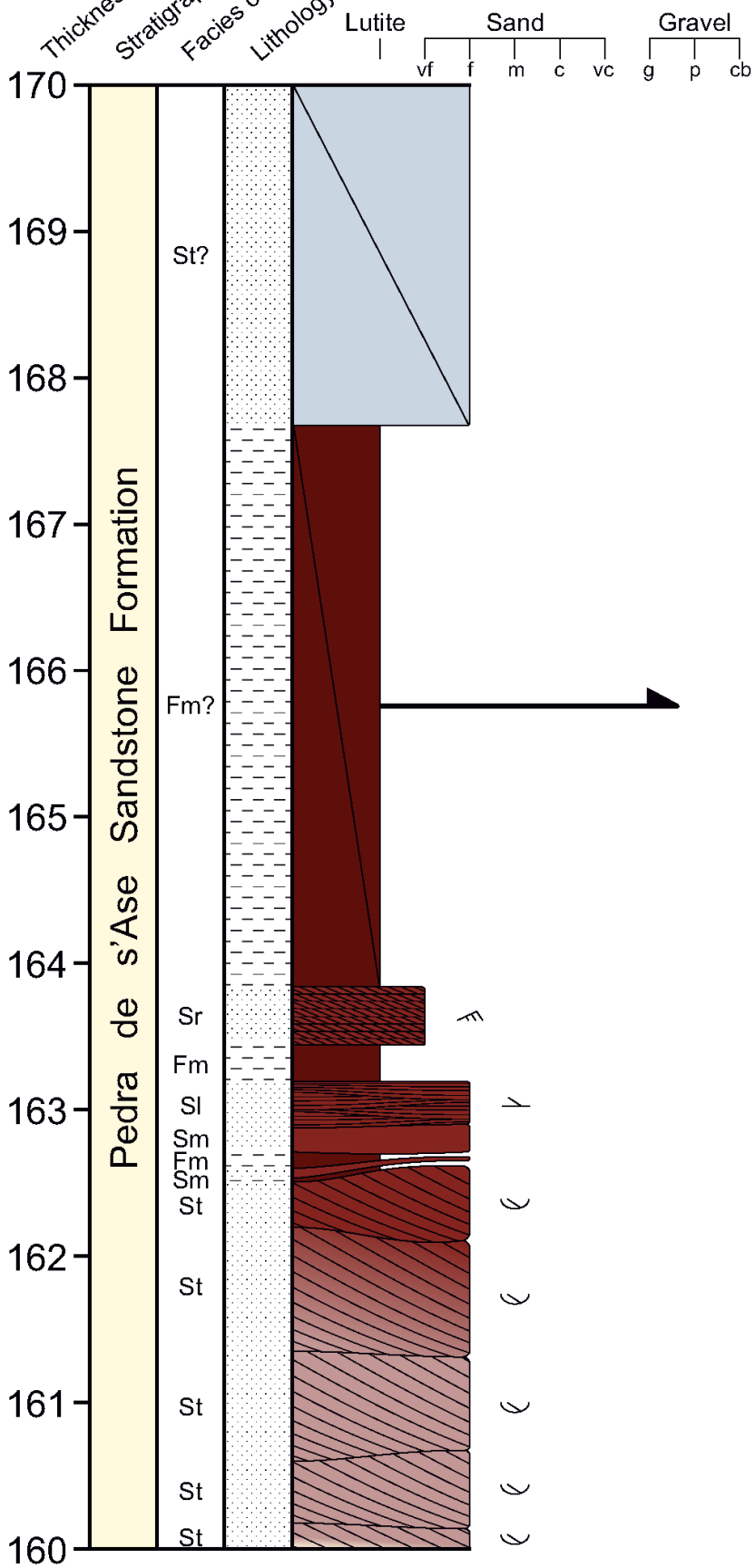

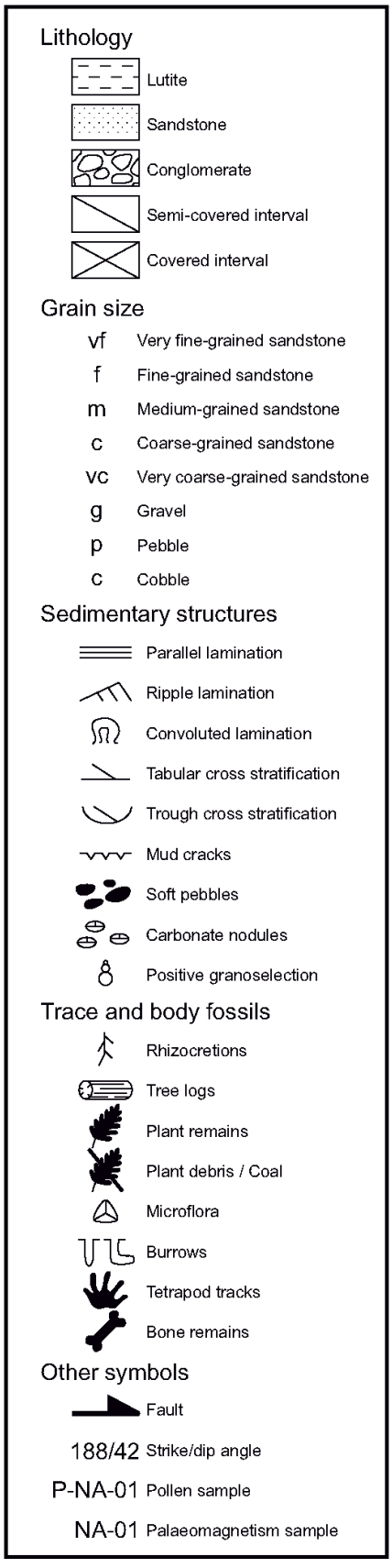

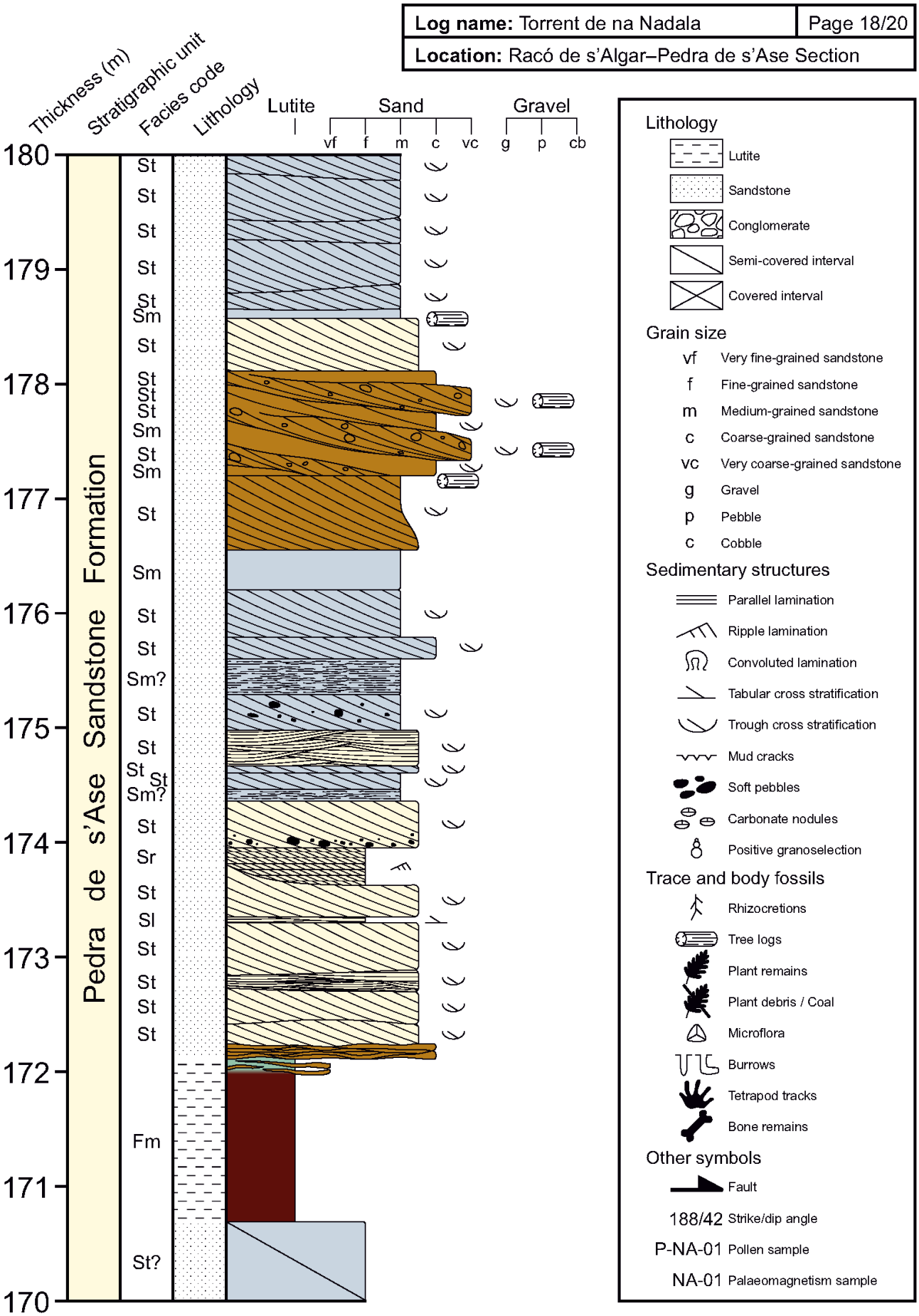
Log name: Torrent de na Nadala
Page 18/20
Location: Racó de s'Algar–Pedra de s'Ase Section
Thickness (m)
Stratigraphic unit
Facies code
Lithology
Lutite
Sand
Gravel
vf f m c vc g p cb
Pedra de s'Ase Sandstone Formation
180
179
178
177
176
175
174
173
172
171
170
St
Sm
Sr
Sl
Fm
St?
Sm?
Lithology
Lutite
Sandstone
Conglomerate
Semi-covered interval
Covered interval
Grain size
vf Very fine-grained sandstone
f Fine-grained sandstone
m Medium-grained sandstone
c Coarse-grained sandstone
vc Very coarse-grained sandstone
g Gravel
p Pebble
c Cobble
Sedimentary structures
Parallel lamination
Ripple lamination
Convoluted lamination
Tabular cross stratification
Trough cross stratification
Mud cracks
Soft pebbles
Carbonate nodules
Positive granoselection
Trace and body fossils
Rhizocretions
Tree logs
Plant remains
Plant debris / Coal
Microflora
Burrows
Tetrapod tracks
Bone remains
Other symbols
Fault
188/42 Strike/dip angle
P-NA-01 Pollen sample
NA-01 Palaeomagnetism sample

Log name: Torrent de na Nadala	Page 19/20
Location: Racó de s'Algar–Pedra de s'Ase Section	

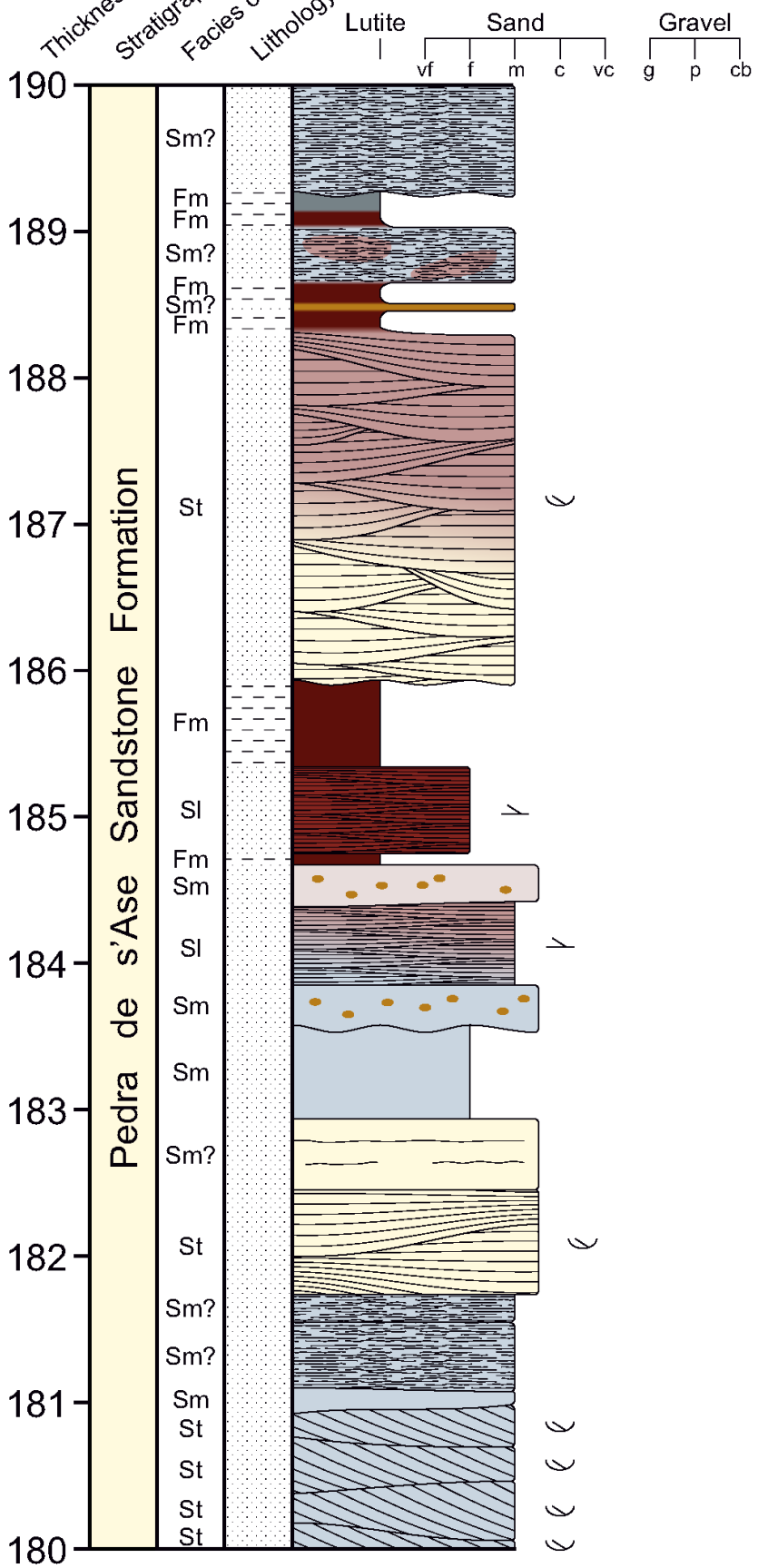

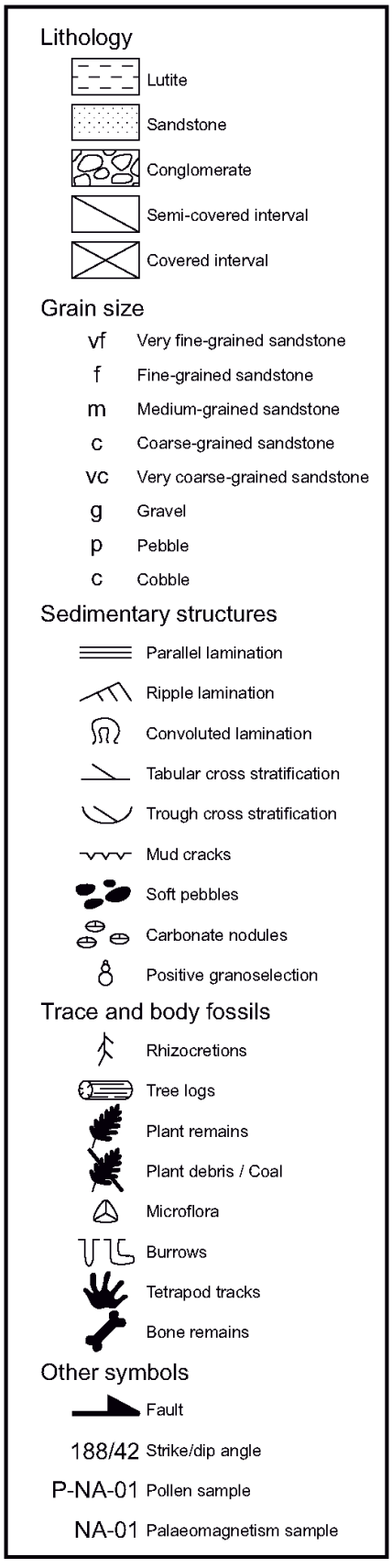

Log name: Torrent de na Nadala	Page 20/20
Location: Racó de s'Algar–Pedra de s'Ase Section	

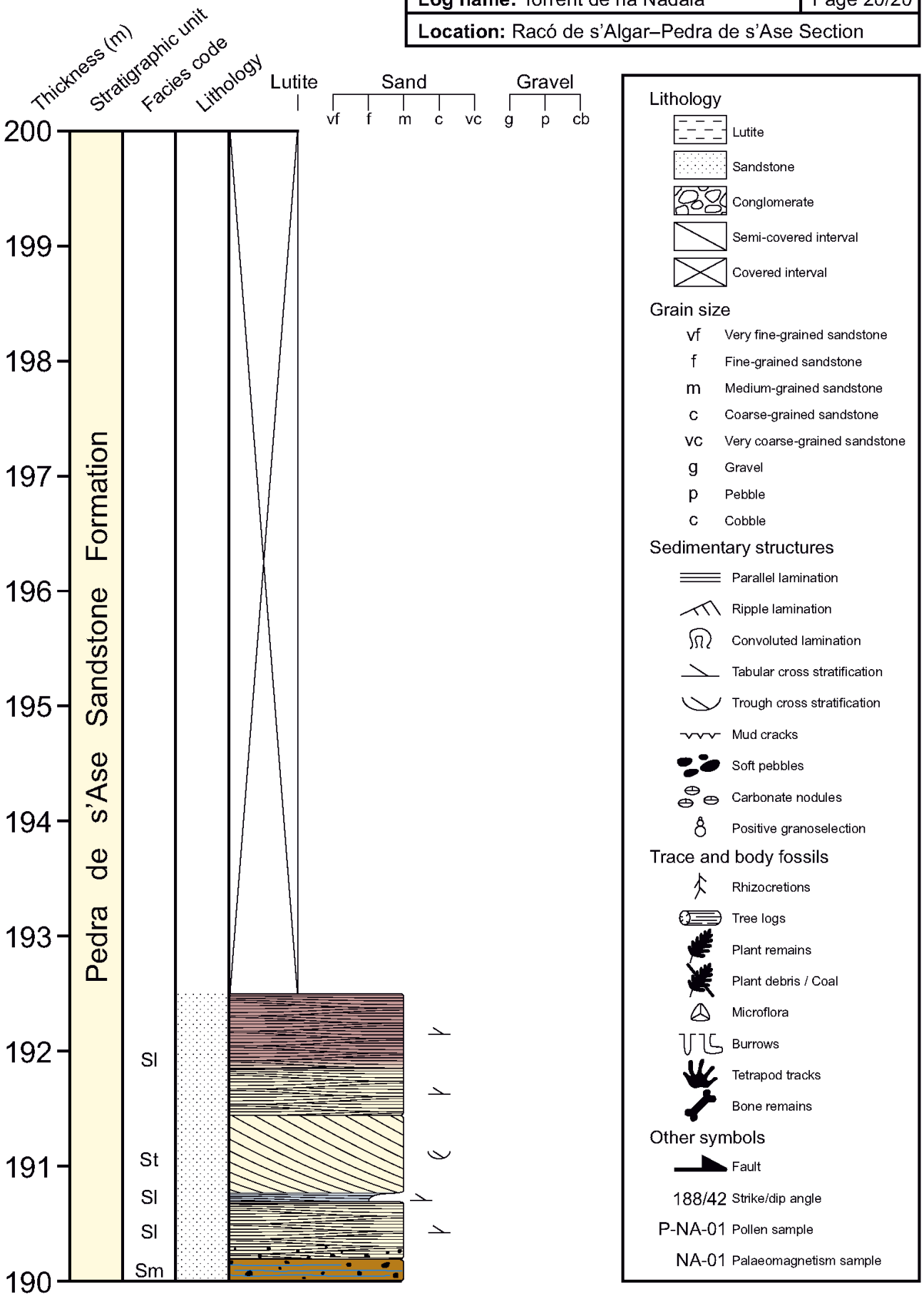

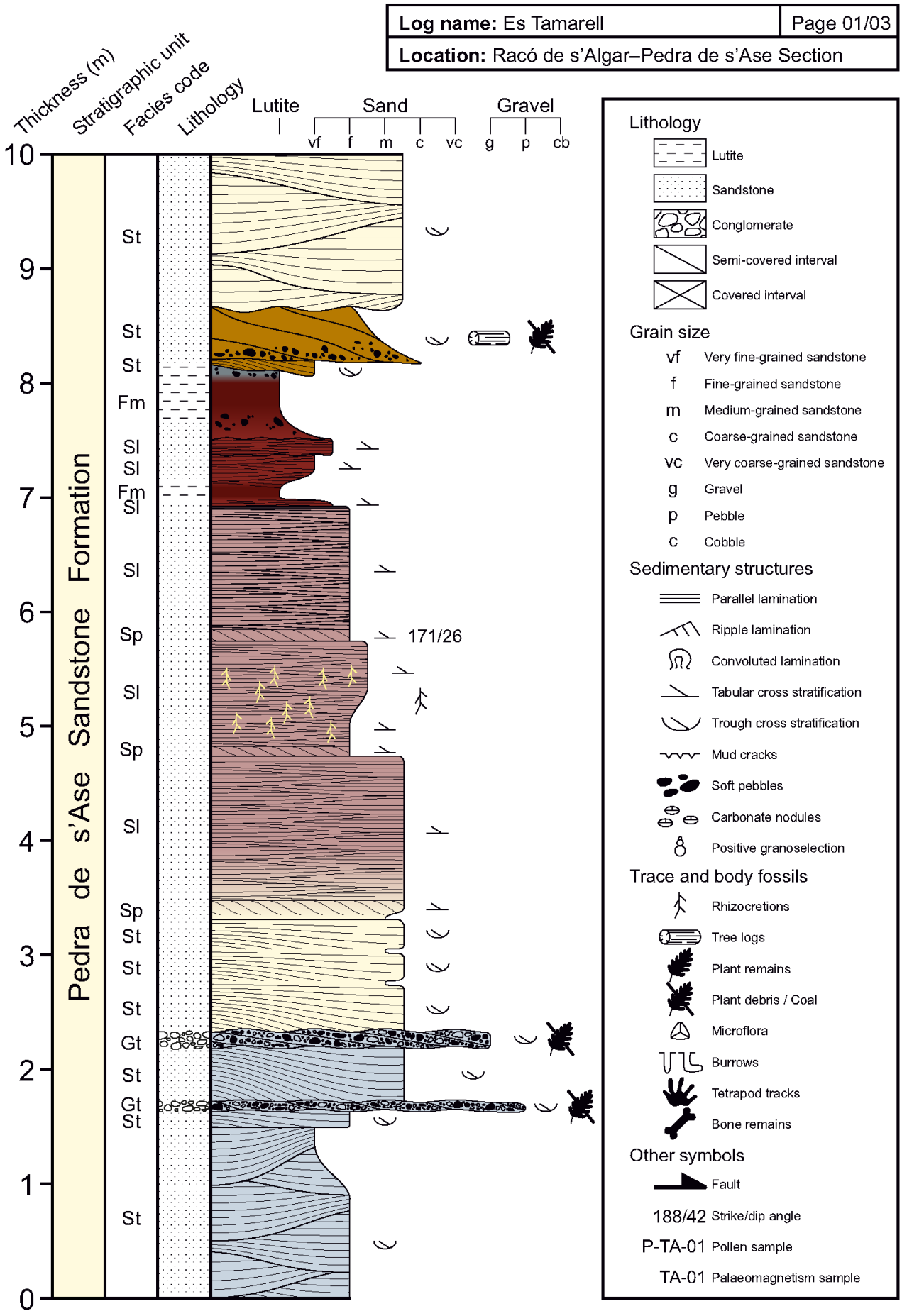
Log name: Es Tamarell
Page 01/03
Location: Racó de s'Algar–Pedra de s'Ase Section
Thickness (m)
Stratigraphic unit
Facies code
Lithology
Lutite
Sand
Gravel
vf f m c vc g p cb
Pedra de s'Ase Sandstone Formation
St
St
St
Fm
Sl
Sl
Fm
Sl
Sl
Sp
171/26
Sl
Sp
Sl
Sp
St
St
St
Gt
St
Gt
St
St
Lithology
Lutite
Sandstone
Conglomerate
Semi-covered interval
Covered interval
Grain size
vf Very fine-grained sandstone
f Fine-grained sandstone
m Medium-grained sandstone
c Coarse-grained sandstone
vc Very coarse-grained sandstone
g Gravel
p Pebble
c Cobble
Sedimentary structures
Parallel lamination
Ripple lamination
Convoluted lamination
Tabular cross stratification
Trough cross stratification
Mud cracks
Soft pebbles
Carbonate nodules
Positive granoselection
Trace and body fossils
Rhizocretions
Tree logs
Plant remains
Plant debris / Coal
Microflora
Burrows
Tetrapod tracks
Bone remains
Other symbols
Fault
188/42 Strike/dip angle
P-TA-01 Pollen sample
TA-01 Palaeomagnetism sample

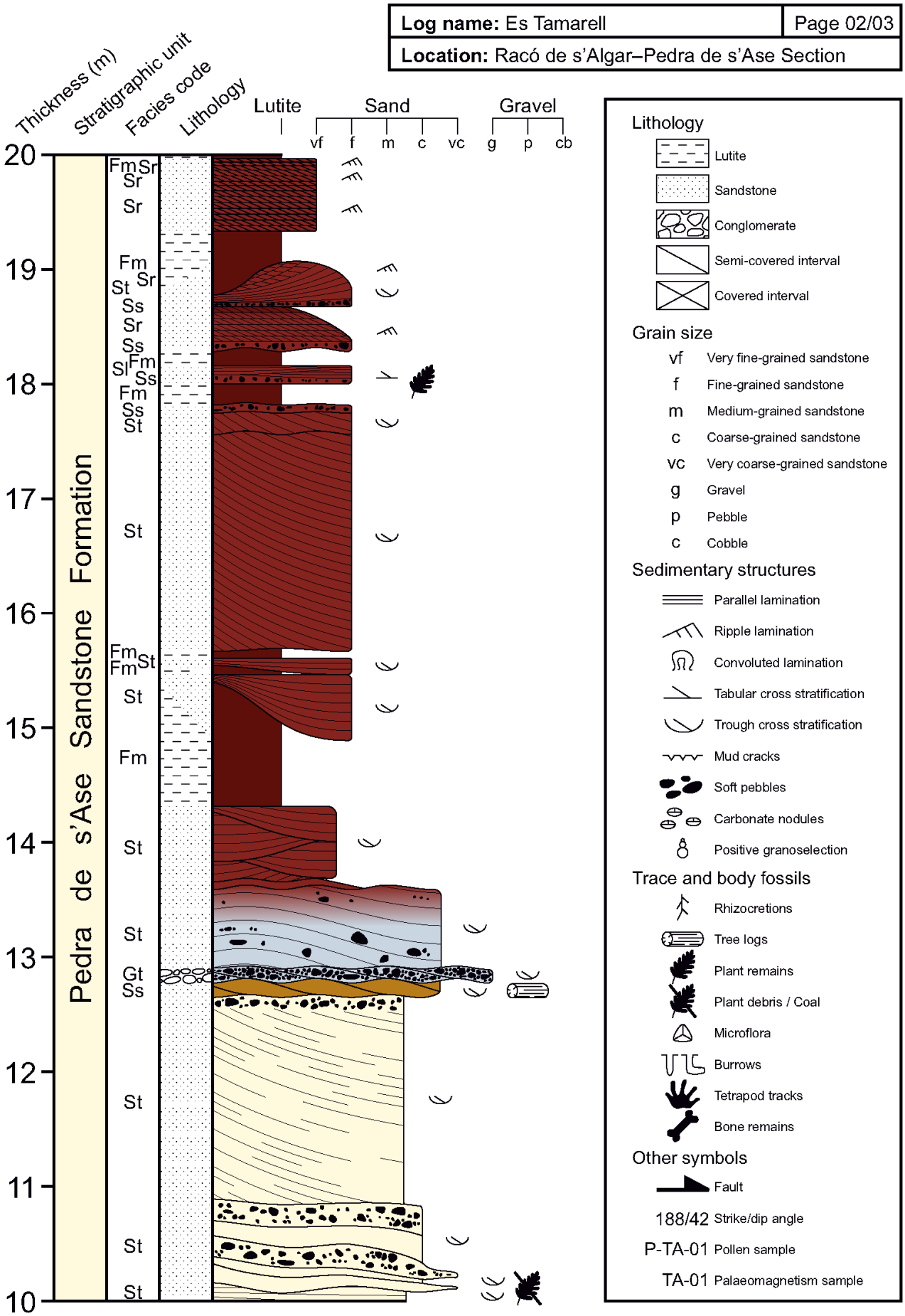
Log name: Es Tamarell
Page 02/03
Location: Racó de s'Algar–Pedra de s'Ase Section
Thickness (m)
Stratigraphic unit
Facies code
Lithology
Lutite
Sand
Gravel
vf f m c vc g p cb
Pedra de s'Ase Sandstone Formation
20
19
18
17
16
15
14
13
12
11
10
Lithology
Lutite
Sandstone
Conglomerate
Semi-covered interval
Covered interval
Grain size
vf Very fine-grained sandstone
f Fine-grained sandstone
m Medium-grained sandstone
c Coarse-grained sandstone
vc Very coarse-grained sandstone
g Gravel
p Pebble
c Cobble
Sedimentary structures
Parallel lamination
Ripple lamination
Convoluted lamination
Tabular cross stratification
Trough cross stratification
Mud cracks
Soft pebbles
Carbonate nodules
Positive granoselection
Trace and body fossils
Rhizocretions
Tree logs
Plant remains
Plant debris / Coal
Microflora
Burrows
Tetrapod tracks
Bone remains
Other symbols
Fault
188/42 Strike/dip angle
P-TA-01 Pollen sample
TA-01 Palaeomagnetism sample

Log name: Es Tamarell	Page 03/03
Location: Racó de s'Algar–Pedra de s'Ase Section	

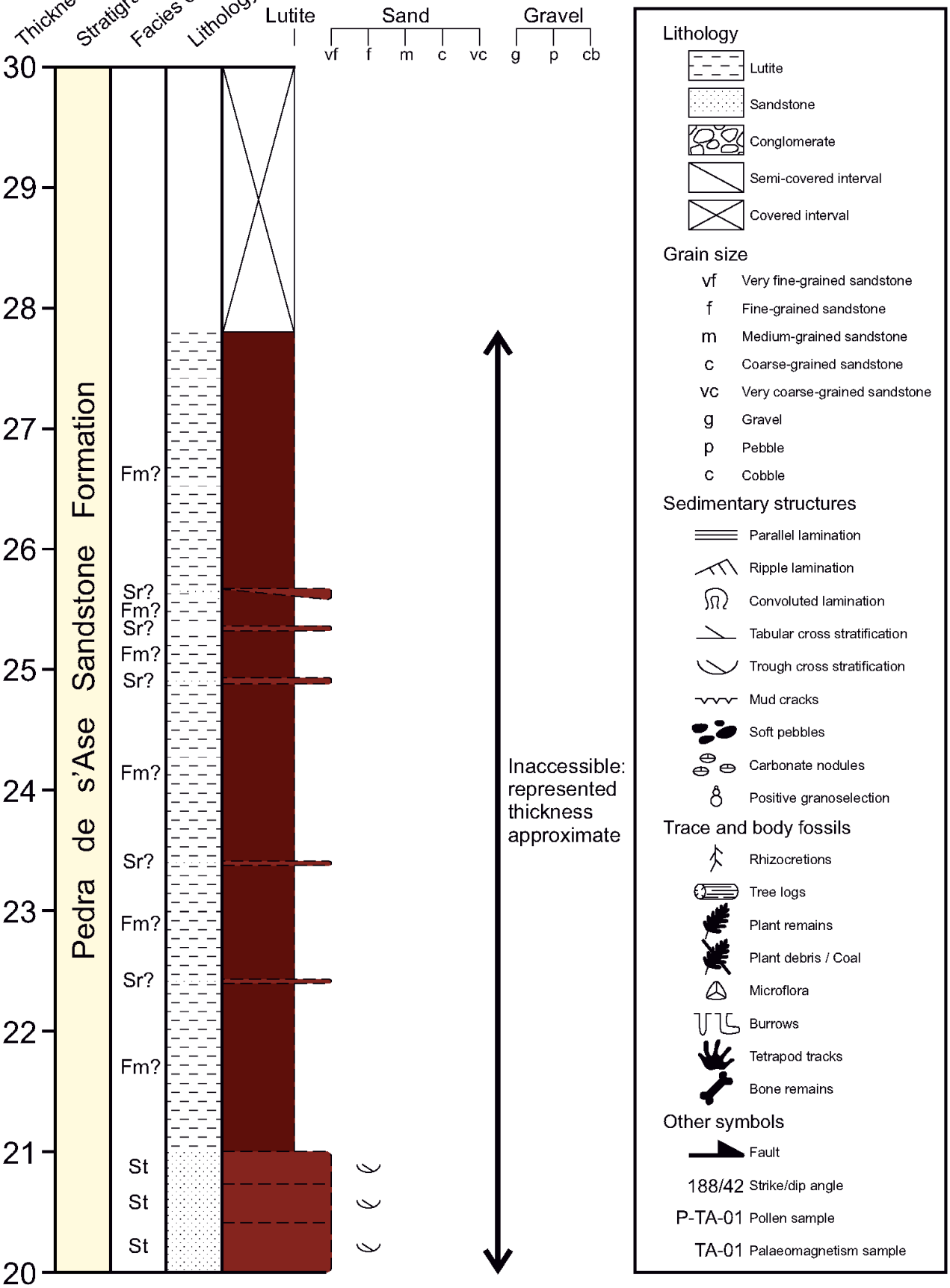

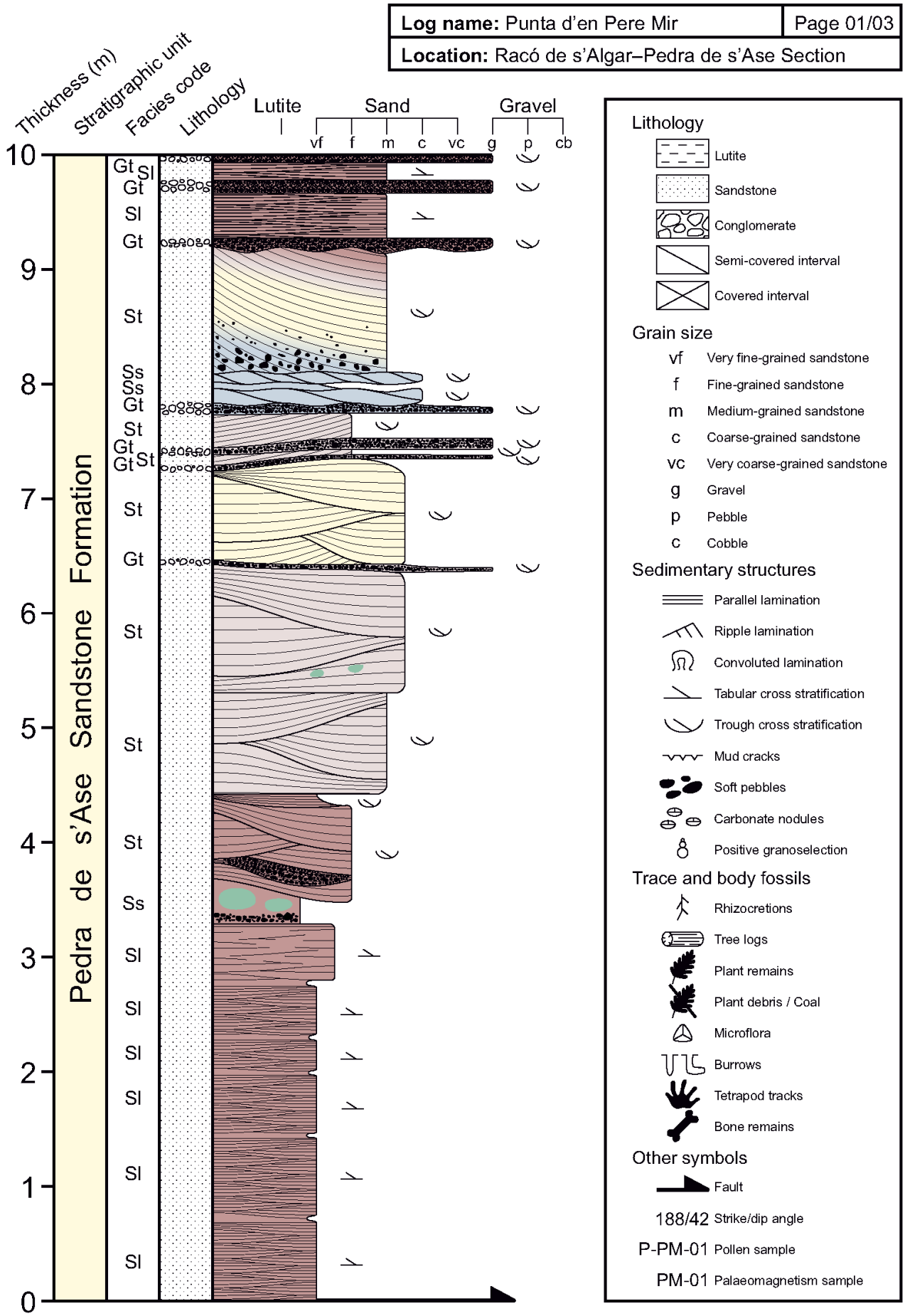
Log name: Punta d'en Pere Mir
Page 01/03
Location: Racó de s'Algar–Pedra de s'Ase Section
Thickness (m)
Stratigraphic unit
Facies code
Lithology
Lutite
Sand
Gravel
vf f m c vc g p cb
Pedra de s'Ase Sandstone Formation
10
9
8
7
6
5
4
3
2
1
0
Gt Sl
Gt
Sl
Gt
St
Ss
Ss
Gt
St
Gt
Gt St
St
Gt
St
St
St
Ss
Sl
Sl
Sl
Sl
Sl
Sl
Lithology
Lutite
Sandstone
Conglomerate
Semi-covered interval
Covered interval
Grain size
vf Very fine-grained sandstone
f Fine-grained sandstone
m Medium-grained sandstone
c Coarse-grained sandstone
vc Very coarse-grained sandstone
g Gravel
p Pebble
c Cobble
Sedimentary structures
Parallel lamination
Ripple lamination
Convoluted lamination
Tabular cross stratification
Trough cross stratification
Mud cracks
Soft pebbles
Carbonate nodules
Positive granoselection
Trace and body fossils
Rhizocretions
Tree logs
Plant remains
Plant debris / Coal
Microflora
Burrows
Tetrapod tracks
Bone remains
Other symbols
Fault
188/42 Strike/dip angle
P-PM-01 Pollen sample
PM-01 Palaeomagnetism sample

Log name: Punta d'en Pere Mir	Page 02/03
Location: Racó de s'Algar–Pedra de s'Ase Section	

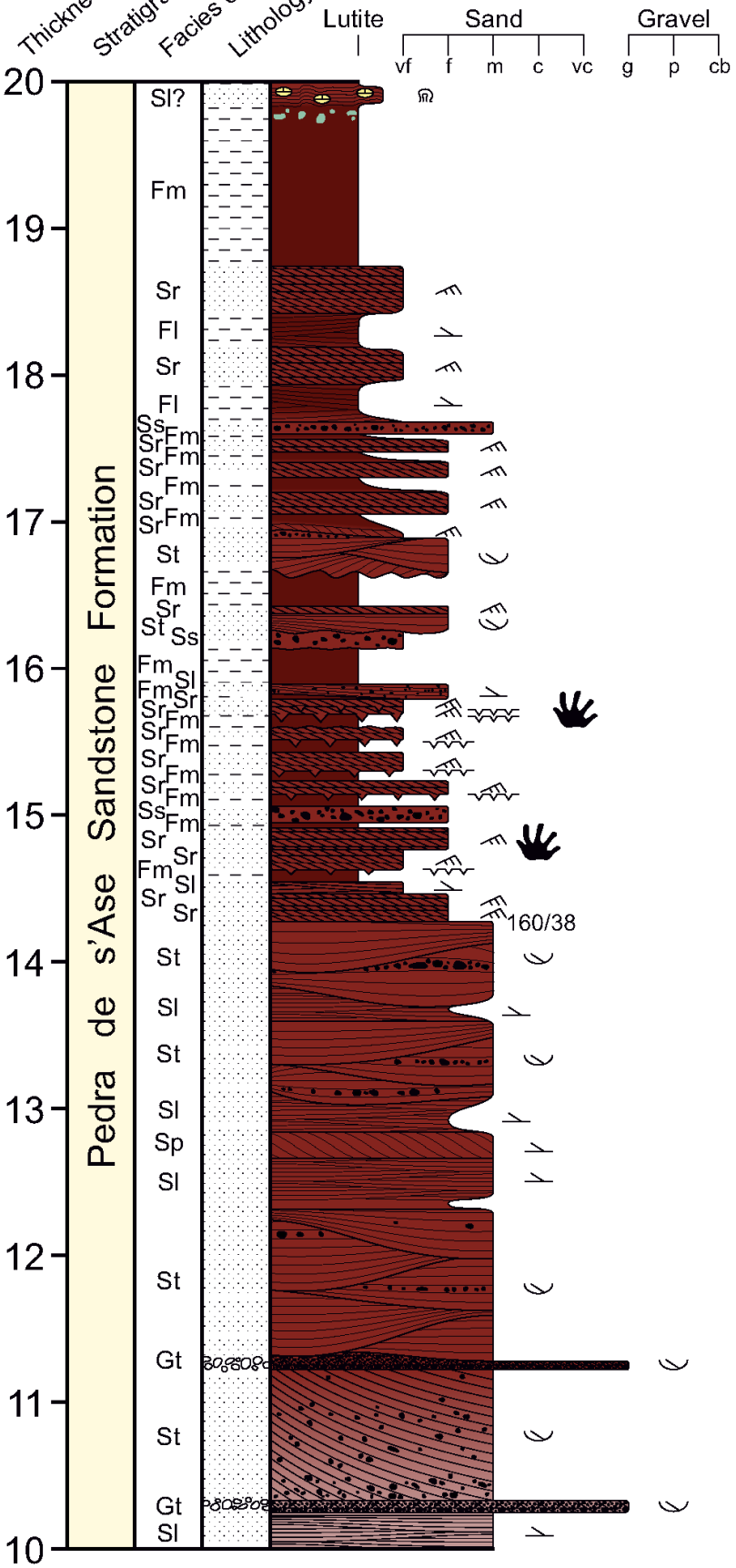

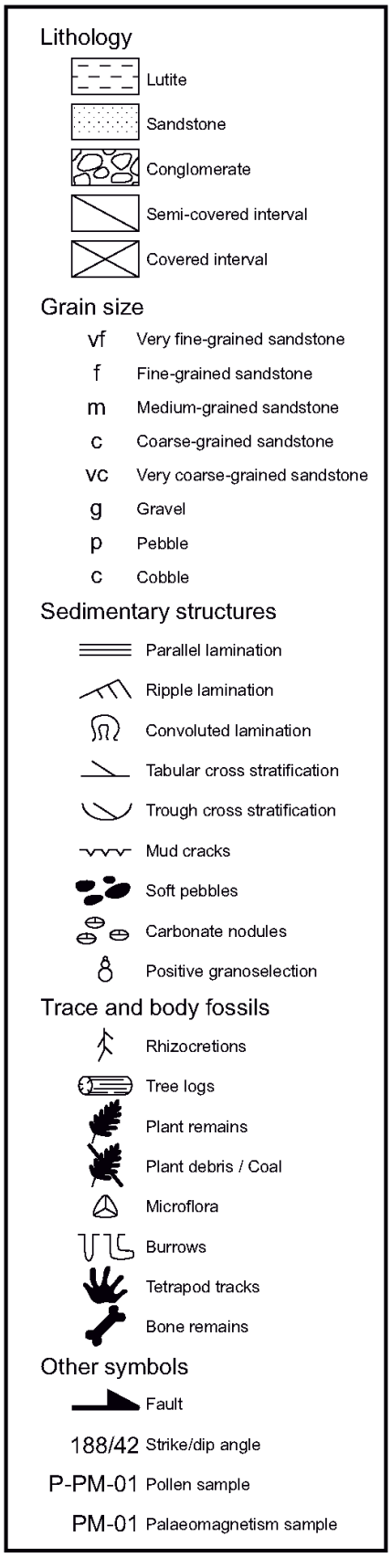

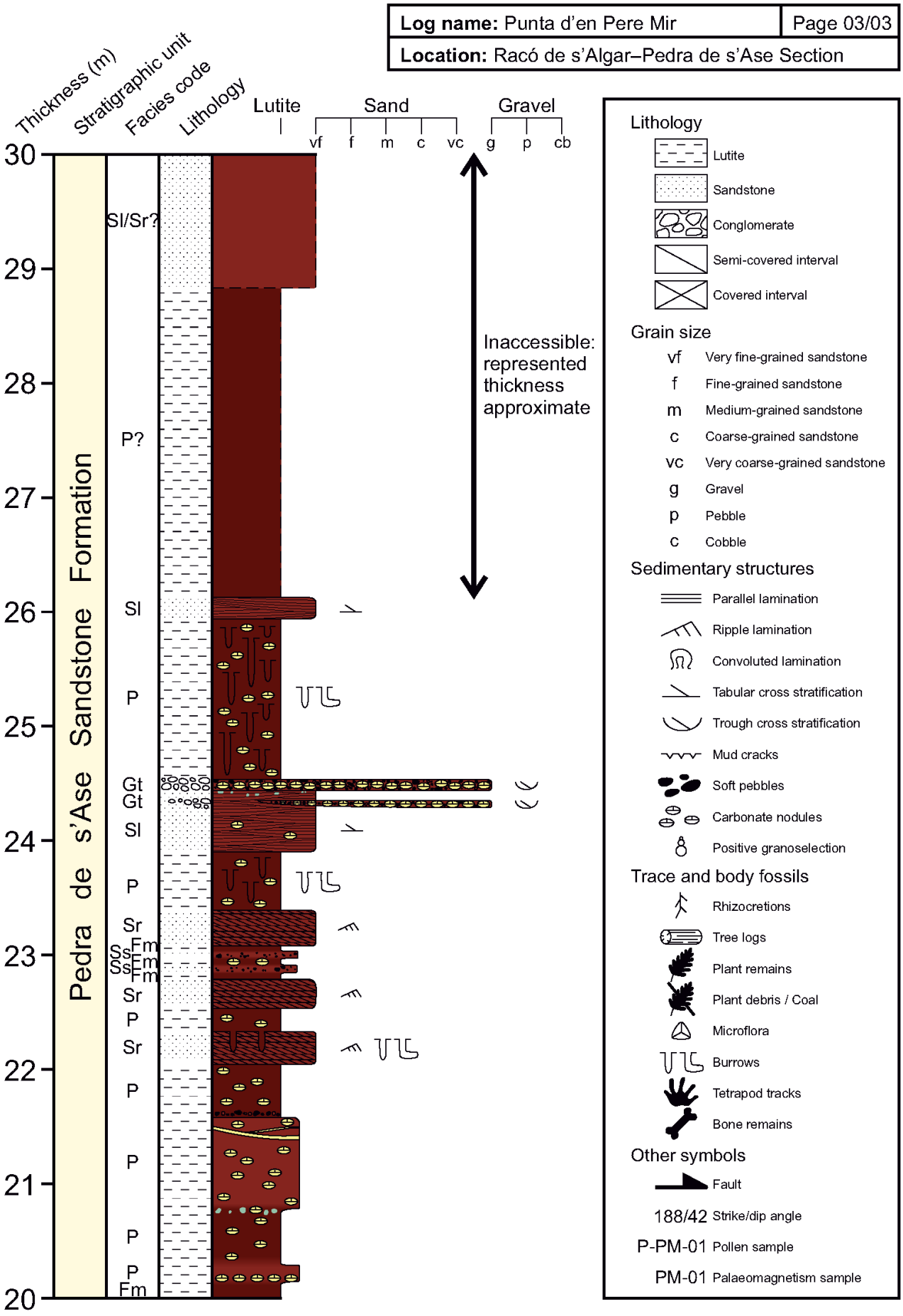
Log name: Punta d'en Pere Mir
Page 03/03
Location: Racó de s'Algar–Pedra de s'Ase Section
Thickness (m)
Stratigraphic unit
Facies code
Lithology
Lutite
Sand
Gravel
vf f m c vc g p cb
Pedra de s'Ase Sandstone Formation
Inaccessible: represented thickness approximate
Lithology
Lutite
Sandstone
Conglomerate
Semi-covered interval
Covered interval
Grain size
vf Very fine-grained sandstone
f Fine-grained sandstone
m Medium-grained sandstone
c Coarse-grained sandstone
vc Very coarse-grained sandstone
g Gravel
p Pebble
c Cobble
Sedimentary structures
Parallel lamination
Ripple lamination
Convoluted lamination
Tabular cross stratification
Trough cross stratification
Mud cracks
Soft pebbles
Carbonate nodules
Positive granoselection
Trace and body fossils
Rhizocretions
Tree logs
Plant remains
Plant debris / Coal
Microflora
Burrows
Tetrapod tracks
Bone remains
Other symbols
Fault
188/42 Strike/dip angle
P-PM-01 Pollen sample
PM-01 Palaeomagnetism sample

Log name: Pedra de s'Ase	Page 01/17
Location: Racó de s'Algar–Pedra de s'Ase Section	

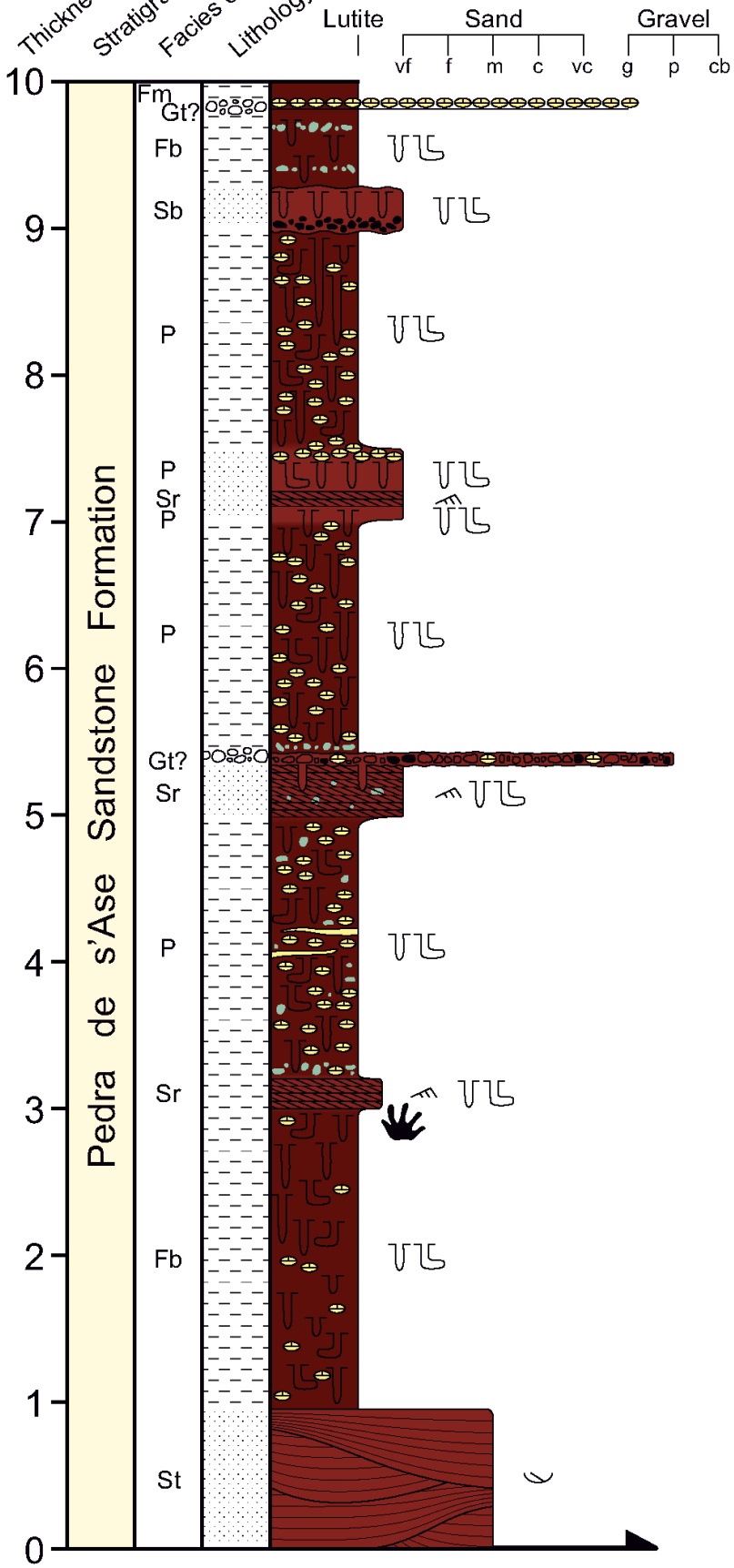

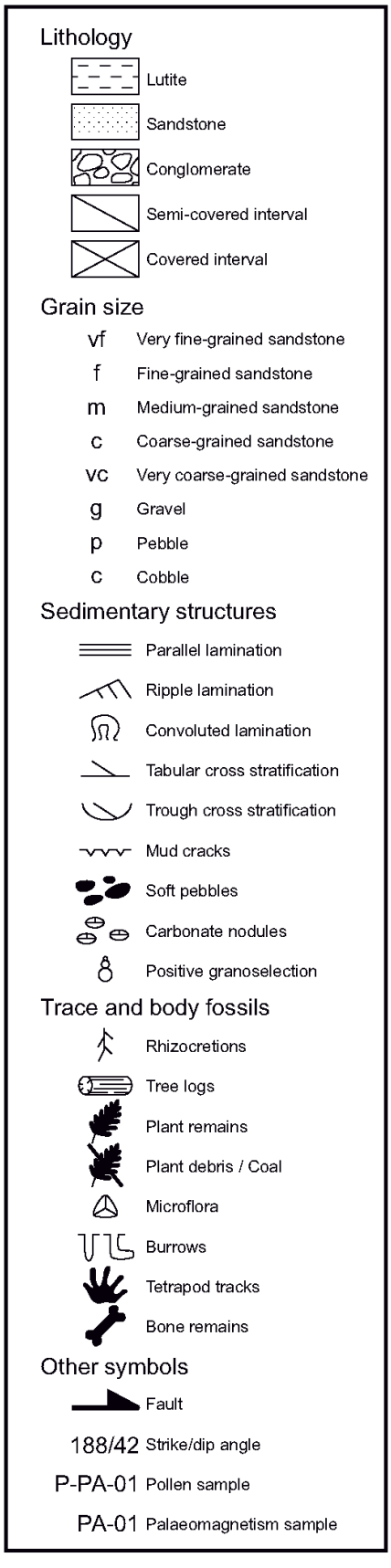

Log name: Pedra de s'Ase	Page 02/17
Location: Racó de s'Algar–Pedra de s'Ase Section	

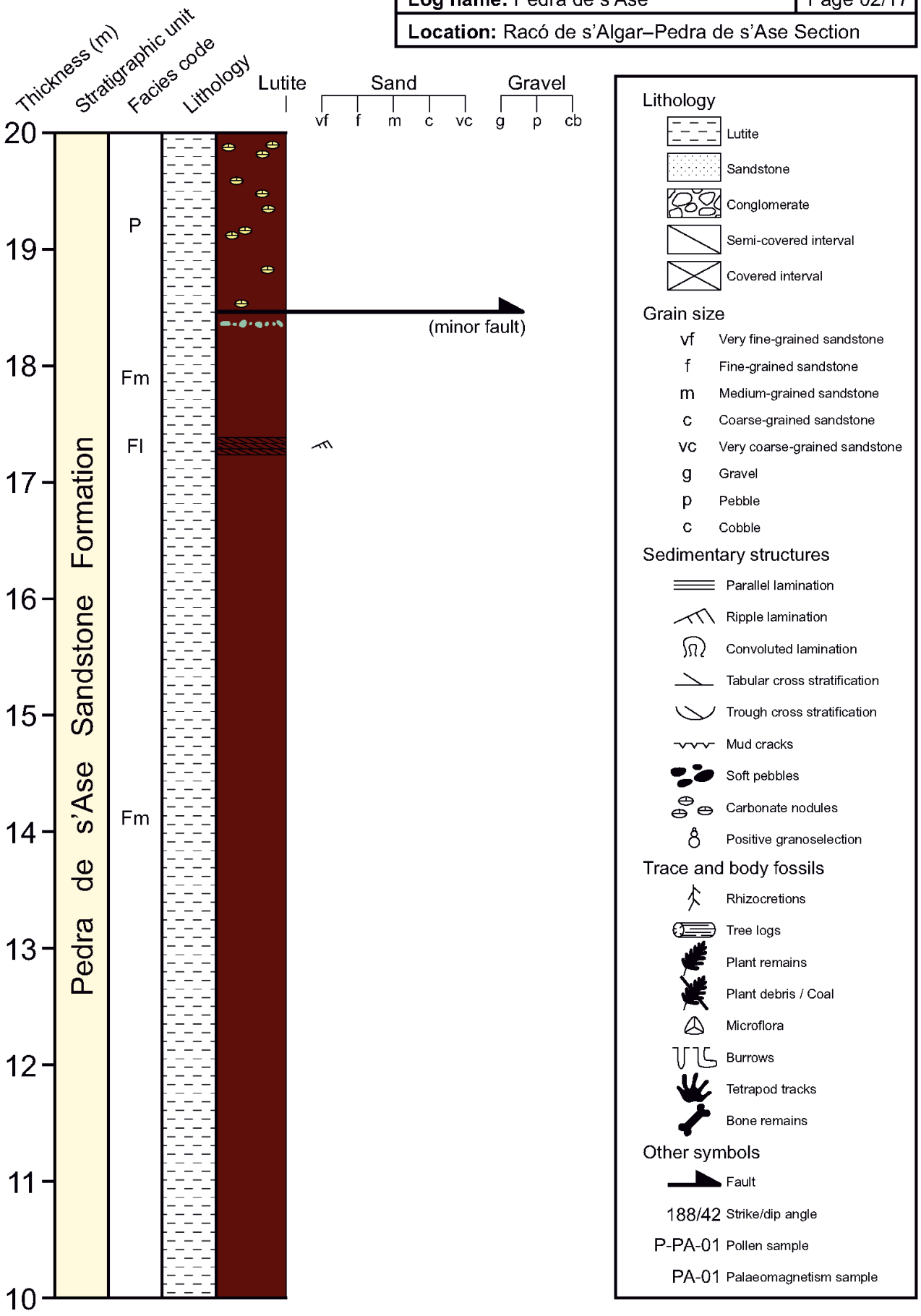

Log name: Pedra de s'Ase	Page 03/17
Location: Racó de s'Algar–Pedra de s'Ase Section	

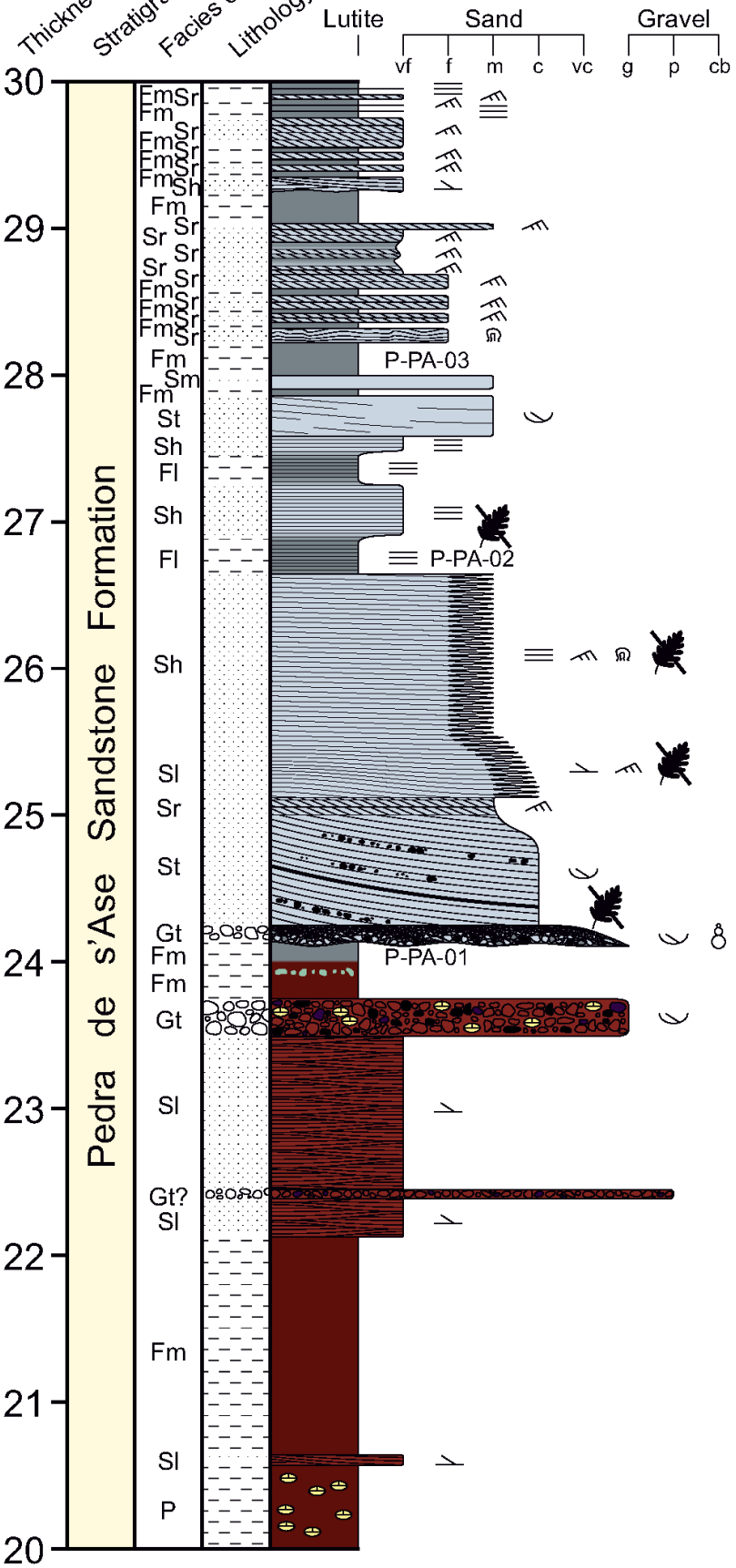

Lithology
- Lutite
- Sandstone
- Conglomerate
- Semi-covered interval
- Covered interval

Grain size
- vf Very fine-grained sandstone
- f Fine-grained sandstone
- m Medium-grained sandstone
- c Coarse-grained sandstone
- vc Very coarse-grained sandstone
- g Gravel
- p Pebble
- c Cobble

Sedimentary structures
- Parallel lamination
- Ripple lamination
- Convoluted lamination
- Tabular cross stratification
- Trough cross stratification
- Mud cracks
- Soft pebbles
- Carbonate nodules
- Positive granoselection

Trace and body fossils
- Rhizocretions
- Tree logs
- Plant remains
- Plant debris / Coal
- Microflora
- Burrows
- Tetrapod tracks
- Bone remains

Other symbols
- Fault
- 188/42 Strike/dip angle
- P-PA-01 Pollen sample
- PA-01 Palaeomagnetism sample

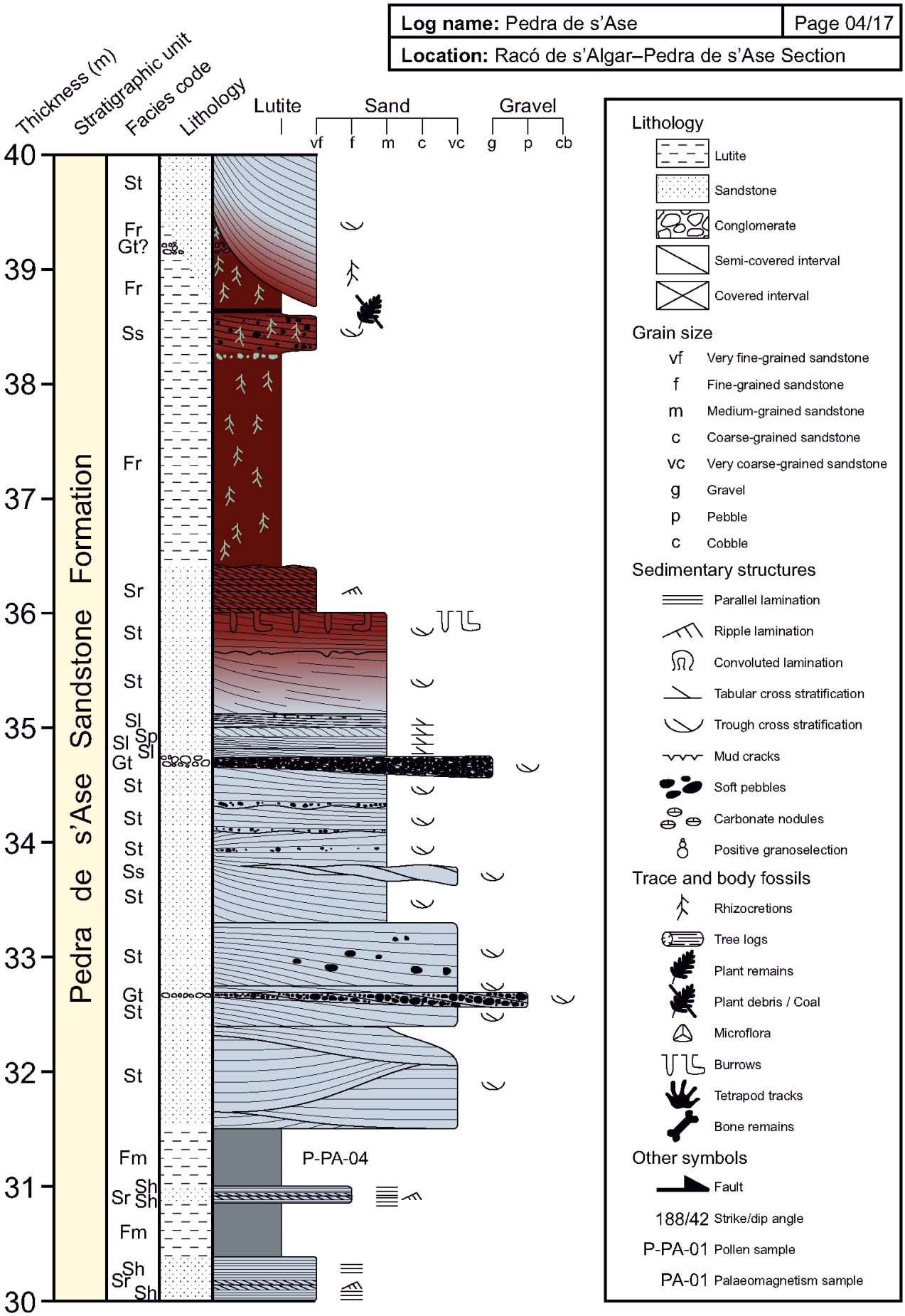
Log name: Pedra de s'Ase
Page 04/17
Location: Racó de s'Algar–Pedra de s'Ase Section
Thickness (m)
Stratigraphic unit
Facies code
Lithology
Lutite
Sand
Gravel
vf f m c vc g p cb
Pedra de s'Ase Sandstone Formation
40
39
38
37
36
35
34
33
32
31
30
St
Fr
Gt?
Fr
Ss
Fr
Sr
St
St
Sl
Sl Sp
Sl
Gt
St
St
St
Ss
St
St
Gt
St
St
Fm
Sr Sh
Fm
Sr Sh
P-PA-04
Lithology
Lutite
Sandstone
Conglomerate
Semi-covered interval
Covered interval
Grain size
vf Very fine-grained sandstone
f Fine-grained sandstone
m Medium-grained sandstone
c Coarse-grained sandstone
vc Very coarse-grained sandstone
g Gravel
p Pebble
c Cobble
Sedimentary structures
Parallel lamination
Ripple lamination
Convoluted lamination
Tabular cross stratification
Trough cross stratification
Mud cracks
Soft pebbles
Carbonate nodules
Positive granoselection
Trace and body fossils
Rhizocretions
Tree logs
Plant remains
Plant debris / Coal
Microflora
Burrows
Tetrapod tracks
Bone remains
Other symbols
Fault
188/42 Strike/dip angle
P-PA-01 Pollen sample
PA-01 Palaeomagnetism sample

Log name: Pedra de s'Ase	Page 05/17
Location: Racó de s'Algar–Pedra de s'Ase Section	

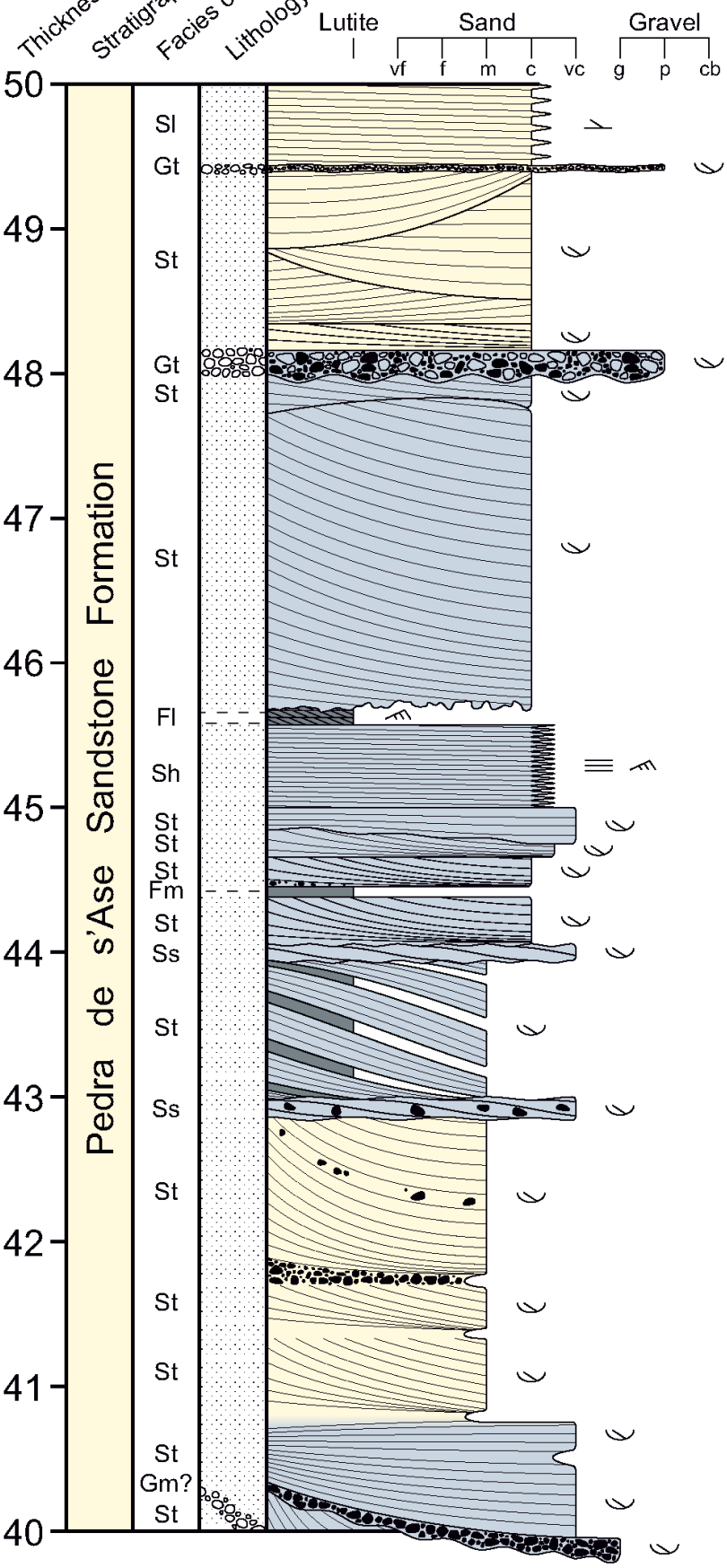

Lithology
- Lutite
- Sandstone
- Conglomerate
- Semi-covered interval
- Covered interval

Grain size
- vf Very fine-grained sandstone
- f Fine-grained sandstone
- m Medium-grained sandstone
- c Coarse-grained sandstone
- vc Very coarse-grained sandstone
- g Gravel
- p Pebble
- c Cobble

Sedimentary structures
- Parallel lamination
- Ripple lamination
- Convoluted lamination
- Tabular cross stratification
- Trough cross stratification
- Mud cracks
- Soft pebbles
- Carbonate nodules
- Positive granoselection

Trace and body fossils
- Rhizocretions
- Tree logs
- Plant remains
- Plant debris / Coal
- Microflora
- Burrows
- Tetrapod tracks
- Bone remains

Other symbols
- Fault
- 188/42 Strike/dip angle
- P-PA-01 Pollen sample
- PA-01 Palaeomagnetism sample

Log name: Pedra de s'Ase | Page 06/17

Location: Racó de s'Algar–Pedra de s'Ase Section

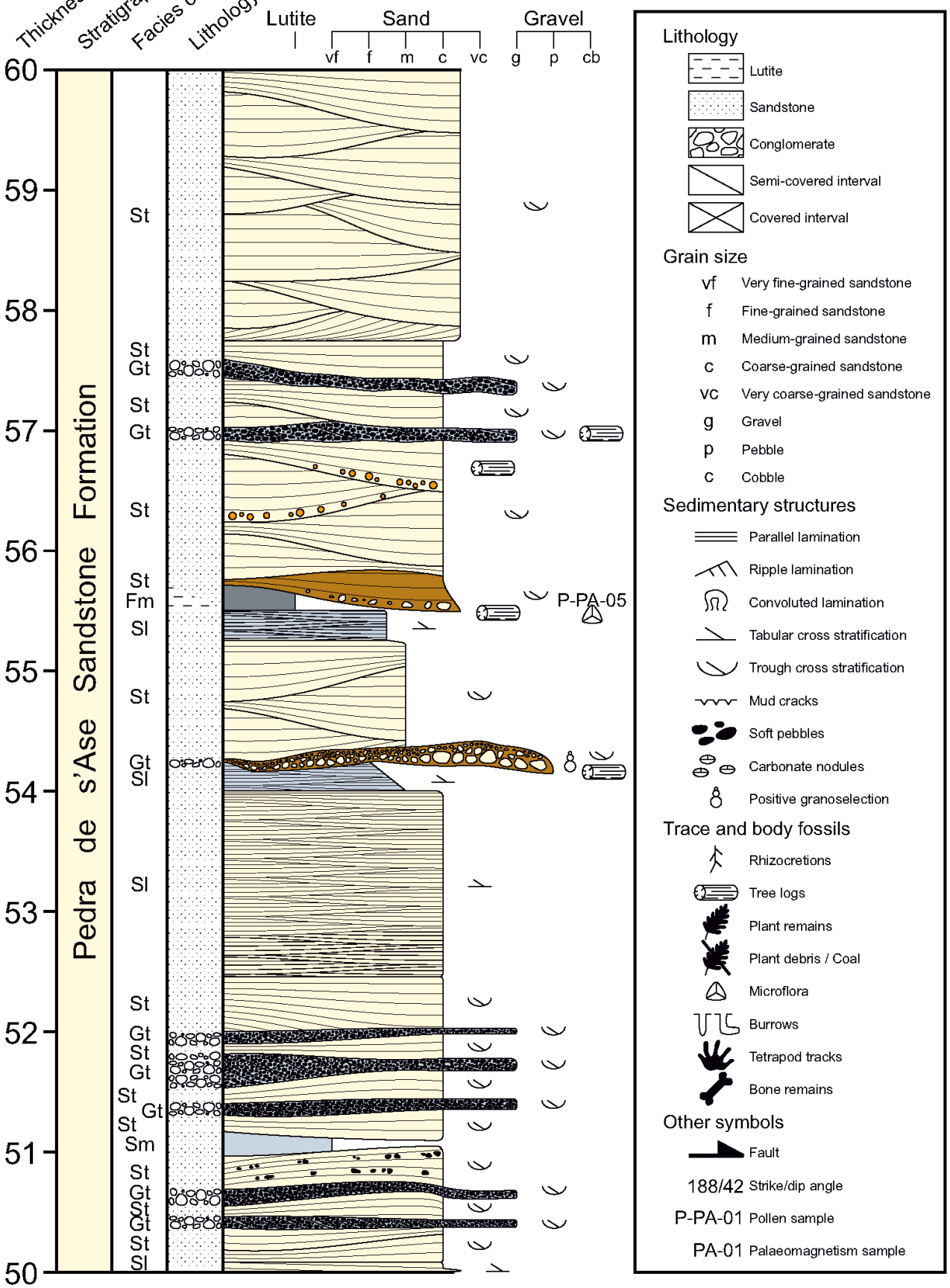

Log name: Pedra de s'Ase	Page 07/17
Location: Racó de s'Algar–Pedra de s'Ase Section	

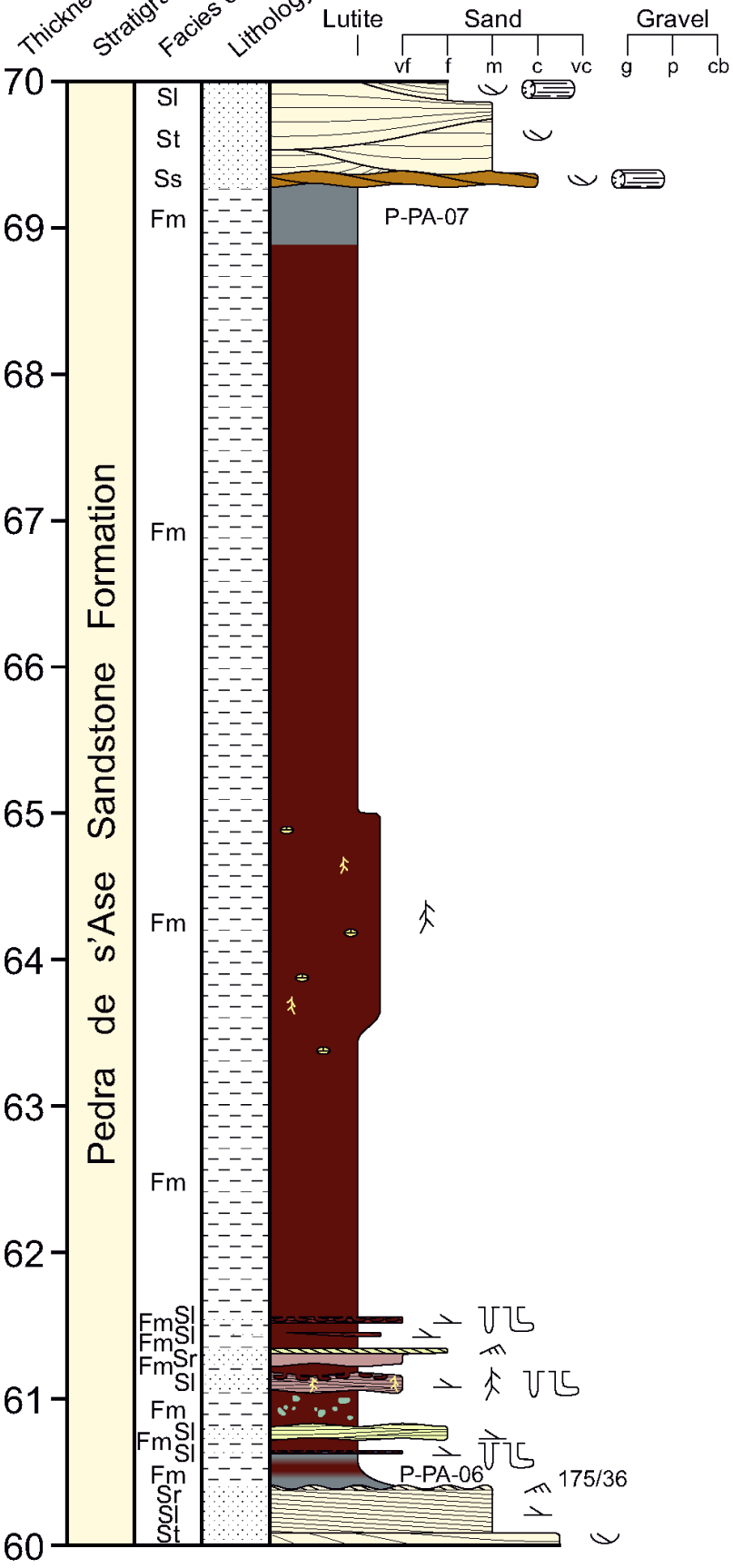

Lithology
- Lutite
- Sandstone
- Conglomerate
- Semi-covered interval
- Covered interval

Grain size
- vf Very fine-grained sandstone
- f Fine-grained sandstone
- m Medium-grained sandstone
- c Coarse-grained sandstone
- vc Very coarse-grained sandstone
- g Gravel
- p Pebble
- c Cobble

Sedimentary structures
- Parallel lamination
- Ripple lamination
- Convoluted lamination
- Tabular cross stratification
- Trough cross stratification
- Mud cracks
- Soft pebbles
- Carbonate nodules
- Positive granoselection

Trace and body fossils
- Rhizocretions
- Tree logs
- Plant remains
- Plant debris / Coal
- Microflora
- Burrows
- Tetrapod tracks
- Bone remains

Other symbols
- Fault
- 188/42 Strike/dip angle
- P-PA-01 Pollen sample
- PA-01 Palaeomagnetism sample

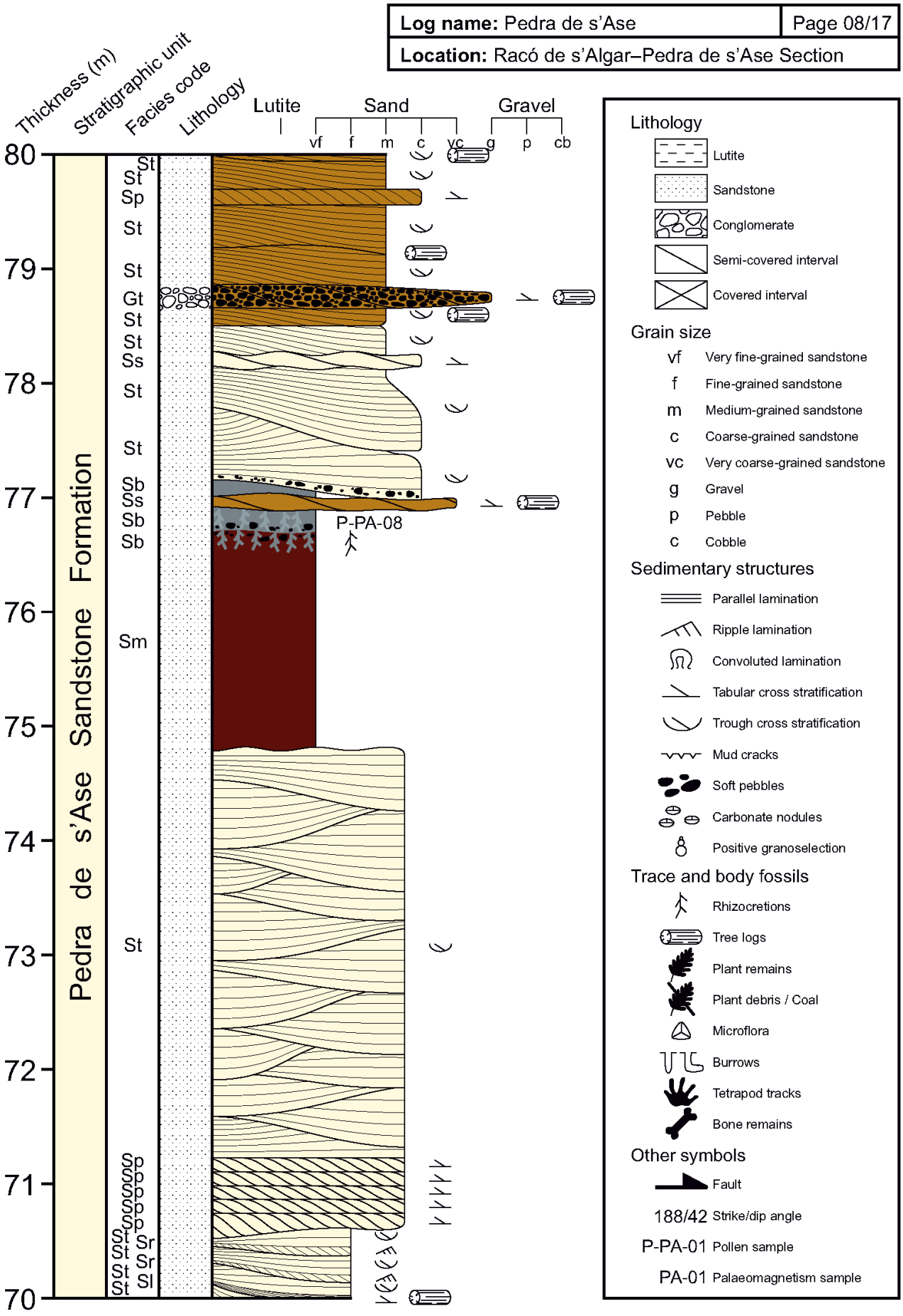
Log name: Pedra de s'Ase
Page 08/17
Location: Racó de s'Algar–Pedra de s'Ase Section
Thickness (m)
Stratigraphic unit
Facies code
Lithology
Lutite
Sand
Gravel
vf f m c vc g p cb
Pedra de s'Ase Sandstone Formation
80
79
78
77
76
75
74
73
72
71
70
St
St
Sp
St
St
Gt
St
St
Ss
St
St
Sb
Ss
Sb
Sb
Sm
St
Sp
Sp
Sp
Sp
Sp
St Sr
St Sr
St Sl
St
P-PA-08
Lithology
Lutite
Sandstone
Conglomerate
Semi-covered interval
Covered interval
Grain size
vf Very fine-grained sandstone
f Fine-grained sandstone
m Medium-grained sandstone
c Coarse-grained sandstone
vc Very coarse-grained sandstone
g Gravel
p Pebble
c Cobble
Sedimentary structures
Parallel lamination
Ripple lamination
Convoluted lamination
Tabular cross stratification
Trough cross stratification
Mud cracks
Soft pebbles
Carbonate nodules
Positive granoselection
Trace and body fossils
Rhizocretions
Tree logs
Plant remains
Plant debris / Coal
Microflora
Burrows
Tetrapod tracks
Bone remains
Other symbols
Fault
188/42 Strike/dip angle
P-PA-01 Pollen sample
PA-01 Palaeomagnetism sample

Log name: Pedra de s'Ase	Page 09/17
Location: Racó de s'Algar–Pedra de s'Ase Section	

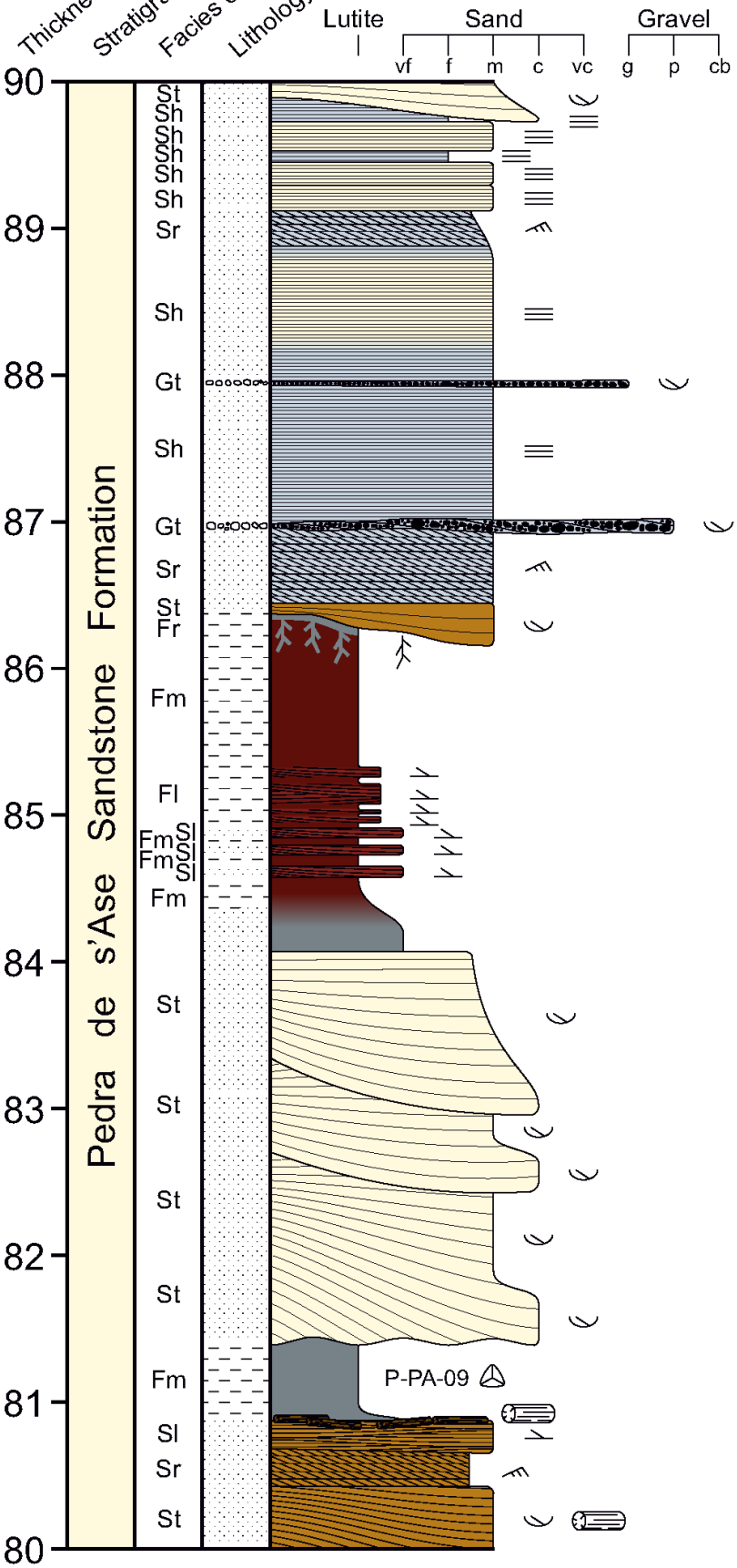

Lithology
- Lutite
- Sandstone
- Conglomerate
- Semi-covered interval
- Covered interval

Grain size
- vf Very fine-grained sandstone
- f Fine-grained sandstone
- m Medium-grained sandstone
- c Coarse-grained sandstone
- vc Very coarse-grained sandstone
- g Gravel
- p Pebble
- c Cobble

Sedimentary structures
- Parallel lamination
- Ripple lamination
- Convoluted lamination
- Tabular cross stratification
- Trough cross stratification
- Mud cracks
- Soft pebbles
- Carbonate nodules
- Positive granoselection

Trace and body fossils
- Rhizocretions
- Tree logs
- Plant remains
- Plant debris / Coal
- Microflora
- Burrows
- Tetrapod tracks
- Bone remains

Other symbols
- Fault
- 188/42 Strike/dip angle
- P-PA-01 Pollen sample
- PA-01 Palaeomagnetism sample

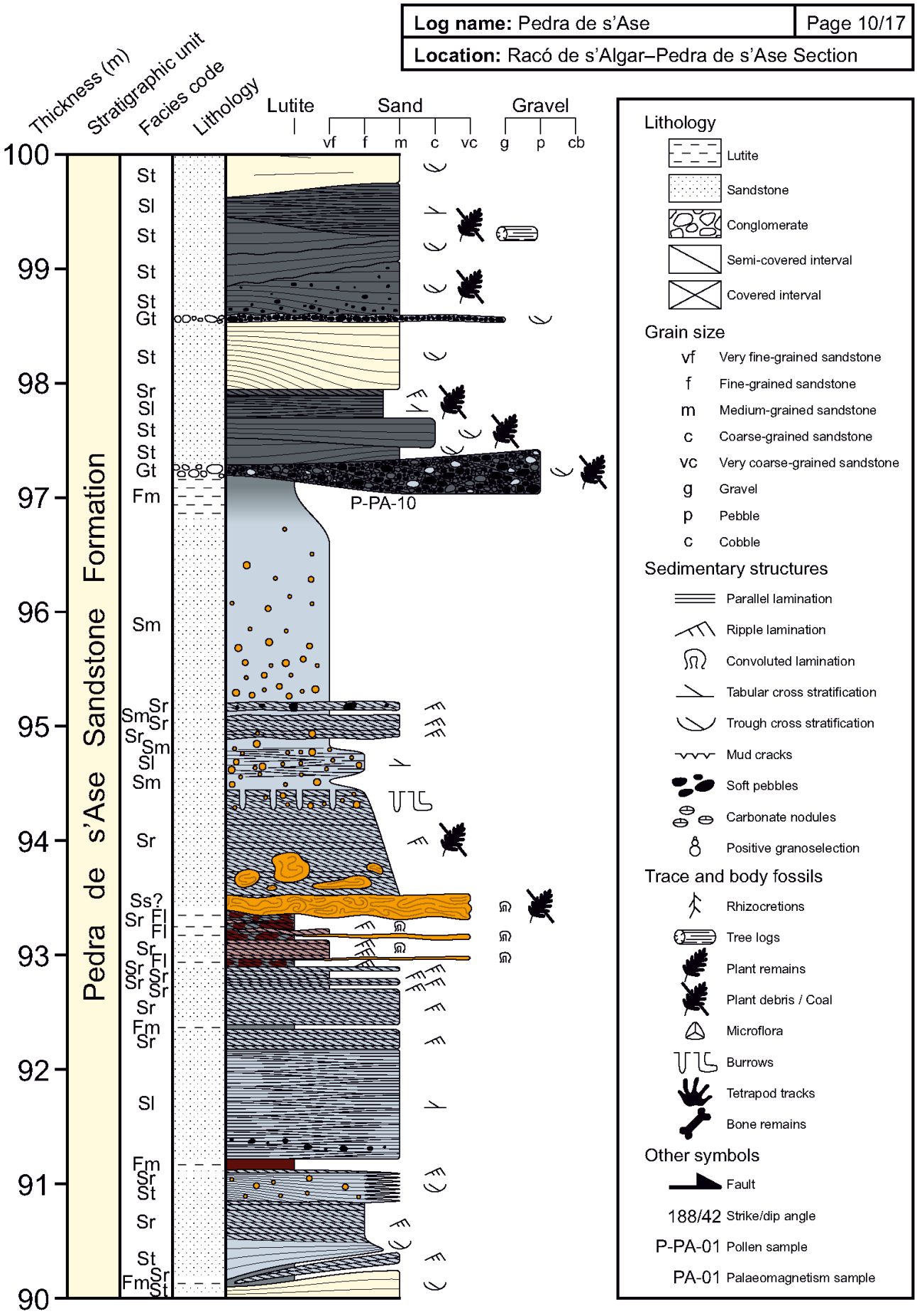
Log name: Pedra de s'Ase
Page 10/17
Location: Racó de s'Algar–Pedra de s'Ase Section
Thickness (m)
Stratigraphic unit
Facies code
Lithology
Lutite
Sand
Gravel
vf f m c vc g p cb
Pedra de s'Ase Sandstone Formation
P-PA-10
Lithology
Lutite
Sandstone
Conglomerate
Semi-covered interval
Covered interval
Grain size
vf Very fine-grained sandstone
f Fine-grained sandstone
m Medium-grained sandstone
c Coarse-grained sandstone
vc Very coarse-grained sandstone
g Gravel
p Pebble
c Cobble
Sedimentary structures
Parallel lamination
Ripple lamination
Convoluted lamination
Tabular cross stratification
Trough cross stratification
Mud cracks
Soft pebbles
Carbonate nodules
Positive granoselection
Trace and body fossils
Rhizocretions
Tree logs
Plant remains
Plant debris / Coal
Microflora
Burrows
Tetrapod tracks
Bone remains
Other symbols
Fault
188/42 Strike/dip angle
P-PA-01 Pollen sample
PA-01 Palaeomagnetism sample

Log name: Pedra de s'Ase	Page 11/17
Location: Racó de s'Algar–Pedra de s'Ase Section	

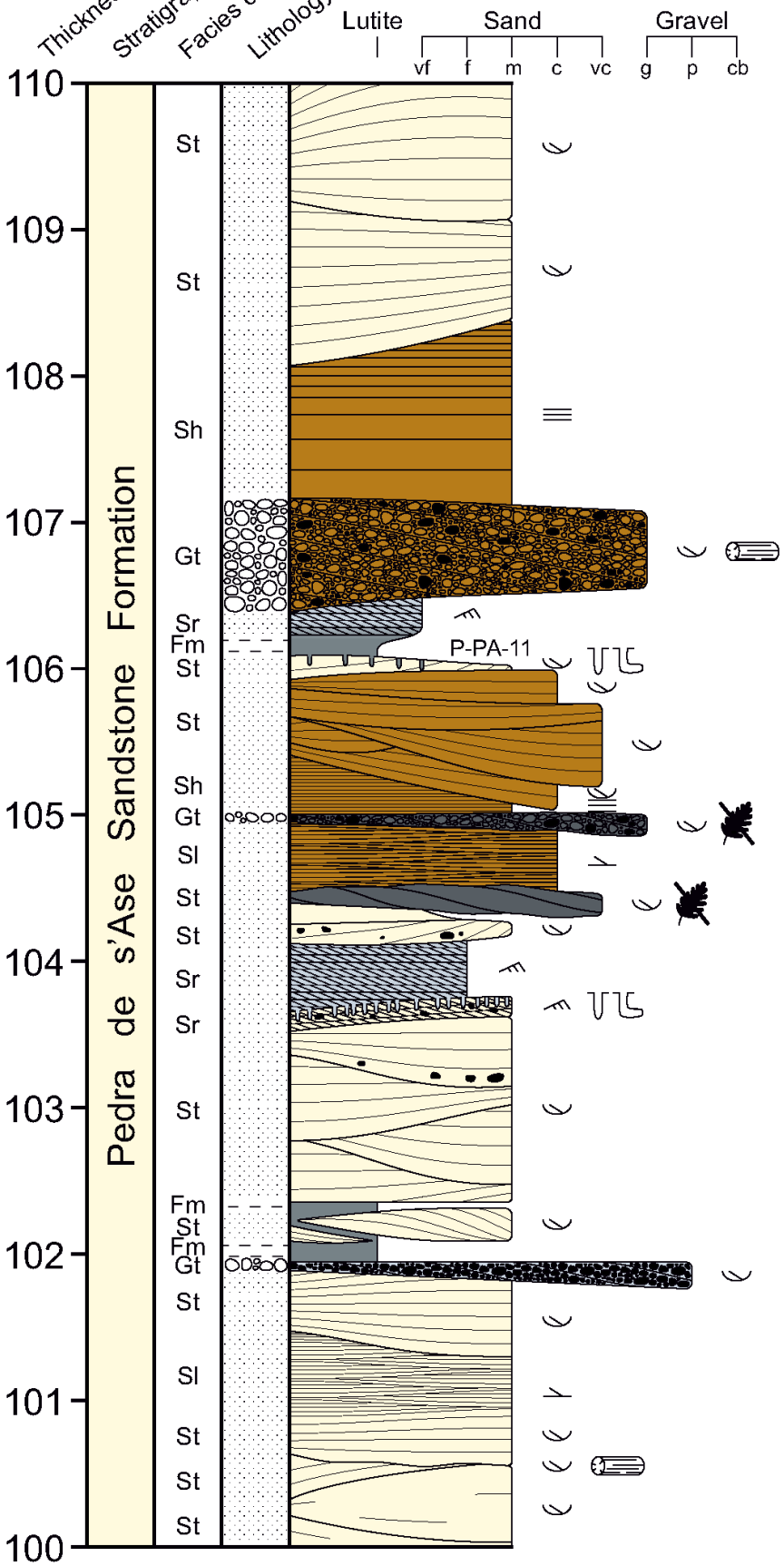

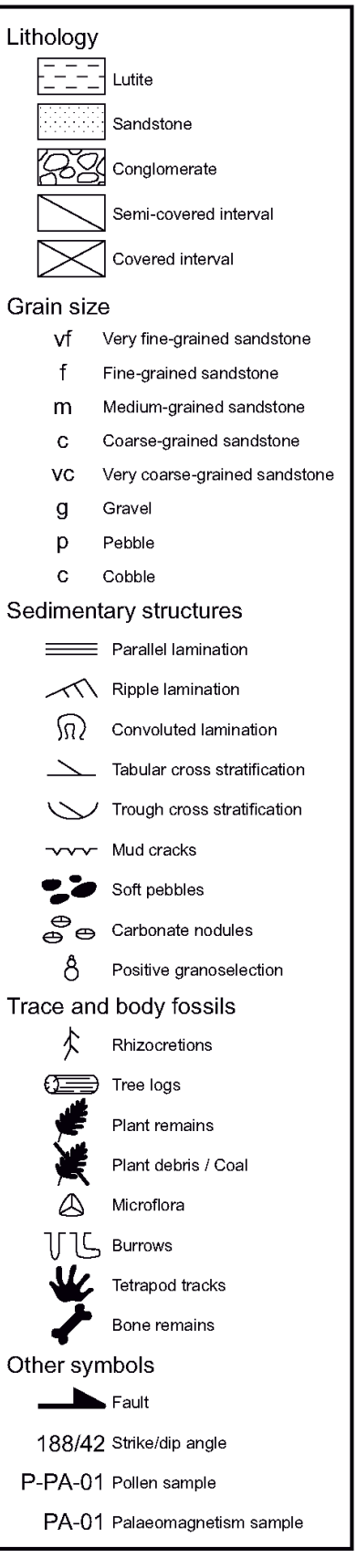

Log name: Pedra de s'Ase | Page 12/17

Location: Racó de s'Algar–Pedra de s'Ase Section

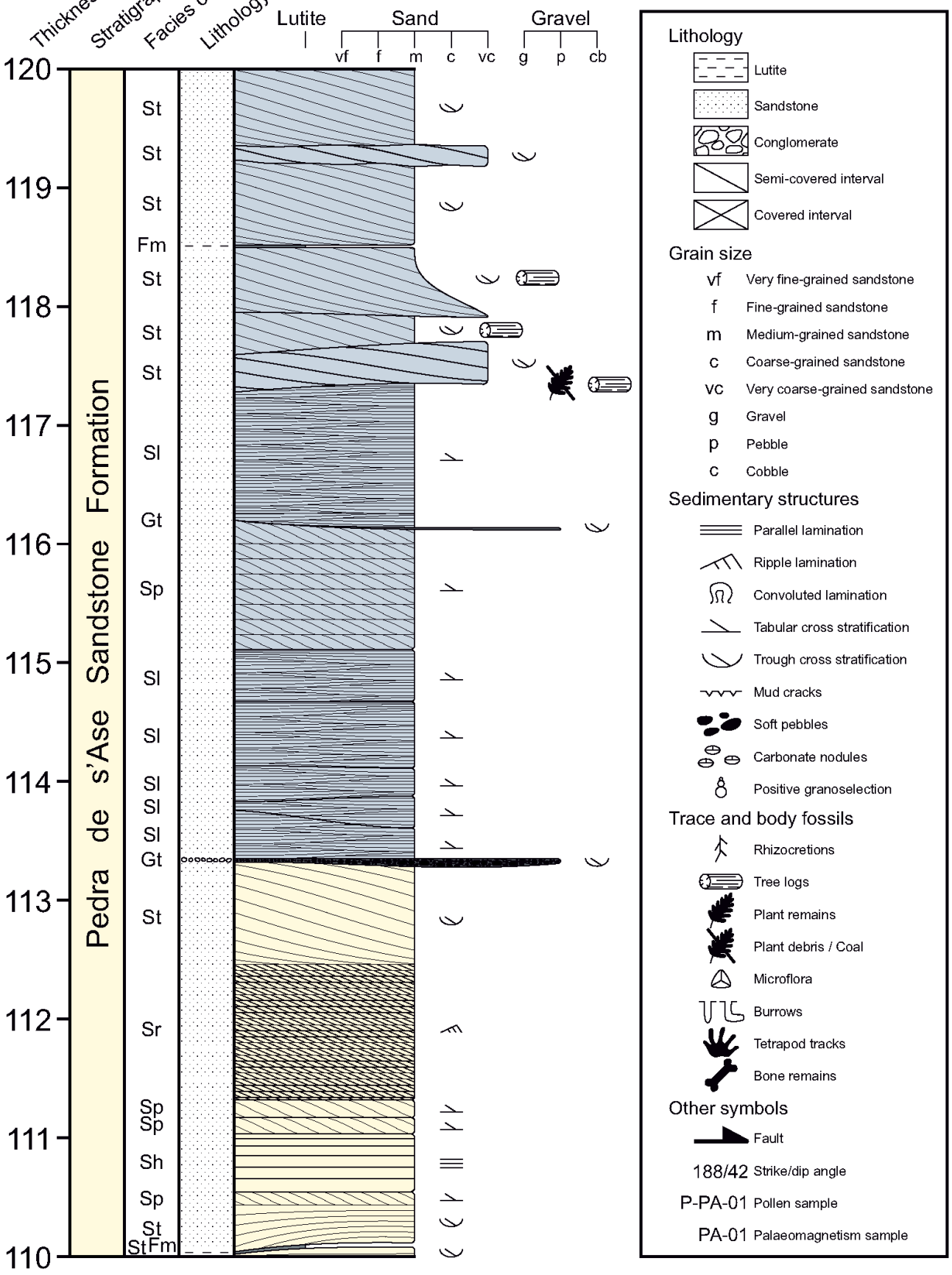

Log name: Pedra de s'Ase	Page 13/17
Location: Racó de s'Algar–Pedra de s'Ase Section	

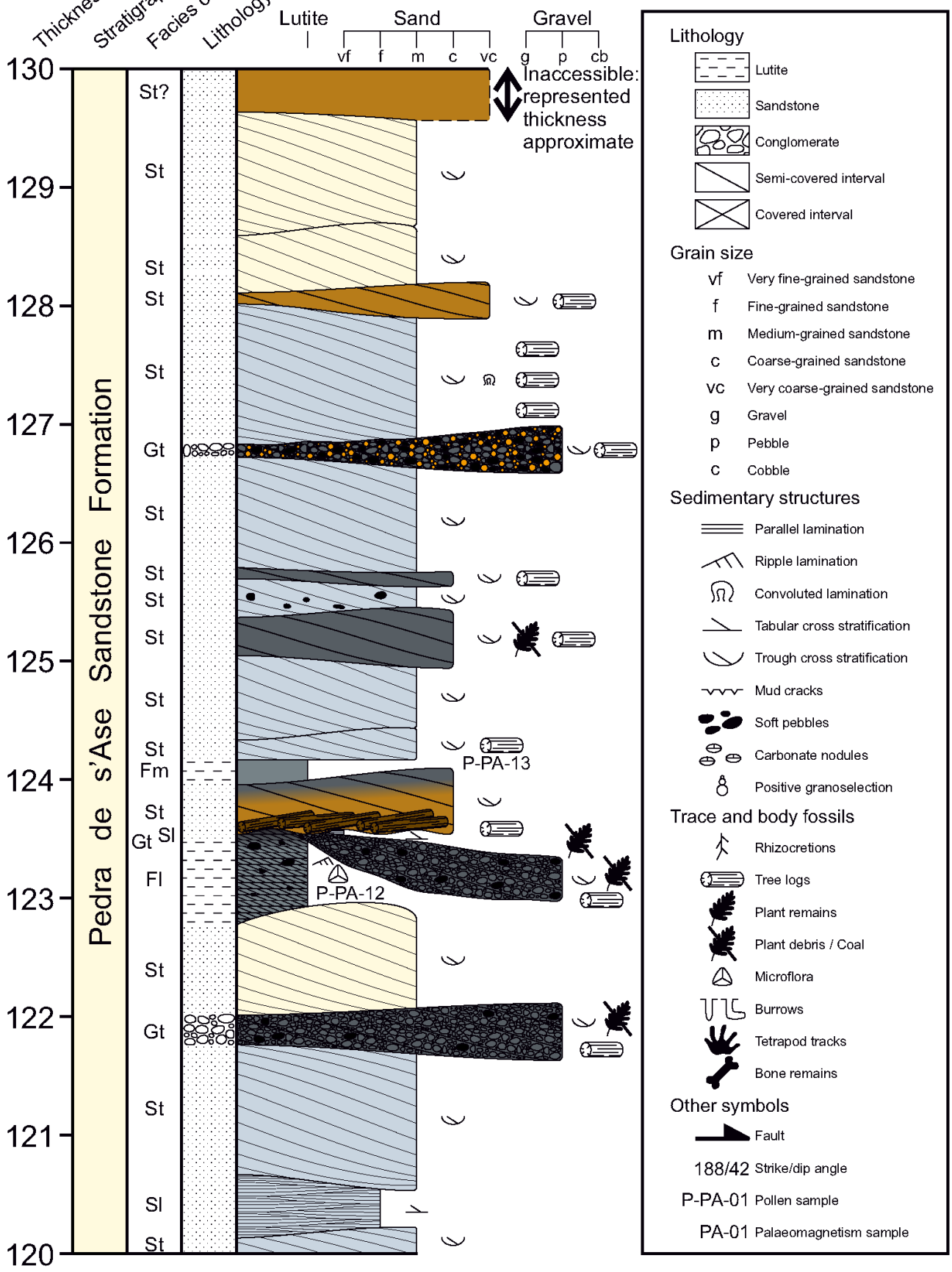

Log name: Pedra de s'Ase	Page 14/17
Location: Racó de s'Algar–Pedra de s'Ase Section	

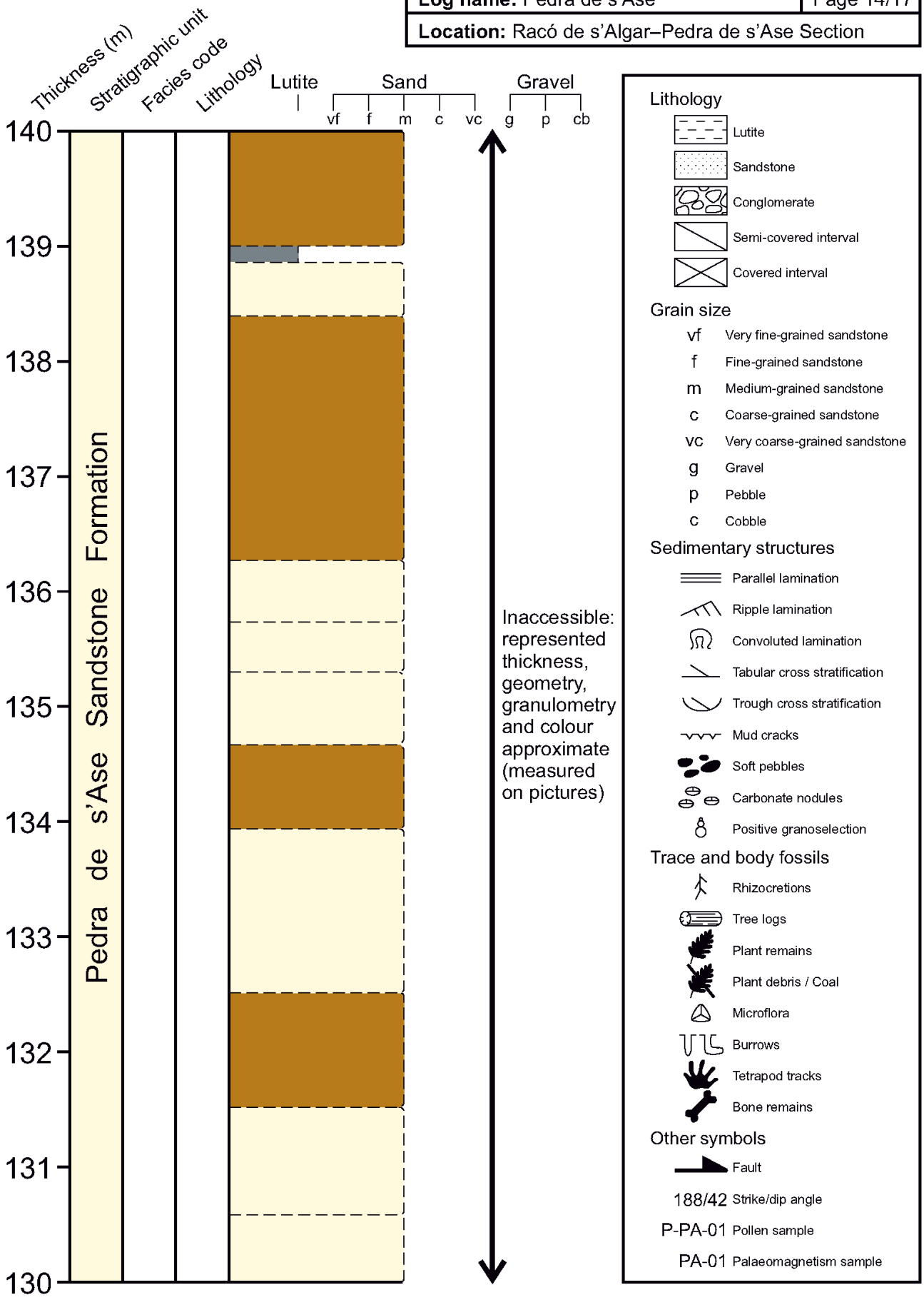

Log name: Pedra de s'Ase	Page 15/17
Location: Racó de s'Algar–Pedra de s'Ase Section	

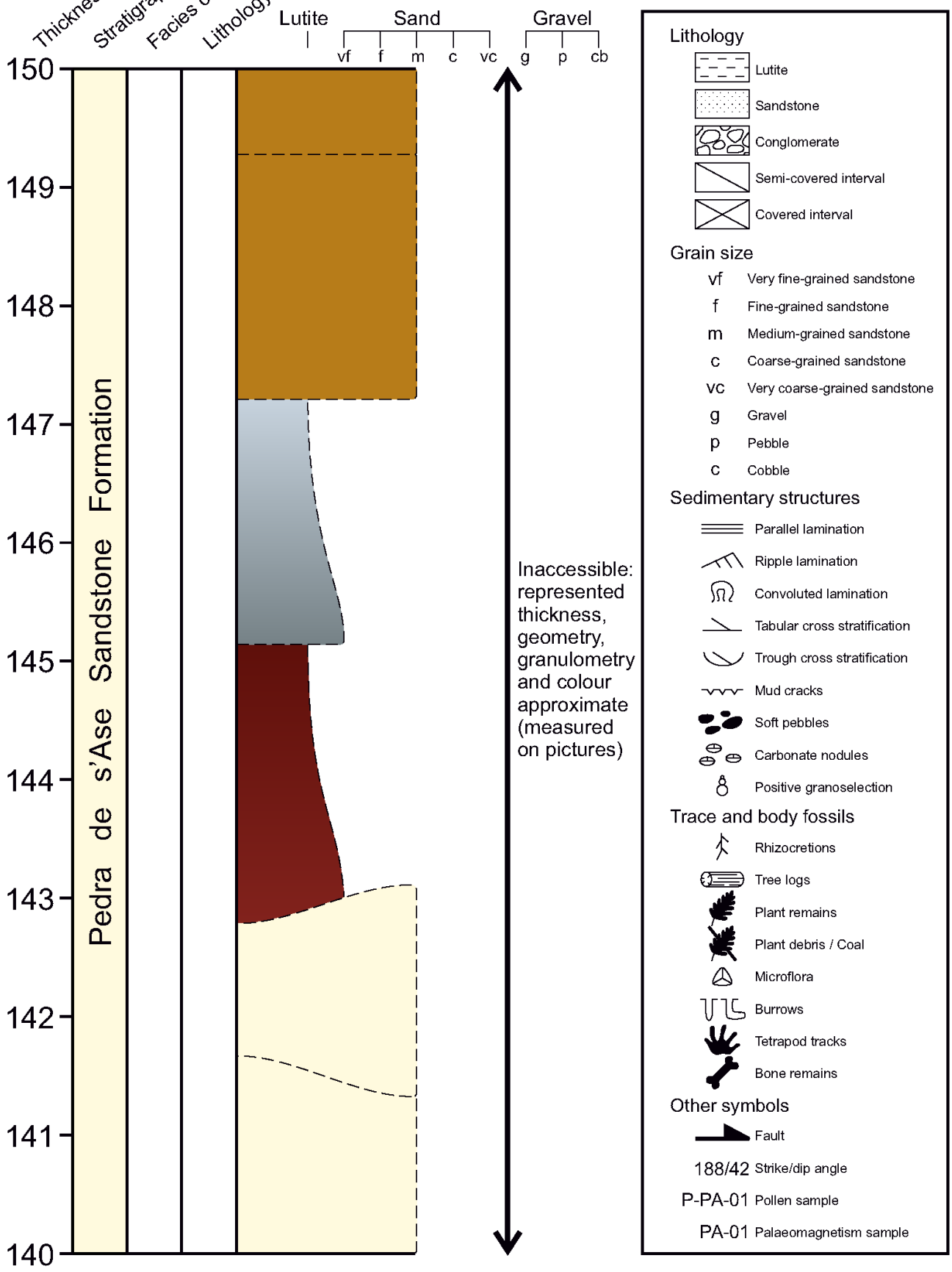

Log name: Pedra de s'Ase	Page 16/17
Location: Racó de s'Algar–Pedra de s'Ase Section	

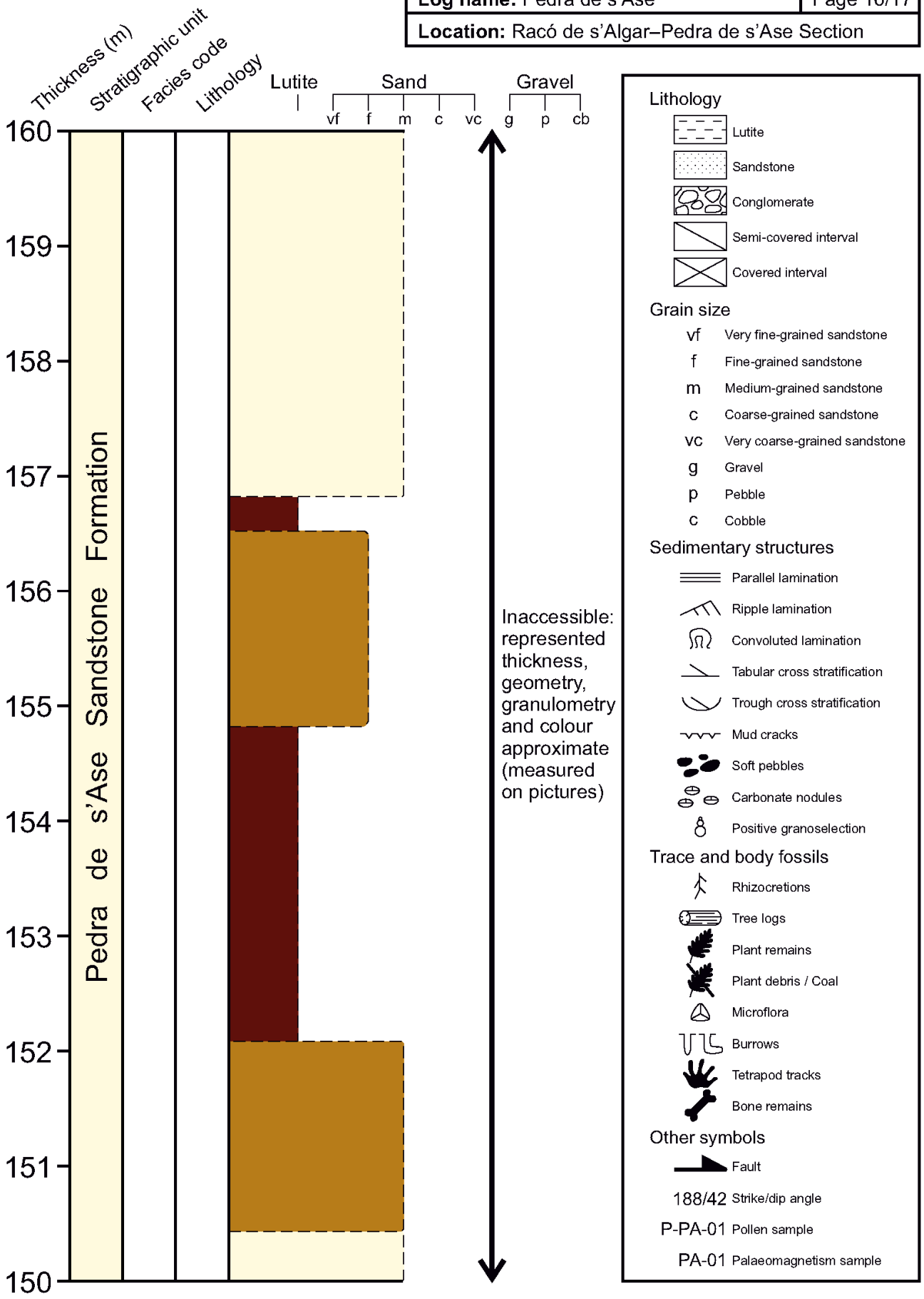

Log name: Pedra de s'Ase	Page 17/17
Location: Racó de s'Algar–Pedra de s'Ase Section	

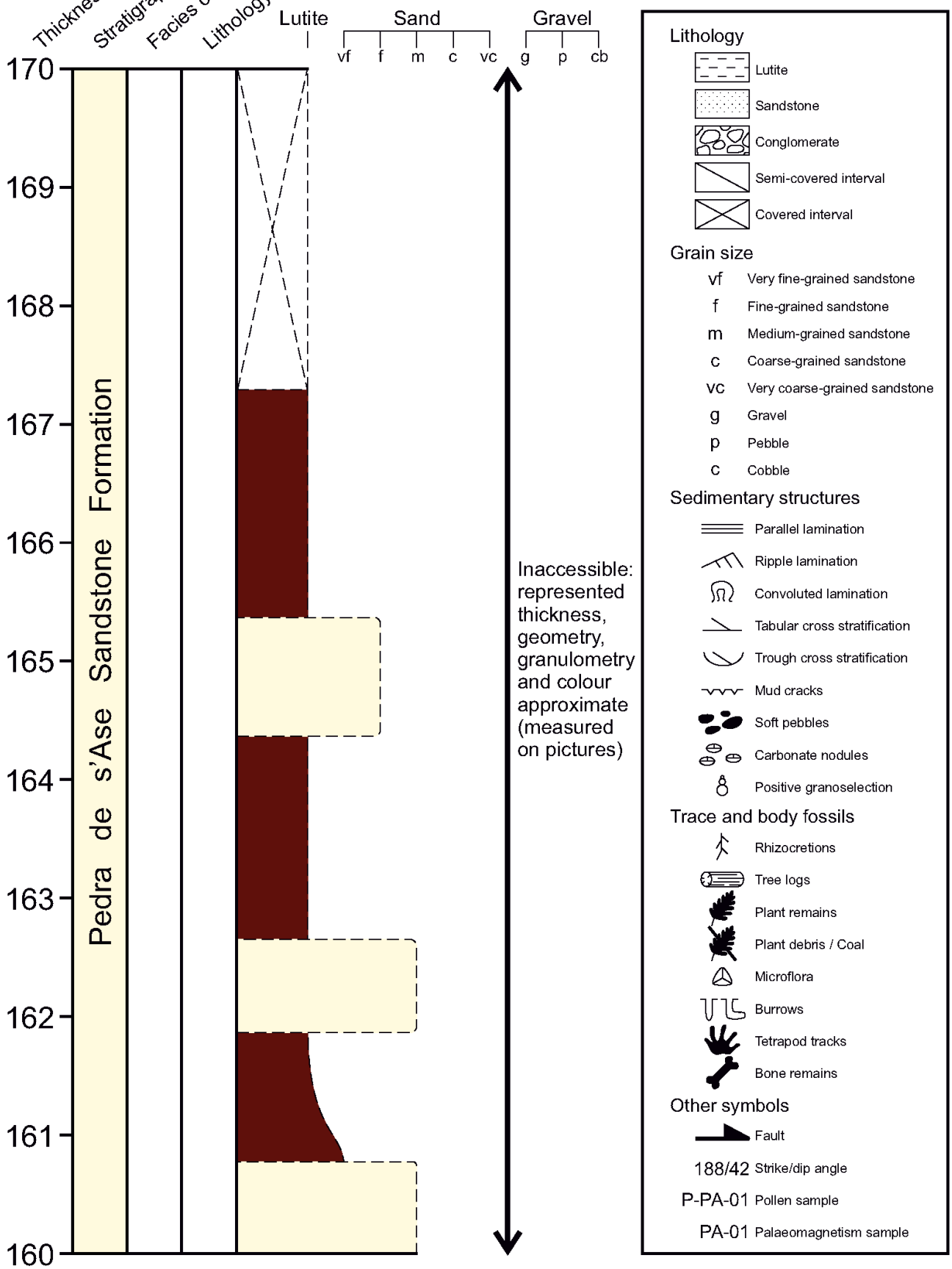

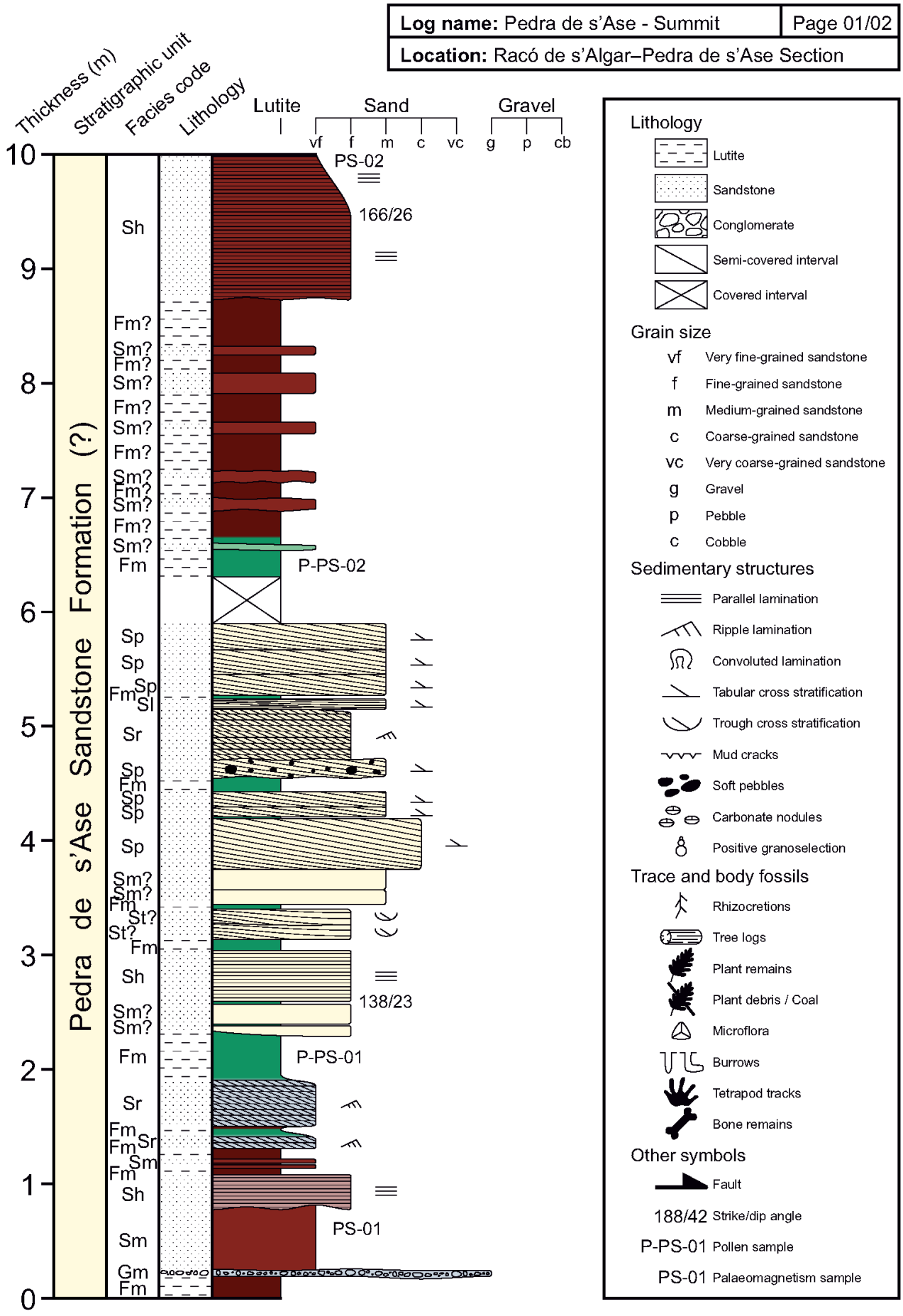
Log name: Pedra de s'Ase - Summit
Page 01/02
Location: Racó de s'Algar–Pedra de s'Ase Section
Thickness (m)
Stratigraphic unit
Facies code
Lithology
Lutite
Sand
Gravel
vf f m c vc g p cb
Pedra de s'Ase Sandstone Formation (?)
PS-02
166/26
P-PS-02
138/23
P-PS-01
PS-01
Lithology
Lutite
Sandstone
Conglomerate
Semi-covered interval
Covered interval
Grain size
vf Very fine-grained sandstone
f Fine-grained sandstone
m Medium-grained sandstone
c Coarse-grained sandstone
vc Very coarse-grained sandstone
g Gravel
p Pebble
c Cobble
Sedimentary structures
Parallel lamination
Ripple lamination
Convoluted lamination
Tabular cross stratification
Trough cross stratification
Mud cracks
Soft pebbles
Carbonate nodules
Positive granoselection
Trace and body fossils
Rhizocretions
Tree logs
Plant remains
Plant debris / Coal
Microflora
Burrows
Tetrapod tracks
Bone remains
Other symbols
Fault
188/42 Strike/dip angle
P-PS-01 Pollen sample
PS-01 Palaeomagnetism sample

Log name: Pedra de s'Ase - Summit	Page 02/02
Location: Racó de s'Algar–Pedra de s'Ase Section	

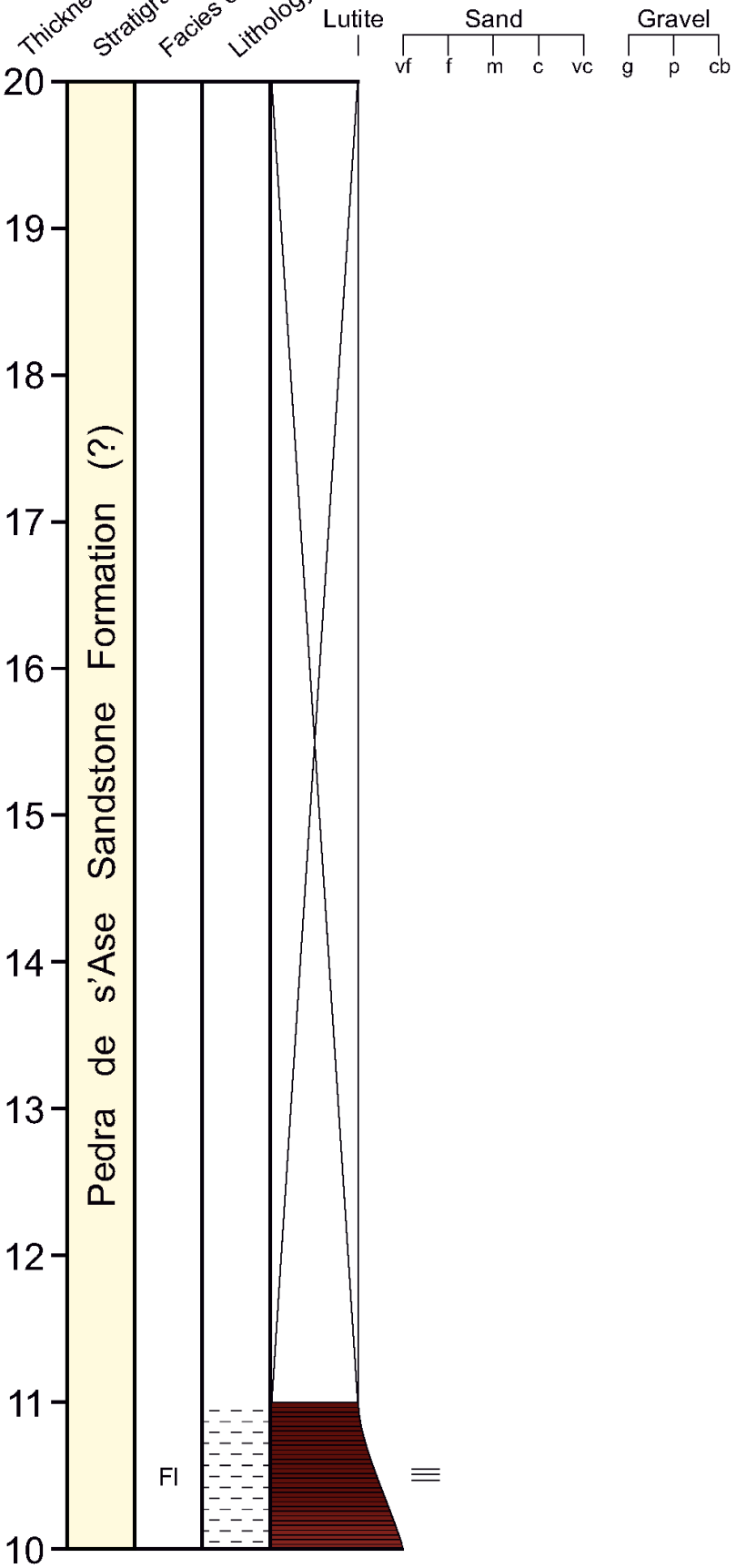

Lithology
- Lutite
- Sandstone
- Conglomerate
- Semi-covered interval
- Covered interval

Grain size
- vf Very fine-grained sandstone
- f Fine-grained sandstone
- m Medium-grained sandstone
- c Coarse-grained sandstone
- vc Very coarse-grained sandstone
- g Gravel
- p Pebble
- c Cobble

Sedimentary structures
- Parallel lamination
- Ripple lamination
- Convoluted lamination
- Tabular cross stratification
- Trough cross stratification
- Mud cracks
- Soft pebbles
- Carbonate nodules
- Positive granoselection

Trace and body fossils
- Rhizocretions
- Tree logs
- Plant remains
- Plant debris / Coal
- Microflora
- Burrows
- Tetrapod tracks
- Bone remains

Other symbols
- Fault
- 188/42 Strike/dip angle
- P-PS-01 Pollen sample
- PS-01 Palaeomagnetism sample

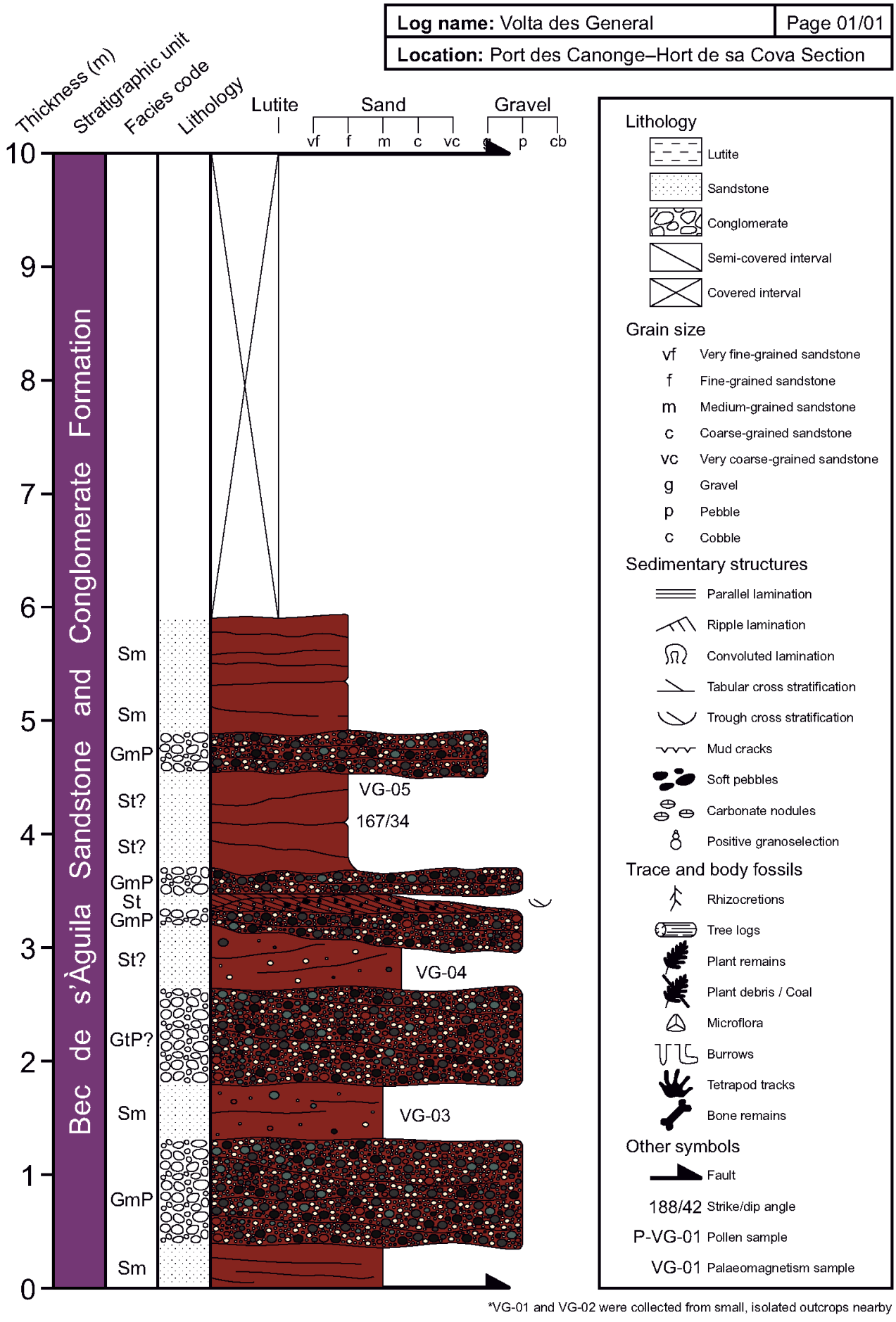

*VG-01 and VG-02 were collected from small, isolated outcrops nearby

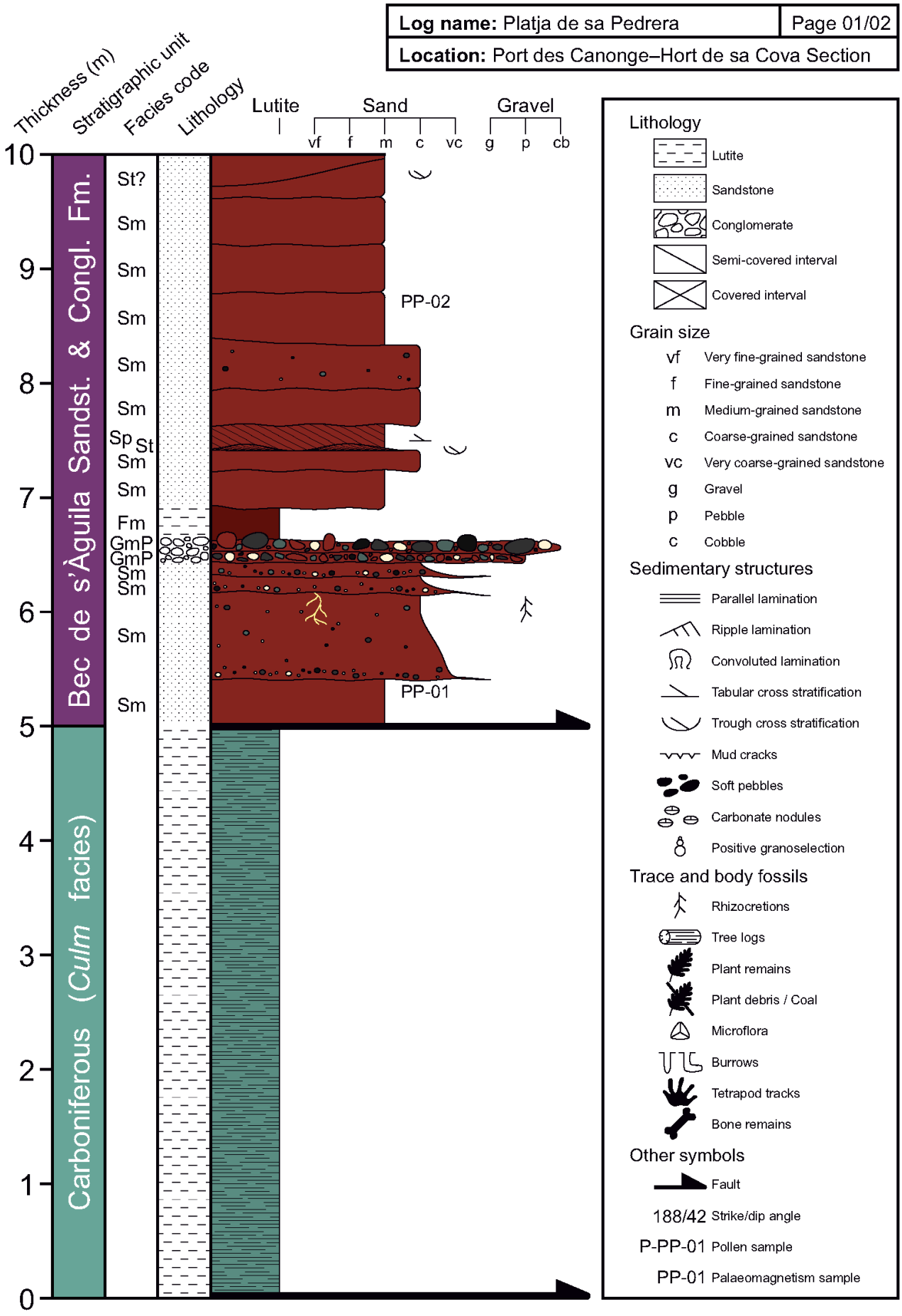
Log name: Platja de sa Pedrera
Page 01/02
Location: Port des Canonge–Hort de sa Cova Section
Thickness (m)
Stratigraphic unit
Facies code
Lithology
Lutite
Sand
Gravel
vf f m c vc g p cb
Bec de s'Àguila Sandst. & Congl. Fm.
Carboniferous (Culm facies)
St?
Sm
Sm
Sm
Sm
Sm
Sp St
Sm
Sm
Fm
GmP
GmP
Sm
Sm
Sm
Sm
PP-02
PP-01
10
9
8
7
6
5
4
3
2
1
0
Lithology
Lutite
Sandstone
Conglomerate
Semi-covered interval
Covered interval
Grain size
vf Very fine-grained sandstone
f Fine-grained sandstone
m Medium-grained sandstone
c Coarse-grained sandstone
vc Very coarse-grained sandstone
g Gravel
p Pebble
c Cobble
Sedimentary structures
Parallel lamination
Ripple lamination
Convoluted lamination
Tabular cross stratification
Trough cross stratification
Mud cracks
Soft pebbles
Carbonate nodules
Positive granoselection
Trace and body fossils
Rhizocretions
Tree logs
Plant remains
Plant debris / Coal
Microflora
Burrows
Tetrapod tracks
Bone remains
Other symbols
Fault
188/42 Strike/dip angle
P-PP-01 Pollen sample
PP-01 Palaeomagnetism sample

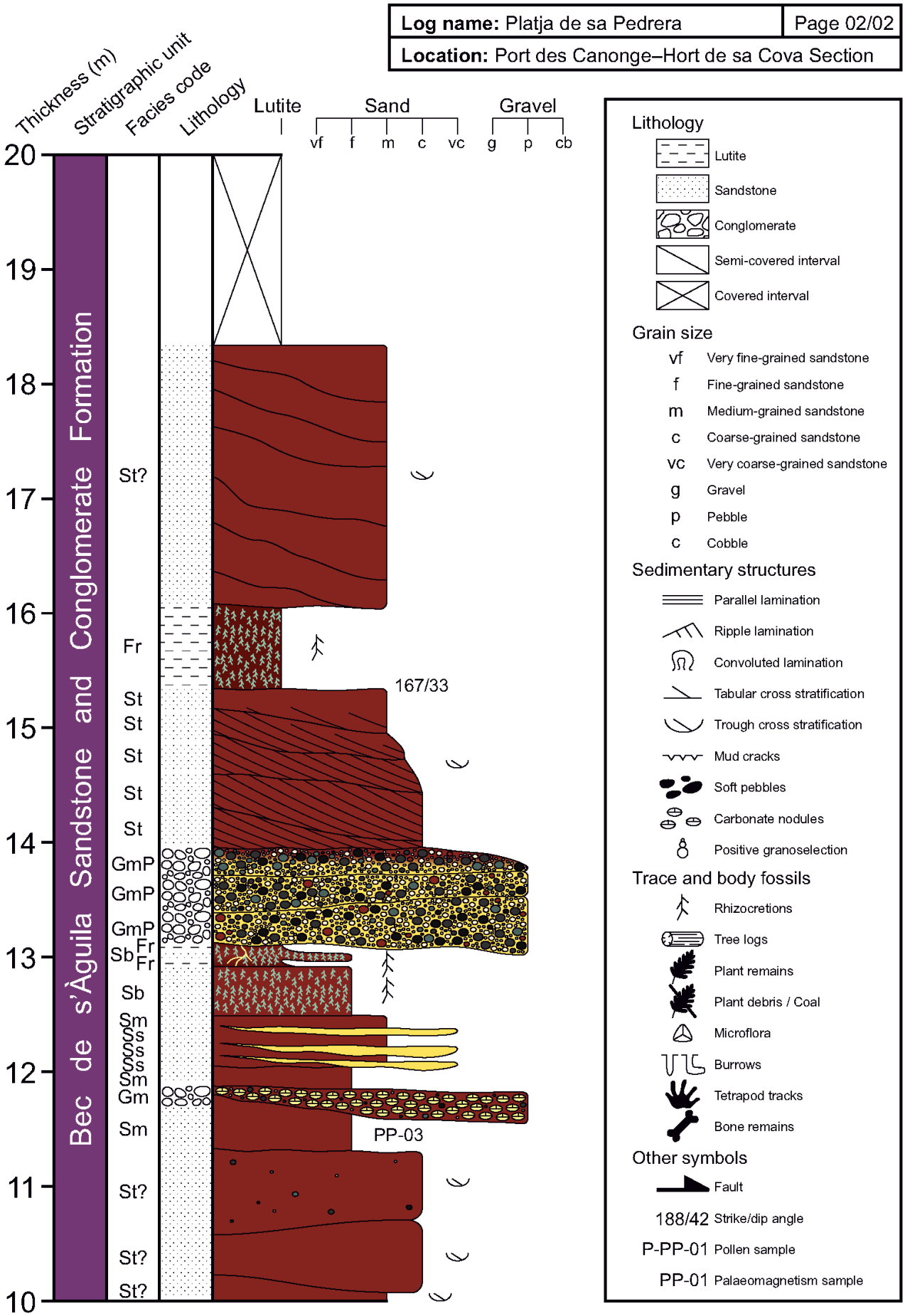
Log name: Platja de sa Pedrera
Page 02/02
Location: Port des Canonge–Hort de sa Cova Section
Thickness (m)
Stratigraphic unit
Facies code
Lithology
Lutite
Sand
Gravel
vf f m c vc g p cb
Bec de s'Àguila Sandstone and Conglomerate Formation
20
19
18
17
16
15
14
13
12
11
10
St?
Fr
St
St
St
St
St
GmP
GmP
GmP
Sb Fr
Fr
Sb
Sm
Ss
Ss
Ss
Sm
Gm
Sm
St?
St?
St?
167/33
PP-03
Lithology
Lutite
Sandstone
Conglomerate
Semi-covered interval
Covered interval
Grain size
vf Very fine-grained sandstone
f Fine-grained sandstone
m Medium-grained sandstone
c Coarse-grained sandstone
vc Very coarse-grained sandstone
g Gravel
p Pebble
c Cobble
Sedimentary structures
Parallel lamination
Ripple lamination
Convoluted lamination
Tabular cross stratification
Trough cross stratification
Mud cracks
Soft pebbles
Carbonate nodules
Positive granoselection
Trace and body fossils
Rhizocretions
Tree logs
Plant remains
Plant debris / Coal
Microflora
Burrows
Tetrapod tracks
Bone remains
Other symbols
Fault
188/42 Strike/dip angle
P-PP-01 Pollen sample
PP-01 Palaeomagnetism sample

Log name: Port des Canonge	Page 01/61
Location: Port des Canonge–Hort de sa Cova Section	

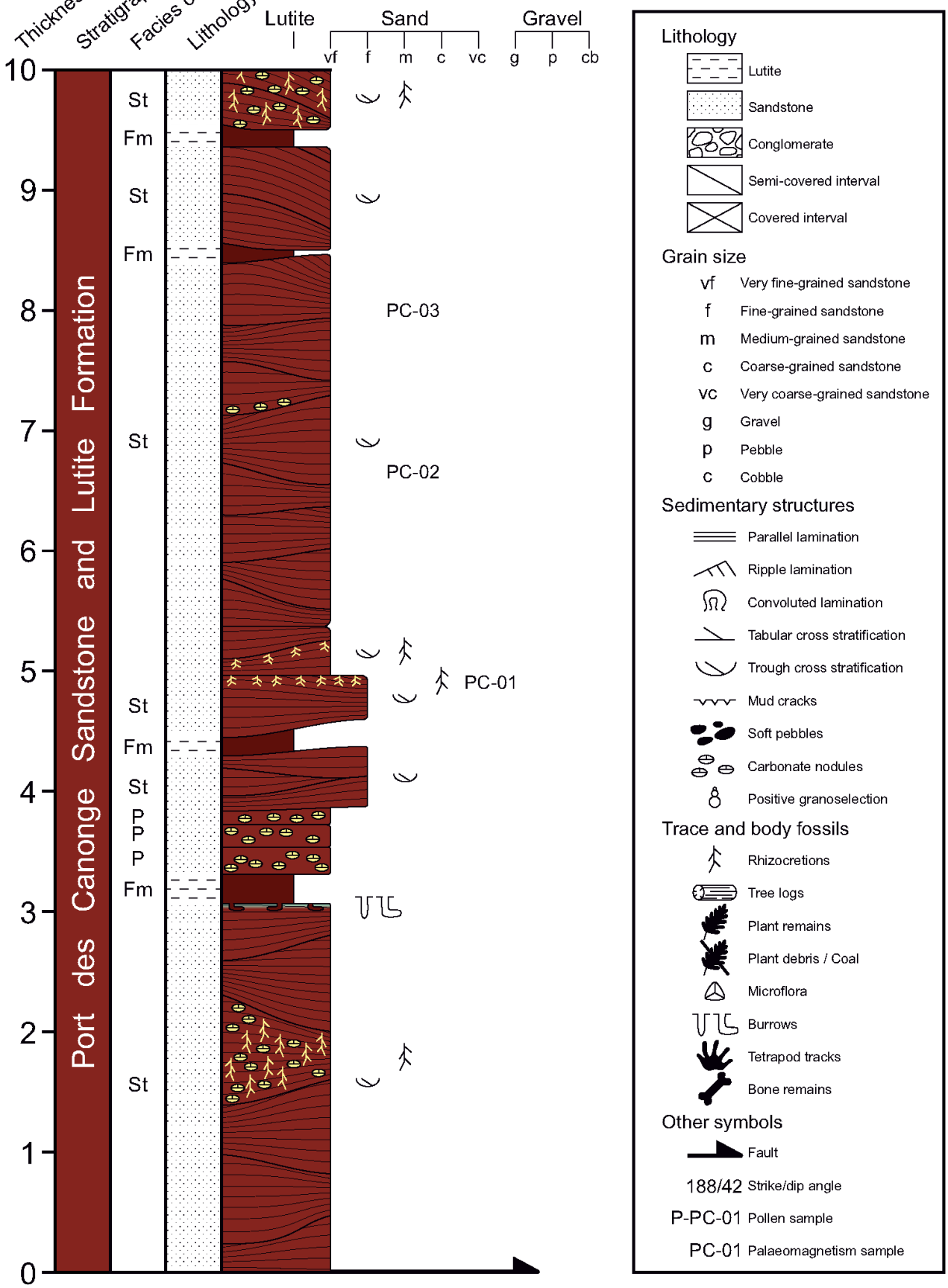

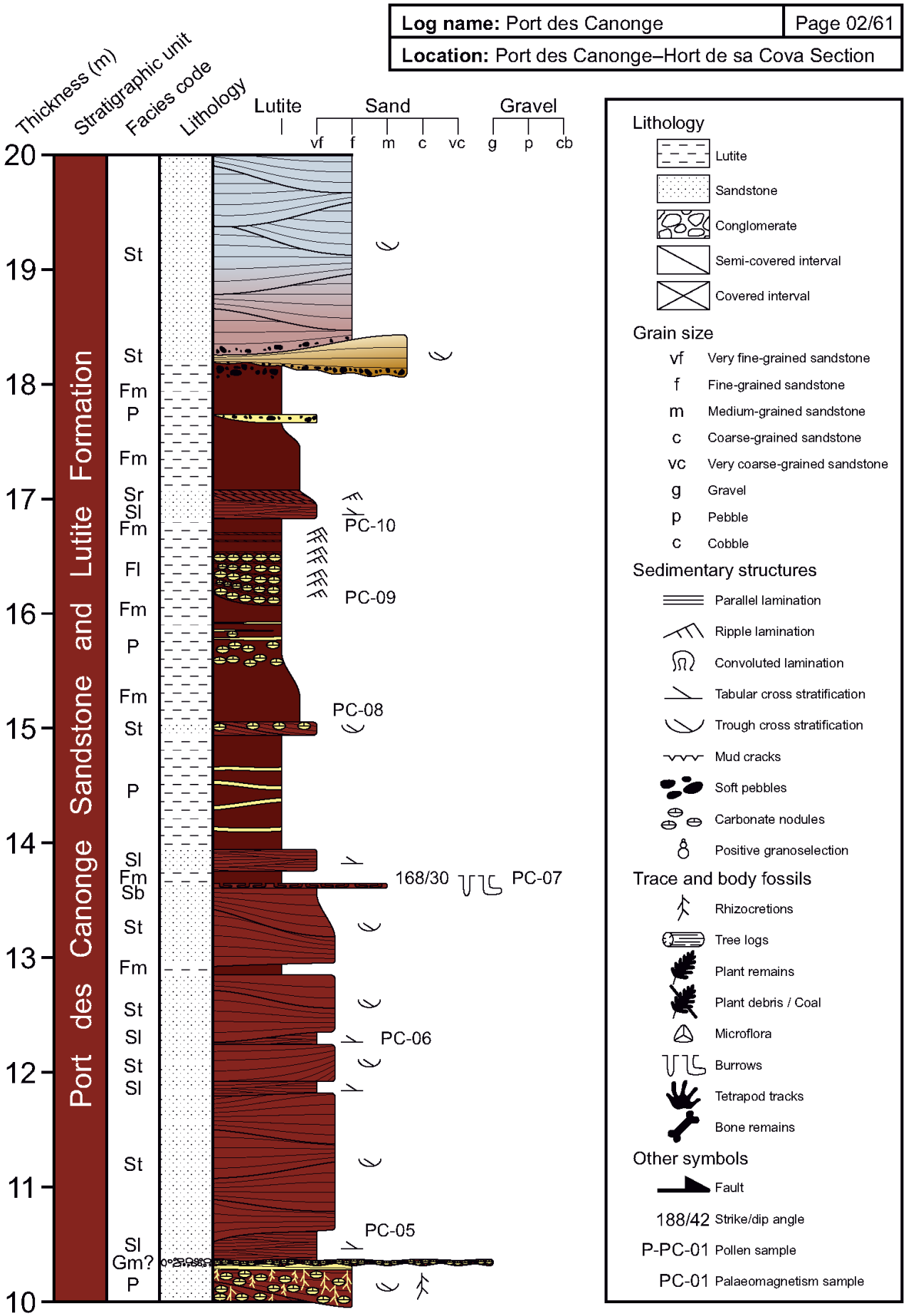
Log name: Port des Canonge
Page 02/61
Location: Port des Canonge–Hort de sa Cova Section
Thickness (m)
Stratigraphic unit
Facies code
Lithology
Lutite
Sand
Gravel
vf f m c vc g p cb
Port des Canonge Sandstone and Lutite Formation
20
19
18
17
16
15
14
13
12
11
10
St
St
Fm
P
Fm
Sr
Sl
Fm
Fl
Fm
P
Fm
St
P
Sl
Fm
Sb
St
Fm
St
Sl
St
Sl
St
Sl
Gm?
P
PC-10
PC-09
PC-08
168/30
PC-07
PC-06
PC-05
Lithology
Lutite
Sandstone
Conglomerate
Semi-covered interval
Covered interval
Grain size
vf Very fine-grained sandstone
f Fine-grained sandstone
m Medium-grained sandstone
c Coarse-grained sandstone
vc Very coarse-grained sandstone
g Gravel
p Pebble
c Cobble
Sedimentary structures
Parallel lamination
Ripple lamination
Convoluted lamination
Tabular cross stratification
Trough cross stratification
Mud cracks
Soft pebbles
Carbonate nodules
Positive granoselection
Trace and body fossils
Rhizocretions
Tree logs
Plant remains
Plant debris / Coal
Microflora
Burrows
Tetrapod tracks
Bone remains
Other symbols
Fault
188/42 Strike/dip angle
P-PC-01 Pollen sample
PC-01 Palaeomagnetism sample

Log name: Port des Canonge	Page 03/61
Location: Port des Canonge–Hort de sa Cova Section	

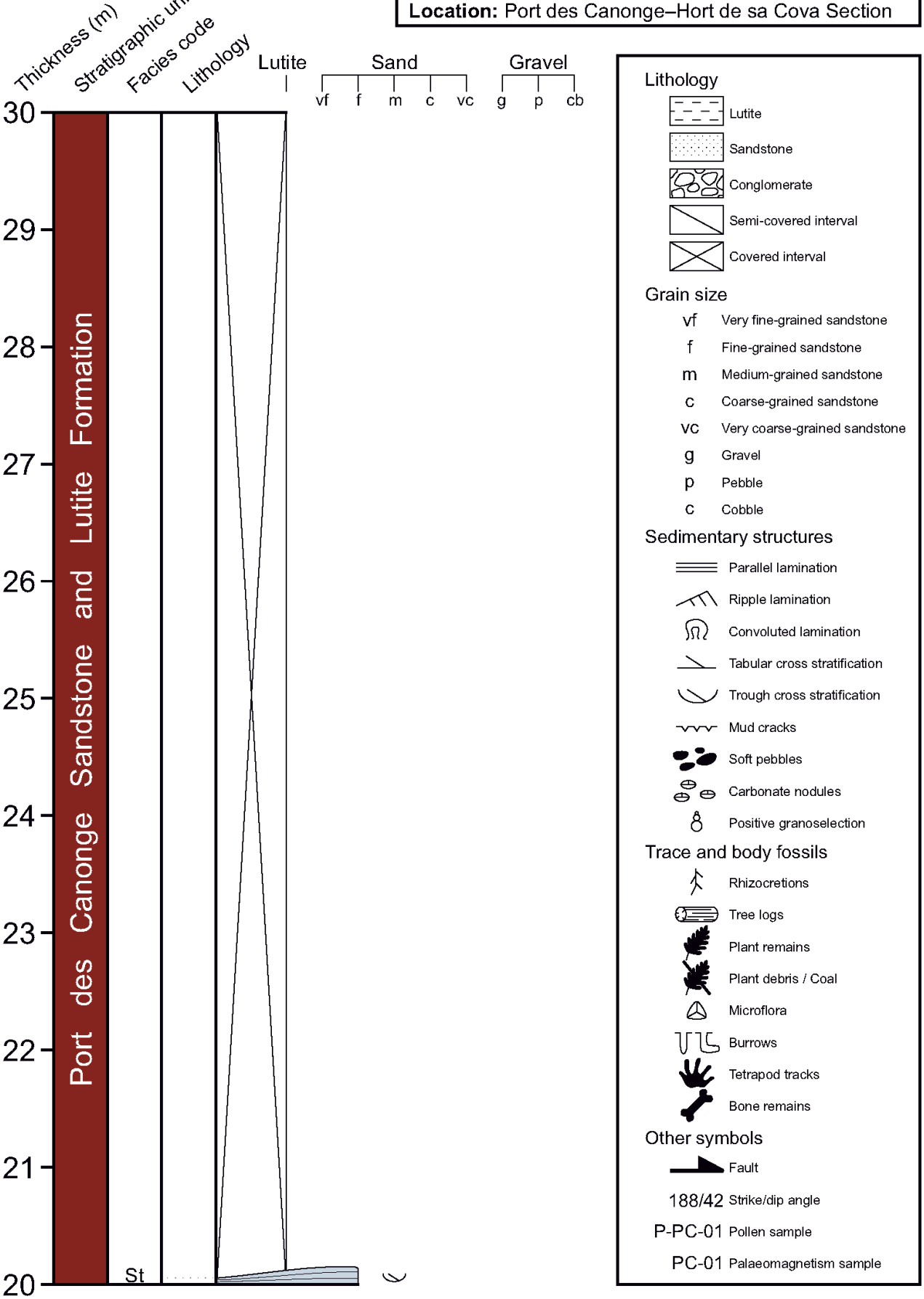

Log name: Port des Canonge	Page 04/61
Location: Port des Canonge–Hort de sa Cova Section	

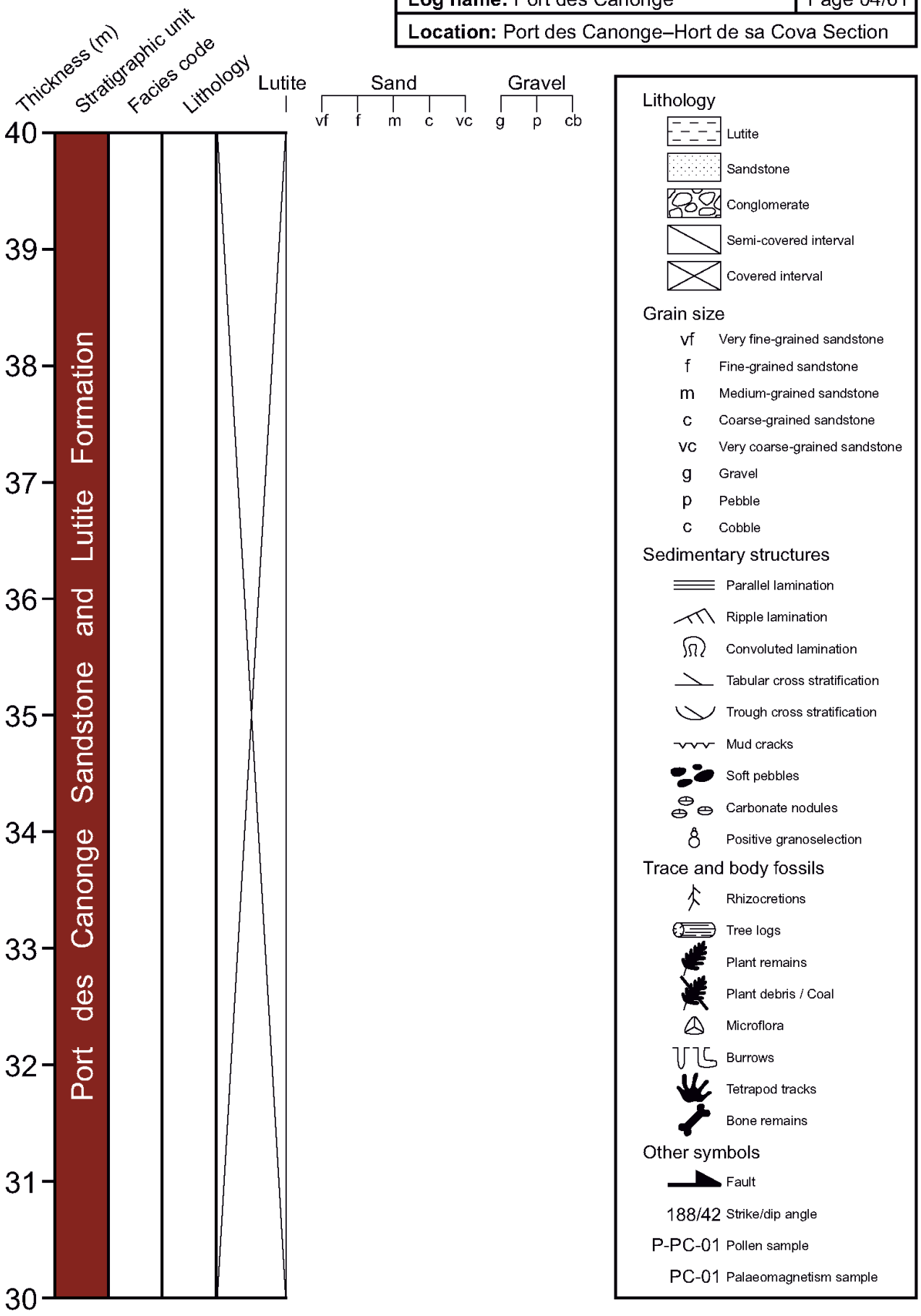

Log name: Port des Canonge	Page 05/61
Location: Port des Canonge–Hort de sa Cova Section	

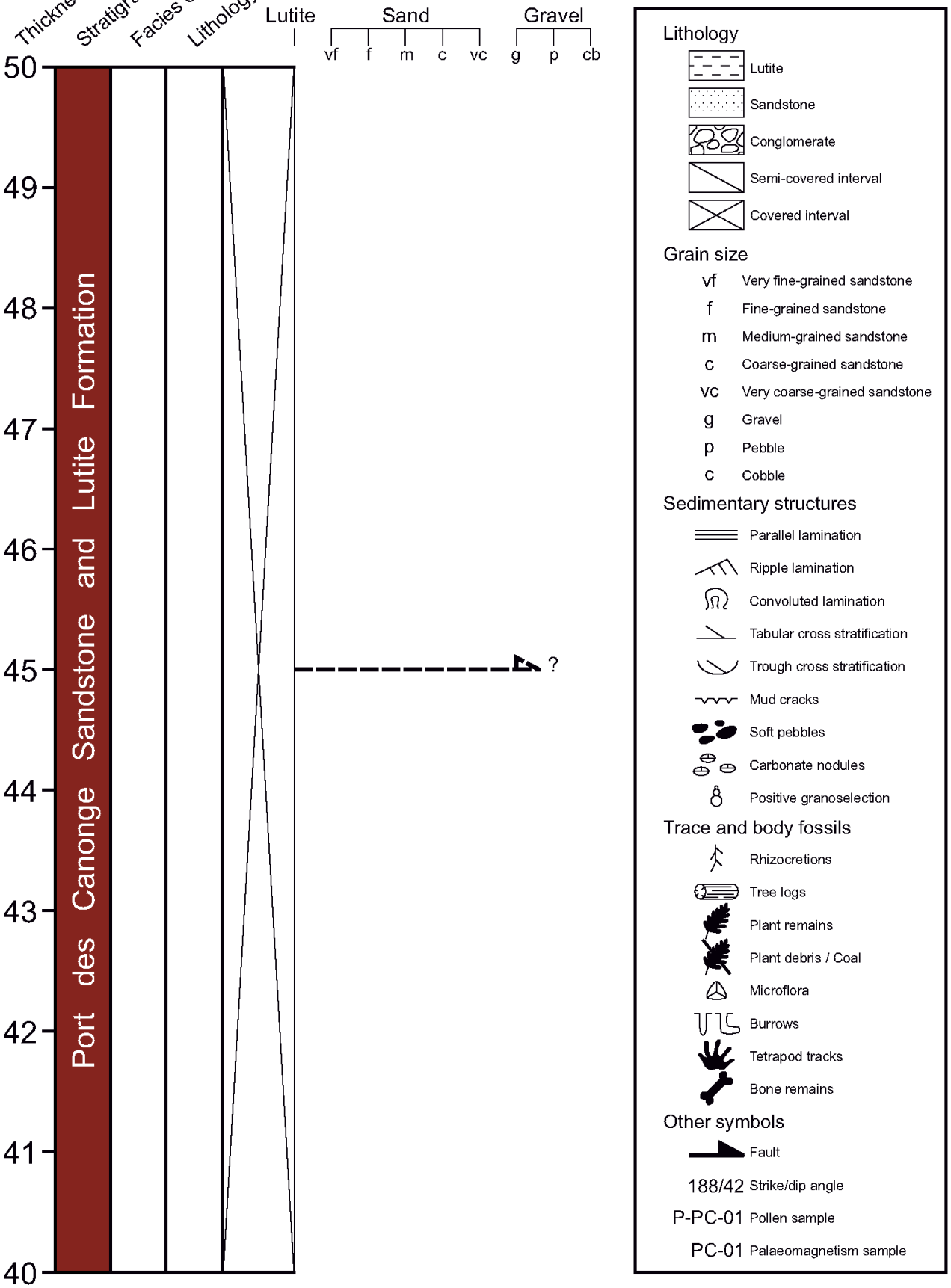

Log name: Port des Canonge	Page 06/61
Location: Port des Canonge–Hort de sa Cova Section	

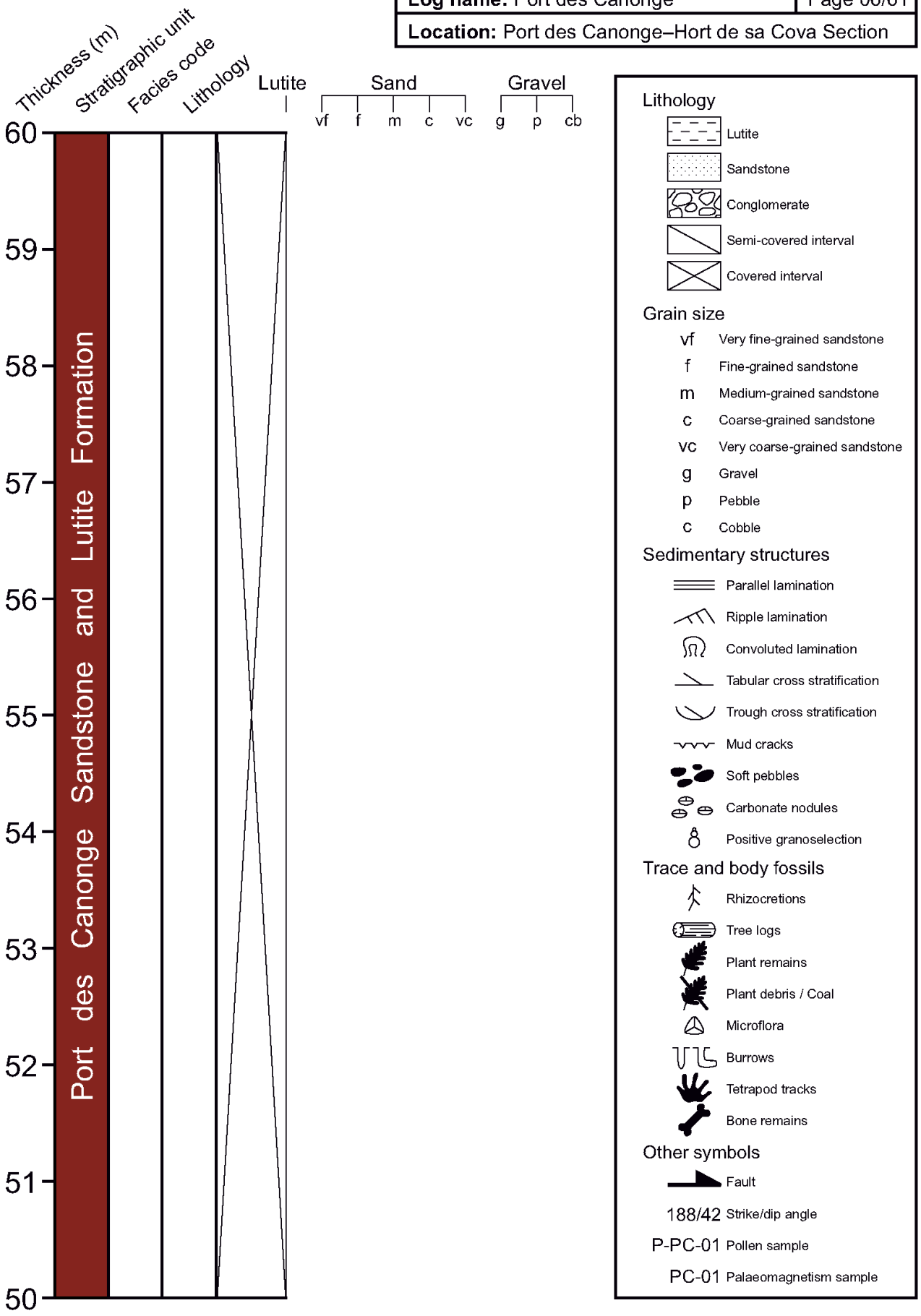

Log name: Port des Canonge	Page 07/61
Location: Port des Canonge–Hort de sa Cova Section	

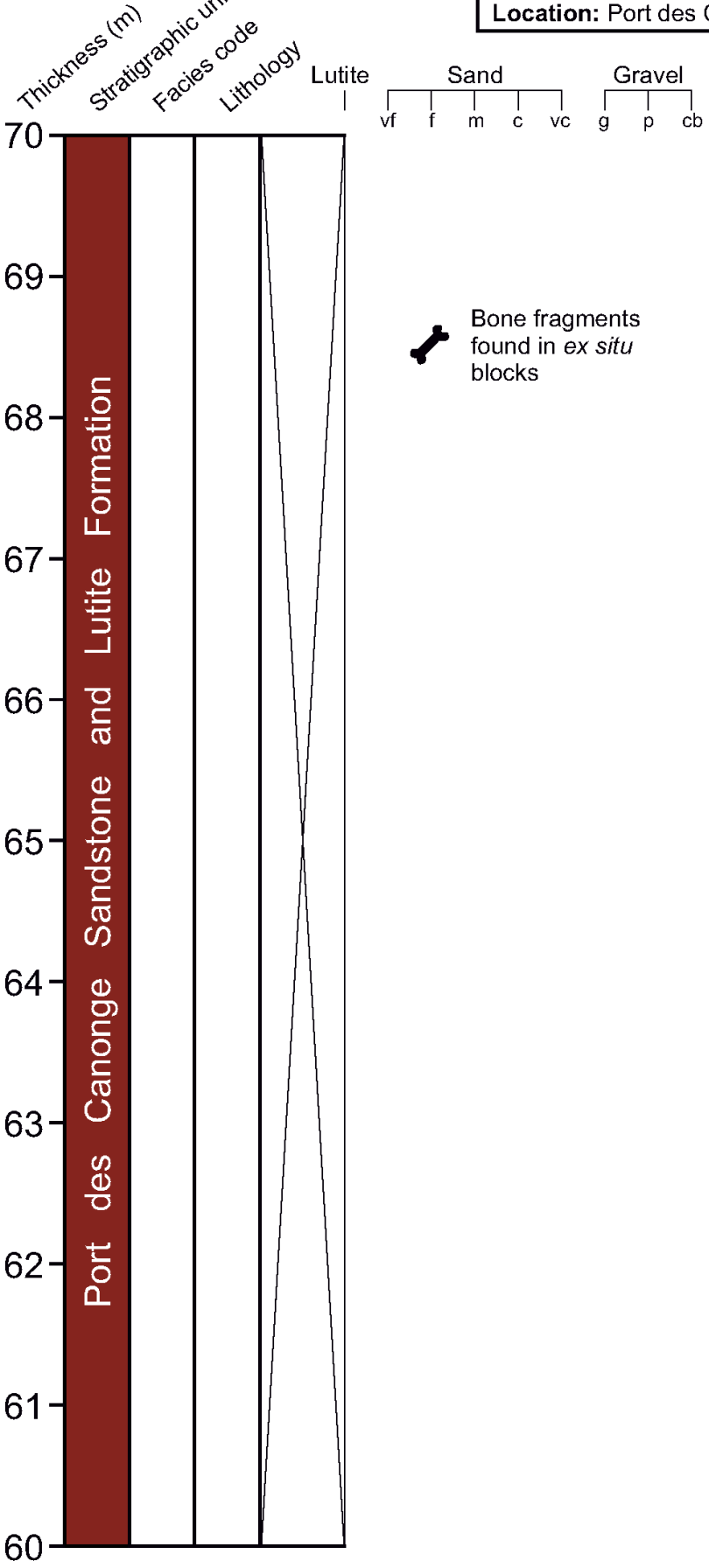

Lithology
- Lutite
- Sandstone
- Conglomerate
- Semi-covered interval
- Covered interval

Grain size
- vf Very fine-grained sandstone
- f Fine-grained sandstone
- m Medium-grained sandstone
- c Coarse-grained sandstone
- vc Very coarse-grained sandstone
- g Gravel
- p Pebble
- c Cobble

Sedimentary structures
- Parallel lamination
- Ripple lamination
- Convoluted lamination
- Tabular cross stratification
- Trough cross stratification
- Mud cracks
- Soft pebbles
- Carbonate nodules
- Positive granoselection

Trace and body fossils
- Rhizocretions
- Tree logs
- Plant remains
- Plant debris / Coal
- Microflora
- Burrows
- Tetrapod tracks
- Bone remains

Other symbols
- Fault
- 188/42 Strike/dip angle
- P-PC-01 Pollen sample
- PC-01 Palaeomagnetism sample

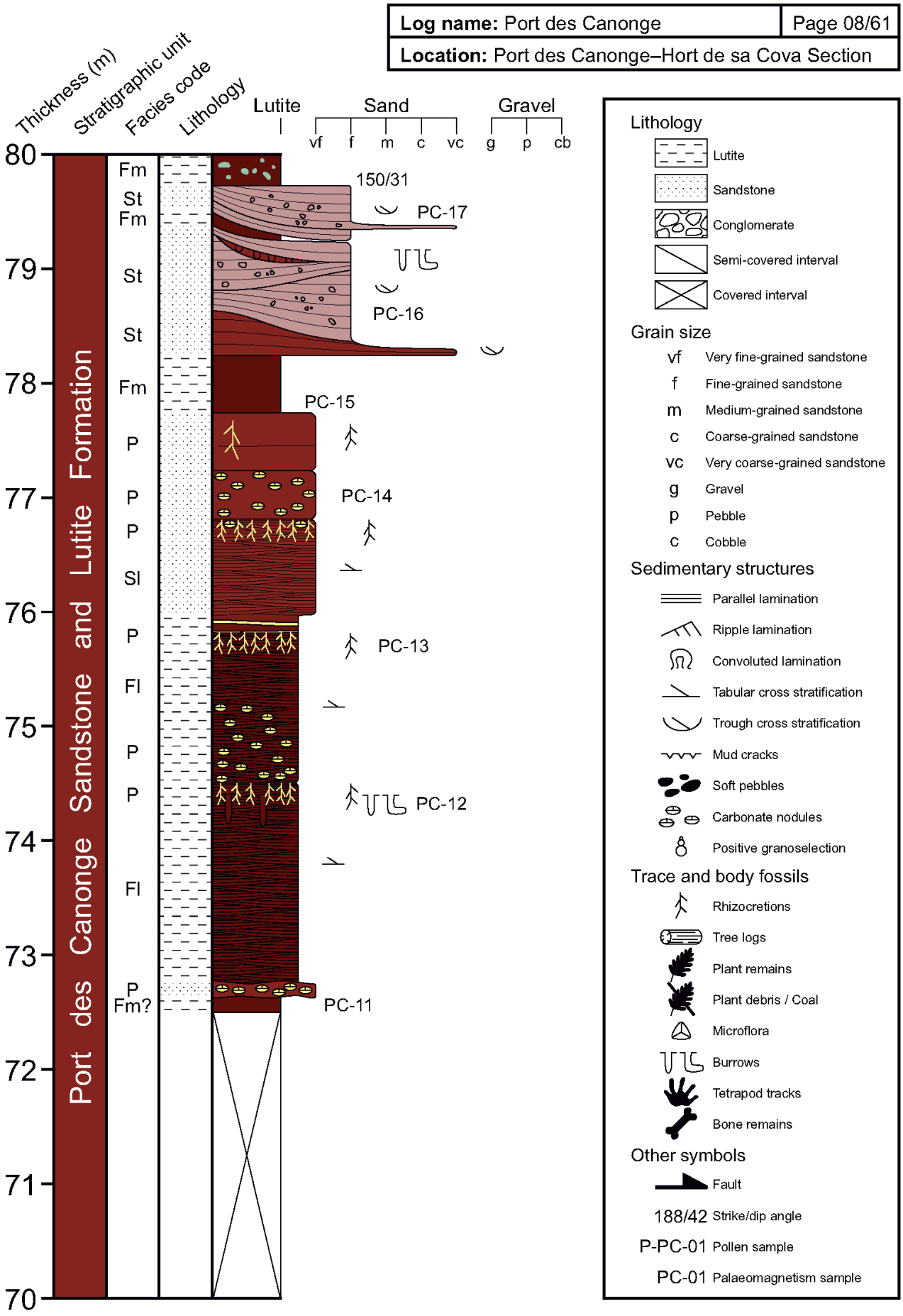
Log name: Port des Canonge
Page 08/61
Location: Port des Canonge–Hort de sa Cova Section
Thickness (m)
Stratigraphic unit
Facies code
Lithology
Lutite
Sand
Gravel
vf f m c vc g p cb
Port des Canonge Sandstone and Lutite Formation
80
79
78
77
76
75
74
73
72
71
70
Fm
St
Fm
St
St
Fm
P
P
P
Sl
P
Fl
P
P
Fl
P
Fm?
150/31
PC-17
PC-16
PC-15
PC-14
PC-13
PC-12
PC-11
Lithology
Lutite
Sandstone
Conglomerate
Semi-covered interval
Covered interval
Grain size
vf Very fine-grained sandstone
f Fine-grained sandstone
m Medium-grained sandstone
c Coarse-grained sandstone
vc Very coarse-grained sandstone
g Gravel
p Pebble
c Cobble
Sedimentary structures
Parallel lamination
Ripple lamination
Convoluted lamination
Tabular cross stratification
Trough cross stratification
Mud cracks
Soft pebbles
Carbonate nodules
Positive granoselection
Trace and body fossils
Rhizocretions
Tree logs
Plant remains
Plant debris / Coal
Microflora
Burrows
Tetrapod tracks
Bone remains
Other symbols
Fault
188/42 Strike/dip angle
P-PC-01 Pollen sample
PC-01 Palaeomagnetism sample

Log name: Port des Canonge	Page 09/61
Location: Port des Canonge–Hort de sa Cova Section	

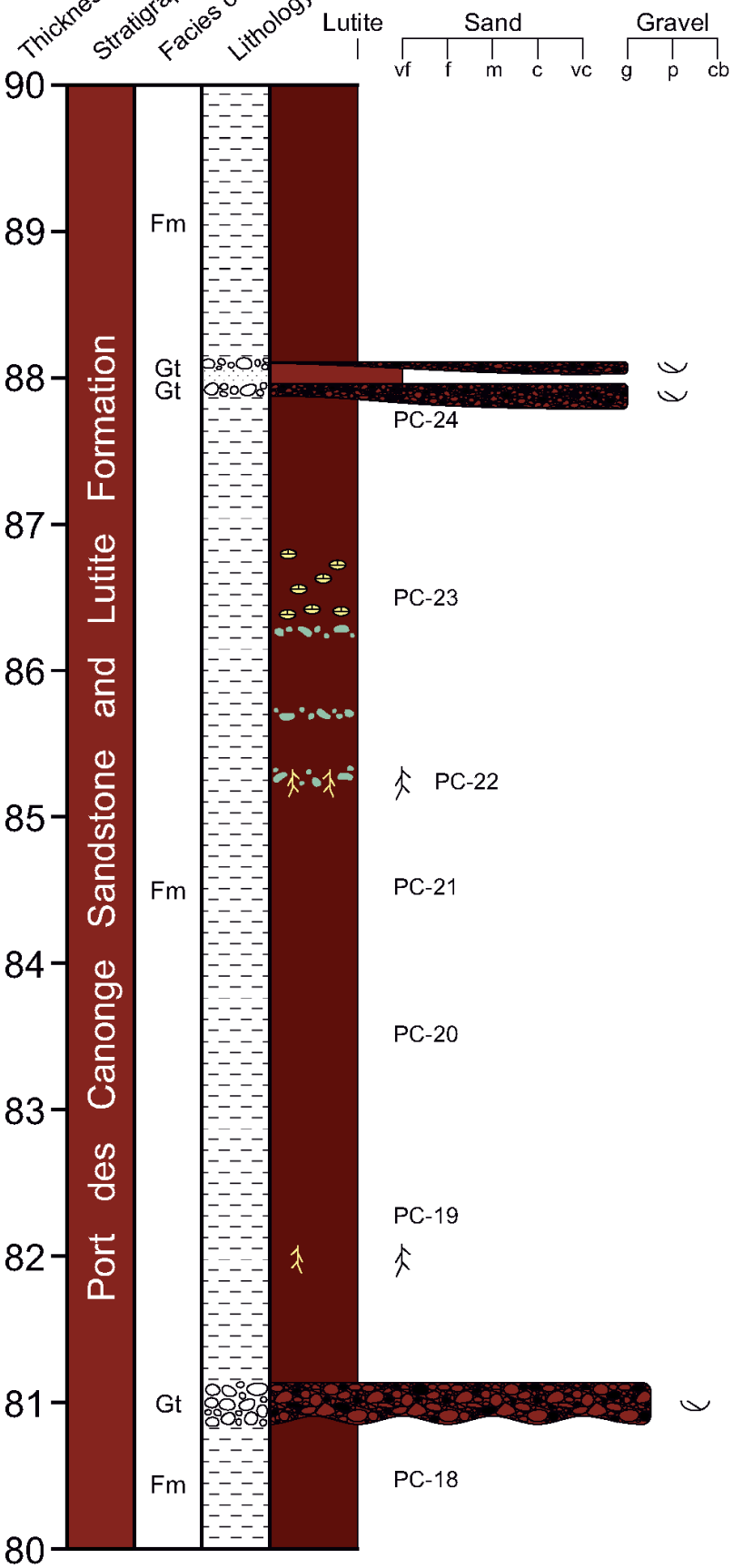

Lithology
- Lutite
- Sandstone
- Conglomerate
- Semi-covered interval
- Covered interval

Grain size
- vf Very fine-grained sandstone
- f Fine-grained sandstone
- m Medium-grained sandstone
- c Coarse-grained sandstone
- vc Very coarse-grained sandstone
- g Gravel
- p Pebble
- c Cobble

Sedimentary structures
- Parallel lamination
- Ripple lamination
- Convoluted lamination
- Tabular cross stratification
- Trough cross stratification
- Mud cracks
- Soft pebbles
- Carbonate nodules
- Positive granoselection

Trace and body fossils
- Rhizocretions
- Tree logs
- Plant remains
- Plant debris / Coal
- Microflora
- Burrows
- Tetrapod tracks
- Bone remains

Other symbols
- Fault
- 188/42 Strike/dip angle
- P-PC-01 Pollen sample
- PC-01 Palaeomagnetism sample

Log name: Port des Canonge | Page 10/61

Location: Port des Canonge–Hort de sa Cova Section

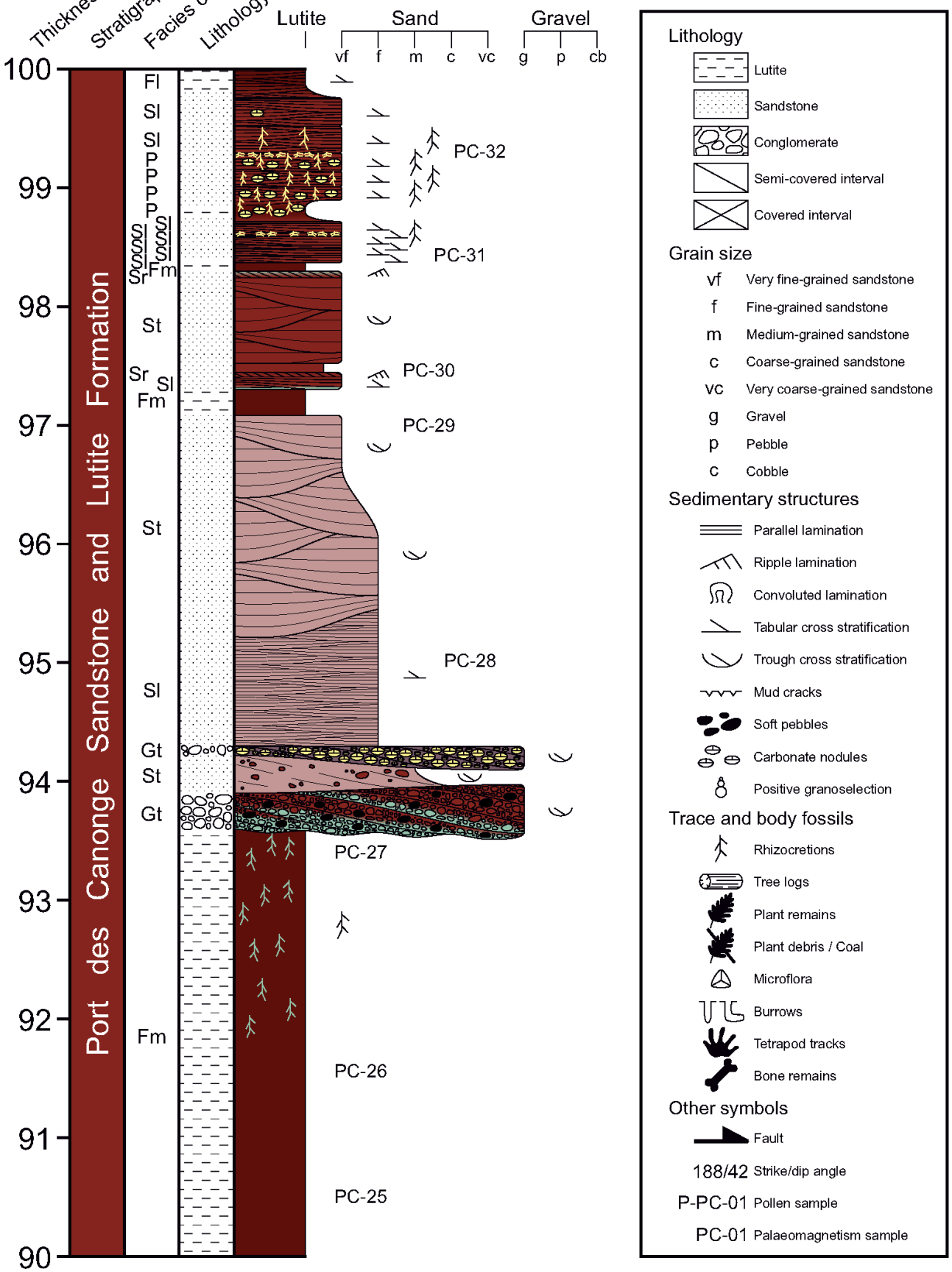

Log name: Port des Canonge	Page 11/61
Location: Port des Canonge–Hort de sa Cova Section	

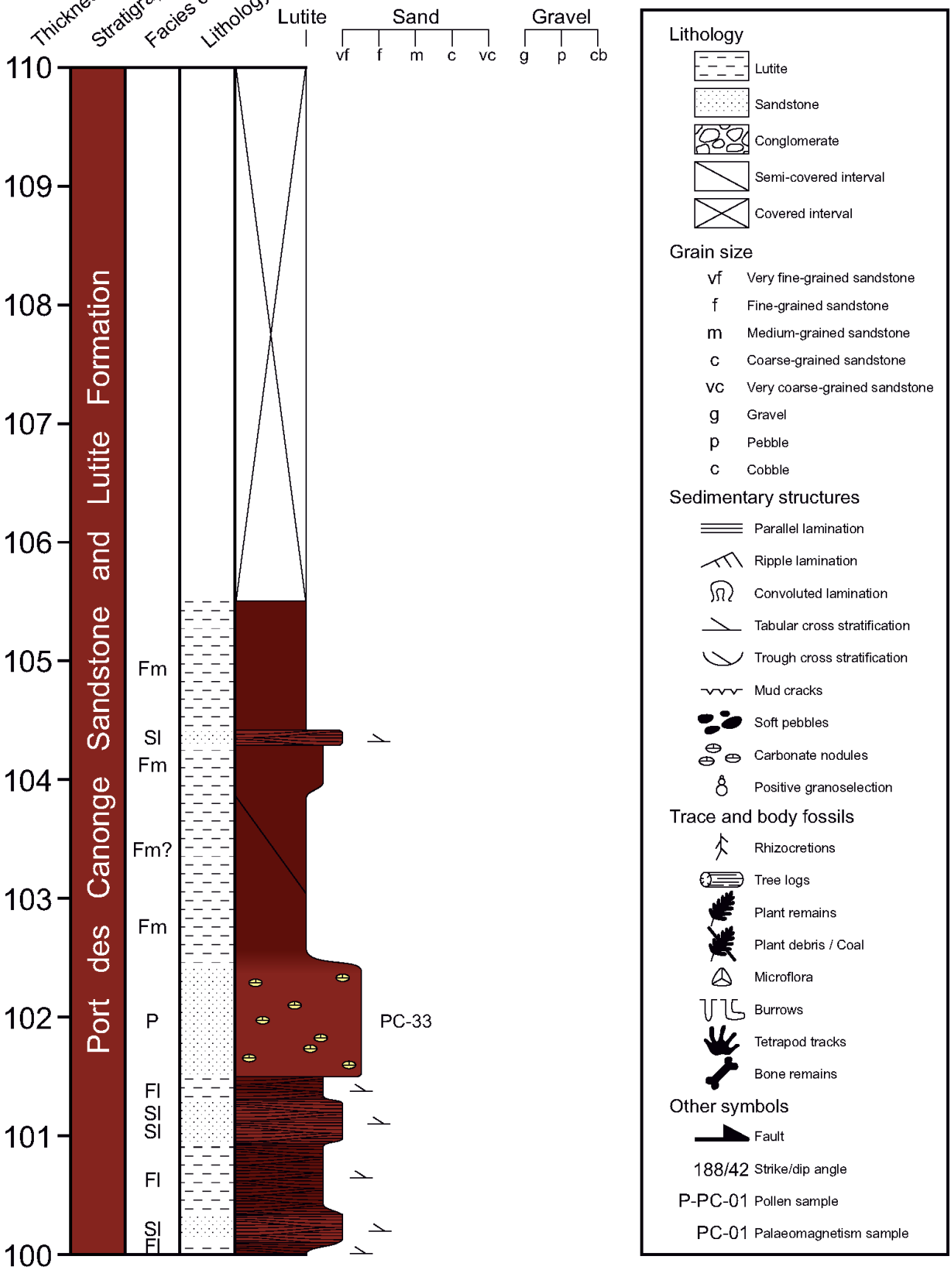

Log name: Port des Canonge	Page 12/61
Location: Port des Canonge–Hort de sa Cova Section	

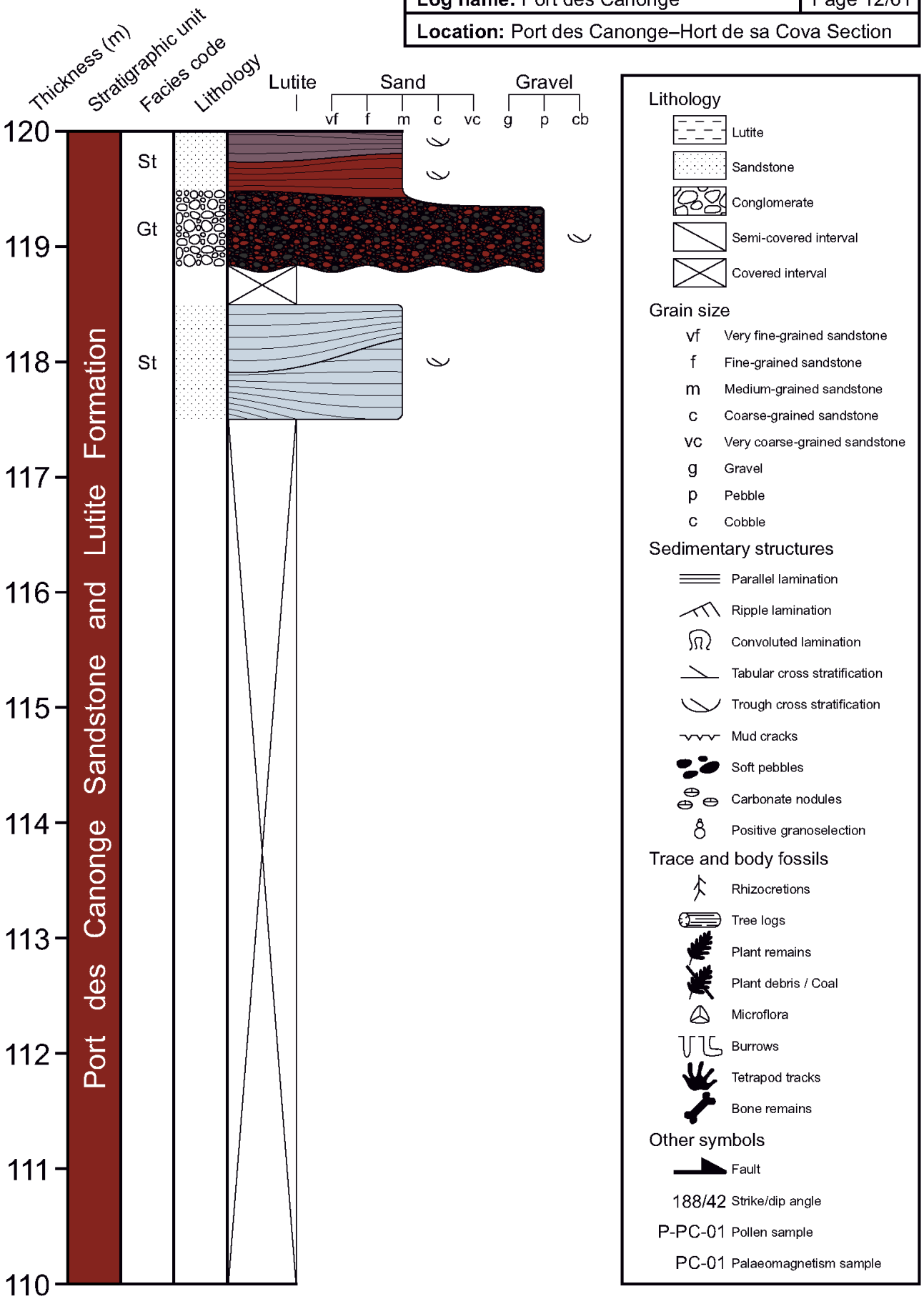

Log name: Port des Canonge	Page 13/61
Location: Port des Canonge–Hort de sa Cova Section	

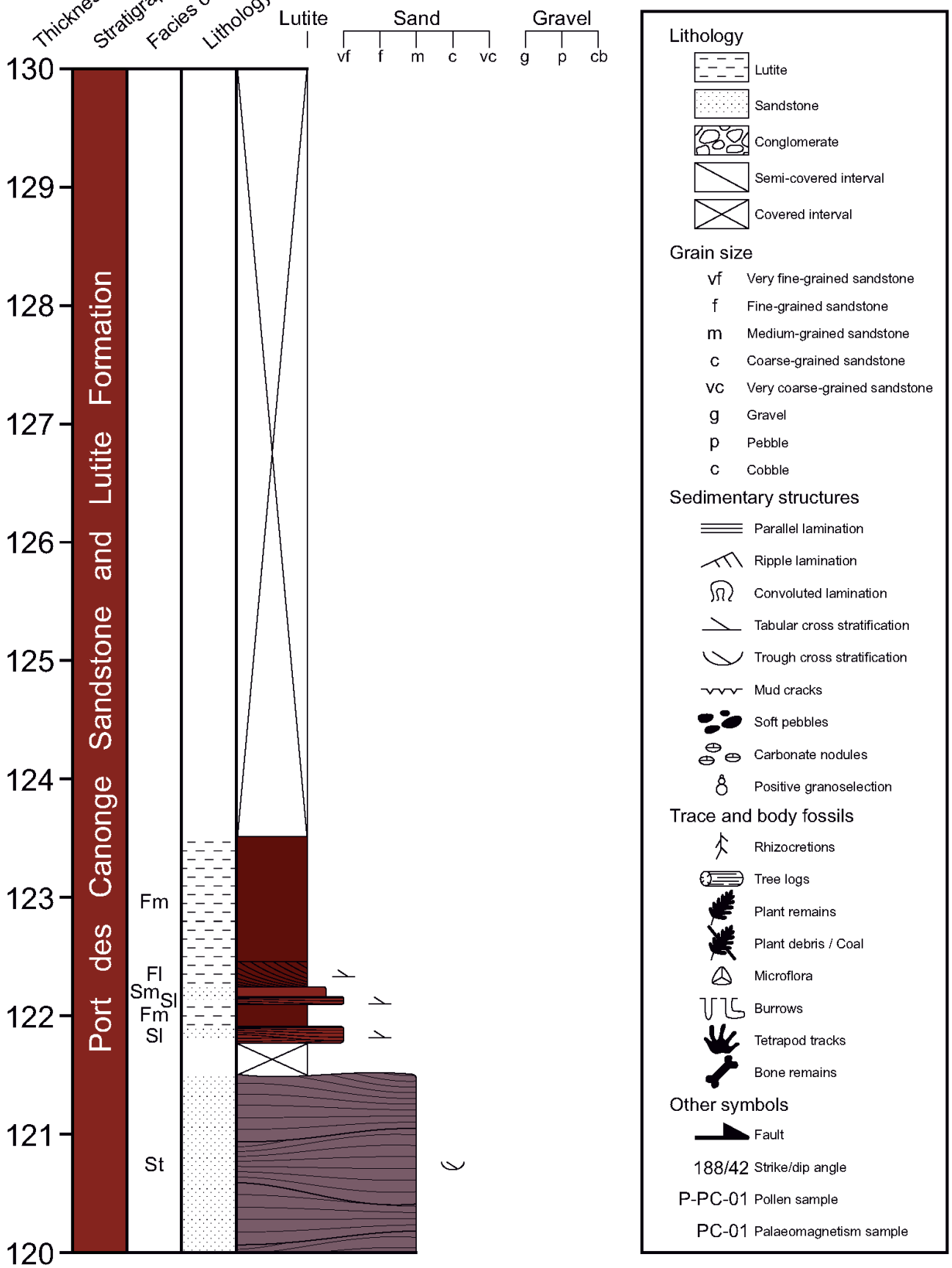

Log name: Port des Canonge	Page 14/61
Location: Port des Canonge–Hort de sa Cova Section	

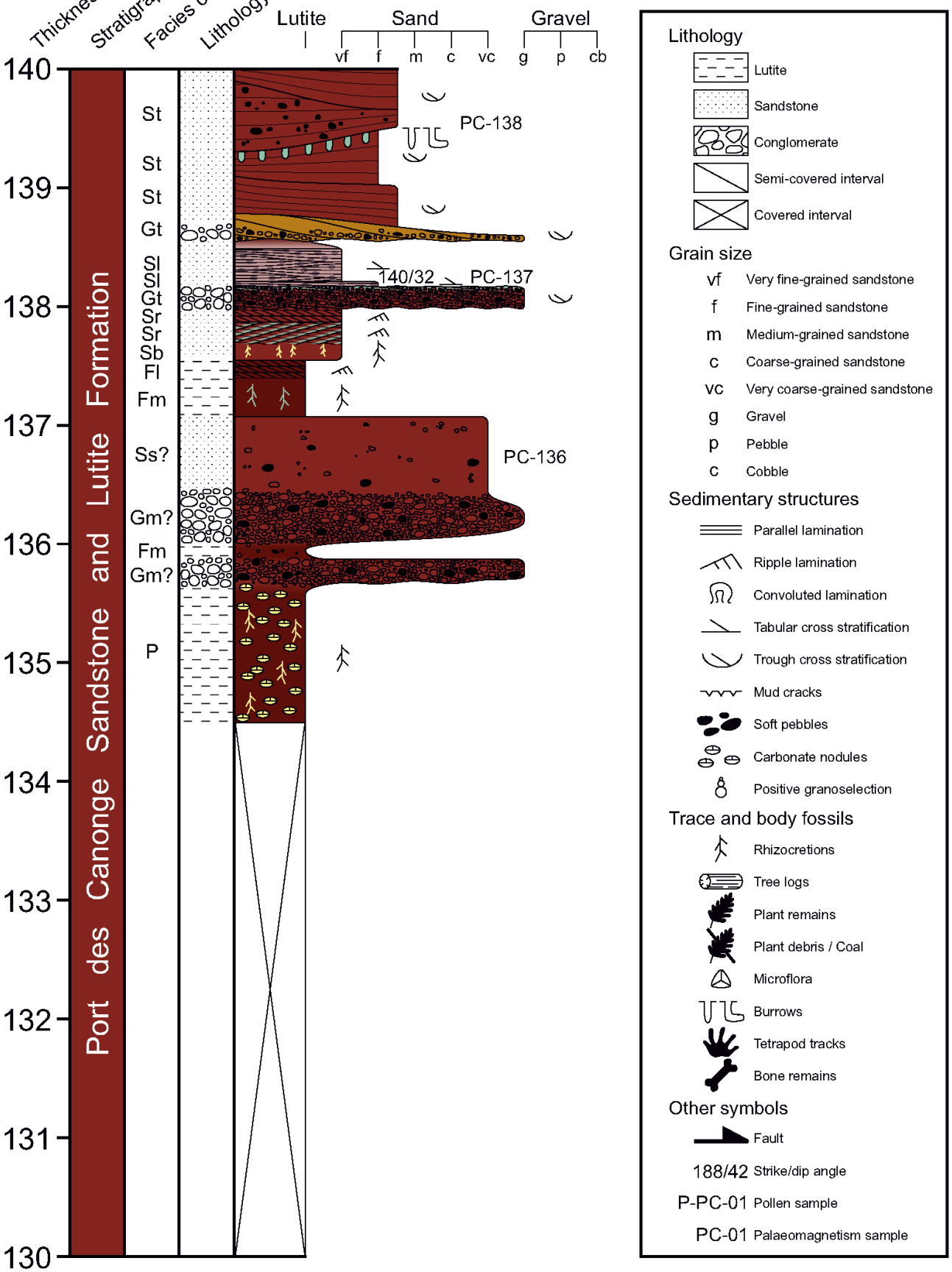

Log name: Port des Canonge	Page 15/61
Location: Port des Canonge–Hort de sa Cova Section	

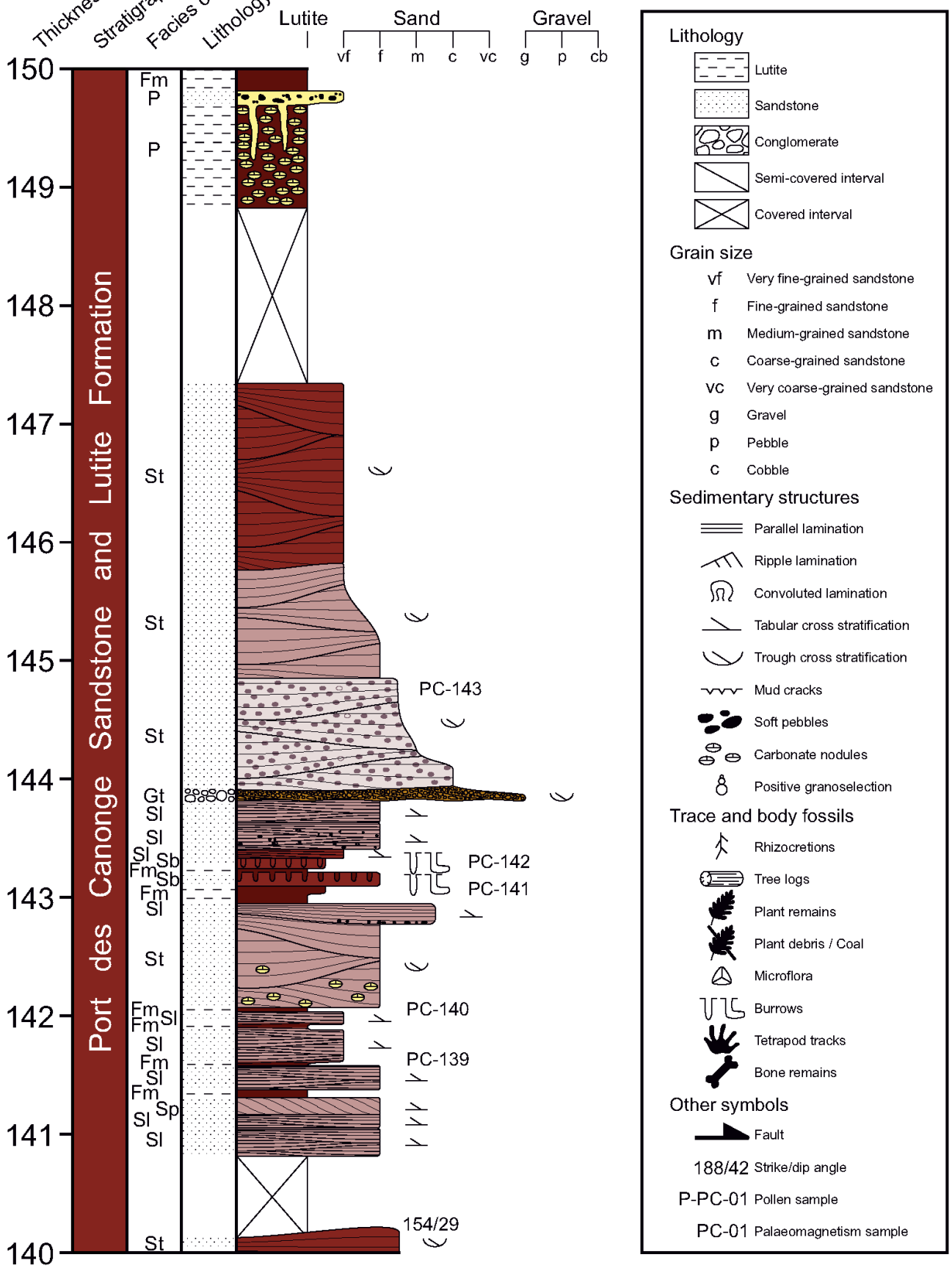

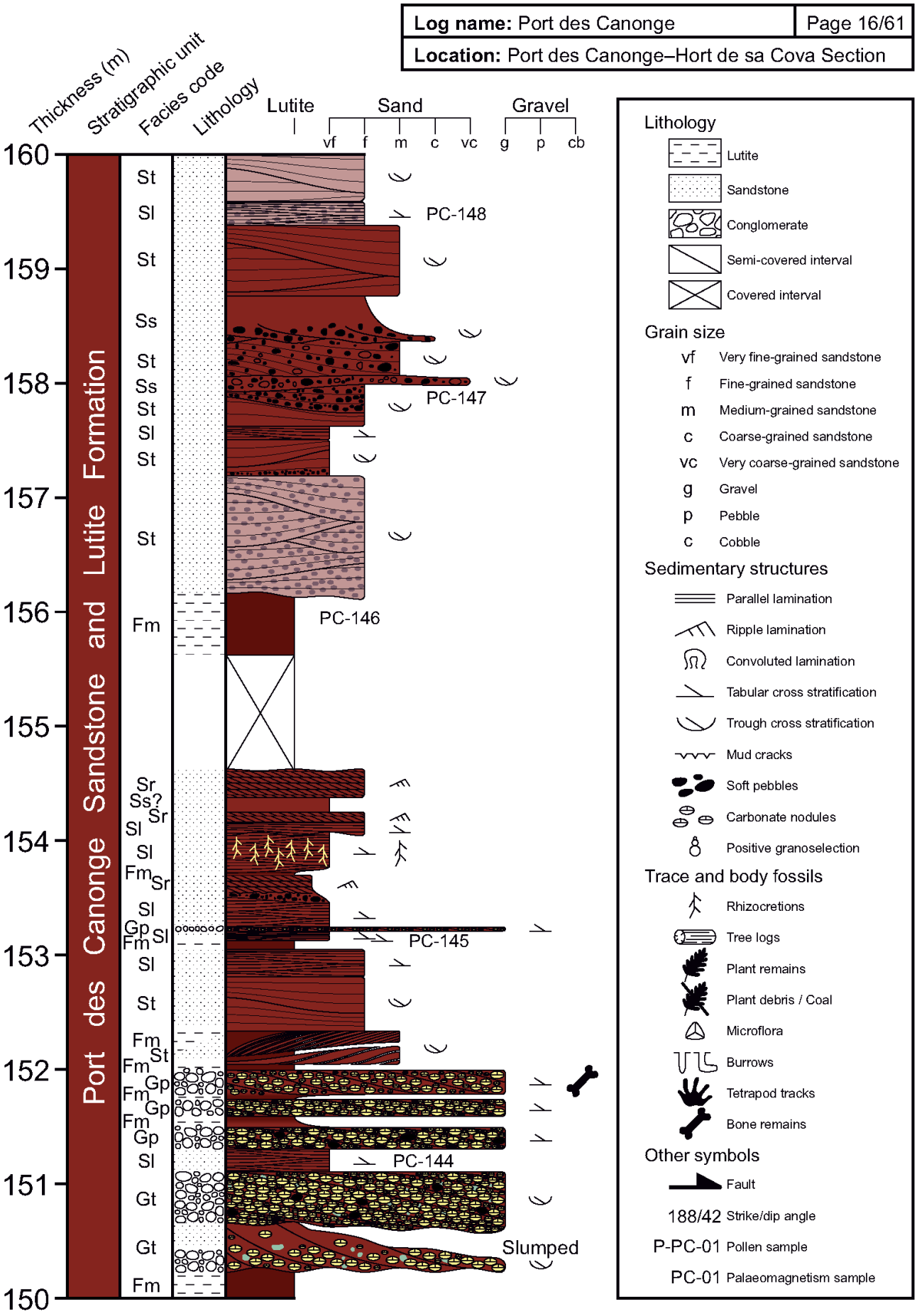
Log name: Port des Canonge
Page 16/61
Location: Port des Canonge–Hort de sa Cova Section
Thickness (m)
Stratigraphic unit
Facies code
Lithology
Lutite
Sand
Gravel
vf f m c vc g p cb
Port des Canonge Sandstone and Lutite Formation
160
159
158
157
156
155
154
153
152
151
150
St
Sl
St
Ss
St
Ss
St
Sl
St
St
Fm
Sr
Ss?
Sr
Sl
Sl
Fm
Sr
Sl
Gp
Fm
Sl
Sl
St
Fm
Fm
St
Fm
Gp
Fm
Gp
Fm
Gp
Sl
Gt
Gt
Fm
PC-148
PC-147
PC-146
PC-145
PC-144
Slumped
Lithology
Lutite
Sandstone
Conglomerate
Semi-covered interval
Covered interval
Grain size
vf Very fine-grained sandstone
f Fine-grained sandstone
m Medium-grained sandstone
c Coarse-grained sandstone
vc Very coarse-grained sandstone
g Gravel
p Pebble
c Cobble
Sedimentary structures
Parallel lamination
Ripple lamination
Convoluted lamination
Tabular cross stratification
Trough cross stratification
Mud cracks
Soft pebbles
Carbonate nodules
Positive granoselection
Trace and body fossils
Rhizocretions
Tree logs
Plant remains
Plant debris / Coal
Microflora
Burrows
Tetrapod tracks
Bone remains
Other symbols
Fault
188/42 Strike/dip angle
P-PC-01 Pollen sample
PC-01 Palaeomagnetism sample

Log name: Port des Canonge	Page 17/61
Location: Port des Canonge–Hort de sa Cova Section	

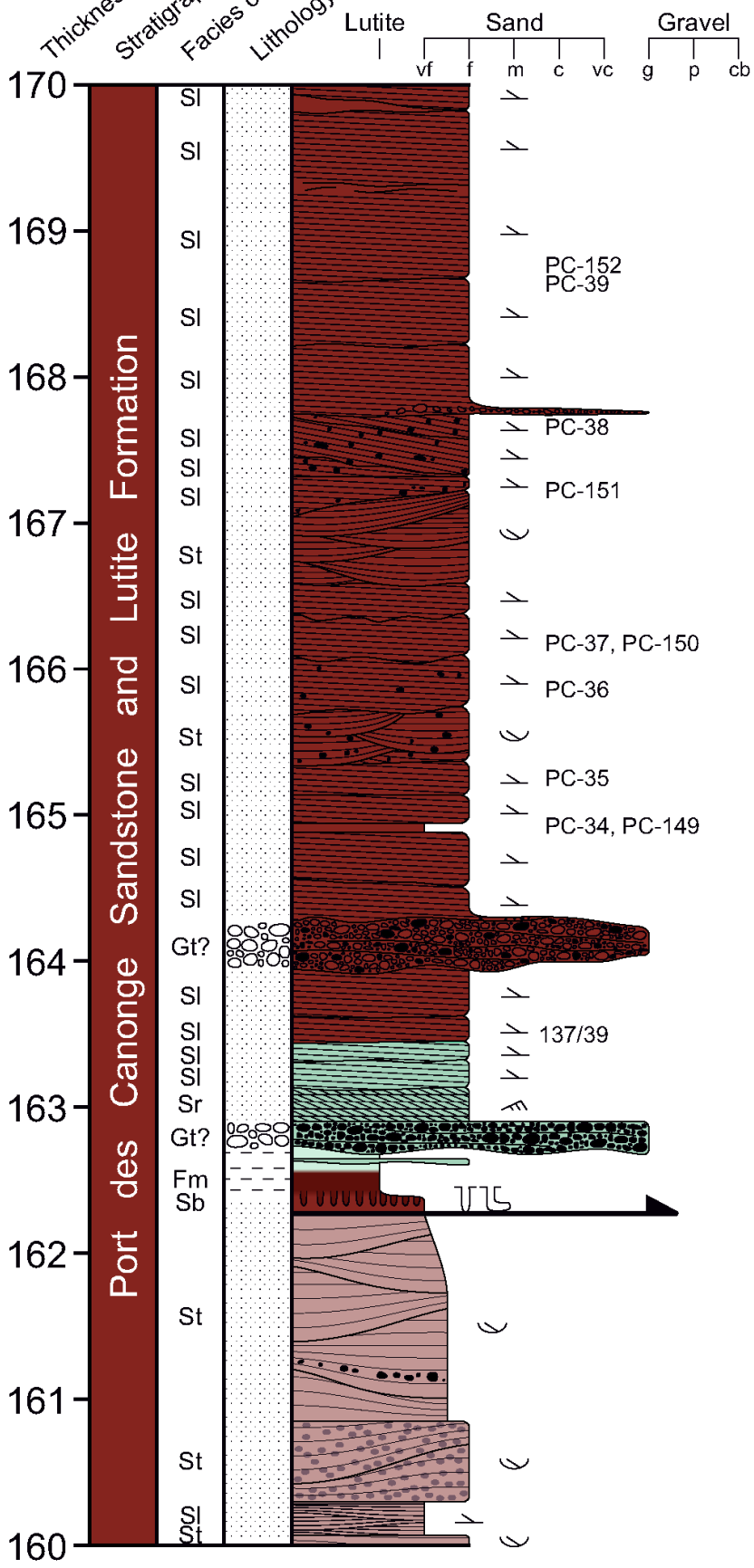

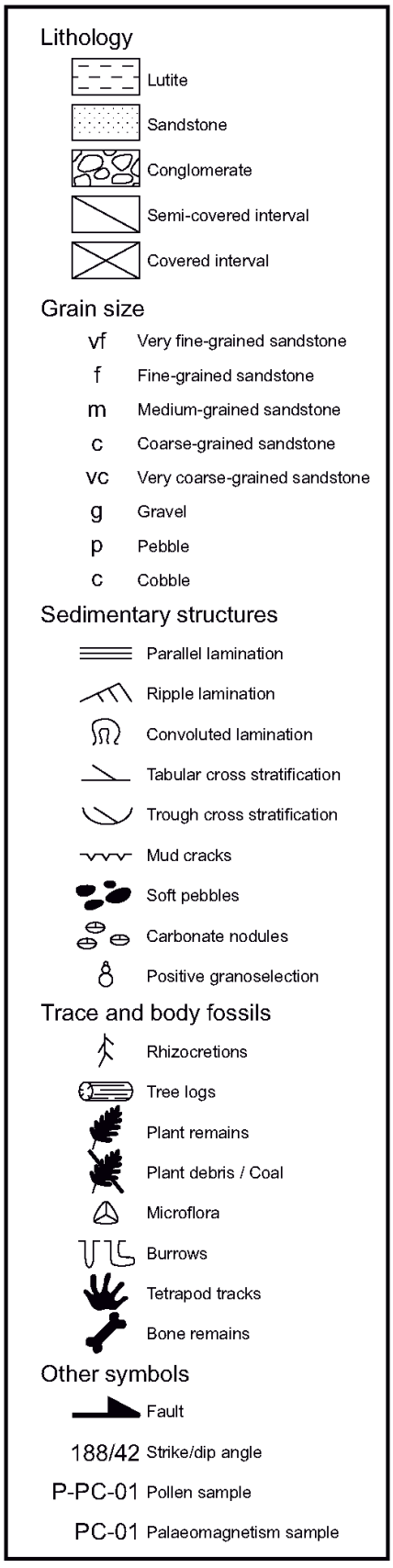

Log name: Port des Canonge	Page 18/61
Location: Port des Canonge–Hort de sa Cova Section	

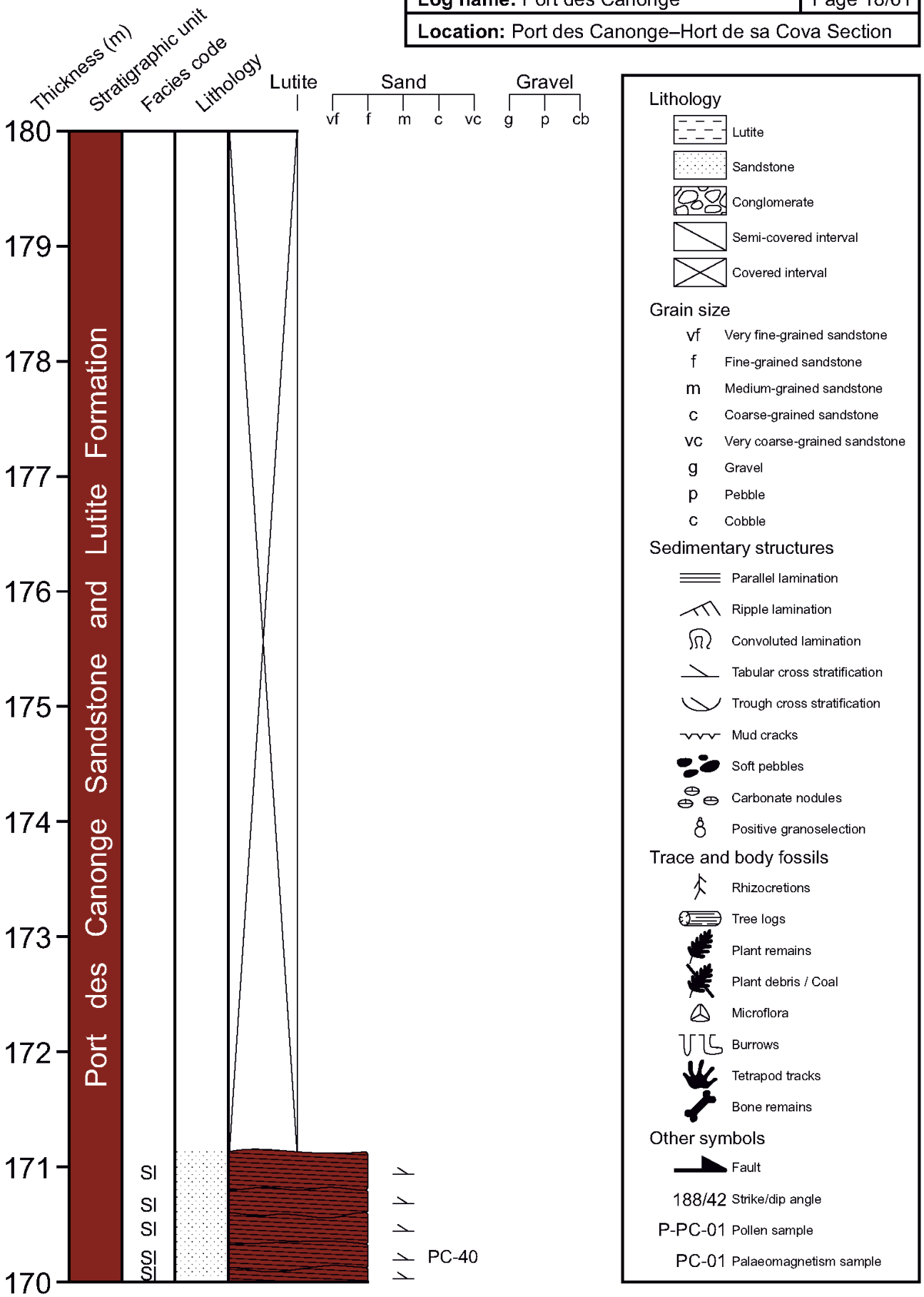

Log name: Port des Canonge	Page 19/61
Location: Port des Canonge–Hort de sa Cova Section	

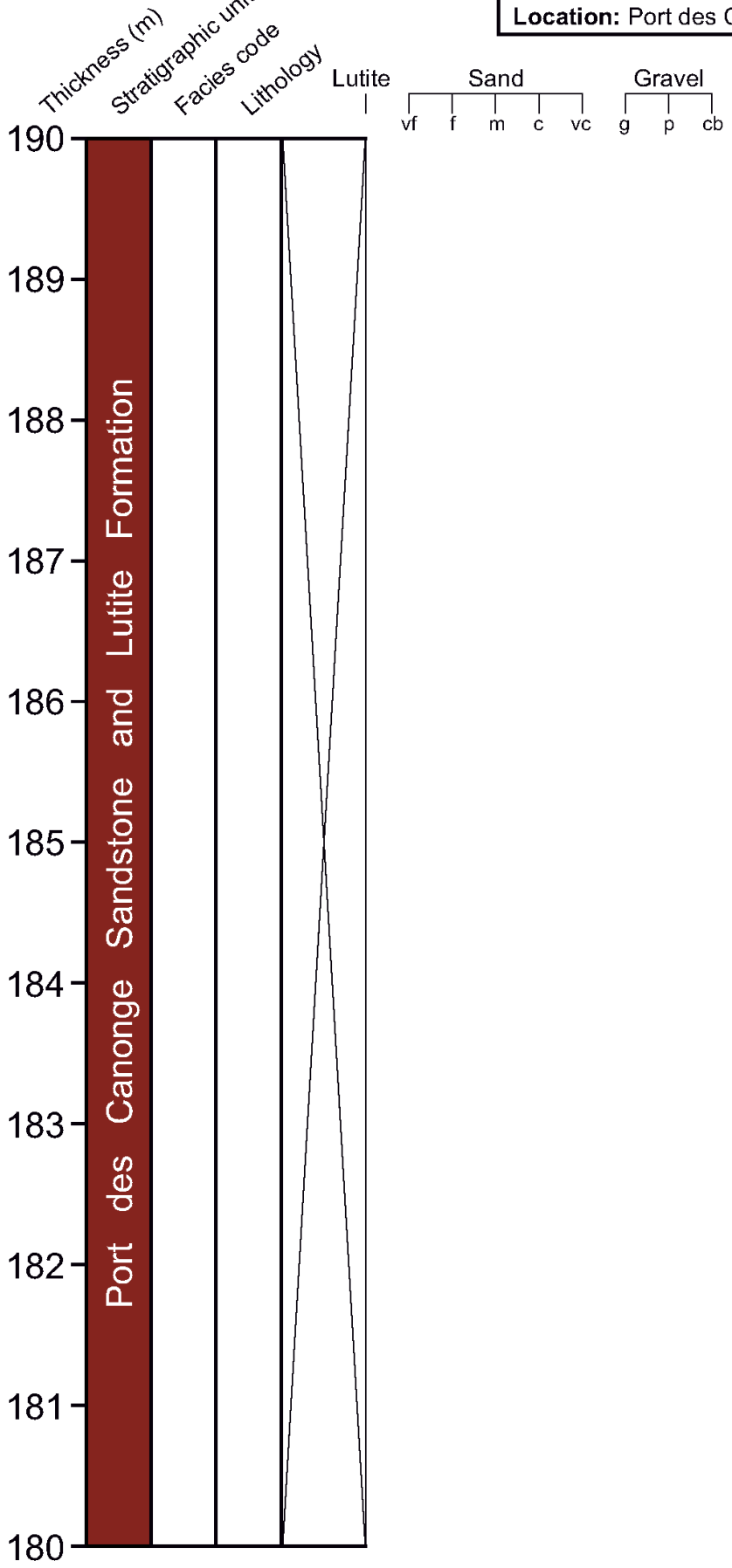

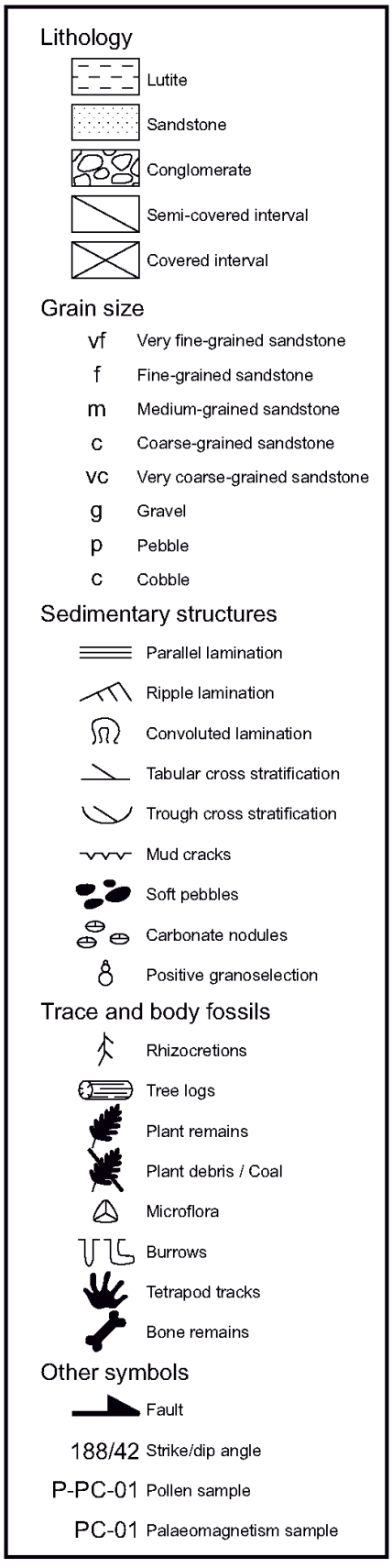

Log name: Port des Canonge	Page 20/61
Location: Port des Canonge–Hort de sa Cova Section	

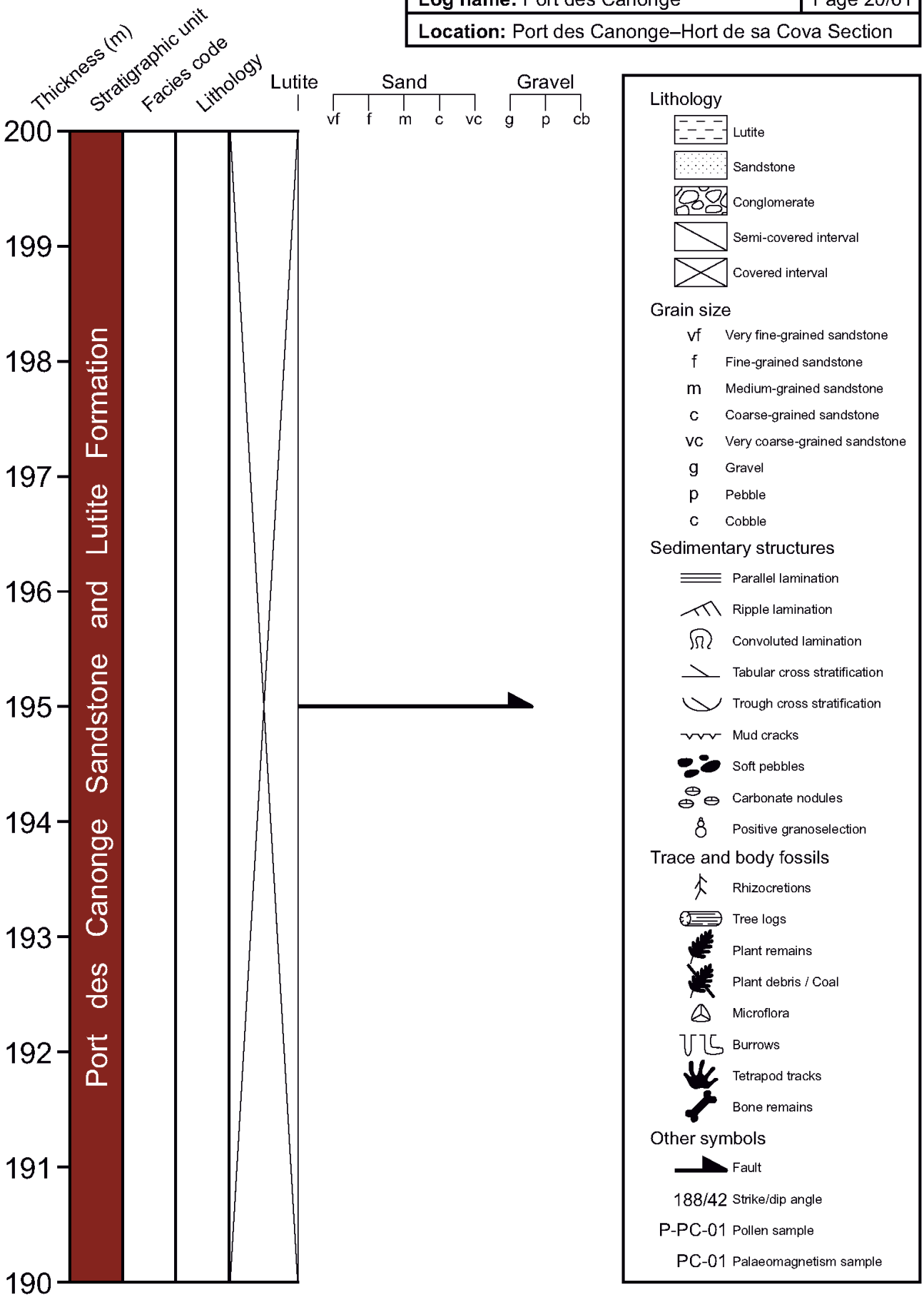

Log name: Port des Canonge	Page 21/61
Location: Port des Canonge–Hort de sa Cova Section	

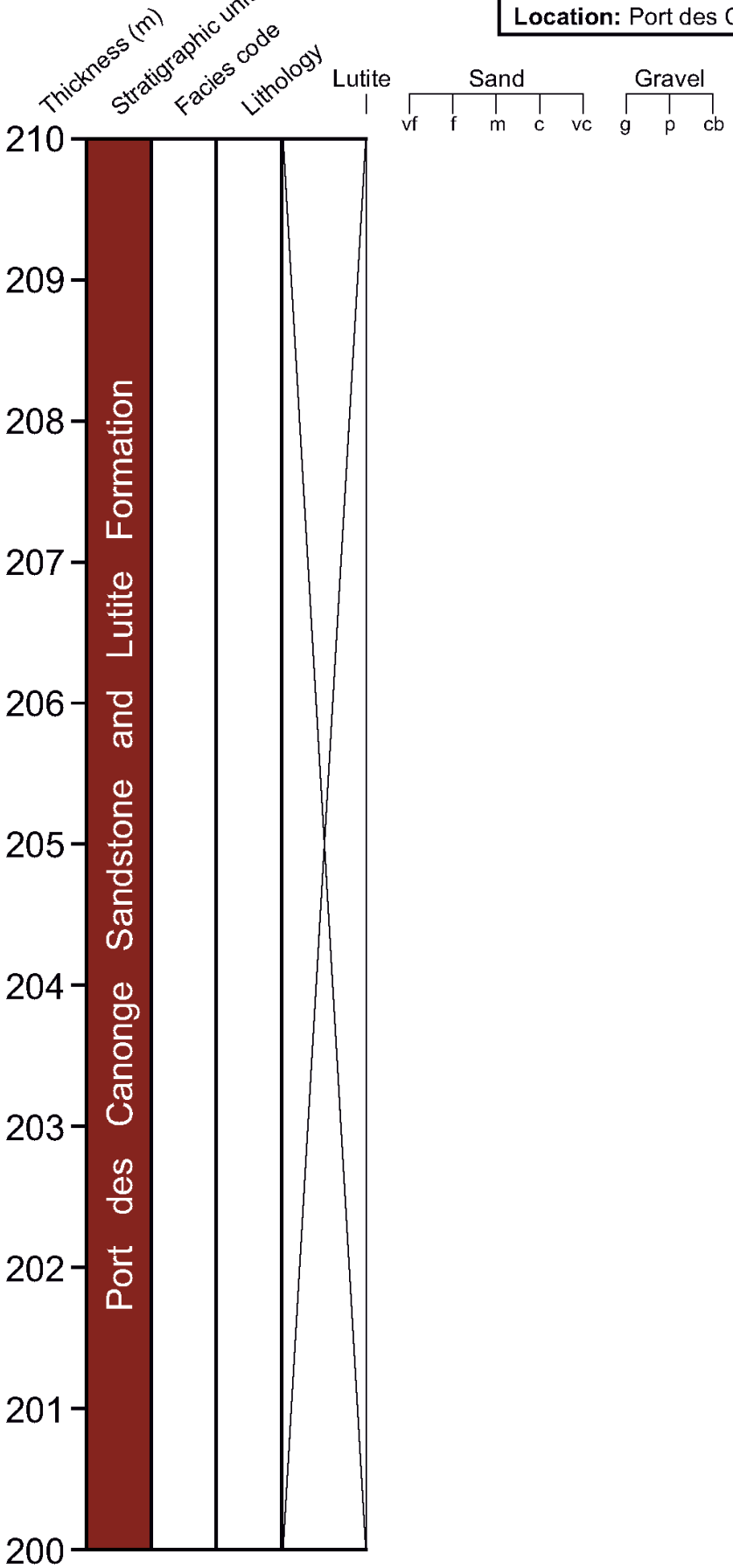

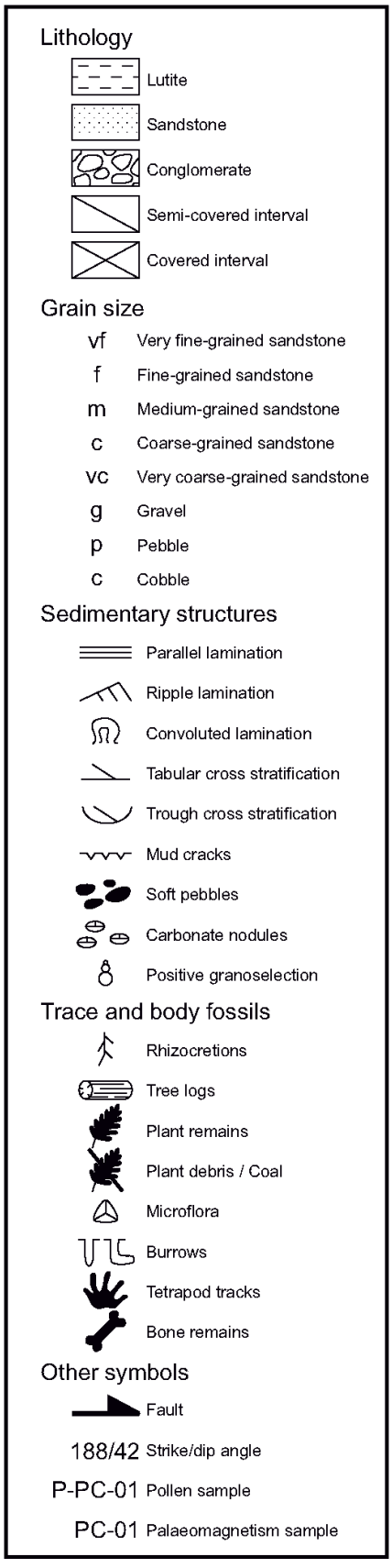

Log name: Port des Canonge	Page 22/61
Location: Port des Canonge–Hort de sa Cova Section	

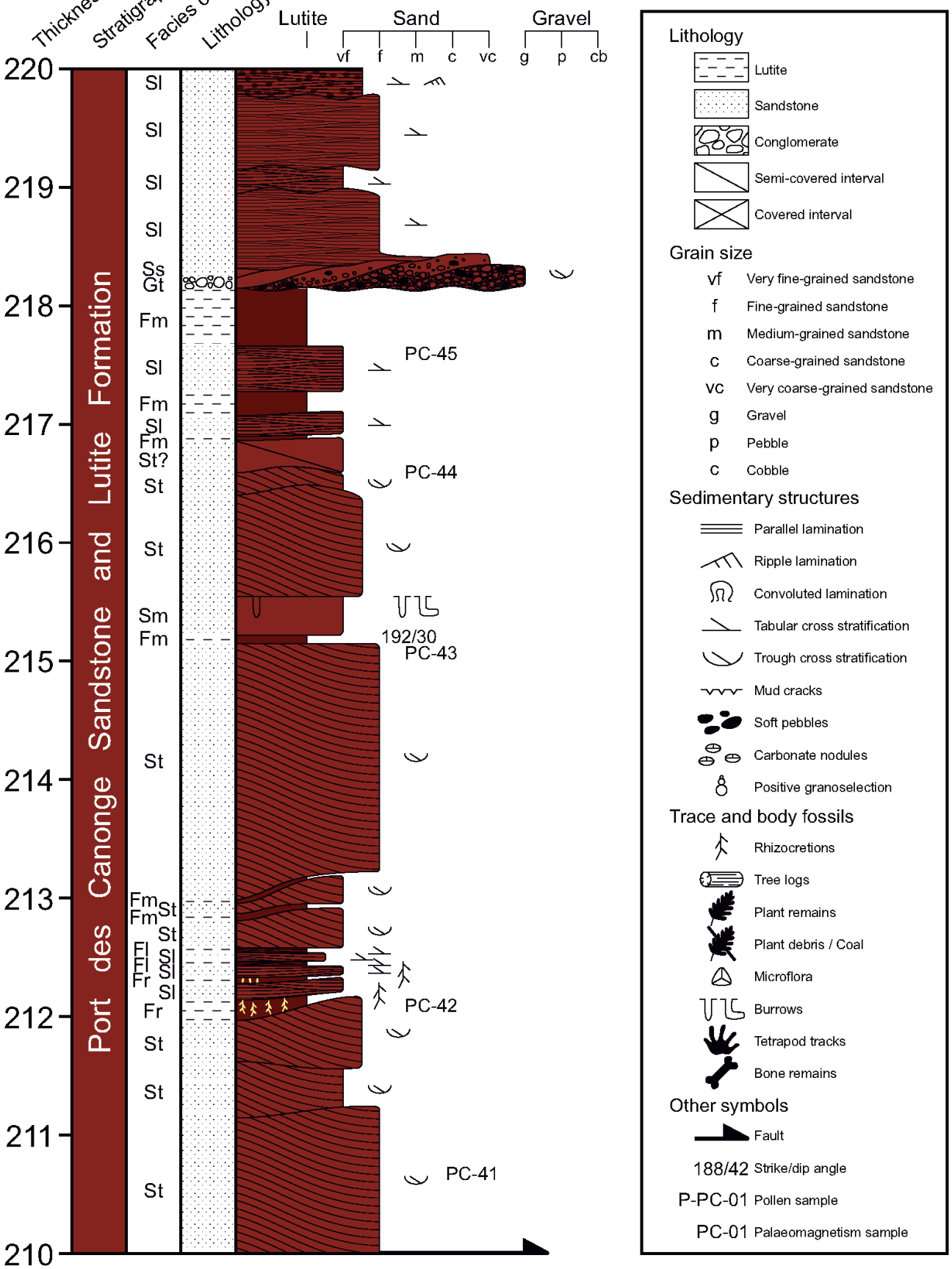

Log name: Port des Canonge	Page 23/61
Location: Port des Canonge–Hort de sa Cova Section	

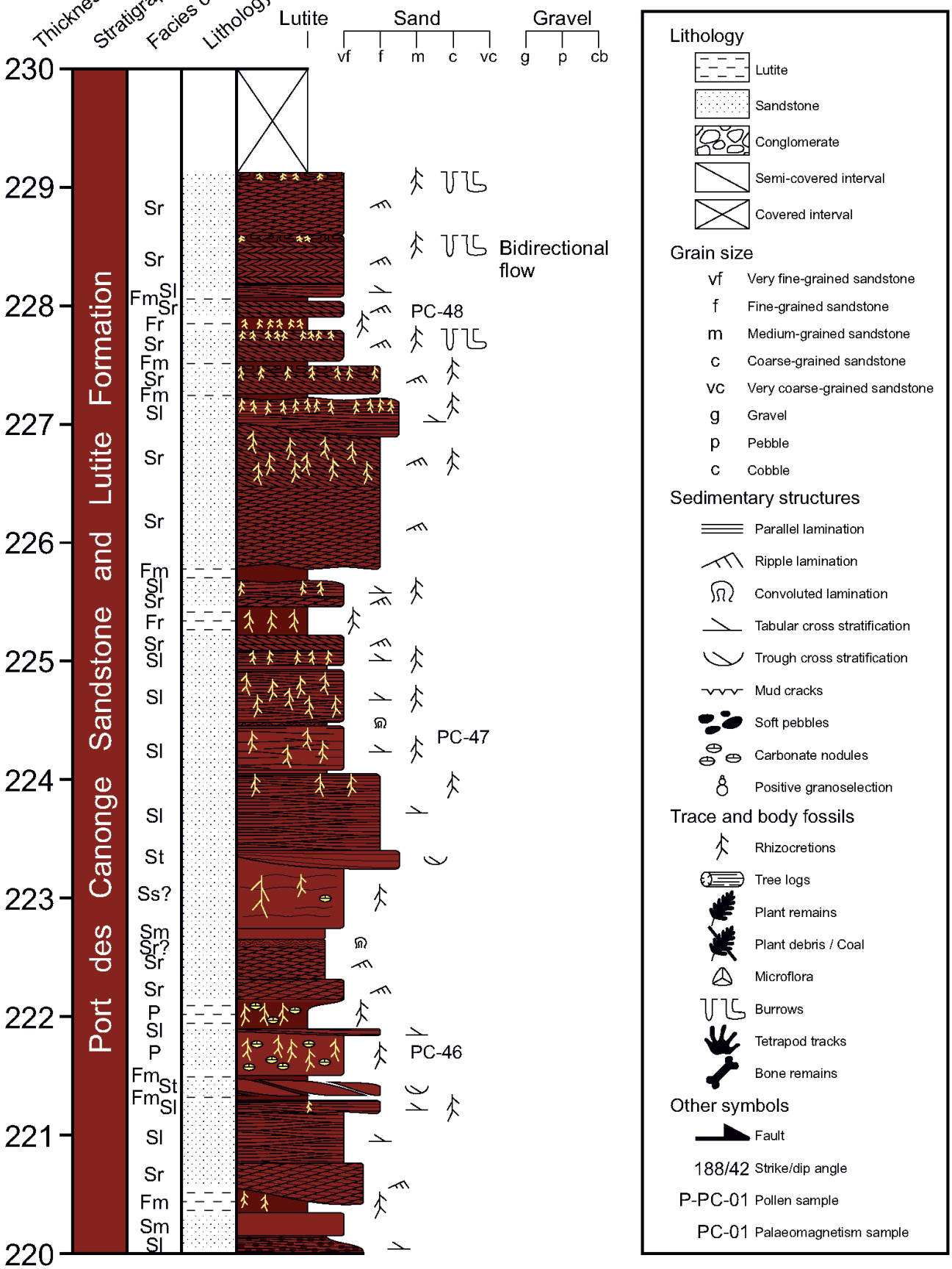

Log name: Port des Canonge | Page 24/61

Location: Port des Canonge–Hort de sa Cova Section

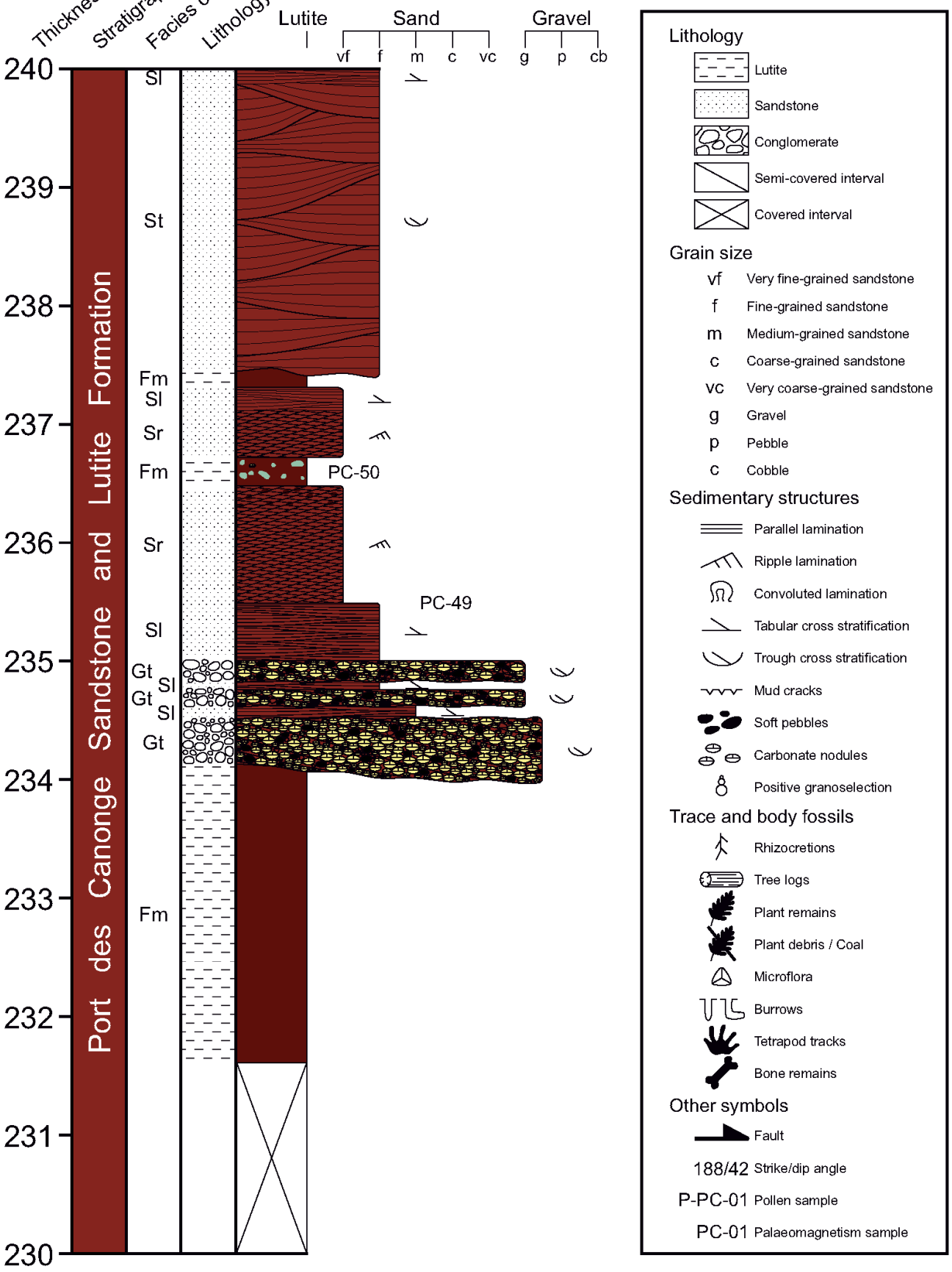

Log name: Port des Canonge	Page 25/61
Location: Port des Canonge–Hort de sa Cova Section	

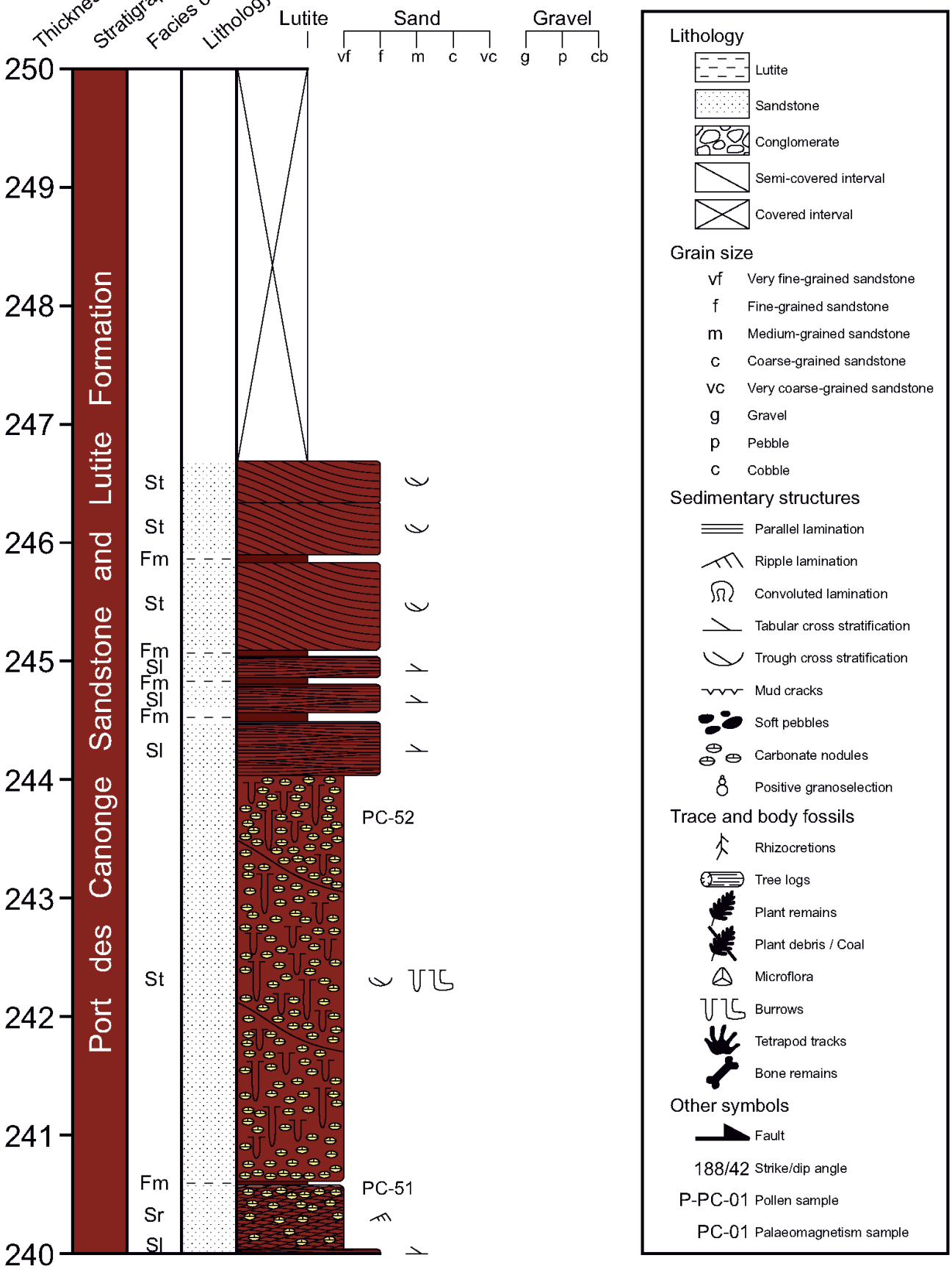

Log name: Port des Canonge	Page 26/61
Location: Port des Canonge–Hort de sa Cova Section	

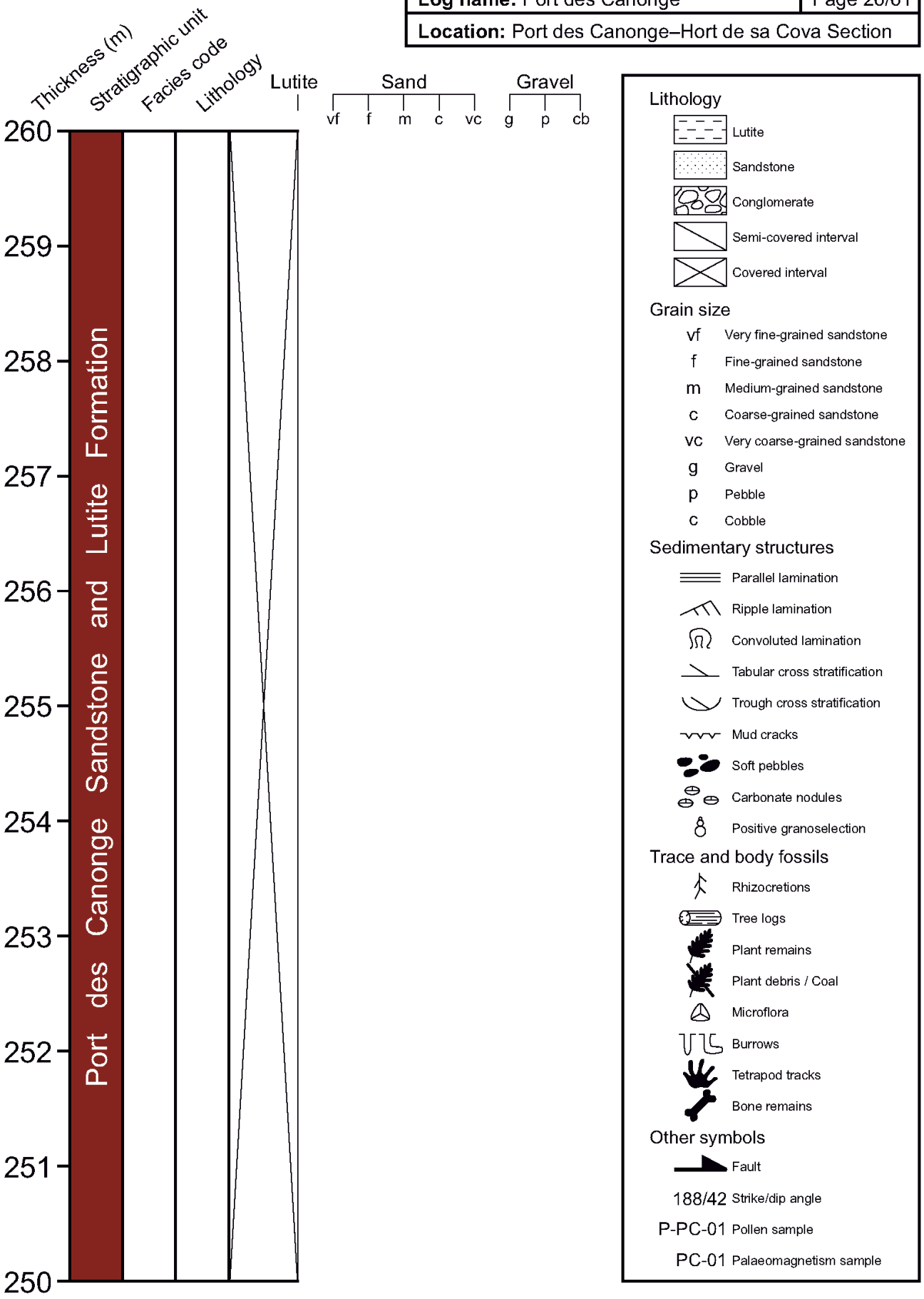

Log name: Port des Canonge	Page 27/61
Location: Port des Canonge–Hort de sa Cova Section	

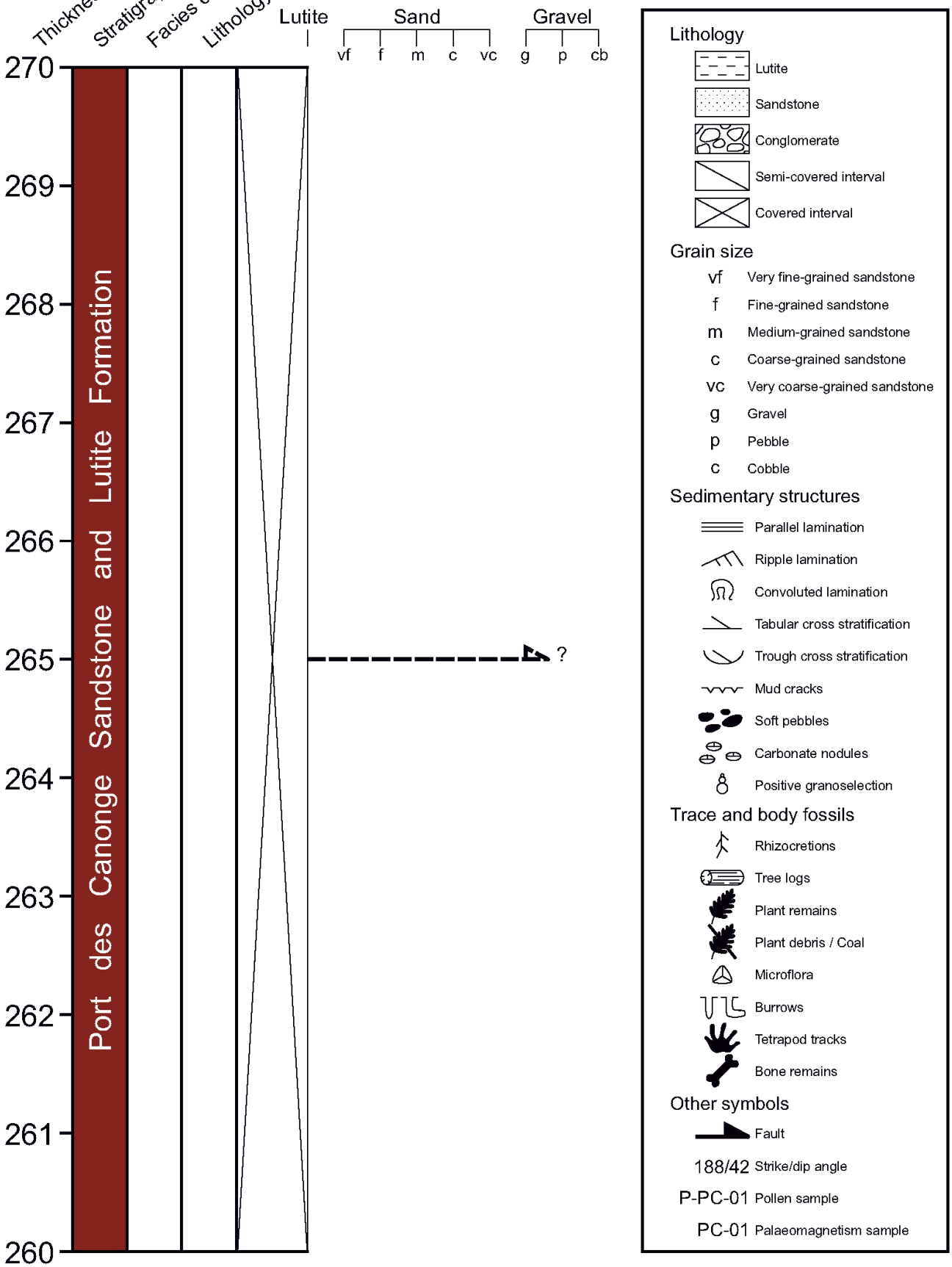

Log name: Port des Canonge	Page 28/61
Location: Port des Canonge–Hort de sa Cova Section	

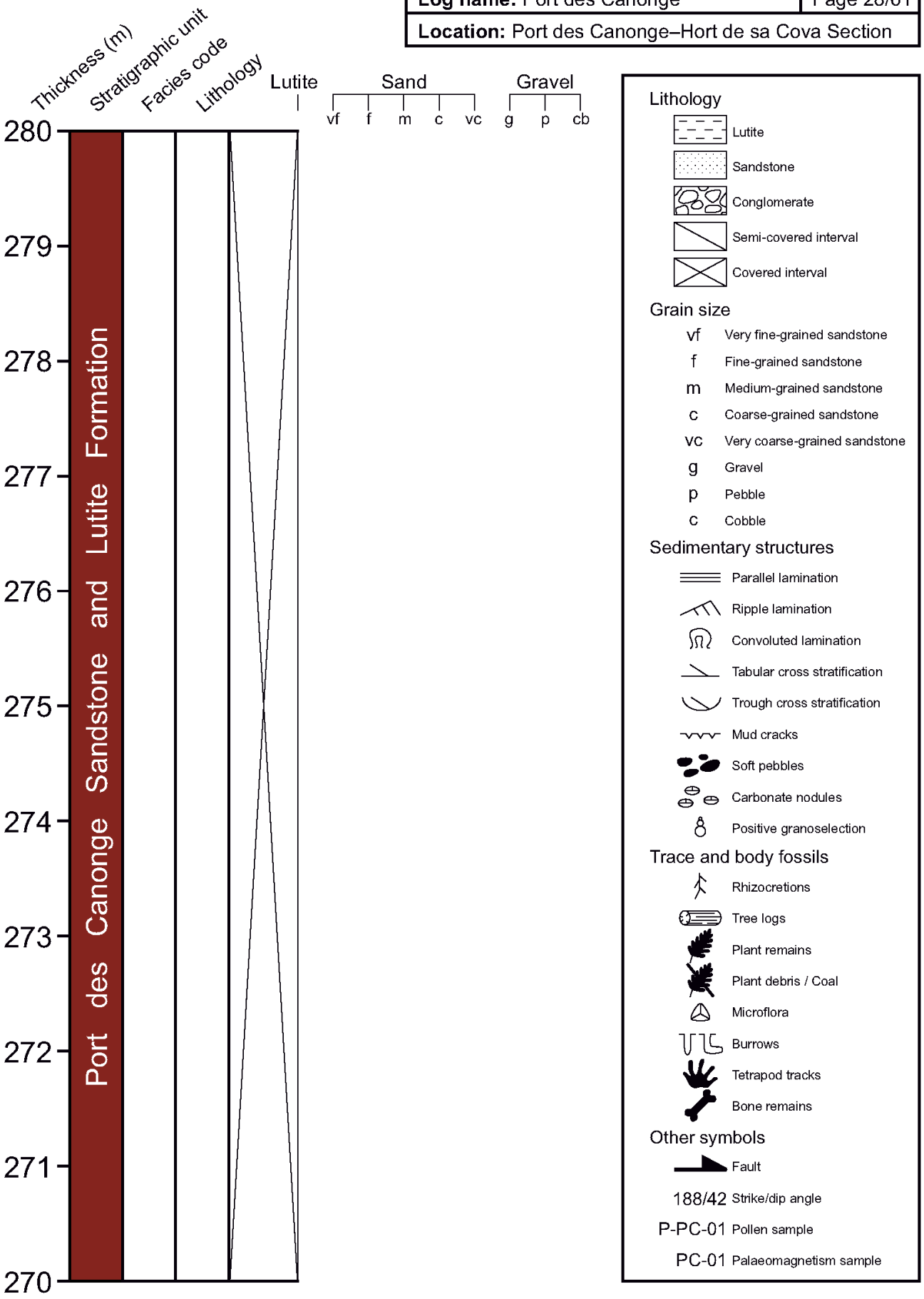

Log name: Port des Canonge	Page 29/61
Location: Port des Canonge–Hort de sa Cova Section	

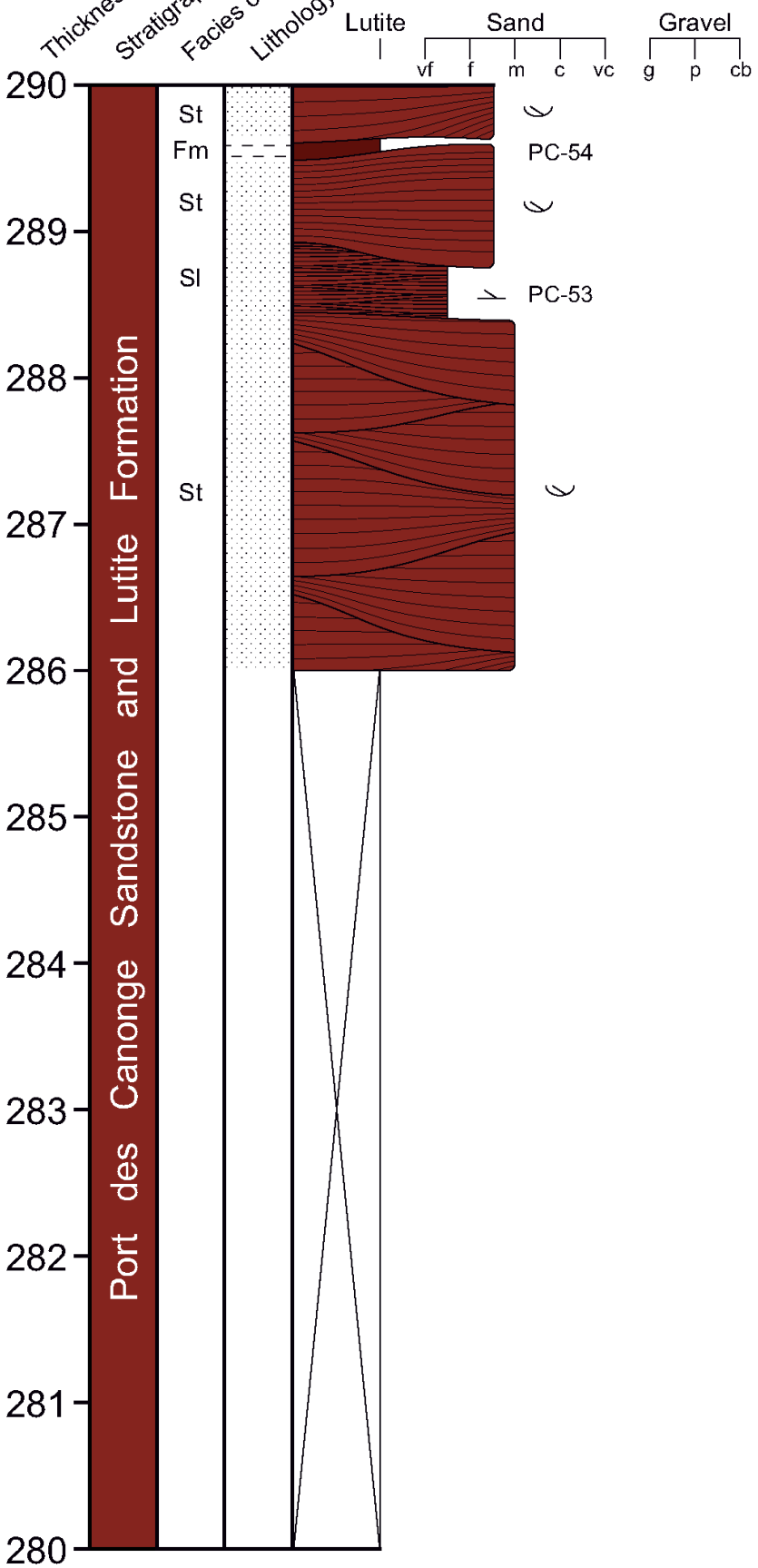

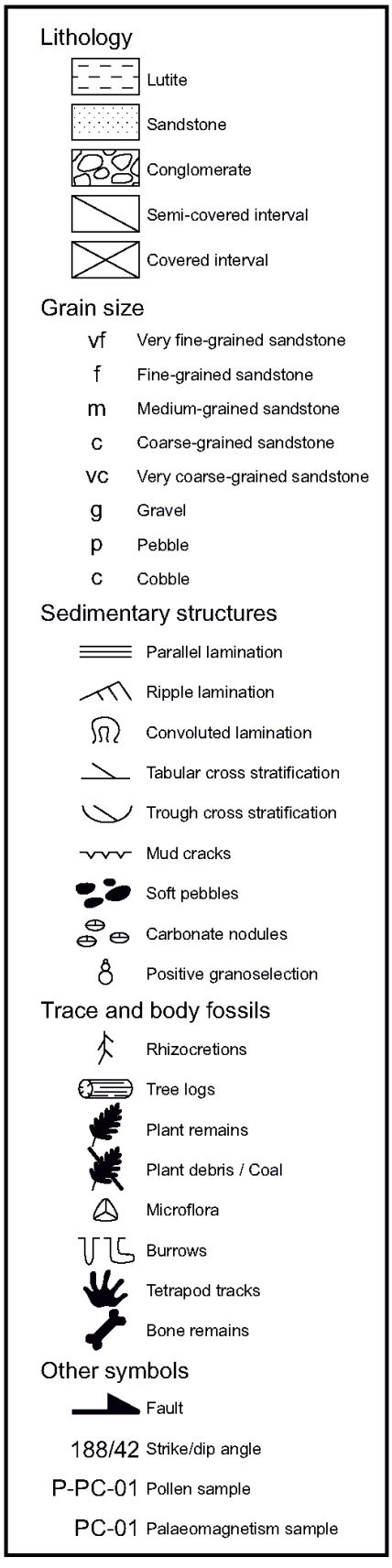

Log name: Port des Canonge	Page 30/61
Location: Port des Canonge–Hort de sa Cova Section	

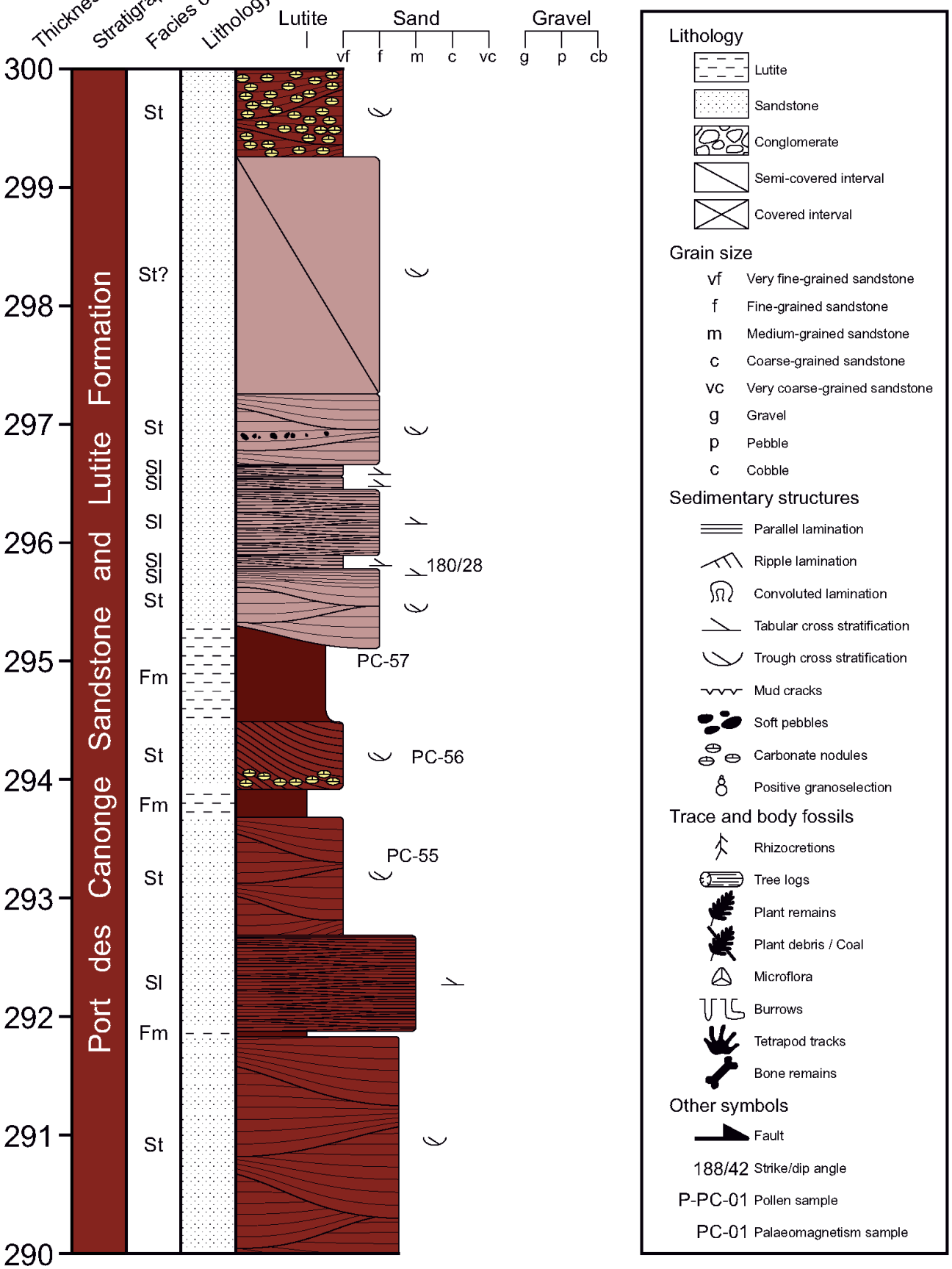

Log name: Port des Canonge	Page 31/61
Location: Port des Canonge–Hort de sa Cova Section	

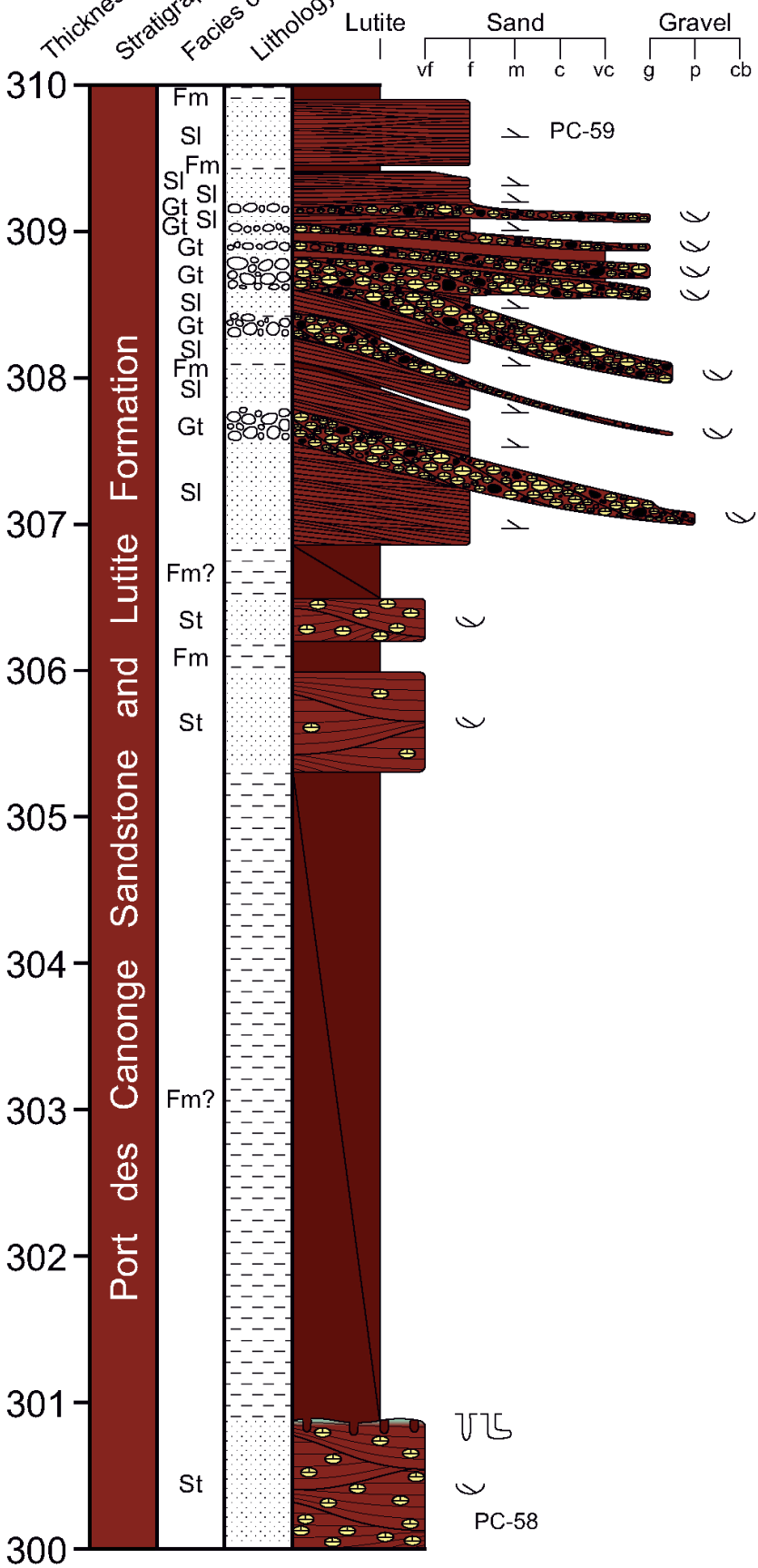

Lithology
- Lutite
- Sandstone
- Conglomerate
- Semi-covered interval
- Covered interval

Grain size
- vf Very fine-grained sandstone
- f Fine-grained sandstone
- m Medium-grained sandstone
- c Coarse-grained sandstone
- vc Very coarse-grained sandstone
- g Gravel
- p Pebble
- c Cobble

Sedimentary structures
- Parallel lamination
- Ripple lamination
- Convoluted lamination
- Tabular cross stratification
- Trough cross stratification
- Mud cracks
- Soft pebbles
- Carbonate nodules
- Positive granoselection

Trace and body fossils
- Rhizocretions
- Tree logs
- Plant remains
- Plant debris / Coal
- Microflora
- Burrows
- Tetrapod tracks
- Bone remains

Other symbols
- Fault
- 188/42 Strike/dip angle
- P-PC-01 Pollen sample
- PC-01 Palaeomagnetism sample

Log name: Port des Canonge	Page 32/61
Location: Port des Canonge–Hort de sa Cova Section	

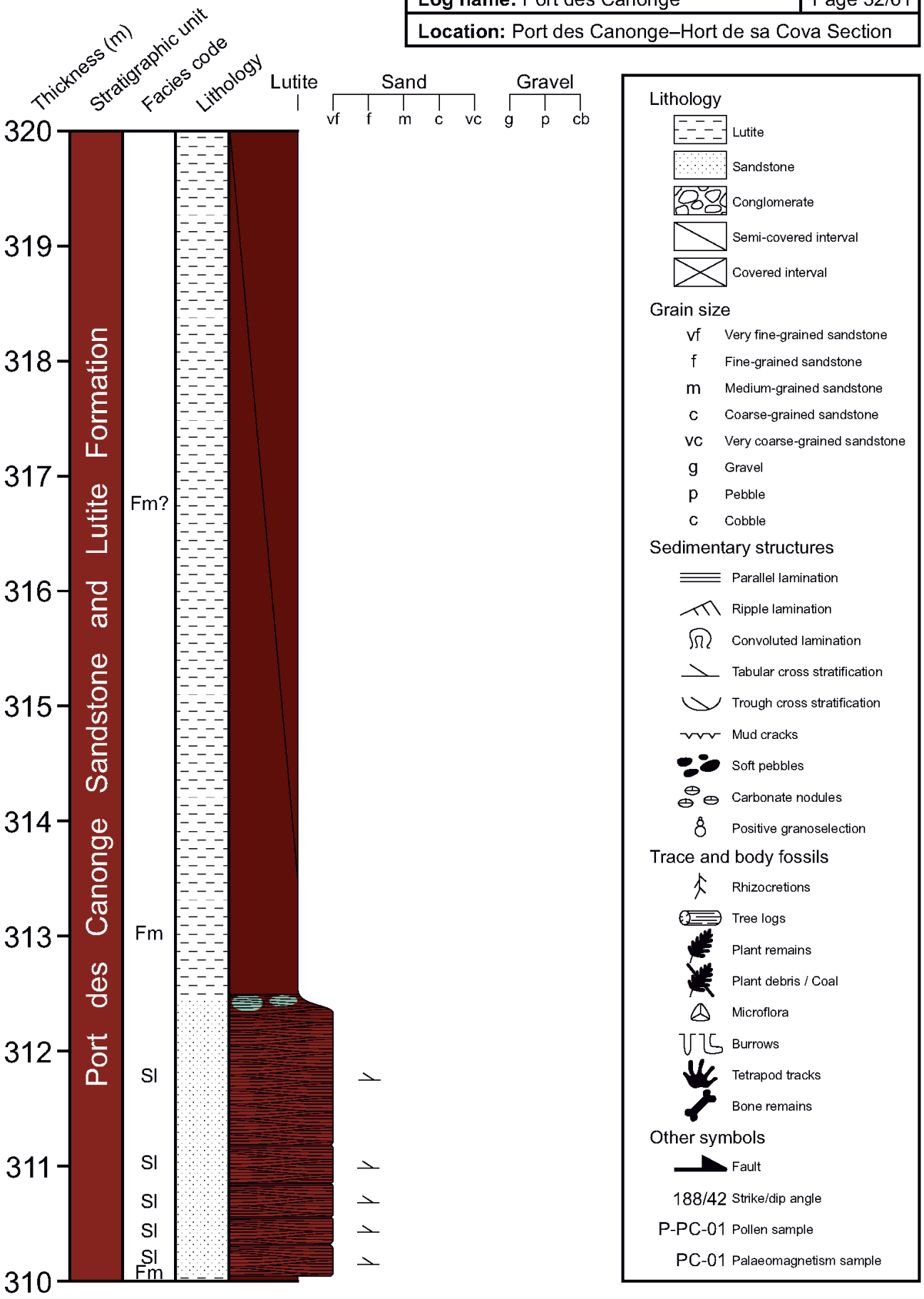

Log name: Port des Canonge	Page 33/61
Location: Port des Canonge–Hort de sa Cova Section	

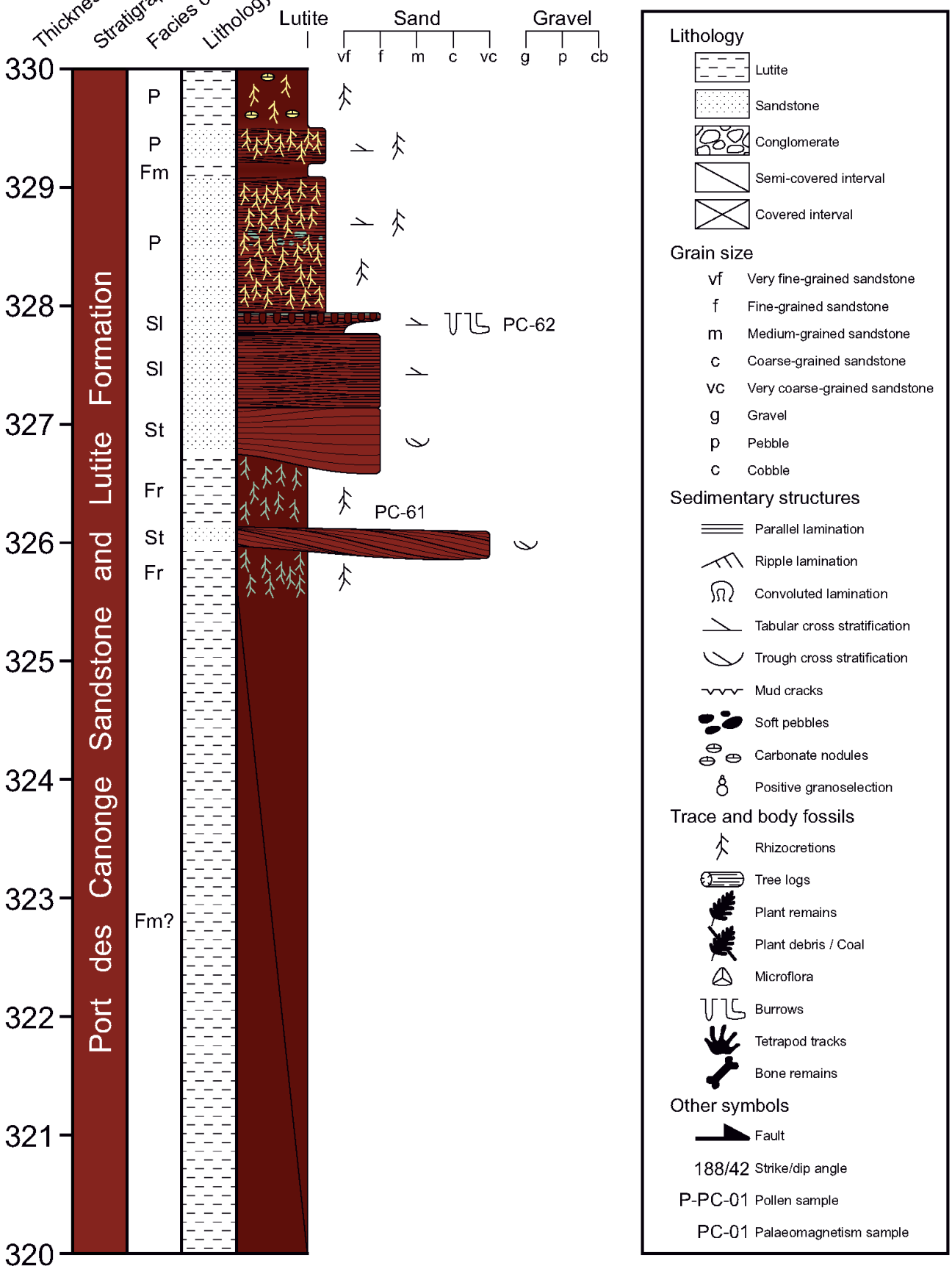

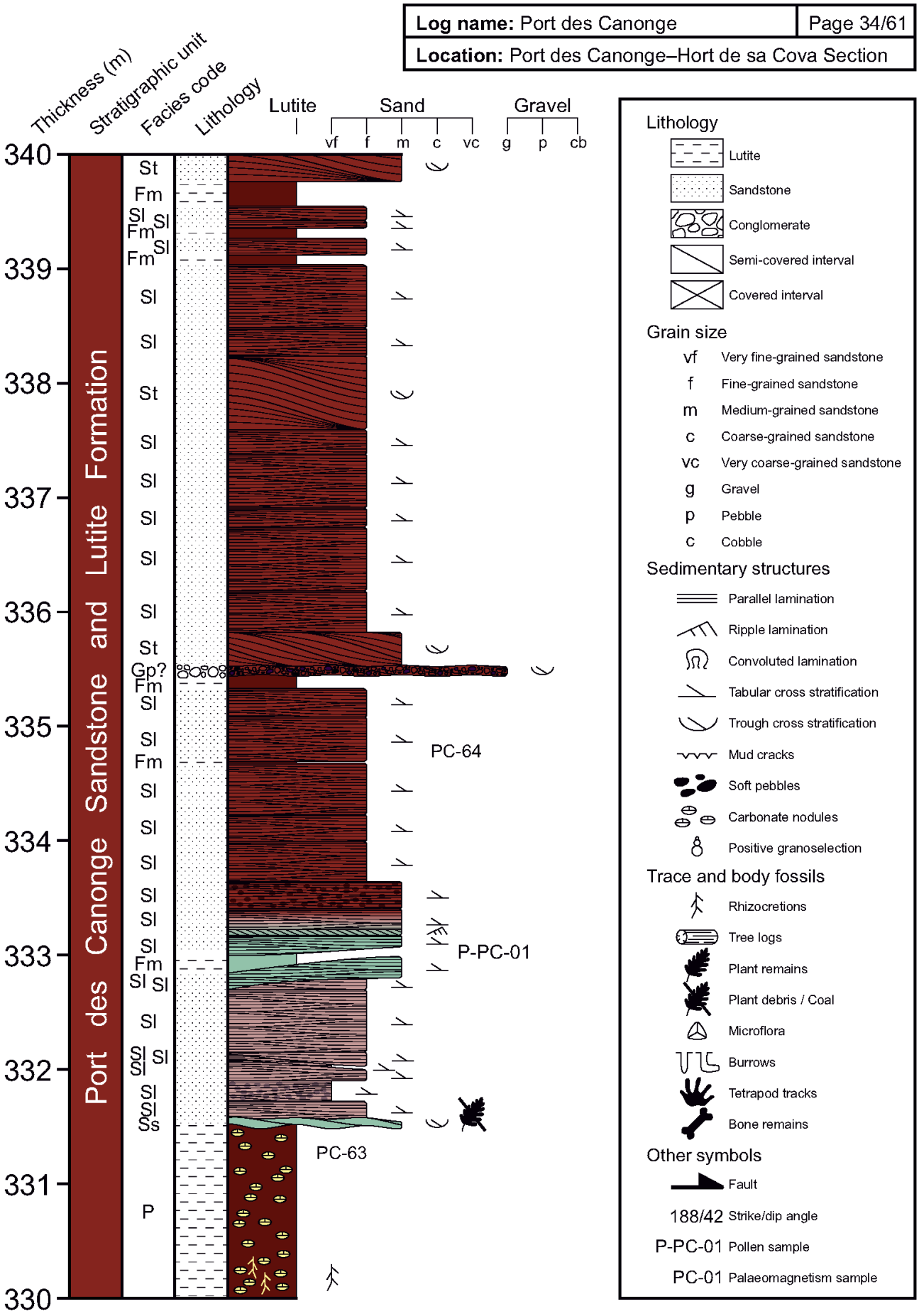
Log name: Port des Canonge
Page 34/61
Location: Port des Canonge–Hort de sa Cova Section
Thickness (m)
Stratigraphic unit
Facies code
Lithology
Lutite
Sand
Gravel
vf f m c vc g p cb
Port des Canonge Sandstone and Lutite Formation
340
339
338
337
336
335
334
333
332
331
330
St
Fm
Sl
Ss
P
Gp?
PC-64
P-PC-01
PC-63
Lithology
Lutite
Sandstone
Conglomerate
Semi-covered interval
Covered interval
Grain size
vf Very fine-grained sandstone
f Fine-grained sandstone
m Medium-grained sandstone
c Coarse-grained sandstone
vc Very coarse-grained sandstone
g Gravel
p Pebble
c Cobble
Sedimentary structures
Parallel lamination
Ripple lamination
Convoluted lamination
Tabular cross stratification
Trough cross stratification
Mud cracks
Soft pebbles
Carbonate nodules
Positive granoselection
Trace and body fossils
Rhizocretions
Tree logs
Plant remains
Plant debris / Coal
Microflora
Burrows
Tetrapod tracks
Bone remains
Other symbols
Fault
188/42 Strike/dip angle
P-PC-01 Pollen sample
PC-01 Palaeomagnetism sample

Log name: Port des Canonge	Page 35/61
Location: Port des Canonge–Hort de sa Cova Section	

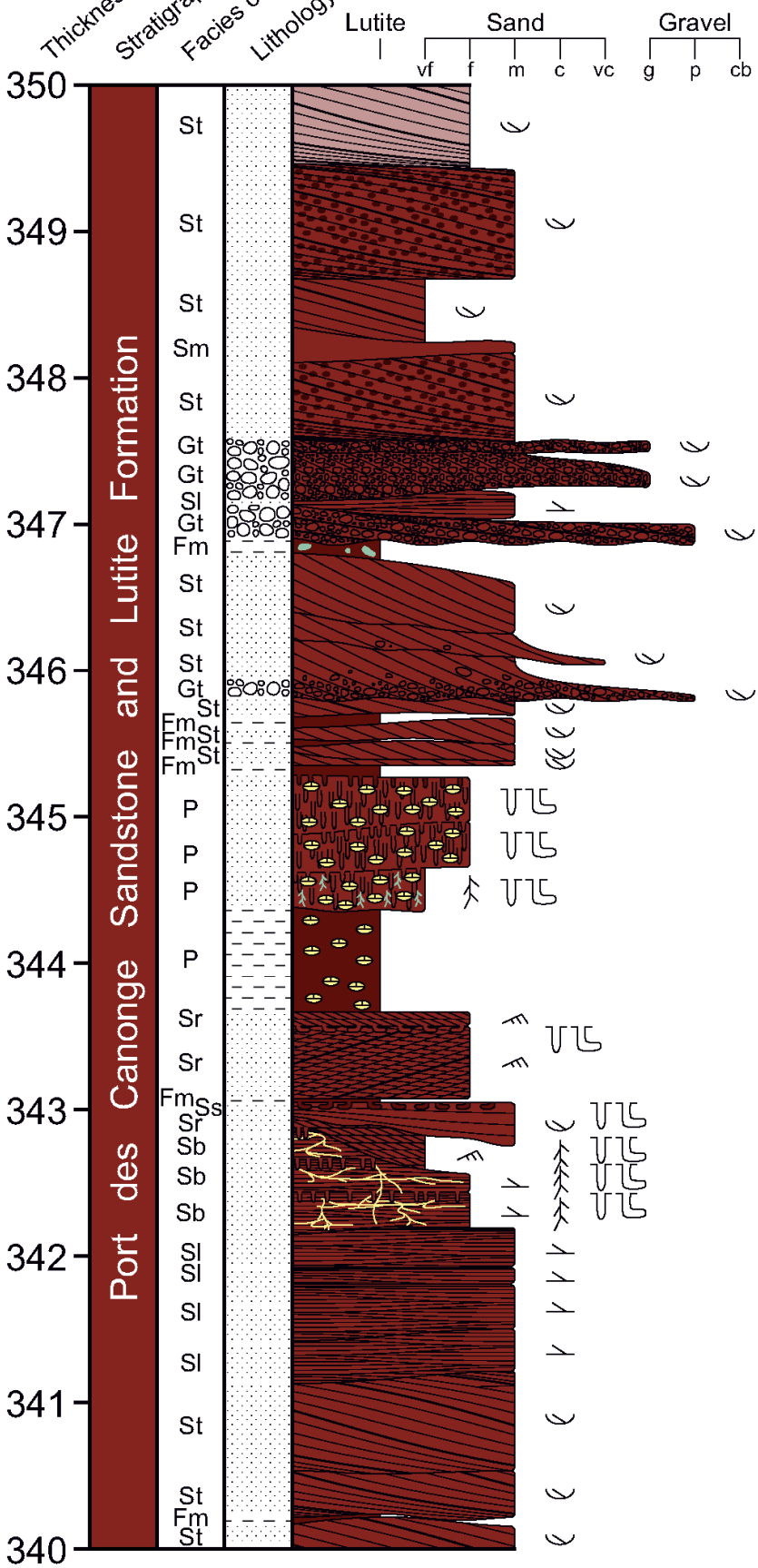

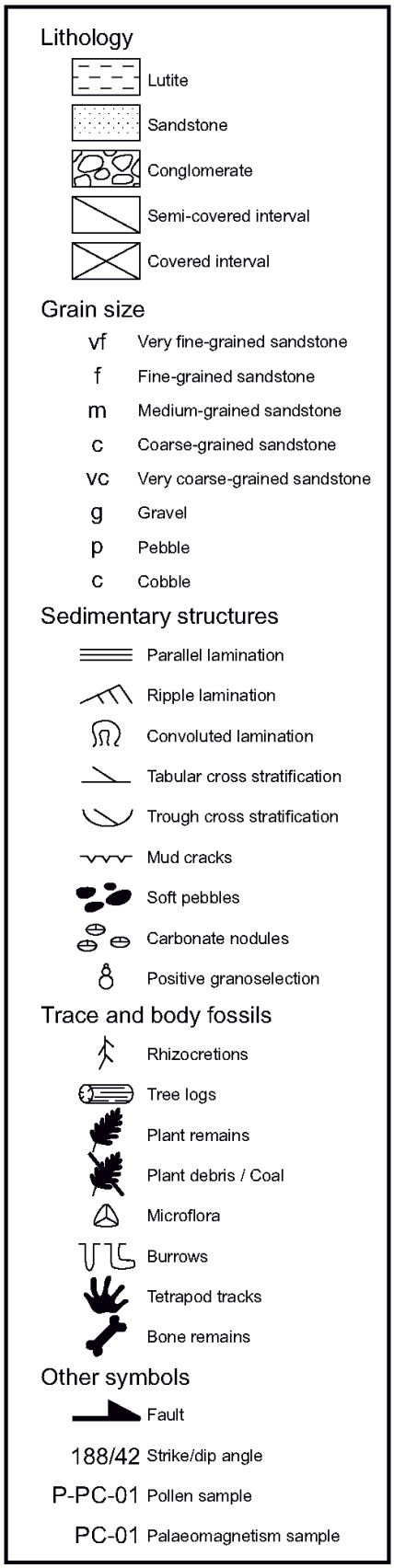

Log name: Port des Canonge | Page 36/61

Location: Port des Canonge–Hort de sa Cova Section

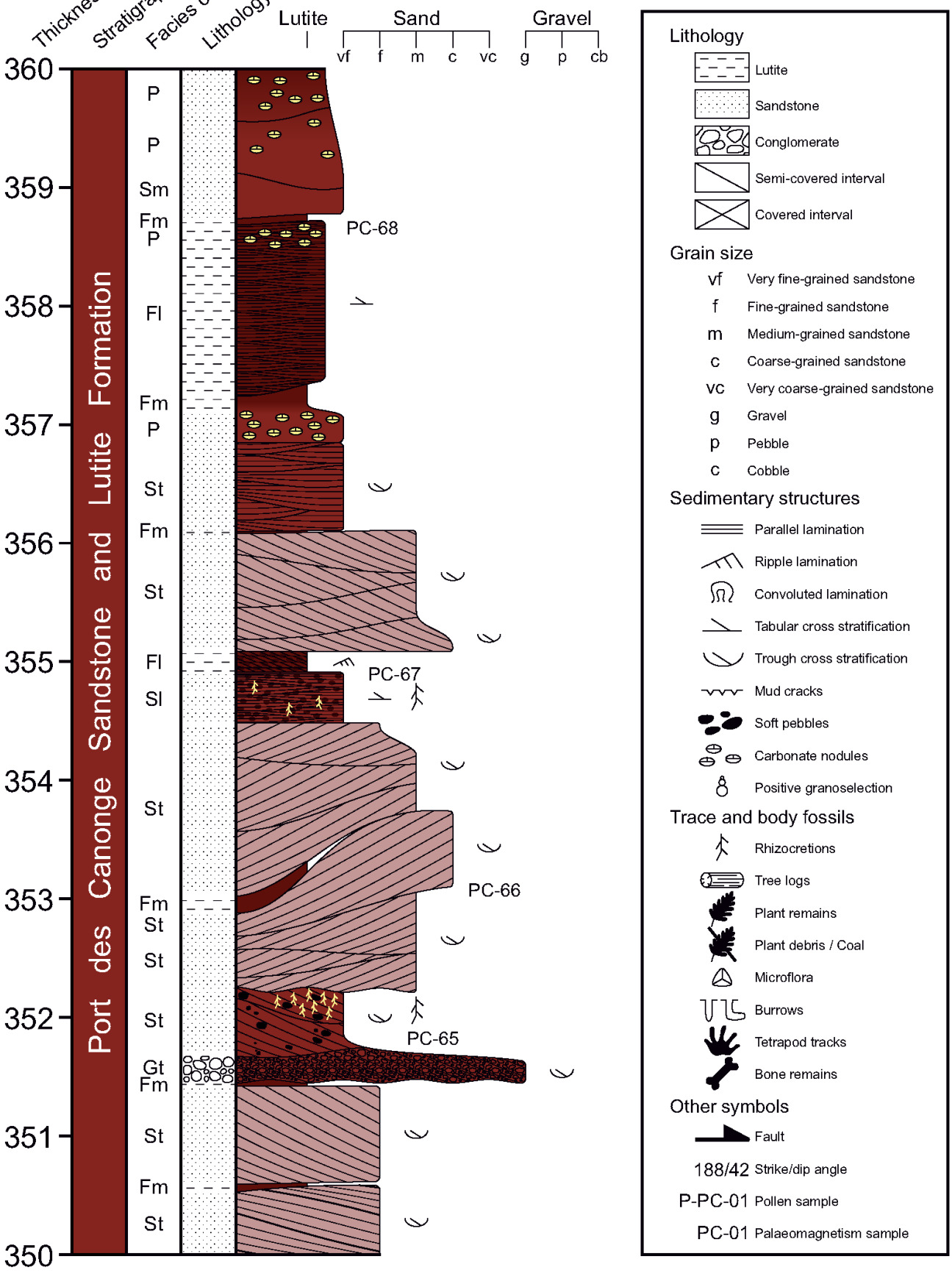

Log name: Port des Canonge	Page 37/61
Location: Port des Canonge–Hort de sa Cova Section	

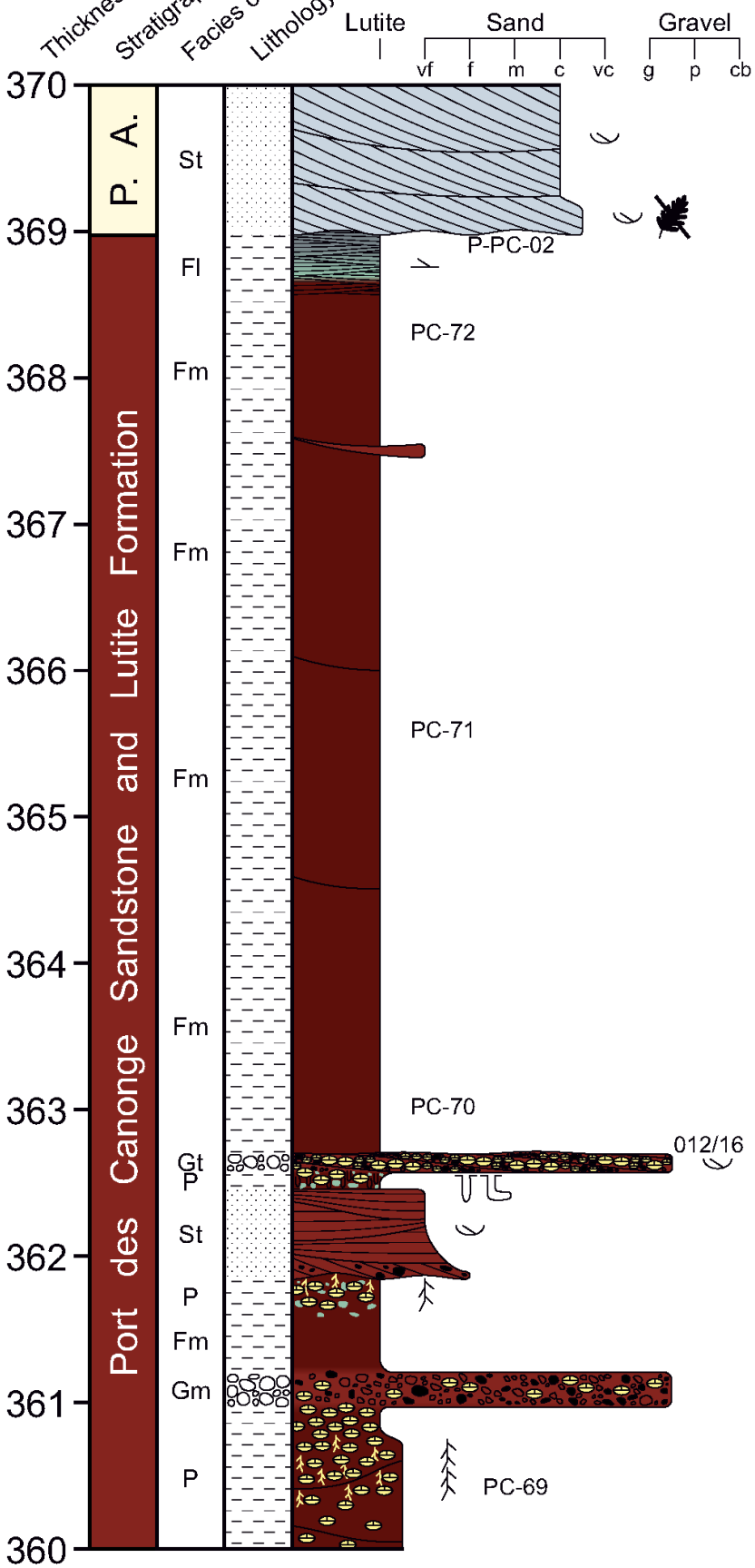

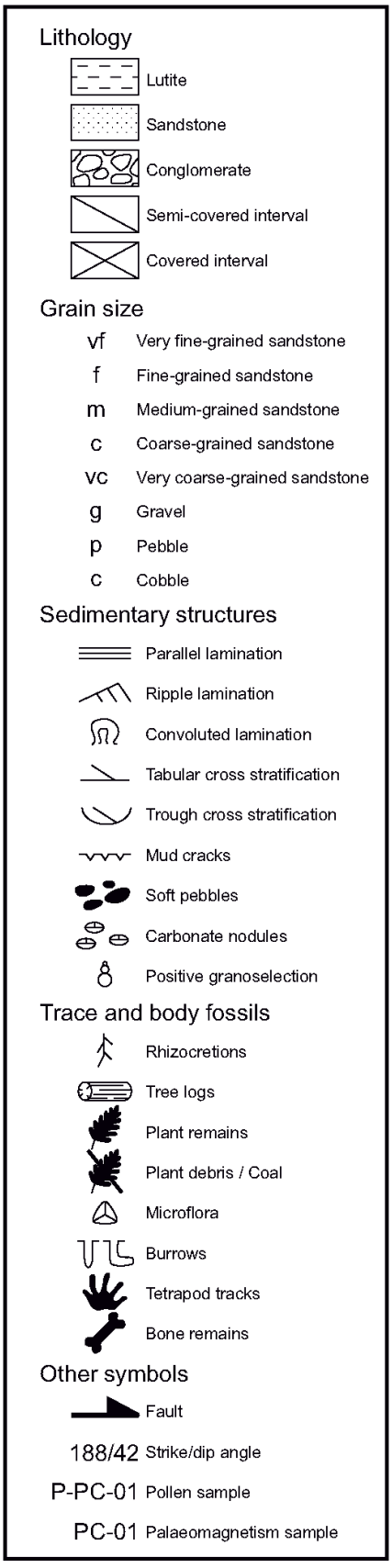

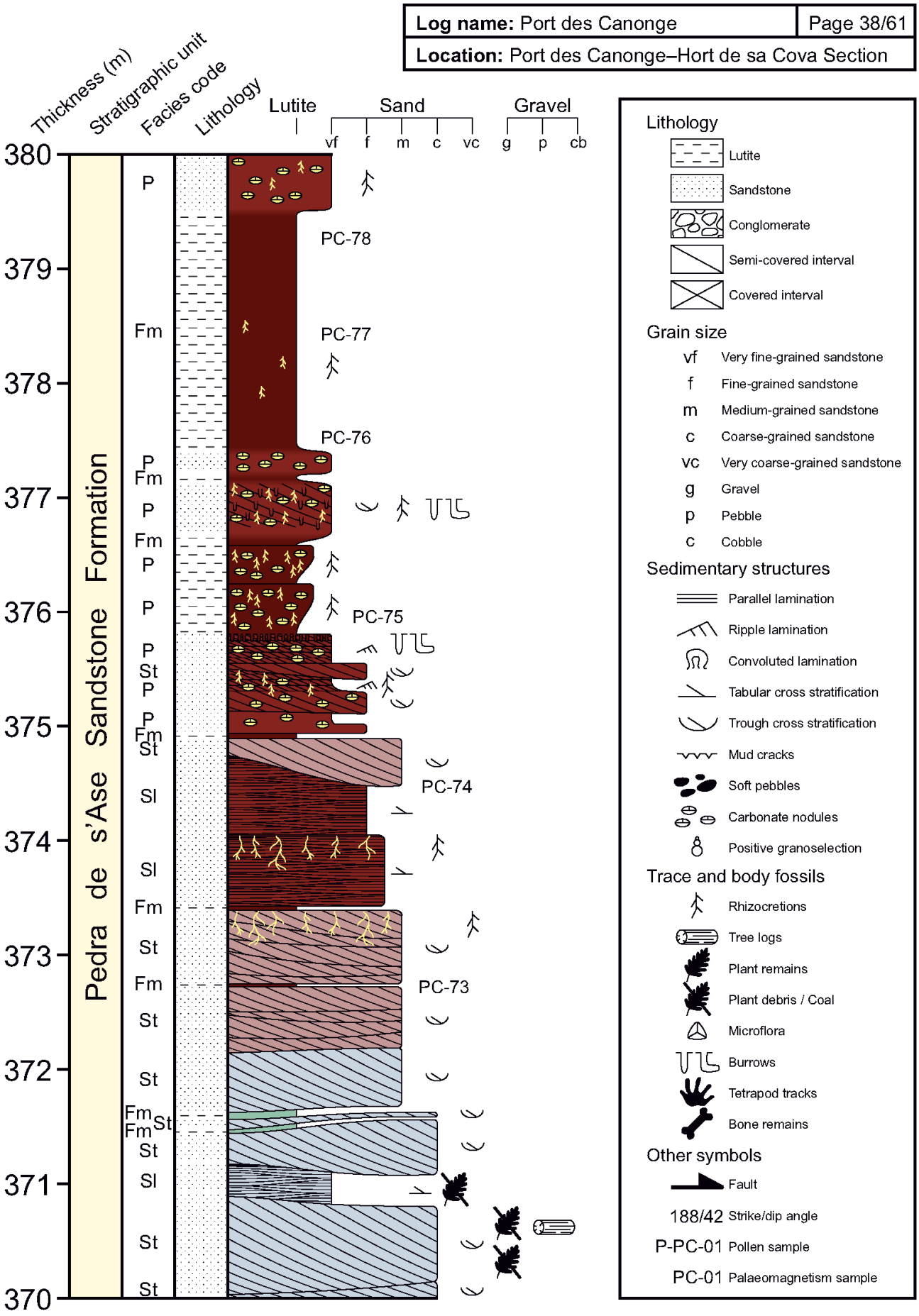
Log name: Port des Canonge
Page 38/61
Location: Port des Canonge–Hort de sa Cova Section
Thickness (m)
Stratigraphic unit
Facies code
Lithology
Lutite
Sand
Gravel
vf f m c vc g p cb
Pedra de s'Ase Sandstone Formation
380
379
378
377
376
375
374
373
372
371
370
PC-78
PC-77
PC-76
PC-75
PC-74
PC-73
Lithology
Lutite
Sandstone
Conglomerate
Semi-covered interval
Covered interval
Grain size
vf Very fine-grained sandstone
f Fine-grained sandstone
m Medium-grained sandstone
c Coarse-grained sandstone
vc Very coarse-grained sandstone
g Gravel
p Pebble
c Cobble
Sedimentary structures
Parallel lamination
Ripple lamination
Convoluted lamination
Tabular cross stratification
Trough cross stratification
Mud cracks
Soft pebbles
Carbonate nodules
Positive granoselection
Trace and body fossils
Rhizocretions
Tree logs
Plant remains
Plant debris / Coal
Microflora
Burrows
Tetrapod tracks
Bone remains
Other symbols
Fault
188/42 Strike/dip angle
P-PC-01 Pollen sample
PC-01 Palaeomagnetism sample

Log name: Port des Canonge	Page 39/61
Location: Port des Canonge–Hort de sa Cova Section	

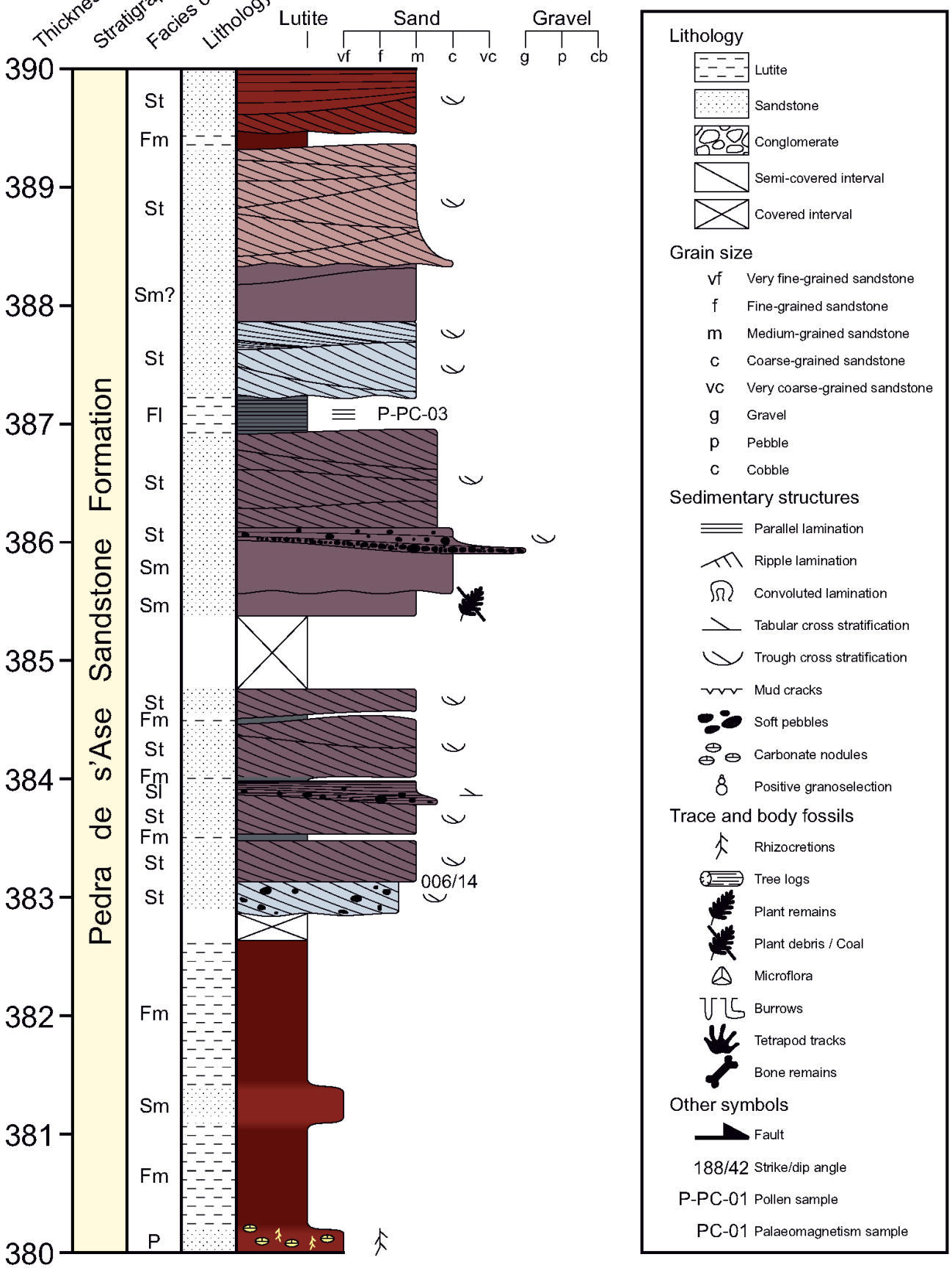

Log name: Port des Canonge	Page 40/61
Location: Port des Canonge–Hort de sa Cova Section	

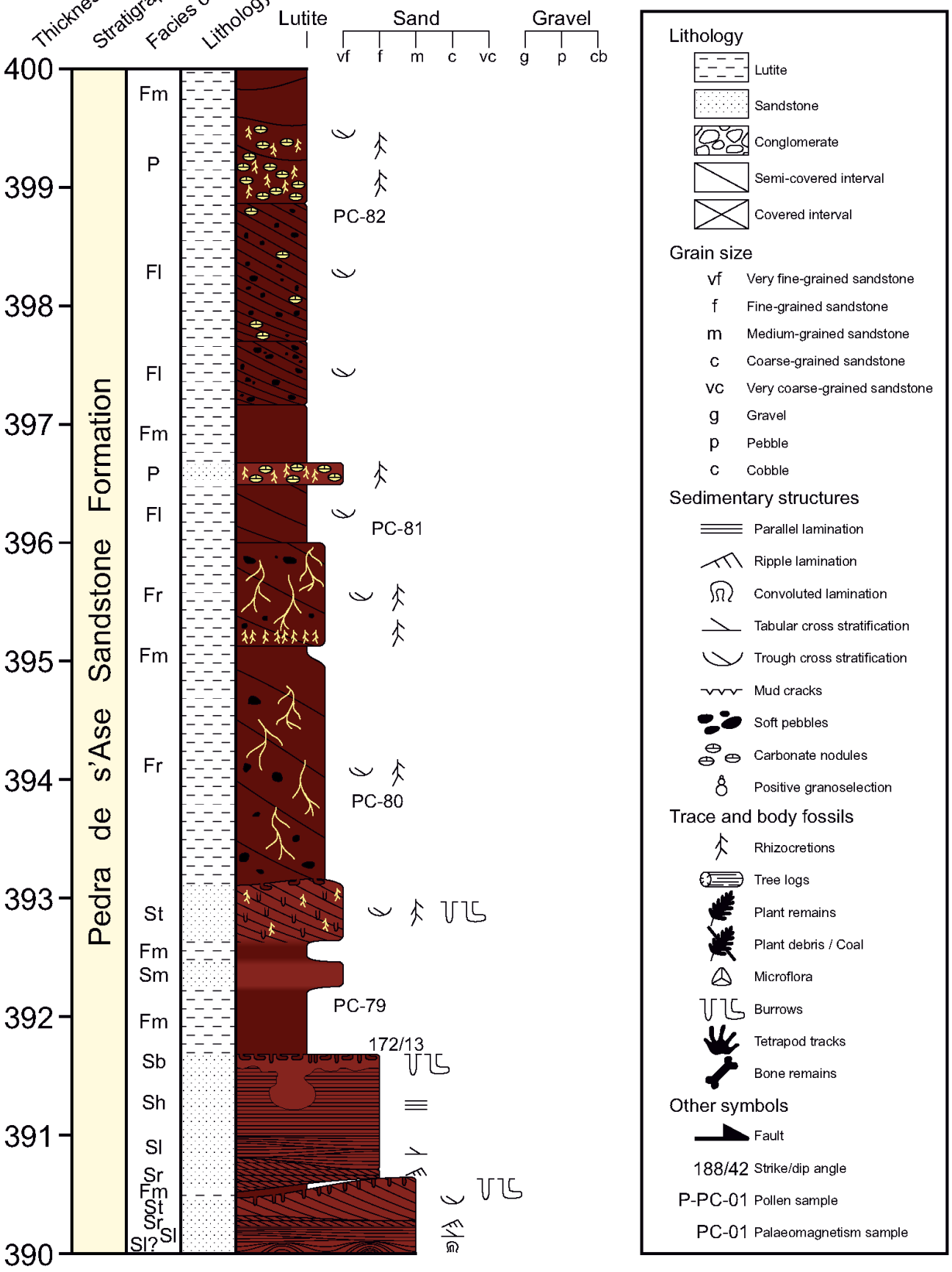

Log name: Port des Canonge	Page 41/61
Location: Port des Canonge–Hort de sa Cova Section	

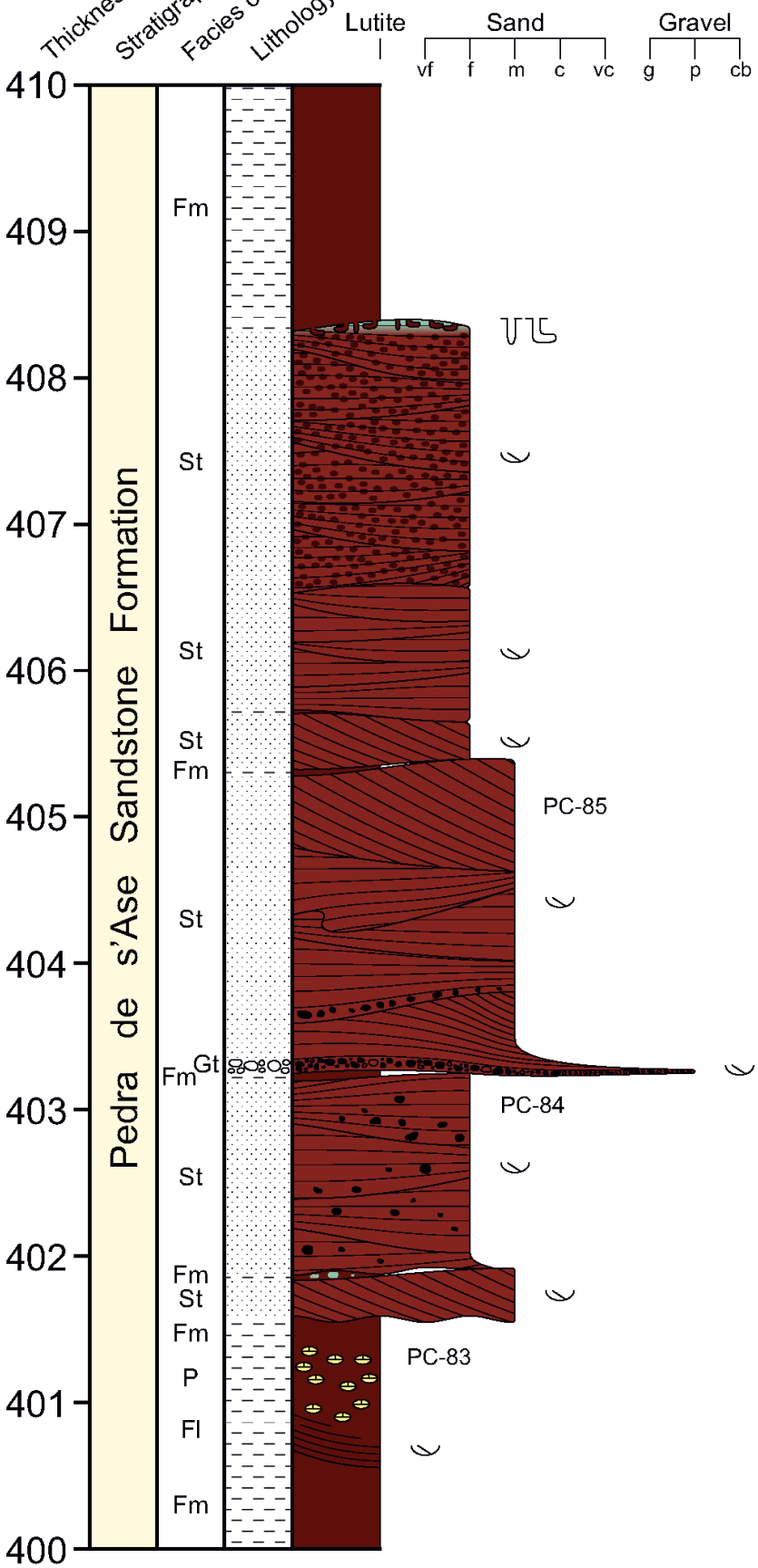

Lithology
- Lutite
- Sandstone
- Conglomerate
- Semi-covered interval
- Covered interval

Grain size
- vf Very fine-grained sandstone
- f Fine-grained sandstone
- m Medium-grained sandstone
- c Coarse-grained sandstone
- vc Very coarse-grained sandstone
- g Gravel
- p Pebble
- c Cobble

Sedimentary structures
- Parallel lamination
- Ripple lamination
- Convoluted lamination
- Tabular cross stratification
- Trough cross stratification
- Mud cracks
- Soft pebbles
- Carbonate nodules
- Positive granoselection

Trace and body fossils
- Rhizocretions
- Tree logs
- Plant remains
- Plant debris / Coal
- Microflora
- Burrows
- Tetrapod tracks
- Bone remains

Other symbols
- Fault
- 188/42 Strike/dip angle
- P-PC-01 Pollen sample
- PC-01 Palaeomagnetism sample

Log name: Port des Canonge	Page 42/61
Location: Port des Canonge–Hort de sa Cova Section	

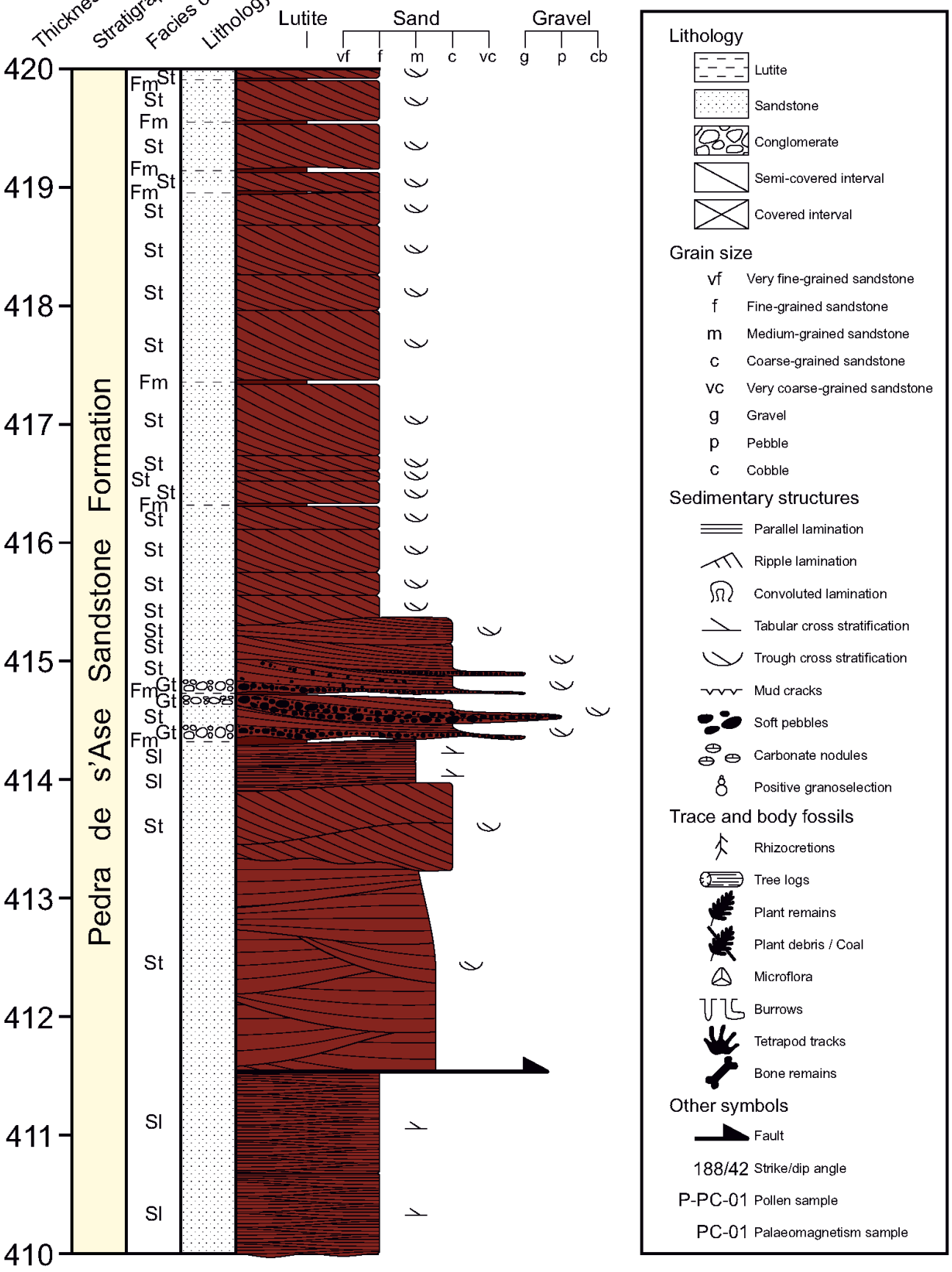

Log name: Port des Canonge	Page 43/61
Location: Port des Canonge–Hort de sa Cova Section	

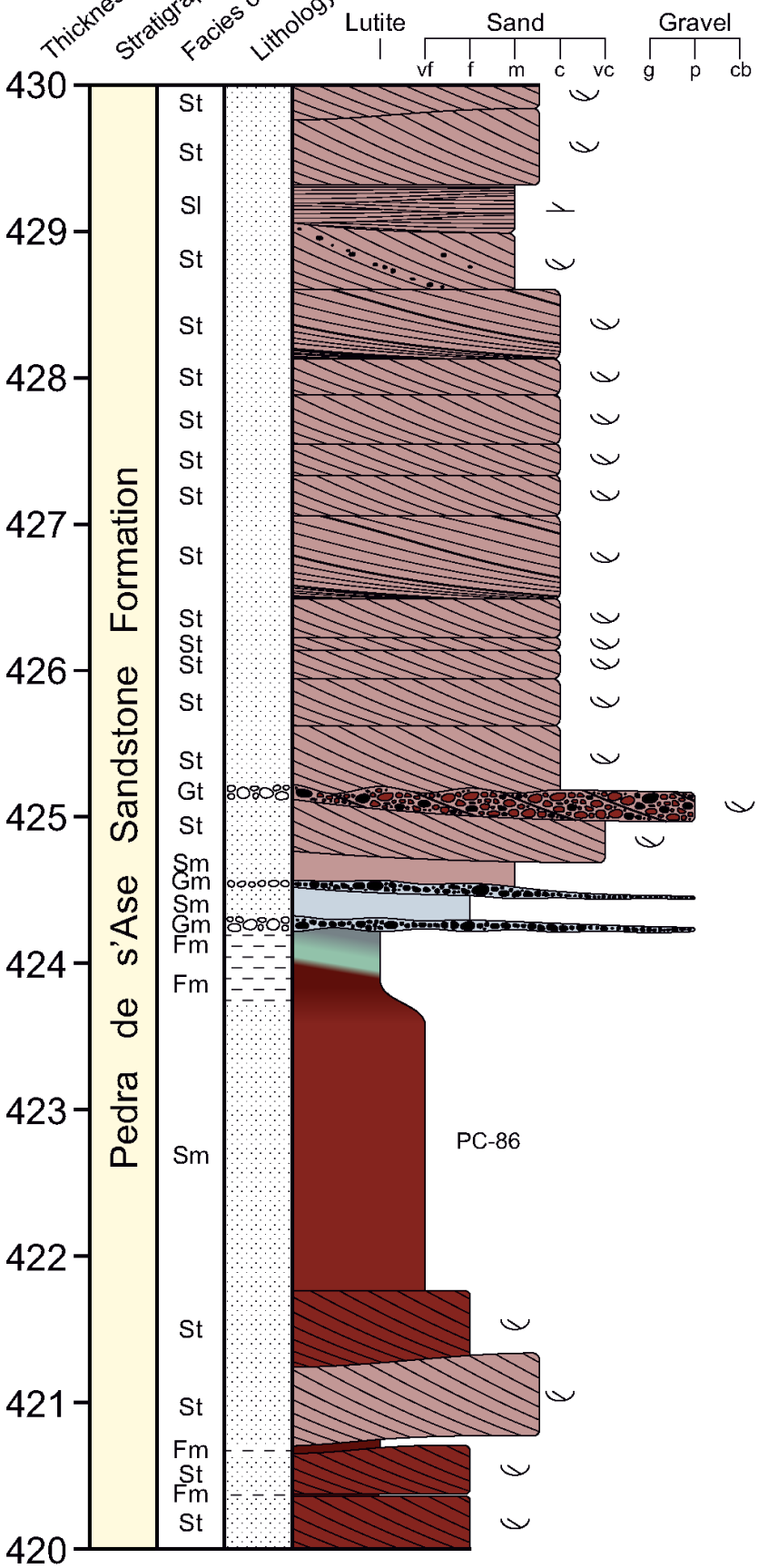

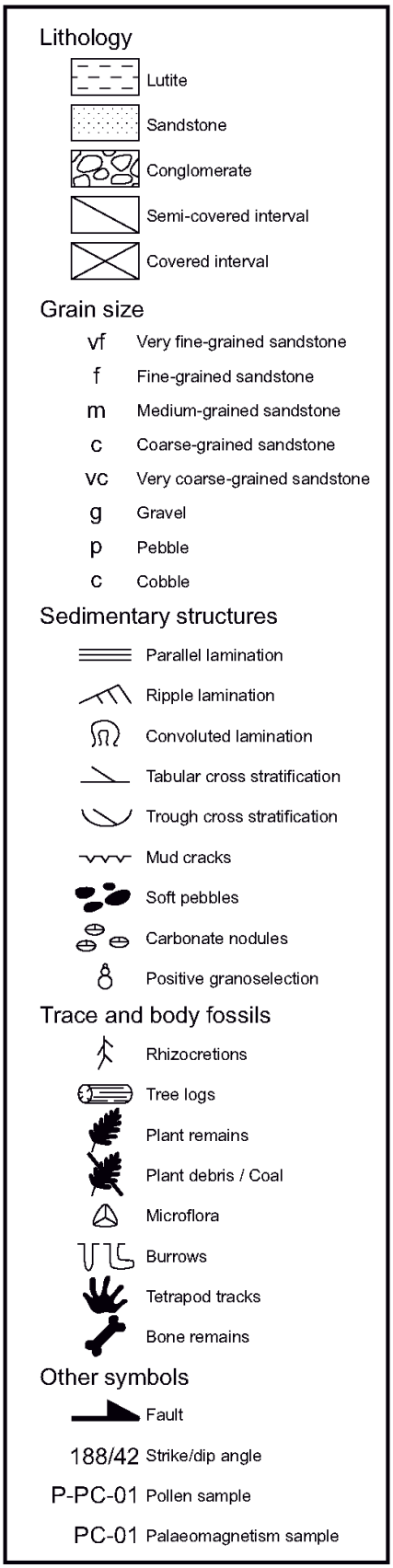

Log name: Port des Canonge	Page 44/61
Location: Port des Canonge–Hort de sa Cova Section	

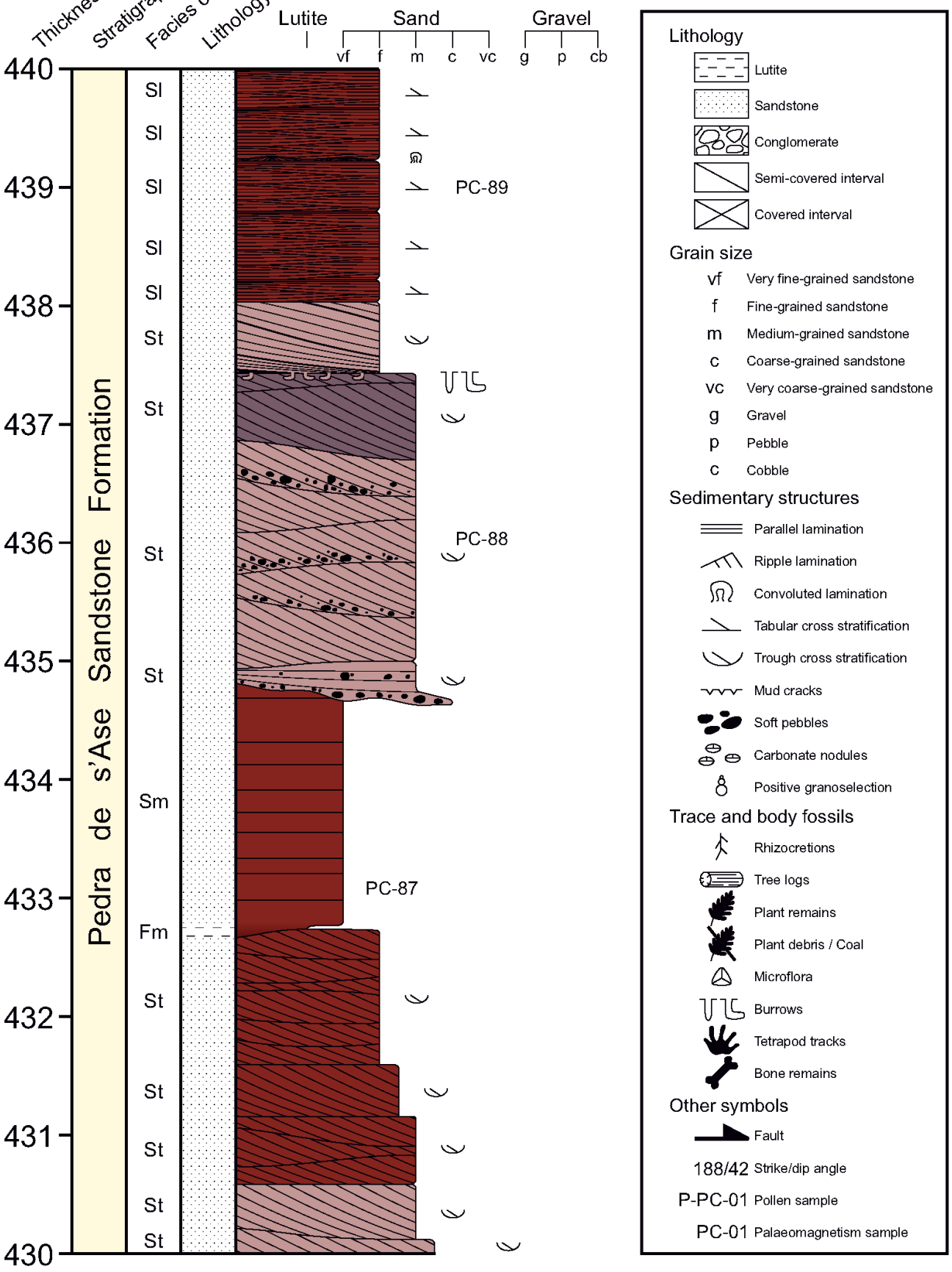

Log name: Port des Canonge	Page 45/61
Location: Port des Canonge–Hort de sa Cova Section	

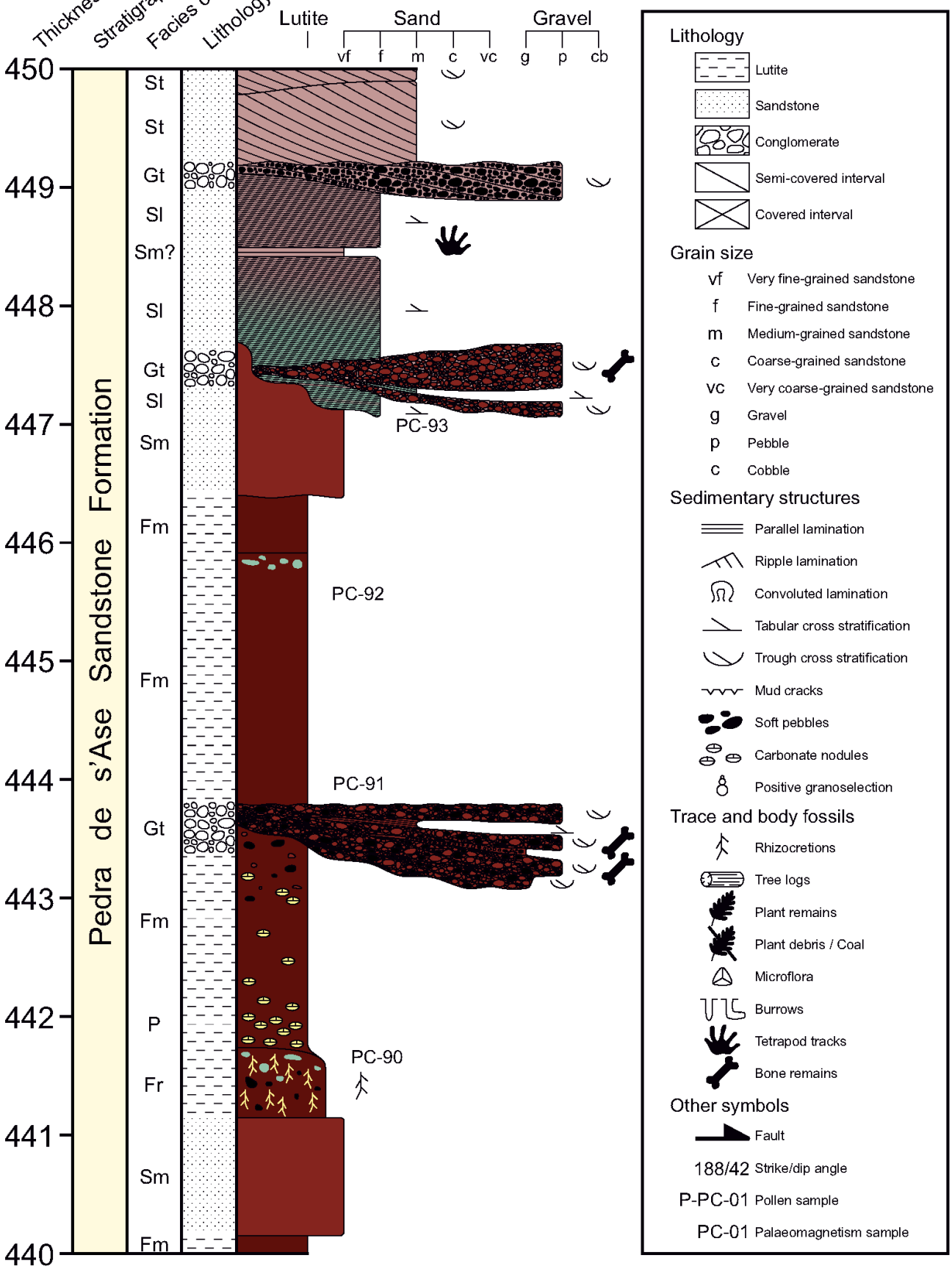

Log name: Port des Canonge	Page 46/61
Location: Port des Canonge–Hort de sa Cova Section	

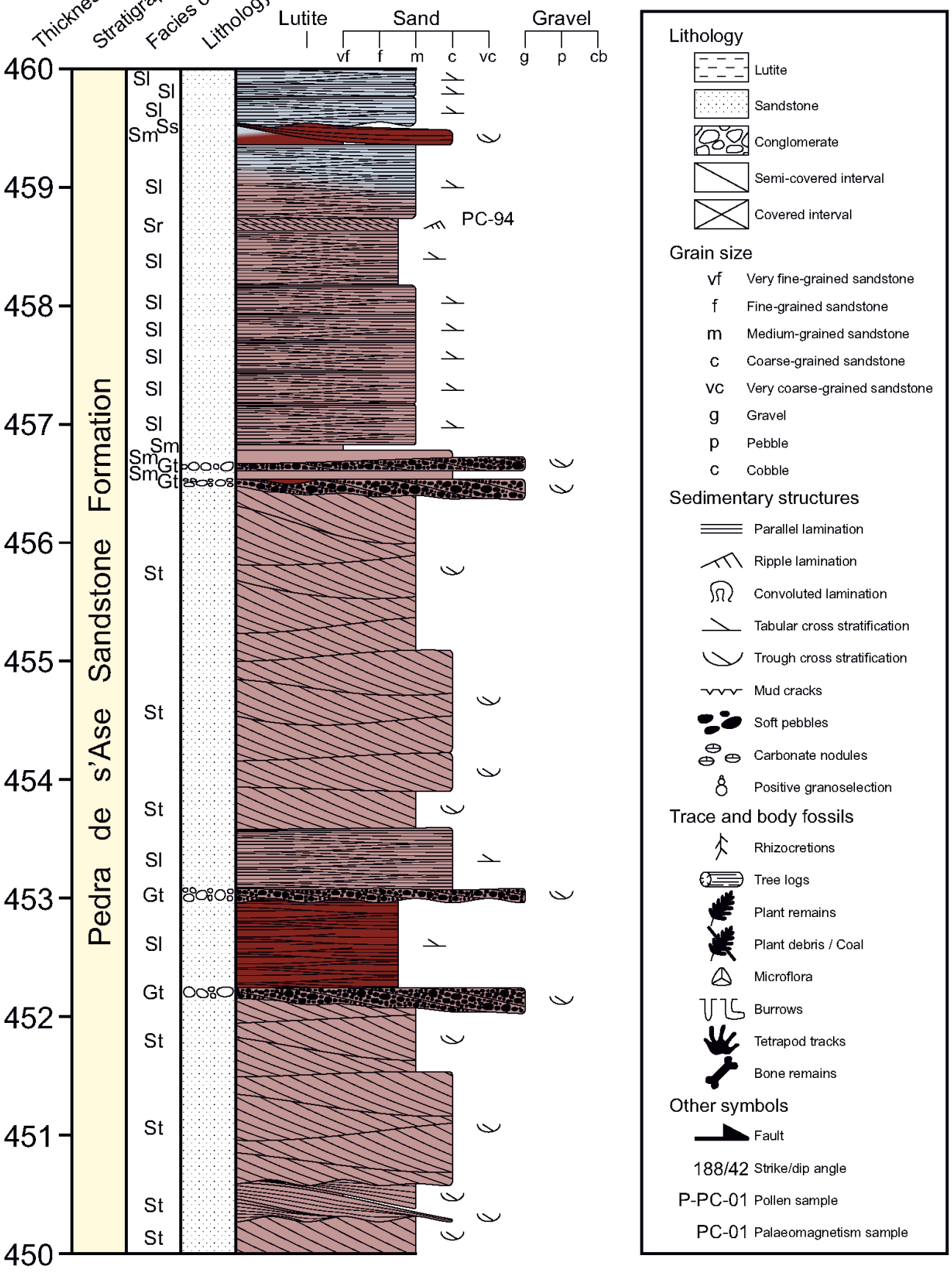

Log name: Port des Canonge	Page 47/61
Location: Port des Canonge–Hort de sa Cova Section	

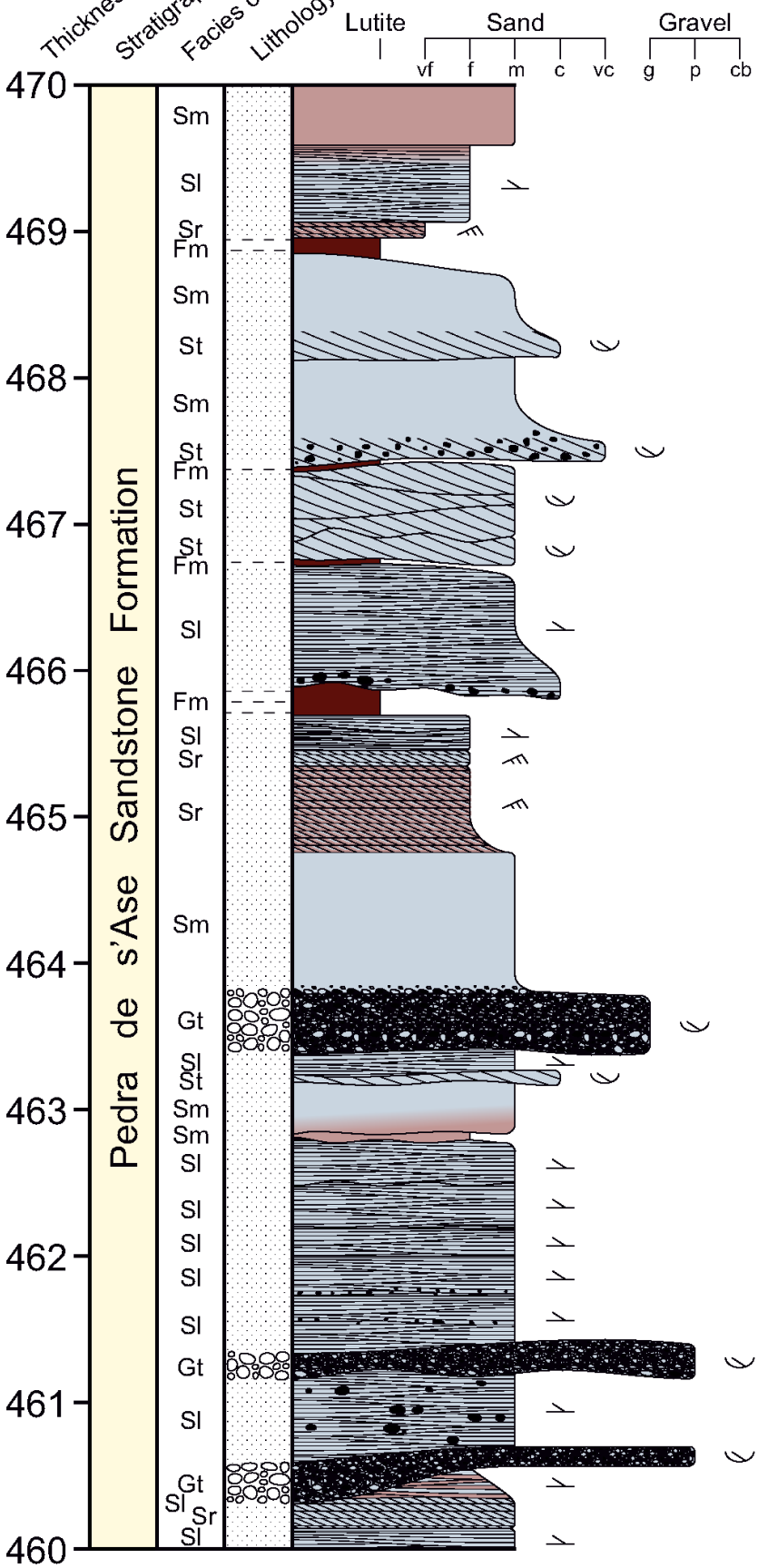

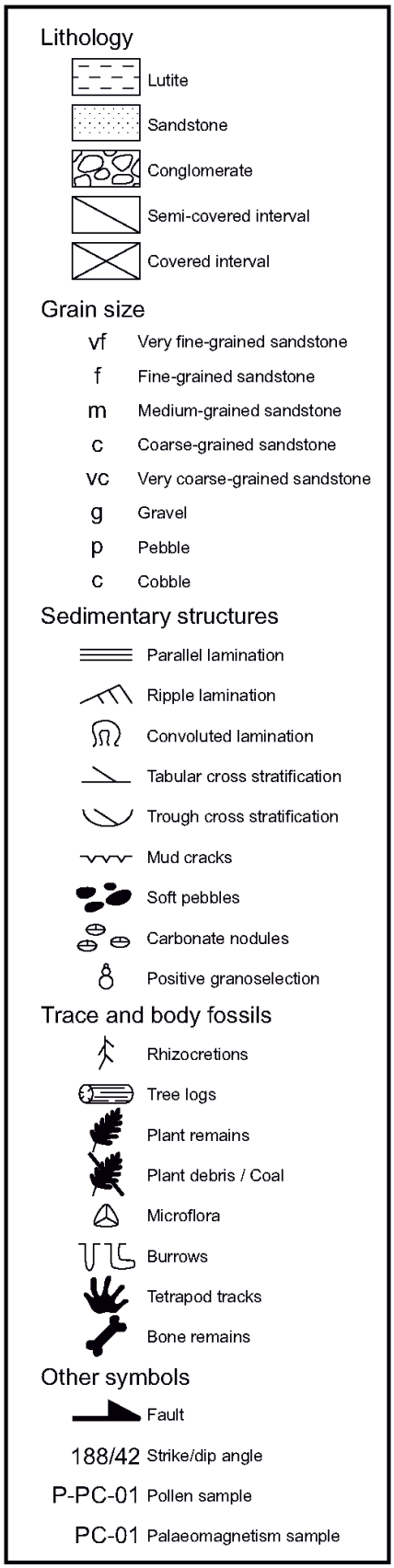

Log name: Port des Canonge	Page 48/61
Location: Port des Canonge–Hort de sa Cova Section	

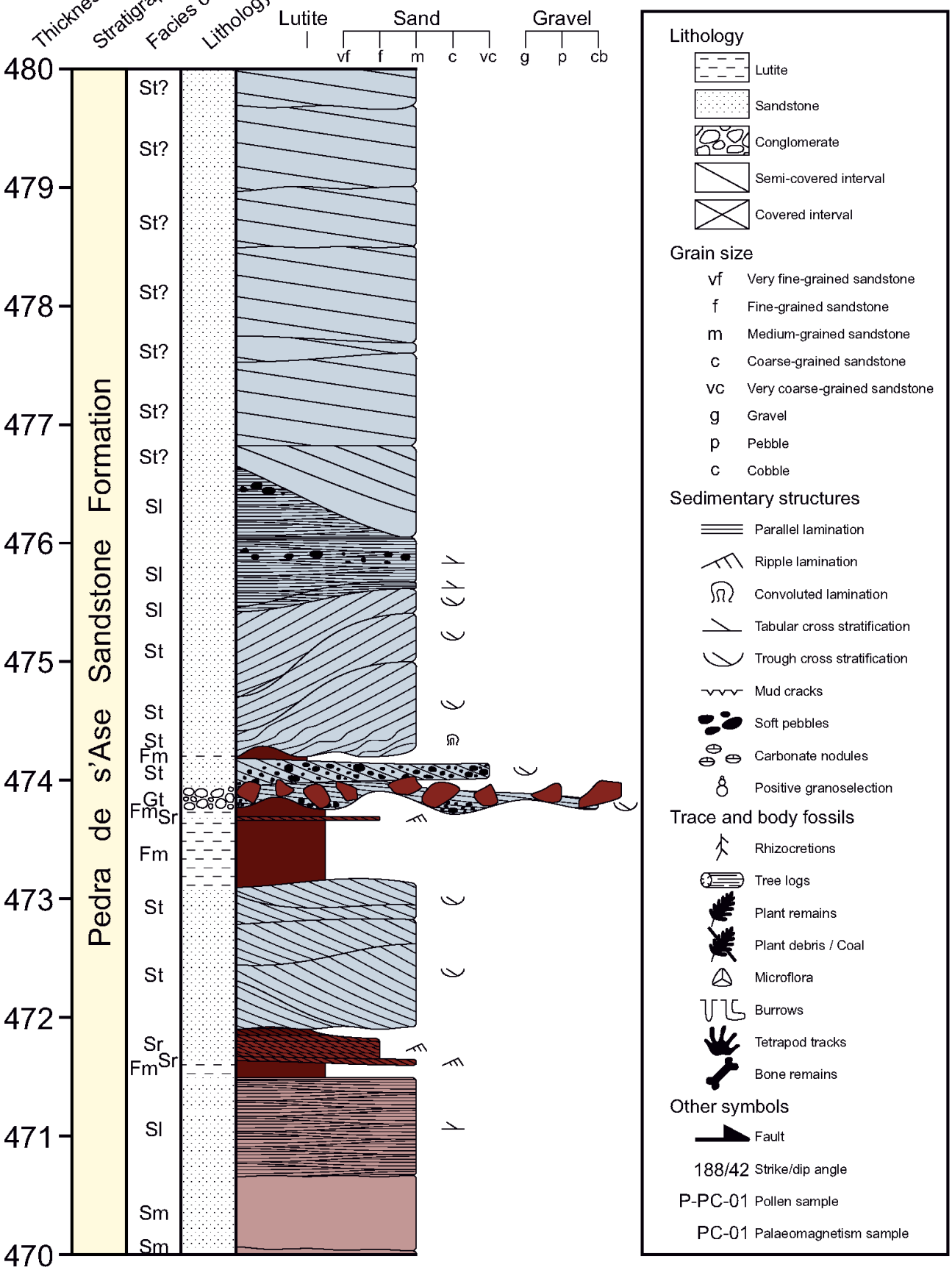

Log name: Port des Canonge	Page 49/61
Location: Port des Canonge–Hort de sa Cova Section	

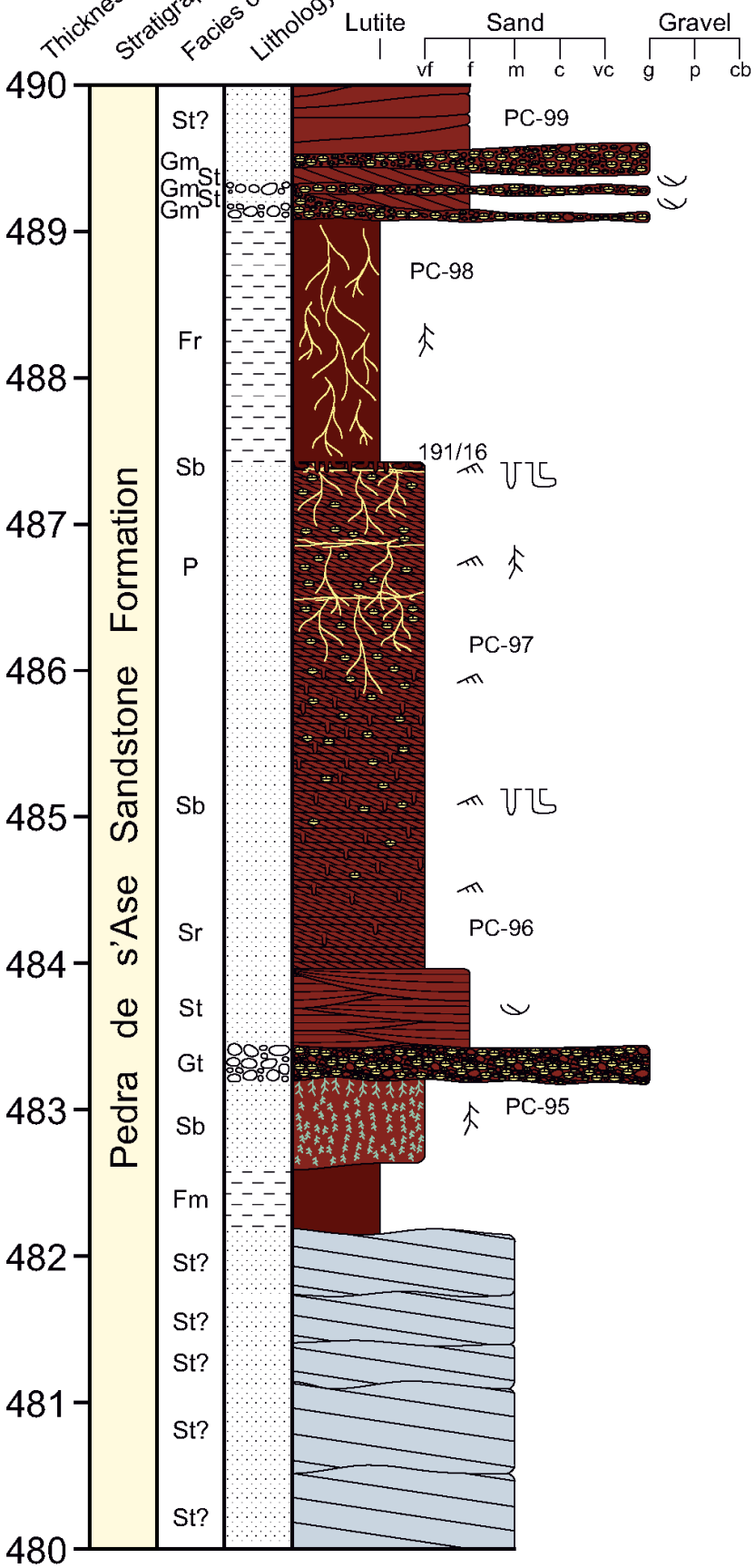

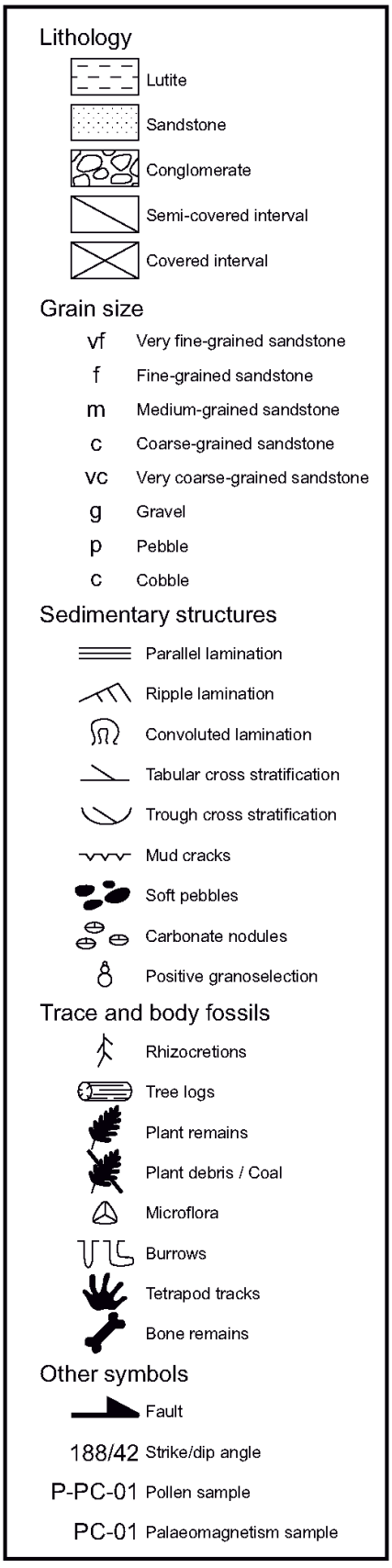

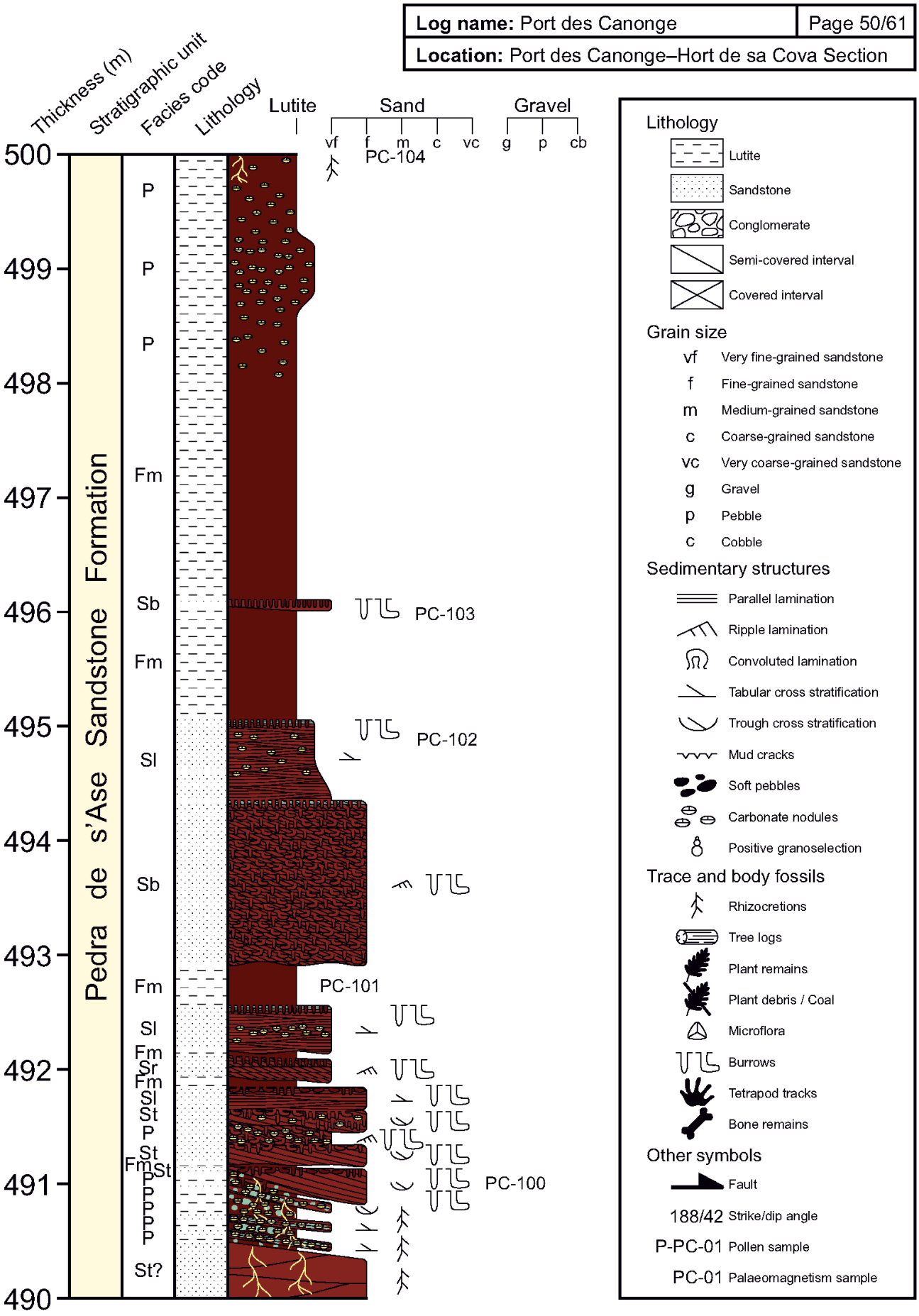
Log name: Port des Canonge
Page 50/61
Location: Port des Canonge–Hort de sa Cova Section
Thickness (m)
Stratigraphic unit
Facies code
Lithology
Lutite
Sand
Gravel
vf f m c vc
g p cb
PC-104
PC-103
PC-102
PC-101
PC-100
Pedra de s'Ase Sandstone Formation
500
499
498
497
496
495
494
493
492
491
490
P
Fm
Sb
Sl
Sr
St
Lithology
Lutite
Sandstone
Conglomerate
Semi-covered interval
Covered interval
Grain size
vf Very fine-grained sandstone
f Fine-grained sandstone
m Medium-grained sandstone
c Coarse-grained sandstone
vc Very coarse-grained sandstone
g Gravel
p Pebble
c Cobble
Sedimentary structures
Parallel lamination
Ripple lamination
Convoluted lamination
Tabular cross stratification
Trough cross stratification
Mud cracks
Soft pebbles
Carbonate nodules
Positive granoselection
Trace and body fossils
Rhizocretions
Tree logs
Plant remains
Plant debris / Coal
Microflora
Burrows
Tetrapod tracks
Bone remains
Other symbols
Fault
188/42 Strike/dip angle
P-PC-01 Pollen sample
PC-01 Palaeomagnetism sample

Log name: Port des Canonge	Page 51/61
Location: Port des Canonge–Hort de sa Cova Section	

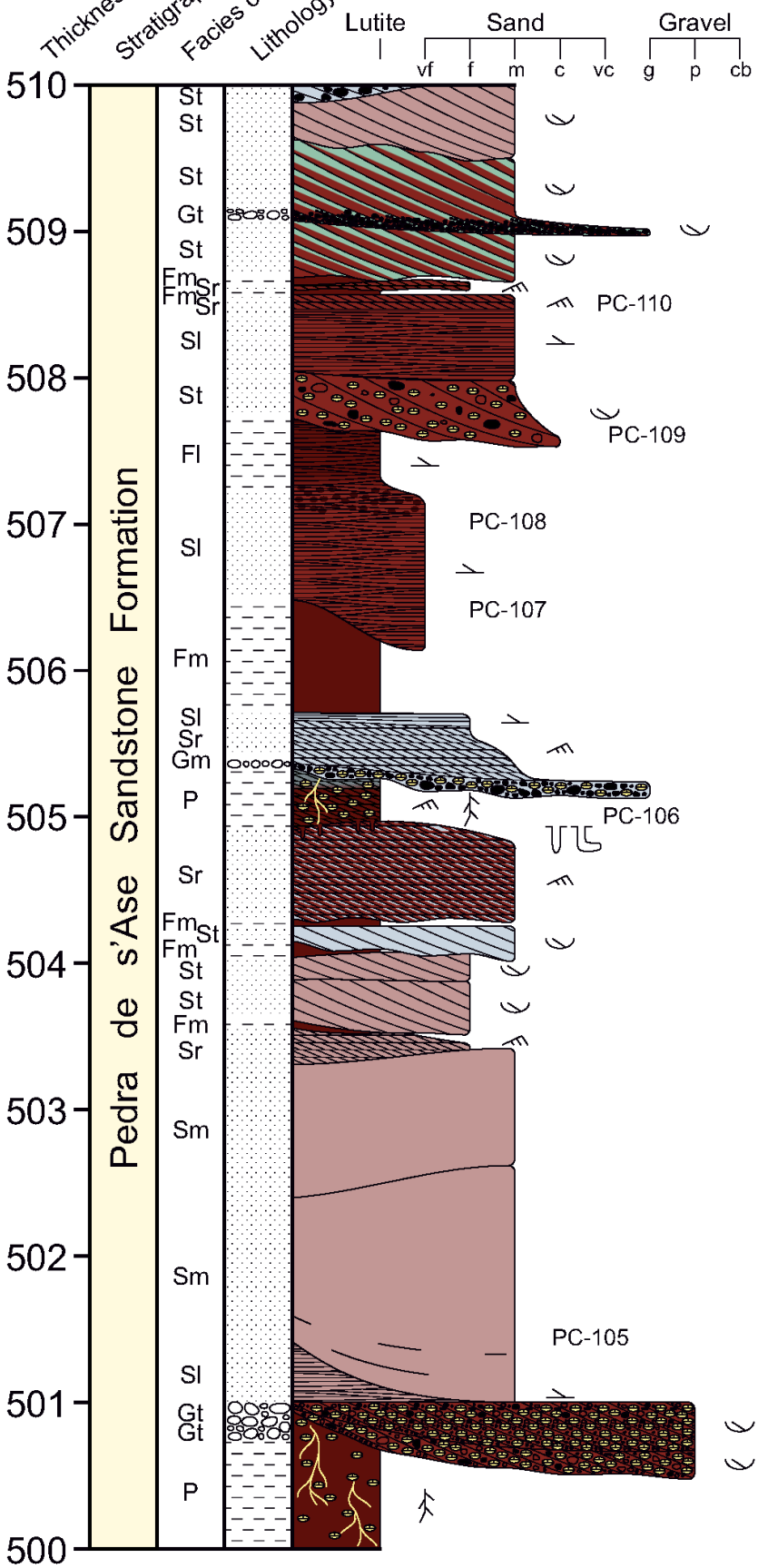

Lithology
- Lutite
- Sandstone
- Conglomerate
- Semi-covered interval
- Covered interval

Grain size
- vf Very fine-grained sandstone
- f Fine-grained sandstone
- m Medium-grained sandstone
- c Coarse-grained sandstone
- vc Very coarse-grained sandstone
- g Gravel
- p Pebble
- c Cobble

Sedimentary structures
- Parallel lamination
- Ripple lamination
- Convoluted lamination
- Tabular cross stratification
- Trough cross stratification
- Mud cracks
- Soft pebbles
- Carbonate nodules
- Positive granoselection

Trace and body fossils
- Rhizocretions
- Tree logs
- Plant remains
- Plant debris / Coal
- Microflora
- Burrows
- Tetrapod tracks
- Bone remains

Other symbols
- Fault
- 188/42 Strike/dip angle
- P-PC-01 Pollen sample
- PC-01 Palaeomagnetism sample

Log name: Port des Canonge | Page 52/61

Location: Port des Canonge–Hort de sa Cova Section

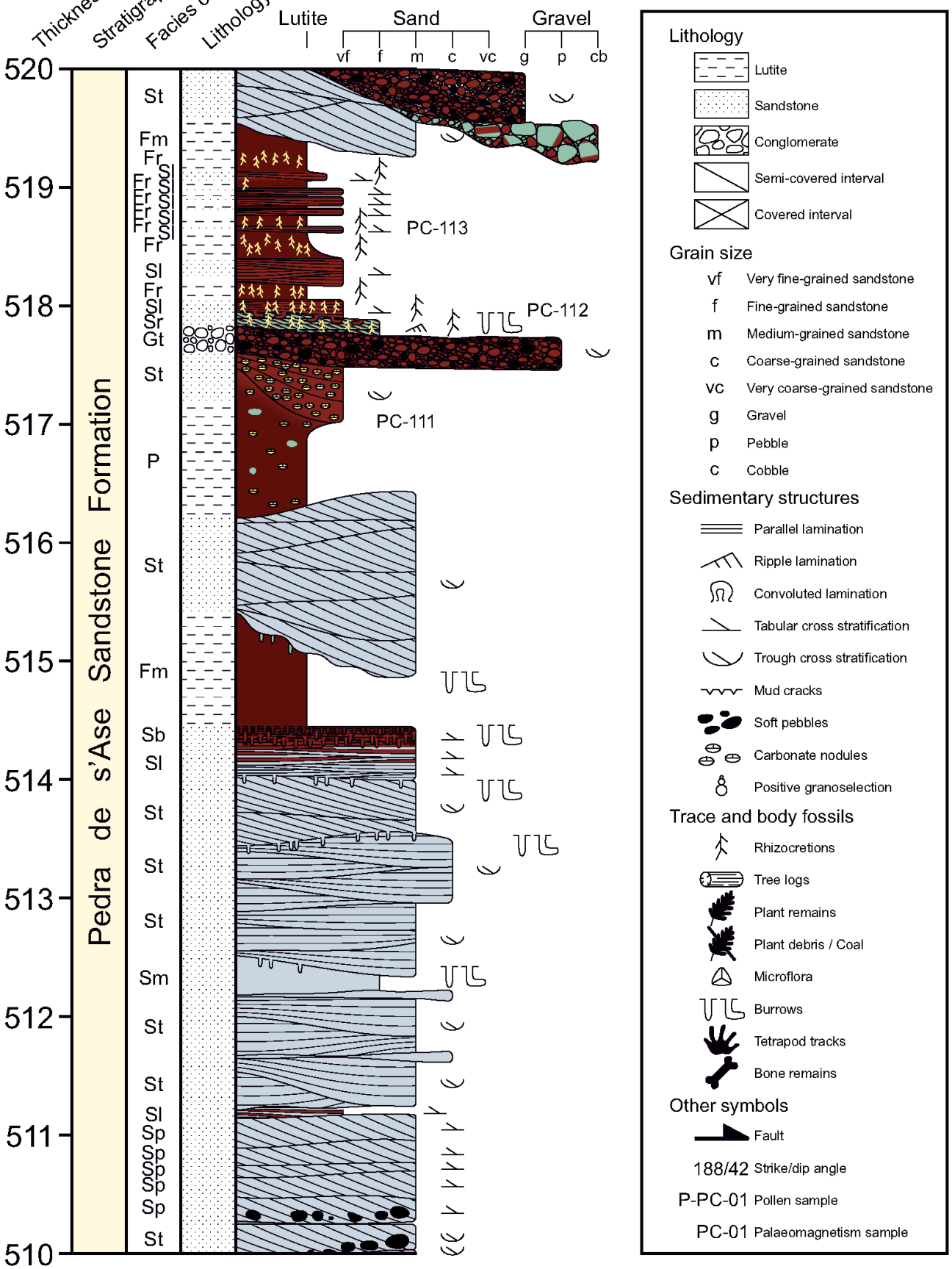

Lithology
- Lutite
- Sandstone
- Conglomerate
- Semi-covered interval
- Covered interval

Grain size
- vf Very fine-grained sandstone
- f Fine-grained sandstone
- m Medium-grained sandstone
- c Coarse-grained sandstone
- vc Very coarse-grained sandstone
- g Gravel
- p Pebble
- c Cobble

Sedimentary structures
- Parallel lamination
- Ripple lamination
- Convoluted lamination
- Tabular cross stratification
- Trough cross stratification
- Mud cracks
- Soft pebbles
- Carbonate nodules
- Positive granoselection

Trace and body fossils
- Rhizocretions
- Tree logs
- Plant remains
- Plant debris / Coal
- Microflora
- Burrows
- Tetrapod tracks
- Bone remains

Other symbols
- Fault
- 188/42 Strike/dip angle
- P-PC-01 Pollen sample
- PC-01 Palaeomagnetism sample

Log name: Port des Canonge	Page 53/61
Location: Port des Canonge–Hort de sa Cova Section	

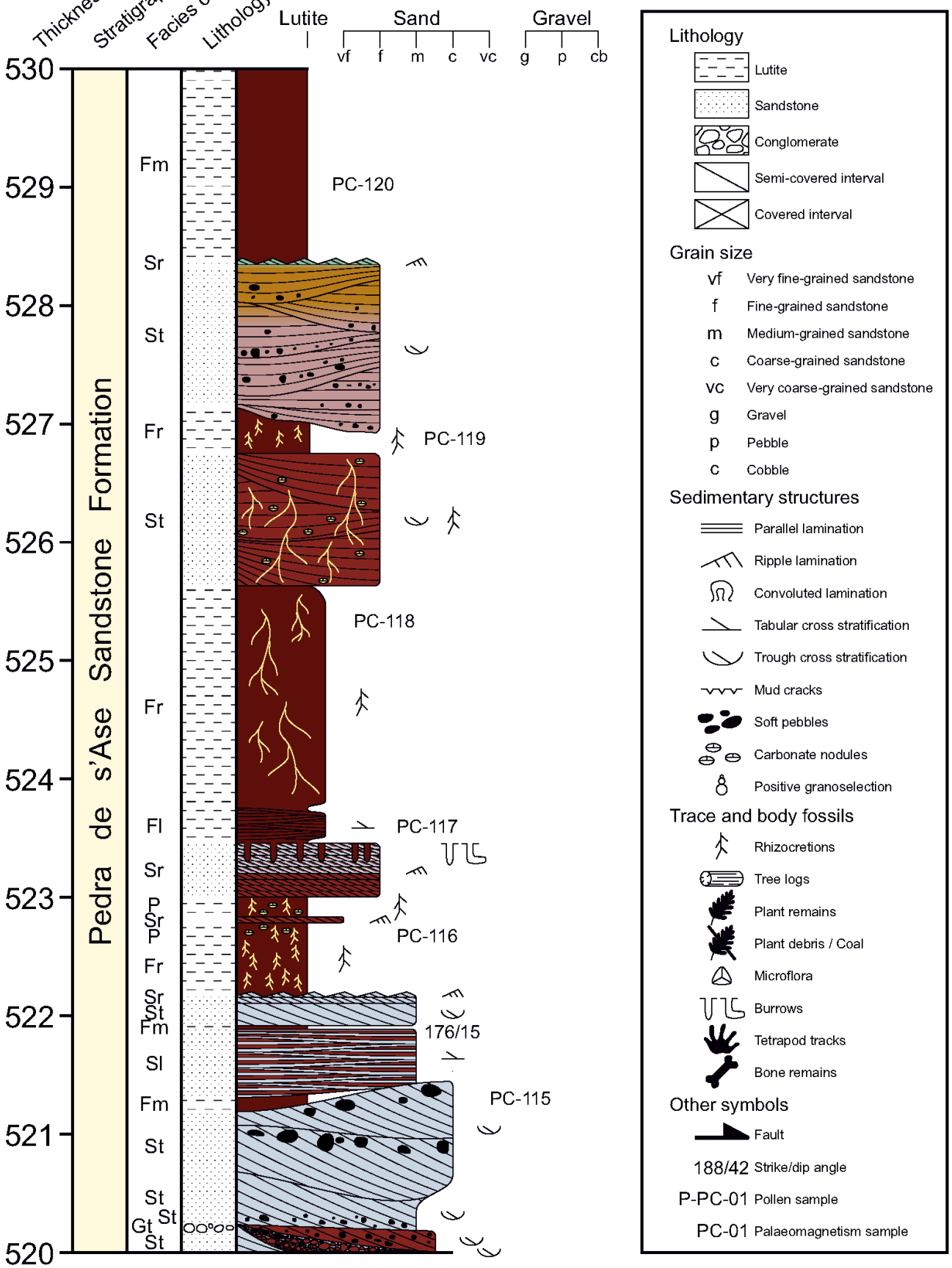

Log name: Port des Canonge	Page 54/61
Location: Port des Canonge–Hort de sa Cova Section	

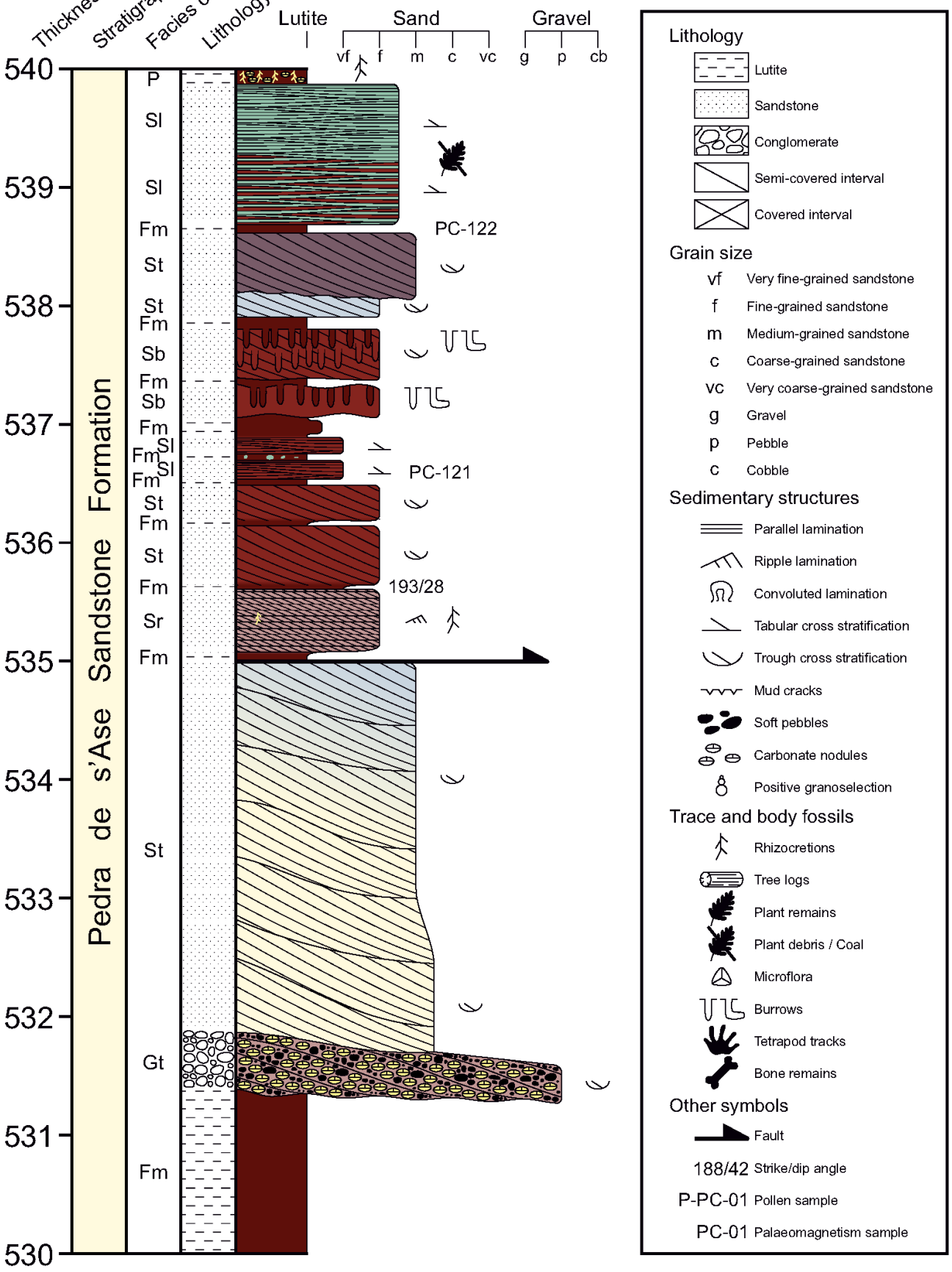

Log name: Port des Canonge	Page 55/61
Location: Port des Canonge–Hort de sa Cova Section	

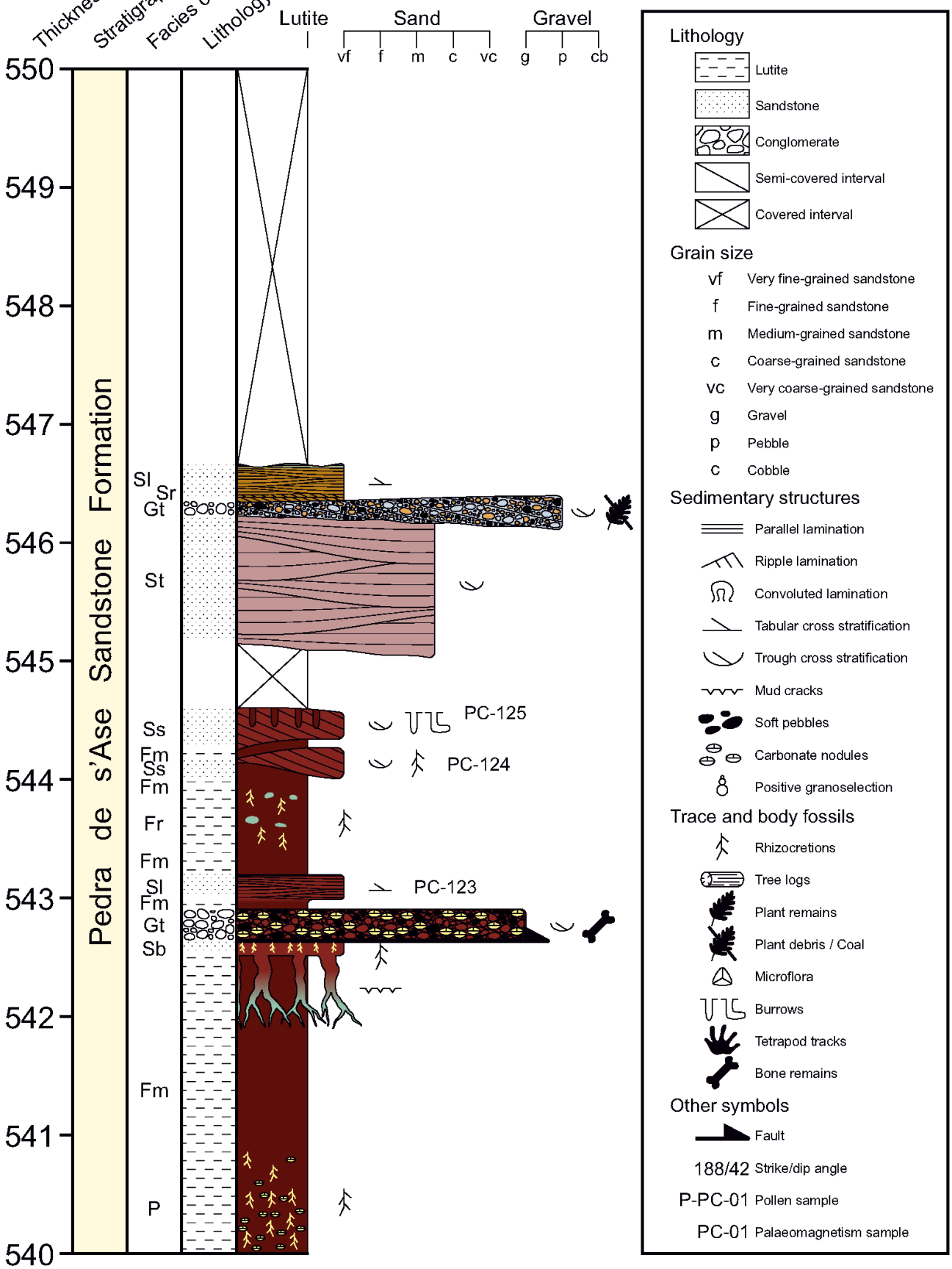

Log name: Port des Canonge	Page 56/61
Location: Port des Canonge–Hort de sa Cova Section	

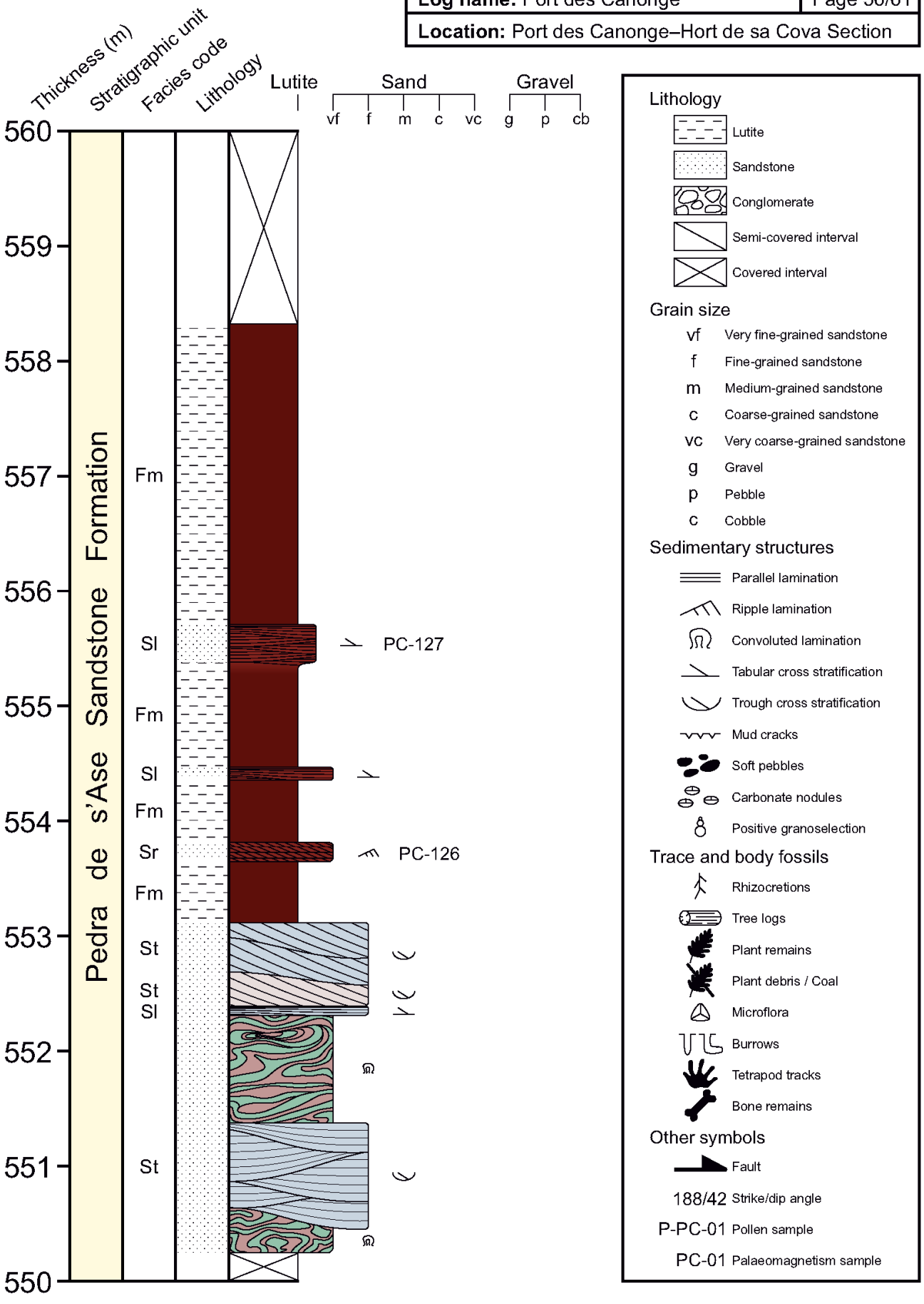

Log name: Port des Canonge	Page 57/61
Location: Port des Canonge–Hort de sa Cova Section	

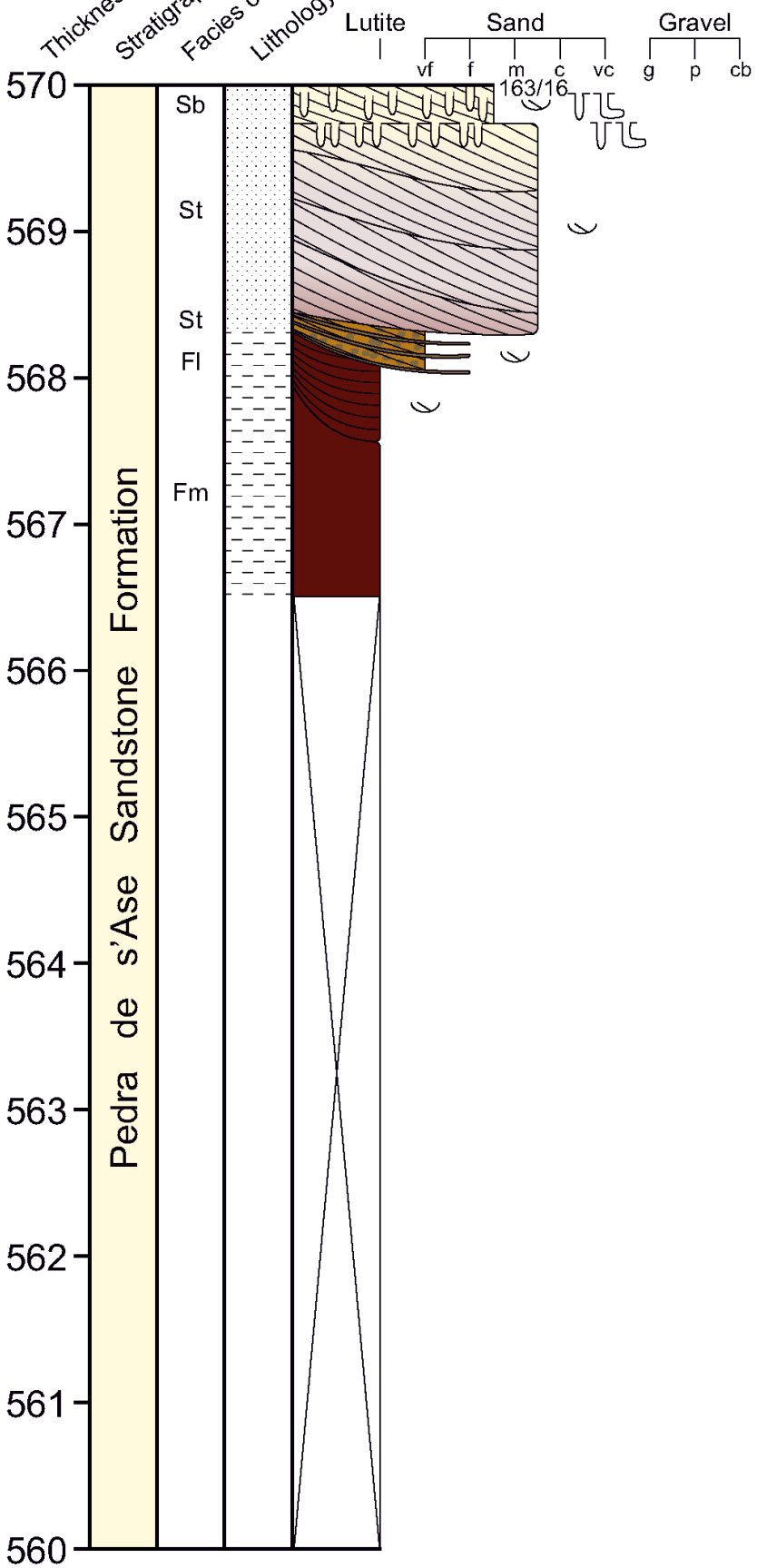

Lithology
- Lutite
- Sandstone
- Conglomerate
- Semi-covered interval
- Covered interval

Grain size
- vf Very fine-grained sandstone
- f Fine-grained sandstone
- m Medium-grained sandstone
- c Coarse-grained sandstone
- vc Very coarse-grained sandstone
- g Gravel
- p Pebble
- c Cobble

Sedimentary structures
- Parallel lamination
- Ripple lamination
- Convoluted lamination
- Tabular cross stratification
- Trough cross stratification
- Mud cracks
- Soft pebbles
- Carbonate nodules
- Positive granoselection

Trace and body fossils
- Rhizocretions
- Tree logs
- Plant remains
- Plant debris / Coal
- Microflora
- Burrows
- Tetrapod tracks
- Bone remains

Other symbols
- Fault
- 188/42 Strike/dip angle
- P-PC-01 Pollen sample
- PC-01 Palaeomagnetism sample

Log name: Port des Canonge | Page 58/61

Location: Port des Canonge–Hort de sa Cova Section

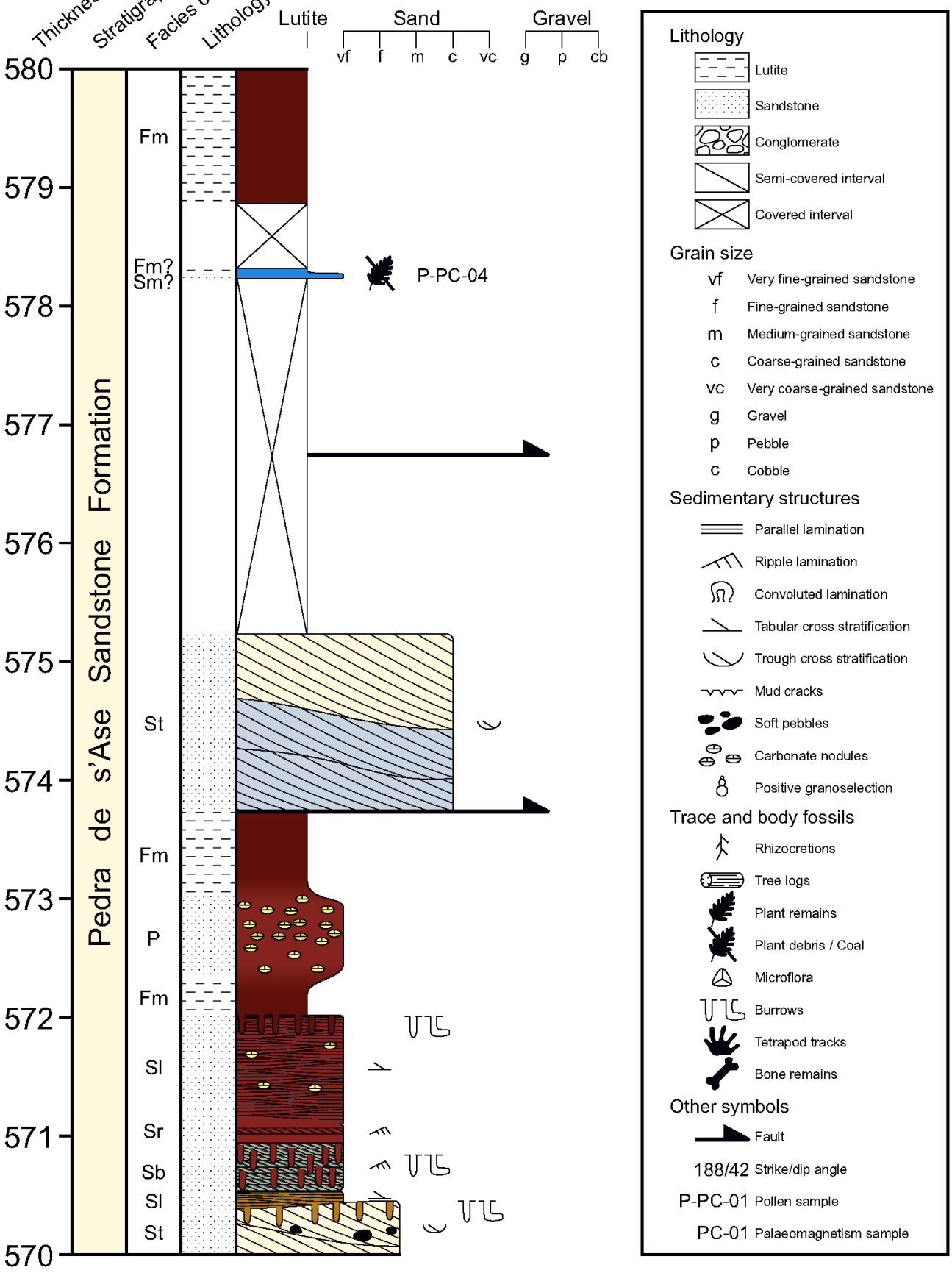

Lithology
- Lutite
- Sandstone
- Conglomerate
- Semi-covered interval
- Covered interval

Grain size
- vf Very fine-grained sandstone
- f Fine-grained sandstone
- m Medium-grained sandstone
- c Coarse-grained sandstone
- vc Very coarse-grained sandstone
- g Gravel
- p Pebble
- c Cobble

Sedimentary structures
- Parallel lamination
- Ripple lamination
- Convoluted lamination
- Tabular cross stratification
- Trough cross stratification
- Mud cracks
- Soft pebbles
- Carbonate nodules
- Positive granoselection

Trace and body fossils
- Rhizocretions
- Tree logs
- Plant remains
- Plant debris / Coal
- Microflora
- Burrows
- Tetrapod tracks
- Bone remains

Other symbols
- Fault
- 188/42 Strike/dip angle
- P-PC-01 Pollen sample
- PC-01 Palaeomagnetism sample

Log name: Port des Canonge	Page 59/61
Location: Port des Canonge–Hort de sa Cova Section	

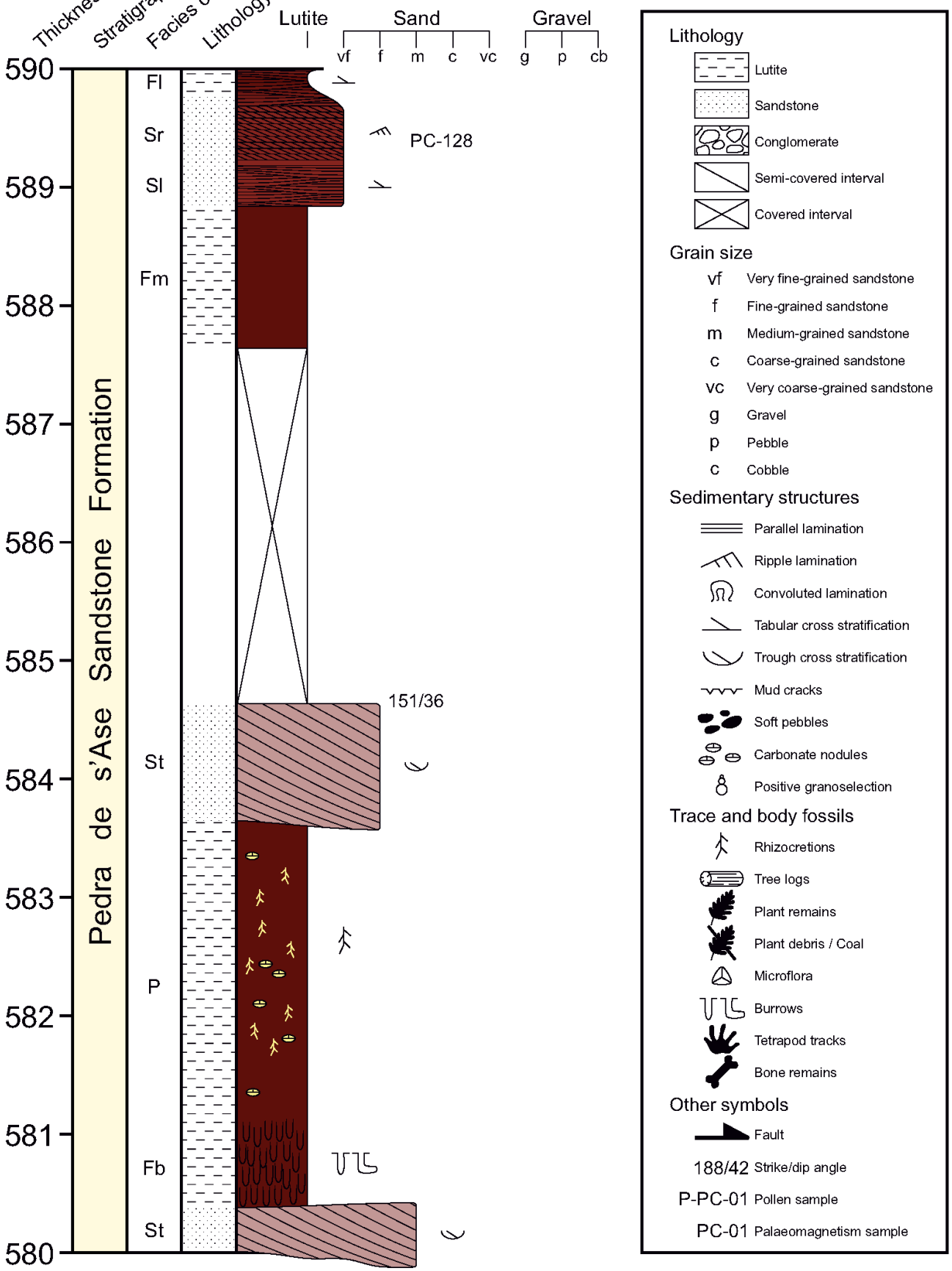

Log name: Port des Canonge | Page 60/61

Location: Port des Canonge–Hort de sa Cova Section

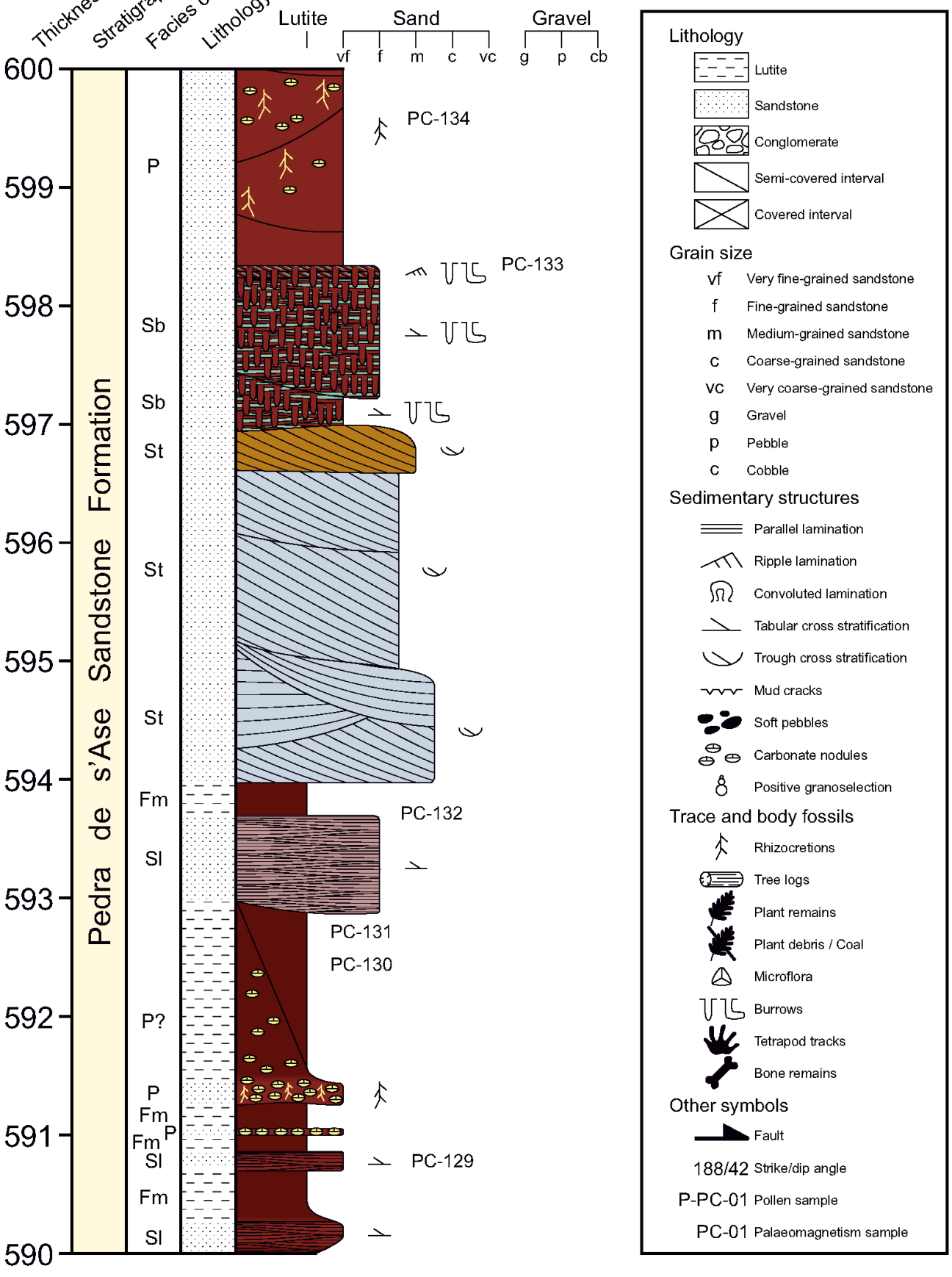

Log name: Port des Canonge	Page 61/61
Location: Port des Canonge–Hort de sa Cova Section	

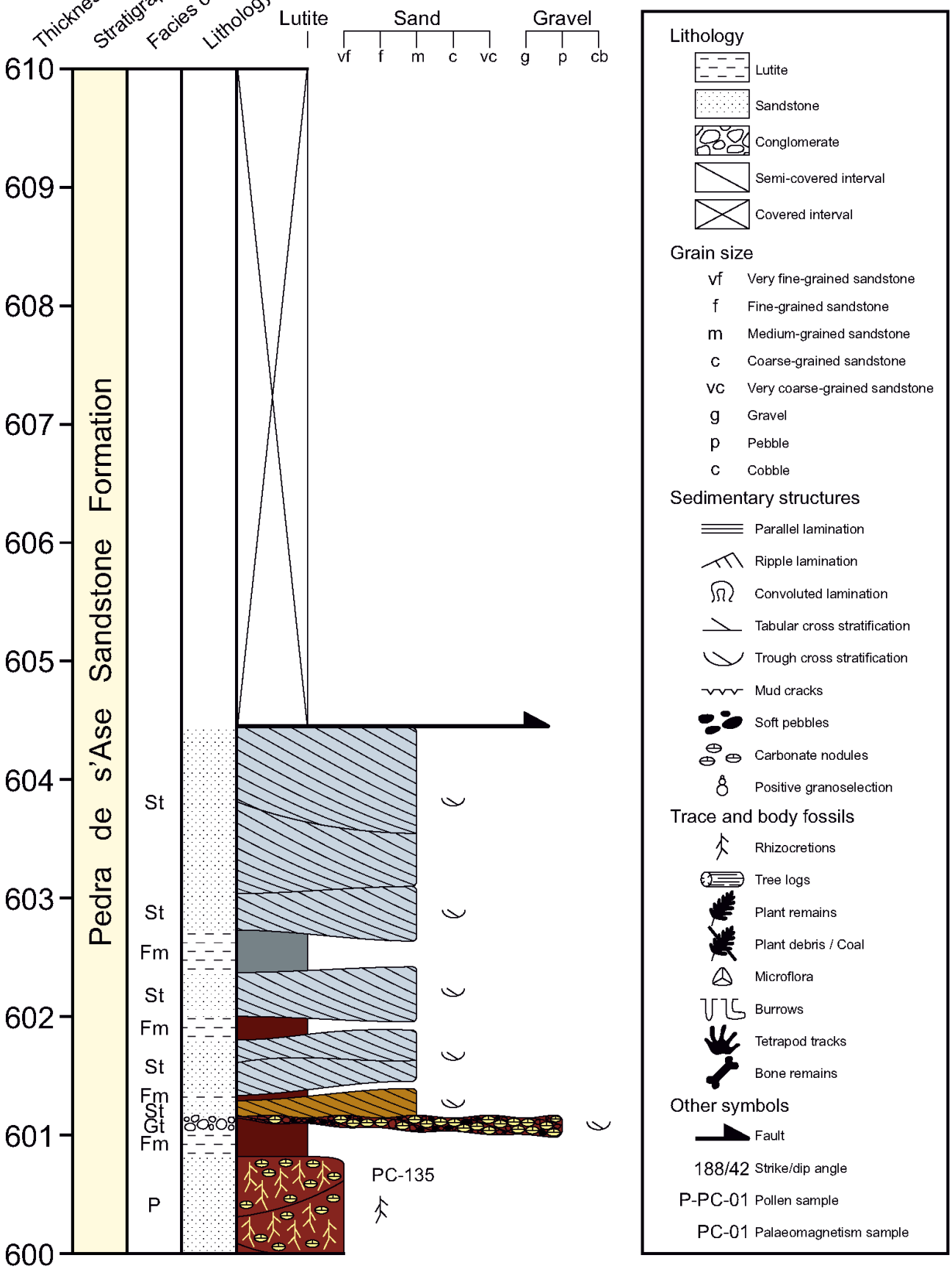

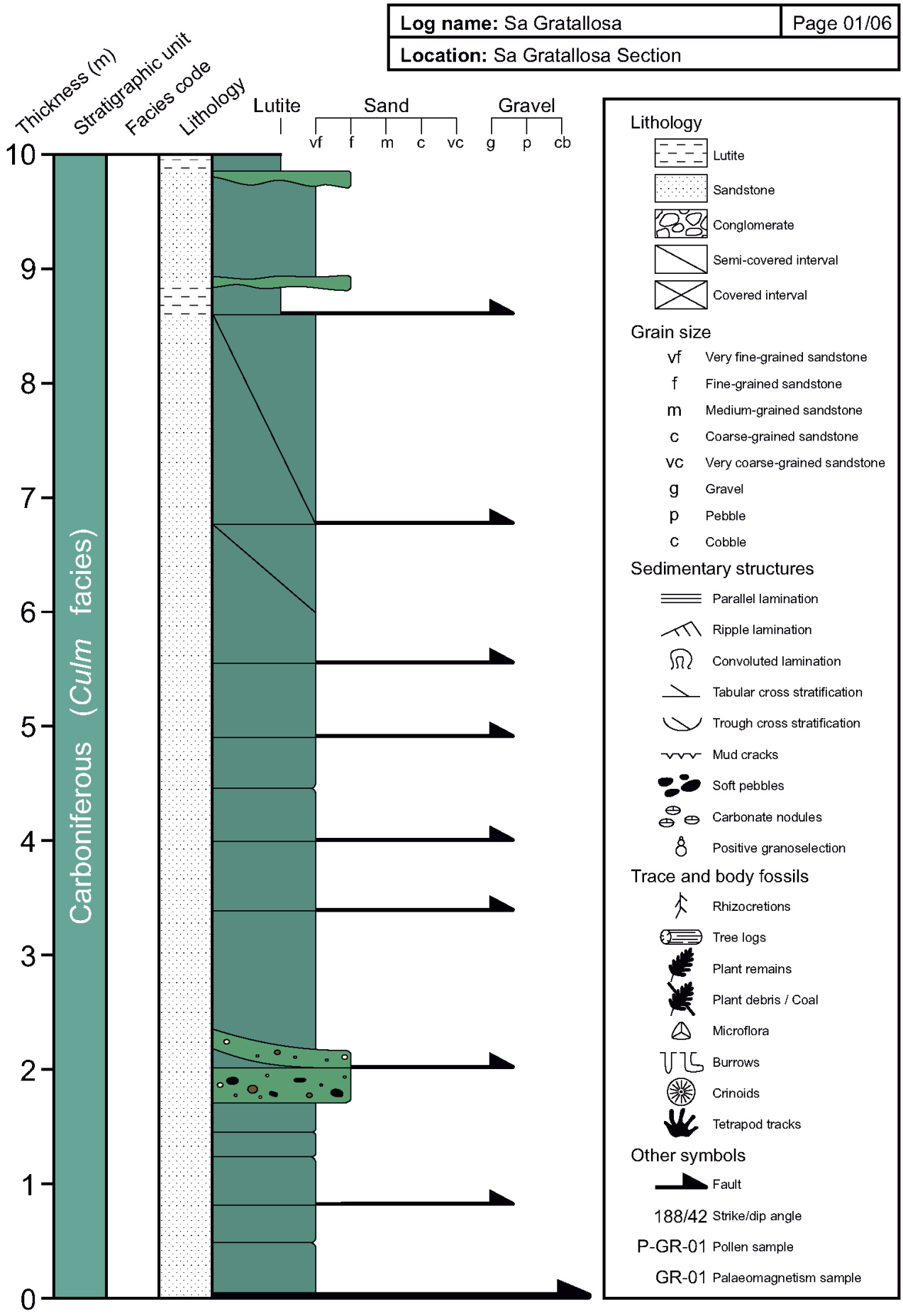
Log name: Sa Gratallosa
Page 01/06
Location: Sa Gratallosa Section
Thickness (m)
Stratigraphic unit
Facies code
Lithology
Lutite
Sand
Gravel
vf f m c vc g p cb
10
9
8
7
6
5
4
3
2
1
0
Carboniferous (Culm facies)
Lithology
Lutite
Sandstone
Conglomerate
Semi-covered interval
Covered interval
Grain size
vf Very fine-grained sandstone
f Fine-grained sandstone
m Medium-grained sandstone
c Coarse-grained sandstone
vc Very coarse-grained sandstone
g Gravel
p Pebble
c Cobble
Sedimentary structures
Parallel lamination
Ripple lamination
Convoluted lamination
Tabular cross stratification
Trough cross stratification
Mud cracks
Soft pebbles
Carbonate nodules
Positive granoselection
Trace and body fossils
Rhizocretions
Tree logs
Plant remains
Plant debris / Coal
Microflora
Burrows
Crinoids
Tetrapod tracks
Other symbols
Fault
188/42 Strike/dip angle
P-GR-01 Pollen sample
GR-01 Palaeomagnetism sample

Log name: Sa Gratallosa	Page 02/06
Location: Sa Gratallosa Section	

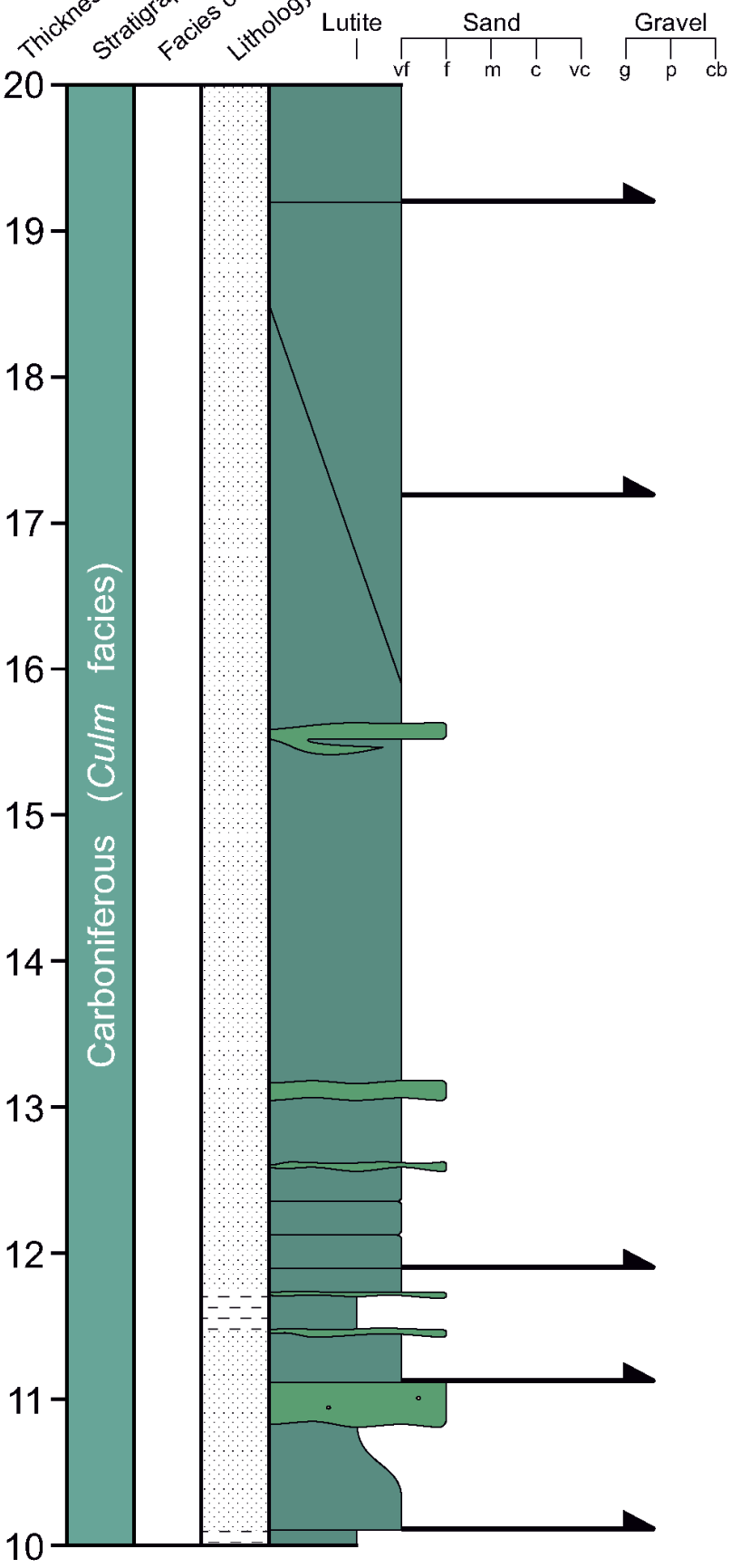

Lithology
- Lutite
- Sandstone
- Conglomerate
- Semi-covered interval
- Covered interval

Grain size
- vf Very fine-grained sandstone
- f Fine-grained sandstone
- m Medium-grained sandstone
- c Coarse-grained sandstone
- vc Very coarse-grained sandstone
- g Gravel
- p Pebble
- c Cobble

Sedimentary structures
- Parallel lamination
- Ripple lamination
- Convoluted lamination
- Tabular cross stratification
- Trough cross stratification
- Mud cracks
- Soft pebbles
- Carbonate nodules
- Positive granoselection

Trace and body fossils
- Rhizocretions
- Tree logs
- Plant remains
- Plant debris / Coal
- Microflora
- Burrows
- Crinoids
- Tetrapod tracks

Other symbols
- Fault
- 188/42 Strike/dip angle
- P-GR-01 Pollen sample
- GR-01 Palaeomagnetism sample

Log name: Sa Gratallosa	Page 03/06
Location: Sa Gratallosa Section	

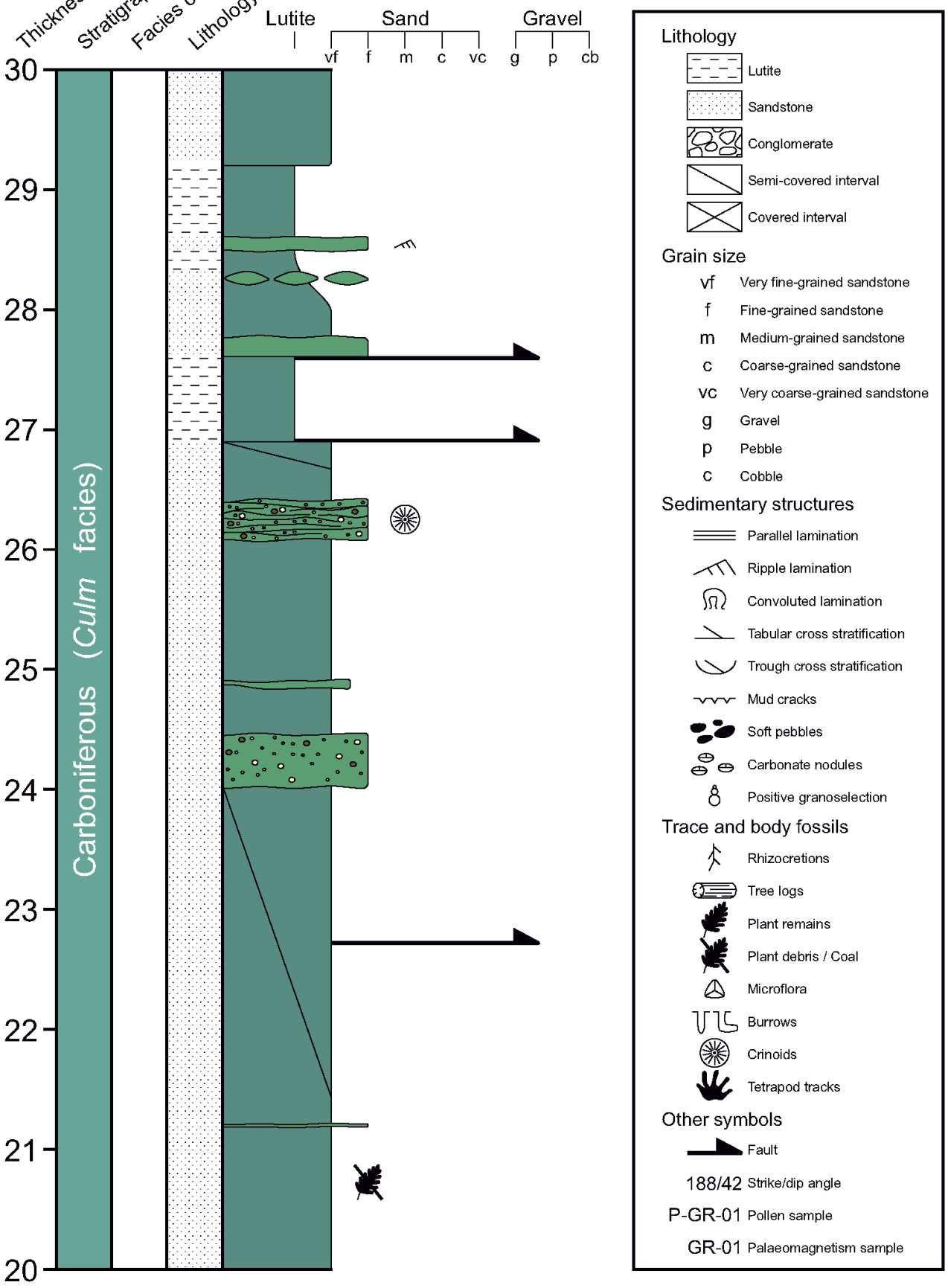

Log name: Sa Gratallosa	Page 04/06
Location: Sa Gratallosa Section	

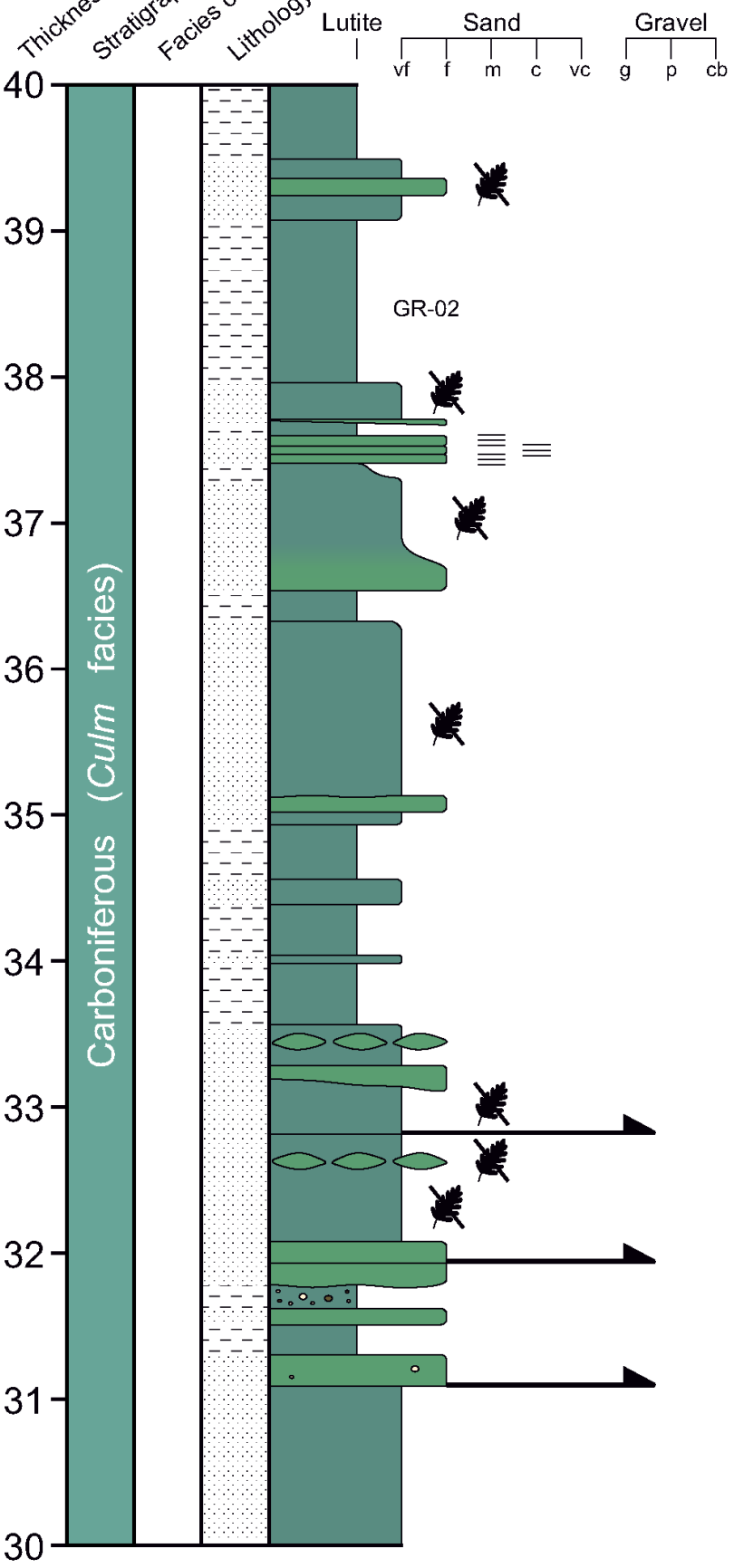

Lithology
- Lutite
- Sandstone
- Conglomerate
- Semi-covered interval
- Covered interval

Grain size
- vf Very fine-grained sandstone
- f Fine-grained sandstone
- m Medium-grained sandstone
- c Coarse-grained sandstone
- vc Very coarse-grained sandstone
- g Gravel
- p Pebble
- c Cobble

Sedimentary structures
- Parallel lamination
- Ripple lamination
- Convoluted lamination
- Tabular cross stratification
- Trough cross stratification
- Mud cracks
- Soft pebbles
- Carbonate nodules
- Positive granoselection

Trace and body fossils
- Rhizocretions
- Tree logs
- Plant remains
- Plant debris / Coal
- Microflora
- Burrows
- Crinoids
- Tetrapod tracks

Other symbols
- Fault
- 188/42 Strike/dip angle
- P-GR-01 Pollen sample
- GR-01 Palaeomagnetism sample

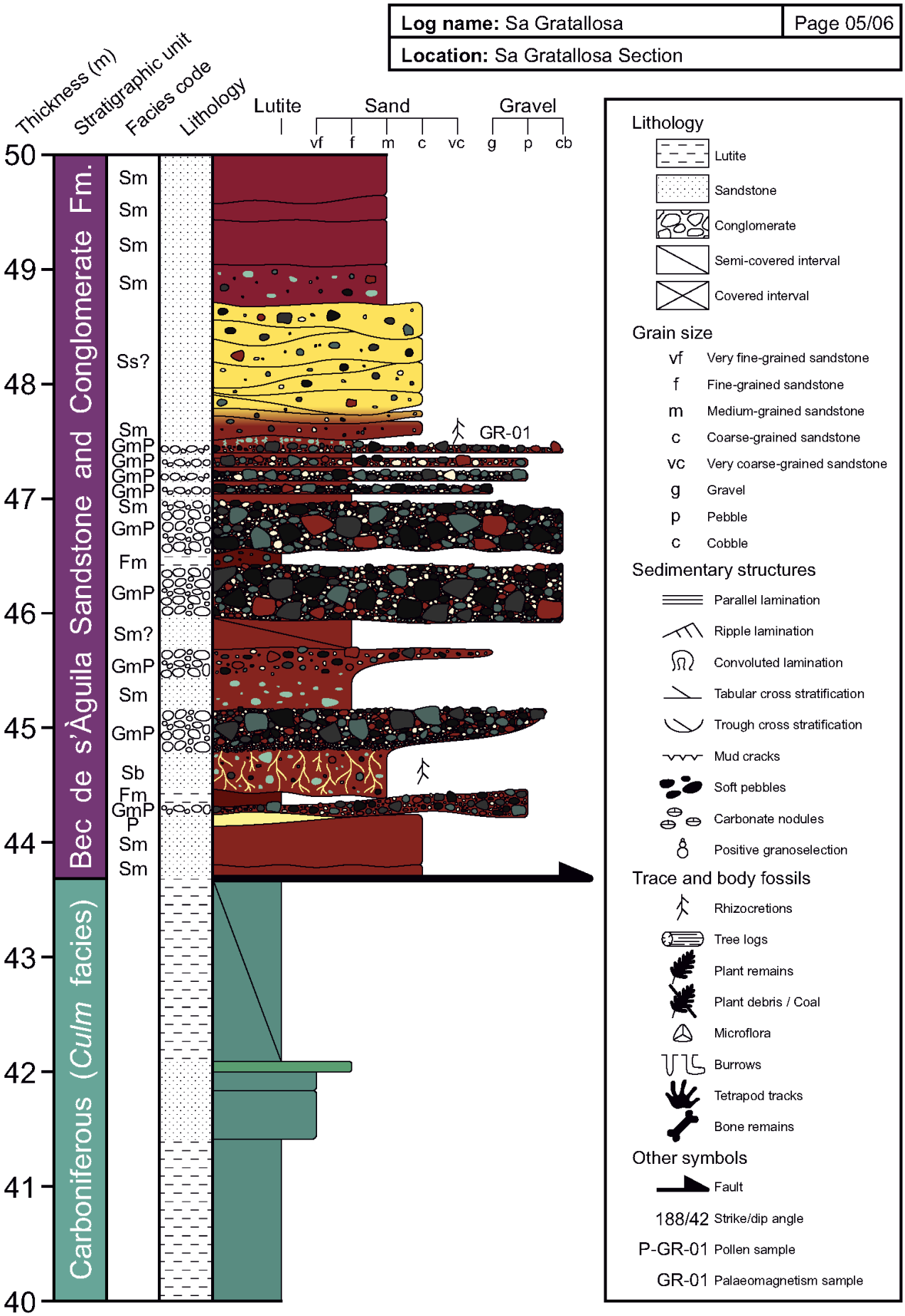
Log name: Sa Gratallosa
Page 05/06
Location: Sa Gratallosa Section
Thickness (m)
Stratigraphic unit
Facies code
Lithology
Lutite
Sand
Gravel
vf f m c vc g p cb
50
49
48
47
46
45
44
43
42
41
40
Bec de s'Àguila Sandstone and Conglomerate Fm.
Carboniferous (Culm facies)
Sm
Sm
Sm
Sm
Ss?
Sm
GmP
GmP
GmP
GmP
Sm
GmP
Fm
GmP
Sm?
GmP
Sm
GmP
Sb
Fm
GmP
P
Sm
Sm
GR-01
Lithology
Lutite
Sandstone
Conglomerate
Semi-covered interval
Covered interval
Grain size
vf Very fine-grained sandstone
f Fine-grained sandstone
m Medium-grained sandstone
c Coarse-grained sandstone
vc Very coarse-grained sandstone
g Gravel
p Pebble
c Cobble
Sedimentary structures
Parallel lamination
Ripple lamination
Convoluted lamination
Tabular cross stratification
Trough cross stratification
Mud cracks
Soft pebbles
Carbonate nodules
Positive granoselection
Trace and body fossils
Rhizocretions
Tree logs
Plant remains
Plant debris / Coal
Microflora
Burrows
Tetrapod tracks
Bone remains
Other symbols
Fault
188/42 Strike/dip angle
P-GR-01 Pollen sample
GR-01 Palaeomagnetism sample

Log name: Sa Gratallosa	Page 06/06
Location: Sa Gratallosa Section	

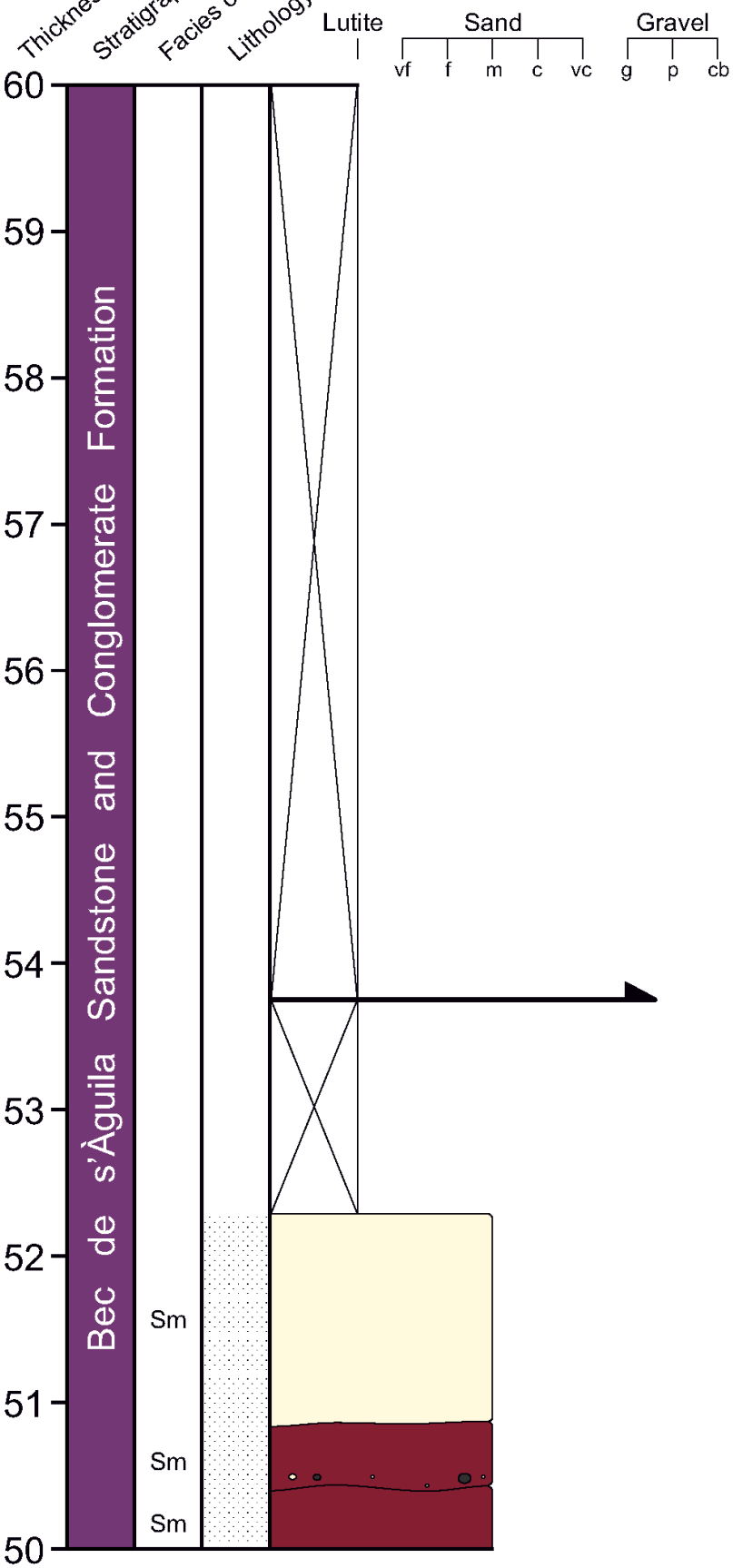

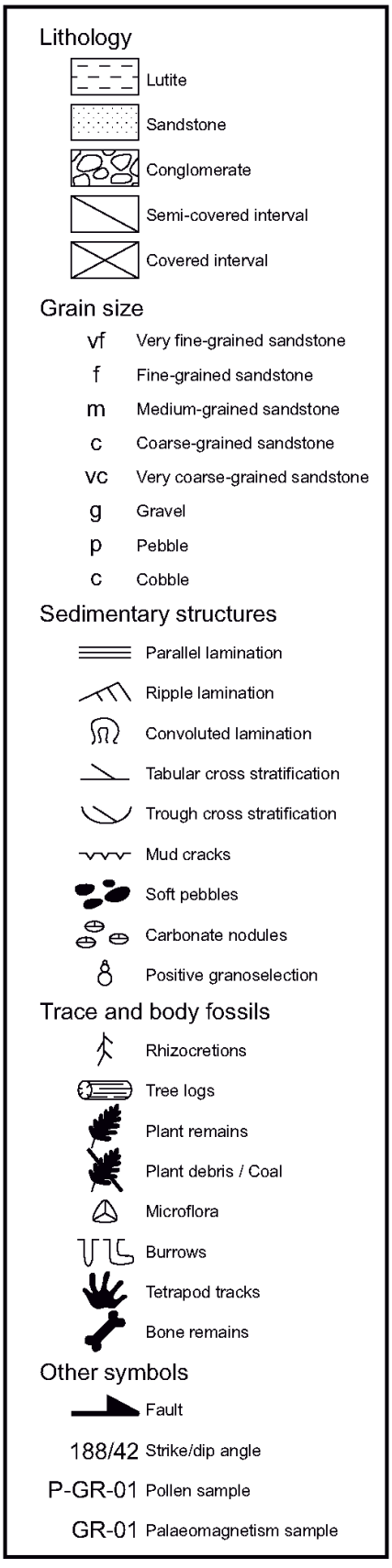

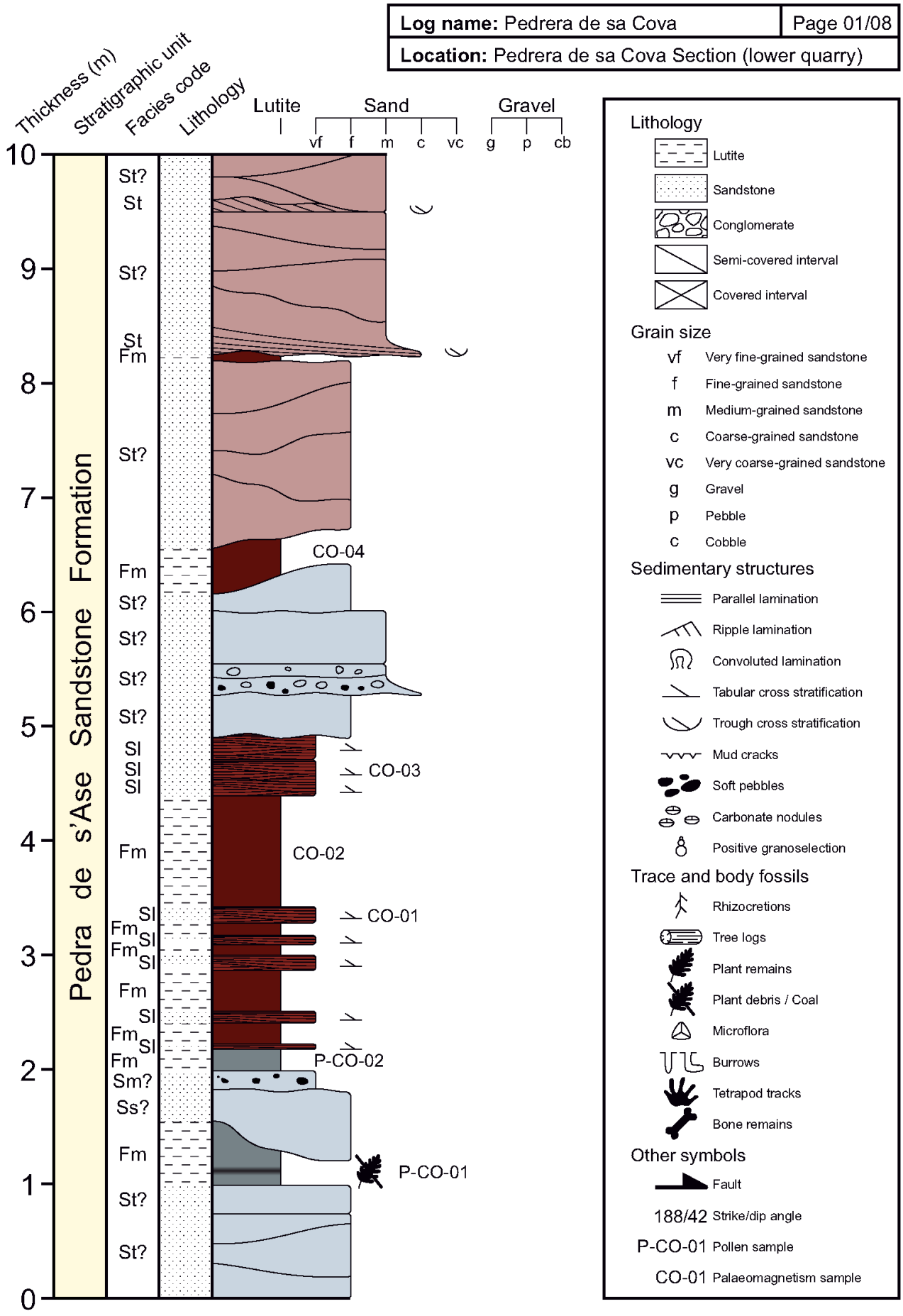
Log name: Pedrera de sa Cova
Page 01/08
Location: Pedrera de sa Cova Section (lower quarry)
Thickness (m)
Stratigraphic unit
Facies code
Lithology
Lutite
Sand
Gravel
vf f m c vc g p cb
Pedra de s'Ase Sandstone Formation
St? St St? St Fm St? Fm St? St? St? St? Sl Sl Sl Fm Sl Fm Sl Fm Sl Fm Fm Sl Fm Sl Fm Sm? Ss? Fm St? St?
CO-04
CO-03
CO-02
CO-01
P-CO-02
P-CO-01
Lithology
Lutite
Sandstone
Conglomerate
Semi-covered interval
Covered interval
Grain size
vf Very fine-grained sandstone
f Fine-grained sandstone
m Medium-grained sandstone
c Coarse-grained sandstone
vc Very coarse-grained sandstone
g Gravel
p Pebble
c Cobble
Sedimentary structures
Parallel lamination
Ripple lamination
Convoluted lamination
Tabular cross stratification
Trough cross stratification
Mud cracks
Soft pebbles
Carbonate nodules
Positive granoselection
Trace and body fossils
Rhizocretions
Tree logs
Plant remains
Plant debris / Coal
Microflora
Burrows
Tetrapod tracks
Bone remains
Other symbols
Fault
188/42 Strike/dip angle
P-CO-01 Pollen sample
CO-01 Palaeomagnetism sample

Log name: Pedrera de sa Cova	Page 02/08
Location: Pedrera de sa Cova Section (lower quarry)	

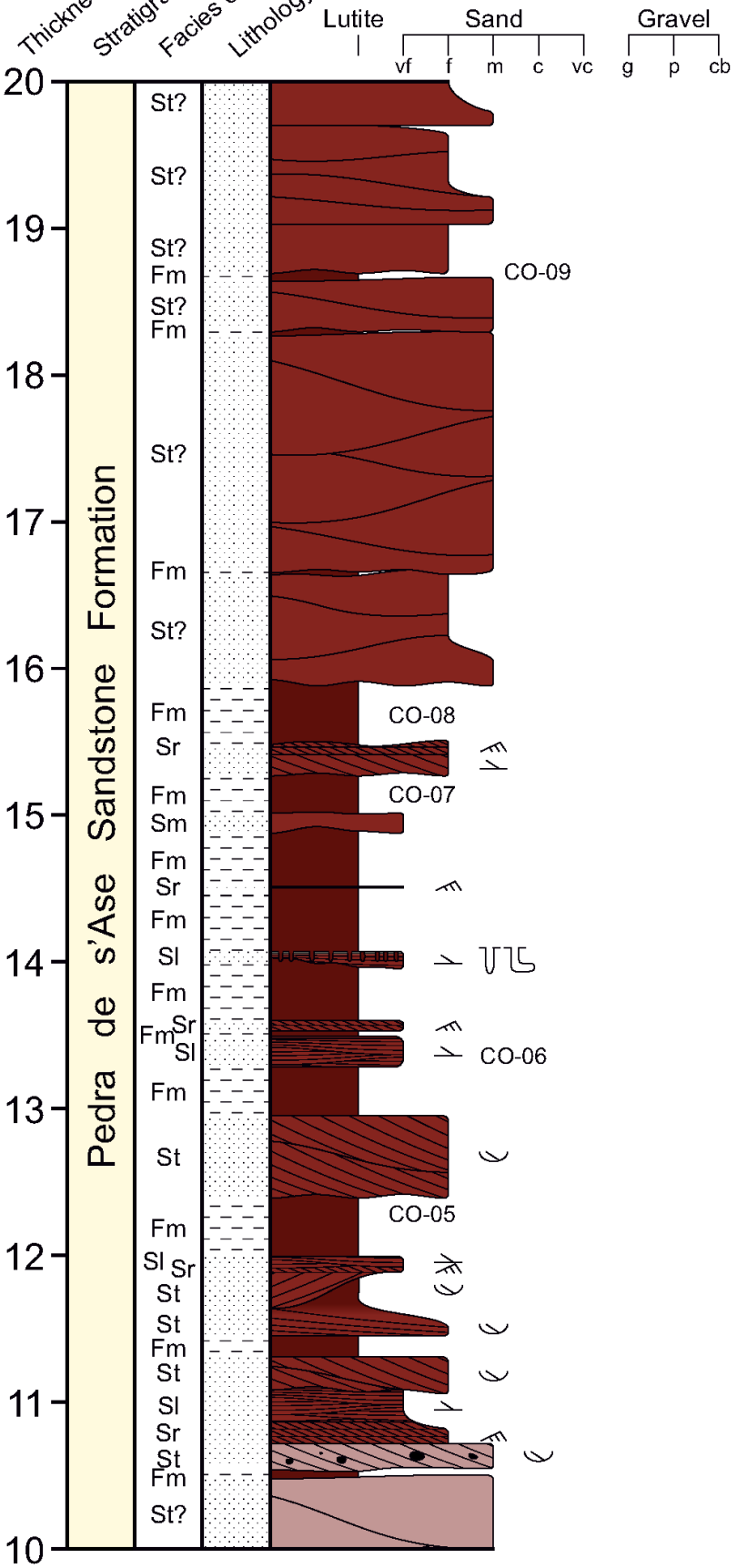

Lithology
- Lutite
- Sandstone
- Conglomerate
- Semi-covered interval
- Covered interval

Grain size
- vf Very fine-grained sandstone
- f Fine-grained sandstone
- m Medium-grained sandstone
- c Coarse-grained sandstone
- vc Very coarse-grained sandstone
- g Gravel
- p Pebble
- c Cobble

Sedimentary structures
- Parallel lamination
- Ripple lamination
- Convoluted lamination
- Tabular cross stratification
- Trough cross stratification
- Mud cracks
- Soft pebbles
- Carbonate nodules
- Positive granoselection

Trace and body fossils
- Rhizocretions
- Tree logs
- Plant remains
- Plant debris / Coal
- Microflora
- Burrows
- Tetrapod tracks
- Bone remains

Other symbols
- Fault
- 188/42 Strike/dip angle
- P-CO-01 Pollen sample
- CO-01 Palaeomagnetism sample

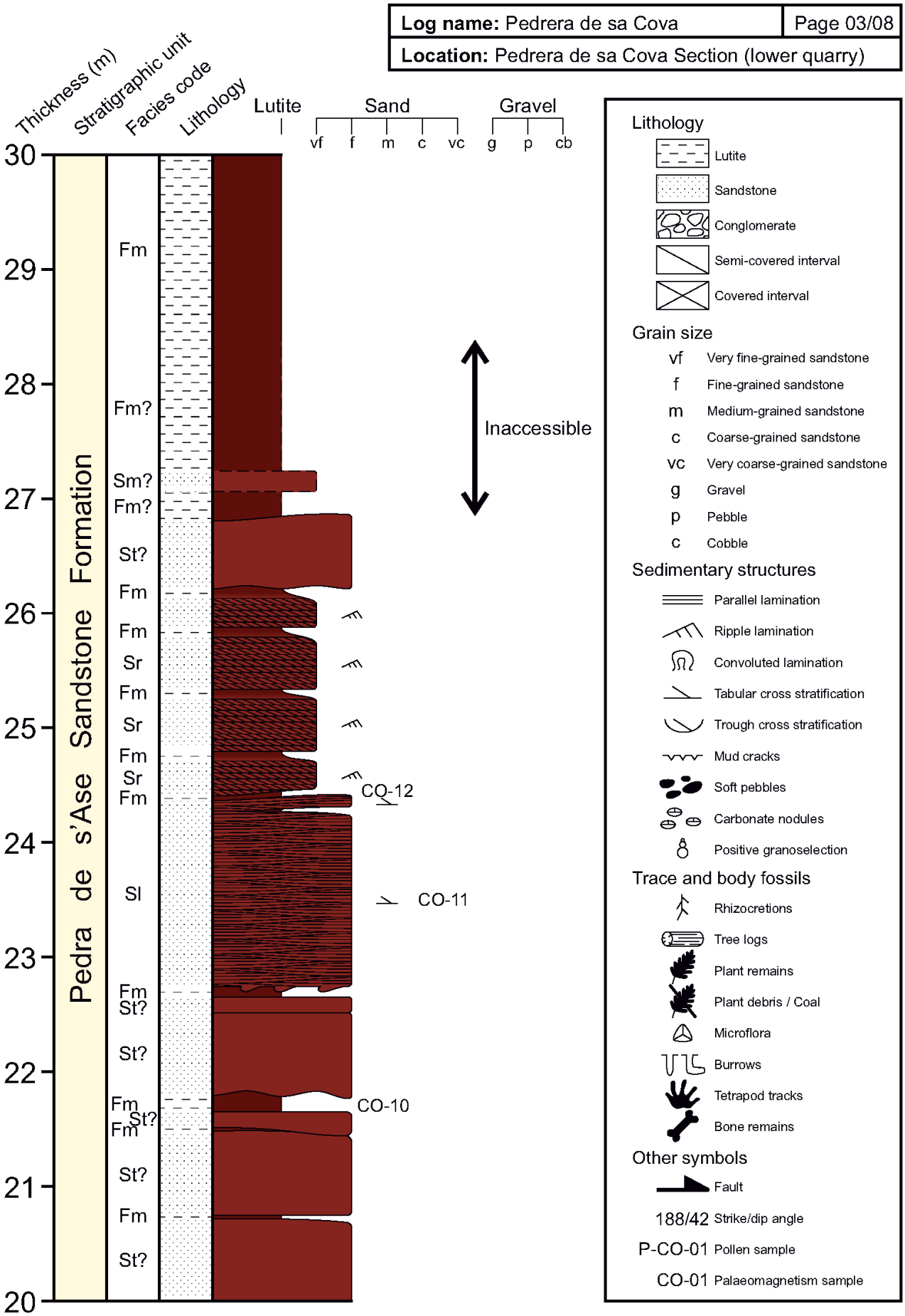
Log name: Pedrera de sa Cova
Page 03/08
Location: Pedrera de sa Cova Section (lower quarry)
Thickness (m)
Stratigraphic unit
Facies code
Lithology
Lutite
Sand
Gravel
vf f m c vc g p cb
Pedra de s'Ase Sandstone Formation
30
29
28
27
26
25
24
23
22
21
20
Fm
Fm?
Sm?
Fm?
St?
Fm
Fm
Sr
Fm
Sr
Fm
Sr
Fm
Sl
Fm
St?
St?
Fm
St?
Fm
St?
Fm
St?
Inaccessible
CO-12
CO-11
CO-10
Lithology
Lutite
Sandstone
Conglomerate
Semi-covered interval
Covered interval
Grain size
vf Very fine-grained sandstone
f Fine-grained sandstone
m Medium-grained sandstone
c Coarse-grained sandstone
vc Very coarse-grained sandstone
g Gravel
p Pebble
c Cobble
Sedimentary structures
Parallel lamination
Ripple lamination
Convoluted lamination
Tabular cross stratification
Trough cross stratification
Mud cracks
Soft pebbles
Carbonate nodules
Positive granoselection
Trace and body fossils
Rhizocretions
Tree logs
Plant remains
Plant debris / Coal
Microflora
Burrows
Tetrapod tracks
Bone remains
Other symbols
Fault
188/42 Strike/dip angle
P-CO-01 Pollen sample
CO-01 Palaeomagnetism sample

Log name: Pedrera de sa Cova	Page 04/08
Location: Pedrera de sa Cova Section (lower quarry)	

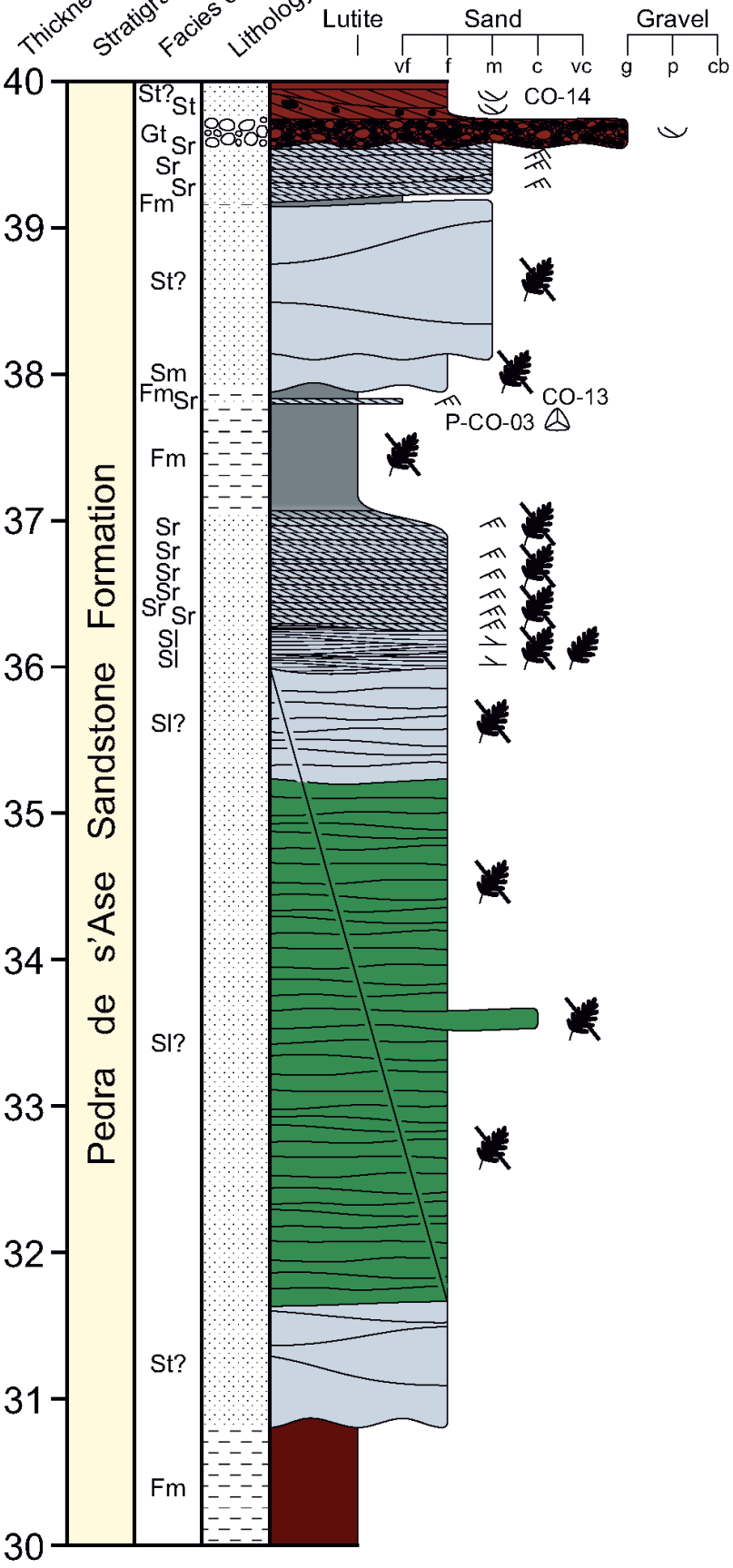

Lithology
- Lutite
- Sandstone
- Conglomerate
- Semi-covered interval
- Covered interval

Grain size
- vf Very fine-grained sandstone
- f Fine-grained sandstone
- m Medium-grained sandstone
- c Coarse-grained sandstone
- vc Very coarse-grained sandstone
- g Gravel
- p Pebble
- c Cobble

Sedimentary structures
- Parallel lamination
- Ripple lamination
- Convoluted lamination
- Tabular cross stratification
- Trough cross stratification
- Mud cracks
- Soft pebbles
- Carbonate nodules
- Positive granoselection

Trace and body fossils
- Rhizocretions
- Tree logs
- Plant remains
- Plant debris / Coal
- Microflora
- Burrows
- Tetrapod tracks
- Bone remains

Other symbols
- Fault
- 188/42 Strike/dip angle
- P-CO-01 Pollen sample
- CO-01 Palaeomagnetism sample

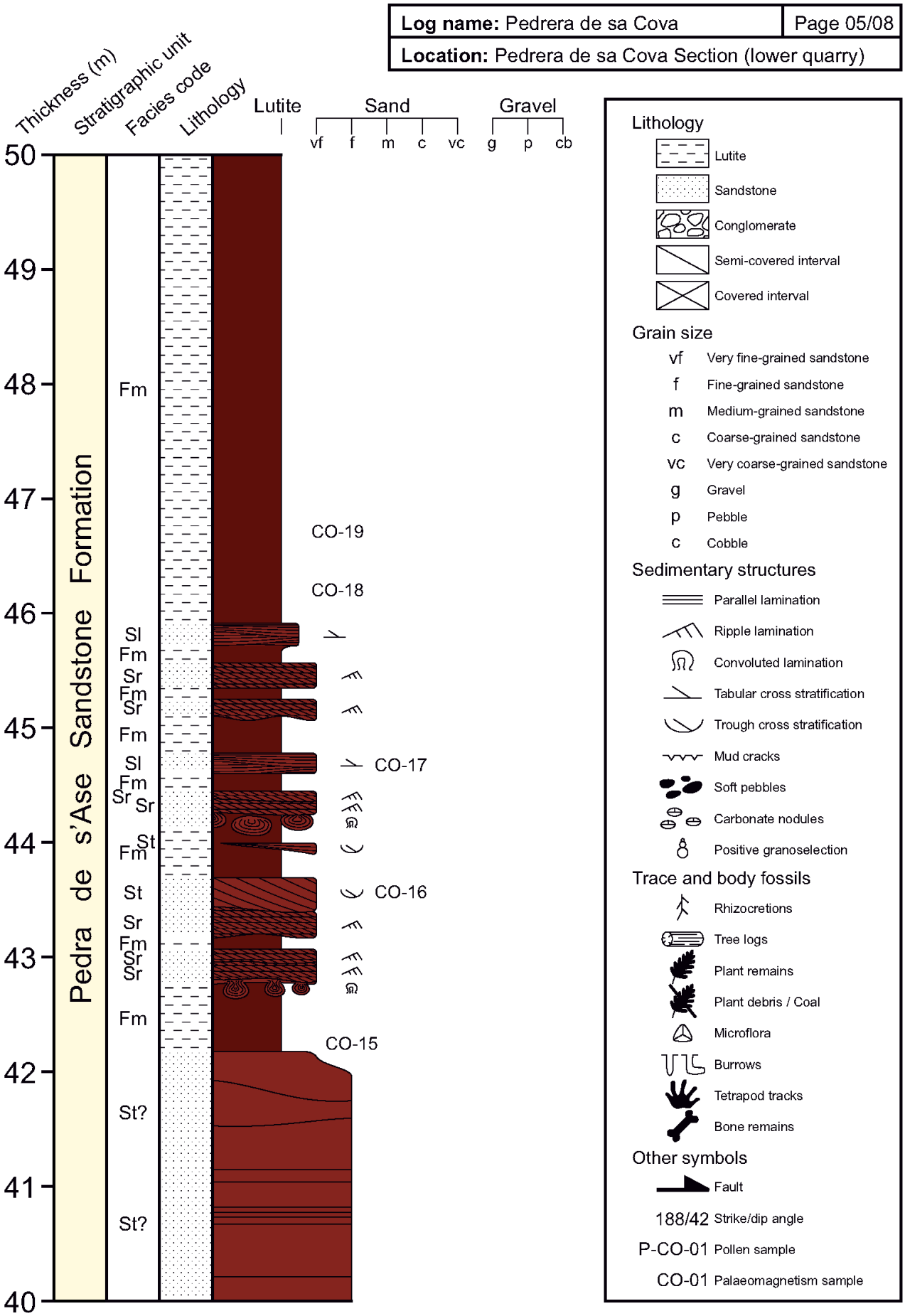
Log name: Pedrera de sa Cova
Page 05/08
Location: Pedrera de sa Cova Section (lower quarry)
Thickness (m)
Stratigraphic unit
Facies code
Lithology
Lutite
Sand
Gravel
vf f m c vc g p cb
Pedra de s'Ase Sandstone Formation
50
49
48
47
46
45
44
43
42
41
40
Fm
Sl
Fm
Sr
Fm
Sr
Fm
Sl
Fm
Sr Sr
St
Fm
St
Sr
Fm
Sr
Sr
Fm
St?
St?
CO-19
CO-18
CO-17
CO-16
CO-15
Lithology
Lutite
Sandstone
Conglomerate
Semi-covered interval
Covered interval
Grain size
vf Very fine-grained sandstone
f Fine-grained sandstone
m Medium-grained sandstone
c Coarse-grained sandstone
vc Very coarse-grained sandstone
g Gravel
p Pebble
c Cobble
Sedimentary structures
Parallel lamination
Ripple lamination
Convoluted lamination
Tabular cross stratification
Trough cross stratification
Mud cracks
Soft pebbles
Carbonate nodules
Positive granoselection
Trace and body fossils
Rhizocretions
Tree logs
Plant remains
Plant debris / Coal
Microflora
Burrows
Tetrapod tracks
Bone remains
Other symbols
Fault
188/42 Strike/dip angle
P-CO-01 Pollen sample
CO-01 Palaeomagnetism sample

Log name: Pedrera de sa Cova	Page 06/08
Location: Pedrera de sa Cova Section (lower quarry)	

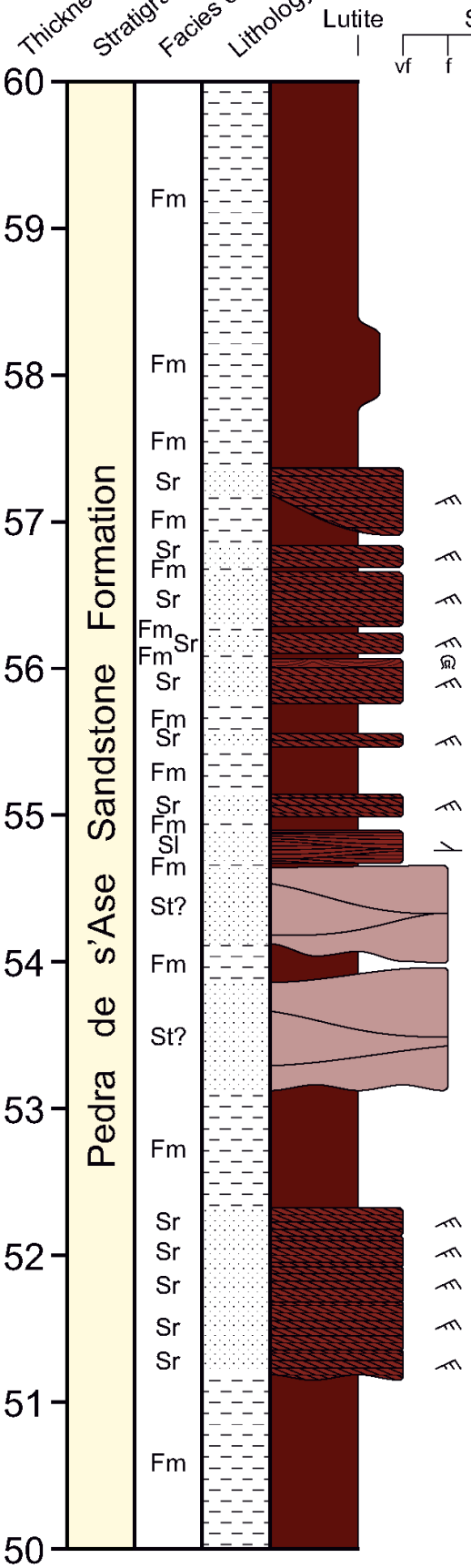

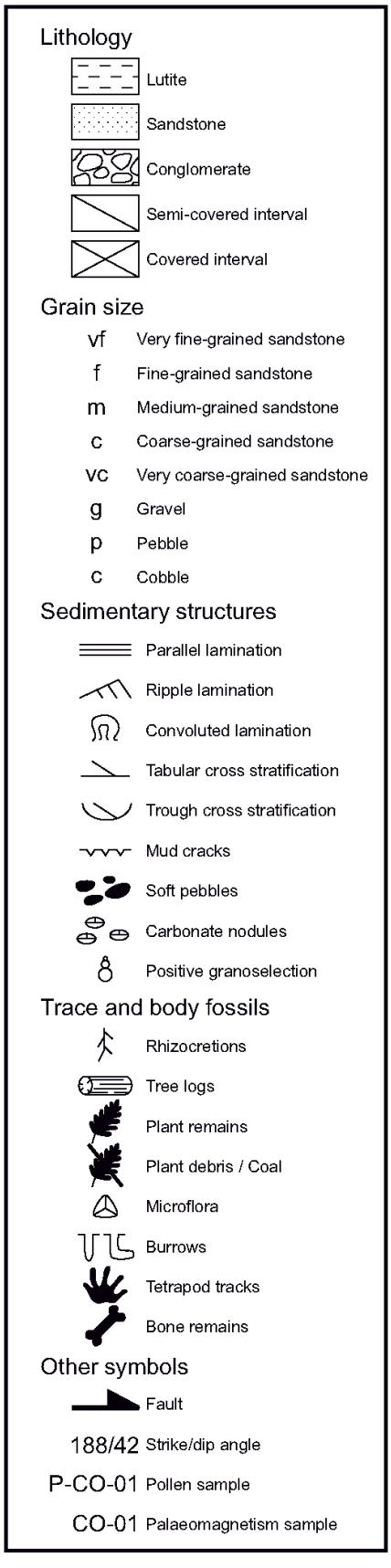

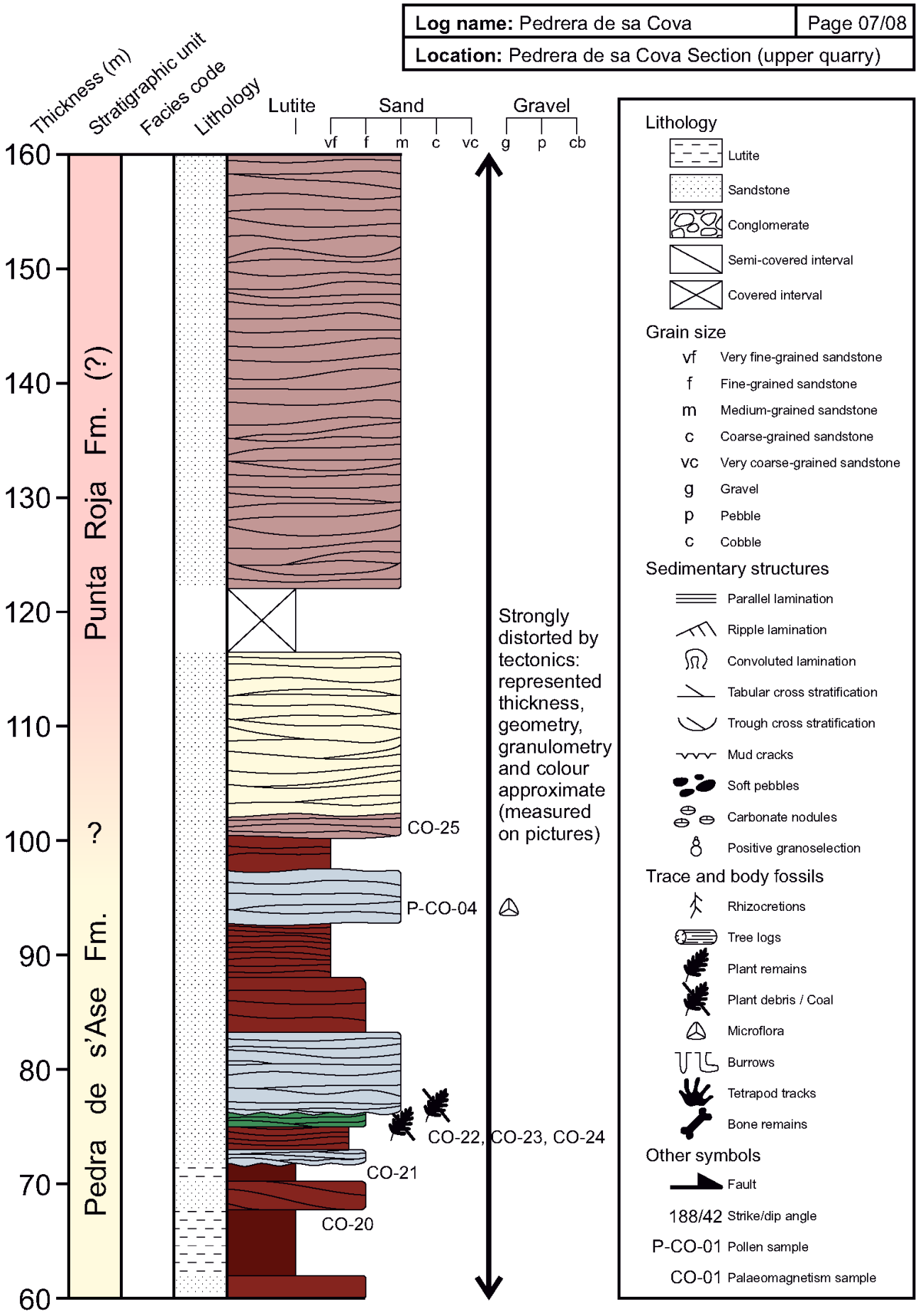
Log name: Pedrera de sa Cova
Page 07/08
Location: Pedrera de sa Cova Section (upper quarry)
Thickness (m)
Stratigraphic unit
Facies code
Lithology
Lutite
Sand
Gravel
vf f m c vc g p cb
160
150
140
130
120
110
100
90
80
70
60
Punta Roja Fm. (?)
?
Pedra de s'Ase Fm.
CO-25
P-CO-04
CO-22, CO-23, CO-24
CO-21
CO-20
Strongly distorted by tectonics: represented thickness, geometry, granulometry and colour approximate (measured on pictures)
Lithology
Lutite
Sandstone
Conglomerate
Semi-covered interval
Covered interval
Grain size
vf Very fine-grained sandstone
f Fine-grained sandstone
m Medium-grained sandstone
c Coarse-grained sandstone
vc Very coarse-grained sandstone
g Gravel
p Pebble
c Cobble
Sedimentary structures
Parallel lamination
Ripple lamination
Convoluted lamination
Tabular cross stratification
Trough cross stratification
Mud cracks
Soft pebbles
Carbonate nodules
Positive granoselection
Trace and body fossils
Rhizocretions
Tree logs
Plant remains
Plant debris / Coal
Microflora
Burrows
Tetrapod tracks
Bone remains
Other symbols
Fault
188/42 Strike/dip angle
P-CO-01 Pollen sample
CO-01 Palaeomagnetism sample

Log name: Pedrera de sa Cova	Page 08/08
Location: Pedrera de sa Cova Section (upper quarry)	

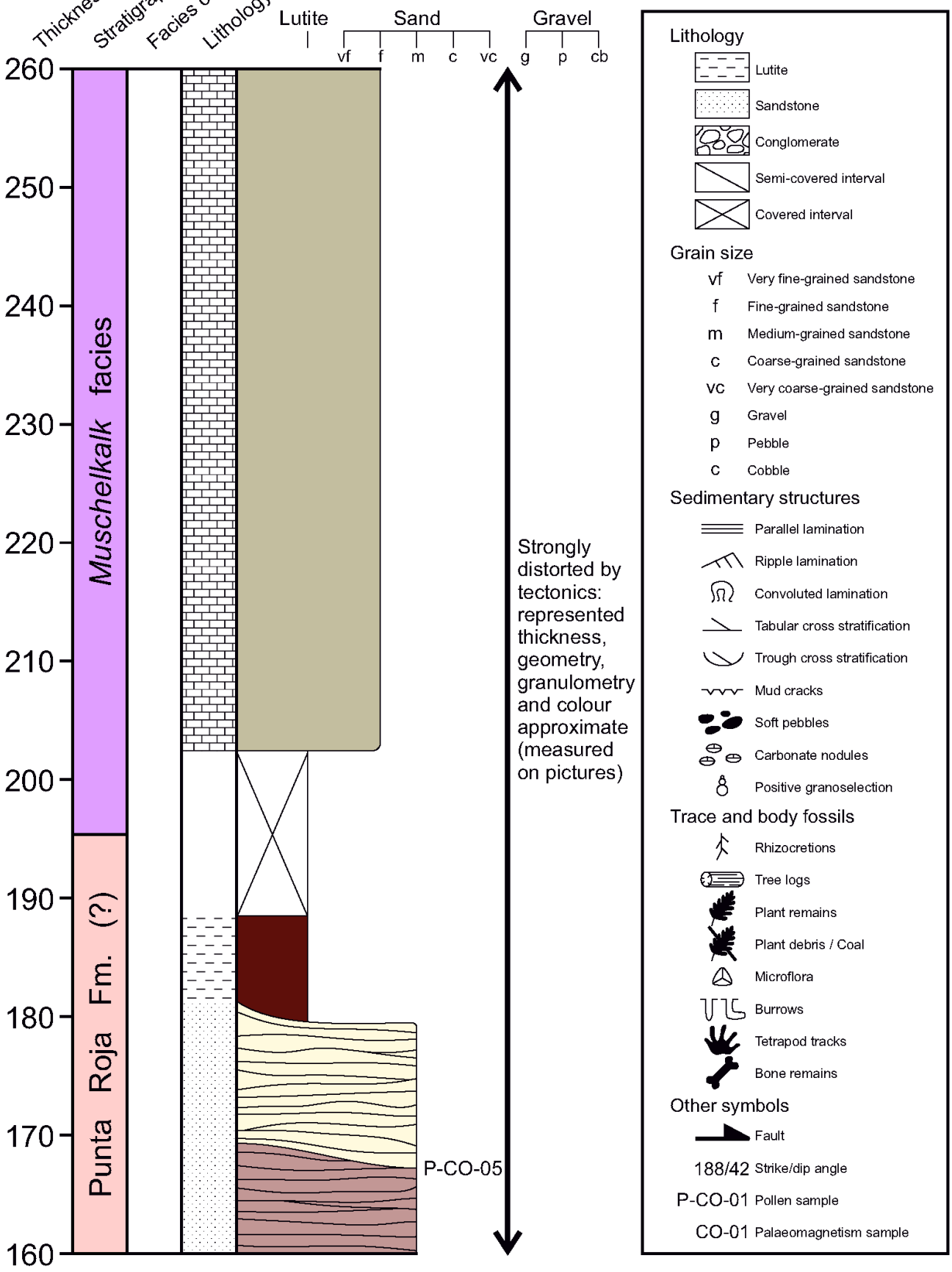

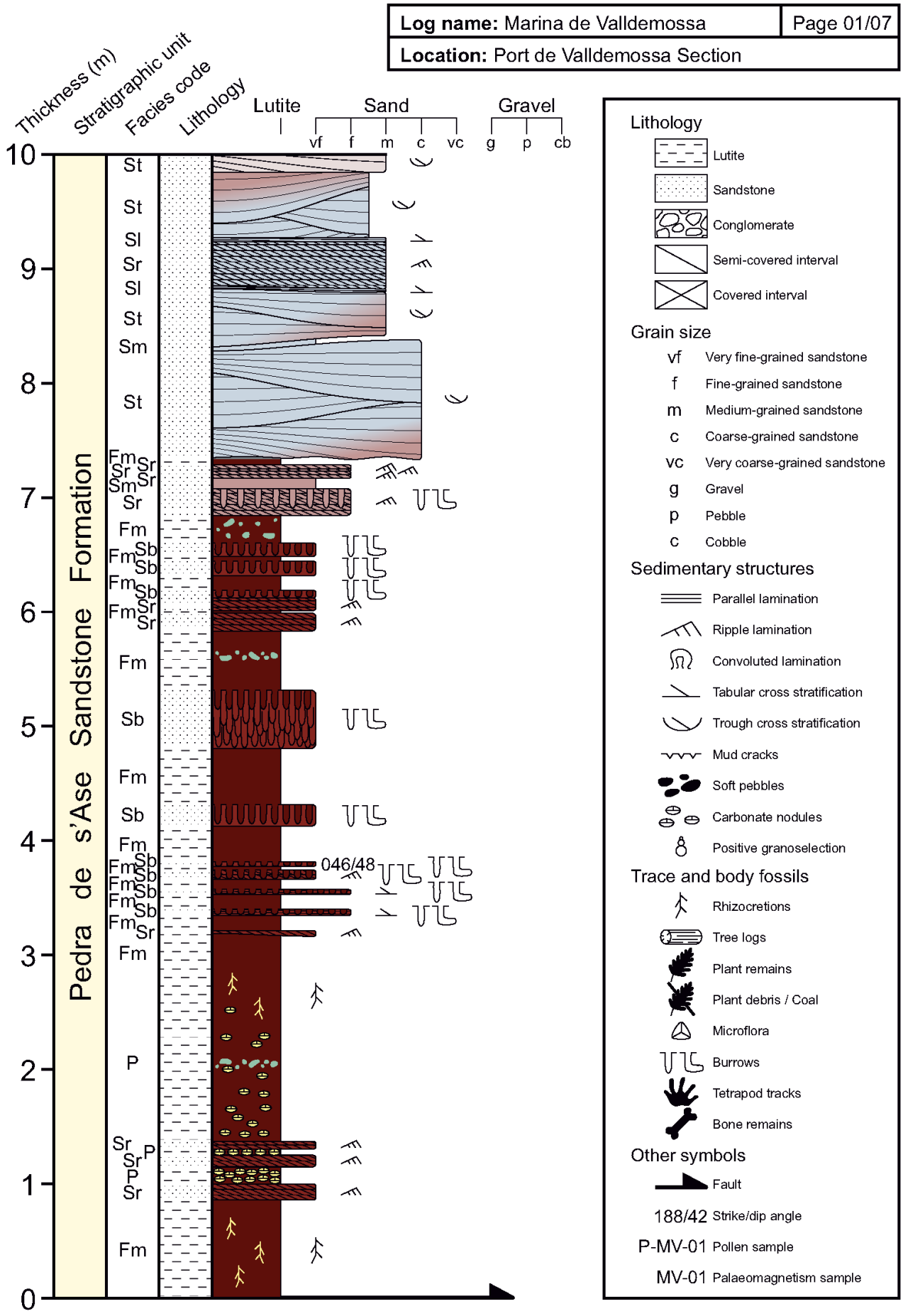
Log name: Marina de Valldemossa
Page 01/07
Location: Port de Valldemossa Section
Thickness (m)
Stratigraphic unit
Facies code
Lithology
Lutite
Sand
Gravel
vf f m c vc g p cb
Pedra de s'Ase Sandstone Formation
046/48
Lithology
Lutite
Sandstone
Conglomerate
Semi-covered interval
Covered interval
Grain size
vf Very fine-grained sandstone
f Fine-grained sandstone
m Medium-grained sandstone
c Coarse-grained sandstone
vc Very coarse-grained sandstone
g Gravel
p Pebble
c Cobble
Sedimentary structures
Parallel lamination
Ripple lamination
Convoluted lamination
Tabular cross stratification
Trough cross stratification
Mud cracks
Soft pebbles
Carbonate nodules
Positive granoselection
Trace and body fossils
Rhizocretions
Tree logs
Plant remains
Plant debris / Coal
Microflora
Burrows
Tetrapod tracks
Bone remains
Other symbols
Fault
188/42 Strike/dip angle
P-MV-01 Pollen sample
MV-01 Palaeomagnetism sample

Log name: Marina de Valldemossa	Page 02/07
Location: Port de Valldemossa Section	

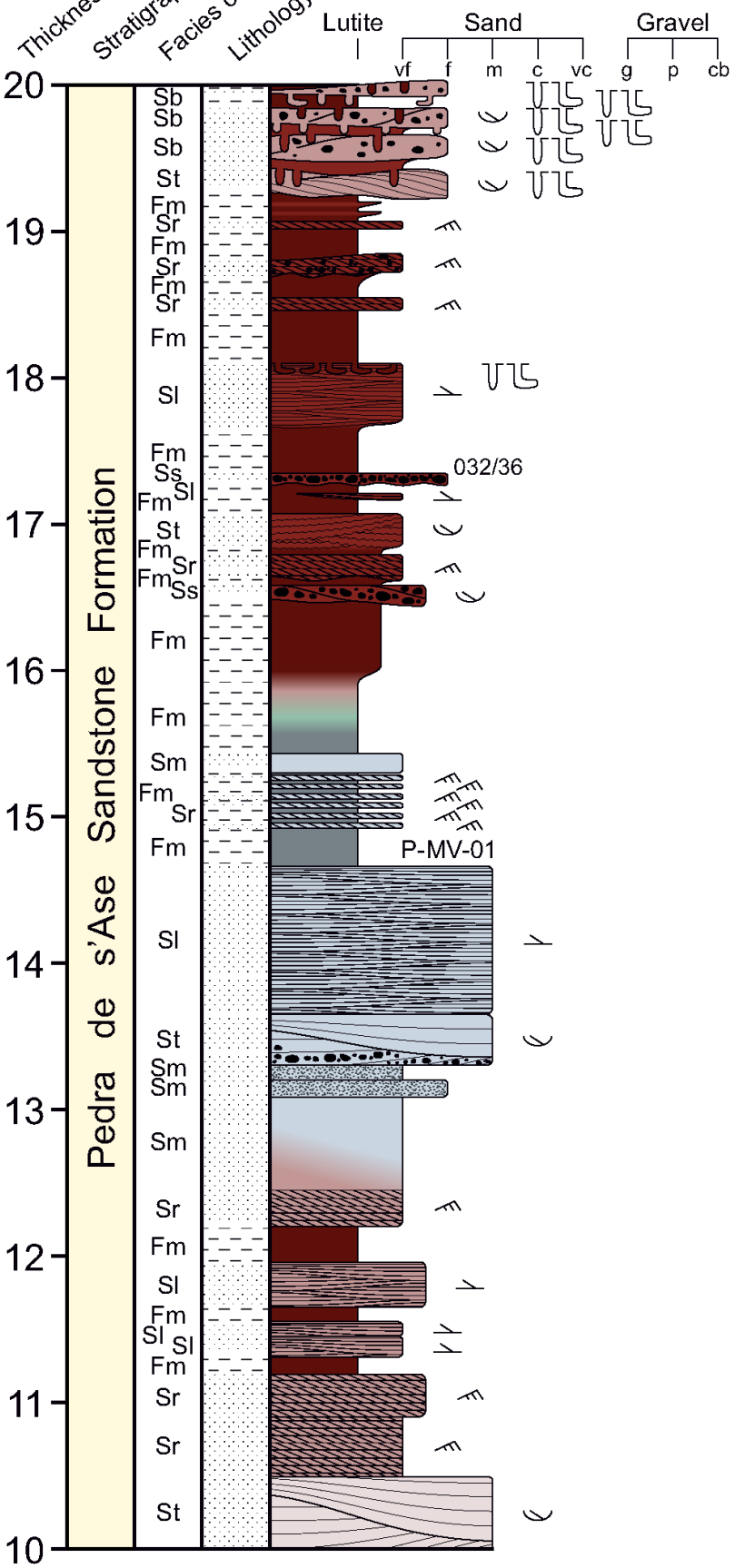

Lithology
- Lutite
- Sandstone
- Conglomerate
- Semi-covered interval
- Covered interval

Grain size
- vf Very fine-grained sandstone
- f Fine-grained sandstone
- m Medium-grained sandstone
- c Coarse-grained sandstone
- vc Very coarse-grained sandstone
- g Gravel
- p Pebble
- c Cobble

Sedimentary structures
- Parallel lamination
- Ripple lamination
- Convoluted lamination
- Tabular cross stratification
- Trough cross stratification
- Mud cracks
- Soft pebbles
- Carbonate nodules
- Positive granoselection

Trace and body fossils
- Rhizocretions
- Tree logs
- Plant remains
- Plant debris / Coal
- Microflora
- Burrows
- Tetrapod tracks
- Bone remains

Other symbols
- Fault
- 188/42 Strike/dip angle
- P-MV-01 Pollen sample
- MV-01 Palaeomagnetism sample

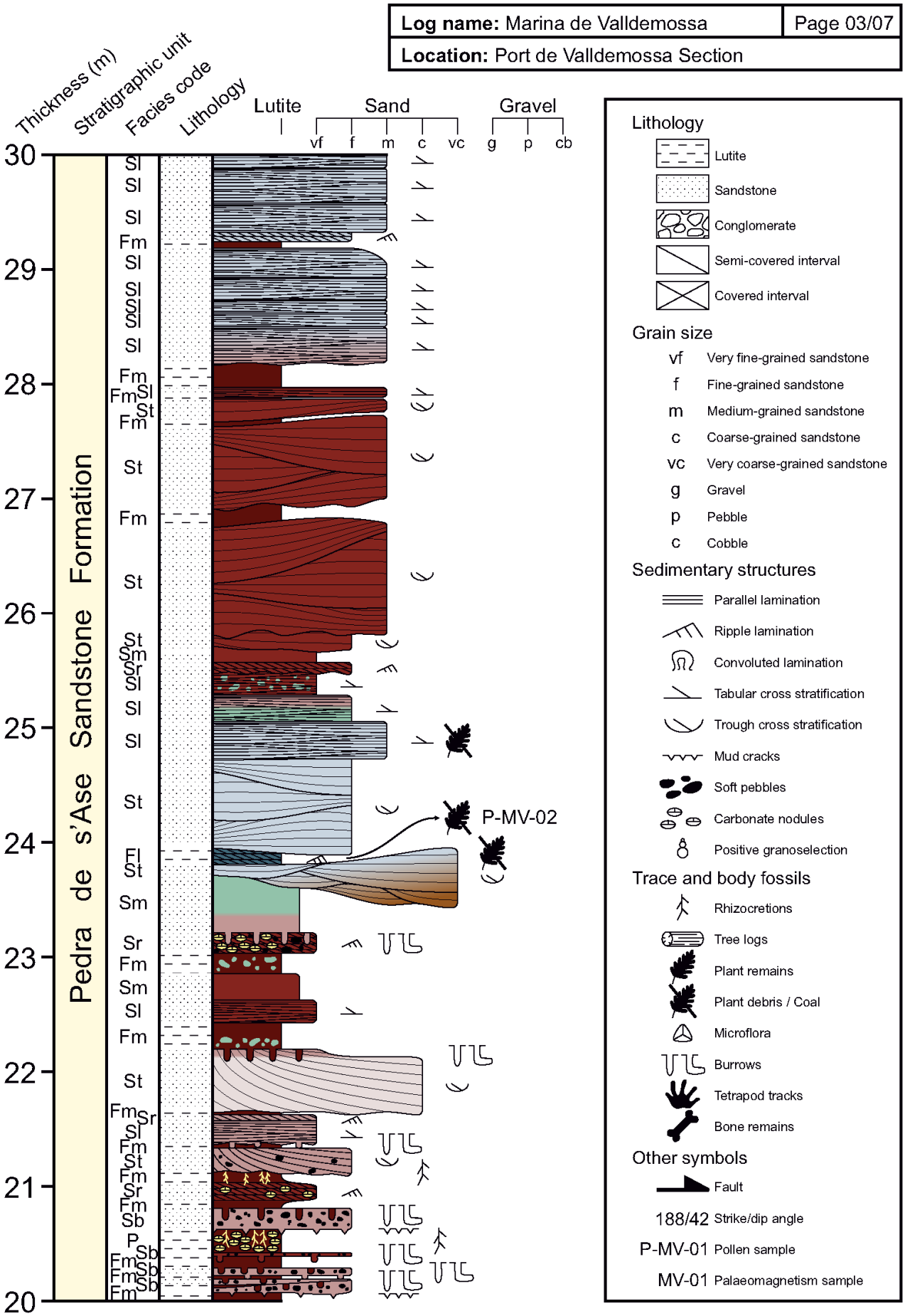
Log name: Marina de Valldemossa
Page 03/07
Location: Port de Valldemossa Section
Thickness (m)
Stratigraphic unit
Facies code
Lithology
Lutite
Sand
Gravel
vf f m c vc g p cb
Pedra de s'Ase Sandstone Formation
P-MV-02
Lithology
Lutite
Sandstone
Conglomerate
Semi-covered interval
Covered interval
Grain size
vf Very fine-grained sandstone
f Fine-grained sandstone
m Medium-grained sandstone
c Coarse-grained sandstone
vc Very coarse-grained sandstone
g Gravel
p Pebble
c Cobble
Sedimentary structures
Parallel lamination
Ripple lamination
Convoluted lamination
Tabular cross stratification
Trough cross stratification
Mud cracks
Soft pebbles
Carbonate nodules
Positive granoselection
Trace and body fossils
Rhizocretions
Tree logs
Plant remains
Plant debris / Coal
Microflora
Burrows
Tetrapod tracks
Bone remains
Other symbols
Fault
188/42 Strike/dip angle
P-MV-01 Pollen sample
MV-01 Palaeomagnetism sample

Log name: Marina de Valldemossa	Page 04/07
Location: Port de Valldemossa Section	

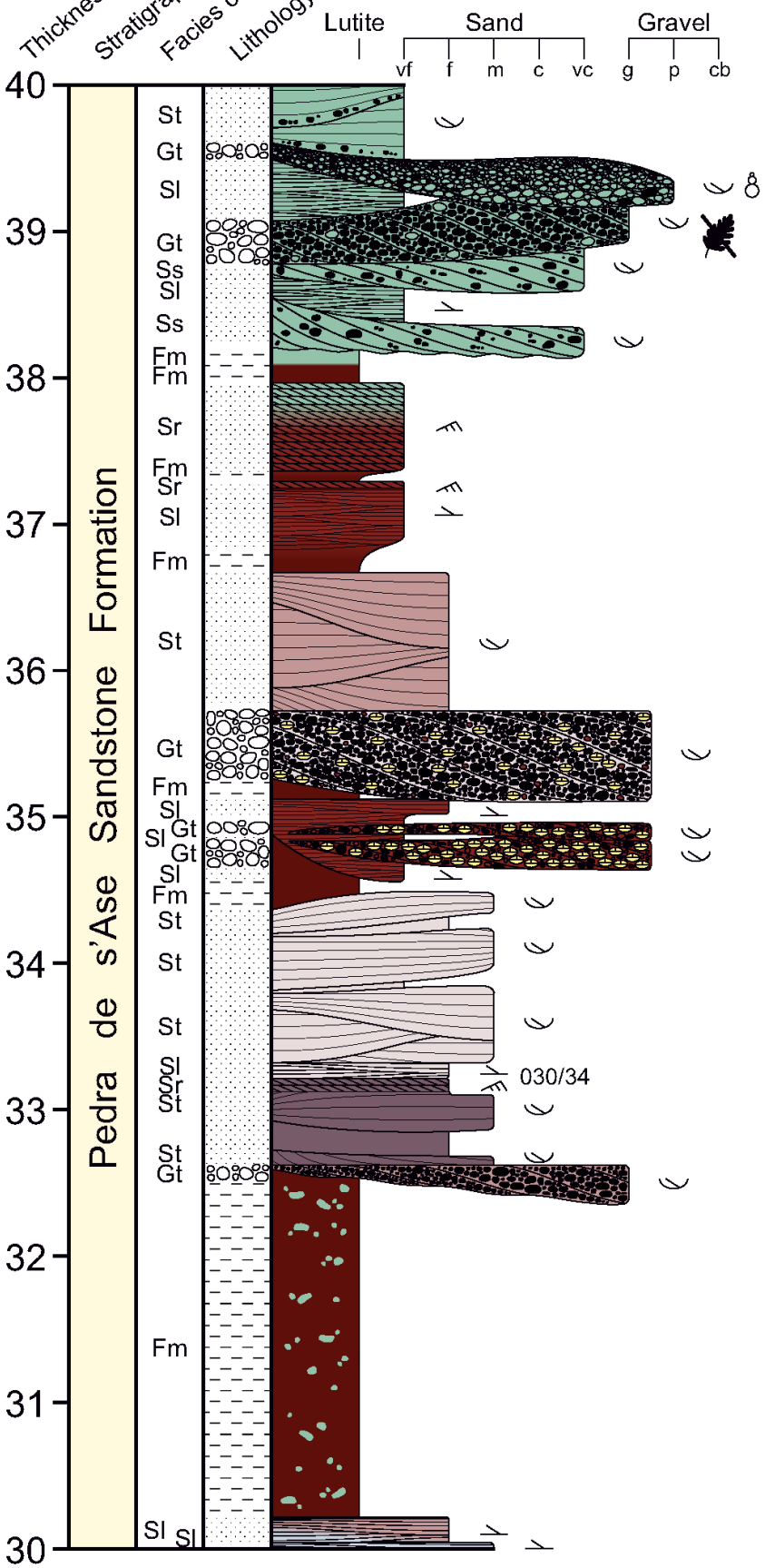

Lithology
- Lutite
- Sandstone
- Conglomerate
- Semi-covered interval
- Covered interval

Grain size
- vf Very fine-grained sandstone
- f Fine-grained sandstone
- m Medium-grained sandstone
- c Coarse-grained sandstone
- vc Very coarse-grained sandstone
- g Gravel
- p Pebble
- c Cobble

Sedimentary structures
- Parallel lamination
- Ripple lamination
- Convoluted lamination
- Tabular cross stratification
- Trough cross stratification
- Mud cracks
- Soft pebbles
- Carbonate nodules
- Positive granoselection

Trace and body fossils
- Rhizocretions
- Tree logs
- Plant remains
- Plant debris / Coal
- Microflora
- Burrows
- Tetrapod tracks
- Bone remains

Other symbols
- Fault
- 188/42 Strike/dip angle
- P-MV-01 Pollen sample
- MV-01 Palaeomagnetism sample

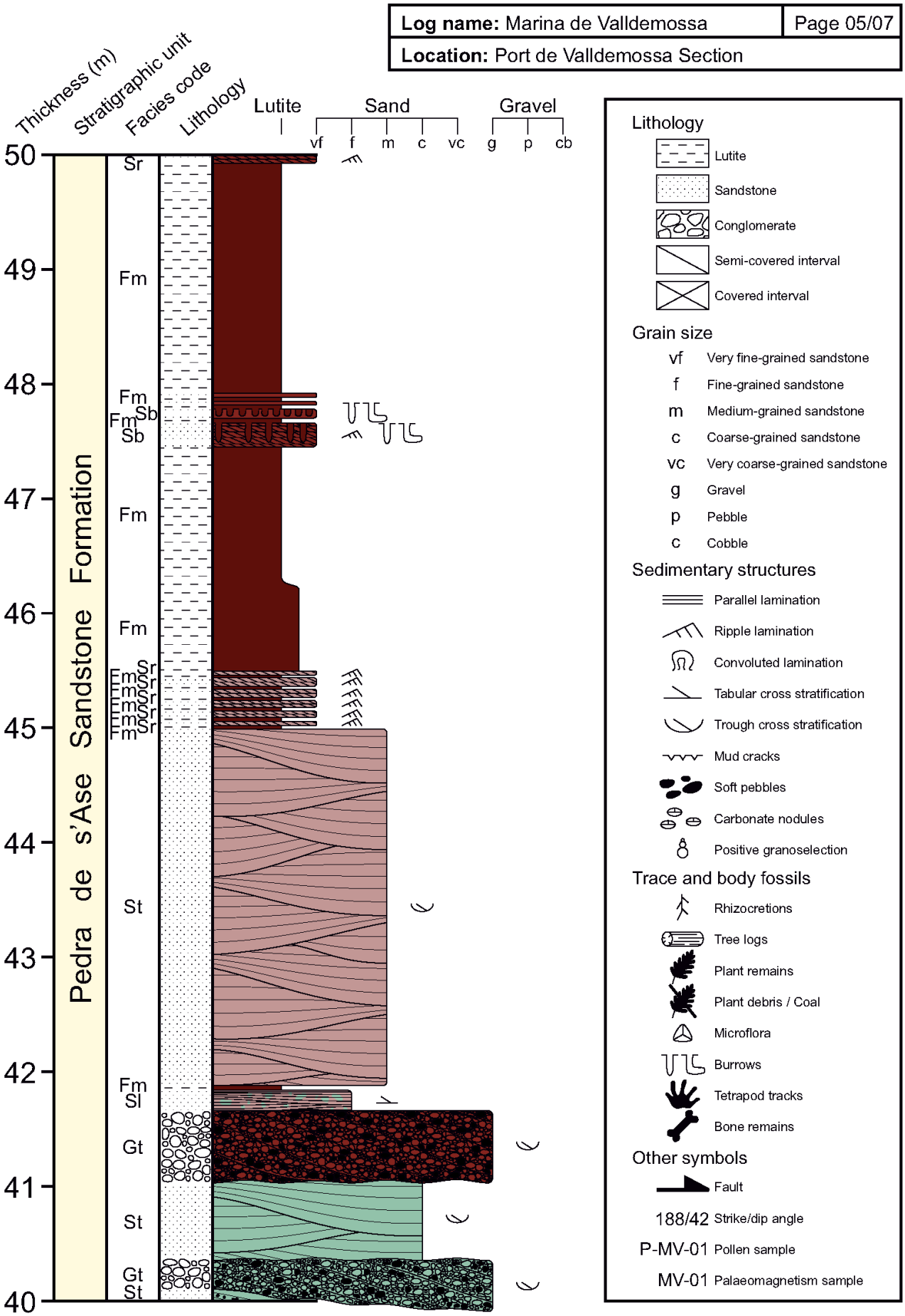
Log name: Marina de Valldemossa
Page 05/07
Location: Port de Valldemossa Section
Thickness (m)
Stratigraphic unit
Facies code
Lithology
Lutite
Sand
Gravel
vf f m c vc g p cb
50
49
48
47
46
45
44
43
42
41
40
Pedra de s'Ase Sandstone Formation
Sr
Fm
Fm
Sb
Fm
Sb
Fm
Fm
Sr
Sr
Sr
Sr
Sr
St
Fm
Sl
Gt
St
Gt
St
Lithology
Lutite
Sandstone
Conglomerate
Semi-covered interval
Covered interval
Grain size
vf Very fine-grained sandstone
f Fine-grained sandstone
m Medium-grained sandstone
c Coarse-grained sandstone
vc Very coarse-grained sandstone
g Gravel
p Pebble
c Cobble
Sedimentary structures
Parallel lamination
Ripple lamination
Convoluted lamination
Tabular cross stratification
Trough cross stratification
Mud cracks
Soft pebbles
Carbonate nodules
Positive granoselection
Trace and body fossils
Rhizocretions
Tree logs
Plant remains
Plant debris / Coal
Microflora
Burrows
Tetrapod tracks
Bone remains
Other symbols
Fault
188/42 Strike/dip angle
P-MV-01 Pollen sample
MV-01 Palaeomagnetism sample

Log name: Marina de Valldemossa	Page 06/07
Location: Port de Valldemossa Section	

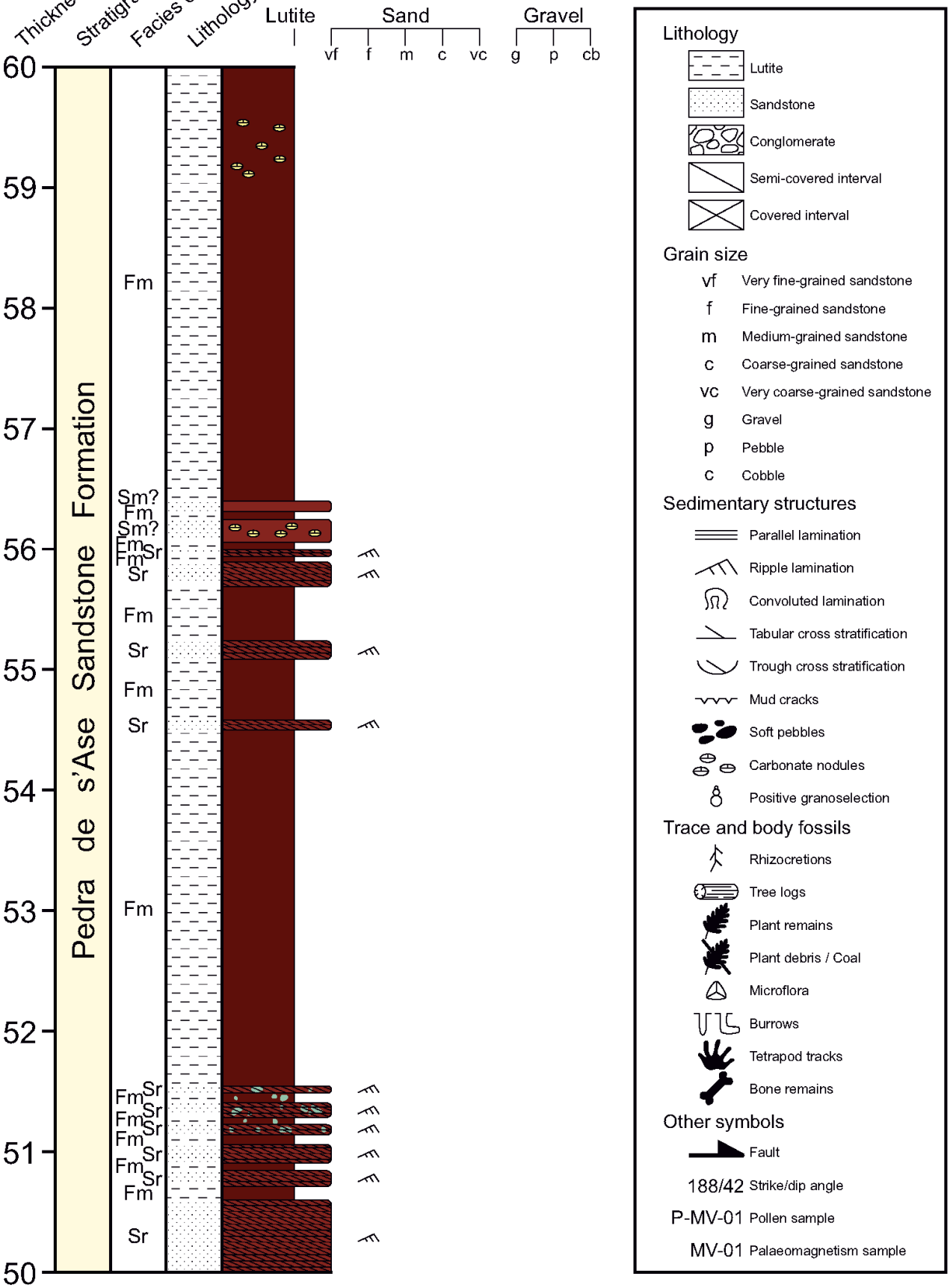

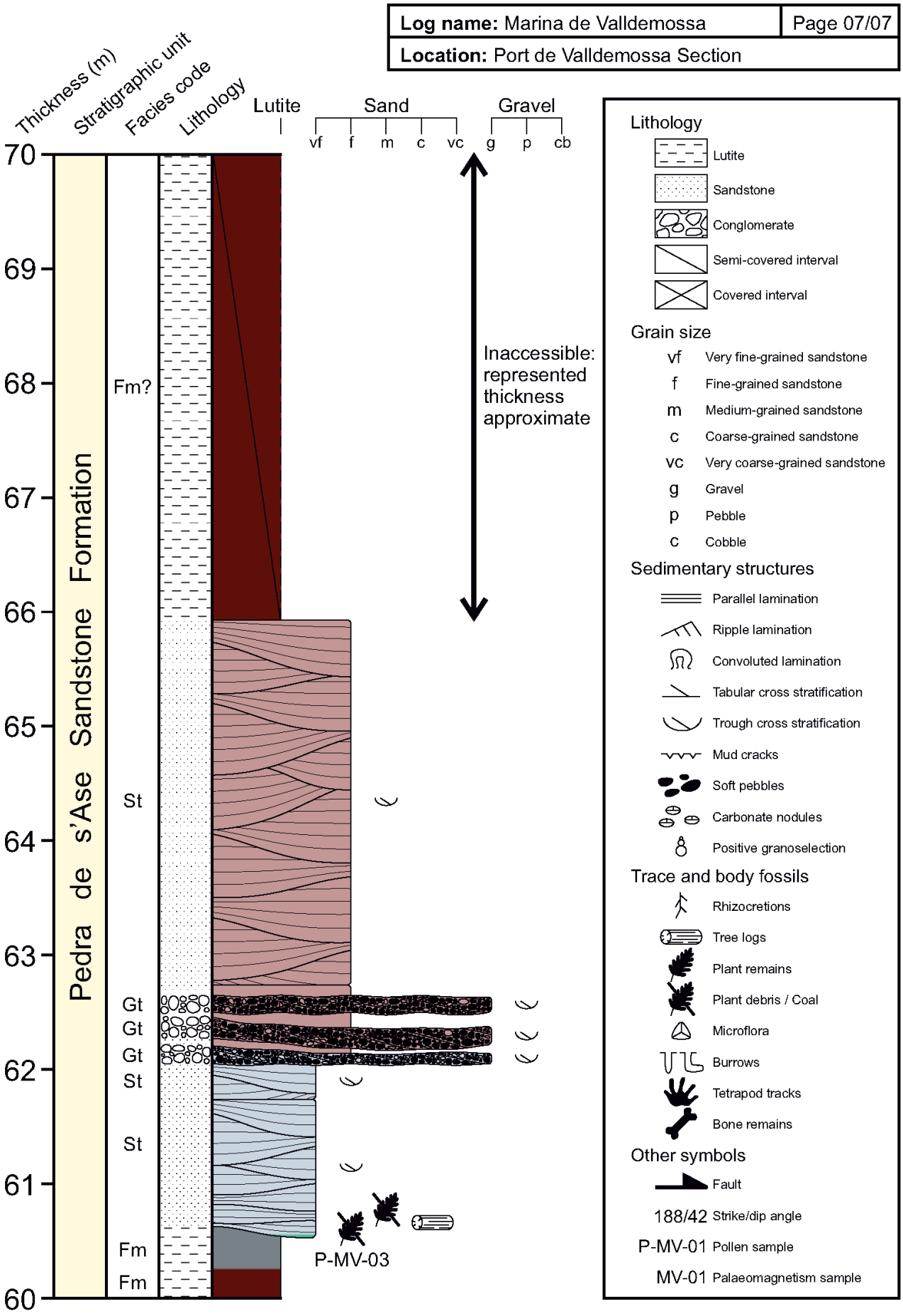
Log name: Marina de Valldemossa
Page 07/07
Location: Port de Valldemossa Section
Thickness (m)
Stratigraphic unit
Facies code
Lithology
Lutite
Sand
Gravel
vf f m c vc g p cb
70
69
68
67
66
65
64
63
62
61
60
Pedra de s'Ase Sandstone Formation
Fm?
St
Gt
Gt
Gt
St
St
Fm
Fm
P-MV-03
Inaccessible: represented thickness approximate
Lithology
Lutite
Sandstone
Conglomerate
Semi-covered interval
Covered interval
Grain size
vf Very fine-grained sandstone
f Fine-grained sandstone
m Medium-grained sandstone
c Coarse-grained sandstone
vc Very coarse-grained sandstone
g Gravel
p Pebble
c Cobble
Sedimentary structures
Parallel lamination
Ripple lamination
Convoluted lamination
Tabular cross stratification
Trough cross stratification
Mud cracks
Soft pebbles
Carbonate nodules
Positive granoselection
Trace and body fossils
Rhizocretions
Tree logs
Plant remains
Plant debris / Coal
Microflora
Burrows
Tetrapod tracks
Bone remains
Other symbols
Fault
188/42 Strike/dip angle
P-MV-01 Pollen sample
MV-01 Palaeomagnetism sample

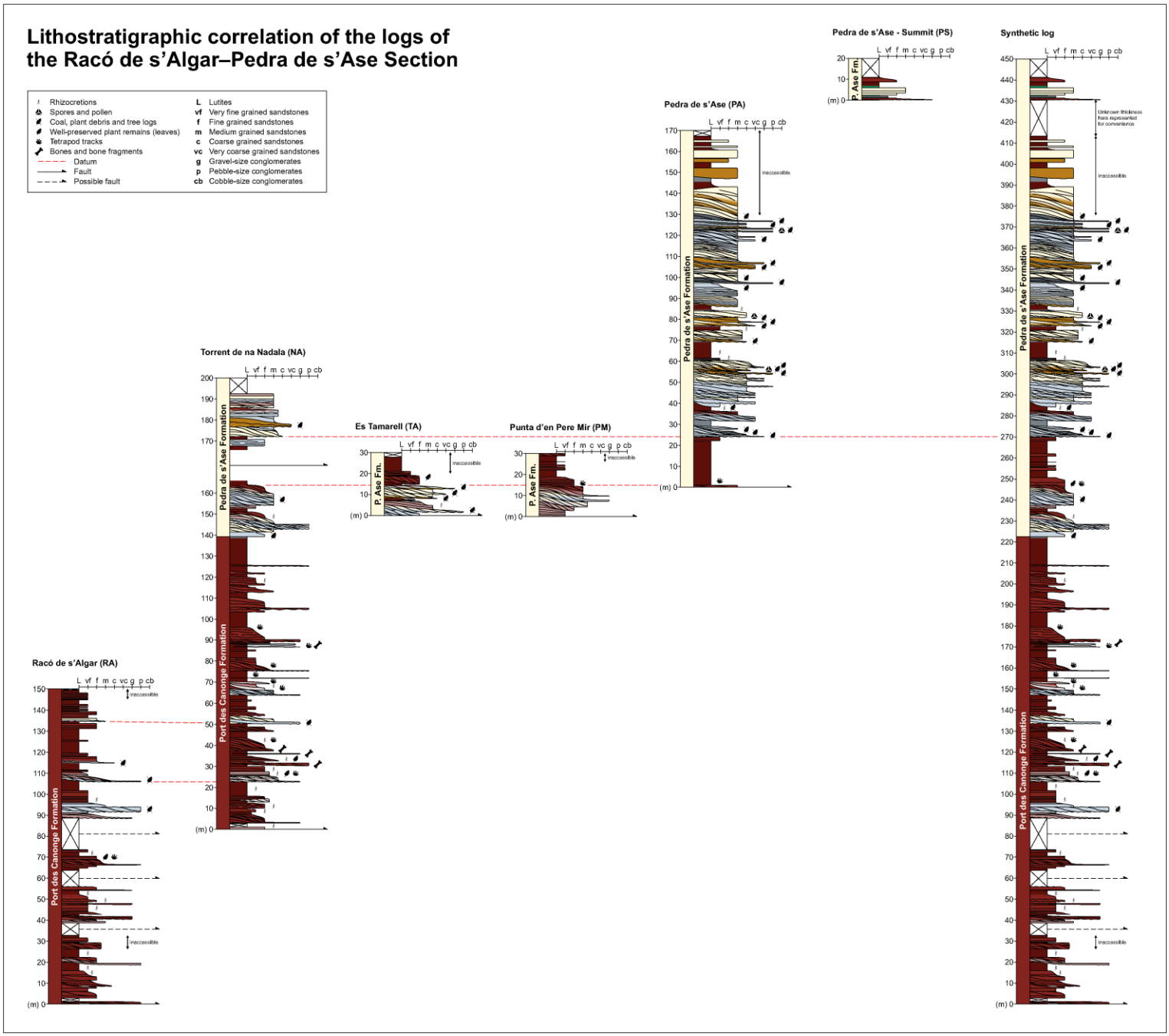
Lithostratigraphic correlation of the logs of the Racó de s'Algar–Pedra de s'Ase Section
Rhizocretions
Spores and pollen
Coal, plant debris and tree logs
Well-preserved plant remains (leaves)
Tetrapod tracks
Bones and bone fragments
Datum
Fault
Possible fault
L Lutites
vf Very fine grained sandstones
f Fine grained sandstones
m Medium grained sandstones
c Coarse grained sandstones
vc Very coarse grained sandstones
g Gravel-size conglomerates
p Pebble-size conglomerates
cb Cobble-size conglomerates
Racó de s'Algar (RA)
Torrent de na Nadala (NA)
Es Tamarell (TA)
Punta d'en Pere Mir (PM)
Pedra de s'Ase (PA)
Pedra de s'Ase - Summit (PS)
Synthetic log
Pedra de s'Ase Formation
Port des Canonge Formation
P. Ase Fm.
inaccessible
Unknown thickness here represented for convenience
(m)

Lithostratigraphic correlation of the logs of the Port des Canonge–Hort de sa Cova Section

Rhizocretions	L Lutites
Spores and pollen	vf Very fine grained sandstones
Coal, plant debris and tree logs	f Fine grained sandstones
Well-preserved plant remains (leaves)	m Medium grained sandstones
Tetrapod tracks	c Coarse grained sandstones
Bones and bone fragments	vc Very coarse grained sandstones
Datum	g Gravel-size conglomerates
Fault	p Pebble-size conglomerates
Possible fault	cb Cobble-size conglomerates

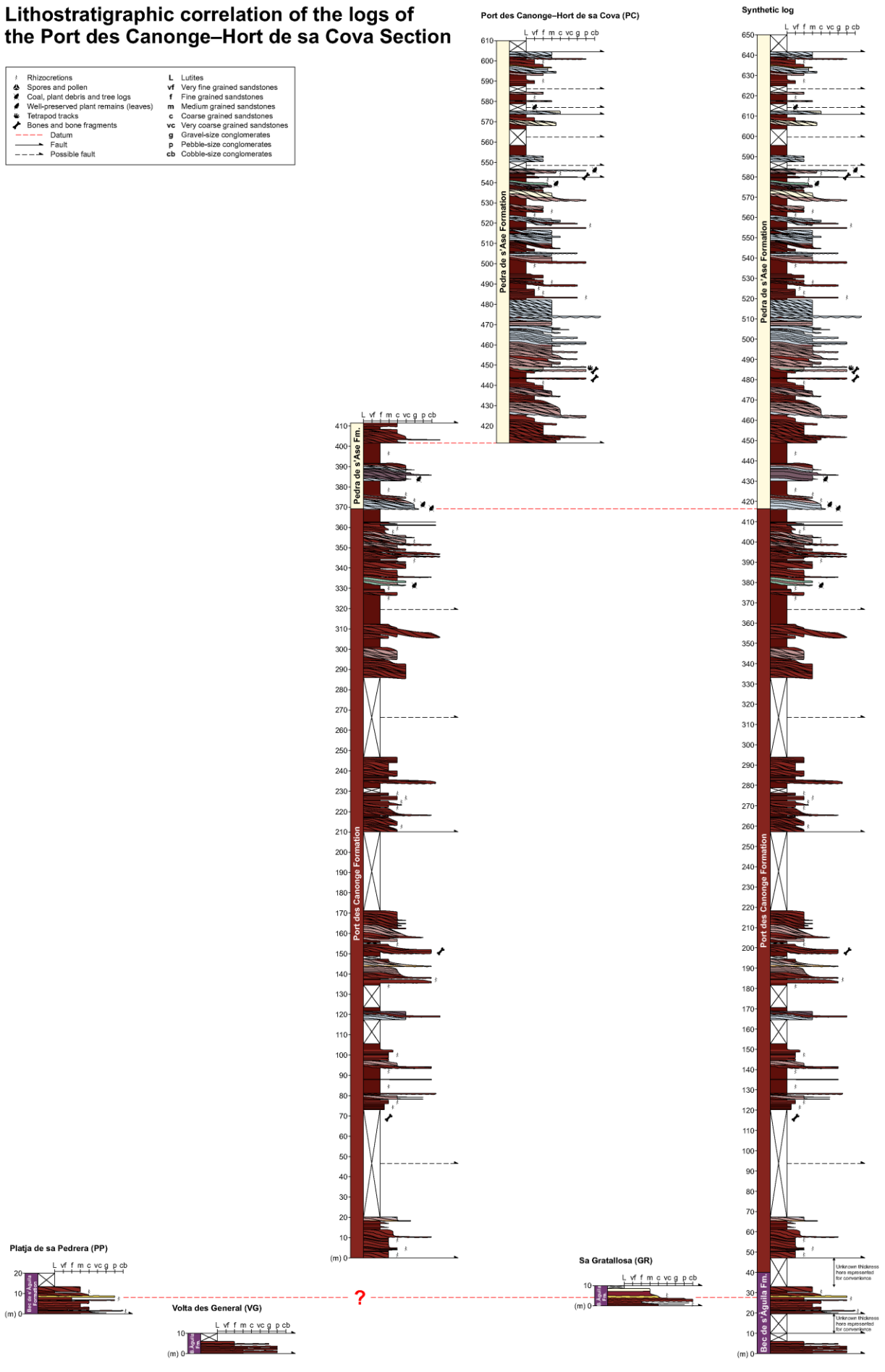

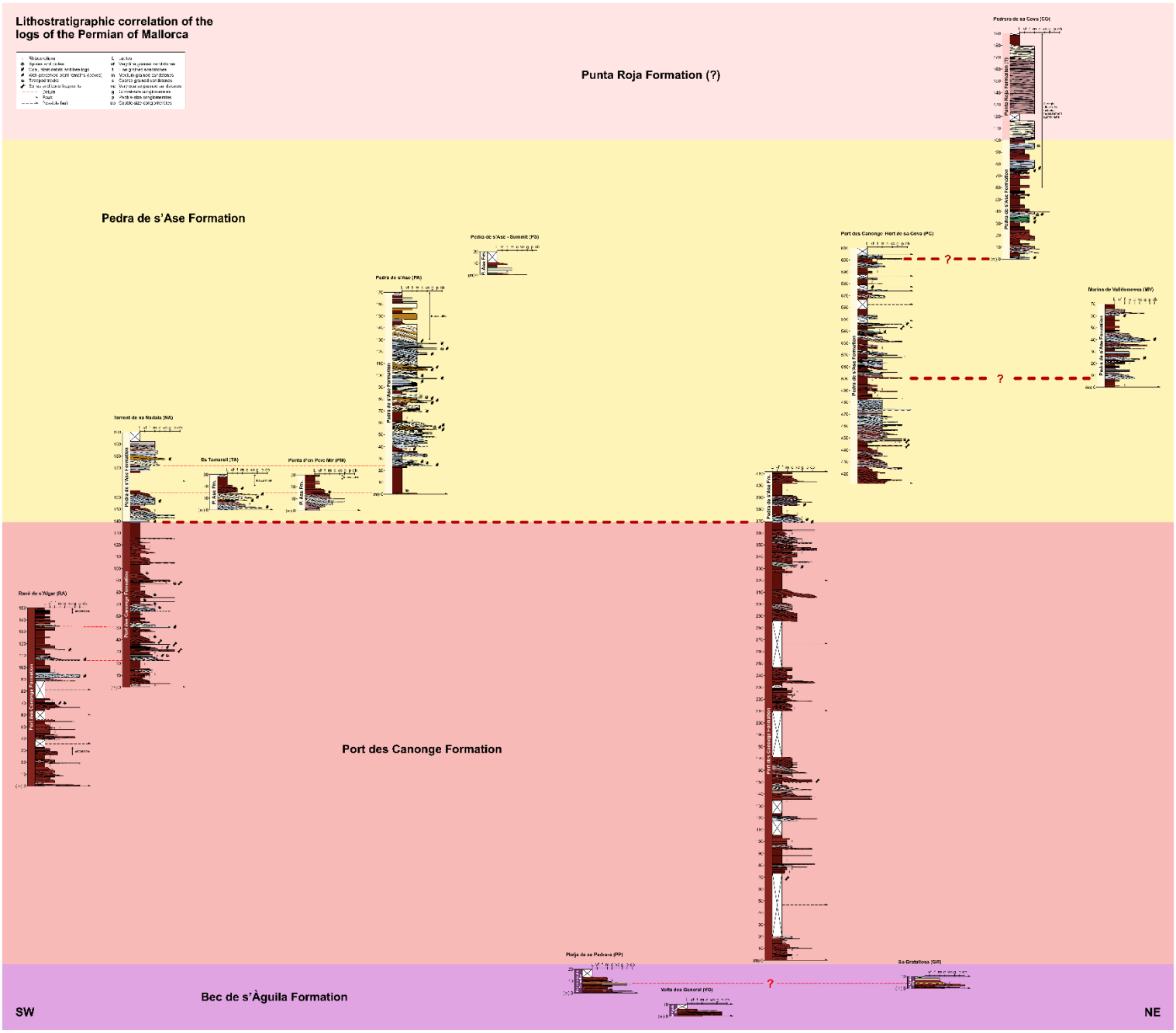
Lithostratigraphic correlation of the logs of the Permian of Mallorca
Punta Roja Formation (?)
Pedra de s'Ase Formation
Port des Canonge Formation
Bec de s'Àguila Formation
SW
NE
Pedrera de sa Geva (CG)
Port des Canonge- Hort de sa Geva (PC)
Marina de Valldemossa (MV)
Pedra de s'Ase - Summit (PS)
Pedra de s'Ase (PA)
Torrent de na Nadala (NA)
Es Tomaresll (TA)
Punta d'en Pere Mir (PM)
Raxó de s'Alger (RA)
Platja de sa Pedrera (PP)
Volta des General (VG)
Sa Gratallosa (GR)

Supplementary Table 2

Supplementary Table 2. ChRM and VGP computed directions for all samples from the three studied sections. Type τ1 denote principal component analysis linear fits and τ1 (τ3) represent directions derived from great circle fit.

Pedrera de sa Cova section_CO_NTC

sample	declination	inclination	reference	core azimuth	core dip	bedding strike	bedding dip	level_m	MAD	type	VGP_long	VGP_lat
CO1A	173,40	-12,80	tectonic	156	26	66	26	3,25	11,20	τ1 (τ3)	160,66	-82,35
CO2A	161,40	-27,40	tectonic	156	26	66	26	4,00	14,40	τ1 (τ3)	163,86	-68,09
CO3A	187,10	-7,30	tectonic	156	26	66	26	4,50	7,52	τ1 (τ3)	300,74	-82,83
CO4A	187,60	-28,80	tectonic	156	26	66	26	6,50	15,03	τ1 (τ3)	249,58	-75,17
CO6A	175,40	-21,20	tectonic	156	26	66	26	13,50	2,89	τ1 (τ3)	191,42	-80,44
CO7A	171,70	-16,00	tectonic	156	26	66	26	15,25	12,31	τ1 (τ3)	164,10	-80,03
CO8A	172,00	-25,40	tectonic	156	26	66	26	15,75	11,51	τ1 (τ3)	183,87	-76,62
CO10A	162,00	-25,80	tectonic	156	26	66	26	21,75	3,10	τ1 (τ3)	162,46	-69,07
CO11A	182,40	-9,30	tectonic	156	26	66	26	23,50	9,31	τ1 (τ3)	268,24	-86,81
CO12A	182,80	-9,30	tectonic	156	26	66	26	24,50	9,78	τ1 (τ3)	272,55	-86,50
CO13A	192,30	28,10	tectonic	156	26	66	26	37,75	24,96	τ1	5,25	-68,66
CO14A	177,90	-17,10	tectonic	156	26	66	26	39,75	9,14	τ1 (τ3)	201,10	-83,48
CO15A	192,70	-5,20	tectonic	156	26	66	26	42,25	32,14	τ1 (τ3)	309,25	-77,31
CO16A	178,00	-10,60	tectonic	156	26	66	26	43,50	24,51	τ1 (τ3)	184,05	-86,58
CO17A	189,50	53,00	tectonic	156	26	66	26	44,75	14,49	τ1	26,56	-52,77
CO18A	182,30	-33,40	tectonic	156	26	66	26	46,25	6,16	τ1 (τ3)	227,73	-74,16
CO19A	210,10	-3,30	tectonic	156	26	66	26	46,75	3,41	τ1	310,84	-59,91
CO20A	210,90	11,60	tectonic	156	26	66	26	67,00	2,29	τ1	325,05	-58,01
CO22A	180,90	10,00	tectonic	156	26	66	26	73,00	13,30	τ1	32,96	-82,34
CO23A	154,30	2,60	tectonic	156	26	66	26	74,00	10,62	τ1	121,42	-64,02
CO25A	224,40	-24,70	tectonic	156	26	66	26		18,58	τ1 (τ3)	293,92	-44,88

Racó de s'Algar–Pedra de s'Ase section_RA_NA_NTC

sample	declination	inclination	reference	core azimuth	core dip	bedding strike	bedding dip	level_m	MAD	type	VGP_long	VGP_lat
RA1A	171,18	-29,16	tectonic	80	32	350	32	67,75	11,77	t1 (t3)	186,74	-74,27
RA2A	179,59	-11,47	tectonic	80	32	350	32	69	1,32	t1 (t3)	212,83	-86,66
RA4A	166,85	-32,77	tectonic	80	32	350	32	73,4	18,74	t1 (t3)	180,64	-69,97
NA2A	175,84	-24,73	tectonic	295	52	350	32	95,46	35,40	t1 (t3)	198,22	-78,74
NA4A	219,81	-2,62	tectonic	115	14	25	14	98,96	14,29	t1	310,63	-50,21
NA5A	168,84	-21,08	tectonic	80	32	350	32	99,46	19,07	t1 (t3)	167,37	-76,05
NA6A	189,03	-17,94	tectonic	80	32	350	32	101,46	8,66	t1	272,54	-78,83
NA9A	188,57	-7,52	tectonic	80	32	350	32	105,71	12,36	t1	301	-81,32
NA10A	168,36	-33,05	tectonic	80	32	350	32	107,96	14,53	t1 (t3)	184,16	-70,77
NA12A	176,63	-18,78	tectonic	80	32	350	32	110,96	29,98	t1 (t3)	194,58	-82,07
NA14A	138,79	-1,46	tectonic	80	32	350	32	113,46	8,35	t1	127,96	-48,78
NA17A	167,46	22,41	tectonic	80	32	350	32	117,71	15,13	t1	80,75	-71,18
NA18A	159,96	-6,58	tectonic	80	32	350	32	119,46	13,10	t1	132,51	-70,01
NA20A	178,81	-13,97	tectonic	80	32	350	32	124,96	16,27	t1	205,19	-85,23
NA22A	146,69	-14,91	tectonic	80	32	350	32	128,21	23,01	t1	139,65	-56,46
NA23A	144,57	-8,66	tectonic	80	32	350	32	137,71	13,99	t1	133,72	-54,62
NA24A	183,16	-26,34	tectonic	80	32	350	32	139,21	5,33	t1	235,01	-78,18
NA25A	176,53	-22,90	tectonic	80	32	350	32	140,21	25,12	t1 (t3)	199,66	-79,95
NA26A	197,50	-13,01	tectonic	80	32	350	32	140,71	6,83	t1	295,86	-72,08
NA28A	217,35	-6,59	tectonic	80	32	350	32	142,96	6,29	t1	307,47	-52,74
NA30A	191,19	-1,07	tectonic	104	30	14	30	146,21	36,02	t1 (t3)	319,32	-78,64
NA32A	175,43	-21,47	tectonic	80	32	350	32	149,96	5,87	t1 (t3)	192,08	-80,22
NA34A	181,04	-5,74	tectonic	104	30	14	30	153,71	1,01	t1	289,47	-88,94
NA36A	187,66	-24,73	tectonic	104	30	14	30	158,21	6,51	t1	255,33	-77,06
NA38A	178,15	4,80	tectonic	104	30	14	30	162,71	6,22	t1	60,9	-84,75
NA40A	196,73	-30,02	tectonic	104	30	14	30	165,71	20,65	t1	269,01	-68,66
NA41A	198,10	-0,06	tectonic	80	32	350	32	166,71	11,28	t1	317,08	-71,74
NA42A	178,40	-19,15	tectonic	104	30	14	30	168,71	21,00	t1 (t3)	207,51	-82,5
NA44A	176,59	-2,64	tectonic	104	30	14	30	170,21	0,86	t1	110,44	-86,4
NA46A	182,71	-10,53	tectonic	104	30	14	30	173,71	6,10	t1 (t3)	263,43	-86,11

Port des Canonge–Hort de sa Cova section_VG_PP_PC_NTC												
sample	declination	inclination	reference	core azimuth	core dip	bedding strike	bedding dip	level_m	MAD	type	VGP_long	VGP_lat
VG2A	173,55	-20,79	tectonic	305	65	347	34		10,57	t1	140,64	-65,81
VG1A	156,05	-13,38	tectonic	250	90	7	9		9,89	t1 (t3)	182,25	-79,62
VG3A	184,18	1,46	tectonic	365	25	347	34	1,5	19,81	t1 (t3)	347,81	-84,66
VG4A	183,03	-14,52	tectonic	290	65	347	34	3	12,63	t1	251,4	-84,33
VG5A	191,54	-4,15	tectonic	77	34	347	34	4,5	23,49	t1 (t3)	311,94	-78,5
PP1A	234,45	-25,62	tectonic	77	33	347	33	20,01	2,46	t1	295,01	-35,07
PP2A	172,61	0,07	tectonic	77	33	347	33	23,26	5,96	t1	110,44	-82,16
PC1A	182,65	-11,28	tectonic	85	32	355	32	52,12	17,27	t1 (t3)	260,09	-85,85
PC3A	209,52	-63,69	tectonic	255	45	355	32	55,12	17,30	t1 (t3)	246,57	-40,01
PC4A	181,47	-10,38	tectonic	330	85	355	32	55,87	9,44	t1 (t3)	248,71	-86,92
PC6A	181,64	-40,03	tectonic	80	42	355	32	59,37	22,58	t1	223,96	-69,73
PC8A	154,80	0,65	tectonic	35	45	355	32	62,12	7,06	t1	123,6	-64,65
PC9A	214,84	9,52	tectonic	85	32	355	32	63,37	20,49	t1	321,59	-54,47
PC10A	183,13	4,96	tectonic	130	30	355	32	63,87	26,11	t1	8,16	-84,07
PC11A	167,80	15,20	tectonic	85	32	330	31	119,62	5,97	t1	89,4	-74,06
PC12A	185,72	-19,74	tectonic	60	31	330	31	121,37	6,69	t1	256,13	-80,52
PC13A	157,70	13,19	tectonic	85	32	330	31	122,87	12,02	t1	107,05	-65,9
PC15A	181,66	-38,46	tectonic	85	32	330	31	124,87	2,50	t1	224,51	-70,79
PC16A	180,44	20,12	tectonic	85	32	330	31	125,62	6,46	t1	37,94	-77,07
PC18A	114,04	-58,17	tectonic	85	32	330	31	127,62	3,22	t1	170,46	-20,13
PC20A	123,96	3,66	tectonic	85	32	330	31	130,62	4,27	t1	125,75	-33,84
PC22A	148,32	17,15	tectonic	85	32	330	31	132,37	0,00	t1	109,67	-56,44
PC24A	119,61	-40,62	tectonic	85	32	330	31	134,87	1,99	t1	154,74	-28,1
PC25A	180,44	-8,54	tectonic	60	31	330	31	137,62	20,46	t1 (t3)	232,73	-88,23
PC27A	185,57	3,26	tectonic	60	31	330	31	140,62	3,57	t1	346,53	-83
PC29A	154,82	2,45	tectonic	60	31	330	31	144,12	2,48	t1	121,52	-64,53
PC31A	208,12	5,66	tectonic	60	31	330	31	145,62	11,00	t1	320,41	-61,39
PC33A	175,60	-2,76	tectonic	60	31	330	31	149,12	20,44	t1	115,14	-85,46
PC138A	200,27	-23,36	tectonic	55	35	325	35	186,62	5,41	t1	283,01	-67,7
PC141A	144,54	-7,76	tectonic	55	35	325	35	190,12	3,37	t1	132,87	-54,53
PC145A	157,21	-6,09	tectonic	55	35	325	35	200,37	1,94	t1	131,53	-67,22
PC146A	208,60	-11,66	tectonic	55	35	325	35	203,12	4,96	t1	302,04	-61,29
PC147A	148,89	-5,23	tectonic	55	35	325	35	204,87	13,67	t1	130,52	-58,93
PC149A	169,75	-15,42	tectonic	55	35	325	35	212,12	2,41	t1	157,61	-78,55
PC34A	191,32	-0,68	tectonic	70	32	340	32	212,12	27,25	t1 (t3)	320,54	-78,49
PC35A	188,88	-27,23	tectonic	70	32	340	32	212,37	7,29	t1	255,72	-75,24
PC36A	180,93	-7,55	tectonic	70	32	340	32	212,62	3,24	t1	256,14	-88,49
PC38A	195,22	1,78	tectonic	70	32	340	32	214,87	18,70	t1 (t3)	322,31	-74,42
PC152A	181,54	-7,35	tectonic	55	35	325	35	215,62	6,22	t1	273	-88,13
PC40A	201,64	-12,32	tectonic	70	32	340	32	217,37	3,72	t1	299,3	-68,16
PC42A	172,54	-16,66	tectonic	102	30	12	30	259,12	26,86	t1 (t3)	168,71	-80,44
PC44A	170,13	-22,30	tectonic	102	30	12	30	263,62	5,58	t1 (t3)	172,83	-76,66
PC46A	184,32	-21,00	tectonic	102	30	12	30	268,87	4,28	t1	246,67	-80,65
PC47A	180,80	-12,23	tectonic	102	30	12	30	271,62	9,93	t1 (t3)	232,1	-86,29
PC48A	151,43	-7,69	tectonic	102	30	12	30	275,12	0,00	t1	133,1	-61,42
PC49A	192,17	-26,44	tectonic	102	30	12	30	282,62	0,00	t1	265,64	-73,42
PC50A	150,70	-47,16	tectonic	102	30	12	30	283,62	14,22	t1 (t3)	175,35	-51,97
PC52A	178,29	-9,33	tectonic	102	30	12	30	290,87	15,55	t1	181,22	-87,28
PC54A	229,97	-46,89	tectonic	102	30	12	30	336,62	30,79	t1 (t3)	276,3	-35,97
PC56A	201,28	-11,59	tectonic	102	30	12	30	341,12	11,94	t1 (t3)	300,15	-68,5
PC58A	195,59	-10,92	tectonic	90	28	355	28	347,37	17,85	t1	298,48	-74,16
PC60A	171,95	-15,92	tectonic	90	28	355	28	358,12	12,46	t1 (t3)	164,91	-80,29
PC61A	177,31	-17,58	tectonic	90	28	355	28	373,87	14,32	t1 (t3)	197,25	-83
PC63A	235,78	16,99	tectonic	90	28	355	28	378,37	1,60	t1	321,83	-33,25
PC64A	185,82	13,96	tectonic	90	28	355	28	381,87	4,00	t1	8,79	-78,74
PC65A	198,77	-14,06	tectonic	90	28	355	28	398,87	17,62	t1 (t3)	295,2	-70,71
PC67A	143,24	-4,06	tectonic	90	28	355	28	401,87	3,46	t1	129,72	-53,23
PC68A	221,15	-15,66	tectonic	90	28	355	28	405,62	12,18	t1 (t3)	300,48	-48,64
PC70A	167,03	-22,95	tectonic	90	28	355	28	410,12	8,97	t1 (t3)	166,4	-74,07
PC72A	164,34	-54,45	tectonic	90	28	355	28	415,37	7,44	t1 (t3)	197,33	-54,4
PC74A	204,69	-1,25	tectonic	90	24	360	24	421,62	8,10	t1	313,68	-65,24
PC75A	155,98	-6,18	tectonic	90	24	360	24	423,12	2,67	t1	131,62	-66,02
PC76A	179,31	-13,42	tectonic	90	24	360	24	424,62	13,92	t1 (t3)	210,39	-85,7
PC78A	186,15	-4,51	tectonic	90	24	360	24	426,37	13,19	t1 (t3)	312,35	-83,9

PC79A	183,04	-14,18	tectonic	90	24	360	24	439,12	3,85	t1 (t3)	252,26	-84,46
PC81A	178,36	-9,32	tectonic	90	24	360	24	443,12	6,75	t1	182,9	-87,34
PC83A	160,27	-25,26	tectonic	2	34	360	24	448,37	13,09	t1 (t3)	159,65	-67,75
PC84A	183,50	16,34	tectonic	90	24	360	24	450,12	4,63	t1	21,93	-78,59
PC85A	247,04	-4,91	tectonic	90	24	360	24	452,12	12,25	t1	308,12	-23,07
PC86A	165,05	-19,05	tectonic	90	24	360	24	469,87	36,10	t1 (t3)	156,2	-73,44
PC87A	179,01	-13,62	tectonic	90	24	360	24	480,12	27,06	t1 (t3)	206,83	-85,54
PC90A	177,62	-14,14	tectonic	90	24	360	24	488,87	4,12	t1 (t3)	192,37	-84,81
PC91A	205,00	8,54	tectonic	90	24	360	24	491,12	21,99	t1 (t3)	324,92	-64,1
PC92A	191,80	-8,41	tectonic	90	24	360	24	492,62	7,55	t1 (t3)	301,3	-78,1
PC93A	157,26	-20,14	tectonic	70	10	340	10	494,62	14,07	t1 (t3)	149,87	-66,15
PC94A	247,24	-72,45	tectonic	70	10	340	10	505,87	13,22	t1 (t3)	250,32	-14,18
PC95A	157,85	-28,30	tectonic	70	10	340	10	530,12	14,19	t1 (t3)	160,78	-64,79
PC98A	198,81	-11,55	tectonic	85	26	355	26	535,87	7,55	t1 (t3)	299,08	-70,96
PC101A	193,95	-6,66	tectonic	85	26	355	26	539,87	11,40	t1 (t3)	306,01	-76,1
PC102A	176,10	1,29	tectonic	85	26	355	26	541,87	22,21	t1	90,37	-84,96
PC103A	128,73	3,38	tectonic	85	26	355	26	543,12	14,63	t1 (t3)	125,49	-38,54
PC104A	208,84	-1,31	tectonic	85	26	355	26	547,12	4,74	t1 (t3)	312,99	-61,15
PC107A	173,23	-16,69	tectonic	85	26	355	26	553,62	31,59	t1 (t3)	171,45	-80,97
PC109A	187,33	-6,93	tectonic	85	26	355	26	554,62	3,66	t1 (t3)	302,38	-82,65
PC111A	149,56	-36,38	tectonic	85	26	355	26	564,12	23,34	t1 (t3)	162,8	-55,47
PC114A	157,62	-18,29	tectonic	85	26	355	26	566,37	10,88	t1 (t3)	147,73	-66,71
PC116A	186,59	-7,41	tectonic	85	26	355	26	569,87	4,90	t1 (t3)	299,5	-83,31
PC119A	183,90	-7,68	tectonic	85	26	355	26	574,12	12,74	t1 (t3)	290,91	-85,89
PC126A	169,32	-5,88	tectonic	76	24	346	24	600,87	6,06	t1	132,14	-79,3
PC128A	172,95	-21,23	tectonic	76	24	346	24	628,37	7,55	t1 (t3)	180,53	-79,08
PC130A	155,42	-36,09	tectonic	76	24	346	24	631,62	20,86	t1 (t3)	167,58	-60,3
PC133A	167,71	-29,31	tectonic	76	24	346	24	637,62	7,92	t1 (t3)	177,73	-72,14
PC135A	169,12	-19,64	tectonic	76	24	346	24	639,87	7,25	t1 (t3)	165,06	-76,8

Supplementary Table 3

Supplementary Table 3. Palaeomagnetic ChRM section and overall means and corresponding statistical parameters in geographic (NTC) and tectonic (TC) coordinates.

N	Ns	L	GC	Cutoff	S	Dec	Inc	R	k	α_{95}	K	A95	A95min	A95max	ΔDx	ΔIx	λ
Pedrera de sa Cova section_CO_NTC																	
21	21	6	15	45	20,45	183,1	-9,15	18,97	9,87	10,66	16,1	8,17	3,55	12,05	8,2	16,04	-4,6
Pedrera de sa Cova section_CO_TC																	
20	21	6	15	45	19,25	185,6	-31,4	18,24	10,82	10,4	18,05	7,9	3,62	12,42	8,26	12,59	-17
Racó de s'Algar–Pedra de s'Ase section_RA_NA_NTC																	
29	30	18	12	45	17,95	169,7	-12,7	27,07	14,54	7,27	20,75	6,02	3,12	9,83	6,06	11,6	-6,4
Racó de s'Algar–Pedra de s'Ase section_RA_NA_TC																	
30	30	18	12	45	19,11	178,8	-14,1	27,99	14,44	7,16	18,47	6,28	3,08	9,62	6,33	12,01	-7,2
Port des Canonge–Hort de sa Cova section_VG_PP_PC_NTC																	
86	93	46	47	45	20,5	171,2	-14,5	79,12	12,35	4,53	16,01	3,94	2,02	4,96	3,97	7,51	-7,4
Port des Canonge–Hort de sa Cova section_VG_PP_PC_TC																	
83	93	46	47	45	18,96	178,4	-11,4	77,09	13,88	4,33	18,64	3,7	2,05	5,07	3,72	7,18	-5,7
All_samples_NTC																	
134	144	70	74	45	19,65	172,7	-13,4	123,5	12,64	3,57	17,41	3,01	1,69	3,75	3,03	5,77	-6,8
All_samples_TC																	
133	144	70	74	45	19,49	179,4	-14,9	122,3	12,37	3,63	17,66	3	1,7	3,77	3,02	5,69	-7,6

Supplementary Table 4

	The present work																												
	P-PA-05	P-PA-09	P-PA-12	P-CO-03	P-CO-04	Ramos & Doubinger (1989)	Diez (2000) (MA-1)	Juncal (2019) (MA-1)		Bercovici *et al.* (2009)		"Thuringian"	Pre-Permian	Asselian	Sakmarian	Artinskian	Kungurian	Roadian	Wordian	Capitanian	Wuchiapingian	Changhsingian	Induan	Olenekian	Anisian	Ladinian	Post-Ladinian
Spores																													
Calamospora pedata Kosanke, 1950										x			x	(x)	(x)	(x)	(x)	x	(x)	(x)	x	x	x					
Calamospora sp.							x	x		x																			
Deltoidospora sp.								x																					
Densoisporites nejburgii (Schulz) Balme, 1970										x												x	x	x	x	x	x		
Densoisporites sp.								x																					
Endosporites velatus Leschik, 1956						x						x									x	(x)	(x)	x	x	x		
Endosporites hexareticulatus Klaus, 1963										cf.									?x	(x)	x	x							
Endosporites sp.			x				x	x		x																			
Granulatisporites sp.	x	x		x																									
Kraeuselisporites spinosus Jansonius, 1962							cf.	cf.											?x	x	(x)	x	x	x	x				
Leiotriletes sp.							x																						
Lundbladispora sp.							x			x																			
Lycospora sp.								x																					
Osmundacidites sp.			x																										
Palaeospongisporis europeus Schulz, 1965										x															x	x	x		
Playfordispora cancellosa (Playford *et* Dettmann) Mahesl										x												x	x	x	x	(x)	x		
Reticulatisporites sp.	x																												
Uvaesporites sp.								x																					
Verrucosisporites sp.								x																					
Pollen																													
Alisporites opii Daugherty, 1941							x	x														x	(x)	(x)	x				
Alisporites splendens (Leschik) Foster, 1941	x	x	x				x						?x	x	(x)	(x)	x	x	x	x	x	x	(x)	(x)	x				
Alisporites spp.		x	x				x	x																					
Bascanisporites sp.							?	x																					
Chordasporites sp.	x	x		x			x	x		x																			
Cordaitina sp.		?					x	x		x																			
Crucisaccites variosulcatus Djupina, 1971						x	x	x		x						x	x	x	x	x	x	x	x						
Crustaesporites sp.						x																							
Falcisporites stabilis Balme, 1970										x												x	x	x	x	x	x		
Falcisporites zapfei (Potonié *et* Klaus) Klaus, 1963			x			x	x	x		x		x	?x	(x)	(x)	x	x	x	x	(x)	x	x	x	x	x				
Falcisporites sp.	x	x						x		x																			
Gardenasporites heisseli Klaus, 1963								x				x			?x	(x)	(x)	x	x	x	x								
Gardenasporites leonardii Klaus, 1963			x									x						x	x	x	x	x							
Gardenasporites sp.		x		x			x	x																					
Gigantosporites aletoides Klaus, 1963	x	x															x	(x)	(x)	(x)	x	x							
Illinites unicus Kosanke emend. Jansonius *et* Hills, 1976										x			x	x	x	x	(x)	x	x	(x)	x	x	(x)	(x)	x	x			
Illinites sp.	x		x							x																			
Jugasporites delasaucei (Potonié *et* Klaus) Leschik, 1956			x			x						x					x	(x)	(x)	(x)	x	x	x					
Jugasporites sp.			x							x																			
Klausipollenites schaubergeri (Potonié *et* Klaus) Jansoniu	x	x	x		x	x	x	x				x					x	(x)	?x	x	x	x	x	x	x	x	x		
Klausipollenites sp.		x		x			x	x		x																			
Limitisporites rectus Leschik, 1956	x												x	(x)	(x)	(x)	x	(x)	(x)	(x)	x	x	(x)	(x)	x				
Limitisporites sp.	x		x	x	x																								
Lueckisporites globosus Klaus, 1963		x						x		x		x						x	x	x	x	x							
Lueckisporites hyalinus Schaarschmidt, 1963							x													?x	x	x	(x)	x	x				
Lueckisporites parvus Klaus, 1963	x			x						x								x	x	x	x	x	(x)	(x)	x				
Lueckisporites singhii Balme, 1970								x		x		x		?x	(x)	x	(x)	x	(x)	(x)	(x)	x	(x)	(x)	x				
Lueckisporites virkkiae (Potonié *et* Klaus) Klaus, 1963	x	x	x	x	x	x	x	x		x		x					x	x	?x	x	x	x	x	(x)	(x)	(x)	x		
Lueckisporites sp.						x	x	x																					
Lunatisporites albertae Jansonius, 1962								x															x	x					
Lunatisporites noviaulensis (Leschik) Fischer, 1979							x	x		x					?x	(x)	(x)	(x)	x	x	x	x	x	x	x	x	x	x	
Lunatisporites pellucidus (Goubin, 1965) De Jersey, 1971		cf.						x		x					x	(x)	(x)	(x)	x	x	(x)	x	x	x	x	x	x	x	
Lunatisporites variesectus Archangelsky *et* Gamerro, 1979								x							x	(x)	x	(x)	(x)	(x)	x	x							
Lunatisporites sp.				x	x		x																						
Maculatasporites sp.							x			x																			
Marsupipollenites sp.			x																										
Minutosaccus sp. 1		x																											
Nuskoisporites dulhuntyi Potonié *et* Klaus, 1954		x				x	x	x				x		x	x	(x)	(x)	(x)	x	x	x	x	(x)	(x)	x				
Nuskoisporites klausii Grebe, 1957							cf.	x		cf.							x	x	(x)	(x)	x	x							
Nuskoisporites sp.	x	x					x			x																			
Paravesicaspora splendens (Leschick) Klaus, 1963						x	cf.	cf.				x					x	x	x	x	x	x							
Paravesicaspora sp.	x									x																			
Platysaccus leschikii Hart, 1960	x						x			x					x	x	(x)	x	x	(x)	(x)	x	(x)	x	x				
Playfordispora cancellosa (Playford *et* Dettmann) Mahesl	x									x								x	x	x	(x)	x	x	x	x	(x)	x		
Platysaccus papilionis Grebe, 1957								x				x						x	x	x	x	x	x	x	x				
Platysaccus sp.										x																			
Potonieisporites novicus Bharadway, 1954							x	x					x	x	x	x	(x)	(x)	(x)	(x)	(x)	x	x	(x)	x	x			
Potonieisporites sp.								x																					

Protohaploxypinus microcorpus (Schaarschmidt) Balme, 1						x	x	x		x				x	x	x	(x)	(x)	x	x	x	x	x	x	x	
Protohaploxypinus limpidus (Balme *et* Hennely) Balme *et*	x									x					x	x	(x)	(x)	x	(x)	x	x	x	(x)	x	x
Protohaploxypinus perfectus (Naumova ex. Kara-Murza) S										x					x	(x)	x	x	x	(x)	x	x				
Protohaploxypinus sp.		x																								
Sahnisporites saarensis Bharabwaj, 1954							x	x				x	(x)	(x)	(x)	(x)	(x)	(x)	(x)	x	x					
Striatoabieites richteri (Potonié et Klaus) Hart, 1964	x									x			x	(x)	x	x	(x)	(x)	(x)	x	x	x	x	(x)	x	
Striatoabieites sp.										x																
Striatopodocarpites sp.								x																		
Strotersporites sp.			x							x																
Taeniaesporites sp.										x																
Tiwariasporis sp.										x																
?*Triadispora* spp.	x																									
Vesicaspora sp.	x	x								x																
Vitreisporites sp.		x								x																
Vittatina angulistriata Klaus, 1963										x								x	x	(x)	x					
Vittatina sp.		x																								
	20	19	14	8	4	11	30			44																
Thuringian sensu Visscher (1968) = Late Permian = Zechstein																										
Today Zechstein = Wuchiapingian *p.p.* - Changhsingian *p.p.* (see Legler & Schneider, 2013)																										

Supplementary Table 5

Museum collection number	UIB174620						Left *in situ*		
IDENTIFICATION	*Hyloidichnus bifurcatus*, large morphotype						*Hyloidichnus bifurcatus*, large morphotype		
Specimen	NA-25.6-01a	NA-25.6-01b	NA-25.6-01c	NA-25.6-01d	NA-25.6-01e	NA-25.6-01f	NA-26.0-02c	NA-26.0-02d	NA-26.0-02e
Anatomy	Right manus	Left pes	Left manus	Right pes	Left pes	Left manus	Right pes	Right manus	Left pes
PARAMETERS OF THE TRACKS									
Length (cm)		9,36	8,04	9,46	9,03	7,79	10,12	7,56	9,77
Width (cm)		11,23	10,02		11,55	9,32	11,92	9,42	
Length sole (cm)		4,09	5,12	4,86	3,91	3,16	4,78	3,28	4,30
Width sole (cm)		6,72	7,29	6,58	5,99	6,10		5,30	
Length I (cm)			1,63	4,20	1,93	2,81	3,62	2,46	3,06
Length II (cm)			2,43	4,34	2,50	3,59	3,99	3,12	4,99
Length III (cm)		4,03		4,42	5,50	4,74	5,35	4,29	5,88
Length IV (cm)		6,12	3,81	5,53	6,39	5,42		5,40	
Length V (cm)	2,48	4,07	2,00			2,62			
Divergence angle I–II (º)			45,25	10,52	24,72	19,56		17,38	38,33
Divergence angle II–III (º)		18,80	35,60	24,34	22,38	14,58	27,06	24,42	21,07
Divergence angle III–IV (º)			14,02	10,26	16,15	16,85		10,65	
Divergence angle IV–V (º)		63,58	39,70			26,52		29,72	
Divergence angle I–V (º)			134,43			77,74		82,77	
Divergence angle II–V (º)		85,67	89,77		63,34	58,04		52,93	
Divergence angle II–IV (º)		21,85	49,96	35,27	38,66	31,47		35,74	
PARAMETERS OF THE TRACKWAYS									
Pace angulation pes (º)		92,94							
Pace angulation manus (º)	95,62								
Divergence angle pes (º)		-8,38		3,37		36,61	-1,43		-0,71
Divergence angle manus (º)			37,48		1,41			34,16	
Stride pes (cm)		41,99							
Stride manus (cm)			42,68						
Pace pes (cm)		30,36		27,54			33,82		
Pace manus (cm)									
Length pace pes (cm)		22,86		19,12			21,14		
Length pace manus (cm)									
Width pace pes (cm)		19,95		19,68					
Width pace manus (cm)									
Interpes distance (cm)									
Intermanus distance (cm)	11,85								
Manus-pes distance (cm)			13,51		14,48		13,17		
Width external (cm)									
Width internal (cm)							9,70		
Glenoacetabular distance (cm)	35,47								

Note 1: Cells in yellow indicate approximate or extrapolated values.
Note 2: Negative numbers in divarication angles indicate lateral (outwards) rotation of the track.
Note 3: For measurements of cf. *Dimetropus* isp., see Matamales-Andreu *et al.* (2021b).

Left *in situ*					DA21/15-14-01		TS-3		DA21/15-07-09	
Hyloidichnus bifurcatus, large morphotype					*Hyloidichnus bifurcatus*, large morphotype		*Hyloidichnus bifurcatus*, small morphotype		*Hyloidichnus bifurcatus*, small morphotype	
NA-77.5-01a	NA-77.5-01b	NA-77.5-01c	NA-77.5-01d	NA-77.5-01e	PM-15.7-01a	PM-15.7-01b	NA-26.0-09r	NA-26.0-09s	NA-60.4-02a	NA-60.4-02b
Left pes	Left manus	Left pes	Left manus	Right pes	Right pes	Right manus	Right pes	Right manus	Left pes	Left manus
9,57	8,39	8,73	7,69	7,14	8,33	6,29	4,01	3,03	4,99	3,53
10,19		12,06	8,80				5,18	4,65		4,86
4,78	4,44	4,16	3,40	3,54	2,93	2,71	1,77	0,95	1,45	1,23
5,89		5,68	4,85	5,20	5,85	5,69	2,27	2,17		2,88
3,33	2,19	3,64	2,21	3,24	3,84	1,62	1,55			1,54
4,22	2,84	4,10	3,21	3,87	4,53	3,38	1,70	1,69	2,49	1,69
4,57	3,15	4,79	4,57		5,06	3,59	2,18	2,12	2,96	2,32
5,75	4,53	5,02	4,84	4,55	5,82	4,20	2,78	2,24	3,78	2,68
		4,08	3,09				1,77			1,75
33,88	13,57	20,88	16,38	37,13	18,23	10,17	39,77	45,96		31,43
		32,75	11,31	21,48	30,26		19,30	21,47	22,03	23,81
25,85	10,10	17,61	20,31	23,03	9,00	16,46	29,57	25,19	21,13	30,67
		62,93	36,65				33,06	42,74		23,23
		134,94	85,10				122,15	135,03		110,51
		71,31	48,15	81,89			81,51	89,54		79,13
27,96	8,83	50,29	31,56	44,51	39,83	20,65	48,45	46,79	42,85	55,08
			18,58			29,20		20,40		47,11
19,90		11,72		8,15			4,93		6,47	

Left *in situ*		Left *in situ*	Left *in situ*	DA21/15-07-06	UIB174620	UIB174620	Left *in situ*	
Hyloidichnus bifurcatus, small morphotype		*Dromopus* isp.	*Dromopus* isp.	*Pachypes* cf. *ollieri*	*Dimetropus leisnerianus*	*Dimetropus leisnerianus*	*Dimetropus leisnerianus*	
NA-60.4-04a	NA-60.4-04b	NA-77.5-01f	NA-77.5-01g	NA-60.6-01a	NA-25.6-01g	NA-25.6-01h	NA-26.0-02f	NA-26.0-02g
Left pes	Left manus	Right ?pes	Right ?pes	Right pes	Left pes	Right pes	Right pes	Right manus
5,63	4,58	1,09	2,58	9,52	4,00			
6,07	5,12		2,11	9,49	3,91			
1,38	1,84	0,27	1,04	5,25	1,60		2,98	
3,10	2,88	0,44	0,71	7,56	2,50			
	1,48	0,28	0,80	3,25	1,81			
3,09	2,39	0,50	1,10	3,76	2,10			
4,13	2,78	0,71	1,82	4,22	2,26			
4,50		0,92	2,44	5,17	2,44			1,98
	1,84			2,16	1,40			
	31,01	32,00			27,68			
20,90	22,61	23,36	30,98	19,39	2,91		29,56	
12,84	21,21	28,12	29,09	18,60	20,45		3,73	
24,01	17,95	43,56		45,16	0,81		51,82	
	92,99			81,79	54,07			
57,37	62,20			83,30	23,10		85,76	
33,79	43,97	51,07	58,66	38,22	23,52		33,70	
	11,62							
4,77								

Left *in situ*									
Dimetropus leisnerianus									
NA-26.0-03b	NA-26.0-03c	NA-26.0-03d	NA-26.0-03e	NA-26.0-03f	NA-26.0-03g	NA-26.0-03h	NA-26.0-03i	NA-26.0-03j	NA-26.0-03k
Left pes	Left manus	Right pes	Right manus	Left pes	Left manus	Right pes	Right manus	Left pes	Left manus
					4,40				
			4,32					5,16	
		3,12	3,03		2,30			1,90	
		3,58	2,57		2,68			2,83	
			0,82			1,46	0,85	1,78	
					1,48			1,90	
				1,67	1,78				
	1,50			2,45	2,31				
	12,75		1,03		1,19				
		60,06	52,36					28,65	
								13,06	
		10,23		1,75	22,19			9,03	
	39,96	56,32	49,00		21,98				
		117,50	144,31						
		61,15	92,78		33,32				
			43,61		11,33			51,38	
		9,45		-2,77				9,36	
					20,38				
		25,07		25,60					
	23,24		30,26		20,99				
		15,75		16,54		14,64			
	14,99		15,29		17,28		13,97		
		11,72		13,41		12,27			
	12,13		11,08		13,94		12,24		
		10,32		9,80		8,19			
	8,89		10,50		10,26		6,82		
						3,32			
		5,25		4,61		5,19		5,16	
	15,63								
	3,32								
		19,45				18,12			

TS-3										
Dimetropus leisnerianus										
NA-26.0-09g	NA-26.0-09h	NA-26.0-09i	NA-26.0-09j	NA-26.0-09k	NA-26.0-09l	NA-26.0-09m	NA-26.0-09n	NA-26.0-09o	NA-26.0-09p	NA-26.0-09q
Left manus	Right pes	Right manus	Left pes	Left manus	Right pes	Right manus	Left pes	Left manus	Right pes	Right manus
3,70						4,90	6,16	3,95		
4,81	6,30					4,81	5,40	3,87		
1,83	3,21	2,97				2,68	3,23	2,21		
2,50						3,15	3,51	2,58		
	1,37	0,61	1,84			0,96	1,98	0,79		
	2,04					1,41	2,20	1,39		
						2,72	2,83	1,74		
2,33		0,71				1,07	3,18	2,01	2,10	
68,73		0,82				0,54	1,77	1,24		0,75
	19,33		28,61			12,65	34,35	51,91		
	29,68					28,30	19,01	27,35		
1,52						65,56	13,41	5,67		
2,01		67,58				23,95	15,13	34,38		
1,10						129,96	82,71	121,07		
		136,37				117,14	48,27	67,50		
		70,00				94,95	32,73	32,97	32,25	
			98,74		101,05		97,48			
		113,44		100,57		99,05		105,47		
	10,78						9,66			
35,07				38,10		53,52		38,89		
	24,43		24,72		24,17					
26,65		26,18		23,15		23,44				
	16,89		15,08		16,94		14,81			
14,60		17,68		16,39		14,02		15,41		
	13,03		11,34		13,38		10,76			
12,86		13,79		12,36		10,70		12,74		
	10,79		9,97		10,38		10,26			
6,91		10,99		10,79		8,98		8,78		
	4,61		4,31		5,01		4,31			
3,47						5,04				
	5,92		6,76		7,76		5,10		7,08	
16,30										
4,61										
	20,35		18,37		18,98					

DA21/15-05-03	DA21/15-10-01	Left *in situ*
Characichnos isp.	*Characichnos* isp.	*Characichnos* isp.
RA-exs-02a	NA-72.4-02a	PM-14.8-01a

Appendix 3

Locomotion in cf. *Dimetropus*, Permian of Mallorca

Appendix 3 was published as:

Matamales-Andreu, R.; Mujal, E.; Galobart, À. & Fortuny, J. (2021). Insights on the evolution of synapsid locomotion based on tetrapod tracks from the lower Permian of Mallorca (Balearic Islands, western Mediterranean). *Palaeogeography, Palaeoclimatology, Palaeoecology*, 579: 110589.

DOI: https://doi.org/10.1016/j.palaeo.2021.110589

In this work, R. Matamales-Andreu contributed in:

A. Direct examination of all the collections and outcrops containing cf. *Dimetropus* isp. fossils from the Permian of Mallorca.
B. Co-direction of all fieldwork campaigns (prospections and excavations). Sampling of tetrapod tracks.
C. 3D modelling and measurement of relevant parameters on tetrapod tracks and trackways.
D. Stratigraphic and sedimentological analysis.
E. Vertebrate palaeoichnology, including identification and description of the cf. *Dimetropus* isp. morphotype.
F. Interpretation and discussion of the results.
G. Writing of the original draft.
H. Preparation of all the tables (1–2), and figures (1–5).
I. Collaboration in obtaining funding for fieldwork.

Palaeogeography, Palaeoclimatology, Palaeoecology 579 (2021) 110589

Contents lists available at ScienceDirect

Palaeogeography, Palaeoclimatology, Palaeoecology

journal homepage: www.elsevier.com/locate/palaeo

Insights on the evolution of synapsid locomotion based on tetrapod tracks from the lower Permian of Mallorca (Balearic Islands, western Mediterranean)

Rafel Matamales-Andreu [a,b,*], Eudald Mujal [a,c], Àngel Galobart [a,d], Josep Fortuny [a]

[a] Institut Català de Paleontologia Miquel Crusafont, Universitat Autònoma de Barcelona, Edifici ICTA-ICP, c/ Columnes s/n, Campus de la UAB, 08193 Cerdanyola del Vallès, Barcelona, Spain
[b] Museu Balear de Ciències Naturals, ctra. Palma-Port de Sóller km 30, 07100 Sóller, Mallorca, Illes Balears, Spain
[c] Staatliches Museum für Naturkunde Stuttgart, Rosenstein 1, 70191 Stuttgart, Germany
[d] Museu de la Conca Dellà, c/ del Museu 4, 25650 Isona i Conca Dellà, Lleida, Spain

ARTICLE INFO

Editor: Howard Falcon-Lang

Keywords:
Ichnology
Photogrammetry
"Pelycosauria"
Functional prevalence
Equatorial Pangaea

ABSTRACT

"Pelycosaur"-grade synapsids were a successful group of terrestrial tetrapods that lived during the Carboniferous and Permian, utilising a wide diversity of ecological niches. They are considered the trackmakers of the ichnogenera *Dimetropus* and possibly also *Dromopus* and *Tambachichnium*, found in upper Palaeozoic deposits of North America, North Africa and Europe. Here we describe a new morphotype from the lower Permian of Mallorca (Balearic Islands, western Mediterranean), identified as cf. *Dimetropus* isp., which was purportedly produced by caseid synapsids. The trackmaker identity is inferred based on the digit proportions, as caseids are the only pelycosaurs with species showing mesaxonic autopodia, and a relative depth pattern (corresponding to the functional prevalence of the autopodia of the trackmaker) showing an overall similarity to that of *Dimetropus osageorum*, which is also attributed to caseids. A detailed study of the expulsion rims and drag traces makes it possible to infer the mode of locomotion of the trackmaker, with a gait alternating the movement of manus and pedes of the two sides of the body and lateral undulation of the spine. Our results provide new information concerning the locomotion of early synapsids, which would undergo important functional modifications later in their evolutionary history such as a shift from abducted to adducted posture and lateral to sagittal bending of the axial skeleton.

1. Introduction

Synapsids were a key tetrapod clade in late Palaeozoic terrestrial ecosystems, including herbivores with high-fibre diet, small predators and large hypercarnivores, which occupied a variety of ecological niches (Kemp, 2005; Angielczyk and Kammerer, 2018). Carboniferous and Permian synapsids are nowadays included in two major clades: "pelycosaur"-grade synapsids, comprising the most basal groups (Romer and Price, 1940), and non-mammalian therapsids, which diversified over the middle and late Permian (Angielczyk and Kammerer, 2018). Regarding their ichnological record, late Palaeozoic synapsids are represented by nine different ichnogenera, three of which correspond to pelycosaurs (*Dromopus*, *Tambachichnium* and *Dimetropus*) and six to therapsids (*Brontopus*, *Karoopes*, *Capitosauroides*, *Dicynodontipus*, *Dolomitipes* and *Procolophonichnium*; the latter four also present in Triassic deposits) (Marchetti et al., 2019a, 2019b; Spindler et al., 2019). Some common traits of these ichnogenera (albeit not always present) are the deeper impression of the median-lateral region of the tracks (median-lateral functional prevalence of autopodia), tracks with paw-like shape (with faintly imprinted proximal part of digits and conspicuos metatarso-/metacarpophalangeal pad and digit tip imprints) because of the digital arcade of synapsid phalanges, and well-imprinted palms and soles (Marchetti et al., 2019a; Mujal et al., 2020).

The only ichnogenus attributed to synapsids that had been (preliminarily) reported so far from the lower Permian beds of Mallorca (Balearic Islands, western Mediterranean) was *Dimetropus* (Matamales-Andreu et al., 2019), with forms similar to *Dimetropus leisnerianus*. The present work analyses newly discovered tetrapod tracks and a trackway that purportedly correspond to a second, hitherto unkown morphotype of *Dimetropus*. Those ichnites, attributable to a synapsid trackmaker,

* Corresponding author.
E-mail address: rafel.matamales@icp.cat (R. Matamales-Andreu).

https://doi.org/10.1016/j.palaeo.2021.110589
Received 14 May 2021; Received in revised form 22 July 2021; Accepted 22 July 2021
Available online 26 July 2021
0031-0182/© 2021 Elsevier B.V. All rights reserved.

possibly a caseid, enlarge the ichnofaunal diversity of the lower Permian of central equatorial Pangaea, and also provide new insights on the evolution of synapsid locomotion.

2. Geographical and geological context

Mallorca is the largest of the Balearic Islands (western Mediterranean) (Fig. 1A), and it is broadly structured in three mountain ranges of SW–NE orientation, with rocks ranging from the Carboniferous to the middle Miocene, and basins filled with sediments ranging from the upper Miocene to the Holocene. The nomenclature of the Permian and Triassic lithostratigraphic units of Mallorca is in need of a thorough revision, as each of the main authors who studied them (Calafat, 1988; Gómez-Gras, 1993; Ramos, 1995) established different names and boundaries for the units, which have never been formally described. However, such a review is beyond the scope of the present work, which uses a nomenclature of correlative letters (from lowermost to uppermost: A, B and C) for the three main lithostratigraphic units (Fig. 1B), based on the stratigraphic logs of Gómez-Gras (1993), which are herein considered to be the most exhaustive of those so far published.

The Racó de s'Algar tracksite (Calafat et al., 1986, 1986–1987; Calafat, 1988), where the ichnites studied herein were discovered, corresponds to the bases of two fine-grained sandstone beds located in Unit B (metre 32 of the log "E" of Calafat, 1988) (Fig. 1B–C). These two beds are mostly tabular, although they wedge laterally, and show climbing ripple lamination, corresponding to two successive point bars of a meandering river deposit separated by a thin bed of mudstones, probably representing seasonal stagnation and desiccation of the channel (Fig. 1D–E). Their bases preserve, as natural casts, the sedimentary (large mud-cracks) and biogenic (tetrapod ichnites) structures recorded on the surfaces of the underlying sandy mudstone beds, which nowadays are mostly eroded. The irregularity of the ichnite-bearing surfaces, reminiscent of "wrinkle structures", points to algal mat development, which probably also contributed to the mode of impression and preservation of the tracks. The succession encompassing the tetrapod tracks is here interpreted as a waterhole environment, with a facies assemblage that is similar to that of the seasonally-dry fluvial palaeoenvironments from the upper Carboniferous of Nova Scotia (Falcon-Lang et al., 2004, 2007). In the succession of Mallorca, such a sedimentary setting can be inferred based on the presence of wave ripples developed on the channel bed, suggesting stagnation of the water, and subsequent desiccation of the pool, as indicated by the large mud cracks (Fig. 1C, E).

Placed in the general framework of the Permian lithostratigraphic units of Mallorca (Fig. 1B), this tracksite is located in the upper part of what is herein called Unit B (="Racó de s'Algar unit" of Calafat, 1988; ="Stretch a" of Gómez-Gras, 1993; ="Port des Canonge unit" of Ramos, 1995), which was interpreted as a meandering river system (Calafat, 1988; Gómez-Gras, 1993; Ramos, 1995). This unit was dated as Permian based on the discovery of moradisaurine captorhinid eureptiles, both in the form of bones (Liebrecht et al., 2017) and tracks (Gand et al., 2010, revising the ichnites figured by Calafat et al., 1986–1987). More recently, Matamales-Andreu et al. (2019) tentatively suggested that the age could be narrowed down to the lower Permian based on the presence of *Dimetropus* (possibly *D. leisnerianus*), and further constrained it to the upper part of the Cisuralian (Artinskian–Kungurian) because of the great abundance of tracks attributed to eureptiles (*Hyloidichnus*) and the rarity of tracks produced by anamniotes (see discussion on the Artinskian–Kungurian reptile radiation by Marchetti et al., 2015, 2019c).

3. Material and methods

Five slabs with ichnites (natural casts) from the same stratigraphic surface of the Racó de s'Algar tracksite (upper ichnite-bearing bed; Fig. 1C) are described in the present work. The material collected *in situ* for the present study consists of a right manus imprint (DA21/15-05-01), housed at the Museu de Mallorca (Palma, Mallorca, Spain, acronym DA21/15-##-##). Moreover, three more slabs were found *in situ* but not collected (it was not possible, as they were in the base of an unstable cliff; field acronym NA-26-##): one with a poorly preserved left manus-pes set (NA-26-02), one with a poorly preserved right pes imprint (NA-26-03), and one with a left manus imprint (NA-26-05). Lastly, from the Tomeu Sáez collection (private collection, Binissalem, Mallorca, Spain; acronym TS-#), we have examined one slab with a trackway comprising three manus-pes sets (TS-3), collected *in situ* in the early 1980s. Ichnites within a same slab have been identified with correlative lowercase letters. In the preservation scale of Marchetti et al. (2019d), most of the tracks studied herein score a 2 (good preservation), although some could be attributed to 1 (intermediate preservation) or even 0 (poor preservation). Therefore, and although they appear to be sensibly different from previously known ichnotaxa of this age, no new ichnospecies will be defined here.

Digital 3D models of all the surfaces with ichnites have been produced using the photogrammetry technique, mostly based on the procedure explained by Mujal et al. (2020). Agisoft Photoscan standard version 1.1.4. (http://www.agisoft.com) has been used to align the photographs, to create the meshes and textures, and to crop the model. MeshLab version 2016.12 (http://meshlab.sourceforge.net) has been used to clean, align, scale and measure the mesh. ParaView version 4.1.0 64-bit (http://www.paraview.org) has been used to create the false colour-coded depth maps with contours. ImageJ version 1.52d (https://imagej.nih.gov/ij) has been used to measure the main descriptive parameters for each footprint and the trackway (see Leonardi, 1987; Hasiotis et al., 2007), herein presented in Tables 1–2. In order to compare the tracks from Mallorca to their possible trackmaker, bones of the caseid *Ennatosaurus tecton* were measured on the scaled 3D model provided by Romano et al. (2017).

4. Systematic palaeoichnology

Ichnogenus *Dimetropus* Romer and Price, 1940
cf. *Dimetropus* isp.
Figures 2–3; Tables 1–2.

4.1. Studied material

DA21/15-05-01, a natural cast of a right manus imprint. NA-26-02, a poorly-preserved natural cast of a left manus-pes set (not collected). NA-26-03, a poorly-preserved natural cast of a right pes imprint (not collected). NA-26-05, a natural cast of a left manus imprint (not collected). TS-3, a natural cast of a trackway with two left manus-pes sets and a right manus-pes set. All from the lower Permian of the upper ichnite-bearing bed of the Racó de s'Algar tracksite, Banyalbufar, Mallorca, Balearic Islands, western Mediterranean.

4.2. Description

Pes track semiplantigrade, pentadactyl, almost as long as wide (*ca.* 7.3–8.3 cm). The digit imprints are slender, strongly curved laterally (outwards) and relatively long. Preservation is quite variable: in some cases, the distal parts of the digits are not well imprinted (especially of digits II and III) (Fig. 2A–B), whereas in other cases digit I seems to be imprinted twice (Figs. 2C, 3A). No clear claw traces have been observed on any specimen. The relative length of the digit imprints is ordered as follows: V<I≈II≈IV≈III (very weakly mesaxonic) (Table 1). However, digit imprints are dragged, deformed and partly incomplete with mud-collapsed distal ends, so it cannot be decided with certainty whether digit III is really longest, because digit IV may not show its true length. The total divergence angle between digits I–V of pes tracks (measured on the proximal part of the digit imprints due to their strong distal curvature) ranges from 77° to 95°. The digit imprints usually have sharp posterolateral margins, whereas their anteromedial margins have gentler slopes. The sole imprint is oval, with an almost straight to weakly

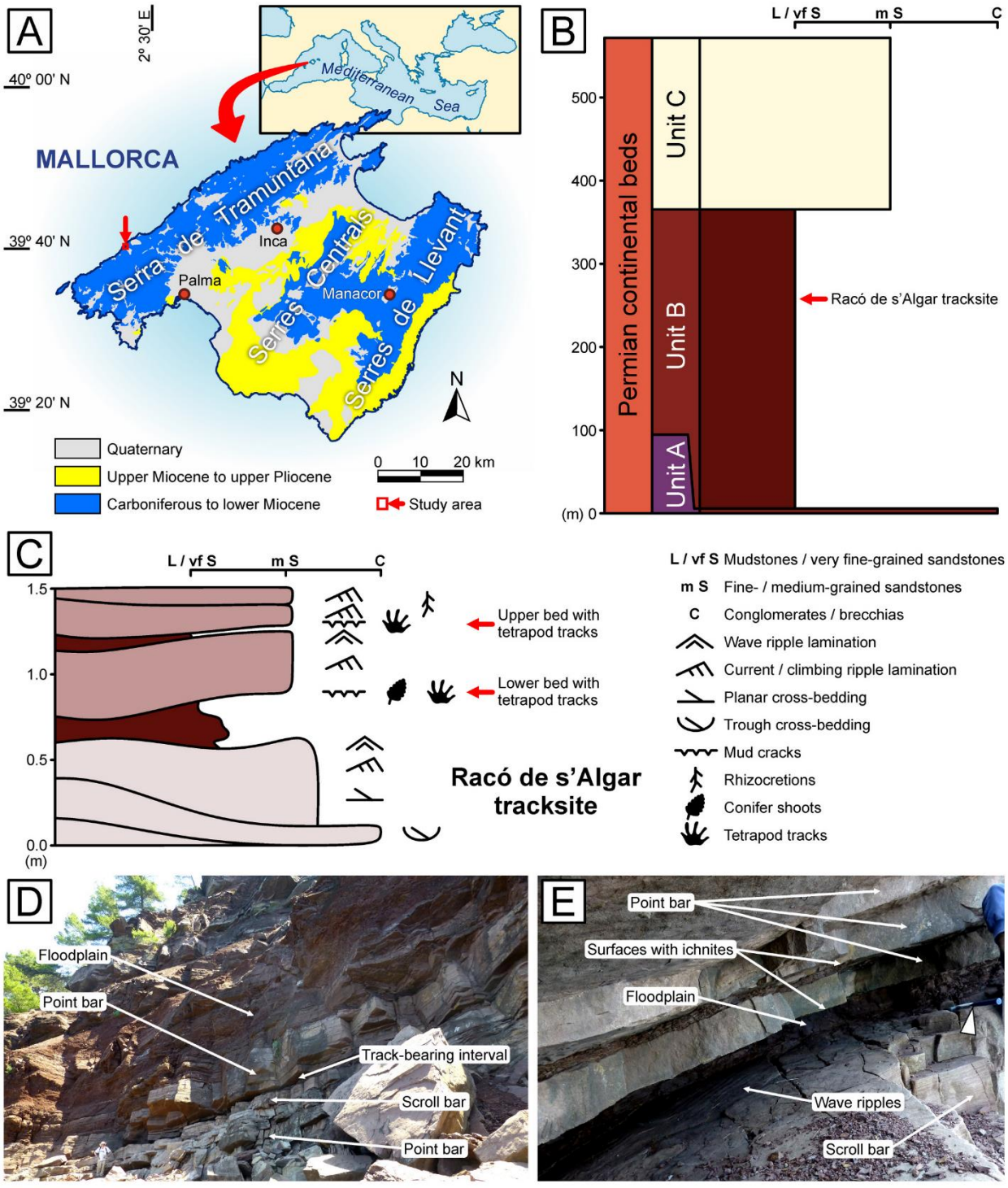

Fig. 1. Geographical and geological context for the Racó de s'Algar tracksite, Permian of Mallorca (Balearic Islands, western Mediterranean). A: Simplified geological map of Mallorca (based on Sevillano and Barnolas, 2019), with indication of the location of the studied site. B: Simplified stratigraphic log of the Permian of Mallorca (thicknesses based on Gómez-Gras, 1993), distinguishing the three main lithostratigraphic units and indicating the location of the studied site. C: Detailed stratigraphic log of the Racó de s'Algar tracksite, indicating the position of the two track-bearing beds and the dominant sedimentary structures and fossil content. D: Field photograph of the Racó de s'Algar tracksite with indication of the main sedimentary environments and the track-bearing beds. See person for scale. E: Close-up photograph of the Racó de s'Algar tracksite showing the two beds with ichnites. See hammer for scale (30 cm), pointed by an arrowhead.

Table 1
Measurements taken on the studied specimens of cf. *Dimetropus* isp. from Mallorca. Numbers in brackets correspond to parameters that have not been confidently measured on poorly preserved ichnites. Hyphens (-) mark measurements impossible to obtain. In the divarication angles, positive values correspond to ichnites rotated medially (inwards), whereas negative values ( ) correspond to ichnites rotated laterally (outwards).

Parameters of the tracks											
Slab	DA21/15-05-01	TS-3						NA-26-02		NA-26-03	NA-26-05
Fig.	2D	2A–C						3A		3B	2E
Ichnite	-	a	b	c	d	e	f	a	b	-	-
Anatomy	Right manus	Right pes	Right manus	Left pes	Left manus	Right pes	Right manus	Left pes	Left manus	Right pes	Left manus
Length (cm)	7.14	(7.78)	(8.21)	8.27	6.86	(7.37)	7.02	-	6.66	-	6.49
Width (cm)	6.69	(13.46)	(13.15)	(8.35)	9.50	7.70	8.22	-	(7.11)	-	-
Length palm (cm)	4.03	(5.25)	-	5.57	3.83	4.17	3.77	-	3.57	-	3.93
Width palm (cm)	3.40	(8.64)	-	6.00	3.63	6.47	4.67	-	4.10	-	3.07
Length I (cm)	1.57	(5.18)	-	(4.97)	2.53	2.66	2.90	-	2.43	-	3.20
Length II (cm)	2.96	(5.68)	-	-	3.01	3.22	3.71	-	2.77	-	3.30
Length III (cm)	3.30	(2.98)	-	-	3.59	3.61	3.92	-	3.49	-	3.83
Length IV (cm)	2.57	3.79	-	4.17	(5.22)	(2.77)	3.26	-	3.00	-	-
Length V (cm)	(2.04)	2.21	2.15	2.08	(1.62)	-	2.69	-	(1.40)	-	-
Divergence angle I–II (°)	45.83	(4.18)	(63.57)	4.80	15.70	8.52	12.93	-	23.37	-	36.72
Divergence angle II–III (°)	23.42	(76.54)	-	6.32	31.38	14.60	22.58	-	14.93	-	18.68
Divergence angle III–IV (°)	40.40	(3.27)	43.91	36.01	42.44	28.24	39.31	-	35.41	-	24.26
Divergence angle IV–V (°)	37.18	(10.76)	45.08	41.51	35.98	25.86	44.45	-	68.96	-	48.03
Divergence angle I–V (°)	147.41	(95.12)	152.45	89.19	125.39	77.65	118.92	-	143.36	-	117.30
Divergence angle II–IV (°)	63.79	(80.12)	(42.06)	43.22	73.67	42.72	62.57	-	50.67	-	42.72
Divergence angle II–V (°)	101.07	(90.40)	(88.97)	84.76	110.34	68.73	106.16	-	120.00	-	91.38
Divarication from midline (°)	-	(−90.70)	(−23.03)	−31.26	9.01	−22.25	26.10	-	-	-	-

Table 2
Mean trackway measurements taken on the studied specimens of cf. *Dimetropus* isp. from Mallorca. Brackets mean that that parameter has been partially inferred. Hyphens (-) mark measurements impossible to obtain.

Parameters of the trackway					
Slab	DA21/15-05-01	TS-3	NA-26-02	NA-26-03	NA-26-05
Fig.	2D	2A–C	3A	3B	2E
Pace angulation pes (°)	-	83.15	-	-	-
Pace angulation manus (°)	-	93.90	-	-	-
Stride pes (cm)	-	34.63	-	-	-
Stride manus (cm)	-	38.64	-	-	-
Pace pes (cm)	-	26.33	-	-	-
Pace manus (cm)	-	27.31	-	-	-
Length pace pes (cm)	-	17.22	-	-	-
Length pace manus (cm)	-	21.05	-	-	-
Width pace pes (cm)	-	19.57	-	-	-
Width pace manus (cm)	-	14.17	-	-	-
Interpes distance (cm)	-	12.07	-	-	-
Intermanus distance (cm)	-	6.00	-	-	-
Pes-manus distance (cm)	-	14.32	(13.12)	-	-
Width external (cm)	-	26.91	-	-	-
Width internal (cm)	-	6.00	-	-	-
Glenoacetabular distance (cm)	-	32.53	-	-	-

convex posteromedial margin and a length of about 1/2 of the whole track. Metatarsophalangeal pads are well impressed, especially at the bases of digits I–III. The most deeply imprinted areas of the pes tracks are the metatarsophalangeal pads of digits I–III (medial functional prevalence). There is an expulsion rim surrounding the pes track posterolaterally.

Manus track plantigrade, pentadactyl, usually slightly wider (6.9–7.1 cm) than long (6.7–9.5 cm). Digit I–IV imprints are slender, relatively long and show clawed tips. The proximal parts of the digit imprints are directed medially, whereas the imprints of the tips are curved laterally, giving digit imprints a "hook-shaped" appearance, especially in digit III (Figs. 2B–E, 3A). They become thinner and gradually decrease in depth distally. Digit V imprint, which is the shortest, is almost as short as digit I, slender and usually straight, although its tip is often not well impressed (Figs. 2B–C, 3A). Some digit imprints, especially I and II, may have drag traces in front of their tips (Fig. 2B–E). The relative lengths of the digit imprints are ordered as follows: V≈I<II≈IV<III (weakly mesaxonic) (Table 1). Digits radiate from the palm, usually without significative overlapping, although the bases of digits I and II can be slightly superimposed. The total divergence angle between the imprints of digit I–V is wide, ranging between 115° and 150°. The palm imprint is posterolaterally elongated, with a concave medial margin ("lunate shape"). Metacarpophalangeal pads are rounded and well-impressed, especially at the bases of digits I–IV with slight overlap in I and II. The most deeply imprinted areas of the manus track are the metacarpophalangeal pads of digits II–III (medial-median functional prevalence of the autopodium), followed by those of digits I and IV. The imprints of the phalangeal parts of the digits are shallower, with that of digit III being the deepest, followed by those of digits II and IV, and then the rest of the palm. There are well-marked expulsion rims posteromedially, laterally and between the imprints of digits II and III, and slightly less marked ones between the other digit imprints.

Trackway produced by a quadrupedal animal, with pes tracks slightly larger than manus tracks (weak heteropody). The manus-pes sets are alternately arranged, with the manus tracks positioned at the height of the mid-proximal portion of the pes track of the next couple (Fig. 2A). The pace angulations of the pes and the manus imprints are of about 80° and 90°, respectively, and thus consistent with an abducted (sprawling) limb posture. Respect to the trackway midline, pes imprints are rotated laterally (outwards) by 20–30°, whereas manus imprints are rotated medially (inwards) by 9–26° and are located anteriorly from the pes imprints. Manus tracks can be positioned medially or laterally from the pes tracks; this trait is variable, as in other synapsid tracks (*e.g.*, Marchetti et al., 2019d) The glenoacetabular distance is of about 32.5 cm (Table 2). No tail traces have been observed.

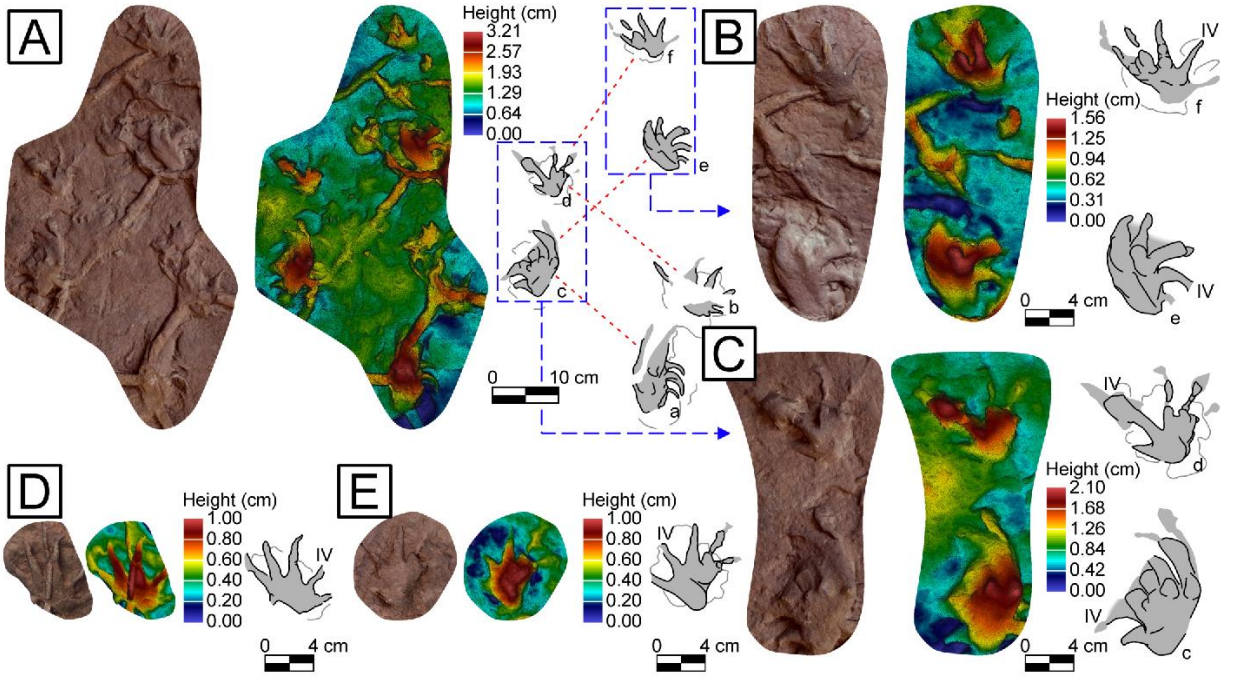

Fig. 2. Selection of the best preserved specimens of cf. *Dimetropus* isp. studied herein, all as textured 3D models, false colour-coded 3D models with contours and interpretative drawings. A: TS-3, natural cast of a trackway with two left manus-pes sets and a right manus-pes set. B: Close-up of the natural cast of the third manus-pes set of TS-3. C: Close-up of the natural cast of the second manus-pes set of TS-3. D: NA-26-05, natural cast of a left manus imprint. E: DA21/15-05-01, natural cast of a right manus imprint. All from the Racó de s'Algar tracksite (Mallorca, Balearic Islands, western Mediterranean), lower Permian.

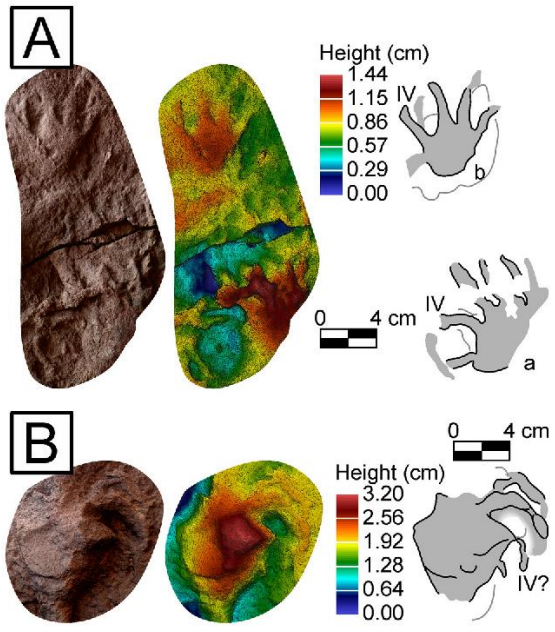

Fig. 3. Other specimens attributed to cf. *Dimetropus* isp., both as textured 3D models, false colour-coded 3D models with contours and interpretative drawings. A: NA-26-02, natural cast of a left manus-pes set. B: NA-26-03, natural cast of a right pes imprint. Both from the Racó de s'Algar tracksite (Mallorca, Balearic Islands, western Mediterranean), lower Permian.

5. Discussion

5.1. Comparison of cf. Dimetropus isp. from Mallorca to other Permian ichnogenera

The tracks here identified as cf. *Dimetropus* isp. are pentadactyl, mesaxonic and have anteroposteriorly elongated palm and sole imprints (Fig. 4A), which makes it possible to rule out all the Permian ichnogenera attributed to anamniotes, "reptiliomorphs", eureptiles and parareptiles (compare to Lucas, 2019), thus placing them in the synapsid group. The ichnogenera currently attributed to synapsid trackmakers are: *Dromopus*, of non-varanopine varanopids and some other groups of diapsids (Spindler et al., 2019; Fig. 4B); *Tambachichnium*, of varanopids (Voigt, 2005; Marchetti et al., 2019a; Fig. 4C); *Dimetropus*, of edaphosaurids, sphenacodontids, ophiacodontids and caseids (Voigt and Ganzelewski, 2010; Sacchi et al., 2014; Marchetti et al., 2019a; Fig. 4D–J); *Brontopus*, of dinocephalians (Marchetti et al., 2019a; Fig. 4K–L); *Dolomitipes*, of dicynodonts (Marchetti et al., 2019a; Fig. 4M–N); *Karoopes*, of gorgonopsians (Marchetti et al., 2019a; Fig. 4O); *Capitosauroides* and at least some ichnospecies of *Procolophonichnium*, of therocephalians (Marchetti et al., 2019a, 2019b; Buchwitz et al., 2020; Fig. 4P–Q); and *Dicynodontipus*, of cynodonts (Marchetti et al., 2019a; Fig. 4R).

Although the specimens herein identified as cf. *Dimetropus* isp. cannot readily be attributed to any of these known ichnogenera (hence the open nomenclature at ichnogenus-level; see Fig. 4), their manus imprints are very similar to other tracks attributed to the ichnogenus *Dimetropus* in the shape of the palm/sole and the digit imprints (compare to Gand, 1987: fig. 52D; Haubold et al., 1995: fig. 23A; Voigt, 2005: fig. 35D). The strong outwards rotation of the pes imprint, the general proportions, the pace angulation and the stride could be also compared to those of *Capitosauroides* (see Buchwitz et al., 2020). The latter, however, has hitherto not been found in lower Permian deposits (Buchwitz et al., 2020), and thus here the assignation to *Dimetropus* (in

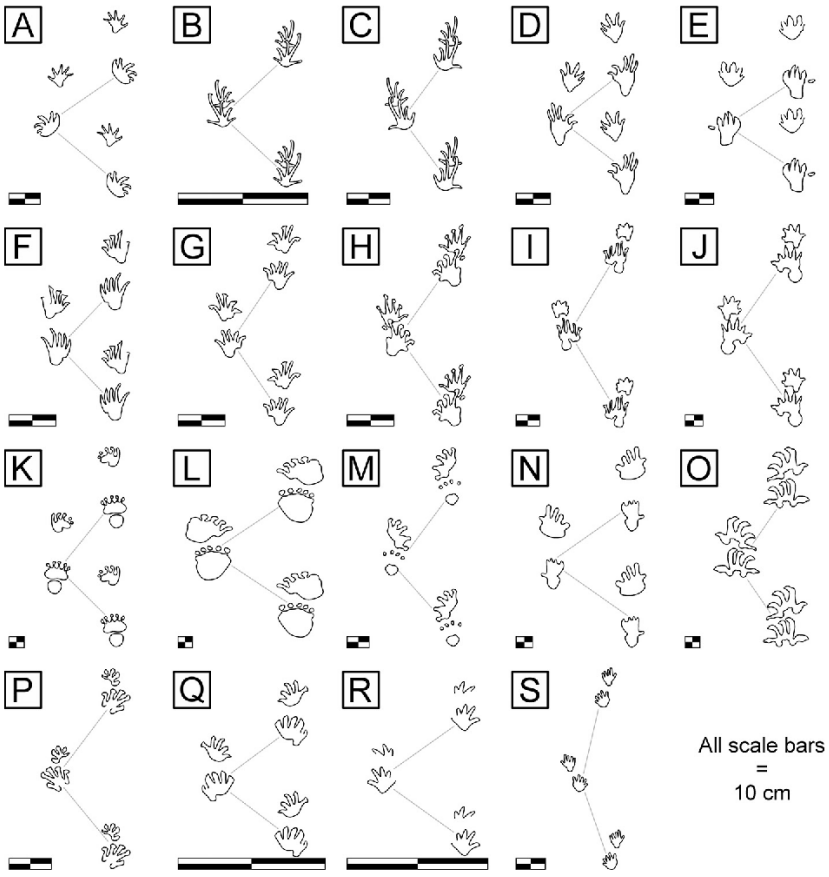

Fig. 4. Schematic drawings of morphotypes of Permian and Triassic tetrapod tracks attributed to non-mammalian synapsids. They are idealised and based on the best-preserved tracks, arranged symmetrically in the usual trackway disposition of each form. A: cf. *Dimetropus* isp. from Mallorca. B: *Dromopus lacertoides*, based on Voigt (2005) and Buchwitz et al. (2021). C: *Tambachichnium schmidti*, based on Voigt (2005). D: *Dimetropus* isp., based on Voigt and Ganzelewski (2010). E: cf. *Dimetropus* isp., based on Marchetti et al. (2019d). F: *Dimetropus leisnerianus*, based on Voigt (2005). G: *Dimetropus leisnerianus*, based on Voigt (2005). H: *Dimetropus leisnerianus*, based on Voigt (2005). I: *Dimetropus* isp., based on Gand (1987). J: *Dimetropus osageorum*, based on Sacchi et al. (2014). K: *Brontopus antecursor*, based on Gand et al. (2000). L: *Brontopus giganteus*, based on Marchetti et al. (2019a). M: *Dolomitipes accordii*, based on Marchetti et al. (2019e). N: *Dolomitipes icelsi*, based on Marchetti et al. (2019a). O: *Karoopes gansfonteinensis*, based on Marchetti et al. (2019a). P: *Capitosauroides bernburgensis*, based on Marchetti et al. (2019a). Q: *Capitosauroides* isp., based on Buchwitz et al. (2020). R: *Procolophonichnium haarmuehlensis*, based on Klein et al. (2015). S: *Dicynodontipus geinitzi*, based on Marchetti et al. (2019a).

open nomenclature) is favoured.

5.2. Comparison of cf. Dimetropus isp. from Mallorca with other ichnospecies of Dimetropus

Sacchi et al. (2014) considered five valid ichnospecies within the ichnogenus *Dimetropus*: *D. leisnerianus* (Geinitz, 1863), *D. osageorum* Sacchi, Cifelli, Citton, Nicosia et Romano, 2014, and perhaps *D. berea* (Tilton, 1931), *D. salopensis* Haubold and Sarjeant, 1973, and *D. nicolasi* Gand and Haubold, 1984. However, the last three need revision to rule out that they are undertracks of *D. leisnerianus* (*e.g.*, Voigt, 2005).

The cf. *Dimetropus* isp. tracks from Mallorca differ from *D. leisnerianus* (Fig. 4E–F) by the following features: (1) the manus imprints are weakly mesaxonic in the former, whereas in the latter they are clearly ectaxonic; (2) the digit tips of the manus imprints (especially digit III) are "hook-shaped" in the former, whereas they are mostly straight in the latter; (3) the digits of the manus imprints of the former usually have relatively higher divergence angles than those of the latter; (4) the depth of the digits of the manus imprints decreases distally in the former, whereas in the latter they are deepest proximally and distally, with a shallower region in between; (5) the pes imprints are rotated outwards (laterally) in the former, whereas in the latter they are subparallel to the trackway midline or even slightly rotated inwards (medially); (6) the digits of the pes imprint of the former are all strongly rotated outwards (laterally), whereas they are straight in the former; (7) the sole imprint is anteroposteriorly short and oval in the former, whereas it is usually posteriorly extended in the latter; (8) the autopodial functional prevalence inferred from the relative depth pattern of the manus and pes imprints of the former is medial-median and medial, respectively, whereas in the latter they are both lateral. For comparison, see tracks and trackways of *D. leisnerianus* in Voigt (2005, 2012), Voigt and Ganzelewski (2010), Voigt et al. (2011, 2012), Lucas et al. (2016), Mujal et al. (2016a, 2020), Marchetti et al. (2019a).

The material from Mallorca differs from *D. berea*, *D. salopensis* and *D. nicolasi* essentially in the same characters listed above for *D. leisnerianus* (see specimens in Haubold and Sarjeant, 1973; Gand and Haubold, 1984; Gand, 1987; Haubold et al., 1995, Lucas et al., 2016). However, these three ichnospecies are of dubious validity (*e.g.*, Voigt, 2005), with definitions based on a few isolated ichnites and manus-pes sets that have slightly different digit lengths, pace angulation and distribution of depths than those of *D. leisnerianus* (see Sacchi et al., 2014). Further research on the type specimens or new materials from the type localities could elucidate this matter, although such a revision is beyond the scope of the present work. Moreover, cf. *Dimetropus* isp. from Mallorca is also different from the Carboniferous *Dimetropus* isp. figured by Voigt and Ganzelewski (2010), *Dimetropus* isp. figuerd by Lagnaoui et al. (2018) and cf. *Dimetropus* isp. figured by Marchetti et al. (2019c), because of the reasons listed above for *D. leisnerianus*.

The cf. *Dimetropus* isp. tracks from Mallorca differ from *D. osageorum* (Fig. 4H) by the following features: (1) the digits of the manus imprints of the former are long, slender and digit III is "hook-shaped", whereas in the latter they are straight, very short and thick; (2) the sole imprints are posteriorly short in the former, whereas in the latter they are elongated, with a marked medial embayment; (3) the pes imprints are strongly rotated outwards (laterally) in the former, whereas in the latter they are subparallel to the trackway midline or even slightly rotated inwards (medially); (4) the pes imprints are only slightly larger than the manus imprints in the former, whereas the latter is notably heteropodic; (5) the

functional prevalence of autopodia inferred for the former is medial-median and medial, respectively for the manus and pes imprints, whereas for the latter it is medial-median in both cases (see examples in Sacchi et al., 2014; Romano et al., 2016, 2020).

It is at this point important to note that the purported *D. leisnerianus* figured by Gand (1987) (Fig. 4I) show a general size, proportions, heteropody and trackway parameters that are comparable to those reported for *D. osageorum* by Sacchi et al. (2014) (Fig. 4J). Their main difference is that the specimens from Europe have ectaxonic tracks (although relative lengths of the digit imprints appear to be very variable), whereas the North American forms have mesaxonic tracks. Although this aspect is beyond the scope of the present work, future studies should compare these two morphotypes to clarify whether they represent only one ichnospecies (and its range of variability and extramorphological deformation) or they are distinct forms. Moreover, taxonomic status of the footprints illustrated by Gand (1987) (Fig. 4I) should probably be reassessed, given the apparent high degree of heretopody of those tracks, atypical of *D. leisnerianus* (Voigt, 2005; Sacchi et al., 2014) (Fig. 4F–H).

5.3. Trackmaker of cf. Dimetropus isp. from Mallorca

Dimetropus is an ichnogenus that has been attributed to various clades of "pelycosaur"-grade synapsids, except for varanopids, which are considered to be the trackmakers of *Dromopus* and *Tambachichnium* (see Voigt and Ganzelewski, 2010; Marchetti et al., 2019a; Spindler et al., 2019). The phylogenetic position of varanopids has recently been questioned, suggesting they are actually diapsids (Ford and Benson, 2020), which would also be consistent with some of the parameters of their footprints (Mujal et al., 2020; Buchwitz et al., 2021). However, some other lines of research suggest that they are indeed more closely related to synapsids, as the morphology of their maxillary canals is more similar to ophiacodonts and therapsids than to other reptiles (Benoit et al., 2021). Given their contentious affinities, varanopids will be not further discussed here. In any case and specifically within *Dimetropus*, *D. leisnerianus* has been indistinctly attributed to edaphosaurids, sphenacodontids, ophiacodontids and caseids, which have relatively similar manus and pes proportions (see references in Voigt and Ganzelewski, 2010; Sacchi et al., 2014), whereas *D. osageorum* was proposed to have been produced by large caseids or perhaps edaphosaurids (Sacchi et al., 2014).

Mujal et al. (2020) showed that most ichnogenera currently attributed to Carboniferous–Triassic synapsid trackmakers share a median-lateral functional prevalence of the autopodia. Interestingly enough, the ichnogenus *Tambachichnium*, purportedly produced by varanopids, showed a different functional prevalence (median), typical of diapsids. Mujal et al. (2020) hypothesised that the basal position of varanopids within synapsids could explain their having this particular type of functional prevalence, or that it could be regarded as a trait evolved convergently in a similar functionality.

Interestingly, the ichnospecies *D. osageorum* also appears to be at odds with the hypothesis that the median-lateral functional prevalence is a trait typical of all synapsids. In the touch-down phase (posterior part of the ichnite), the functional prevalence of *D. osageorum* was considered to be median-lateral, but during the kick-off phase (anterior part of the ichnite) it appeared to be medial-median (Romano et al., 2016, 2020). *D. osageorum* was attributed to large caseid trackmakers (Sacchi et al., 2014), which are also a synapsid clade that diverged before the eupelycosaurs, the latter containing all ichnogenera that display a median-lateral functional prevalence according to Mujal et al. (2020). Moreover, both manus and pes tracks of *D. osageorum* are mesaxonic (Sacchi et al., 2014), whereas the autopodia of all non-therapsid eupelycosaurs have a digit IV longer than digit III, being caseids the only pelycosaurs with species known to have subequal digit II–IV lengths (*e.g.*, Romer and Price, 1940; Olson, 1968).

In this sense, cf. *Dimetropus* isp. from Mallorca is similar to *D. osageorum* in that they both share a medial-median functional prevalence (with only slight differences), especially in the anterior portion of the tracks, and that they are both mesaxonic, being their digit III imprint slightly longer than that of digit IV. Following the reasoning explained above, it is here tentatively suggested that caseids could also be considered the trackmakers of these cf. *Dimetropus* isp. tracks. Nevertheless, as noted by Sacchi et al. (2014), the complete structure of edaphosaurid autopodia is unknown, so they cannot be fully excluded from being the trackmakers of these two morphotypes of *Dimetropus*. In any case, the size of manus and pes tracks of cf. *Dimetropus* isp. from Mallorca is consistent with the general proportions and dimensions of the autopodia of the middle Permian genus *Ennatosaurus*, which is the only caseid of relatively small size with digits III and IV being subequal in length (*e.g.*, Olson, 1968; Romano et al., 2017); all other small-sized genera have a digit IV that is clearly longer than digit III (*e.g.*, Spindler et al., 2016; Berman et al., 2020). Moreover, the manus/pes proportions (1.02 in *Ennatosaurus* and 0.83–0.95 in cf. *Dimetropus* isp. from Mallorca) and the glenoacetabular distance in relation to the pes length (4.97 in *Ennatosaurus* and 3.93–4.41 in cf. *Dimetropus* isp. from Mallorca) are also similar (measurements of *Ennatosaurus* based on the complete skeleton figured by Romano et al., 2017). Interestingly, a partial vertebra tentatively attributed to cf. *Ennatosaurus tecton*, of notably larger size than the Russian specimens, was reported from the middle Permian of the Pyrenees (Mujal et al., 2016b), which were palaeogeographically close to the Mallorcan basin.

Taking all of the above into account, a caseid identity for the trackmaker of cf. *Dimetropus* isp. from Mallorca becomes feasible; specifically, a relatively small-sized form with digits III and IV subequal in length, similar to *Ennatosaurus*. Nevertheless, further osteological discoveries are needed to confirm this attribution, especially of autopodial material of more small forms of caseids and also edaphosaurs.

5.4. Locomotion of the trackmaker of cf. Dimetropus isp. from Mallorca

Despite the abundant record of upper Palaeozoic ichnites (*e.g.*, Lucas, 2019), detailed studies of functionality and locomotion are all relatively recent (Voigt et al., 2007; Nyakatura et al., 2015, 2019; Romano et al., 2016, 2020; Marchetti et al., 2017; Buchwitz and Voigt, 2018; Mujal and Marchetti, 2020; Mujal et al., 2020; Buchwitz et al., 2021; Logghe et al., 2021). Therefore, although the general patterns of locomotion are well understood, work remains to be done on the evolutionary timing of the locomotion style of different clades. In this sense, a detailed study of the distribution of trackway parameters and the depth patterns of the ichnites and associated expulsion rims makes it possible to infer different phases in the step cycle and the mode of locomotion of cf. *Dimetropus* isp. from Mallorca (Fig. 5), thus adding new insight on the locomotion patterns of primitive "pelycosaur"-grade synapsids.

The general functional interpretation for the manus track of cf. *Dimetropus* isp. from Mallorca differs little from that offered by Romano et al. (2016) for *D. osageorum*. In fact, expulsion rims of different height arranged around the tracks further complement this interpretation. In the touch-down phase, the weight was mostly applied on the pad below the ulnare, proximally to digit V (lateral functional prevalence). In the manus tracks of cf. *Dimetropus* isp. from Mallorca, this is not only represented by a relatively deep imprint of the posterolaterally part of the palm, but also by a high expulsion rim located around it (Figs. 2B–E, 5A). After that, the weight shifted towards the pad below the radiale and the metacarpophalangeal pads of digits I, II and III (medial-median functional prevalence) during the kick-off phase, making them the deepest-imprinted areas of the track (Fig. 5B). Digit drag traces (Figs. 2B–C, E, 5C) were also formed during this phase evidencing an initial movement of the manus towards the medial-anterior part.

The functional interpretation of the pes track of cf. *Dimetropus* isp. from Mallorca is, on the other hand, quite different to that of *D. osageorum* by Romano et al. (2016). Possibly, the most noteworthy trait of the pes tracks of cf. *Dimetropus* isp. from Mallorca is their strong

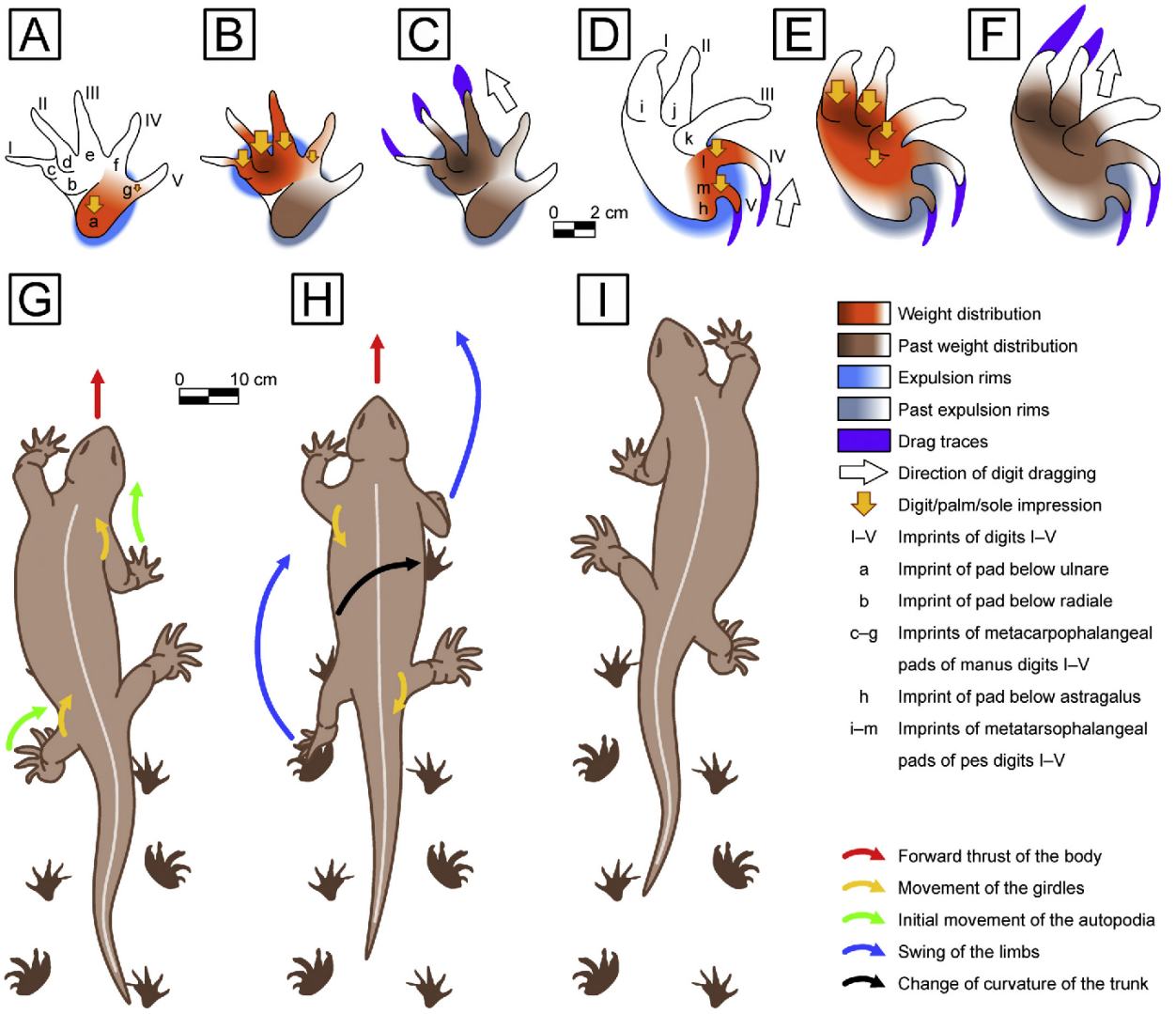

Fig. 5. Functional interpretation of cf. *Dimetropus* isp. from Mallorca. A: Manus track in touch-down phase. B: Manus track in kick-off phase. C: Manus track after the forefoot was lifted. D: Pes track in touch-down phase. E: Pes track in kick-off phase. F: Pes track after the hindfoot was lifted. G–I: Reconstruction of the step cycle of the trackmaker (based on *Ennatosaurus tecton* illustrated by Romano et al., 2017), with indication of the main movements occurring. G: Initial phase of the step cycle, rotating the autopodia slightly medially and lining the pectoral and pelvic girdles perpendicular to the body axis to gain a forward thrust. H: Swing phase moving the limbs to the new position simultaneously to bending the trunk and finishing the movement of the girdles. I: Final phase of the step cycle.

lateral rotation, coupled with an additional lateral curvature of the imprints of digits III–V. It is likely that, during locomotion, the trackmaker used an alternate lateral bending of the trunk, as inferred for other pelycosaurs (Hopson, 2015). It is herein interpreted that in the touch-down phase, there was an initial dragging of the tips of digits IV and V (and, to a lesser extent, digit III), and then the weight was applied on the pad below the astragalus and the metatarsophalangeal pads of digits IV and V (lateral functional prevalence), developing a moderately high expulsion rim between digits IV and V, and around the posterior region of the ichnite (Figs. 2A–C, 3A–B, 5D). Shortly after, and as a readjustment of the body weight when the trunk was bent towards the opposite side, the pes slightly rotated medially and the imprints of digits IV, V and, to a lesser extent, digit III, became curved laterally (Fig. 5G). This movement obscured the original imprints of digits III–V and the posterolateral part of the sole. In the kick-off phase, the weight shifted towards the anterior part of the autopodium, specifically, on the metatarsophalangeal pads of digits I and II (medial functional prevalence), where the deepest impression of the track was left (Figs. 2A–C, 3A–B, 5E). The fact that the anteromedial margins of the pes digit imprints have a much gentler slope than the posterolateral margins (Fig. 2B–C) further supports that the pes was risen off the ground with an anteromedial movement (Fig. 5G). Drag traces of digits I (in some cases imprinted twice) and II (Figs. 2C, 3A, 5F) reveal an initial anterolateral movement of the pes when it was taken off the ground (Fig. 5H).

Therefore, in both the manus and the pes imprints, the functional prevalence of the autopodia changed from being lateral in the touch-down phase (posterolateral region of the ichnites) to being medial-median in the kick-off phase (anterior region of the ichnites, being the deepest imprinted part overall), similarly to what Romano et al. (2016) observed in *D. osageorum*. As interpreted herein, the gait would have had

lateral sequence (Hildebrand, 1980), that is, the sequence of movement of manus and pedes would have alternated the left and right side of the body of the trackmaker (Fig. 5G–I).

5.5. Notes on the evolution of synapsid locomotion

The particular functional prevalence inferred for these purported caseid tracks may provide new insights on the evolution of the synapsid mode of locomotion. Anamniotes and basal amniotes (*i.e.*, seymouriamorphs, diadectomorphs, captorhinomorphs) produced ichnites that showed a medial-median functional prevalence of their autopodia (Mujal et al., 2020). On the other hand, eupelycosaurs, which include all the more derived synapsids, seem to homogeneously feature a median-lateral functional prevalence of their autopodia (Mujal et al., 2020). Therefore, a transition between these two states of functional prevalence probably occurred between those basal amniotes and the eupelycosaurs. Caseids, the purported trackmakers of the ichnites studied here, correspond to a clade that diverged quite early in the synapsid tree (Ford and Benson, 2020). Their tracks, as interpreted herein, show a mixture of lateral (posterior part) and medial-median (anterior part) functional prevalence of their autopodia, which could be referred to the transitional state referred above.

Caseids with mesaxonic autopodia, such as *Ennatosaurus* and *Cotylorhynchus*, nest highly within the phylogeny of caseasaurs (Maddin et al., 2008). This could appear to conflict with the foregoing hypotheses, as the most derived caseids would have the "intermediate" state of functional prevalence argued above, whereas small, primitive forms would not. Therefore, it must be stressed that the present work does not necessarily consider mesaxony as a primitive state of caseids, and the fact that two mesaxonic track morphotypes (cf. *Dimetropus* isp. from Mallorca and *D. osageorum*) show a combination of posterolateral and anteromedial-median deeper areas does not exclude ectaxonic tracks having a similar pattern. It must be noted, however, that the relative depth patterns of small tracks attributed to *Dimetropus* have not been exhaustively described in the literature so far, and in fact, they are known only from five specimens from the West Midlands, the Thüringer Wald, the Massif Central and the Pyrenees (Meade et al., 2016; Mujal et al., 2016a, 2020; Marchetti et al., 2019a). Since *Dimetropus* is thought to have been produced by a wide variety of "pelycosaur"-grade synapsids, it is likely that there are forms with different types of relative depth patterns among the pool of specimens from different ages and formations. Further research is needed to confirm this aspect, but it would be expected for a part of the typical *D. leisnerianus* to show a relative depth pattern similar to that of cf. *Dimetropus* isp. from Mallorca and *D. osageorum*. Especially interesting would be to assess this aspect in the Carboniferous *Dimetropus* specimens (*e.g.*, Van Allen et al., 2005; Voigt and Ganzelewski, 2010; Meade et al., 2016; Lagnaoui et al., 2018; Marchetti et al., 2019c), as they may show other traits closer to the primitive state of synapsids, some of them already pointed out by Buchwitz et al. (2021).

6. Conclusions

The present work describes a trackway and several isolated ichnites from the lower Permian of Mallorca (Balearic Islands, western Mediterranean) identified as cf. *Dimetropus* isp. This form differs from *Dimetropus leisnerianus* and allied forms because cf. *Dimetropus* isp. from Mallorca has mesaxonic manus and pes imprints, the pes imprints are strongly rotated laterally (outwards), and the deepest regions of both manus and pes imprints are located laterally in their posterior half and medial-median in their anterior half. It differs from *Dimetropus osageorum* because cf. *Dimetropus* isp. from Mallorca has long and slender manus and pes digit imprints, and pes imprints that are strongly rotated laterally (outwards). It has been here suggested that the trackmaker of cf. *Dimetropus* isp. from Mallorca can probably be attributed to caseid synapsids, based on the proportions of the autopodia and its relative depth pattern being similar to that of *D. osageorum*, which was also purportedly produced by caseids. The general relative depth pattern (which corresponds to the functional prevalence of the autopodia of the trackmaker) of cf. *Dimetropus* isp. from Mallorca, which is deeper in the lateral region of the posterior half and in the medial-median region of the anterior half, appears to be transitional from the primitive state of anamniotes and basal amniotes (medial-median functional prevalence), to the derived state of eupelycosaur synapsids (lateral-median functional prevalence). This has important implications for the evolution of the mode of locomotion throughout the synapsid line, as caseids, occupying a basal position in the synapsid tree, probably produced footprints with a relative depth pattern (and thus functional prevalence of the autopodia) that was intermediate between that of anamniotes/basal amniotes and eupelycosaurs.

Declaration of Competing Interest

The authors declare that they have no known competing financial interests or personal relationships that could have appeared to influence the work reported in this paper.

Acknowledgements

To Tomeu Sáez, who kindly let us study and make a 3D model of the trackway specimen in his collection, as well as the precise indications on its discovery and exact stratigraphic position. To Sebastià Matamalas for aid in fieldwork. To the reviewers, Michael Buchwitz and Hendrik Klein, for their critical review of the manuscript that substantially improved it. To Prof. Howard Falcon-Lang, editor, for reviewing and handling the manuscript. We acknowledge support from the CERCA program (Generalitat de Catalunya, Spain). R.M.A. was supported by the predoctoral grant FPU17/01922 (Ministerio de Ciencia, Innovación y Universidades, Spain). À.G. is member of the consolidated research group 2017 SGR 1666 GRC (Generalitat de Catalunya, Spain). J.F. is member of the consolidated research group 2017 SGR 086 GRC (Generalitat de Catalunya, Spain). We acknowledge support from the project "Mallorca abans dels dinosaures: estudi dels ecosistemes continentals del Permià i Triàsic amb especial èmfasi en les restes de vertebrats" (ref. 15 - 619/2020), based at the ICP and funded by the Departament de Cultura, Patrimoni i Política Lingüística (Consell Insular de Mallorca).

References

Angielczyk, K.D., Kammerer, C.F., 2018. Non-Mammalian synapsids: the deep roots of the mammalian family tree. In: Zachos, F., Asher, R. (Eds.), Mammalian Evolution, Diversity and Systematics. De Gruyter, pp. 117–198.
Benoit, J., Ford, D.P., Miyamae, J.A., Ruf, I., 2021. Can maxillary canal morphology inform varanopid phylogenetic affinities? Acta Palaeontol. Pol. 66 (2), 389–393.
Berman, D.S., Maddin, H.C., Henrici, A.C., Sumida, S.S., Scott, D., Reisz, R.R., 2020. New primitive caseid (Synapsida, Caseasauria) from the early Permian of Germany. Ann. Carnegie Museum 86 (1), 43–75.
Buchwitz, M., Voigt, S., 2018. On the morphological variability of *Ichniotherium* tracks and evolution of locomotion in the sistergroup of amniotes. PeerJ 6, e4346.
Buchwitz, M., Marchetti, L., Jansen, M., Falk, D., Trostheide, F., Schneider, J.W., 2020. Ichnotaxonomy and trackmaker assignment of tetrapod tracks and swimming traces from the middle Permian Hornburg Formation of Saxony-Anhalt (Germany). Ann. Soc. Geol. Pol. 90, 291–320.
Buchwitz, M., Jansen, M., Renaudie, J., Marchetti, L., Voigt, S., 2021. Evolutionary change in locomotion close to the origin of amniotes inferred from trackway data in an ancestral state reconstruction approach. Front. Earth Sci. 9, 674779.
Calafat, F., 1988. Estratigrafía y sedimentología de la litofacies Buntsandstein de Mallorca.. Bachelor's Thesis Universitat de Barcelona, 127 pp. + 31 annexed figs.
Calafat, F., Fornós, J.J., Marzo, M., Ramos, E., Rodríguez-Perea, A., 1986. Icnología de vertebrados de las facies Buntsandstein de Mallorca. In: Cabrera, L. (Ed.), XI Congreso Español de Sedimentología. Libro de Resúmenes, p. 40.
Calafat, F., Fornós, J.J., Marzo, M., Ramos-Guerrero, E., Rodríguez-Perea, A., 1986–1987. Icnología de vertebrados de las facies Buntsandstein de Mallorca. Acta Geol. Hisp. 21–22, 515–520.
Falcon-Lang, H.J., Rygel, M.C., Calder, J.H., Gibling, M.R., 2004. An early Pennsylvanian waterhole deposit and its fossil biota in a dryland alluvial plain setting, Joggins, Nova Scotia. J. Geol. Soc. Lond. 161, 209–222.
Falcon-Lang, H.J., Benton, M.J., Stimson, M., 2007. Ecology of earliest reptiles inferred from basal Pennsylvanian trackways. J. Geol. Soc. Lond. 164, 1113–1118.

Ford, D.P., Benson, R.B.J., 2020. The phylogeny of early amniotes and the affinities of Parareptilia and Varanopidae. Nat. Ecol. Evolut. 4, 57–65.

Gand, G., Garric, J., Demathieu, G., Ellenberger, P., 2000. La palichnofaune de vertébrés tétrapodes du Permien supérieur du bassin de Lodève (Languedoc-France). Palaeovertebrata 29, 1–82.

Gand, G., Haubold, H., 1984. Traces de Vertèbrés tetrapodes du Permien du Bassin de Saint-Affrique (Description, datation, comparaison avec celle du bassin de Lodève). Géologie Méditerranéenne 11 (4), 321–348.

Gand, G., 1987. Les traces de vertébrés tétrapodes du Permien français: paléontologie, stratigraphie, paléoenvironnements.. State Ph.D. Thesis Université de Bourgogne, 368 pp.

Gand, G., De La Horra, R., Galán-Abellán, B., López-Gómez, J., Barrenechea, J.F., Arche, A., Benito, M.I., 2010. New ichnites from the Middle Triassic of the Iberian Ranges (Spain): palaeoenvironmental and paleogeographical implications. Hist. Biol. 22 (1–3), 40–56.

Geinitz, H.B., 1863. Beiträge zur Kenntnis der organischen Überreste in der Dyas. Neues Jahrbuch für Mineralogie, Geologie und Paläontologie 1863, 385–398 + pl. III–IV.

Gómez-Gras, D., 1993. El Permotrías de las Baleares y de la vertiente mediterránea de la Cordillera Ibérica y del Maestrat: Facies y Petrología Sedimentaria (Parte II). Bol. Geol. Min. 104, 467–515.

Hasiotis, S.T., Platt, B.F., Hembree, D.I., Everhart, M.J., 2007. The trace-fossil record of vertebrates. In: William Miller, I.I.I. (Ed.), Trace Fossils: Concepts, Problems, Prospects. Elsevier, pp. 196–218.

Haubold, H., Sarjeant, W.A.S., 1973. Tetrapodenfährten aus den Keele und Enville Groups (Permokarbon: Stefan und Autun) von Shropshire und South Staffordshire, Großbritannien. Z. Geol. Wiss. 1, 895–933.

Haubold, H., Hunt, A.P., Lucas, S.G., Lockley, M.G., 1995. Wolfcampian (Early Permian) vertebrate tracks from Arizona and New Mexico. N. M. Mus. Nat. Hist. Sci. Bull. 6, 135–165.

Hildebrand, M., 1980. The adaptive significance of tetrapod gait selection. Am. Zool. 20 (1), 255–267.

Hopson, J.A., 2015. Fossils, trackways, and transitions in locomotion: a case study of *Dimetrodon*. In: Dial, K.P., Shubin, N., Brainerd, E.L. (Eds.), Great Transformations in Vertebrate Evolution. University of Chicago Press, Chicago & London, 424 pp.

Kemp, T.S., 2005. The Origin and Evolution of Mammals. Oxford University Press, New York, 331 pp.

Klein, H., Lucas, S.G., Voigt, S., 2015. Revision of the ?Permian-Triassic tetrapod ichnogenus *Procolophonichnium* Nopcsa 1923 with description of the new ichnospecies *P. lockleyi*. Ichnos 22, 155–176.

Lagnaoui, A., Voigt, S., Belahmira, A., Saber, H., Klein, H., Hminna, A., Schneider, J.W., 2018. Late Carboniferous Tetrapod Footprints from the Souss Basin, Western High Atlas Mountains, Morocco. Ichnos 25 (2–3), 81–93.

Leonardi, G., 1987. Glossary and Manual of Tetrapod Footprint Palaeoichnology. Departamento Nacional de Produção Mineral, Brasília, 117 pp.

Liebrecht, T., Fortuny, J., Galobart, A., Müller, J., Sander, P.M., 2017. A large, multiple-tooth-rowed captorhinid reptile (Amniota: Eureptilia) from the Upper Permian of Mallorca (Balearic Islands, Western Mediterranean). J. Vertebr. Paleontol. 37 (1), 1–6 e1251936.

Logghe, A., Mujal, E., Marchetti, L., Nel, A., Pouillon, J.-M., Giner, S., Garrouste, R., Steyer, J.-S., 2021. *Hyloidichnus* trackways with digit and tail drag traces from the Permian of Gonfaron (Var, France): New insights on the locomotion of captorhinomorph eureptiles. Palaeogeogr. Palaeoclimatol. Palaeoecol. 573, 110436.

Lucas, S.G., 2019. An ichnological perspective on some major events of Paleozoic tetrapod evolution. Boll. Soc. Paleontol. Ital. 58 (3), 223–266.

Lucas, S.G., Kollar, A.D., Berman, D.S., Henrici, A.C., 2016. Pelycosaurian-grade (Amniota: Synapsida) footprints from the lower Permian Dunkard Group of Pennsylvania and West Virginia. Ann. Carnegie Museum 83 (4), 287–294.

Maddin, H.C., Sidor, C.A., Reisz, R.R., 2008. Cranial anatomy of *Ennatosaurus tecton* (Synapsida: Caseidae) from the Middle Permian of Russia and the evolutionary relationships of Caseidae. J. Vertebr. Paleontol. 28, 160–180.

Marchetti, L., Ronchi, A., Santi, G., Schirolli, P., Conti, M.A., 2015. Revision of a classic site for Permian tetrapod ichnology (Collio Formation, Trompia and Caffaro valleys, N. Italy), new evidences for the radiation of captorhinomorph footprints. Palaeogeogr. Palaeoclimatol. Palaeoecol. 433, 140–155.

Marchetti, L., Mujal, E., Bernardi, M., 2017. An unusual *Amphisauropus* trackway and its implication for understanding seymouriamorph locomotion. Lethaia 50, 162–174.

Marchetti, L., Klein, H., Buchwitz, M., Ronchi, A., Smith, R.M.H., De Klerk, W.J., Sciscio, L., Groenewald, G.H., 2019a. Permian-Triassic vertebrate footprints from South Africa: Ichnotaxonomy, producers and biostratigraphy through two major faunal crises. Gondwana Res. 72, 139–168.

Marchetti, L., van der Donck, H., van Hylckama Vlieg, M., During, M.A.D., 2019b. Leaving only trace fossils-the unknown visitors of Winterswijk. Staringia 16, 250–257.

Marchetti, L., Voigt, S., Lucas, S.G., Francischini, H., Dentzien-Dias, P., Sacchi, R., Mangiacotti, M., Scali, S., Gazzola, A., Ronchi, A., Millhouse, A., 2019c. Tetrapod ichnotaxonomy in eolian paleoenvironments (Coconino and De Chelly formations, Arizona) and late Cisuralian (Permian) sauropsid radiation. Earth Sci. Rev. 190, 148–170.

Marchetti, L., Belvedere, M., Voigt, S., Klein, H., Castanera, D., Díaz-Martínez, I., Marty, D., Xing, L., Feola, S., Melchor, R.N., Farlow, J.O., 2019d. Defining the morphological quality of fossil footprints. Problems and principles of preservation in tetrapod ichnology with examples from the Palaeozoic to the present. Earth Sci. Rev. 193, 109–145.

Marchetti, L., Voigt, S., Klein, H., 2019e. Revision of Late Permian tetrapod tracks from the Dolomites (Trentino-Alto Adige, Italy). Hist. Biol. 31 (6), 748–783.

Matamales-Andreu, R., Fortuny, J., Mujal, E., Galobart, À., 2019. Tetrapod tracks from the Permian of Mallorca (western Mediterranean): preliminary data, biostratigraphic and biogeographic inferences. In: The Palaeontological Association, 63rd annual meeting, 15th–21st December 2019, p. 107.

Meade, L.E., Jones, A.S., Butler, R.J., 2016. A revision of tetrapod footprints from the late Carboniferous of the West Midlands, UK. PeerJ 4, e2718.

Mujal, E., Marchetti, L., 2020. *Ichniotherium* tracks from the Permian of France, and their implications for understanding the locomotion and palaeobiogeography of large diadectomorphs. Palaeogeogr. Palaeoclimatol. Palaeoecol. 547, 109698.

Mujal, E., Fortuny, J., Oms, O., Bolet, A., Galobart, À., Anadón, P., 2016a. Palaeoenvironmental reconstruction and early Permian ichnoassemblage from the NE Iberian Basin (Pyrenean Basin). Geol. Mag. 153 (4), 578–600.

Mujal, E., Gretter, N., Ronchi, A., López-Gómez, J., Falconnet, J., Diez, J.B., De la Horra, R., Bolet, A., Oms, O., Arche, A., Barrenechea, J.F., Steyer, J.-S., Fortuny, J., 2016b. Constraining the Permian/Triassic transition in continental environments: Stratigraphic and palaeontological record from the Catalan Pyrenees (NE Iberian Peninsula). Palaeogeogr. Palaeoclimatol. Palaeoecol. 445, 18–37.

Mujal, E., Marchetti, L., Schoch, R.R., Fortuny, J., 2020. Upper Paleozoic to lower Mesozoic tetrapod ichnology revisited: photogrammetry and relative depth pattern inferences on functional prevalence of autopodia. Front. Earth Sci. 8 (248), 1–23.

Nyakatura, J.A., Allen, V.R., Lauströer, J., Andikfar, A., Danczak, M., Ullrich, H.-J., Hufenbach, W., Martens, T., Fischer, M.S., 2015. A three-dimensional skeletal reconstruction of the stem amniote *Orobates pabsti* (Diadectidae): analyses of body mass, centre of mass position, and joint mobility. PLoS One 10 (9), e0137284.

Nyakatura, J.A., Melo, K., Horvat, T., Karakasiliotis, K., Allen, V.R., Andikfar, A., Andrada, E., Arnold, P., Lauströer, J., Hutchinson, J.R., Fischer, M.S., Ijspeert, A.J., 2019. Reverse-engineering the locomotion of a stem amniote. Nature 565, 351–355.

Olson, E.C., 1968. The family Caseidae. Fieldiana: Geology 17 (3), 225–349.

Ramos, A., 1995. Transition from alluvial to coastal deposits (Permian–Triassic) on the Island of Mallorca, western Mediterranean. Geol. Mag. 132 (4), 435–447.

Romano, M., Citton, P., Nicosia, U., 2016. Corroborating trackmaker identification through footprint funcional analysis: the case study of *Ichniotherium* and *Dimetropus*. Lethaia 49, 102–116.

Romano, M., Brocklehurst, N., Fröbisch, J., 2017. The postcranial skeleton of *Ennatosaurus tecton* (Synapsida, Caseidae). J. Syst. Palaeontol. 16 (13), 1097–1122.

Romano, M., Citton, P., Nicosia, U., 2020. A review of the concepts of 'axony' and their bearing on tetrapod ichnology. Hist. Biol. 32 (5), 611–619.

Romer, A.S., Price, L.I., 1940. Review of the Pelycosauria. Geol. Soc. Am. Spec. Pap. 28, 1–538.

Sacchi, E., Cifelli, R., Citton, P., Nicosia, U., Romano, M., 2014. *Dimetropus osageorum* n. isp. from the Early Permian of Oklahoma (USA): A Trace and its Trackmaker. Ichnos 21, 175–192.

Sevillano, A., Barnolas, A., 2019. Mapa Geológico Digital Continuo E. 1:50.000, Zona Mallorca (Zona-2210). In: GEODE. Mapa Geológico Digital Continuo de España. GEODE,. Available online at. http://info.igme.es/visorweb/ (last accessed on 26/07/2019).

Spindler, F., Falconnet, J., Fröbisch, J., 2016. *Callibrachion* and *Datheosaurus*, two historical and previously mis-taken basal caseasaurian synapsids from Europe. Acta Palaeontol. Pol. 61 (3), 597–616.

Spindler, F., Werneburg, R., Schneider, J.W., 2019. A new mesenosaurine from the lower Permian of Germany and the postcrania of *Mesenosaurus*: implications for early amniote comparative osteology. Paläontol. Z. 93, 303–344.

Tilton, J.L., 1931. Permian vertebrate tracks in West Virginia. Bull. Geol. Soc. Am. 42, 547–556.

Van Allen, H.E.K., Calder, J.H., Hunt, A.P., 2005. The trackway record of a tetrapod community in a walchian conifer forest from the Permo-Carboniferous of Nova Scotia. N. M. Mus. Nat. Hist. Sci. Bull. 30, 322–332.

Voigt, S., 2005. Die Tetrapodenichnofauna des kontinentalen Oberkarbon und Perm im Thüringer Wald - Ichnotaxonomie, Paläoökologie und Biostratigraphie. Cuvillier Verlag, Göttingen, 308 pp.

Voigt, S., 2012. Tetrapodenfährten im Rotliegend. In: Lützner, H., Kowalczyk, G. (Eds.), *Stratigraphie von Deutschland X. Rotliegend. Teil I: Innervariscische Becken*. Schriftenreihe der Deutschen Gesellschaft für Geowissenschaften, 61, pp. 161–175.

Voigt, S., Ganzelewski, M., 2010. Toward the origin of amniotes: Diadectomorph and synapsid footprints from the early Late Carboniferous of Germany. Acta Palaeontol. Pol. 55 (1), 57–72.

Voigt, S., Berman, D.S., Henrici, A.C., 2007. First well-established track-trackmaker association of paleozoic tetrapods based on *Ichniotherium* trackways and diadectid skeletons from the Lower Permian of Germany. J. Vertebr. Paleontol. 27 (3), 553–570.

Voigt, S., Lagnaoui, A., Hminna, A., Saber, H., Schneider, J.W., 2011. Revisional notes on the Permian tetrapod ichnofauna from the Tiddas Basin, central Morocco. Palaeogeogr. Palaeoclimatol. Palaeoecol. 302, 474–483.

Voigt, S., Niedźwiedzki, G., Raczyński, P., Mastalerz, K., Ptaszyński, T., 2012. Early Permian tetrapod ichnofauna from the Intra-Sudetic Basin, SW Poland. Palaeogeogr. Palaeoclimatol. Palaeoecol. 313–314, 173–180.

Appendix 4

A new moradisaurine captorhinid and its locomotion

Appendix 4 was prepared as:

Matamales-Andreu, R.; Mujal, E.; Galobart, À. & Fortuny, J. (under review). A new medium-sized moradisaurine captorhinid eureptile from the Permian of Mallorca (Balearic Islands, western Mediterranean) and correlation with the co-occurring ichnogenus *Hyloidichnus*.

In this work, R. Matamales-Andreu contributed in:

A. Logging of the stratigraphic section.
B. Co-direction of all fieldwork campaigns (prospections and excavations). Sampling of tetrapod tracks and bones.
C. 3D modelling of tetrapod tracks and trackways.
D. Stratigraphic and sedimentological analysis.
E. Vertebrate palaeontology, including description of the new genus and species.
F. Coding of character matrix and phylogenetic analysis.
G. Interpretation and discussion of the results.
H. Writing of the original draft and supplementary materials, except for section 'Correlation of *Tramuntanasaurus tiai* gen. *et* sp. nov. with ichnites from the same area' (palaeoichnology).
I. Preparation of figures 1–6. Adaptation of figures 7 and SF1.
J. Collaboration in obtaining funding for fieldwork and fossil preparation.

Taxonomical disclaimer:

The name of the new taxon described in Appendix 4 is not valid under the rules of the International Code of Zoological Nomenclature. The publication where it will be formally erected is in process of review, and the name proposed here will be retained if possible.

A new medium-sized moradisaurine captorhinid eureptile from the Permian of Mallorca (Balearic Islands, western Mediterranean) and correlation with the co-occurring ichnogenus *Hyloidichnus*

Rafel Matamales-Andreu[1,2]‡, Eudald Mujal[3,2]*‡, Àngel Galobart[2,4], Josep Fortuny[2]

[1] Museu Balear de Ciències Naturals, FJBS-MBCN, ctra. Palma-Port de Sóller km 30.5, 07100 Sóller, Mallorca, Illes Balears, Spain.

[2] Institut Català de Paleontologia Miquel Crusafont, Universitat Autònoma de Barcelona, Edifici ICTA-ICP, c/ Columnes s/n, Campus de la UAB, 08193 Cerdanyola del Vallès, Barcelona, Catalunya, Spain.

[3] Staatliches Museum für Naturkunde Stuttgart, Rosenstein 1, 70191 Stuttgart, Germany.

[4] Museu de la Conca Dellà, c/ del Museu 4, 25650 Isona i Conca Dellà, Lleida, Catalunya, Spain.

*Corresponding author: rafel.matamales@icp.cat

‡ These authors contributed equally to this paper.

Abstract

Moradisaurine captorhinid eureptiles are one of the best-known groups of Permian herbivorous tetrapods. Moradisaurines, with several rows of teeth on the maxillae and jaws, first appeared in the Cisuralian and became extinct at the end of the Lopingian, and were especially abundant in the equatorial latitudes of Pangaea. However, the postcranial skeleton of this clade is relatively poorly known, as most of the species described have been based on skulls. This fact has precluded a detailed correlation to coeval tracks. The present work describes a new moradisaurine genus and species, *Tramuntanasaurus tiai* gen. *et* sp. nov., based on an almost complete, semi-articulated skeleton from the Port des Canonge Formation of Mallorca (Balearic Islands, western Mediterranean), identifying it as the trackmaker of the co-ocurring small-sized traces of the ichnogenus *Hyloidichnus*. Apart from documenting the new moradisaurine species, the results presented herein strongly support that *Hyloidichnus* was produced by both non-moradisaurine captorhinids and moradisaurines, which, at least those of small to medium size, had a very conserved autopodial morphology and gait. Therefore, this study provides new data to infer the trackmakers of *Hyloidichnus* where bone remains are missing, and thus contributes to the understanding of Permian tetrapod ichnofaunas and tetrapod communities.

Keywords: Permian, Moradisaurinae, Captorhinidae, eureptile, *Hyloidichnus*

1. Introduction

Moradisaurine captorhinids were a moderately diverse clade of eureptiles with species that lived in the low latitudes of Pangaea during the Permian (*e.g.*, Cisneros *et al.*, 2020; Matamales-Andreu *et al.*, 2021a). They were among the first tetrapod clades to develop high-fibre herbivory, with tooth plates on the maxilla and the dentary used to grind and shred plant material using a propalinal motion of the lower jaw (Dodick & Modesto, 1995; Reisz & Sues, 2000; Modesto *et al.*, 2007, 2014, 2019). The genus *Captorhinikos* Olson, 1954, the most basal and oldest of the subfamily Moradisaurinae de Ricqlès & Taquet, 1982, has been found in the Artinskian (Cisuralian) of North and South America (Cisneros *et al.*, 2020 and references therein). The most recent genera, of Guadalupian–Lopingian epoch, are: *Acrodenta* Dutuit, 1976, from northern Africa; *Gansurhinus* Reisz, Liu, Li *et* Müller, 2011, from Asia; *Gecatogomphius* Vjushkov *et* Chudinov, 1957, from eastern Europe; *Kahneria* Olson, 1962a, from southern North America; and *Moradisaurus* Taquet, 1969, from central Africa (Olson, 1962a; Jalil & Dutuit, 1996; O'Keefe *et al.*, 2005; Hmich *et al.*, 2006; Ivakhnenko, 2008; Reisz *et al.*, 2011; Olroyd & Sidor, 2017; Modesto *et al.*, 2019; Laurin & Hook, 2022; Sidor *et al.*, 2022). Almost all known species have been described based on cranial material, and semi-complete skeletons are only well known in the case of the species *Captorhinikos chozaensis* Olson, 1954 (Olson, 1962b; Jung, 2018). Other moradisaurine genera with preserved postcranial remains are *Gansurhinus* (see Reisz *et al.* 2011), *Kahneria* (see Olson, 1962a), *Moradisaurus* (see O'Keefe *et al.*, 2005), and *Rothianiscus* Kuhn, 1961 (see Olson & Barghusen, 1962).

The tetrapod ichnofossil record generally mirrors that of captorhinomorph eureptiles. The ichnogenus *Hyloidichnus* Gilmore, 1927, first described from the Cisuralian of Colorado, North America (Gilmore, 1927) and extensively known from many localities of equatorial Pangaea (Logghe *et al.*, 2021; Matamales-Andreu *et al.*, 2021a), has been classically attributed to captorhinomorph trackmakers. This has been recently demonstrated on an anatomy-based correlation with a detailed reconstruction of the step cycles based on well-preserved trackways (Logghe *et al.*, 2021; see also Holmes, 2003). *Hyloidichnus* tracks, especially those of larger size (>5 cm long), have been referred to moradisaurines (Voigt *et al.*, 2010). In addition, the ichnogenus *Merifontichnus* Gand, Garric, Demathieu *et* Ellenberger, 2000, is also correlated with moradisaurines (Marchetti, 2016). This interpretation is consistent with the relative depth patterns of this ichnogenus, because they are the same as those of *Hyloidichnus*, hence suggesting an equivalent functional prevalence of autopodia of the trackmakers of both ichnogenera (Mujal *et al.*, 2020).

Body fossils of moradisaurines are scarce in the deposits of the southeastern part of the Variscan mountains, with seven reported specimens comprising at least three different species, all from the present-day Balearic Islands (western Mediterranean), although only one has been named formally. From an indeterminate Permian level (probably Guadalupian–Lopingian) of the P3 unit of the island of Menorca, Matamales-Andreu *et al.* (2021a) reported four specimens: (1) a new, large moradisaurine with a unique teeth ornamentation of ridges and furrows, named *Balearosaurus bombardensis* Matamales-Andreu, Roig-Munar, Oms, Galobart *et* Fortuny, 2021; (2) a second specimen of large size consisting of several cranial and postcranial remains that was tentatively also attributed to the same species; (3) a vertebra of an indeterminate, smaller species; and (4) a fragment of lower jaw

with three rows of teeth that also belonged to a medium-sized, indeterminate species. Additionally, from the Cisuralian–?Guadalupian of the Port des Canonge Formation of Mallorca (see Matamales-Andreu *et al.* 2022; **Appendix 5** of the present dissertation), Liebrecht *et al.* (2017) reported a fragment with parts of the palate and the maxilla, with three rows of teeth, that belonged to a large, indeterminate species of moradisaurine. Recently, Matamales-Andreu *et al.* (2021b) preliminarily reported two more moradisaurine specimens from that formation, (1) an essentially complete and mostly articulated skeleton of a medium-sized species, and (2) a small specimen, probably juvenile, consisting of several semi-articulated cranial, axial and appendicular remains. The present work is focused on the former, providing a detailed description of what is the most complete moradisaurine skeleton known to date, and introducing a new genus and species. Moreover, the presence of tracks corresponding to the ichnospecies *Hyloidichnus bifurcatus* Gilmore, 1927, in stratigraphically close beds (see Matamales-Andreu *et al.* 2022), is utilised to propose a track-trackmaker correlation considering the specimen herein studied.

2. Geographical and geological setting

Mallorca is the largest island of the Balearic Archipelago, a group of five islands and many islets located in the western Mediterranean basin. Permian rocks crop out on Menorca (Matamales-Andreu *et al.*, 2021a) and Mallorca (Matamales-Andreu *et al.*, 2022), although in the latter the majority of outcrops are very small and inaccessible. Despite this, the fossil record is very rich compared to nearby regions, with spores, pollen, macroplant remains, invertebrate ichnofossils, and tetrapod tracks and bones (Calafat *et al.*, 1986–1987; Calafat, 1988; Liebrecht *et al.*, 2017; Matamales-Andreu *et al.*, 2021b; 2021c; 2021d; 2022). The fossils studied in the present work were collected *in situ* at the Torrent de na Nadala fossil site, located in the northwestern margin of the Serra de Tramuntana, the main mountain range of the island (**Figure 1A**).

During the Permian, the region nowadays corresponding to Mallorca was located in the equatorial latitudes of the supercontinent Pangaea, under a semi-arid, seasonal climate (see Matamales-Andreu *et al.*, 2022). Three units that encompass the Permian sequence of Mallorca have been recently described (Matamales-Andreu *et al.*, 2022), from lower to upper: (1) Bec de s'Àguila Formation, made up of colluvial and alluvial-fan conglomerates; (2) Port des Canonge Formation, of floodplain and meandering river mudstones and sandstones; and (3) Pedra de s'Ase Formation, of meandering river, sheetflood sandstones and, less commonly, floodplain mudstones (Matamales-Andreu *et al.*, 2022). A Cisuralian epoch (Artinskian/Kungurian) was attributed to the Port des Canonge Formation based on the tetrapod ichnoassemblage (Matamales-Andreu *et al.*, 2022), but a lowermost Guadalupian stage, even though unlikely, cannot be excluded for the uppermost part of the unit (**Appendix 5** of the present dissertation). The Pedra de s'Ase Formation has been dated as Guadalupian (Roadian/Wordian) based on the palynoassemblages and palaeomagnetic data (Matamales-Andreu *et al.*, 2022).

The Torrent de na Nadala fossil site (**Figure 1B–C**) is located at the lower part of the Racó de s'Algar–Pedra de s'Ase section, and corresponds to the Port des Canonge Formation (see all names of stratigraphic sections and localities from Mallorca in Matamales-Andreu *et al.*, 2022). The fossiliferous beds comprise a thickness of about

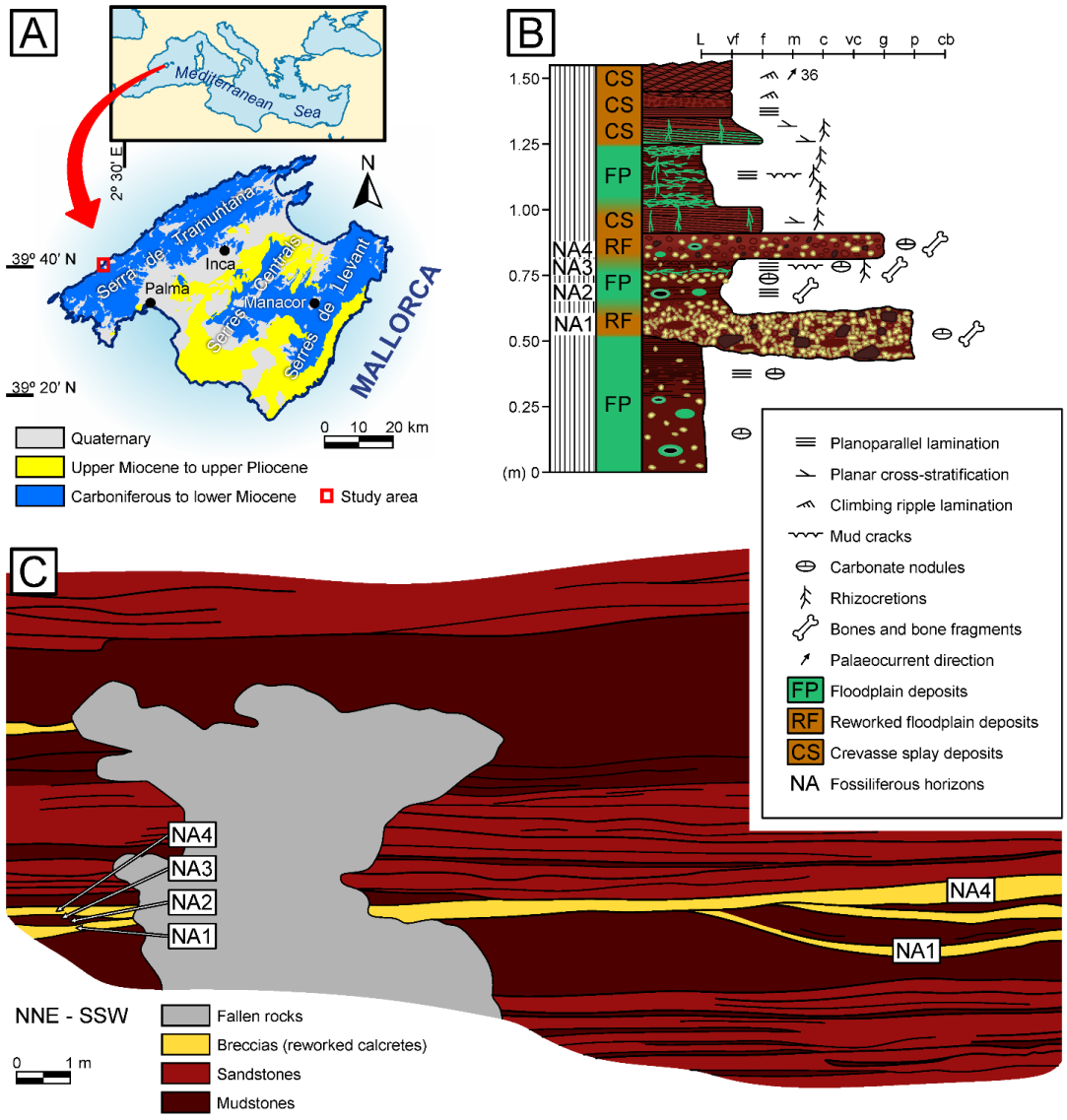

Figure 1. A: Geological synthetic map of the island of Mallorca, with indication of the study area. **B:** Detailed stratigraphic log of the Torrent de na Nadala site (for general stratigraphic context, see Matamales-Andreu *et al.*, 2022). Colours of beds and layers in the log represent approximate rock colours at the outcrop. Clasts depicted in the log represent: reworked carbonate nodules (yellow with outline), sandstone clasts (red and maroon with outline), clay chips (dark red without outline) and gleyed patches (green, sometimes surrounding black coalified plant remains). Rhizocretions have been represented as vertical or horizontal based on their arrangement at the outcrop. Abbreviations: L = mudstones, vf = very fine-grained sandstones, f = fine-grained sandstones, m = medium-grained sandstones, c = coarse-grained sandstones, vc = very coarse-grained sandstones, g = gravel-sized breccia, p = pebble-sized breccia, cb = cobble-sized breccia. **C:** Sketch of the outcrop at Torrent de na Nadala, showing the geometry of the sedimentary bodies containing the fossils.

40 cm of silty sandstones with four distinct horizons that have yielded bone remains here named, from lower to upper, Torrent de na Nadala 1–4 (NA1–4). Specifically, the specimen described in the present work was collected *in situ* from the horizon NA3. Just above its cranium, in the horizon NA4, there was a semi-articulated skeleton of another, much smaller captorhinid with multiple tooth rows (Matamales-Andreu *et al.*, 2021c), which is not considered here because it is still under preparation. The horizon NA2 also contained several multiple tooth-rowed captorhinid skeletons that will be the subject of future studies.

In terms of depositional environments, the four fossiliferous horizons of Torrent de na Nadala correspond to levée, crevase splay and floodplain deposits of slightly different nature. NA1 is herein interpreted as the deposits of ephemeral floodplain channels, as it is equivalent to the 'Type 1' reworked calcretes described by Gómez-Gras & Alonso-Zarza (2003). The breccia deposits herein observed are certainly of a larger scale (about 20–30 cm thick and several metres wide) than those studied by the aforementioned authors, but all the other traits match relatively well, with the presence of a scouring base, crude cross-bedding, and lack of extraformational clasts. In NA1, bones always appear isolated and with random orientations, evidencing that that horizon was formed by dense flows (*e.g.*, Miall, 2006). The horizon NA2 corresponds to the sandy muds deposited when the flow waned. It represents a stage of no deposition in which mud cracks and palaeosols formed. These deposits contain abundant carbonate nodules, rhizocretions and sporadic carbonised plant debris. The beds show no clear lamination, and essentially fill the depressions of the irregular top of NA1. The bones found in this horizon show no signs of transport by water, and thus, the fact that they are disarticulated and some elements are missing, probably points to long periods of exposure on the floodplain (cf. Behrensmeyer, 1982). Carbonate nodules and small rhizocretions are especially abundant near the bones, sometimes forming crusts over them. Above, there is a horizon of larger (2–3 cm) carbonate nodules followed by abundant horizontal, gleyed fossil roots; the latter may indicate a brief period of high water table. NA3 overlies these horizons, being lithologically very similar to NA2, *i.e.*, with mud cracks, carbonate nodules and rhizocretions. The skeletons found in NA3 do not show signs of transport by water either, and are slightly disarticulated, probably because of weathering or scavenging (cf. Behrensmeyer, 1982). NA4 can be attributed to the 'Type 2' reworked calcretes as described by Gómez-Gras & Alonso-Zarza (2003), thus corresponding to the deposits of the proximal part of crevasse splay lobes. These intraformational breccias are essentially tabular elements with cross-bedding, containing some isolated bones in random orientation but also semi-articulated skeletons. The sequence ends with several very fine- to fine-grained sandstones with low-angle cross-bedding and climbing ripple lamination corresponding to crevasse splay deposits.

In outcrop view (**Figure 1C**), it has been established that the sequence of fossiliferous horizons was deposited in a slightly depressed area of the floodplain. This is because the sandy mudstone deposits that have yielded bones and skeletons wedge laterally, where the breccia beds directly underlay the crevasse splay sandstones. That zone might have acted as an ephemeral waterhole frequented by the local fauna, as indicated by the presence of mud cracks and horizontal, gleyed root traces. Smith (1993) argued that such environments ('Taphonomic Pathway 6') were areas of bone accumulation through predation, and that the trampling of the bones by other animals accelerated their incorporation into the substrate.

3. Material and methods

3.1. The studied skeleton

The specimen herein studied was extracted from an in situ layer of the Torrent de na Nadala 3 fossil site (NA3) in 2019, with the legal permission of the Comissió Insular de Patrimoni Històric del Consell de Mallorca (file number 306-2019). Then, it was transported to the Institut Català de Paleontologia Miquel Crusafont (ICP, Cerdanyola del Vallès, Spain), where it was prepared using airscribes and micro-air abrasives. The skull and jaws were separated from the surrounding matrix and scanned at the Centro Nacional de Investigación sobre Evolución Humana (CENIEH, Burgos, Spain) using a high-resolution X-ray tomography scanner µCT model V|Tome|X s 240 (GE Sensing & Inspections Technologies). The micro-CT acquisition was carried out at 240 kV and a current of 520 µA, obtaining a voxel size of 65.50 µm. The X-ray beam was filtered by a 0.2 mm-thick copper absorber. The low contrast between some of the bones and the surrounding matrix precluded detailed segmentation of the complete skull. Nevertheless, a preliminary segmentation was carried out and, although the results were good for the maxilla and the jaw, it was not possible to delimit sutures among bones or internal cranial structures. The fossil is now housed at the Museu de Mallorca (Palma, Spain), under the collection number DA21/17-01-03.

3.2. Phylogenetic analysis

The present study used the matrix provided by Albright *et al.* (2021) for the Captorhinomorpha, with the modifications for Moradisaurus introduced by Sidor *et al.* (2022). The character states for *Kahneria seltina* Olson, 1962a, have been added to the matrix following Brocklehurst (2020). The character states for *Captorhinus kierani* deBraga, Bevitt *et* Reisz, 2019, have been added following deBraga *et al.* (2019). The character states for *Labidosauriscus richardi* Modesto, Scott *et* Reisz, 2018, were also added following Modesto *et al.* (2018), but this taxon was finally excluded from the analysis because it caused large polytomies. The moradisaurines reported from the Permian of the Balearic Islands (Liebrecht *et al.*, 2017; Matamales-Andreu *et al.*, 2021a) were also excluded from the analysis due to the large amount of missing data, which caused large polytomies. This was especially because of the recognition of incorrect character states in the matrix by Liebrecht *et al.* (2017) (and all the subsequent works that included that specimen), regarding the indeterminate large moradisaurine from the Permian of Mallorca, and in the matrix by Matamales-Andreu *et al.* (2021a), concerning the holotype of Balearosaurus bombardensis from the Permian of Menorca. Both specimens are fragments of maxillae, and thus tooth counts cannot be carried out with reasonable confidence. For this reason, characters 6, 7 and 9 must, in both cases, be coded as indeterminate ('?') instead.

Phylogenetic analysis was run using PAUP* v.4.0 (Swofford, 2003) as a branch-and-bound search with parsimony as the optimality criterion, with unordered and unweighted characters. Then, a strict consensus tree was computed, and bootstrap support values were calculated with 100 repetitions, not showing values under 50.

3.3. Ichnology and track-trackmaker correlation

For the ichnological study, this work follows Matamales-Andreu *et al.* (2022), who provided detailed descriptions of the tracks attributed to *Hyloidichnus bifurcatus*. Terminology of track and trackway parameters follows the conventions of Leonardi (1987).

Matamales-Andreu *et al.* (2022) identified two morphotypes of this ichnospecies, mainly differentiated by their size (*i.e.*, designated as small and large morphotypes) and by slight differences in the relative depth patterns in both manus and pes imprints. Considering the size of the tracks, in this work those of the small morphotype of *Hyloidichnus bifurcatus* from Mallorca are used to perform a track-trackmaker correlation following the approaches by Voigt *et al.* (2007), Marchetti *et al.* (2017) and Logghe *et al.* (2021), the latter being focused on the correlation of *Hyloidichnus* to captorhinomorph trackmakers. Of relevance, this is a similar case to that reported by Voigt *et al.* (2007), in which tracks and the purported trackmakers were found in close stratigraphic levels.

Herein, a slab preserving a trackway (specimen DA21/15-13-02) is analysed. The trackway, preserved in convex hyporelief in a laminated fine-grained sandstone slab, is composed of three consecutive manus imprints, two of which are coupled with pes imprints (*i.e.*, the trackway consists of two manus-pes sets and an isolated manus imprint), and a slightly sinuous tail trace. They score a 1–2 (intermediate–good) in the track preservation scale of Marchetti *et al.* (2019). A 3D photogrammetric model of the specimen was created based on a set of 73 photographs taken with the digital camera Panasonic Lumix DMC-TZ27. The workflow mainly follows Mallison & Wings (2014) and Mujal *et al.* (2020) for photograph acquisition, and Mujal *et al.* (2020) for the generation of the model. The dense point cloud and triangular mesh with original colour texture was generated by using Agisoft Photoscan (standard version 1.1.4), and the mesh was edited using Meshlab (v.2020.07), a false colour-coded depth map with contours was obtained from the 3D model using ParaView (v.4.1.0). The specimen was collected from the Platjola des munt de Pedres 4 site (Matamales-Andreu *et al.*, 2022), representing floodplain settings cut by meandering fluvial channels, which correspond to the upper part of the Port des Canonge Formation (Cisuralian–?Guadalupian). The specimen is housed at the Museu de Mallorca (Palma, Spain).

4. Systematic palaeoichnology

Reptilia Laurenti, 1768

Eureptilia Olson, 1947

Captorhinomorpha Carroll *et* Baird, 1972

Family Captorhinidae Case, 1911

Subfamily Moradisaurinae de Ricqlès *et* Taquet, 1982

Genus *Tramuntanasaurus* gen. nov.[1]

Type species: *Tramuntanasaurus tiai* gen. *et* sp. nov.

Origin of the name: From 'Tramuntana', the main mountain range of Mallorca, where the holotype specimen was found, and 'saurus', Latin for 'lizard'. Gender: masculine.

Diagnosis: Medium-sized moradisaurine with a broad snout relative to skull length (unlike *Labidosaurikos*, *Moradisaurus* and *Rothianiscus*), anteriormost dentary teeth pointing rostrally (unlike *Captorhinikos* and *Gecatogomphius*), a double row of teeth anterior to the tooth plate (unlike *Captorhinikos* and *Moradisaurus*), and without a diastema (unlike *Gansurhinus* and *Kahneria*) (Olson, 1962a, 1962b, 1965; de Ricqlès & Taquet, 1982; Dodick & Modesto, 1995; Ivakhnenko, 2008; Reisz *et al.*, 2011; LeBlanc *et al.*, 2015; Jung, 2018; Sidor *et al.*, 2022).

Tramuntanasaurus tiai gen. *et* sp. nov.[2]

Figures 2, 3, 4, 5, Supplementary Figure 1

Holotype: DA21/17-01-03, a nearly complete, semi-articulated skeleton.

Origin of the name: Dedicated to Sebastià (Tià) Matamalas Riera, father of the first author (R.M.A.) and discoverer of the holotype specimen.

Type level, locality and age: Torrent de na Nadala 3 fossil site (NA3), Port des Canonge Formation (Cisuralian–?Guadalupian, Permian), Racó de s'Algar–Pedra de s'Ase section, Banyalbufar, Mallorca, Balearic Islands.

Diagnosis: Medium-sized moradisaurine captorhinid characterised by the following combination of characters: triangular skull with relatively broad snout, postorbital cheek with little lateral convexity, anterior process of frontal long, anterior process of jugal reaching anterior orbital margin, pterygoid without teeth, maxilla and dentary with five tooth rows, lack of diastema, anteriormost dentary teeth pointing rostrally.

Description: *Skull*: The skull is medium-sized (maximum width 70.0 mm, although it is crushed and slightly deformed, it was slightly wider originally; anteroposterior length 83.1 mm) and distinctly triangular in shape. In dorsal view, it tapers progressively towards its anterior end, without an abrupt decrease of width in the snout zone (unlike most moradisaurines). The posterior margin of the skull is, in dorsal view, slightly convex. The ventral margin is somewhat sigmoidal in lateral view, being convex in the post-orbital area (jugal and quadratojugal) and straight in the maxilla/splenial. The anteriormost portion of the skull is not well preserved, and thus it is unknown whether it is recurved ventrally (like most captorhinids) or not. All the bones of the skull roof are externally ornamented with a dense honeycomb pattern. The sutures between bones are straight or gently curved, without dense interfingering

[1] This genus description is not valid under the ICZN code, as this work is still under review. See the cover page of this appendix for more information.
[2] This species description is not valid under the ICZN code, as this work is still under review. See the cover page of this appendix for more information.

9

Figure 2. (previous page) Holotype specimen of *Tramuntanasaurus tiai* gen. *et* sp. nov. (DA21/17-01-03), from the Cisuralian–?Guadalupian Port des Canonge Formation at Torrent de na Nadala 3. Scale bar represents 25 mm.

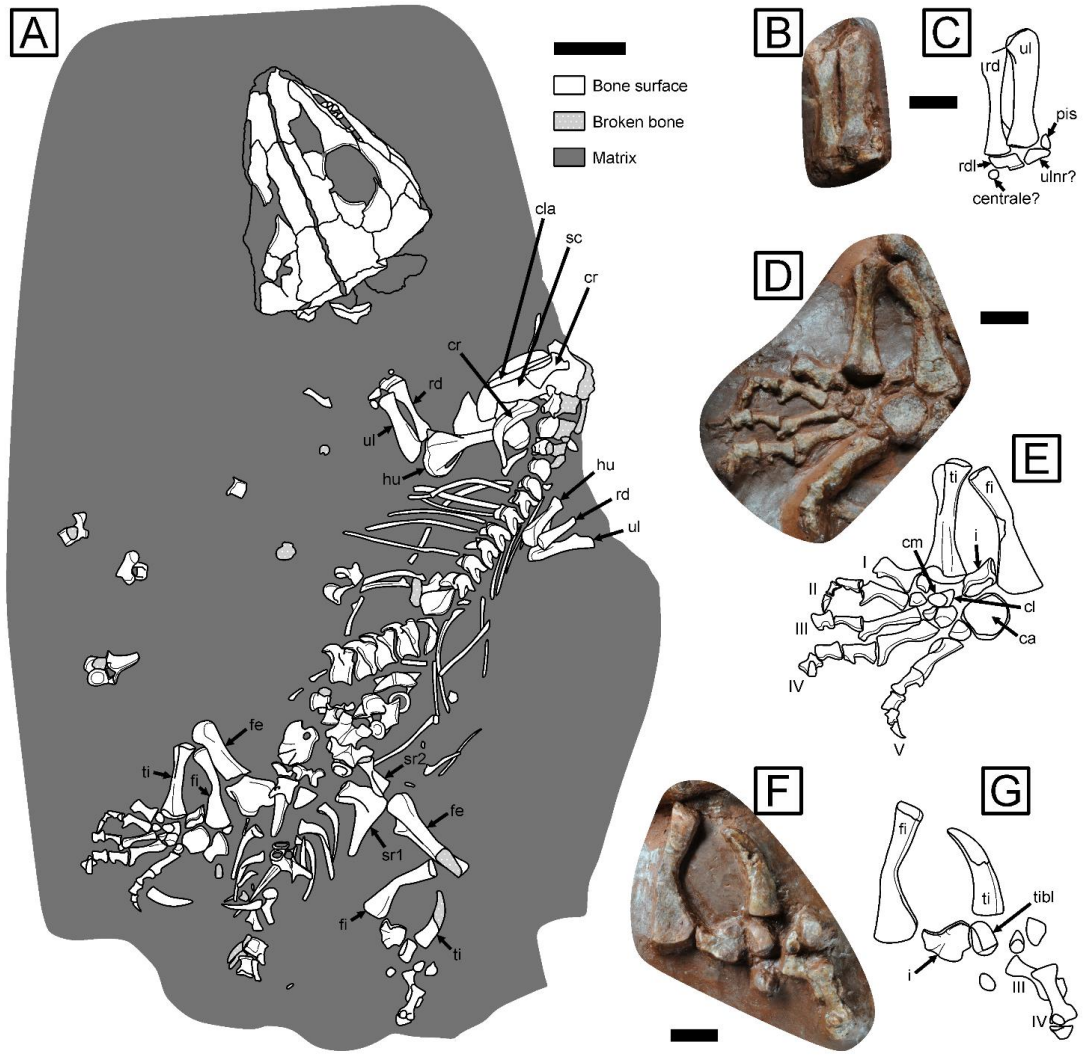

Figure 3. **A:** Interpretative drawing of the holotype specimen of *Tramuntanasaurus tiai* gen. *et* sp. nov. (DA21/17-01-03) from the Cisuralian–?Guadalupian Port des Canonge Formation at Torrent de na Nadala 3. **B:** Detail of left forelimb. **C:** Interpretative drawing of left forelimb. **D:** Detail of left hindlimb. **E:** Interpretative drawing of left hindlimb. **F:** Detail of right hindlimb. **G:** Interpretative drawing of right hindlimb. Abbreviations: I–V = metatarsals I–V, ca = calcaneum, cl = lateral centrale, cla = clavicle, cm = medial centrale, cr = cervical rib, fe = femur, fi = fibula, hu = humerus, i = intermedium (astragalus), rd = radius, sc = scapulocoracoid, sr1–2 = first and second sacral ribs, respectively, ti = tibia, tibl = tibiale (astragalus), pis = pisiform, rd = radius, rdl = radiale, ul = ulna, ulnr = ulnare. Scale bars represent: 25 mm (A); 10 mm (B–G).

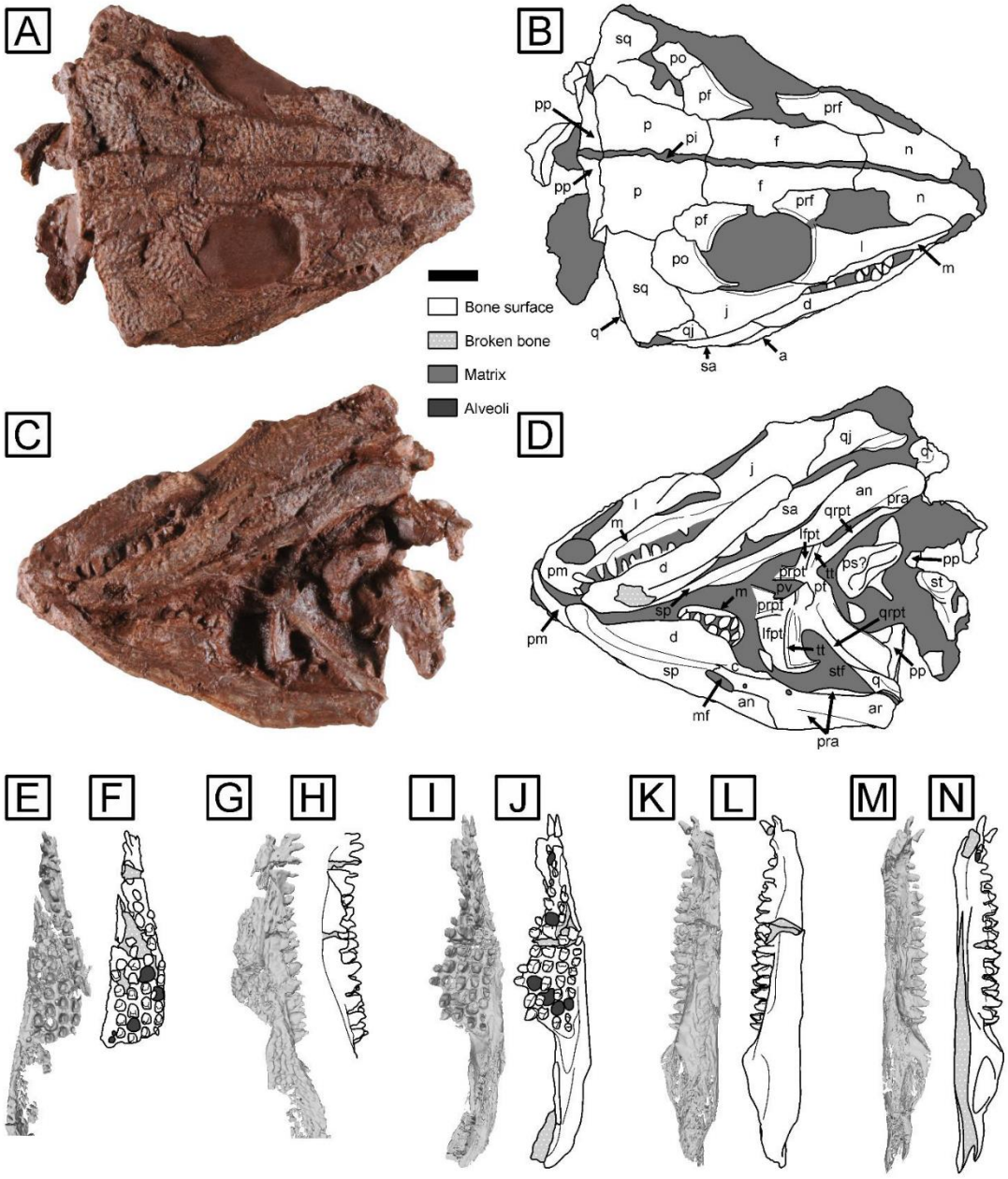

Figure 4. Skull and jaws of the holotype specimen of *Tramuntanasaurus tiai* gen. *et* sp. nov. (DA21/17-01-03), from the Cisuralian–?Guadalupian Port des Canonge Formation at Torrent de na Nadala 3. **A:** Dorsal view of the skull of the specimen DA21/17-01-03. **B:** Interpretative drawing of dorsal view. **C:** Ventral view of the skull of the specimen DA21/17-01-03. **D:** Interpretative drawing of ventral view. **E–F:** 3D model and interpretative drawing of right maxilla in occlusal view. **G–H:** 3D model and interpretative drawing of right maxilla in lateral view. **I–J:** 3D model and interpretative drawing of right jaw in occlusal view. **K–L:** 3D model and interpretative drawing of right jaw in lateral view. **M–N:** 3D model and interpretative drawing of right jaw in medial view.Abbreviations: an = angular, ar = articular, c = coronoid, d = dentary, q = quadrate, qj = quadratojugal, qrpt = pterygoid quadrate ramus, j = jugal, l = lacrimal, lfpt = pterygoid lateral flange, m = maxilla, mf = Meckelian foramen, n = nasal,

p = parietal, pi = pineal foramen, pf = postfrontal, pm = premaxilla, po = postorbital, pp = postparietal, pra = preangular, prf = prefrontal, prpt = pterygoid palatine ramus, ps = parasphenoid, pt = pterygoid, pv = interpterygoid vacuity, sa = surangular, sp = splenial, sq = squamosal, st = stapes, stf = subtemporal fossa, tt = torosus transiliens. Scale bar represents 10 mm.

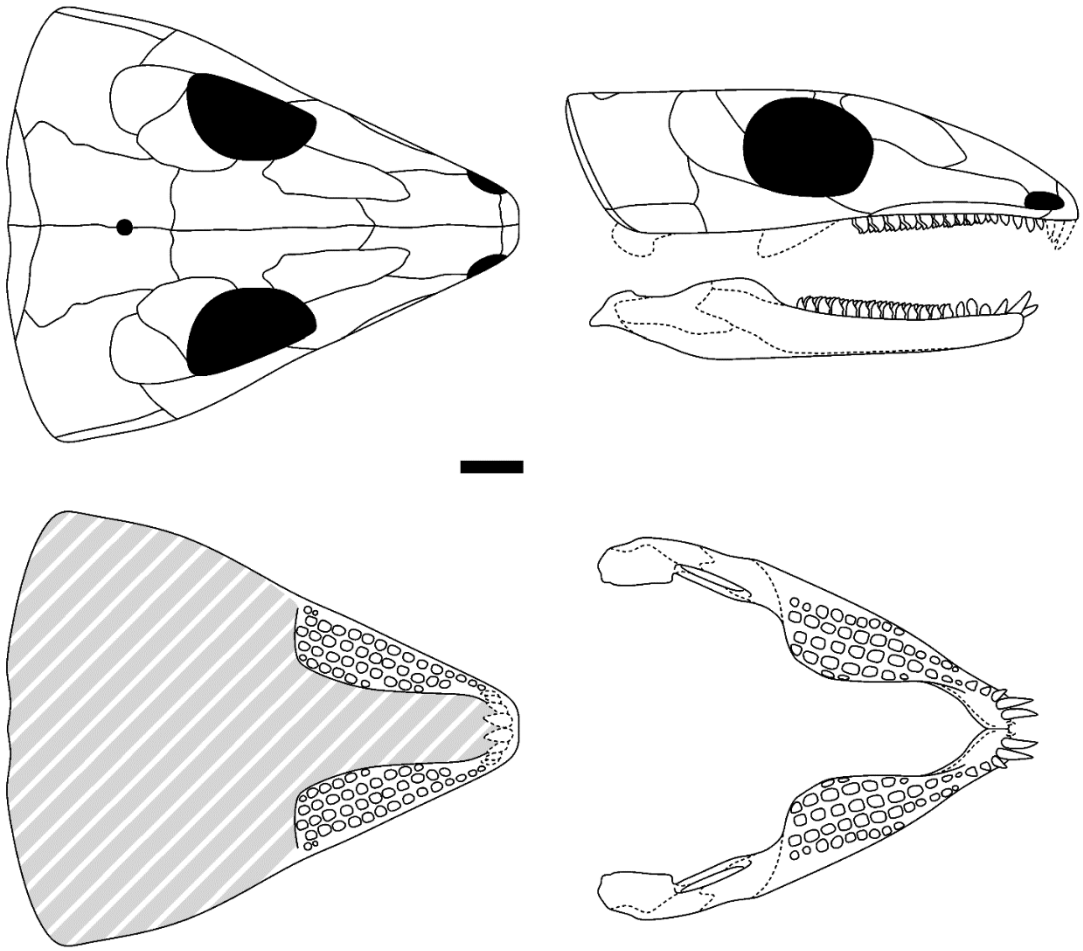

Figure 5. Reconstruction of the skull and jaws of *Tramuntanasaurus tiai* gen. *et* sp. nov. based on the holotype specimen. Dashed lines represent inferred bones or sutures. Scale bar represents 10 mm.

patterns. The orbits (22.0 mm length; 14.7 mm height) are located slightly posterior to the midlength of the skull, and their rims are slightly elevated but not above the dorsal skull table. The nares (8.7 mm length; 6.0 mm height) are located in the anteriormost part of the skull, and face laterally and slightly anteriorly.

Both premaxillae are poorly preserved in the holotype specimen, and so it has not been possible to trace their limits with other bones. They correspond to the anteriormost part of the skull, located anteriorly to the nares, and they appear to bear two teeth each.

The maxillae are long, low bones (34.6 mm length; 4.1 mm maximum height) extending from the naris to the contact between the lacrimal and the jugal, below the anterior end of the orbits. Dorsally, the maxillae contact the lacrimal, with mostly straight sutures. Posteroventrally, the maxillae form plates extending medially, bearing five rows of teeth each. After an anteriormost single-rowed area with four teeth (c. 1.3–2.1 mm high; 0.9–1.7 mm wide), more teeth rows start to appear, up to five, arranged diagonally to each other. These teeth are bulbous, with constricted bases, and with a subquadrate/subtrapezoidal section (c. 2.3–2.8 mm high; 1.9–3.1 mm wide). They clearly show wear facets on their distal side, producing a 'heeled' lateral outline. Their mode of insertion has not been determined.

Nasals are long (25.6 mm length; 10.0 mm maximum width) and flat paired bones that contact the nares and premaxillae anteriorly, the lacrimals laterally and the frontals and prefrontals posteriorly. The sutures with the premaxillae have not been observed; those with the lacrimals are undulated; those with the frontals are directed posterolaterally; those with the prefrontals are 'V'-shaped, convex anteriorly; and the suture between the two nasals is essentially straight.

Lacrimals are also long, flat, slender bones (32.1 mm length; 11.3 mm maximum height), contacting the nares anteriorly, the nasals and prefrontals dorsally, the orbits and jugals posteriorly and the maxillae ventrally. These bones are lowest anteriorly, and become progressively higher towards the orbits, of which they form the anteroventral margins. Below the orbits, the sutures with the jugals are slightly curved and directed posterodorsally.

Prefrontals are long, flat, lanceolate bones (23.0 mm length; 7.1 mm maximum width), contacting the frontals and orbits posterodorsally, the lacrimals posteroventrally and the nasals anteriorly. The sutures with the frontals, lacrimals and the other prefrontal are all essentially straight. A conspicuous anterior process is wedged between the two posterior processes of the nasal, with a suture forming a distinct 'V' shape.

Frontals are long, flat, rectangular bones (30.0 mm length; 9.7 mm maximum width) contacting the prefrontals, orbits and postfrontals laterally, the nasals frontally and the parietals posteriorly. They are narrowest anteriorly between the prefrontals, then they expand posterolaterally to form a small part of the dorsal margin of the orbits, and then they become slightly narrower again posteriorly between the postfrontals. The sutures with the posterior part of the prefrontals are 'V'-shaped (convex posteriorly), and all the other sutures are straight or slightly curved.

Jugals are triangular, flat bones (32.7 mm maximum length; 12.0 mm maximum height) contacting the maxillae and lacrimals anteriorly, the postorbitals and the orbits dorsally and the quadratojugal and squamosal posteriorly. They are highest posteriorly and taper progressively towards the suture with the maxillae and the lacrimals. Their ventral margin is convex. Most of their dorsal parts form the ventral margin of the orbits. The posterodorsal part of the jugals wedges between the postorbitals and squamosals, forming an almost right angle. The posterior margin of the element then runs slightly anteroventrally until the ventral margin of the skull.

Quadratojugals are flat, rectangular bones (18.4 mm length; 9.4 mm height) that contact the jugals anteriorly, the squamosals dorsally and the ventral and posterior margins of the skull. In its posteroventral part, they develop lappets that extend medioventrally to articulate with the quadrates.

Postorbitals are semicircular bones (10.0 mm length; 11.2 mm height), probably convex originally, contacting the orbits anteriorly, the postfrontals and parietals dorsally, the squamosals posteriorly and the jugals ventrally. The sutures with the postfrontals are relatively undulated and directed posterodorsally, whereas the sutures with the other bones form an arch contacting the orbits posteroventrally, forming distinctly pointed anterior processes for the postorbitals.

Postfrontals are flat, triangular bones (10.4 mm length; 15.9 mm width) that articulate to the frontals and parietals dorsally, and contact the postorbitals and the orbits ventrally. Their anterodorsal and posteroventral projections taper progressively, forming the posterodorsal portion of the orbit rim. Their posterodorsal projections are wedged between the postorbitals and the parietals.

Squamosals are high, rectangular bones (13.7 mm maximum length; 22.6 mm height), probably somewhat convex originally, articulated ventrally to the quadratojugals, anteriorly to the jugals and postorbitals and dorsally to the parietals and probably to a small portion of the postparietals. They also contribute to part of the posterior surface of the skull, lacking ornamentation. Sutures with all the other bones are relatively straight except for those with the postorbital, which are concave.

Parietals are flat, long (19.7 mm), subtrapezoidal paired bones, which are wider posteriorly (17.5 mm) than anteriorly (8.5 mm). They articulate with the frontals and postfrontals anteriorly, the postorbitals and squamosals laterally and the postparietals posteriorly. The posterolateral notch to accommodate the supratemporals can be distinguished, although the latter bones have not been recognised. Both parietals articulate with each other medially by means of a straight suture. The pineal foramen is relatively small (1.9 mm of diameter) and located anteriorly from the midlength.

Postparietals are thin, paired bones (6.0 mm maximum length; 17.3 mm width; 3.5 mm height), articulated with the posterior edges of parietals and squamosals. They form a narrow band in the posteriormost part of the skull roof, also contributing to the dorsal part of the posterior surface of the skull, where they lack ornamentation.

The pterygoid is the only identifiable bone of the palate that has been partially exposed. Only the most posterior portion of the palatine ramus is visible as two branches projecting anteriorly (9.3 mm preserved length), surrounding the interpterygoid vacuity between them (3.6 mm wide). The pterygoid flanges extend laterally (14.2 mm) rhoughly perpendicular to the main anteroposterior axis of the skull. The flanges consist of laminae of bone becoming broader laterally (c. 11.6 mm), transversally divided into two by a conspicuous ridge representing the ventral margin of the torosus transiliens. The anterior part is tilted anteriorly and bears no palatal teeth. The posterior part is tilted posteriorly, suggesting a post-mortem deformation of this bone with a dominant anterior direction. The quadrate rami extend posteriorly from the pterygoid neck (16.7 mm long), forming an angle of about 86°. Laterally,

they show a thickened margin (2.6 mm thick) limiting the subtemporal fossa. Medially, the rami project in the form of laminae of bone (c. 7.6 mm wide) slanting dorsally. Posterolaterally, they contact the quadrates.

The quadrates are bones that are somewhat 'T'-shaped in posterior view, as a result of the three main plates that extend dorsally, medially and ventrally (only the latter two are well visible in the holotype specimen). The concave surface between the ventral (4.4 mm) and lateral (4.0 mm) plates articulates to the angular bone of the lower jaw; the area between the lateral and dorsal (2.2 mm preserved) plates appears to be attached to the posteromedial end of the squamosal/quadratojugal; and the concave area between the dorsal and ventral plates is free in the preserved skull, but it was probably articulated with the braincase (which is missing in the holotype specimen).

One right stapes is preserved (16.3 mm long). Medially, it has a concave, oval foot plate, with the anterior margin slightly broader (7.7 mm wide dorsoventrally; 7.9 mm wide mediolaterally). Laterally from it, there is the stapedial shaft, which is rather stout (8.9 mm long; c. 3.5 mm thick). No stapedial foramen can be observed. At midlength of the shaft, the dorsal process appears, being strongly directed dorsally (3.2 mm) and then medially (5.0 mm) towards the foot plate.

Other bones of the braincase are not well visible. One poorly-preserved, displaced bone (7.4 mm long; 13.7 mm wide; c. 4.6 mm high) is present near the posterior part of the skull. Given its structure with two clear lobes present ventrally, it may correspond to the basioccipital, but there are not any other characters to confirm this assignation.

Lower jaws: The mandibles are relatively slender bones (70.2 mm long; c. 6.0 mm wide; 11.1 mm high just after the tooth plate). The lateral portions of the dentaries, splenials, angulars and surangulars are ornamented with a profuse honeycomb pattern. The majority of suture lines are not well visible in the lower jaws. In ventral view, their anterior 75% are essentially straight, whereas their posterior part curve medially. In lateral view, the dorsal and ventral margins of the jaws have slightly sigmoidal shapes, with the coronoid processes elevating dorsally posterior to the teeth, at about halfway of the jaws and comprising about 30% of their height. The jaws taper posteriorly, with an acuminate retroarticular process.

The dentaries are long (49.2 mm), slender bones that form the anterodorsal portion of the jaw. They are expanded medially, forming tooth plates, wider posteriorly, overhanging in the lingual side of the jaws. The anteriormost two teeth are conical, enlarged (c. 4.1 mm high; 1.3 mm wide) and directed anteriorly. Posteriorly to them, the teeth are smaller (c. 2.5 mm high; 1.3 mm wide), forming a single row and directed occlusally. After three teeth, multiple rows start to appear, arranged diagonally. In the broadest area of the tooth plates, five tooth rows can be distinguished. The teeth have a subquadrate/subtrapezoidal section (c. 1.5–3.3 mm high; 1.3–2.2 mm wide) and are bulbous, with a constricted base. Tooth wear is conspicuous, developing a 'saddle' on the mesial side of the teeth. The mode of insertion of the teeth cannot be established. The dentaries are broader on their lateral sides (c. 6.4 mm), which are ventrally convex and contact the splenials and the angulars. Posteriorly, they articulate with the surangulars and coronoids. On their medial side, the dentaries extend posteromedially forming the overhanging tooth plates described above. The coronoids, contacting the dentaries posteriorly, may also participate in the tooth

plates, although the sutures between those two bones have not been traced precisely. On the medial side, the dentaries are also articulated with the splenials and prearticulars ventrally.

The splenials are also long (c. 25.6 mm) and slender bones that constitute the anteroventral regions of the jaws. They are broader (c. 6.6 mm) on the medial sides, where they appear from the base of the tooth rows to the ventral margins of the jaws. Posteriorly, the splenials are articulated with the prearticulars and angulars, and form the most anterior margin of the Meckelian foramen. The sutures with the dentaries are slightly arched, whereas those with the prearticulars are somewhat undulated.

The angulars form the most posterolateral part of the jaws, extending from about midlength to the ventral parts of the retroarticular processes (c. 34.6 mm, approximately the 47–49% of the jaw length). Their ventral margins describe a sigmoidal outline up to the retroarticular processes. On its lateral side, it contacts the surangular dorsally with a similarly sigmoidal suture. On the medial side, it forms the posterior margin of the Meckelian foramen and contacts the prearticular dorsally.

The surangulars are elongated bones (c. 38.0 mm) with anterior ends wedged between the maxillae and the angulars, and posterior ends constituting the posterodorsal part of the jaw, laterally to the articular bones (which are not exposed in the studied specimen).

The prearticulars are long bones (35.6 mm) that appear on the posteromedial side of the jaws, form approximately midlength to the retroarticular processes below the angulars. They form the dorsal margin of the Meckelian foramen.

Axial skeleton: The studied specimen preserves a fairly complete vertebral column. The most anterior cervical vertebrae are missing (the head is disarticulated), and the dorsal region of the spine is divided into three strings of eleven, five and two vertebrae, respectively. Together with the disarticulated vertebrae scattered around the specimen, there are about 24–25 presacral vertebrae. They slightly increase in size posteriorly (height of 13.2 mm in the most anterior measurable vertebrae and 14.8 mm in the most posterior measurable dorsal). Pleurocentra are amphicoelous, cylindrical, with flared cortical rims and a length/height ratio of 1.1 (slightly longer than high). The neural arches surround the neural canal and are considerably swollen. Transversal processes are quite inconspicuous and correspond to a low ridge that runs from the anterior laterodorsal region of the pleurocentrum (just below the pedicels) to the space between pre- and postzygapophyses. The prezygapophyses are almost always partially or completely covered by the postzygapophyses of the preceding vertebra, and have only been observed in some elements. They are essentially directed laterally and have an articular surface slightly tilted medially. Postzygapophyses are swollen and extend laterally. Neural spines are generally low (about the 7% of the total vertebral height), in the form of a thin anteroposterior lamina (about the 8% of the total width). In some cases, however, the neural spine appears to be stouter (25% of the total width) and slightly higher (17% of the total height). Such particular vertebrae do not appear to follow any consistent arrangement. No intercentra have been observed. All the sacral and caudal vertebrae observed are disarticulated and somewhat scattered. Only preparation of those closer to the surface has been possible, but more elements were observed below when the block was fractured

during excavation, probably corresponding to caudal vertebrae and parts of the pelvis, which remain unexposed. Two sacral vertebrae and 9–10 caudals can be observed on the surface. The first sacral vertebra is only exposed in dorsal view, so its assignment is relatively uncertain. Nevertheless, it is here considered to be the first sacral because it contacts the confirmed second sacral vertebra anteriorly. It is 13.9 mm wide, the prezygapophyses are broad and extend anterolaterally, the postzygapophyses are smaller, and the neural spine is of the low and narrow type. The second sacral vertebra is 13.2 mm high, 16.1 mm wide and 10.5 mm long. Prezygapophyses are wide and extended anterolaterally, whereas the postzygapophyses seem to be considerably reduced. The neural spine is rather thin. It preserves a sacral rib articulated on the right side. Proximal caudal vertebrae are smaller and show a distinctly high, posteriorly-projected neural spine. Their pleurocentra are cylindrical and deeply amphicoelous. They have a broad area for the articulation of ribs (26–31% of total height) placed on both the pleurocentrum and the pedicels of the neural arch. Pre- and postzygapophyses are greatly reduced, and the neural spine makes up for 44% of the total height.

The most anteriorly preserved ribs are quite broad. One of them has expanded ends of subequal width (8.5 mm) separated by a narrower neck (3.5 mm), and the other has a relatively broad anterior area (6.3 mm), and it extends laterally until it turns posteriorly, similarly to the proximal caudal ribs. In the dorsal ribs where the head has been preserved, the capitulum is united to the tuberculum by an osseous lamina (distance of 5.7 mm), giving a triangular shape to the head. The ribs are about 2.7 mm thick and slightly curved. The longest measured dorsal rib, albeit not complete, is of 44.1 mm. The first sacral rib is quite expanded and falciform. The articular surface measures 7.7 mm dorsally, and is followed by a neck of 6.7 mm. Distally, this rib extends posteriorly up to an anteroposterior length of 20.5 mm. The second sacral rib is still attached to the vertebra, which has been anteriorly displaced. It consists of a spatulate structure, smaller than the first sacral rib. In dorsal view, its articular surface measures 6.2 mm, the neck that follows is of 3.5 mm, and the broader distal area measures 10.5 mm. The first three caudal ribs have a single, broad (4.3–5.1 mm) articular surface, then the ribs extend slightly lateroposteriorly and finally they recurve sharply posteriorly. From this point on, the vertebral column is completely disarticulated. There is at least another vertebra with an articulated rib, although it is unknown whether it corresponds to the fourth or fifth caudal. That rib is straight (proximal end of 3.8 mm and maximum length of 12.8 mm) and presents a relatively deep furrow anteriorly that runs from the articular surface to midlength of the rib. Based on known information about other captorhinids (Sumida, 1990), this latter rib probably corresponds to the fifth caudal, whereas the fourth, usually of recurved type as well, may be covered or missing in the studied specimen. Distal caudal vertebrae are probably present below the prepared surface, and thus cannot be accessed at present. Caudal chevrons (if present) are not observable either.

Pectoral girdle and forelimb: The dorsal part of the left clavicle is exposed in the specimen herein studied. This element consists of an osseous plate (7.1 mm wide) that tapers dorsally, with a preserved length of up to 23.2 mm. Just below there is a broad plate of bone that corresponds to the left scapulocoracoid. This element is relatively horizontal in its medial part (coracoid), but it laterally recurves dorsally forming the scapular blade (41.0 mm high). The interclavicle is not exposed.

Both humeri are present; the left one is complete, exposed in dorsal view, and the right one preserves only its distal part and is exposed in lateral view. This description focuses on the former. The element is 35.8 m long, with a moderately expanded proximal end (11.3 mm, may be partially covered), a thin shaft (4.0 mm) and a greatly expanded distal end (18.5 mm). In the latter, the ectepicondyle can be seen in its lateral margin, constituting the distal end of an elevated area of the lateral margin. The supinator process has not been observed. The entepicondyle corresponds to a broad and slightly convex area in the medial part of the distal epiphysis. Just above the ridge forming the entepicondyle, the surface of the bone is pierced by the entepicondylar foramen, of 3.7 mm long proximodistally and about 1.0 mm wide. Both left and right radii and ulnae are also present, but only those on the left side are complete. The radius is a long element (23.0 mm), very slender and thin, with slightly expanded ends (proximal end = 6.1 mm; shaft = 2.4 mm; distal end = 6.7 mm). The ulna is long (25.2 mm) and slender, with both ends slightly expanded (proximal end = 7.6 mm; shaft = 4.7 mm; distal end = 7.5 mm). The proximal end is slightly curved laterally, with the olecranon slightly covering the proximal end of the ulna.

The right manus is not preserved in the studied specimen, and unfortunately, the left manus is also very fragmentary, preserving only three bones of the carpus and an isolated metacarpal or phalanx. Attached distally to the radius there is the radiale bone, of about 5.6 mm wide mediolaterally and 3.2 mm long proximodistally. Medially from it there is a small piece of bone (4.1 mm wide; 2.9 mm long), which may correspond to one of the centralia. Just below the distal end of the ulna, there is another small bone of triangular shape (5.4 mm wide; 2.7 mm long) that may correspond to the ulnare. Medially to it, the pisiform can be observed in the form of an ovoid, small bone (2.7 mm wide; 3.9 mm long). Disarticulated but near the manus, there is one metatarsal or phalanx of 9.2 mm long and about 2.4 mm thick.

Pelvic girdle and hindlimb: No elements of the pelvic girdle have been clearly recognised. A plate-like fragment (14.5 mm high; 19.5 mm wide) with undulated margins, located just below the second sacral vertebra, could correspond to (part of) the pubis. However, there are no morphological characters to confirm this assignation.

Both femora are present; the left one is complete and the right one lacks its distal end. The former is preserved in ventromedial view, whereas the latter is in medial view. The femora are stout bones of 40.1 mm long, with a proximal head of about 14.0 mm wide and a shaft of 10.5 mm wide (the distal end has not been measured because it is partially covered in the left femur and broken in the right one). The femora show a well-developed ventral intertrochanteric fossa, with the internal trochanter on its lateral edge. A fourth trochanter has not ben observed in any of the two, the surface distal from the intertrochanteric fossa being rather smooth. Regarding the condyles, only the posterior one can be observed in the left femur, and therefore it is impossible to compare its size with the anterior one. Both tibiae are also present, although only the left one is complete, and thus this description is only based on this element, exposed in lateral view. It is a long (26.9 mm), slender element, somewhat convex laterally, with expanded ends (proximal end = 9.1 mm; shaft = 3.8 mm; distal end = 5.7 mm). The proximal end is wider in the mediolateral axis, whereas the distal end is wider in the dorsoventral axis. The cnemial crest can be observed on the studied specimen, bearing no conspicuous knob. Both fibulae are completely preserved and

exposed in ventral view. They correspond to long (27.8 mm) and slender elements, curved medially, with expanded ends (proximal end = 5.8 mm; shaft = 3.6 mm; distal end = 9.2 mm).

Both pedes are present, exposed in ventral view. Except for the astragalus, this description is based on the left pes, which is almost completely preserved, just lacking a few phalanges and parts of the astragalus. The calcaneum is present near the distal end of the fibula, as a relatively flat plate of subquadrate shape (7.8 mm wide; 9.4 mm long), with straight and amost orthogonal medial and distal margins, and a rounded proximolateral margin. Part of the astragalus (intermedium) of the left pes can be observed medial to the calcaneum, between the distal ends of the tibia and the fibula. It is slightly displaced, and only the articulation surfaces for the fibula and the proximal centrale are exposed. The astragalus (intermedium and tibiale) of the right pes, although disarticulated, is completely exposed in ventromedial view. The intermedium (10.0 mm wide; 9.1 mm long) is somewhat 'L'-shaped, with a concave proximolateral margin to accommodate the part of the tibia, a lateral straight margin that contacted the tibiale, a concave laterodistal margin to articulate with the proximal centrale, a slightly concave mediodistal margin that was articulated to the calcaneum, and a slightly concave proximomedial margin forming the articulation with the fibula. The right tibiale, located lateral to the intermedium, is a subrectangular bone (4.0 mm wide; 7.1 mm long; 3.4 mm high). The lateral centrale is probably present distally from the left intermedium, although it is partially covered a small, round bone corresponding to the medial centrale (3.8 mm wide; 3.6 mm long). Tarsals 1 to 5 are all present in the left pes; the 1, 2 and 3 are also small, subquadrangular/round bones (respectively, 3.9 mm wide; 3.2 mm long; 3.4 mm wide; 3.1 mm long; 2.6 mm wide; 3.0 mm long) contacting the lateral centrale distally, the 4 is a somewhat round bone (4.2 mm wide; 2.5 mm long) just distally from the medial centrale, and the 5 is a rectangular bone (3.8 mm wide; 3.5 mm long) attached to the distal end of the calcaneum. Metatarsals I to V are also all present in the left pes as slender bones with expanded ends. They increase in length from I to IV, being the V slightly smaller again (respective lengths of 9.1, 9.6, 13.9, 14.5 and 11.2 mm). Distally, metatarsals I–IV have a medially pointed tuberosity. Digit I does not preserve any phalanges. Digit II is complete, with two phalanges with expanded ends and one ungual phalanx (respective lengths of 5.4, 3.6 and 2.8 mm). Digit III only preserves the two most proximal phalanges (respective lengths of 5.5 and 4.6 mm), probably lacking two more (if compared to the pes of *Captorhinus* by Holmes 2003, and *Captorhinikos* by Olson 1962b). Digit IV preserves three proximal phalanges (respective lengths of 6.8, 5.5 and 4.2 mm), probably lacking two more (cf. Holmes 2003). Digit V is complete, with three proximal phalanges and a terminal, ungual phalanx (respective lengths of 6.8, 4.5, 3.6 and 3.6 mm).

Remarks: *Tramuntanasaurus tiai* gen. *et* sp. nov. shows a combination of morphological characters that differ from all other moradisaurines known to date. Its skull is triangular and with a slightly convex posterior margin, being more reminiscent of primitive captorhinomorphs (cf. Clark & Carroll, 1973) rather than all other known moradisaurines (cf. Albright *et al.*, 2021). Apart from that, the general arrangement of the cranial bones is similar to that of *Captorhinus* (cf. Fox & Bowman, 1966; Heaton, 1979) and other captorhinids. The arrangement of the dentition is typical of moradisaurines, with five rows of teeth in the upper and lower jaws. However, it differs from all the other known moradisaurines in the following combination of characters: presence of a double row of teeth anterior to the tooth plate (unlike *Captorhinikos* and *Moradisaurus*), lack of diastema (unlike *Gansurhinus* and

Kahneria), anteriormost dentary teeth pointing rostrally (unlike *Captorhinikos* and *Gecatogomphius*) and a broad snout relative to skull length (unlike *Labidosaurikos* Stovall, 1950, *Moradisaurus* and *Rothianiscus*) (Olson, 1962a, 1962b, 1965; de Ricqlès & Taquet, 1982; Dodick & Modesto, 1995; Ivakhnenko, 2008; Reisz *et al.*, 2011; LeBlanc *et al.*, 2015; Jung, 2018; Sidor *et al.*, 2022).

Tramuntanasaurus tiai shows the general postcranial morphology of other captorhinids, being very similar to the postcranial skeleton of the well-known species *Captorhinus aguti* (Cope, 1896) (*e.g.*, Fox & Bowman, 1966; Sumida, 1990; Holmes, 2003). Dorsal vertebrae present alternation of neural spine height, similarly to other species of the family (Sumida, 1990). The astragalus of *Tramuntanasaurus tiai* shows a condition similar to that observed in *Captorhinus magnus* Kissel, Dilkes *et* Reisz, 2002, in which the intermedium and the tibiale still constitute separate units in subadult specimens (cf. Kissel *et al.*, 2002: fig. 8). This stands in contrast with what has been described for *Captorhinus aguti*, with a well-fused astragalus even in juveniles (*e.g.*, Holmes, 2003; Meyer & Anderson, 2013). Although the rest of the skeleton of the holotype specimen of *Tramuntanasaurus tiai* seems to be well-ossified, the partitioned astragalus probably indicates that it was still growing when it died. It is unknown whether the third centrale (if present in *Tramuntanasaurus tiai*) also formed part of the astragalus, a condition seen in juvenile moradisaurines such as *Captorhinikos chozaensis* and *Moradisaurus* (O'Keefe *et al.*, 2006). In the specimen studied herein, putative medial and lateral centralia have been identified, although they are poorly preserved and exposed. If this were correct, the specimen from Mallorca would show a pes structure similar to that of *Captorhinikos chozaensis* (cf. Olson, 1962b). Other captorhinids, such as *Captorhinus aguti*, *Labidosaurus hamatus* (Cope, 1895) and *Moradisaurus grandis* Taquet, 1969, have only one centrale (Sumida, 1989; Holmes, 2003; O'Keefe *et al.*, 2005).

5. Discussion

5.1. Phylogeny

The phylogenetic tree obtained (**Figure 6**) places *Tramuntanasaurus tiai* gen. *et* sp. nov. in the monophyletic clade Moradisaurinae. As stated above, this subfamily is characterised by multiple tooth-rowed plates on the maxillae and jaws. Nevertheless, other captorhinids, such as *Captorhinus aguti* and *Rhodotheratus parvus* (Olson, 1970), also evolved multiple-rowed dentition independently (*e.g.*, LeBlanc & Reisz, 2015; Albright *et al.*, 2021), but the combination of all other morphological traits places them outside the moradisaurines.

Specifically, the taxon herein described is situated in a polytomy with *Kahneria*, *Labidosaurikos* and the group of most derived moradisaurines (*Gansurhinus*, *Moradisaurus* and *Rothianiscus*). This heterogeneous clade contains species of disparate sizes, including the largest known moradisaurine (*Moradisaurus*).

5.2. Comparison of Tramuntanasaurus tiai *gen. et sp. nov. to other forms from the peri-Tethys*

Comparing *Tramuntanasaurus tiai* gen. *et* sp. nov. to the other moradisaurine captorhinids from the peri-Tethys is especially interesting, given their scarcity and their palaeogeographical closeness. The indeterminate large

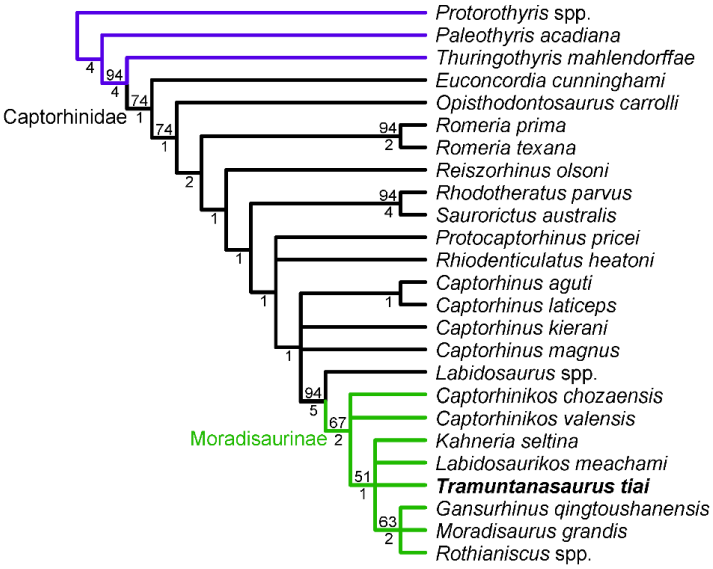

Figure 6. Strict consensus of the best 180 trees recovered (tree length = 218 steps) of the Captorhinomorpha, including *Tramuntanasaurus tiai* gen *et* sp. nov., using a branch-and-bound search. Consistency index (CI) = 0.4977; retention index (RI) = 0.7054. Double-digit numbers on the branches represent the bootstrap support values (n = 100, values under 50 not shown), and single digits below represent the Bremer decay support value of that node.

moradisaurine from Mallorca reported by Liebrecht *et al.* (2017) was collected in the same lithostratigraphic unit as *Tramuntanasaurus tiai* (Port des Canonge Formation) but from a different locality (Platja de son Bunyola) (see Matamales-Andreu *et al.*, 2022). Based on the described fragment of maxilla, that form is much larger than *Tramuntanasaurus tiai* and only possesses three rows of teeth on the mid-posterior part of the maxilla (Liebrecht *et al.*, 2017), contrarily to the specimen herein studied, with five rows. Considering that *Tramuntanasaurus tiai* is much smaller, these two specimens cannot be part of a same ontogenetic series, as in moradisaurines the number of teeth increases over time (Jung & Sumida, 2017). Therefore, they were probably two different biological species that coexisted in the same environment, as demonstrated by the co-occurrence of two consistent size populations of the ichnogenus *Hyloidichnus* (purportedly produced by moradisaurines, among other captorhinomorphs, see 5.3 below) in the Port des Canonge Formation (Matamales-Andreu *et al.*, 2022). Of note, coexistence of large and small species of captorhinomorphs has been documented elsewhere (Cisneros *et al.*, 2020), as well as different size populations of *Hyloidichnus* tracks in the palaeogeographically close localities of the Catalan Pyrenees (Voigt & Haubold, 2015; Mujal *et al.*, 2016) and Provençe (Logghe *et al.*, 2021; Marchetti *et al.*, 2022) (see also Matamales-Andreu *et al.*, 2021a).

From the neighbouring island of Menorca, Matamales-Andreu *et al.* (2021a) reported two forms of moradisaurine captorhinids that are probably slightly younger than *Tramuntanasaurus tiai* in terms of geochronological age. They were found in the P3 unit, with an upper part dated as Lopingian (Bercovici *et al.*,

2009; Matamales-Andreu *et al.*, 2022) but with no precise age constraints for its lower part (Matamales-Andreu *et al.*, 2021a). Based on the lithological correlation with the sequences of Mallorca, the P3 unit could range from the Guadalupian to the lower part of the Lopingian (Matamales-Andreu *et al.*, 2022). The large form from Menorca corresponds to the species *Balearosaurus bombardensis*, with a holotypic fragment of maxilla preserving three rows of conical teeth with an ornamentation of thin grooves and ridges (Matamales-Andreu *et al.*, 2021a). The actual number of tooth rows is uncertain, since the fragment is none too well preserved, but the dental ornamentation is sufficiently diagnostic. In addition to its smaller size, *Tramuntanasaurus tiai* lacks ornamentation on its teeth. The smaller form from Menorca, identified based on a posterior jaw fragment and a vertebra (Matamales-Andreu *et al.*, 2021a), is of roughly the same size as *Tramuntanasaurus tiai*. However, this unnamed moradisaurine from Menorca has only three rows of teeth on the tooth plates, whereas *Tramuntanasaurus tiai* has five. Because of this, herein they are thought not to be conspecific, but this discussion can only be settled by finding more specimens of both forms.

Two other forms of moradisaurine captorhinids were reported from the Argana Formation of the Argana Basin, in northwestern Africa (Dutuit, 1976; Jalil & Dutuit, 1996), of Lopingian epoch (Hmich *et al.*, 2006). The first one (ARG 506, formerly 69.Ir.1.JMD) corresponds to a poorly-preserved fragment of maxilla with three rows of long, needle-like acrodont teeth. The second form is based on two other fragments of maxillae (ARG 507 and ARG 508, formerly 74.XXIII.1.JMD and 74.XXIII.2.JMD, respectively), slightly larger and with 3–4 rows of bulbous subthecodont teeth. Regarding the nomenclature, Dutuit (1976) stated that naming the specimen ARG 506 was premature with only that material; specimens ARG 507 and ARG 508 were assigned the new name *Acrodenta irerhi* Dutuit, 1976, which constitutes a valid name (based on two syntypes) following the articles 8.1 and 73.2 of the International Code of Zoological Nomenclature (Ride *et al.*, 1999). However, Jalil & Dutuit (1996) described and illustrated the specimen ARG 506 under the name '*Acrodonta irerhi* Dutuit, 1976', and the specimens ARG 507 and ARG 508 as Moradisaurinae gen. *et* sp. indet., effectively reversing the identifications of the previous work. Therefore, '*Acrodonta irerhi*' *sensu* Jalil & Dutuit (1996) *non* Dutuit (1976) is not a valid name, as it was not described as a new species but cited as if it had been described by Dutuit (1976). In reality, Dutuit (1976) described *Acrodenta irerhi* to accommodate two other specimens (ARG 507 and ARG 508), which are identified as indeterminate moradisaurines by Jalil & Dutuit (1996). ARG 506 shows an acrodont mode of implantation of the thin and needle-like teeth, which differs from *Tramuntanasaurus tiai*, whose teeth are bulbous and bullet-shaped, and probably with a thecodont mode of implantation. ARG 507 and ARG 508 (syntypes of *Acrodenta irerhi*) are fragments with very few diagnostic characters and should, at best, be considered indeterminate moradisaurines in line with Jalil & Dutuit (1996).

Additionally, another fragmentary moradisaurine captorhinid was described from the Guadalupian of the East European Plain: *Gecatogomphius kavejevi* Vjushkov *et* Chudinov, 1957. Even though it is similar to *Tramuntanasaurus tiai* in terms of size, the eastern European species shows anteriormost dentary teeth that are very enlarged and point dorsally (Ivakhnenko, 2008), whereas in the species herein studied, those teeth are comparatively smaller and point anteriorly.

5.3. Correlation of Tramuntanasaurus tiai *gen. et sp. nov. with ichnites from the same area*

The Racó de s'Algar–Pedra de s'Ase section is locally very rich in fossil tetrapod tracks. Among those, Matamales-Andreu *et al.* (2022) identified the ichnospecies *Hyloidichnus bifurcatus*, which is broadly correlated to captorhinomorph trackmakers (Logghe *et al.*, 2021; Marchetti *et al.*, 2022). Matamales-Andreu *et al.* (2022) noted that there were two clearly differentiated size classes of this ichnospecies in Mallorca, with also slightly different relative depth patterns (see further discussion below). As Matamales-Andreu *et al.* (2022) suggested, the large tracks (pes length of c. 70–100 mm) are tentatively attributed to large moradisaurine trackmakers such as the one reported by Liebrecht *et al.* (2017), whereas the smaller tracks (pes length of c. 40–55 mm), as further discussed herein, are correlated to *Tramuntanasaurus tiai* gen. *et* sp. nov.

Although the specimen DA21/17-01-03 is an almost complete skeleton, some parts are partially disarticulated or missing (**Figures 2**, **3A**, **7A**). This is especially true for the autopodia (**Figure 3B–G**): the right manus is missing because that part of the rock had been eroded when it was found; the left manus appears to have been disarticulated and scattered, so almost all the bones are missing; the right pes is also disarticulated, with some bones missing; and the left pes is mostly complete, only with some distal phalanges and some parts of the astragalus missing. Therefore, regarding the autopodia, only the pes retains enough information for a suitable reconstruction of *Tramuntanasaurus tiai* (**Figure 3D–G**). Given the overall size similarity and phylogenetic proximity to *Captorhinikos*, the manus of *Tramuntanasaurus tiai* is here reconstructed based on the manus of *Captorhinikos chozaensis* illustrated and reconstructed by Olson (1962b: figure 14B). Similarly, available information on the structure of the pes of *Tramuntanasaurus tiai* is completed with the reconstruction of Olson (1962b: figure 15C) for *Captorhinikos chozaensis*, including the astragalus anatomy described by O'Keefe *et al.* (2006) for that species. Other missing and/or poorly preserved elements (*e.g.*, the pelvic girdle) in the moradisaurine herein studied are reconstructed based on the skeletal reconstructions of *Captorhinus* by Heaton & Reisz (1980) and Holmes (2003).

The skeletal reconstruction of *Tramuntanasaurus tiai* makes it possible to propose a detailed correlation with the *Hyloidichnus* specimens found in the same area (**Figure 7**). Of the small morphotype of *Hyloidichnus bifurcatus* from Mallorca, Matamales-Andreu *et al.* (2022: figure 10D–F) illustrated three manus-pes sets, without any complete trackways. Here we report an additional specimen (DA21/15-13-02) consisting of three consecutive manus-pes sets, two complete and one preserving only the manus imprint, as well as a slightly sinuous and thin trace of the tail (**Figure 7B, C**). The general morphology of the tracks, the relative length of the digit imprints (increasing in length from digits I to IV) and the trackway patterns (with alternating manus-pes sets and a relatively narrow pace angulation) are characteristic of *Hyloidichnus bifurcatus* (*e.g.*, Gand, 1988; Marchetti, 2016; Logghe *et al.*, 2021; Marchetti *et al.*, 2022; **Table 1**).

This new trackway makes it possible to measure the paces of both pes and manus (129.4 mm and 113.8–134.5 mm, respectively) and the stride length of the manus (c. 187.7 mm), giving a relatively accurate size approximation of the potential trackmaker, with an estimated trackmaker glenoacetabular distance (*i.e.*, trunk length: half of the stride length of the pes, plus manus-pes distance; see Leonardi, 1987) of 117.9–125.0 mm. This value is in the range of the estimated glenoacetabular distance of *Tramuntanasaurus tiai* considering a shortening

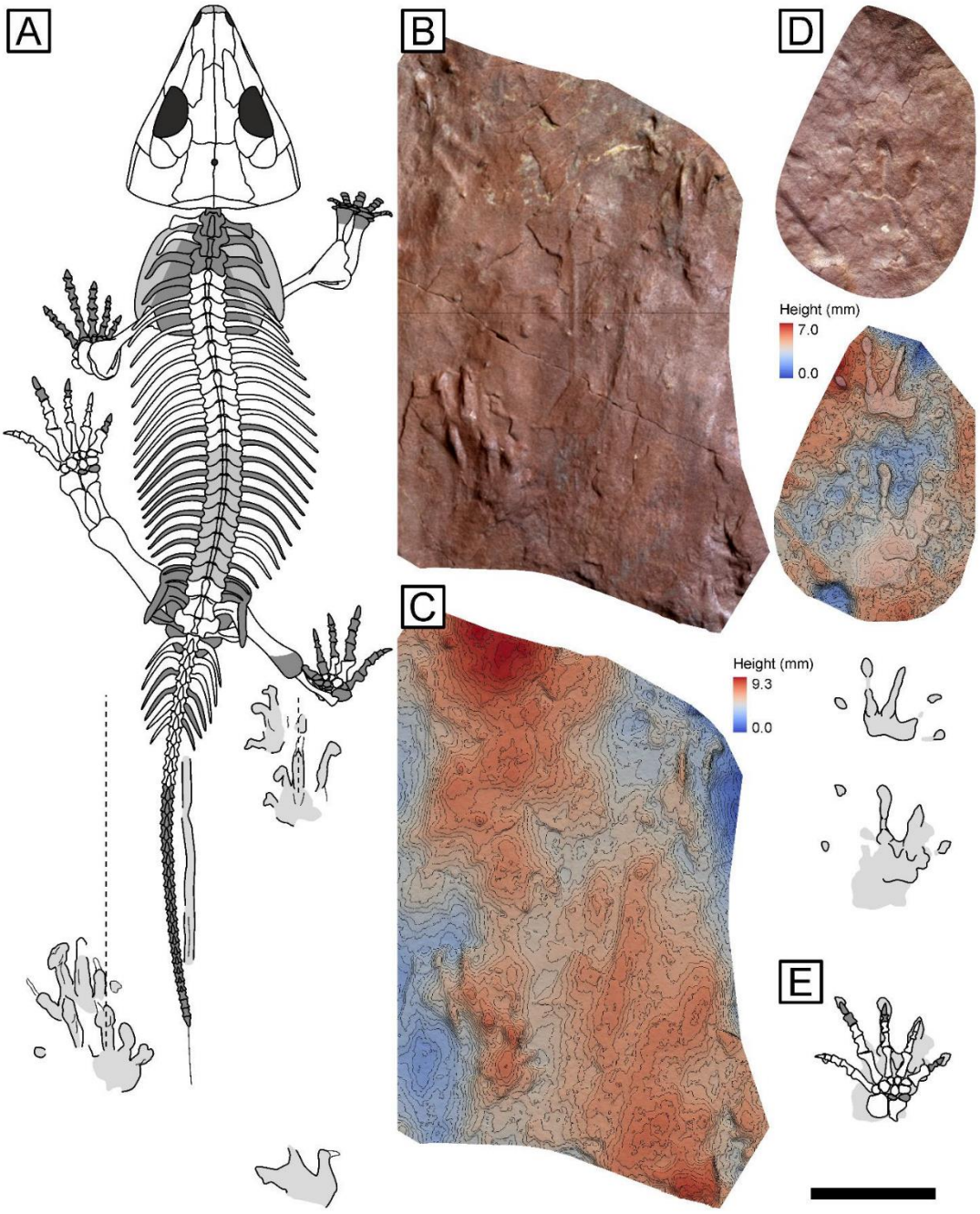

Figure 7. Skeletal reconstruction of *Tramuntanasaurus tiai* gen. *et* sp. nov. and correlation with *Hyloidichnus bifurcatus* Gilmore, 1927 from Mallorca. **A:** Skeletal reconstruction based on the holotype DA21/17-01-03; white elements are known bones, light grey elements are bones present but of unknown shape, dark grey elements are missing bones reconstructed on the basis of other known captorhinids (see text for references). **B, C:** Orthophoto (B) and false-colour depth map and contours (C) of the 3D model of the trackway DA21/15-13-02; the interpretative drawing of tracks and tail trace is on the left side of the false-colour depth map; black dashed line corresponds to the axis of the pes tracks (base of digit III imprints), showing a narrower pace than the one inferred from the skeletal

reconstruction. **D:** Right manus-pes set in convex hyporelief including orthophoto (top), false-colour depth map and contours with superimposed interpretative drawing (middle) and interpretative drawing (bottom) (modified from Matamales-Andreu *et al.*, 2022: figure 10D). **E:** Interpretative drawing of the pes imprint in D with superimposed reconstruction of the left pes of DA21/17-01-03. Note that the skeletal reconstructions, tracks and trackway are all at the same scale. Scale bar represents 50 mm.

of this value due to rapid movement (**Table 1**; see below). The relatively short length of the sole impressions in *Hyloidichnus* in comparison with the size of the tarsals plus calcaneum and astragalus of the proposed trackmaker indicates that the latter two bones were not impressed during locomotion; as further discussed below, this is in line with the relative depth pattern of the pes tracks in the reported trackway (**Figure 7C**), with the sole impression mostly only represented by the medial portion. Of note, in the reported trackway, pes tracks partially overstep manus tracks (**Figure 7B, C**), a feature not common, but still present, in trackways of this ichnospecies (Logghe *et al.*, 2021).

This overstepping, together with the elongated (slightly dragged), thin and straight digit imprints, and with both manus and pes tracks being parallel to the trackway midline, indicate a relatively high-speed locomotion of the trackmaker (cf. Peabody, 1956; Logghe *et al.*, 2021). This is supported by the correlation of the skeletal reconstruction of *Tramuntanasaurus tiai* to the trackway herein reported and the tracks of *Hyloidichnus bifurcatus* analysed by Matamales-Andreu *et al.* (2022): while the trackway is notably narrower than the pace inferred from the idealised locomotion of the reconstructed skeleton (**Figure 7A–C**), the pes fits in both morphology and size with the tracks of *Hyloidichnus bifurcatus* (**Figure 7D–E**; **Table 1**). This indicates that, in order to generate such a narrow trackway, the limbs were more upright and located closer to the body trunk. Of note, the tail impression is only slightly sinuous, especially when compared with other *Hyloidichnus* trackways with inferred walking gait (see also discussion in Logghe *et al.*, 2021). This indicates that in faster gaits the body trunk was more rigid (yet still with some slight lateral torsion) than during walking locomotion. Furthermore, in the trackway, both manus and pes imprints are parallel to the midline, whereas in the isolated manus-pes sets of *Hyloidichnus* from Mallorca (Matamales-Andreu *et al.*, 2022: figure 10D–F; **Figure 7D**), the pes does not overstep the manus, and the latter is inwardly rotated towards the hypothetical trackway midline. These latter features are more commonly found in *Hyloidichnus* specimens, being associated to a walking gait (see Logghe *et al.*, 2021 and references therein). Therefore, this may also be in line with a more rigid body trunk with limbs more erect and closer to the body during fast locomotion. The tracks parallel to the trackway midline would then be indicative of a lack of rotation of the autopodia (see further discussion below), which might be explained by a reduced movement between the different carpal and tarsal bones.

Regarding the track-trackmaker correlation, as stated above, the ichnogenus *Hyloidichnus* is generally attributed to captorhinomorphs (Logghe *et al.*, 2021). Previously, Voigt *et al.* (2010) correlated this ichnogenus with moradisaurines, based on the supposed Lopingian epoch of the North African succession studied in that work. The co-occurrence of *Hyloidichnus* and moradisaurine skeletal remains in Mallorca and the close matching of the tracks and the reconstructed skeleton (**Figure 7**; **Table 1**) show that moradisaurines were indeed trackmakers of *Hyloidichnus*. Yet, as pointed out by Logghe *et al.* (2021), other members of Captorhinomorpha (*e.g.*, *Captorhinus*)

Table 1. Comparison between the left pes of *Tramuntanasaurus tiai* gen. *et* sp. nov. and pes tracks of the small morphotype of *Hyloidichnus bifurcatus* from Mallorca.

Tramuntanasaurus tiai **gen. *et* sp. nov.**	
Museum collection number	DA21/17-01-03
Specimen field number	RA-19b-35
Left autopodium of the hindlimb	
Total length (mm)[1]	45.7
Total width (mm)[1]	51.4
Tarsal elements length (mm)[1]	10.9
Tarsal elements width (mm)[1]	15.9
Digit I length (metatarsal)[2]	9.1*
Digit II length (metatarsal + phalanges)	21.4 (9.6+(5.4+3.6+2.8))
Digit III length (metatarsal + (phalanges))[2]	24.0* (13.9+(5.5+4.6))
Digit IV length (metatarsal + (phalanges))[2]	31.0* (14.5+(6.8+5.5+4.2))
Digit V length (metatarsal + (phalanges))	29.7 (11.2+(6.8+4.5+3.6+3.6))
Glenoacetabular distance[1]	120.9

Note: The digit length of the tracks is notably shorter than that of the metatarsals + phalanges, because the digit length measured on the footprints start at the mid-distal portion of each impression of the metatarsal. Similarly, the length and width of all tarsal elements is shorter than the length and width of the sole impressions because the latter include part of the metatarsal impressions. Therefore, the values provided here are mainly to show that the skeletal elements and the pes tracks fall within the same size range and are proportionate. For further track and trackway parameters, see Matamales-Andreu *et al.* (2022).

[1]Estimated from the skeletal reconstruction

[2]Incomplete (skeletal elements missing)

*Approximate value

Hyloidichnus bifurcatus, **small morphotype**					
Museum collection number	TS-3	DA21/15-07-09	Left *in situ*	DA21/15-13-02	
Specimen field number	NA-26.0-09 (Figure 7D)	NA-60.4-02	NA-60.4-04	NA-87?-02 (Figure 7B, C)	
Anatomy	Right pes	Left pes	Left pes	Right pes	Left pes
Length (mm)	40.1	49.9	56.3	42.1	34.4
Width (mm)	51.8	-	60.7	46.7	-
Length sole (mm)	17.7	14.5	13.8	16.4	13.5
Width sole (mm)	22.7	-	31.0	18.2*	18.8*
Length I (mm)	15.5	-	-	8.3	6.6
Length II (mm)	17.0	24.9	30.9	12.0	12.5
Length III (mm)	21.8	29.6	41.3	16.7	19.3
Length IV (mm)	27.8	37.8	45.0	26.0	22.5
Length V (mm)	17.7	-	-	20.0*	-
Glenoacetabular distance				117.9	125.0
Manus-pes distance (mm)	49.3*	64.7*	47.7*	24.0	31.1
Stride length manus (mm)				187.7	
Pace pes (mm)				129.4	-
Pace manus (mm)				113.8	134.5
Pace angulation manus (degrees)				95.7	

could have produced this track morphotype as well. This is in line with the relatively long time span and widespread distribution of *Hyloidichnus* (Schneider *et al.*, 2020; Logghe *et al.*, 2021). Therefore, the conserved morphology of the appendicular skeleton of captorhinomorphs is also reflected in the ichnological record. Nonetheless, other ichnotaxa, such as *Merifontichnus*, have been also correlated to large moradisaurines (Marchetti, 2016). In this

sense, the presence of large-sized *Hyloidichnus bifurcatus* in the Permian successions of Mallorca (Matamales-Andreu *et al.*, 2022), which may be attributed to the large moradisaurine osteological remains recovered from nearby outcrops (Liebrecht *et al.*, 2017; Matamales-Andreu *et al.*, 2022), suggests a relatively higher morphological diversity of the postracranial skeleton of moradisaurines.

Such diversity of the postcranial skeleton of moradisaurines may also be reflected in the two size classes of *Hyloidichnus bifurcatus* from Mallorca. As described by Matamales-Andreu *et al.* (2022), the relative depth patterns (linked to the functional prevalence of autopodia, see Mujal *et al.*, 2020) are slightly different: in the small morphotype, the manus and pes tracks suggest a medial and medial-median functional prevalence, respectively; in the large morphotype, the manus and pes tracks suggest a medial-median and medial functional prevalence, respectively. This shows that the weight distribution was different between small and large moradisaurines, and this may be linked to different size proportions of the head with respect to the body, and/or notably different morphologies of the postcranium. This would result in different orientations of the fore- and hindlimbs on the substrate, eventually producing tracks with slightly different relative depth patterns. Noteworthy, in the *Hyloidichnus* trackway herein reported (**Figure 7B**), the relative depth patterns of the tracks suggest a medial-median functional prevalence for the manus and a medial functional prevalence for the pes (**Figure 7C**), just like the large morphotype of *Hyloidichnus bifurcatus* from Mallorca (Matamales-Andreu *et al.*, 2022) and opposite to those of the tracks of the small morphotype. In this case, differences in relative depth patterns among the small morphotype of this ichnotaxon from Mallorca are probably linked to different locomotion gaits that resulted in a shift in the distribution of the weight of the trackmaker, *i.e.*, in a slightly different functional prevalence of the autopodia (though still showing the general condition of the tetrapod group as suggested by Mujal *et al.*, 2020). As discussed above, the trackway DA21/15-13-02 (**Figure 7B–C**) is suggestive of a fast gait, whereas the isolated manus-pes sets reported by Matamales-Andreu *et al.* (2022) are compatible with a walking (slower) gait (those tracks do not show overstepping and the manus tracks are rotated inwards with respect to a hypothetical trackway midline). In a faster gait, the manus would have been less rotated, with the weight shifted towards the median carpals due to a lack of rotation of the autopodium. Similarly, in the hindlimb, the ankle would have also had a reduced rotation, resulting in the medial (inner) portion of the pes being the main part touching the substrate. Comparisons with the postcranium of other moradisaurines and captorhinomorphs, together with ichnological studies, may provide further insights on the locomotion of the group and on potential differences between taxa of notably different size, and the significance for the habitats of this diverse group of Permian eureptiles.

6. Conclusions

Tramuntanasaurus tiai gen. *et* sp. nov. (**Figure 8**) has been described as a new medium-sized moradisaurine captorhinid eureptile from the recently discovered Permian bone-bearing beds of Mallorca (Balearic Islands, western Mediterranean). It features a triangular skull with five rows of teeth on the maxilla and jaws, and a particular configuration of the cranial bones. This new taxon is related to other genera found in palaeoequatorial latitudes, such as *Kahneria* and *Labidosaurikos*. The holotype of *Tramuntanasaurus tiai*, a semi-articulated subadult skeleton,

is the most complete moradisaurine specimen found so far. The well-preserved pes, together with the overall body configuration, as shown in the skeletal reconstruction, has made it possible to correlate *Hyloidichnus* tracks to moradisaurines with a high degree of confidence, based on the exceptional case of having bones and tracks in geographically and stratigraphically close deposits. The different size classes of the *Hyloidichnus* found on Mallorca, with slight differences in relative depth patterns, suggest diversity of morphologies and/or proportions in the postcranium of moradisaurines. The correlation of the ichnogenus *Merifontichnus* to moradisaurine trackmakers further supports this hypothesis of morphological diversity, apparently higher than what has been observed in more basal groups of captorhinomorphs.

Figure 8. Life reconstruction of *Tramuntanasaurus tiai* gen. *et* sp. nov., depicting an adult specimen (foreground) and two juvenile specimens (background) among horsetails, in a floodplain setting. Created by Henry Sutherland Sharpe. © 2022 Henry Sutherland Sharpe. Used under license.

7. Acknowledgements

The authors of the present paper thank Sebastià Matamalas for aid in fieldwork. To Marina Rull and Xènia Aymerich (ICP, Cerdanyola del Vallès) for preparation of the specimen. To Amy Henrici (CMNH, Pittsburgh) for advice on the preparation. To the Hospital Universitari Mútua de Terrassa (Terrassa) for the preliminary medical CT scan of the rock containing the specimen DA21/17-01-03. To Alejandro Serrano-Martínez (ICP, Cerdanyola del Vallès) for his help on the CT scanning and segmentation of the skull of the holotype specimen. The μCT scan was performed at the CENIEH facilities (Burgos) with the collaboration of the CENIEH staff. To Enric Vicens (UAB, Cerdanyola del Vallès) for granting us access to the photographic equipment of the Palaeontology Unit of the UAB. To the reviewers (Spencer G. Lucas and one anonymous), publications officer (Sally Thomas) and editor (Lorenzo Marchetti) for their insightful comments and corrections that contributed to improving the original manuscript. To the Comissió Insular de Patrimoni Històric (Consell Insular de Mallorca) for granting us the excavation permits (file numbers 306/2019 and 75/2021) and funding for preparation (ref. 2 - 295/2021). R.M.A. was supported by the predoctoral grant FPU17/01922 (Ministerio de Ciencia, Innovación y Universidades) and the grant Synthesys+ DE-TAF-23 (European Commission). It has been further supported by the Generalitat de Catalunya (CERCA Programme and consolidated research groups 2021 SGR 01184 to J.F. and 2021 SGR 01192 to À.G.). This work is part of the Ramon y Cajal grant to J.F. [RYC2021-032857-I] financed by MCIN/AEI/10.13039/501100011033 and the European Union 'NextGenerationEU'/PRTR. We acknowledge support from the project 'Mallorca abans dels dinosaures: estudi dels ecosistemes continentals del Permià i Triàsic amb especial èmfasi en les restes de vertebrats' (ref. 15 - 619/2020), based at the Institut Català de Paleontologia Miquel Crusafont and funded by the Departament de Cultura, Patrimoni i Política Lingüística (Consell Insular de Mallorca).

8. References

Albright, G.M.; Sumida, S.S. & Jung, J.P. (2021). A new genus of captorhinid reptile (Amniota: Eureptilia) from the lower Permian Hennessey Formation of central Oklahoma, and consideration of homoplasy in the family Captorhinidae. *Annals of Carnegie Museum*, 87(2): 89–116.

Behrensmeyer, A.K. (1982). Time resolution in fluvial vertebrate assemblages. *Paleobiology*, 8(3): 211–227.

Bercovici, A.; Diez, J.B.; Broutin, J.; Bourquin, S.; Linol, B.; Villanueva-Amadoz, U.; López-Gómez, J. & Durand, M. (2009). A palaeoenvirnomental analysis of Permian sediments in Minorca (Balearic Islands, Spain) with new palynological and megafloral data. *Review of Palaeobotany and Palynology*, 158: 14–28.

Brocklehurst, N. (2020). Olson's Gap or Olson's Extinction? A Bayesian tip-dating approach to resolving stratigraphic uncertainty. *Proceedings of the Royal Society B*, 287: 20200154.

Calafat, F. (1988). *Estratigrafía y sedimentología de la litofacies Buntsandstein de Mallorca*. Bachelor's Thesis. Universitat de Barcelona, Barcelona. 127 pp. + 31 annexed figs.

Calafat, F.; Fornós, J.J.; Marzo, M.; Ramos-Guerrero, E. & Rodríguez-Perea, A. (1986–1987). Icnología de vertebrados de las facies Buntsandstein de Mallorca. *Acta Geològica Hispànica*, 21–22: 515–520.

Carroll, R.L. & Baird, D. (1972). Carboniferous stem-reptiles of the family Romeriidae. *Bulletin of the Museum of Comparative Zoology*, 143(5): 321–363.

Case, E.C. (1911). A revision of the Cotylosauria of North America. *Carnegie Institution of Washington Publication*, 145: 1–121.

Cisneros, J.C.; Angielczyk, K.; Kammerer, C.F.; Smith, R.M.H.; Fröbisch, J.; Marsicano, C.A. & Richter, M. (2020). Captorhinid reptiles from the lower Permian Pedra de Fogo Formation, Piauí, Brazil: the earliest herbivorous tetrapods in Gondwana. *PeerJ*, 8: e8719.

Clark, J. & Carroll, R.L. (1973). Romeriid reptiles from the lower Permian. *Bulletin of the Museum of Comparative Zoology*, 144(5): 353–407.

Cope, E.D. (1896). The reptilian order Cotylosauria. *Proceedings of the American Philosophical Society*, 34: 436–457.

deBraga, M.; Bevitt, J.J. & Reisz, R.R. (2019). A new captorhinid from the Permian cave system near Richards Spur, Oklahoma, and the taxic diversity of *Captorhinus* at this locality. *Frontiers in Earth Science*, 7:112.

de Ricqlès, A. & Taquet, P. (1982). La faune de vertébrés du Permien Supérieur du Niger. I. Le captorhinomorphe *Moradisaurus grandis* (Reptilia, Cotylosauria). Le crane. *Annales de Paléontologie (Vert.-Invert.)*, 68: 33–106.

Dodick, J.T. & Modesto, S.P. (1995). The cranial anatomy of the captorhinid reptile *Labidosaurikos meachami* from the lower Permian of Oklahoma. *Palaeontology*, 38(3): 687–711.

Dutuit, J.M. (1976). Il est probable que les Rhynchocéphales sont représentés dans la faune du Trias marocain. *Comptes Rendus Hebdomadaires des Séances de l'Académie des Sciences, Paris, s. D*, 283: 483–486.

Fox, R.C. & Bowman, M.C. (1966). Osteology and relationships of *Captorhinus aguti* (Cope) (Reptilia: Captorhinomorpha). *The University of Kansas Paleontological Contributions*, 11: 1–79.

Gand, G. (1988). *Les traces de vertébrés tétrapodes du Permien français, paléontologie, stratigraphie, paléoenvironnements*. PhD dissertation. Université de Bourgogne, Dijon. 341 pp.

Gand, G.; Garric, J.; Demathieu, G. & Ellenberger, P. (2000). La palichnofaune de vertébrés tétrapodes du permien supérieur du Bassin de Lodève (Languedoc-France). *Palaeovertebrata*, 29: 1–82.

Gilmore, G.W. (1927). Fossil footprints from the Grand Canyon: second contribution. *Smithsonian Miscellaneous Collections*, 80: 1–78.

Gómez-Gras, D. & Alonso-Zarza, A.M. (2003). Reworked calcretes: their significance in the reconstruction of alluvial sequences (Permian and Triassic, Minorca, Balearic Islands, Spain). *Sedimentary Geology*, 158: 299–319.

Heaton, M.J. (1979). Cranial anatomy of primitive captorhinid reptiles from the late Pennsylvanian and early Permian Oklahoma and Texas. *Oklahoma Geological Survey Bulletin*, 127: 1–84.

Hmich, D.; Schneider, J.W.; Saber, H.; Voigt, S. & El Wartiti, M. (2006). New continental Carboniferous and Permian faunas of Morocco: implications for biostratigraphy, palaeobiogeography and palaeoclimate. *Geological Society, London, Special Publications*, 265(1): 297–324.

Holmes, R.B. (2003). The hind limb of *Captorhinus aguti* and the step cycle of basal amniotes. *Canadian Journal of Earth Sciences*, 40: 515–526.

Ivakhnenko, M.F. (2008). Podklass Captorhinomorpha [Subclass Captorhinomorpha]. *In*: Ivakhnenko, M.F. & Kurotchkin, E.N. (Eds.). *Iskopaemye pozvonotchnye Rossii i sopredel'nykh stran: Iskopaemye reptilii i ptitsy, Tchast' 1 [Fossil vertebrates of Russia and adjacent countries: Fossil reptiles and birds, Part 1]*. GEOS, Moskva: 86–94. [in Russian]

Jalil, N.E. & Dutuit, J.M. (1996). Permian captorhinid reptiles from the Argana Formation, Morocco. *Palaeontology*, 39: 907–918.

Jung, J.P. (2018). *Redescription and phylogenetic analysis of the materials assigned to the taxon* "Captorhinikos" chozaensis. Master's Thesis. California State University, San Bernardino. 79 pp.

Jung, J.P. & Sumida, S.S. (2017). A juvenile of the multiple-tooth-rowed reptile *Labidosaurikos* (Eureptilia, Captorhinidae, Moradisaurinae) from the Lower Permian of north-central Texas. *PaleoBios*, 34: 1–5.

Kissel, R.A.; Dilkes, D.W. & Reisz, R.R. (2002). *Captorhinus magnus*, a new captorhinid (Amniota: Eureptilia) from the Lower Permian of Oklahoma, with new evidence on the homology of the astragalus. *Canadian Journal of Earth Sciences*, 39: 1363–1372.

Kuhn, O. (1961). *Fossilium Catalogus. I: Animalia. Pars 99. Reptilia (Supplementum 1(2))*. Uitgeverij Dr. W. Junk, The Hague. 163 pp.

Laurenti, J.N. (1768). *Specimen Medicum, Exhibens Synopsin Reptilium Emendatam cum Experimentis Circa Venena et Antidota Reptilium Austriacorum*. Typis Joannis Thomae Nobilis de Trattnern, Wien. 214 pp + 5 pl.

Laurin, M. & Hook, R.W. (2022). The age of North America's youngest Paleozoic continental vertebrates: a review of data from the Middle Permian Pease River (Texas) and El Reno (Oklahoma) Groups. *BSGF - Earth Sciences Bulletin*, 193: 10.

LeBlanc, A.R.H. & Reisz, R.R. (2015). Patterns of tooth development and replacement in captorhinid reptiles: a comparative approach for understanding the origin of multiple tooth rows. *Journal of Vertebrate Paleontology*, 35: e919928.

LeBlanc, A.R.H.; Brar, A.K.; May, W. & Reisz, R.R. (2015). Multiple tooth-rowed captorhinids from the early Permian fissure fills of the Bally Mountain Locality of Oklahoma. *Vertebrate Anatomy Morphology Palaeontology*, 1: 35–49.

Leonardi, G. (1987). *Glossary and Manual of Tetrapod Footprint Palaeoichnology*. Departamento Nacional de Produção Mineral, Brasília. 117 pp.

Liebrecht, T.; Fortuny, J.; Galobart, À.; Müller, J. & Sander, P.M. (2017). A large, multiple-tooth-rowed captorhinid reptile (Amniota: Eureptilia) from the Upper Permian of Mallorca (Balearic Islands, Western Mediterranean). *Journal of Vertebrate Paleontology*, 37(1): e1251936.

Logghe, A.; Mujal, E.; Marchetti, L.; Nel, A.; Pouillon, J.M.; Giner, S.; Garrouste, R. & Steyer, J.-S. (2021). *Hyloidichnus* trackways with digit and tail drag traces from the Permian of Gonfaron (Var, France): New insights on the locomotion of captorhinomorph eureptiles. *Palaeogeography, Palaeoclimatology, Palaeoecology*, 573: 110436.

Mallison, H. & Wings, O. (2014). Photogrammetry in paleontology – a practical guide. *Journal of Paleontological Techniques*, 12: 1–31.

Marchetti, L. (2016). New occurrences of tetrapod ichnotaxa from the Permian Orobic Basin (Northern Italy) and critical discussion of the age of the ichnoassociation. *Papers in Palaeontology*, 2: 363–386.

Marchetti, L.; Mujal, E. & Bernardi, M. (2017). An unusual *Amphisauropus* trackway and its implication for understanding seymouriamorph locomotion. *Lethaia*, 50: 162–174.

Marchetti, L.; Belvedere, M.; Voigt, S.; Klein, H.; Castanera, D.; Díaz-Martínez, I.; Marty, D.; Xing, L.; Feola, S.; Melchor, R.N. & Farlow, J.O. (2019). Defining the morphological quality of fossil footprints. Problems and principles of preservation in tetrapod ichnology with examples from the Palaeozoic to the present. *Earth-Science Reviews*, 193: 109–145.

Marchetti, L.; Logghe, A.; Mujal, E.; Barrier, P.; Montenat, C.; Nel, A.; Pouillon, J.M.; Garrouste, R. & Steyer, J.-S. (2022). Vertebrate tracks from the Permian of Gonfaron (Provence, Southern France) and their implications for the late Capitanian extinction event. *Palaeogeography, Palaeoclimatology, Palaeoecology*, 599: 111043.

Matamales-Andreu, R.; Roig-Munar, F.X.; Oms, O.; Galobart, À. & Fortuny, J. (2021a). A captorhinid-dominated assemblage from the palaeoequatorial Permian of Menorca (Balearic Islands, western Mediterranean). *Earth and Environmental Science Transactions of the Royal Society of Edinburgh*, 112(2): 125–145.

Matamales-Andreu, R.; Galobart, À. & Fortuny, J. (2021b). New occurrences of small moradisaurine captorhinid eureptiles from the Permian of Mallorca (western Mediterranean). *In*: Belvedere, M.; Díez Díaz, V.; Mecozzi, B. & Sardella, R. (Eds.). *Abstract book of the XVIII annual conference of the European Association of Vertebrate Palaeontologists, online, 5th–9th July 2021. Palaeovertebrata*, 44: p. 115.

Matamales-Andreu, R.; Mujal, E.; Galobart, À. & Fortuny, J. (2021c). Insights on the evolution of synapsid locomotion based on tetrapod tracks from the lower Permian of Mallorca (Balearic Islands, western Mediterranean). *Palaeogeography, Palaeoclimatology, Palaeoecology*, 579: 110589.

Matamales-Andreu, R.; Oms, O. & Fortuny, J. (2021d). Paleoecosistemes del Permià i Triàsic continental de Mallorca (Illes Balears, Mediterrània occidental): síntesi i prespectives futures. *In*: Gómez-Pujol, Ll.; Roig-Munar, F.X.; Gelabert, B. & Martín, J.A. (Eds.). *De la terra a la mar i de la mar a la terra. Homenatge a Antonio Rodríguez-Perea. Monografies de la Societat d'Història Natural de Balears*, 34. Societat d'Història Natural de les Balears, Palma: 17–39.

Matamales-Andreu, R.; Mujal, E.; Dinarès-Turell, J.; Kustatscher, E.; Roghi, G.; Oms, O.; Galobart, À. & Fortuny, J. (2022). Early-middle Permian ecosystems of equatorial Pangaea: integrated multi-stratigraphic and palaeontological review of the Permian of Mallorca (Balearic Islands, western Mediterranean). *Earth-Science Reviews*, 228: 103948.

Meyer, T.E. & Anderson, J.S. (2013). Tarsal fusion and the formation of the astragalus in *Hylonomus lyelli*, the earliest amniote, and other early tetrapods. *Journal of Vertebrate Paleontology*, 33(2): 488–492.

Miall, A.D. (2006). *The Geology of Fluvial Deposits: Sedimentary Facies, Basin Analysis, and Petroleum Geology*. 4th ed. Springer, Berlin, Heidelberg, New York. 582 pp.

Modesto, S.P.; Scott, D.M.; Berman, D.S.; Müller, J. & Reisz, R.R. (2007). The skull and the palaeoecological significance of *Labidosaurus hamatus*, a captorhinid reptile from the Lower Permian of Texas. *Zoological Journal of the Linnean Society*, 149: 237–262.

Modesto, S.P.; Lamb, A.J. & Reisz, R.R. (2014). The captorhinid reptile *Captorhinikos valensis* from the lower Permian Vale Formation of Texas, and the evolution of herbivory in eureptiles. *Journal of Vertebrate Paleontology*, 34(2): 291–302.

Modesto, S.P.; Scott, D.; Reisz, R.R. (2018). A new small captorhinid reptile from the lower Permian of Oklahoma and resource partitioning among small captorhinids in the Richards Spur fauna. *Papers in Palaeontology*, 4(2): 293–307.

Modesto, S.P.; Richards, C.D.; Ide, O. & Sidor, C.A. (2019). The vertebrate fauna of the upper Permian of Niger — X. The mandible of the captorhinid reptile *Moradisaurus grandis*. *Journal of Vertebrate Paleontology*, 38(6): e1531877.

Mujal, E.; Fortuny, J.; Oms, O.; Bolet, A.; Galobart, À. & Anadón, P. (2016). Palaeoenvironmental reconstruction and early Permian ichnoassemblage from the NE Iberian Basin (Pyrenean Basin). *Geological Magazine*, 153(4): 578–600.

Mujal, E.; Marchetti, L.; Schoch, R.R. & Fortuny, J. (2020). Upper Paleozoic to lower Mesozoic tetrapod ichnology revisited: photogrammetry and relative depth pattern inferences on functional prevalence of autopodia. *Frontiers in Earth Science*, 8:248.

O'Keefe, F.R.; Sidor, C.A.; Larsson, H.C.; Maga, A. & Ide, O. (2005). The vertebrate fauna of the upper Permian of Niger—III, Morphology and ontogeny of the hindlimb of *Moradisaurus grandis* (Reptilia, Captorhinidae). *Journal of Vertebrate Paleontology*, 25(2): 309–319.

O'Keefe, F.R.; Sidor, C.A.; Larsson, H.C.E.; Maga, A. & Ide, O. (2006). Evolution and homology of the astragalus in early amniotes: new fossils, new perspectives. *Journal of Morphology*, 267: 415–425.

Olroyd, S.L. & Sidor, C.A. (2017). A review of the Guadalupian (middle Permian) global tetrapod fossil record. *Earth-Science Reviews*, 171: 583–597.

Olson, E.C. (1947). The family Diadectidae and its bearing on the classification of reptiles. *Fieldiana: Geology*, 11: 1–53.

Olson, E.C. (1954). Fauna of the Vale and Choza: 9. Captorhinomorpha. *Fieldiana: Geology*, 10(19): 211–218.

Olson, E.C. (1962a). Late Permian terrestrial vertebrates, U.S.A. and U.S.S.R. *Transactions of the American Philosophical Society*, 52: 1–224.

Olson, E.C. (1962b). Permian vertebrates from Oklahoma and Texas. Part II. — The osteology of *Captorhinikos chozaensis* Olson. *Oklahoma Geological Survey Circular*, 59: 49–68.

Olson, E.C. (1965). New Permian vertebrates from the Chickasha Formation in Oklahoma. *Oklahoma Geological Survey Circular*, 70: 1–70.

Olson, E.C. & Barghusen, H. (1962). Permian vertebrates from Oklahoma and Texas. Part I. — Vetrbrates from the Flowerpot Formation, Permian of Oklahoma. *Oklahoma Geological Survey Circular*, 59: 6–48.

Reisz, R.R. & Sues, H.-D. (2000). Herbivory in late Paleozoic and Triassic terrestrial vertebrates. *In*: Sues, H.-D. (Ed.). *Evolution of Herbivory in Terrestrial Vertebrates*. Cambridge University Press: 9–41.

Reisz, R.R.; Liu, J.; Li, J.-L. & Müller, J. (2011). A new captorhinid reptile, *Gansurhinus qingtoushanensis*, gen. et sp. nov., from the Permian of China. *Naturwissenschaften*, 98: 435–441.

Ride, W.D.L.; Cogger, H.G.; Dupuis, C.; Kraus, O.; Minelli, A.; Thompson, F.C. & Tubbs, P.K. (1999). *International Code of Zoological Nomenclature*. Fourth Edition (updated 2012). The International Trust for Zoological Nomenclature, London. Accessible online on: https://www.iczn.org/the-code/the-code-online/ (last accessed on 22/05/2022).

Schneider, J.W.; Lucas, S.G.; Scholze, F.; Voigt, S.; Marchetti, L.; Klein, H.; Opluštil, S.; Werneburg, R.; Golubevb, V.K.; Barrick, J.E.; Nemyrovska, Y.; Ronchi, A.; Day, M. O.; Silantiev, V.V.; Rößler, R.; Saber, H.; Linnemann,

U.; Zharinova, V. & Shen, S.-Z. (2020). Late Paleozoic–early Mesozoic continental biostratigraphy — links to the Standard Global Chronostratigraphic Scale. *Palaeoworld*, 29(2): 186–238.

Sidor, C.A.; Ouide, O.; Larsson, H.C.E.; O'Keefe, F.R.; Smith, R.M.H.; Steyer, J.-S. & Modesto, S.P. (2022). The vertebrate fauna of the upper Permian of Niger—XI. Cranial material of a juvenile *Moradisaurus grandis* (Reptilia: Captorhinidae). *Journal of Vertebrate Paleontology*, 41(5): e2030345.

Smith, R.M.H. (1993). Vertebrate taphonomy of late Permian floodplain deposits in the southwestern Karoo Basin of South Africa. *Palaios*, 8: 45–67.

Stovall, J.W. (1950). A new cotylosaur from North Central Oklahoma. *American Journal of Science*, 248(1): 46–54.

Sumida, S.S. (1989). The appendicular skeleton of the early Permian genus *Labidosaurus* (Reptilia, Captorhinomorpha, Captorhinidae) and the hind limb musculature of captorhinid reptiles. *Journal of Vertebrate Paleontology*, 9(3): 295–313.

Sumida, S.S. (1990). Vertebral morphology, alternation of neural spine height, and structure in Permo-Carboniferous tetrapods, and a reappraisal of primitive modes of terrestrial locomotion. *University of California Publications in Zoology*, 122: 1–129 + 3 pls.

Swofford, D.L. (2003). *PAUP*: phylogenetic analysis using parsimony (*and other methods)*. Version 4. Sunderland, Massachusetts: Sinauer Associates.

Taquet, P. (1969). Première découverte en Afrique d'un reptile captorhinomorphe (cotylosaurien). *Comptes Rendus Hebdomadaires des Séances de l'Académie des Sciences, Paris, s. D*, 268: 779–781.

Vjushkov, B.P. & Chudinov, P.K. (1957). Otkrytie Kaptorinid v verkhnnej Permi SSSR [Discovery of a captorhinid in the upper Permian of the USSR]. *Doklady Akademii Nauk SSSR*, 112: 523–536. [in Russian]

Voigt, S. & Haubold, H. (2015). Permian tetrapod footprints from the Spanish Pyrenees. *Palaeogeography, Palaeoclimatology, Palaeoecology*, 417: 112–20.

Voigt, S.; Berman, D.S. & Henrici, A.C. (2007). First well-established track-trackmaker association of Paleozoic tetrapods based on *Ichniotherium* trackways and diadectid skeletons from the Lower Permian of Germany. *Journal of Vertebrate Paleontology*, 27: 553–570.

Voigt, S.; Hminna, A.; Saber, H.; Schneider, J.W. & Klein, H. (2010). Tetrapod footprints from the uppermost level of the Permian Ikakern Formation (Argana Basin, Western High Atlas, Morocco). *Journal of African Earth Sciences*, 57: 470–478.

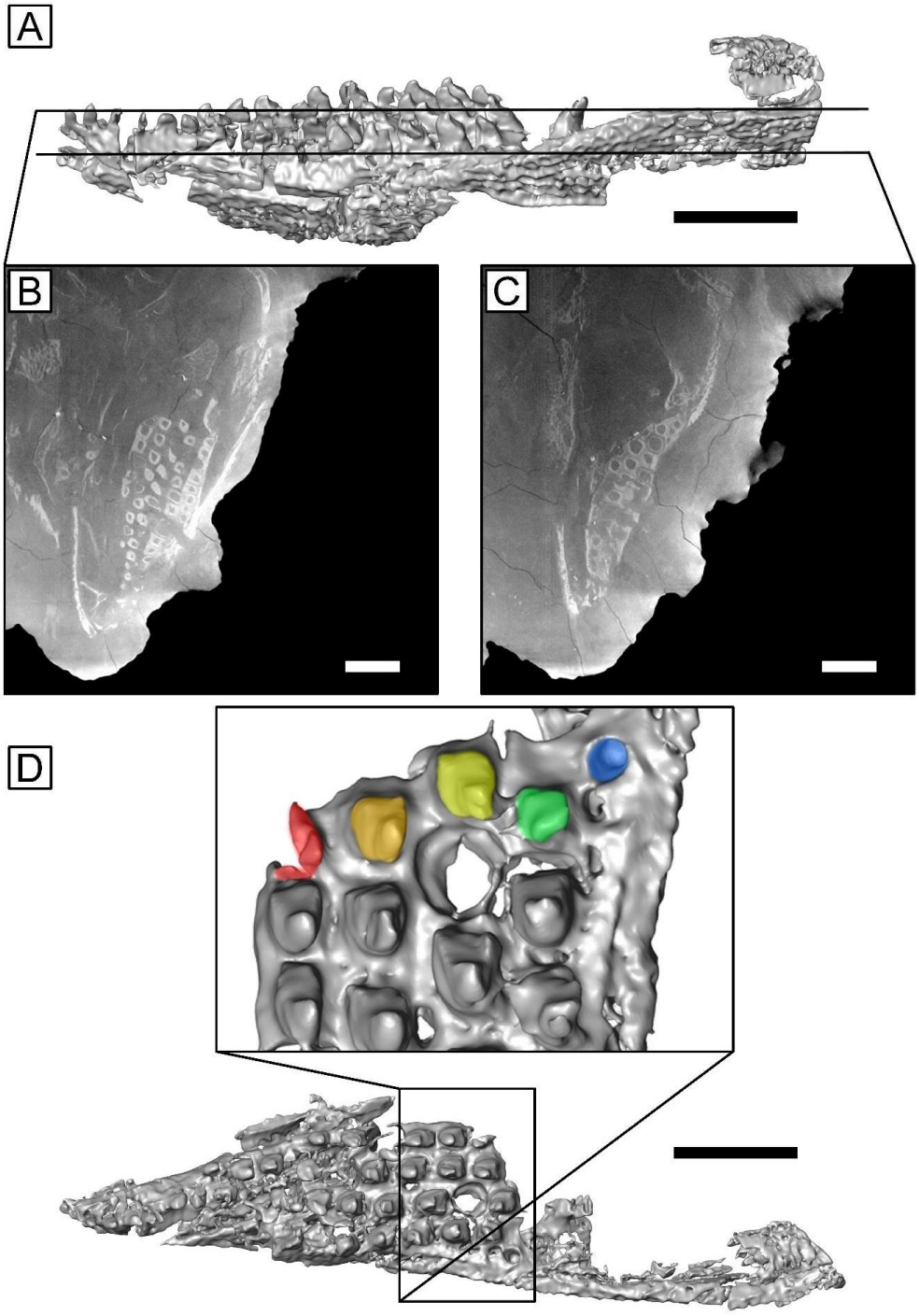

Supplementary Figure 1. Detail of the 3D model of the right maxilla of the holotype specimen of *Tramuntanasaurus tiai* gen. *et* sp. nov. **A:** Complete 3D model in lateral-occlusal view with indication of the position of the slices in (B) and (C). **B–C:** Slices of the maxilla in two different heights, showing the teeth. **D:** Maxilla in occlusal view, with posteriormost teeth of each row painted in a different colour. Note that, although teeth of one of the rows are very small, there are five rows of teeth. Scale bars represent 10 mm.

Supplementary Material 2. Phylogenetic Matrix

Protorothyris spp.

0000000000000000000000000000000000000000000000000000000000000000000000000000000000000000?000??

Paleothyris acadiana

00000000010000000100000020100000100000000010?000000000000???000000000000000000000000

Thuringothyris mahlendorffae

000000101100010101000000100000000000000001000000000000000????000100100??0000??10100

Euconcordia cunninghami

000101111100011 0??000000101001000?0?00000101 0?000000?0000???0?0100000100 0??????????

Opisthodontosaurus carrolli

0???111?????00100?001???10?????????0?020001100 0?????1?000110100030000301001?0??110??

Romeria prima

00111010000?00110000110 00?000100?01?0???0100000??0?1?0000???00110000010 10?0?1?1?1??

Romeria texana

001110??000?00110000010 01?000100101 00?00010?0?00?0?100000???00110000010 10??????????

Reiszorhinus olsoni

10111010000?01100100000010111011111?????????????000?1?000?11?00110000110 10??????????

Protocaptorhinus pricei

00111011000101110?00101010010101 10???10?010?0??00011?0000???10110000110?011?00111??

Rhiodenticulatus heatoni

00111011110101101100000??1?0101?1?0?10100010000 0?00?1000001???00100000101 01?1??111??

Saurorictus australis

00?1111?010?0100110012220001012?00????????1?????0?????0????????1100000101 0??????????

Rhodotheratus parvus

000111100100010011001222100101211010000 01?01010?00110000010110120101110101111???????

Captorhinus magnus

00111111001201101101 0?10100?01?2???102100?00100000??000101 0?2011000011110111??111??

Captorhinus kierani

10101111000?01101101 0?10110101221?10021001001000001100 01?10?10111000 01?10??????????

Captorhinus aguti

00111111000201101101001010010111210110210010010000011000101002011100121111111111111111

Captorhinus laticeps

00111111000200101101001010010111210110210101001000001100010100101100001111 0111111111111

Labidosauriscus richardi

001111110?0?010????1????10?????2??110210021010?????1?0011100?0120000110 10??????????

Labidosaurus spp.

1111111000111110110101101101011211110110011020011111011111111011001012110111121111 1

Captorhinikos valensis

1????1????????????????????????????????000???????????????????????120123??2211????????

Captorhinikos chozaensis

1011111?0?0??0??????????10??????????01100??0????11?1?1111???111120123?0221?111101?1

Labidosaurikos meachami

1111111000111110111111111101111211110111111021011111011110111112211332122??????????

Kahneria seltina

1???????????1??11101?????1??????????????21?????????1?1?010?????110123?1??1?0??1????

Moradisaurus grandis

1(0 1)1?101?1???11001102???111??11?1??1111111210211110?111111111111220033212221???1?1?1

Rothianiscus spp.

111?10???????1????12???111?????1??111?112210?????????111????111311123?122211????1??

Gansurhinus qingtoushanensis

1?1?1???1?????????1??????????320123???2211???1???

Tramuntanasaurus tiai

10??1110001?1110110011??110111?11??????12????????????1111?0121?221123111211?1?111?0

Balearosaurus bombardensis

1???

Moradisaurine Son Bunyola

1????????????1???3???2??????????

Appendix 5

First gorgonopsian therapsid from equatorial Pangaea

Appendix 5 was prepared as:

Matamales-Andreu, R.; Kammerer, C.F.; Angielczyk, K.D.; Mujal, E.; Hellert, S.M., Galobart, À. & Fortuny, J. (in preparation). First gorgonopsian from the Mediterranean demonstrates ancient equatorial distribution of therapsids.

In this work, R. Matamales-Andreu contributed in:

A. Logging of the stratigraphic section.
B. Co-direction of all fieldwork campaigns (prospections and excavations). Sampling of tetrapod bones.
C. Stratigraphic and sedimentological analysis.
D. Interpretation and discussion of the results.
E. Collaboration in writing of the original draft and supplementary materials, except for section Results, the part of the Discussion comparing the specimen to other therapsids and gorgonopsians, and the Extended Description in the Supplementary Material.
F. Preparation of figures 1, 3 and SF1–SF6.
G. Collaboration in obtaining funding for fieldwork and fossil preparation.

First gorgonopsian from the Mediterranean demonstrates ancient equatorial distribution of therapsids

Rafel Matamales-Andreu[1,2*], Christian F. Kammerer[3], Kenneth D. Angielczyk[4], Eudald Mujal[5,2], Spencer M. Hellert[4], Àngel Galobart[2,6], Josep Fortuny[2]

[1] Museu Balear de Ciències Naturals, FJBS-MBCN, ctra. Palma-Port de Sóller km 30.5, 07100 Sóller, Mallorca, Illes Balears, Spain.

[2] Institut Català de Paleontologia Miquel Crusafont, Universitat Autònoma de Barcelona, Edifici ICTA-ICP, c/ Columnes s/n, Campus de la UAB, 08193 Cerdanyola del Vallès, Barcelona, Catalunya, Spain.

[3] North Carolina Museum of Natural Sciences, 11 W. Jones Street, Raleigh, North Carolina 27604 U.S.A.

[4] Field Museum of Natural History, 1400 South DuSable Lake Shore Drive, Chicago, Illinois 60605 U.S.A.

[5] Staatliches Museum für Naturkunde Stuttgart, Rosenstein 1, 70191 Stuttgart, Germany.

[6] Museu de la Conca Dellà, c/ del Museu 4, 25650 Isona i Conca Dellà, Lleida, Spain.

*Corresponding author: rafel.matamales@icp.cat

Abstract

Therapsids, the group of tetrapods that eventually gave rise to mammals during the early Mesozoic, were a dominant component of middle–late Permian terrestrial ecosystems worldwide. Their skeletal fossil record is biased towards the temperate palaeolatitudes of Pangaea, with only highly fragmentary remains recorded from the palaeotropics. This uneven geographic coverage of the group, together with their obscure phylogenetic origins in the form of a lengthy ghost lineage, has made their early history one of the most enigmatic questions in synapsid palaeontology. Here we describe a partial gorgonopsian therapsid skeleton from the lower–?middle Permian of Mallorca (western Mediterranean), which at that time was located near the equator of Pangaea. This specimen represents the oldest gorgonopsian record worldwide, and possibly the oldest therapsid as well. Its palaeobiogeographic position and purported age show that therapsids lived in the palaeotropics and were diverse and specialised near the early–middle Permian transition, providing new insight into the timing of the phylogenetic and morphological

diversification of therapsids. Therefore, this study provides novel data that help to fill a major gap in the evolutionary and palaeobiogeographic history of therapsids, underscoring the importance of the southwestern European sites to answering persistent questions about the forerunners of mammals.

Keywords: Gorgonopsia, Therapsida, Synapsida, Permian, Mallorca

1. Introduction

Therapsida is a clade of diverse and ecologically successful tetrapods, with mammals as their modern representatives. The roots of the clade extend back to the late Palaeozoic, when non-mammalian therapsids were important, often dominant, components of terrestrial ecosystems. The oldest known unequivocal therapsid is *Raranimus dashankouensis*, from the Roadian (lower part of the middle Permian) of central-east Asia (Liu *et al.*, 2009; Duhamel *et al.*, 2021). Yet, phylogenetic analyses consistently suggest that therapsids are the sister group of sphenacodontid "pelycosaur"-grade synapsids that diverged in the late Mississippian (Hopson & Barghusen, 1986; Sidor & Hopson, 1998; Liu *et al.*, 2009; Amson & Laurin, 2011; Fröbisch *et al.*, 2011; Benson, 2012; Brink *et al.*, 2015; Didier & Laurin, 2020; Huttenlocker *et al.*, 2021; Brocklehurst *et al.*, 2022). This result implies a long therapsid ghost lineage spanning about 30 million years, in which fossils of this clade have never been found.

This knowledge gap in part may be due to the uneven geographic sampling of Permian tetrapods worldwide. The best-known lower Permian tetrapod-bearing formations, in North America (eastern shelf of the Midland Basin and northern shelf of the Anadarko Basin) and in western Europe (Central European Basin), correspond to palaeoequatorial ecosystems and have not yielded any definitive therapsid fossils so far (Angielczyk & Kammerer, 2018; Laurin & Hook, 2022). On the other hand, the sites with the best middle and upper Permian tetrapod record are those in the Cis-Urals and southern Africa, representing ecosystems of northern and southern palaeotemperate latitudes with abundant representation of therapsids (Bernardi *et al.*, 2017 and references therein; Olroyd & Sidor, 2017 and references therein). The historical lack of a spatiotemporal link between these regions has obscured the early history of therapsid evolution and diversification.

Here we describe the first unequivocal therapsid from equatorial Pangaea, collected in the upper Cisuralian (lower Permian)–lowermost Guadalupian? (middle Permian) of Mallorca (Balearic Islands, western Mediterranean) (see Matamales-Andreu *et al.*, 2022) (**Figure 1a–c**, **Supplementary Text 1**, **Supplementary Figure 1**), showing that, contrary to conventional wisdom, therapsids were not excluded from the palaeoequator at the beginning of their history. We discuss the identity, age and palaeobiogeographical implications of this new specimen, which reveal that it is the oldest known gorgonopsian (**Figure 1d**) and possibly the oldest therapsid reported worldwide, as it likely dates to the early Permian.

2. Results

Synapsida Osborn, 1903

Therapsida Broom, 1905

Gorgonopsia Seeley, 1894

Gorgonopsia indet.

Figure 2, Supplementary Figures 2–5

Studied material: DA21/17-01-01, a disarticulated, partial skeleton consisting of partial snout roof, partial basicranium, pterygoid, ectopterygoid?, hyoid?, left dentary, one upper canine, four lower? incisors, four presacral vertebrae, two proximal caudal vertebrae, eight distal caudal vertebrae, two right dorsal ribs and fragments of others, left femur, left tibia, left fibula, left calcaneum, left astragalus, possible left distal tarsal 3, left metatarsals 3 and 4, right metatarsals 1 and 5, first phalanges of right digits I, IV and V, second phalanx of right digit IV, one penultimate phalanx of digit III, IV or V, and one ungual phalanx. All the bones were found near the base of bed NA2 (Torrent de na Nadala 2, Banyalbufar, Mallorca, western Mediterranean; see **Supplementary Text 1**, **Supplementary Figure 1a–b**) except for one of the presacral vertebrae, which was extracted from the upper part of the same bed (c. 4–5 cm above), in a conglomerate horizon (**Supplementary Figure 1b**).

Description: See **Supplementary Text 2** and **Supplementary Figures 2–6** for a detailed description and illustration of all the elements. DA21/17-01-01 represents a small gorgonopsian (estimated skull length ~18 cm) known from various cranial fragments, several portions of the axial column (including a large portion of the tail), and most of the left hind limb. Cranial elements consist of a badly-flattened dorsal portion of the snout, fused basicranium incorporating at least the basioccipital, opisthotic, and prootic, and an isolated pterygoid. The pterygoid exhibits prominently "wing-shaped", backswept transverse processes (seen in other early gorgonopsians, such as *Eriphostoma* and *Gorgonops*) and bears anterior articular facets for the ectopterygoids. The left dentary is preserved in almost its entirety, with preserved alveoli indicating a tooth count of i4/c1/pc5. The dentary has a prominent mentum at the ventral edge of the symphysis and a clear inflection point dorsally where the incisor roots would have been housed. Several serrated, weakly spatulate teeth probably represent the lower incisors. A much larger, compressed, blade-like tooth represents a canine, probably an upper based on size.

Preserved axial elements include two probable cervical vertebrae, two intact dorsal ribs and fragments of additional ribs, two isolated anterior caudal vertebrae, and an articulated caudal series including evidence for 14 vertebrae. The vertebrae are similar to those known in other gorgonopsians. The left hind limb includes the femur, tibia, fibula, astragalus, calcaneum, and several metatarsals and phalanges, including one ungual. The tibia and fibula are both bowed, indicating the presence of a large interosseous space. The femur is weakly curved with a notably offset head, which is the typical morphology of small gorgonopsians (Sigogneau-Russell, 1989). In general,

the postcranial anatomy of the gorgonopsian from Mallorca is very consistent with that known in other small-bodied members of the group (*e.g.*, *Cyonosaurus*), with no clear autapomorphies.

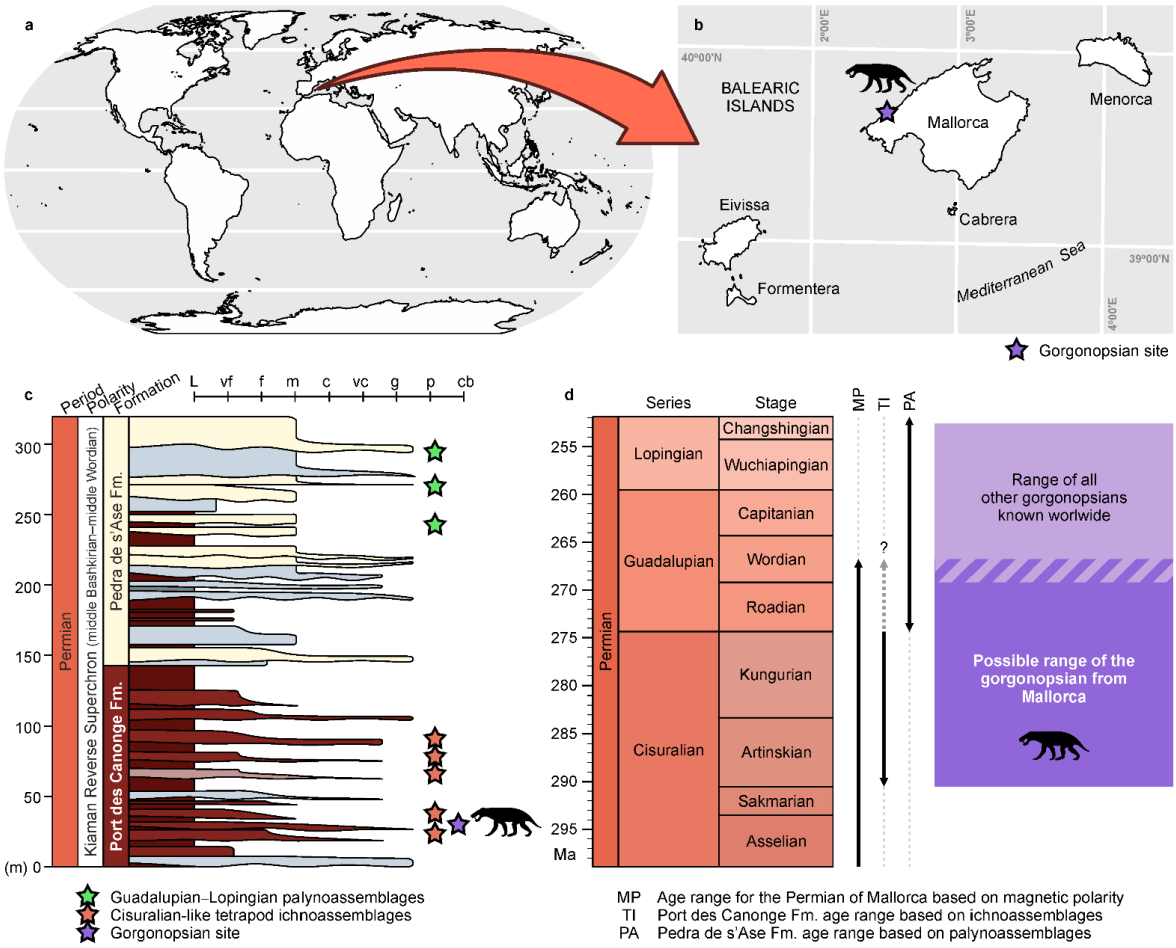

Figure 1. Context of the studied gorgonopsian specimen. **a**: World map showing the location of the island of Mallorca, **b**: Map of the Balearic Islands with indication of the study area, **c**: Synthetic stratigraphic log for the Racó de s'Algar-Pedra de s'Ase section (simplified from Matamales-Andreu *et al.*, 2022), indicating the beds that contain tetrapod tracks, spores and pollen, and the gorgonopsian, **d**: Chronostratigraphic chart for the Permian with age ranges for the formations of Mallorca, obtained from the study of palaeomagnetism, tetrapod ichnoassemblages and palynoassemblages, and the possible age range of the gorgonopsian from Mallorca compared to all the other known specimens from this clade (also see **Supplementary Figure 1**).

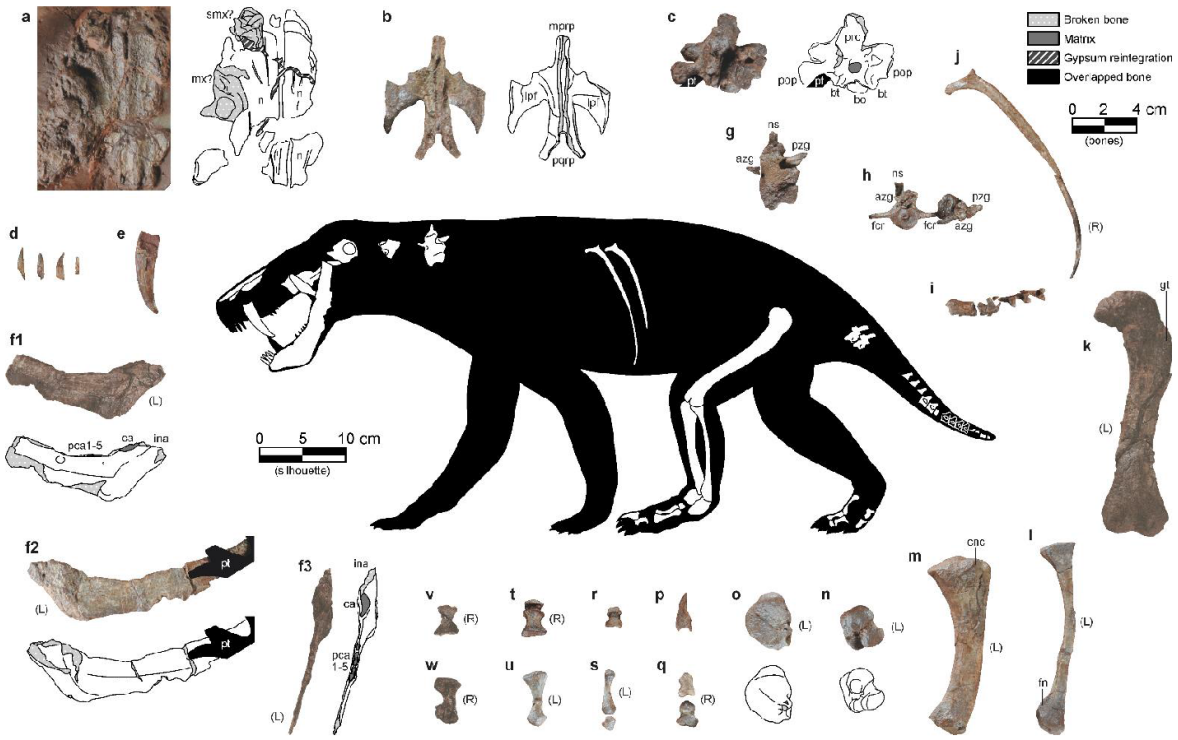

Figure 2. Most relevant elements of the specimen DA21/17-01-01 and silhouette showing their positions (see also **Supplementary Figures 2–6**). **a**: snout fragment, **b**: pterygoid, **c**: basicranium, **d**: incisors, **e**: canine, **f1-3**: left dentary, **g**: cervical? vertebra, **h**: proximal caudal vertebrae, **i**: distal caudal vertebrae, **j**: right dorsal rib, **k**: left femur, **l**: left fibula, **m**: left tibia, **n**: left astragalus, **o**: left calcaneum, **p**: ungual, **q**: right first metatarsal (below) and first phalanx of right digit I (above), **r**: penultimate phalanx, **s**: left third distal tarsal (below) and left third metatarsal (above), **t**: first (below) and second (above) phalanges of right digit IV, **u**: left fourth tarsal, **v**: first phalanx of right digit V, **w**: right fifth metatarsal. Abbreviations: azg = prezygapophysis, bo = basioccipital, bt = basal tuber, ca = alveolus of canine, cnc = cnemial crest, fcr = fused caudal ribs, ina = alveoli of incisors, lpf = lateral pterygoid flange, mprp = median palatal ramus of the pterygoid, mx = maxilla, n = nasal, ns = neural spine, pca = alveoli of postcanines, pop = paroccipital process (opisthotic), pqrp = pterygoid posterior quadrate rami, pro = prootic, pt = pterygoid, pzg = postzygapophysis, smx = septomaxilla, tp = transverse process, fn = fibular notch, gt = greater trochanter. (L) and (R) next to the elements refer to the left and right sides of the skeleton, respectively.

3. Discussion

A suite of characters clearly demonstrates that specimen DA21/17-01-01 represents a gorgonopsian therapsid. The dentary is characteristic for this clade, showing the combination of a steeply inclined mandibular symphysis, canine-postcanine diastema, relatively short postcanine tooth row, and anterodorsally-to-posteroventrally angled postcanine tooth row. Together, this combination of characters is only known in Gorgonopsia among Permian taxa. A steep mandibular symphysis is also present in anteosaurs (Kammerer, 2011) and some

biarmosuchians (*e.g.*, *Hipposaurus*; Sigogneau, 1970), but in these taxa no diastema exists between the lower canine and the (usually extensive) postcanine tooth row. In therocephalians, the symphysis is generally weak, with a low convex anterior face (van den Heever, 1994); this is also true of some biarmosuchians (*e.g.*, *Herpetoskylax*; Sidor & Rubidge, 2006). Anterodorsal-to-posteroventral angulation of the postcanine tooth row is typical of biarmosuchians and therocephalians in addition to gorgonopsians, but this character excludes identification as a dinocephalian or a non-therapsid synapsid ("pelycosaur"). Furthermore, the triangular anterodorsal projection housing the incisor tooth row is seen in almost all small gorgonopsians. The canine is mesiodistally serrated and extremely compressed (although this may be exaggerated by taphonomic distortion); this tooth is more circular in cross-section in other early synapsid groups with serrated canines (biarmosuchians, anteosaurs, and stemward therocephalians; also the caniniforms of some sphenacodontids). The pterygoid shows a backswept 'wing'-like morphology of the transverse processes, which is frequently observed in early gorgonopsians and differs strongly from the more robust-edged transverse processes of biarmosuchians and dinocephalians, which lack attenuate tips. Some early therocephalians also have backswept transverse processes of the pterygoid (*e.g.*, lycosuchids; van den Heever, 1994), but in therocephalians the ectopterygoid is located lateral to this process, such that there is not an anterior facet for the ectopterygoid as in DA21/17-01-01. The general morphology of the femur (sinuous with the head sharply offset from the shaft; low, rounded fourth trochanter; and greatly expanded distal end) is characteristically gorgonopsian, and the fibula and especially the tibia bow strongly away from one another (indicating a large interosseous space), a morphology unique to gorgonopsians among therapsids (Colbert, 1948).

Because of the incompleteness of this specimen, it is difficult to identify it more precisely than Gorgonopsia, especially considering the notorious morphological conservatism of this group. Some types of gorgonopsians can clearly be excluded as possibilities, however. The morphology of the pterygoids is unlike that of rubidgeines and related taxa (*e.g.*, *Arctops*), in which the transverse processes are generally swollen towards their tips and not backswept (Kammerer, 2016, 2017). The presence of five lower postcanines also excludes several rubidgeine taxa (*e.g.*, *Clelandina*, *Rubidgea*) as well as various others with absent (*e.g.*, *Inostrancevia*) or reduced (*e.g.*, *Eriphostoma*) lower postcanine tooth rows (Kammerer *et al.*, 2015). However, the same tooth count is known in, *e.g.*, *Aelurosaurus felinus* (Sigogneau, 1970). A variety of other features distinguish this specimen from rubidgeines and *Inostrancevia*, but these may be more size-related than strictly phylogenetic. For example, the inflected anterior face of the mandibular symphysis and the sinuous femoral shape differ from the straight, massive symphysis and nearly-straight femur of large gorgonopsians, but they are known in most small-bodied members of the clade regardless of relationships. Ontogenetic variation in these features is poorly understood, and whether they change with increasing in body size during the life of an individual is currently unknown. However, this specimen likely represents an osteologically mature individual, based on the extremely well-ossified limb and ankle elements and fused basicranium, so it does not seem to be a "giant" (skull length 40 cm or greater) species. Although the exact size of the animal is hard to determine given the paucity of elements and limited basis for postcranial comparisons in the group, based on dentary length, and assuming comparable proportions to *Gorgonops*, this individual would have had a skull length of ~18 cm.

Presence of a steep mandibular symphysis suggests that the specimen from Mallorca is more derived than the current earliest-diverging gorgonopsian, *Nochnitsa* (following the character polarity of Kammerer & Masyutin, 2018), but otherwise its cranial characters are generally plesiomorphic. The elongate, backswept transverse processes of the pterygoids are seen in *Eriphostoma*, *Gorgonops*, and *Cynariops* (Kammerer *et al.*, 2015; Bendel *et al.*, 2018) among African taxa, but also in the earlier-diverging *Viatkogorgon*, suggesting that this morphology may be ancestral for the major lineages of gorgonopsians. The relatively anterior position of divergence between the quadrate rami of the pterygoids is also observed in *Gorgonops*, *Scylacocephalus*, and *Cyonosaurus*, and the close proximity between the basal tubera and the occipital condyle is comparable to that of *Gorgonops*, *Suchogorgon*, and *Sauroctonus*. Overall, the gorgonopsian from Mallorca shows features most consistent with stemward members of the "African clade" (*sensu* Kammerer & Masyutin, 2018), but as these are plesiomorphic, it could also fall outside of this subclade (as either an early-diverging member of the "Russian clade", like *Suchogorgon*, or outside of the major divergence altogether, like *Viatkogorgon*).

Regarding its age, the bone-bearing beds containing the new gorgonopsian were argued to belong to the Artinskian or Kungurian stages of the Cisuralian series (lower Permian) by Matamales-Andreu *et al.* (2022), based on five lines of evidence. First, magnetostratigraphic analysis showed that the uppermost levels of the succession, 250 m stratigraphically above the bone-bearing levels, belong to the Kiaman Reverse Superchron, which dates to the middle Bashkirian to middle Wordian (early Pennsylvanian to middle Permian) (Aretz *et al.*, 2020; Henderson & Shen, 2020). This indicates that the gorgonopsian from Mallorca must at least be older than middle Wordian, and the considerable stratigraphic thickness between the top of the section and the fossil site (**Figure 1c**) suggests a much older age for the specimen because of the abundance of mudstones with carbonate palaeosols (Matamales-Andreu *et al.*, 2022), a type of rock with low sedimentation rates (Machette, 1985; Kraus, 1999). Second, palynoassemblages provided additional evidence for a Guadalupian (middle Permian) age for the uppermost part of the section (**Figure 1c**, **Supplementary Figure 1c**). Third, the tetrapod tracks and trackways located stratigraphically below and above the gorgonopsian site (**Figure 1c**) possess the typical components of Cisuralian ichnoassemblages elsewhere (**Supplementary Figure 1c**), including the ichnogenus *Dimetropus*, unknown from rocks younger than the Kungurian (upper part of the lower Permian) (Marchetti *et al.*, 2019a). Fourth, these ichnoassemblages lack the ichnogenera *Erpetopus* (middle Artinskian–middle Wuchiapingian) and *Brontopus* (Roadian–middle Capitanian), which commonly appear in mostly younger strata in palaeogeographically proximate basins (Gand & Durand, 2006; Marchetti *et al.*, 2019a, 2019b, 2022a). Fifth, "pelycosaur"-dominated ichnoassemblages, such as those from Mallorca, are typical of the Cisuralian worldwide, regardless of the sedimentary palaeoenvironment (Marchetti *et al.*, 2019a, 2022b).

All this said, the presence of a gorgonopsian is, in itself, at odds with the age attribution proposed by Matamales-Andreu *et al.* (2022). Gorgonopsians are unknown from deposits older than Guadalupian, with the oldest confirmed record being Wordian (Kammerer & Rubidge, 2022) (**Figure 1d**). Additionally, even though there is no record of the ichnogenus *Dimetropus* (purportedly produced by non-varanopid "pelycosaurs": Marchetti *et al.*, 2019b) after the Cisuralian, the Mezen assemblage of the Cis-Urals (upper Kungurian–middle Capitanian)

(Sennikov & Golubev, 2017), the San Angelo (lower Roadian) and Chickasha (Roadian–lower Wordian) formations of southern North America (Laurin & Hook, 2022), and the Cala del Vino Formation of Sardigna (Roadian) (Romano *et al.*, 2019) do contain definite "pelycosaur" body fossil records. Therefore, it would not be entirely unexpected for this ichnogenus to appear in at least part of the range of the Guadalupian as well (**Supplementary Figure 1c**). Nevertheless, the abundance of these tracks in the Port des Canonge Formation seems to be more typical of the upper part of the Cisuralian (Marchetti *et al.*, 2019a).

Based on the above arguments, the age of the gorgonopsian from Mallorca should be expressed in a possible range between the Artinskian (Cisuralian, lower Permian) and, perhaps, the lower half of the Wordian (Guadalupian, middle Permian) (**Figure 1d**). This places it among the oldest known gorgonopsians worldwide, only rivalled by an indeterminate gorgonopsian from the *Eodicynodon* Assemblage Zone of South Africa, dated as Wordian (Kammerer & Rubidge, 2022). As stated above, because the stratigraphic position of the specimen from Mallorca is 250 m below the last bed of the section, still part of the Kiaman Reverse Superchron (**Figure 1c**), it is probably older than Wordian, therefore making it the oldest record of gorgonopsians worldwide. By extension, the specimen from Mallorca is also among the oldest therapsids known, possibly older than *Raranimus*, from the Roadian of Asia (Duhamel *et al.*, 2021).

Currently, no definitive early Permian therapsids are known, despite the therapsid ghost lineage extending back to the Pennsylvanian (Angielczyk & Kammerer, 2018; Huttenlocker *et al.*, 2021). Although the unusual taxon *Tetraceratops* has at times been proposed to represent a therapsid (Laurin & Reisz, 1990, 1996; Amson & Laurin, 2011), debate continues as to whether it is actually a non-therapsid eupelycosaur (Spindler, 2020). No recognizable members of the major therapsid subclades (Biarmosuchia, Dinocephalia, Anomodontia, Gorgonopsia, Therocephalia, and Cynodontia) are known from the early Permian, so if the gorgonopsian from Mallorca does date to that time, it would pull the entire therapsid radiation (generally considered to have occurred explosively in the Guadalupian; see Kemp, 2006) back to at least the late part of the early Permian.

The new specimen has important implications for the origin and early palaeobiogeography of therapsids. Historically, the geographical sampling disjunction between low-palaeolatitude early Permian "pelycosaurs" and high-palaeolatitude middle–late Permian therapsids had raised questions about where the latter originated (Angielczyk & Kammerer, 2018) (**Figure 3**). Until the present work, the tropical therapsid record was extremely poor, with only fragmentary remains from central Africa (Smiley *et al.*, 2008), which were not very informative regarding the origin of the clade. The new specimen described herein confirms that therapsids, and more specifically, gorgonopsians, were indeed present at the palaeoequatorial latitudes of Pangaea since very early in their evolutionary history. Kemp (2006) hypothesised that the first therapsids evolved from sphenacodont "pelycosaurs" during the late part of the early Permian, acquiring a unique combination of traits that allowed them to expand into the more seasonally arid tropical biomes of the supercontinent. There, they would have persisted as medium-sized carnivores until the middle Permian, when the tropical and temperate biomes became connected, allowing therapsids to colonise higher latitudes. It would have been in these new areas where the clade diversified into the main groups classically known from the cis-Urals and south Africa.

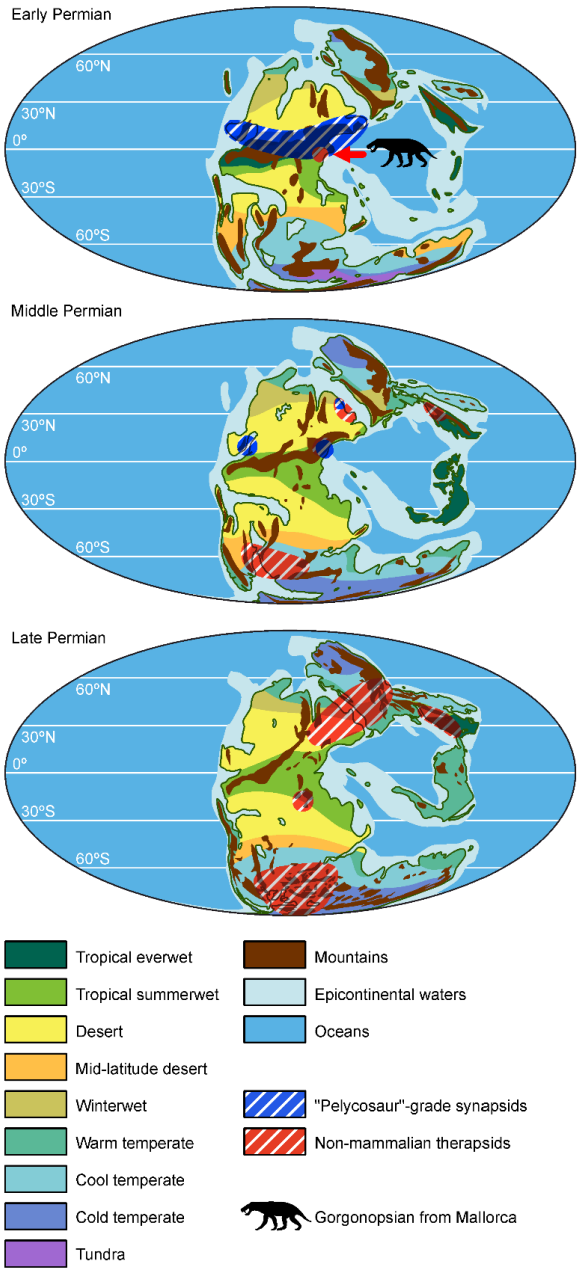

Figure 3. Palaeobiogeographical distribution of Permian synapsids (excluding varanopids) through time. Note a dominant tropical distribution of "pelycosaur"-grade synapsids during the early and early part of the middle Permian, and a trans-Pangaean distribution of non-mammalian therapsids during the middle and late Permian. The specimen studied herein has been displayed on the early Permian map because it is its most probable age, although it could also be from the earliest middle Permian. Maps after Scotese (2014), and climate zones after Rees *et al.* (2002) for the early and middle Permian, and Smith *et al.* (2015) for the late Permian. Synapsid distribution after Bernardi *et al.* (2017), Olroyd & Sidor (2017), Marchetti *et al.* (2019a), Romano *et al.* (2019) and Laurin & Hook (2022).

The gorgonopsian from Mallorca sheds new light on some of these uncertainties. First, it confirms that near the early–middle Permian transition, medium-sized carnivorous therapsids were indeed present in the summerwet biomes of equatorial Pangaea. Moreover, the fact that DA21/17-01-01 is clearly diagnosable as a gorgonopsian indicates that both the phylogenetic and morphological diversification of major therapsid clades was underway by the latest part of the early Permian–earliest part of the middle Permian. Therefore, and as Kemp (2006) hypothesised, it does appear that an important part of the early evolution of therapsids occurred in the tropical latitudes of Pangaea, which have not been well sampled to date. The new specimen clearly represents a specialized form that was probably the apex predator of the ecosystem based on the fossil track record of its locality (Matamales-Andreu *et al.*, 2022), which is dominated by moradisaurine captorhinids and small-sized "pelycosaur"-grade synapsids.

This new discovery underscores the need for more sampling in poorly studied areas of northern Africa and southern Europe that preserve Permian tropical ecosystems. Available data suggest that, at least during the late Permian, tropical tetrapod assemblages consisted of an 'atypical' mixture of classical middle–late Permian elements (pareiasaur parareptiles, therapsids) and relict groups otherwise widespread during the late Carboniferous and early Permian (cochleosaurid temnospondyls, diplocaulid lepospondyls, moradisaurine captorhinids) (de Ricqlès & Taquet, 1982; Jalil & Dutuit, 1996; Jalil & Janvier, 2005; Sidor *et al.*, 2005; Smiley *et al.*, 2008; Germain, 2010; Tsuji *et al.*, 2013). The assemblage from Mallorca is also unique but in a different sense, as in this case it shows a mixture of early Permian tetrapods ("pelycosaurs" and moradisaurine captorhinids) and a therapsid. These observations hint at a complex tetrapod palaeobiogeographical history in the tropical regions of Pangaea, with therapsids as one of their most notable components, that has not been studied in depth so far. In this context, the new fossil site from Mallorca represents a potentially key locality to help unravel the origin and early evolution of therapsids.

4. Conclusions

Here we have shown that gorgonopsian therapsids inhabited equatorial Pangaea during the early–?middle Permian. Specifically, the described remains are the first record for this clade in western Europe, and correspond to a medium-sized taxon. Several independent lines of evidence (palaeomagnetism, palynoassemblages and tetrapod ichnoassemblages) point to an upper Cisuralian/?lowermost Guadalupian (certainly lower than middle Wordian) stage for the beds containing it, implying that this specimen (**Figure 4**) is the oldest (albeit not most stemward) gorgonopsian worldwide. By extension, it can also be placed among the oldest therapsids, and it might represent the first early Permian therapsid worldwide. The new specimen shows that therapsids lived in the palaeoequator and had already undergone a significant degree of diversification and specialisation by, at most, the earliest part of the middle Permian. Therefore, the present work shows that lower and middle Permian sites of palaeoequatorial Pangaea have the potential to yield highly significant new specimens that help resolve the early evolution of therapsids, the group that ultimately gave rise to mammals.

Figure 4. Life reconstruction of the gorgonopsian from Mallorca in a floodplain setting. Created by Henry Sutherland Sharpe. © 2023 Henry Sutherland Sharpe. Used under license.

5. Acknowledgements

The authors of the present paper thank Sebastià Matamalas and Chabier De Jaime for aid in fieldwork. To Marina Rull and Xènia Aymerich (ICP, Cerdanyola del Vallès) for preparation of the specimen. To Enric Vicens (UAB, Cerdanyola del Vallès) for granting us access to the photographic equipment of the Palaeontology Unit of the UAB. To the Comissió Insular de Patrimoni Històric (Consell Insular de Mallorca) for granting us the excavation permits (file numbers 306/2019 and 75/2021) and funding for preparation (ref. 26 - 374/2020). R.M.A. was supported by the predoctoral grant FPU17/01922 (Ministerio de Ciencia, Innovación y Universidades) and the grant Synthesys+ DE-TAF-23 (European Commission). It has been further supported by the Generalitat de Catalunya (CERCA Programme and consolidated research groups 2021 SGR 01184 to J.F. and 2021 SGR 01192 to À.G.). This work is part of the Ramon y Cajal grant to J.F. [RYC2021-032857-I] financed by MCIN/AEI/10.13039/501100011033 and the European Union 'NextGenerationEU'/PRTR. We acknowledge support from the project "Mallorca abans dels dinosaures: estudi dels ecosistemes continentals del Permià i Triàsic amb especial èmfasi en les restes de vertebrats" (ref. 15 - 619/2020), based at the Institut Català de Paleontologia

Miquel Crusafont and funded by the Departament de Cultura, Patrimoni i Política Lingüística (Consell Insular de Mallorca).

6. References

Amson, E. & Laurin, M. (2011). On the affinities of *Tetraceratops insignis*, an Early Permian synapsid. *Acta Palaeontologica Polonica*, 56(2): 301–312.

Angielczyk, K. & Kammerer, C. (2018). Non-mammalian synapsids: the deep roots of the mammalian family tree. *In*: Zachos, F. & Asher, R. (Eds.). *Mammalian evolution, diversity and systematics*. De Gruyter; Berlin: 117–198.

Aretz, M.; Herbig, H.G. & Wang, X.D. (2020). Chapter 23 - The Carboniferous Period. *In*: Gradstein, F.M.; Ogg, J.G.; Schmitz, M.D. & Ogg, G.M. (Eds.). *Geologic Time Scale 2020*. Elsevier: 811–874.

Becq-Giraudon, J.-F.; Montenat, C. & Van Den Driessche, J. (1996). Hercynian high-altitude phenomena in the French Massif Central: tectonic implications. *Palaeogeography, Palaeoclimatology, Palaeoecology*, 122: 227–241.

Bendel, E.-M., Kammerer, C.F.; Kardjilov, N.; Fernandez, V. & Fröbisch, J. (2018). Cranial anatomy of the gorgonopsian *Cynariops robustus* based on CT-reconstruction. *PLoS ONE*, 13(11): e0207367.

Benson, R.B.J. (2012). Interrelationships of basal synapsids: cranial and postcranial morphological partitions suggest different topologies. *Journal of Systematic Palaeontology*, 10(4): 601–624.

Bernardi, M.; Petti, F.M., Kustatscher, E.; Franz, M.; Hartkopf-Fröder, C.; Labandeira, C.C.; Wappler, T.; van Konijnenburg-van Cittert, J.H.A.; Peecook, B.R. & Angielczyk, K.D. (2017). Late Permian (Lopingian) terrestrial ecosystems: A global comparison with new data from the low-latitude Bletterbach Biota. *Earth-Science Reviews*, 175: 18–43.

Brink, K.S.; Maddin, H.C.; Evans, D.C. & Reisz, R.R. (2015). Re-evaluation of the historic Canadian fossil *Bathygnathus borealis* from the Early Permian of Prince Edward Island. *Canadian Journal of Earth Sciences*, 52(12): 1109–1120.

Brocklehurst, N.; Ford, D.P. & Benson, R.B. (2022). Early origins of divergent patterns of morphological evolution on the mammal and reptile stem-lineages. *Systematic Biology*, 71(5): 1195–1209.

Broom, R. (1905). On the use of the term Anomodontia. *Records of the Albany Museum*, 1: 266–269.

Colbert, E.H. (1948). The mammal-like reptile *Lycaenops*. *Bulletin of the American Museum of Natural History*, 89(6): 353–404.

Didier, G. & Laurin, M. (2020). Exact distribution of divergence times from fossil ages and tree topologies. *Systematic Biology*, 69(6): 1068–1087.

Duhamel, A.; Benoit, J.; Rubidge, B.S & Liu, J. (2021). A re-assessment of the oldest therapsid *Raranimus* confirms its status as a basal member of the clade and fills Olson's gap. *The Science of Nature*, 108: 26.

Fröbisch, J.; Schoch, R.R.; Müller, J.; Schindler, T. & Schweiss, D. (2011). A new basal sphenacodontid synapsid from the Late Carboniferous of the Saar–Nahe Basin, Germany. *Acta Palaeontologica Polonica*, 56(1): 113–120.

Gand, G. & Durand, M. (2006). Tetrapod footprint ichno-associations from French Permian basins. Comparisons with other Euramerican ichnofaunas. *Geological Society, London, Special Publications*, 265: 157–177.

Glennie, K.W. (1972). Permian Rotliegendes of northwest Europe interpreted in light of modern desert sedimentation studies. *American Association of Petroleum Geologists Bulletin*, 56(6): 1048–1071.

Henderson, C.M. & Shen, S.Z. (2020). Chapter 24 - The Permian Period. *In*: Gradstein, F.M.; Ogg, J.G.; Schmitz, M.D. & Ogg, G.M. (Eds.). *Geologic Time Scale 2020*. Elsevier: 875–902.

Hopson, J.A. & Barghusen, H.R. (1986). An analysis of therapsid relationships. *In*: Hotton, N.; MacLean, P.D.; Roth, J.J. & Roth, E.C. (Eds.). *The ecology and biology of mammal-like reptiles*. Smithsonian Institution Press: 83–106.

Huttenlocker, A.H.; Singh, S.A.; Henrici, A.C. & Sumida, S.S. (2021). A Carboniferous synapsid with caniniform teeth and a reappraisal of mandibular size-shape heterodonty in the origin of mammals. *Royal Society Open Science*, 8: 211237.

Kammerer, C.F. (2011). Systematics of the Anteosauria (Therapsida: Dinocephalia). *Journal of Systematic Palaeontology*, 9(2): 261–304.

Kammerer, C.F. (2016). Systematics of the Rubidgeinae (Therapsida: Gorgonopsia). *PeerJ*, 4: e1608.

Kammerer, C.F. & Masyutin, V. (2018). Gorgonopsian therapsids (*Nochnitsa* gen. nov. and *Viatkogorgon*) from the Permian Kotelnich locality of Russia. *PeerJ*, 6: e4954.

Kammerer, C.F. & Rubidge, B.S. (2022). The earliest gorgonopsians from the Karoo Basin of South Africa. *Journal of African Earth Sciences*, 194: 104631.

Kammerer, C.F.; Smith, R.M.H.; Day, M.O. & Rubidge, B.S. (2015). New information on the morphology and stratigraphic range of the mid-Permian gorgonopsian *Eriphostoma microdon* Broom, 1911. *Papers in Palaeontology*, 1: 201–221.

Kemp, T.S. (2006). The origin and early radiation of the therapsid mammal-like reptiles: a palaeobiological hypothesis. *Journal of Evolutionary Biology*, 19(4): 1231–1247.

Kraus, M.J. (1999). Paleosols in clastic sedimentary rocks: their geologic applications. *Earth-Science Reviews*, 47: 41–70.

Laurin, M. & Hook, R.W. (2022). The age of North America's youngest Paleozoic continental vertebrates: a review of data from the Middle Permian Pease River (Texas) and El Reno (Oklahoma) Groups. *BSGF - Earth Sciences Bulletin*, 193: 10.

Laurin, M. & Reisz, R.R. (1990). *Tetraceratops* is the oldest known therapsid. *Nature*, 345: 249–250.

Laurin, M. & Reisz, R.R. (1996). The osteology and relationships of *Tetraceratops insignis*, the oldest known therapsid. *Journal of Vertebrate Paleontology*, 16(1): 95–102.

Liu, J. & Yang, W. (2022). A gorgonopsian from the Wutonggou Formation (Changhsingian, Permian) of Turpan Basin, Xinjiang, China. *Palaeoworld*, 31: 383–388.

Liu, J.; Rubidge, B. & Li, J. (2009). New basal synapsid supports Laurasian origin for therapsids. *Acta Palaeontologica Polonica*, 54(3): 393–400.

Machette, M.N. (1985). Calcic soils of the southwestern United States. *Geological Society of America, Special Papers*, 203: 1–21.

Marchetti, L.; Voigt, S.; Lucas, S.G.; Francischini, H.; Dentzien-Dias, P.; Sacchi, R.; Mangiacotti, M.; Scali, S.; Gazzola, A.; Ronchi, A. & Millhouse, A. (2019a). Tetrapod ichnotaxonomy in eolian paleoenvironments (Coconino and De Chelly formations, Arizona) and late Cisuralian (Permian) sauropsid radiation. *Earth-Science Reviews*, 190: 148–170.

Marchetti, L.; Klein, H.; Buchwitz, M.; Ronchi, A.; Smith, R.M.H.; De Klerk, W.J.; Sciscio, L. & Groenewald, G.H. (2019b). Permian-Triassic vertebrate footprints from South Africa: Ichnotaxonomy, producers and biostratigraphy through two major faunal crises. *Gondwana Research*, 72: 139–168.

Marchetti, L.; Logghe, A.; Mujal, E.; Barrieri, P.; Montenat, C.; Nel, A.; Pouillon, J.-M.; Garrouste, R. & Steyer, J.-S. (2022a). Vertebrate tracks from the Permian of Gonfaron (Provence, Southern France) and their implications for the late Capitanian terrestrial extinction event. *Palaeogeography, Palaeoclimatology, Palaeoecology*, 599: 111043.

Marchetti, L.; Forte, G.; Kustatscher, E.; DiMichele, W.A.; Lucas, S.G.; Roghi, G.; Juncal, M.A.; Hartkopf-Fröder, C.; Krainer, K.; Morelli, C. & Ronchi, A. (2022b). The Artinskian Warming Event: an Euramerican change in climate and the terrestrial biota during the early Permian. *Earth-Science Reviews*, 226: 103922.

Matamales-Andreu, R.; Mujal, E.; Dinarès-Turell, J.; Kustatscher, E.; Roghi, G.; Oms, O.; Galobart, À. & Fortuny, J. (2022). Early–middle Permian ecosystems of equatorial Pangaea: Integrated multi-stratigraphic and palaeontological review of the Permian of Mallorca (Balearic Islands, western Mediterranean). *Earth-Science Reviews*, 228: 103948.

Mujal, E.; Fortuny, J.; Pérez-Cano, J.; Dinarès-Turell, J. Ibáñez-Insa, J.; Oms, O.; Vila, I.; Bolet, A. & Anadón, P. (2017). Integrated multi-stratigraphic study of the Coll de Terrers late Permian–Early Triassic continental succession from the Catalan Pyrenees (NE Iberian Peninsula): A geologic reference record for equatorial Pangaea. *Global and Planetary Change*, 159: 46–60.

Nowak, H.; Vérard, C. & Kustatscher, E. (2020). Palaeophytogeographical patterns across the Permian–Triassic boundary. *Frontiers in Earth Science*, 8: 613350.

Olroyd, S.L. & Sidor, C.A. (2017). A review of the Guadalupian (middle Permian) global tetrapod fossil record. *Earth-Science Reviews*, 171: 583–597.

Osborn, H.F. (1903). On the primary division of the Reptilia into two sub-classes, Synapsida and Diapsida. *Science*, 17: 275–276.

Pfeifer, L.S.; Birkett, B.A.; Van Den Driessche, J.; Pochat, S. & Soreghan, G.S. (2021). Ice-crystal traces imply ephemeral freezing in early Permian equatorial Pangea. *Geology*, 49: 1397–1401.

Rees, P.M.; Ziegler, A.M.; Gibbs, M.T.; Kutzbach, J.E.; Behling, P.J. & Rowley, D.B. (2002). Permian phytogeographic patterns and climate data/model comparisons. *The Journal of Geology*, 110: 1–31.

Romano, M.; Citton, P.; Maganuco, S.; Sacchi, E.; Caratelli, M.; Ronchi, A. & Nicosia, U. (2019). New basal synapsid discovery at the Permian outcrop of Torre del Porticciolo (Alghero, Italy). *Geological Journal*, 54(3): 1554–1566.

Scotese, C.R. (2014). Atlas of Middle & Late Permian and Triassic Paleogeographic Maps, maps 43 – 48 from Volume 3 of the PALEOMAP Atlas for ArcGIS (Jurassic and Triassic) and maps 49 – 52 from Volume 4 of the PALEOMAP Atlas for ArcGIS (Late Paleozoic), Mollweide Projection, PALEOMAP Project, Evanston, IL.

Seeley, H.G. (1894). Researches on the structure, organisation, and classification of the fossil reptilia.—Part IX., Section 1. On the Therosuchia. *Philosophical Transactions of the Royal Society of London B*, 185: 987–1018.

Sennikov, A.G. & Golubev, V.K. (2017). Sequence of Permian tetrapod faunas of Eastern Europe and the Permian–Triassic ecological crisis. *Paleontological Journal*, 51(6): 600–611.

Sidor C.A. & Hopson J.A. (1998). Ghost lineages and "mammalness": assessing the temporal pattern of character acquisition in the Synapsida. *Paleobiology*, 24: 254–273.

Sidor, C.A. & Rubidge, B.S. (2006). *Herpetoskylax hopsoni*, a new biarmosuchian (Therapsida: Biarmosuchia) from the Beaufort Group of South Africa. *In*: Carrano, M.T.; Gaudin, T.J.; Blob, R.W. & Wible, J.R. (Eds.). *Amniote Paleobiology, prespectives on the evolution of mammals, birds and reptiles*. Chicago University Press: 76–113.

Sidor, C.A.; O'Keefe, F.R.; Damiani, R.; Steyer, J.S.; Smith, R.M.H.; Larsson, H.C.E.; Sereno, P.C.; Ide, O. & Maga, A. (2005). Permian tetrapods from the Sahara show climate-controlled endemism in Pangaea. *Nature*, 434: 886–889.

Sigogneau, D. (1970). *Révision systématique des gorgonopsiens sud-africains*. Centre National de la Recherche Scientifique; Paris. 417 pp.

Sigogneau-Russell, D. (1989). *Handbuch der Paläoherpetologie / Encyclopedia of Paleoherpetology. Teil 17 B/I / Part 17 B/I: Theriodontia I. Phthinosuchia, Biarmosuchia, Eotitanosuchia, Gorgonopsia*. Gustav Fischer Verlag; Stuttgart, New York. 127 pp.

Smiley, T.M.; Sidor, C.A.; Maga, A. & Ide, O. (2008). The vertebrate fauna of the upper Permian of Niger. VI. First evidence of a gorgonopsian therapsid. *Journal of Vertebrate Paleontology*, 28(2): 543–547.

Smith, R.M.H.; Sidor, C.A.; Tabor, N.J. & Steyer, J.S. (2015). Sedimentology and vertebrate taphonomy of the Moradi Formation of northern Niger: A Permian wet desert in the tropics of Pangaea. *Palaeogeography, Palaeoclimatology, Palaeoecology*, 440: 128–141.

Spindler, F. (2020). The skull of *Tetraceratops insignis* (Synapsida, Sphenacodontia). *Palaeovertebrata*, 43(1): 1–11.

van den Heever, J.A. (1994). The cranial anatomy of the early Therocephalia (Amniota: Therapsida). *Universiteit van Stellenbosch Annale*, 1: 1–59.

Supplementary Text 1: Material and methods

Specimen collection

The specimen DA21/17-01-01 was collected from the Torrent de na Nadala site (Port des Canonge Formation, Mallorca, Balearic Islands, western Mediterranean) (Matamales-Andreu *et al.*, 2022; **Figure 1a–c** of the main text). All the outcrops of this formation are located at the base of coastal cliffs in the northwestern margin of the Serra de Tramuntana, the main mountain range of the island, and have been interpreted as meandering river systems and associated floodplains deposited under a semi-arid, seasonal climate (Matamales-Andreu *et al.*, 2022). The horizon where the gorgonopsian fossil was collected (**Figure 1c** of the main text, **Supplementary Figure 1a–b**) consists of silty, very fine-grained, red sandstones with carbonate nodules and rhizocretions (indicating the formation of carbonate palaeosols), and fragments of coalified plant remains. Bones were scattered with no preferential orientation nor selection of elements (**Supplementary Figure 1b**), indicating a relatively prolonged exposure and a late stage of decay without (major) transportation of the remains (Behrensmeyer, 1978). In outcrop view, the fossil site corresponds to the infill of a depressed part of the floodplain, wedging laterally (see **Appendix 4** of the present dissertation). Considering this morphology, the very fine grain size, and the abundance of tetrapod bones (seven semi-complete, partially disarticulated adult and juvenile skeletons found so far), this deposit probably corresponded to a shrinking waterhole, similar to those grouped under the taphonomical class B1 of Smith *et al.* (2022). In the Karoo Basin of South Africa, waterhole deposits (corresponding to abandoned chute channels or floodplain depressions) contain abundant and well-preserved tetrapod skeletons that probably accumulated because of increased predation in such environments (Smith, 1993) and transportation of mummified carcasses by sheet flows (Smith *et al.*, 2022).

Collection and preparation was carried out with the permission of the *Comissió Insular de Patrimoni Històric* of the *Consell Insular de Mallorca* (excavations with file numbers 306/2019 and 75/2021, preparation with file numbers 374/2020 and 295/2021). The tetrapod bones are very brittle and were collected in the matrix and subsequently prepared using air scribes. The bones glow under UV light (wavelength of 365 nm), which made it possible to distinguish them from the surrounding matrix, which is usually of almost the same colour. The original material is housed at the *Museu de Mallorca* (Palma, Spain), and casts of all the elements have been deposited at the *Institut Català de Paleontologia Miquel Crusafont* (Sabadell, Spain).

Institutional abbreviations

AMNH FARB: American Museum of Natural History, Fossil Amphibian, Reptile, and Bird Collection, New York, U.S.A.

DA/21: Museu de Mallorca, Palma, Mallorca, Balearic Islands, Spain.

KPM: Vyatka Paleontological Museum, Kirov, Russia.

MB.R: Museum für Naturkunde, Berlin, Germany.

NHCC LB: National Heritage Conservation Commission, Lusaka, Zambia.

NHMUK PV R: The Natural History Museum, London, United Kingdom.

PIN: Paleontological Institute of the Russian Academy of Sciences, Moscow, Russia.

SAM-PK: Iziko South African Museum, Cape Town, South Africa.

Supplementary Text 2: Detailed description

Craniomandibular elements

Preserved definite cranial elements consist of a flattened portion of the snout roof, a partial basicranium, and a pterygoid. The snout portion (**Supplementary Figure 2a**) is largely made up of the paired nasals. Preservation of the snout is very poor, and because of crushing, it is difficult to even determine whether the exposed bone surface is external or internal. Based on the apparent presence of sculpturing on what is here interpreted as the anterior right nasal, it seems to be external, but this is not certain. The median suture between the nasals is slightly raised. A large semicircular element on the left side of the snout piece is interpreted as the left maxilla; its surface is extremely poorly preserved, but a rounded thickening near its anterior edge may represent the root of an upper canine. Another very poor section of bone is an amorphous mass at the anterolateral tip of the snout; based on position this could be part of the septomaxilla, but it is too incomplete to say anything about its morphology.

The pterygoid (**Supplementary Figure 2b**) is the best-preserved and most informative of the cranial elements. It is nearly complete, missing only the posterior tips of the quadrate rami and part of the anterior margin of the right transverse process. It is exposed in dorsal view, so it is uncertain whether the palatal bosses are preserved. Anteriorly, the pterygoid bears a short (1.7 cm from anterior tip to base of transverse process), attenuate process that would have fit between the palatines. The anterior tip is broken, so it is uncertain whether it would have extended to contact the vomer (inferred to be the plesiomorphic condition in gorgonopsians; see Kammerer & Masyutin, 2018) or whether such a contact was excluded by a midline suture of the palatines, as in most known gorgonopsians (Hopson & Barghusen, 1986; Sigogneau-Russell, 1989; but reconstructed as a synapomorphy of the "African clade" of Kammerer & Masyutin, 2018). The median septum of the pterygoids is preserved as a low (~0.4 cm dorsoventral height) ridge on the anterior process, which becomes taller (~1.0 cm) beginning at the anterior margin of the transverse process, but this likely reflects incomplete preservation, as this is still quite low compared to that observed in intact skulls (see, *e.g.*, Kemp, 1969; Bendel *et al.*, 2018). Lateral to the median septum, weak depressions are present, which expand anterolaterally towards the anterior margins of the transverse processes. Bounding these depressions laterally are weak ridges connecting the transverse processes to the quadrate rami. Posterior to the

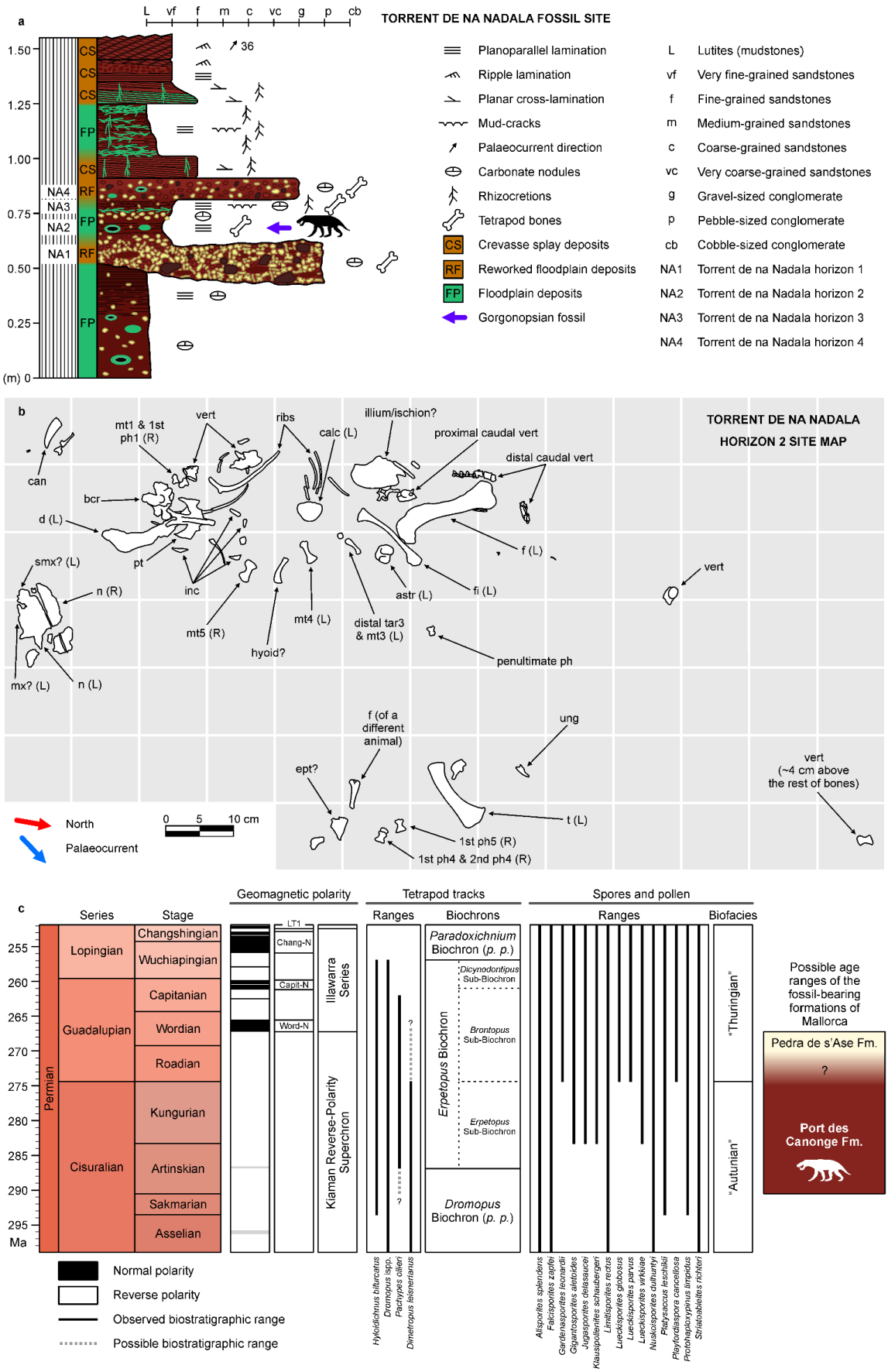
a
TORRENT DE NA NADALA FOSSIL SITE
L vf f m c vc g p cb
1.50
1.25
1.00
0.75
0.50
0.25
(m) 0
CS
FP
RF
NA4
NA3
NA2
NA1
36
Planoparallel lamination
Ripple lamination
Planar cross-lamination
Mud-cracks
Palaeocurrent direction
Carbonate nodules
Rhizocretions
Tetrapod bones
Crevasse splay deposits
Reworked floodplain deposits
Floodplain deposits
Gorgonopsian fossil
L Lutites (mudstones)
vf Very fine-grained sandstones
f Fine-grained sandstones
m Medium-grained sandstones
c Coarse-grained sandstones
vc Very coarse-grained sandstones
g Gravel-sized conglomerate
p Pebble-sized conglomerate
cb Cobble-sized conglomerate
NA1 Torrent de na Nadala horizon 1
NA2 Torrent de na Nadala horizon 2
NA3 Torrent de na Nadala horizon 3
NA4 Torrent de na Nadala horizon 4
b
TORRENT DE NA NADALA
HORIZON 2 SITE MAP
can
mt1 & 1st ph1 (R)
vert
ribs
calc (L)
illium/ischion?
proximal caudal vert
distal caudal vert
bcr
d (L)
pt
inc
smx? (L)
n (R)
mx? (L)
n (L)
mt5 (R)
hyoid?
mt4 (L)
distal tar3 & mt3 (L)
astr (L)
fi (L)
f (L)
penultimate ph
vert
f (of a different animal)
ung
ept?
t (L)
1st ph5 (R)
1st ph4 & 2nd ph4 (R)
vert (~4 cm above the rest of bones)
North
Palaeocurrent
0 5 10 cm
c
Series
Stage
Geomagnetic polarity
Tetrapod tracks
Spores and pollen
Ranges
Biochrons
Ranges
Biofacies
255
260
265
270
275
280
285
290
295
Ma
Permian
Lopingian
Guadalupian
Cisuralian
Changshingian
Wuchiapingian
Capitanian
Wordian
Roadian
Kungurian
Artinskian
Sakmarian
Asselian
LT1
Chang-N
Capit-N
Word-N
Illawarra Series
Kiaman Reverse-Polarity Superchron
Paradoxichnium Biochron (p. p.)
Dicynodontipus Sub-Biochron
Brontopus Sub-Biochron
Erpetopus Sub-Biochron
Erpetopus Biochron
Dromopus Biochron (p. p.)
"Thuringian"
"Autunian"
Possible age ranges of the fossil-bearing formations of Mallorca
Pedra de s'Ase Fm.
?
Port des Canonge Fm.
Normal polarity
Reverse polarity
Observed biostratigraphic range
Possible biostratigraphic range
Hyloidichnus bifurcatus
Dromopus ispp.
Pachypes cillieri
Dimetropus leisnerianus
Alisporites splendens
Falcisporites zapfei
Gardenasporites leonardii
Gigantosporites aletoides
Jugasporites delasaucei
Klausipollenites schaubergeri
Limitisporites rectus
Lueckisporites globosus
Lueckisporites parvus
Lueckisporites virkkiae
Nuskoisporites duthuntyi
Platysaccus leschikii
Playfordiaspora cancellosa
Protohaploxypinus limpidus
Striatoabieites richteri

Supplementary Figure 1. (previous page) Stratigraphy, site map and age attributions. **a:** Detailed stratigraphic log of the Torrent de na Nadala fossil site with indication of the lithology, palaeoenvironment and location of fossiliferous horizons, **b:** Site map of the Torrent de na Nadala horizon 2, with all the bones attributed to the gorgonopsian, **c:** Magneto- and biostratigraphic criteria used to date the Permian formations of Mallorca (modified from Matamales-Andreu *et al.*, 2022, with additional data from Marchetti *et al.*, 2022). Abbreviations: astr = astragalus, bcr = basicranium, calc = calcaneum, can = canine, d = dentary, ept = ectopterygoid, f = femur, fi = fibula, inc = incisor, (L) = left element, mt = metatarsal, mx = maxilla, n = nasal, ph = phalanx, pt = pterygoid, (R) = right element, smx = septomaxilla, t = tibia, tar = tarsal, ung = ungual, vert = vertebra.

median septum is a median facet that would have accommodated the parasphenoid, bounded on either side by weak ridges along the medial edges of the quadrate rami.

The transverse processes of the pterygoid are 'wing'-like, with extremely elongate, attenuate, backswept tips. These are unlike the pterygoids of rubidgeines (Kammerer, 2016) and related African gorgonopsians (*e.g.*, *Arctops;* Kammerer, 2017), in which the lateral edges are thickened, without extensive tapering. However, similar transverse processes are known in earlier-diverging taxa, such as *Cynariops* (Bendel *et al.*, 2018). The anterior margin of the transverse process bears a prominent notch (best preserved on the left side), which would have accommodated the ectopterygoid. The shape and position of this notch is extremely similar to that of *Cynariops* (Bendel *et al.*, 2018). The quadrate rami begin to diverge in a relatively anterior position in this specimen, at the level of the tips of the transverse processes. Generally in gorgonopsians, the quadrate rami diverge at a more posterior point on the basicranial girder (*e.g.*, Kemp, 1969; Kammerer, 2015, 2016, 2017; Bendel *et al.*, 2018). However, some early-diverging gorgonopsians such as *Eriphostoma* and *Gorgonops* show comparable proportions (see, *e.g.*, Kammerer *et al.*, 2015).

The basicranial element (**Supplementary Figure 2c**) consists of a fused complex composed minimally of basioccipital, opisthotic, and prootic (the exoccipitals are not exposed, but likely are also included in this complex). Fusion between these braincase elements is common (if not universal) in adult gorgonopsians (Sigogneau, 1970; Bendel *et al.*, 2018; but see Araújo *et al.*, 2017, for delimitations based on a supposed juvenile). The complex is exposed anteroventrally, with a large median cavity where the parabasisphenoid (or parasphenoid-basipresphenoid *sensu* Araújo *et al.*, 2017) would have attached. The basioccipital contributions to the basal tubera project posterolaterally. The articular facets that would have connected to the parabasisphenoid are exposed; these are mostly flat, but with a weak median ridge. This morphology of the basal tubera (with the bulbous contributions of the parabasisphenoid overlapping those of the basioccipital ventrally) is observed in many gorgonopsians. The occipital condyle is not fully exposed, but appears to be a single, reniform structure (1.7 cm in transverse width) as is typical of gorgonopsians, rather than the tripartite element of various other therapsid clades (*e.g.*, dinocephalians, anomodonts; King, 1988). The paroccipital process of the opisthotic is relatively short (1.6 cm in length). It is separated from the prootic by a gap of 0.4 cm.

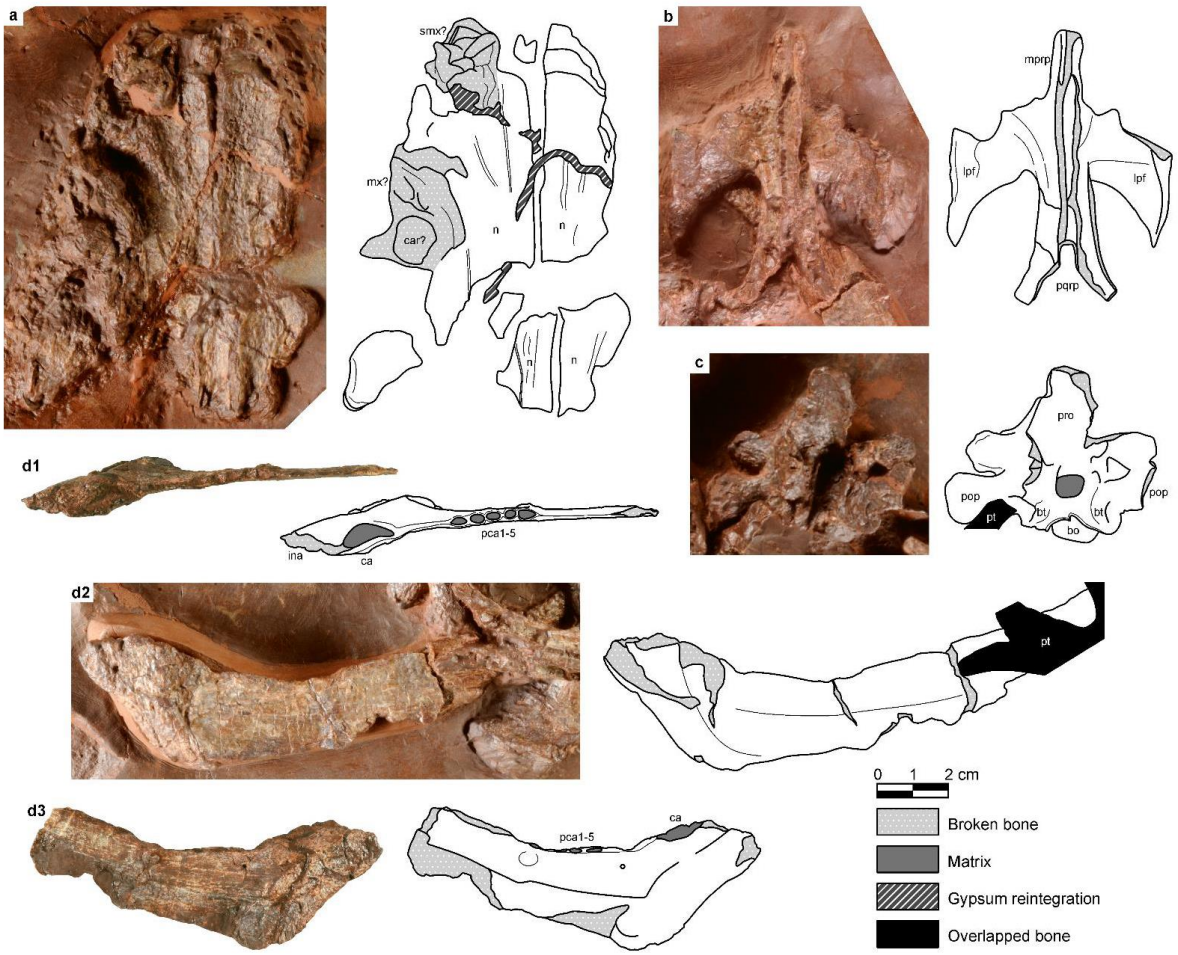

Supplementary Figure 2. Photographs and interpretative drawings of craniomandibular elements of the gorgonopsian from Mallorca. **a:** nasals and possible fragments of left maxilla and septomaxilla, dorsal view, **b:** pterygoid, dorsal view, **c:** basicranium, anterior view, **d1:** left dentary, dorsal view, **d2:** left dentary, labial view, **d3:** left dentary, lingual view. Abbreviations: bo = basioccipital, bt = basal tuber, ca = alveolus of canine, car = root of the canine, ina = alveoli of incisors, lpf = lateral pterygoid flange, mprp = median palatal ramus of the pterygoid, mx = maxilla, n = nasal, pca = alveoli of postcanines, pop = paroccipital process (opisthotic), pqrp = pterygoid posterior quadrate rami, pro = prootic, pt = pterygoid, smx = septomaxilla.

The only preserved mandibular element is the left dentary (**Supplementary Figure 2d1–d3**). The bone surface is poorly preserved; some sculpturing and possibly foramina appear to have been present on the external surface of the mandibular symphysis, but it is not possible to provide more specific details. The posterior portion of the dentary, including the coronoid process, is preserved beneath the pterygoid and thus is poorly exposed. What can be seen of the coronoid process demonstrates that it was weakly sloping, forming an angle of roughly 160° relative to the long axis of the dentary. Overall, the dentary is relatively elongate (visible preserved length 14.0 cm, with

symphyseal height 4.2 cm from ventral edge to anterior margin of canine alveolus, with ramus height 2.4 cm immediately anterior to pc1 and 2.0 cm immediately posterior to pc5). This morphology differs from that observed in *Aelurosaurus felinus* (NHMUK PV R339) and *Cynariops robustus* (MB.R.999; see Bendel *et al.*, 2018), where the dentary is anteroposteriorly shorter with a taller, more sharply sloping coronoid process in, but it is similar to the morphology present in many other gorgonopsians (*e.g.*, *"Delphaciognathus paucidens"*, AMNH FARB 5562; see Broom, 1915).

The dentary symphysis is angled roughly 120° relative to the long axis of the dentary. Its anterior face is concave in lateral view. This concavity is the result of an anterodorsal projection in front of the canine root that houses the incisors; otherwise, the symphysis sharply but evenly slopes posteroventrally-to-anterodorsally, creating the prominent mentum characteristic of gorgonopsians. This morphology (steep symphysis around the canine root, but inflecting anteriorly around the incisor roots) is present in almost all small gorgonopsians, with the apparent exception of the basal taxon *Nochnitsa* (the lack of an incisor inflection in this taxon is probably due to it having only a weakly sloping dentary symphysis to begin with, like that of basal therocephalians; Kammerer & Masyutin, 2018). In larger gorgonopsians, the symphysis is usually massive, with a straight, steeply sloping anterior face lacking an inflection point around the incisors (*e.g.*, in rubidgeines; Kammerer, 2016). An articular facet for the splenial is visible on the internal surface of the dentary. The splenial would have contributed to the base of the symphysis and was roughly half the height of the mandibular ramus (facet height 1.0 cm and total height of ramus 2.1 cm at level of pc3).

The incisor alveoli are poorly preserved, but the standard gorgonopsian count of four (Sigogneau, 1970) appears to be present. A single, large canine alveolus is present (1.6 cm in length, 0.5 cm maximum width). The canine root can be discerned in the form of a ridge along the side of the symphysis, immediately anterior to a dorsoventrally elongate depression that would have accommodated the upper canine. The postcanine tooth row is separated from the canine alveolus by a diastema (1.4 cm in length), as is usual for gorgonopsians. Five small (0.3 cm long and 0.2 cm wide) postcanine alveoli are present. The postcanine tooth row is angled anterodorsally-to-posteroventrally, such that the anteriormost tooth is also the most dorsally-positioned. This configuration of the dentary postcanine row is present in all gorgonopsians (with the exception of those lacking multiple postcanines), and is also usual for biarmosuchians (*e.g.*, *Ustia atra*, PIN 4548/155) and therocephalians (*e.g.*, *Glanosuchus macrops*, SAM-PK-11942). Five lower postcanines is a relatively high count for gorgonopsians, but equivalent counts are present in some taxa (*e.g.*, *Aelurosaurus felinus*, NHMUK PV R339), and greater numbers are known in others (*e.g.*, *Nochnitsa geminidens*, KPM 310, with six).

At least four small, isolated teeth (**Supplementary Figure 3a–d**) are scattered on the block adjacent to the craniomandibular elements. All appear to be incisors: they are elongate, very weakly recurved, and somewhat spatulate. No striations or facets are present on the enamel surface, but all are serrated, and where both mesial and distal carinae are visible, both show serrations. Given their count, size, and proximity to the dentary, it is possible that these teeth represent the left lower incisors, but this is speculation.

Supplementary Figure 3. Photographs and interpretative drawings of teeth of the gorgonopsian from Mallorca. **a–d:** possible incisors, **e:** possible upper canine. Colours and patterns as in **Supplementary Figure 2**.

A single isolated canine is preserved (**Supplementary Figure 3e**). Although roughly in the same area of the block as the craniomandibular elements, it was found much further from these bones than the incisors and is less likely to have originated in the left dentary (although this cannot be excluded as a possibility). The canine is weakly recurved and blade-like—laterally compressed with mesially and distally serrated edges. It is 1.5 cm wide at its base, and the length of the intact tooth is 4.4 cm (5.3 cm long if including the impression of an additional, missing portion). Serrations run 3.1 cm up the mesial edge of the tooth, suggesting that the entirety of the crown is preserved and the base of this element represents the start of the root. The serrations are very fine, four per millimetre on the better-exposed mesial carina. An indeterminate, splint-like fragment of bone is preserved close to (2.0 cm from) the canine.

A possible additional palatal element is preserved widely separated from the other craniomandibular bones, closer to the tibia. It is a broad, very poorly preserved bone bearing two ridges perpendicular to one another, which bound a depression covering most of its surface (**Supplementary Figure 4a**). If part of the skull, this could represent the ectopterygoid or a portion of the palatine (if exposed dorsally), but given the preservation of this element, precise identification is not possible. Near it is another mass of bone, which is an unidentifiable fragment. Another mysterious element is a small (~4.5 cm total length, tip broken off but impression of it present), weakly sinuous bone that may represent a hyoid (**Supplementary Figure 4b**). Hyoid elements have not been described in gorgonopsians, but are commonly preserved in therocephalians and cynodonts, where they are simple, slightly bowed rods. Alternatively,

this could represent a rib from the posterior portion of the dorsal series, near the sacrum. Although gorgonopsians do not have true lumbar ribs, their ribs do tend to become proportionally thicker and more curved towards the end of the series.

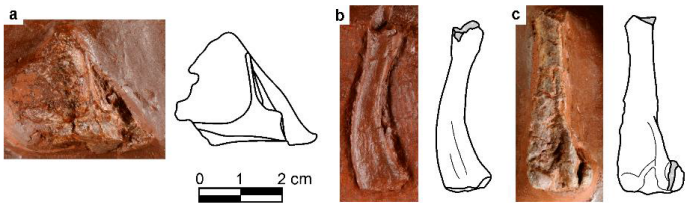

Supplementary Figure 4. Photographs and interpretative drawings of elements of the gorgonopsian from Mallorca with uncertain identifications, and an element of another animal associated with the studied skeleton. **a:** possible ectopterygoid, **b:** possible hyoid element or posterior dorsal rib, **c:** distal fragment of a small femur of another animal, posterior view. Colours and patterns as in **Supplementary Figure 2**.

Postcranial elements

Preserved axial elements are few, consisting of various isolated ribs and vertebrae plus a large section of the tail. Ten posterior caudal vertebrae are preserved (**Supplementary Figure 5a**), split into two articulated groups (the anterior consisting of six and the posterior of four) separated by a gap of 4.5 cm. When collected, this gap area, originally exposed on the outcrop, showed impressions of additional vertebrae, indicating that an additional three or four vertebrae would have been present. All of the articulated vertebrae are very small (0.7–0.9 cm in length) and the posteriormost ones would have been very close to the termination of the series. Tail length variation in Gorgonopsia is poorly understood due to limited material; in complete skeletons (*e.g.*, *Viatkogorgon ivakhnenkoi*, see Tatarinov, 2005), between 16 and 19 caudal vertebrae are present, suggesting that the majority of the tail is preserved in this specimen. Two more anterior caudals are preserved in isolation (**Supplementary Figure 5b**). The larger of the two (1.5 cm anterior centrum width, 1.1 cm centrum length) is nearly complete (missing only the neural spine) and bears large, posterolaterally oriented transverse processes. The smaller one (1.2 cm anterior centrum width, 1.0 cm centrum length) is more crushed, and only preserves a fragment of the right transverse process.

Adjacent to the cranial elements, two fragmentary, probable cervical vertebrae are preserved. The more complete of the two is exposed in left lateral view (**Supplementary Figure 5c**); it has suffered shear and most of the lateral face of the centrum is missing. Identification as a cervical is based on its proportions, it is relatively short and tall (centrum length 2.1 cm, height at anterior face 2.2 cm, height of vertebra at base of neural spine 3.4 cm). The neural spine and prezygapophyses are broken, but the right postzygapophysis is intact and shows that it was largely flat, but angled slightly dorsolaterally at its tip. The other vertebra is a fragment consisting mostly of the neural arch with prezygapophyses (**Supplementary Figure 5d**), preserved close to the basicranium. The prezygapophyses are close together, with flat articular facets that are weakly angled dorsolaterally.

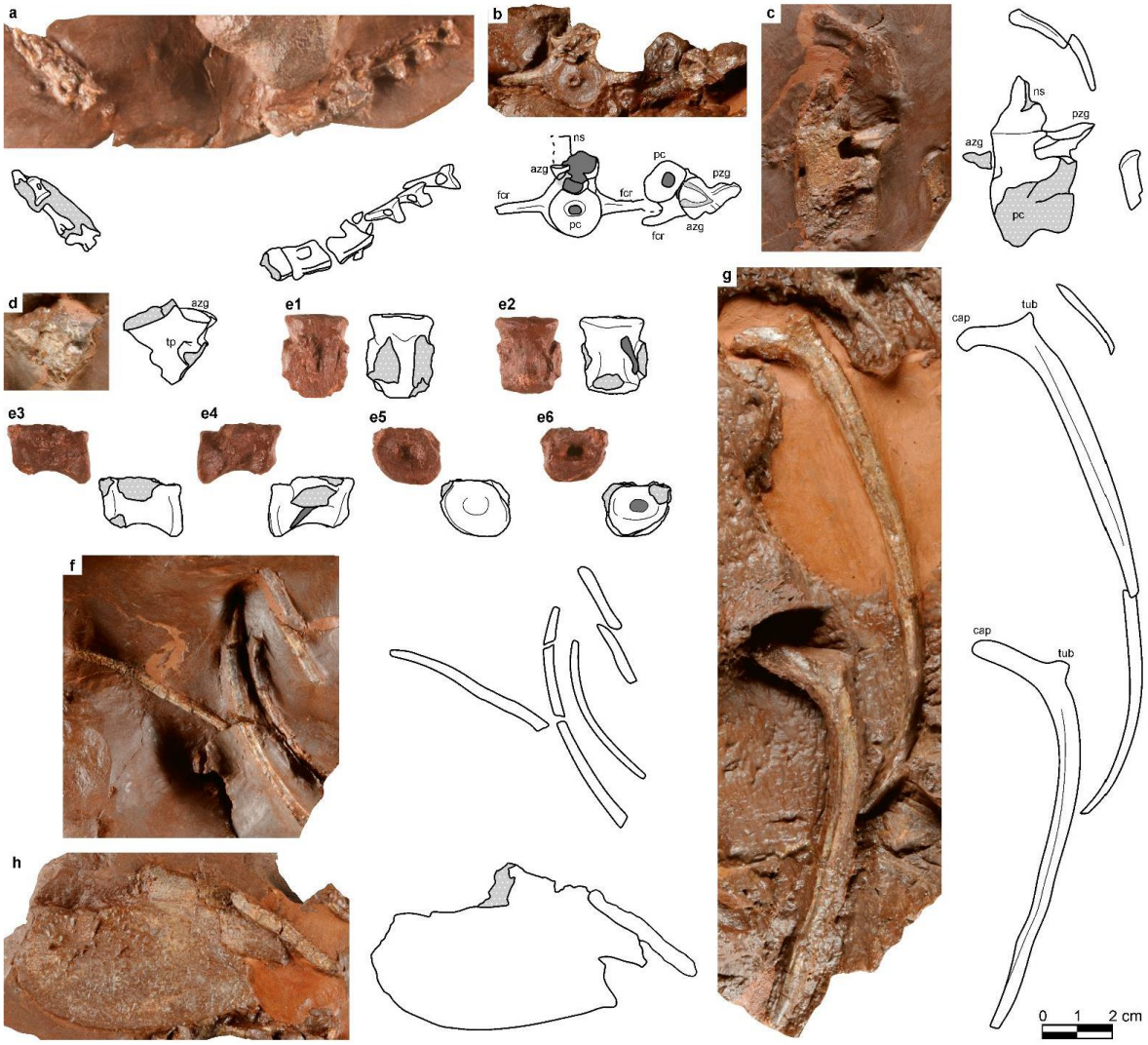

Supplementary Figure 5. Photographs and interpretative drawings of axial and possible girdle elements of the gorgonopsian from Mallorca. **a**: articulated distal caudal vertebrae, **b**: proximal caudal vertebrae, **c**: possible cervical vertebra and fragmentary ribs, **d**: possible cervical vertebral neural arch, **e1**: vertebral pleurocentrum, dorsal view, **e2**: vertebral pleurocentrum, ventral view, **e3**: vertebral pleurocentrum, right lateral view, **e4**: vertebral pleurocentrum, left lateral view, **e5**: vertebral pleurocentrum, anterior view, **e6**: vertebral pleurocentrum, posterior view, **f**: fragmentary ribs, **g**: right dorsal ribs, **h**: possible part of the pelvis (illium or ischion). Abbreviations: azg = prezygapophysis, cap = capitulum, fcr = fused caudal ribs, ns = neural spine, pc = pleurocentrum, pzg = postzygapophysis, tp = transverse process, tub = tubercle. Colours and patterns as in **Supplementary Figure 2**.

Two additional partial vertebrae, of uncertain position, were found widely separated from the other elements, and consist of a distorted centrum (**Supplementary Figure 5e1–e6**) and a badly damaged vertebral fragment (mostly centrum), with centrum lengths of 2.3 cm and 1.7 cm, respectively.

Two right dorsal ribs (**Supplementary Figure 5g**) are preserved on the underside of the block section containing the dentary, pterygoid, and basicranium. Both were complete as preserved, but one has had its tip split off through the original separation of the blocks. They have been exposed posterior side up. They are indistinguishable from those of other gorgonopsians (see, *e.g.*, Tatarinov, 2005; Gebauer, 2014), with bicipital heads and weakly curved bodies. The total length of the complete rib along its curvature is 17.5 cm. The tips of at least four additional ribs (**Supplementary Figure 5f**) are preserved near the tarsals and fibula.

Several well-preserved limb elements are present, but few, if any, girdle elements are preserved. A large (preserved dimensions 7.9 × 4.5 cm), laminar bone fragment near the caudal series probably represents part of the pelvic girdle (either the ilium or ischium) (**Supplementary Figure 5h**), but it is too incomplete and poorly preserved for definite identification.

The left femur has been prepared out in the round (**Supplementary Figure 6a1–a6**). It is 14.9 cm in total length. Proximally it is 3.9 cm wide, 2.0 cm at mid-length (5.0 cm circumference), and 4.1 cm wide distally. The head is well-ossified and not confluent with the greater trochanter, which is a low, curved structure extending 4.5 cm down the anterolateral margin of the shaft. The distal condyles are massive, but with shallow intertrochanteric and popliteal fossae. In general, this element is similar to that of other small-to-mid-sized gorgonopsians, showing sinuous curvature (Colbert, 1948; Sigogneau-Russell, 1989; Gebauer, 2014) as opposed to the more straight-shafted morphology in larger taxa (Sigogneau-Russell, 1989; Blob *et al.*, 2015).

The left fibula (**Supplementary Figure 6b**) was preserved disarticulated from but in contact with the femur. It is a very narrow, elongate element whose shaft is weakly bowed. The proximal and distal tips are greatly expanded where it would have articulated with the femur/tibia and tarsals, respectively. The proximal articular surface is convex, whereas the distal articular surface is nearly flat. The fibula is 11.5 cm in total length, and mediolaterally is 1.9 cm wide at its proximal end, 0.7 cm at wide at mid-length, and 2.0 cm wide at its distal end.

The left tibia is exposed in posterior view (**Supplementary Figure 6c**), and shows the typical gorgonopsian morphology (Colbert, 1948; Sigogneau-Russell, 1989; Gebauer, 2014), being robust and strongly bowed. The weak cnemial crest is visible at the anteromedial edge of the exposed bone. The tibia is 10.2 cm in total length, and mediolaterally is 3.8 cm wide at its proximal end, 1.7 cm wide at mid-length, and 2.3 cm wide at its distal end.

An additional element preserved in the same general area as the tibia appears to represent the distal half of another femur (**Supplementary Figure 4c**). However, this bone is much smaller (length of preserved portion 4.1 cm) than the other femur, with a much more gracile morphology. Identification as a femur is based on general shape and presence of well-ossified anterior and posterior trochanters at the inferred distal tip. This is the only element in the block that seems to belong to an individual other than the gorgonopsian. Damage to this bone makes taxonomic identification difficult, but it is consistent with the morphology of small reptiles (Romer, 1956).

A variety of pedal elements are scattered across the block; they represent a mixture of left and right elements, suggesting a complex history of disarticulation. Although incomplete, enough of the tarsals, metatarsals (mt), and

phalanges (ph) are preserved to recognise that this animal had a typical gorgonopsian pes (Sigogneau-Russell, 1989; Hopson, 1995; Sidor, 2022).

The only definitely preserved tarsal elements are the left calcaneum and astragalus. Both are typical for gorgonopsians, and previous descriptions of these elements (*e.g.*, Schaeffer, 1941; Colbert, 1948; Sidor, 2022) could also apply to this specimen. The calcaneum (**Supplementary Figure 6d**) has the standard primitive therapsid condition, being disc-shaped and notched medially. Its dimensions are 3.5 × 2.8 cm. The astragalus (**Supplementary Figure 6e**) is a multilobate element with bulbous surfaces for articulation with the tibia and fibula and a channel for the perforating artery. Its dimensions are 2.4 × 2.3 cm.

The metatarsal preserved closest to the craniomandibular elements has been prepared out in the round (**Supplementary Figure 6f1–f6**). It measures 2.8 cm in total length, and mediolaterally it is 1.6 cm wide at its proximal end, 0.7 cm wide at mid-length, and 1.5 cm wide at its distal end. It is very thin dorsoventrally (0.2 cm at mid-length), suggesting taphonomic compression. Considering the great degree of expansion of its proximal and distal ends, and their asymmetry, it is identified as the right mt5. In general morphology, it is similar to the equivalent element described in NHCC LB1073 by Sidor (2022), with dorsally oriented proximal and ventrally oriented distal articular facets, but it differs in some minor details. The proximal articular facets are more asymmetrical than in NHCC LB1073, with the medial portion wider (1.0 cm) than the lateral (0.5 cm). In proximal view, the surface is attenuate at both the medial and lateral edges (it is only attenuate laterally in NHCC LB1073), but the lateral portion is thicker, with the median ridge dividing the proximolateral portions into equal dorsal and ventral portions (in NHCC LB1073, the dorsal portion is dominant). Although these differences may be partially influenced by taphonomy, that is unlikely to explain all of them, particularly considering that the thicker proximal surface would seem to be opposite from the observed direction of compression for the rest of this element.

Two additional metatarsals were preserved in isolation closer to the femur/fibula, which are identified as the left mt4 and mt3. The mt4 (exposed ventral side up) (**Supplementary Figure 6g**) is the longest preserved metatarsal (total length 3.2 cm, mediolateral width of proximal end 1.0 cm, mid-length 0.5 cm, and distal end 1.5 cm). Its proximal end is notably more compact than in mt5, and it bears a dorsomedial facet for articulation with mt3. The mt3 (**Supplementary Figure 6h**) is preserved on its side; its identity is inferred from being morphologically nearly identical to that of the mt4, except smaller (total length 2.6 cm, other measures not possible to take precisely because of angle of exposure). Close (0.8 cm) to the proximal tip of mt3 is a small, cuboidal bone, which may represent the third distal tarsal (**Supplementary Figure 6h**).

Two pedal elements are preserved immediately adjacent to the basicranium, consisting of the right mt1 and ph1 of digit I (**Supplementary Figure 6i**). The metatarsal is 1.6 cm in total length, and mediolaterally it is 1.5 cm wide at its proximal end, 0.8 cm wide at mid-length, and 1.0 cm wide at its distal end. The phalanx is 1.3 cm in total length, and mediolaterally it is 1.0 cm wide at its proximal end, 0.5 cm wide at mid-length, and 0.8 cm wide at its distal end. Although disarticulated, these elements are still in contact, suggesting that disarticulation occurred late in the depositional history of the specimen, probably shortly before burial. Both are exposed ventrally, showing

the morphology of the distal articular facet of the metatarsal and proximal articular facet of the phalanx. The proximal articular facet of the metatarsal is not visible, indicating that it was dorsally oriented, as in other early synapsids (Kümmell & Frey, 2014). Unlike the other metatarsals, mt1 is short, thick, and highly asymmetrical, with an enlarged medial but reduced lateral lobe at its proximal end. The distal articular region is narrow and also asymmetrical, with the medial facet for articulation with the phalanx wider than the lateral. This asymmetry is reflected in the morphology of the distal portion of the phalanx: the medial condyle is mediolaterally broader and flatter, whereas the lateral condyle is shorter but more bulbous. The articular head of the phalanx bears a weak, distally-oriented protrusion, as in other gorgonopsians (Kümmell & Frey, 2012).

An additional three phalanges are preserved near the small femur. Two of these appear to represent ph1 and ph2 of the right digit IV, exposed dorsally (**Supplementary Figure 6j**). The second phalanx of this set is discoidal, indicating that these must be from digit III, IV, or V (Hopson, 1995). Ph1 is highly asymmetrical proximally, with a pointed expansion medially (ruling out digit III by comparison to other gorgonopsians; Sigogneau-Russell, 1989; Sidor, 2022). The phalanges of digits IV and V are difficult to distinguish in isolation, but the third phalanx preserved in this part of the block (see below) is more consistent with being the ph1 of digit V, because it is larger and more elongate. The proximal articular facet of the digit IV ph1 is dorsally oriented, with a ventrally expanded 'lip' (more prominent medially). The phalanx is roughly 'dumbbell'-shaped, but with the proximal expansions greater than the distal. The distal articular facet is ventrally oriented. The discoidal phalanx is only semi-disarticulated, exposing its proximal articular facet. This facet is weakly concave, with greater curvature laterally than medially, following the edge of the distal ph1. The ph1 is 1.7 cm in total length, and mesiodistally is 1.4 cm wide at its proximal end, 0.8 cm wide at mid-length, and 1.2 cm wide at its distal end. The discoidal ph2 is 0.2 cm long and 1.2 cm wide. The third phalanx (here interpreted as the ph1 of digit IV) (**Supplementary Figure 6k1–k6**) is very similar to the other ph1, but with slightly different proportions (1.9 cm total length, mediolateral width of proximal end 1.5 cm, 0.6 cm at mid-length, and 1.2 cm at distal end).

An additional dorsally-exposed phalanx (**Supplementary Figure 6l**) is preserved in an isolated position roughly equidistant between the tibia and femur. Based on size and general morphology, it is definitely a penultimate phalanx, but its digital identity is uncertain; for digits III–V these phalanges are very difficult to distinguish in isolation. Like the other non-discoidal phalanges it is a 'dumbbell'-shaped element that is broader proximally than distally (total length 1.2 cm, mediolateral width 1.1 cm distally, 0.6 cm at mid-length, and 0.8 cm distally). At its proximal end, it has an expanded lateral lobe protruding proximally; its distal end is trapezoidal, with a broad trochlea for articulation with the ungual.

A single ungual phalanx (**Supplementary Figure 6m**) is preserved on the underside of the block containing the tibia. Known gorgonopsian unguals are generally conservative in morphology, and it is consistent with previously described examples (e.g., Sidor, 2022). The articular facet is prominently cupped, and a well-developed flexor tubercle is visible on the exposed proximoventral portion of the bone. The ungual is elongate and only weakly curved (ungual tip extends at an angle of roughly 20° from the dorsal and ventral edges of the articular facet).

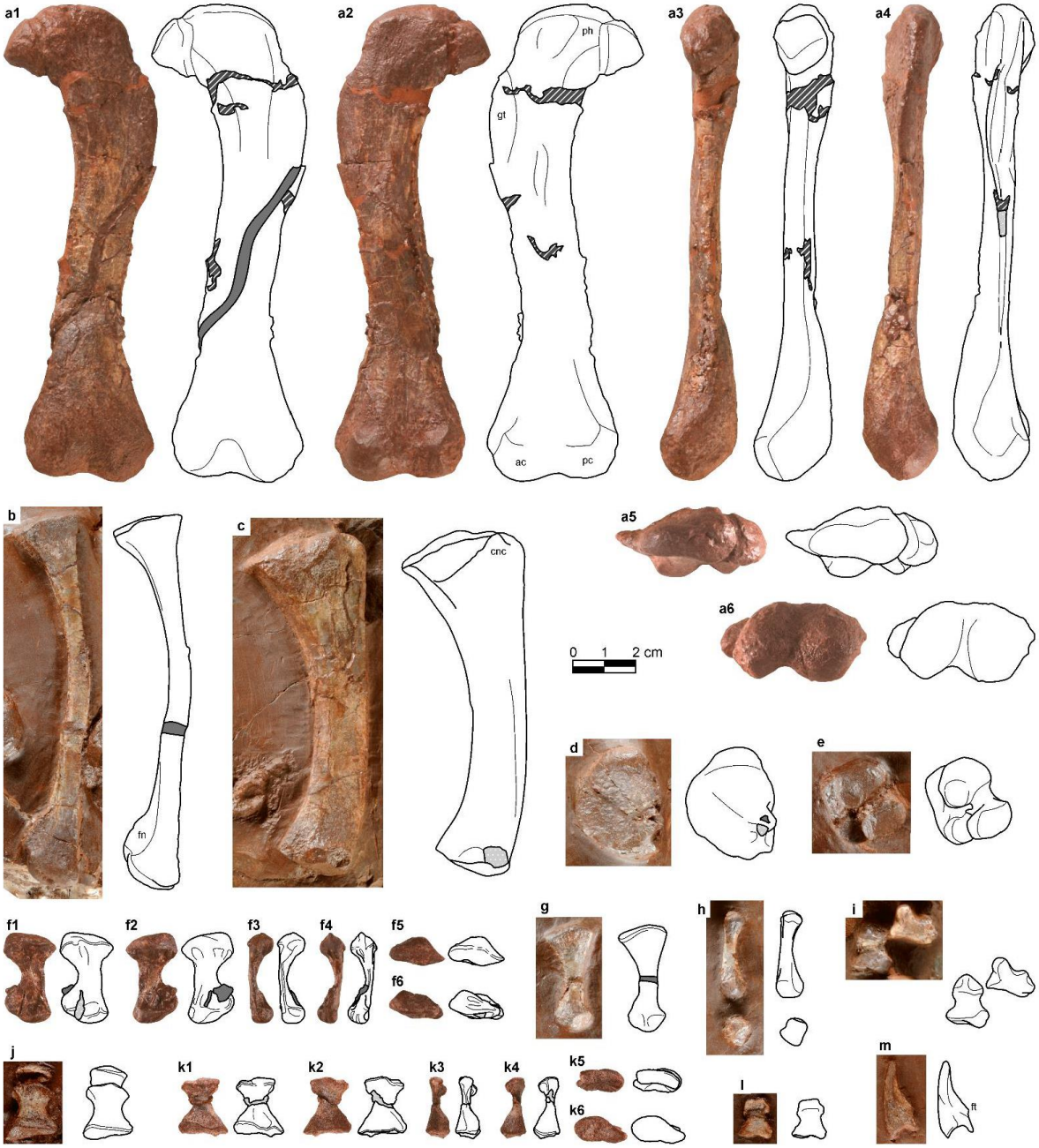

Supplementary Figure 6. Photographs and interpretative drawings of hindlimb and pedal elements of the gorgonopsian from Mallorca. **a1**: left femur, anterior view, **a2**: left femur, posterior view, **a3**: left femur, medial view, **a4**: left femur, lateral view, **a5**: left femur, proximal view, **a6**: left femur, distal view, **b**: left fibula, anterior view, **c**: left tibia, posterior view, **d**: left calcaneum, dorsal view, **e**: left astragalus, dorsal view, **f1**: right fifth metatarsal, dorsal view, **f2**: right fifth metatarsal, ventral view, **f3**: right fifth metatarsal, lateral view, **f4**: right fifth metatarsal, medial view, **f5**: right fifth metatarsal, distal view, **f6**: right fifth metatarsal, proximal view, **g**: left fourth metatarsal, ventral view, **h**: left third distal tarsal and left third metatarsal, lateral view, **i**: right first metatarsal and first phalanx of right digit I, ventral view, **j**: first and second phalanges of right digit IV, dorsal view, **k1**: first phalanx

of right digit V, dorsal view, **k2:** first phalanx of right digit V, ventral view, **k3:** first phalanx of right digit V, lateral view, **k4:** first phalanx of right digit V, medial view, **k5:** first phalanx of right digit V, distal view, **k6:** first phalanx of right digit V, proximal view, **l:** penultimate phalanx, dorsal view, **m:** ungual (terminal phalanx), lateral or medial view. Abbreviations: ac = anterior condyle, cnc = cnemial crest, fn = fibular notch, ft = flexor tubercle, gt = greater trochanter, pc = posterior condyle, ph = proximal head of femur. Colours and patterns as in **Supplementary Figure 2**.

Supplementary References

Araújo, R.; Fernandez, V.; Polcyn, M.J.; Fröbisch, J. & Martins, R.M.S. (2017). Aspects of gorgonopsian paleobiology and evolution: insights from the basicranium, occiput, osseous labyrinth, vasculature, and neuroanatomy. *PeerJ*, 5: e3119.

Behrensmeyer, A.K. (1978). Taphonomic and ecologic information from bone weathering. *Paleobiology*, 4(2): 150–162.

Bendel, E.-M.; Kammerer, C.F.; Kardjilov, N.; Fernandez, V. & Fröbisch, J. (2018). Cranial anatomy of the gorgonopsian *Cynariops robustus* based on CT-reconstruction. *PLoS ONE*, 13(11): e0207367.

Blob, R.W.; Huttenlocker, A.K.; Kammerer, C.F. & Sidor, C.A. (2015). Comparative allometry of femoral curvature in gorgonopsian versus therocephalian therapsids. *In*: Meeting Program and Abstracts, SVP 75th Annual Meeting, Society of Vertebrate Paleontology: p. 91.

Broom, R. (1915). Catalogue of types and figured specimens of fossil vertebrates in the American Museum of Natural History; ii Permian, Triassic and Jurassic reptiles of South Africa. *Bulletin of the American Museum of Natural History*, 25: 105–164.

Colbert, E.H. (1948). The mammal-like reptile *Lycaenops*. *Bulletin of the American Museum of Natural History*, 89(6): 353–404.

Gebauer, E.V.I. (2014). Re-assessment of the taxonomic position of the specimen GPIT/RE/7113 (*Sauroctonus parringtoni* comb. nov., Gorgonopsia). *In*: Kammerer, C.F.; Angielczyk, K.D. & Fröbisch, J. (Eds.). *Early Evolutionary History of the Synapsida*. Springer; Dordrecht, Heidelberg, New York, London: 185–207.

Hopson, J.A. (1995). Patterns of evolution in the manus and pes of non-mammalian therapsids. *Journal of Vertebrate Paleontology*, 15(3): 615–639.

Hopson, J.A. & Barghusen, H.B. (1986). An analysis of therapsid relationships. *In*: Hotton, N. III; MacLean, P.D.; Roth, J.J. & Roth, E.C. (Eds.). *The Ecology and Biology of the Mammal-Like Reptiles*. Smithsonian Institution Press; Washington, D.C: 83–106.

Kammerer, C.F. (2015). Cranial osteology of *Arctognathus curvimola*, a short-snouted gorgonopsian from the Late Permian of South Africa. *Papers in Palaeontology*, 1(1): 41–58.

Kammerer, C.F. (2016). Systematics of the Rubidgeinae (Therapsida: Gorgonopsia). *PeerJ*, 4: e1608.

Kammerer, C.F. (2017). Anatomy and relationships of the South African gorgonopsian *Arctops* (Therapsida, Theriodontia). *Papers in Palaeontology*, 3: 583–611.

Kammerer, C.F. & Masyutin, V. (2018). Gorgonopsian therapsids (*Nochnitsa* gen. nov. and *Viatkogorgon*) from the Permian Kotelnich locality of Russia. *PeerJ*, 6: e4954.

Kammerer, C.F.; Smith, R.M.H.; Day, M.O. & Rubidge, B.S. (2015). New information on the morphology and stratigraphic range of the mid-Permian gorgonopsian *Eriphostoma microdon* Broom, 1911. *Papers in Palaeontology*, 1(1): 201–221.

Kemp, T.S. (1969). On the functional morphology of the gorgonopsid skull. *Philosophical Transactions of the Royal Society B*, 256(801): 1–83.

King, G.M. (1988). *Handbuch der Paläoherpetologie / Encyclopedia of Paleoherpetology. Teil 17C / Part 17C: Anomodontia*. Gustav Fischer Verlag; Stuttgart, New York. 174 pp.

Kümmell, S.B. & Frey, E. (2012). Digital arcade in the autopodia of Synapsida: Standard position of the digits and dorsoventral excursion angle of digital joints in the rays II–V. *Palaeobiodiversity and Palaeoenvironments*, 92(2): 171–196

Kümmell, S.B. & Frey, E. (2014). Range of movement in ray I of manus and pes and the prehensility of the autopodia in early Permian to Late Cretaceous non-anomodont Synapsida. *PLoS One*, 9: e113911.

Marchetti, L.; Logghe, A.; Mujal, E.; Barrier, P.; Montenat, C.; Nel, A.; Pouillon, J.-M.; Garrouste, R. & Steyer, J.S. (2022). Vertebrate tracks from the Permian of Gonfaron (Provence, Southern France) and their implications for the late Capitanian terrestrial extinction event. *Palaeogeography, Palaeoclimatology, Palaeoecology*, 599: 111043.

Matamales-Andreu, R.; Mujal, E.; Dinarès-Turell, J.; Kustatscher, E.; Roghi, G.; Oms, O.; Galobart, À. & Fortuny, J. (2022). Early–middle Permian ecosystems of equatorial Pangaea: Integrated multi-stratigraphic and palaeontological review of the Permian of Mallorca (Balearic Islands, western Mediterranean). *Earth-Science Reviews*, 228: 103948.

Romer, A.S. (1956). *Osteology of the Reptiles*. University of Chicago Press; Chicago, London. 772 pp.

Schaeffer, B. (1941). The morphological and functional evolution of the tarsus in amphibians and reptiles. *Bulletin of the American Museum of Natural History*, 78: 395–472.

Sidor, C.A. (2022). New information on gorgonopsian pedal morphology based on articulated material from Zambia. *Journal of African Earth Sciences*, 191: 104533.

Sigogneau, D. (1970). *Révision systématique des gorgonopsiens sud-africains*. Centre National de la Recherche Scientifique; Paris. 417 pp.

Sigogneau-Russell, D. (1989). *Handbuch der Paläoherpetologie / Encyclopedia of Paleoherpetology. Teil 17B/I / Part 17B/I: Theriodontia I. Phthinosuchia, Biarmosuchia, Eotitanosuchia, Gorgonopsia*. Gustav Fischer Verlag; Stuttgart, New York. 127 pp.

Smith, R.M.H. (1993). Vertebrate taphonomy of late Permian floodplain deposits in the southwestern Karoo Basin of South Africa. *Palaios*, 8: 45–67.

Smith, R.M.H.; Botha, J. & Viglietti, P.A. (2022). Taphonomy of drought afflicted tetrapods in the Early Triassic Karoo Basin, South Africa. *Palaeogeography, Palaeoclimatology, Palaeoecology*, 604: 111207.

Tatarinov, L.P. (2005). A postcranial skeleton of the gorgonopian *Viatkogorgon ivachnenkoi* (Reptilia, Theriodontia) from the Upper Permian Kotelnich locality, Kirov Region. *Paleontological Journal*, 38: 437–447.

Appendix 6

Permian gorgonopsian tracks from Mallorca

Appendix 6 was prepared as:

Matamales-Andreu, R.; Mujal, E.; Galobart, À. & Fortuny, J. (in preparation). Track-trackmaker correlation of co-occurring gorgonopsian bones and footprints from the Permian of equatorial Pangaea.

In this work, R. Matamales-Andreu contributed in:

A. Logging of the stratigraphic section.
B. Co-direction of all fieldwork campaigns (prospections and excavations). Sampling of tetrapod tracks.
C. 3D modelling of tetrapod tracks and trackways.
D. Stratigraphic and sedimentological analysis.
E. Interpretation and discussion of the results.
F. Collaboration in writing of the original draft except for the section Systematic Palaeoichnology and part of the Discussion.
G. Preparation of figure 1.
H. Collaboration in obtaining funding for fieldwork and fossil preparation.

Track-trackmaker correlation of co-occurring gorgonopsian bones and footprints from the Permian of equatorial Pangaea

Rafel Matamales-Andreu[1,2]‡, Eudald Mujal[3,2]*‡, Àngel Galobart[2,4], Josep Fortuny[2]

[1] Museu Balear de Ciències Naturals, FJBS-MBCN, ctra. Palma-Port de Sóller km 30.5, 07100 Sóller, Mallorca, Illes Balears, Spain.

[2] Institut Català de Paleontologia Miquel Crusafont, Universitat Autònoma de Barcelona, Edifici ICTA-ICP, c/ Columnes s/n, Campus de la UAB, 08193 Cerdanyola del Vallès, Barcelona, Catalunya, Spain.

[3] Staatliches Museum für Naturkunde Stuttgart, Rosenstein 1, 70191 Stuttgart, Germany.

[4] Museu de la Conca Dellà, c/ del Museu 4, 25650 Isona i Conca Dellà, Lleida, Catalunya, Spain.

*Corresponding author: eudald.mujalgrane@smns-bw.de

‡ These authors contributed equally to this paper.

Abstract

Therapsids are a group of terrestrial tetrapods that gave rise to mammals during the Triassic. The oldest confirmed record of this group dates to the Permian, showing the acquisition of a suite of morphological traits that resulted in substantial physiological changes, drifting away from the "reptilian" body plan. One of these modifications affected the girdle and limb joint anatomy and had a profound impact on posture, and, by extension, locomotion. Therefore, trackways can be used as a fairly reliable proxy to track down the mode and tempo of those changes. However, references to lower/middle Permian tracks attributed to therapsids are still scarce in the literature. Here we report a new ichnotaxon from the palaeoequatorial lower/?middle Permian of Mallorca (western Mediterranean), correlating it to gorgonopsian trackmakers. This is because the pes tracks match almost exactly, in terms of size and proportions, with the gorgonopsian body fossils found in the same section and formation. The narrow gauge and the wide values of pace angulation of the studied trackways suggest an upright posture with a parasagittal mode of locomotion. These results shed light on the palaeoequatorial tetrapod communities and their importance in the diversification of early therapsids, as well as on the evolution of locomotion in this group, showing that modifications that would result in the "mammalian" gait were already underway by the lower/?middle Permian.

Keywords: western Mediterranean, Mallorca, Therapsida, Gorgonopsia, Ichnology, Functional prevalence

1. Introduction

Gorgonopsians were a group of sabre-toothed, predatory therapsids that became key components of the Lopingian terrestrial ecosystems, replacing dinocephalian and large therocephalian therapsids as top predators after the Guadalupian (Sigogneau-Russell, 1989; Day *et al.*, 2015; Kammerer, 2016; Day & Rubidge, 2021; Kammerer & Rubidge, 2022). The origin of the group dates back, probably, to the late Cisuralian (Kammerer & Rubidge, 2022; **Appendix 5** of the present dissertation), disappearing at the end of the Permian (Ward *et al.*, 2005). Their fossil record presents a mostly disjunct distribution, occurring in high palaeolatitudes of the northern (*e.g.*, Tatarinov, 1974; Ivakhnenko, 2003; Liu & Yang, 2022) and southern (*e.g.*, Sigogneau, 1970; Smith *et al.*, 2020) hemispheres. Only the palaeoequatorial floodplains of Mallorca (western Mediterranean) (Matamales-Andreu *et al.*, 2022; **Appendix 5** of the present dissertation) and the palaeotropical "wet desert" of Moradi (central Africa) (Smiley *et al.*, 2008; Smith *et al.*, 2015) have produced low-latitude gorgonopsians, demonstrating a trans-Pangaean distribution for this group. Still, separation of most gorgonopsians into two greater monophyletic clades ("Russian clade" and "African clade": Kammerer & Masyutin, 2018) may suggest their dispersion potential decreased after their initial dispersal event.

So far, footprints attributed to gorgonopsians have been reported from South Africa (Marchetti *et al.*, 2019a) and perhaps from Uruguay as well (Piñeiro *et al.*, 2022). In South Africa, tracks attributed to gorgonopsians were found in the uppermost *Tapinocephalus* to uppermost *Pristerognathus* assemblage zones (uppermost Guadalupian), and assigned to the ichnotaxon *Karoopes gansfonteinensis* (Marchetti *et al.*, 2019a). It corresponds to medium to large, pentadactyl, weakly ectaxonic, semiplantigrade/digitigrade tracks with curved digits and with the lateral side relatively deeper, indicating a lateral functional prevalence of autopodia (Mujal *et al.*, 2020). The trackways show homopody and very high pace angulation values (Marchetti *et al.*, 2019a). The track material from the Guadalupian–Lopingian of Uruguay is, at present, much scarcer, corresponding to large, pentadactyl, ectaxonic tracks with curved digits that have been doubtfully identified as cf. *Karoopes* by Piñeiro *et al.* (2022). Ichnites correlated to gorgonopsians represent a small fraction of the relatively diverse record of therapsid (and more generally synapsid) tracks and trackways (Marchetti *et al.*, 2019a); however, they are relevant to understand the evolution of the locomotion of therapsids, because their trackways are usually narrow, with long strides and high pace angulations, differing from trackways attributed to other Permian synapsids (Marchetti *et al.*, 2019a).

Recent fieldwork on Mallorca (Balearic Islands) has discovered rich Permian tetrapod assemblages consisting of both tracks and bone remains (Matamales-Andreu *et al.*, 2021, 2022; **Appendices 4** and **5** of the present dissertation). Among those, stands out the discovery of body fossils belonging to the first unequivocal gorgonopsian from equatorial Pangaea, possibly the oldest of its clade worldwide (**Appendix 5** of the present dissertation). Some mysterious tetrapod tracks and trackways (identified as "indeterminate synapsid tracks" by Matamales-Andreu *et al.*, 2022) were found 46 m stratigraphically above the bones, still in the Port des Canonge Formation. The present contribution describes those footprints, potentially identifying them as a new ichnotaxon, and, by means of an analysis of their morphology and arrangement, attributes them to the clade Gorgonopsia. In the light of the track-trackmaker correlation, this work aims to contribute to the understanding of the locomotion of early therapsids.

2. Geographical and geological context

2.1. General context

Mallorca is the largest of the Balearic Islands, an archipelago located at the western Mediterranean. Permian outcrops appear in the lowermost tectonic unit of the Serra de Tramuntana, the main mountain range of the island (**Figure 1A**). They have been recently divided into three formal lithostratigraphic units (Matamales-Andreu *et al.*, 2022), from lower to upper: Bec de s'Àguila Formation, corresponding to alluvial fans and high-energy meandering river deposits, Port des Canonge Formation, interpreted as the deposits of low-energy meandering rivers and floodplains, and Pedra de s'Ase Formation, representing high-energy meandering river, sheetflood and floodplain deposits (Matamales-Andreu *et al.*, 2022). Among those, the most fossiliferous is the Port des Canonge Formation, dated in a possible range between the upper Cisuralian (Artinskian/Kungurian) to perhaps (although unlikely) the lowermost Guadalupian (Roadian?/Wordian?) (**Appendix 5** of the present dissertation). It contains macroplant remains (conifers ?*Feysia* and *Hermitia*), invertebrate trace fossils indicative of freshwater settings with several degrees of transience (*Arenicolites*, *Cochlichnus*, *Cruziana*, *Palaeophycus*, *Planolites* and *Taenidium*), and tetrapod tracks and skeletons (Matamales-Andreu *et al.*, 2022; **Appendix 4** of the present dissertation). Footprints are represented by the ichnogenera *Hyloidichnus* (two morphotypes attributed to medium-sized and large moradisaurine captorhinid amniotes, respectively), *Dromopus* (attributed to araeoscelidian diapsid reptiles or non-varanodontine varanopids), cf. *Pachypes* (attributed to nycteroletid non-pareiasaur pareiasauromorphs), *Dimetropus* (attributed to indeterminate "pelycosaur"-grade synapsids), cf. *Dimetropus* (attributed with doubts to caseasaurian "pelycosaurs"), *Characichnos* (indeterminate tetrapod swimming traces) and the new tracks herein studied (Matamales-Andreu *et al.*, 2021, 2022; **Appendix 4** of the present dissertation). Among bone remains, there is record of a medium-sized moradisaurine (*Tramuntanasaurus tiai*: **Appendix 4** of the present dissertation), an indeterminate large moradisaurine (Liebrecht *et al.*, 2017), and a medium-sized gorgonopsian (**Appendix 5** of the present dissertation).

2.2. Stratigraphy and sedimentology of the tracksite

The footprints studied herein were found in a single stratigraphic surface corresponding to the base of a very-fine grained sandstone bed in the upper part of the Port des Canonge Formation, designated as "Platjola des munt de Pedres 3" (PMP3) (see Matamales-Andreu *et al.* 2022, for its position in the detailed stratigraphic log of the section) (**Figure 1B**). Therefore, they are all preserved as convex hyporeliefs infilling the original footprints that were imprinted on the underlying mudstones, now eroded. The same surface contains *Hyloidichnus*, *Dromopus*, *Dimetropus*, mud cracks and abundant groove casts.

The detailed stratigraphic log (**Figure 1C**) shows that, below the tracksite, there is a sandstone unit corresponding to, at least, seven cycles of infill of a fluvial channel. After an initial bed of intrabasinal breccias made up of carbonate nodules and soft pebbles, there is an alternation of fine- to medium-grained sandstone beds with trough cross-bedding and internal reactivation surfaces, and beds of mudstones to very fine-grained sandstones with low-angle cross-bedding, separated by erosive surfaces with occasional soft pebbles. It represents a channel

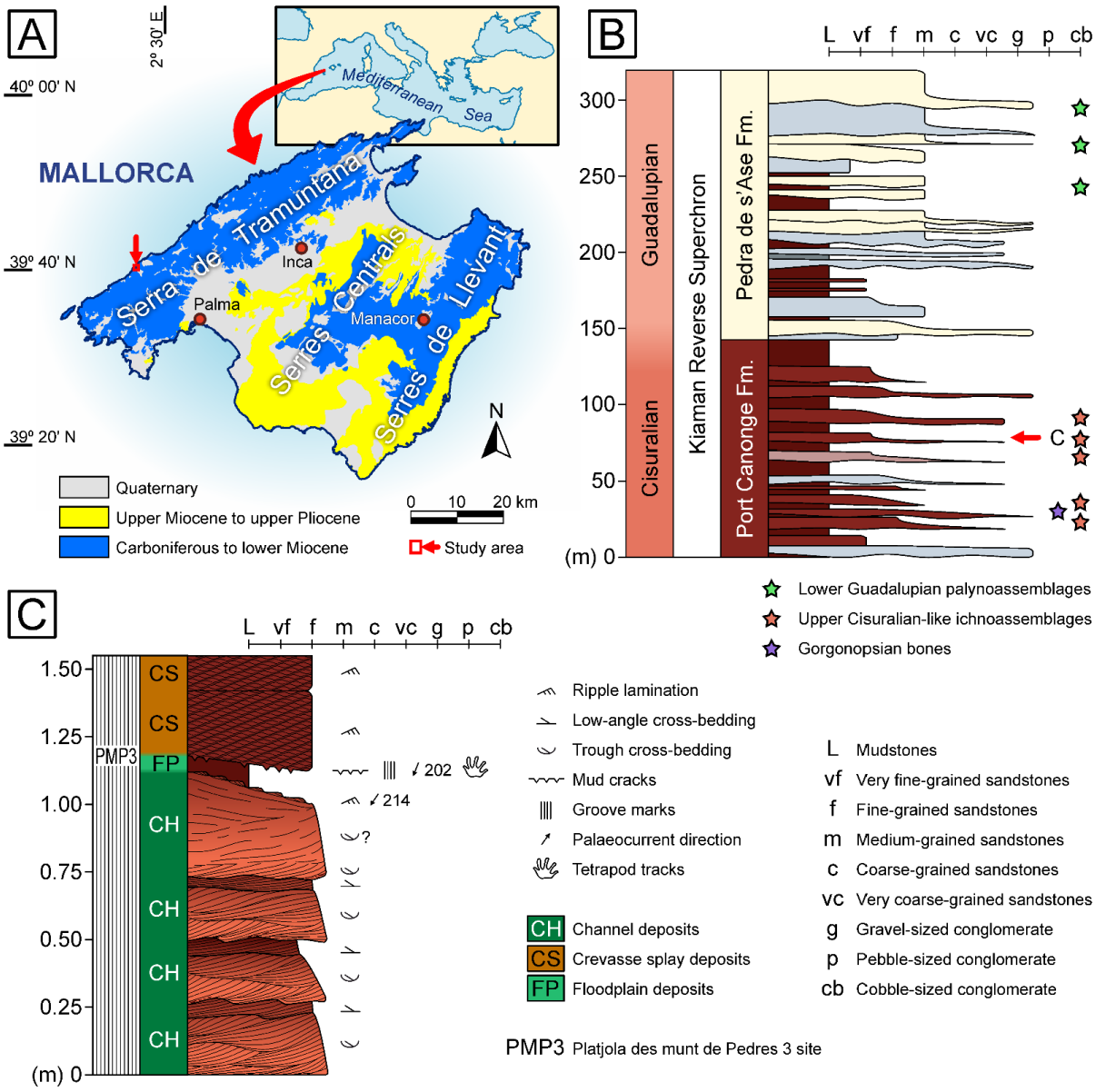

Figure 1. Geographical and geological context for the studied samples. **A:** Simplified geological map of Mallorca, showing the location of the studied section. **B:** Synthetic stratigraphic log of the Racó de s'Algar-Pedra de s'Ase section, with magneto- and biostratigraphic information, with the position of the detailed log in C. Simplified after Matamales-Andreu *et al.* (2022). **C:** Detailed stratigraphic log of the Platjola des munt de Pedres 3 tracksite (PMP3), indicating the track-bearing surface.

subjected to currents of varying energy and periods of still waters. Since all the cycles follow the same dynamics, each of them could correspond to a full seasonal, yearly cycle. The lack of palaeosols would also agree with this interpretation, since it indicates a rapid and essentially continuous deposition of the sediments. In any case, the last

cycle is topped by a linguoid climbing-ripple carpet overlain by a thick bed of mudstones. Those mudstones wedge laterally, indicating that the channel may have, at that time, acted as a waterhole that ended up drying, as suggested by the presence of mud cracks. It is on this surface that the tetrapod footprints were imprinted and, interestingly, they are more abundant and better preserved in what appears to be the deepest zone of the waterhole, *i.e.*, the one that dried up the last. The mud cracks on the trampled surface are relatively thin (~1.6–5.0 mm wide) and with T-junctions (*i.e.*, the intersection between two cracks is at about 90°), which is suggestive of a low number of cycles of desiccation-hydration of the substrate (Goehring *et al.*, 2010). Therefore, it is likely that the surface was not exposed for a long time. Above these mudstones, the dynamics of the system changed completely, with tabular, fine-grained sandstone beds with climbing-ripple lamination, probably corresponding to crevasse splay deposits of another nearby channel. The lowermost bed of those sandstones is the one that produced the natural casts of the tracks.

3. Material and methods

3.1. Collected specimens

Two specimens (DA21/15-12-02 [RA-21-58], and RA-22-20) were collected directly from the *in situ* layer using chisels, hammers and buzzsaws, with permission of the Comissió Insular de Patrimoni Històric of the Consell Insular de Mallorca (excavations/prospections with file numbers 75/2021 and 259/2022). The original material is housed at the Museu de Mallorca (Palma, Spain), acronym: DA21.

3.2. Three-dimensional models and silicone moulds

Digital three-dimensional (3D) models of the studied specimens were produced using photogrammetry, following the exact same methodology as in Matamales-Andreu *et al.* (2022) and references therein. It consists in taking a set of pictures (between 50 and 200, depending on the size of the area to modelise), capturing all the elements in different (and overlapping) perspectives, and then processing it with the software Agisoft Metashape (professional license, educational version, v.1.8.3), MeshLab (v.2020.07) and ParaView (v.4.1.0). The result is a false-coloured height map that may include contours (when necessary) and facilitates the interpretation of the reliefs (*e.g.*, Mujal *et al.*, 2020). The camera used was a Panasonic Lumix DMC-TZ27, and 3D models were made of the complete trackways and of specific tracks separately, in order to attain different levels of detail.

Apart from the 3D models, six silicone moulds were made (MBCN-M-RA-21-07, MBCN-M-RA-21-08, MBCN-M-RA-21-09, MBCN-M-RA-21-11, MBCN-M-RA-21-18, MBCN-CM-RA-21-18, MBCN-M-RA-22-02), comprising all the tracks herein studied that remain *in situ*. To make them, the surface was first covered in petroleum jelly. In the case of individual footprints, the polyaddition silicone paste ClayGum was applied and left to dry for about 10 minutes. For larger surfaces such as the trackway surfaces, the silicone with a thixotroping agent Silicast Tixo was used instead. First, a thin layer of about 1–3 mm thick was applied on the surface and left to dry. Once it had dried, another silicone layer, slightly thicker (5 mm), was applied over it. After drying for one night, a jacket was

made using Triaxial D-5 glass fibre and Plasticrete acrylic resin in order to maintain the shape of the silicone mould. After a few hours, the silicone was peeled off the track-bearing surface, obtaining the mould. Once in the lab, casts of the moulds were produced by using Acrylic One resin, obtaining a high-fidelity copy of the original surface and allowing for a further detailed first-hand study of tetrapod ichnites. All the moulds and casts are housed at the Museu Balear de Ciències Naturals (Sóller, Spain), acronym: MBCN.

3.3. Ichnological study

Tetrapod tracks and trackways were described and measured following the conventions of Leonardi (1987). The relative depth pattern of the footprints (*sensu* Mujal *et al.*, 2020) was also assessed, since it appears to be a consistent ichnotaxobase. Specimens were first studied in the field, and further observations were made in the lab from the recovered specimens, resin casts, and 3D photogrammetric models. The morphological preservation of the tracks *sensu* Marchetti *et al.* (2019b) ranges from 0.5 to 3, with most of the footprints (mainly pes tracks, only two manus tracks) scoring around 2–2.5. This, together with the presence of complete step cycles (building two different trackways), allows for a confident ichnotaxonomic identification.

4. Systematic palaeoichnology

Gorgonopsian tracks, igen. nov.

Diagnosis: Tetrapod pentadactyl ichnites of a remarkably heteropodic trackmaker, with manus tracks (46.97–47.55 mm long) smaller than pes tracks (70.72–118.22 mm long). Pes track semiplantigrade, weakly ectaxonic (digit IV the longest) with digit V longer than digit III. Pes digit imprints relatively long, thick, all of them inwardly curved and displaying large, oval-shaped claw traces. Sole imprint composed of the metatarsal-phalangeal joint mainly of digits II to V, and an oval-shaped anteroposteriorly elongated imprint located posterolaterally (calcaneum area), at the height of the digit V metatarsal-phalangeal joint, and separated from the rest of the pes imprint. Pes track more deeply impressed laterally (digit IV and corresponding metatarsal-phalangeal joint usually the deepest). Manus track plantigrade, weakly mesaxonic (digit IV only slightly shorter than digit III), and more deeply impressed median-laterally (digit III and outer half of the palm more deeply impressed). Proximal margin of the palm strongly convex. Narrow trackway with regular alternating manus-pes sets; long pace and stride (pes length/stride ratio: 0.15–0.34), and very high pace angulation (125,54°–147,61°); manus tracks closer to the midline and completely overstepped by pes tracks, with the latter anterolaterally positioned with respect to the former (different from any other upper Palaeozoic ichnotaxon); manus tracks strongly rotated inwards, pes tracks slightly rotated outwards.

Gorgonopsian tracks, igen. *et* isp. nov.

Figures 2–4, Tables 1, 2

Material: Trackway, MBCN-M-RA-21-18 (field number NA-77.5-01) (**Figure 2**); left manus-pes set (field number RA-22-20 / NA-77.5-05) (**Figure 3A**); right manus-pes set, DA21/15-12-02 /// MBCN-M-RA-21-07 /// MBCN-M-RA-21-18 /// MBCN-CM-RA-21-18 (field numbers RA-21-58 / NA-77.5-01) (**Figure 3B**); isolated manus-pes sets (field number NA-77.5-04) (**Figure 3C**), MBCN-M-RA-21-18 (field number NA-77.5-01) (**Figure 3D**); isolated manus-pes set of large size, MBCN-M-RA-21-18 (field number NA-77.5-01) (**Figure 4A**); trackway composed of large tracks, and other isolated tracks MBCN-M-RA-22-02 (NA-77.5-02) (**Figure 4B**). All tracks in convex hyporelief.

Level, locality and age: Platjola des munt de Pedres 3 fossil site (PMP3), Port des Canonge Formation (upper Cisuralian–?lowermost Guadalupian, Permian), Racó de s'Algar–Pedra de s'Ase section (Matamales-Andreu *et al.*, 2022), Banyalbufar, Mallorca, Balearic Islands.

Description: Remarkably heteropodic ichnites (differing in both size and shape) produced by a quadrupedal tetrapod with manus tracks overprinted by pes tracks (**Figure 2**).

Manus: Ichnites produced by the manus are generally poorly preserved, mostly represented by circular to oval-shaped impressions of the palm, with some narrower, elongated branches corresponding to digit imprints. Of note, the manus track coupled with the best-preserved pes (**Figure 3B**), even if only shallowly impressed, presents five digit imprints, confirming the pentadactylity of the manus tracks of this morphotype. Besides this manus track, only another one (**Figure 3A**), preserving four digit imprints, makes it possible to identify the morphology of the manus, and thus this description is mainly based on these specimens. The manus tracks are markedly plantigrade, slightly wider than long (in the best preserved specimen: 46.0 mm long, 47.8 mm wide; **Figure 3A**). Digit I is substantially shorter than digits II, III and IV. Digit III imprint is the longest, with digit IV subequal in length (only slightly shorter than digit III). Digit V is slightly longer than digit I. The digit tip imprints are generally round, only slightly angular, denoting the presence of relatively wide claws in the autopodium. The digit imprints are generally straight, digits I to IV are slightly curved inwards and digit V is slightly curved outwards. They all are radially distributed from the palm impression, with the angulation of digits I and II being higher than the others. The proximal part of the digit I to IV imprints is defined by a faint, convex (proximally curved) relief, better observed in the false-colour depth map of the 3D model and in the imprints of digits II and III. In front of the tips of all four digit imprints, there are shallow and short, inwardly oriented drag traces. The palm impression is only slightly wider than long, with a marked proximally convex margin. The lateral (outer) half of the palm is the most deeply impressed part of the footprint, followed by the digit III. As stated above, the poorly-preserved manus tracks are mostly represented by the palm, denoting the strong plantigrady of these ichnites; in addition, the lateral half of these tracks is also generally more deeply impressed. This is indicative of a median-lateral functional prevalence of the manus autopodium.

Pes: Imprints of the pes (70,72–118.22 mm long, 72.30–143.88 mm wide) are notably larger and generally better preserved than those of the manus. Pes tracks are semiplantigrade and pentadactyl, with digit impressions being the most prominent part of the ichnites. Digit imprints increase in length from I to IV, and digit V imprint is slightly shorter than digit III. The relative depth of the digits parallels its relative length: I<II<III<V<IV; though occasionally the digit V imprint is the deepest (**Figure 3B**). All digit imprints are curved inwards, with the tip imprint more markedly bent. The tips display large and deep claw traces that are anteroposteriorly elongated, giving an

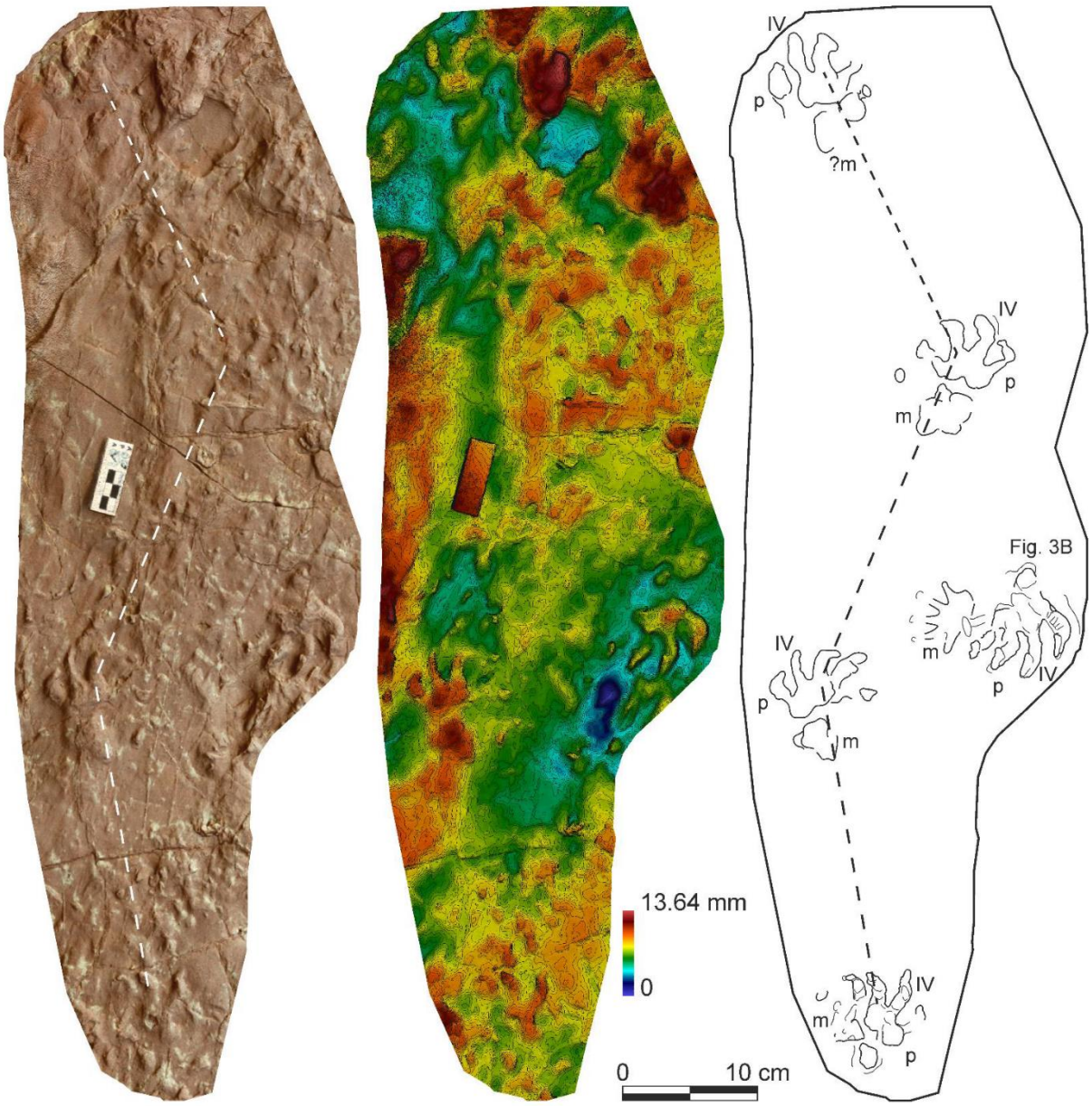

Figure 2. Gorgonopsian tracks, igen. *et* isp. nov. (MBCN-M-RA-21-18 [mould], MBCN-CM-RA-21-18 [cast], NA-77.5-01 [field identificator of track surface]), including orthophoto (left) and false colour depth map with contours (middle) of the 3D photogrammetric model, and interpretative outline (right). The surface also preserves tracks from other ichnotaxa, not represented in the interpretative outline. Dashed lines: pace of the pes tracks. Abbreviations: m, manus; p, pes; IV, pedal digit IV.

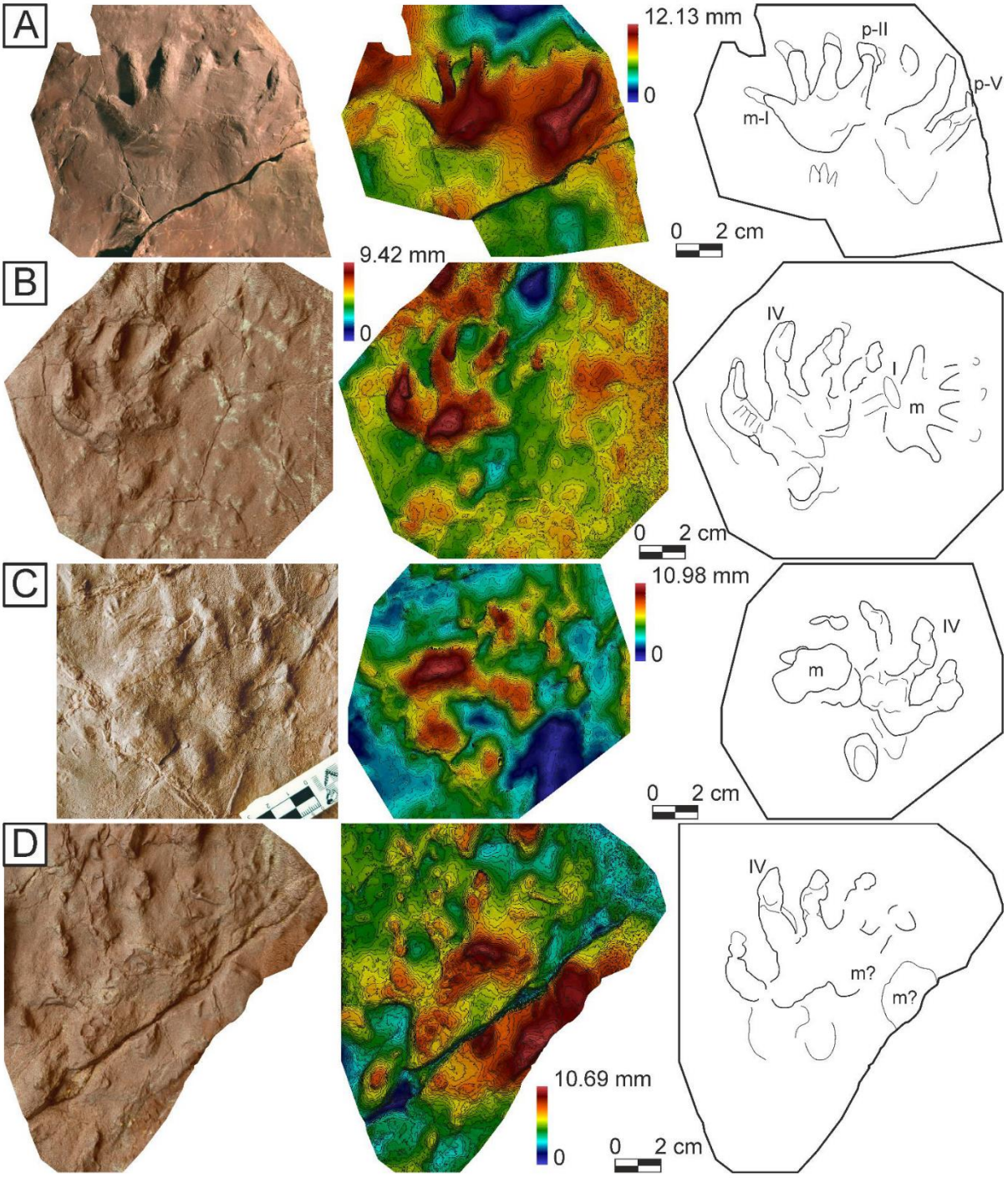

Figure 3. Gorgonopsian tracks, igen. *et* isp. nov. **A:** Left couple with well-preserved manus track (RA-22-20 [field number of collected specimen] NA-77.5-05 [field identificator of track surface]). **B:** Right couple with very well-preserved pes track (DA21/15-12-02 [collected specimen], MBCN-M-RA-21-07 [mould], MBCN-M-RA-21-18 [mould], MBCN-CM-RA-21-18 [cast], RA-21-58 [field number of collected specimen], NA-77.5-01 [field identificator of track surface]). **C:** Left couple (NA-77.5-04 [field identificator of track surface]). **D:** Right couple (MBCN-M-RA-21-18 [mould], MBCN-CM-RA-21-18 [cast], NA-77.5-01 [field identificator of track surface]).

Specimens include, from left to right: photograph (A, C) or orthophoto from the 3D photogrammetric model with original texture (B, D); false-colour depth map with contours; and interpretative outline of the tracks. Dashed lines in A correspond to the pace of the pes tracks. Abbreviations: m, manus; p, pes; I, II, and IV, digits I, II, and IV, respectively.

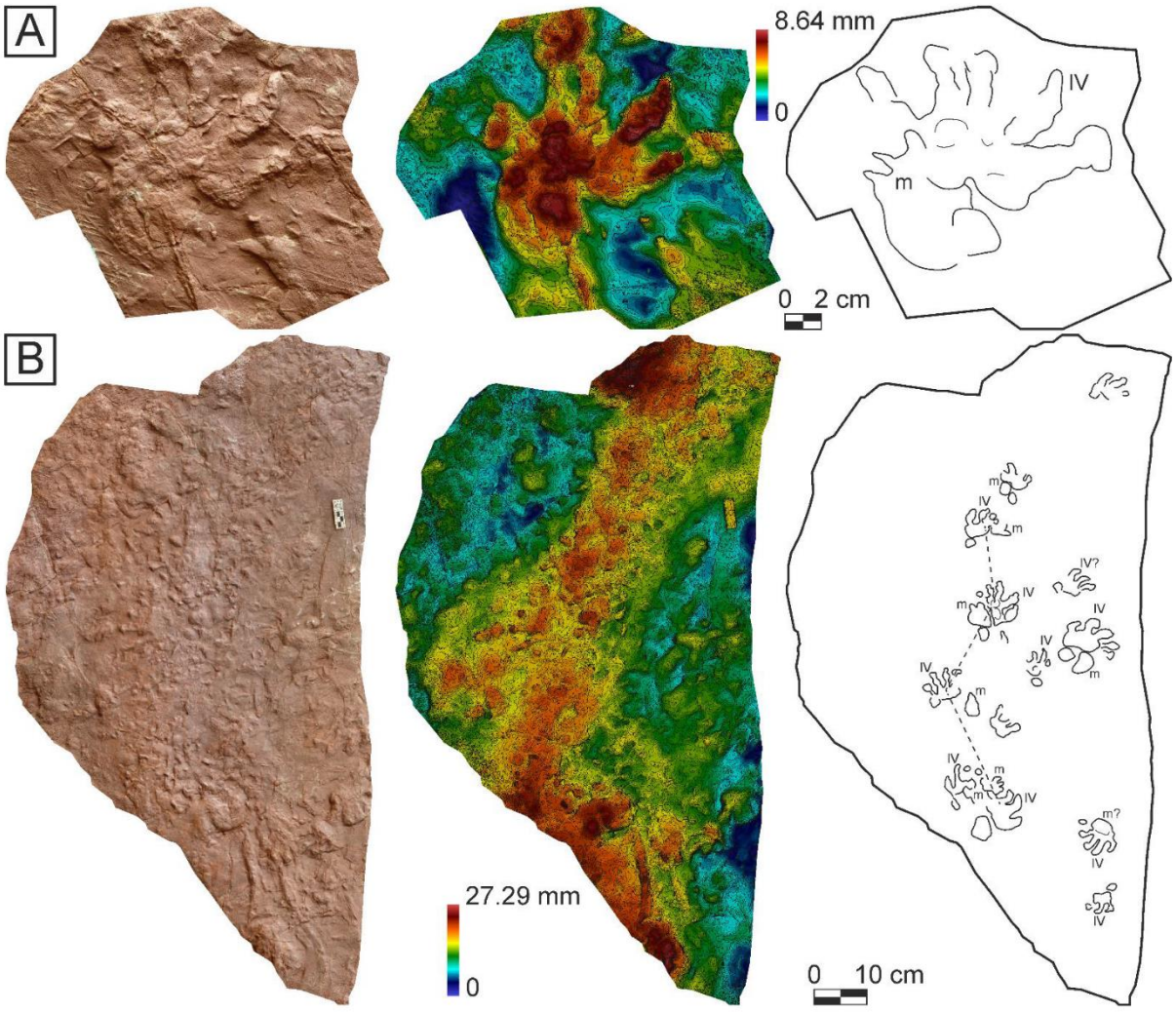

Figure 4. Large-sized gorgonopsian tracks, igen. *et* isp. nov. **A:** Isolated left couple (MBCN-M-RA-21-18 [mould], MBCN-CM-RA-21-18 [cast], NA-77.5-01 [field identificator of track surface]). **B:** Trackway and isolated tracks (MBCN-M-RA-22-02 [mould], NA-77.5-02 [field identificator of track surface]); dashed line corresponds to pes paces; the surface also preserves tracks from other ichnotaxa, not represented in the interpretative outline. All specimens include orthophoto from the 3D photogrammetric model with original texture, false-colour depth map with contours, and interpretative outline of the tracks. Abbreviations: m, manus; IV, pedal digit IV.

Table 1. Track parameters of gorgonopsian tracks, igen. *et* isp. nov.

Museum collection number (Field number)	MBCN-M-RA-21-18 /// MBCN-CM-RA-21-18 (NA-77.5-01)							
IDENTIFICATION	Gorgonopsian tracks							
Specimen	Fig. 2	Fig. 2	Fig. 2	Fig. 2	Fig. 2	Fig. 2	Fig. 2	Fig. 2
Anatomy	Left manus (Set #1)	Left pes (Set #1)	Right manus (Set #2)	Right pes (Set #2)	Left manus (Set #3)	Left pes (Set #3)	Right manus (Set #4)	Right pes (Set #4)
PARAMETERS OF THE TRACKS								
Length (mm)	25,96	70,72	25,95	73,85	33,04	79,67	-	90,31
Width (mm)	22,47	82,33	35,19	75,81	40,14	88,91	-	72,30
Length palm/sole (mm)	-	35,95	-	45,68	-	44,21	-	47,22
Width palm/sole (mm)	-	44,81	-	32,29	-	42,63	-	33,88
Length I (mm)	-	19,07	-	24,63	-	20,35	-	24,86
Length II (mm)	-	28,23	-	27,32	-	23,45	-	29,98
Length III (mm)	-	31,12	-	30,13	-	30,50	-	42,06
Length IV (mm)	-	38,38	-	37,06	-	34,46	-	48,65
Length V (mm)	-	26,88	-	28,39	-	28,36	-	39,13
Divergence angle I–II (°)	-	36,63	-	42,67	-	28,30	-	29,75
Divergence angle II–III (°)	-	10,79	-	23,81	-	36,02	-	45,27
Divergence angle III–IV (°)	-	22,11	-	17,56	-	31,92	-	17,69
Divergence angle IV–V (°)	-	33,17	-	21,80	-	25,79	-	9,34
Divergence angle I–V (°)	-	108,94	-	101,82	-	119,93	-	82,26
Divergence angle I–IV (°)	-	76,51	-	81,79	-	92,17	-	72,31
Divergence angle II–V (°)	-	66,05	-	70,13	-	94,42	-	65,05
Divergence angle II–IV (°)	-	35,65	-	45,42	-	64,74	-	59,40

Note 1: Cells in yellow indicate approximate or extrapolated values.

Table 1. Track parameters of gorgonopsian tracks, igen. *et* isp. nov. (continued)

Museum collection number (Field number)	(RA-22-20 / NA-77.5-05)		DA21/15-12-02 /// MBCN-M-RA-21-07 /// MBCN-M-RA-21-18 /// MBCN-CM-RA-21-18 (RA-21-58 / NA-77.5-01)		(NA-77.5-04)		MBCN-M-RA-21-18 /// MBCN-CM-RA-21-18 (NA-77.5-01)		MBCN-M-RA-21-18 /// MBCN-CM-RA-21-18 (NA-77.5-01)	
IDENTIFICATION	Gorgonopsian tracks		Gorgonopsian tracks		Gorgonopsian tracks		Gorgonopsian tracks		Gorgonopsian tracks	
Specimen	Fig. 3A	Fig. 3A	Fig. 3B	Fig. 3B	Fig. 3C	Fig. 3C	Fig. 3D	Fig. 3D	Fig. 4A	Fig. 4A
Anatomy	Left manus	Left pes	Right manus	Right pes	Left manus	Left pes	Right manus	Right pes	Left manus	Left pes
PARAMETERS OF THE TRACKS										
Length (mm)	47,55	67,72	46,97	79,27	34,14	75,51	-	86,69	76,56	112,49
Width (mm)	47,34	-	51,55	78,70	32,95	77,26	-	86,18	59,83	143,88
Length palm/sole (mm)	23,05	29,26	22,27	39,01	-	39,91	-	45,73	-	65,47
Width palm/sole (mm)	25,56	-	22,96	36,01	-	34,41	-	47,04	-	59,80
Length I (mm)	16,50	-	15,85	21,15	-	26,72	-	26,46	-	40,78
Length II (mm)	21,92	36,01	23,37	31,20	-	31,36	-	32,57	-	49,24
Length III (mm)	24,97	36,28	22,74	35,58	-	36,15	-	33,00	-	53,81
Length IV (mm)	23,69	40,44	22,39	42,38	-	38,81	-	39,32	-	64,17
Length V (mm)	-	28,56	17,07	39,53	-	31,44	-	32,50	-	60,80
Divergence angle I–II (°)	45,50	-	33,54	43,53	-	35,11	-	31,69	-	38,09
Divergence angle II–III (°)	19,79	20,08	27,27	32,75	-	20,37	-	26,41	-	17,99
Divergence angle III–IV (°)	16,27	9,54	20,25	11,56	-	28,24	-	13,53	-	24,69
Divergence angle IV–V (°)	64,05	14,01	54,40	27,39	-	30,91	-	30,55	-	26,94
Divergence angle I–V (°)	146,22	-	133,77	113,46	-	111,36	-	91,59	-	99,16
Divergence angle I–IV (°)	83,39	-	88,42	80,78	-	86,21	-	60,63	-	75,11
Divergence angle II–V (°)	96,46	44,37	98,79	75,98	-	82,98	-	70,56	-	64,79
Divergence angle II–IV (°)	35,98	30,85	53,72	44,60	-	59,28	-	34,92	-	43,29

Note 1: Cells in yellow indicate approximate or extrapolated values.

Table 1. Track parameters of gorgonopsian tracks, igen. *et* isp. nov. (continued)

Museum collection number (Field number)	MBCN-M-RA-22-02 (NA-77.5-02)									
IDENTIFICATION	Gorgonopsian tracks									
Specimen	Fig. 4B	Fig. 4B	Fig. 4B	Fig. 4B	Fig. 4B	Fig. 4B	Fig. 4B	Fig. 4B	Fig. 4B	Fig. 4B
Anatomy	Right manus (large isolated couple)	Right pes (large isolated couple)	Left manus (Set #1)	Left pes (Set #1)	Right manus (Set #2)	Right pes (Set #2)	Left manus (Set #3)	Left pes (Set #3)	Right manus (Set #4)	Right pes (Set #4)
PARAMETERS OF THE TRACKS										
Length (mm)	35,28	108,82	-	113,02	30,28	-	46,86	118,22	-	86,99
Width (mm)	44,06	103,50	-	-	42,69	-	44,90	86,17	-	-
Length palm/sole (mm)	-	65,48	-	83,95	-	-	-	72,62	-	48,24
Width palm/sole (mm)	-	47,48	-	67,10	-	44,95	-	38,29	-	33,81
Length I (mm)	-	39,60	-	-	-	-	-	25,57	-	-
Length II (mm)	-	40,22	-	-	-	38,61	-	32,93	-	26,87
Length III (mm)	-	42,48	-	43,50	-	43,80	-	46,70	-	31,13
Length IV (mm)	-	45,38	-	48,84	-	48,47	-	56,50	-	41,81
Length V (mm)	-	36,10	-	41,95	-	40,30	-	50,19	-	40,44
Divergence angle I–II (°)	-	20,89	-	-	-	-	-	39,12	-	-
Divergence angle II–III (°)	-	26,19	-	36,56	-	17,03	-	23,90	-	21,58
Divergence angle III–IV (°)	-	43,69	-	15,47	-	18,87	-	37,83	-	30,70
Divergence angle IV–V (°)	-	14,71	-	10,99	-	20,00	-	9,47	-	14,55
Divergence angle I–V (°)	-	107,95	-	-	-	-	-	105,90	-	-
Divergence angle I–IV (°)	-	87,14	-	-	-	-	-	94,25	-	-
Divergence angle II–V (°)	-	96,04	-	63,78	-	57,69	-	80,09	-	64,14
Divergence angle II–IV (°)	-	73,89	-	39,63	-	36,19	-	71,26	-	48,38

Note 1: Cells in yellow indicate approximate or extrapolated values.

Table 2. Trackway parameters of gorgonopsian tracks, igen. *et* isp. nov.

Museum collection number	MBCN-M-RA-21-18 /// MBCN-CM-RA-21-18 (NA-77.5-01)				MBCN-M-RA-22-02 (NA-77.5-02)		
IDENTIFICATION	Gorgonopsian tracks				Gorgonopsian tracks		
Specimen	Fig. 2				Fig. 4B		
PARAMETERS OF THE TRACKWAYS							
Pace angulation pes (°)	147,61	132,91			125,54	142,34	
Pace angulation manus (°)							
Divergence angle pes (°)	4,54	5,03	-7,22	32,12	74,57	19,32	8,80
Divergence angle manus (°)							
Stride pes (mm)	488,57	451,07			380,44	317,85	
Stride manus (mm)					400,98		
Pace pes (mm)	246,58	262,21	230,12		237,37	193,44	144,12
Pace manus (mm)							
Length pace pes (mm)	236,43	253,21	207,86		215,16	183,86	132,03
Length pace manus (mm)							
Width pace pes (mm)	70,71	71,43	97,50		94,87	50,86	52,81
Width pace manus (mm)							
Interpes distance (mm)	0,00	0,00	17,14		28,36	0,00	0,00
Intermanus distance (mm)							
Manus-pes distance (mm)							
Manus-pes divergence (°)							
Width external (mm)	143,57	151,43	184,29		179,95	142,79	137,90
Width internal (mm)							
Glenoacetabular distance (mm)	242,14	226,07			190,71	162,35	

Note 1: Cells in yellow indicate approximate or extrapolated values.

Note 2: Negative numbers in divarication angles indicate medial (inwards) rotation of the track.

overall hook shape to the digit tip imprints. In addition to their large size, claw traces are also the deepest part of the digit imprints, followed by the distal third of the phalangeal region (**Figures 3B–D**, **4A**). The digit imprints are generally well-defined, except for digit I, which is mostly only represented by a shallow imprint of the tip (the claw) and a very faint impression (if present) of the distal phalangeal portion. The same is true for the proximal half of digit II, usually not preserved or only shallowly impressed. In the best-preserved pes track (**Figure 3B**), the digit V imprint displays laterally elongated creases (*i.e.*, perpendicular to the digit axis), more developed to the inner side and forming blocky rectangular reliefs; they most likely correspond to skin creases (similar to those found in *Dimetropus*: Calábková *et al.*, 2023). The digit imprints are radially distributed from the sole imprint, which is mainly represented by the impressions of the basal pad of each digit, corresponding to the metatarsal-phalangeal joint. Each basal pad is circular and altogether form a tight bulbous impression, being deepest below digit IV and usually not imprinted below digit I. In most of the pes ichnites, a separate, slightly anteroposteriorly elongated oval-shaped

imprint is present; it is usually well-defined, even surrounded by an expulsion rim. This oval-shaped imprint represents the most proximal part of the pes tracks, and most likely corresponds to the impression of the tarsal pad. This imprint may appear connected to the basal pad of digit V by a shallow, faint relief that would correspond to the tarsal bones associated to digits IV and V. The inner-proximal part of the sole is not imprinted; in fact, the manus imprints are often located in this area. In this sense, considering the imprinted parts of the sole and the relative depth pattern of the digit imprints (with digits IV and V being the deepest), pes tracks indicate a marked lateral functional prevalence of the autopodium.

Trackway: Tracks are arranged in couples or sets, with pes tracks overstepping (overprinting) manus tracks, the latter usually located in the inner-proximal part of the former (in the region where the sole would appear), therefore, manus tracks are closer to the midline than pes tracks. The divergence angle between manus and pes is markedly high, sometimes being over 80° (**Figure 3B**), though it can also be below 30° (**Figure 3A**). The trackways are composed of completely alternating manus-pes sets, they are relatively narrow, with a high pace angulation (125.54–147.61° for the pes) and long paces and strides (pace: 144.12–237.37 mm for the pes; stride length: 317.85–488.57 mm for the pes). No tail nor belly traces are preserved. All these features denote a narrow gauge and a relatively upright posture of the limbs of the trackmaker, denoting a parasagittal locomotion (see 5. Discussion below). The glenoacetabular distance of the trackmaker inferred from the trackways is of 162.35–242.14 mm. Pes tracks are slightly rotated outwards, whereas manus tracks are strongly rotated inwards. In the trackways, pes imprints are notably much better preserved than manus imprints. In fact, the manus morphology cannot be assessed in the ichnites composing the trackways (**Figure 2**), and sometimes the imprints are even difficult to identify, also because the trampled surfaces display many other reliefs and other tetrapod tracks (**Figures 2**, **4B**).

5. Discussion

5.1. Ichnotaxonomic remarks

The size range of the studied tracks herein is relatively wide (**Table 1**), yet their morphology and trackway parameters remain quite constant (**Figures 2–4**; **Table 2**). Therefore, all these tracks are referred to the same morphotype.

The combination of features from both the tracks and trackways from Mallorca herein described show that they were produced by quadrupedal tetrapods with strong heteropody, with both manus and pes being pentadactyl and with clawed digits. This readily rules out *Limnopus* and *Batrachichnus* (the latter being also <20 mm long; Voigt, 2005), which have tetradactyl manus and are attributed to anamniotes (usually temnospondyls). The presence of claw traces also rules out *Amphisauropus* and *Ichniotherium*, which have pentadactyl manus but are clawless. Besides, these ichnogenera display a notably different morphology of both manus and pes, and a much weaker heteropody than the tracks from Mallorca. In the same way, the strong heteropody (pes much larger than manus tracks) plus the weak ectaxony of the pes and mesaxony of the manus in the tracks from Mallorca differ from coeval (or similarly aged) ichnotaxa such as *Hyloidichnus* (represented by two morphotypes on Mallorca, see Matamales-

Andreu *et al.*, 2022), *Merifontichnus*, *Varanopus*, *Erpetopus*, *Dromopus* (also present on Mallorca, see Matamales-Andreu *et al.*, 2022), *Tambachichnium*, and *Rhynchosauroides*. The tracks studied herein also differ from *Pachypes* (potentially present on Mallorca, see Matamales-Andreu *et al.*, 2022) because it displays relatively short and wide digit imprints (Marchetti *et al.*, 2021). Another major difference is in the relative depth pattern: in the specimens from Mallorca, manus imprints are deeper median-laterally, and pes imprints are notably deeper laterally, whereas tracks attributed to all aforementioned ichnotaxa are deeper medially or median-medially (see Mujal *et al.*, 2020). As discussed by these authors, relative depth patterns of the tracks correlate to the functional prevalence of autopodia, which may be linked to phylogeny. In this sense, the tracks of Mallorca indicate a lateral (or median-lateral) functional prevalence of autopodia, which is a state generally attributed to synapsids (Mujal *et al.*, 2020). Indeed, this is in agreement with the anatomical features of the studied tracks that, as detailed below, are comparable to those observed in ichnotaxa correlated to synapsid, and more specifically therapsid, trackmakers.

The morphologies of both manus and pes tracks of the morphotype herein studied differ from most Permian/Triassic ichnotaxa correlated to synapsid trackmakers (*e.g.*, Marchetti *et al.*, 2019a: fig 9; Matamales-Andreu *et al.*, 2021: fig 4): *Dimetropus* presents proportionally longer sole imprints, thinner and straight digit imprints, usually with only the distal part well impressed; *Tambachichnium* presents low heteropody, a very marked ectaxony, relatively long digit imprints, and a digit V imprint in both manus and pes rotated outwards and proximally positioned, separated from the rest of the digit imprints; *Brontopus*, *Dolomitipes* and *Dicynodontipus* show a much lower degree of heteropody (even with the manus larger than the pes in some *Dolomitipes*), relatively shorter and more rounded digit imprints, and no overstepping, with the manus imprint always anteriorly positioned with respect to the pes imprint. Therefore, the tracks from Mallorca cannot be attributed to any of these ichnotaxa either.

The morphotype herein studied is most similar to the ichnospecies *Capitosauroides talus* and *Karoopes gansfonteinensis* (**Figure 5**), known from the Permian of central and southern Pangaea, respectively. These ichnotaxa show some anatomical characters and relative depth patterns consistent with biarmosuchian, dinocephalian, gorgonopsian, and therocephalian trackmakers, but their absolute sizes, degree of heteropody and age ranges suggest that *Capitosauroides* was produced by therocephalians and *Karoopes* by gorgonopsians (Marchetti *et al.*, 2019a).

The shape of the manus tracks from Mallorca are somewhat similar to those of *C. talus*, known from the Guadalupian of the Central European Basin and the Massif Central (Buchwitz *et al.*, 2020; Marchetti *et al.*, 2022) and the Lopingian of the Alps (Marchetti *et al.*, 2019c, 2022). They present a similar overall shape, with slender digit imprints and a deeply impressed palm (**Figure 5B, E**). However, two morphological (anatomical) differences exist: (1) the imprint of manus digit IV of *C. talus* is slightly longer than digit III (though not in all specimens, see parameters in Buchwitz *et al.*, 2020; Marchetti *et al.*, 2022), whereas in the manus tracks of the morphotype herein studied, the digit IV imprint is slightly shorter than digit III (**Table 1**); (2) the proximal margin of the palm imprint is concave in *C. talus*, whereas it is convex in the tracks of Mallorca. It should be noted that the relative length of the manus digit imprints of the specimens from Mallorca can only be confidently identified in two tracks (**Figures 3A, B, 5B, C**); nonetheless, these imprint are reasonably well preserved, without extramorphological features (even if short

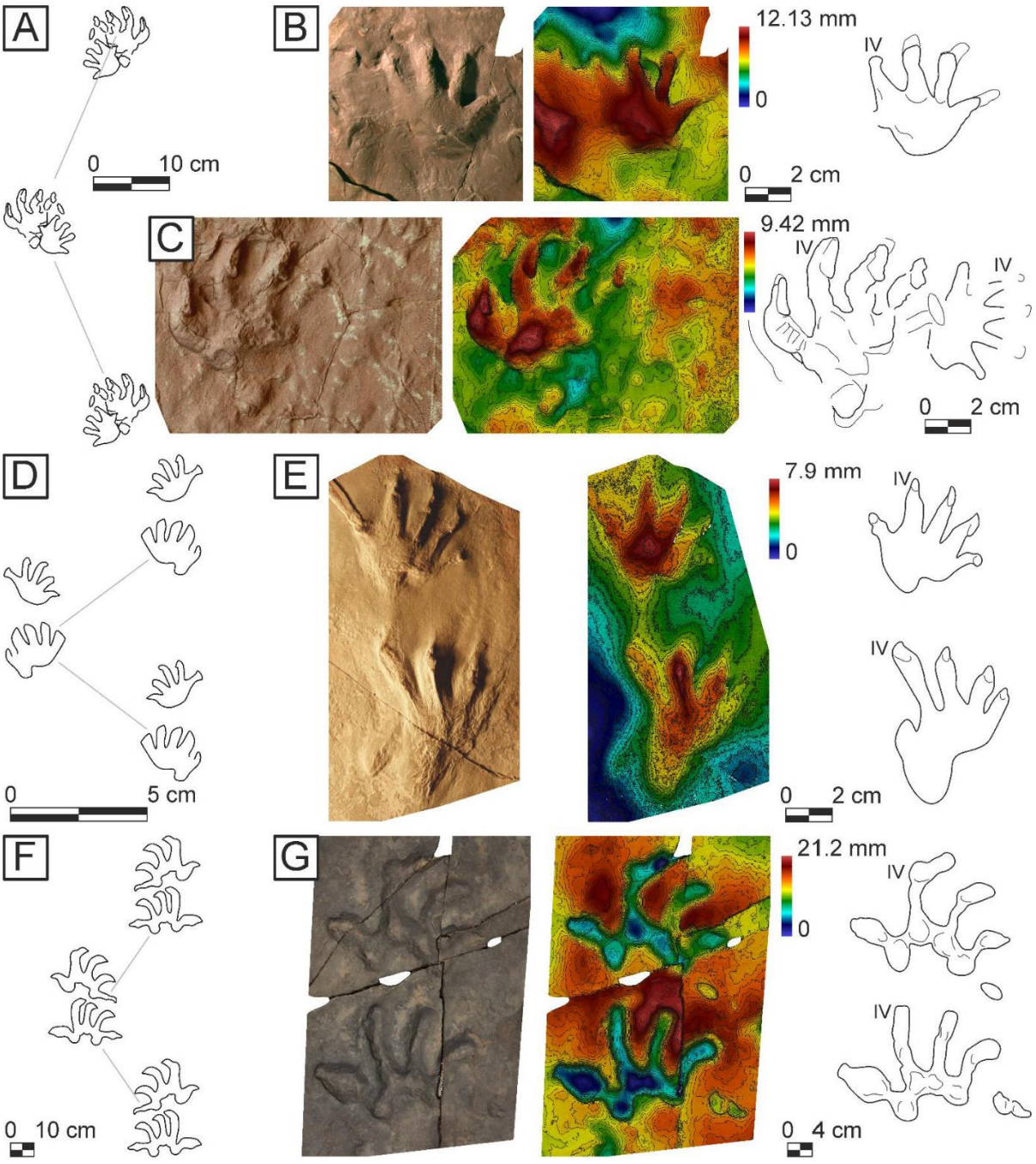

Figure 5. Comparison of the gorgonopsian tracks igen. *et* isp. nov. (**A–C**) with *Capitosauroides talus* (**D, E**) and *Karoopes gansfonteinensis* (**F, G**), including idealised trackways (**A, D, F**) and exemplary manus and pes tracks (**B, C, E, G**) of the three ichnospecies. Specimens in **B** and **G** are mirrored for a better comparison. Idealised trackways of *C. talus* (**D**) and *K. gansfonteinensis* (**F**) modified from Matamales-Andreu *et al.* (2021). 3D model of *K. gansfonteinensis* (**G**) modified from Marchetti *et al.* (2019a) and Mujal *et al.* (2020), photograph of *C. talus* (**E**) modified from Marchetti *et al.* (2022).

digit drag traces are present, the tip and the proximal end of all digit imprints are well defined). The digit V imprint, though shallow, is only recognised in a single track (**Figure 3B**), being slightly longer than digit I, as in *C. talus*.

The pes tracks of the morphotype herein studied also resemble those of *C. talus*, although the tracks from Mallorca are morphologically more similar to those of *Karoopes gansfonteinensis*, known from the uppermost Guadalupian of South Africa (Marchetti *et al.*, 2019a). However, significant differences exist in the pes track morphology of those ichnotaxa (**Figure 5C, E, G**), indicating that they were produced by animals with a different pes anatomy: (1) The relative position, proportions and shape of digit V is notably different; in the tracks of Mallorca the digit V is more proximally positioned (close to digit IV, not separated from the group I–IV as it is in *K. gansfonteinesis* and *C. talus*), anteriorly oriented, proportionally longer (longer than digit III in the tracks from Mallorca), and curved inwards (being straight and directed, even curved outwards in both *K. gansfonteinesis* and *C. talus*). (2) The pes of the morphotype herein studied displays an oval-shaped imprint proximolaterally positioned (at the height of digit V), which is generally separated from the rest of the track, and may correspond to the impression of the tarsal pad; in both *K. gansfonteinensis* and *C. talus*, such proximolateral imprint is also present, but it is always connected to the rest of the pedal imprint through the outer side of the metatarsal-phalangeal joint. (3) The digit imprints of the pes tracks of Mallorca are more inwardly curved than those of *K. gansfonteinensis* and, especially, *C. talus*. (4) The digit tips of the pes tracks of Mallorca are characterised by notably large and deep claw traces, which are oval-shaped and located in the inner side of the digits, giving a hook shape to the digit tip imprints; instead, in *K. gansfonteinensis* claw traces are smaller and less well-differentiated from the rest of the digit imprints, and in *C. talus*, claw traces are circular and located anteriorly to the digit imprints. The relative depth pattern of the pes tracks is more similar between the morphotype herein studied and *K. gansfonteinensis* (tracks markedly deeper laterally) than with *C. talus* (tracks deeper median-laterally). The overall set of differences is most likely linked to the anatomy of the autopodium, rather than to different locomotion gaits. Of note, even if pes tracks are somewhat reminiscent to those of *K. gansfonteinensis*, the manus track morphology is markedly different. In that ichnospecies, manus and pes tracks are of similar morphology and size, whereas the morphotype herein studied is strongly heteropodal and the overall morphology and proportions between manus and pes imprints are different (**Table 1**).

The trackways of the morphotype herein studied (**Figures 2**, **4B**, **5A**) present a combination of features that have not been observed in any other Permian/Triassic ichnotaxon correlated to synapsid trackmakers, which generally present a relative depth pattern that indicates a lateral, and/or median-lateral, functional prevalence of autopodia (see Mujal *et al.*, 2020). This unique combination of features includes: (1) marked heteropody, with pes tracks notably larger than manus tracks, (2) complete overstepping of the manus by the pes, (3) narrow gauge with high pace angulation, and (4) long strides and paces (**Figure 5A**; **Table 2**). The morphological consistency of all the tracks and trackways, with important size differences (pes length 70.72–118.22 mm), suggests that the unique morphology of the tracks herein studied is not a result of trackmaker size, ontogeny, extramorphology, or peculiar gait, but represents a strong anatomical signal of the producer. Of note, *K. gansfonteinensis* trackways are also narrow and with high pace angulation, but the pes overstepping is weak, only reaching half of the manus palm impression (**Figure 5F**; Marchetti *et al.*, 2019a). Conversely, in *C. talus* trackways the pace angulation is relatively low, resulting in short stride lengths and an overall wide trackway (**Figure 5D**; Buchwitz *et al.*, 2020), being

significantly different to the morphotype herein studied (**Figure 5A**). For the reasons above, attribution of the morphotype herein studied to *Capitosauroides* or *Karoopes* is ruled out (*Karoopes* is so far monospecific, and the other ichnospecies of *Capitosauroides*, *C. bernburgensis* from the Triassic of the Central European Basin, displays a notably different track morphology, especially in the manus imprints, see Buchwitz *et al.*, 2020). Furthermore, the morphology of the pes tracks and trackway patterns of the morphotype herein studied remain invariable despite the relatively wide range of sizes of the sample (**Table 2**). This suggests that most of (if not all) the described features rely on the anatomy of the autopodia and bauplan of the trackmaker, and thus no extramorphological features play a significant role in the described tracks and trackways. Therefore, all the specimens from Mallorca herein described are here attributed to the same morphotype. In the subsequent section, these tracks are correlated to the potential trackmakers, most probably gorgonopsian therapsids.

5.2. Track-trackmaker correlation

The relatively good morphological preservation (*sensu* Marchetti *et al.*, 2019b) of most of the pes tracks and two manus tracks, as well as the presence of complete step cycles, makes it possible to propose a detailed anatomy-based correlation to the potential producer(s) (**Figure 6**). This has been done with other Permian ichnotaxa, such as *Amphisauropus*-seymouriamorphs (Marchetti *et al.*, 2017), *Ichniotherium*-diadectomorphs (Voigt *et al.*, 2007), *Hyloidichnus*-captorhinomorphs (Logghe *et al.*, 2021), *Hyloidichnus*-moradisaurine captorhinids (**Appendix 4** of the present dissertation), and *Pachypes*-pareiasauromorphs (Marchetti *et al.*, 2021). The lateral and median-lateral functional prevalence inferred from the tracks herein studied points to synapsids as the potential trackmakers (Mujal *et al.*, 2020), and this is in accordance with the resemblance the morphotype herein studied with *Capitosauroides talus* and *Karoopes gansfonteinensis* (see section 5.1 above), which have been correlated to theriodont therapsids (Marchetti *et al.*, 2019a, 2022; Buchwitz *et al.*, 2020). Indeed, the relative length of the imprints of the pes digits of the morphotype herein studied and their proportions with respect to the sole impression, and the oval-shaped impression posterolaterally positioned, are consistent with the pedal morphology of several groups of early therapsids such as biarmosuchians, dinocephalians, gorgonopsians and therocephalians (*e.g.*, Colbert, 1948; Romer, 1956; Orlov, 1958; Boonstra, 1964, 1965, 1966; Sigogneau & Tchudinov, 1972; Sigogneau-Russell, 1989; Gebauer, 2014; Sidor, 2022; **Figure 6A–E**). Detailed features include: (1) ectaxony, with pedal digit IV being the longest, and a relative long digit V (only slightly shorter than digit IV); (2) large claw impressions that fit well with the large unguals of those groups; (3) deeply impressed metatarsal-phalangeal joint (characteristic of synapsid tracks) that corresponds to the wide ends of the metatarsals, particularly those of digits III to IV; and (4) oval-shaped impression posterlaterally positioned in the sole that is agrees with the large calcaneum and its position in those groups (**Figure 6F, G**). Attributing the morphotype herein studied to one of the early therapsid groups mentioned above is not an easy task, as the autopodial morphology remains undescribed for most of their species. Moreover, even considering the taxa in which the autopodia are well-known, their appear to have a fairly conserved morphology, showing a remarkably similar general structure. In such cases, resorting to the co-occurring body fossil record is the only way to shed some light on this question.

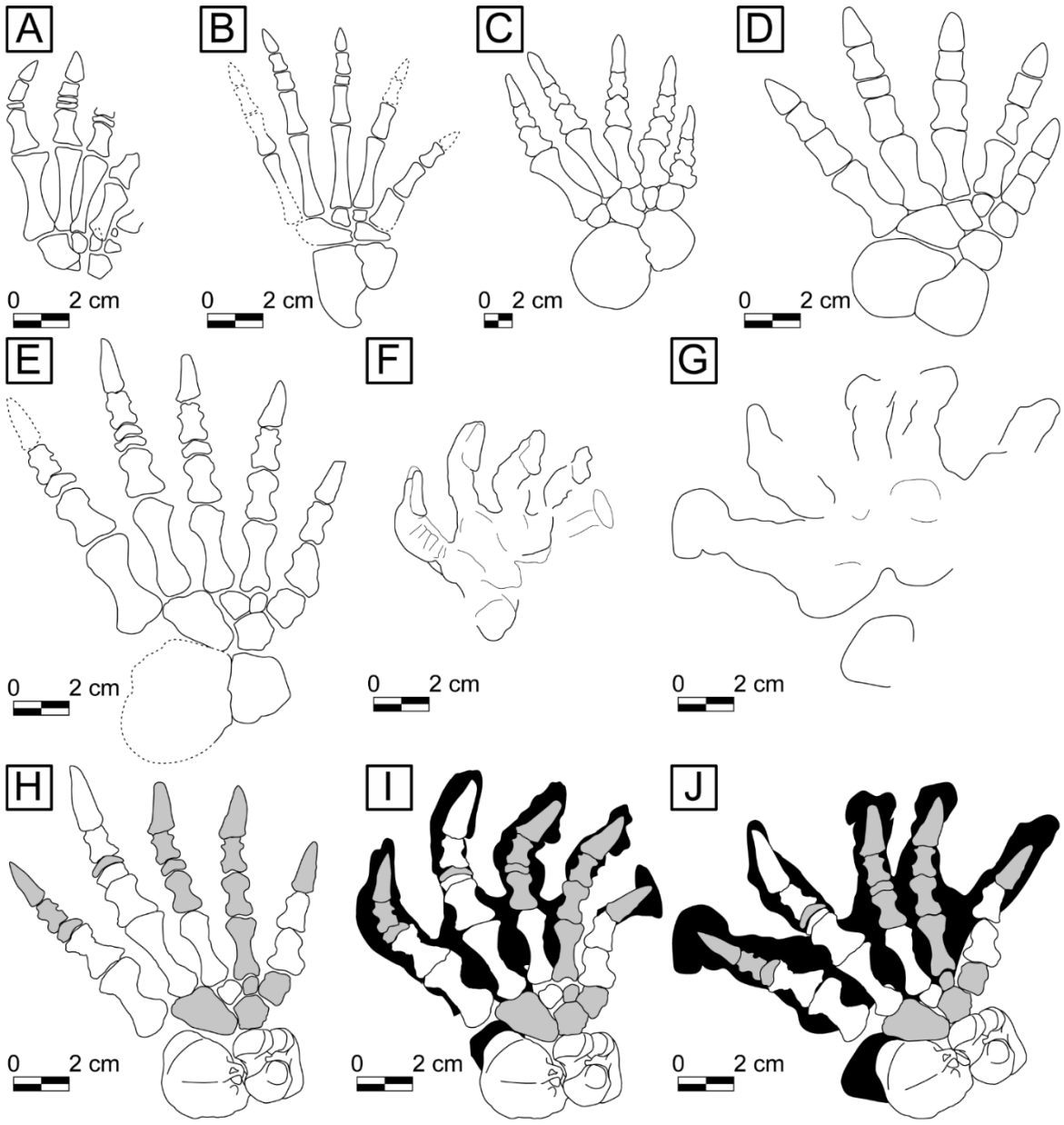

Figure 6. Track-trackmaker correlation for the gorgonopsian tracks, igen. *et* isp. nov. **A–E:** Left pedes of biarmosuchian *Biarmosuchus tener* (**A**, redrawn and mirrored from Sigogneau & Tchudinov, 1972), biarmosuchian *Hipposaurus boonstrai* (**B**, redrawn and mirrored from Boonstra, 1956), dinocephalian *Titanophoneus potens* (**C**, redrawn and mirrored from Orlov, 1958), gorgonopsian *Lycaenops ornatus* (**D**, redrawn from Colbert, 1948), Gorgonopsia indet. (**E**, redrawn and mirrored from Sidor, 2022). **F, G:** Pes tracks of the morphotype herein studied, including the best-preserved (**F**) and largest (**G**) specimens. **H:** Reconstructed left pes of the gorgonopsian from Mallorca (DA21/17-01-01, grey elements are missing from the original specimen, some are mirrored; see details in **Appendix 5** of the present dissertation). **I, J:** Correlation and reconstruction of the gorgonopsian pes from Mallorca on pedes of the morphotype herein studied; note that track in **I** is enlarged to fit with the bones and track and bones in **J** are at the same scale.

Apart from tetrapod tracks, the Port des Canonge Formation contains several bone beds that have produced remains of different tetrapod taxa. Particularly interesting is a partial skeleton of a gorgonopsian therapsid that has been found 46 m stratigraphically below the tracksite containing the morphotype herein studied, (**Appendix 5** of the present dissertation; **Figure 1B**). This specimen (DA21/17-01-01) preserves several elements of the left and right pedes, allowing for a nearly complete reconstruction of the pes (**Figure 6H**). Such reconstruction, with the missing elements taken from Sidor (2022), fits exactly with the tracks of the morphotype herein studied: in the tracks depicted in **Figures 2** and **3B** the only difference is size (**Figure 6I**), but in the largest track (**Figure 4A**) and the surface with the trackway composed of large tracks (**Figure 4B**) the bones fit also in size (**Figure 6J**). This provides a reasonably confident correlation of the pes tracks and skeletons. In addition, the complete overstepping of the pes tracks to the manus tracks of the morphotype herein studied (**Figure 5A**) might be in agreement with the proportionally long hindlimbs inferred for the gorgonopsian of Mallorca (**Appendix 5** of the present dissertation).

5.3. Locomotion

Therapsid synapsids developed a suite of morphological innovations from the basal "pelycosaur" body plan. Those affected different aspects of their biology, including, among others, a more specialised dentition, the possible presence of a soft secondary palate and more complex nasoturbinals, the beginning of reorganisation of the bones associated to sound reception, and the modification of girdle joints, shifting from a sprawled to a more upright posture (Kemp, 2006).

This change of posture had a profound impact on the locomotion and, as a consequence, on the track arrangement in the produced trackways (Kubo & Benton, 2009). The study of the girdle joints of early therapsids suggests that their front legs were still anatomically constrained to adopt a sprawled posture, whereas the hind legs could facultatively switch between a sprawled and a more upright posture (Kemp, 1982, 2005). Therefore, early therapsids could produce trackways with low pace angulation values and wide gauges, similar to those made by "pelycosaurs" and other amniotes, but they also were able to move with a narrower gauge and a wider pace angulation (Marchetti *et al.*, 2019a; Matamales-Andreu *et al.*, 2021).

The potentially new ichnotaxon reported herein, based on at least two preserved trackways of different size, shows a distinctly narrow gauge and a wide pace angulation (**Figure 5A**), especially when compared to other latest Cisuralian–early Guadalupian ichnotaxa attributed to synapsids (see Marchetti *et al.*, 2019a). The Permian ichnogenera *Capitosauroides* and *Karoopes*, with tracks reminiscent to the morphotype herein studied (**Figure 5**), show trackway values indicative of a different locomotion style (see Marchetti *et al.*, 2019a, 2022; Buchwitz *et al.*, 2020), possibly with a more sprawled posture in both the front and hind legs. This is especially interesting in the case of *Karoopes*, which has been attributed to large-sized gorgonopsians (Marchetti *et al.*, 2019a). A remarkable feature of the trackways of the morphotype herein studied is the complete overstepping of the pes to the manus tracks, plus the strong inward rotation of the manus imprints. This combination of unusual distribution among early therapsid trackways (*e.g.*, Marchetti *et al.*, 2019a) can be explained by a proportionally long hind leg of the producer

(as observed in the gorgonopsian of Mallorca: **Appendix 5** of the present dissertation) and the anatomical constraint of the front legs to a sprawled posture (Kemp, 1982, 2005).

Overall, such trackway variability in an otherwise morphologically conservative group is striking, but it could be explained by the effect of size and stoutness, as well as by slight morphological variations on the leg and manus/pes structure among species. Most of the studies on gorgonopsian anatomy have focused on the skull remains, and the postcrania of most species remain undescribed or are yet to be found, so this question cannot be solved at present. In any case, the correlation of the morphotype herein studied to gorgonopsian trackmakers proposed herein confirms that the ability to walk in an upright posture had been already acquired in the earliest middle Permian by, at least, some species of medium-sized gorgonopsians.

6. Conclusions

The present paper has described a new tetrapod ichnotaxon from the palaeoequatorial Permian of Mallorca (western Mediterranean), gorgonopsian tracks, igen. *et* isp. nov., correlating it to gorgonopsian therapsid trackmakers. This attribution has been possible thanks to the gorgonopsian pes bones present in the same section and formation, which match the pes tracks almost exactly in terms of morphology, proportions and size. The tracks herein described are among the oldest ichnofossils confidently attributed to therapsid trackmakers, as they date to the lower/?middle Permian. Despite its age, the trackway parameters, with narrow gauges and wide pace angulation values, show that the trackmakers walked in an upright posture and parasagittal gait. This suggests that lower/?middle Permian therapsids had already acquired part of the anatomical modifications that contributed to the shift from sprawled posture, typical of sauropsids and "pelycosaur"-grade synapsids, to the upright posture that would characterise the derived therapsids, *i.e.*, mammals and their kin.

7. Acknowledgements

The authors of the present paper thank Sebastià Matamalas, Josep Juárez and Chabier De Jaime-Soguero for aid in fieldwork. We are grateful to Christian F. Kammerer for fruitful discussions. To the Comissió Insular de Patrimoni Històric (Consell Insular de Mallorca) for granting us the excavation permits (file number 75/2021). R.M.A. was supported by the predoctoral grant FPU17/01922 (Ministerio de Ciencia, Innovación y Universidades) and the grant Synthesys+ DE-TAF-23 (European Commission). It has been further supported by the Generalitat de Catalunya (CERCA Programme and consolidated research groups 2021 SGR 01184 to J.F. and 2021 SGR 01192 to À.G.). This work is part of the Ramon y Cajal grant to J.F. [RYC2021-032857-I] financed by MCIN/AEI/10.13039/501100011033 and the European Union 'NextGenerationEU'/PRTR. We acknowledge support from the project "Mallorca abans dels dinosaures: estudi dels ecosistemes continentals del Permià i Triàsic amb especial èmfasi en les restes de vertebrats" (ref. 15 - 619/2020), based at the Institut Català de Paleontologia Miquel Crusafont and funded by the Departament de Cultura, Patrimoni i Política Lingüística (Consell Insular de Mallorca).

8. References

Boonstra, L.D. (1964). The girdles and limbs of the pristerognathid therocephalia. *Annals of the South African Museum*, 48(5): 121–165 + 1 pl.

Boonstra, L.D. (1965). The girdles and limbs of the Gorgonopsia of the *Tapinocephalus* Zone. *Annals of the South African Museum*, 48(13): 237–249.

Boonstra, L.D. (1966). The dinocephalian manus and pes. *Annals of the South African Museum*, 50(2): 13–26.

Buchwitz, M.; Marchetti, L.; Jansen, M.; Falk, D.; Trostheide, F. & Schneider, J.W. (2020). Ichnotaxonomy and trackmaker assignment of tetrapod tracks and swimming traces from the middle Permian Hornburg Formation of Saxony-Anhalt (Germany). *Annales Societatis Geologorum Poloniae*, 90: 291–320.

Calábková, G.; Březina, J.; Nosek, V. & Madzia, D. (2023). Synapsid tracks with skin impressions illuminate the terrestrial tetrapod diversity in the earliest Permian of equatorial Pangea. *Scientific Reports*, 13: 1130.

Colbert, E.H. (1948). The mammal-like reptile *Lycaenops*. *Bulletin of the American Museum of Natural History*, 89(6): 353–404.

Day, M.O. & Rubidge, B.S. (2021). The late Capitanian mass extinction of terrestrial vertebrates in the Karoo Basin of South Africa. *Frontiers in Earth Science*, 9: 631198.

Day, M.O.; Ramezani, J.; Bowring, S.A.; Sadler, P.M.; Erwin, D.H.; Abdala, F. & Rubidge, B.S. (2015). When and how did the terrestrial mid-Permian mass extinction occur? Evidence from the tetrapod record of the Karoo Basin, South Africa. *Proceedings of the Royal Society B*, 282: 20150834.

Gebauer, E.V.I. (2014). Re-assessment of the taxonomic position of the specimen GPIT/RE/7113 (*Sauroctonus parringtoni* comb. nov., Gorgonopsia). *In*: Kammerer, C.F.; Angielczyk, K.D. & Fröbisch, J. (Eds.). *Early Evolutionary History of the Synapsida*. Springer; Dordrecht, Heidelberg, New York, London: 185–207.

Goehring, L.; Conroy, R.; Akhter, A.; Clegg, W.J. & Routh, A.F. (2010). Evolution of mud-crack patterns during repeated drying cycles. *Soft Matter*, 6: 3562–3567.

Ivakhnenko, M.F. (2003). Eotherapsids from the East European Placket (late Permian). *Paleontological Journal*, 37(4): S339–S465.

Kammerer, C.F. (2016). Systematics of the Rubidgeinae (Therapsida: Gorgonopsia). *PeerJ*, 4: e1608.

Kammerer, C.F. & Masyutin, V. (2018). Gorgonopsian therapsids (*Nochnitsa* gen. nov. and *Viatkogorgon*) from the Permian Kotelnich locality of Russia. *PeerJ*, 6: e4954.

Kammerer, C.F. & Rubidge, B.S. (2022). The earliest gorgonopsians from the Karoo Basin of South Africa. *Journal of African Earth Sciences*, 194: 104631.

Kemp, T.S. (1982). *Mammal-like reptiles and the origin of mammals*. Academic Press; New York. xiv + 364 pp.

Kemp, T.S., 2005. *The origin and evolution of mammals*. Oxford University Press; New York, Auckland, Bangkok, Buenos Aires, Cape Town, Chennai, Dar es Salaam, Delhi, Hong Kong, Istanbul, Karachi, Kolkata, Kuala Lumpur, Madrid, Melbourne, Mexico City Mumbai, Nairobi, São Paulo, Shanghai, Taipei, Tokyo, Toronto. x + 331 pp.

Kemp, T.S. (2006). The origin and early radiation of the therapsid mammal-like reptiles: a palaeobiological hypothesis. *Journal of Evolutionary Biology*, 19(4): 1231–1247.

Kubo, T. & Benton, M.J. (2009). Tetrapod postural shift estimated from Permian and Triassic trackways. *Palaeontology*, 52(5): 1029–1037.

Leonardi, G. (1987). *Glossary and Manual of Tetrapod Footprint Palaeoichnology*. Departamento Nacional de Produção Mineral, Brasília. 117 pp.

Liebrecht, T.; Fortuny, J.; Galobart, À.; Müller, J. & Sander, P.M. (2017). A large, multiple-tooth-rowed captorhinid reptile (Amniota: Eureptilia) from the Upper Permian of Mallorca (Balearic Islands, Western Mediterranean). *Journal of Vertebrate Paleontology*, 37(1): e1251936.

Liu, J. & Yang, W. (2022). A gorgonopsian from the Wutonggou Formation (Changhsingian, Permian) of Turpan Basin, Xinjiang, China. *Palaeoworld*, 31: 383-388.

Logghe, A.; Mujal, E.; Marchetti, L.; Nel, A.; Pouillon, J.-M.; Giner, S.; Garrouste, R. & Steyer, J.-S. (2021). *Hyloidichnus* trackways with digit and tail drag traces from the Permian of Gonfaron (Var, France): New insights on the locomotion of captorhinomorph eureptiles. *Palaeogeography, Palaeoclimatology, Palaeoecology*, 573: 110436.

Marchetti, L.; Mujal, E. & Bernardi, M. (2017). An unusual *Amphisauropus* trackway and its implication for understanding seymouriamorph locomotion. *Lethaia*, 50: 162–174.

Marchetti, L.; Belvedere, M.; Voigt, S.; Klein, H.; Castanera, D.; Díaz-Martínez, I.; Marty, D.; Xing, L.; Feola, S.; Melchor, R.N. & Farlow, J.O. (2019b). Defining the morphological quality of fossil footprints. Problems and principles of preservation in tetrapod ichnology with examples from the Palaeozoic to the present. *Earth-Science Reviews*, 193: 109–145.

Marchetti, L.; Klein, H.; Buchwitz, M.; Ronchi, A.; Smith, R.M.H.; De Klerk, W.J.; Sciscio, L. & Groenewald, G.H. (2019a). Permian-Triassic vertebrate footprints from South Africa: Ichnotaxonomy, producers and biostratigraphy through two major faunal crises. *Gondwana Research*, 72: 139–168.

Marchetti, L.; Voigt, S. & Klein, H. (2019c). Revision of Late Permian tetrapod tracks from the Dolomites (Trentino-Alto Adige, Italy). *Historical Biology*, 31(6): 748–783.

Marchetti, L.; Voigt, S.; Mujal, E.; Lucas, S.G.; Francischini, H.; Fortuny, J. & Santucci, V.L. (2021). Extending the footprint record of Pareiasauromorpha to the Cisuralian: earlier appearance and wider palaeobiogeography of the group. *Papers in Palaeontology*, 7(3): 1297–1319.

Marchetti, L.; Logghe, A.; Mujal, E.; Barrier, P.; Montenat, C.; Nel, A.; Pouillon, J.-M.; Garrouste, R. & Steyer, J.S. (2022). Vertebrate tracks from the Permian of Gonfaron (Provence, Southern France) and their implications for the late Capitanian terrestrial extinction event. *Palaeogeography, Palaeoclimatology, Palaeoecology*, 599: 111043.

Matamales-Andreu, R.; Mujal, E.; Galobart, À. & Fortuny, J. (2021). Insights on the evolution of synapsid locomotion based on tetrapod tracks from the lower Permian of Mallorca (Balearic Islands, western Mediterranean). *Palaeogeography, Palaeoclimatology, Palaeoecology*, 579: 110589.

Matamales-Andreu, R.; Mujal, E.; Dinarès-Turell, J.; Kustatscher, E.; Roghi, G.; Oms, O.; Galobart, À. & Fortuny, J. (2022). Early-middle Permian ecosystems of equatorial Pangaea: integrated multi-stratigraphic and palaeontological review of the Permian of Mallorca (Balearic Islands, western Mediterranean). *Earth-Science Reviews*, 228: 103948.

Mujal, E.; Marchetti, L.; Schoch, R.R. & Fortuny, J. (2020). Upper Paleozoic to lower Mesozoic tetrapod ichnology revisited: photogrammetry and relative depth pattern inferences on functional prevalence of autopodia. *Frontiers in Earth Science*, 8:248, 1–23.

Orlov, J.A. (1958). [Predatory dinocephalians from the Isheevo Fauna (titanosuchians)]. *Trudy Paleontologicheskogo Instituta, Akademiya Nauk SSSR*, 72: 1–114. [in Russian]

Piñeiro, G.; Marchetti, L.; Mármol, S.; Celio, A.; Xavier, P.; Francia, M. & Schultz, C. (2022). Enigmatic wood and first evidence of tetrapods in the Yaguarí Formation (Middle-Late Permian), Uruguay. *Agrociencia Uruguay*, 26(NE1): e504.

Romer, A.S. (1956). *Osteology of the Reptiles*. University of Chicago Press; Chicago, London. 772 pp.

Sidor, C.A. (2022). New information on gorgonopsian pedal morphology based on articulated material from Zambia. *Journal of African Earth Sciences*, 191: 104533.

Sigogneau, D. (1970). *Révision systématique des gorgonopsiens sud-africains*. Centre National de la Recherche Scientifique; Paris. 417 pp.

Sigogneau-Russell, D. (1989). *Handbuch der Paläoherpetologie / Encyclopedia of Paleoherpetology. Teil 17 B/I / Part 17 B/I: Theriodontia I. Phthinosuchia, Biarmosuchia, Eotitanosuchia, Gorgonopsia*. Gustav Fischer Verlag; Stuttgart, New York. 127 pp.

Sigogneau, D. & Tchudinov, P.K. (1972). Reflections on some Russian eotheriodonts (Reptilia, Synapsida, Therapsida). *Palaeovertebrata*, 5: 79–109.

Smiley, T.M.; Sidor, C.A.; Maga, A. & Ide, O. (2008). The vertebrate fauna of the upper Permian of Niger. VI. First evidence of a gorgonopsian therapsid. *Journal of Vertebrate Paleontology*, 28(2): 543–547.

Smith, R.M.H.; Sidor, C.A.; Tabor, N.J. & Steyer, J.S. (2015). Sedimentology and vertebrate taphonomy of the Moradi Formation of northern Niger: A Permian wet desert in the tropics of Pangaea. *Palaeogeography, Palaeoclimatology, Palaeoecology*, 440: 128–141.

Smith, R.M.H.; Rubidge, B.S.; Day, M.O. & Botha, J. (2020). Introduction to the tetrapod biozonation of the Karoo Supergroup. *South African Journal of Geology*, 123(2): 131–140.

Tatarinov, L.P. (1974). [Terriodont of USSR]. *Trudy Paleontologicheskogo Instituta, Akademiya Nauk SSSR*, 143: 1–226. [in Russian]

Voigt, S. (2005). *Die Tetrapodenichnofauna des kontinentalen Oberkarbon und Perm im Thüringer Wald - Ichnotaxonomie, Paläoökologie und Biostratigraphie*. Cuvillier Verlag, Göttingen. 308 pp.

Voigt, S.; Berman, D.S. & Henrici, A.C. (2007). First well-established track-trackmaker association of paleozoic tetrapods based on *Ichniotherium* trackways and diadectid skeletons from the Lower Permian of Germany. *Journal of Vertebrate Paleontology*, 27(3): 553–570.

Ward, P.D.; Botha, J.; Buick, R.; De Kock, M.O.; Erwin, D.H.; Garrison, G.H.; Kirschvink, J.L. & Smith, R. (2005). Abrupt and gradual extinction among late Permian land vertebrates in the Karoo Basin, South Africa. *Science*, 307: 709–714.

Appendix 7

Supplementary Material, continental Triassic of Mallorca

Appendix 7 was published as the supplementary material of:

Matamales-Andreu, R.; Peñalver, E.; Mujal, E.; Oms, O.; Scholze, F.; Juárez, J.; Galobart, À. & Fortuny, J. (2021). Early–Middle Triassic fluvial ecosystems of Mallorca (Balearic Islands): Biotic communities and environmental evolution in the equatorial western peri-Tethys. *Earth-Science Reviews*, 222: 103783.

DOI: https://doi.org/10.1016/j.earscirev.2021.103783

Also, refer to:

Chapter 3: Matamales-Andreu *et al.* (2021), *Earth-Science Reviews*

APPENDIX A. SUPPLEMENTARY DATA

Early–Middle Triassic fluvial ecosystems of Mallorca (Balearic Islands): biotic communities and palaeoenvironmental evolution in the equatorial western peri-Tethys

Rafel Matamales-Andreu[a,b,*], Enrique Peñalver[c], Eudald Mujal[a,d], Oriol Oms[e], Frank Scholze[f], Josep Juárez[b], Àngel Galobart[a,g] & Josep Fortuny[a]

[a] Institut Català de Paleontologia Miquel Crusafont, Universitat Autònoma de Barcelona, Edifici ICTA-ICP, c/ Columnes s/n, Campus de la UAB, 08193 Cerdanyola del Vallès, Barcelona, Spain.

[b] Museu Balear de Ciències Naturals, ctra. Palma-Port de Sóller km 30, 07100 Sóller, Mallorca, Illes Balears, Spain.

[c] Instituto Geológico y Minero de España (Museo Geominero), c/ Cirilo Amorós 42, 46004 València, València, Spain.

[d] Staatliches Museum für Naturkunde Stuttgart, Rosenstein 1, 70191 Stuttgart, Germany.

[e] Departament de Geologia, Universitat Autònoma de Barcelona, av. de l'Eix Central s/n, Campus de la UAB, 08193 Cerdanyola del Vallès, Barcelona, Spain.

[f] Institut für Geowissenschaften, Friedrich-Schiller-Universität Jena, Burgweg 11, 07749 Jena, Germany.

[g] Museu de la Conca Dellà, c/ del Museu 4, 25650 Isona i Conca Dellà, Lleida, Spain.

*Corresponding author: rafel.matamales@icp.cat

Supplementary Text 1. Previous works

Hermite (1879, 1888) and Lozano (1884) were the first authors to carry out a detailed geological survey near Cala d'Estellencs, attributing the red-beds there cropping out to the Lower Triassic based on the finding of purported specimens of the horsetail plant *Equisetum arenaceum* Brogniart, 1828. Subsequent works, such as those by Nolan (1887, 1888), Darder (1914) and Fallot (1922), somewhat increased the knowledge on the red-beds near Estellencs, Banyalbufar, Port des Canonge and Port de Valldemossa, without supplying any further evidence to infer their age. It was not until several decades later that Cuevas-López (1958a, 1958b) put forward the hypothesis that only part of the red-beds could be assigned to the Triassic (which he named lower, middle and upper *Buntsandstein*), the bulk of them actually belonging to the Permian (*Rothliegende*, *Zechstein* + *Kupferschiefer*) (Supplementary Table 1). This proposal was in part followed by Pomar-Gomà (1979), Martí *et al*. (1985), Rodríguez-Perea *et al*. (1987) and Barnolas (1991a, 1991b), who accepted that the lowermost units of the sequence could be of Permian age. Concurrently, Ramos *et al*. (1985) attempted to provide a lithostratigraphic framework for the red-beds of Mallorca, but the lithological similarity of some Permian and Triassic units led to miscorrelations that ultimately rendered that scheme unusable. Calvet & Marzo *in* Santanach (1986) reproduced that framework with very small changes. Banda *et al*. (1986) performed preliminary palaeomagnetic analyses on some beds of Cala d'Estellencs, and concluded that the natural remanent magnetisation characteristic directions were similar to the ones of the *Buntsandstein* facies of Menorca and the Catalan Coastal Ranges (further discussed by Parés *et al*., 1989, 1992a, 1992b).

Calafat (1986, 1987, 1988) carried out a comprehensive stratigraphic and sedimentological study on the red-beds of Mallorca (both Permian and Triassic), distinguishing several lithostratigraphic units (Supplementary Table 1). By means of the study of the fossil palynomorphs, the two uppermost units (Estellencs Sandstone and Lutite Unit and Son Serralta Lutite Unit), cropping out between the Cala d'Estellencs and the Punta de Son Serralta, were attributed to the Anisian (Middle Triassic). They were interpreted to represent floodplains (sporadically inundated) traversed by braided sandy rivers. Further palynological analyses were performed by several authors (Ramos & Doubinger, 1989; Grauvogel-Stamm & Álvarez-Ramis, 1994, 1996; Ramos, 1995; Diez, 2000; Diez *et al*., 2005, 2010), confirming an Anisian age (Aegean to Pelsonian) for several horizons of those two units.

Calafat (1988) also recorded and illustrated well-preserved fossil plants in the Estellencs Sandstone and Lutite Unit (Supplementary Table 1), from which Bauzá (1971, 1981) had reported *Equisetum arenaceum* and other plant remains several years before. The specimens mentioned by Calafat (1988) were later studied in detail by Álvarez-Ramis *et al*. (1989, 1995) and Grauvogel-

Stamm & Álvarez-Ramis (1994, 1996), recognising an assemblage of plants with representation of the clades Pteridophylla, Articulata, Cycadophyta, Ginkgophyta and Coniferophyta (with *in situ* pollen that allowed the description of a new species of cone: *Willsiostrobus hexasacciphorus* Grauvogel-Stamm & Álvarez-Ramis, 1996). The study of those fossil plants was recently resumed by Juárez-Ruiz & Wachtler (2015), describing a rich palaeobotanical assemblage including several new taxa (*Estellencsia saezii* Juárez-Ruiz & Wachtler, 2015; *Ortiseia collii* Juárez-Ruiz & Wachtler, 2015; and *Sagenopteris nadalii* Juárez-Ruiz & Wachtler, 2015).

On one of the uppermost sandstone beds of the Estellencs Sandstone and Lutite Unit, Calafat *et al.* (1986, 1986–1987) and Calafat (1988) reported the presence of several circular, concave structures of 30–40 cm of diameter, which were thought to correspond to very large tetrapod ichnites (named 'ichnites of the upper stretch' in Calafat *et al.*, 1986; 'type D ichnites' in Calafat *et al.*, 1986–1987; and 'type E ichnites' in Calafat, 1988). In the present work, they are reinterpreted as some kind of non-biological sedimentary structures (see Supplementary Figure 1). Moreover, Juárez-Ruiz & Wachler (2015) figured a trackway consisting of two small ichnites from the lower beds of the Estellencs Sandstone and Lutite Unit (Supplementary Table 1), which they identified as *Rhynchosauroides* isp. (here illustrated in Figure 5C of the main text). The other icnites that these authors illustrated (purported *Rotodactylus* isp.), come from the Racó de s'Algar site and are thus of Permian age (Calafat, 1988; Ramos & Doubinger, 1989).

Calafat & Sáez (1987) and Calafat (1988) also reported the presence of well-preserved crustaceans, insects and a fish in some lutitic beds of the Estellencs Sandstone and Lutite Unit (Supplementary Table 1). Specifically, they mentioned the abundant presence of clam shrimps ("conchostracans") (here illustrated in Figure 6A of the main text), and sporadic findings of larval and adult stages of insects that purportedly belonged to the orders Coleoptera, Lepidoptera and Ephemeroptera (Shcherbakov *et al.*, 1995 considered that one of the illustrated specimens could also belong to the order Diptera)[1]. Calafat & Sáez (1987) and Calafat (1988) also found a small fish of unknown affinities (here illustrated in Figure 9 of the main text). Those beds were resampled by Ansorge (1997), who reported three wings of the order "Blattaria". Several years later, Zessin (2008a, 2008b) listed the presence of clam shrimps (*Euestheria* sp.), insects of the orders "Blattaria", Coleoptera, Diptera, Heteroptera, (?)Megaloptera, Homoptera and (?)Orthopteroidea, indeterminate insect traces and hybodontid egg capsules (*Palaeoxyris* isp.). From the same beds, Aristov & Zessin (2009) described a new grylloblattid species: *Mallorcagryllus hispanicus* Aristov & Zessin, 2009. Additionally, some of the crustaceans and

[1] The purported coleopteran, which was figured in quite a poor quality by Calafat (1988), has not been detected by the authors of the present work in the Tomeu Sáez collection; the lepidopteran is in fact a mayfly (see Figure 7B–C of the main text); and the dipteran sensu Shcherbakov *et al.* (1995), herein figured in Supplementary Figure 2A–B, is actually a mayfly as well.

insects originally illustrated in Calafat (1988) were refigurated by Gallemí *in* Gallemí (1988), Martínez *in* Gallemí (1988) and Juárez-Ruiz & Wachtler (2015), without commenting them further.

The most recent detailed works concerning the Lower–Middle Triassic *Buntsandstein* facies of Mallorca are the ones by Gómez-Gras (1992, 1993) and Ramos (1995). The latter followed the framework proposed by Ramos *et al.* (1985), and thus the interpretations presented therein ought to be considered with caution given the confusion with the correlation of the different lithostratigraphic units (see above). It is also important to note that subsequent reviews (Arche *et al.*, 2002; López-Gómez *et al.*, 2002, 2019; Vera *et al.*, 2004; Bourquin *et al.*, 2007, 2011; Cassinis *et al.*, 2012) were also based on this conception. In any case, Ramos (1995) asserted that the succession represented by the 65 m-thick Son Serralta lutites and sandstones (Supplementary Table 1) corresponded to a distal braidplain depositional setting transitioning towards a marine influenced plain just after the first appearance of the *Muschelkalk* facies. Conversely, Gómez-Gras (1992, 1993) reinterpreted the whole red-bed sequence of Mallorca, including in his study some outcrops that Calafat (1988) had not considered due to their inaccessibility. Gómez-Gras (1992, 1993) divided the Triassic succession of Mallorca in four different units (Supplementary Table 1): 'Stretch d', which had been considered of Permian age until then (Calafat, 1988), and 'Stretch e', which was in turn divided in three: a lower part with abundance of red lutites and sandstones, a middle part constituted mainly by whitish sandstones, and an upper part constituted by red lutites. The 'Stretch d' was interpreted as braided rivers, whereas all the subunits of the 'Stretch e' were thought to represent floodplains and meandering rivers. The thickest sandstone packs would represent intervals of little accommodation space generation, prompting the amalgamation of the meandering bars that could be mistaken for braided river deposits. Finally, inter- and supratidal structures in the uppermost subunit would anticipate the transition to the *Muschelkalk* shallow marine platforms (Gómez-Gras, 1992, 1993).

Supplementary Figures and Tables

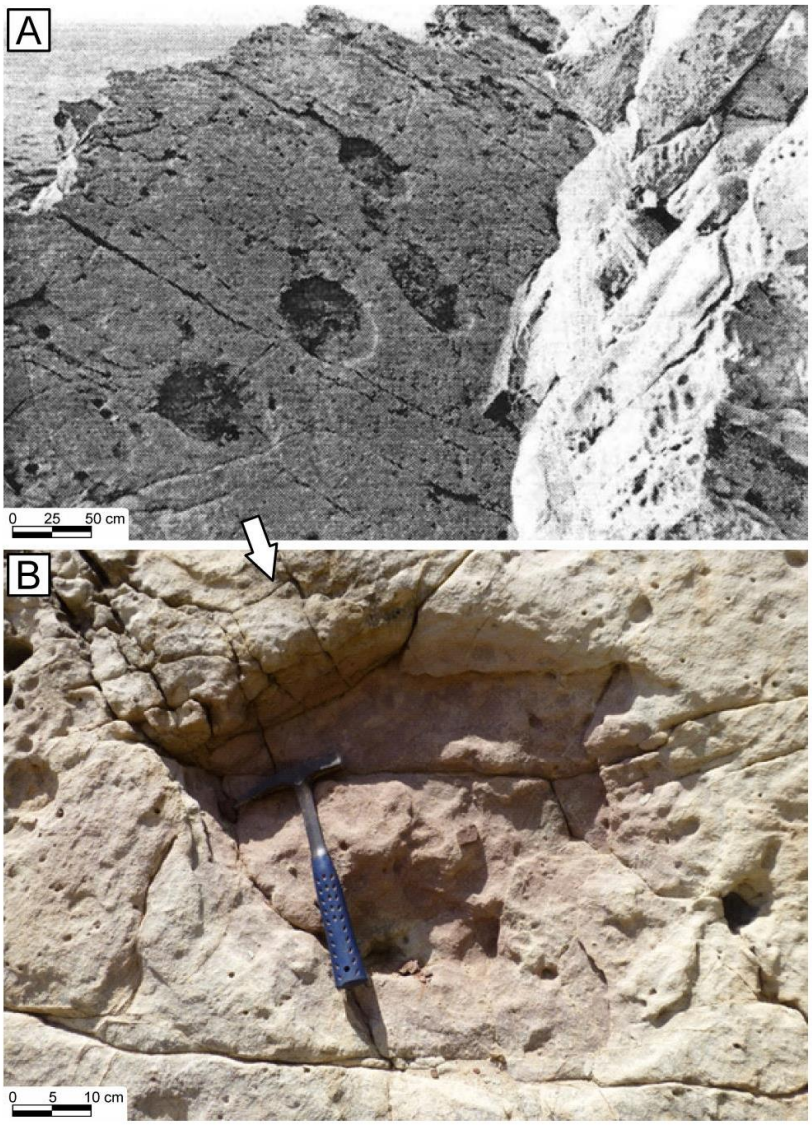

Supplementary Figure 1. A: Sedimentary structures called 'ichnites of the upper stretch' by Calafat *et al.* (1986), 'type D ichnites' by Calafat *et al.* (1986–1987) and 'type E ichnites' by Calafat (1988), metre 5.2 of the Tenassa de sa Tanca log (see Supplementary Logs). They are not ichnites, given their very large size and the lack of expulsion rims or any distinct pes or manus-like shape. Nowadays, most of them are covered by large boulders and complete observation has not been possible. Picture courtesy of Feliu Calafat, taken in mid 1980s. **B:** Detailed picture of the current aspect of one of the structures shown in A. Specifically, this picture corresponds to the one in the bottom-left-hand-corner.

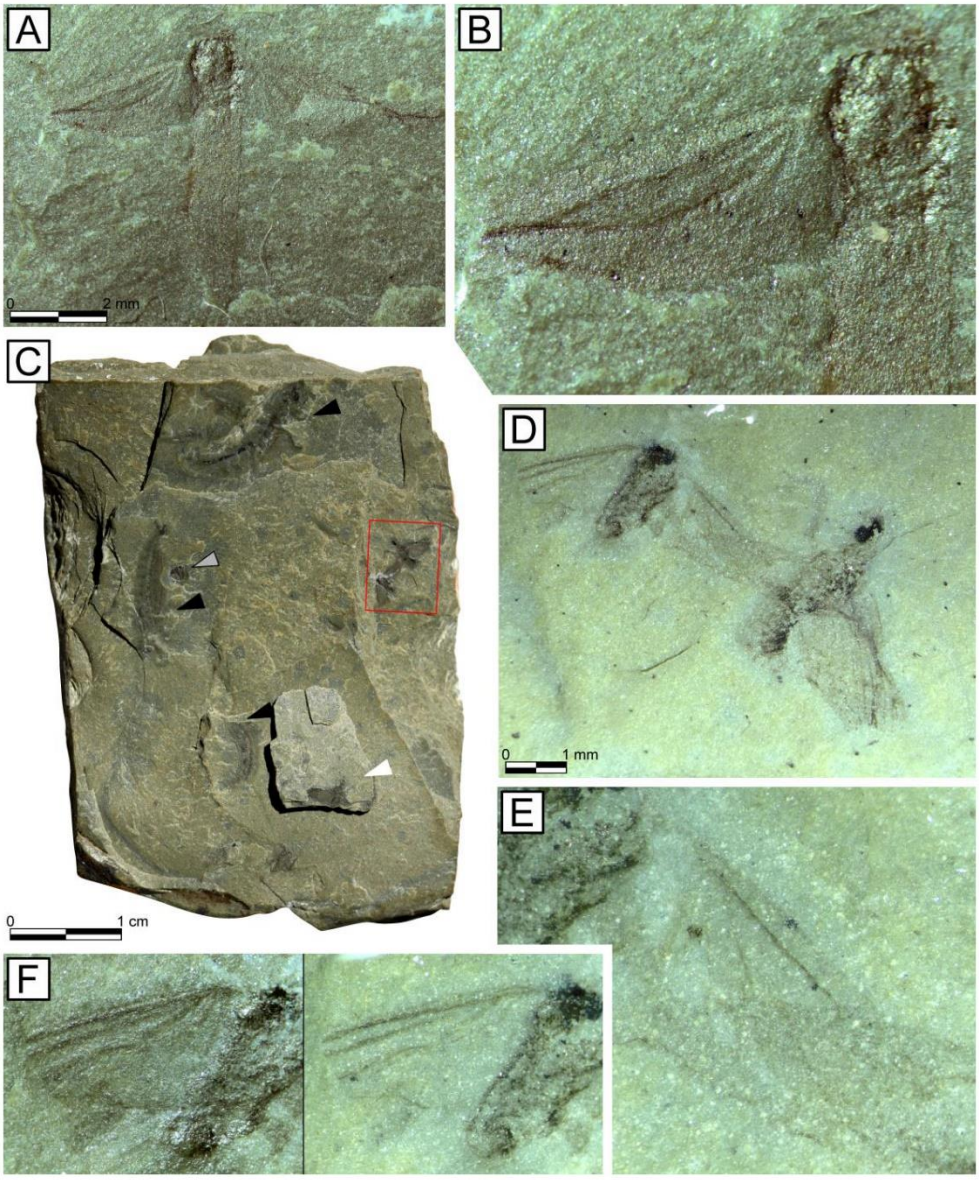

Supplementary Figure 2. Adult mayflies from Pedra Alta section, upper part of the Estellencs Formation, Aegean. **A–B:** Habitus and left forewing detail of the specimen in TS-B-1 figured by Calafat (1988) and misinterpreted as a dipteran by Shcherbakov *et al.* (1995). **C:** Slab TS-G (part) with a flake of the counterpart (white arrowhead: note an adult specimen in the flake) on top (black arrowheads indicate three nymphs and grey arrowhead indicates a clam shrimp). **D–F:** Adult morphotype 1 (family indet.), TS-G-1a and TS-G-2, adult specimens (see red square in C and partial counterpart of one specimen in the flake) and details of the fore wings (F shows the same forewing photographed using tangential light and under alcohol, respectively). Photographs D–F (right) taken with the specimens wet with alcohol. Scale of B referred to graphic scale in A, and of E and F referred to graphic scale in D.

Supplementary Table 1. Synonymy of the different names for the Middle Triassic *p.p.* units (*Buntsandstein* facies) of Mallorca.

<table>
<tr><th>Cuevas-López (1958a, 1958b)</th><th>Pomar-Gomà (1979)</th><th>Martí et al. (1985)</th><th>Ramos et al. (1985), Ramos & Doubinger (1989)</th><th>Calvet & Marzo in Santanach et al. (1986)</th><th>Calafat (1986), Calafat et al. (1987)</th><th colspan="2">Calafat (1987)</th><th>Rodríguez-Perea et al. (1987)</th><th colspan="2">Calafat (1988), Álvarez-Ramis et al. (1995), Gauvogel-Stamm & Álvarez-Ramis (1996), Diez (2000), Juárez-Ruiz & Wachtler (2015)</th><th>Barnolas (1991a, 1991b)</th><th colspan="2">Gómez-Gras (1992, 1993)</th><th>Ramos (1995), Arche et al. (2002), López-Gómez et al. (2002, 2019), Vera et al. (2004), Bourquin et al. (2007, 2011), Cassinis et al. (2012)</th><th>The present work</th><th></th></tr>
<tr><td colspan="14">Middle Triassic Muschelkalk facies</td><td>TRIASSIC</td></tr>
<tr><td>Level V, top (100 m)</td><td rowspan="4">(not studied)</td><td rowspan="5">(not studied)</td><td>Son Serralta Lutites and Sandstones (65 m)</td><td>Son Serralta Lutites and Sandstones (120 m)</td><td>Transit unit (25 m)</td><td colspan="2">Son Serralta Lutite formation (27 m)</td><td rowspan="4">(not studied)</td><td colspan="2">Son Serralta Lutite Unit (27 m)</td><td rowspan="4">(not studied)</td><td rowspan="2">Stretch e) (160 m)</td><td>Upper Pelites and Sandstones</td><td>Son Serralta Lutites and Sandstones (65 m)</td><td>Son Serralta Formation (22 m)</td><td></td></tr>
<tr><td>Level IV (40 m)</td><td rowspan="3">Asá Sandstones (140 m)</td><td rowspan="3">Pedra de s'Ase Sandstones (100 m)</td><td>Upper unit (100 m)</td><td colspan="2">Estellencs Sandstone and Lutite formation (124 m)</td><td colspan="2">Estellencs Sandstone and Lutite Unit (124 m)</td><td>Middle Sandstones</td><td rowspan="3">Asá Sandstones (110 m)</td><td>Pedra Alta Formation (48 m)</td><td></td></tr>
<tr><td>Level III (50–60 m)</td><td rowspan="2">Middle unit (100 m)</td><td rowspan="2">Pedra de s'Ase Sandstone formation (150 m)</td><td rowspan="2">Punta Roja Sandstone member (25 m)</td><td rowspan="2">Upper Pelite-Sandstone Stretch (≈80 m)</td><td rowspan="2">Pedra de s'Ase Sandstone Unit (150 m)</td><td rowspan="2">Punta Roja Sandstone Sub-Unit (25 m)</td><td>Lower Pelites and Sandstones</td><td>Estellencs Formation (55 m)</td><td></td></tr>
<tr><td>Level V, base (30–40 m)</td><td colspan="2">Stretch d) (58 m)</td><td>Punta Roja Formation (>53 m)</td><td></td></tr>
<tr><td>Level III (50–60 m)</td><td>Last Lutitic Stretch (≈80 m)</td><td rowspan="2">Pedra de s'Ase Sandstone member (125 m)</td><td>Red and green lutites (>20 m)</td><td colspan="2">Stretch c) (135 m)</td><td rowspan="3">(not studied here)</td><td>PERMIAN</td></tr>
<tr><td>Level II (200 m)</td><td>Light-coloured Sandstone Stretch (127 m)</td><td>Sandstone Stretch</td><td>Middle Light-Coloured Sandstones (127 m)</td><td>White and red sandstones (120 m)</td><td colspan="2">Stretch b) (110 m)</td></tr>
<tr><td rowspan="2">Level I (800 m)</td><td rowspan="2">Lower Lutitic Stretch (213 m)</td><td>Lower Pelitic Stretch</td><td rowspan="2">Port des Canonge Sandstones and Lutites (176 m)</td><td rowspan="2">Port d'es Canonge Sandstones and Lutites (260 m)</td><td>Lower unit (150–250 m)</td><td colspan="2">Racó de s'Algar Sandstone and Lutite formation (144 m)</td><td>Lower Sandstone-Pelitic Stretch (213 m)</td><td colspan="2">Racó de s'Algar Sandstone and Lutite Unit (144 m)</td><td>Red lutites (>100 m)</td><td colspan="2" rowspan="2">Stretch a) (403 m)</td><td rowspan="2">Port des Canonge Sandstones and Lutites (160 m)</td><td rowspan="2"></td><td></td></tr>
<tr><td>Polygenic Breccia</td><td>Basal unit (10 m)</td><td colspan="2">Bec de s'Àguila Sandstone and Conglomerate formation (25 m)</td><td>Basal Conglomerate-Sandstone Stretch (<20 m)</td><td colspan="2">Bec de s'Àguila Sandstone and Conglomerate Unit (25 m)</td><td>(not studied)</td><td></td></tr>
<tr><td colspan="14">Carboniferous Culm facies</td><td></td></tr>
</table>

Supplementary Table 2. Measurements taken on the footprints herein studied. In brackets, measurements inferred on poorly defined imprints.

Determination	*Rhynchosauroides* isp. 1	Indeterminate morphotype		*Rhynchosauroides* isp. 2		Indeterminate morphotype				cf. *Prorotodactylus mesaxonichnus*	*Prorotodactylus mesaxonichnus*		cf. *Prorotodactylus mesaxonichnus*		*Rhynchosauroides* isp. 1	
Footprint slab field code	PN-7.6?-01	PN-7.6?-02		PN-7.6?-03		PN-7.6-01				PN-14.6-01	PN-14.6-02		PN-14.6-03		PN-14.7-01	
Figure	5A of main text	5H of main text		5C of main text		5G of main text				5F of main text	5D of main text		5E of main text		5B of main text	
Footprint letter	a	a	b	a	b	a	b	c	d	a	a	b	a	b	a	b
Anatomy	Right manus	Left ?manus	Right ichnite	Left manus	Left pes	Left manus	Left pes	Right manus	Right pes	Left manus	Left manus	Left pes	Left manus	Left pes	Left manus	?Left pes
Length (mm)	37.5	39.1	42.8	-	-	30.6	-	31.3	-	-	18.6	29.0	-	-	29.5	-
Width (mm)	29.5	30.7	44.3	-	23.6	37.6	-	-	-	21.6	15.6	18.6	-	-	22.6	-
Length palm/sole (mm)	24.3	21.4	-	-	-	18.3	-	16.2	-	-	9.2	(9.2)	-	-	15.7	-
Width palm/sole (mm)	14.7	24.6	-	-	-	28.4	-	-	-	-	(9.5)	-	-	-	12.8	-
Length I (mm)	4.5	8.3	13.1	-	-	10.1	-	-	-	-	4.1	8.6	5.5	7.1	5.0	-
Length II (mm)	10.4	14.2	-	-	-	11.2	-	8.5	-	8.7	8.1	15.3	6.9	8.8	13.3	-
Length III (mm)	14.0	18.2	-	-	-	14.2	-	15.0	-	(11.5)	9.6	20.6	7.9	-	15.1	-
Length IV (mm)	17.0	15.0	-	-	-	13.0	-	11.6	-	-	(7.8)	(19.3)	-	-	14.8	-
Length V (mm)	9.6	6.0	-	-	-	5.0	-	5.8	-	-	3.8	-	-	-	7.8	-
Divergence angle I–II (°)	36.0	82.8	6.9	(30.2)	(7.2)	23.8	-	-	-	-	50.8	9.9	(5.4)	7.9	28.0	-
Div. angle II–III (°)	38.8	17.8	-	(16.9)	(4.8)	31.3	-	28.8	-	25.9	18.5	9.8	(17.6)	5.5	25.5	-
Div. angle III–IV (°)	42.5	12.4	-	(26.8)	(27.8)	-	-	18.0	-	(19.3)	22.0	(4.7)	-	-	38.7	-
Div. angle IV–V (°)	29.7	-	-	-	-	62.5	-	64.6	-	-	37.2	(30.8)	-	-	33.0	-
Div. angle I–V (°)	-	113.9	-	-	-	123.5	-	-	-	-	128.5	(54.8)	-	-	125.1	-
Div. angle II–IV (°)	85.7	44.9	-	(46.5)	(29.9)	33.8	-	51.6	-	(42.4)	41.5	(11.3)	-	-	65.9	-
Div. angle II–V (°)	112.5	18.6	27.0	(43.4)	(31.1)	101.2	-	86.9	-	(51.5)	75.8	(51.4)	-	-	95.9	-

Supplementary Table 3. Review of all the age attributions to the Mallorcan Lower–Middle Triassic formations by previous works based on palynology.

Stratigraphic position \ Authors	**Calafat (1988)**	**Ramos & Doubinger (1989)**	**Grauvogel-Stamm & Álvarez-Ramis (1994, 1996)**	**Diez (2000)**	**Diez *et al.* (2005)**	**Diez *et al.* (2010)**	**Synthesis of all previous works**
Middle part of Son Serralta Formation (approximately m 35 of the TT log)	Anisian			Aegean–Pelsonian *[Revised from Calafat, 1988]*	Anisian *[Revised from Calafat, 1988]*	Anisian *[Revised from Calafat, 1988]*	Indeterminate Anisian
Lowermost part of Pedra Alta Formation (approximately m 37–42 of the PN log)				Aegean (perhaps upper Aegean)	Aegean *[Revised from Diez, 2000]*	Aegean *[Revised from Diez, 2000]*	Aegean
Upper part of Estellencs Formation (m 9.5 of the PI log and lateral equivalent at Platja de sa Marina)	Anisian		Anisian (perhaps lower Anisian)	Aegean–Pelsonian *[Revised from Calafat, 1988]*	Anisian *[Revised from Calafat, 1988]*	Lower Anisian *[Revised from Calafat, 1988]*	Aegean
Unknown bed, probably somewhere in the Son Serralta Formation (TT log)		Middle–upper Anisian, perhaps even lower Ladinian		Aegean–Pelsonian *[Revised from Ramos & Doubinger, 1989]*	Aegean–Pelsonian *[Revised from Ramos & Doubinger, 1989]*	Aegean–Pelsonian *[Revised from Ramos & Doubinger, 1989]*	Aegean–Pelsonian

Supplementary References

Álvarez-Ramis, C.; Solé, N. & Calafat, F. (1989). Paleoflora del Triásico inferior de Mallorca. *In*: *Abstracts of the II European Paleobotanical Conference*. Madrid: p. 12.

Álvarez-Ramis, C.; Fernández-Marrón, T. & Calafat, F. (1995). Avance sobre la megaflora triásica, en facies germánica, de Estellencs (sector noroccidental de la sierra de Tramontana, Mallorca). *Revista Española de Paleontología*, nº homenaje al Dr. Guillermo Colom: 55–58.

Ansorge, J. (1997). Insekten aus dem Buntsandstein (Untere Trias) von Mallorca (Spanien). *In*: *Abstracts für 4. Fachgespräch "Fossile Insekten"*. Clausthal-Zellerfeld: 1 pp.

Arche, A.; López-Gómez, J. & Vargas, H. (2002). Propuesta de correlación entre los sedimentos Pérmicos y Triásicos de la Cordillera Ibérica Este y de las Islas Baleares. *Geogaceta*, 32: 275–278.

Aristov, D. & Zessin, W. (2009). *Mallorcagryllus hispanicus* n. get. et sp. - eine neue Grylloblattide (Insecta: Grylloblattida: Blattogryllidae) aus dem Buntsadstein der Insel Mallorca, Spanien. *Virgo, Mitteilungsblatt des Entomologischen Vereins Mecklenburg*, 12(1): 30–34.

Banda, E.; Parés, J.M. & Freeman, R. (1986). La técnica del paleomagnetismo. Estudio piloto en los bordes de la cuenca balear. *Estudios Geológicos*, 42: 147–165.

Barnolas, A. (1991a). *Mapa Geológico de España. Escala 1:50.000. Andraitx*. Segunda serie, primera edición. Instituto Tecnológico GeoMinero de España, Madrid. 56 pp. + 1 map + 5 stratigraphic logs.

Barnolas, A. (1991b). *Mapa Geológico de España. Escala 1:50.000. Sóller*. Segunda serie, primera edición. Instituto Tecnológico GeoMinero de España, Madrid. 62 pp. + 1 map + 8 stratigraphic logs.

Bauzá, J. (1971). Ciento ochenta millones de años de la flora y fauna de Mallorca. *In*: Mascaró, J. (Coord.). *Historia de Mallorca*. Gráficas Miralles, Palma: 331–430.

Bauzá, J. (1981). Contribuciones a la paleontología de Mallorca. *Bolletí de la Societat d'Història Natural de Balears*, 25: 7–20.

Bourquin, S.; Durand, M.; Diez, J.B.; Broutin, J. & Fluteau, F. (2007). The Permian-Triassic boundary and Early Triassic sedimentation in Western European Basins: an overview. *Journal of Iberian Geology*, 33(2): 221–236.

Bourquin, S.; Bercovici, A.; López-Gómez, J.; Diez, J.B.; Broutin, J.; Ronchi, A.; Durand, M.; Arche, A.; Linol, B. & Amour, F. (2011). The Permian–Triassic transition and the onset of Mesozoic sedimentation at the northwestern peri-Tethyan domain scale: Palaeogeographic maps and geodynamic implications. *Palaeogeography, Palaeoclimatology, Palaeoecology*, 299: 265–280.

Brogniart, A.T. (1828). *Prodrome d'une histoire des végétaux fossiles*. F.G. Levrault, Paris and Strasbourg. 223 pp. + 8 pls.

Calafat, F. (1986). Estratigrafía y sedimentología de la litofacies Buntsandstein de Mallorca. *In*: Cabrera, L. (Ed.). *Resúmenes del XI Congreso Español de Sedimentología*. Grupo Español de Sedimentología, Barcelona: p. 39.

Calafat, F. (1987). Paleoambients de les facies Buntsandstein de Mallorca. *In*: *Llibre de resums de les I Jornades del Medi Ambient de les Illes Balears*. Palma: 16–17.

Calafat, F. (1988). *Estratigrafia y sedimentología de la litofacies Buntsandstein de Mallorca*. Bachelor's thesis. Universitat de Barcelona, Barcelona. 127 pp. + 31 annexed fig.

Calafat, F. & Sáez, B. (1987). Paleofauna lacustre del Triàsic Inferior de Mallorca. *In*: *Llibre de resums de les I Jornades del Medi Ambient de les Illes Balears*. Palma: 18–19.

Calafat, F.; Fornós, J.J.; Marzo, M.; Ramos, E. & Rodríguez-Perea, A. (1986). Icnología de vertebrados de las facies Buntsandstein de Mallorca. *In*: Cabrera, L. (Ed.). *Resúmenes del XI Congreso Español de Sedimentología*. Grupo Español de Sedimentología, Barcelona: p. 40.

Calafat, F.; Fornós, J.J.; Marzo, M.; Ramos-Guerrero, E. & Rodríguez-Perea, A. (1986–1987). Icnología de vertebrados de las facies Buntsandstein de Mallorca. *Acta Geològica Hispànica*, 21–22: 515–520.

Cassinis, G.; Perotti, C.R. & Ronchi, A. (2012). Permian continental basins in the Southern Alps (Italy) and peri-mediterranean correlations. *International Journal of Earth Sciences/GR Geologische Rundschau*, 101: 129–157.

Cuevas-López, F. (1958a). *Informe geológico y minero de los yacimientos de cobre de Banyalbufar y Estallenchs, Mallorca*. Barcelona. 37 pp. + 8 fig.

Cuevas-López, F. (1958b). *Informe geológico y minero de los yacimientos de cobre de Banyalbufar y Valldemosa, Mallorca*. Barcelona. 23 pp. + 7 fig.

Darder, B. (1914). El Triásico de Mallorca. *Trabajos del Museo Nacional de Ciencias Naturales, Serie Geológica*, 7: 85 pp. + 1 map + 1 tab.

Diez, J.B. (2000). *Geología y Paleobotánica de la Facies Buntsandstein en la Rama Aragonesa de la Cordillera Ibérica. Implicaciones paleogeográficas en el Peritethys Occidental*. Ph.D. dissertation. Universidad de Zaragoza–Université Pierre & Marie Curie, Paris VI, Zaragoza and Paris. 424 pp.

Diez, J.B.; Broutin, J. & Ferrer, J. (2005). Difficulties encountered in defining the Permian–Triassic boundary in Buntsandstein facies of the western Peritethyan domain based on palynological data. *Palaeogeography, Palaeoclimatology, Palaeoecology*, 229: 40–53.

Diez, J.B.; Broutin, J.; Grauvogel-Stamm, L.; Bourquin, S.; Bercovici, A. & Ferrer, J. (2010). Anisian floras from the NE Iberian Peninsula and Balearic Islands: A synthesis. *Review of Palaeobotany and Palynology*, 162: 522–542.

Fallot, P. (1922). *Étude Géologique de la Sierra de Majorque*. Librairie Polytechnique Ch. Béranger, Paris and Liège. 16 pp. + 8 ps. + 476 pp. + 9 pl.

Gallemí, J.; Riba, O.; Reguant, S.; Agustí, J.; Álvarez, G.; Calzada, S.; Caus, M.; López, C.; Martinell, J.; Martínez, R.; Martínez, X.; Porta, J. de; Sanz de Siria, A.; Solé, N.; Truyols, J.; Truyols, M. & Via, Ll. (1988). *Història Natural dels Països Catalans, 15: Registre Fòssil*. Enciclopèdia Catalana, Barcelona. 478 pp.

Gómez-Gras, D.M. (1992). *El Permotrías de las Baleares, de la Cordillera Costero Catalana y de la vertiente mediterránea de la Cordillera Ibérica: Facies y Petrología Sedimentaria*. Ph.D. dissertation. Universitat Autònoma de Barcelona, Barcelona. XIX + 242 pp. + 55 fig. + 7 tab.

Gómez-Gras, D. (1993). El Permotrías de las Baleares y de la vertiente mediterránea de la Cordillera Ibérica y del Maestrat: Facies y Petrología Sedimentaria (Parte II). *Boletín Geológico y Minero*, 104: 467–515.

Grauvogel-Stamm, L. & Álvarez-Ramis, C. (1994). Macroflore et microflore in situ du Buntsandstein de l'île de Majorque (Baléares, Espagne). *In*: Arche, A. (Ed.). *Resúmenes del III Coloquio de Estratigrafía y Paleogeografía del Pérmico y Triásico de España*. Consejo Superior de Investigaciones Científicas and Universidad Complutense de Madrid, Cuenca: 51–53.

Grauvogel-Stamm, L. & Álvarez-Ramis, C. (1996). Conifères et pollen in situ du Buntsandstein de l'île de Majorque (Baléares, Espagne). *Cuadernos de Geología Ibérica*, 20: 229–243.

Hermite, H. (1879). *Études géologiques sur les îles Baléares. Première partie: Majorque et Minorque*. Pichon et Savy, Paris. 362 pp. + 5 pl.

Hermite, H. (1888). Estudios Geológicos de las Islas Baleares. *Boletín de la Comisión del Mapa Geológico*, 15: 1–244 + 4 pl.

Juárez-Ruiz, J. & Wachtler, M. (2015). Early–middle Triassic (Anisian) fossil flora from Majorca (Spain). *Dolomythos*, 2015: 1–49.

López-Gómez, J.; Arche, A. & Pérez-López, A. (2002). Permian and Triassic. *In*: Gibbons, W. & Moreno, M.T. (Eds.). *The Geology of Spain*. Geological Society, London: 185–212.

López-Gómez, J.; Alonso-Azcárate, J.; Arche, A.; Arribas, J.; Fernández-Barrenechea, J.; Borruel-Abadía, V.; Bourquin, S.; Cadenas, P.; Cuevas, J.; De la Horra, R.; Díez, J.B.; Escudero-Mozo, M.J.; Fernández-Viejo, G.; Galán-Abellán, B.; Galé, C.; Gaspar-Escribano, J.; Gisbert-Aguilar, J.; Gómez-Gras, D.; Goy, A.; Gretter, N.; Heredia-Carballo, N.; Lago, M.; Lloret, J.; Luque, J.; Márquez, L.; Márquez-Aliaga, A.; Martín-Algarra, A.; Martín-Chivelet, J.; Martín-González, F.; Marzo, M.; Mercedes-Martín, R.; Ortí, F.; Pérez-López, A.; Pérez-Valera, F.; Pérez-Valera, J.A.; Plasencia, P.; Ramos, E.; Rodríguez-Méndez, L.; Ronchi, A.; Salas, R.; Sánchez-Fernández, D.; Sánchez-Moya, Y.; Sopeña, A.; Suárez-Rodríguez, Á.; Tubía, J.M.; Ubide, T.; Valero-Garcés, B.; Vargas,

H. & Viseras, C. (2019). Permian-Triassic rifting stage. *In*: Vergés, J. & Kullberg, J.C. (Coord.). *The Geology of Iberia: A Geodynamic Approach. Volume 3: The Alpine Cycle*. Springer, Cham: 29–112.

Lozano, R. (1884). *Anotaciones fisicas y geológicas de la isla de Mallorca para las aplicaciones del mapa: dedicado á la Excma. Diputación Provincial de Baleares*. Imprenta de la Casa de la Misericordia, Palma. 68 pp.

Martí, J.; Paniello, X.; Pomar, L.; Ramos, E. & Rodríguez-Perea, A. (1985). El Triásico de las Baleares. *In*: Mateu Ibars, F. & Marzo, M. (Eds.). *Resúmenes del II Coloquio de Estratigrafia y Paleogeografia del Pérmico y Triásico de España.* Institut d'Estudis Ilerdencs and Grupo Español del Mesozoico, La Seu d'Urgell: 84–85.

Nolan, H. (1887). Note sur le Trias de Minorque et Majorque. *Bulletin de la Société géologique de France*, 15: 592–599.

Nolan, H. (1888). El Trias de Mallorca y Menorca. *Boletín de la Comisión del Mapa Geológico*, 15: 234–241.

Parés, J.M.; Freeman, R. & Sàbat, F. (1989). Síntesis de los resultados paleomagnéticos de los bordes de la Cuenca Catalano-Balear. *Cuadernos de Geología Ibérica*, 12: 59–74.

Parés, J.M.; Freeman, R. & Roca, E. (1992a). Neogene structural development in the Valencia trough margins from palaeomagnetic data. *Tectonophysics*, 203: 111–124.

Parés, J.M.; Roca, E. & Freeman, R. (1992b). Datos paleomagnéticos de los márgenes del surco de Valencia. Papel de las rotaciones en la estructuración neógena. *Física de la Tierra*, 4: 231–246.

Pomar-Gomà, L. (1979). *The Triassic of the Balearic Islands*. Geology Department, Palma de Mallorca University, Palma. 49 pp. + 7 Petrologic Logs.

Ramos, A. (1995). Transition from alluvial to coastal deposits (Permian–Triassic) on the Island of Mallorca, western Mediterranean. *Geological Magazine*, 132(4): 435–447.

Ramos, A. & Doubinger, J. (1989). Premières datations palynologiques dans le facies Buntsandstein de l'île de Majorque (Baléares, Espagne). *Comptes Rendus de l'Académie des Sciences de Paris*, 2nd series, 309: 1089–1094.

Ramos, A.; Olmo, P. del & Alvaro, M. (1985). El Buntsandstein de la isla de Mallorca. *In*: Mateu Ibars, F. & Marzo, M. (Eds.). *Resúmenes del II Coloquio de Estratigrafia y Paleogeografia del Pérmico y Triásico de España.* Institut d'Estudis Ilerdencs and Grupo Español del Mesozoico, La Seu d'Urgell: 103–104.

Rodríguez-Perea, A.; Ramos-Guerrero, E.; Pomar, L.; Paniello, X.; Obrador, A. & Martí, J. (1987). El Triásico de las Baleares. *Cuadernos de Geología Ibérica*, 11: 295–321.

Santanach, P.; Banda, E.; Calvet, F.; Carreras, J.; Casas, J.M.; Fontboté, J.M.; Fornós, J.; Gisbert, J.; Julivert, M.; Marzo, M.; Rodríguez-Perea, A.; Salas, R. & Souquet, P. (1988). *Història Natural dels Països Catalans, 1: Geologia (I)*. Enciclopèdia Catalana, Barcelona. 439 pp.

Shcherbakov, D.E.; Lukashevich, E.D. & Blagoderov, V.A. (1995). Triassic Diptera and initial radiation of the order. *Journal of Dipterological Research*, 6(2): 75–115.

Vera, J.-A.; Alonso-Chaves, F.M.; Andreo, B.; Arias, C.; Azañón, J.M.; Balanyá, J.C.; Barón, A.; Booth-Rea, G.; Castro, J.M.; Chacón, B.; Company, M.; Crespo-Blanc, A.; Delgado, F.; Díaz de Federico, A.; Esteras, M.; Estévez, A.; Fernández, J.; Fornós, J.J.; Galindo-Zaldívar, J.; García-Casco, A.; García-Dueñas, V.; García-Hernández, M.; Garrido, C.J..; Gea, G.A. de; Gelabert, B.; Gervilla, F.; González-Lodeiro, F.; Jabaloy, A.; López-Garrido, A.C.; Luján, M.; Martín-Algarra, A.; Martín-Chivelet, J.; Martín-Martín, M.; Molina, J.M.; Morata, D.; Nieto, J.M.; Obrador, A.; O'Dogherty, L.; Orozco, M.; Pérez-López, A.; Pomar, L.; Puga, E.; Ramos, E.; Rey, J.; Rivas, P.; Rodríguez-Cañero, R.; Ruiz-Cruz, M.D.; Ruiz-Ortiz, P.A.; Sàbat, F.; Sánchez-Gómez, M.; Sánchez-Navas, A.; Sandoval, J.; Sanz de Galdeano, C.; Soto, J.I.; Torres-Roldán, R.L. & Villas, L. (2004). Cordillera Bética y Baleares. *In*: Vera, J.-A. (Ed.). *Geología de España*. IGME, Madrid: 346–464.

Zessin, W. (2008a). Einige neue Insekten aus der Unteren Trias (Buntsandstein) von Mallorca, Spanien (Blattaria, Coleoptera, Diptera, Heteroptera und Megaloptera). *Deutschen Gesellschaft für allgemeine und angewandte Entomologie – Nachrichten*, 22(1): 20–21.

Zessin, W. (2008b). Neue Insekten aus der Unteren Trias (Buntsadstein) von Mallorca, Spanien (Blattaria, Coleoptera, Diptera, Heteroptera, Orthopteroidea und Homoptera). *Virgo, Mitteilungsblatt des Entomologischen Vereins Mecklenburg*, 11(1): 99–101.

Supplementary Logs

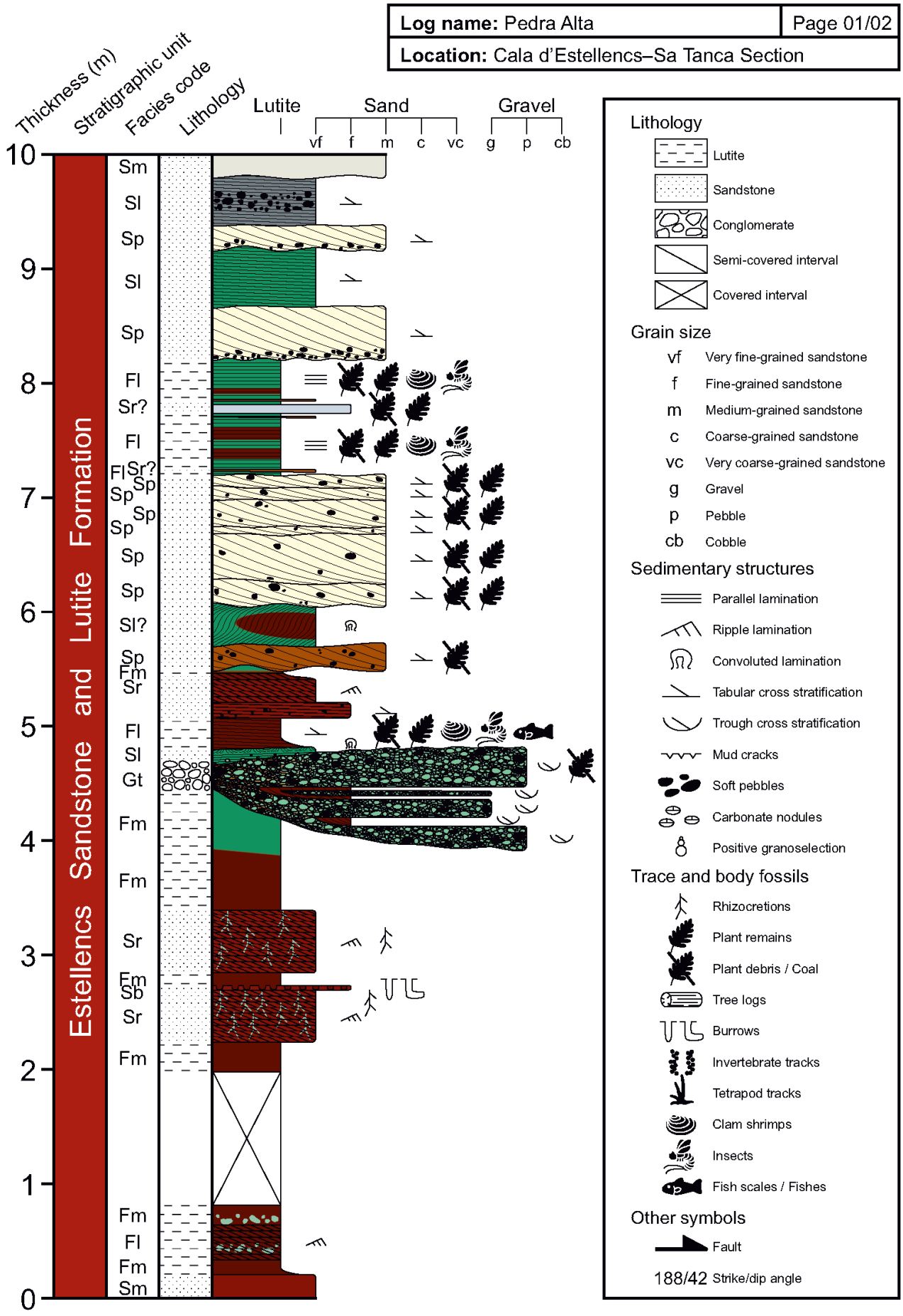
Log name: Pedra Alta
Page 01/02
Location: Cala d'Estellencs–Sa Tanca Section
Thickness (m)
Stratigraphic unit
Facies code
Lithology
Lutite
Sand
Gravel
vf f m c vc g p cb
Estellencs Sandstone and Lutite Formation
Sm Sl Sp Sl Sp Fl Sr? Fl Fl Sr? Sp Sp Sp Sp Sp Sl? Sp Fm Sr Fl Sl Gt Fm Fm Sr Fm Sb Sr Fm Fm Fl Fm Sm
Lithology
Lutite
Sandstone
Conglomerate
Semi-covered interval
Covered interval
Grain size
vf Very fine-grained sandstone
f Fine-grained sandstone
m Medium-grained sandstone
c Coarse-grained sandstone
vc Very coarse-grained sandstone
g Gravel
p Pebble
cb Cobble
Sedimentary structures
Parallel lamination
Ripple lamination
Convoluted lamination
Tabular cross stratification
Trough cross stratification
Mud cracks
Soft pebbles
Carbonate nodules
Positive granoselection
Trace and body fossils
Rhizocretions
Plant remains
Plant debris / Coal
Tree logs
Burrows
Invertebrate tracks
Tetrapod tracks
Clam shrimps
Insects
Fish scales / Fishes
Other symbols
Fault
188/42 Strike/dip angle

Log name: Pedra Alta	Page 02/02
Location: Cala d'Estellencs–Sa Tanca Section	

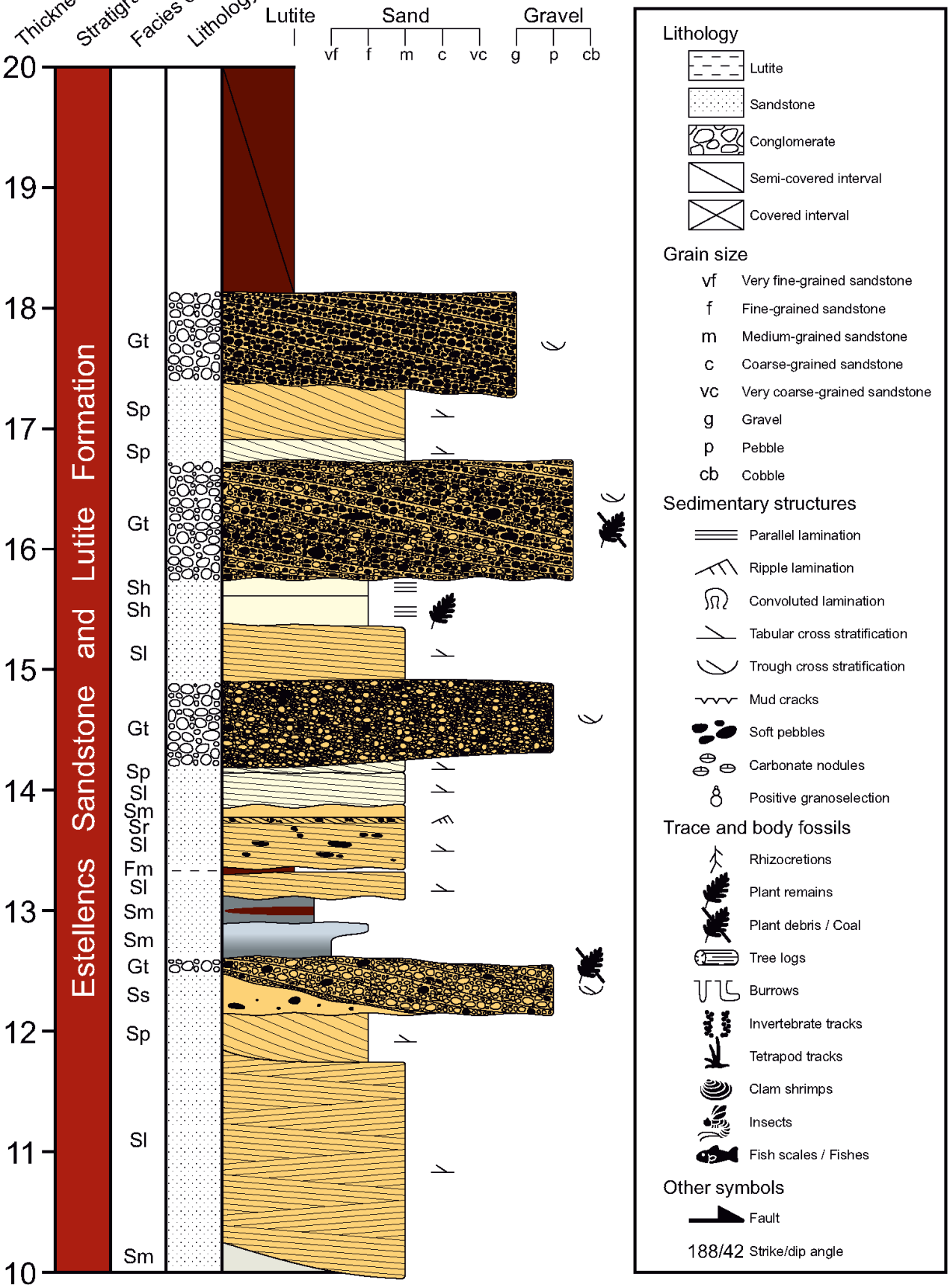

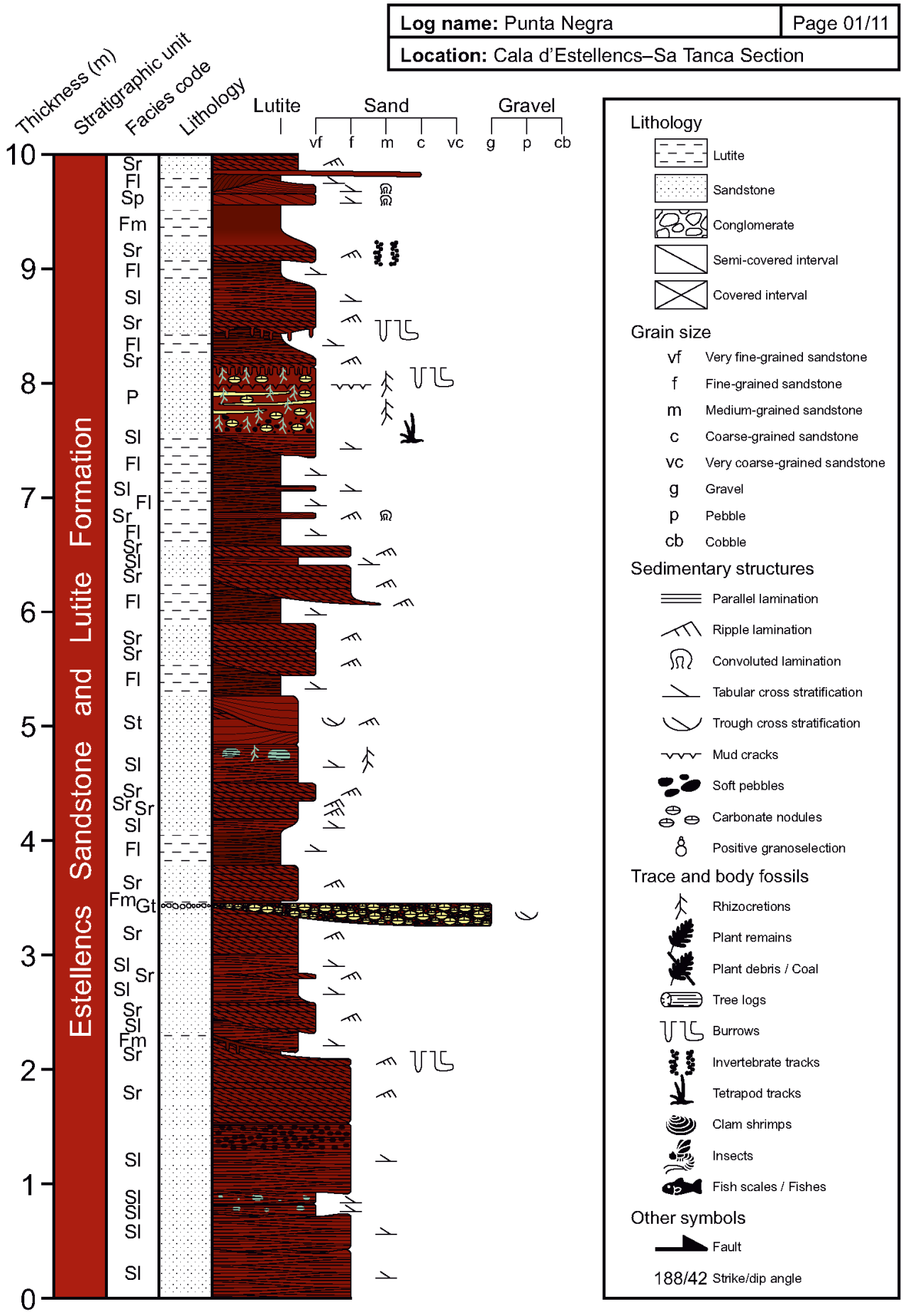
Log name: Punta Negra
Page 01/11
Location: Cala d'Estellencs–Sa Tanca Section
Thickness (m)
Stratigraphic unit
Facies code
Lithology
Lutite
Sand
Gravel
vf f m c vc g p cb
Estellencs Sandstone and Lutite Formation
Lithology
Lutite
Sandstone
Conglomerate
Semi-covered interval
Covered interval
Grain size
vf Very fine-grained sandstone
f Fine-grained sandstone
m Medium-grained sandstone
c Coarse-grained sandstone
vc Very coarse-grained sandstone
g Gravel
p Pebble
cb Cobble
Sedimentary structures
Parallel lamination
Ripple lamination
Convoluted lamination
Tabular cross stratification
Trough cross stratification
Mud cracks
Soft pebbles
Carbonate nodules
Positive granoselection
Trace and body fossils
Rhizocretions
Plant remains
Plant debris / Coal
Tree logs
Burrows
Invertebrate tracks
Tetrapod tracks
Clam shrimps
Insects
Fish scales / Fishes
Other symbols
Fault
188/42 Strike/dip angle

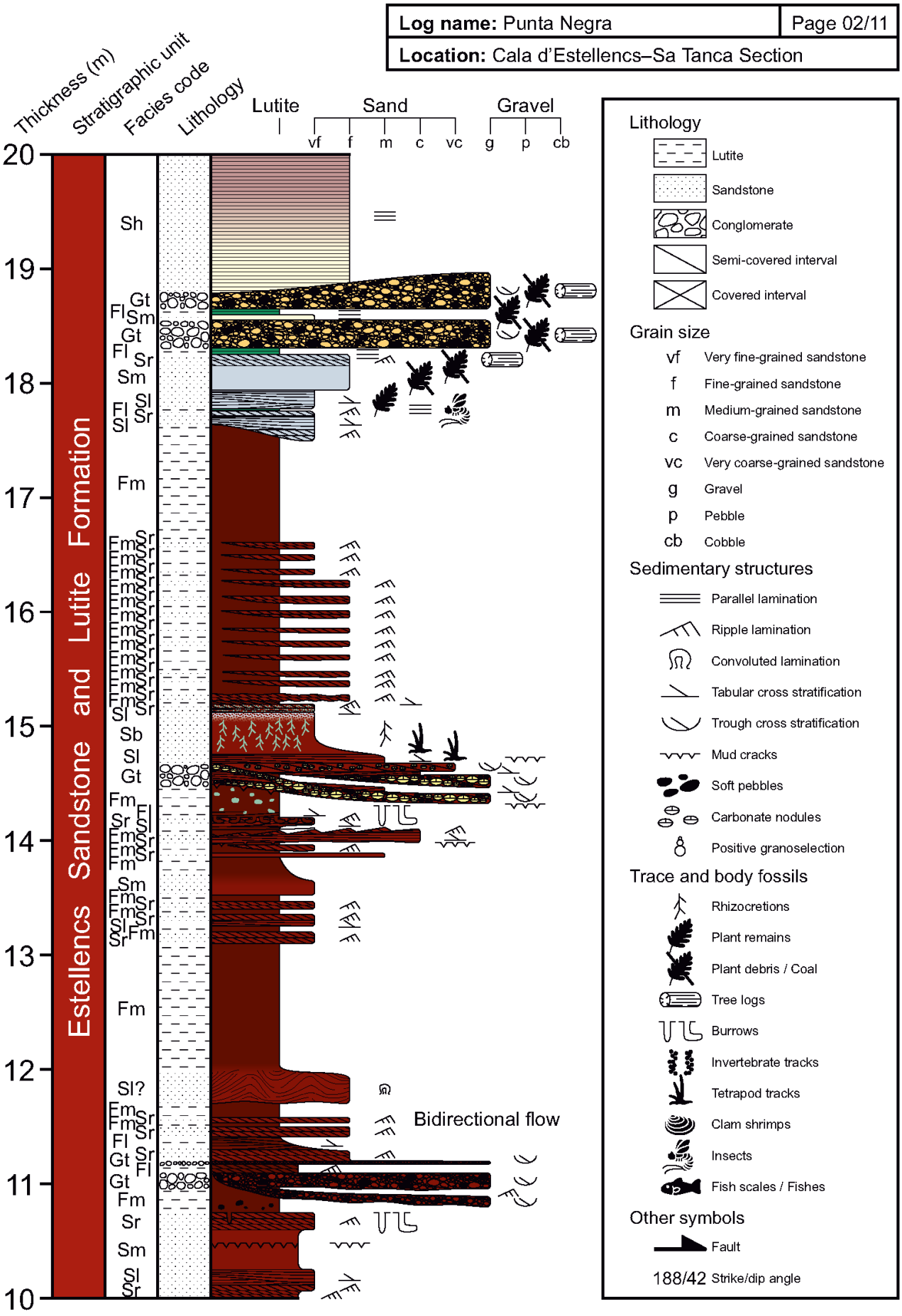
Log name: Punta Negra
Page 02/11
Location: Cala d'Estellencs–Sa Tanca Section
Thickness (m)
Stratigraphic unit
Facies code
Lithology
Lutite
Sand
Gravel
vf f m c vc g p cb
Estellencs Sandstone and Lutite Formation
Bidirectional flow
Lithology
Lutite
Sandstone
Conglomerate
Semi-covered interval
Covered interval
Grain size
vf Very fine-grained sandstone
f Fine-grained sandstone
m Medium-grained sandstone
c Coarse-grained sandstone
vc Very coarse-grained sandstone
g Gravel
p Pebble
cb Cobble
Sedimentary structures
Parallel lamination
Ripple lamination
Convoluted lamination
Tabular cross stratification
Trough cross stratification
Mud cracks
Soft pebbles
Carbonate nodules
Positive granoselection
Trace and body fossils
Rhizocretions
Plant remains
Plant debris / Coal
Tree logs
Burrows
Invertebrate tracks
Tetrapod tracks
Clam shrimps
Insects
Fish scales / Fishes
Other symbols
Fault
188/42 Strike/dip angle

Log name: Punta Negra	Page 03/11
Location: Cala d'Estellencs–Sa Tanca Section	

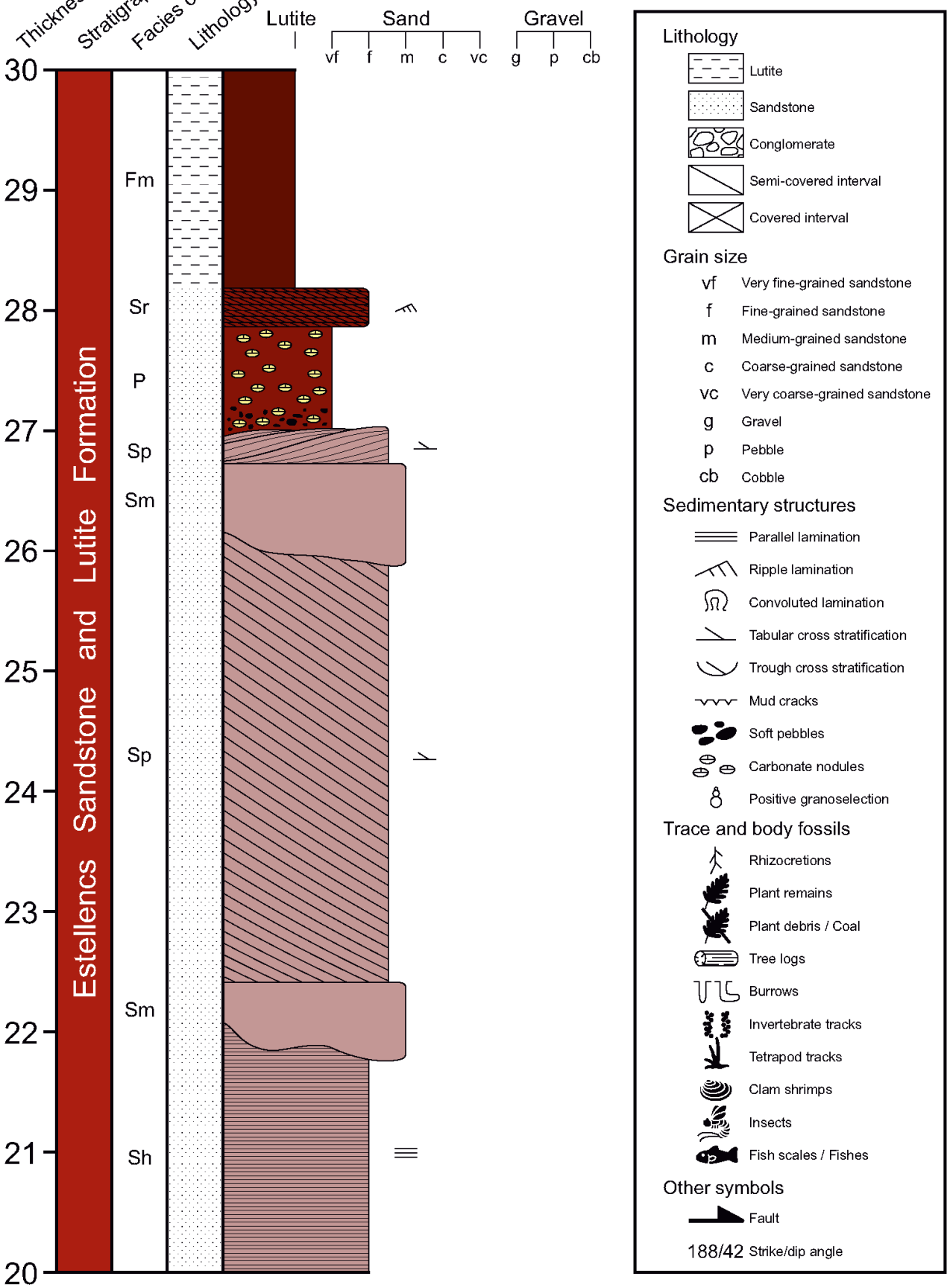

Log name: Punta Negra | Page 04/11

Location: Cala d'Estellencs–Sa Tanca Section

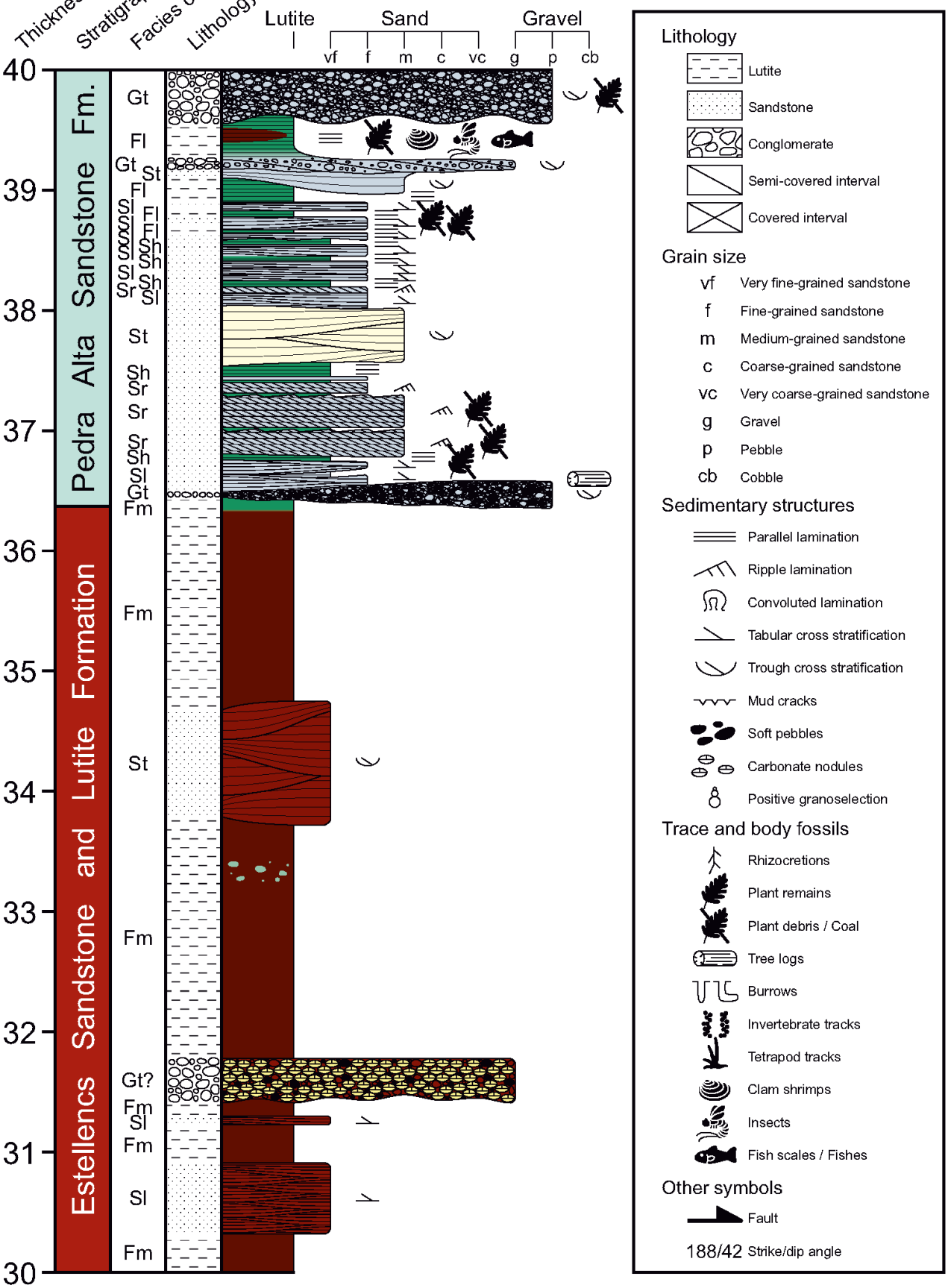

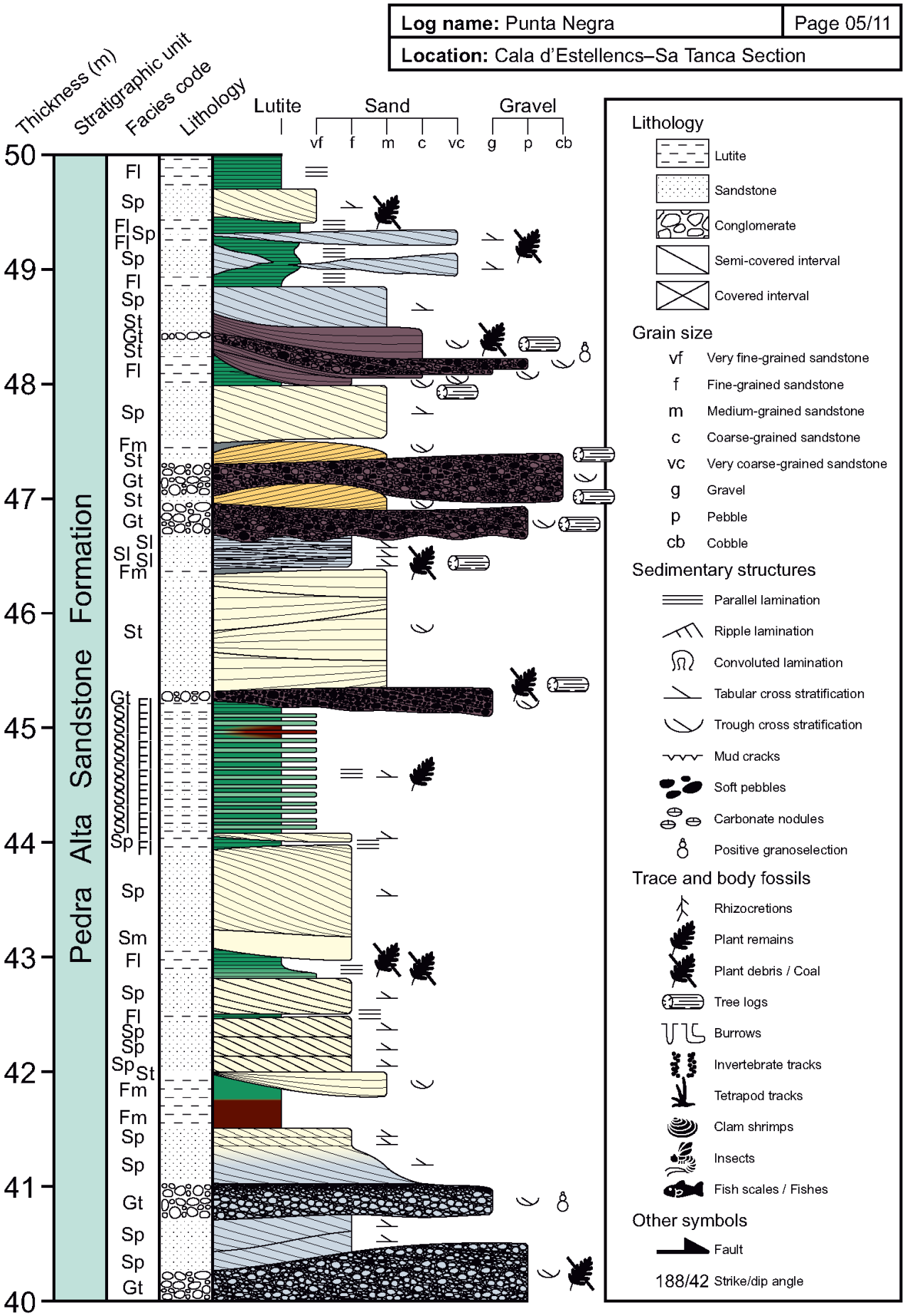
Log name: Punta Negra
Page 05/11
Location: Cala d'Estellencs–Sa Tanca Section
Thickness (m)
Stratigraphic unit
Facies code
Lithology
Lutite
Sand
Gravel
vf f m c vc g p cb
Pedra Alta Sandstone Formation
50
49
48
47
46
45
44
43
42
41
40
Fl Sp Fl Sp Fl Sp Fl Sp St Gt St Fl Sp Fm St Gt St Gt Sl Sl Fm St Gt Fl Sp Fl Sp Sm Fl Sp Fl Sp Sp Sp St Fm Fm Sp Sp Gt Sp Sp Gt
Lithology
Lutite
Sandstone
Conglomerate
Semi-covered interval
Covered interval
Grain size
vf Very fine-grained sandstone
f Fine-grained sandstone
m Medium-grained sandstone
c Coarse-grained sandstone
vc Very coarse-grained sandstone
g Gravel
p Pebble
cb Cobble
Sedimentary structures
Parallel lamination
Ripple lamination
Convoluted lamination
Tabular cross stratification
Trough cross stratification
Mud cracks
Soft pebbles
Carbonate nodules
Positive granoselection
Trace and body fossils
Rhizocretions
Plant remains
Plant debris / Coal
Tree logs
Burrows
Invertebrate tracks
Tetrapod tracks
Clam shrimps
Insects
Fish scales / Fishes
Other symbols
Fault
188/42 Strike/dip angle

Log name: Punta Negra | Page 06/11

Location: Cala d'Estellencs–Sa Tanca Section

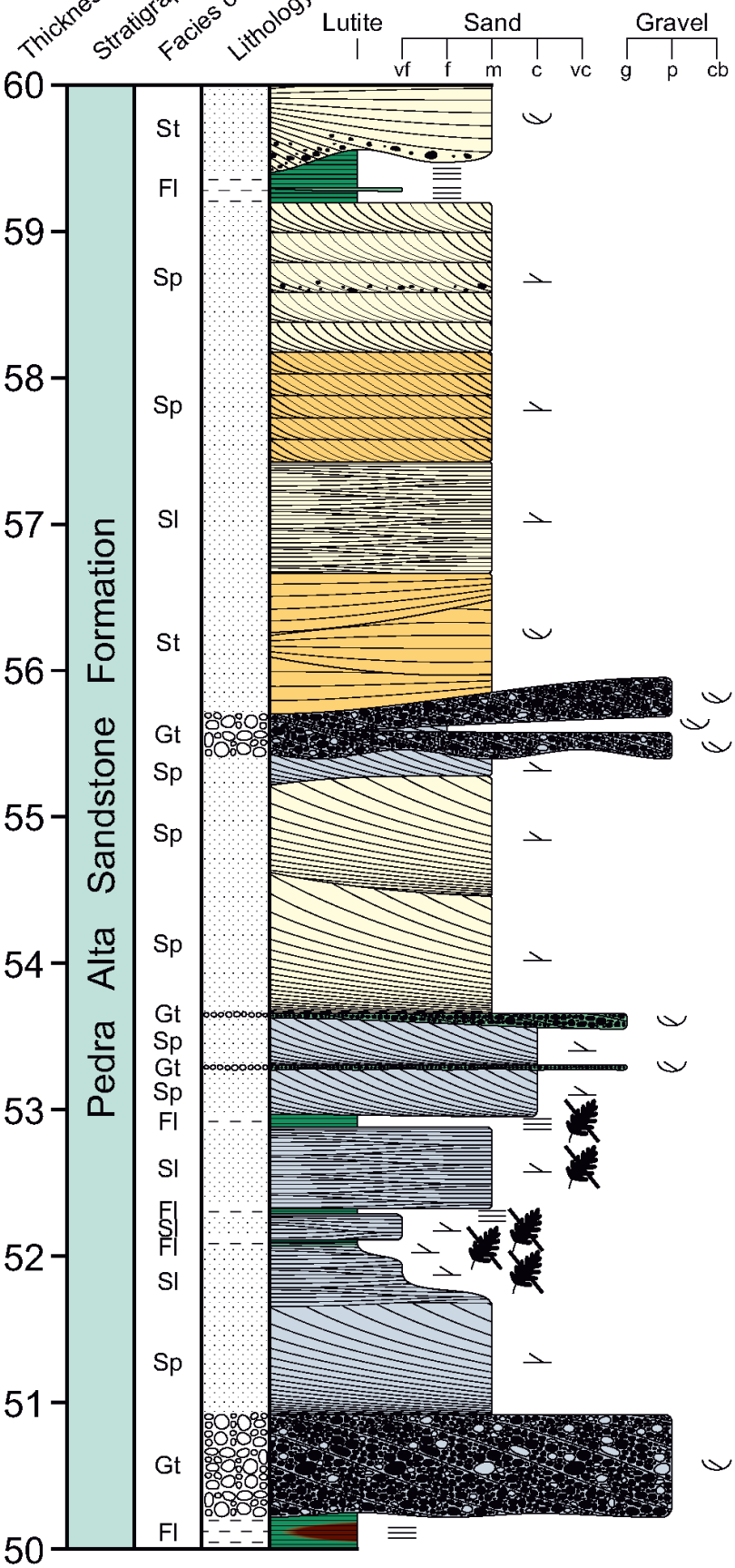

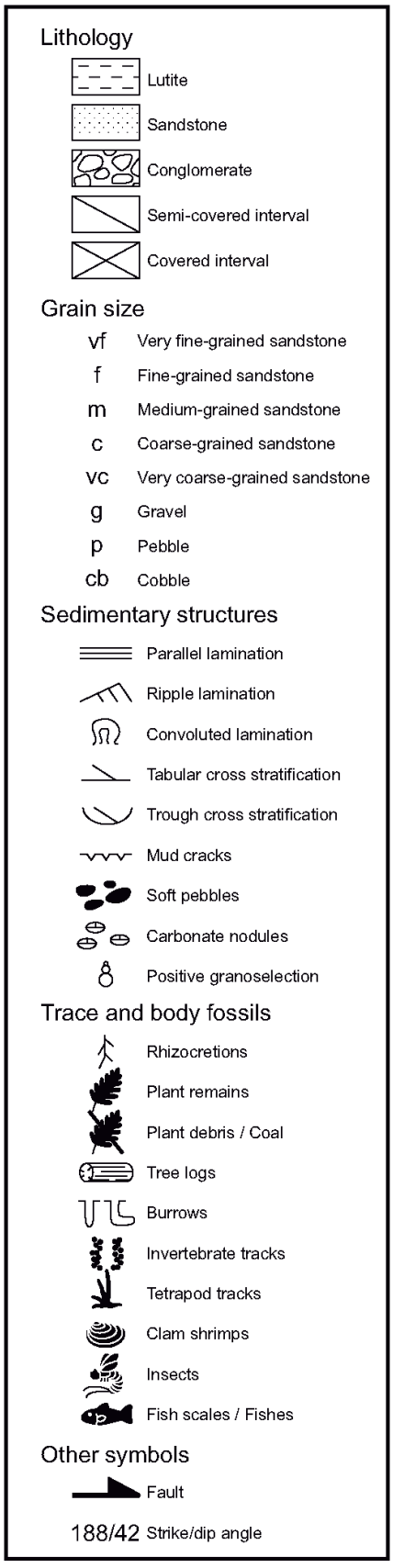

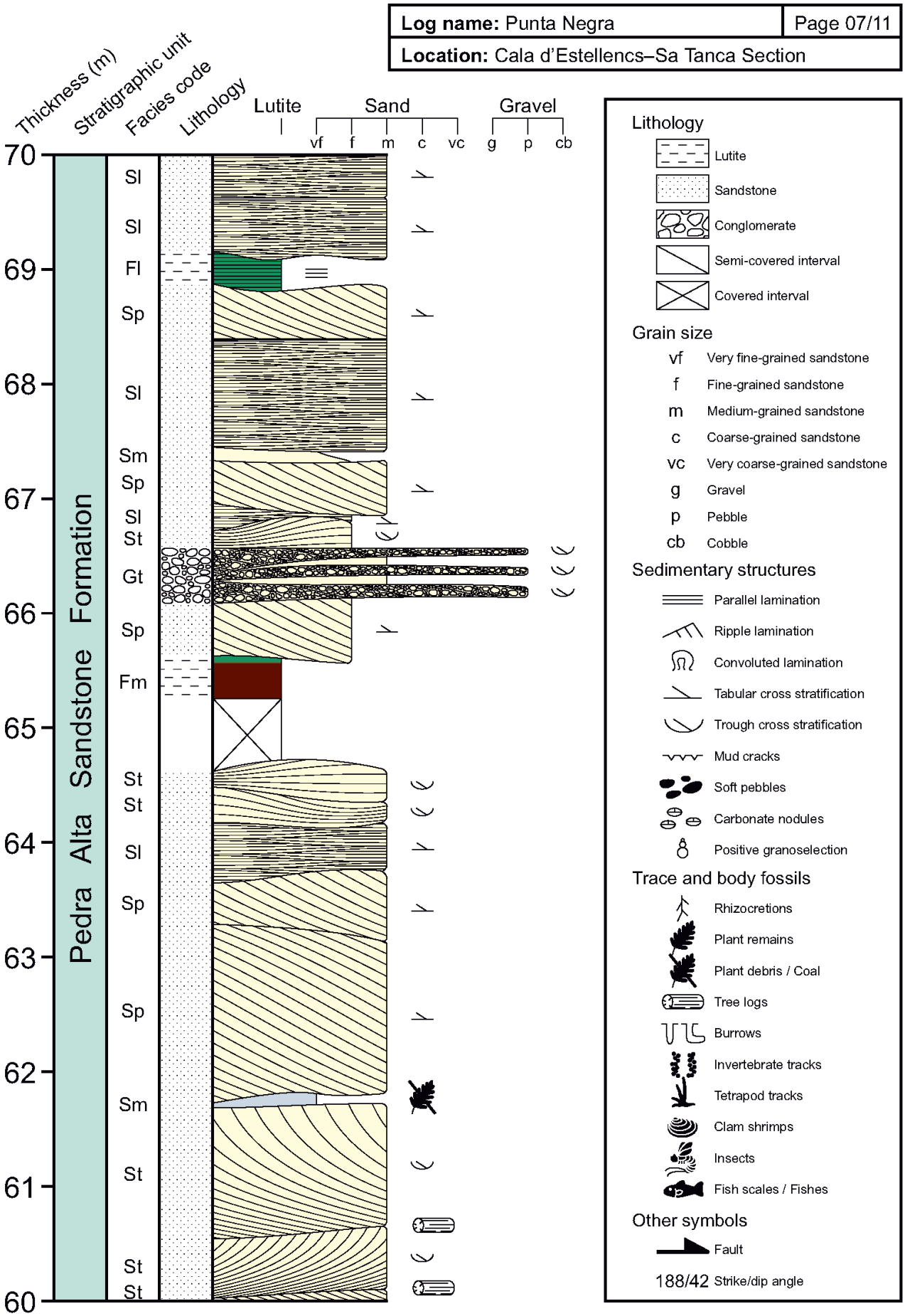
Log name: Punta Negra
Page 07/11
Location: Cala d'Estellencs–Sa Tanca Section
Thickness (m)
Stratigraphic unit
Facies code
Lithology
Lutite
Sand
Gravel
vf f m c vc g p cb
70
69
68
67
66
65
64
63
62
61
60
Pedra Alta Sandstone Formation
Sl
Sl
Fl
Sp
Sl
Sm
Sp
Sl
St
Gt
Sp
Fm
St
St
Sl
Sp
Sp
Sm
St
St
St
Lithology
Lutite
Sandstone
Conglomerate
Semi-covered interval
Covered interval
Grain size
vf Very fine-grained sandstone
f Fine-grained sandstone
m Medium-grained sandstone
c Coarse-grained sandstone
vc Very coarse-grained sandstone
g Gravel
p Pebble
cb Cobble
Sedimentary structures
Parallel lamination
Ripple lamination
Convoluted lamination
Tabular cross stratification
Trough cross stratification
Mud cracks
Soft pebbles
Carbonate nodules
Positive granoselection
Trace and body fossils
Rhizocretions
Plant remains
Plant debris / Coal
Tree logs
Burrows
Invertebrate tracks
Tetrapod tracks
Clam shrimps
Insects
Fish scales / Fishes
Other symbols
Fault
188/42 Strike/dip angle

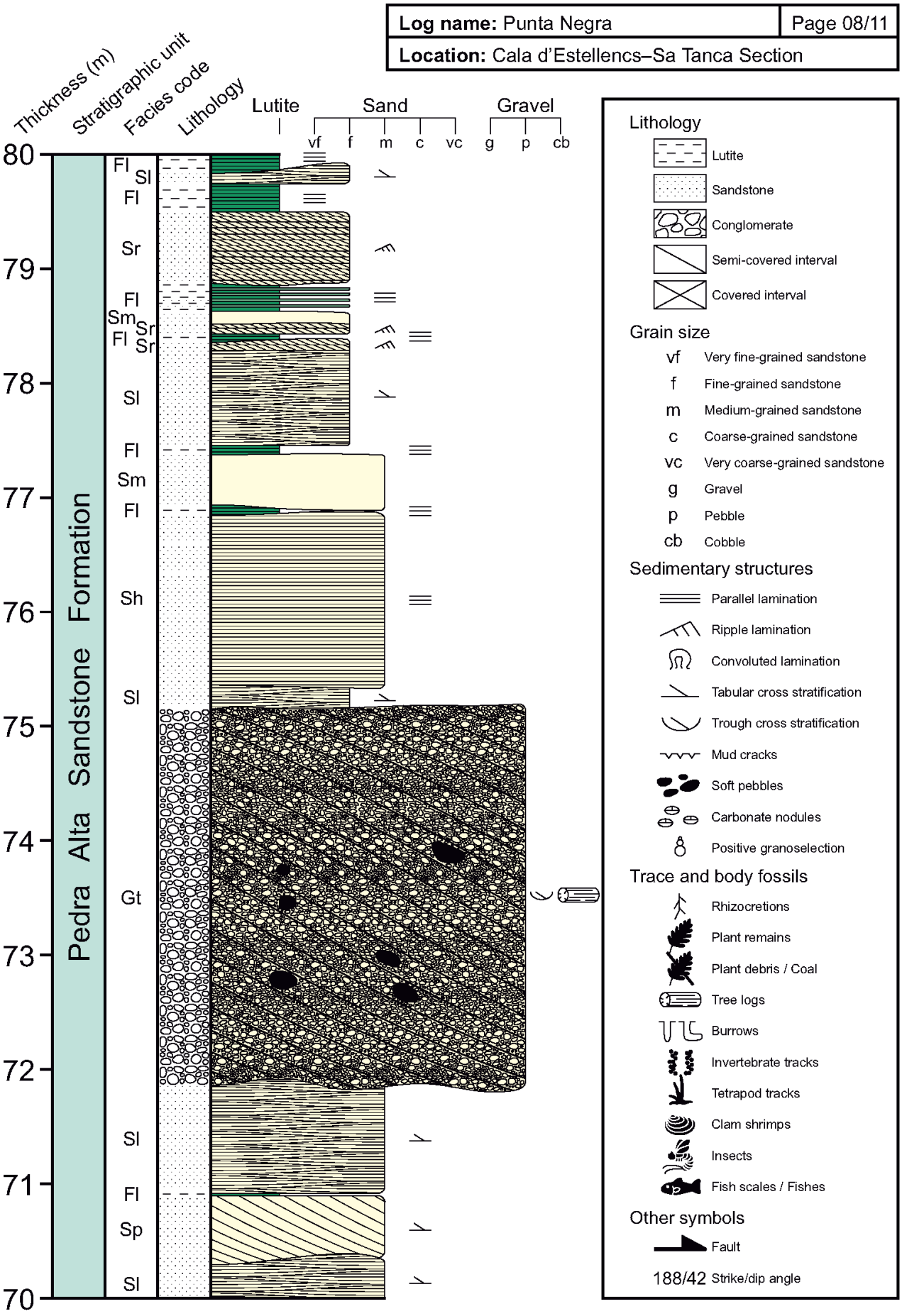
Log name: Punta Negra
Page 08/11
Location: Cala d'Estellencs–Sa Tanca Section
Thickness (m)
Stratigraphic unit
Facies code
Lithology
Lutite
Sand
Gravel
vf f m c vc g p cb
80
79
78
77
76
75
74
73
72
71
70
Pedra Alta Sandstone Formation
Fl Sl
Fl
Sr
Fl
Sm Sr
Fl Sr
Sl
Fl
Sm
Fl
Sh
Sl
Gt
Sl
Fl
Sp
Sl
Lithology
Lutite
Sandstone
Conglomerate
Semi-covered interval
Covered interval
Grain size
vf Very fine-grained sandstone
f Fine-grained sandstone
m Medium-grained sandstone
c Coarse-grained sandstone
vc Very coarse-grained sandstone
g Gravel
p Pebble
cb Cobble
Sedimentary structures
Parallel lamination
Ripple lamination
Convoluted lamination
Tabular cross stratification
Trough cross stratification
Mud cracks
Soft pebbles
Carbonate nodules
Positive granoselection
Trace and body fossils
Rhizocretions
Plant remains
Plant debris / Coal
Tree logs
Burrows
Invertebrate tracks
Tetrapod tracks
Clam shrimps
Insects
Fish scales / Fishes
Other symbols
Fault
188/42 Strike/dip angle

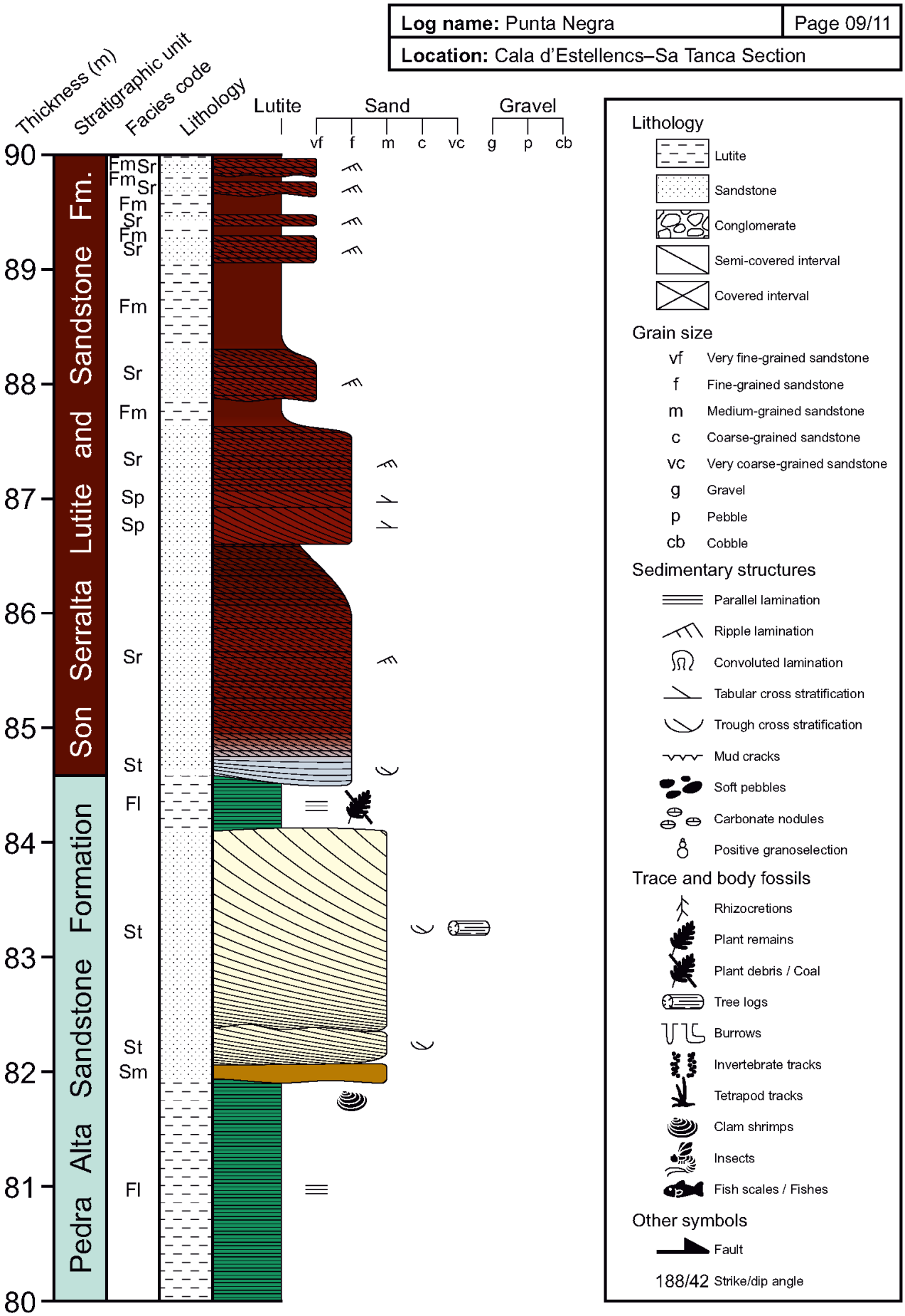
Log name: Punta Negra
Page 09/11
Location: Cala d'Estellencs–Sa Tanca Section
Thickness (m)
Stratigraphic unit
Facies code
Lithology
Lutite
Sand
Gravel
vf f m c vc g p cb
90
89
88
87
86
85
84
83
82
81
80
Son Serralta Lutite and Sandstone Fm.
Pedra Alta Sandstone Formation
Fm Sr Fm Sr Fm Sr Fm Sr Fm Sr Sp Sp Sr St Fl St St Sm Fl
Lithology
Lutite
Sandstone
Conglomerate
Semi-covered interval
Covered interval
Grain size
vf Very fine-grained sandstone
f Fine-grained sandstone
m Medium-grained sandstone
c Coarse-grained sandstone
vc Very coarse-grained sandstone
g Gravel
p Pebble
cb Cobble
Sedimentary structures
Parallel lamination
Ripple lamination
Convoluted lamination
Tabular cross stratification
Trough cross stratification
Mud cracks
Soft pebbles
Carbonate nodules
Positive granoselection
Trace and body fossils
Rhizocretions
Plant remains
Plant debris / Coal
Tree logs
Burrows
Invertebrate tracks
Tetrapod tracks
Clam shrimps
Insects
Fish scales / Fishes
Other symbols
Fault
188/42 Strike/dip angle

Log name: Punta Negra	Page 10/11
Location: Cala d'Estellencs–Sa Tanca Section	

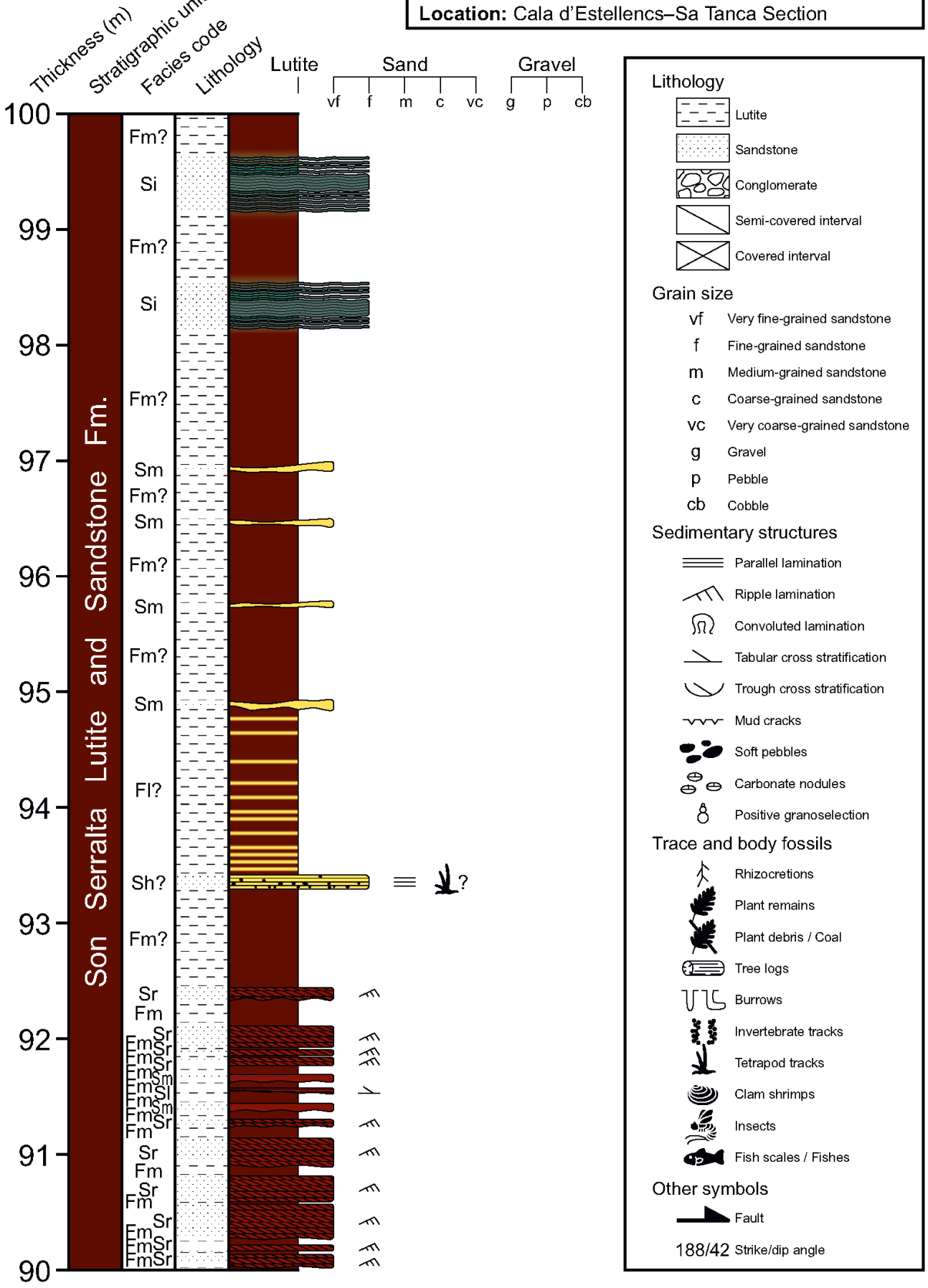
Thickness (m)
Stratigraphic unit
Facies code
Lithology
Lutite
Sand
Gravel
vf f m c vc g p cb
100
99
98
97
96
95
94
93
92
91
90
Son Serralta Lutite and Sandstone Fm.
Fm?
Si
Fm?
Si
Fm?
Sm
Fm?
Sm
Fm?
Sm
Fm?
Sm
Fl?
Sh?
Fm?
Sr
Fm
Sr
Fm
Sr
Fm
Sm
Fm
Sl
Fm
Sm
Fm
Sr
Fm
Sr
Fm
Sr

Log name: Punta Negra | Page 11/11

Location: Cala d'Estellencs–Sa Tanca Section

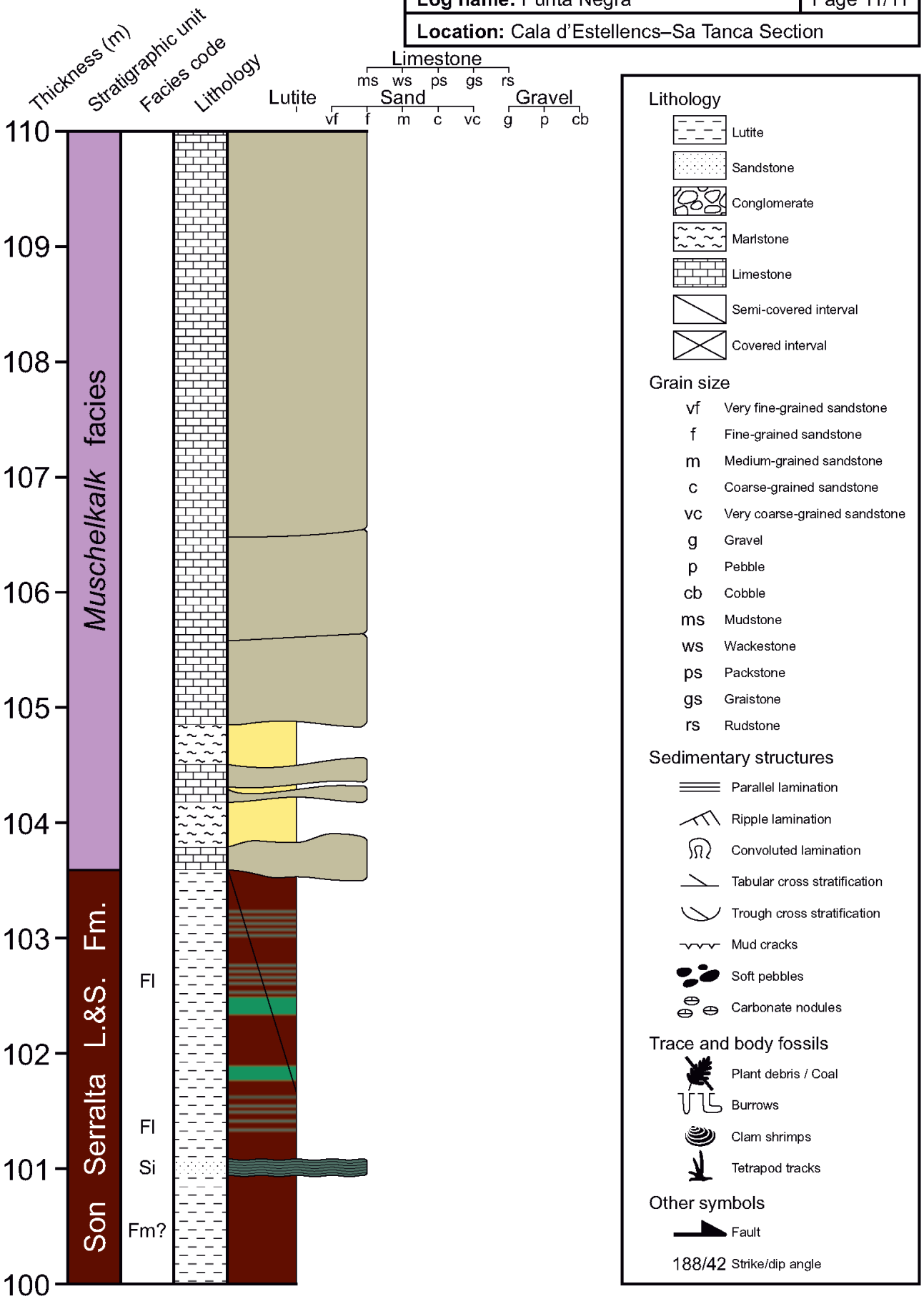

Log name: Punta Roja	Page 01/13
Location: Cala d'Estellencs–Sa Tanca Section	

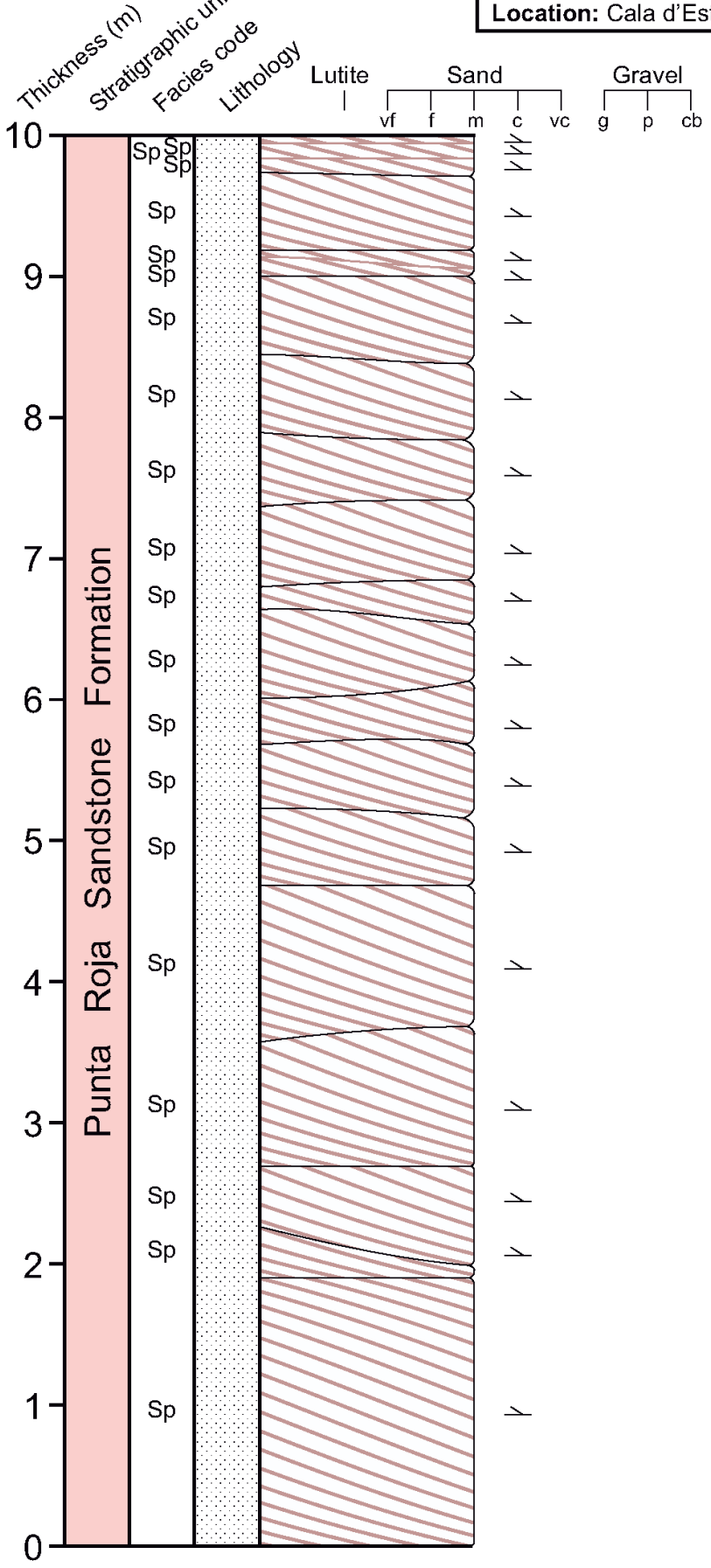

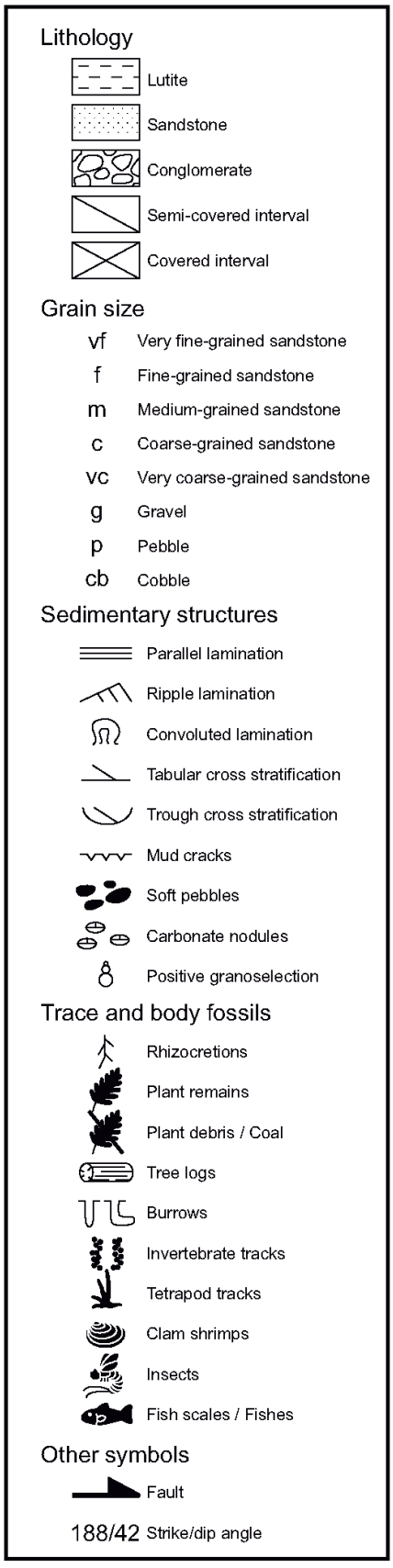

Log name: Punta Roja | Page 02/13

Location: Cala d'Estellencs–Sa Tanca Section

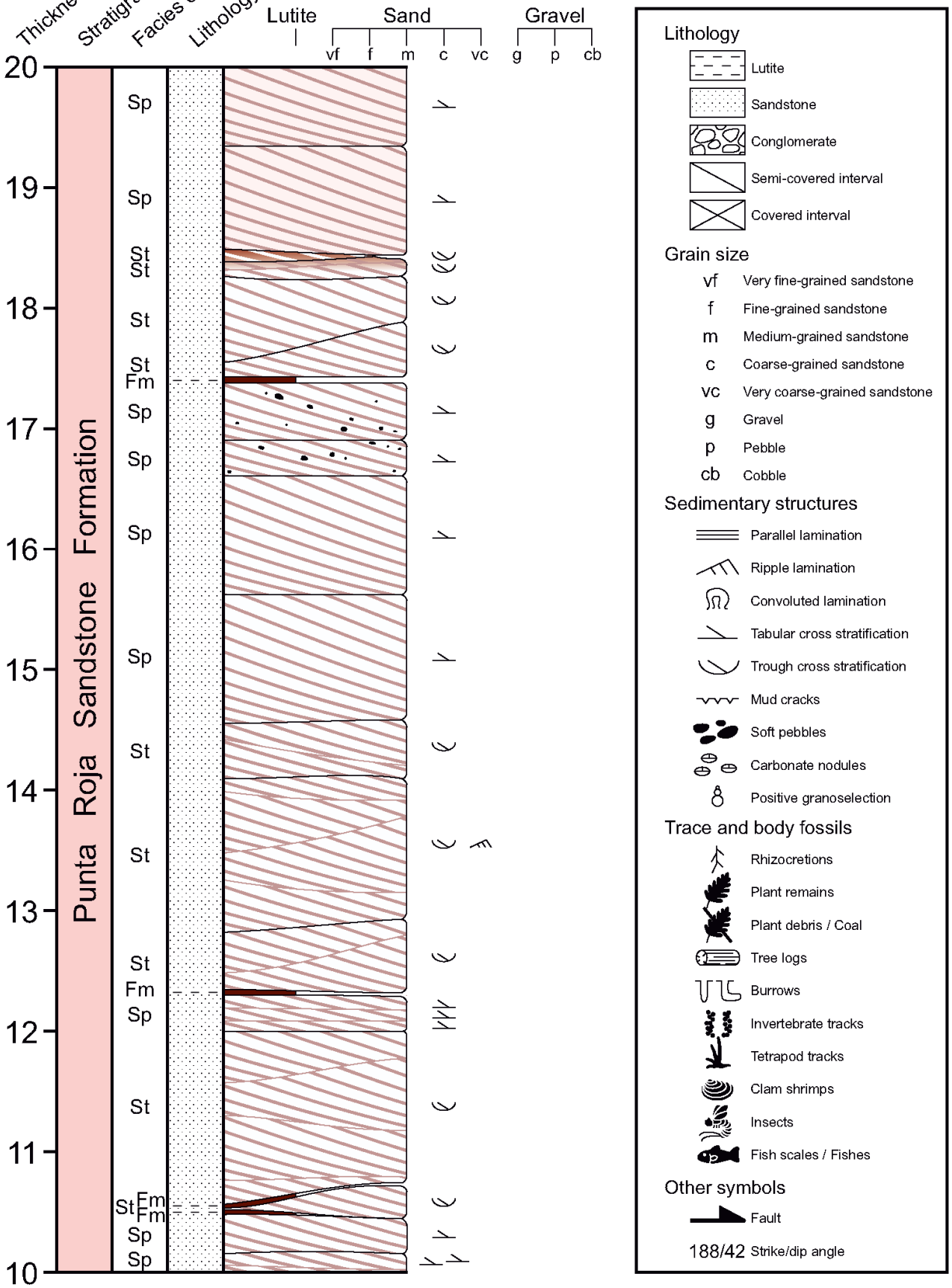

Log name: Punta Roja	Page 03/13
Location: Cala d'Estellencs–Sa Tanca Section	

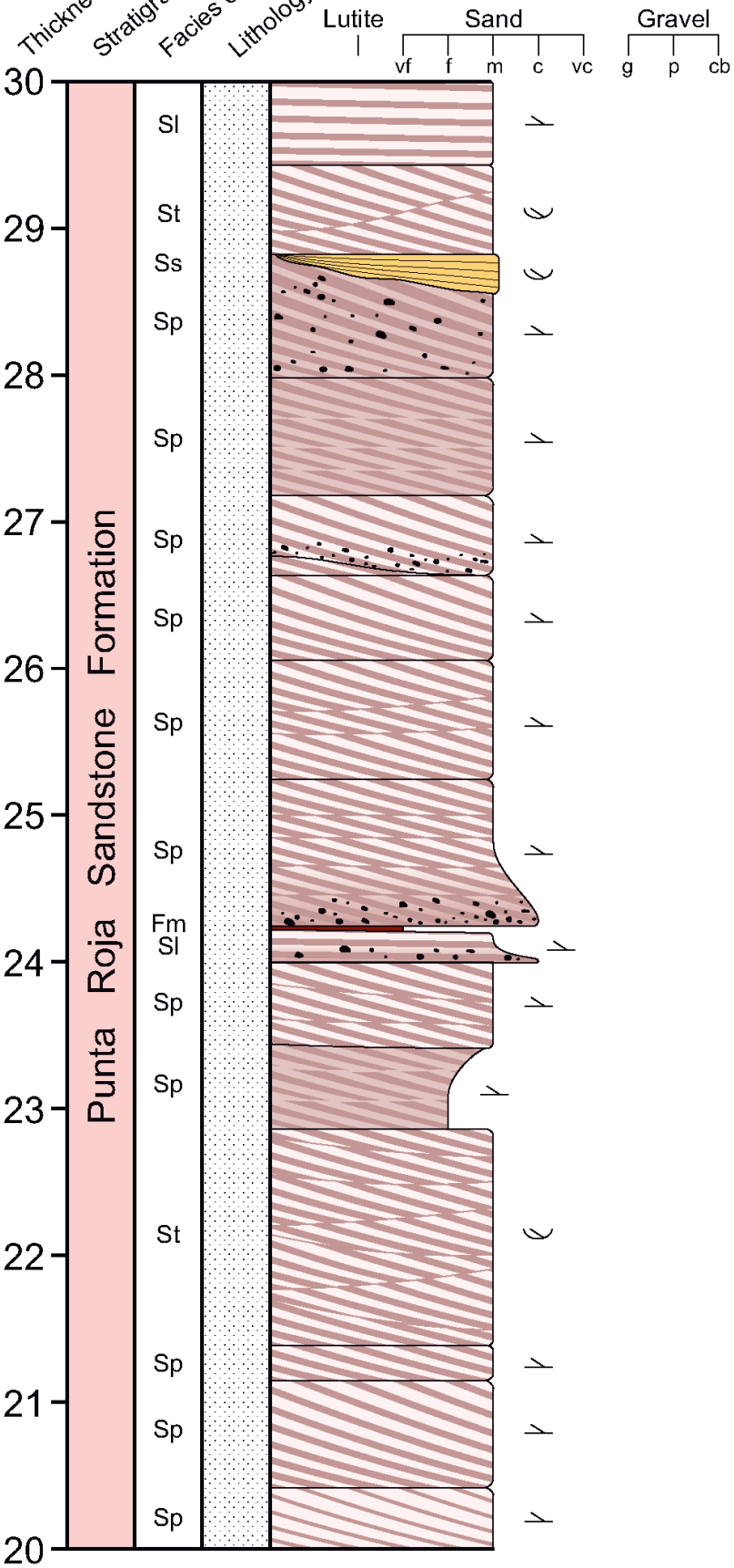

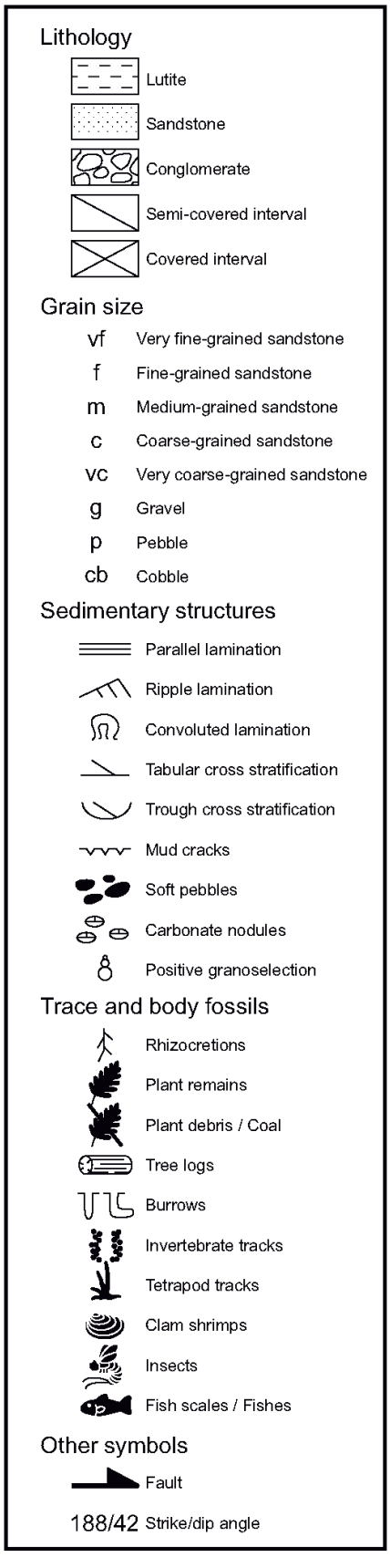

Log name: Punta Roja | Page 04/13

Location: Cala d'Estellencs–Sa Tanca Section

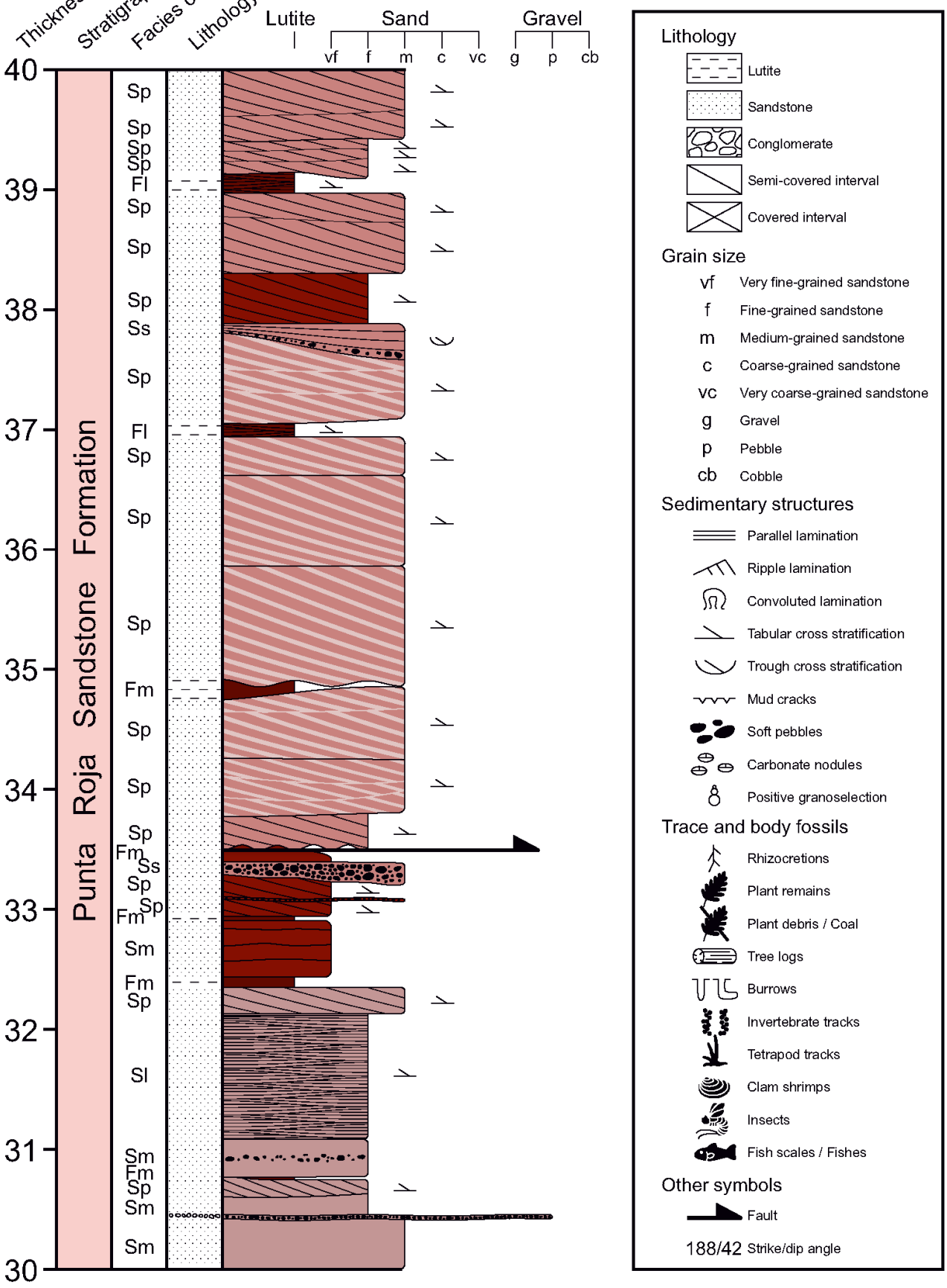

Lithology
- Lutite
- Sandstone
- Conglomerate
- Semi-covered interval
- Covered interval

Grain size
- vf Very fine-grained sandstone
- f Fine-grained sandstone
- m Medium-grained sandstone
- c Coarse-grained sandstone
- vc Very coarse-grained sandstone
- g Gravel
- p Pebble
- cb Cobble

Sedimentary structures
- Parallel lamination
- Ripple lamination
- Convoluted lamination
- Tabular cross stratification
- Trough cross stratification
- Mud cracks
- Soft pebbles
- Carbonate nodules
- Positive granoselection

Trace and body fossils
- Rhizocretions
- Plant remains
- Plant debris / Coal
- Tree logs
- Burrows
- Invertebrate tracks
- Tetrapod tracks
- Clam shrimps
- Insects
- Fish scales / Fishes

Other symbols
- Fault
- 188/42 Strike/dip angle

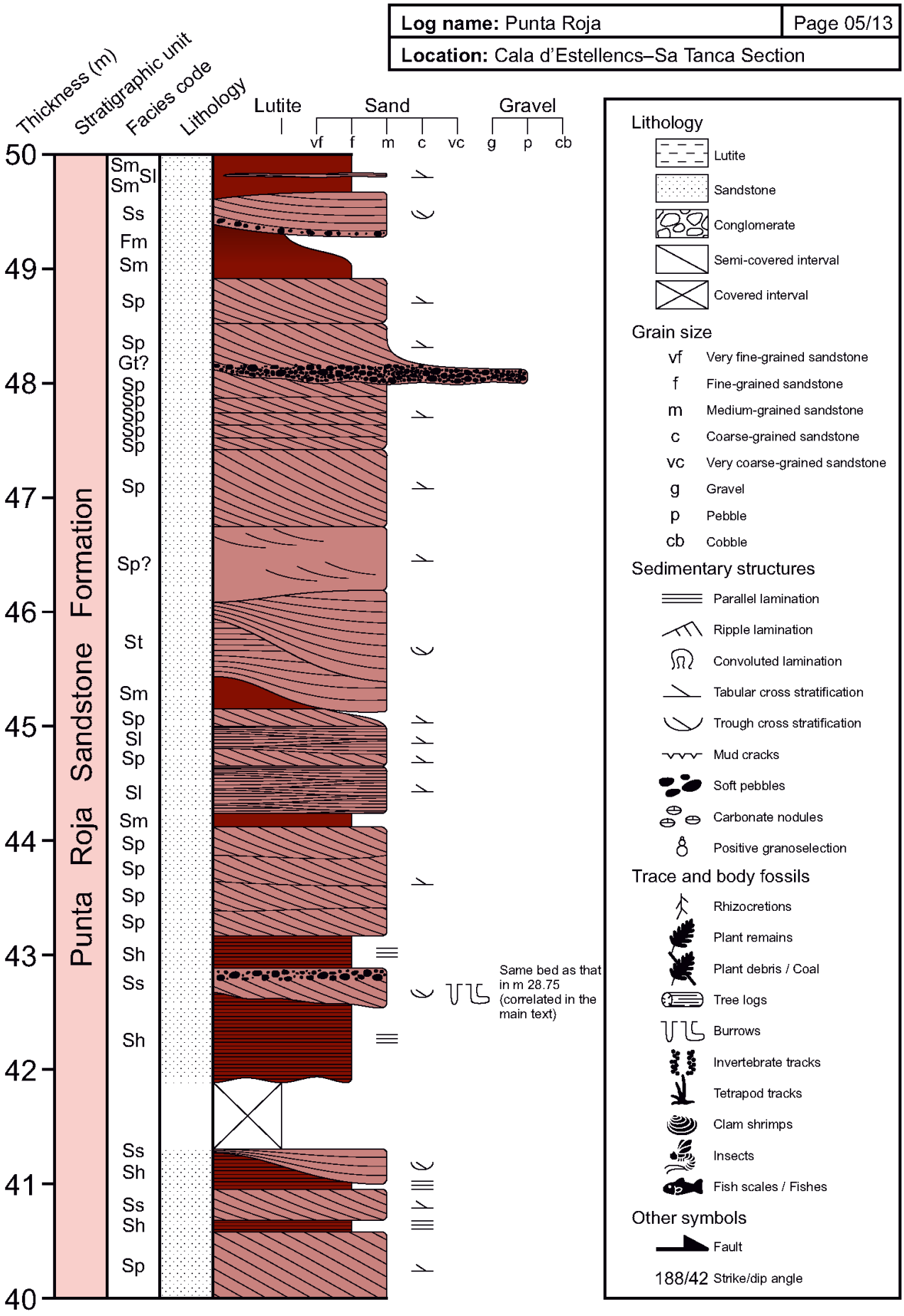
Log name: Punta Roja
Page 05/13
Location: Cala d'Estellencs–Sa Tanca Section
Thickness (m)
Stratigraphic unit
Facies code
Lithology
Lutite
Sand
Gravel
vf f m c vc g p cb
Punta Roja Sandstone Formation
50
49
48
47
46
45
44
43
42
41
40
Sm Sl
Sm
Ss
Fm
Sm
Sp
Sp
Gt?
Sp
Sp
Sp
Sp
Sp
Sp
Sp?
St
Sm
Sp
Sl
Sp
Sl
Sm
Sp
Sp
Sp
Sp
Sh
Ss
Sh
Ss
Sh
Ss
Sh
Sp
Same bed as that in m 28.75 (correlated in the main text)
Lithology
Lutite
Sandstone
Conglomerate
Semi-covered interval
Covered interval
Grain size
vf Very fine-grained sandstone
f Fine-grained sandstone
m Medium-grained sandstone
c Coarse-grained sandstone
vc Very coarse-grained sandstone
g Gravel
p Pebble
cb Cobble
Sedimentary structures
Parallel lamination
Ripple lamination
Convoluted lamination
Tabular cross stratification
Trough cross stratification
Mud cracks
Soft pebbles
Carbonate nodules
Positive granoselection
Trace and body fossils
Rhizocretions
Plant remains
Plant debris / Coal
Tree logs
Burrows
Invertebrate tracks
Tetrapod tracks
Clam shrimps
Insects
Fish scales / Fishes
Other symbols
Fault
188/42 Strike/dip angle

Log name: Punta Roja | Page 06/13

Location: Cala d'Estellencs–Sa Tanca Section

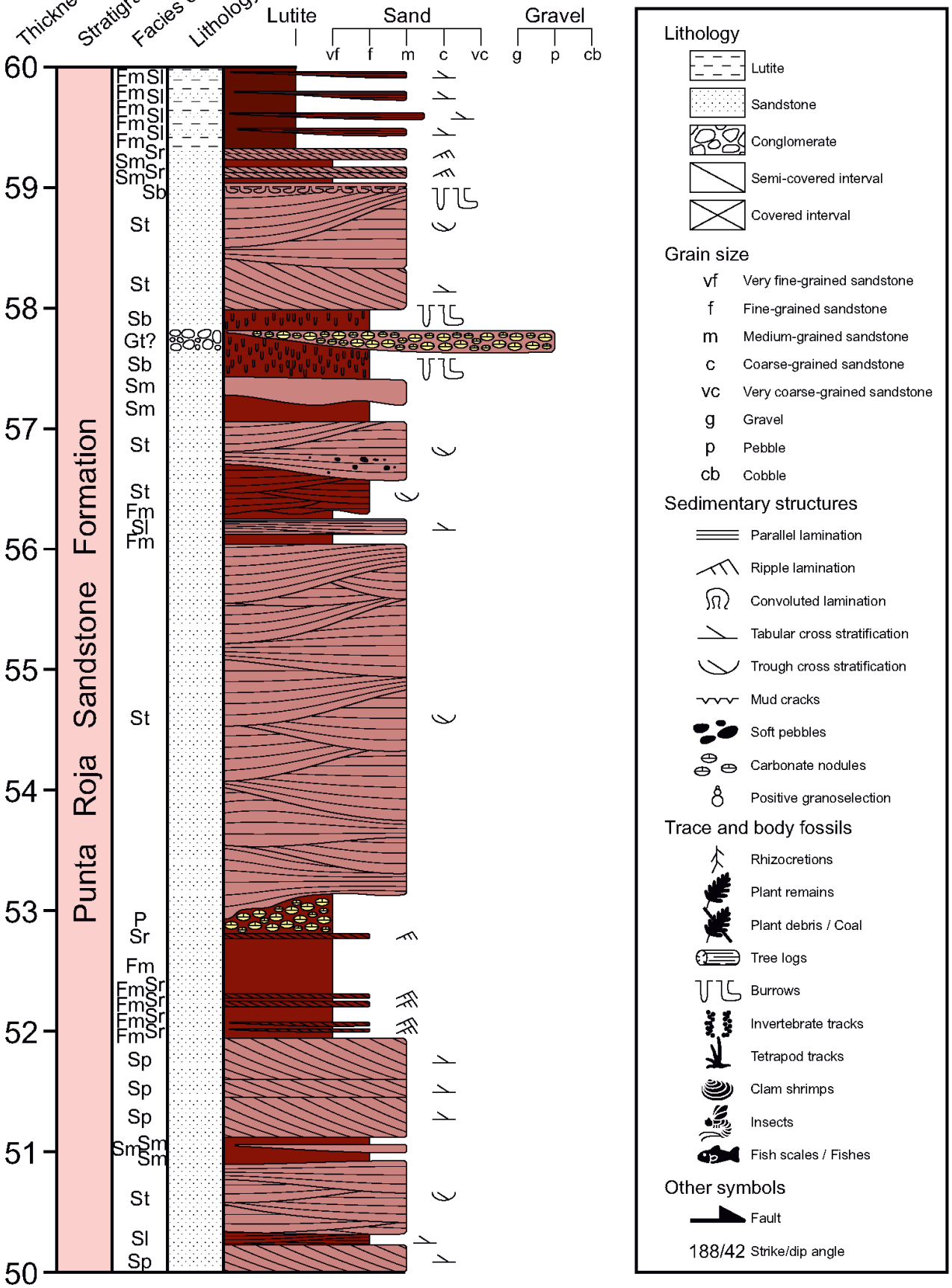

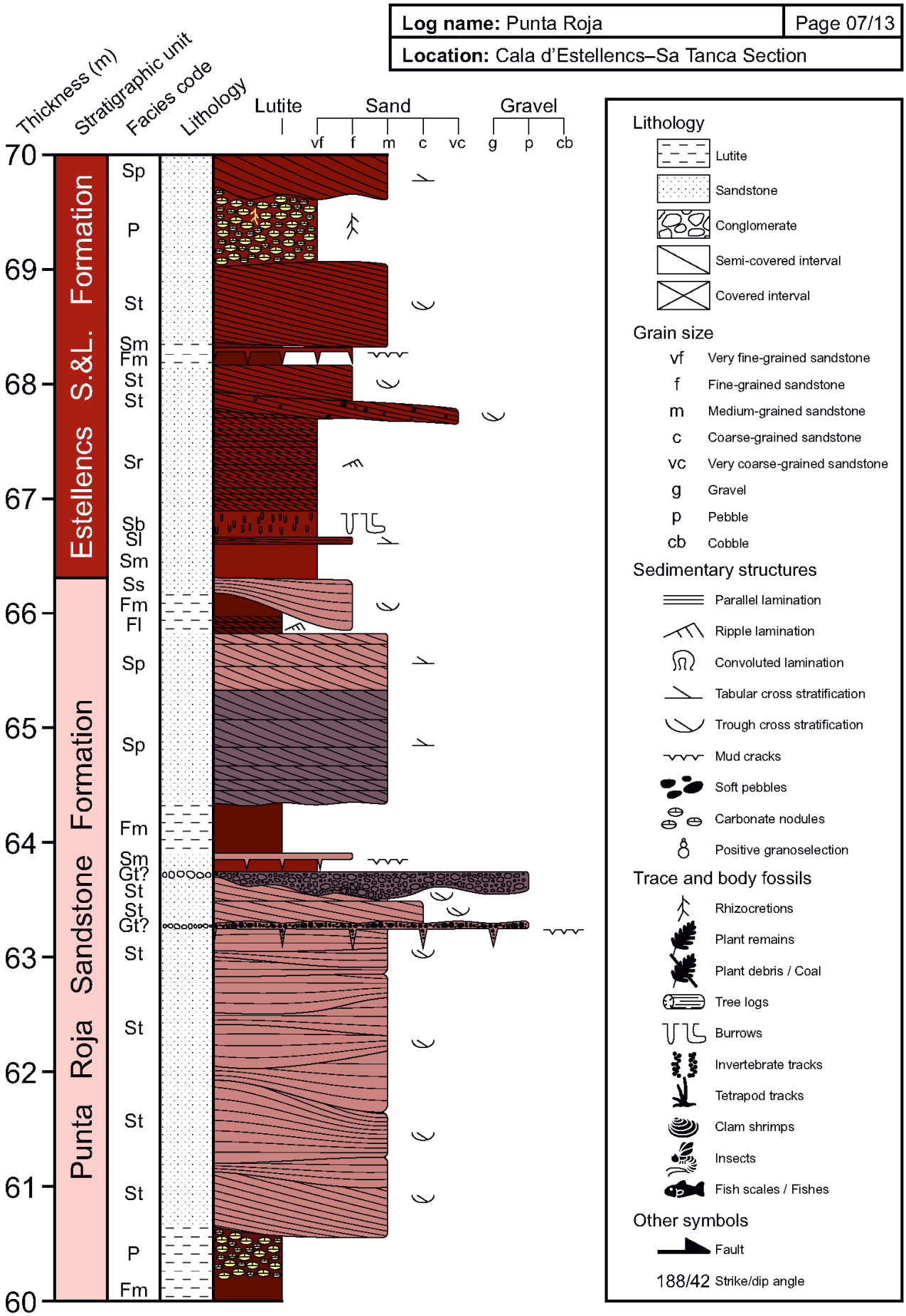
Log name: Punta Roja
Page 07/13
Location: Cala d'Estellencs–Sa Tanca Section
Thickness (m)
Stratigraphic unit
Facies code
Lithology
Lutite
Sand
Gravel
vf f m c vc g p cb
70
69
68
67
66
65
64
63
62
61
60
Estellencs S.&L. Formation
Punta Roja Sandstone Formation
Sp
P
St
Sm
Fm
St
St
Sr
Sb
Sl
Sm
Ss
Fm
Fl
Sp
Sp
Fm
Sm
Gt?
St
St
Gt?
St
St
St
St
P
Fm
Lithology
Lutite
Sandstone
Conglomerate
Semi-covered interval
Covered interval
Grain size
vf Very fine-grained sandstone
f Fine-grained sandstone
m Medium-grained sandstone
c Coarse-grained sandstone
vc Very coarse-grained sandstone
g Gravel
p Pebble
cb Cobble
Sedimentary structures
Parallel lamination
Ripple lamination
Convoluted lamination
Tabular cross stratification
Trough cross stratification
Mud cracks
Soft pebbles
Carbonate nodules
Positive granoselection
Trace and body fossils
Rhizocretions
Plant remains
Plant debris / Coal
Tree logs
Burrows
Invertebrate tracks
Tetrapod tracks
Clam shrimps
Insects
Fish scales / Fishes
Other symbols
Fault
188/42 Strike/dip angle

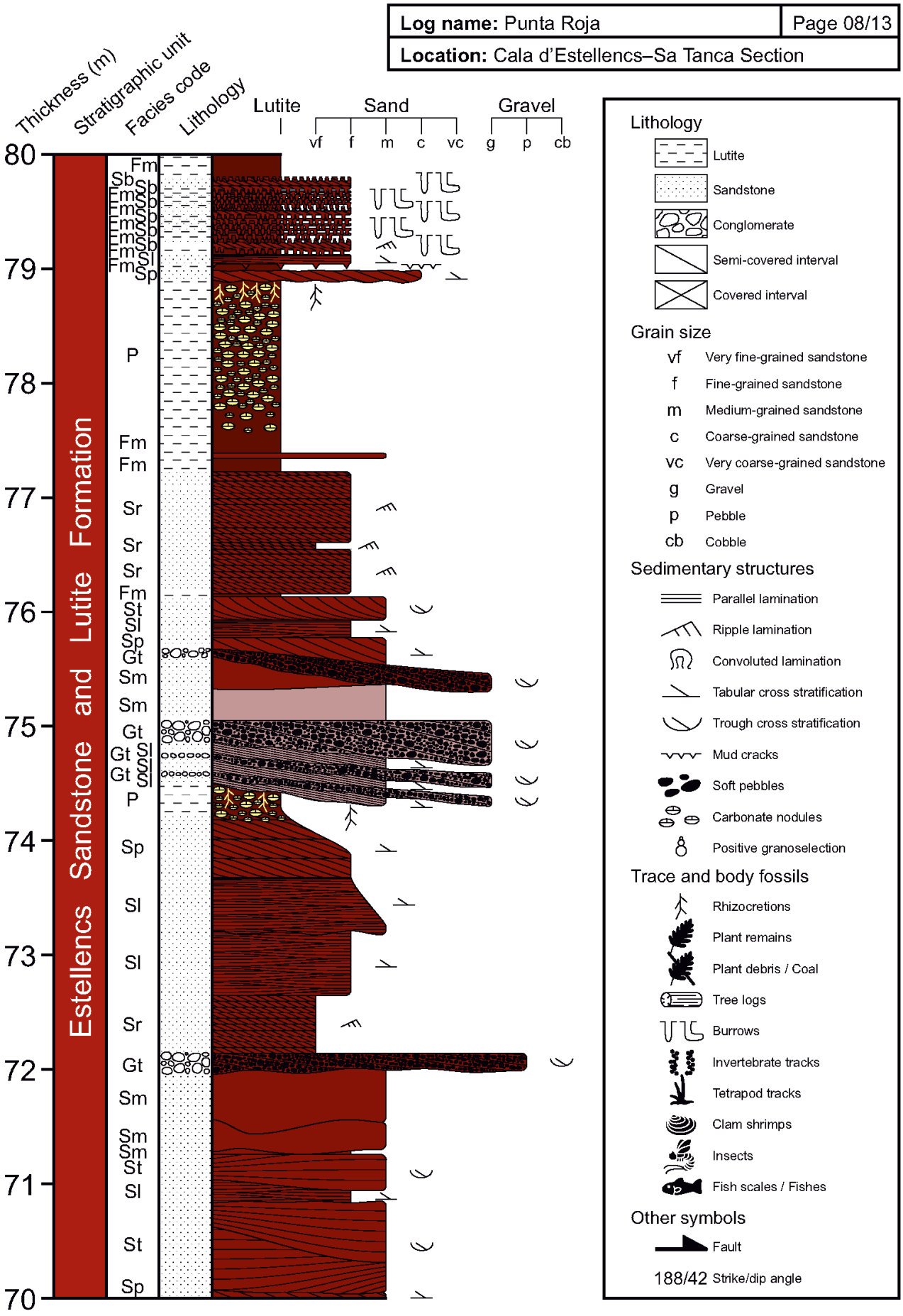
Log name: Punta Roja
Page 08/13
Location: Cala d'Estellencs–Sa Tanca Section
Thickness (m)
Stratigraphic unit
Facies code
Lithology
Lutite
Sand
Gravel
vf f m c vc g p cb
Estellencs Sandstone and Lutite Formation
80
79
78
77
76
75
74
73
72
71
70
Fm
Sb
Sm
Sl
Sp
P
Sr
St
Gt
Lithology
Lutite
Sandstone
Conglomerate
Semi-covered interval
Covered interval
Grain size
vf Very fine-grained sandstone
f Fine-grained sandstone
m Medium-grained sandstone
c Coarse-grained sandstone
vc Very coarse-grained sandstone
g Gravel
p Pebble
cb Cobble
Sedimentary structures
Parallel lamination
Ripple lamination
Convoluted lamination
Tabular cross stratification
Trough cross stratification
Mud cracks
Soft pebbles
Carbonate nodules
Positive granoselection
Trace and body fossils
Rhizocretions
Plant remains
Plant debris / Coal
Tree logs
Burrows
Invertebrate tracks
Tetrapod tracks
Clam shrimps
Insects
Fish scales / Fishes
Other symbols
Fault
188/42 Strike/dip angle

Log name: Punta Roja	Page 09/13
Location: Cala d'Estellencs–Sa Tanca Section	

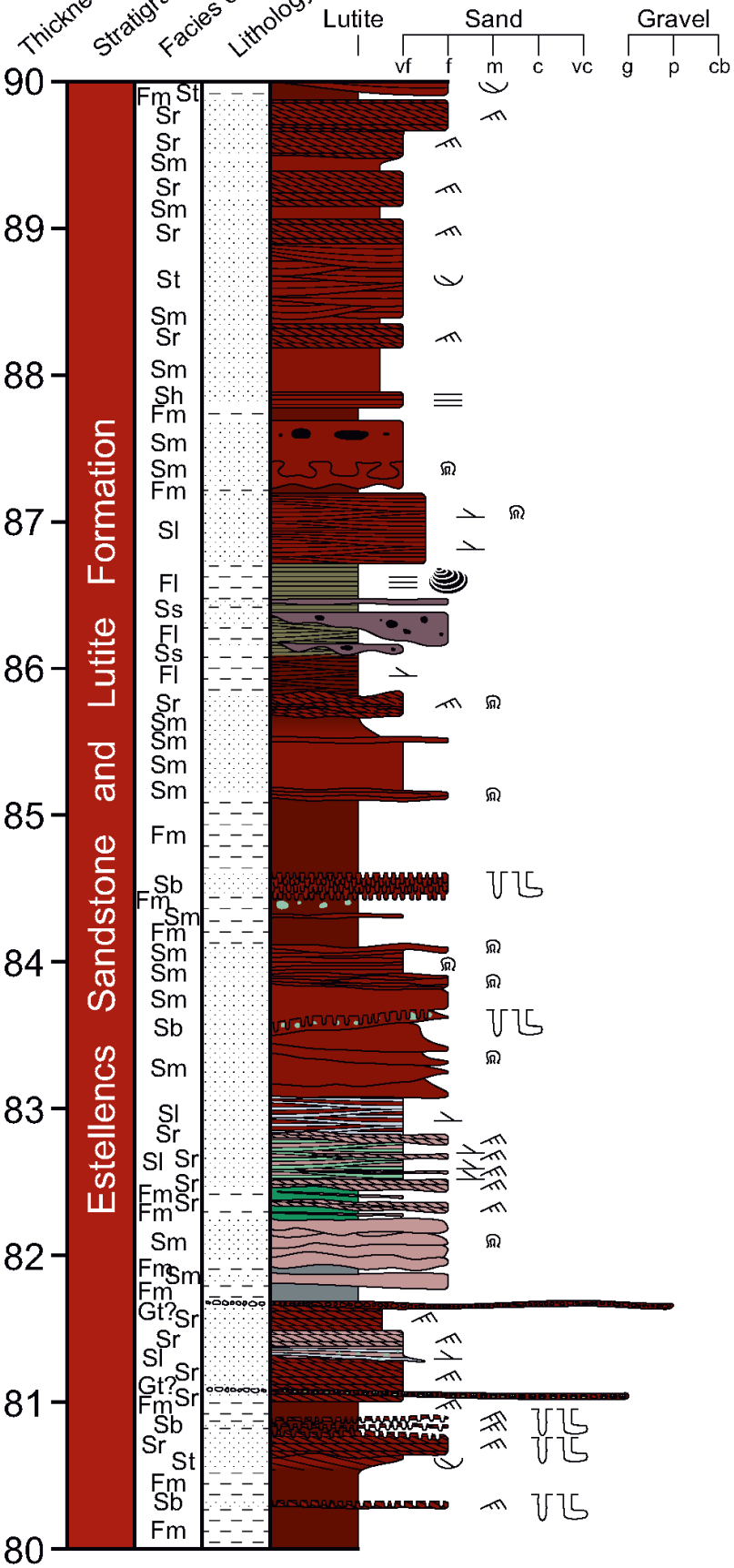

Lithology
- Lutite
- Sandstone
- Conglomerate
- Semi-covered interval
- Covered interval

Grain size
- vf Very fine-grained sandstone
- f Fine-grained sandstone
- m Medium-grained sandstone
- c Coarse-grained sandstone
- vc Very coarse-grained sandstone
- g Gravel
- p Pebble
- cb Cobble

Sedimentary structures
- Parallel lamination
- Ripple lamination
- Convoluted lamination
- Tabular cross stratification
- Trough cross stratification
- Mud cracks
- Soft pebbles
- Carbonate nodules
- Positive granoselection

Trace and body fossils
- Rhizocretions
- Plant remains
- Plant debris / Coal
- Tree logs
- Burrows
- Invertebrate tracks
- Tetrapod tracks
- Clam shrimps
- Insects
- Fish scales / Fishes

Other symbols
- Fault
- 188/42 Strike/dip angle

Log name: Punta Roja | Page 10/13

Location: Cala d'Estellencs–Sa Tanca Section

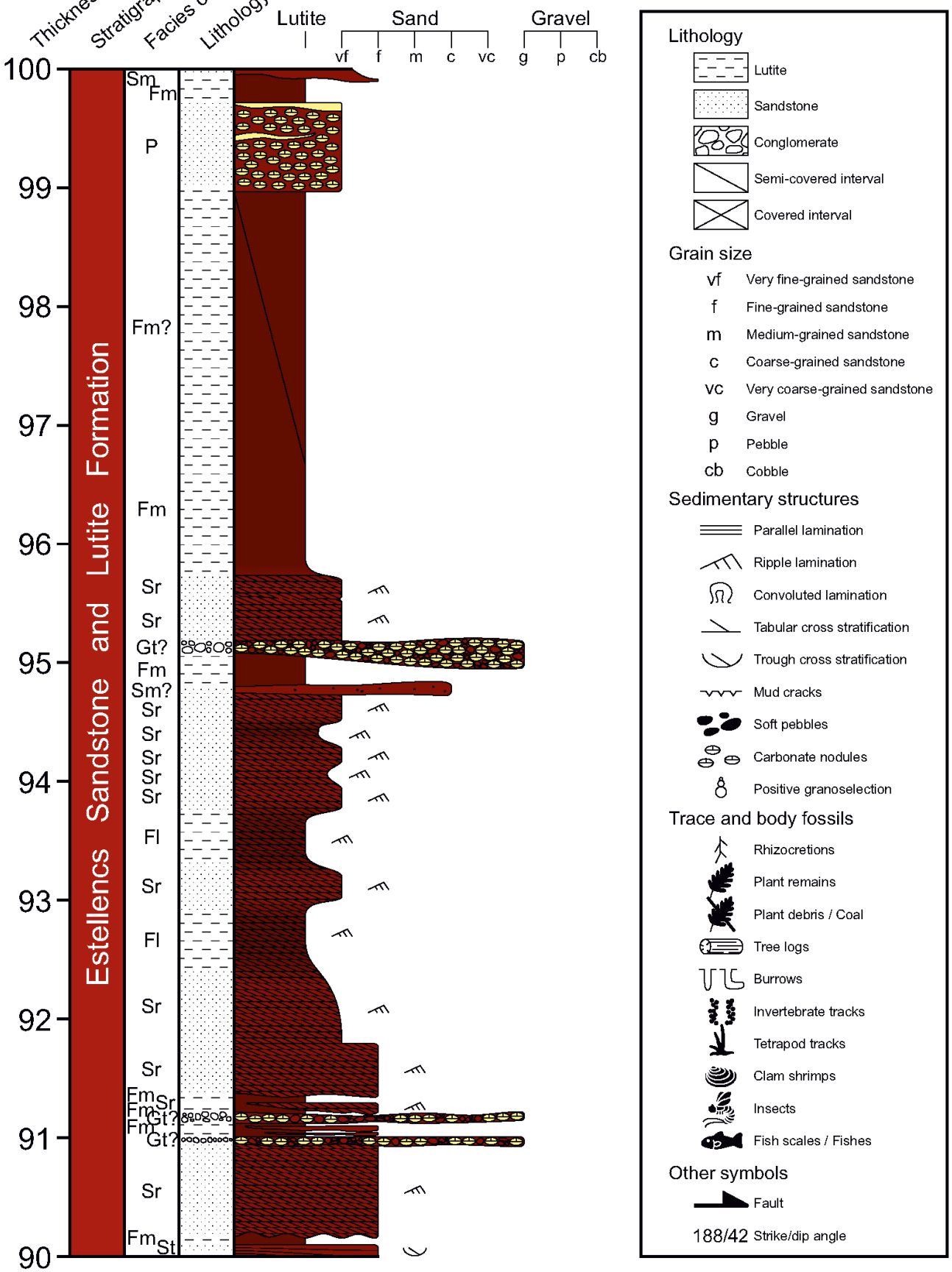

Log name: Punta Roja	Page 11/13
Location: Cala d'Estellencs–Sa Tanca Section	

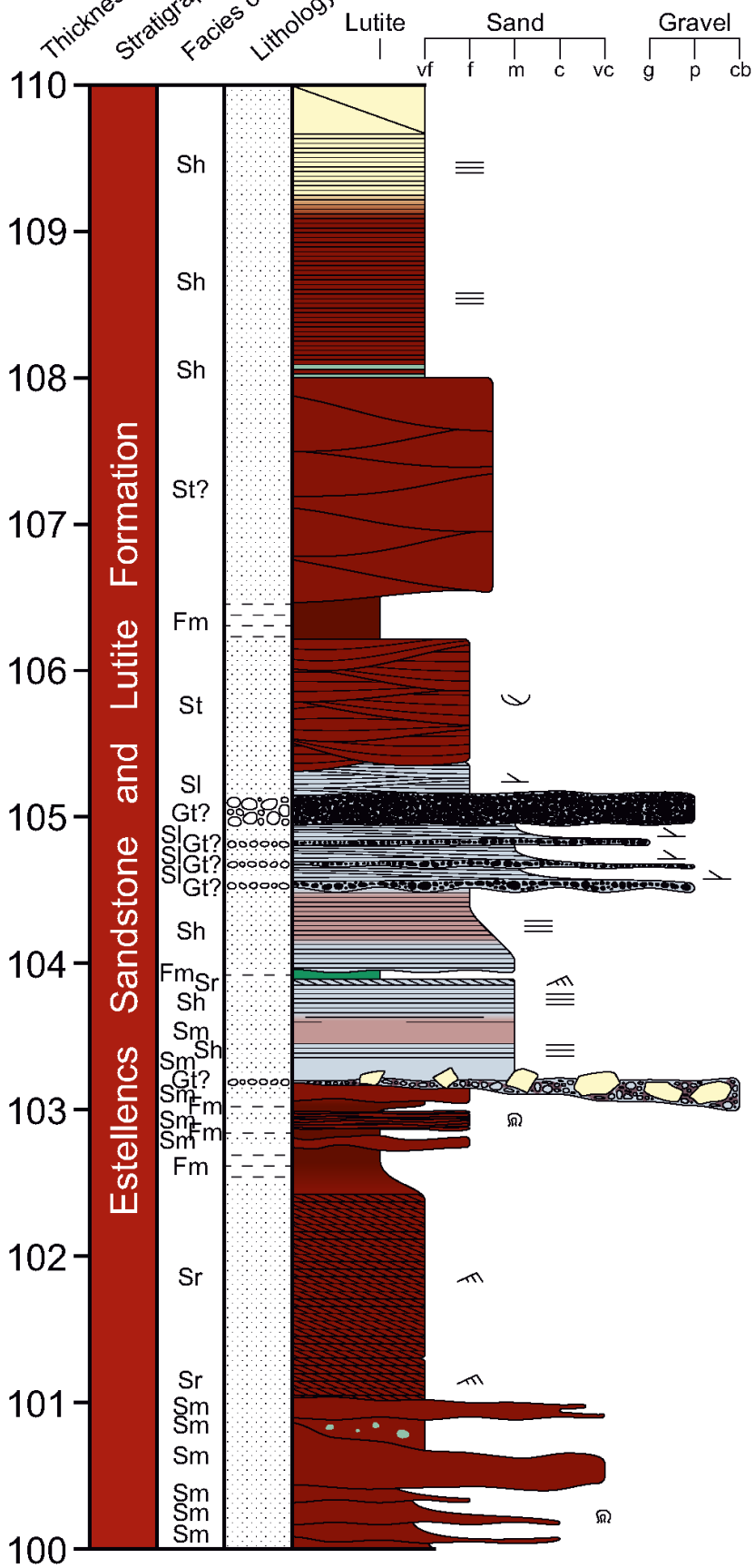

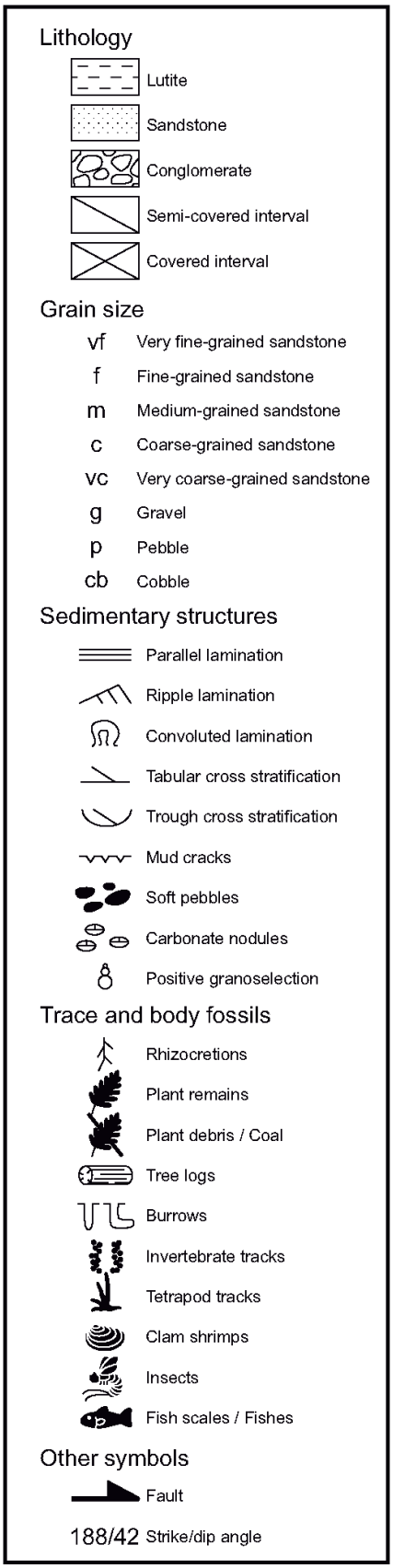

Log name: Punta Roja	Page 12/13
Location: Cala d'Estellencs–Sa Tanca Section	

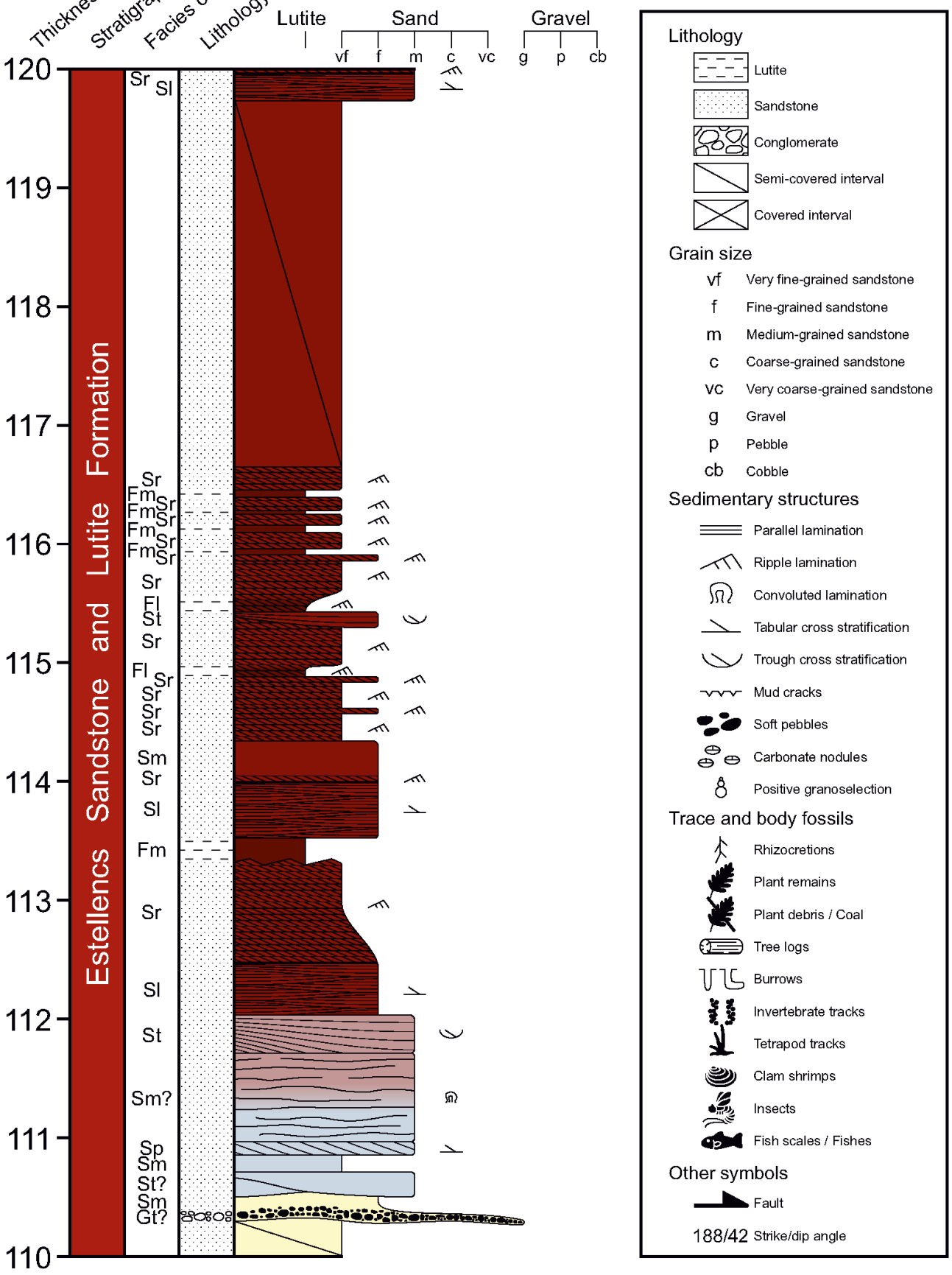

Log name: Punta Roja	Page 13/13
Location: Cala d'Estellencs–Sa Tanca Section	

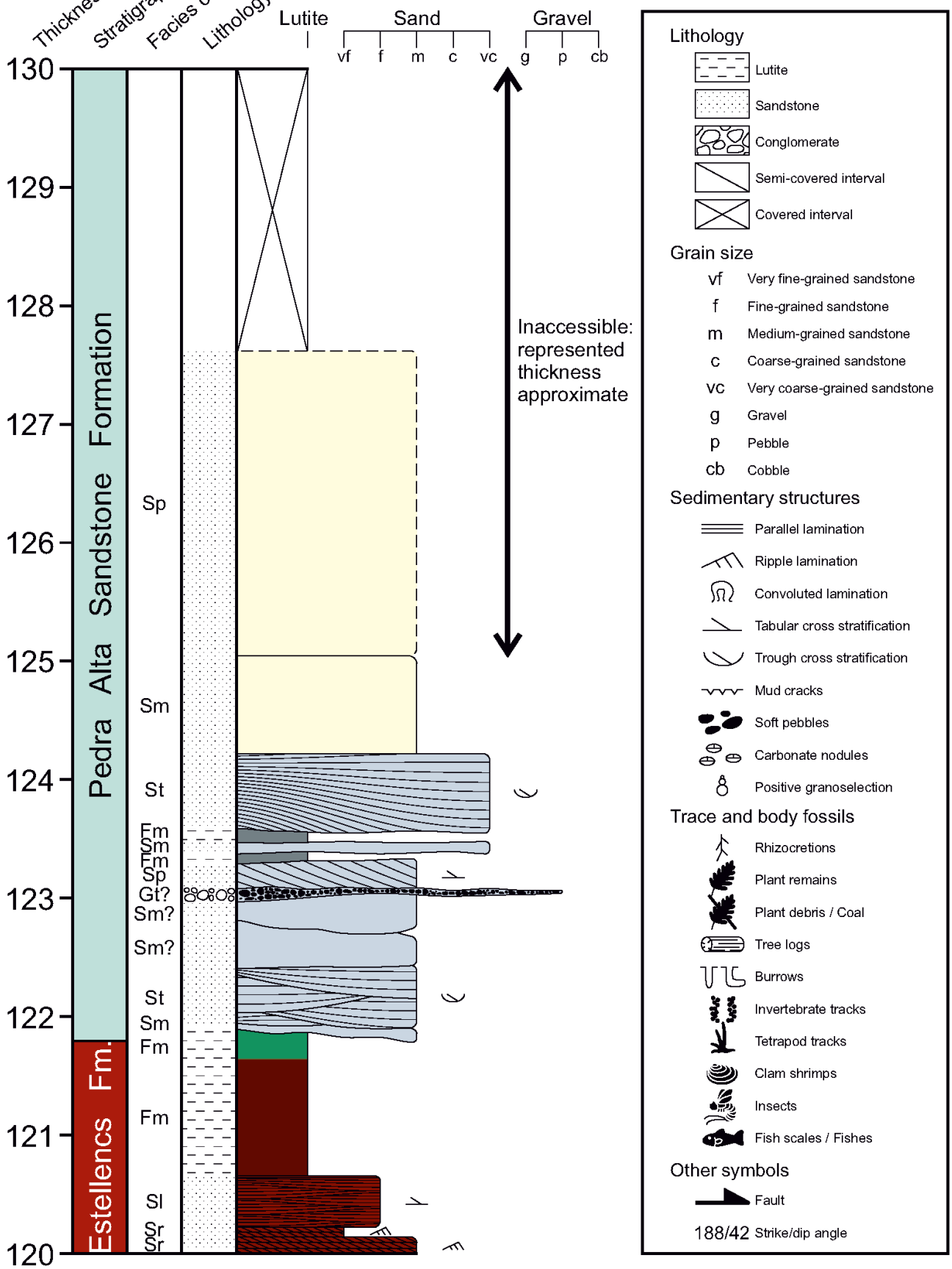

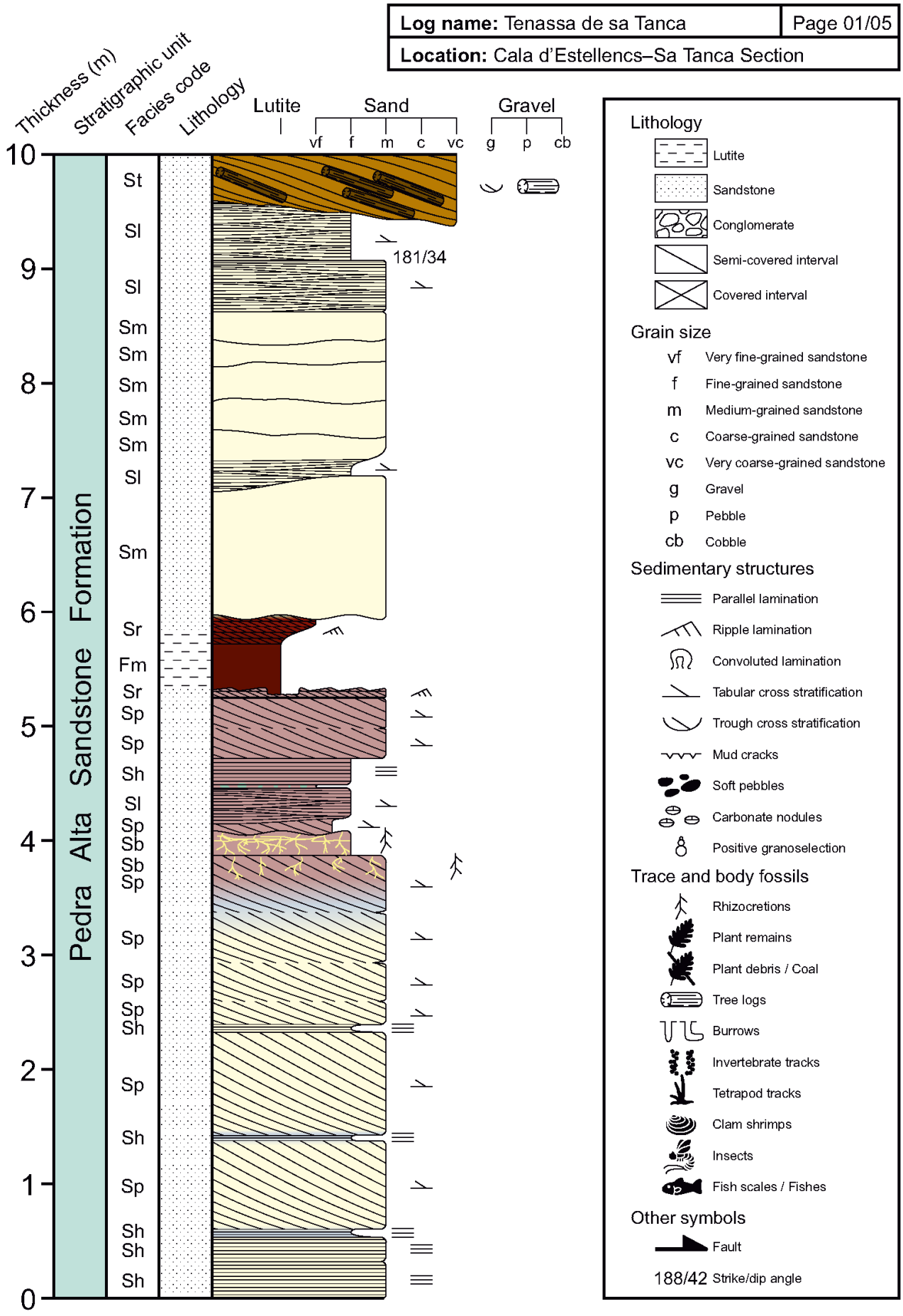
Log name: Tenassa de sa Tanca
Page 01/05
Location: Cala d'Estellencs–Sa Tanca Section
Thickness (m)
Stratigraphic unit
Facies code
Lithology
Lutite
Sand
Gravel
vf f m c vc
g p cb
Pedra Alta Sandstone Formation
181/34
Lithology
Lutite
Sandstone
Conglomerate
Semi-covered interval
Covered interval
Grain size
vf Very fine-grained sandstone
f Fine-grained sandstone
m Medium-grained sandstone
c Coarse-grained sandstone
vc Very coarse-grained sandstone
g Gravel
p Pebble
cb Cobble
Sedimentary structures
Parallel lamination
Ripple lamination
Convoluted lamination
Tabular cross stratification
Trough cross stratification
Mud cracks
Soft pebbles
Carbonate nodules
Positive granoselection
Trace and body fossils
Rhizocretions
Plant remains
Plant debris / Coal
Tree logs
Burrows
Invertebrate tracks
Tetrapod tracks
Clam shrimps
Insects
Fish scales / Fishes
Other symbols
Fault
188/42 Strike/dip angle

Log name: Tenassa de sa Tanca	Page 02/05
Location: Cala d'Estellencs–Sa Tanca Section	

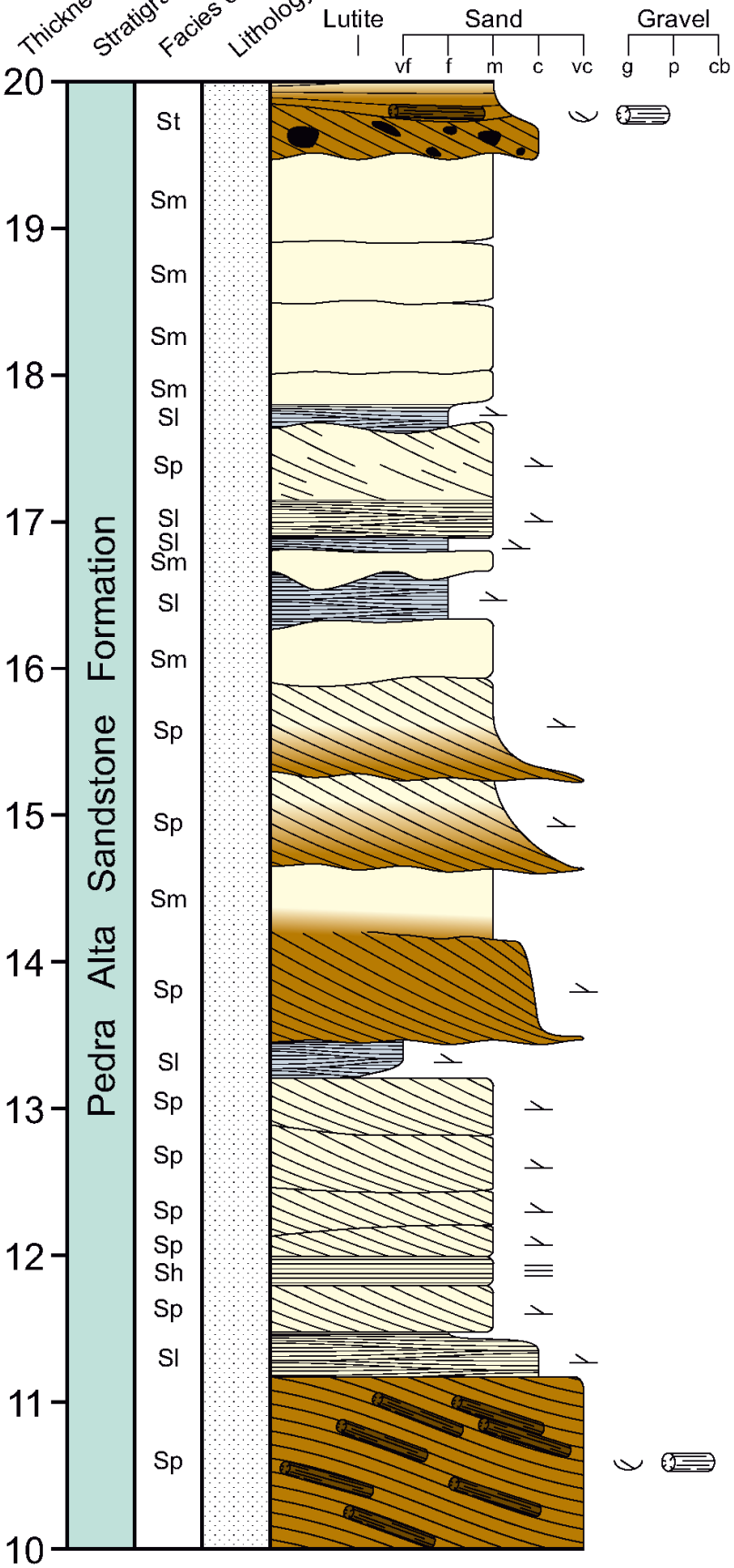

Lithology
- Lutite
- Sandstone
- Conglomerate
- Semi-covered interval
- Covered interval

Grain size
- vf Very fine-grained sandstone
- f Fine-grained sandstone
- m Medium-grained sandstone
- c Coarse-grained sandstone
- vc Very coarse-grained sandstone
- g Gravel
- p Pebble
- cb Cobble

Sedimentary structures
- Parallel lamination
- Ripple lamination
- Convoluted lamination
- Tabular cross stratification
- Trough cross stratification
- Mud cracks
- Soft pebbles
- Carbonate nodules
- Positive granoselection

Trace and body fossils
- Rhizocretions
- Plant remains
- Plant debris / Coal
- Tree logs
- Burrows
- Invertebrate tracks
- Tetrapod tracks
- Clam shrimps
- Insects
- Fish scales / Fishes

Other symbols
- Fault
- 188/42 Strike/dip angle

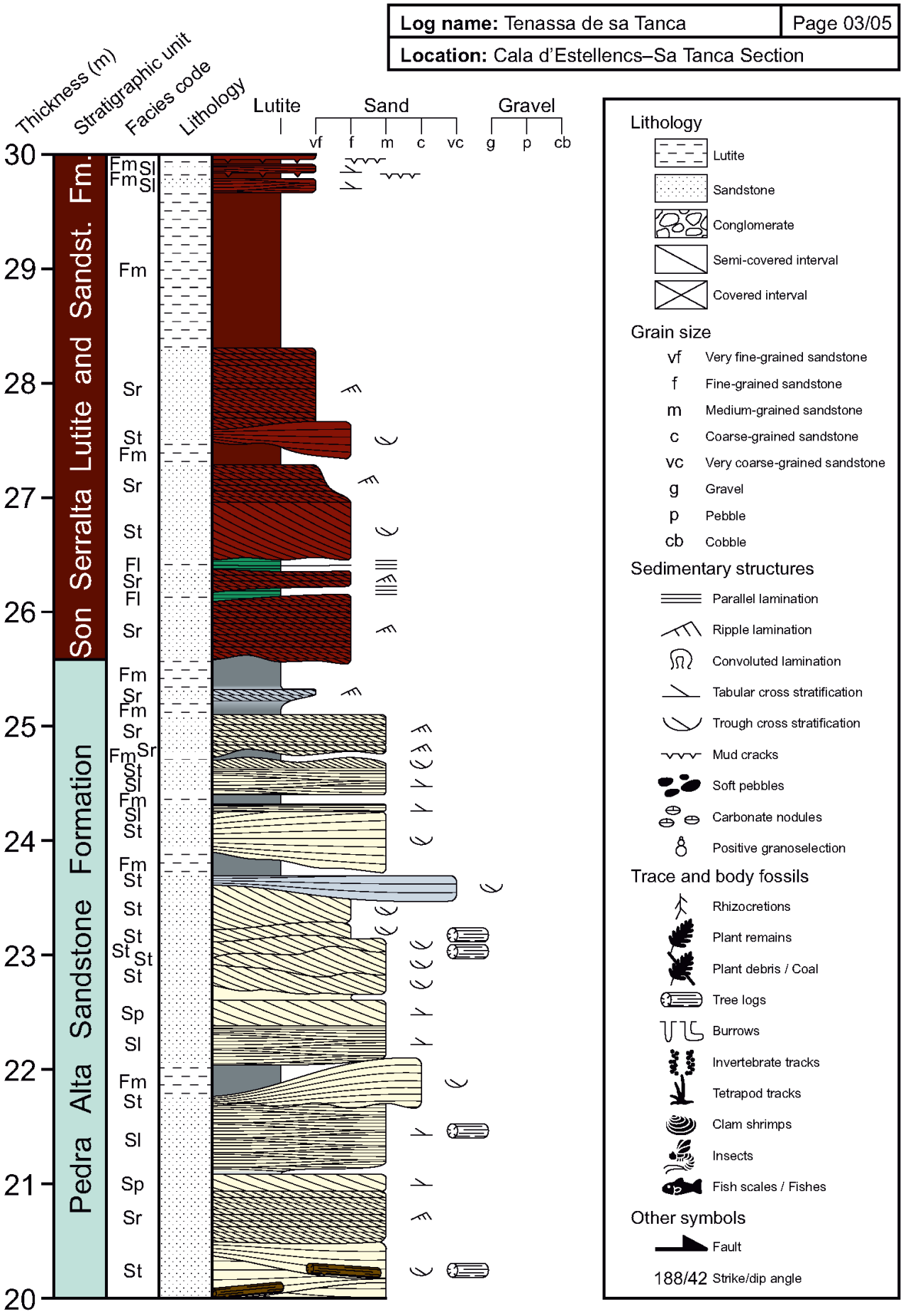
Log name: Tenassa de sa Tanca
Page 03/05
Location: Cala d'Estellencs–Sa Tanca Section
Thickness (m)
Stratigraphic unit
Facies code
Lithology
Lutite
Sand
Gravel
vf f m c vc g p cb
Son Serralta Lutite and Sandst. Fm.
Pedra Alta Sandstone Formation
30
29
28
27
26
25
24
23
22
21
20
Lithology
Lutite
Sandstone
Conglomerate
Semi-covered interval
Covered interval
Grain size
vf Very fine-grained sandstone
f Fine-grained sandstone
m Medium-grained sandstone
c Coarse-grained sandstone
vc Very coarse-grained sandstone
g Gravel
p Pebble
cb Cobble
Sedimentary structures
Parallel lamination
Ripple lamination
Convoluted lamination
Tabular cross stratification
Trough cross stratification
Mud cracks
Soft pebbles
Carbonate nodules
Positive granoselection
Trace and body fossils
Rhizocretions
Plant remains
Plant debris / Coal
Tree logs
Burrows
Invertebrate tracks
Tetrapod tracks
Clam shrimps
Insects
Fish scales / Fishes
Other symbols
Fault
188/42 Strike/dip angle

Log name: Tenassa de sa Tanca	Page 04/05
Location: Cala d'Estellencs–Sa Tanca Section	

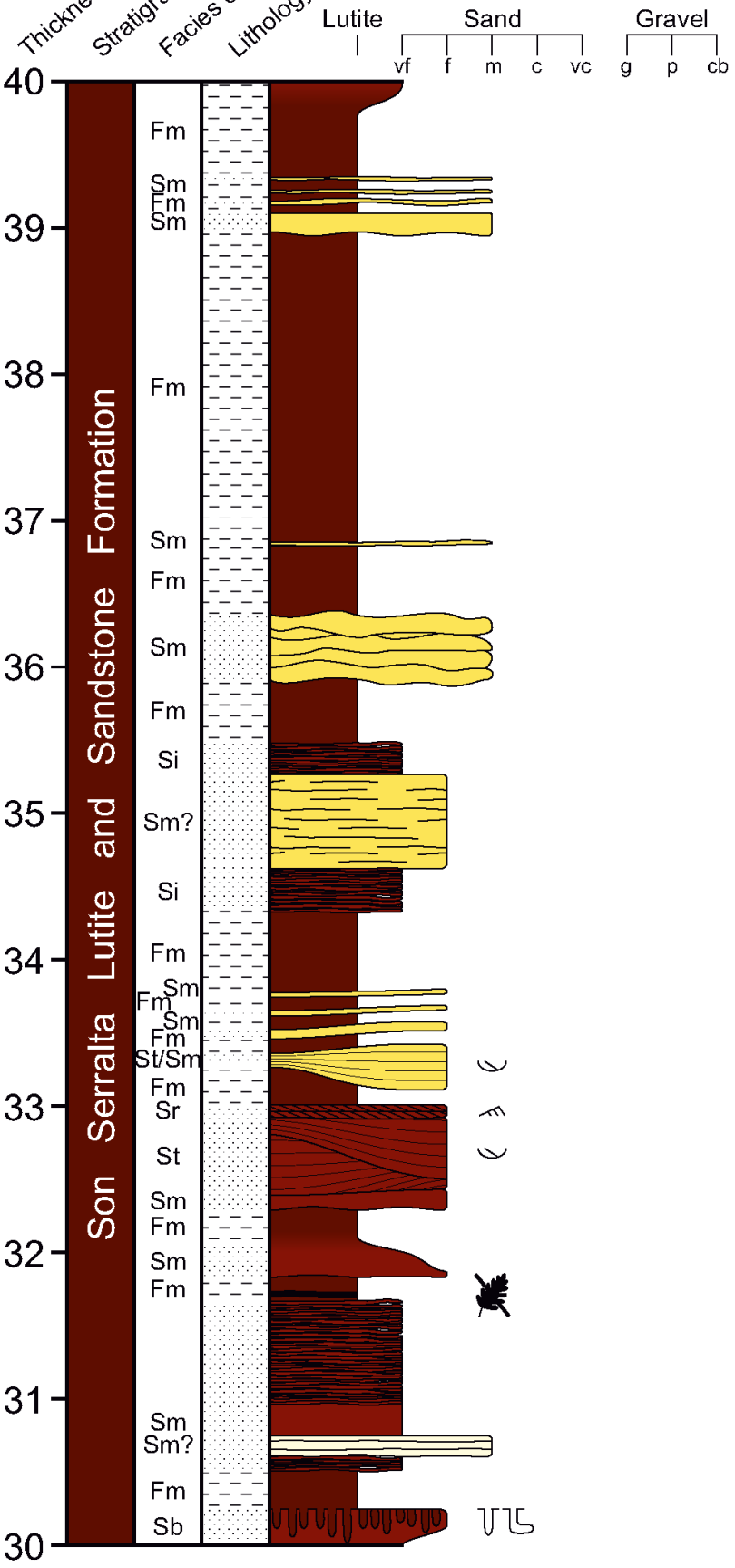

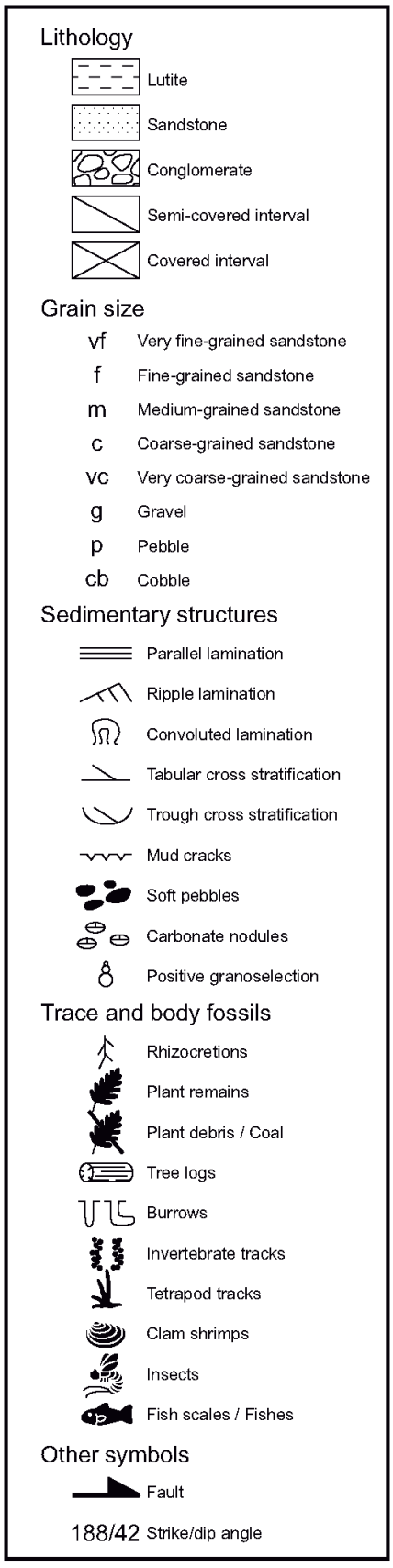

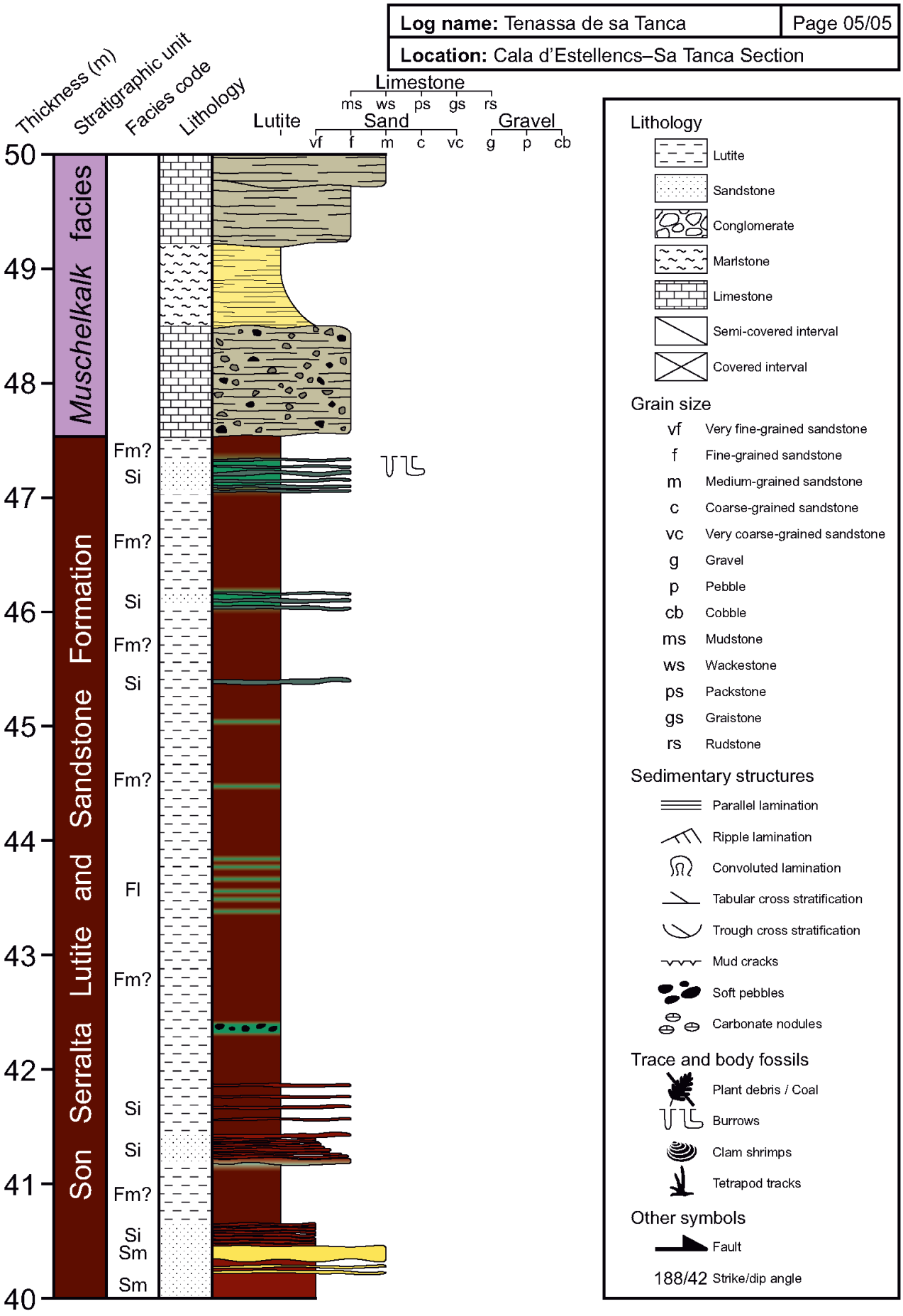
Log name: Tenassa de sa Tanca
Page 05/05
Location: Cala d'Estellencs–Sa Tanca Section
Thickness (m)
Stratigraphic unit
Facies code
Lithology
Limestone
ms ws ps gs rs
Lutite
Sand
vf f m c vc
Gravel
g p cb
50
49
48
47
46
45
44
43
42
41
40
Muschelkalk facies
Son Serralta Lutite and Sandstone Formation
Fm?
Si
Fm?
Si
Fm?
Si
Fm?
Fl
Fm?
Si
Si
Fm?
Si
Sm
Sm
Lithology
Lutite
Sandstone
Conglomerate
Marlstone
Limestone
Semi-covered interval
Covered interval
Grain size
vf Very fine-grained sandstone
f Fine-grained sandstone
m Medium-grained sandstone
c Coarse-grained sandstone
vc Very coarse-grained sandstone
g Gravel
p Pebble
cb Cobble
ms Mudstone
ws Wackestone
ps Packstone
gs Graistone
rs Rudstone
Sedimentary structures
Parallel lamination
Ripple lamination
Convoluted lamination
Tabular cross stratification
Trough cross stratification
Mud cracks
Soft pebbles
Carbonate nodules
Trace and body fossils
Plant debris / Coal
Burrows
Clam shrimps
Tetrapod tracks
Other symbols
Fault
188/42 Strike/dip angle

Appendix 8

Triassic clam shrimps from Mallorca

Appendix 8 was published as:

Scholze, F. & **Matamales-Andreu, R.** (2021). Triassic clam shrimps ("Conchostraca"; Branchiopoda: Diplostraca) from Mallorca: Taxonomic description and interregional comparisons. *Zootaxa*, 4964(3): 471–496.

DOI: https://doi.org/10.11646/zootaxa.4964.3.3

In this work, R. Matamales-Andreu contributed in:

A. Logging of the stratigraphic section.
B. Co-direction of all fieldwork campaigns (prospections and excavations). Sampling of clam shrimp fossils.
C. Stratigraphic and sedimentological analysis.
D. Writing of the Geologic Setting section of the original draft.
E. Review and editing of the manuscript.
F. Preparation of Figure 1.
G. Collaboration in obtaining funding for fieldwork.

Zootaxa 4964 (3): 471–496
https://www.mapress.com/j/zt/
Copyright © 2021 Magnolia Press

Article

ISSN 1175-5326 (print edition)
ZOOTAXA
ISSN 1175-5334 (online edition)

https://doi.org/10.11646/zootaxa.4964.3.3
http://zoobank.org/urn:lsid:zoobank.org:pub:B31AA81E-5462-4B4A-A686-B9C21890347C

Triassic clam shrimps ("Conchostraca"; Branchiopoda: Diplostraca) from Mallorca: Taxonomic description and interregional comparisons

FRANK SCHOLZE[1] & RAFEL MATAMALES-ANDREU[2,3]
[1]*Institut für Geowissenschaften, Friedrich-Schiller-Universität Jena, Burgweg 11, 07749 Jena, Germany.*
Frank.Scholze@uni-jena.de; https://orcid.org/0000-0001-7298-9741
[2]*Institut Català de Paleontologia Miquel Crusafont (ICP), C/ de les Columnes s/n, Edifici Z (ICTA-ICP), Campus de la Universitat Autònoma de Barcelona, 08193 Cerdanyola del Vallès, Barcelona, Catalunya, Spain.*
rafel.matamales@icp.cat; https://orcid.org/0000-0001-9914-0510
[3]*Museu Balear de Ciències Naturals, Carretera Palma–Port de Sóller Km. 30, 07100 Sóller, Mallorca, Illes Balears, Spain.*

Abstract

We describe four upper Lower Triassic to lower Middle Triassic clam shrimp-bearing intervals from Mallorca, which include the clam shrimp species *Hornestheria* sp. aff. *Hornestheria sollingensis* and several other forms of carapace valve morphology: *Hornestheria*? Morphotype 1, *Hornestheria*? Morphotype 2, and other undetermined carapace valves. All of this material was obtained from red-bed units cropping out in the Serra de Tramuntana mountains of Mallorca (western Mediterranean). Except for a few morphologically similar carapace valves of Middle Triassic age from China, *Hornestheria* is known only from the type locality of its type species, *Hornestheria sollingensis* Kozur et Lepper, in the Solling Formation (Middle Buntsandstein Subgroup) in the German part of the Central European Basin. According to its original definition, the larval carapace valve of *Hornestheria* Kozur et Lepper is characterized by a radial sculpture, but this characteristic apparently is only variably developed. Due to both a limited number of previously known occurrences of *Hornestheria* and its poorly known carapace valve morphology, open nomenclature is applied to the taxonomy herein. The studied specimens were freshly collected from outcrop sections composed of greyish-green to greyish-red laminated claystones and siltstones that accumulated in a fluvial facies. The clam shrimp specimens are accompanied by remains of insects and fishes, invertebrate and tetrapod ichnofossils, and micro-/macroplant remains, all of which either have been described by previous workers or are currently part of a separate study.

Key words: Crustacea, Spinicaudata, *Hornestheria*, Pangaea, Balearic Islands, western Mediterranean

Introduction

The traditional term 'conchostracans' designates a group of small-sized branchiopod crustaceans, which are known from Devonian to recent times (e.g., Tasch 1969; Hegna & Astrop 2020). They have a chitinous, bivalved carapace, composed of two symmetric valves laterally enclosing their crustacean body. However, it is difficult to link their fossil forms to the zoological classification scheme of their recent relatives (i.e., clam shrimps and waterfleas) due to the often poorly preserved morphological characteristics of fossil carapace valves. Therefore, fossil 'Conchostraca' are treated as a paraphyletic taxonomic group corresponding to a composite of the extant monophyletic suborders Spinicaudata, Laevicaudata, Cyclestherida, and Cladocera (e.g., Rogers & Hegna 2020). In both fossil and recent taxonomic systematics, these four suborders comprise the order Diplostraca within the class Branchiopoda. Occurrences of modern clam shrimps in continental deposits are known from all continents other than Antarctica (Frank 1988). Fossil clam shrimps are mostly found in continental bodies of water, but can also be found in both brackish and shallow marine deposits (e.g., Webb 1979; Liu & He 2000; Scholze *et al.* 2020).

Both modern and fossil clam shrimps are (palaeo-) geographically widely distributed from the Devonian to the present, because of the very high dispersal potential of their minute, drought and/or frost resistant, wind-transportable dormant eggs. Their eggs can also be attached to other animals or survive passage through the digestive system of predators, thus adding to their geographic dispersal mechanisms (e.g., Vanschoenwinkel *et al.* 2008). As noticed

Accepted by M. Alonso: 17 Mar. 2021; published: 23 Apr. 2021

by previous workers (e.g., Schneider *et al.* 2020), clam shrimp habitats changed during the late Palaeozoic from perennial lakes to seasonal and temporary lakes, ponds, and puddles, coincident with a nearly global palaeoclimate aridification that began at that time. Like other pioneering organisms, many clam shrimp species (including all modern species of spinicaudatans and laevicaudatans) became adapted to thrive in ephemeral freshwater pools, as well as in water bodies with elevated salinities because of evaporation, where their carapace valves often accumulated in mass occurrences that are useful for biostratigraphy.

Here, we study the clam shrimps from the lower Middle Triassic continental units of Mallorca. The deposits of the study area are known for their occurrences of insects (Calafat & Sáez 1987; Calafat 1988; Zessin 2008a, 2008b; Aristov & Zessin 2009; Juárez-Ruiz & Wachtler 2015) and tetrapod trace fossils (Juárez-Ruiz & Wachtler 2015). Additionally, records of clam shrimps ("*Euestheria* sp."), shark egg capsules ("*Palaeoxyris* sp."), a fish of unknown affinities, and arthropod trace fossils also have been mentioned by Calafat & Sáez (1987), Calafat (1988), and Zessin (2008b). Moreover, occurrences of conifers and other micro- and macroplant remains have been reported in detail by previous workers (e.g., Álvarez-Ramis *et al.* 1995; Grauvogel-Stamm & Álvarez-Ramis 1996; Diez *et al.* 2010; Juárez-Ruiz & Wachtler 2015). All of these records open a window into a local biota that succeeded the aftermath of the end-Permian (e.g., Joachimski *et al.* 2012; Shen & Bowring 2014; Biswas *et al.* 2020) to the Early Triassic (e.g., Galfetti *et al.* 2007; Stanley 2009; Hochuli *et al.* 2016; Zhang *et al.* 2019) mass extinction event, which is known to be the most profound biotic crisis in the history of multicellular life on Earth (e.g., Benton 1995, 2018; Stanley 2016; Delfino *et al.* 2020). From the upper Lower Triassic to the lower Middle Triassic, fossil clam shrimps are known from only a few of localities apart from the ones studied herein, such as France (e.g., Gall & Grauvogel-Stamm 2005), Germany (e.g., Kozur *et al.* 1993; Mahler & Sell 2015), Poland (e.g., Żyła *et al.* 2013), Tunisia (Soussi *et al.* 2017), and Argentina (e.g., Tassi *et al.* 2015). Comparing these occurrences with our new data from Mallorca contributes to a better understanding of the Early–Middle Triassic post-crisis fauna within a wider palaeogeographic realm than has been previously possible. Additionally, it is hoped that our present study will motivate future working groups to improve the general knowledge on transitional Lower Triassic–Middle Triassic clam shrimp biostratigraphy through additional future studies, as clam shrimps have great potential for both fine-scale biozonation and regional to interregional biostratigraphic correlations (e.g., Kozur & Weems 2010; Scholze *et al.* 2016; Schneider *et al.* 2020).

Geologic setting

The study area is located in the Serra de Tramuntana, a mountainous area in the northwest of the island of Mallorca (western Mediterranean). The studied sections, comprising a Lower(?)–Middle Triassic interval of predominantly siliciclastic red-beds ('*Buntsandstein* facies'), crop out along the coastal cliffs between Cala d'Estellencs and Punta de son Serralta (Figure 1A). Gómez-Gras (1993) recognised four (herein called A–D) main lithostratigraphic units in these outcrops (Figure 1B): (A) a basal sandstone unit representing braided rivers, (B) a lower sandstone and siltstone unit corresponding to meandering rivers, (C) a middle sandstone unit of meandering or braided river deposits, and (D) an upper siltstone and sandstone unit deposited in tidal flats transitional to the overlying shallow marine deposits of the so-called '*Muschelkalk* facies' (e.g., Matamales-Andreu *et al.* 2020). The lithostratigraphic units A–D have not been formally described so far. Diez *et al.* (2010) provided age attributions based on their review of palynomorphs found in some beds of the units B, C, and D, attributing the lowest two to the Aegean Substage (lower Anisian Stage, lower Middle Triassic), and the upper one to an indeterminate substage within the Anisian.

Clam shrimps studied in the present work were all collected *in situ* from four different stratigraphic horizons, all of them consisting of greenish or reddish grey, finely laminated claystones/siltstones, possibly representing small, dysoxic pools formed on fluvial floodplains near meandering channels or in abandoned channels of the braided rivers during low-water intervals. The four sites have been named (in ascending stratigraphic order) "Punta Roja" (middle part of Unit B; Figure 1C), "Pedra Alta" (upper part of Unit B; Figure 1D), "Punta Negra 1" (base of Unit C; Figure 1E) and "Punta Negra 2" (top of Unit C; Figure 1F). Figure 1B shows a synthetic stratigraphic log that indicates the location of the four sites.

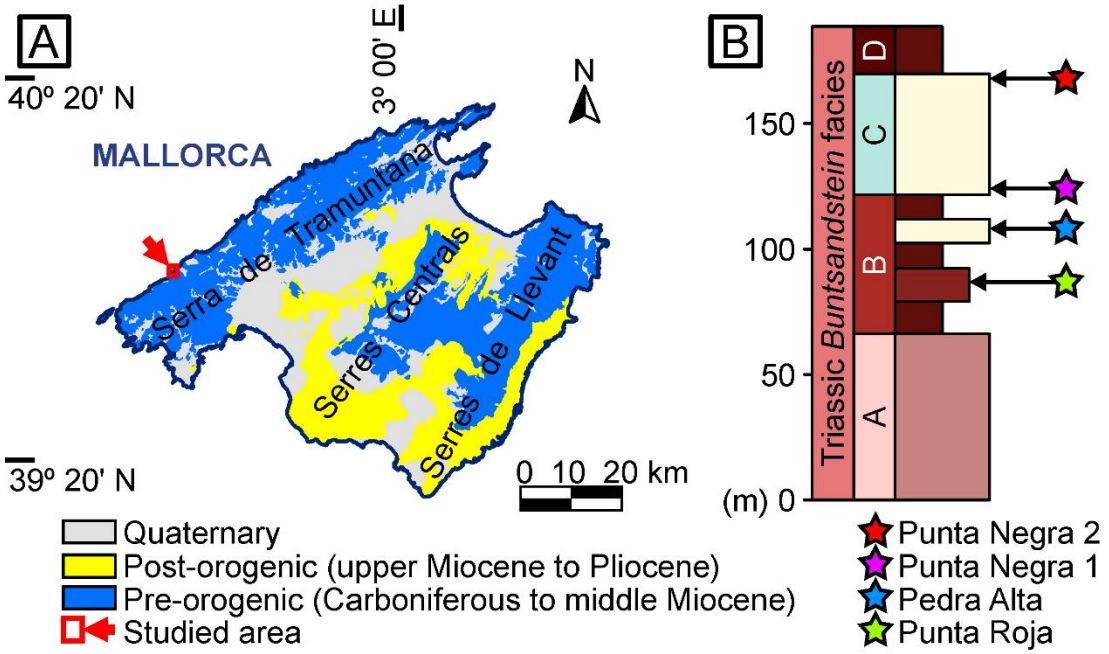

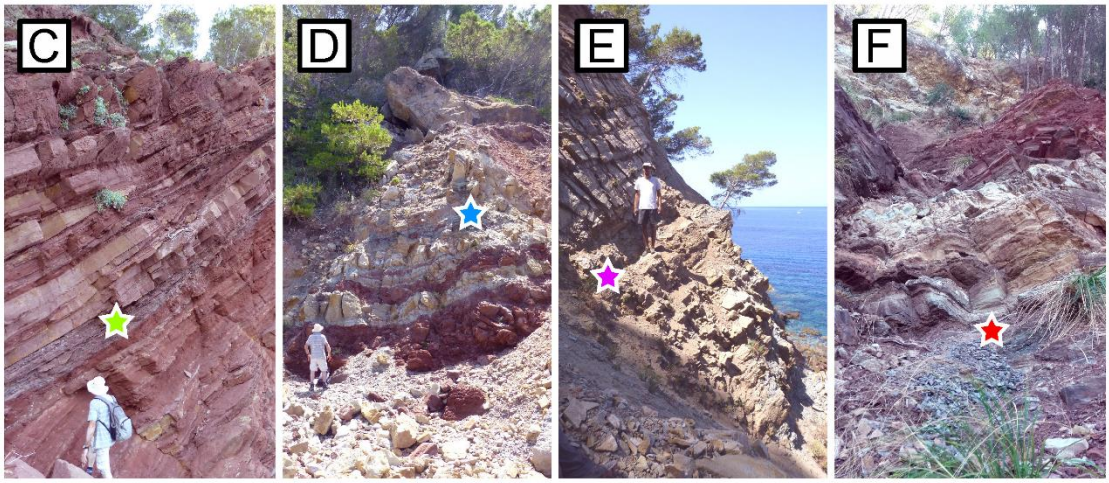

FIGURE 1. Position of the study area, lithostratigraphy, and field photographs of outcrop sections with respective clam shrimp occurrences. A, simplified geological map of the island of Mallorca with indication of the location of the study area. B, lithostratigraphic framework of the Lower(?)–Middle Triassic red-beds of Mallorca, indicating the four main units (lithostratigraphic units A–D) and the stratigraphic position of the clam shrimp-bearing horizons. The colour of each unit represents the dominant colour of the rocks that constitute it. C–F, outcrop conditions of the Punta Roja site (C), Pedra Alta site (D), Punta Negra 1 site (E), and Punta Negra 2 site (F), with stars marking the respective fossiliferous horizons.

Material and methods

Systematic, bed-by-bed collection of freshly exposed claystone and siltstone slabs from the studied outcrop sections was carried out during a field campaign in 2019 (which was authorized through an excavation permit granted by the Consell de Mallorca under the ref. 305-19, code 0313JUL2019ARQ.305-19.estellencs). About 47 slabs were obtained, each containing between one and 20 clam shrimp carapace valves, resulting in a total collection of 112

individual carapace valves. The best preserved individuals (25 in total) were selected for both microscope drawing and photography of their carapace valves, using a LEICA MZ12 stereo-microscope with a WILD drawing mirror tube, and a BRESSER MikroCamII digital camera. Multiple photographs were taken of each of these clam shrimp carapace valves at different focus distances, which were later vertically stacked automatically using the software ADOBE Photoshop CS4. To make the microscope line drawings by hand with the drawing mirror tube, a cold light source equipped with a flexible rubber light guide was used for variable illumination of the specimens. The vector graphic software COREL DRAW 20 was used for digitizing the microscope line drawings.

The microscope drawings were used for precisely measuring a set of carapace valve parameters (e.g., total valve height [H], valve length [L], dorsal margin length [l], larval valve height [h], total number of growth lines), according to the procedure and terminology proposed by Scholze & Schneider (2015). In order to make a taxonomic determination of the clam shrimp material, carapace valve parameters such as the total size values (valve length and height) and their ratio values (total valve height/total valve length, dorsal margin length/total valve length), as well as the positions of points of maximum curvature at the outer margins of the carapace valve, were used for comparison with literature data, which primary includes Triassic clam shrimps (e.g., Reible 1962; Gall 1971; Chang *et al.* 1976; Kozur & Seidel 1983a; Kozur & Weems 2010).

During the stereomicroscopic investigation, it was observed that some microstructures (i.e., remnants of ornamentation on the carapace valves) were partially preserved on a few individuals. Initial attempts to photograph these ornamentation patterns under higher magnifications, utilizing a KEYENCE VHX 6000 digital microscope failed due to ineffective illumination through the inner lens of this digital microscope. Therefore, selected individuals were permanently coated with gold films, and then photographed using a PHILIPS XL30 Environmental Scanning Electron Microscope (ESEM) with an acceleration voltage of 10 kV and up to 600x magnification. The resulting descriptions on observed microstructures could serve as additional criteria in clam shrimp taxonomy, as generally discussed in previous studies on other clam shrimp occurrences (e.g., Orlova 1978; Li 2017).

All specimens figured herein are permanently stored at Museu de Mallorca in the city of Palma (Mallorca, Balearic Islands, Spain).

Results

The studied clam shrimp carapaces are preserved as a dark greyish to slightly patchy yellowish brown-coloured substance with irregular thicknesses, which represent either remnants of organic materials and/or a derivate of the primary (chitinous) shell substance. An overview of their occurrences in their respective fossiliferous sites, along with a summary of the coordinates, lithostratigraphy, and the taxonomy of the recorded clam shrimp occurrences, is given in Table 1.

TABLE 1. Summary of the upper Lower Triassic(?)–lower Middle Triassic clam shrimp occurrences from the present study.

Name of the fossil site	Coordinates	Lithostratigraphy	Identified clam shrimp taxa
Punta Negra 2	39°39'41"N, 02°28'33"E	Uppermost part of Unit C	*Hornestheria? Morphotype* 1; *Hornestheria? Morphotype* 2
Punta Negra 1	39°39'42"N, 02°28'31"E	Lowermost part of Unit C	Indeterminate
Pedra Alta	39°39'41"N, 02°28'28"E	Upper part of Unit B	*Hornestheria* sp. aff. *Hornestheria sollingensis*
Punta Roja	39°39'54"N, 02°28'39"E	Middle part of Unit B	Indeterminate

For the following morphologic description of the clam shrimp carapace valves, the terminology proposed by Scholze & Schneider (2015) is used. The systematic hierarchy (see below Subchapter 'Systematic palaeontology') follows Kozur & Weems (2010), Hegna & Astrop (2020), and Hegna & Olesen (2020), except for taxonomically indeterminate individuals (see Subchapter 'Indeterminate clam shrimps').

Systematic palaeontology

Class Branchiopoda Lamarck, 1801

Subclass Phyllopoda Preuss, 1951

Order Diplostraca Gerstaecker, 1866

Superfamily Lioestheriacea Raymond, 1946 emended Holub et Kozur, 1981

Family Xiangxiellidae Shen in Chang *et al.*, 1976

Remarks. Xiangxiellidae was defined as a subfamily in Chang *et al.* (1976) and attributed therein to the family Vertexiidae Kobayashi, 1954. Carapace valves of Vertexiidae have concavely recurved growth lines along the upper posterior margin below the dorsal margin, and sometimes a spine-like sculpture on its larval carapace valve (Kobayashi 1954; Astrop & Hegna 2015). These two characteristics are absent in Xiangxiellinae, which excludes this taxon from the family Vertexiidae sensu stricto. Instead, Xiangxiellidae became elevated to family rank by Kozur & Weems (2010), which is followed herein.

Genus *Hornestheria* Kozur et Lepper in Kozur et Weems, 2010

Type species. *Hornestheria sollingensis* Kozur et Lepper (in Kozur & Weems, 2010); from the Frohrieper Berg Quarry (East of the town of Lauenförde, Lower Saxony, Germany), Solling Formation (Middle Buntsandstein Subgroup, Buntsandstein Group), uppermost Spathian (uppermost Olenekian, uppermost Lower Triassic) (Kozur & Weems 2010: p. 395). *Hornestheria sollingensis* was used in stratigraphic charts (e.g., Bachmann & Kozur 2004) before the taxonomic characteristics for its genus and species levels were formally published by Kozur & Weems (2010: appendix 1).

Remarks. A diagnosis of this genus was proposed by H.W. Kozur and J. Lepper (in Kozur & Weems 2010), but metric values for total carapace valve length and height were not provided. Besides a low convexity of the carapace valves and their almost straight dorsal margin, other characteristics of *Hornestheria* included the location of points of maximum curvature of the anterior margin in the horizontal midline of the carapace valve and of the posterior margin below the horizontal midline (Kozur & Weems 2010). The larval carapace valve (=umbonal area of the valve free of growth lines) bore a rather enigmatic radial element, which was either "often quite distinct" (Kozur & Weems 2010: p. 395) or unrecognizable, depending on the respective preservation state of individual carapace valves.

Based on the description of *Hornestheria* in Kozur & Weems (2010), the radial element on the larval carapace valves of *Hornestheria* most closely resembles that of *Lioestheria* Depéret et Mazeran, 1912, which has both nodular and radial sculptures on its larval carapace valves (e.g., Kozur *et al.* 1981). In contrast, however, the size of the larval carapace valve in adult individuals of *Lioestheria* is greater than 1/3 of the total carapace valve length (Holub & Kozur 1981), and this is much larger relatively than the size of the larval valve seen in the carapace of the genus *Hornestheria.* This difference provides a clear distinction between *Hornestheria* and *Lioestheria* sensu Holub & Kozur (1981).

Prominent sculptures are also found on the larval carapace valves of the clam shrimp genus *Cornia* Lutkevich, 1937, which is widely distributed in the Lower Triassic (e.g., Kozur & Seidel 1983a; Kozur & Mock 1993; Tassi *et al.* 2013; Scholze *et al.* 2016). This genus is characterized by an umbonal spine with a circular base located on the larval carapace valve. The spine can be variably preserved (Kozur 1983), being either perpendicular or obliquely embedded in the sediment or being broken, due to variable deformation (e.g., sedimentary compaction) of the rock. According to the description for *Hornestheria* provided by Kozur & Weems (2010), the generally radial shape of its larval sculpture makes it consistently different from the circular shape of the base of the umbonal spine in *Cornia.*

A further characteristic of *Hornestheria* in the sense of H.W. Kozur and J. Lepper (in Kozur & Weems 2010) is the presence of certain types of microsculpture (ornamentation) located on the growth bands of the carapace valves.

The ornamentation of the genus *Hornestheria* was originally described as a dense, fine reticulation, which became replaced by fine, short, radial lines in the outer margins in adult individuals (Kozur & Weems 2010). However, it should be noted that the figures of *H. sollingensis* in Kozur & Weems (2010: fig. A2) show only indistinct reticulation.

In lateral view, the carapace valves of *Hornestheria* are morphologically similar to *Euestheria* Depéret et Mazeran, 1912, and *Magniestheria* Kozur, 1982. However, in contrast to *Hornestheria*, the carapace valves of *Euestheria* have a more strongly convex shape with its highest convexity in the umbonal area. The highest convexity in carapace valves of *Magniestheria* is located in its central area. Both *Euestheria* and *Magniestheria* differ in their ornamentation from *Hornestheria*. The ornamentation of *Euestheria* is either finely dotted to weakly reticulated (Kozur & Seidel 1983a) or very finely pitted, having pits of round to round-oval shapes with diameters of about 10 µm (Sell 2018), that appear generally to be more regular and smoother than the ornamentation seen in *Hornestheria*. The ornamentation of *Magniestheria* is indistinct, varying between coarse pits and very short, irregular, radial lines (Kozur & Seidel 1983a); their expression is less intense than in *Hornestheria*.

Occurrence. Uppermost Spathian (uppermost Olenekian; upper Lower Triassic) and Anisian (lower Middle Triassic) in Germany (Kozur & Weems 2010), China (see discussions on "*Protomonocarina*" in Kozur & Weems 2010: p. 395), and Mallorca (the present study).

Hornestheria sp. aff. *Hornestheria sollingensis* Kozur et Lepper (in Kozur & Weems 2010)

(Figures 2–7)

Material. DA21/03/02/58, DA21/03/02/68, DA21/03/02/72, DA21/03/02/75, DA21/03/02/77, DA21/03/02/78, DA21/03/02/80, DA21/03/02/81.

Description. Carapace valve medium-sized to large, elongated-oval to oval shape; dorsal margin straight, short to long; larval carapace valve very small; umbo located submedial and marginal to inframarginal; anterior and posterior margins sharply curved to very sharply curved; points of maximum curvature along the anterior and posterior margins located in the median-dorsal to median-ventral region, and along the ventral margin in the median to median-posterior region; ornaments fine, indistinct or irregularly reticulated.

Size. Height (H) of the carapace valve between 1.6–3.9 mm; length (L) of the valve between 2.5–3.9 mm; 0.57<H/L<0.7; dorsal margin length (l) between 1.8–2.3 mm; 0.51<l/L<0.70; larval carapace valve height (h) between 0.1–0.5 mm; 0.04<h/H<0.19; up to 20 growth lines; all measurements based on 8 valves.

Occurrence. Pedra Alta site; upper part of Unit B; lower Anisian (lower Middle Triassic), dated as Aegean by Diez *et al.* (2010).

Remarks. H.W. Kozur and J. Lepper (in Kozur & Weems 2010) first defined *Hornestheria sollingensis* as a new species, providing the following parameters: total carapace valve length between 3.0–3.8 mm, total height between 1.95–2.85 mm, length/height ratio values between 1.3–1.66 (Kozur & Weems 2010). The morphotype of the specimens in the present study identified as *Hornestheria* sp. aff. *H. sollingensis* (Figures 2–6) differ from *H. sollingensis* Kozur et Lepper in their larger size and wider range of the height/length ratio values. Additionally, the larval carapace valve (="free umbonal area" in Kozur & Weems 2010: p. 397) of *H. sollingensis* is smaller than that of *Hornestheria* sp. aff. *H. sollingensis*. In accordance to the general description of the genus *Hornestheria* by Kozur & Weems (2010), the presence of a radial element on the larval carapace valve of *Hornestheria* sp. aff. *H. sollingensis* cannot be clearly observed, except for two individuals (collection numbers DA21/03/02/80, DA21/03/02/81; Figure 2B–E). Problematically, in most specimens the small larval carapace valve seems to be poorly preserved and the umbonal area has been almost without exception affected by deformation (i.e., sedimentary compaction). Generally, large sample sets, preferably including layers of mass occurrence (see Figure 2A), need to be analysed in order to better understand the full spectrum of preservation variability found in specimens attributable to *Hornestheria*.

When the radial sculpture cannot be clearly seen on the larval carapace valves, both *H. sollingensis* Kozur et Lepper (in Kozur & Weems 2010) and *Hornestheria* sp. aff. *H. sollingensis* (the present study) are morphologically reminiscent of both *Euestheria albertii albertii* (in the sense of Kozur *et al.* 1993; formerly designated as "*Isaura minuta albertii* (Voltz, 1835)" by Reible 1962) and *Euestheria albertii mahlerselli* Kozur et Lepper (in Kozur & Weems 2010). By comparison with the literature, *E. albertii albertii* (figured by Kozur *et al.* 1993: figs. 3.1–3.2) shows a more rounded shape, whereas *E. albertii mahlerselli* (figured by Kozur *et al.* 1993: figs. 3.4, 3.6;

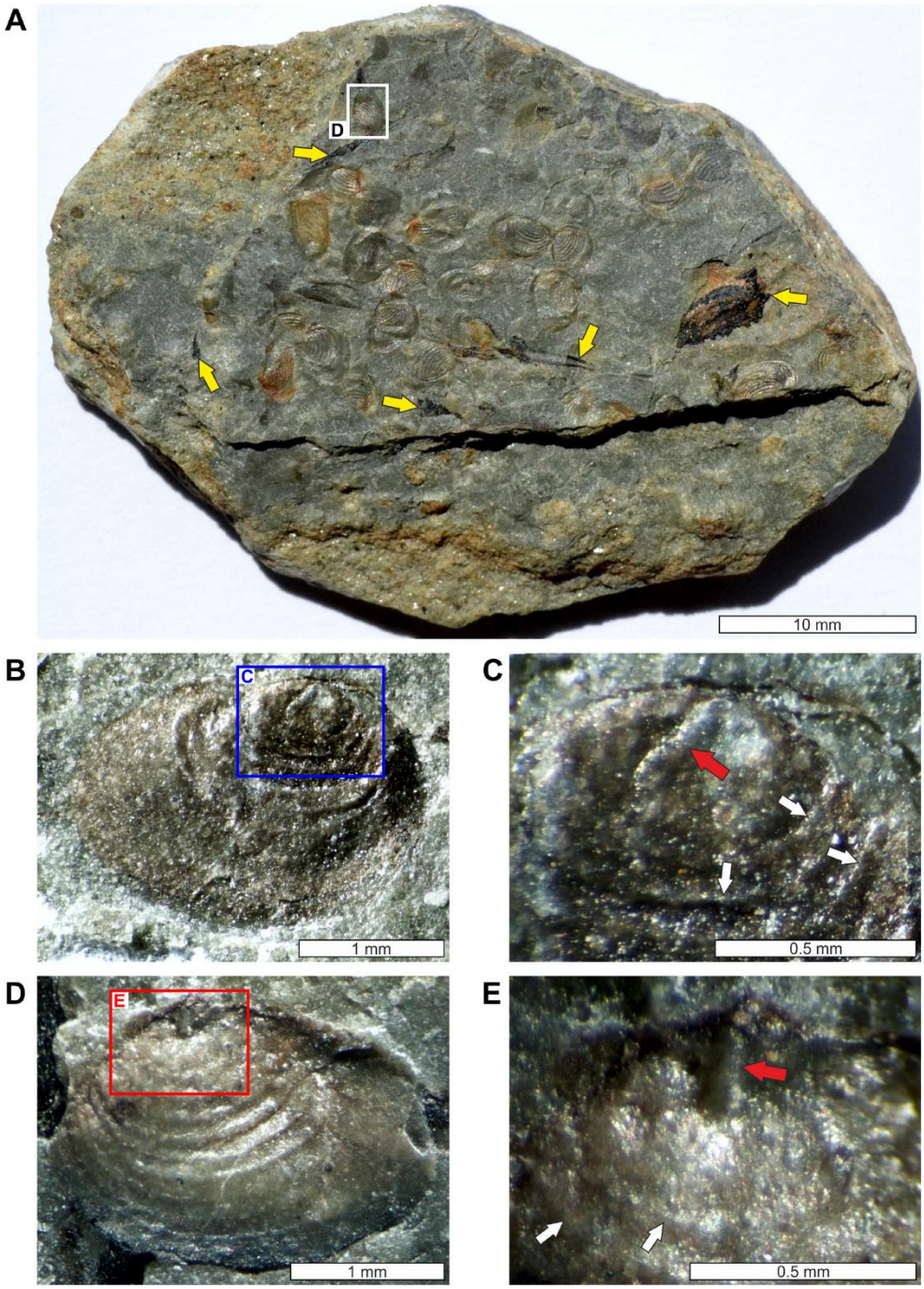

FIGURE 2. Clam shrimps and plants from Pedra Alta site; upper part of Unit B, lower Anisian. A, mass-occurrence of *Hornestheria* sp. aff. *Hornestheria sollingensis* and coalified plant remains (marked with yellow arrows); DA21/03/02/80. B, external view on a right carapace valve of *Hornestheria* sp. aff. *Hornestheria sollingensis*. C, radial sculpture on the larval carapace valve (marked by red arrow), which is a diagnostic character for the genus *Hornestheria*; white arrows mark concentric growth lines in the umbonal area of the carapace valve; DA21/03/02/81. D, detail framed in A, external view on a left carapace valve of *Hornestheria* sp. aff. *Hornestheria sollingensis*; DA21/03/02/80. E, detail framed in D, showing an indistinct radial sculpture on the larval carapace valve (red arrow) and earliest growth lines (white arrows).

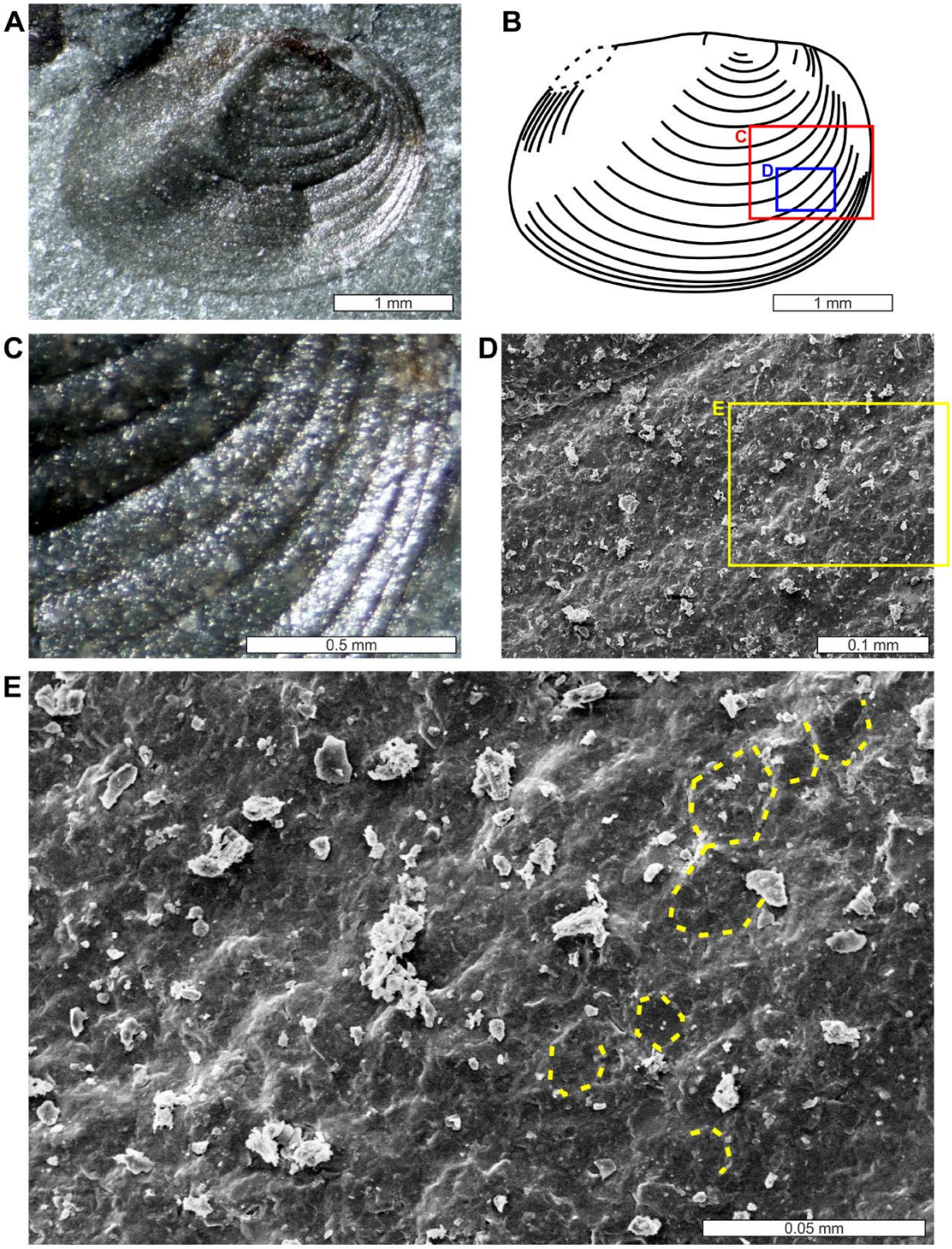

FIGURE 3. Light microscopic photographs (Figs. A, C), line drawings, and ESEM images (D, E) of *Hornestheria* sp. aff. *Hornestheria sollingensis* from Pedra Alta site; upper part of Unit B, lower Anisian. A–B, external view on a right carapace valve (DA21/03/02/75). C–E, details of the same individual showing finely reticulated ornaments (highlighted by yellow dashed lines) on the growth bands.

for references to further figures see the synonymy list in Kozur & Weems 2010: p. 391) shows a more elongated shape than *Hornestheria* sp. aff. *H. sollingensis*. Additionally, *E. albertii albertii* and *E. albertii mahlerselli* have the strongest carapace valve convexity in the umbonal area, whereas in *Hornestheria* sp. aff. *H. sollingensis* it is more or less at the centre of the carapace valve.

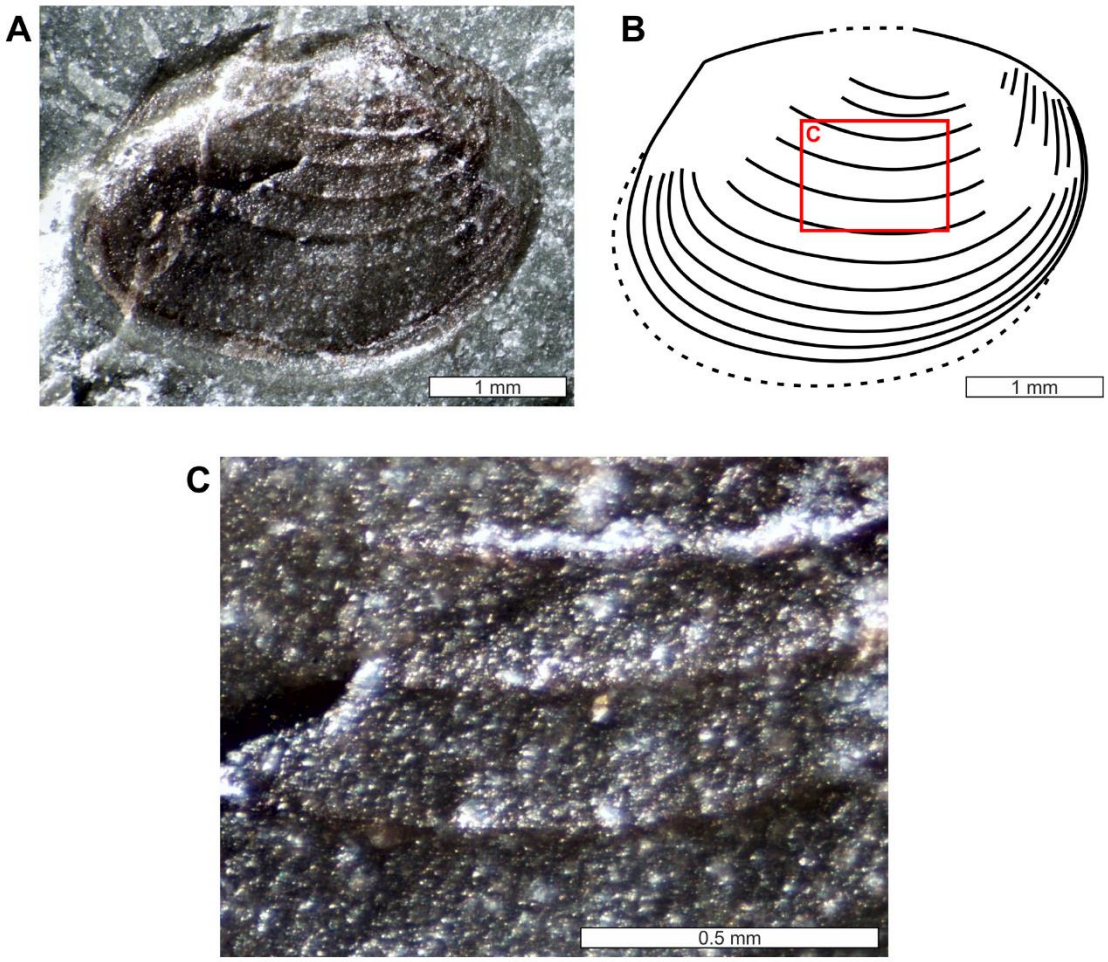

FIGURE 4. Light microscopic photographs and line drawing of *Hornestheria* sp. aff. *Hornestheria sollingensis* from Pedra Alta site; upper part of Unit B, lower Anisian. A–B, external view on a right carapace valve (DA21/03/02/72). C, details of the same individual showing indistinct fine ornaments on the growth bands.

Hornestheria? Morphotype 1

(Figures 8, 9)

Material. DA21/03/04/01, DA21/03/04/02, DA21/03/04/07-1a, DA21/03/04/07-2a, DA21/03/04/07-1c, DA21/03/04/07-2c, DA21/03/04/07-1d, DA21/03/04/10, DA21/03/04/11, DA21/03/04/12-1, DA21/03/04/12-2, DA21/03/04/13a, DA21/03/04/13b.

Description. Carapace valves very large and round in shape; dorsal margin straight, very short to short; larval carapace valve very small; position of the umbo anterior to slightly submedial and inframarginal to slightly marginal; anterior and posterior margins sharply curved to very sharply curved; points of maximum curvature of the anterior margin located median-dorsal to median-ventral, in the posterior margin median-ventral, and in the ventral margin median-anterior; ventral margin is often indented in its median-posterior area.

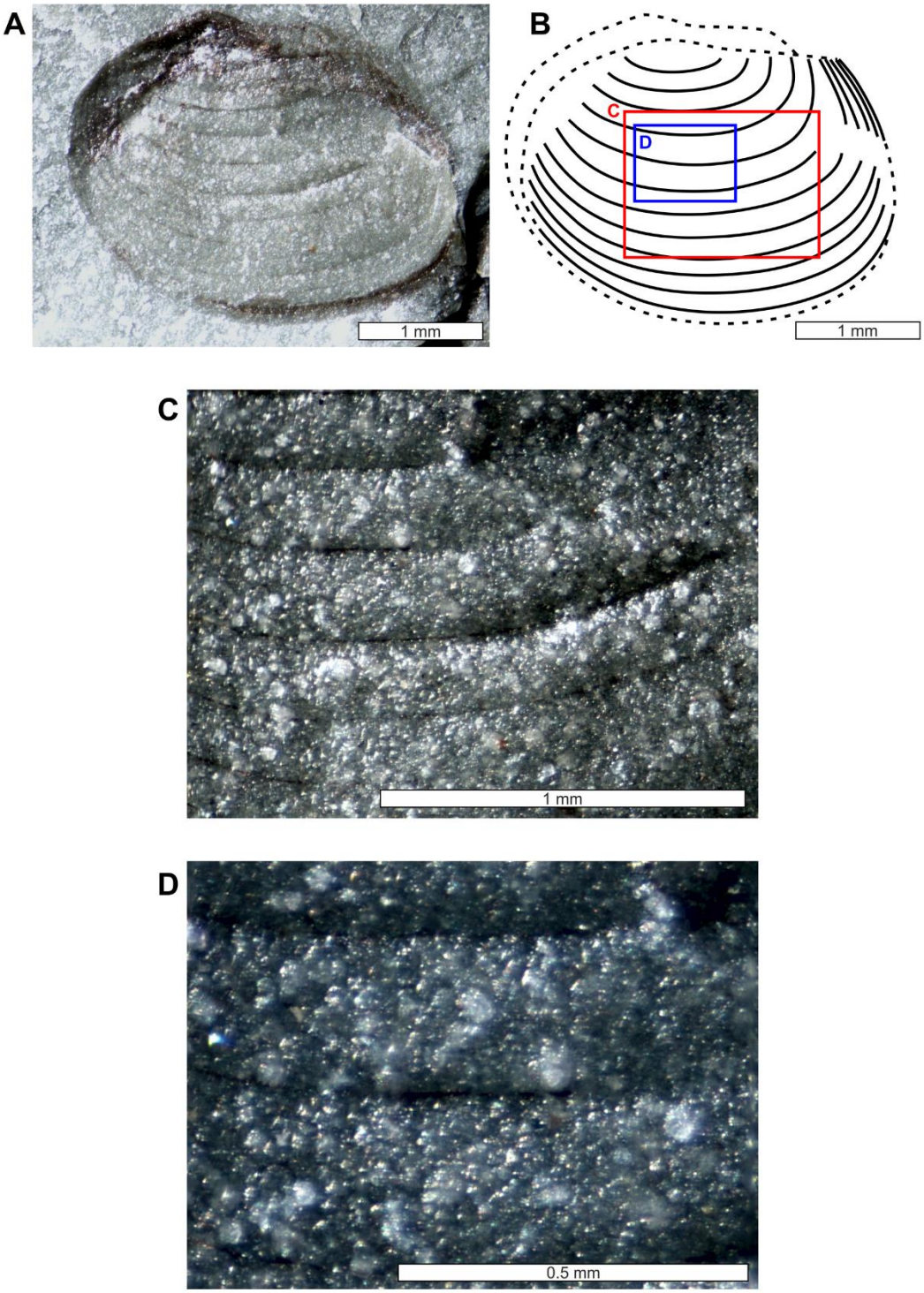

FIGURE 5. Light microscopic photographs and line drawing of *Hornestheria* sp. aff. *Hornestheria sollingensis* from Pedra Alta site; upper part of Unit B, lower Anisian. A–B, external view on a left carapace valve, slightly shifted against the underlying internal side of the right carapace valve (DA21/03/02/77). C–D, details of the same individual showing indistinct fine ornaments on the growth bands.

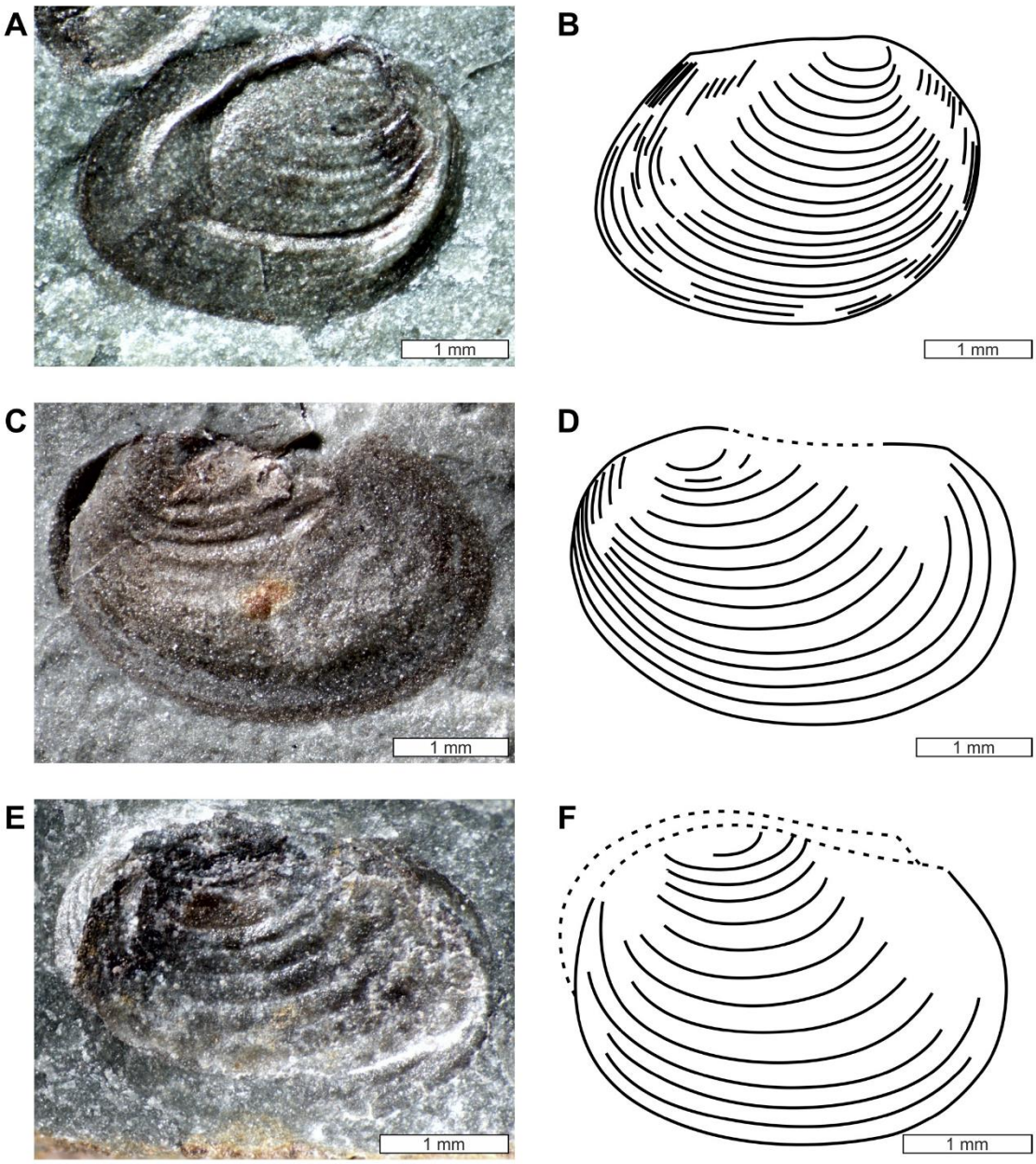

FIGURE 6. Light microscopic photographs and line drawings of *Hornestheria* sp. aff. *Hornestheria sollingensis* from Pedra Alta site; upper part of Unit B, lower Anisian. A–B, external view on a right carapace valve (DA21/03/02/58). C–D, external view on a left carapace valve (DA21/03/02/78). E–F, external view on a left carapace valve (DA21/03/02/68).

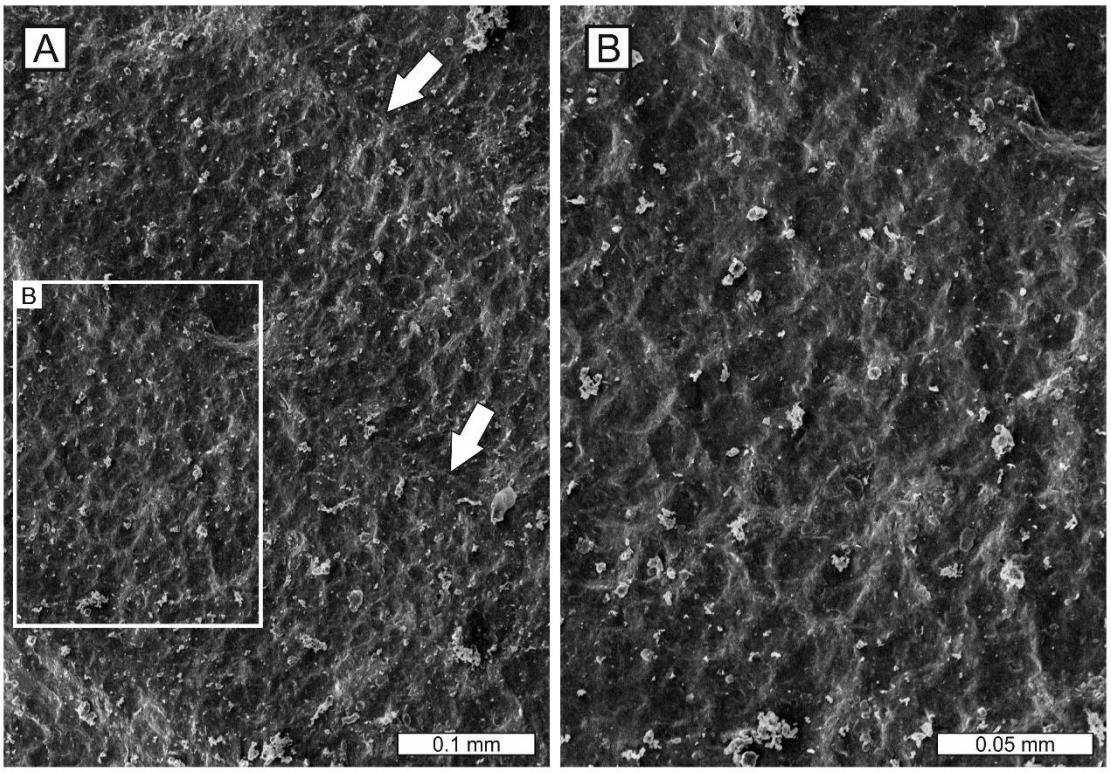

FIGURE 7. ESEM image of the ornamentation on the external side of a right carapace valve of *Hornestheria* sp. aff. *Hornestheria sollingensis* from the Pedra Alta site; upper part of Unit B, lower Anisian; collection number DA21/03/02/72. A, image taken in the central area of the carapace valve; concentric growth lines are marked by white arrows. B, detail showing irregularly reticulated ornaments on the growth band.

Size. Height (H) of the carapace valve between 4.9–7.8 mm; length (L) of the carapace valve between 6.0–9.9 mm; 0.76<H/L<0.87; dorsal margin length (l) between 2.7–4.6 mm; 0.38<l/L<0.56; larval carapace valve height (h) between 0.3–0.9 mm; 0.05<h/H<0.16; up to 55 growth lines, 5–7 growth lines/1 mm towards growth direction; all measurements based on 10 valves plus counterparts.

Occurrence. Punta Negra 2 site; uppermost Unit C; Aegean (Diez *et al.* 2010), lower Anisian (lower Middle Triassic).

Remarks. The use of open nomenclature at the species level is preferred for this set of specimens, due to the small sample available for study. This careful practice follows previous clam shrimp studies by Schneider *et al.* (2005: p. 11) and Schneider & Scholze (2018: p. 369), in order to prevent the creation of new definitions for what may prove to be synonymous species. A formal species diagnosis for *Hornestheria*? Morphotype 1 should be made only when more congeneric material from a wider study area is available.

Large clam shrimps identified as "*Dictyonatella* sp." (Żyła *et al.* 2013: figs. 5A, B) and "cf. *Dictyonatella*" (Soussi *et al.* 2017: figs. 13A, B) from the upper Lower Triassic–Middle Triassic of Poland and Tunisia, respectively, have a rounded shape similar to *Hornestheria*? Morphotype 1. According to Kozur (1982), the genus *Dictyonatella* has, among other characteristics, an ornamentation on the growth bands represented by a coarse reticulation and a recurvature of posterior growth lines below the dorsal margin. These two characteristics clearly differ from the generally small reticulated ornaments of *Hornestheria* sensu lato and its non-concave recurvature in the posterodorsal margin of the carapace valve. Notably, in *Hornestheria*? Morphotype 1, a recurved posterodorsal margin is absent.

Shen *et al.* (2002) described "*Euestheria* (*Magniestheria*) *truempyi*" from the basal Olenekian (basal upper Lower Triassic), which has a large size and a rounded carapace valve shape similar to the *Hornestheria*? Morpho-

type 1. Additionally, a minute reticulated ornamentation noted by Shen *et al.* (2002: plate 2, fig. 2) resembles that of *Hornestheria* sp. aff. *H. sollingensis* (Figure 7). "*Euestheria* (*Magniestheria*) *truempyi*" of Shen *et al.* (2002), however, shows pronounced concentric ribs in the umbonal and central areas of the carapace valves, whereas the growth bands in all the specimens of the present study are both narrower and their convex curvature is less intense, lacking pronounced concentric ribs.

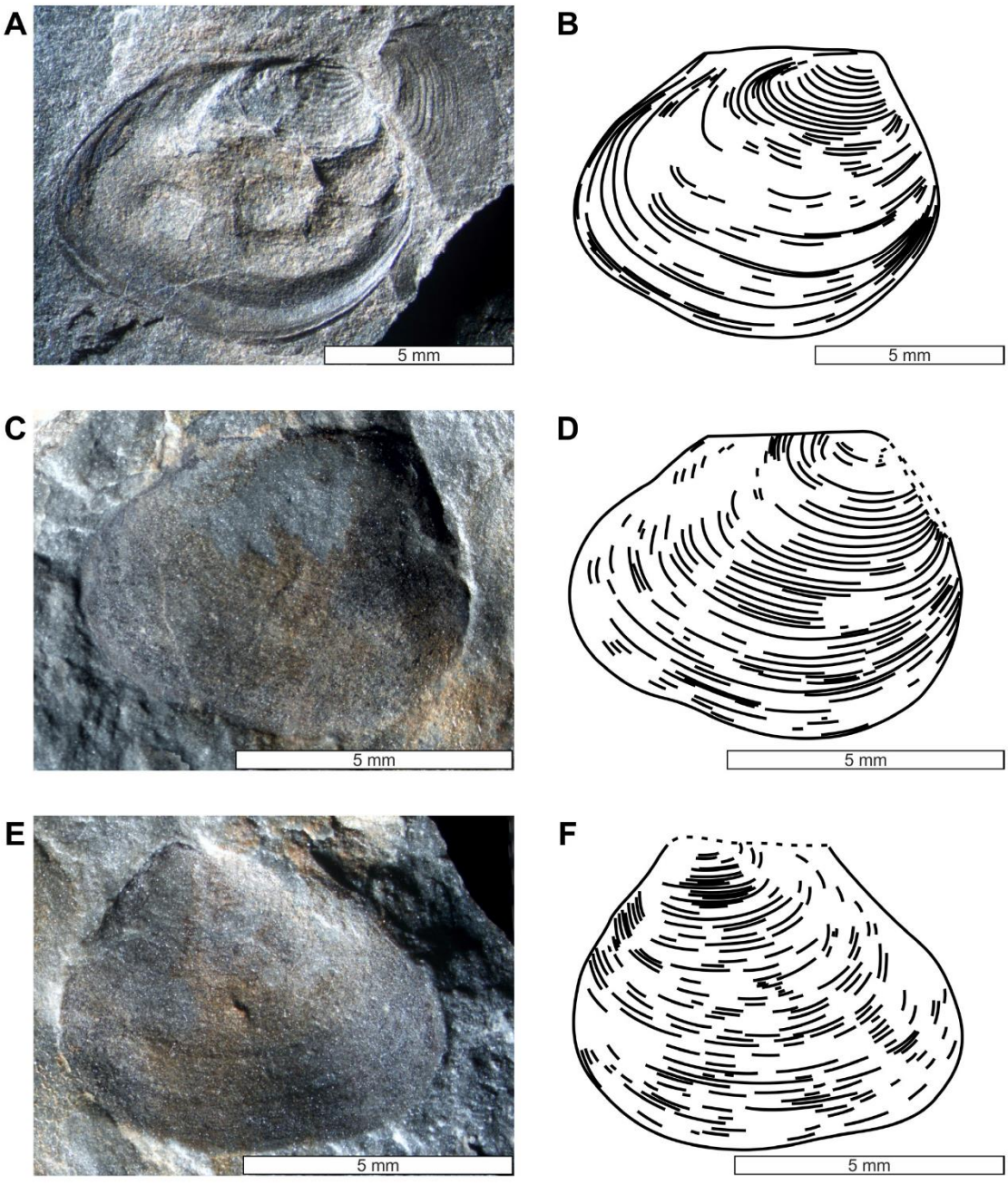

FIGURE 8. Light microscopic photographs and line drawings of *Hornestheria*? Morphotype 1 from Punta Negra 2 site; uppermost part of Unit C, lower Anisian. A–B, compacted carapace in lateral view (DA21/03/04/11). C–D, external view on a right carapace valve (DA21/03/04/07-1a). E–F, internal side of a right carapace valve, appearing optically inverted through artificial shallow-angle illumination (DA21/03/04/07-2a).

More recently, Scholze *et al.* (2020: fig. 9E) described a Lower Triassic clam shrimp fauna from the Jialingjiang Formation in southwestern China, which also contained a species designated preliminarily as *Magniestheria* sp. aff. *Magniestheria subcircularis* (Chernyshev, 1934). Its size, shape, and the position of points of maximal curvature of the outer margins of the carapace valve are similar to those of *Hornestheria*? Morphotype 1 (Figures 8, 9), but the umbo of *Magniestheria* sp. aff. *M. subcircularis* is located in a more submedial position. Additionally, the strongest convexity of the carapace valves, in lateral view, is located in the umbonal area in the case of *Hornestheria*? Morphotype 1, whereas in *Magniestheria* sp. aff. *M. subcircularis* it is located in the central area of the carapace valve.

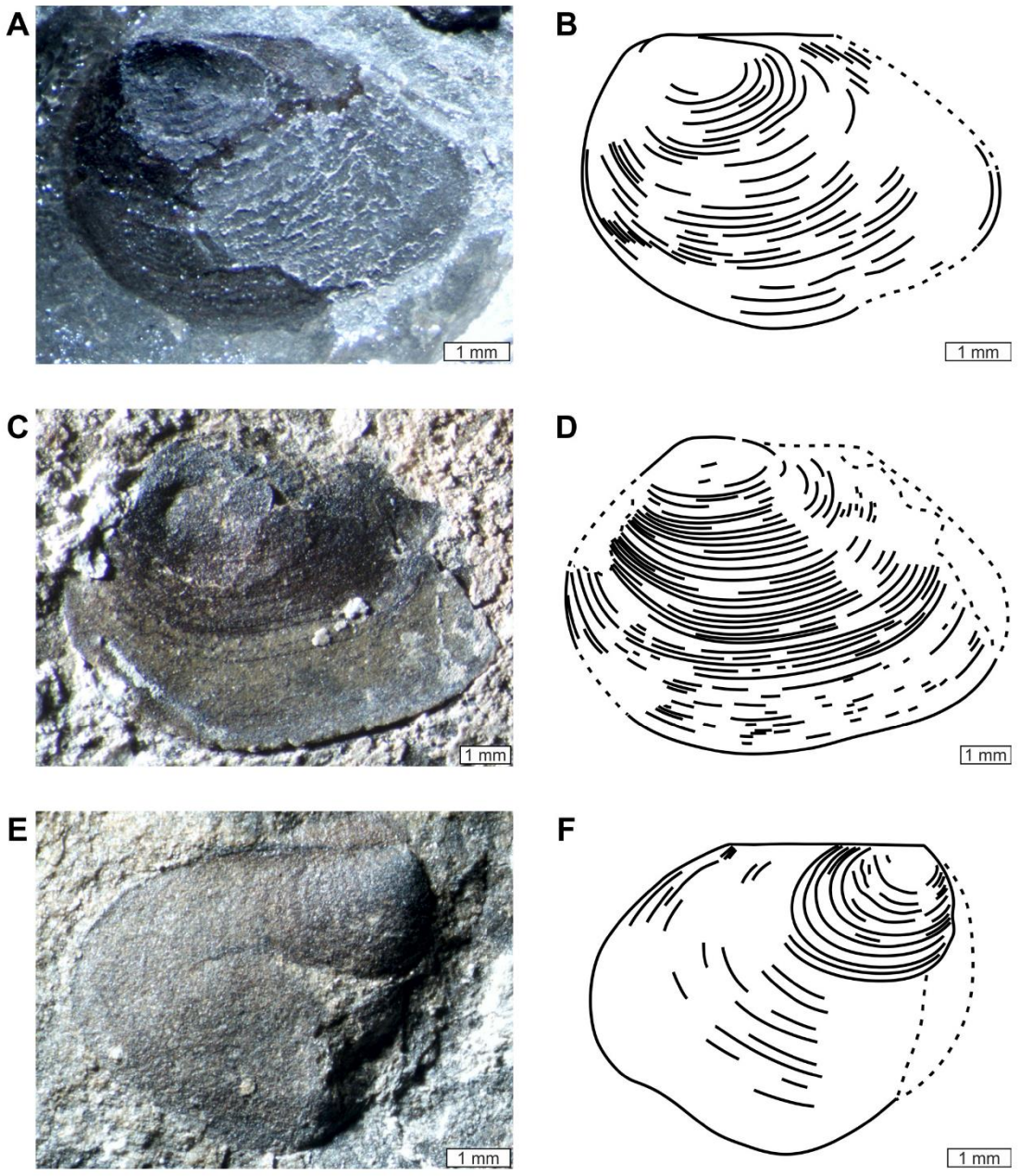

FIGURE 9. Light microscopic photographs and line drawings of *Hornestheria*? Morphotype 1 from Punta Negra 2 site; uppermost part of Unit C, lower Anisian. A–B, compacted carapace in lateral view; rock surface was covered with adhesive (DA21/03/04/07-1d). C–D, external side of a left carapace valve (DA21/03/04/12-1). E–F, external side of a fragmented right carapace valve (DA21/03/04/13a).

***Hornestheria*? Morphotype 2**
(Figures 10, 11)

Material. DA21/03/04/04a, DA21/03/04/06, DA21/03/04/07-1b, DA21/03/04/07-2b, DA21/03/04/08, DA21/03/04/09.

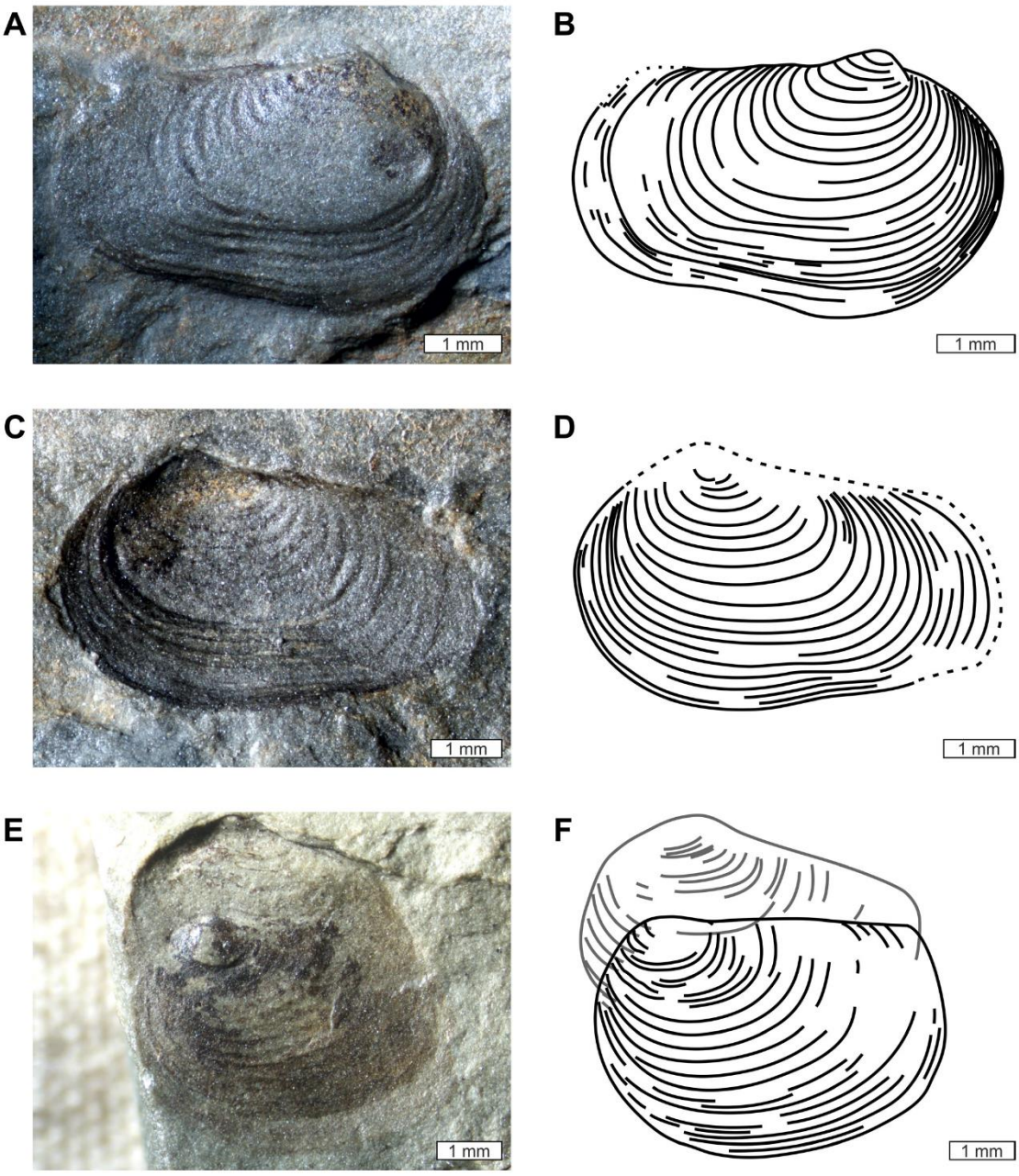

FIGURE 10. Light microscopic photographs and line drawings of *Hornestheria*? Morphotype 2 from Punta Negra 2 site, showing more or less developed concave bending of the ventral margin in the median-posterior area of the carapace valve; uppermost part of Unit C, lower Anisian. A–B, Right carapace valve, almost completely preserved as a steinkern (DA21/03/04/07-1b). C–D, imprint of a right carapace valve, appearing optically inverted through shallow illumination (DA21/03/04/07-2b). E–F, external side of a left carapace valve, overlying the internal side of the corresponding right carapace valve; both carapace valves are shifted relative to each other (DA21/03/04/08).

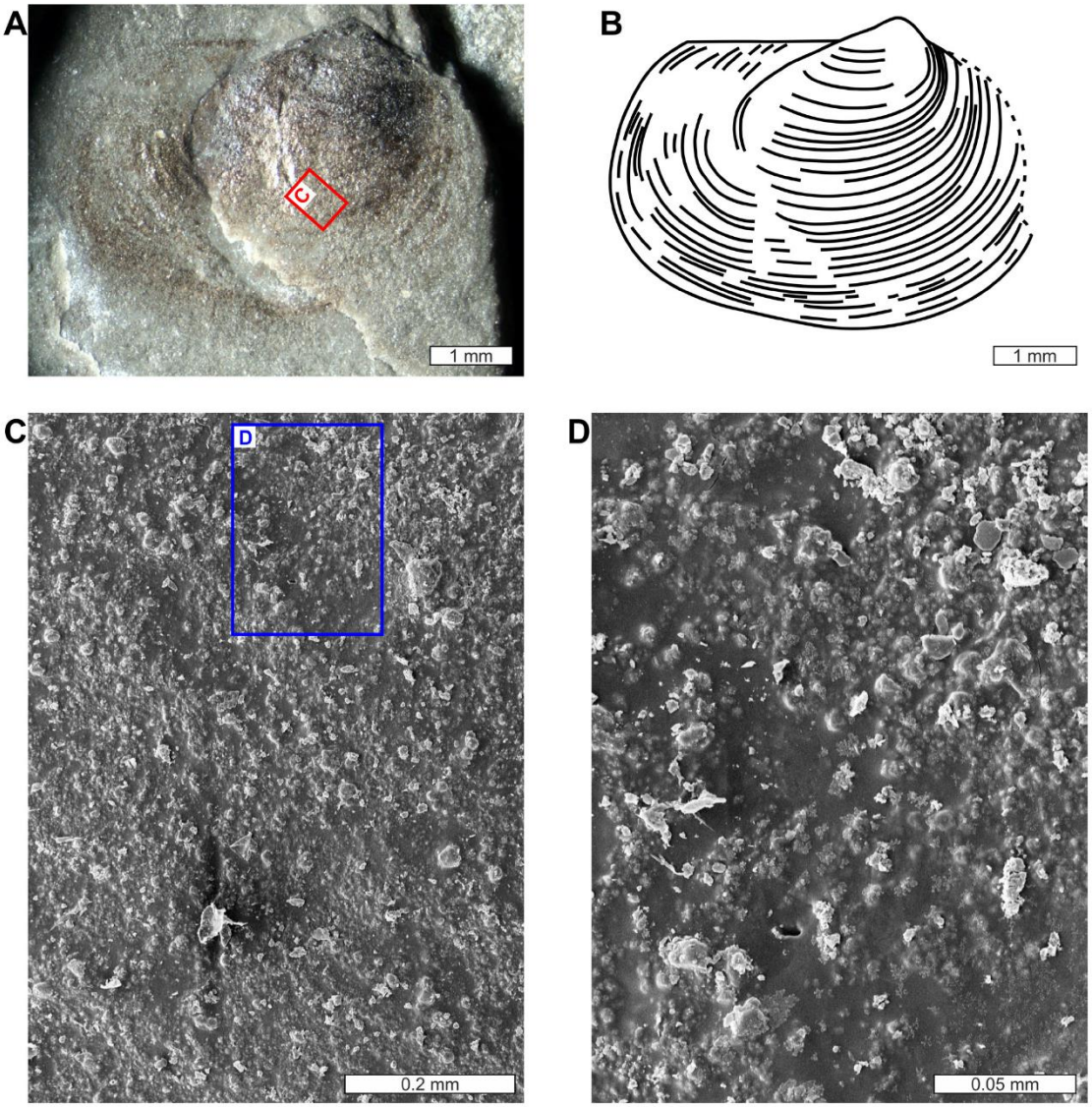

FIGURE 11. A–B, light microscopic photograph and line drawing of external view on a right carapace valve (DA21/03/04/09), showing the positions of the ESEM images. C–D, ESEM images of *Hornestheria*? Morphotype 2 from Punta Negra 2 site; uppermost part of Unit C, lower Anisian; irregularly (not smoothly) preserved surface, the ornamentation is not clearly detectable even under high magnification.

Description. Carapace valves very large and elongated oval to oval in shape; dorsal margin slightly curved to curved, very short to long; larval carapace valve very small; position of the umbo submedial and marginal to supramarginal; anterior and posterior margins sharply curved to very sharply curved; points of maximum curvature of the anterior and posterior margins located median or slightly median-dorsal, and in the ventral margin median-anterior; the ventral margin is concavely indented in the median-posterior region of the carapace valve.

Size. Height (H) of the carapace valve between 3.2–4.9 mm; length (L) of the valve between 5.3–7.5 mm; $0.57<H/L<0.71$; dorsal margin length (l) between 3.0–4.0 mm; $0.48<l/L<0.70$; larval carapace valve height (h) between 0.2–0.9 mm; $0.06<h/H<0.2$; often between 25–30 growth lines; all measurements based on 6 valves.

Occurrence. Punta Negra 2 site; uppermost part of Unit C, Aegean (Diez *et al.* 2010), lower Anisian (lower Middle Triassic).

Remarks. The genus name is written with a question mark, because neither its characteristic radial sculpture in the umbonal area nor microstructures (ornamentation) of the carapace valves could be clearly identified, possibly due to the imperfection of their preservation. Instead of a formal species name, open nomenclature is applied to this distinctive carapace valve morphology. This morphotype co-occurs with the above described *Hornestheria*? Morphotype 1 (Figures 8, 9). The latter mentioned morphotype reaches greater total carapace valve height values than *Hornestheria*? Morphotype 2 (Figures 10, 11). It also differs from *Hornestheria*? Morphotype 2 in having a more rounded shape.

Hornestheria? Morphotype 2 is of larger size than both *H. sollingensis* sensu stricto and *Hornestheria* sp. aff. *H. sollingensis* (Figures 2–6). The large carapace valves of *Hornestheria*? Morphotype 2 resemble similarly-sized clam shrimps, such as "*Isaura minuta albertii*" (see Reible 1962: plate 7-fig. 7) or *E. albertii albertii* (see Kozur *et al.* 1993: fig. 3), but differ from them in both its concavely recurved ventral margin and the morphology of the umbo.

Indeterminate clam shrimps

Punta Roja site. Clam shrimps occur rarely in the Punta Roja site, in the lower part of Unit B (upper Olenekian(?)–lower Anisian). So far, the sample from this site is limited to three individuals (specimen numbers DA21/03/01/01a, DA21/03/01/01b, DA21/03/01/02; Figure 12A–D) that possess the following characteristics (with semi-quantitative measurements based on both microscope line drawings and attempted line drawing reconstruction of fragments): small to medium-sized carapace valves (L=2.3–3.5 mm; H=1.6–2.6 mm), rounded in shape (0.57<H/L<0.74); dorsal margin straight, short to long (l=1.6–1.9 mm; 0.51<l/L<0.70); larval valve very small (h=0.1–0.5 mm; 0.04<h/H<0.19); position of the umbo submedial and inframarginal; anterior and posterior margins sharply curved to very sharply curved; points of maximum curvature along the anterior margin located medial to slightly medial-dorsal, in the posterior margin medial, and in the ventral margin medial to slightly medial-posterior; about 13–19 growth lines.

Punta Negra 1 site. Two clam shrimps carapace valves were collected from the Punta Negra 1 site, in the base of Unit C, of lower Anisian (Aegean; Diez *et al.* 2010) age. In both individuals, the outline of the carapace valves is incomplete; specimen DA21/03/03/02 (Figure 12E, F) appears to be strongly compressed by diagenesis; specimen DA21/03/03/01 (Figure 12G, H) is a fragment of an anterior part of a probably juvenile carapace valve.

Discussion

Taxonomic remarks on the genus *Hornestheria*

In lateral view, the genus *Hornestheria* often shows a low convexity with its maximal curvature located in the umbonal to central areas of the carapace valve and its umbo lying against or slightly overtopping the dorsal margin. The presence of a radial sculpture on the larval carapace valve represents an important taxonomic characteristic; however, its degree of development is quite variable (Kozur & Weems 2010). This might be a consequence of taphonomic variability, i.e., variable compression could flatten out that feature when the carapace is not well-supported by sediment underneath during the early diagenesis. The radial sculpture seems to be well preserved in only a few of the specimens figured by Kozur & Weems (2010: fig. A2), showing a generally high morphologic variability. This is also true for the material in our present study, wherein such a radial structure cannot be clearly observed in any specimens of *Hornestheria*? Morphotype 1 and *Hornestheria*? Morphotype 2, due to the only moderately good preservation seen in the larval carapace valve areas. Therefore, *Hornestheria*? is written with a question mark in order to indicate that this variability is a problem at our current state of knowledge, which does particularly account for these two morphotypes. More data on well-preserved specimens are required, which would also involve making a detailed re-study of either the *Hornestheria* type material of Kozur & Weems (2010) or new material from its type locality, in order to better understand the undeformed larval carapace valve morphology of this genus.

Other species with radial sculptures on their larval carapace valves were discussed by H.W. Kozur and J. Lepper (in Kozur & Weems, 2010: p. 395), including *Protomonocarina* spp. Shen (in Chang *et al.*, 1976). Among these species, one individual of *Protomonocarina sinensis* figured in Chang *et al.* (1976: plate 14, fig. 6) showed a radial rib running from the umbo towards the ventral margin of the carapace valve, which agrees with the taxonomic range

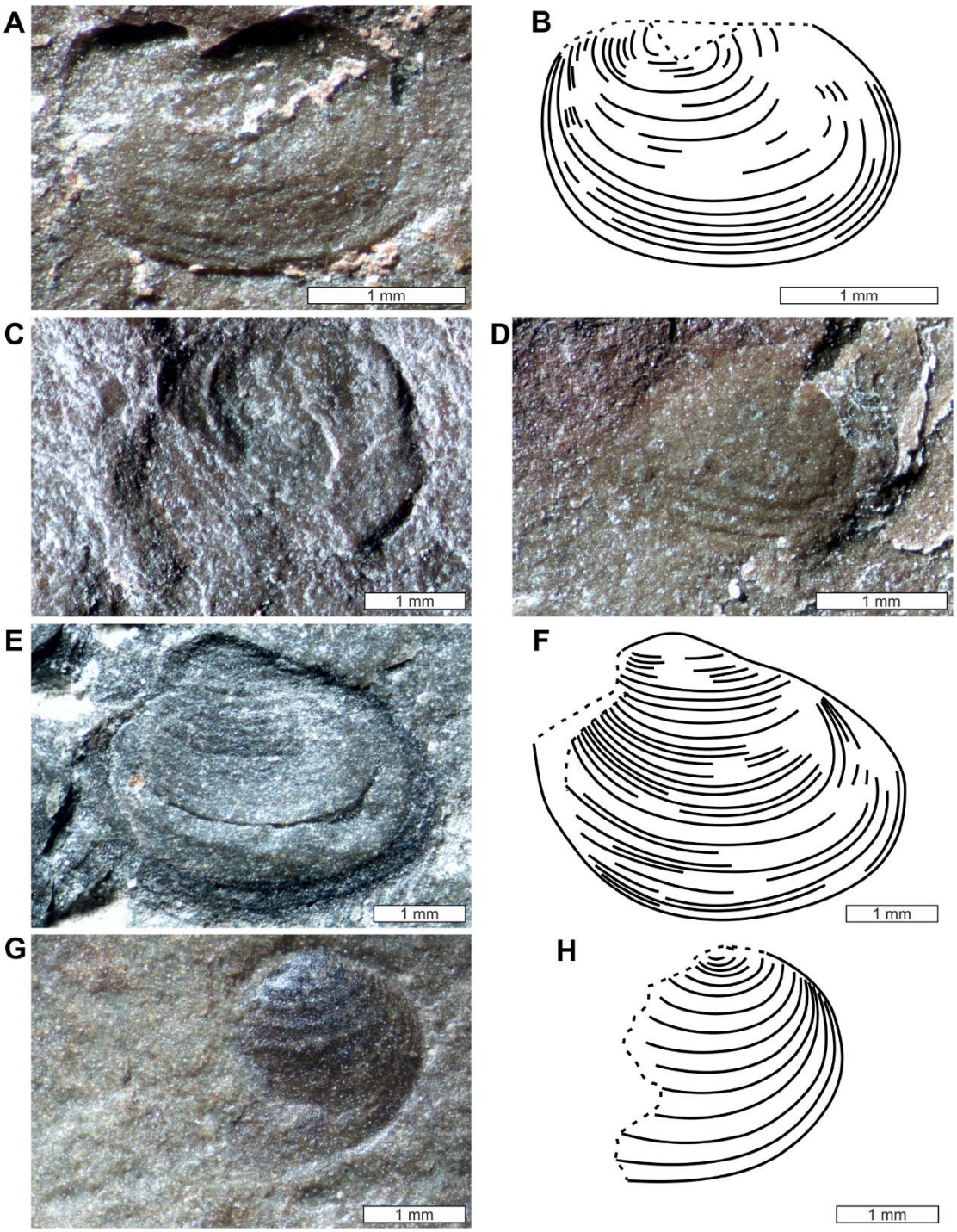

FIGURE 12. Light microscopic photographs and line drawings of indeterminate clam shrimp fragments; specimens from Punta Roja site, middle part of Unit B, upper Olenekian(?)–lower Anisian (A–D); and from Punta Negra 1 site, lowermost part of Unit C, lower Anisian (E–H). A–B, compacted fragments of the left and right carapace valves (DA21/03/01/01a). C, compacted carapace fragment (DA21/03/01/01b). D, steinkern of a right carapace valve (DA21/03/01/02). E–F, compacted carapace in lateral view (DA21/03/03/02). G–H, external view on an anterior fragment of a right carapace valve (DA21/03/03/01).

of the genus *Protomonocarina* Tasch, 1962. The other species, *P. carinata* Shen (in Chang *et al.*, 1976: plate 15, figs. 1, 2), *P. oblonga* Shen (in Chang *et al.*, 1976: plate 15, figs. 11, 12), *P. ziguiensis* Shen (in Chang *et al.*, 1976: plate 15, figs. 3–7), *P. hubeiensis* Shen (in Chang *et al.,* 1976: plate 15, figs. 8, 9), *P. buzhuangheensis* Shen (in Chang *et al.*, 1976: plate 15, fig. 10), and *P. xiangxiensis* Shen (in Chang *et al.*, 1976: plate 15, fig. 13), were assigned to the genus *Hornestheria* by Kozur & Weems (2010), based on the presence in those species of a radial sculpture on their larval carapace valves. These species of *Protomonocarina* spp. can be readily differentiated from *Hornestheria* sp. aff. *H. sollingensis* (Figures 2–6) by the relatively smaller size of the larval carapace valve and the radial sculpture of the latter species. Additionally, values for total carapace valve length and height of *Protomonocarina* spp. sensu Shen (in Chang *et al.*, 1976) range between 1.9–2.9 mm and 1.2–1.8 mm, respectively; these dimensions are distinctly smaller than those of *Hornestheria* sp. aff. *H. sollingensis*.

In contrast to specimens of *Hornestheria* sp. aff. *H. sollingensis* (Figures 2–6), specimens of both *Hornestheria*? Morphotype 1 (Figures 8, 9) and *Hornestheria*? Morphotype 2 (Figures 10, 11) are less well-preserved, showing a mixture of brownish carapace fragments and sedimentary imprints or moulds. Microstructures are present in *Hornestheria*? Morphotype 2 but cannot be clearly seen or imaged (Figure 11C, D), which is most likely a consequence of its poor preservation. Therefore, an open nomenclature is preferred instead of a formal species name for these specimens, even though *Hornestheria*? Morphotype 1 and *Hornestheria*? Morphotype 2 probably represent new taxa. Both of these carapace valve morphologies are known from a single stratigraphic horizon at the same fossil site (i.e., Punta Negra 2), so they are here separated into two different forms because of the consistently observed differences in the carapace valve morphology of each of these morphotypes. In particular, *Hornestheria*? Morphotype 1 (Figures 8, 9) has a rounded shape, whereas *Hornestheria*? Morphotype 2 (Figures 10, 11) is much more elongated. This might be an expression of sexual dimorphism; it is known from other studies of fossil clam shrimps that sexual dimorphism can be recognised within a single population by the presence of two carapace forms (e.g., Astrop *et al.* 2012; Weems & Lucas 2015). By comparison with the literature, similarly high degrees of shape variation are known from other late Olenekian–early Anisian clam shrimp species, such as *E. albertii mahlerselli*. According to H.W. Kozur and J. Lepper (in Kozur & Weems 2010: p. 392), this differentiation is based on the length (L)/height (H) ratio values of the carapace valves, resulting in the definition of a slender morphotype (L/H=1.57–1.74) and a stout morphotype (L/H= 1.11–1.44). Another example of a high degree of carapace valve shape variation representing a differentiation into two morphotypes is *H. sollingensis* Kozur et Lepper (in Kozur & Weems 2010), as shown in the photographs of the type material: round carapace valves (see Kozur & Weems 2010: figs. A2.1, A2.4) represent a stout morphotype, whereas elongated-oval carapace valves represent a slender morphotype (see Kozur & Weems 2010: figs. A2.3, A2.5–2.7).

In analogy to these examples of slender and stout morphotypes, one may assume that the assemblage of *Hornestheria*? Morphotype 1 and *Hornestheria*? Morphotype 2 specimens represents a monospecific fauna, which is composed of a morphologically highly variable species that could be differentiated by its total carapace valve height (H)/total carapace valve length (L) ratio values into a stout morphotype (=*Hornestheria*? Morphotype 1; 0.76<H/L<0.87) and slender morphotype (=*Hornestheria*? Morphotype 2; 0.57<H/L<0.71). The stout morphotype would be characterized by both larger total carapace valve sizes and a more round shape. Generally, separation into slender and stout morphotypes seems to be a well-established practice for describing high morphological variability in clam shrimps (e.g., Astrop *et al.* 2012; Weems & Lucas 2015). As exemplified by *Magniestheria mangaliensis* (Jones, 1862) from Lower Triassic deposits of the Buntsandstein Group in Germany (e.g., Kozur & Seidel 1983a; Scholze *et al.* 2015, 2016), the presence of slender and stout morphotypes within a single species can be best recognized by studying large numbers of specimens within single layers of mass occurrences. In the best case, both morphotypes occur in a single population in direct association on a bedding plane. The latter has not been possible to observe in most slabs of the present study, due to both a low amount of available specimens within layers of mass occurrences and the predominantly moderate to poor preservation of *Hornestheria*? Morphotype 1 and *Hornestheria*? Morphotype 2 specimens. Consequently, both forms are treated as two separate morphotypes by using open nomenclature at the species level owing the rather limited state of knowledge at present.

Implications for biostratigraphy

The sedimentary succession in the wider study area is interrupted by a widespread hiatus at the Permian–Triassic transition. The onset of this stratigraphic gap in the upper Permian has been identified on the Balearic Islands (e.g., Rosell *et al.* 1988), and has been suggested to range upward approximately to the early Olenekian or locally

even up to the early Anisian (e.g., Linol *et al.* 2009). This gap is also present in the Iberian Ranges (e.g., López-Gómez *et al.* 2012) and other neighbouring regions in the western peri-Tethys (Bourquin *et al.* 2011). On Mallorca, such a gap has not been recognised so far, because the uppermost part of the Permian sequence and the lowermost part of the Triassic sequence do not crop out anywhere on the island (Calafat 1988; Gómez-Gras 1993). Previous works have dated the herein called units B–D as lower Anisian (Diez *et al.* 2010), but an upper Olenekian age cannot be excluded for (part of) Unit A. Records of conifer cones and other plant remains from Unit B reveal a flora similar to that of the Grès à Voltzia Formation of the Vosges, and this was considered to be an indicator for an Anisian age (Álvarez-Ramis *et al.* 1995; Grauvogel-Stamm & Álvarez Ramis 1996; Gall & Grauvogel-Stamm 2005). Our new data on clam shrimp occurrences on Mallorca generally support assumptions on an uppermost Olenekian–Anisian age for this sequence of strata, because index species typical of the lower Lower Triassic (Induan) were not recorded in the present study, as discussed in the following paragraphs.

Clam shrimp biostratigraphic zonation for the upper Permian–Lower Triassic transition on the northern hemisphere of the supercontinent Pangaea were initially established by Kozur & Seidel (1983b) and Kozur (1993), which became later expanded by Kozur & Weems (2010) to cover a wider time span ranging from the uppermost Permian to the lowermost Jurassic. These biozones have been critically tested (e.g., Becker 2015; Scholze *et al.* 2016) and partially refined, based on new data from multiple stratigraphic intervals of different regions (e.g., Weems & Lucas 2015; Sell 2018; Scholze *et al.* 2019). Recently published studies on new finds of Lower Triassic clam shrimps, such as from European Russia (Scholze *et al.* 2015), Germany (Scholze *et al.* 2016), Jordan (Scholze *et al.* 2017), and southwestern China (Scholze *et al.* 2020), have been summarized by Schneider & Scholze (2018) and Schneider *et al.* (2020).

According to the biozonation schema proposed by Schneider *et al.* (2020), an interval of the so-called *Euestheria gutta* Fauna (Schneider *et al.* 2020) correlates to the basal Lower Triassic (lowermost Induan). Apart from occurrences of both *Euestheria* sp. and the lowermost Triassic index species *Euestheria gutta* (Lutkevich, 1937), this fauna also includes *Palaeolimnadiopsis vilujensis* Varentsov, 1955, *Palaeolimnadiopsis* sp., and one carapace valve form morphologically resembling *Rossolimnadiopsis* Novozhilov, 1958. The latter three taxa also have records in the upper Permian (Scholze *et al.* 2019), so they slightly straddle the Permian–Triassic boundary. According to Schneider *et al.* (2020), this fauna is directly followed by the so-called *Cornia germari* Fauna of Lower Triassic (Induan) age, which is composed of its index species *Cornia germari* (Beyrich, 1857) and several radially ribbed species belonging to the genus *Estheriella* Weiss, 1875. The species of both the *Euestheria gutta* Fauna and the *Cornia germari* Fauna can be accompanied by *Magniestheria mangaliensis* (Jones, 1862), which is widely distributed during the Early Triassic (e.g., Jones 1862; Kozur & Seidel 1983a; Liu & He 2000; Goretzki 2003; Ghosh 2011; Hauschke 2014; Scholze *et al.* 2015, 2016; Chu *et al.* 2019). The studied outcrop sections on Mallorca lack all these species characteristically found in Lower Triassic (Induan) deposits of other regions. Therefore, an age younger than Induan is inferred for the clam shrimp faunas found in the Mallorcan Unit B and Unit C; the Mallorcan clam shrimp faunas show much closer affinities with the Olenekian–Anisian interval clam shrimp faunas, specifically those designated as the *Hornestheria sollingensis* Zone and "*Magniestheria-Euestheria-Hornestheria* Fauna" by Kozur & Weems (2010) and Schneider *et al.* (2020), respectively.

According to Kozur & Weems (2010), the occurrence of *H. sollingensis* in the Solling Formation (Buntsandstein Group) in the German part of the Central European Basin is biostratigraphically indicative of the so-called *Hornestheria sollingensis* Zone within the uppermost Spathian Substage (uppermost Olenekian, uppermost Lower Triassic). Kozur & Weems (2010) also re-assigned several Anisian-aged species of the genus *Protomonocarina* from China (see Chang *et al.* 1976: p. 112–115) to *Hornestheria*. An Olenekian age for records of *Protomonocarina sinensis* in northern China was also reported by Liu & He (2000). These re-assignments extend the stratigraphic range of the genus *Hornestheria* upward from the uppermost Olenekian into the Anisian.

Other occurrences of upper Olenekian–Anisian clam shrimps were reported by Żyła *et al.* (2013) from the Samsonów Formation (Buntsandstein Group) in the Polish part of the Central European Basin, which includes an assemblage of *Dictyonatella* sp. and *Palaeolimnadia mecsekensis* Nagy, 1960. The genus *Dictyonatella* was first described by Kozur (1982) and so far is only known from Anisian occurrences in Poland ("*Dictyonatella* spp." in Żyła *et al.* 2013: fig. 5A, B) and France ("*Palaeolimnadiopsis dictyonata*" in Reible 1962: plate 10, figs. 1–3; Gall 1971: plate IX, fig.2; which was later designated as *Dictyonatella dictyonata* in Kozur & Weems 2010). In the Grès à Voltzia Formation of the uppermost Buntsandstein Group in the French part of the Central European Basin, *Dictyonatella* is accompanied by *Palaeolimnadia alsatica* (=*Palaeolimnadia alsatica alsatica* in Kozur & Seidel

1983a) and *Euestheria albertii* (="*Isaura minuta albertii*" in Reible 1962). According to Kozur & Weems (2010), these species belong to the *Euestheria albertii albertii* Zone of the Bithynian Substage (middle Anisian). Further occurrences of large-sized forms morphologically similar to *Dictyonatella* were also reported from Anisian–lower Ladinian deposits in Tunisia (Soussi *et al.* 2017). The common occurrence of *Dictyonatella* in all of these deposits might suggest a biostratigraphic correlation between all of these sections in Poland, France and Tunisia, while the absence of this genus in the clam shrimp faunas from the units B and C of Mallorca studied herein suggest that the Mallorcan clam shrimp faunas are of a different age. Notably, other typical Anisian index species like *E. albertii* and *P. alsatica* are absent as well. Consequently, a slightly older age is inferred for the faunas from Mallorca studied here. For these reasons, forms similar to *H. sollingensis* are, at our current state of knowledge, considered to be indicative of an upper Spathian (upper Olenekian) to Anisian stratigraphic range.

Remarks on taphonomy

In contrast to the exceptionally well-preserved thorax, furca, and appendages of both *Palaeolimnadia alsatica* Reible, 1962 (=*P. alsatica alsatica* sensu Kozur & Seidel 1983a) (see Gall 1971: plate 7, fig. 4) and *Palaeolimnadiopsis dictyonata* Reible, 1962 (=*Dictyonatella dictyonata* sensu Kozur 1982) (see Reible 1962: fig. 8) from the Grès à Voltzia Formation in France, segments of the crustacean body are not preserved in *Hornestheria* sp. aff. *H. sollingensis* (Figures 2–6), *Hornestheria*? Morphotype 1 (Figures 8, 9), or *Hornestheria*? Morphotype 2 (Figures 10, 11) from the units B and C of Mallorca. The fact that the majority of observed carapace valves are preserved with intact outlines indicates that there was no significant long-distance post-mortem transport through water currents, which is consistent with the low energy conditions inferred for the deposition of the fine-grained beds containing the fossils. Additionally, there is no indication of abrasion, scavenging, or predation on these clam shrimp carapace valves. Occasional fragmentation of some carapace valves most likely is an artefact resulting from the splitting of claystone and siltstone slabs during fieldwork. This was difficult to avoid because these rocks have been pervasive affected by the development of microfractures generated during diagenesis. This pervasive microfracturing likely also is the cause of loss of flexibility and other carapace properties during diagenesis, at which time mineral changes in the shell substance increased its susceptibility to fragmentation (Monferran *et al.* 2018).

As known from studies of modern spinicaudatan clam shrimps, their carapace valves consist of a multi-layered cuticle of chitin, which can be taxa-specifically strengthened by integrating calcium carbonate minerals within them (Astrop *et al.* 2015; Hegna *et al.* 2020). Microstructures (i.e., ornamentation) of the carapace valve can appear as different morphologies depending on the preservation of the respective cuticle layers (Monferran *et al.* 2018). Accordingly, the lack of clearly observable ornaments in most of the carapace valves from Mallorca studied here is interpreted to be the result of incomplete preservation or even the absence of primarily mineralized outer cuticles in their respective carapace valves. As the colours of clam shrimp carapace can serve as indicator for fossilization temperatures (P. Tasch, cited in Monferran *et al.* 2018: p. 1062–1063), the slightly brownish coloured remnants of the carapace substance in *Hornestheria* sp. aff. *H. sollingensis* from the Pedra Alta site (e.g., Figures 2, 4) indicate temperatures between 450°C–600°C during diagenesis. Besides heat resulting from burial depth, such relatively high temperatures might also reflect a magmatic heat input, possibly derived from alkaline basaltic flows that are present in the Upper Triassic strata found in the Serra de Tramuntana mountains (e.g., Navidad & Álvaro 1985; Sanz *et al.* 2013).

Summary

The transitional upper Olenekian (upper Lower Triassic) to lower Anisian (lower Middle Triassic) deposits of the "*Buntsandstein* facies" in the Serra de Tramuntana mountains on Mallorca have yielded a clam shrimp fauna composed of *Hornestheria* sp. aff. *H. sollingensis*, *Hornestheria*? Morphotype 1, *Hornestheria*? Morphotype 2, and a few undetermined specimens. *Hornestheria* sp. aff. *H. sollingensis* shows finely reticulated ornamentation, in agreement with the original taxonomic description of *H. sollingensis* Kozur et Lepper (in Kozur & Weems, 2010). This taxon, in comparison with literature data, shows strong morphological similarities with the group of *Euestheria albertii albertii* (Reible, 1962) and *Euestheria albertii mahlerselli* Kozur et Lepper (in Kozur & Weems, 2010) in respect to their carapace valve size and shape. The taxonomically characteristic radial sculpture on the larval carapace valve region of *Hornestheria* is demonstrably well developed in very few individuals, but this is likely due, at

least in part, to its generally small-sized larval carapace valve and only a moderate level of preservation due to deformation (i.e., sedimentary compaction) during diagenesis. According to both the biostratigraphic zonation schema of Kozur & Weems (2010) and the stratigraphic range of the genus *Hornestheria*, the new records of *Hornestheria* sp. aff. *H. sollingensis* from Mallorca indicate that these strata formed during the *Hornestheria sollingensis* Zone, corresponding to the latest Olenekian–Anisian interval.

Large-sized carapace valves, reported here on Mallorca for the first time, are designated preliminarily as *Hornestheria*? Morphotype 1 and *Hornestheria*? Morphotype 2; they show a high degree of variability in their valve shape, best expressed by the variation of the total valve height/length ratio values. This degree of variability may reflect the occurrence of either a single morphologically variable species, possibly divided into a slender and a stout morphotype, or two new species previously unknown. First results from ESEM observations suggest that there is microsculpturing on the carapace valve surface of *Hornestheria*? Morphotype 2, but the exact geometry of the shape of these ornaments is not well-preserved in the analysed sample set.

Consequently, future studies are recommended to more completely document the full spectrum of carapace valve morphologies in *Hornestheria* from Mallorca and other regions, such as from its type area in the Solling Formation (Upper Buntsandstein) in the German part of the Central European Basin. This future study needs to include a more detailed re-study of the rather enigmatic radial sculpture on its larval carapace valve, both by reinvestigating the holotype material of *H. sollingensis* Kozur et Lepper and any other material found in the holotype region. Nevertheless, the new data presented here on clam shrimp occurrences in the studied outcrop sections on Mallorca emphasizes the great potential of clam shrimps for achieving a detailed biostratigraphy of Permian–Triassic continental deposits.

Acknowledgements

R.M.A. was supported by the predoctoral grant FPU17/01922 (Ministerio de Ciencia, Innovación y Universidades, Spain), the CERCA program (Generalitat de Catalunya, Spain) and the project "Mallorca abans dels dinosaures: estudi dels ecosistemes continentals del Permià i Triàsic amb especial èmfasi en les restes de vertebrats" (ref. 15 – 619/2020), based at the ICP and funded by the Departament de Cultura, Patrimoni i Política Lingüística (Consell Insular de Mallorca). Fieldwork campaigns on Mallorca were carried out with permission of the Servei de Patrimoni Històric of the Consell de Mallorca (file number 305-2019, reference code 0313JUL2019ARQ.305-19.estellencs), with the aid of Josep Juárez-Ruiz, Francesc Baiget and Sebastià Matamalas for sampling. R.M.A. also acknowledges Josep Fortuny, Àngel Galobart, Oriol Oms and Eudald Mujal for funding and discussion on the stratigraphy and sedimentology. F.S. acknowledges Peter Frenzel for making photographs with the ESEM. The reviewers Thomas Hegna and Robert E. Weems are greatly acknowledged for their critical comments that improved the initial manuscript. The editor Miguel Alonso is thanked for proper handling of the manuscript.

References

Álvarez-Ramis, C., Fernández-Marrón, T. & Calafat, F. (1995) Avance sobre la megaflora triásica, en facies germánica, de Estellencs (sector noroccidental de la sierra de Tramontana, Mallorca). *Revista Española de Paleontología,* nº homenaje al Dr. Guillermo Colom, 55–58.

Aristov, D. & Zessin, W. (2009) *Mallorcagryllus hispanicus* n. gen. et sp. - eine neue Grylloblattide (Insecta: Grylloblattida: Blattogryllidae) aus dem Buntsandstein der Insel Mallorca, Spanien. *Virgo, Mitteilungsblatt des Entomologischen Vereins Mecklenburg*, 12 (1), 30–34.

Astrop, T.I. & Hegna, T.A. (2015) Phylogenetic relationships between living and fossil spinicaudatan taxa (Branchiopoda Spinicaudata): Reconsidering the evidence. *Journal of Crustacean Biology*, 35 (3), 339–354. https://doi.org/10.1163/1937240X-00002317

Astrop, T.I., Park, L.E., Brown, B. & Weeks, S.C. (2012) Sexual discrimination at work: Spinicaudatan 'Clam Shrimp' (Crustacea: Branchiopoda) as a model organism for the study of sexual system evolution. *Palaeontologia Electronica*, article number 15.2.20A. https://doi.org/10.26879/307

Astrop, T.I., Sahni, V., Blackledge, T.A. & Stark, A.Y. (2015) Mechanical Properties of the Chitin-Calcium-Phosphate "Clam Shrimp" Carapace (Branchiopoda: Spinicaudata): Implications for Taphonomy and Fossilization. *Journal of Crustacean Biology*, 35 (2), 123–131. https://doi.org/10.1163/1937240X-00002332

Bachmann, G.H. & Kozur, H.W. 2004. The Germanic Triassic: correlations with the international chronostratigraphic scale, numerical ages and Milankovitch cyclicity. *Hallesches Jahrbuch für Geowissenschaften, Reihe B*, 26, 17–62.

Becker, A. (2015) Ambiguities in Conchostracan Biostratigraphy: A Case Study of the Permian–Triassic Boundary. *Annales Societatis Geologorum Poloniae*, 85, 697–701. https://doi.org/10.14241/asgp.2015.035

Benton, M.J. (1995) Diversification and Extinction in the History of Life. *Science*, 268, 52–58. https://doi.org/10.1126/science.7701342

Benton, M.J. (2018) Hyperthermal-driven mass extinctions: killing models during the Permian–Triassic mass extinction. *Philosophical Transactions of the Royal Society A*, 376 (2130), 20170076. https://doi.org/10.1098/rsta.2017.0076

Beyrich, W. (1857) 2. Protokoll der Juni-Sitzung. *Zeitschrift der Deutschen Geologischen Gesellschaft*, 9, 374–377.

Biswas, R.K., Kaiho, K., Saito, R., Tian, L. & Shi, Z. (2020) Terrestrial ecosystem collapse and soil erosion before the end-Permian marine extinction: Organic geochemical evidence from marine and non-marine records. *Global and Planetary Change*, 195, 103327. https://doi.org/10.1016/j.gloplacha.2020.103327

Bourquin, S., Bercovici, A., López-Gómez, J., Díez, J.B., Broutin, J., Ronchi, A., Durand, M., Arche, A., Linol, B. & Amour, F. (2011) The Permian–Triassic transition and the onset of Mesozoic sedimentation at the northwestern peri-Tethyan domain scale: palaeogeographic maps and geodynamic implications. *Palaeogeography, Palaeoclimatology, Palaeoecology*, 299 (1–2), 265–280. https://doi.org/10.1016/j.palaeo.2010.11.007

Calafat, F. (1988) *Estratigrafia y sedimentología de la litofacies Buntsandstein de Mallorca*. Bachelor's Thesis, Universitat de Barcelona, Barcelona, 127 pp., 31 annexed figs.

Calafat, F. & Sáez, B. (1987) Paleofauna lacustre del Triàsic Inferior de Mallorca. *Jornades del Medi Ambient de les Illes Balears*, 1, 18–19.

Chang, W.-T., Chen, P.-J. & Shen, Y.-B. (1976) *Fossil Conchostraca of China*. Science Press, Beijing, 325 pp., 138 pls.

Chernyshev, B.I. (1934) O nekotorykh Branchiopoda iz kuznetskogo basseyna. *Trudy leningradskogo obshchestva yestestvoispytateley*, 63 (2), 115–125. [in Russian]

Chu, D., Tong, J., Benton, M.J., Yu, J. & Huang, Y. (2019) Mixed continental-marine biotas following the Permian-Triassic mass extinction in South and North China. *Palaeogeography, Palaeoclimatology, Palaeoecology*, 519, 95–107. https://doi.org/10.1016/j.palaeo.2017.10.028

Delfino, M., Kustatscher, E., Lavezzi, F. & Bernardi, M. (2020) The End-Permian Mass Extinction: Nature's Revolution. *In*: Martinetto, E., Tschopp, E. & Gastaldo, R.A. (Eds.), *Nature through Time. Springer Textbooks in Earth Sciences, Geography and Environment*. Springer, Cham, pp. 253–267. https://doi.org/10.1007/978-3-030-35058-1_10

Depéret, C. & Mazeran, P. (1912) Les *Estheria* du Permien d'Autun. *Bulletin de la Société d'Histoire Naturelle d'Autun*, 25, 165–174.

Diez, J.B., Broutin, J., Grauvogel-Stamm, L., Bourquin, S., Bercovici, A. & Ferrer, J. (2010) Anisian floras from the NE Iberian Peninsula and Balearic Islands: A synthesis. *Review of Palaeobotany and Palynology*, 162 (3), 522–542. https://doi.org/10.1016/j.revpalbo.2010.09.003

Frank, P.W. (1988) Conchostraca. *Palaeogeography, Palaeoclimatology, Palaeoecology*, 62, 399–403. https://doi.org/10.1016/0031-0182(88)90064-8

Galfetti, T., Hochuli, P.A., Brayard, A., Bucher, H., Weissert, H. & Vigran, J.O. (2007) Smithian-Spathian boundary event: evidence for global climatic change in the wake of the end-Permian biotic crisis. *Geology*, 35, 291–294. https://doi.org/10.1130/G23117A.1

Gall, J.-C. (1971) Faunes et paysages du Grès à Voltzia du Nord des Vosges. Essai paléoécologique sur le Buntsandstein supérieur. *Mémoires du Service de la Carte Géologique d'Alsace et de Lorraine*, 34, 1–318.

Gall J.-C. & Grauvogel-Stamm, L. (2005) The early Middle Triassic 'Grès à Voltzia' Formation of eastern France: a model of environmental refugium. *Comptes Rendus Palevol*, 4, 637–652. https://doi.org/10.1016/j.crpv.2005.04.007

Gerstaecker, A. (1866–1879) Die Klassen und Ordnungen der Arthropoden wissenschaftlich dargestellt in Wort und Bild. Erste Abtheilung Crustacea (Erste Hälfte). *In*: Bronn, H.G. (Ed.), *Die Klassen und Ordnungen des Thier-Reichs wissenschaftlich dargestellt in Wort und Bild. Fünfter Band Gliederfüssler (Arthropoda)*. C.F. Winter, Leipzig, Heidelberg, 1320 pp. https://doi.org/10.5962/bhl.title.9999

Ghosh, S.C. (2011) Estheriids (fossil conchostraca) of Indian Gondwana. *Palaeontologia Indica*, 54, 1–145.

Gómez-Gras, D. (1993) El Permotrías de la Cordillera Costero Catalana Facies y Petrología Sedimentaria (Parte I). *Boletín geológico y minero*, 104 (2), 3–49.

Goretzki, J. (2003) *Biostratigraphy of Conchostracans: A Key for the Interregional Correlations of the Continental Palaeozoic and Mesozoic – Computer-aided Pattern Analysis and Shape Statistics to Classify Groups Being Poor in Characteristics*. PhD thesis, Technische Universität Bergakademie Freiberg, Freiberg, 243 pp., 64 pls.

Grauvogel-Stamm, L. & Álvarez Ramis, C. (1996) Conifères et pollen in situ du Buntsandstein de l'île de Majorque (Baléares, Espagne). *Cuadernos de Geología Ibérica*, 20, 229–243.

Hauschke, N. (2014) Conchostraken als Zeitmarken und Faziesanzeiger in kontinentalen Ablagerungen der Trias: Fallbeispiele aus Sachsen-Anhalt und dem östlichen Niedersachsen. *Abhandlungen und Berichte für Naturkunde*, 34, 19–55.
Hegna, T.A. & Astrop, T.I. (2020) The Fossil Record of the Clam Shrimp (Crustacea; Branchiopoda). *Zoological Studies*, 59, 43. https://doi.org/10.6620/zs.2020.59-43
Hegna, T.A. & Olesen, J. (2020) Branchiopoda J.-B. Lamarck 1801 [T.A. Hegna and J. Olesen], converted clade name. *In:* de Queiroz, K., Cantino, P.D. & Gauthier, J.A. (Eds.), *Phylonyms: A Companion to the PhyloCode*. CRC Press, Boca Raton, pp. 587–593.
Hegna T.A., Czaja A.D. & Rogers, D.C. (2020) Raman spectroscopic analysis of the composition of the clam-shrimp carapace (Branchiopoda: Laevicaudata, Spinicaudata, Cyclestherida): a dual calcium phosphatecalcium carbonate composition. *Journal of Crustacean Biology*, 40 (6), 756–760. https://doi.org/10.1093/jcbiol/ruaa078
Hochuli, P., Sanson-Barrera, A., Schneebeli-Hermann, E. & Bucher, H. (2016) Severest crisis overlooked—Worst disruption of terrestrial environments postdates the Permian–Triassic mass extinction. *Scientific Reports*, 6, Article number: 28372. https://doi.org/10.1038/srep28372
Holub, V. & Kozur, H. (1981) Revision einiger Conchostracen-Faunen des Rotliegenden und biostratigraphische Auswertung der Conchostracen des Rotliegenden. *Geologisch-Paläontologische Mitteilungen Innsbruck*, 11 (2), 39–94.
Joachimski, M.M., Lai, X., Shen, S., Jiang, H., Luo, G., Chen, B., Chen, J. & Sun, Y. (2012) Climate warming in the latest Permian and the Permian–Triassic mass extinction. *Geology*, 40, 195–198. https://doi.org/10.1130/G32707.1
Jones, R. (1862) *A Monograph of the Fossil Estheriae*. Palaeontological Society, London, 134 pp., 5 pls. https://doi.org/10.5962/bhl.title.52947
Juárez-Ruiz, J. & Wachtler, M. (2015) *Early-Middle Triassic (Anisian) Fossil Floras from Majorca (Spain)*. Dolomythos, Innichen, 49 pp.
Kobayashi, T. (1954) Fossil Estherians and allied fossils. *Journal of the Faculty of Science, University of Tokyo section 2*, 9, 1–192.
Kozur, H. (1982) Beiträge zur Taxonomie und stratigraphischen Auswertung der untertriassischen Conchostracen. *Geologisch-Paläontologische Mitteilungen Innsbruck*, 11 (11), 355–398.
Kozur, H. (1983) Intraspezifische und erhaltungsbedingte Variabilität der Conchostraca-Arten *Cornia germari* (BEYRICH) und *Estheriella nodoscostata* (GIEBEL) aus dem Unteren Buntsandstein (Bernburg-Formation, Oberes Brahmanian, höheres Unterskyth). *Neues Jahrbuch für Geologie und Paläontologie, Abhandlungen*, 166 (3), 404–430.
Kozur, H.W. (1993) Range charts of conchostracans in the Germanic Buntsandstein. *New Mexico Museum of Natural History & Science Bulletin*, 3, 249–253.
Kozur, H.W. & Mock, R. (1993) The importance of conchostracans for the correlation of continental and marine beds. *New Mexico Museum of Natural History & Science Bulletin*, 3, 261–266.
Kozur, H. & Seidel, G. (1983a) Revision der Conchostracen-Faunen des unteren und mittleren Buntsandsteins. Teil I. *Zeitschrift für Geologische Wissenschaften*, 11 (3), 295–423.
Kozur, H. & Seidel, G. (1983b) Die Biostratigraphie des unteren und mittleren Buntsandsteins des Germanischen Beckens unter besonderer Berücksichtigung der Conchostracen. Teil II zur Revision der Conchostracen-Faunen des unteren und mittleren Buntsandsteins. *Zeitschrift für Geologische Wissenschaften*, 11 (4), 429–464.
Kozur, H.W. & Weems, R.E. (2010) The biostratigraphic importance of conchostracans in the continental Triassic of the northern hemisphere. *Geological Society, London, Special Publications*, 334, 315–417. https://doi.org/10.1144/SP334.13
Kozur, H., Martens, T. & Pacaud, G. (1981) Revision von *„Estheria" (Lioestheria) lallyensis* Depéret & Mazeran, 1912 und *„Euestheria" autunensis* Raymond, 1946. *Zeitschrift für Geologische Wissenschaften*, 9, 1437–1445.
Kozur, H.W., Mahler, H. & Sell, J. (1993) Stratigraphic and paleobiologic importance of the latest Olenekian and Early Anisian conchostracans of Middle Europe. *New Mexico Museum of Natural History & Science Bulletin*, 3, 255–259.
Lamarck, J.B. (1801) *Système des animaux sans vertèbres*. Dèterville, Paris, 432 pp.
Li, G. (2017) SEM plays an important role in the study of fossil clam shrimps. *Journal of Environmental Geology*, 1 (1), 22–23. https://doi.org/10.4172/2591-7641.1000006
Linol, B., Bercovici, A., Bourquin, S., Diez, J. B., López-Gómez, J., Broutin, J., Durand, M. & Villanueva-Amadoz, U. (2009) Late Permian to Middle Triassic correlations and palaeogeographical reconstructions in south-western European basins: New sedimentological data from Minorca (Balearic Islands, Spain). *Sedimentary Geology*, 220 (1–2), 77–94. https://doi.org/10.1016/j.sedgeo.2009.06.003
Liu, S.W. & He, Z.J. (2000) Marine conchostracans from the "Sunjiagou Formation" of Qishan, Shaanxi. *Acta Palaeontologica Sinica*, 39 (2), 230–236. [in Chinese with English summary]
López-Gómez, J., Galán-Abellán, A.B., De la Horra, R., Barrenechea, J.F., Arche, A., Bourquin, S., Marzo, M. & Durand, M. (2012) Sedimentary evolution of the continental Early–Middle Cañizar Formation (Central Spain): implications for life recovery after the Permian–Triassic crisis. *Sedimentary Geology*, 249/250, 26–44. https://doi.org/10.1016/j.sedgeo.2012.01.006
Lutkevich, E.M. (1937) O nekotorykh Phyllopoda SSSR. *Ezhegodnik Vsesoyuznogo Paleontologicheskogo Obshchestva*, 11, 60–70. [in Russian with English summary]

Mahler, H. & Sell, J. (2015) Profile im Oberen Buntsandstein (Röt 4-Subformation) von Unterfranken und Südthüringen. *Naturwissenschaftliches Jahrbuch Schweinfurt*, 27, 27–93.
Matamales-Andreu, R., Oms, O., Galobart, À. & Fortuny, J. (2020) Middle–Upper Triassic marine vertebrates of Mallorca (Balearic Islands, western Mediterranean). *Historical Biology*. https://doi.org/10.1080/08912963.2020.1810682
Monferran, M., D'Angelo, J., Cabaleri, N., Gallego, O. & Garban, G. (2018) Chemical taphonomy and preservation modes of Jurassic spinicaudatans from Patagonia: A chemometric approach. *Journal of Paleontology*, 92 (6), 1054–1065. https://doi.org/10.1017/jpa.2018.40
Nagy, E. (1960) A Mecsek-Hegység Mezozóos Phyllopodá. *Földtani Közlöny*, 90 (1), 137–141.
Navidad, M. & Álvaro, M. (1985) El vulcanismo alcalino del Triásico Superior de Mallorca (Mediterráneo Occidental). *Boletín Geológico y Minero*, 96 (1), 10–22.
Novozhilov, N.I. (1958) Recueil D'Articles sur les Phyllopodes Conchostracés. *Annales du Service d'Information Géologique du Bureau de Recherches Géologiques, Géophysiques et Minières*, 26, 1–135.
Orlova, E.F. (1978) The use of replicas to study fossil conchostracans. *Paleontological Journal*, 3, 401–404.
Preuss, G. (1951) Die Verwandtschaft der Anostràca und Phyllopoda. *Zoologischer Anzeiger*, 147, 49–64.
Raymond, P.E. (1946) The genera of fossil Conchostraca – An order of bivalved crustaceans. *Bulletin of the Museum of Comparative Zoology*, 96, 217–370.
Reible, P. (1962) Die Conchostraken (Branchiopoda, Crustacea) der Germanischen Trias. *Neues Jahrbuch für Geologie und Paläontologie Abhandlungen*, 114, 169–244.
Rogers, D.C. & Hegna, T.A. (2020) Fossil and Modern Clam Shrimp (Branchiopoda: Spinicaudata, Laevicaudata): The World's First Clam Shrimp Symposium and a Celebration of Brian V. Timms. *Zoological Studies*, 59, 32. https://doi.org/10.6620/zs.2020.59-32
Rosell, J., Arribas, J., Elízaga, E. & Gómez-Gras, D. (1988) Caracterización sedimentológica y petrográfica de la serie roja permo–triásica de la isla de Menorca. *Boletín Geológico y Minero*, 99 (1), 71–82.
Sanz, T., Lago, M., Galé, C., Ubide, T., Pocoví, A. & Gil, A. (2013) Las rocas magmáticas de la Sierra de Tramuntana (N de Mallorca, España): contexto estratigráfico. *Geogaceta*, 54, 39–42. https://doi.org/10.5209/rev_JIGE.2013.v39.n1.41759
Schneider, J.W. & Scholze, F. (2018) Late Pennsylvanian–Early Triassic conchostracan biostratigraphy: a preliminary approach. *Geological Society, London, Special Publications*, 450, 365–386. https://doi.org/10.1144/SP450.6
Schneider, J.W., Goretzki, J. & Rössler, R. (2005) Biostratigraphisch relevante nicht-marine Tiergruppen im Karbon der variscischen Vorsenke und der Innensenken. *Courier Forschungsinstitut Senckenberg*, 254, 103–118.
Schneider, J.W., Lucas, S., Scholze, F., Voigt, S., Marchetti, L., Klein, H., Opluštil, S., Werneburg, R., Golubev, V., Barrick, J., Nemyrovska, T., Ronchi, A., Day, M., Silantiev, V., Rößler, R., Saber, H., Linnemann, U., Zharinova, V. & Shen, S. (2020) Late Paleozoic–early Mesozoic continental biostratigraphy — links to the Standard Global Chronostratigraphic Scale. *Palaeoworld*, 29 (2), 186–238. https://doi.org/10.1016/j.palwor.2019.09.001
Scholze, F. & Schneider, J.W. (2015) Improved methodology of 'conchostracan' (Crustacea: Branchiopoda) classification for biostratigraphy. *Newsletters on Stratigraphy*, 48, 287–298. https://doi.org/10.1127/nos/2015/0065
Scholze, F., Golubev, V.K., Niedźwiedzki, G., Sennikov, A.G., Schneider, J.W. & Silantiev, V.V. (2015) Early Triassic Conchostracans (Crustacea: Branchiopoda) from the terrestrial Permian–Triassic boundary sections in the Moscow syncline. *Palaeogeography, Palaeoclimatology, Palaeoecology*, 429, 22–40. https://doi.org/10.1016/j.palaeo.2015.04.002
Scholze, F., Schneider, J.W. & Werneburg, R. (2016) Conchostracans in continental deposits of the Zechstein-Buntsandstein transition in central Germany: Taxonomy and biostratigraphic implications for the position of the Permian-Triassic boundary within the Zechstein Group. *Palaeogeography, Palaeoclimatology, Palaeoecology*, 449, 174–193. https://doi.org/10.1016/j.palaeo.2016.02.021
Scholze, F., Abu Hamad, A., Schneider, J.W., Golubev, V.K., Sennikov, A.G., Voigt, S. & Uhl, D. (2017) An enigmatic 'conchostracan' fauna in the eastern Dead Sea region of Jordan: First records of *Rossolimnadiopsis* Novozhilov from the Early Triassic Ma'in Formation. *Palaeogeography, Palaeoclimatology, Palaeoecology*, 466, 314–325. https://doi.org/10.1016/j.palaeo.2016.11.047
Scholze, F., Golubev, V.K., Niedźwiedzki, G., Schneider, J.W. & Sennikov, A.G. (2019) Late Permian conchostracans (Crustacea, Branchiopoda) from continental deposits in the Moscow Syneclise, Russia. *Journal of Paleontology*, 93 (1), 72–97. https://doi.org/10.1017/jpa.2018.58
Scholze, F., Shen, S., Backer, M., Wei, H., Hübner, M., Cui, Y., Feng, Z. & Schneider, J.W. (2020) Reinvestigation of conchostracans (Crustacea: Branchiopoda) from the Permian–Triassic transition in Southwest China. *Palaeoworld*, 29 (2), 368–390. https://doi.org/10.1016/j.palwor.2019.04.007
Sell, J. (2018) Die Euestheriidae (Conchostraca) des Oberen Muschelkalks und Unteren Keupers von Unterfranken. *Semana*, 33, 55–90.
Shen, S.-z. & Bowring, S.A. (2014) The end-Permian mass extinction: a still unexplained catastrophe. *National Science Review*,

1 (4), 492–495.
https://doi.org/10.1093/nsr/nwu047
Shen, Y., Garassino, A. & Teruzzi, G. (2002) Studies on Permo-Trias of Madagascar. 4. Early Triassic Conchostracans from Madagascar. *Atti della Società italiana di scienze naturali e del Museo civico di storia naturale di Milano*, 143 (1), 3–11.
Soussi, M., Niedźwiedzki, G., Tałanda, M., Dróżdż, D., Sulej, T., Boukhalfa, K., Mermer, J. & Błażejowski, B. (2017) Middle Triassic (Anisian-Ladinian) Tejra red beds and Late Triassic (Carnian) carbonate sedimentary records of southern Tunisia, Saharan Platform: Biostratigraphy, sedimentology and implication on regional stratigraphic correlations. *Marine and Petroleum Geology*, 79, 222–256.
https://doi.org/10.1016/j.marpetgeo.2016.10.019
Stanley, S.M. (2009) Evidence from ammonoids and conodonts for multiple Early Triassic mass extinctions. *PNAS*, 106 (36), 15264–15267.
https://doi.org/10.1073/pnas.1613094113
Stanley, S.M. (2016) Estimates of the magnitudes of major marine mass extinctions in earth history. *PNAS*, 113 (42), E6325–E6334.
https://doi.org/10.1073/pnas.1613094113
Tasch, P. (1962) Taxonomic and evolutionary significance of two new conchostracan genera from the midcontinent Wellington Formation. *Journal of Paleontology*, 36 (4), 817–821.
Tasch, P. (1969) Branchiopoda, Order Conchostraca. *In*: Moore, R.C. (Edi.), *Treatise on Invertebrate Paleontology. Part R. Arthropoda 4*. The University of Kansas and The Geological Society of America, Lawrence, pp. R141–R163.
Tassi, L.V., Monti, M., Gallego, O.F., Zavattieri, A.M. & Lara, M.B. (2013) The first spinicaudatan (Crustacea: Diplostraca) from Permo-Triassic continental sequences in South America and its palaeoecological context. *Alcheringa*, 37, 189–202.
https://doi.org/10.1080/03115518.2013.736793
Tassi, L.V., Zavattieri, A.M. & Gallego, O.F. (2015) Triassic spinicaudatan fauna from the Cerro de Las Cabras Formation (Cuyo Basin), Mendoza Province (Argentina): description of new species and revision of previous records. *Ameghiniana*, 52, 241–264.
https://doi.org/10.5710/AMGH.29.11.2014.2823
Vanschoenwinkel, B., Gielen, S., Vandewaerde, H., Seaman, M. Brendonck, L. (2008) Relative importance of different dispersal vectors for small aquatic invertebrates in a rock pool metacommunity. *Ecography*, 31, 567–577.
https://doi.org/10.1111/j.0906-7590.2008.05442.x
Varentsov, I.M. (1955) O sostave i rasprostranenii roda dvustvorchatykh listonogikh rakoobraznykh *Palaeolimnadiopsis* v paleozoe. *Doklady Akademii Nauk S.S.S.R.*, 104, 310–312. [in Russian]
Voltz, P.L. (1835) Notice sur le grès bigarré de la grande carrière de Soultz-les-Bains: avec observations de M. Schimper. *Mémoires de la Société du Muséum d'Histoire Naturelle de Strasbourg*, 2, 1–14.
Webb, J.A. (1979) A Reappraisal of the Palaeoecology of Conchostracans (Crustacea: Branchiopoda). *Neues Jahrbuch für Geologie und Paläontologie Abhandlungen*, 158, 259–275.
Weems, R.E. & Lucas, S.G. (2015) A revision of the Norian conchostracan zonation in North America and its implications for Late Triassic North American tectonic history. *New Mexico Museum of Natural History and Science Bulletin*, 67, 303–317.
Weiss, W. (1875) 1. Protokoll der Juli-Sitzung. *Zeitschrift der Deutschen geologischen Gesellschaft*, 27, 709–712.
Zessin, W. (2008a) Einige neue Insekten aus der Unteren Trias (Buntsandstein) von Mallorca, Spanien (Blattaria, Coleoptera, Diptera, Heteroptera und Megaloptera). *DGaaE-Nachrichten*, 22 (1), 20–21.
Zessin, W. (2008b) Neue Insekten aus der Unteren Trias (Buntsandstein) von Mallorca, Spanien (Blattaria, Coleoptera, Diptera, Heteroptera, Orthopteroidea und Homoptera). *Virgo, Mitteilungsblatt des Entomologischen Vereins Mecklenburg*, 11 (1), 99–101.
Zhang, L., Orchard, M.J., Brayard, A., Algeo, T.J., Zhao, L., Chen, Z.-Q. & Lyu, Z. (2019) The Smithian/Spathian boundary (late Early Triassic): A review of ammonoid, conodont, and carbon-isotopic criteria. *Earth-Science Reviews*, 195, 7–36.
https://doi.org/10.1016/j.earscirev.2019.02.014
Żyła, D., Wegierek, P., Krzysztof, O. & Niedźwiedzki, G. (2013) Insects and crustaceans from the latest Early–early Middle Triassic of Poland. *Palaeogeography, Palaeoclimatology, Palaeoecology*, 371, 136–144.
https://doi.org/10.1016/j.palaeo.2013.01.002

Appendix 9

Triassic sedimentivorous mayfly nymphs from Mallorca

Appendix 9 was published as:

Peñalver, E.; **Matamales-Andreu, R.**; Juárez-Ruiz, J.; Nel, A.; Lozano, R. & Pérez-de la Fuente, R. (2023). Early detritivory and sedimentivory in insects based on insitu gut contents from Triassic aquatic immatures. *Papers in Palaeontology*, in press.

DOI: https://doi.org/10.1002/spp2.1478

In this work, R. Matamales-Andreu contributed in:

A. Logging of the stratigraphic section.
B. Co-direction of all fieldwork campaigns (prospections and excavations).
C. Stratigraphic and sedimentological analysis and interpretation.
D. Writing of the Geographical and Geological Context section of the original draft.
E. Review and editing of the manuscript.
F. Preparation of Figure 1.
G. Collaboration in obtaining funding for fieldwork.

S P P 2	1478 / PALA-08-22-5366-OA.R1	WILEY	Dispatch: 27.12.22	CE: Geetha M
Journal Code	Manuscript No.		No. of pages: 18	PE: Raymond Appavoo M.

[Papers in Palaeontology, 2022, e1478]

Early detritivory and sedimentivory in insects based on *in situ* gut contents from Triassic aquatic nymphs

by ENRIQUE PEÑALVER[1,*], RAFEL MATAMALES-ANDREU[2,3], JOSEP JUÁREZ RUIZ[2], ANDRÉ NEL[4], RAFAEL PABLO LOZANO[1] *and* RICARDO PÉREZ-DE LA FUENTE[5]

[1]Instituto Geológico y Minero de España (IGME), CSIC, C/Cirilo Amorós 42, 46004, València, Comunitat Valenciana, Spain; e.penalver@igme.es; r.lozano@igme.es
[2]Museu Balear de Ciències Naturals, Carretera Palma–Port de Sóller Km. 30.5, 07100, Sóller, Mallorca, Illes Balears, Spain; rafel.matamales@icp.cat
[3]Institut Català de Paleontologia Miquel Crusafont, Universitat Autònoma de Barcelona, Edifici ICTA-ICP, C/ Columnes s/n, Edifici Z (ICTA-ICP), Campus de la Universitat Autònoma de Barcelona, Campus de la UAB, 08193, Cerdanyola del Vallès, Barcelona, Catalunya, Spain
[4]Institut de Systématique, Évolution, Biodiversité (ISYEB), Muséum national d'Histoire naturelle, CNRS, Sorbonne Université, EPHE, Université des Antilles, CP50, 57 rue Cuvier, F-75005, Paris, France; andre.nel@mnhn.fr
[5]Oxford University Museum of Natural History, Parks Road, OX1 3PW, Oxford, UK; ricardo.perez-de-lafuente@oum.ox.ac.uk
*Corresponding author

Typescript received 9 August 2022; accepted in revised form 24 November 2022

Abstract: The colonization of freshwater by insects is one of the milestones in the establishment of continental ecosystems and, thus, of life on our planet. However, several key aspects of this process such as patterns of origination, early adaptations and palaeoecological relationships of the groups involved remain poorly known, namely due to the scarcity of significant assemblages. The Palaeozoic fossil record of freshwater insects is poor and unstudied in suitable detail. Here we analyse exceptionally preserved, three-dimensional cololites (*in situ* gut contents) in abundant mayfly nymphs from Pedra Alta (lower Anisian, lowermost Middle Triassic; Mallorca, Spain), which probably inhabited lentic waters (pools) in a riverine ecosystem. This Konservat-Lagerstätte shows an aquatic insect assemblage *c.* 2 myr older than the similar locality of Grès à Voltzia (Northern Vosges, France). Detailed morphological and elemental analysis show that the cololites are composed of the same very fine-grained claystone as the fossil-bearing rock. This study presents the oldest direct evidence of insect detritivory, as well as most probably that of sedimentivory. The trophic niche represented by insect sedimentivory in the early continental aquatic ecosystem of Pedra Alta is not known for the subsequent *c.* 240 myr of insect evolutionary history and up to the present. This lifestyle in extant insects is extremely infrequent and is known only in a few species of burrowing mayfly nymphs. Our findings illuminate the role of insects in detritus processing in relatively complex food webs shortly after the end-Permian mass extinction event.

Key words: insect evolution, palaeoecology, trophic net, detritivory, sedimentivory, Mesozoic.

One of the milestones in the history of continental ecosystems is the colonization of the continental waters by insects. The Palaeozoic record of aquatic insects is scarce and often ambiguous, with the first records of aquatic insects not known until the late Permian (Wootton 1988; Sinitshenkova 2002, 2003; Zherikhin 2002). Insects play a crucial role in extant aquatic ecosystems, including in key aspects of trophic nets, as recyclers of organic matter (Cummins 1973). The available fossil record indicates that such ecological predominance had already been achieved by, at least, the Middle Triassic (Anisian) based on the rich insect assemblage from the Grès à Voltzia locality in France (Sinitshenkova *et al.* 2005; Lukashevich *et al.* 2010). This view was recently supported by a preliminary palaeoecological assessment of the aquatic insect fauna from the slightly older Pedra Alta deposit in Spain (Matamales-Andreu *et al.* 2021). A few other localities of similar age are known, but these are either very poor in aquatic insects (e.g. Sinitshenkova *et al.* 2015) or lack them, at least for certain (e.g. Bashkuev *et al.* 2012). During the Triassic, continental ecosystems underwent a profound remodelling largely due to biotic turnovers, and many of the key structural features of modern ecosystems became established (Sinitshenkova 2002; Benton & Wu 2022), especially for the aquatic ones (Zhao *et al.* 2020). Changes in the insect palaeofaunas around the end-Permian mass extinction and the subsequent early recovery are poorly known due to the lack of Lower Triassic palaeoentomological outcrops (but see Briggs & Gall 1990). This gap has been considered one of the most important in the fossil insect record (Zherikhin 2002).

© 2022 The Authors.
Papers in Palaeontology published by John Wiley & Sons Ltd on behalf of The Palaeontological Association.
This is an open access article under the terms of the Creative Commons Attribution License, which permits use, distribution and reproduction in any medium, provided the original work is properly cited.

doi: 10.1002/spp2.1478

Exceptional preservation deposits provide high-quality ecological data on past ecosystems, mostly those related to aquatic (i.e. compression deposits: e.g. Gall 1972; Kopylov *et al.* 2020) or forested environments (i.e. amber: e.g. Grimaldi 2000; Sánchez-García *et al.* 2021). Even though the evolution of larval stages in insects has classically been one of the most neglected topics in (palaeo)entomology (Peñalver & Pérez-de la Fuente 2014), compression deposits provide rich assemblages of aquatic preimaginal stages of insects, including egg lays, larvae, nymphs, or exuviae. Because compression deposits (particularly those offering exceptional preservation) have their origin in aquatic environments, they are crucial to understand some of the key topics in the evolution of insects in freshwater habitats (Martínez-Delclòs *et al.* 2004). In the case of Triassic insects, virtually known only as compression fossils, the studies are scarce and our knowledge on them is not based on strong taphonomic analyses. Indeed, although has been studied in detail from the taphonomic, taxonomic and palaeoecological standpoints (Gall 1996, 1972, 1983; Gall & Grauvogel-Stamm 2005), including its aquatic insect forms (e.g. Sinitshenkova *et al.* 2005; Lukashevich *et al.* 2010; Sroka & Staniczek 2022), a detailed analysis of the insect preservation is yet to be carried out.

The evolution of feeding habits in insects is a poorly known subject and largely relies on indirect evidence, such as inferences based on extant relatives, analogous anatomical features (e.g. mouthparts) and ichnofossils (e.g. plant–insect interactions). A few fossils provide direct evidence of feeding habits. These include food sources in association with their potential consumers (e.g. pollen loads clumped to long-proboscid flies; Peñalver *et al.* 2015), coprolites (Richter & Baszio 2001; Peñalver 2002), or preserved gut contents, particularly palynomorphs, in the form of gastroliths (stomach contents) or cololites (intestinal contents) (e.g. Krassilov & Rasnitsyn 1997; Wedmann *et al.* 2021). Fossilized gut contents represent a source of remarkable palaeobiological and palaeoenvironmental data (Seilacher 2002). Although cololites are not rare in arthropods and occur in diverse groups, ages and outcrop types (Knaust 2020), they are easily overlooked or ignored. For instance, they are present in Devonian aquatic isopod relatives preserved as compressions (Robin *et al.* 2021, fig. 1c) and in terrestrial isopods preserved in Cretaceous amber (Sánchez-García *et al.* 2021, figs 7B, 9B). The three-dimensional (3D) cololites preserved in arthropods are usually present in body fossils, and not isolated as more commonly occurs in fossil vertebrates (Seilacher 2002).

Here we provide a detailed analysis of 3D, *in situ* cololites of the most abundant mayfly nymph morphotype from the Spanish earliest Middle Triassic aquatic assemblage of Pedra Alta (Matamales-Andreu *et al.* 2021). The taphonomic study of these mayfly nymphs and their cololites indicates a probable sedimentivorous lifestyle, a peculiar strategy in insects that could had played an important role during their early colonization of aquatic ecosystems.

GEOGRAPHICAL AND GEOLOGICAL CONTEXT

Mallorca is the largest island of the Balearic Archipelago, located in the western Mediterranean. It was uplifted during the Alpine Orogeny, and it is structurally composed of three main southwest–northeast mountain ranges that range from the Carboniferous to the middle Miocene, surrounded by upper Miocene–Holocene material. A few small and poorly accessible outcrops of Lower–Middle Triassic continental facies, the only ones of Mallorca, appear along the coastal cliffs between Cala d'Estellencs and Punta de son Serralta, at the northwest margin of the Serra de Tramuntana mountains (Fig. 1A). There, four formal lithostratigraphic units have been recently defined (Matamales-Andreu *et al.* 2021), from lower to upper: Punta Roja Formation (Fm.), Estellencs Fm., Pedra Alta Fm. and Son Serralta Fm. (Fig. 1B).

All of the insect fossils considered herein were collected from greenish (sometimes sandy) siltstone beds in the Pedra Alta outcrop (Fig. 1C), which can be included in the upper part of the Estellencs Fm. (Matamales-Andreu *et al.* 2021; Peñalver *et al.* 2022). Although this formation was interpreted to mostly correspond to meandering river and associated floodplain deposits, its upper part consistently possesses a coarser interval that was argued to represent deposits of braided rivers that developed during a period of more energetic water flow (Matamales-Andreu *et al.* 2021). The Pedra Alta palaeoentomological outcrop is part of that interval, and contains a succession consisting of alternating beds of white medium-grained sandstones with tabular cross-bedding, and beds of red or green very finely grained claystones with sub-horizontal lamination, sometimes with intercalated thin horizons of siltstones or very fine-grained sandstones (Fig. 1C). The white sandstones are interpreted as the levée deposits of a braided river, formed during the high-water phases, whereas the siltstones and claystones correspond to the sedimentation of the suspended load when the water table fell and the backswamp was isolated from the main channel (Matamales-Andreu *et al.* 2021; Peñalver *et al.* 2022).

The pools that developed in the backswamp were probably quite persistent in time, perhaps during a whole wet season. Their deepest parts were dysoxic or completely anoxic, as represented by the reduced sediments rich in organic matter (green siltstones), whereas the parts closer to the surface were heavily oxidized (red siltstones) and barely preserve any fossil remains (Matamales-Andreu *et al.* 2021). Such deposits are generally devoid of

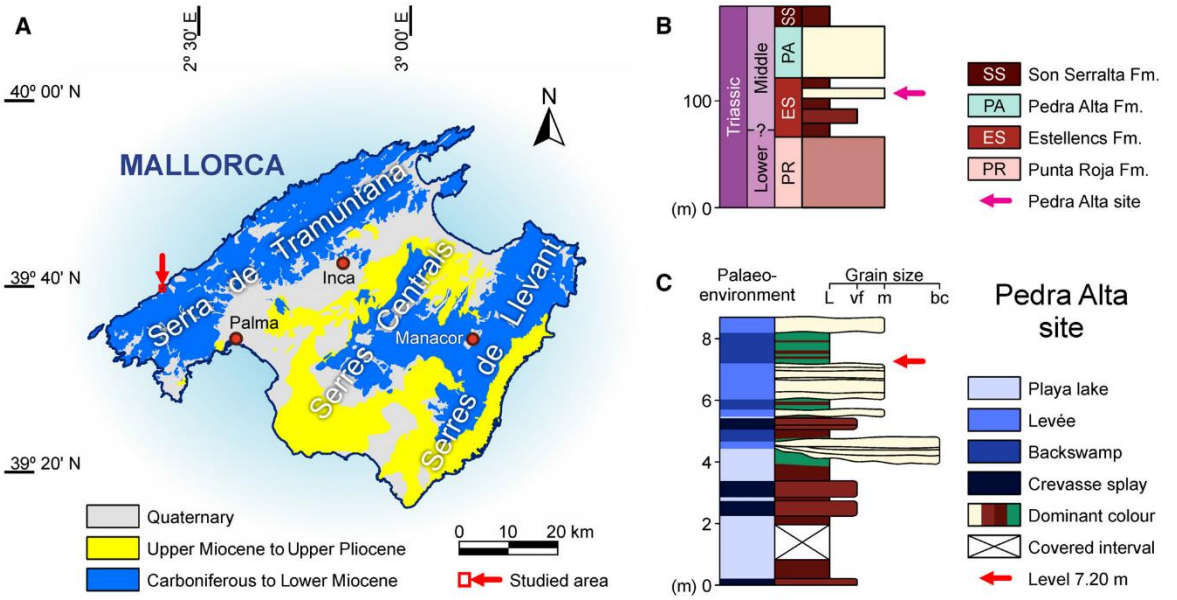

Color 3

FIG. 1. Geographical and geological context of the Pedra Alta palaeontological site. A, simplified geological map of Mallorca showing the location of the study area. B, stratigraphic framework of the Lower–Middle Triassic continental units of Mallorca, showing the position of the studied section. C, stratigraphic log of the studied section, with the location of the fossiliferous horizons and the four recognized depositional palaeoenvironments (indicated with different shades of blue). *Abbreviations*: bc, xxx; L, xxx; m, xxx; vf, xxx. B–C simplified after Matamales-Andreu *et al.* (2021).

bioturbation, although some particular horizons have a local abundance of small, horizontal and vertical burrows. Similar environments to those of the Pedra Alta outcrop were described in the slightly younger locality of Grès à Voltzia of the northern Vosges (France) (e.g. Gall 1972, 1983).

In the upper part of the Estellencs Fm. abundant macrofossils are documented. One example of this is a clam shrimp assemblage that characterizes various of the palaeontological beds, and is distinguished by the presence of valves from *Hornesteria* Kozur & Lepper *in* Kozur & Weems, 2010 (Scholze & Matamales-Andreu 2021). A single record of an indeterminate fish corresponds to the siltstone beds as well (Matamales-Andreu *et al.* 2021). Finally, a macrofloristic assemblage completes the fossil content of the siltstones from the Upper Estellencs Fm., mostly characterized by the presence of branches of the genera *Albertia* Schimper *in* Voltz, 1837 and *Voltzia* Brongniart, 1828, and other coniferous remains (cones and bracts; Juárez Ruiz & Wachtler 2015).

The Konservat-Lagerstätte of Pedra Alta was most recently dated as Aegean (lower Anisian, Middle Triassic) (Matamales-Andreu *et al.* 2021). Palynomorph analysis pointed to an Anisian age (Calafat 1988). Later, Diez *et al.* (2010) revised the list of species, confirming the attribution to the Anisian and positing that the age could be further constrained in the lower Anisian (= Aegean substage). Recently, Scholze & Matamales-Andreu (2021) studied the clam shrimp fossils present in the Pedra Alta outcrop and argued that the finding of specimens identified as *Hornestheria* aff. *H. sollingensis* Kozur & Lepper *in* Kozur & Weems, 2010 (Xiangxiellidae) was indicative of the *H. sollingensis* Zone, characteristic of the uppermost Spathian to Aegean (uppermost Olenekian to lower Anisian). Therefore, both the palynomorphs and the clam shrimps are consistent with an Aegean (lower Anisian) age for this outcrop. This contrasts with the similar palaeoenvironments of the Grès à Voltzia (Gall & Grauvogel-Stamm 2005; Matamales-Andreu *et al.* 2021), which have been attributed to the Bithynian substage (middle Anisian) based on its clam shrimp fauna (*E. albertii albertii* Zone of Kozur & Weems 2010). This means that Pedra Alta is up to *c.* 2 myr older than Grès à Voltzia.

MATERIAL AND METHOD

The more than 50 specimens included in this study come from the Pedra Alta section (at 4.75 m and 7.20–7.30 m), the upper part of the Estellencs Fm. (Mallorca, Balearic Islands, Spain). These specimens are present in two collections, one public and the other a historical private collection. Field sampling was carried out under the excavation permits from the Comissió Insular de Patrimoni Històric

of the Consell de Mallorca number 305-2019, reference code 0313JUL2019ARQ305-19.estellencs. The specimens collected during this palaeontological excavation, and the samples prepared from them for the present study, are part of the public collection and are housed at Museu de Mallorca (Palma, Mallorca, Balearic Islands, Spain) with an abbreviation in the form: DA21/[campaign number]-[horizon number]-[specimen number]. All figured specimens in this study belong to this collection.

The fossilized exoskeletons studied herein are better visualized using low-angle light due to the contrast of their shiny surface with the matt sheen of the rock matrix. The cololites have been observed in preparations under optic microscopy, namely by transparency using transmitted light. These preparations were made as follows. Small sections (S1–S7) of the 3D cololites were easily obtained by pressing with a pin on one side and were prepared on microscope slides using glue (instant cyanoacrylate adhesive; Ethyl-cyanoacrylate, LOCTITE®, Henkel Adhesives) (Fig. S1); two additional samples of the rock matrix, in association with cololites but outside the body perimeter, were obtained for comparison (Sa1 matrix and Sa2 matrix). All of the sections were prepared in longitudinal position except S5 and one of the two portions obtained from S7. The contents of the cololite sample in the glue drop were strongly contrasted and enhanced, being semitransparent under the optic microscope. The glue drop needed several minutes to harden, allowing time to add the cololite sample and to take photographs and/or camera lucida drawings. When the cololite hardened, the glue could be cut easily using a scalpel under the stereomicroscope, exposing the core of the cololite and obtaining a thin preparation of the sample to be observed using scanning electron microscopy (SEM), including serial transversal sections while avoiding sampling deformation due to the glue consistency. A similar methodology was conducted for the 'Sa2 matrix' sample, whereas the 'Sa1 matrix' sample was obtained and mounted directly on the SEM sample holder (Fig. S2).

SEM images of a cololite/digestive tube and a rock matrix sample were taken using a HITACHI Tabletop Microscope TM4000Plus, without gold sputtering; and element analysis (energy dispersive x-ray spectroscopy: EDS) of a cololite section fragment and a rock matrix sample were obtained using a Hitachi S4800 Electronic Microscope, both at the Microscopy Services (SCSIE) of the University of Valencia (Spain). Margarite pseudomorphs after chiastolite have been studied using a JEOL JSM-6010 Plus scanning electron microscope equipped with an energy-dispersive x-ray microanalyser and a back-scattered electron detector (BSE) at the laboratories of the Instituto Geológico y Minero de España (IGME, Madrid), CSIC. The photographs of complete slab surfaces were taken using a Canon EOS 40D digital camera. Some photographs were taken with a Canon EOS 650D digital camera using Macrofotografía version 1.1.0.5 (IGME-CSIC, Madrid, Spain), which integrates the Helicon Focus software to create composite photographs by integrating sequential images obtained at different focal planes. Microphotographs were taken with a ColorView IIIu Soft Imaging System digital camera attached to an Olympus BX51 microscope (IGME-CSIC, Madrid, Spain). An Olympus BX53 compound microscope equipped with an attached camera lucida tube was used to make the drawings of the fossil insects and their gut contents (IGME-CSIC, Valencia). The non-prepared specimens were examined, drawn and photographed dried and/or wet with a mixture of alcohol and water (the alcohol–water mixture enhances the contrast of the carbonaceous film against the matrix). Photography was enhanced in Photoshop CS2 version 9.0 (https://www.adobe.com) for increased contrast, and composite figures were prepared using the same software.

RESULTS

The mayfly nymphal morphotype bearing the cololites analysed herein occurs in Pedra Alta under diverse developmental stages, with body lengths ranging from *c.* 3–4 mm to 6.6–7.0 mm. These nymphs constitute the most abundant insect record in some beds, including slabs indicative of mass records (Fig. 2). All of the specimens are articulated and show differential preservation. The exoskeleton is generally preserved as a transparent film imprinting a fine relief in the rock matrix. Some external areas are fossilized as darker (originally more sclerotized) carbonaceous films, such as the cephalic capsule and the mouthparts. However, the most evident structures in the fossil nymphs are generally the gut tubes, either directly due to their sclerotization or indirectly due to the general presence of cololites inside them (Figs 3, 4D, E). Details of the foregut can be distinguished in one particularly well-preserved specimen as darker structures, showing an originally greater degree of sclerotization by the presence of cuticle due to the ectodermal origin of the foregut (Chapman 2013; Holtof *et al.* 2019); visible parts include the pharynx and proventriculus, and the anterior part of the oesophagus (Fig. 4C). The remaining parts of the gut in these nymphs are also visible, indicating a differential resistance to decay. In a transversal cut of a cololite section covered by the gut epithelium under SEM, the epithelium is preserved as a carbonaceous film without cuticle layers (Fig. 5), which indicates that this section is most likely to have belonged to the midgut. In any case, the limits between the fore-, mid- and hind gut are not evident in these fossils. These nymphs can be accurately attributed to Ephemeroptera because of the typical three apical abdominal appendages. A general description of this mayfly nymph morphotype is provided by Matamales-Andreu *et al.* (2021).

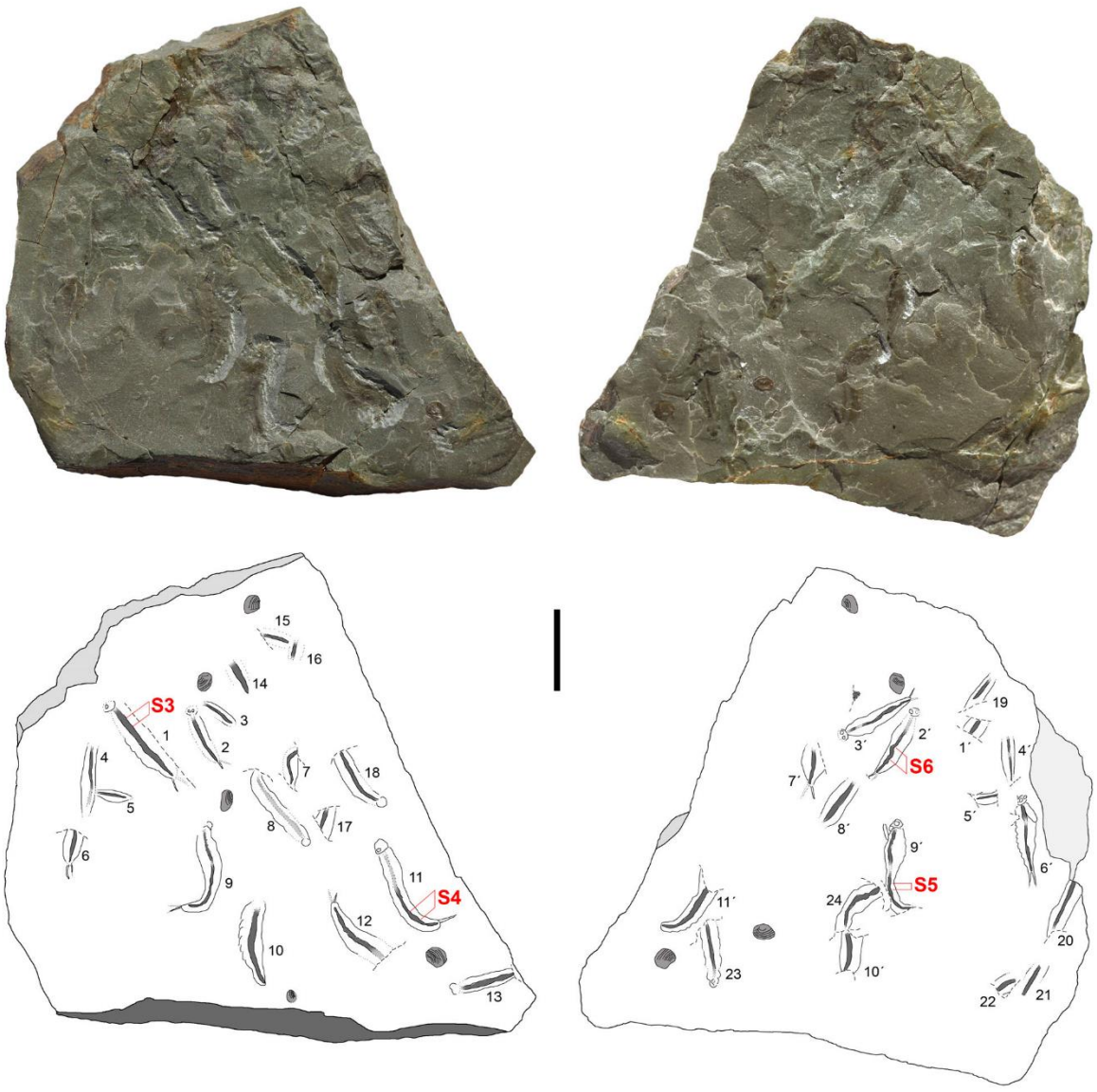

Color

FIG. 2. Part (left) and counterpart of slab DA21/14-02-01 showing a mass record of the mayfly nymph morphotype with cololitic content from Pedra Alta (24 specimens) and six specimens of clam shrimp *Hornestheria* aff. *H. sollingensis*. Not all of the specimens are in the same surface (note that parts and counterparts share the same numbers). Digestive guts that lack distinction of their cololite portions (see the detailed drawings of selected guts in Fig. 6), are shown in grey. S3–S6 indicate sections of cololites removed and prepared. Scale bar represents 1 cm.

The majority of the mayfly nymphs from Pedra Alta have gut contents, which are preserved in three dimensions and *in situ*. These cololites are so conspicuous that nymphs were often detected in the field because of these structures. The cololites are easily detachable, more commonly during rock exfoliation. They are sometimes split into part and counterpart. Detached cololites leave a conspicuous mark as a negative relief (Fig. 3). The width of the cololites depends on the stage of nymph development, ranging from 0.1 to 0.6 mm, with an average of 0.48 mm (n = 20) (Fig. 4). The cololites are not homogeneous along their lengths, showing constrictions and/or different regions separated by short sections of gut tube that were apparently empty (Fig. 6). Moreover, the cololites are present in the midgut and the hind gut, and are practically absent in the foregut (Fig. 6).

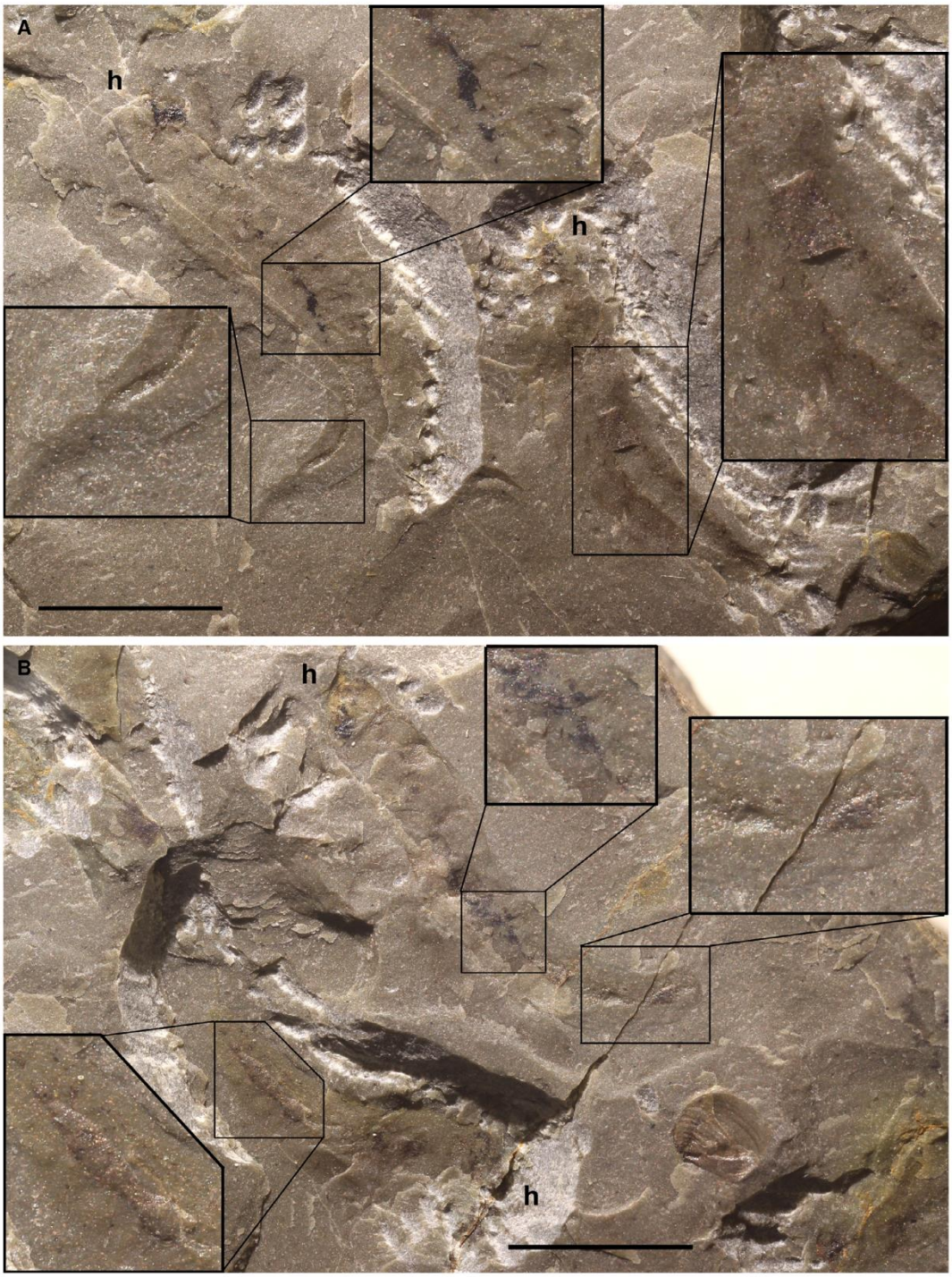

Color

FIG. 3. Detail of four mayfly nymphs from the part of mass record slab DA21/14-02-01 in Fig. 2. A, specimens 9 (left) and 10 (right): details of the negative relief left in the hind gut by a lost 3D cololite (left inset), an undetached cololite section in midgut (right inset), and the carbonaceous film preserved of a gut section in midgut (top inset). B, specimens 12 (left) and 11 (right) showing similar details as in (A); note the clam shrimp *Hornestheria* aff. *H. sollingensis* at the right. *Abbreviation*: h, head or anterior part of the body. Images created from consecutive pictures taken at successive focal planes. Scale bars represent 5 mm.

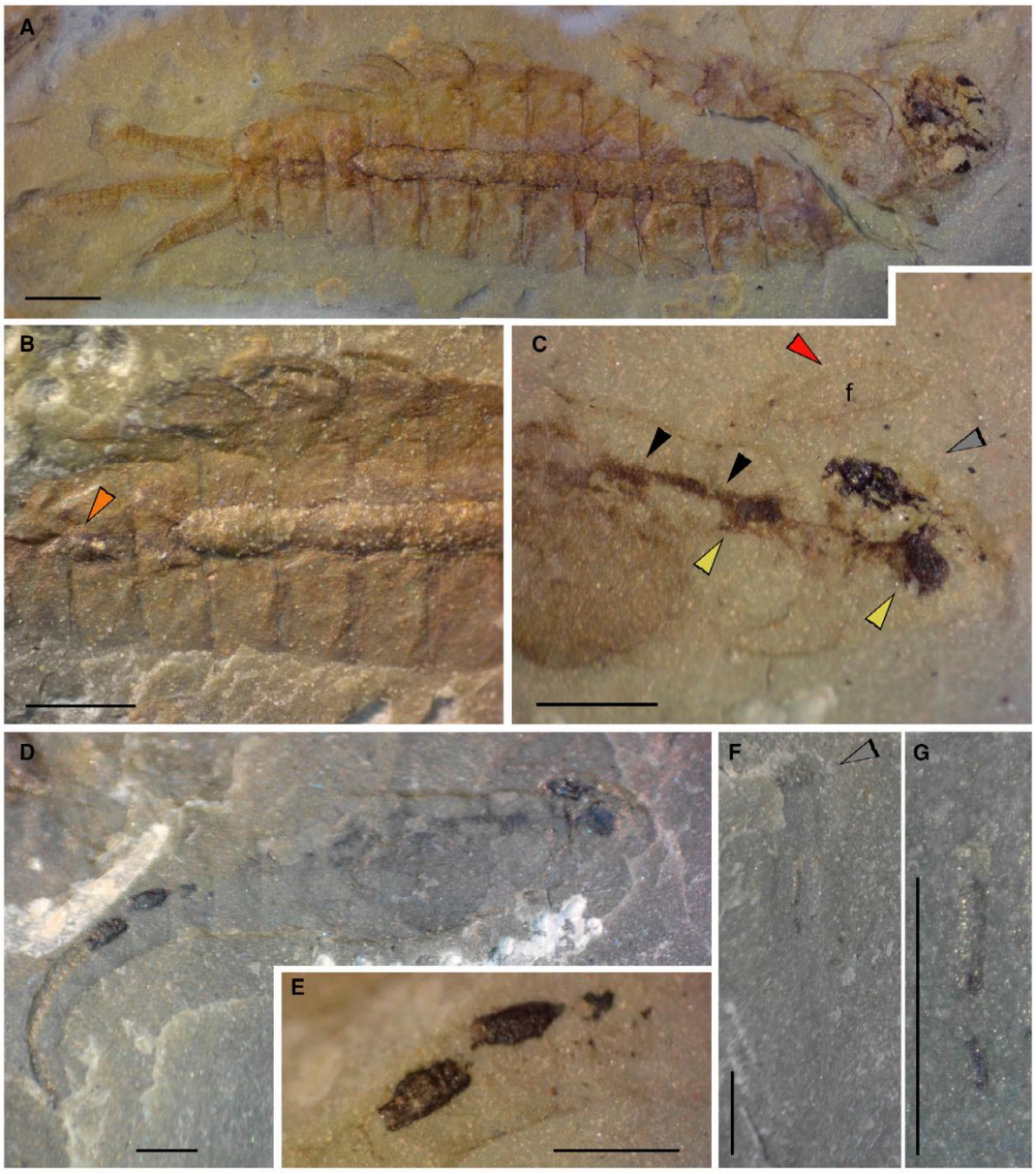

Color

FIG. 4. Digestive guts of selected virtually complete mayfly nymphs from Pedra Alta, showing diverse typologies of 3D cololites and anatomical details of the foregut. A, specimen DA21/03-02-19 showing a massive cololite, virtually infilling its gut. B, detail of the same specimen showing the terminal section of the cololite and a small terminal cololite part in the rectum or nearby (orange arrowhead). C, detail of the head (grey arrowhead) of specimen 9′ in DA21/14-02-01 (Fig. 2) with an anterior dark mass corresponding to the mouthparts and the carbonaceous foregut showing the pharynx (the anterior yellow arrowhead most likely indicates the pharynx and the posterior indicates the proventriculus) and the anterior part of the oesophagus (black arrowheads) (red arrowhead indicates the swollen femur of the foreleg). D, habitus of the same specimen showing a cololite in several portions as a combination of the 3D content and the carbonaceous epithelium of the gut covering it. E, detail of the cololite parts of the same specimen (Fig. 5; Fig. S1). F, minute specimen, DA21/03-02-05, showing a small cololite in two parts along one-third of the body length, as an example of poorly preserved small mayfly nymphs that are identifiable only due to their preserved cololite. Habitus of specimen in A, head in C, and cololite in E, photographed wet using a mixture of alcohol and water, the rest were photographed dry. *Abbreviation*: f, fore femur. Scale bars represent 1 mm.

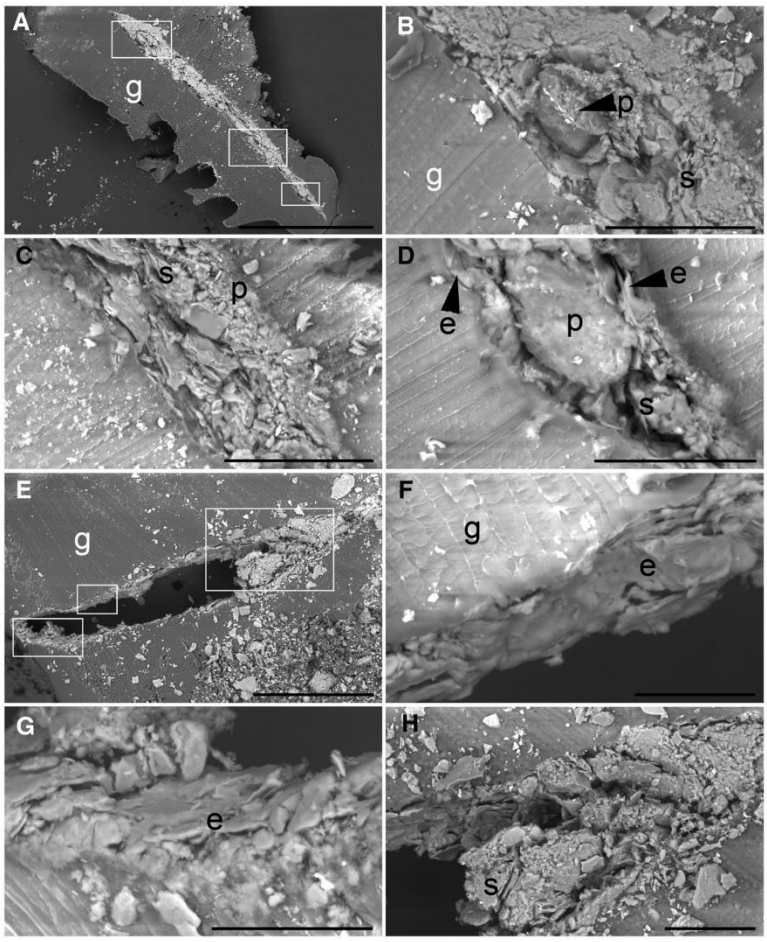

FIG. 5. SEM images of the digestive tube and its content (cololite) of specimen 9′ in DA21/14-02-01, in two transversal cuts from a preparation using instant glue to externally fix the structures (Fig. S1). A, E, general views of two cuts; B–D, details from A; F–H, details from E. A, cut 1 showing a strongly compacted sectioned sample (13:1 compaction ratio); B–C, details of gut content showing large particles (sedimentary particles or compacted sedimentary material not exfoliated by the scalpel) and squamous parts; D, gut tube epithelium preserved as a carbonaceous film. E, cut 2 with loss of cololite content during cutting (given that the glue did not harden the sample, obtaining the compaction ratio was not possible); F–G, details of gut tube epithelium preserved as a carbonaceous film in direct contact with the glue that fixed the cololite sectioned sample; H, gut content or cololite, mostly with a squamous aspect. *Abbreviations*: e, epithelium of the digestive tube, most likely from the midgut; g, glue, p, particle (non-squamous); s, squamous digestive content. Scale bars represent: 300 μm (A); 50 μm (B, C, H); 30 μm (D, G); 200 μm (E); 20 μm (F).

The cololites are composed of inorganic and organic detrital particles as well as small aggregates. The inorganic particles are the main components, and consist mostly of very fine-grained claystone, a few conspicuous sand grains of varied size, and abundant mineral crystals with a dark nucleus, 35 μm in average dimension (n = 40 from specimen 11 in

FIG. 6. Digestive guts of selected virtually complete mayfly nymphs from Pedra Alta. Camera lucida drawings of 22 specimens indicating the 3D cololite sections (S1–S6) and rock matrix samples (Sa1 matrix–Sa2 matrix) obtained and prepared (to the same scale); only the gut has been drawn, with its boundaries schematically drafted (head position and base of cerci), except for specimen (I), in which other anatomical features have been drawn. Specimens grouped together correspond to specimens present in the same rock slab. A, DA21/03-02-109. B, DA21/03-02-97. C, DA21/03-02-20. D, DA21/03-02-45. E, DA21/03-02-19. F, DA21/03-02-89. G, DA21/03-02-98. H, DA21/03-02-87. I, DA21/03-02-23. J, DA21/03-02-05. K, DA21/03-02-117. L, DA21/03-02-90. M, DA21/14-02-01 (specimens 1, 11, 6′, 9′, 3′and 2′, respectively, in Fig. 2). N, some of the drawn specimens (not to the same scale). White arrowheads indicate separation of gut content between different stages of intake in some selected specimens. Scale bars represent 1 mm.

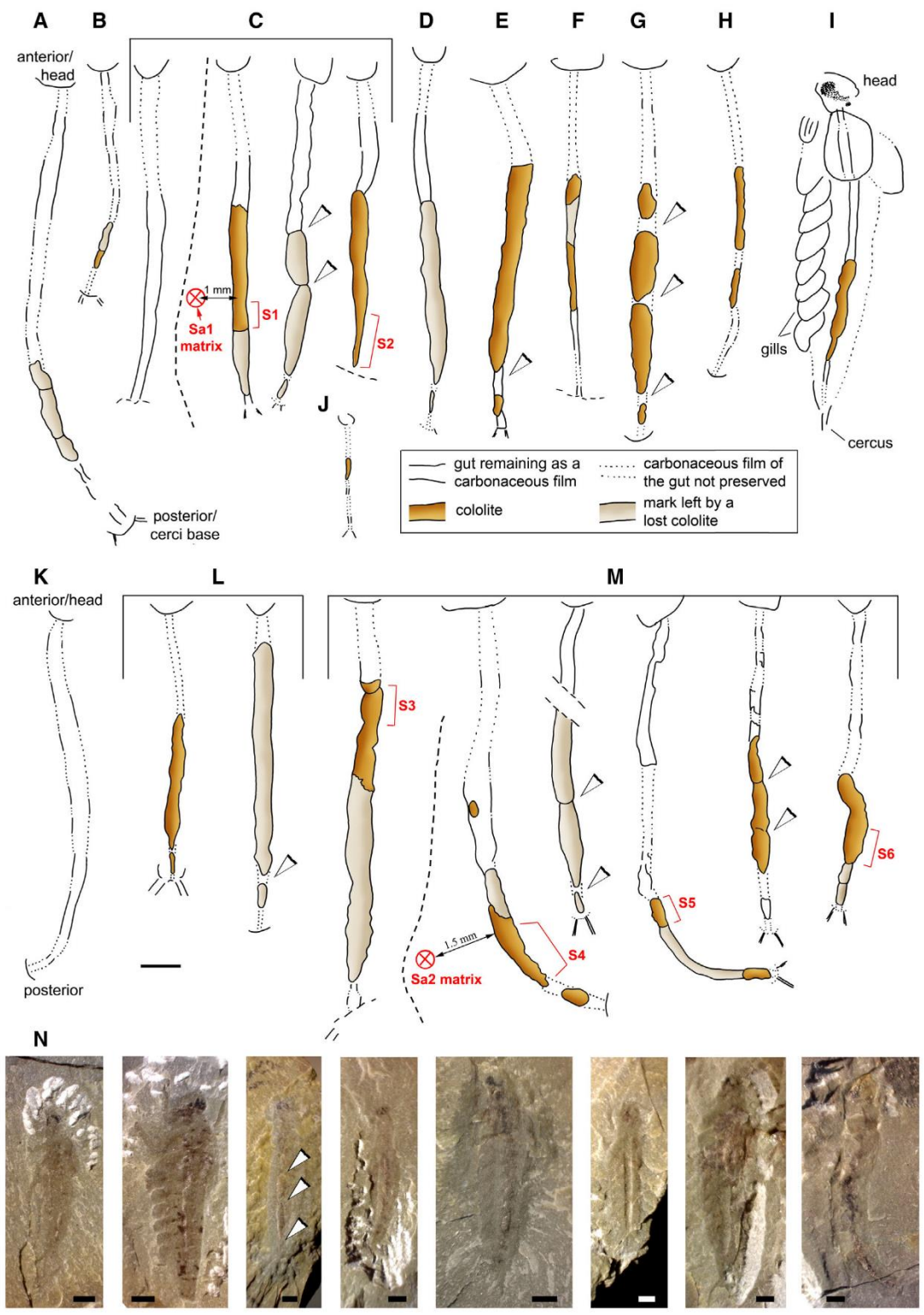
A
B
C
D
E
F
G
H
I
anterior/
head
1 mm
Sa1
matrix
S1
S2
J
head
gills
cercus
posterior/
cerci base
gut remaining as a
carbonaceous film
carbonaceous film of
the gut not preserved
cololite
mark left by a
lost cololite
K
L
M
anterior/head
S3
S4
S5
S6
1.5 mm
Sa2 matrix
posterior
N

color

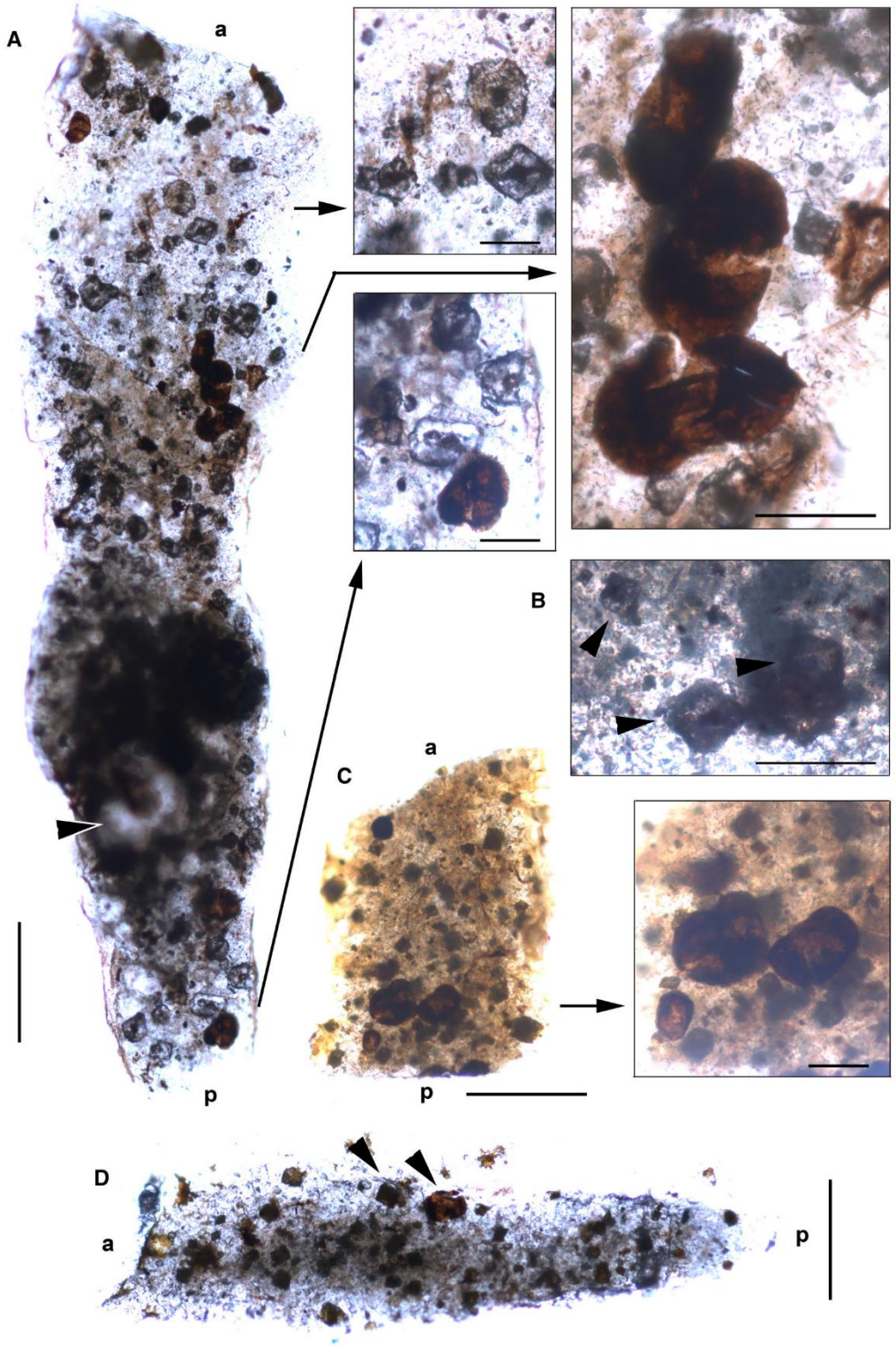

color

FIG. 7. Preparations of three representative 3D cololite sections and one rock matrix sample. A, long portion of a cololite from specimen 11 in DA21/14-02-01 (section S4, Fig. 2; Fig. S3) and details of the margarite pseudomorphs and refractive organic matter, being bisaccate pollen grains of cf. *Alisporites* sp. and/or cf. *Lunatisporites* sp., the only organic remains that could be identified; arrowhead indicates a relatively large sand grain (out of focus in this microphotograph). B, margarite pseudomorphs after chiastolite (arrowheads point to three of them) in a sample from the nymph-bearing rock. C, short cololite portion from a specimen in slab DA21/03-02-20 (section S1; Fig. 6) showing its content in refractive organic matter including pollen grains of cf. *Alisporites* sp. and/or cf. *Lunatisporites* sp. D, long portion of a small cololite sampled from another specimen in slab DA21/03-02-20 (section S2; Fig. 6; Fig. S1); arrowheads indicate a margarite pseudomorph (left) and a well-preserved pollen grain (right). *Abbreviations*: a, anterior end; p, posterior end. Scale bars represent: 0.2 mm (A–D); 0.05 mm (insets from A and C).

DA21/14-02-01, Fig. 7A). The organic detrital particles represent a low percentage of the total cololite content, and include: (1) very particulate debris, most likely to be due to plant decomposition/fragmentation and thus cellulosic in nature; (2) conspicuous bisaccate pollen grains, up to *c.* 90 µm long, of cf. *Alisporites* sp. and/or cf. *Lunatisporites* sp. (E. Barrón, pers. comm., 2021; Diez 2000; Diez *et al.* 2010); the type of preparations and the suboptimal preservation of the pollen grains prevent a confident identification (Fig. 7; Fig. S3); and (3) small aggregates. Last, the cololites also contain a few small indeterminate tubular structures, suggestive of filamentous microbial remains but which cannot be identified with confidence. Under SEM, the few areas observed of cololite content samples were very homogeneous in appearance, and sand grains, mineral crystals or organic detritus were not evident (Fig. 5; Fig. S2). Although
6 the cololites were flattened due to the compaction of the host sediment, it was less intense than that of the host bodies. This is evident in the cololite section that was prepared for observation of its transversal section (650 × 50 µm, to avoid sample deformation; Fig. 5; Fig. S1).

The nymph-bearing rock is composed of the same constituents as the cololites: very fine-grained inorganic detrital particles, crystals with a dark nucleus, and organic components such as conspicuous bisaccate pollen grains (Fig. 7; Fig. S3). EDS analyses (in areas without the crystals described above) indicated the same elemental composition, with a predominance of Si, Al and O (Fig. 8).
7 Removed cololite sections showed the same squamous breaking parallel to the slab plane as the nymph-bearing rock when sampled (Fig. 5; Fig. S2).

DISCUSSION

Cololite origin and composition

The mayfly nymphs bearing cololites studied herein are remarkably abundant, in some cases fossilized in mass records (Fig. 2). An extensive record of transported lotic insects, where burial under suitable preservational conditions typically occurs, would be implausible, given the taphonomic processes that usually occur in continental compression deposits. The extraordinary abundance of the present mayfly nymphs strongly suggests that these aquatic insects lived in the standing waters that produced the sediments and, thus, that they underwent minimal transport (para-autochthony).

The pervasiveness of cololites in the nymph morphotype addressed herein and their preservation, generally present beyond the anterior third of the gut length, and sometimes still present in the rectum or nearby (Figs 4A, 6), are evidence of food intake. Thus, an accidental and
8 abundant ingestion of sediment due to the physical external forces in an early biostratinomic phase conducive to the death and burial of these nymphs can be ruled out. Further evidence is provided by the fact that most of the cololites are composed of several sections, both in consecutive contact in the gut or with gaps between them, indicating different intake stages (Fig. 6A, C, E, G, H, I, M). The shared appearance and similar composition, consistent with that of claystone (constituted by phyllosilicates) (Fig. 8), of the rock matrix and the cololites, show that the mayfly nymphs ingested virtually the same sediment that buried their carcasses but in an oxygenated environment while alive, further indicating para-autochthony for this mayfly nymph assemblage.

The crystals with a dark nucleus that are present in both the cololites and the rock matrix (Fig. S3) are margarite pseudomorphs after chiastolite (andalusite). The presence of Si, Al and Ca in the crystals and of C in the nucleus obtained with EDS analysis indicates that this phyllosilicate occurs as a pseudomorphic replacement of previous chiastolite (Guidotti *et al.* 1979). Thus, the margarite pseudomorphs are diagenetic rather than representing detrital particles in the original sediment ingested. Due to the simi-
9 lar composition of the cololites and the rock matrix, it is expected that the same effects of diagenesis would be observed. In organic matter-rich fossiliferous claystone, chiastolite is formed by low-grade thermal metamorphism. Probably, this was due to the intrusion of volcanic or subvolcanic rocks in Permian–Triassic rocks of nearby areas of the Serra de Tramuntana (Enrique 1986), during Upper Triassic magmatic episodes (Sanz *et al.* 2013).

Food processing in the gut must have been fast, given that the sediment that originated the claystone was poor

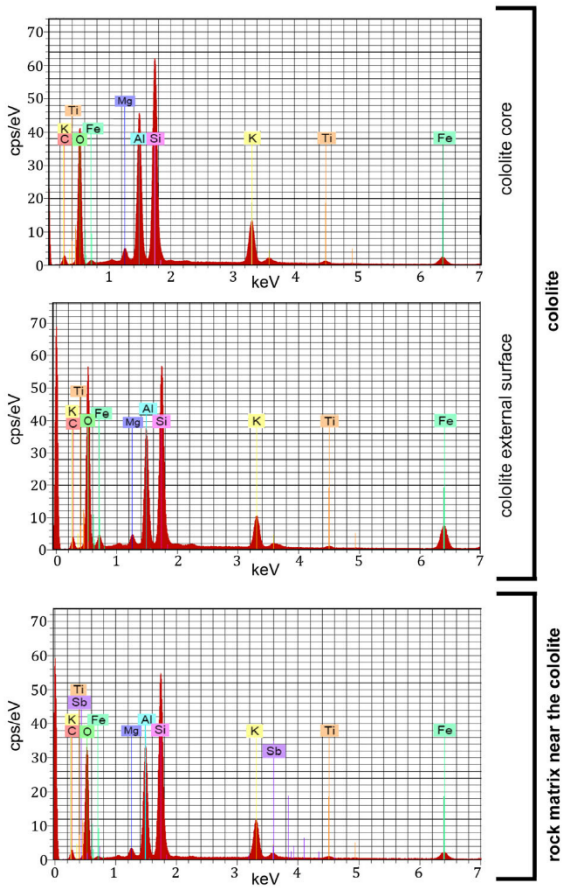

FIG. 8. Elemental analyses of sub-square areas with sides *c.* 0.1 × 0.05 mm of the cololite (sample from section S1) and rock matrix surfaces, of a specimen in slab DA21/03-02-20 (specimen drawn in Fig. 6C), for comparison (Fig. S2). The top and middle panels show the analyses of the core of the cololite, cut using a surgical scalpel, and its external surface (both of the same sample). The bottom panel shows the analysis of a fresh surface of a flake (Sa1 matrix; Fig. 6) from the rock matrix 1 mm from the removed cololite section (S1). Note the elemental similitude between the two types of materials and that the analysed areas did not contain margarite pseudomorphs.

in organic matter. This could explain the lack of cololite remains in some studied nymph specimens (e.g. Fig. 6K). In any case, the available specimens show that the sediment transit towards the midgut was probably fast. In some extant mayfly nymphs such as *Baetis* Leach, 1815 or *Cloeon* Leach, 1815 species, it takes only *c.* 30 min for the ingested matter to pass through the gut (Sartori & Britain 2015).

Seilacher (2002) showed that coprolites and cololites usually retain their original three-dimensionality and so they are partly resistant to flattening. This also occurs in deposits where other organic remains, such as ammonite shells, are strongly flattened. However, that is not always the case: abundant coprolites in the Iberian Peninsula Miocene lacustrine deposits of the Bicorb-Quesa and Rubielos de Mora basins (oil-shales) and the Ribesalbes-Alcora Basin (laminated dolomicrites), produced by salamanders (in the latter two) or by fishes (Peñalver 2002; Peñalver & Gaudant 2010; Peñalver *et al.* 2016), are strongly flattened as carbonaceous films. The 3D cololites studied herein are different from those discussed by Seilacher (2002), in that slight flattening has occurred and they are preserved *in situ*.

The exceptional preservation of the cololites in Pedra Alta and the absence of complete flattening produced by both lithostatic pressure and decomposition can be explained by: (1) the very same nature of the original very fine-grained clay-dominated sediment both in the gut content and in the host matrix; (2) the high sediment content in some parts of the gut due to ingestion, and the differential resistance of the gut content (ingested incompressible particles or sediment) with regards to the nymphal body when subjected to compaction; and (3) the similar early processes of mineralization in the gut sediment and the surrounding sediment of burial. An early mineralization of the cololites induced by bacteria seems not to have occurred or, at least, it was not the main cause of their three-dimensionality. The similar squamous breaking of the cololites and the rock matrix suggests similar processes of compaction during diagenesis.

Considering that the cololite of specimen 9′ in the counterpart of the slab DA21/14-02-01 was originally circular in transversal section when infilled, and that fossil diagenetic flattening did not alter the lateral dimensions of the whole original carcass in the position of burial, based on the expected or 'natural' dimensions of this and the other mayfly nymphs, the compaction ratio of the sediment as gut content can be calculated. The transversal preparation of the cololite section from specimen 9′ is shown in Figure 5A and Figure S1C (see Fig. 4D, E for the cololite section after removal). The current dimensions of the transversal section imply a *c.* 13:1 compaction ratio, but apparently, it was slightly lower in the case of cololite sections from guts that are more infilled by sediment, for instance in the specimen DA21/03-02-19 (Fig. 4A), in contrast to sections of small isolated cololite portions due to poor sediment intake. This compaction ratio is consistent with that generally found in fine-grained muds (Whittington 1978). The compaction ratio for the rest of the body was extreme, considering the typical preservation as a carbonaceous film in compression fossils when early intense mineralization processes are absent (Peñalver *et al.* 1996).

Three-dimensional structures similar to the cololites herein reported have been observed in some Cambrian arthropods from the Burgess Shale and Chengjiang localities. These were first interpreted as guts infilled by mud in sedimentivorous forms (e.g. in the paracrustacean *Canadaspis laevigata* (Hou & Bergström, 1991); see Hou & Bergström 1997), but later were deemed as serially repeated midgut glands preferentially permineralized by early diagenetic phosphate (Butterfield 2002*a*, 2002*b*; also see Vannier *et al.* 2014). Some of the photographs in Hou & Bergström (1997) show 3D gut tubes very similar to mud cololites, instead of the clear 3D glands also figured in that work and others. Vannier & Chen (2002) also considered that these 3D gut tubes in naraoiids apparently infilled with mud are taphonomic artefacts, and also noted the possibility of accidental mud ingestion by individuals trapped alive in turbiditic flows. As Butterfield (2002*a*) and Hou & Bergström (1997) noted, the gut contents of these fossils were not analysed in detail to clarify their nature and origin. In contrast, Vannier *et al.* (2014, fig. 1a) presented a lobopodian from the Chengjiang biota with its seriate 3D glands flanking a 3D cololite located in the main part of the gut, but the analysis of its content was not detailed or conclusive.

Detritivorous lifestyle of the mayfly nymphs

Extant mayfly nymphs (adults do not feed) are usually scrapers or collectors (Cummins 1973; Sartori & Brittain 2015). Based on feeding mechanism, Cummins (1973) classified collectors into filter or suspension feeders and sediment or deposit (surface) feeders, the latter considered as fine particle detritivores (decomposing organic matter) according to the type of dominant food ingested. The same author defined detritivory as 'the intake of nonliving particulate organic matter and the nonphotosynthetic microorganisms that are always associated with it (detritus)'. The mayfly nymph morphotype bearing the cololites reported herein was recently described as a 'detritivore nymph type' (Matamales-Andreu *et al.* 2021) following the preliminary optic assessment of the cololites, which showed that most of their content was composed of inorganic particles and that organic detritus was present only in very small amounts. The detailed analysis of the cololites herein provides an insight into the specific feeding habits of the Triassic freshwater mayfly nymphs containing them.

The nymphs of the extant burrowing mayfly *Hexagenia limbata* (Serville, 1829) feed using two strategies, which have been repeatedly observed in the field and in experimental conditions (Hunt 1953; Zimmerman & Wissing 1980; Dermott 1981). First, they create a water flux inside their burrows by movements of their abdominal respiratory gills, which brings the organic and inorganic particles suspended in the water (seston) to their mouthparts for processing. Second, they feed directly on the sediment, at times on macroscopic particles such as plant fragments, that is present at their burrow entrances with the aid of their forelegs. *Hexagenia limbata* nymphs feed continuously during the day and night and ingest over 100% of their dry body weight per day (Zimmerman & Wissing 1980; Sartori & Brittain 2015), sometimes reaching 192% (Dermott 1981). Research on the ingestion rate of this species suggested that its main food source is the sediment directly consumed rather than the seston brought into the burrows by the gill movements (Dermott 1981). This could also be the case for other *Hexagenia* species, given that 90% of the gut contents of *H. munda* Eaton, 1883 consisted of sand and clay (Walker 1970; Zimmerman & Wissing 1980).

The high quantity of original sediment in the cololites studied herein suggests that the Triassic mayfly nymphs largely fed on selected portions of deposited sediment directly, together with (or instead of) other strategies to obtain organic matter, such as suspension feeding through the active production of currents, implying the concomitant ingestion of abundant suspended detrital clays. The presence of several sand grains in the cololite from specimen 11 in DA21/14-02-01 (Fig. 7A; Fig. S3), several orders of magnitude larger in size than the clay particles, supports the hypothesis of the ingestion of selected portions of benthic sediment. Furthermore, the richer content of organic matter particles in the cololites than in the nymph-bearing rock, particularly evident in the differential abundance of pollen grains, suggests selection of sediment rich in organic matter and/or a different concentration of organic matter in the oxygenated areas (shallow, sublittoral areas) in respect to the dysoxic or completely anoxic areas of sedimentation and burial. Aside from the fine particulate organic matter and small remains such as pollen grains present in the sediment, the ingestion of mud would have also entailed feeding on the microbial community in the sediment. Bacteria, protozoans, fungi and algae present in the sediment play an important role in the feeding of the extant *Hexagenia limbata* nymphs (Zimmerman & Wissing 1980).

Although *Hexagenia* species such as *H. limbata* and *H. munda* could represent plausible extant ecological analogues of the Pedra Alta Triassic mayfly nymphs regarding their feeding habits, there is no evidence of typical mayfly burrows in the Pedra Alta locality, unlike in Grès à Voltzia, where U-shaped burrows tentatively attributed to ephemeroid mayflies are present (Sinitshenkova 2002, 2003). Although the structure of the forelegs of the nymph morphotype studied herein may be compatible with that of a burrowing detritivore (Fig. 4C), it is also possible that the legs were simply used to obtain selected

small portions for ingestion as occurs in *Hexagenia*. Given that the Pedra Alta detritivorous mayfly nymphs do not preserve mouthpart details and their body preservation is poor (Figs 3, 4C), a filter-feeding habit in burrows as occurs in extant *Hexagenia* species, and perhaps complementary to mud-eating, can be neither ascertained nor ruled out.

Single instances of other mayfly nymph taxa (Sinitshenkova *et al.* 2005) (*Triassoephemera punctata* Sinitshenkova & Marchal-Papier, 2005 (Triassoephemeridae), *Triassonurus doliiformis* Sinitshenkova & Marchal-Papier, 2005 (Siphlonuridae) and cf. *Voltziaephemera fossoria* Sinitshenkova & Marchal-Papier, 2005 (Voltziaephemeridae)) have been found in Pedra Alta, but they all lack guts with mud infilling (Matamales-Andreu *et al.* 2021). Thus, a similar detritivorous lifestyle cannot be ruled out for these as well. Although these taxa are also present in the slightly younger lower Middle Triassic Grès à Voltzia locality, according to the published descriptions and the figured specimens, none of these mayfly taxa or others from this last locality has cololite content (Sinitshenkova *et al.* 2005). Differences in the nature of the pool sediments was not likely to be the cause of the absence of gut content in the mayfly nymphs, considering that the insects in Grès à Voltzia have also been found in very fine-grained laminated clay (Briggs & Gall 1990) and are mostly articulated, indicating limited biostratinomic transport, similar to the case of Pedra Alta. Two species from Grès à Voltzia, *Mesoplectopteron longipes* Handlirsch, 1918 and *Vogesonympha ludovici* Sinitshenkova & Papier *in* Sinitshenkova *et al.*, 2005, were recently regarded as passive filter feeders by Sroka & Staniczek (2022), based on their double row of pronounced setae along the prothoracic leg and their dense mouthpart setation. Details enabling the determination of feeding habits with confidence have not been described from other Grès à Voltzia mayfly nymphs, but they probably were detritus collectors or algal feeders, while burrowing forms could filter detritus (Sinitshenkova *et al.* 2005). Sinitshenkova (2000) considered that one of the specimens from Pedra Alta, which had been previously reported and figured by Calafat (1988), was a burrowing form. Later, the same author suggested that this morphotype from Pedra Alta had a filter-feeding habit (Sinitshenkova 2002), as was also presumed for the burrowing taxa of Grès à Voltzia (Sinitshenkova *et al.* 2005). Note that the specimen from the Pedra Alta outcrop discussed by Sinitshenkova (2000, 2002) was tentatively identified by Matamales-Andreu *et al.* (2021) as *Voltziaephemera fossoria*. The current knowledge indicates that the detritivorous nymph morphotype from Pedra Alta studied herein was probably absent in the Grès à Voltzia aquatic palaeoenvironment. Exuviae belonging to this morphotype have not been found in Pedra Alta, which is probably related to their lower preservation potential.

Early detritivory in insects of aquatic environments

There is evidence of Palaeozoic detritivory in groups such as myriapods and arachnids (mites) (e.g. Falcon-Lang *et al.* 2015). Among the Hexapoda, the Collembola and other so-called 'apterygotes' were probably detritivorous since the Devonian (Labandeira 2019). It is highly probable that detritivory also occurred in some Palaeozoic adults or preimaginal stages of winged insects, but the lack of direct evidence as well as the scarcity and poor study of indirect evidence renders this topic highly speculative (Zherikhin 2002). The latter author concluded that the Palaeozoic record is not informative about detritivorous habits among roachoids (stem group of modern Dictyoptera, including Blattodea), and the disparate and diverse Mesozoic groups were most likely to have been opportunistic detritivores more specialized in habitat than diet, but direct evidence or clear indirect evidence of detritivory is lacking. Slater *et al.* (2012) showed several middle Permian cases of terrestrial detritivory through the study of coprolites, some of which they tentatively attributed to myriapods or insects.

There is no evidence of detritivory in Palaeozoic aquatic insects. Even if, at least by the late Permian, insects had already colonized aquatic environments, the diversity of aquatic insects was clearly lower during the Palaeozoic than during the Triassic (Sinitshenkova 2002, 2003). One reason could be that the Palaeozoic fossil record is rich in terrestrial insect adults but very poor in preimaginal stages, either terrestrial or potentially aquatic. Shcherbakov (2008) noted that 'there are no reasons to assume a terrestrial mode of life in the Palaeozoic for larvae of those insect groups that now develop in the water', but this reasoning ignores that substantial ecological differences could have existed between stem and crown groups of a clade. Kukalová-Peck (2009) studied a Carboniferous aquatic nymph of Meganisoptera (carnivorous Odonatoptera). No further Permian nymph of this superorder is currently known, although all of the numerous and diverse 'Protozygoptera', Protanisoptera and stem Panodonata certainly had aquatic or subaquatic preimaginal stages. Few Triassic nymphs with a 'zygopterous' morphology are known in the Middle Triassic (Nel *et al.* 2022). Numerous mayfly nymphs are recorded from the transitional Permian–Triassic deposits of the Tunguska Basin, Siberia (Sinitshenkova 2013), but there are few Permian nymphs attributed to the stem group of Ephemeroptera, viz. *Kukalova americana* Demoulin, 1970 and *Misthodotes sharovi* Tshernova, 1965 (Demoulin 1970; Wootton 1988; Hubbard & Kukalová-Peck 1980; Sroka *et al.* 2021). Nearly nothing is known about the biology of these nymphs but they are supposed to have been herbivorous. Prokop *et al.* (2019) proposed that the nymphs of the Palaeozoic Paleodictyoptera had either aquatic or

amphibious ways of life. But their specialized sucking mouthparts were unlikely to have been adapted for detritivory. The archaeognathan family Dasyleptidae, potentially detritivorous as their extant relatives, could have been aquatic during the Carboniferous, Permian and Triassic, although this is strongly speculative (Sinitshenkova 2002, 2003). Bechly & Stockar (2011, p. 32) suggested 'a way of life at the marine and brackish drift line and possibly also freshwater shores' for these insects. Ponomarenko & Prokin (2015) considered that the Permian record of aquatic beetles is very scarce, much less abundant than the Triassic one. Furthermore, Prokin *et al.* (2019) described *Kargalarva permosialis* Prokin *et al.*, 2019 from the upper Permian and attributed it to the beetle infraorder Schizophoromorpha. These beetles were likely to have been carnivorous. In contrast, the order Diptera, with numerous taxa having aquatic larvae, is hitherto unknown in the Permian but becomes very diverse in the Triassic, with numerous larvae, some of which could have been detritivorous.

CONCLUSION

The feeding habits determined based on detailed analysis of the exceptionally preserved cololites inside the most abundant mayfly nymph form in the lower Middle Triassic (Anisian) of Pedra Alta shed light on the early ecological role of insects in aquatic ecosystems. These mayfly nymphs were detritivores, recycling finely particulate organic matter in the early Mesozoic freshwater trophic net. This record represents the oldest direct evidence of detritivory known in insects. Furthermore, the sum of available evidence indicates that the detritivorous nymph of Pedra Alta was most likely to have been sedimentivorous, ingesting portions of the benthic muddy sediment. This lifestyle is extremely uncommon in insects and had not been hitherto reported in the palaeoentomological record. Sedimentivory apparently never became common in insects throughout their evolutionary history, including for the mayflies. Although the Pedra Alta mayfly nymphs could have been analogues of some extant burrowing species of the genus *Hexagenia*, an excavating habit cannot be determined at present for them. A detailed study of the mouthparts of this form will be crucial to increase the knowledge on their more specific feeding habits, although that will require the finding of additional material with exceptionally well-preserved heads.

The 3D, *in situ* cololite type described in detail herein is very scarce in the fossil record. The present work shows that fossilized gut contents, particularly if present *in situ*, are able to provide key palaeobiological data on palaeoenvironment and/or palaeoecological relationships.

It is unclear whether the end-Permian mass extinction event played a significant role in the constitution of early Triassic aquatic terrestrial ecosystems or whether it entailed an impoverishment of those existing beforehand, and how it affected the mode and tempo of the changes that took place. This uncertainty is caused by the extensive gap that exists in the fossil record of insect aquatic forms before the early Anisian. Thus, our knowledge on how the end-Permian mass extinction event influenced the different levels of the trophic guilds must await the discovery of older outcrops, particularly those of insects preserving their gut contents (Zherikhin 2002). For now, the rich outcrops of Grès à Voltzia (Gall & Grauvogel-Stamm 2005) and now Pedra Alta illuminate some key aspects of the early specializations of insects in aquatic communities, following the end-Permian mass extinction event.

Acknowledgements. Thanks are due to Sebastià Matamalas, Francesc Baiget, Eduardo Barrón, Ana Rodrigo and Enric Pedrón for aid in fieldwork, and to Pedro Agustín Robledo, Ana Sevillano and José María López García, who facilitated the field palaeontological research. Dr Barrón also provided comments about the pollen grains. We also thank the Comissió Insular de Patrimoni Històric of the Consell de Mallorca for granting the excavation permits (file numbers 305/2019 and 52/2021). We acknowledge support from the CERCA program (Generalitat de Catalunya, Spain). RM-A was supported by a pre-doctoral grant FPU17/01922 (Ministerio de Ciencia, Innovación y Universidades, Spain). We acknowledge support from the project 'Mallorca abans dels dinosaures: estudi dels ecosistemes continentals del Permià i Triàsic amb especial èmfasi en les restes de vertebrats' (ref. 15 - 619/2020), based at the Institut Català de Paleontologia Miquel Crusafont and funded by the Departament de Cultura, Patrimoni i Política Lingüística (Consell Insular de Mallorca, Spain). Dr Torsten Wappler and another, anonymous, reviewer are thanked for their useful comments.

Author contributions. **Conceptualization** E Peñalver (EP); **Investigation** EP, R Matamales-Andreu (RM-A), A Nel (AN), RP Lozano (RPL), R Pérez-de la Fuente (RPF); **Methodology** EP, RM-A, J Juárez Ruiz (JJR); **Visualization** EP, RM-A; **Writing – Original Draft Preparation** EP, RPF; **Writing – Review & Editing** EP, RM-A, JJR, AN, RPL, RPF.

Editor. Michael Engel

SUPPORTING INFORMATION

Additional Supporting Information can be found online (https://doi.org/10.1002/spp2.1478):

Figure S1. Preparation methodology of small sections of cololites on microscope slides using instant glue.

Figure S2. SEM images of the sample surfaces of a cololite (from section S1) from a specimen present in slab DA21/03-02-20 (specimen drawn in Fig. 6C), and the rock matrix near that cololite (Sa1 matrix), the elemental components of which were analysed (Figs 6, 8).

Figure S3. Camera lucida drawing of the components in a long portion of cololite from specimen 11 in DA21/14-02-01 (section S4, Figs 2, 7).

REFERENCES

BACHTERAM, A. M., MAZUREK, K. A. and CIBOROWSKI, J. J. H. 2005. Sediment suspension by burrowing mayflies (*Hexagenia* spp., Ephemeroptera: Ephemeridae). *Journal of Great Lakes Research*, **31** (Suppl. 2), 208–222.

BASHKUEV, A., SELL, J., ARISTOV, D., PONOMARENKO, A., SINITSHENKOVA, N. and MAHLER, H. 2012. Insects from the Buntsandstein of Lower Franconia and Thuringia. *Paläontologische Zeitschrift*, **86**, 175–185.

BECHLY, G. and STOCKAR, R. 2011. The first Mesozoic record of the extinct apterygote insect genus *Dasyleptus* (Insecta: Archaeognatha: Monura: Dasyleptidae) from the Triassic of Monte San Giorgio (Switzerland). *Palaeodiversity*, **4**, 23–37.

BENTON, M. J. and WU, F. 2022. Triassic revolution. *Frontiers in Earth Science*, **10** (899541), 1–19.

BRIGGS, D. E. and GALL, J. C. 1990. The continuum in soft-bodied biotas from transitional environments: a quantitative comparison of Triassic and Carboniferous Konservat-Lagerstätten. *Paleobiology*, **16**, 204–218.

BRONGNIART, A. T. 1828. *Prodrome d'une histoire des végétaux fossiles*. Levrault, Paris, 223 pp.

BUTTERFIELD, N. J. 2002*a*. Permineralization vs. compression; disparate modes of exceptional preservation in the Burgess Shale and their palaeobiological significance. 241–246. *In* DE RENZI, M., PARDO, M., BELINCHÓN, M., PEÑALVER, E., MONTOYA, P. and MÁRQUEZ ALIAGA, A. (eds) *Current topics on taphonomy and fossilization*. Ayuntamiento de Valencia.

BUTTERFIELD, N. J. 2002*b*. *Leanchoilia* guts and the interpretation of three-dimensional structures in Burgess Shale-type fossils. *Paleobiology*, **28**, 155–171.

CALAFAT, F. 1988. Estratigrafía y sedimentología de la litofacies Buntsandstein de Mallorca. Bachelor's thesis. Universitat de Barcelona, 127 pp. + 31 annexed figs.

CHAPMAN, R. F. 2013. *The insects: Structure and function*. Cambridge University Press, 959 pp.

CHEN, J., WANG, B., ENGEL, M. S., WAPPLER, T., JARZEMBOWSKI, E. A., ZHANG, H., WANG, X., ZHENG, X. and RUST, J. 2014. Extreme adaptations for aquatic ectoparasitism in a Jurassic fly larva. *eLife*, **3**, e02844.

CUMMINS, K. W. 1973. Trophic relations of aquatic insects. *Annual Review of Entomology*, **18**, 183–206.

DEMOULIN, G. 1970. Remarques critiques sur des larves "éphéméromorphes" du Permien. *Bulletin de l'Institut Royal des Sciences Naturelles de Belgique*, **46** (3), 1–10.

DERMOTT, R. 1981. Ingestion rate of the burrowing mayfly *Hexagenia limbata* as determined with ^{14}C. *Hydrobiologia*, **83**, 499–503.

DIEZ, J. B. 2000. Geología y Paleobotánica de la Facies Buntsandstein en la Rama Aragonesa de la Cordillera Ibérica. Implicaciones paleogeográficas en el Peritethys Occidental. PhD thesis. Universidad de Zaragoza–Université Pierre & Marie Curie, Paris VI, 424 pp.

DIEZ, J. B., BROUTIN, J., GRAUVOGEL-STAMM, L., BOURQUIN, S., BERCOVICI, A. and FERRER, J. 2010. Anisian floras from the NE Iberian Peninsula and Balearic Islands: a synthesis. *Review of Palaeobotany & Palynology*, **162**, 522–542.

EATON, A. E. 1883–1888. A revisional monograph of recent Ephemeridae or mayflies. *Transactions of the Linnean Society of London, Second Series, Zoology*, **3**, 1–352, 65 pl.

ENRIQUE, P. 1986. Nota sobre les roques hipabissals de la Serra de Tramuntana de Mallorca: algunes característiques petrogràfiques i geoquímiques. *Bolletí de la Societat d'Història Natural de les Balears*, **30**, 19–50.

FALCON-LANG, H. J., LABANDEIRA, C. C. and KIRK, R. 2015. Herbivorous and detritivorous arthropod trace fossils associated with subhumid vegetation in the Middle Pennsylvanian of southern Britain. *PALAIOS*, **30**, 192–206.

GALL, J.-C. 1972. Le rôle de la paléoécologie dans la reconstitution des anciens biotopes. Application aux gisements fossilifères du Trias inférieur des Vosges. *Bulletin de la Société d'Ecologie*, **3**, 354–367.

GALL, J.-C. 1983. The Grès à Voltzia delta. 134–148. *In* GALL, J.-C. (ed.) *Ancient sedimentary environments and the habitats of living organisms: Introduction to palaeoecology*. Springer.

GALL, J.-C. 1996. Triassic insects of Western Europe. *Paleontologia Lombarda*, **5**, 3–4.

GALL, J.-C. and GRAUVOGEL-STAMM, L. 2005. The early Middle Triassic 'Grès à Voltzia' Formation of eastern France: a model of environmental refugium. *Comptes Rendus Palevol*, **4**, 637–652.

GRIMALDI, D. 2000. *Studies on fossils in amber, with particular reference to the Cretaceous of New Jersey*. Backhuys, 498 pp.

GUIDOTTI, C. V., POST, J. L. and CHENEY, J. T. 1979. Margarite pseudomorphs after chiastolite in the Georgetown area, California. *American Mineralogist*, **64**, 728–732.

HANDLIRSCH, A. 1918. Fossile Ephemeridenlarven aus dem Buntsandstein der Vogesen. *Verhandlungen der Kaiserlich-Königlichen Zoologisch-botanischen Gesellschaft in Wien*, **68**, 112–114.

HOLTOF, M., LENAERTS, C., CULLEN, D. and VANDEN BROECK, J. 2019. Extracellular nutrient digestion and absorption in the insect gut. *Cell & Tissue Research*, **377**, 397–414.

HOU, X. and BERGSTRÖM, J. 1991. The arthropods of the Lower Cambrian Chengjiang fauna, with relationships and evolutionary significance. 179–187. *In* SIMONETTA, A. M. and CONWAY MORRIS, S. (eds) *The early evolution of Metazoa and the significance of problematic taxa*. Cambridge University Press.

HOU, X. and BERGSTRÖM, J. 1997. Arthropods of the Lower Cambrian Chengjiang fauna, southwest China. *Fossils & Strata*, **45**, 1–116.

HUBBARD, M. D. and KUKALOVÁ-PECK, J. 1980. Permian mayfly nymphs: new taxa and systematic characters. 19–31. *In* FLANNAGAN, J. F. and MARSCHALL, K. E. (eds) *Advances in Ephemeroptera biology* Proceedings of the 3rd International Conference on Ephemeroptera. Plenum.

HUNT, B. P. 1953. The life history and economic importance of a burrowing mayfly, *Hexagenia limbata*, in Southern Michigan lakes. *Bulletin of the Institute for Fisheries Research*, **4**, 1–151.

JUÁREZ RUIZ, J. and WACHTLER, M. 2015. *Early–Middle Triassic (Anisian) fossil flora from Majorca (Spain)*. Dolomythos, Innichen 40 pp.

KNAUST, D. 2020. Invertebrate coprolites and cololites revised. *Papers in Palaeontology*, **6**, 385–423.

KOPYLOV, D. S., RASNITSYN, A. P., ARISTOV, D. S., BASHKUEV, A. S., BAZHENOVA, N. V., DMITRIEV, V. Y., GOROCHOV, A. V., IGNATOV, M. S., IVANOV, V. D., KHRAMOV, A. V., LEGALOV, A. A., LUKASHEVICH, E. D., MAMONTOV, Y. S., MELNITSKY, S. I., OGŁAZA, B., PONOMARENKO, A. G., PROKIN, A. A., RYZHKOVA, O. V., SHMAKOV, A. S., SINITSHENKOVA, N. D., SOLODOVNIKOV, A. Y., STRELNIKOVA, O. D., SUKACHEVA, I. D., ULIAKHIN, A. V., VASILENKO, D. V., WEGIEREK, P., YAN, E. V. and ZMARZŁY, M. 2020. The Khasurty fossil insect Lagerstätte. *Paleontological Journal*, **54**, 1221–1394.

KOZUR, H. W. and WEEMS, R. E. 2010. The biostratigraphic importance of conchostracans in the continental Triassic of the northern hemisphere. *Geological Society, London, Special Publications*, **334**, 315–417.

KRASSILOV, V. A. and RASNITSYN, A. P. 1997. Pollen in the guts of Permian insects: first evidence of pollinivory and its evolutionary significance. *Lethaia*, **29**, 369–372.

KUKALOVÁ-PECK, J. 2009. Carboniferous protodonatoid dragonfly nymphs and the synapomorphies of Odonatoptera and Ephemeroptera (Insecta: Palaeoptera). *Palaeodiversity*, **2**, 169–198.

LABANDEIRA, C. C. 2019. The fossil record of insect mouthparts: innovation, functional convergence, and associations with other organisms. 567–671. *In* KRENN, H. W. (ed.) *Insect mouthparts: Form, function, development and performance*. Springer International.

LEACH, W. E. 1815. Entomology. *Brewster's Edinburgh Encyclopaedia*, **9**, 57–172.

LUKASHEVICH, E. D., PRZHIBORO, A. A., MARCHAL-PAPIER, F. and GRAUVOGEL-STAMM, L. 2010. The oldest occurrence of immature Diptera (Insecta), Middle Triassic, France. *Annales de la Société Entomologique de France (n.s.)*, **46**, 4–22.

MARTÍNEZ-DELCLÒS, X., BRIGGS, D. E. G. and PEÑALVER, E. 2004. Taphonomy of insects in carbonates and amber. *Palaeogeography, Palaeoclimatology, Palaeoecology*, **203**, 19–64.

MATAMALES-ANDREU, R., PEÑALVER, E., MUJAL, E., OMS, O., SCHOLZE, F., JUÁREZ, J., GALOBART, A. and FORTUNY, J. 2021. Early–Middle Triassic fluvial ecosystems of Mallorca (Balearic Islands): biotic communities and environmental evolution in the equatorial western peri-Tethys. *Earth-Science Reviews*, **222**, 103783.

NEL, A., NAM, G.-S. and JOUAULT, C. 2022. First representative of the odonatan superfamily Triassolestoidea (Odonatoptera: Parazygoptera) from the Upper Triassic of the Korean Peninsula. *Alcheringa*, 1–7. https://doi.org/10.1080/03115518.2022.2130426

PEÑALVER, E. 2002. Los insectos dípteros del Mioceno del Este de la Península Ibérica; Rubielos de Mora, Ribesalbes y Bicorp. Tafonomía y sistemática. PhD thesis. Universitat de València, 548 pp.

PEÑALVER, E. and GAUDANT, J. 2010. Limnic food web and salinity of the Upper Miocene Bicorb palaeolake (eastern Spain). *Palaeogeography, Palaeoclimatology, Palaeoecology*, **297**, 683–696.

PEÑALVER, E. and PÉREZ-DE LA FUENTE, R. 2014. Unearthing the secrets of ancient immature insects. *eLife*, **3**, e03443.

PEÑALVER, E., DE RENZI, M., MARTÍNEZ-DELCLÒS, X. and QUEROL, X. 1996. Actividad fosildiagenética de bacterias sulfato-reductoras en dípteros bibiónidos del Mioceno de Rubielos de Mora (Teruel, España). Un caso de fosilización diferencial. *II Reunión de Tafonomía y Fosilización*, Zaragoza, 299–303.

PEÑALVER, E., ARILLO, A., PÉREZ-DE LA FUENTE, R., RICCIO, M. L., DELCLÒS, X., BARRÓN, E. and GRIMALDI, D. A. 2015. Long-proboscid flies as pollinators of Cretaceous gymnosperms. *Current Biology*, **25**, 1917–1923.

PEÑALVER, E., BARRÓN, E., POSTIGO-MIJARRA, J. M., GARCÍA VIVES, J. A. and SAURA VILAR, M. 2016. *El paleolago de Ribesalbes. Un ecosistema de hace 19 millones de años*. Diputación de Castellón & IGME, 201 pp.

PEÑALVER, E., MATAMALES-ANDREU, R., NEL, A. and PÉREZ-DE LA FUENTE, R. 2022. Early adaptations of true flies (Diptera) to moist and aquatic continental environments. *Papers in Palaeontology*, **8**, e1472.

PÉREZ-DE LA FUENTE, R., DELCLÒS, X., PEÑALVER, E., SPERANZA, M., WIERZCHOS, J., ASCASO, C. and ENGEL, M. S. 2012. Early evolution and ecology of camouflage in insects. *Proceedings of the National Academy of Sciences*, **190**, 21414–21419.

PONOMARENKO, A. G. and PROKIN, A. A. 2015. Review of paleontological data on the evolution of aquatic beetles (Coleoptera). *Paleontological Journal*, **49**, 1383–1412.

PROKIN, A. A., PONOMARENKO, A. G. and KIREJTSHUK, A. G. 2019. Description of a larva of *Kargalarva permosialis* gen. et sp. nov. (Coleoptera: Schizophoromorpha) from the Kargala fossil site. *Paleontological Journal*, **53**, 282–286.

PROKOP, J., KRZEMIŃSKA, E., KRZEMIŃSKI, W., ROSOVÁ, K., PECHAROVÁ, M., NEL, A. and ENGEL, M. S. 2019. Ecomorphological diversification of the Late Palaeozoic Palaeodictyopterida reveals different larval strategies and amphibious lifestyle in adults. *Royal Society Open Science*, **6** (190460), 1–10.

RICHTER, G. and BASZIO, S. 2001. First proof of planctivory/insectivory in a fossil fish: *Thaumaturus intermedius*

from the Eocene Lake Messel (FRG). *Palaeogeography, Palaeoclimatology, Palaeoecology*, **173**, 75–85.

ROBIN, N., GUERIAU, P., LUQUE, J., JARVIS, D., DALEY, A. C. and VONK, R. 2021. The oldest peracarid crustacean reveals a Late Devonian freshwater colonization by isopod relatives. *Biology Letters*, **17**, 20210226.

SÁNCHEZ-GARCÍA, A., PEÑALVER, E., DELCLÒS, X. and ENGEL, M. S. 2021. Terrestrial isopods from Spanish amber (Crustacea: Oniscidea): insights into the Cretaceous soil biota. *American Museum Novitates*, **3974**, 1–32.

SANZ, T., LAGO, M., GALÉ, C., UBIDE, T., POCOVÍ, A. and GIL, A. 2013. Las rocas magmáticas de la Sierra de Tramuntana (N de Mallorca, España): contexto estratigráfico. *Geogaceta*, **54**, 39–42.

SARTORI, M. and BRITTAIN, J. E. 2015. Order Ephemeroptera. 873–891. *In* THORP, J. and ROGERS, D. C. (eds) *Ecology and general biology: Thorp and Covich's freshwater invertebrates*. Academic Press.

SCHOLZE, F. and MATAMALES-ANDREU, R. 2021. Triassic clam shrimps ("Conchostraca"; Branchiopoda: Diplostraca) from Mallorca: taxonomic description and interregional comparisons. *Zootaxa*, **4964**, 471–496.

SEILACHER, A. 2002. Non olet: the strange taphonomy of coprolites and cololites. 233–240. *In* DE RENZI, M., PARDO, M., BELINCHÓN, M., PEÑALVER, E., MONTOYA, P. and MÁRQUEZ ALIAGA, A. (eds) *Current topics on taphonomy and fossilization*. Ayuntamiento de Valencia.

SERVILLE, J. G. 1829. Descripción of *Ephemera limbata*. 2 pp. *In* GUÉRIN-MÉNEVILLE, F. E. and CUVIER, G. (eds) *Iconographie du Règne animal de G. Cuvier*. J. B. Baillière, Paris.

SHCHERBAKOV, D. E. 2008. On Permian and Triassic insect faunas in relation to biogeography and the Permian–Triassic crisis. *Paleontological Journal*, **42**, 15–31.

SINITSHENKOVA, N. D. 2000. A review of Triassic mayflies, with the description of new species from Western Siberia and Ukraine (Ephemerida = Ephemeroptera). *Paleontological Journal*, **34**, S275–S283.

SINITSHENKOVA, N. D. 2002. 3.3. Ecological history of the aquatic insects. 388–426. *In* RASNITSYN, A. P. and QUICKE, D. L. J. (eds) *History of insects*. Kluwer.

SINITSHENKOVA, N. D. 2003. Main ecological events in aquatic insects history. *Acta Zoologica Cracoviensia*, **46**, 381–392.

SINITSHENKOVA, N. D. 2013. New mayflies (Insecta: Ephemerida = Ephemeroptera) from the intertrappean deposits of the Tunguska basin, Siberia. *Paleontological Journal*, **47**, 84–88.

SINITSHENKOVA, N. D., MARCHAL-PAPIER, F., GRAUVOGEL-STAMM, L. and GALL, J.-C. 2005. The Ephemeridea (Insecta) from the Grès à Voltzia (early Middle Triassic) of the Vosges (NE France). *Paläontologische Zeitschrift*, **79**, 377–397.

SINITSHENKOVA, N. D., ARISTOV, D. S., WEGIEREK, P. and ŻYŁA, G. 2015. New mayfly genera from the Middle Triassic of Poland and their evolutionary and paleogeographic implications (Ephemerida: Litophlebiidae, Vogesonymphidae). *Zootaxa*, **3949**, 281–288.

SLATER, B. J., McLOUGHLIN, S. and HILTON, J. 2012. Animal–plant interactions in a Middle Permian permineralised peat of the Bainmedart Coal Measures, Prince Charles Mountains, Antarctica. *Palaeogeography, Palaeoclimatology, Palaeoecology*, **363–364**, 109–126.

SROKA, P. and STANICZEK, A. H. 2022. Evolution of filter-feeding in aquatic insects dates back to the Middle Triassic: new evidence from stem-group mayflies (Insecta, Ephemerida) from Grès à Voltzia, Vosges, France. *Papers in Palaeontology*, **8** (4), e1456.

SROKA, P., GODUNKO, R. J., SINITSHENKOVA, N. D. and PROKOP, J. 2021. Life history, systematics and flight ability of the Early Permian stem-mayflies in the genus *Misthodotes* Sellards, 1909 (Insecta, Ephemerida, Permoplectoptera). *BMC Ecology & Evolution*, **21** (97), 1–18.

TSHERNOVA, O. A. 1965. Some fossil mayflies (Ephemeroptera, Misthodotidae) from Permian-beds of the Ural. *Revue d'Entomologie de l'URSS*, **44**, 353–361.

VANNIER, J. and CHEN, J.-Y. 2002. Digestive system and feeding mode in Cambrian naraoiid arthropods. *Lethaia*, **35**, 107–120.

VANNIER, J., LIU, J., LEROSEY-AUBRIL, R., VINTHER, J. and DALEY, A. C. 2014. Sophisticated digestive systems in early arthropods. *Nature Communications*, **5**, 3641.

VOLTZ, L. 1837. Notice sur le grès bigarré de la Carrière de Soultz-les-Bains. *Société des Amis du Musée d'histoire naturelle Strasbourg*, **2**, 9–14.

WALKER, W. H. 1970. A study of the ecology and distribution of burrowing mayfly nymphs (Ephemeroptera: *Hexagenia munda* Eaton) in Stone Mountain Lake. PhD thesis. Emory University, Atlanta.

WEDMANN, S., HÖRNSCHEMEYER, T. H., ENGEL, M. S., ZETTER, R. and GRÍMSSON, F. 2021. The last meal of an Eocene pollen-feeding fly. *Current Biology*, **31**, 2020–2026.

WHITTINGTON, H. B. 1978. The lobopod animal *Aysheaia pedunculata* Walcott, Middle Cambrian, Burgess Shale, British Columbia. *Philosophical Transactions of the Royal Society B*, **284**, 165–197.

WOOTTON, R. J. 1988. The historical ecology of aquatic insects: an overview. *Palaeogeography, Palaeoclimatology, Palaeoecology*, **62**, 477–492.

ZHAO, X., ZHENG, D., XIE, G., JENKYNS, H. C., GUAN, C. H., FANG, Y., HE, J., YUAN, X., XUE, N., WANG, H., LI, S., JARZEMBOWSKI, E. A., ZHANG, H. and WANG, B. 2020. Recovery of lacustrine ecosystems after the end-Permian mass extinction. *Geology*, **48**, 609–613.

ZHERIKHIN, V. V. 2002. 3.2. Ecological history of terrestrial insects. 331–388. *In* RASNITSYN, A. P. and QUICKE, D. L. J. (eds) *History of insects*. Kluwer.

ZIMMERMAN, M. C. and WISSING, T. E. 1980. Nutritional dynamics of the burrowing mayfly, *Hexagenia limbata*. 231–257. *In* FLANNAGAN, J. F. and MARSHALL, K. E. (eds) *Advances in Ephemeroptera biology*. Plenum Press.

SUPPORTING INFORMATION

Early detritivory and sedimentivory in insects based on in-situ gut contents from Triassic aquatic nymphs

by Enrique Peñalver, Rafel Matamales-Andreu, Josep Juárez Ruiz, André Nel, Rafael Pablo Lozano *and* Ricardo Pérez-De La Fuente

Figures S1–S3

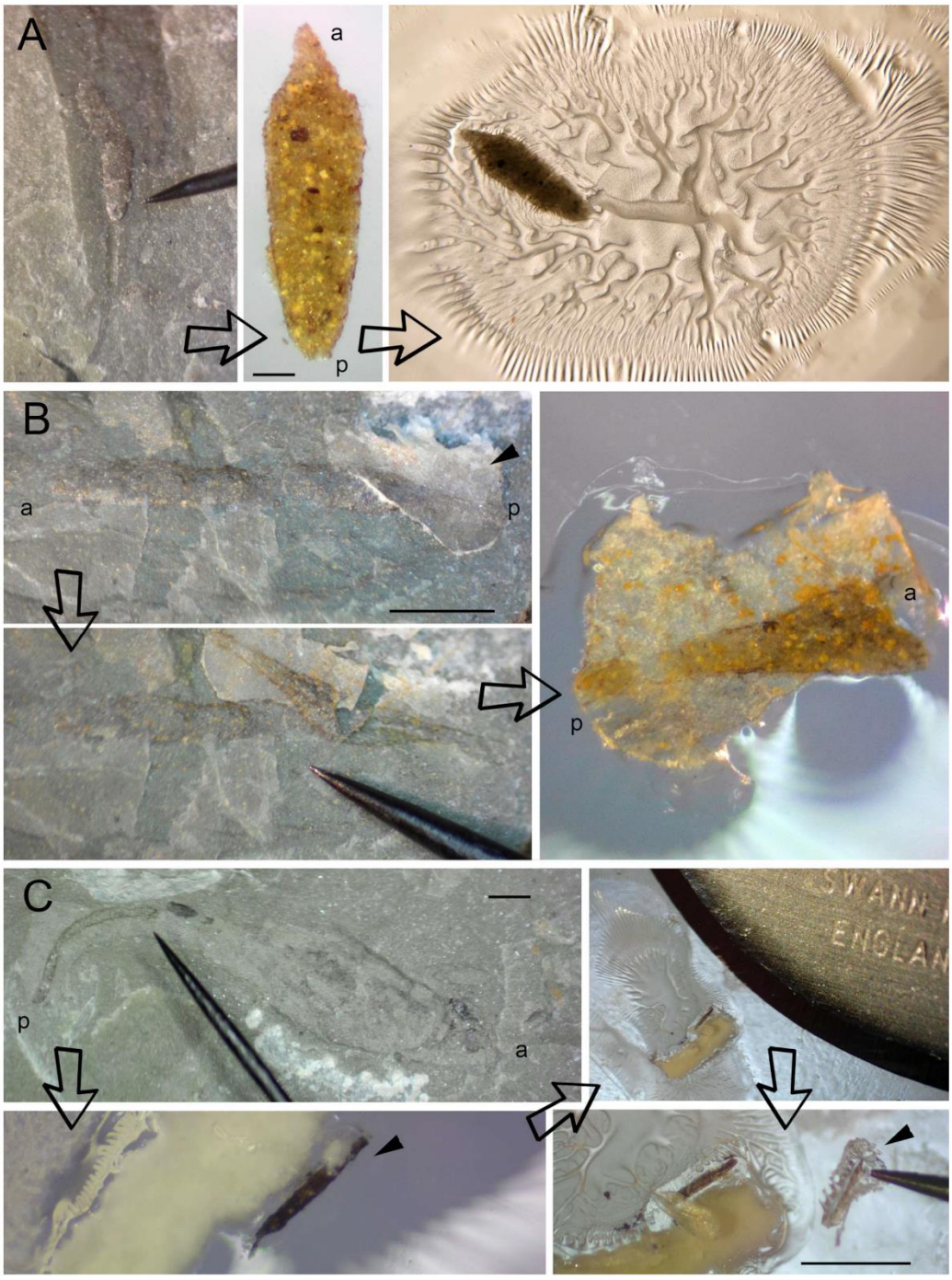

FIG. S1. Preparation methodology of small sections of cololites on microscope slides using instant glue. A, cololite section (S6) detached and obtained using a pin from specimen 2´ at the counterpart of the slab DA21/14-02-01; the external surface of the section prepared horizontally on a microscope slide can be photographed for some minutes before the glue fully hardens –middle photograph– and then can

be thinned using a scalpel. B, cololite section (S2) covered by a mineral plate (arrowhead) detached and obtained using a pin; from specimen DA21/03/02/20 (Fig. 7D shows this sample after thinning using a scalpel). C, extraction of transversal samples for SEM using a scalpel from section (S5) prepared vertically (left arrowhead) on a microscope slide (the transversal section sample is recovered with a pin –right arrowhead– and corresponds to Fig. 5A); the pin in left image indicates the position of the cololite section, possibly of the midgut, that was removed (compare to Fig. 4E) from specimen 9′ in the counterpart of the slab DA21/14-02-01. Abbreviations: a= anterior end, p = posterior end. Scale bars represent: 0.2 mm (A); 1 mm (B, C).

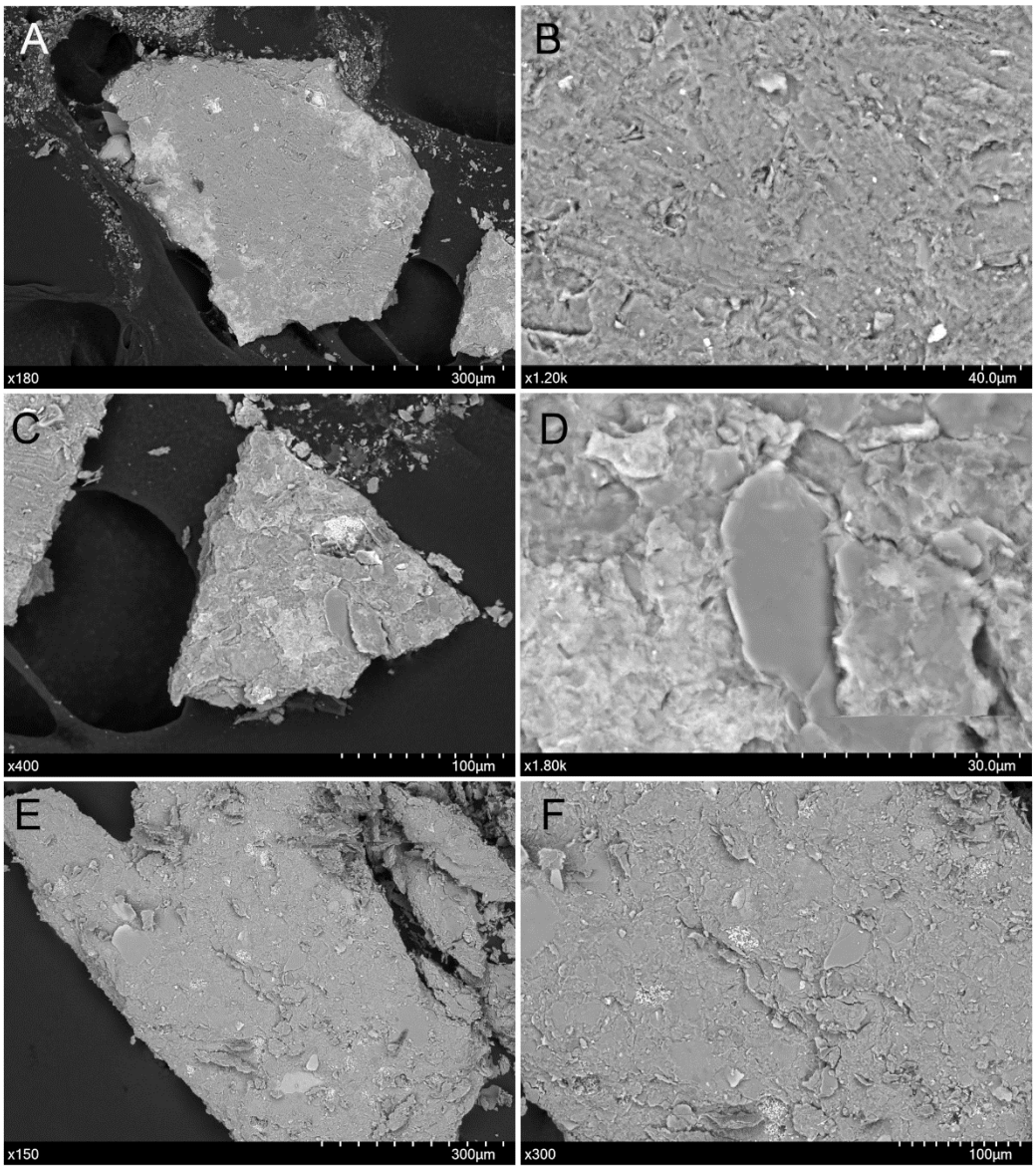

FIG. S2. SEM images of the sample surfaces of a cololite (from section S1) from a specimen present in DA21/03-02-20 slab (specimen drawn in Fig. 6C), and the rock matrix nearby that cololite (Sa1 matrix), the elemental components of which were analysed (see Figs 6, 8). A–B, core of a fragment of the cololite section, surface exposed after cutting using a surgical scalpel, and detail. C–D, external surface of another fragment from the same cololite section, and detail showing squamous breaking parallel to the slab plane. E–F, fresh surface of a flake of the rock matrix (Sa1 matrix) one millimetre distant from the cololite section, and detail.

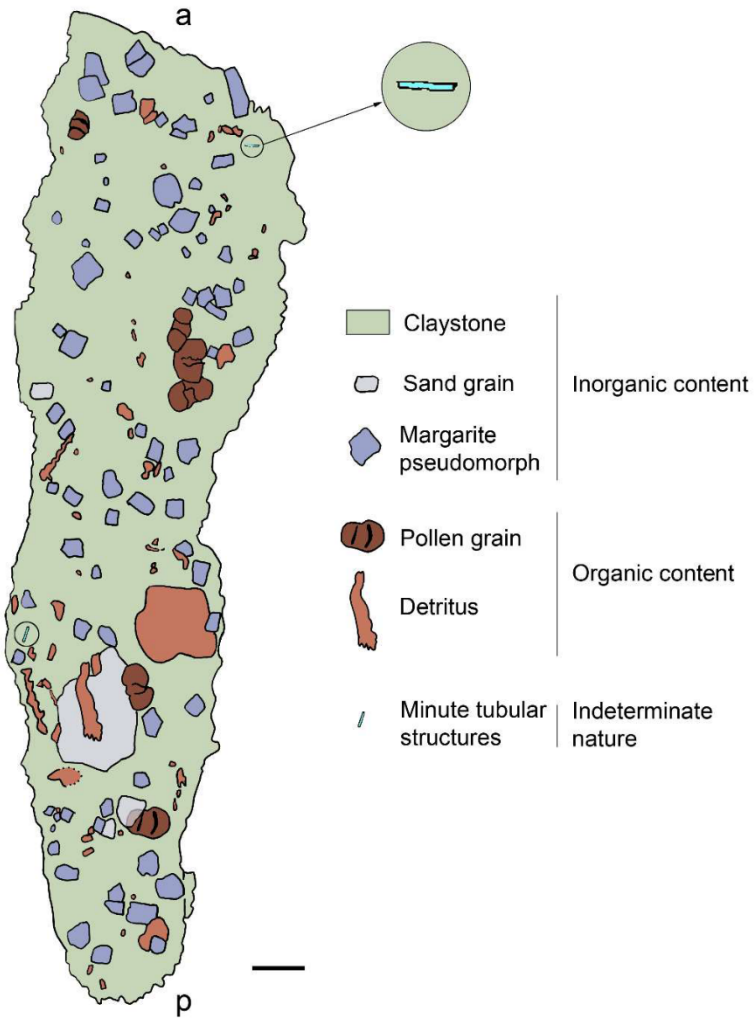

FIG. S3. Camera lucida drawing of the components in a long portion of cololite from specimen 11 in DA21/14-02-01 (section S4, see Figs 2, 7). Bisaccate pollen grains belong to cf. *Alisporites* sp. and/or cf. *Lunatisporites* sp. Detritus are constituted by detrital particles and small aggregates. Small tubular structures apparently are not abundant, only the two most apparent have been drawn (encircled). Note the comparatively large sand grain near the posterior extreme of this cololite section. Abbreviations: a = anterior end, p = posterior end. Scale bar represents 0.1 mm.

Appendix 10

Triassic true flies from Mallorca

Appendix 10 was published as:

Peñalver, E.; **Matamales-Andreu, R.**; Nel, A. & Pérez-de la Fuente, R. (2022). Early adaptations of true flies (Diptera) to moist and aquatic continental environments. *Papers in Palaeontology*, 8(6): e1472.

DOI: https://doi.org/10.1002/spp2.1472

In this work, R. Matamales-Andreu contributed in:

A. Logging of the stratigraphic section.
B. Co-direction of all fieldwork campaigns (prospections and excavations).
C. Stratigraphic and sedimentological analysis and interpretation.
D. Writing of the Geographical and Geological Context section of the original draft.
E. Review and editing of the manuscript.
F. Collaboration in the preparation of figures 1 and 6.
G. Collaboration in obtaining funding for fieldwork.

[Papers in Palaeontology, 2022, e1472]

Early adaptations of true flies (Diptera) to moist and aquatic continental environments

by ENRIQUE PEÑALVER[1,*], RAFEL MATAMALES-ANDREU[2,3], ANDRÉ NEL[4] *and* RICARDO PÉREZ-DE LA FUENTE[5]

[1]Instituto Geológico y Minero de España (IGME), CSIC, C/Cirilo Amorós 42, 46004, València, Comunitat Valenciana, Spain; e.penalver@igme.es
[2]Museu Balear de Ciències Naturals, FJBS-MBCN, ctra. Palma-Port de Sóller km 30, 07100, Sóller, Mallorca, Illes Balears, Spain
[3]Institut Català de Paleontologia Miquel Crusafont, Universitat Autònoma de Barcelona, Edifici ICTA-ICP, c/Columnes s/n, Campus de la UAB, 08193, Cerdanyola del Vallès, Barcelona, Spain; rafel.matamales@icp.cat
[4]Institut de Systématique, Évolution, Biodiversité (ISYEB) Muséum national d'Histoire naturelle, CNRS, Sorbonne Université, EPHE, Université des Antilles, CP50, 57 rue Cuvier, 75005, Paris, France; andre.nel@mnhn.fr
[5]Oxford University Museum of Natural History, Parks Road, Oxford, OX1 3PW, UK; ricardo.perez-de-lafuente@oum.ox.ac.uk
*Corresponding author

Typescript received 26 April 2022; accepted in revised form 4 August 2022

Abstract: Insect colonization of continental aquatic ecosystems and their immediate surroundings was paramount for the establishment of complex trophic nets and organic-matter recycling in those environments. True flies and other insects such as mayflies developed crucial ecological roles in early continental aquatic ecosystems, as early as the Triassic. However, the mode and tempo of these processes remain poorly known, partly due to a critical fossil record gap before the Middle Triassic. Here we study the dipterans from the early Middle Triassic Konservat-Lagerstätte of Pedra Alta (Aegean, early Anisian, Spain), which yields the oldest records of the order. *Protoanisolarva juarezi* gen. et sp. nov., based on an exceptionally preserved larva, shares key features with the extant nematoceran family Anisopodidae. Developing in inferred moist terrestrial environments contiguous with pools inhabited by aquatic organisms, it represents the only known Triassic dipteran larva with terrestrial affinities indicating that the amphipneustic respiratory system of insect larvae extends back to *c.* 247 Ma. Two nematoceran aquatic pupae are also described: one classified as *Voltziapupa* cf. *cornuta*, and the other as an indeterminate taxon. Finally, an egg cluster belonging to the ootaxon *Clavapartus latus* is likely to have been produced by chironomids. These eggs were included in a mucilaginous matrix, a probable adaptation against predation and/or changing conditions, including desiccation. These new findings provide key data on the early evolutionary history of the mega-diverse order Diptera, the ecology of their ancestral pre-adult forms, and the functioning of early Middle Triassic continental aquatic ecosystems.

Key words: insect evolution, palaeoecology, taphonomy, egg-laying, Diptera, Mesozoic.

STUDIES on insect diversity are traditionally biased towards adult forms (Smith 1989). However, fossils representing larval, nymphal or pupal stages are not rare in compression deposit assemblages. These fossils of pre-adult stages have an aquatic origin and were produced under a set of circumstances often conducive to an abundant record of aquatic insects with exceptional preservation, mostly body remains or products of activity or life cycle such as exuviae (e.g. Gall 1972; Peñalver 2002; Martínez-Delclòs *et al.* 2004). Aside from a few exceptional cases (e.g. Fleck *et al.* 2002; Wang *et al.* 2015), recognizing conspecific pre-adult and adult forms in the fossil record is challenging, if not virtually impossible, and will always remain conjectural to a certain extent, even if the two forms from a given taxonomic group are recorded in the same deposit. In addition, formal taxonomic description of pre-adult stages of insects is generally desirable due to the key palaeoecological and/or phylogenetic data that it can provide (e.g. Lukashevich *et al.* 2010; Chen *et al.* 2014). This is particularly true in insect groups, in which adults play a limited role in trophic nets, and might not even feed at all. However, the study of larval stages is one of the most overlooked topics in palaeoentomology (Peñalver & Pérez-de la Fuente 2014). Knowledge on these pre-adult stages is crucial, for example, to reconstruct the organic matter recycling in continental aquatic ecosystems and surrounding areas (e.g. Sinitshenkova 2003; Peñalver *et al.* in press) and the structure of trophic nets (e.g. Peñalver & Gaudant 2010). The study of fossil pre-adult forms is especially useful for phylogenetic analysis in some groups (Lukashevich 2008).

Triassic dipterans, both pre-adults and adults, are of particular interest in palaeoentomology because they are the oldest representatives of one of the four megadiverse insect

© 2022 The Authors.
doi: 10.1002/spp2.1472

Papers in Palaeontology published by John Wiley & Sons Ltd on behalf of The Palaeontological Association.
This is an open access article under the terms of the Creative Commons Attribution-NonCommercial-NoDerivs License, which permits use and distribution in any medium, provided the original work is properly cited, the use is non-commercial and no modifications or adaptations are made.

orders; in fact, arguably the most ecologically disparate insect order (Grimaldi & Engel 2005). Nevertheless, dipterans are not abundant in the few Triassic outcrops yielding insects that have been discovered to date. The Konservat-Lagerstätte of 'Grès à Voltzia' from the Vosges (France) provided a first view of the earliest insect groups to inhabit continental aquatic ecosystems, including the oldest dipterans hitherto known. A detailed study of these specimens enabled the first comprehensive view of early Triassic Diptera as pre-adult stages (Lukashevich *et al.* 2010). Although aquatic dipteran pupae were found abundantly and well preserved in this locality, larvae were scarce and did not provide sound morphological characters to enable a reliable placement at familial level, or even at infraordinal level, and were considered as Culicomorpha indet. (Chironomoidea *incertae familae*) (Lukashevich *et al.* 2010). This circumstance prevented critical palaeoecological inferences based on the pre-adult forms of dipterans from Grès à Voltzia. Several adult dipteran taxa were also described from this locality (Krzemiński *et al.* 1994; Krzemiński & Krzemińska 2003). Moreover, a new species assigned to the Mesozoic dipteran family Nadipteridae was recently described based on an isolated wing from the Röt Formation of Lower Franconia (Germany), roughly coetaneous to Grès à Voltzia (Bashkuev *et al.* 2012; Lukashevich 2021). Triassic Diptera have also been found elsewhere, such as in Great Britain or Argentina (Krzemiński & Krzemińska 2002; Lara & Lukashevich 2013).

Outside of the Central European Basin, some authors (Calafat 1988; Shcherbakov *et al.* 1995) noted the possible presence of an adult dipteran specimen from the Pedra Alta locality (Cala d'Estellencs, Mallorca, Balearic Islands, Spain), Anisian in age. That specimen is in a historical private collection (Tomeu Sáez collection in Binissalem, Mallorca) and was obtained during the early 1980s, before the establishment of laws regulating the fossil collection in Spain. However, a recently published review (Matamales-Andreu *et al.* 2021) identified it as a badly preserved mayfly with strongly folded wings. A small dipteran wing portion from Cala d'Estellencs, currently kept in a private collection in Germany, was figured by Zessin (2008). This specimen was collected under irregular circumstances together with other insect remains in 2007 and has not been assessed for the present work.

Based on material extracted during legal palaeontological excavations in 2019 and 2021, we herein describe terrestrial and aquatic pre-adult forms of dipterans from Pedra Alta: a larva and two pupae, respectively, as well as an egg cluster. These dipteran fossils represent the oldest known records for the entire order, and provide key insights into the early evolution of Diptera and the ecology of early Middle Triassic ecosystems.

GEOGRAPHICAL AND GEOLOGICAL CONTEXT

Mallorca is the largest of the Balearic Islands (Fig. 1), an archipelago located in the western Mediterranean that was uplifted during the Alpine Orogeny. It is essentially structured in several horsts and grabens of broad southwest–northeast orientation. The horsts correspond to the main three mountain ranges of the islands, with rocks that are Carboniferous to Middle Miocene in age, and the grabens are the main Cenozoic basins, with rocks and sediments that range from the Upper Miocene to the Holocene. Triassic outcrops of continental origin are scarce and limited to some cliffs in the northwest margin of the Serra de Tramuntana, between Cala d'Estellencs and Punta de son Serralta (Estellencs municipality). Matamales-Andreu *et al.* (2021) recently described four lithostratigraphic formations that encompass this succession (from stratigraphically lower to upper): Punta Roja Formation, Estellencs Formation, Pedra Alta Formation and Son Serralta Formation. These were dated as ranging from the upper Olenekian to the lower Anisian (Matamales-Andreu *et al.* 2021; Scholze & Matamales-Andreu 2021).

The dipteran fossils herein studied were collected from several horizons in the Pedra Alta site (Fig. 1; see Matamales-Andreu *et al.* 2021; Scholze & Matamales-Andreu 2021, for further details). This site has been correlated to the upper part of the Estellencs Formation (Fig. 1A). The fossils have been found in green siltstone beds (sometimes slightly sandy) with sub-horizontal lamination. These have been interpreted as deposits formed in environments of low-energy to still waters, corresponding to backswamps and pools among sand bars of abandoned channels of the braided river system during the low-water phase (Matamales-Andreu *et al.* 2021).

The fossiliferous beds of the Estellencs Formation of Mallorca are slightly older than the Grès à Voltzia

FIG. 1. The Pedra Alta site and section, lower Anisian. A, simplified geological map of the west end of the island of Mallorca (Balearic Islands), with the position of the study area and Pedra Alta site, and simplified stratigraphic log of the Pedra Alta section (simplified from Matamales-Andreu *et al.* 2021); red arrow indicates the level at which the fossil dipterans were found, and colours in the stratigraphic log indicate variable rock colouration. B, panoramic view of the outcrop of Pedra Alta (arrow indicates a member of excavation team). C, detail of fossiliferous levels with indication of a normal fault and the 7.20 m level at which the anisopodoid larva was found. D–E, detail of level of green claystones with sub-horizontal lamination, and aspect of fossiliferous slabs of green claystones after weathering, respectively.

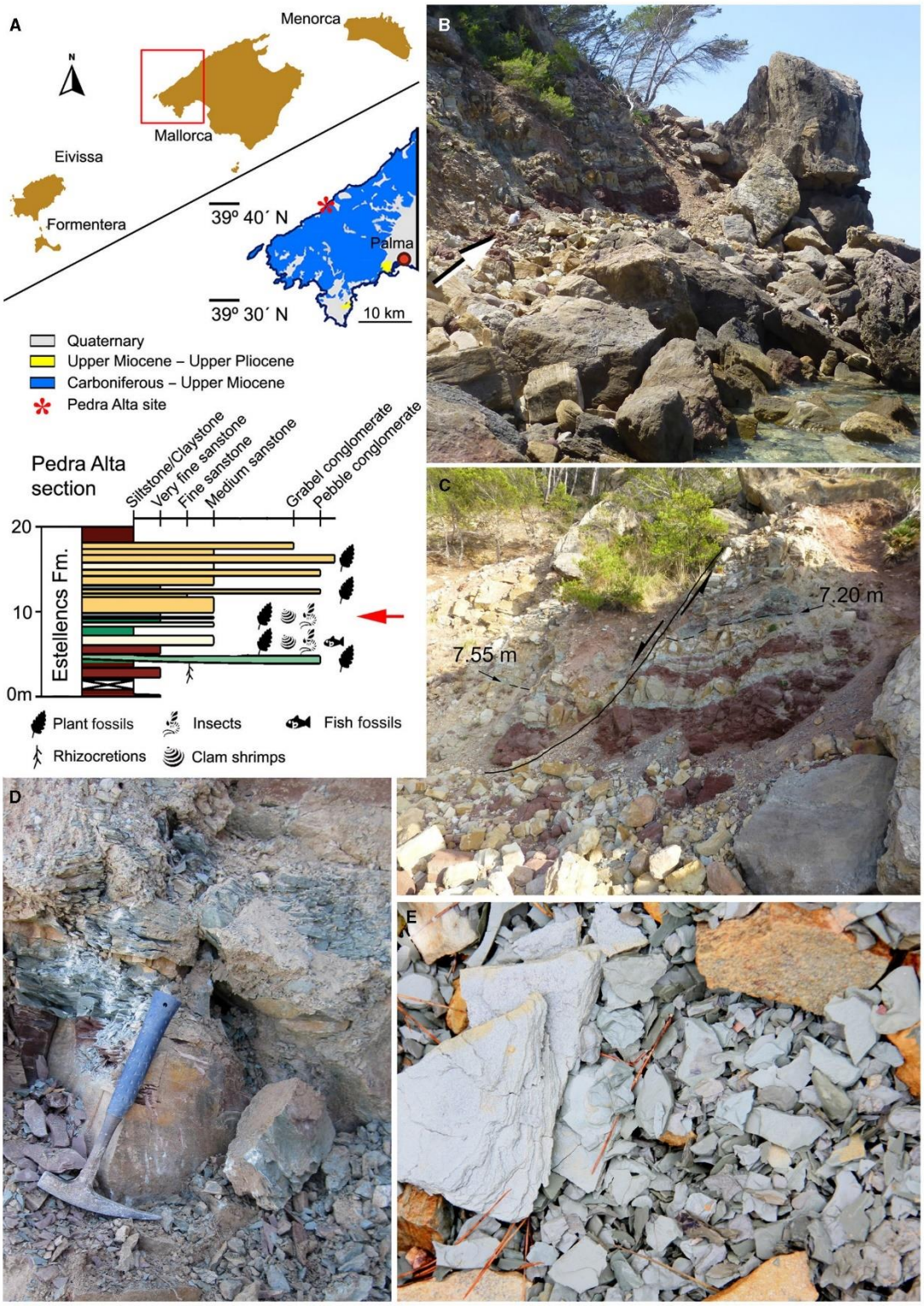
A
Menorca
N
Mallorca
Eivissa
Formentera
39º 40´ N
Palma
39º 30´ N
10 km
Quaternary
Upper Miocene – Upper Pliocene
Carboniferous – Upper Miocene
Pedra Alta site
Pedra Alta section
Siltstone/Claystone
Very fine sanstone
Fine sanstone
Medium sanstone
Grabel conglomerate
Pebble conglomerate
20
10
0m
Estellencs Fm.
Plant fossils
Insects
Fish fossils
Rhizocretions
Clam shrimps
B
C
7.20 m
7.55 m
D
E

deposits (Vosges), which are well known for their rich record of Anisian fossil insects. The age of the Estellencs Formation is essentially constrained by the biostratigraphic data obtained from sporomorphs and clam shrimps. The sporomorphs were studied by Diez *et al.* (2010), who revised some samples collected at the base of the overlying Pedra de s'Ase Formation (Diez 2000; Matamales-Andreu *et al.* 2021) and considered them Aegean in age. The clam shrimps were studied by Scholze & Matamales-Andreu (2021), who identified the species *Hornestheria* aff. *sollingensis* from the same beds as the insects, suggesting an uppermost Olenekian to lowermost Anisian age (Sollingensis Zone) for those beds. In contrast, the age of Grès à Voltzia is more challenging to determine. It is widely accepted that it represents a diachronic facies, younger towards the west, and it has been broadly considered 'lower Anisian' (Durand & Jurain 1969; Gall 1971; Bourquin *et al.* 2006). The most precise age attribution was provided by Kozur & Weems (2010), who considered that the Grès à Voltzia in the Vosges Mountains could be dated as lower Bithynian because of the presence of the clam shrimp *Euestheria albertii albertii* (Albertii albertii Zone). Given that this species appears in the same localities as the insects (cf. Gall 1971; Sinitshenkova *et al.* 2005; Lukashevich *et al.* 2010), the insects can also be considered lower Bithynian in age. All of the above indicates that the specimens from Mallorca are slightly older than those from the Vosges, up to *c.* 1.9 Ma, based on the absolute age attributions for the boundaries of these substages given by Ogg *et al.* (2020). The Röt Formation of Lower Franconia, from which a nadipterid species has been recently described (Bashkuev *et al.* 2012; Lukashevich 2021), is correlated with Grès à Voltzia following the presence of the bivalve *Myophoria vulgaris*, and thus it is also dated as Bithynian (Kozur & Weems 2010; Bashkuev *et al.* 2012).

MATERIAL AND METHOD

The specimens studied herein were found during two palaeontological excavations (further details in Matamales-Andreu *et al.* 2021) and are housed at the Museu de Mallorca (Palma, Mallorca, Balearic Islands, Spain), with an abbreviation in the form: DA21/[campaign number]-[horizon number]-[specimen number].

All of the specimens were moistened with a mixture of alcohol and water for examination, photography and drawing, to enhance the contrast between the carbonaceous parts and the light-coloured rock matrix and thus facilitate the observation of their minute morphological details. It is important to note that moistening caused damage to some of the tiny carbonaceous structures such as the spiracles in the larval specimen, which underwent fracturing and shrinkage, and therefore its use was strongly limited. After examination, the head and spiracles of the part of the larval specimen were consolidated using PRIMAL™ SF-016 ER Acrylic Emulsion Polymer. Photographs (habitus) were taken with the digital camera Canon EOS 650D using Macrofotografía version 1.1.0.5 (IGME-CSIC, Madrid); the software created composite images by integrating photographs obtained at sequential focal planes. Microphotographs of anatomical details were taken with a ColorView IIIu Soft Imaging System digital camera attached to an Olympus BX51 microscope (IGME-CSIC, Madrid). An Olympus BX53 compound microscope equipped with a camera lucida tube was used to create the drawings (IGME-CSIC, Valencia). Photography was enhanced in Photoshop CS2 v9.0 to increase contrast; composite figures were prepared using the same software.

The literature followed for the general description of the larval specimen was Fuller (1935), Keilin & Tate (1940), Peterson (1981), Smith (1989) and Hancock & Amorim (2009). We follow the divisions of the superfamily Anisopodoidea by Krzemiński & Krzemińska (2003) and the conservative approach for the family Anisopodidae by Amorim *et al.* (2016). Description of the pupae follows Lukashevich *et al.* (2010), and that of the egg clusters follows Gall & Grauvogel (1966).

Institutional abbreviation. IGME-CSIC, Instituto Geológico y Minero de España-Consejo Superior de Investigaciones Científicas, Madrid and Valencia, Spain.

SYSTEMATIC PALAEONTOLOGY

by Enrique Peñalver, André Nel & Ricardo Pérez-de la Fuente

Order DIPTERA Linnaeus, 1758
Suborder NEMATOCERA Schiner, 1862
Infraorder BIBIONOMORPHA Hennig, 1948
Superfamily ANISOPODOIDEA Knab, 1912
Stem-group ANISOPODIDAE Knab, 1912

Genus PROTOANISOLARVA nov.

LSID. https://zoobank.org/NomenclaturalActs/69BBB680-8083-46F8-9AFA-AC2D8CD2269F

Derivation of name. Protoanisolarva refers to the oldest known larval stage of anisopodoid flies, using the prefix 'proto', meaning 'first' or 'foremost'. Gender: feminine.

Type species. Protoanisolarva juarezi sp. nov. by monotypy.

Diagnosis. Larva. Body glabrous, lacking conspicuous processes. Abdomen 8-segmented, with anterior intercalary segments; segment VIII the widest, longer than the two previous combined.

Anterior spiracles circular in shape, with a curved row of about six primary openings, circular or subcircular in shape. Segment VIII barely divided, its perianal shield covering the complete ventral surface. Posterior spiracles terminal, subcircular to circular in shape, with over 30 primary circular openings, arranged around the entire perimeter of an inner, heavily sclerotized disc. Posterior spiracles present on a short and broad cuticular process, in a distal position on that process.

Protoanisolarva juarezi sp. nov.
Figures 2, 3, S1

LSID. https://zoobank.org/NomenclaturalActs/7F029393-98E2-422D-A473-9C721C7B6B05

Derivation of name. The specific epithet honours Mr Josep Juárez, from Mallorca, an expert on Mallorcan palaeontology and finder of the holotype specimen.

Holotype. Virtually complete, exceptionally preserved larva as part (preserving the ventral side of the head) and counterpart (preserving the dorsal side of the head), DA21/03-02-91a,b, in small slabs of claystone (part 5.0 × 3.8 cm, counterpart 4.1 × 3.8 cm). The fossil larva in the part was accidentally damaged in the margin of the last abdominal segments in an attempt to prepare the specimen (the same area is not preserved in the counterpart due to imperfect rock exfoliation). The virtually complete posterior spiracle was also damaged as a result of the alcohol–water wetting cycles applied during observation and photography. The holotype, in two slabs, is housed at the Museu de Mallorca (Palma, Mallorca, Balearic Islands, Spain).

Diagnosis. As for the genus, with the following additional character: abdominal segments broader than long.

Type locality. Pedra Alta site, Cala d'Estellencs, Mallorca, Balearic Islands, Spain; Pedra Alta section (7.20 m), upper part of Estellencs Formation (Fig. 1A), Aegean (lower Anisian).

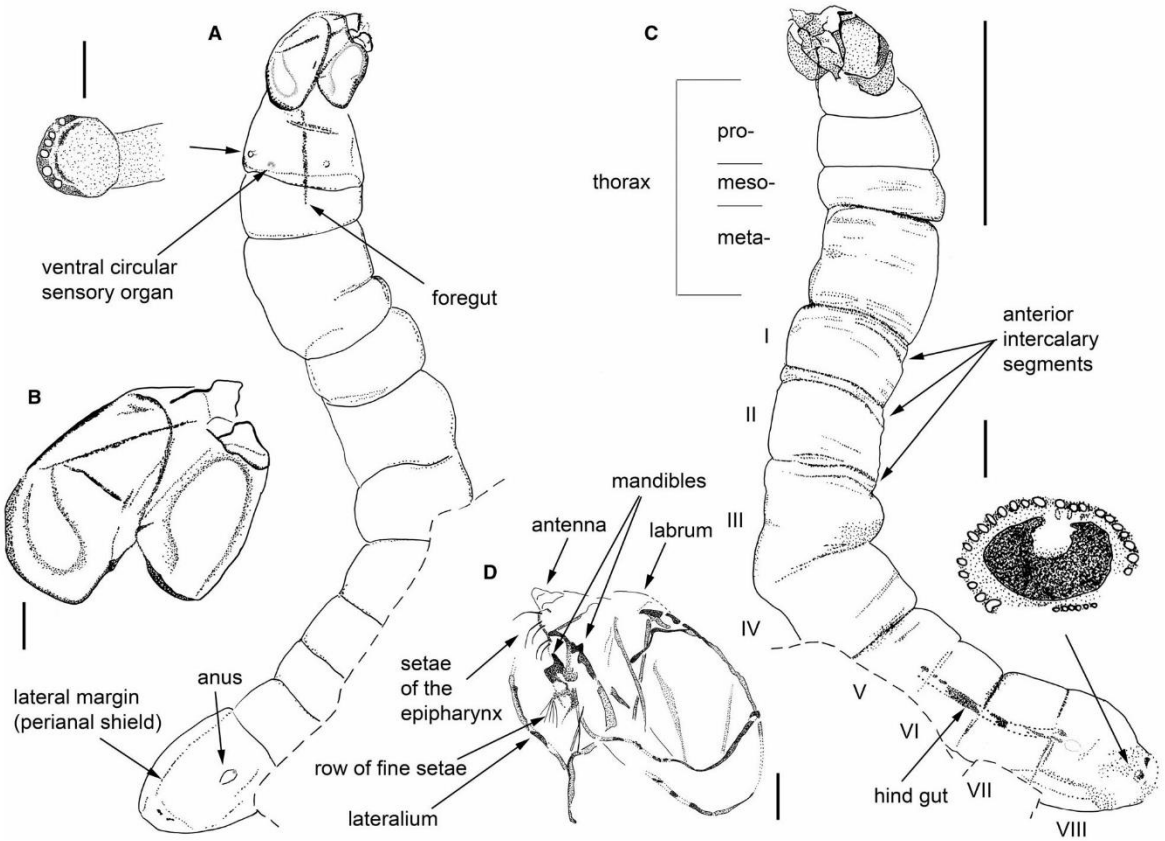

FIG. 2. Triassic terrestrial larva *Protoanisolarva juarezi* gen. et sp. nov. (Diptera, Anisopodoidea, stem-group Anisopodidae), holotype DA21/03-02-91, from the Pedra Alta site, lower Anisian. Camera lucida drawings. A–B, habitus, counterpart (DA21/03-02-91b): A, one of the anterior spiracles enlarged; B, detail of head, showing the dorsal surface. C–D, habitus, part (DA21/03-02-91a): C, one of the posterior spiracles enlarged (one preserved spiracle is complete but some small portions are present in the counterpart); D, detail of head, showing ventral and inner structures. I–VIII indicate abdominal segments. Scale bars represent: 0.02 mm (detail in A, detail in C); 0.1 mm (B, D); 1 mm (C).

Description. Body long and narrow, 4.8 mm long, 0.6 mm greatest width. Body slender, glabrous, and lacking minute spicules, projections, tubercles or conspicuous fleshy processes. Body segments weakly sclerotized, without evident colour patterns.

Head capsule well developed (eucephalic larva), probably not capable of retraction into thorax due to its shape and size (Fig. 2), 0.6 × 0.5 mm, subconical, heavily sclerotized (Figs 2D, 3B, S2B), more sclerotized dorsally than ventrally as evidenced by differential fossilization of head in part (ventral body surface) and counterpart (dorsal surface). Antennae allegedly the visible anterior pair of sclerotized processes, short and without sensory structures. Eye spots probably arranged in a way preventing their observation in the position of fossilization of the carcass. Sensory pits not visible. Labrum apparently without setae. Lateralia with strongly sclerotized margins. Some preserved tentorial rods running longitudinally, their connections to other structures unclear. Head with a preserved row of setae in a ventroanterior position, most probably corresponding to the epipharynx. Mandibles strongly sclerotized and apparently with a single tooth, having a basal piece with a row of fine setae or at least this row very close to mandible base. Maxillae not visible. Labium apparently not preserved.

Thoracic segments not fused and lacking prolegs. Prothoracic segment slightly broader than long, with a narrow anterior intercalary segment (pseudo-segmentation), bearing the anterior spiracles and a ventral circular structure lacking setae tentatively interpreted as a sensory organ (Fig. 3C). Anterior spiracles circular in shape (small, 0.03 mm in diameter), with a distal curved row of around six primary openings circular/subcircular in shape (Figs 2A, 3C); remains of two spiracles close to the posterior limit of prothorax (visible only in counterpart, mostly preserving dorsal features). Mesothoracic segment distinctly short. Metathoracic segment as long as wide. Thorax and first abdominal segment well separated.

Eight abdominal segments, broader than long, lacking prolegs and setae. Abdominal segments I–VII lacking spiracles. Each abdominal segment with an anterior intercalary segment (Fig. 2C). Remains of foregut (part) and hind gut (counterpart; visible in abdominal segments V–VIII, although portion in segments V and VI may correspond to the midgut) present. Segment VIII barely divided (apparently with only a weak terminal division), with a perianal shield on the complete ventral segment surface as evidenced by a markedly thick lateral margin on the segment (Fig. 2A). Segment VIII the widest and the longest (longer than two previous segments combined). Anus anteroposteriorly elongated, wide in anterior apex and acute in posterior one, 0.11 × 0.05 mm (Fig. 3D). Posterior spiracles terminal (one exceptionally preserved and showing its features, the other preserved in a very lateral position, thus with its features strongly distorted and not well discernible), close together, subcircular to circular in shape (not crescent-shaped or oval-shaped as observed in extant Anisopodidae); with 34 primary openings preserved (counted in both part and counterpart), but *c.* 37 estimated, circular in shape, visible around an inner heavily sclerotized disc in its entire perimeter as noted by superposition of its preserved remains in part and counterpart (Fig. 2C). Posterior spiracle area lacking fleshy lobes or setae, but posterior spiracles located distally on a cuticular process, apparently in the shape of a conical frustum (Fig. 3F). Entire abdominal segment VIII devoid of setae. Body apparently terminating in a short conical process (Fig. 2C) as in the extant anisopodid genus *Olbiogaster* (Keilin & Tate 1940).

Remarks. This fossil corresponds to a holometabolous insect due to the presence of three well-separated tagma (head, thorax and abdomen). The vermiform body lacking thoracic legs and subcylindrical in shape is typical of dipteran larvae (Stehr 1991). The absence of thoracic legs allows separation from many holometabolan larval types such as the eruciform larvae of Lepidoptera, Mecoptera, or 'symphytan' Hymenoptera (Teskey 1981). Coleoptera larvae lacking thoracic legs have body shapes deviating from the subcylindrical shape, often with enlarged thoraces or more grub-like bodies (Stehr 1991). Although larvae of apocritan Hymenoptera also lack thoracic legs, these are unknown in the Triassic and live in specialized environments (parasitoids on or in other insects, in galls, in nests etc.). They are quite unlikely to be found in a Triassic lacustrine environment, given that they are also unknown as compression fossils of more recent periods.

Following the key to the fly families of Afrotropical larvae of Borkent & Sinclair (2017), the present fossil would fall in the Anisopodidae because of the following characters: well-differentiated mouthparts, moving against one another obliquely or in horizontal plane (not parallel to one another); head capsule complete and eucephalic, not longitudinally excised dorsally; head, thorax and first abdominal segments distinct; amphipneustic respiratory system (spiracles on prothorax and abdominal segment VIII only); no elongate respiratory siphon at apex of abdomen; thoracic segments individually distinguishable, equal in diameter to widest abdominal segments; prolegs absent on thorax and abdominal segments; terminal abdominal segments without any processes; prothorax and abdominal segments with distinct annulus anteriorly.

Although the anatomical characters of *Protoanisolarva juarezi* generally agree with those of extant anisopodid larvae (Keilin & Tate 1940; Peterson 1981; Smith 1989; Hancock & Amorim 2009), it possesses some peculiarities such as the features of the posterior spiracles, the anus morphology, and some proportions of the body segments. The inner heavily sclerotized disc of the posterior spiracles could be related to the 'dense black external scar near the middle of the concave side of the spiracular tubercle' described by Keilin & Tate (1940) in the extant anisopodid species *Olbiogaster africanus*. It is important to note that the quantities of primary openings in both anterior and posterior spiracles fall within the variability observed in extant species of the family Anisopodidae. The anterior spiracles of *P. juarezi* have around six primary openings. In extant species of the family these spiracles usually have between three and 19 primary openings (Peterson 1981), although Fuller (1935) figured 24 openings in *Olbiogaster insularis*. The posterior spiracles of the fossil have 37 estimated primary openings, but in the extant genera *Olbiogaster*, *Sylvicola* and *Mycetobia* there are only 12–25 (Peterson 1981). Nevertheless, Fuller (1935) figured 35 and 36 primary openings in the posterior spiracles of *Anisopus dubius* and *Olbiogaster insularis*, respectively. A placement in the crown

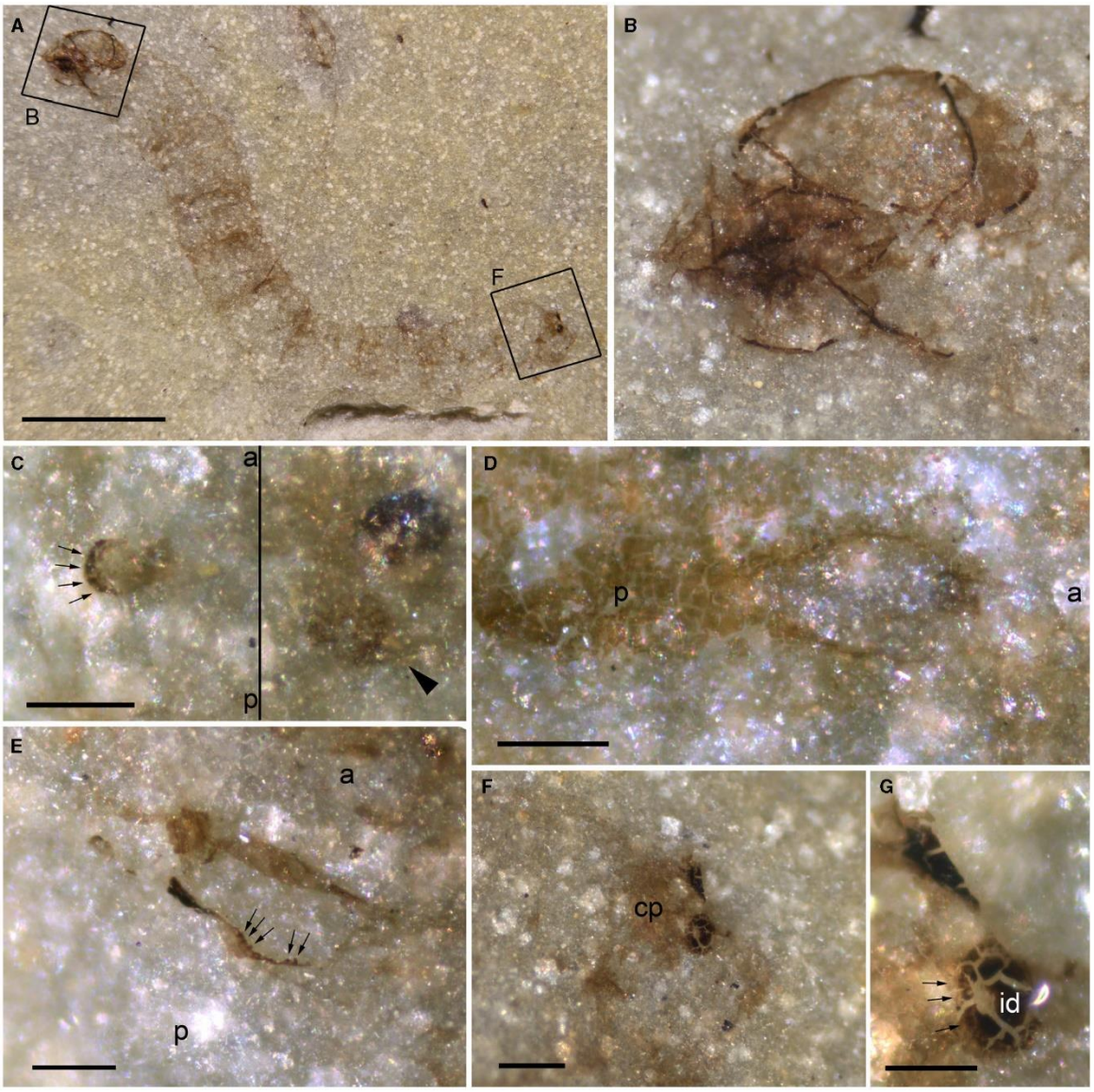

FIG. 3. Triassic terrestrial larva *Protoanisolarva juarezi* gen. et sp. nov. (Diptera, Anisopodoidea, stem-group Anisopodidae), holotype DA21/03-02-91a-b, from the Pedra Alta site, lower Anisian. A–B, habitus and detail of head (part, DA21/03-02-91a). C–E, details of structures preserved in counterpart (DA21/03-02-91b); C, anterior spiracle (left) and a ventral circular structure tentatively interpreted as a sensory organ (arrowhead, right) (vertical line separates two pictures of the same region taken in different focal planes); D, anus; E, preserved remains of posterior spiracles (small portions of posterior margins of both). F–G, details of posterior spiracles (part), showing a spiracle-bearing cuticular process, apparently in the shape of a conical frustum. Arrows indicate some of the preserved circular primary openings. Photographs made with consecutive pictures taken at successive focal planes (except C and E–G) and specimens photographed moistened with a mixture of alcohol and water (except G). Microphotograph in G taken after hardening of spiracles using PRIMAL™; see its appearance before damage in Figure 2C. *Abbreviations*: a, anterior part; cp, cuticular process; id, inner disc; p, posterior part. Scale bars represent: 1 mm (A); 0.05 mm (C–E, G); 0.1 mm (F).

group Anisopodidae cannot be justified on the sole basis of the characters of this larva. Therefore, regarding *P. juarezi* as a stem-group Anisopodidae is the most plausible stance based on the current data. Also, a closer affiliation of *P. juarezi* with the two known extinct families of Anisopodoidea, Protorhyphidae Handlirsch, 1906 and Siberhyphidae Kovalev, 1985 (also in

the stem group of the Anisopodidae, based on adults) cannot be ruled out. Larvae of these two Mesozoic families remain unknown. The oldest fossil of the stem group Anisopodidae that does not belong to the Protorhyphidae or the Siberhyphidae is Early Jurassic (Sinemurian) (Krzemińska *et al.* 2010). The oldest Protorhyphidae is Middle Triassic, and the unique Siberhyphidae (*Siberhyphus lebedevi* Kovalev, 1985) is Jurassic (Kovalev 1985; Krzemiński & Krzemińska 2003).

The body length of the larva is only 4.8 mm, which is small compared with the common sizes of mature larvae of extant Anisopodidae species (Keilin & Tate 1940; Peterson 1981). The body is long and narrow, but less gracile than typical fully grown extant anisopodid larvae. Given that early instars of the extant anisopodid *Anisopus fenestralis* are metapneustic (Keilin & Tate 1940), the size and the presence of an amphipneustic respiratory system suggest that *P. juarezi* does not represent an early instar or a fully grown one.

The excellent preservation of the holotype enables visualization of the gut tube, possessing a straight and narrow hind gut as observed in the extant anisopodid species *Mycetobia pallipes* (Keilin & Tate 1940). Despite the excellent preservation of *P. juarezi*, several interesting head features are not evident, such as eye spots, labium and maxillae. The head is fossilized in a ventrolateral position (part) implying a certain deformation aside from the fossil diagenetic flattening. Even though the head preserves internal characters that can be observed due to transparency, the interpretation of the different parts is challenging and incomplete. Note that the limits between body segments cannot be exactly matched between part and counterpart (Fig. 2) given that each part preferentially preserves one of the body sides. Moreover, a slight difference and/or displacement in the segment limits occurred in one side of the body in relation to the other. A larval morphotype similar to the present Pedra Alta taxon has not been found at Grès à Voltzia.

Infraorder ?PSYCHODOMORPHA Hennig, 1968
Superfamily ?GRAUVOGELIOIDEA Lukashevich & Shcherbakov, 1999
Family ?GRAUVOGELIIDAE Krzemiński, Krzemińska & Papier, 1994
Genus VOLTZIAPUPA Lukashevich *et al.*, 2010
Voltziapupa cornuta Lukashevich *et al.*, 2010

Voltziapupa cf. *cornuta*
Figure 4A–D

Material. An almost complete pupal specimen preserved in lateral position, DA21/14-02-06, from the Pedra Alta site, in Pedra Alta section (7.55 m), upper part of the Estellencs Formation, Aegean (lower Anisian). The specimen lacks fine detail, and the distal abdominal segments are lost.

Description. Pupa subcylindrical, at least *c.* 4.3 mm long as preserved. Head with large frontal horns (at least one preserved). Mesothoracic respiratory horns and antennae not preserved. Dorsum of cephalothorax without large setae. Wing sheaths well preserved, *c.* 1.7 mm long and 0.6 mm wide, with rounded tip, without marks of venation observed, and reaching approximately body mid-length. Mid-dorsal cleft partially preserved. Leg sheaths poorly preserved (only two small remains present). Abdominal segments relatively well preserved, apparently subequal and lacking secondary segmentation, with tergites more sclerotized than sternites and with small spines in posterior margin (a few spines preserved, not arranged in obvious rows).

Remarks. Lukashevich *et al.* (2010) described the genus *Voltziapupa* and the two species *V. tentata* and *V. cornuta* from the aquatic insect assemblage of Grès à Voltzia. These authors considered that these pupae possibly belonged to the extinct family Grauvogeliidae, described from adult remains preserved in Grès à Voltzia, and, if belonging to this family, then they would be assigned to Psychodomorpha in the superfamily Grauvogelioidea close to the Ptychopteroidea (Lukashevich & Shcherbakov 1999). The preserved characters of the new pupa from Pedra Alta agree with those in the diagnosis of the genus *Voltziapupa* but the specimen shows only a few characters. The habitus and measurements are very similar. The presence of one large frontal horn (the only character in the diagnosis of the species) that is identical to those in the holotype and paratype of *V. cornuta* enables the identification of this incomplete specimen. However, we prefer to use open nomenclature until more complete material is discovered, given that the frontal horn is not sufficiently well preserved. The wing sheaths from the Pedra Alta pupa are smaller, but a high degree of intraspecies variation was observed in this character within the genus (i.e. the 15 specimens of *V. tentata* and the 3 specimens of *V. cornuta*). The rows of small spines present along the posterior abdominal margins in *Voltziapupa* have not been observed in the present specimen, which bears only a few spines, two of them close to one another (see Fig. 4D), but this might be due to poor preservation.

NEMATOCERA indet. (pupa)
Figure 4E

Material. One incomplete, poorly preserved pupal specimen preserved in slightly lateral position, DA21/14-02-07, from the Pedra Alta site, in the Pedra Alta section (7.55 m), upper part of the Estellencs Formation, Aegean (lower Anisian). The specimen's distal abdominal segments are lost.

Description. Pupa subcylindrical, at least 4.3 mm long as preserved. Head structures, leg sheaths and wing sheaths not preserved. Mid-dorsal cleft partially preserved. The well-preserved abdominal segments seem subequal and without secondary segmentation; rows of spines along posterior abdominal margins not preserved.

Remarks. This specimen is poorly preserved but it is herein figured due to the sparse record of dipteran pupae in this outcrop and in most Triassic localities, except for Grès à Voltzia (Lukashevich *et al.* 2010). The present specimen could in fact represent another *V. cornuta* specimen, although very poorly preserved.

Ootaxon *Clavapartus latus* Gall & Grauvogel, 1966
Figures 5, S2

Material. One incomplete egg cluster in side b of the slab DA21/14-02-01 from the Pedra Alta site, in the Pedra Alta

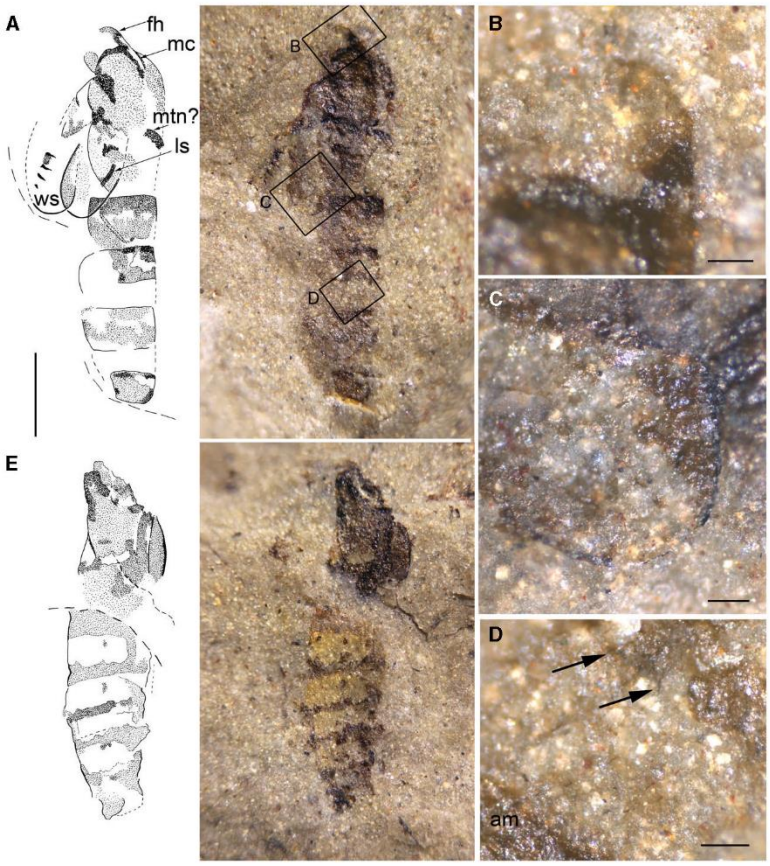

FIG. 4. Triassic aquatic dipteran pupae from the Pedra Alta site, lower Anisian. A–D, habitus of *Voltziapupa* cf. *cornuta* (?Grauvogeliidae), DA21/14-02-06, drawing and photograph, and details of the frontal horn (B), rounded tip of one of the forewing sheaths (C), and two abdominal small spines (D; arrows). E, habitus of incomplete pupa of Nematocera indet., DA21/14-02-07, drawing and photograph. A shares the scale with E. Photographs made with consecutive pictures taken at successive focal planes (except for C and D) and specimens photographed moistened with a mixture of alcohol and water. *Abbreviations*: am, abdominal margin; fh, frontal horn; ls, leg sheath; mc, mid-dorsal cleft; mtn, metanotum remain; ws, forewing sheath. Scale bars represent: 1 mm (A, E); 0.1 mm (B–D).

section (stratigraphic location uncertain, but most likely from 7.2–7.55 m in the section), upper part of the Estellencs Formation, Aegean (lower Anisian). The egg cluster is incomplete due to the limits of the claystone surface that preserved it. Most eggs are badly preserved due to weathering or sampling damage to the slab surface.

Description. Incomplete egg cluster elongated in shape, 21 mm long as preserved, 4 mm wide. Preserved portion containing 250–300 eggs. Eggs oval-shaped, *c.* 0.3 × 0.2 mm (length/width ratio = 1.5), slight brown in colour due to slight sclerotization. Eggs unhatched, some showing two-lobed tips. Eggs randomly distributed but generally distanced from each other; a few appear to be in contact (Fig. 5C) but this is most likely to have resulted from compression; the eggs were probably separated in the vertical plane prior to fossilization.

Remarks. The distribution of the eggs in the cluster indicates that these were almost certainly originally included in a mucilaginous matrix, although the latter is not evident in the fossil. The features of this egg cluster are identical to those of the very abundant *Clavapartus latus* described by Gall & Grauvogel (1966) from Grès à Voltzia, often associated to the similar ootaxon *Monilipartus tenuis* described in the same publication. The present partial specimen contains only 250–300 eggs, but between 500 and 2500 were described from the complete specimens of *C. latus* from Grès à Voltzia. Without doubt, these egg clusters covered by a mucilaginous matrix were directly laid in a water pool. Extant anisopodids lay egg clusters included in mucilaginous matrices in terrestrial substrates (Keilin & Tate 1940; Smith 1989). However, the Grès à Voltzia fossils probably do not correspond to such clusters due to their taphonomic features, which show evidence of absence of transport by

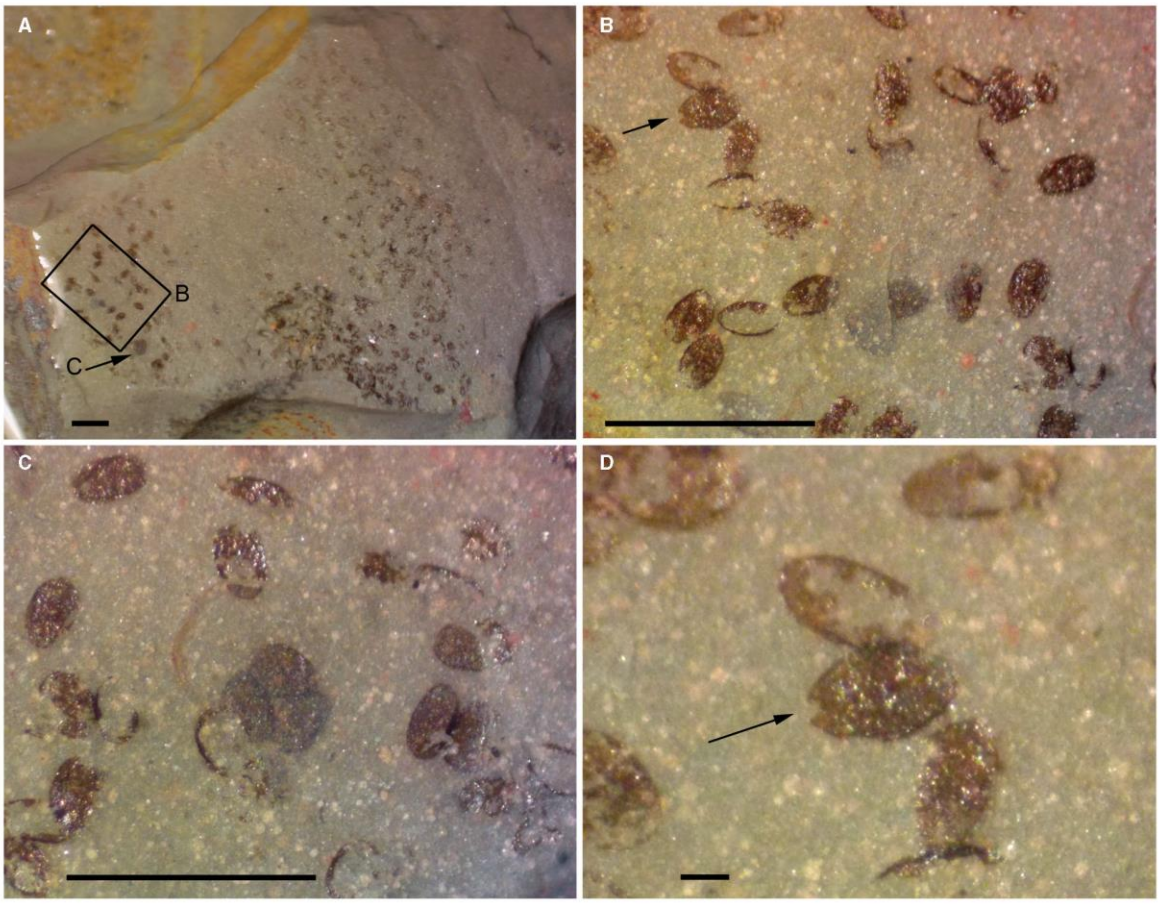

FIG. 5. Elongated, incomplete egg cluster originally in a mucilaginous matrix of the ootaxon *Clavapartus latus* Gall & Grauvogel, most likely produced by a nematoceran, present on the other side of one of the DA21/14-02-01 slab parts from the Pedra Alta site, lower Anisian. A, general view. B, detail from A (arrow indicates two-lobed tip from one oval egg (enlarged in D)). C, detail showing some eggs close together as preserved (three eggs together indicated with an arrow in A). D, detail of B. Specimen photographed moistened with a mixture of alcohol and water. Scale bars represent: 1 mm (A–C); 0.1 mm (D).

strong water currents towards the aquatic environments of burial. This explains the perfect integrity of abundant egg clusters despite their original delicate nature, as well as the lack of debris attached to the sticky mucilaginous matrix.

Gall & Grauvogel (1966) noted that nematocerans of the family Chironomidae were the most probable producers of *C. latus*, which resembles the egg clusters in mucilaginous matrices from extant *Chironomus* species; *Monilipartus tenuis* was also related to chironomids by these authors. Indeed, some Late Triassic representatives of the stem group Chironomidae are known (Krzemiński & Jarzembowski 1999). Gall & Grauvogel (1966) also considered the possibility that those egg clusters were laid by caddisflies (Trichoptera). Because trichopterans were most likely to have been present in running waters, the probability of any potential egg clusters to arrive in the quiet waters of the pools was low; this contradicts the abundance of intact clusters in Grès à Voltzia. Later, Grauvogel-Stamm & Kelber (1996) also suggested anisopteran odonates as possible producers, given the resemblance of the egg clusters to those of some extant Corduliidae as well as the description of a few adult remains of Odonatoptera (Triadophlebiomorpha and Protozygoptera, but no Odonata *s.s.*) in Grès à Voltzia (Nel *et al.* 1996). However, nothing is known on the egg laying of these Triassic Odonatoptera, which are phylogenetically quite distant from the extant Anisoptera. In any case, the herein described egg cluster is similar to those from extant Chironomidae, as well as to egg clusters from the Cenozoic fossil record (Fig. S2) tentatively assigned to Chironomidae and Chaoboridae (see below).

Although here we follow the most plausible attribution indicated in the original publication (Gall & Grauvogel 1966), in a more conservative manner we consider that these egg clusters were most likely produced by nematoceran dipterans. Extant chironomids lay their eggs in the water together with a transparent mucilaginous material produced by a female gland, which

expands in the water and is adhesive, acting as a protection for the eggs against aquatic mites and fishes (Oliver 1981; Pinder 1995). These chironomid egg clusters can be cylindrical and very elongated or spherical. The eggs vary in form and in number depending on each cluster, thus showing some features that are species specific (Richards & Davies 1977), but are usually elliptical in shape, although they can be deltoid in two subfamilies (Nolte 1993; Pinder 1995). The length of the eggs varies between 170 and 612 μm and the length/width ratio of chironomid unhatched eggs ranges from 1.6 to 4.5 (Pinder 1995). Note that the herein unhatched eggs of *Clavapartus latus* have a ratio of 1.5, close to the smallest ratio for extant chironomid eggs, and that hatching slightly deforms the eggs. Extant chaoborid eggs are arranged in the form of a floating disc, which can contain mucilaginous material surrounding the eggs to prevent sinking (Saether 1997), and thus are very different to both Triassic and extant chironomid egg clusters.

Although descriptions of fossil nematoceran egg clusters are scarce, this is probably due to specimen misinterpretation and the paucity of studies, given that their potential for fossilization in lacustrine compression deposits is not as low as expected (Peñalver 2002). Despite the age difference, the Triassic egg clusters noted above share an original protective mucilaginous matrix with some ovoid clusters found in Konservat-Lagerstätten in the USA (Eocene) and Spain (Miocene). The shape of *Clavapartus* is very similar to the eggs found in the middle Eocene of the Kishenehn outcrop (Baranov *et al.* 2022), which are attributed to the genus *Chaoborus* (Chaoboridae), but smaller (Fig. S2); the Eocene egg clusters are 4.6 × 2.3 mm in size and the eggs are 0.47 × 0.20 mm (length/width ratio = 2.35) (from Baranov *et al.* 2022, fig. 22). These Eocene eggs were probably originated by chironomids instead of chaoborids, because the only cluster figured (Baranov *et al.* 2022, fig. 22A) does not have the eggs arranged in a spiral pattern as indicated by these authors in the main text, but instead are arranged without a pattern in a globular mass similar to what has been observed in some extant chironomid egg clusters. The Spanish Miocene clusters were found in Rubielos de Mora and Bicorb outcrops, Burdigalian (Lower Miocene) and Vallesian (Upper Miocene) in age, respectively, and attributed to the family Chironomidae (Peñalver 2002; Peñalver & Gaudant 2010). The mucilaginous matrix can be seen as a clear halo around the egg clusters from these two localities in relation to the rock matrix during the first seconds after moistening the specimens with alcohol (Peñalver 2002). In both Miocene outcrops the egg clusters with evidence of original mucilaginous matrices are very abundant, and the chironomids (pupae, exuviae, and adults) are the most abundant fossils. Trichopteran and odonatan fossils are, on the contrary, very scarce or absent. In these egg clusters, evidence of significant pre-burial transport is present: some organic structures, such as legs and other disarticulated parts from adult and pupal chironomids, were commonly ensnared by the mucilaginous matrices, which are mostly preserved broken (Peñalver 2002). The egg clusters from Rubielos de Mora are small, for instance 4.2 × 2.4 mm in a typical specimen, ovoid-shaped (spherical–globular type), and contain up to 75 fusiform eggs, 0.46 × 0.16 mm in a typical hatched egg (length/width ratio = 2.88); the egg clusters and egg size from Bicorb are very similar: 5.5 × 2.2 mm and 0.37 × 0.16 mm (length/width ratio = 2.31) in typical cluster and hatched egg specimens, respectively (Peñalver 2002; Peñalver & Gaudant 2010). In contrast, the Pedra Alta clusters are of the cylindrical and very elongated type. All of these Mesozoic and Cenozoic fossil eggs fall within the size and length/width ratio ranges observed in eggs of extant chironomids (Pinder 1995).

DISCUSSION

Palaeobiological implications of the new anisopodoid fossil larva

The dipteran fossils described herein represent the earliest known record of the megadiverse order Diptera. *Protoanisolarva juarezi* also represents the oldest anisopodoid dipteran known, and is evidence of the presence of stem-group Anisopodidae back to *c.* 247 Ma. The major lineages of the dipteran infraorder Bibionomorpha *s.l.* (i.e. Sciaroidea, Bibionoidea, Anisopodoidea and Scatopsoidea), as well as most of their families, including Anisopodidae, were supported as monophyletic by a molecular phylogeny combining nuclear and mitochondrial markers (Ševčík *et al.* 2016), and also by morphological data (e.g. Lambkin *et al.* 2013). Wojtoń *et al.* (2019) proposed the following phylogenetic hypothesis for the Anisopodoidea = (Protorhyphidae + (Siberhyphidae + Anisopodidae)) based on adult morphology. Prior to the present study, the oldest representative of the superfamily Anisopodoidea was *Vymrhyphus blagoderovi* Krzemiński & Krzemińska, 2003, of the extinct family Protorhyphidae, found in Grès à Voltzia.

The family Anisopodidae, containing only 120 extant species in seven genera (Grimaldi & Engel 2005), has been proposed as the closest living relative of the diverse suborder Brachycera based on characters from both their essentially terrestrial larvae and adults (Woodley 1989; Oosterbroek & Courtney 1995; Shcherbakov *et al.* 1995; Grimaldi & Engel 2005). Although the clade Anisopodidae + Brachycera was found to be sister to the clade Tipulidae + Trichoceridae based on morphological characters (Oosterbroek & Courtney 1995), Anisopodidae was recovered as sister to the clade Bibionomorpha *s.s.* + Scatopsoidea by Ševčík *et al.* (2016). The oldest certain representatives of crown-group Anisopodidae are Early Jurassic in age (Wojtoń *et al.* 2019), all of them being adult forms. Hennig (1973) used both adult and larval characters in his classic analysis on the evolution and classification of the order Diptera. Larval cephalic features of Bibionomorpha have been found to be very informative from the phylogenetic standpoint (Bauernfeind *et al.* 2015). The discovery of *P. juarezi* illuminates important phylogenetic aspects of Bibionomorpha. The preserved cephalic features also shed light on the palaeobiology of the oldest bibionomorphans *s.l.* in the moist

surroundings of the first continental water bodies colonized with certainty by dipterans.

Protoanisolarva juarezi is interpreted as a terrestrial form based on its morphology and taxonomic affinities. It probably developed in pool marginal areas rich in organic matter. The excellent preservation and completeness of this larva, originally very delicate and with scarcely sclerotized cuticle, indicate that it is para-autochthonous. Thus, after a phase of biostratinomic transport that must have been short, the carcass went from the pool margin areas to the dysoxic or completely anoxic waters of the deepest pool parts.

The amphipneustic respiratory system exhibited by *P. juarezi* is externally evident thanks to the exceptional preservation of only anterior and posterior spiracles (Fig. 6). The new fossil adds this type of respiratory mode (typical of dipteran larvae) to the Pedra Alta Triassic insect assemblage, and represents its earliest known occurrence in the fossil record. In addition, the aquatic mayfly nymphs described from Pedra Alta preserved evidence of abdominal tracheal gills, chiefly observed as conspicuous rounded plates densely fringed on the borders, indicating an apneustic respiratory system as expected for this group (Peñalver *et al.* in press). Last, *Voltziapupa* bears elongate, cylindrical mesothoracic respiratory horns (not preserved in the Pedra Alta specimen), as evidenced by its rich and well-preserved record in Grès à Voltzia. This propneustic respiratory system is in accordance with the suggested semiaquatic mode of life for this taxon (Lukashevich *et al.* 2010).

The great morphological similarities between *P. juarezi* and the larvae of extant Anisopodidae suggest that they had a similar biology. Extant anisopodid larvae are saprophagous and develop in areas with moist to wet decaying and fermenting organic matter of multiple origins (Peterson 1981; Hancock & Amorim 2009). More specifically, the fossil larva possibly fed on fungal mycelia and/or fungal fruiting bodies, as is common among the extant relatives. For Zherikhin (2002), mycetophagy was probably widespread in the Mesozoic and was likely to have been an important condition in insect evolution and diversification. The fossil record of mycetophagy is sparse and has been poorly studied. In the *Protoanisolarva juarezi* specimen the hind gut is partially preserved, with possible gut contents corresponding to a black carbonaceous film that contrasts with the light brown of the preserved foregut, showing that the latter was empty when the larva died. Preparation of a hind gut sample could confirm mycelia and/or other identifiable fungal structures, but the minute size and the exceptional relevance of this holotype precludes partially destructive sampling.

Palaeobiology of the aquatic insect community

The aquatic assemblage of Pedra Alta developed in backswamps or among abandoned sand bars in channel margins (Matamales-Andreu *et al.* 2021) (Fig. 6). Aside from the dipteran taxa described herein, the Pedra Alta palaeoecosystem was inhabited by fishes (only one complete juvenile found) and clam shrimps ('conchostracans'; very abundant) of the species *Hornestheria* aff. *sollingensis* Kozur & Lepper *in* Kozur & Weems, 2010 (Matamales-Andreu *et al.* 2021). Other insects present in Pedra Alta were mayfly nymphs of an indeterminate detritivorous morphotype preserving cololites (abundant) and the species *Triassoephemera punctata* Sinitshenkova & Marchal-Papier *in* Sinitshenkova *et al.*, 2005, *Triassonurus doliiformis* Sinitshenkova & Marchal-Papier *in* Sinitshenkova *et al.*, 2005 and cf. *Voltziaephemera fossoria* Sinitshenkova & Marchal-Papier *in* Sinitshenkova *et al.*, 2005 (all of these rare) (Matamales-Andreu *et al.* 2021; Peñalver *et al.* in press).

All of the organisms found in the Pedra Alta section are considered to be virtually coeval. With regard to the insects, the holotype and only specimen of *Protoanisolarva juarezi* was found at 7.20 m of the Pedra Alta section, whereas the aquatic pupae were recovered from 7.55 m of the same section. An abundant record of mayfly nymphs and adults is present in both of these horizons as well as at 4.75 m (Matamales-Andreu *et al.* 2021; Peñalver *et al.* in press).

Based on their completeness despite their original frailty, all of the pre-adult dipterans and the mayfly nymphs found in this deposit must have undergone relatively little disturbance during transport to the deepest areas of the water pool (Martínez-Delclòs *et al.* 2004). The sedimentivorous mayfly nymphs from this locality were considered as inhabiting lentic habitats, which virtually were those of burial (Peñalver *et al.* in press). However, the other pre-adult forms found in Pedra Alta, such as those described herein, are very sparsely represented and could be considered allochthonous regarding the water pools. Despite the exceptional preservation and abundance of the fossils in Grès à Voltzia, palaeoecological inferences based on the material from that locality must be considered tentative. For Pedra Alta, with a lower number of specimens found and generally more poorly preserved, inferences and conclusions need to be at least equally cautious. The river shorelines with slow currents were deemed as the most plausible habitat for the Grès à Voltzia mayfly nymphs, namely *Voltziaephemera* and *Triassonurus* (Sinitshenkova *et al.* 2005). The same habitat was suggested for the dipteran *Voltziapupa* from Grès à Voltzia, recorded in the same beds as the mayflies, and aquatic or semiaquatic habitats for their unknown larvae (Sinitshenkova *et al.* 2005; Lukashevich *et al.* 2010). Nevertheless, it is not clear from the taphonomic standpoint whether the fossil pupae from Pedra Alta can be attributed to lotic habitats.

The body fossils and invertebrate traces from Pedra Alta provide several insights into the early Middle Triassic

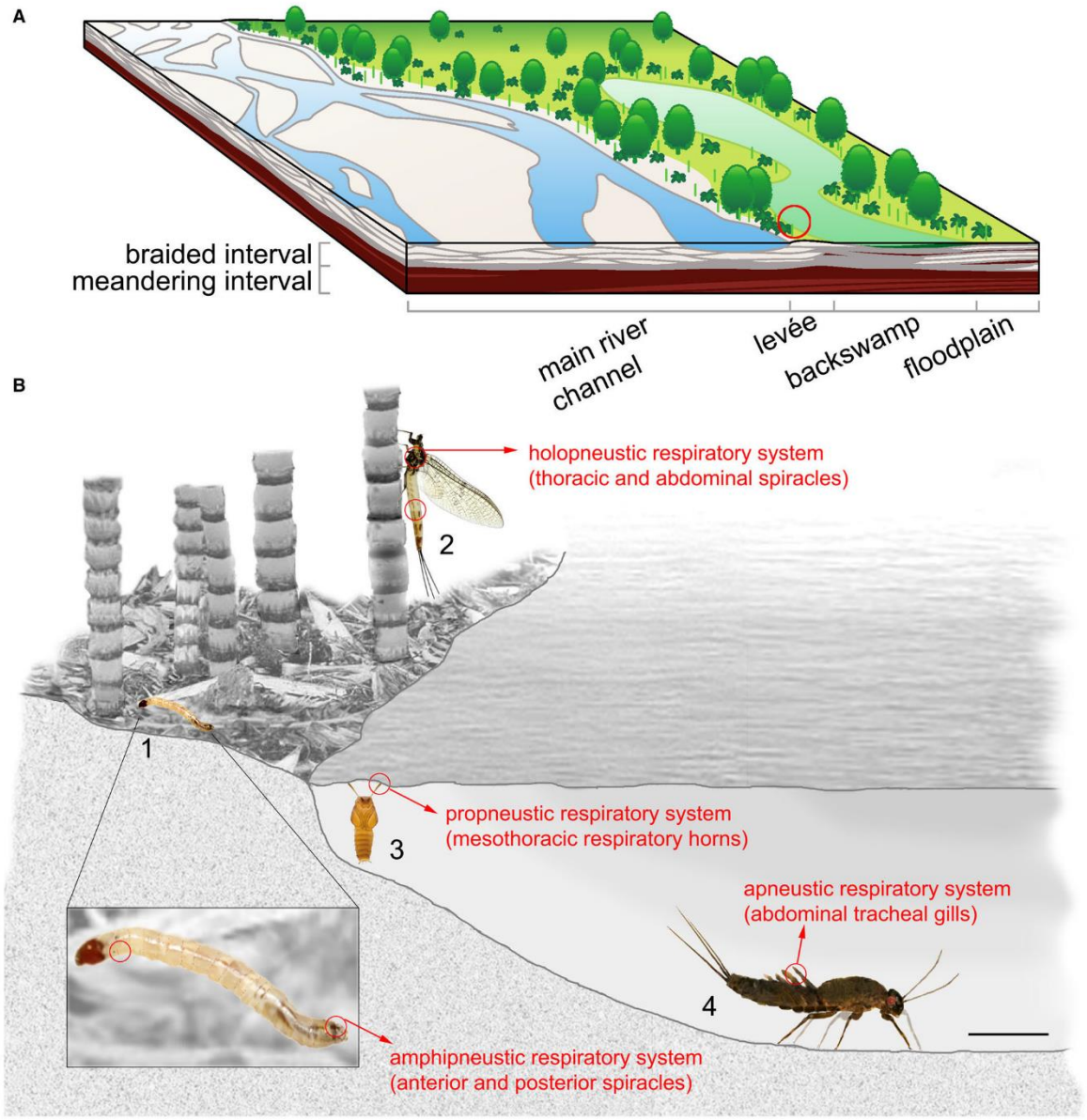

FIG. 6. Reconstruction of the moist and aquatic continental environment represented in the Pedra Alta site (Estellencs Fm., early Anisian), showcasing insect taxa, with different respiratory systems, that inhabited the palaeoecosystem. A, schematic diagram of the different environments of the Estellencs Fm. braided interval, and some of the plants found in the same levels as the insects: *Equisetites* sp., *Pelourdea* sp., *Voltzia* sp. B, schematic representation of a backswamp zone according to the interpretation of the Pedra Alta fossiliferous horizons (red circle in A): 1, dipteran larva *Protoanisolarva juarezi* gen. et sp. nov.; 2, mayfly adult *Hammephemera* cf. *pulchra*; 3, dipteran pupa *Voltziapupa* cf. *cornuta*, reconstructed based on more complete congeneric specimens found at Grès à Voltzia (Lukashevich *et al.* 2010); and 4, mayfly nymph *Triassonurus doliiformis*. All reconstructed insects to the same scale (scale bar applies to the insects only and represents 5 mm).

aquatic trophic net (Matamales-Andreu *et al.* 2021). Phytoplankton and photosynthetic bacteria could have been the primary producers in the palaeoecosystem. Although no direct evidence from the rock of these fossiliferous beds is currently available, it seems that microbial films (not mats) developed in the water–sediment interphase

based on the exfoliation of the Pedra Alta fossiliferous rock following pure planes, where the insects are preserved as carbonaceous films. We infer that the growth of microbial mats on the pond bottom after each sedimentary input formed relatively clean limits separating these layers (Peñalver 2002). Moreover, it is likely that a hygrophytic flora developed around the freshwater body, providing abundant plant organic matter to the ponds and their surrounding terrestrial wet habitats (Matamales-Andreu *et al.* 2021). Clam shrimps and mayfly nymphs were the primary consumers and/or saprophagous. The clam shrimps were most likely filter feeders, consuming plankton and organic detritus suspended in the water, as do most of their extant counterparts (Dodson & Frey 2001). The detritivore mayfly nymph morphotypes from Pedra Alta were sedimentivorous based on the content of their 3D cololites (Peñalver *et al.* in press). The rest of the mayfly nymph forms, also recorded in Grès à Voltzia with at least one burrowing species (cf. *Voltzia-ephemera fossoria*), were most likely detritivores (although not of the sedimentivorous type), grazers and filter-feeders (Sinitshenkova *et al.* 2005). Based on the currently known record, the only predators or secondary consumers were fishes, but direct evidence from the single fish specimen found in Pedra Alta to date is lacking. This palaeoecological scenario is complemented by the data presented herein on early dipterans. *Protoanisolarva juarezi* is interpreted as saprophagous, most likely mycetophagous, and probably developed in moist to wet decaying and fermenting organic matter contiguous to the water pools (Fig. 6). There is no evidence of feeding habits for the pre-adult nematocerans represented by the semiaquatic *Voltziapupa*, but these probably were primary consumers or saprophagous, with food intake by filtering or chewing.

According to the established regional palaeoenvironment and the presence of mass mortality records of mayfly nymphs, it seems clear that the Pedra Alta aquatic ecosystem underwent important shifts in environmental conditions, such as changes in water dynamics, turbidity and bathymetry, salinity, dissolved oxygen, and/or temperature (Matamales-Andreu *et al.* 2021). Under that scenario, the fossil nematoceran egg clusters protected with a mucilaginous matrix present in Pedra Alta and Grès à Voltzia appear to have been an adaptation that minimized the mechanical damage and potential desiccating conditions (Gall & Grauvogel-Stamm 2005), and maybe even predation as well.

CONCLUSION

Following the remarkable gap in the terrestrial fossil record of the Early Triassic, including that of insects, Middle Triassic fossil insect localities remain very scarce globally. Pedra Alta (early Anisian), almost 2 myr older than the well-studied locality of Grès à Voltzia, has yielded the earliest dipterans currently known. Those correspond to the pre-adult stages herein described, which offer valuable palaeoecological data. Moreover, Pedra Alta is, together with Grès à Voltzia, the only Triassic locality that has provided pre-adult dipterans, at both larval and pupal stages. These deposits provide evidence of the role of insects such as dipterans and mayflies in the colonization of the first continental aquatic ecosystems after/during the recovery period from the Permo-Triassic mass extinction event.

Pedra Alta has provided insights into some key putative adaptations in Triassic insects. Now these include specializations of the megadiverse insect order Diptera related to respiratory systems, possible trophic habits, and strategies to protect the eggs; some of these presumed adaptations represent the oldest known direct evidence, and are extended back to *c.* 247 Ma. Although Pedra Alta is generally poor in fossil insects and has only a few productive levels, the assemblage described herein has an exceptional degree of preservation. *Protoanisolarva juarezi* gen. et sp. nov. has an exquisitely preserved body, including external characters and some internal cephalic ones. This terrestrial larva is key to improving the understanding of the evolution and early ecology of true flies.

The new records described herein provide additional faunistic similarities between the Anisian localities of Pedra Alta and Grès à Voltzia. Taking into account differences in preservation and biases between these two localities, our data increase the knowledge on the early Middle Triassic entomofauna and its palaeobiology, with regard to aquatic environments. Furthermore, the presence of the same (or very similar) aquatic insect species in the two deposits indicates that the difference in their ages must be low. The maximum age difference between the two localities of up to *c.* 2 myr is compatible with the 3–10 myr inferred life span of insect species (Grimaldi & Engel 2005).

The study of the palaeoentomofauna from Pedra Alta has just begun. More excavations are necessary to recover new exceptionally preserved specimens. Likewise, increasing the sampling of more aquatic and terrestrial insect taxa from this locality is crucial to complete the current palaeoecological reconstruction. Greater sampling will also increase the taphonomic knowledge and shed light on the proportion of forms from diverse aquatic habitats such as lentic and lotic.

The pre-adult dipterans presently described are small and challenging to detect during palaeontological excavations. Most of the important records described herein were found during laboratory stereomicroscopy of slabs from which other specimens had already been found, namely clam shrimps and mayflies. Therefore, the collections from Pedra Alta would clearly be increased in specimen number and diversity if slabs from productive levels were able to be closely inspected in the laboratory.

According to the preservation observed in this Konservat-Lagerstätte, it is likely that some small insects, both aquatic and terrestrial, and belonging to uncommon groups in the Triassic fossil record, such as Thysanoptera, would be found following this approach.

Acknowledgements. We thank Josep Juárez, Sebastià Matamalas, Francesc Baiget, Eduardo Barrón, Ana Rodrigo and Enric Pedrón for help in fieldwork. We also thank Pedro Agustín Robledo, Ana Sevillano and José María López García for facilitating the field palaeontological research. The Comissió Insular de Patrimoni Històric of the Consell de Mallorca granted the excavation permits (file numbers 305/2019 and 52/2021). We acknowledge support from the IGME, the CERCA program (Generalitat de Catalunya, Spain), and the project 'Mallorca abans dels dinosaures: estudi dels ecosistemes continentals del Permià i Triàsic amb especial èmfasi en les restes de vertebrats' (ref. 15-619/2020), based at the ICP and funded by the Departament de Cultura, Patrimoni i Política Lingüística (Consell Insular de Mallorca, Spain). RM-A was supported by the predoctoral grant FPU17/01922 (Ministerio de Ciencia, Innovación y Universidades, Spain). Two anonymous referees commented on an earlier draft of this manuscript.

Author contributions. **Conceptualization** Enrique Peñalver (EP), Ricardo Pérez-de la Fuente (RPF); **Formal Analysis** EP, Rafel Matamales-Andreu (RM-A), André Nel (AN), RPF; **Investigation** EP, RM-A, AN, RPF; **Methodology** EP, RM-A; **Supervision** EP; **Visualization** EP; **Writing – Review & Editing** EP, RM-A, AN, RPF.

DATA ARCHIVING STATEMENT

This published work and the nomenclatural acts it contains, have been registered in ZooBank: http://zoobank.org/References/B668BD02-B77B-4BE5-BF80-136961F62874

Editor. Michael Engel

SUPPORTING INFORMATION

Additional Supporting Information can be found online (https://doi.org/10.1002/spp2.1472):

Figure S1. Additional microphotographs of the Triassic terrestrial larva *Protoanisolarva juarezi* gen. et sp. nov. (Diptera, Anisopodoidea, stem-group Anisopodidae), holotype DA21/03-02-9b, from Pedra Alta site, lower Anisian.
Figure S2. Putative Mesozoic and Cenozoic nematoceran eggs from egg clusters present in a mucilaginous matrix.

REFERENCES

AMORIM, D. D. S., LOPES FALASCHI, R. and SIQUEIRA OLIVEIRA, S. 2016. Family Anisopodidae. *Zootaxa*, **4122**, 015–019.

BARANOV, V. A., HAUG, J. T., GREENWALT, D. E. and HARBACH, R. 2022. A vanished ecosystem: diversity of culicomorphan dipterans in the Eocene Kishenehn Konservat-Lagerstätte (Montana, USA) and its palaeoecological implications. *Palaeontologia Electronica*, **25** (1), a4.

BASHKUEV, A., SELL, J., ARISTOV, D., PONOMARENKO, A., SINITSHENKOVA, N. and MAHLER, H. 2012. Insects from the Buntsandstein of Lower Franconia and Thuringia. *Paläontologische Zeitschrift*, **86**, 175–185.

BAUERNFEIND, R., SCHNEEBERG, K. and BEUTEL, R. G. 2015. The larval head of *Exechia* (Mycetophilidae) and *Bibio* (Bibionidae) (Diptera). *Arthropod Structure & Development*, **44**, 326–345.

BORKENT, C. J. and SINCLAIR, B. J. 2017. Key to Diptera families – larvae. 357–409. *In* KIRK-SPRIGGS, A. H. and SINCLAIR, B. J. (eds) *Manual of Afrotropical Diptera. Vol. 1. Introductory chapters and keys to Diptera families*. Suricata, **4**, 425 pp.

BOURQUIN, S., PERON, S. and DURAND, M. 2006. Lower Triassic sequence stratigraphy of the western part of the Germanic Basin (west of Black Forest): fluvial system evolution through time and space. *Sedimentary Geology*, **186**, 187–211.

CALAFAT, F. 1988. *Estratigrafía y sedimentología de la litofacies Buntsandstein de Mallorca*. Bachelor thesis. Universitat de Barcelona, 127 pp.

CHEN, J., WANG, B., ENGEL, M. S., WAPPLER, T., JARZEMBOWSKI, E. A., ZHANG, H., WANG, X., ZHENG, X. and RUST, J. 2014. Extreme adaptations for aquatic ectoparasitism in a Jurassic fly larva. *eLife*, **3**, e02844.

DIEZ, J. B. 2000. *Geología y Paleobotánica de la Facies Buntsandstein en la Rama Aragonesa de la Cordillera Ibérica. Implicaciones paleogeográficas en el Peritethys Occidental*. PhD thesis, Universidad de Zaragoza–Université Pierre & Marie Curie, Paris VI, 424 pp.

DIEZ, J. B., BROUTIN, J., GRAUVOGEL-STAMM, L., BOURQUIN, S., BERCOVICI, A. and FERRER, J. 2010. Anisian floras from the NE Iberian Peninsula and Balearic Islands: a synthesis. *Review of Palaeobotany & Palynology*, **162**, 522–542.

DODSON, S. I. and FREY, D. G. 2001. Cladocera and other branchiopoda. 849–913. *In* THORP, J. H. and COVICH, A. P. (eds) *Ecology and classification of North American freshwater invertebrates*. Academic Press, 911 pp.

DURAND, M. and JURAIN, G. 1969. Eléments paléontologiques nouveaux du Trias des Vosges méridionales. *Comptes Rendus de l'Académie des Sciences, Paris, Série D*, **269**, 1047–1049.

FLECK, G., BECHLY, G., NEL, A. and ESCUILLIÉ, F. 2002. The larvae of the Mesozoic family Aeschnidiidae and their phylogenetic implications (Insecta: Odonata: Anisoptera). *Palaeontology*, **45**, 165–184.

FULLER, M. E. 1935. Notes on Australasian Anisopodidae (Diptera). *Proceedings of the Linnean Society of New South Wales*, **60**, 291–302.

GALL, J.-C. 1971. Faunes et paysages du Grès à Voltzia du nord des Vosges. Essai paléoécologique sur le Buntsandstein supérieur. *Service de la Carte Géologique d'Alsace et de Lorraine*, **34**, 1–318.

GALL, J.-C. 1972. Le role de la paléoécologie dans la reconstitution des anciens biotopes. Application aux gisements fossilifères du Trias Inférieur des Vosges. *Bulletin de la Société d'Ecologie*, **3**, 354–367.

GALL, J.-C. and GRAUVOGEL, L. 1966. Faune du Buntsandstein. I. Pontes d'invertébrés du Buntsandstein supérieur. *Annales de Paléontologie (Invertébrés)*, **52**, 155–161.

GALL, J.-C. and GRAUVOGEL-STAMM, L. 2005. The early Middle Triassic 'Grès à Voltzia' Formation of eastern France: a model of environmental refugium. *Comptes Rendus Palevol*, **4**, 637–652.

GRAUVOGEL-STAMM, L. and KELBER, K.-P. 1996. Plant–insect interactions and coevolution during the Triassic in Western Europe. *Paleontologia Lombarda*, **5**, 5–23.

GRIMALDI, D. A. and ENGEL, M. S. 2005. *Evolution of the insects*. Cambridge University Press, 755 pp.

HANCOCK, E. G. and AMORIM, D. D. S. 2009. Anisopodidae (wood gnats or window gnats). 341–345. *In* BROWN, B. V., BORKENT, A., CUMMING, J. M., WOOD, D. M., WOODLEY, N. E. and ZUMBADO, M. A. (eds) *Manual of Central American Diptera*, **1**. NRC Research Press, 714 pp.

HANDLIRSCH, A. 1906. *Die Fossilen Insekten und die Phylogenie der Rezenten Formen. Ein Handbuch fur Palaontologen und Zoologen*. Parts I–IV. Engelmann, Leipzig, 640 pp.

HENNIG, W. 1948. *Die Larvenformen der Dipteren*. Akademie-Verlag, Berlin, 1.

HENNIG, W. 1968. Kritische Bemerkungen über den Bau der Flügelwurzel bei den Dipteren und die Frage nach der Monophylie der Nematocera. *Stuttgarter Beiträge zur Naturkunde*, **193**, 1–23.

HENNIG, W. 1973. Ordnung Diptera (Zweiflügler). *Handbuch der Zoologie*, **4** (2) (Lfg. 20), 1–337.

KEILIN, D. and TATE, P. 1940. The early stages of the families Trichoceridae and Anisopodidae (=Rhyphidae) (Diptera: Nematocera). *Transactions of the Royal Entomological Society of London*, **90**, 39–62.

KNAB, F. 1912. New species of Anisopidae (Rhyphidae) from tropical America. *Proceedings of the Biological Society of Washington*, **25**, 111–113.

KOVALEV, V. G. 1985. Infraorder Bibionomorpha and Asilomorpha. 113–187. *In* KALUGINA, N. S. and KOVALEV, V. G. (eds) *Dvukrylye Yury Sibiri [Insecta Diptera of the Jurassic in Siberia.]*. Akademiya nauk SSSR, Paleontologicheskij Instituta, Moskovskogo Obshchestva Ispytatelej Prirody, 198 pp. [in Russian]

KOZUR, H. W. and WEEMS, R. E. 2010. The biostratigraphic importance of conchostracans in the continental Triassic of the northern hemisphere. *Geological Society, London, Special Publications*, **334**, 315–417.

KRZEMIŃSKA, E., CORAM, A. R. and KRZEMIŃSKI, W. 2010. A new species of *Megarhyphus*, an interesting discovery from the Lower Jurassic of England (Diptera, Anisopodidae). *Acta Geologica Sinica, English Edition*, **84**, 693–695.

KRZEMIŃSKI, W. and JARZEMBOWSKI, E. 1999. *Aenne triassica* sp. n., the oldest representative of the family Chironomidae (Insecta: Diptera). *Polskie Pismo Entomologiczne*, **68**, 445–449.

KRZEMIŃSKI, W. and KRZEMIŃSKA, E. 2002. Rhaetaniidae, a new family of the Diptera from the Upper Triassic of Great Britain (Diptera: Nematocera). *Annales Zoologici*, **52**, 211–213.

KRZEMIŃSKI, W. and KRZEMIŃSKA, E. 2003. Triassic Diptera: descriptions, revisions and phylogenetic relations. *Acta Zoologica Cracoviensia Supplements*, **46**, 153–184.

KRZEMIŃSKI, W., KRZEMIŃSKA, E. and PAPIER, F. 1994. *Grauvogelia arzvilleriana* sp. n.: the oldest Diptera species (Lower/Middle Triassic of France). *Acta Zoologica Cracovensia*, **37**, 95–99.

LAMBKIN, C. L., BRADLEY, J., SINCLAIR, T. P., COURTNEW, G. W., SKEVINGTON, J. H., MEIER, R., YEATES, D. K., BLAGODEROV, V. and WIEGMANN, B. M. 2013. The phylogenetic relationships among infraorders and superfamilies of Diptera based on morphological evidence. *Systematic Entomology*, **38**, 164–179.

LARA, M. B. and LUKASHEVICH, E. D. 2013. The first Triassic dipteran (Insecta) from South America, with review of Hennigmatidae. *Zootaxa*, **3710**, 81–92.

LINNAEUS, C. 1758. *Systema naturae*, **1**. Tenth edition. Laurentius Salvius, Holmiae, 824 pp. https://doi.org/10.5962/bhl.title.542

LUKASHEVICH, E. D. 2008. Larvae: a key to evolution of Culicoidea (Diptera) in the Mesozoic. *Alavesia*, **2**, 59–72.

LUKASHEVICH, E. D. 2021. The oldest Diptera (Insecta) from the Upper Buntsandstein (early Middle Triassic) of Europe. *Zootaxa*, **5067**, 135–143.

LUKASHEVICH, E. D. and SHCHERBAKOV, D. E. 1999. A new Triassic family of Diptera from Australia. 81–89. *In Proceedings of the 1st International Palaeoentomological Conference, Moscow 1998*. AMB Project, Bratislava, 199 pp.

LUKASHEVICH, E. D., PRZHIBORO, A. A., MARCHAL-PAPIER, F. and GRAUVOGEL-STAMM, L. 2010. The oldest occurrence of immature Diptera (Insecta), Middle Triassic, France. *Annales de la Société Entomologique de France (n.s.)*, **46**, 4–22.

MARTÍNEZ-DELCLÒS, X., BRIGGS, D. E. G. and PEÑALVER, E. 2004. Taphonomy of insects in carbonates and amber. *Palaeogeography, Palaeoclimatology, Palaeoecology*, **203**, 19–64.

MATAMALES-ANDREU, R., PEÑALVER, E., MUJAL, E., OMS, O., SCHOLZE, F., JUÁREZ, J., GALOBART, A. and FORTUNY, J. 2021. Early–Middle Triassic fluvial ecosystems of Mallorca (Balearic Islands): biotic communities and environmental evolution in the equatorial western peri-Tethys. *Earth-Science Reviews*, **222**, 103783.

NEL, A., PAPIER, F., GRAUVOGEL-STAMM, L. and GALL, J.-C. 1996. *Voltzialestes triasicus* gen. nov., sp. nov., le premier Odonata Protozygoptera du Trias inferieur des Vosges (France). *Paleontologia Lombarda della Societa Italiana di scienze Naturali e del Museo, Civico di Storia Naturale di Milano (n.s.)*, **5**, 25–35.

NOLTE, U. 1993. Egg masses of Chironomidae (Diptera). A review, including new observations and a preliminary key. *Entomologica Scandinavia Supplement*, **43**, 1–75.

OGG, J. G., CHEN, Z. -Q., ORCHARD, M. J. and JIANG, H. S. 2020. The Triassic period. 903–953. *In* GRADSTEIN,

F. M., OGG, J. G., SCHMITZ, M. D. and OGG, G. M. (eds) *Geologic time scale 2020*. Elsevier, 1357 pp.

OLIVER, D. R. 1981. CHIRONOMIDAE. 423–458. *In* McALPINE, J. F. (ed.) *Manual of Nearctic Diptera. Vol. 1*. Research Branch Agriculture Canada, **27**, cap. 29, 674 pp.

OOSTERBROEK, P. and COURTNEY, G. 1995. Phylogeny of the nematocerous families of Diptera (Insecta). *Zoological Journal of the Linnean Society*, **115**, 267–311.

PEÑALVER, E. 2002. *Los insectos dípteros del Mioceno del Este de la Península Ibérica; Rubielos de Mora, Ribesalbes y Bicorp. Tafonomía y sistemática*. PhD thesis, Universitat de València, Valencia, 548 pp.

PEÑALVER, E. and GAUDANT, J. 2010. Limnic food web and salinity of the Upper Miocene Bicorb palaeolake (eastern Spain). *Palaeogeography, Palaeoclimatology, Palaeoecology*, **297**, 683–696.

PEÑALVER, E. and PÉREZ-DE LA FUENTE, R. 2014. Unearthing the secrets of ancient immature insects. *eLife*, **3**, e03443.

PEÑALVER, E., MATAMALES-ANDREU, R., JUÁREZ RUIZ, J., NEL, A., LOZANO, R. P. and PÉREZ-DE LA FUENTE, R. in press. Early detritivory and sedimentivory in insects based on *in situ* gut contents from Triassic aquatic nymphs. *Papers in Palaeontology*. https://doi.org/10.1002/spp2.1478

PETERSON, B. V. 1981. Anisopodidae. 305–312. *In* McALPINE, J. F., PETERSON, B. V., SHEWELL, G. E., TESKEY, H. J., VOCKEROTH, J. R. and WOOD, D. M. (coors.) *Manual of Nearctic Diptera, Vol. 1*. Agriculture Canada Monograph 27, 674 pp.

PINDER, L. C. V. 1995. Biology of the eggs and first-instar larvae. 87–106. *In* ARMITAGE, P. D., CRANSTON, P. S. and PINDER, L. C. V. (eds) *The Chironomidae: Biology and ecology of non-biting midges*. Springer Science, 572 pp.

RICHARDS, O. W. and DAVIES, R. G. 1977. *Imms' general textbook of entomology. Vol. 2, classification and biology*. Tenth edition. Springer, 1354 pp.

SAETHER, O. A. 1997. Diptera Chaoboridae, phantom midges. 149–161. *In* NILSSON, A. (ed.) *Aquatic insects of North Europe: A taxonomic handbook. Vol. 2. Odonata-Diptera*. Apollo Books, 440 pp.

SCHINER, J. R. 1862. Heft 8 (part). *In Fauna Austriaca. Die Fliegen (Diptera). Theil 1*. Carl Gerolds Sohn, Wien, i–lxxx + 657–674.

SCHOLZE, F. and MATAMALES-ANDREU, R. 2021. Triassic clam shrimps ("Conchostraca"; Branchiopoda: Diplostraca) from Mallorca: taxonomic description and interregional comparisons. *Zootaxa*, **4964**, 471–496.

ŠEVČÍK, J., KASPŘÁK, D., MANTIČ, M., FITZGERALD, S., ŠEVČÍKOVÁ, T., TÓTHOVÁ, A. and JASCHHOF, M. 2016. Molecular phylogeny of the megadiverse insect infraorder Bibionomorpha *sensu lato* (Diptera). *PeerJ*, **4**, e2563.

SHCHERBAKOV, D. E., LUKASHEVICH, E. D. and BLAGODEROV, V. A. 1995. Triassic Diptera and initial radiation of the order. *Dipterological Research*, **6**, 75–115.

SINITSHENKOVA, N. D. 2003. Main ecological events in aquatic insects history. *Acta Zoologica Cracoviensia*, **46**, 381–392.

SINITSHENKOVA, N. D., MARCHAL-PAPIER, F., GRAUVOGEL-STAMM, L. and GALL, J. -C. 2005. The Ephemeridea (Insecta) from the Grès à Voltzia (early Middle Triassic) of the Vosges (NE France). *Paläontologische Zeitschrift*, **79**, 377–397.

SMITH, K. G. V. 1989. *An introduction to the immature stages of British flies. Diptera larvae, with notes on eggs, puparia and pupae. Handbooks for the identification of British Insects*, **10**. Royal Entomological Society of London (14), 280 pp.

STEHR, F. W. (ed.) 1991. *Immature insects. Vol. 2*. Kendall/Hunt, 992 pp.

TESKEY, H. J. 1981. Morphology and terminology: larvae. 65–87. *In* McALPINE, J. F., PETERSON, B. V., SHEWELL, G. E., TESKEY, H. J., VOCKEROTH, J. R. and WOOD, D. M. (coordinators). *Manual of Nearctic Diptera, 1*. Research Branch, Agricultural Canada Monograph, Ottawa, Ontario, 27, 674 pp.

WANG, B., XIA, F., WAPPLER, T., SIMON, E., ZHANG, H., JARZEMBOWSKI, E. A. and SZWEDO, J. 2015. Brood care in a 100-million-year-old scale insect. *eLife*, **4**, e05447.

WOJTOŃ, M., KANIA, I., KRZEMIŃSKI, W. and DONG, R. 2019. Phylogenetic relationships within the superfamily Anisopodoidea (Diptera: Nematocera), with description of new Jurassic species. *Palaeoentomology*, **2**, 119–139.

WOODLEY, N. E. 1989. Phylogeny and classification of the "orthorrhaphous" Brachycera. 1371–1396. *In* McALPINE, J. F. and WOOD, D. M. (eds) *Manual of Nearctic Diptera. Vol. 3*. Agriculture Canada Monograph 32, 248 pp.

ZESSIN, W. 2008. Neue Insekten aus der Unteren Trias (Buntsadstein) von Mallorca, Spanien (Blattaria, Coleoptera, Diptera, Heteroptera, Orthopteroidea und Homoptera). *Virgo, Mitteilungsblatt des Entomologischen Vereins Mecklenburg*, **11**, 99–101.

ZHERIKHIN, V. V. 2002. Ecological history of terrestrial insects. 331–388. *In* RASNITSYN, A. P. and QUICKE, D. L. J. (eds) *History of insects*. Kluwer Academic Publishers, 517 pp.

SUPPORTING INFORMATION

Early adaptations of true flies (Diptera) to moist and aquatic continental environments

by Enrique Peñalver, Rafel Matamales-Andreu, André Nel *and* Ricardo Pérez-de la Fuente

Figures S1, S2

Fig. S1. Additional microphotographs of the Triassic terrestrial larva *Protoanisolarva juarezi* gen. et sp. nov. (Diptera: Anisopodoidea, stem-group Anisopodidae), holotype DA21/03-02-9b, from Pedra Alta site, lower Anisian. **A**) Habitus and detail of head (dorsal surface, counterpart, DA21/03-02-91b). **C**) Detail of prothoracic structures. **D**) Remains in counterpart of posterior spiracle pair showing well-preserved, circular primary openings in the posterior margin of one of them. **E**) Detail of posterior extremity of body. Photographs B and C were obtained from consecutive pictures taken at successive focal planes, and specimen photographed moistened with a mixture of alcohol and water except for A. Abbreviations: a = anterior part, p = posterior part. Scale bars represent: 1 mm (A); 0.1 mm (B, C, E); 0.05 mm (D).

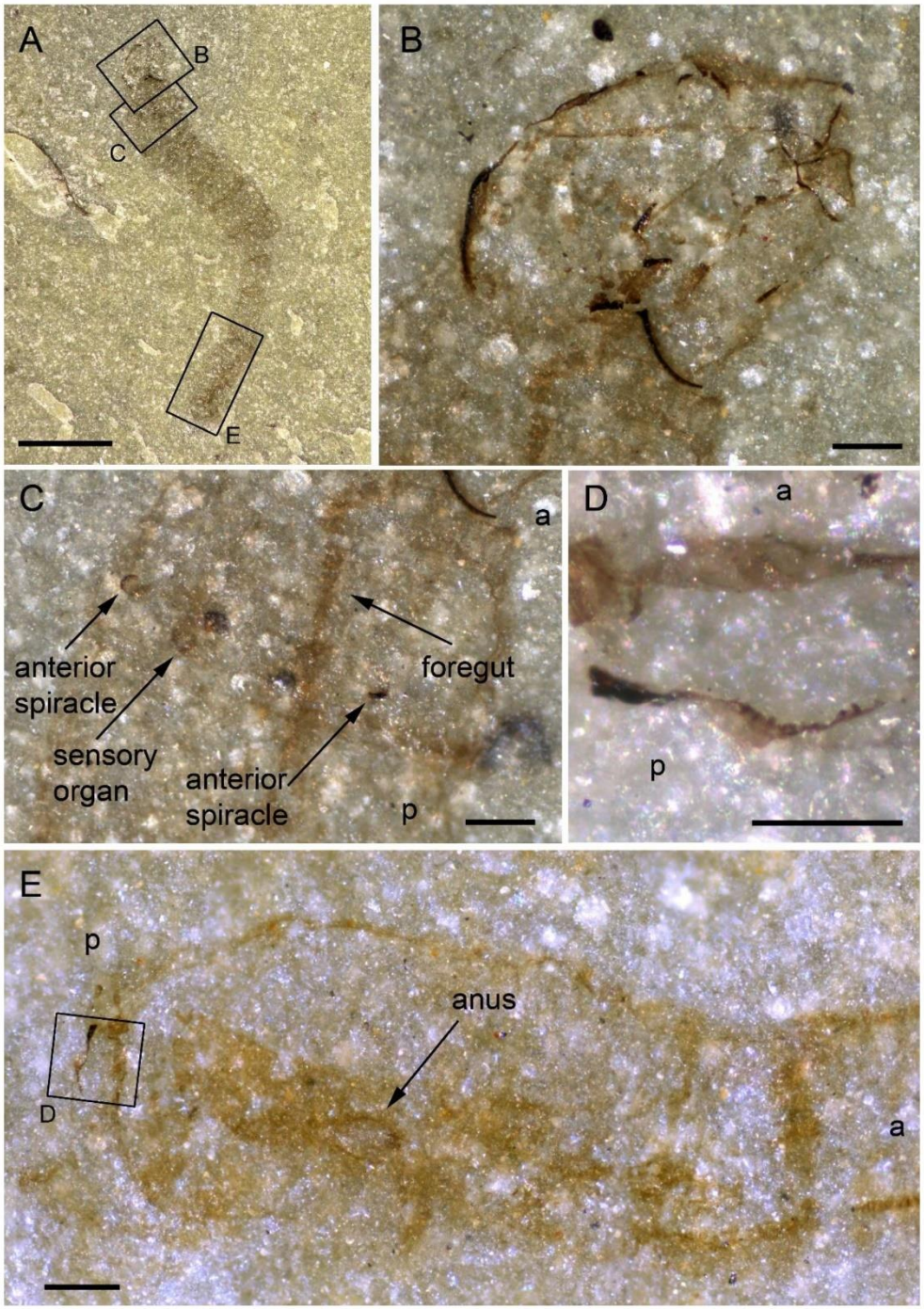
A
B
C
E
B
C
a
anterior
spiracle
foregut
sensory
organ
anterior
spiracle
p
D
a
p
E
p
anus
D
a

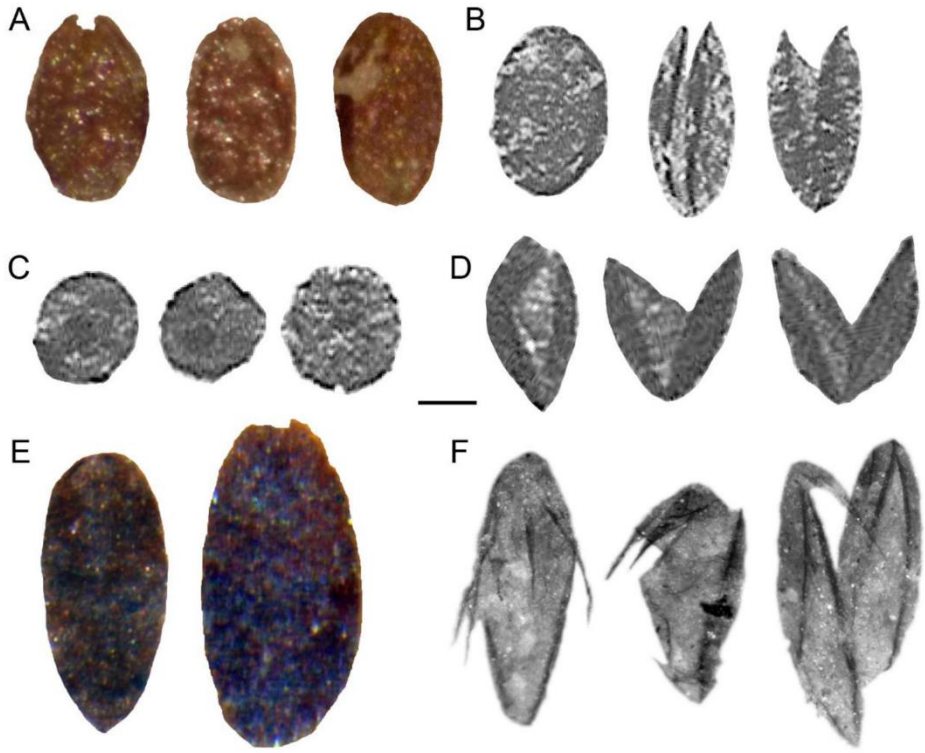

Fig. S2. Putative Mesozoic and Cenozoic nematoceran eggs (A–D and F have been tentatively attributed to Chironomidae, E to Chaoboridae) from egg clusters present in a mucilaginous matrix (except to E, apparently, but eggs of the same morphotype recorded in mucilaginous matrices in the same outcrop). **A**) Three unhatched eggs of *Clavapartus latus* from the only egg cluster found in Pedra Alta site (Triassic: Anisian). **B**) Three hatched eggs of *Clavapartus latus* from 'Grès à Voltzia' (Triassic: Anisian). **C–D**) Unhatched (C) and hatched (D) eggs of *Monilipartus tenuis* from 'Grès à Voltzia' (Triassic: Anisian). **E**) Eggs apparently unhatched and attributed to a new species of *Chaoborus* (Chaoboridae) (middle Eocene), but most likely of Chironomidae. **F**) Four hatched eggs from an egg cluster attributed to Chironomidae found in the Rubielos de Mora outcrop (Miocene: Burdigalian). B–D modified from Gall & Grauvogel (1966), E modified from Baranov *et al.* (2022), and F modified from (Peñalver 2002). Scale bar represents: 0.1 mm; all to the same scale.

References

BARANOV, V. A., HAUG, J. T., GREENWALT, D. E. and HARBACH, R. 2022. A vanished ecosystem: diversity of culicomorphan dipterans in the Eocene Kishenehn Konservat-Lagerstätte (Montana, USA) and its palaeoecological implications. *Palaeontologia Electronica*, **25**(1), a4. https://doi.org/10.26879/1165

GALL, J. -C. and GRAUVOGEL, L. 1966. Faune du Buntsandstein. I. – Pontes d´invertébrés du Buntsandstein supérieur. *Annales de Paléontologie (Invertébrés)*, **LII**(2), 155–161, 5 plates.

PEÑALVER, E. 2002. *Los insectos dípteros del Mioceno del Este de la Península Ibérica; Rubielos de Mora, Ribesalbes y Bicorp. Tafonomía y sistemática*. Published PhD thesis, Universitat de València, Valencia, 548 pp.

Appendix 11

Triassic marine molluscs from Mallorca

Appendix 11 was published as:

Juárez-Ruiz, J. & **Matamales-Andreu, R.** (2021). Mollusca (Ammonoidea, Gastropoda, Bivalvia) from the upper Ladinian (Middle Triassic) of the island of Mallorca (Balearic Islands, western Mediterranean): preliminary data. *Ciências da Terra Procedia*, 1(2021): 21–24. [in Spanish]

DOI: https://doi.org/10.21695/cterraproc.v1i0.397

In this work, R. Matamales-Andreu contributed in:

A. Review and editing of the manuscript.
B. Preparation of all the figures (1–2).

CIÊNCIAS DA TERRA PROCEDIA
EARTH SCIENCES JOURNAL

Check for updates

OPEN ACCESS

Mollusca (Ammonoidea, Gastropoda, Bivalvia) from the upper Ladinian (Middle Triassic) of the island of Mallorca (Balearic Islands, western Mediterranean): preliminary data

Mollusca (Ammonoidea, Gastropoda, Bivalvia) del Ladiniense superior (Triásico Medio) de la isla de Mallorca (Islas Baleares Mediterráneo occidental): datos preliminares

J. Juárez-Ruiz[1] & R. Matamales-Andreu[1, 2]

[1] Museu Balear de Ciències Naturals. Carretera Palma-Sóller km30, 07100, Sóller, Spain.
[2] Institut Català de Paleontologia Miquel Crusafont. C/ de les Columnes s/n, Edifici Z (ICTA-ICP), Campus de la Universitat Autònoma de Barcelona. 08193 Cerdanyola del Vallès, Spain.

Corresponding author:
J. Juárez-Ruiz
nite1988@hotmail.com

Journal webpage:
http://cienciasdaterra.novaidfct.pt/

Copyright:
© 2021 J. Juárez-Ruiz & R. Matamales-Andreu. This is an open access article distributed under the terms and conditions of the Creative Commons Attribution License (CC BY), which permits unrestricted use, distribution, and reproduction in any medium, provided the original author and source are credited.

ISSN: 0254 - 055X
eISSN: 2183 - 4431

Abstract

A group of fossil molluscs with silicified presevation from the Muschelkalk facies (Middle Triassic) of the southwest of Serra de Tramuntana (Mallorca, western Mediterranean), is studied. Due to the biostratigraphical significance of its ammonoids, upper Ladinian is characterized for the first time on the island. In a similar way, the biogeographical context of the area during this interval is analyzed using the ammonoid, gastropoda and bivalvia records in a preliminary approach.

Keywords: Ladinian, ammonoid, bivalve, gastropod, Mallorca.

1. Introducción

Las llamadas facies Muschelkalk corresponden generalmente a ambientes de extensas plataformas carbonáticas desarrolladas durante el Anisiense y el Ladiniense (Triásico Medio). Son el reflejo de ciclos transgresivo-regresivos del mar Neotethys, que inundó paulatinamente grandes extensiones continentales debido a la fragmentación del supercontinente Pangea (Pérez-Valera, 2005). Yacimientos con restos macropaleontológicos en estos episodios son bien conocidos en diversos puntos de Iberia, habiéndose documentado, en el ámbito Balear, en Menorca (Bourrouilh, 1973; Escudero-Mozo *et al.*, 2014, entre otros), Ibiza (Rangheard, 1972) y Mallorca. En lo referente a ésta última, el Muschelkalk es conocido desde el siglo XIX (Hermite, 1879; Nolan, 1887). Durante la primera mitad del siglo siguiente no faltan estudios que dan a conocer una fauna puntualmente rica, compuesta fundamentalmente por moluscos y braquiópodos (Darder, 1914; Fallot, 1922; Schmidt, 1929; Bauzá, 1946) si bien existen aislados hallazgos de vertebrados (Bauzá, 1955). Tiempo después (Rotger, 1952; Virgili, 1952; Bauzá, 1981), se documentan escasos pero relevantes ammonoideos revisados posteriormente en algunos trabajos (Goy, 1986, 1995; Rein, 2008; Pérez-Valera & Goy, 2012; Pérez-Valera, 2016). De estas revisiones se describe la especie *Gevanites virgiliae* (Goy, 1986), del Ladiniense inferior.

A pesar de todas estas contribuciones, el Muschelkalk de Mallorca está falto de estudios recientes que caractericen pormenorizadamente con metodología actualizada su geología y paleontología. En esta breve comunicación se aportan de forma meramente preliminar datos relevantes sobre hallazgos inéditos de una etapa de la historia geológica de la isla aún poco conocida.

El afloramiento aquí estudiado se situa en el municipio de Puigpunyent, en el sector sudoeste de la Serra de Tramuntana, Mallorca (Fig. 1). Consiste en una extensa serie de 150 m de calizas y calizas dolomíticas de plataforma proximal con presencia de ripples y niveles intensamente bioturbados. De forma ocasional, aparecen macrorestos fósiles que son especialmente abundantes en la parte media de la secuencia. La práctica totalidad del registro observado corresponde a moluscos.

2. Material y métodos

El material estudiado proviene de las colecciones del MBCN (Museu Balear de Ciències Naturals), donde está depositado. Para una óptima observación del mismo se ha realizado a los ejemplares más representativos una preparación química a base de ácido acético al 10%, aprovechando la preservación silicificada de los fósiles.

Las divisiones paleobiogeográficas y la biozonación siguen la nomenclatura de Escudero-Mozo *et al.* (2015) y Pérez-Valera (2016). Para la determinación de los ejemplares, además de las fuentes mencionadas, se ha recurrido a Goy (1986, 1995), Tozer (1994) y Bandel (2007).

3. Resultados

El estudio de un afloramiento del Muschelkalk en la región de Puigpunyent y la revisión de su fauna han permitido por vez primera documentar bioestratigráficamente la presencia del Ladiniense superior en el registro geológico de la isla. Los ammonites por ahora identificados (*Protrachyceras hispanicum* Mojsisovics, *Iberites pradoi* Mojsisovics, *Anolcites doleriticus* Mojsisovics, *Thanamites* cf. *schooleri* McLearn y *Nannites* sp.) corresponden en su totalidad a nuevas citas para el registro de la isla, así como la mayor parte de sus gasterópodos (*Naticopsis* sp., *Cassianopsis* aff. *ornata* Münster, *Loxonema* sp.) y bivalvos (*Pseudocorbula gregaria* Münster, *Modiolus* cf. *myconchaeformis* Phillipp) (Fig. 2).

4. Discusión y conclusiones

La presencia de *Protrachyceras hispanicum* e *Iberites pradoi*, observados en asociación, denota claramente una afinidad del Ladiniense superior mallorquín (bizona Hispanicum) con el Triásico Mediterráneo, en el cual ambas especies están bien documentadas (Goy, 1995; Escudero-Mozo *et al.*, 2014, 2015). En cambio, *Anolcites doleriticus* (coincidente estratigráficamente en el afloramiento con los taxones anteriores), taxón poco conocido en Iberia (parte interna de las Béticas) (Goy *et al.*, 2005), es propio del dominio del Tethys (=Dominio Alpino). Este carácter alóctono sugiere una conexión entre éste y la Mediterránea a inicios del Ladiniense superior, ya documentada en trabajos previos (Pérez-Valera, 2016). Ello contrasta con el hasta ahora único conjunto faunístico de ammonoideos del Triásico mallorquín descrito, que pertenece exclusivamente al género *Gevanites*, taxón típico de la provincia Sefardí (Escudero-Mozo *et al.*, 2015; Pérez-Valera, 2016).

Del conjunto de ammonoideos tratado en este trabajo la especie con mayor abundancia relativa es *Thanamites* cf. *schooleri*. Este hecho contrasta fuertemente con la aparente gran rareza de formas de este género documentado desde Canadá hasta la India (Tozer, 1994) y en el Triásico de la Península Ibérica (Goy, 1995; Pérez-Valera, 2016). Los ejemplares de Puigpunyent estudiados en el presente trabajo y pertenecientes al citado taxón podrían tener relación con los previamente documentados, si bien su

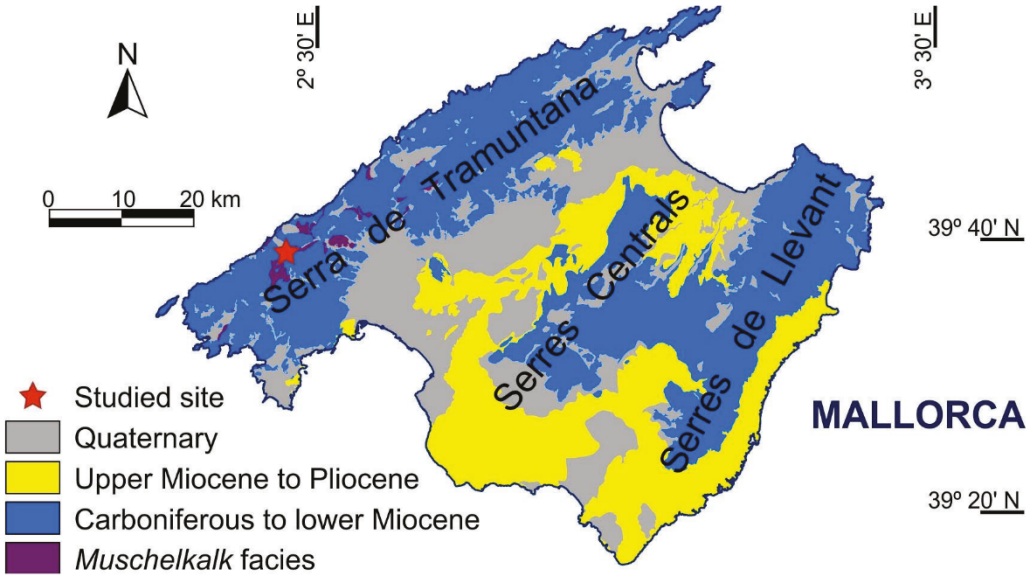

Fig. 1. -Geological map of Mallorca with the location of studied outcrop (red star).

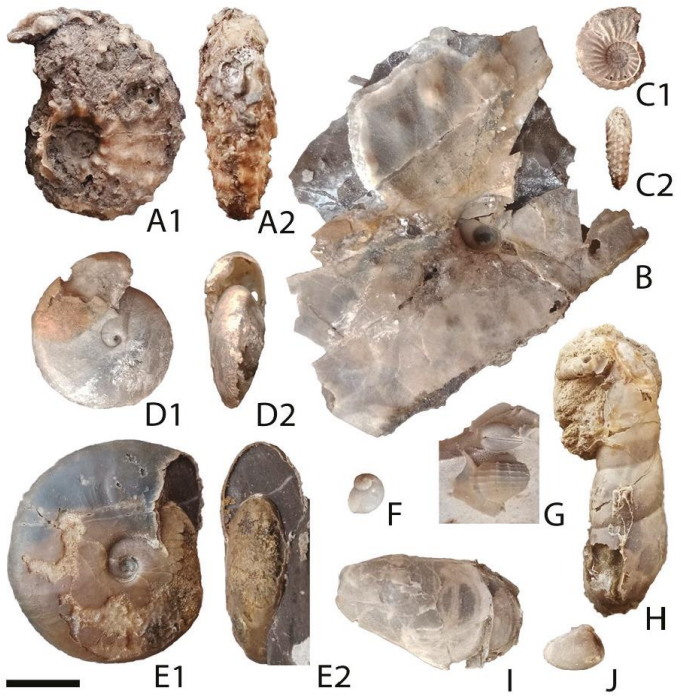

Fig. 2. -Upper Ladinian Mollusca from Puigpunyent outcrop. A- *Protrachyceras hispanicum* (MBCN23365); B- *Iberites pradoi* (MBCN23363); C- *Anolcites doleriticus* (MBCN23369); D- *Thanamites* cf. *schooleri* (MBCN23364); E- *Nannites* sp. (MBCN23360); F- *Naticopsis* sp.(MBCN23368); G- *Cassianopsis* aff. *ornata* (MBCN23362; H- *Loxonema* sp. (MBCN23361); I- *Modiolus* cf. *myconchaeformis* (MBCN23366); J- *Pseudocorbula gregaria* (MBCN23367). Scale bar: 1 cm.

estudio pormenorizado queda pendiente para futuros trabajos. La última especie de este grupo, *Nannites* sp., es un ammonoideo escasamente documentado en el registro de Iberia y Baleares, citándose en Menorca (Goy, 1995). De este taxón únicamente ha sido identificado un solo ejemplar proveniente de Puigpunyent. Estos últimos ammonites también coinciden estratigráficamente en el rango dado en el afloramiento por *P. hispanicum*.

En referencia a los bivalvos, los de mayor abundancia relativa son los taxones cosmopolitas *Pseudocorbula gregaria*, típica del Triásico Mediterráneo, y *Modiolus* cf. *myconchaeformis*, ligada al Triásico Alpino (Escudero-Mozo *et al.*, 2015). Concerniente a la fauna de gasterópodos, *Cassianopsis* aff. *ornata* indica un estrecha relación con dominio del Tethys (Bandel, 2007). Igualmente, existen entre este último grupo taxones de carácter más cosmopolita como *Loxonema* sp. y *Naticopsis* sp. (Bandel, 2007; Escudero-Mozo *et al.*, 2015).

En conclusión, la fauna hasta hoy inédita de moluscos del Ladiniense de Puigpunyent estudiada en el presente trabajo denota la presencia de taxones de diferentes dominios paleogeográficos en el registro del Ladiniense superior mallorquín. Este carácter mixto de su fauna pone de manifiesto que la zona pasó de ser parte del dominio Sefardí durante el Ladiniense inferior a una conexión entre el dominio del Tethys y el Triásico mediterráneo a inicios del superior, si bien con presencia de elementos cosmopolitas.

Agradecimientos

Los autores del presente estudio agradecemos a Joan Arbona (MBCN) y Vicenç Pla, descubridores del yacimiento, su disposición a la hora de comunicar su existencia. A ellos, a Sebastià Matamalas y a Núria Navarro, también agradecemos su inestimable ayuda en el trabajo de campo. Finalmente, agradecemos también el trabajo crítico de los revisores Juan Alberto Pérez-Valera (Universitat d'Alacant) y Ana Márquez-Aliaga (Universitat de València), que contribuyeron a la mejora del manuscrito.

Referencias

Bandel K. (2007) - Description and classification of Late Triassic *Neritimorpha* (Gastropoda, Mollusca) from the St Cassian Formation, Italian Alps. *Bull. Geosci.* 82(3), 215–274.

Bauzá J. (1946) - Nuevo yacimiento fosilífero en el Trias de la Sierra Norte de Mallorca. *Bol. Soc. Esp. Hist. Nat.* XLIV,

335.

Bauzá J. (1955) - Notas paleontológicas de Mallorca: sobre el hallazgo del «*Nothosaurus*» en el Trias. *Bol. Soc. Hist. Nat. Baleares* 1, 87.

Bauzá J. (1981) - Contribuciones a la paleontología de Mallorca. *Boll. Soc. Hist. Nat. Balears.* 25, 7–19.

Bourrouilh R. (1973) - *Stratigraphie, sedimentologie, et tectonique de l'ille de Minorque et du Nord-Est de Majorque (Baleares)*, PhD Thesis. Université Pierre et Marie Curie, 822 p.

Darder B. (1914) - El Triásico de Mallorca. Trabajos del Museo Nacional de Ciencias Naturales. *Sección Geológica* (7), 85 p.

Escudero-Mozo M. J., Márquez-Aliaga A., Goy A., Martín-Chivelet J., López-Gómez J., Márquez L., Arche A., Plasencia P., Pla C., Marzo M. & Sánchez-Fernández D. (2015) - Middle Triassic carbonate platforms in eastern Iberia: Evolution of their fauna and palaeogeographic significance in the western Tethys. *Palaeogeogr. Palaeoclimatol. Palaeoecol.* 417, 236–260.

Escudero-Mozo M. J., Martín-Chivelet J., Goy A. & López-Gómez J. (2014) - Middle-Upper Triassic carbonate platforms in Minorca (Balearic islands): implications for Western Tethys correlations. *Sediment. Geol.* 310, 41–58.

Fallot P. (1922) - *Étude Géologique de la Sierra de Majorque.* Librairie Polytechnique Ch. Béranger, Paris and Liège, 509 p.

Goy A. (1986) - *Ammonoideos del Triásico de España.* Cathedra Thesis, Universidad Complutense de Madrid, 28 p.

Goy A. (1995) - Ammonoideos del Triásico Medio de España: Bioestratigrafía y Correlaciones. *Cuadernos de Geología Ibérica* 19, 21–60.

Goy A., Pérez-López A. & Pérez-Valera F. (2005) - Ammonoideos del Ladiniense en la Unidad de Cabo Cope (zonas internas, Cordillera Bética). *Geo-Temas* 8, 179–182.

Hermite H. (1879) - *Études géologiques sur les îles Baléares. Première partie: Majorque et Minorque*. Pichon et Savy, Paris, 367 p.

Nolan H. (1887) - Note sur le Trias de Minorque et Majorque. *Bulletin Societe Géologique de France* 3(XV), 593–599.

Pérez-Valera F. (2005) - *Estratigrafía y Tectónica del Triásico Sudibérico en el sector oriental de la Cordillera Bética.* PhD Thesis, Universidad de Granada, 237 p.

Pérez-Valera J. A. (2005) - Ammonoideos y bioestratigrafía del Triásico Medio (Anisiense superior-Ladiniense) en la sección de Calasparra (sector oriental de la Cordillera Bética, Murcia, España). *Coloquios de Paleontología* 55, 125–161.

Pérez-Valera J. A. (2016) - *Ammonoideos y bioestratigrafía del Triásico Medio (Ladiniense) del sector oriental de la Cordillera Bética*. PhD Thesis, Univiversidad Complutense de Madrid, 489 p.

Pérez-Valera J. A. & Goy A. (2012) - Ammonoideos del Triásico Medio (Ladiniense) de la Isla de Mallorca. *In:* Liao, J. C., Gámez Vintaned, J. A., Valenzuela-Rios, J. I. & García-Forner, A. (Eds.), *XXVIII Jornadas de La Sociedad Española de Paleontología y Simposios de Los Proyectos No 587 Y 596 Del PICG*. Libro de Resúmenes, Valencia y Sóller, 179– 182.

Rangheard Y. (1972) - *Étude géologique des îles d'Ibiza et da Formentera (Baleares)*. Memorias del Instituto Geológico Minero de España 82, 340 p.

Rein S. (2008) - *Ceratites atavus* auf Mallorca? Die Muschelkalk ammonoideen des Museu Balear de Sciencies Naturals Sóller. *Vernate*, 27, 5–19.

Rotger P. (1952) - Hallazgo de un ammonite tipo *Ceratites* en el Muschelkalk de Canet (Esporlas). *Boll. Soc. Hist. Nat. Balears, January-February 1952,* 1, 6.

Schmidt M. (1929) - Newe funde in der Iberish-Balearischen Trias. *Preuss. Akademie der Wiss.* 25, 16–32.

Tozer E. T. (1994) - Canadian Triassic ammonoid faunas. *Geol. Surv. Can. Bull.* 467, 1–663.

Virgili C. (1952) - Hallazgo de nuevos *Ceratites* en el Triásico Mallorquín. *Memorias y Comunicaciones del Instituto Geológico Provincial* 9, 19–39.

Appendix 12

Supplementary Material, Permian of Menorca

Appendix 12 was published as the supplementary material of:

Matamales-Andreu, R.; Roig-Munar, F.X.; Oms, O.; Galobart, À. & Fortuny, J. (2021). A captorhinid-dominated assemblage from the palaeoequatorial Permian of Menorca (Balearic Islands, western Mediterranean). *Earth and Environmental Science Transactions of the Royal Society of Edinburgh*, 112(2): 125–145.

DOI: https://doi.org/10.1017/S1755691021000268

Also, refer to:

Chapter 5: Matamales-Andreu *et al.* (2021), *Earth and Environmental Science Transactions of the Royal Society of Edinburgh*

A captorhinid-dominated assemblage from the palaeoequatorial Permian of Menorca (Balearic Islands, western Mediterranean)

Rafel Matamales-Andreu[1,2]*, Francesc Xavier Roig-Munar[3], Oriol Oms[4],

Àngel Galobart[1,5] & Josep Fortuny[1]

[1] Institut Català de Paleontologia Miquel Crusafont. Carrer de les Columnes s/n, Edifici Z (ICTA-ICP), Campus de la Universitat Autònoma de Barcelona. 08193, Cerdanyola del Vallès. Barcelona, Catalunya, Spain.

[2] Museu Balear de Ciències Naturals. Carretera Palma–Port de Sóller Km. 30. 07100, Sóller. Mallorca, Illes Balears, Spain.

[3] Carrer Carritxaret 18-6. 07749, es Migjorn Gran. Menorca, Illes Balears, Spain.

[4] Departament de Geologia, Universitat Autònoma de Barcelona. Avinguda de l'eix Central s/n, Campus de la Universitat Autònoma de Barcelona. 08193, Cerdanyola del Vallès. Barcelona, Catalunya, Spain.

[5] Museu de la Conca Dellà. Carrer del Museu 4. 25650, Isona i Conca Dellà. Lleida, Catalunya, Spain.

*Corresponding author. E-mail address: rafel.matamales@icp.cat.

Supplementary Table 1. Lithofacies of Cala del Pilar–Pla de Mar section.

Code	Lithofacies	Sedimentary structures, processes and fossil content
Gt	Stratified, matrix to clast-supported, gravel to pebble-sized breccia (with rounded clasts and rhizocretion fragments) of reworked calcretes and intraformational clasts, and rarely extraformational clasts and tetrapod bones (as clasts).	Crude trough stratification. Usually not graded or imbricated. Sometimes with soft pebbles. It corresponds to 3D megaripples that rework the floodplain and levee palaeosols during sudden floods, or the basal lags of larger channels (Gómez-Gras & Alonso-Zarza, 2003). It sometimes contains tetrapod bones and bone fragments.
Gm	Massive, matrix to clast-supported, gravel to pebble-sized breccia (with rounded clasts and rhizocretion fragments) of reworked calcretes and intraformational clasts, and rarely extraformational clasts and tetrapod bones (as clasts).	Massive. Usually not graded or imbricated. Sometimes with soft pebbles. It corresponds to 3D megaripples that rework the floodplain and levee palaeosols during sudden floods, or the basal lags of larger channels (Gómez-Gras & Alonso-Zarza, 2003). It sometimes contains tetrapod bones and bone fragments.
GmP	Stratified, clast-supported, pebble to cobble-sized breccia (with occasionally rounded clasts) of extraformational clasts.	Crude trough stratification. Not graded or imbricated. Large rhizocretions. It corresponds to high density flows near the footwall scarp of the basin, mixing autochthonous and allochtonous clasts (Gómez-Gras & Alonso-Zarza, 2003). It usually contains large rhizocretions.
St	Stratified, very fine to very coarse-grained sands.	Trough cross stratification. Sometimes with soft pebbles. It corresponds to sinuous or linguoid 3D megaripples of lower flow regime (Miall, 1985, 2006).
Sp	Stratified, medium-grained sands.	Planar cross stratification. It corresponds to transverse 2D megaripples of lower flow regime (Miall, 1985, 2006).
Sr	Stratified, very fine to medium-grained sands.	Ripple-marks, mostly climbing ripples. Sometimes convolute lamination. It corresponds to low regime flows, usually at the top of channel sequences or at crevasse splays (Miall, 1985). They can be affected by rapid suspension fall-out, thus generating water-escaping structures.
Sh	Stratified, very fine to fine-grained sands.	Horizontal stratification and lamination. It corresponds to planar bed flow of lower flow regime (Miall, 1985, Postma, 1990).
Sl	Stratified, very fine to fine-grained sands.	Low-angle cross stratification. Sometimes convolute lamination. It corresponds to crevasse splays (Miall, 1985).
Sm	Massive, very fine to very coarse-grained sands.	Massive. Sometimes soft pebbles. It corresponds to either sediment gravity flows or to heavily bioturbated sediments (Miall, 2006).
Sb	Massive to crudely stratified, very fine to medium-grained sands with bioturbation.	Lamination (almost) obliterated by roots or invertebrate burrows. It corresponds to the reworking of sand-sheet or overbank deposits (Linol *et al.*, 2009). The fossils present in this lithofacies are rhizocretions and bioturbation of the *Scoyenia* ichnofacies, including tetrapod footprints.
Fl	Laminated lutites.	Fine lamination, either horizontal, low angle or ripple lamination. It corresponds to overbank, abandoned channel or waning flood deposits (Miall, 2006).
Fm	Massive lutites.	Massive, sometimes with disperse clasts. Gleyed patches are usual. It corresponds to overbank, abandoned channel or drape deposits (Postma, 1990; Miall, 2006).
Fr	Massive lutites with root traces.	Numerous root traces. It corresponds to settled sediments and incipient palaeosols (Bercovici *et al.*, 2009).
Fb	Massive lutites with bioturbation.	Numerous invertebrate burrows (*Scoyenia* ichnofacies). It corresponds to the reworking of other lutitic lithofacies.
P	Lutites or sandstones with any lamination, with abundance of carbonate nodules, locally forming crusts.	Massive to laminated. Very abundant carbonate nodules, root traces and gleyed patches usual. It corresponds to palaeosols (Mack *et al.*, 1993; Gómez-Gras & Alonso-Zarza, 2003; Bercovici *et al.*, 2009).

Supplementary Logs (following pages). Detailed log of Cala del Pilar–Pla de Mar section (1:40 scale).

Log name: Cala del Pilar–Pla de Mar	Page 01/32
Location: Cala del Pilar–Muntanya Mala Section	

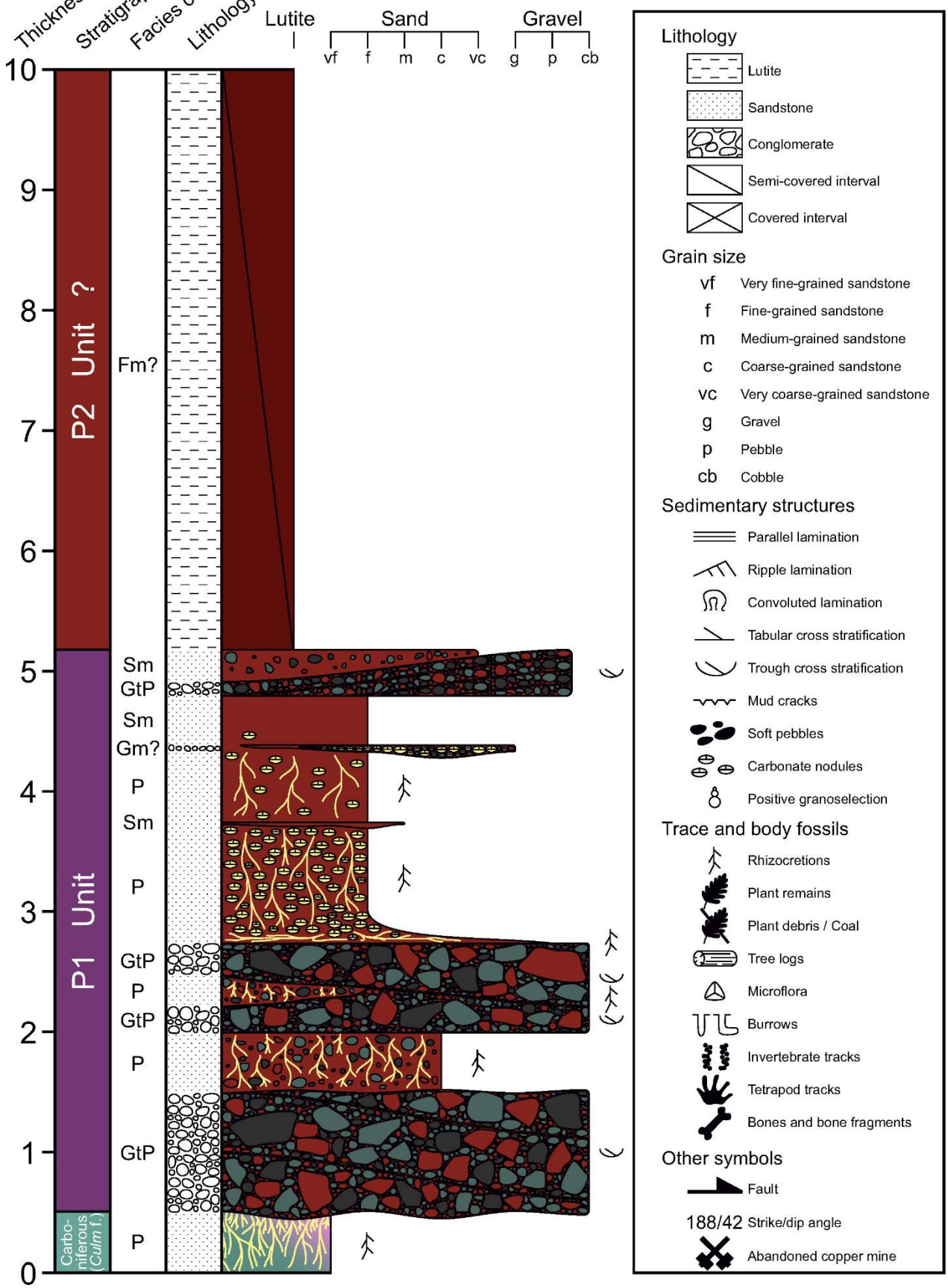

Log name: Cala del Pilar–Pla de Mar	Page 02/32
Location: Cala del Pilar–Muntanya Mala Section	

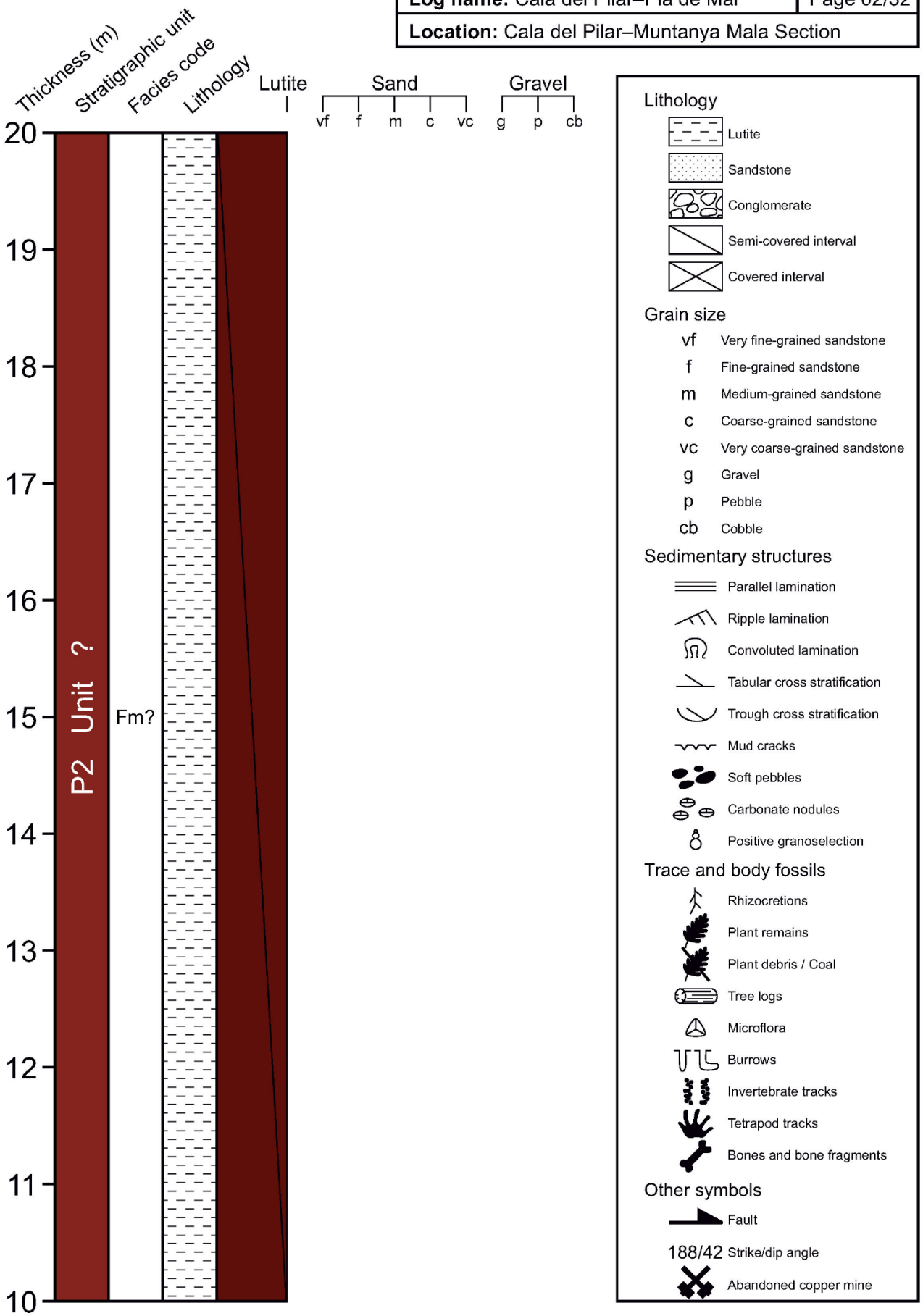

Log name: Cala del Pilar–Pla de Mar	Page 03/32
Location: Cala del Pilar–Muntanya Mala Section	

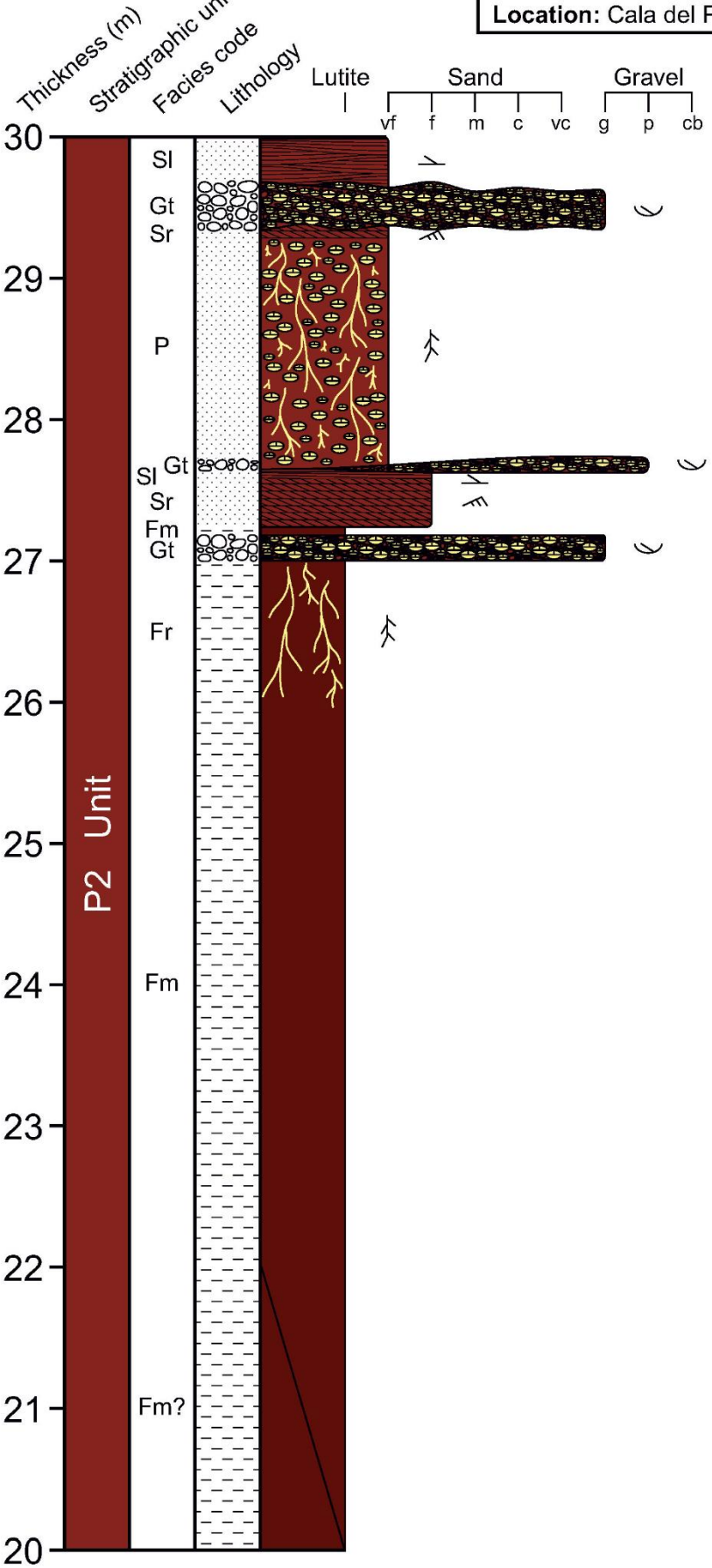

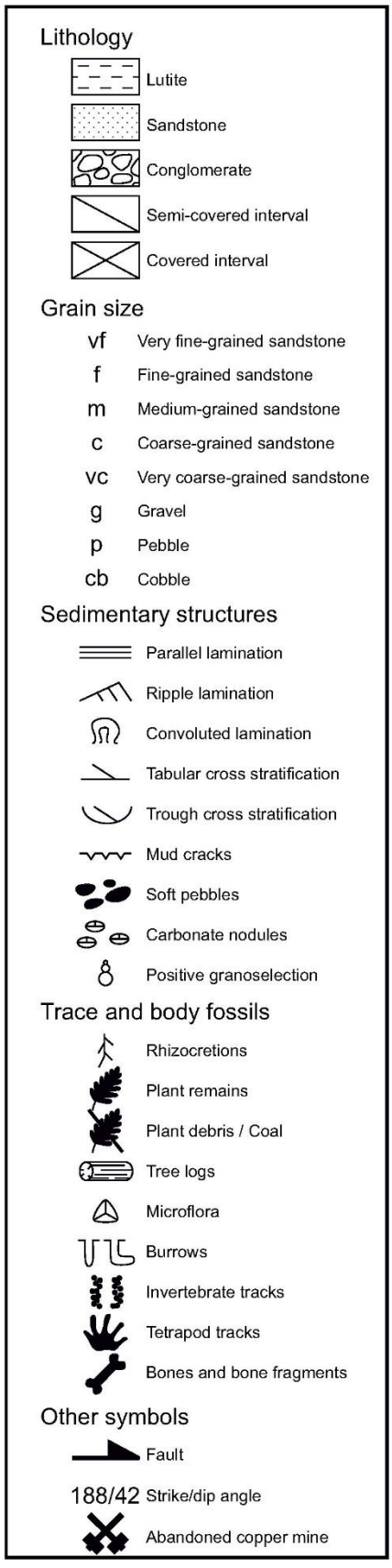

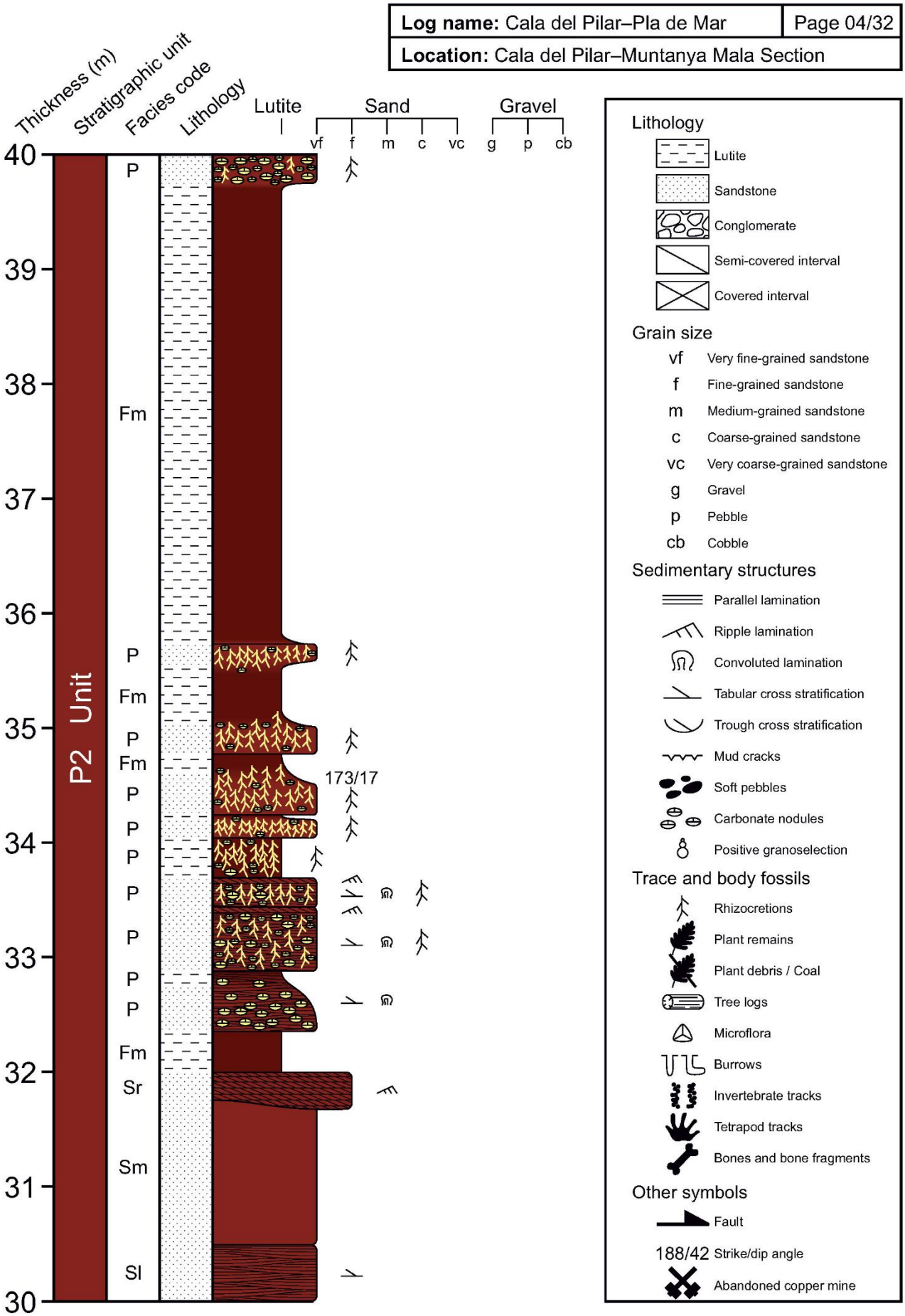
Log name: Cala del Pilar–Pla de Mar
Page 04/32
Location: Cala del Pilar–Muntanya Mala Section
Thickness (m)
Stratigraphic unit
Facies code
Lithology
Lutite
Sand
Gravel
vf f m c vc g p cb
40
39
38
37
36
35
34
33
32
31
30
P2 Unit
P
Fm
Sr
Sm
Sl
173/17
Lithology
Lutite
Sandstone
Conglomerate
Semi-covered interval
Covered interval
Grain size
vf Very fine-grained sandstone
f Fine-grained sandstone
m Medium-grained sandstone
c Coarse-grained sandstone
vc Very coarse-grained sandstone
g Gravel
p Pebble
cb Cobble
Sedimentary structures
Parallel lamination
Ripple lamination
Convoluted lamination
Tabular cross stratification
Trough cross stratification
Mud cracks
Soft pebbles
Carbonate nodules
Positive granoselection
Trace and body fossils
Rhizocretions
Plant remains
Plant debris / Coal
Tree logs
Microflora
Burrows
Invertebrate tracks
Tetrapod tracks
Bones and bone fragments
Other symbols
Fault
188/42 Strike/dip angle
Abandoned copper mine

Log name: Cala del Pilar–Pla de Mar	Page 05/32
Location: Cala del Pilar–Muntanya Mala Section	

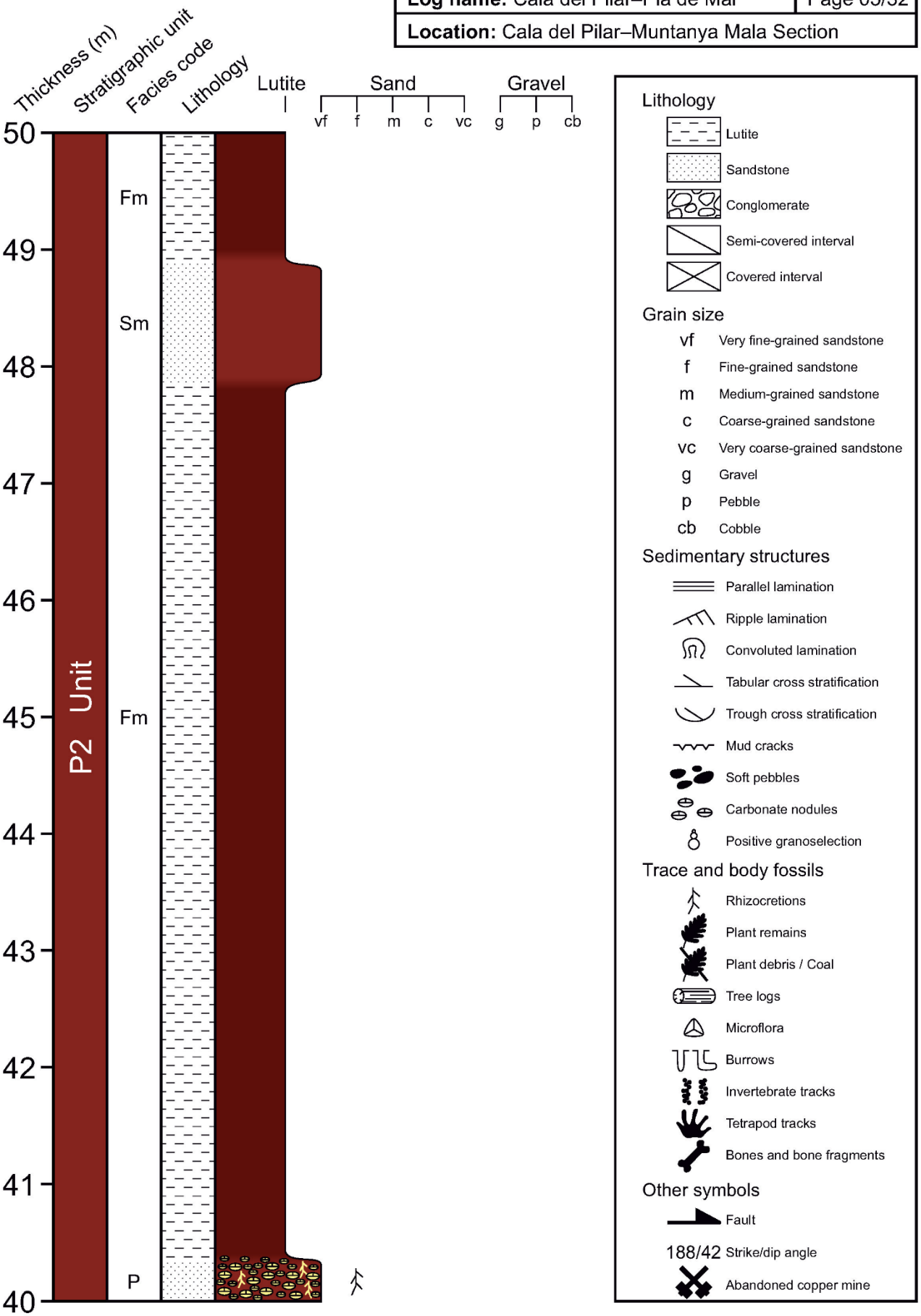

Log name: Cala del Pilar–Pla de Mar	Page 06/32
Location: Cala del Pilar–Muntanya Mala Section	

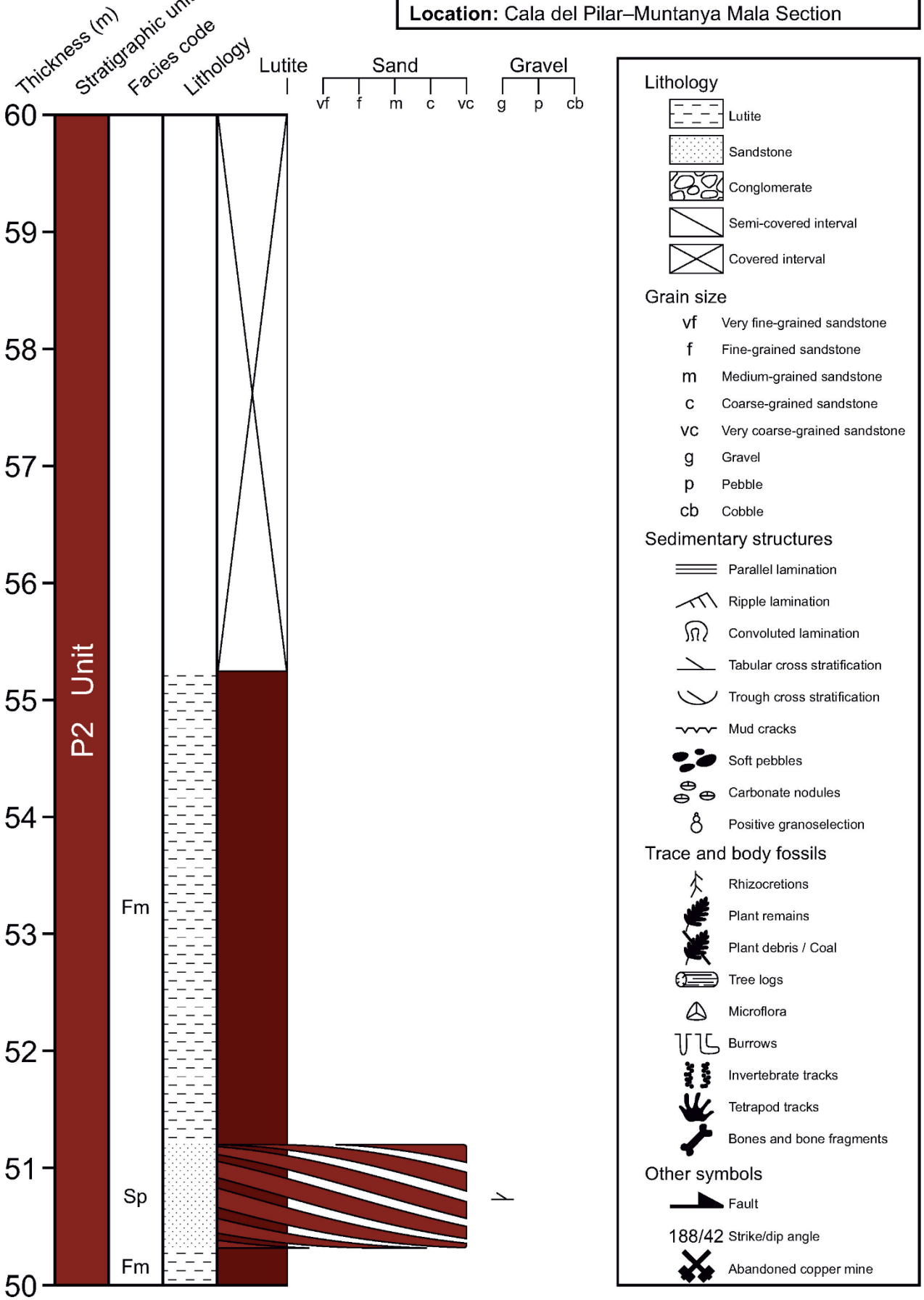

Log name: Cala del Pilar–Pla de Mar	Page 07/32
Location: Cala del Pilar–Muntanya Mala Section	

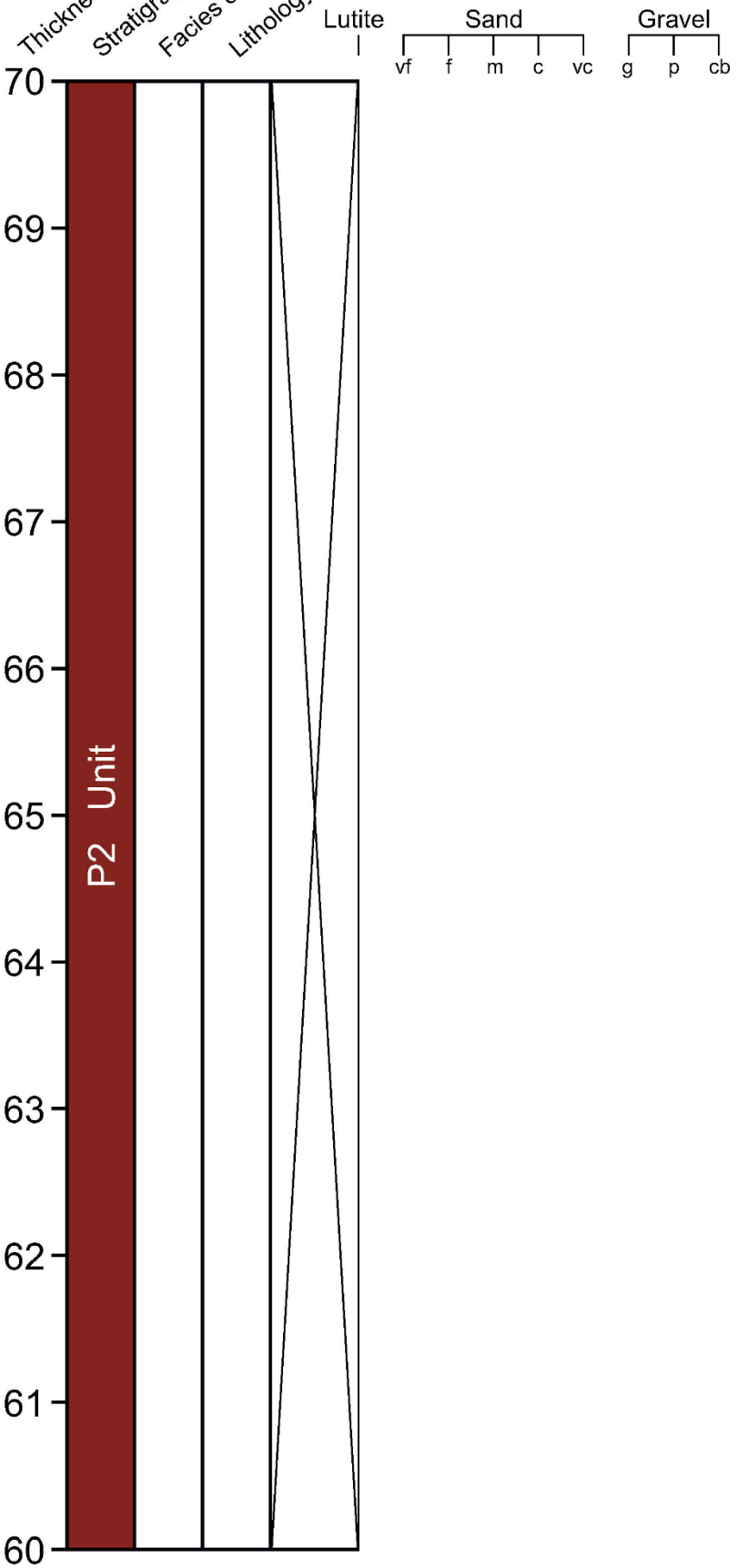

Lithology
- Lutite
- Sandstone
- Conglomerate
- Semi-covered interval
- Covered interval

Grain size
- vf Very fine-grained sandstone
- f Fine-grained sandstone
- m Medium-grained sandstone
- c Coarse-grained sandstone
- vc Very coarse-grained sandstone
- g Gravel
- p Pebble
- cb Cobble

Sedimentary structures
- Parallel lamination
- Ripple lamination
- Convoluted lamination
- Tabular cross stratification
- Trough cross stratification
- Mud cracks
- Soft pebbles
- Carbonate nodules
- Positive granoselection

Trace and body fossils
- Rhizocretions
- Plant remains
- Plant debris / Coal
- Tree logs
- Microflora
- Burrows
- Invertebrate tracks
- Tetrapod tracks
- Bones and bone fragments

Other symbols
- Fault
- 188/42 Strike/dip angle
- Abandoned copper mine

Log name: Cala del Pilar–Pla de Mar	Page 08/32
Location: Cala del Pilar–Muntanya Mala Section	

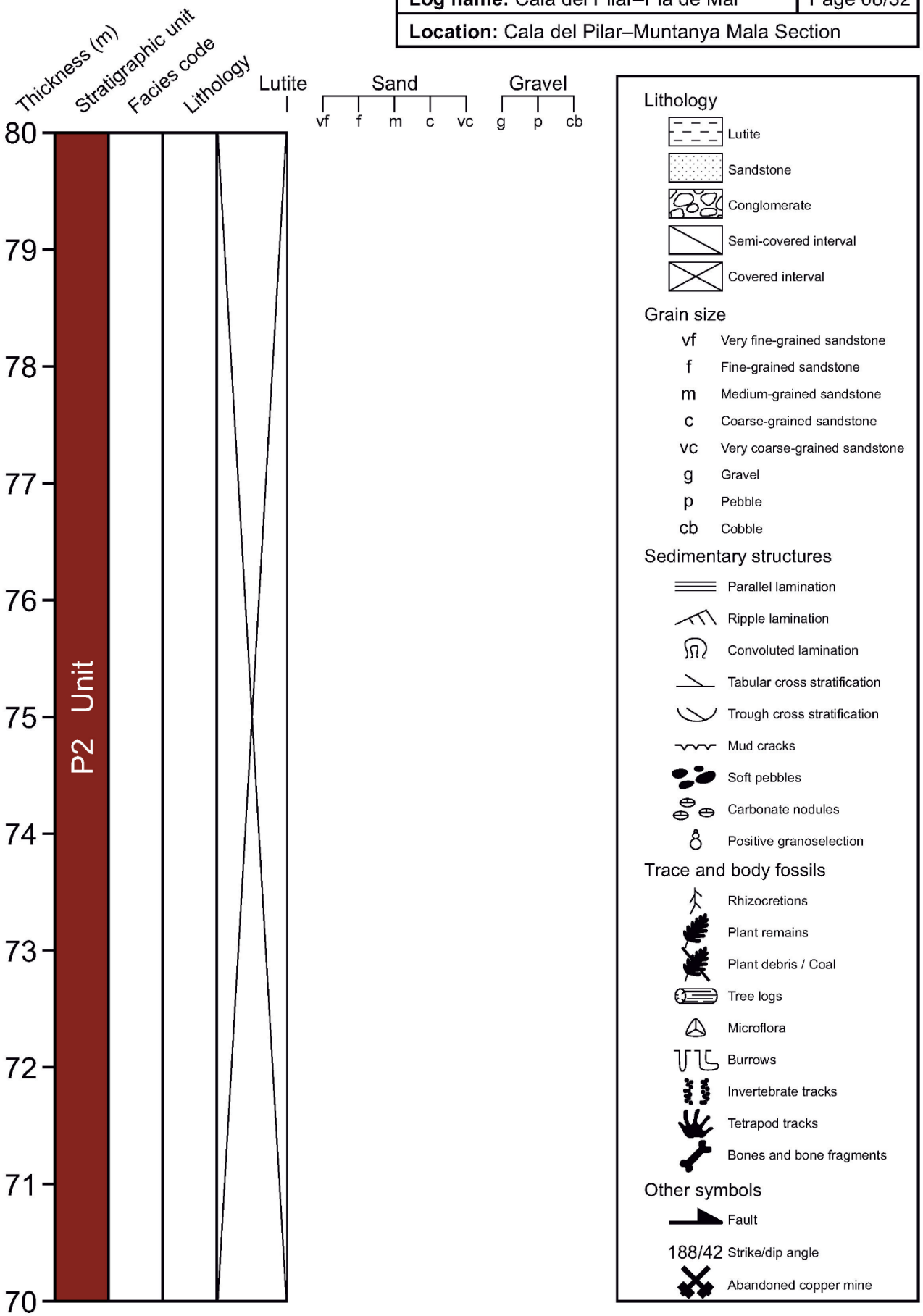

Log name: Cala del Pilar–Pla de Mar	Page 09/32
Location: Cala del Pilar–Muntanya Mala Section	

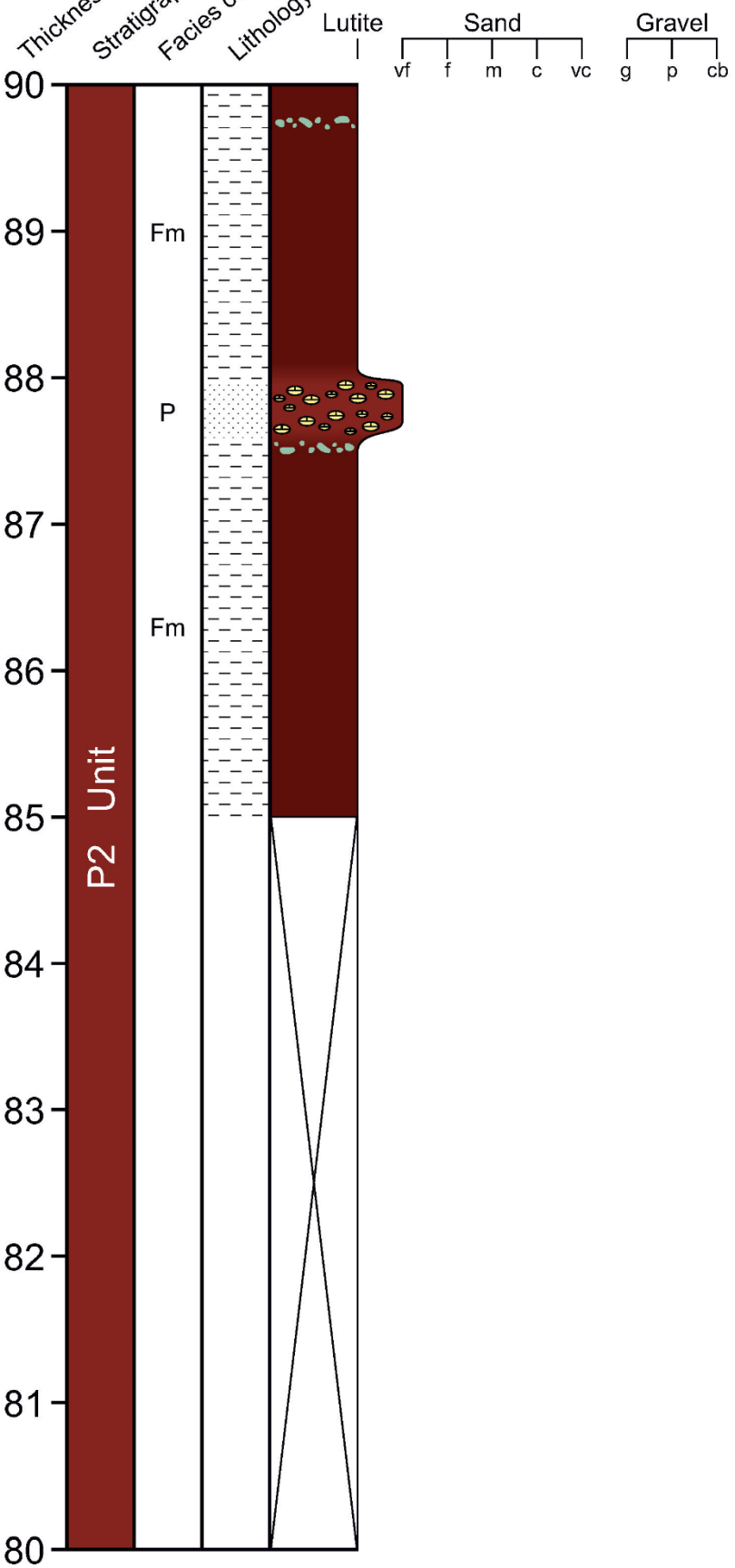

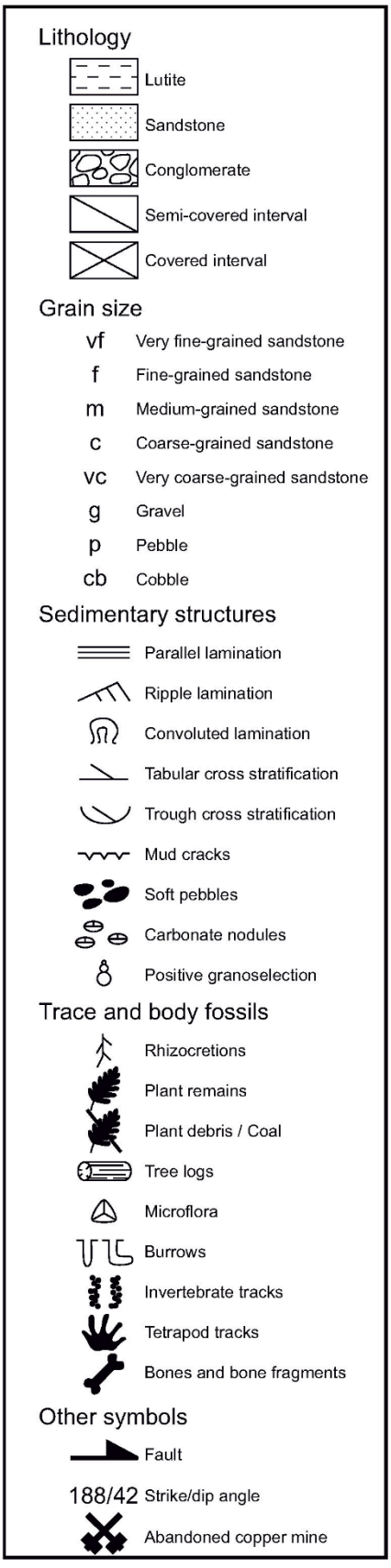

Log name: Cala del Pilar–Pla de Mar	Page 10/32
Location: Cala del Pilar–Muntanya Mala Section	

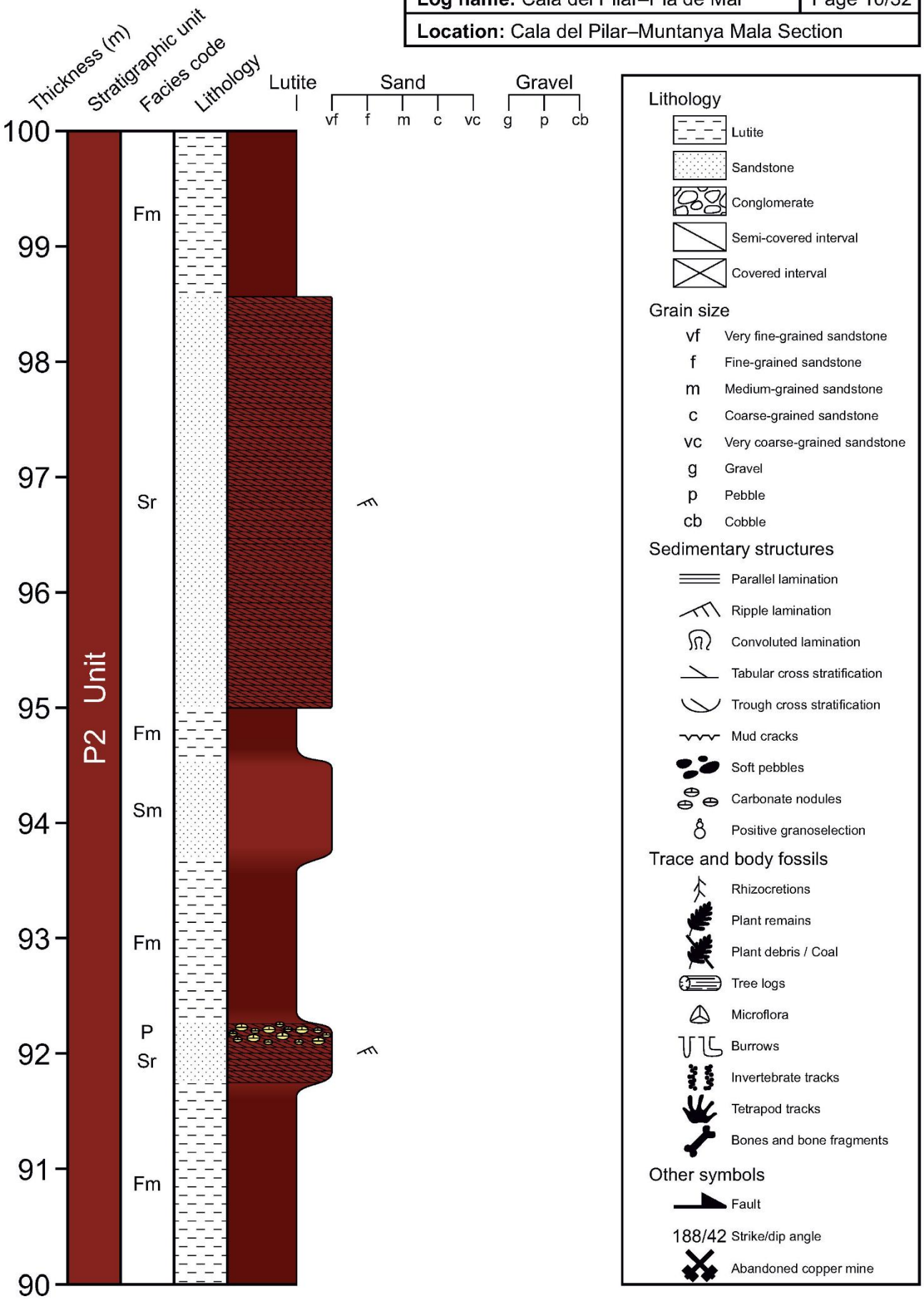

Log name: Cala del Pilar–Pla de Mar	Page 11/32
Location: Cala del Pilar–Muntanya Mala Section	

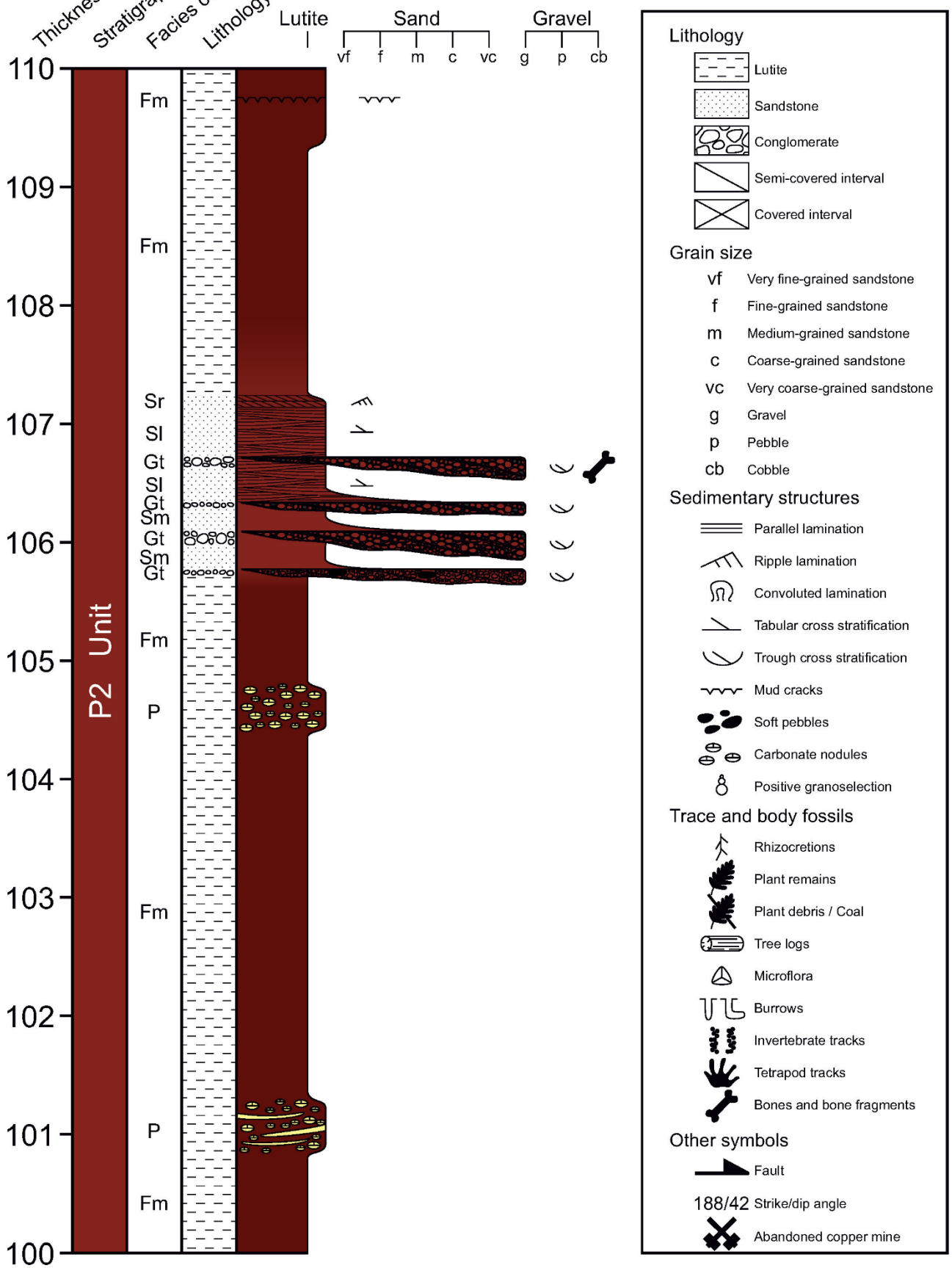

Log name: Cala del Pilar–Pla de Mar	Page 12/32
Location: Cala del Pilar–Muntanya Mala Section	

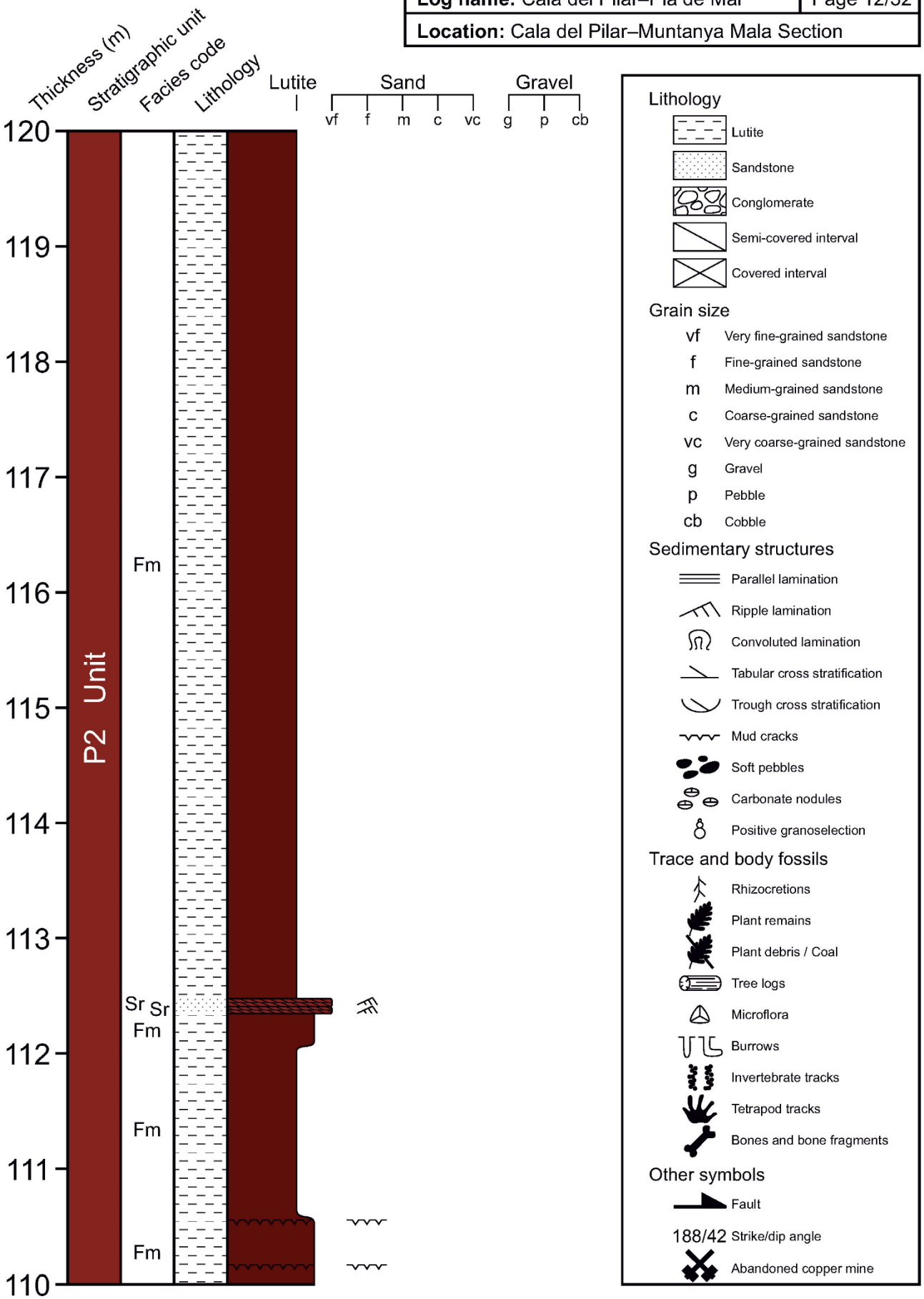

Log name: Cala del Pilar–Pla de Mar	Page 13/32
Location: Cala del Pilar–Muntanya Mala Section	

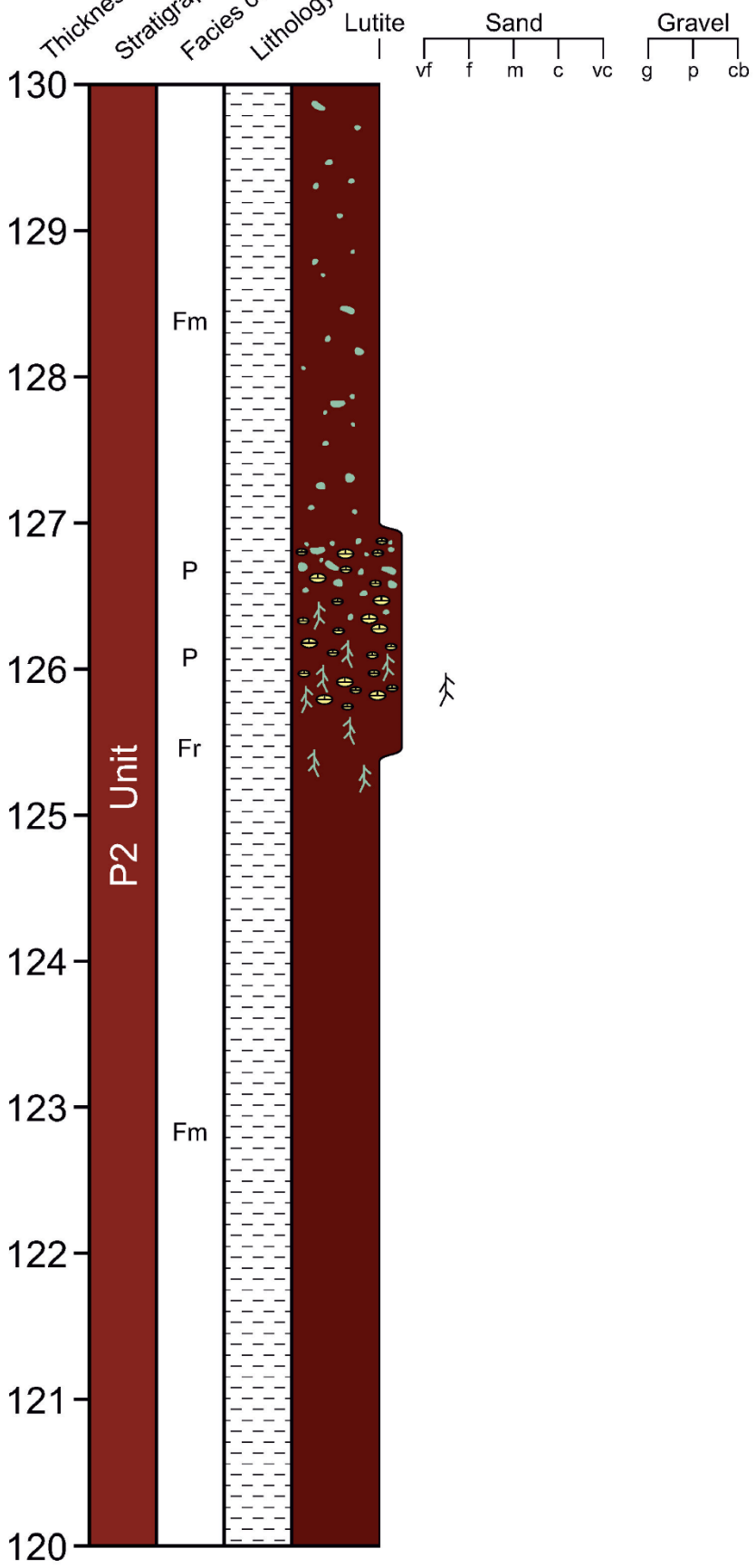

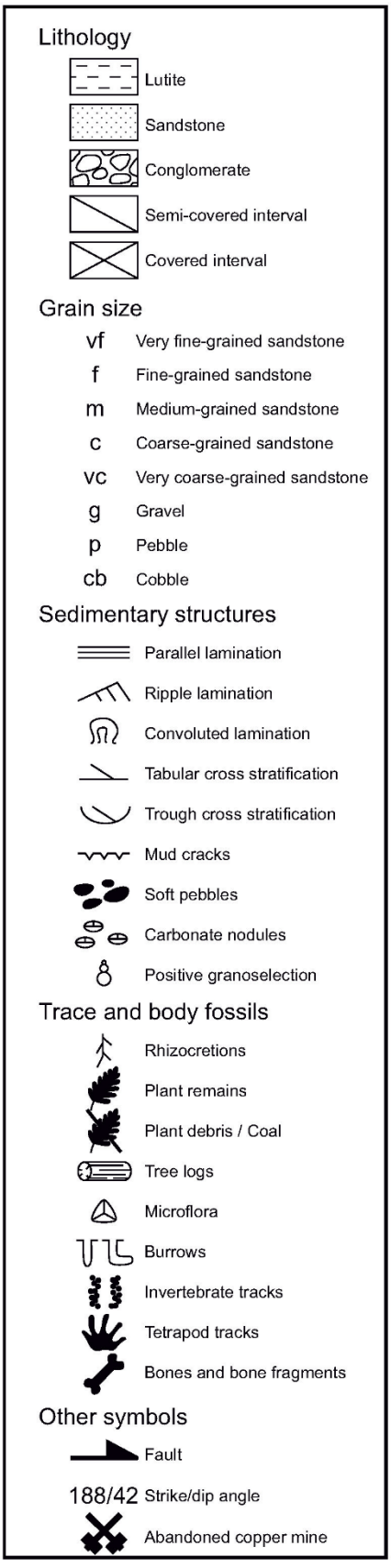

Log name: Cala del Pilar–Pla de Mar	Page 14/32
Location: Cala del Pilar–Muntanya Mala Section	

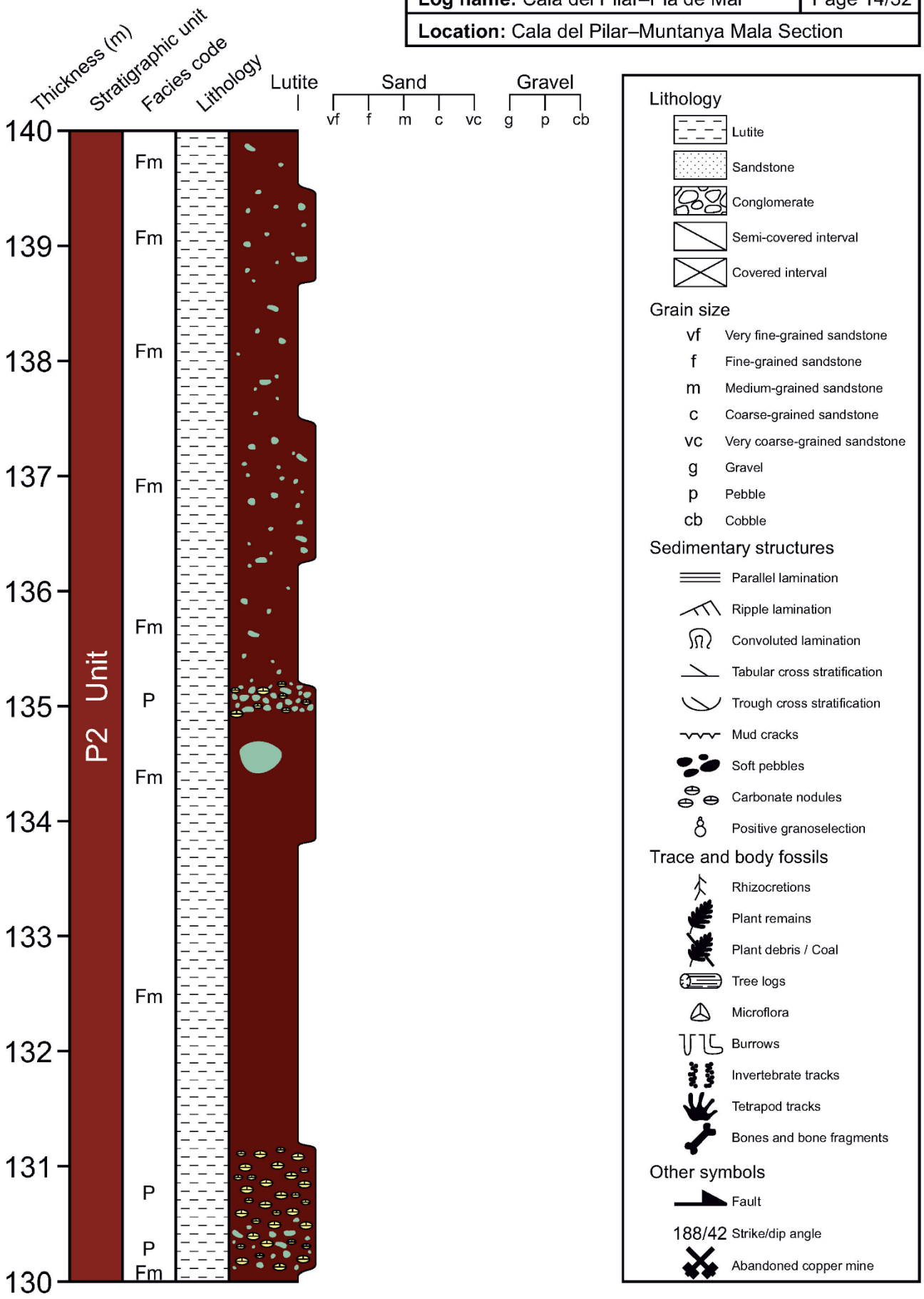

Log name: Cala del Pilar–Pla de Mar	Page 15/32
Location: Cala del Pilar–Muntanya Mala Section	

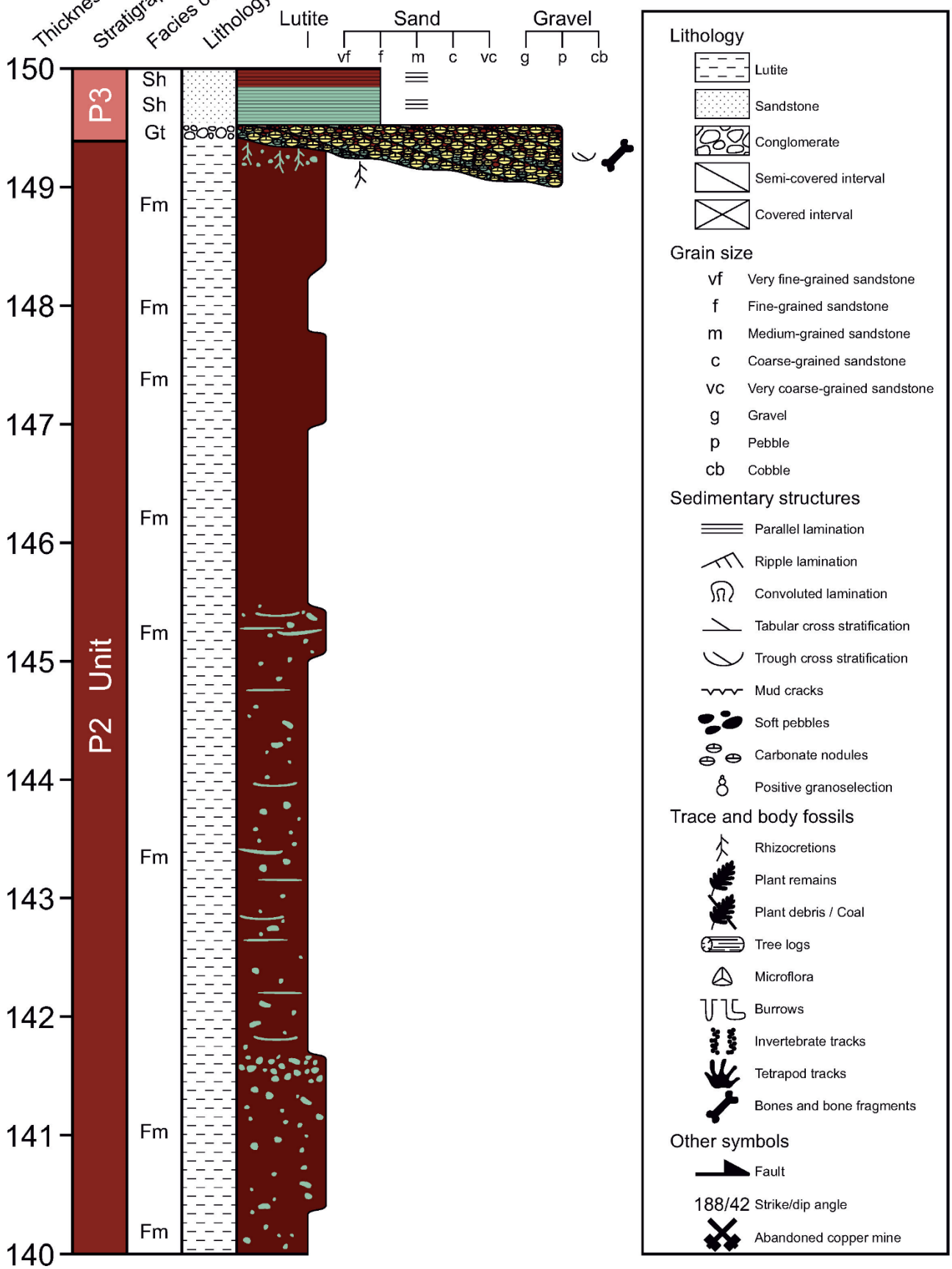

Log name: Cala del Pilar–Pla de Mar | Page 16/32

Location: Cala del Pilar–Muntanya Mala Section

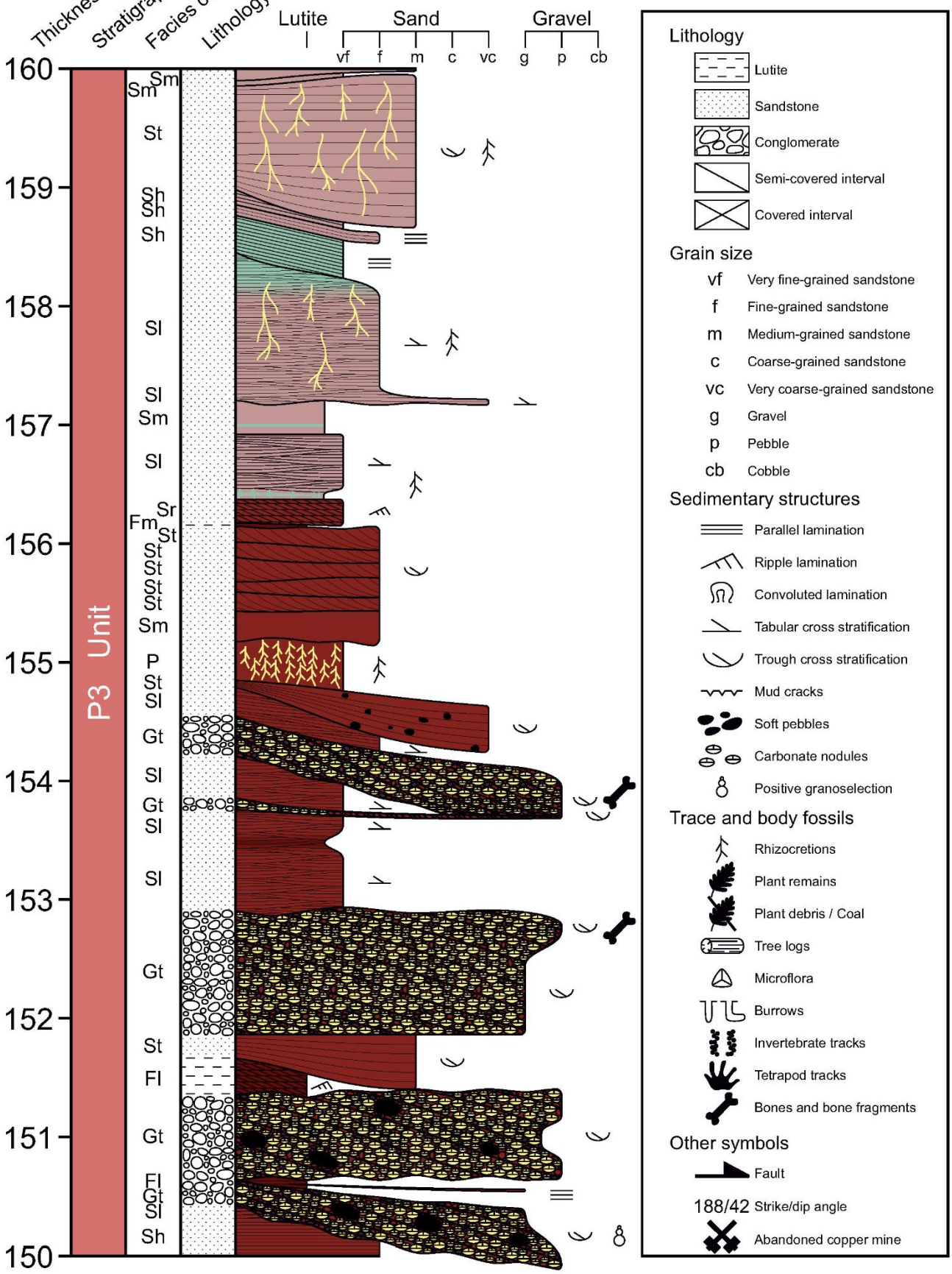

Log name: Cala del Pilar–Pla de Mar	Page 17/32
Location: Cala del Pilar–Muntanya Mala Section	

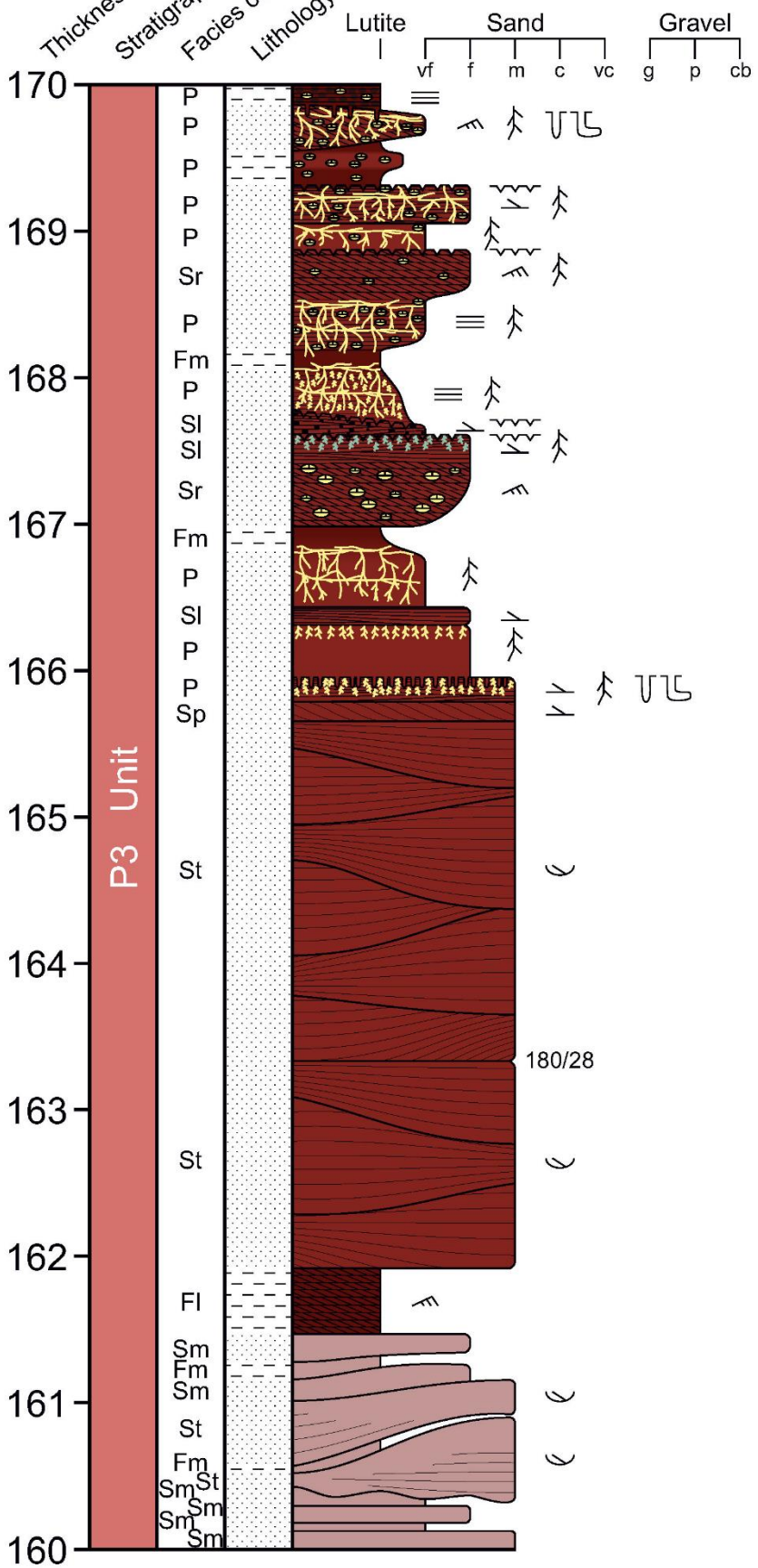

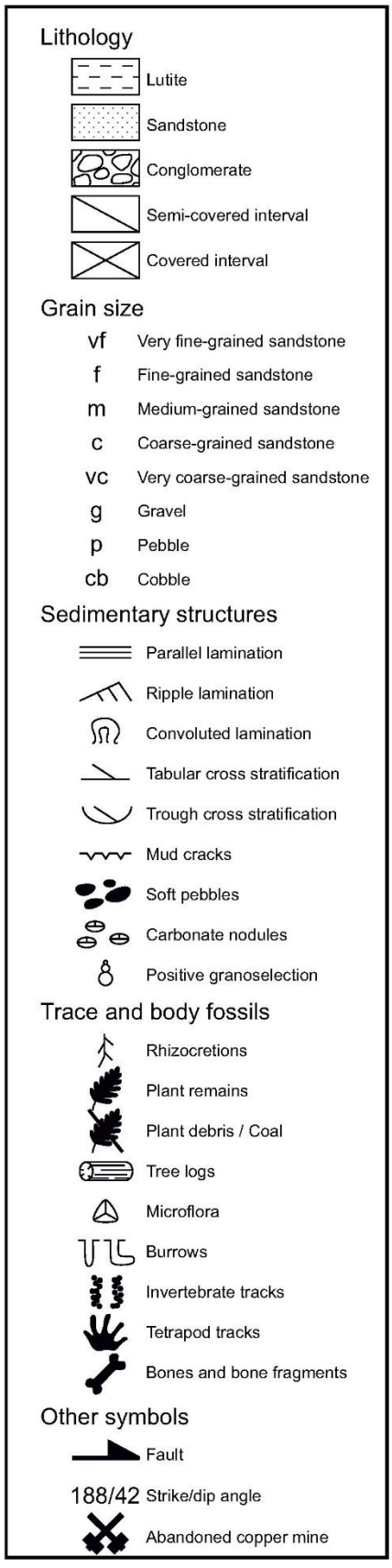

Log name: Cala del Pilar–Pla de Mar	Page 18/32
Location: Cala del Pilar–Muntanya Mala Section	

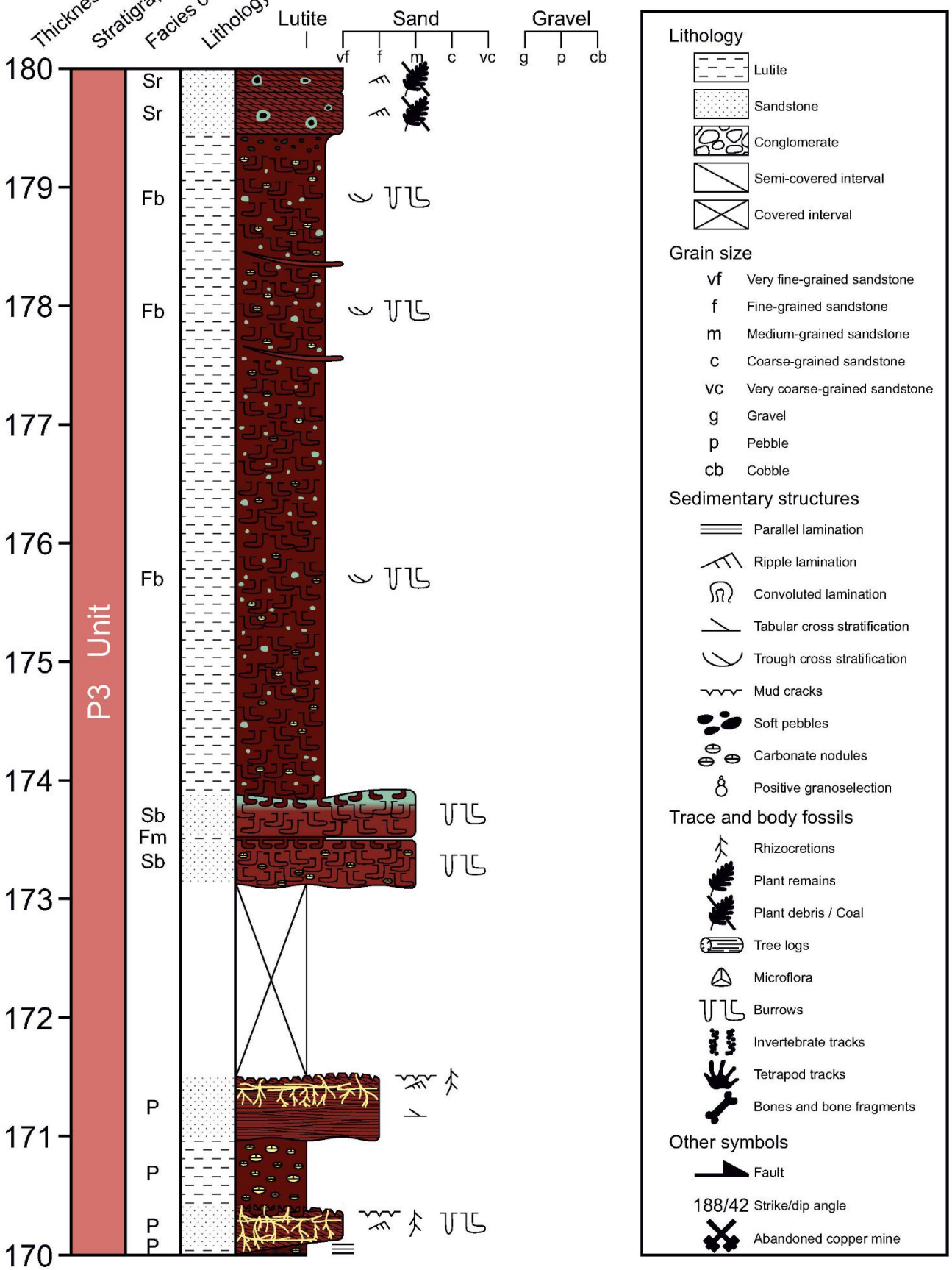

Log name: Cala del Pilar–Pla de Mar	Page 19/32
Location: Cala del Pilar–Muntanya Mala Section	

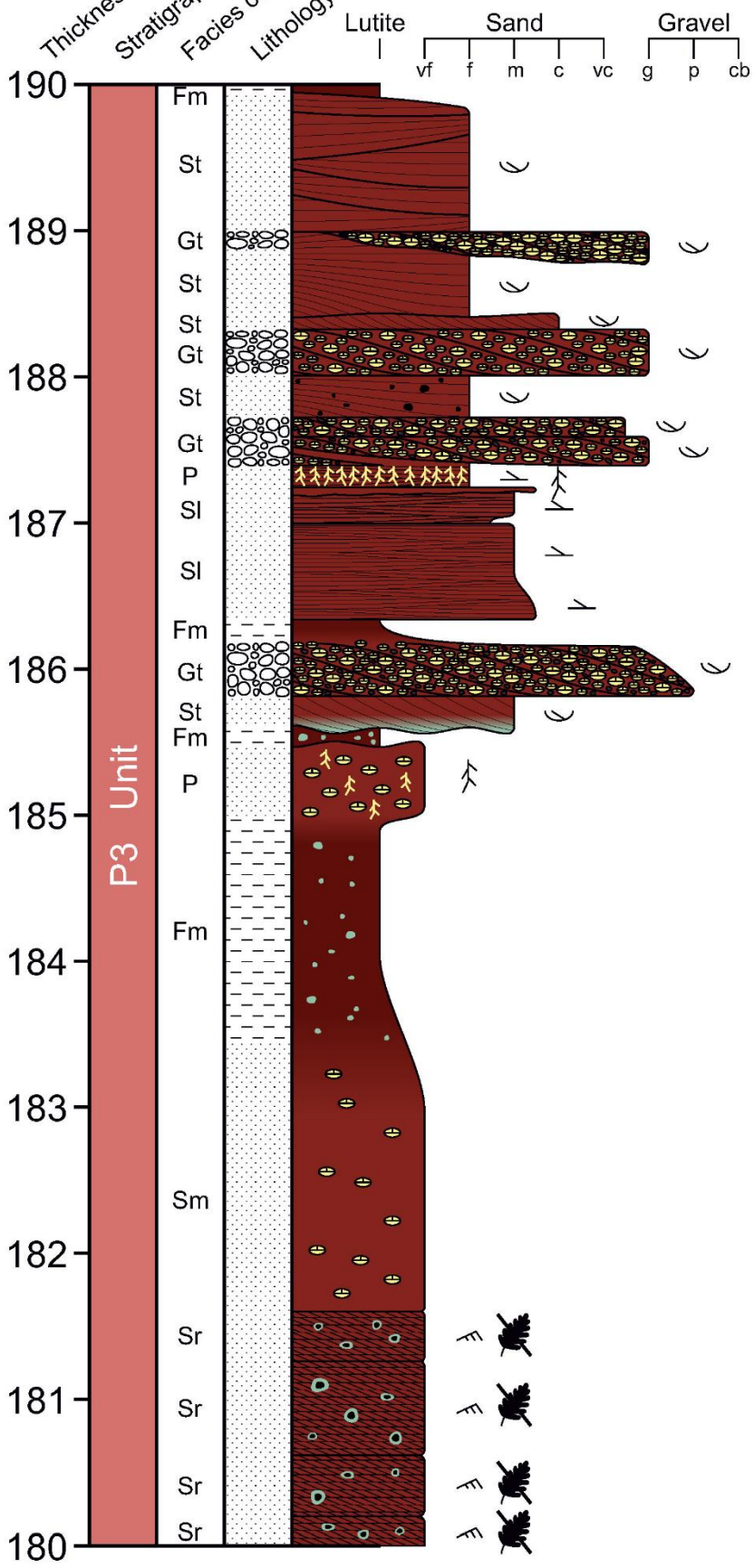

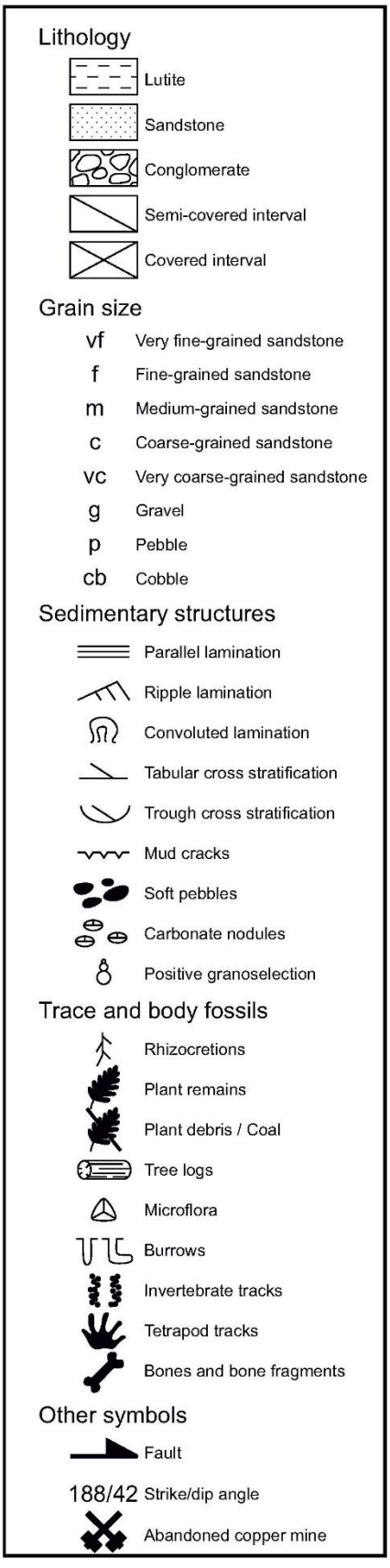

Log name: Cala del Pilar–Pla de Mar	Page 20/32
Location: Cala del Pilar–Muntanya Mala Section	

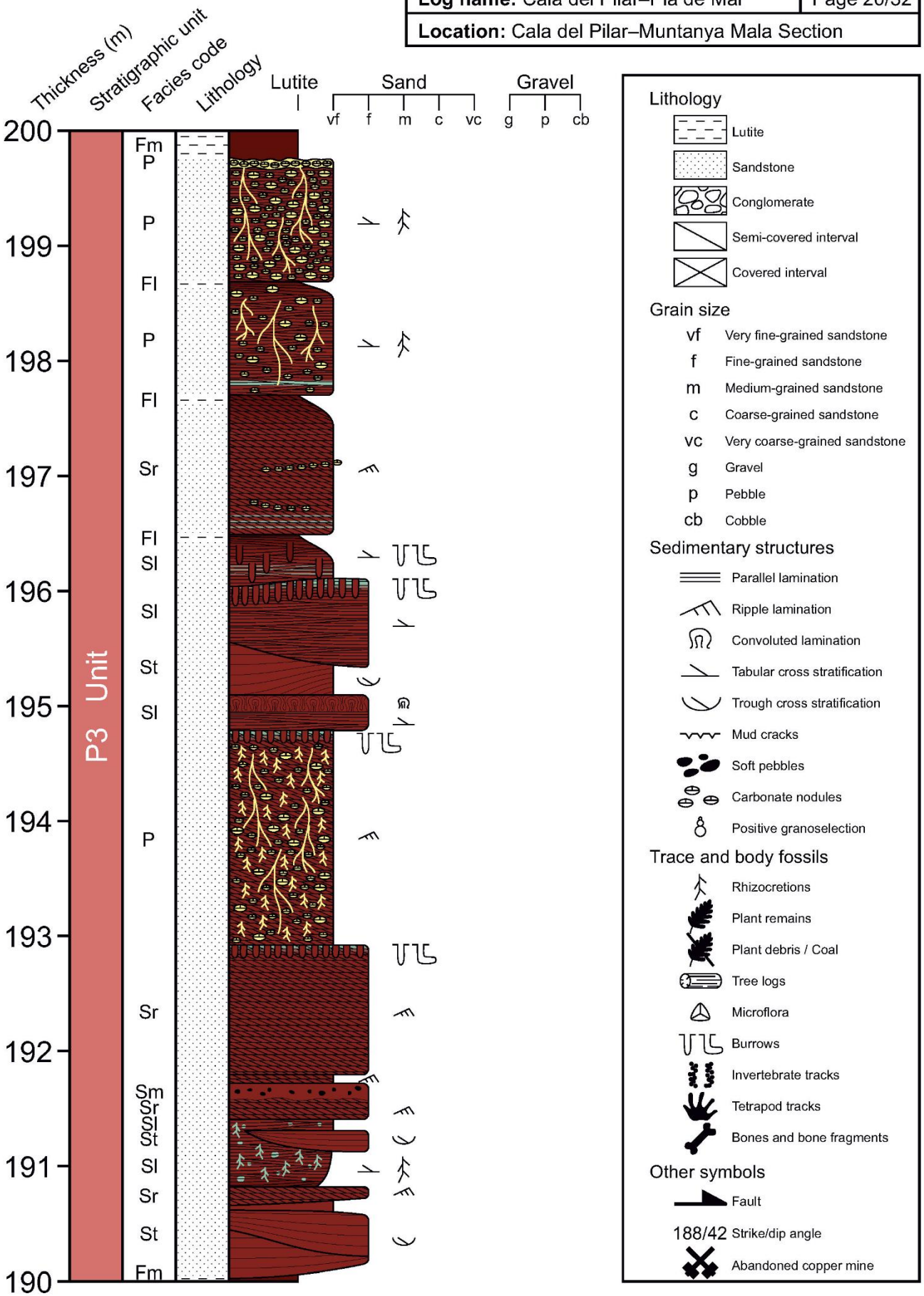

Log name: Cala del Pilar–Pla de Mar	Page 21/32
Location: Cala del Pilar–Muntanya Mala Section	

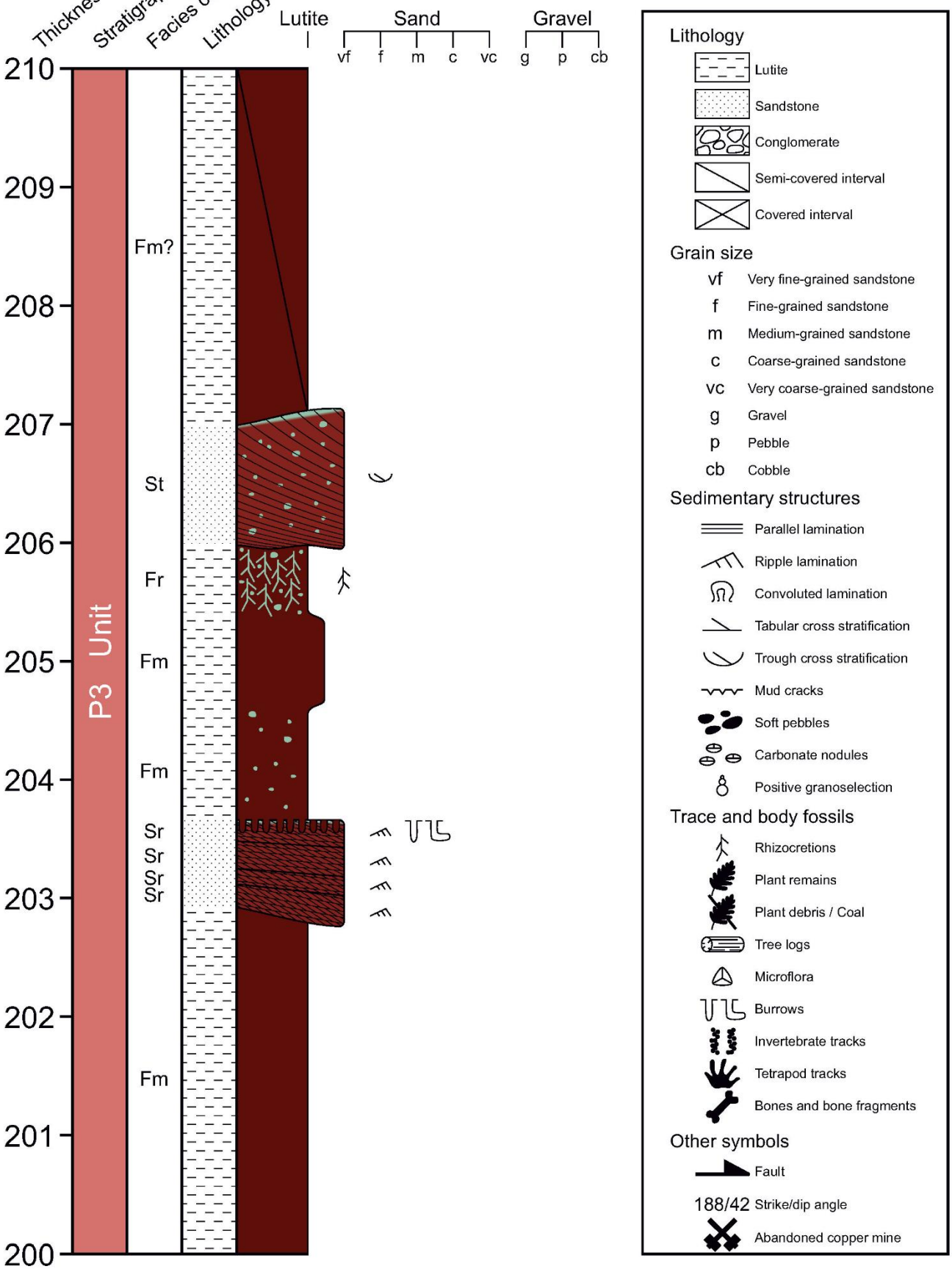

Log name: Cala del Pilar–Pla de Mar	Page 22/32
Location: Cala del Pilar–Muntanya Mala Section	

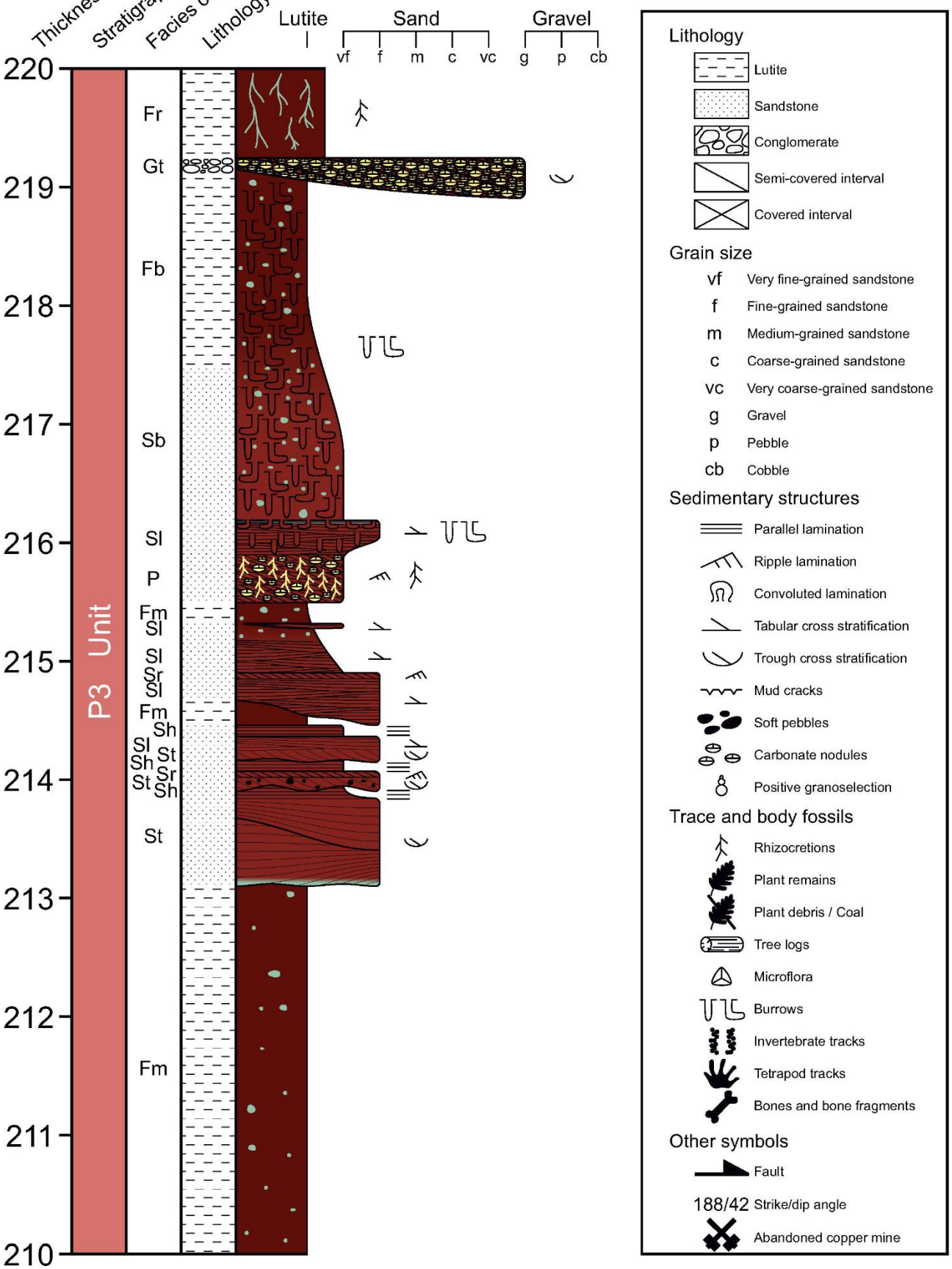

Log name: Cala del Pilar–Pla de Mar	Page 23/32
Location: Cala del Pilar–Muntanya Mala Section	

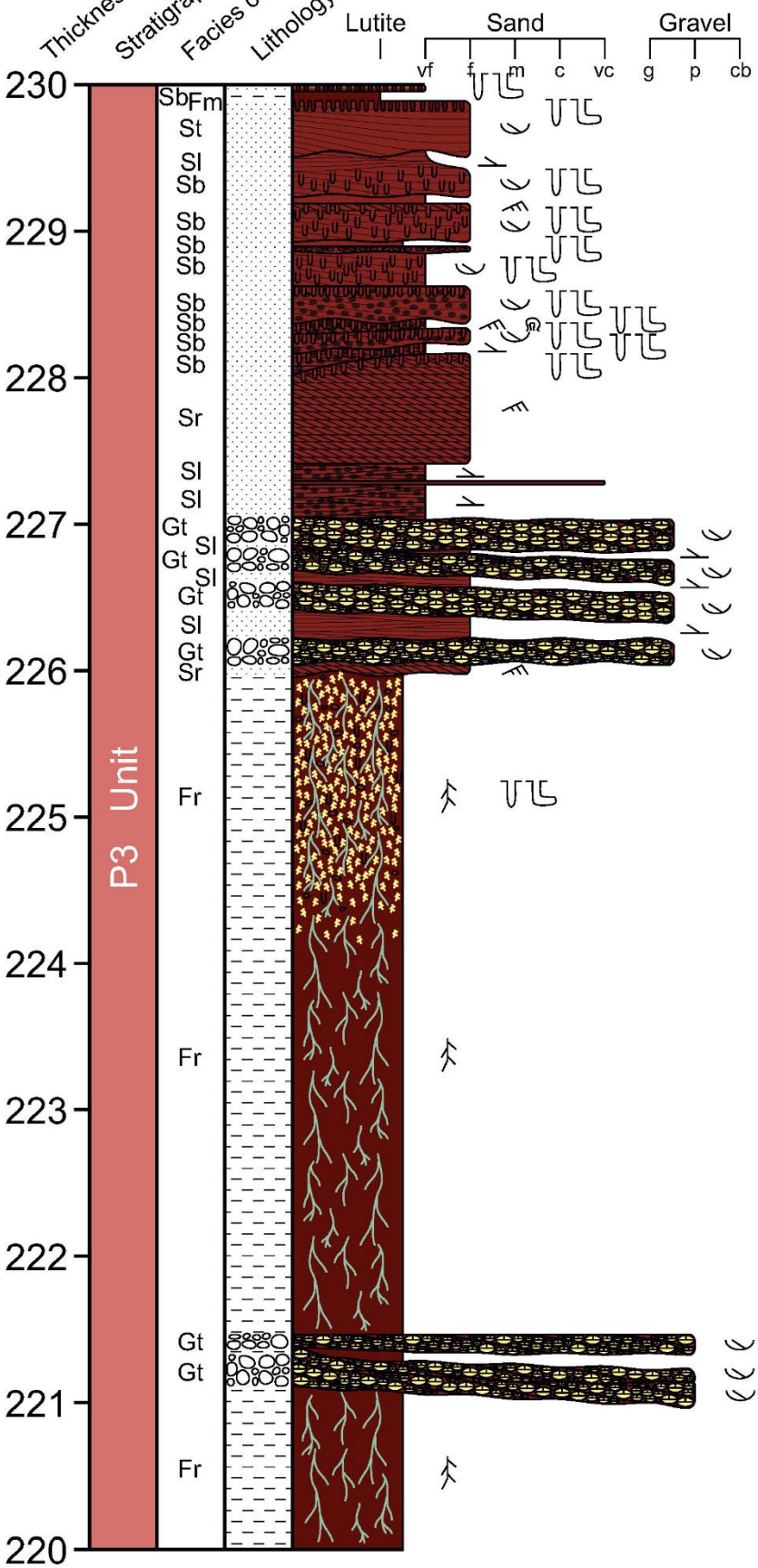

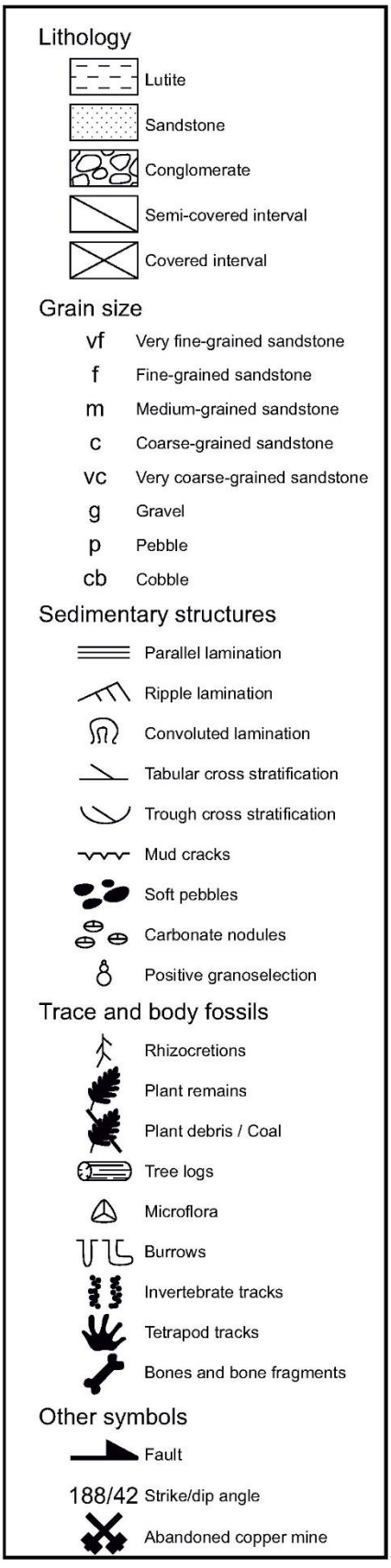

Log name: Cala del Pilar–Pla de Mar	Page 24/32
Location: Cala del Pilar–Muntanya Mala Section	

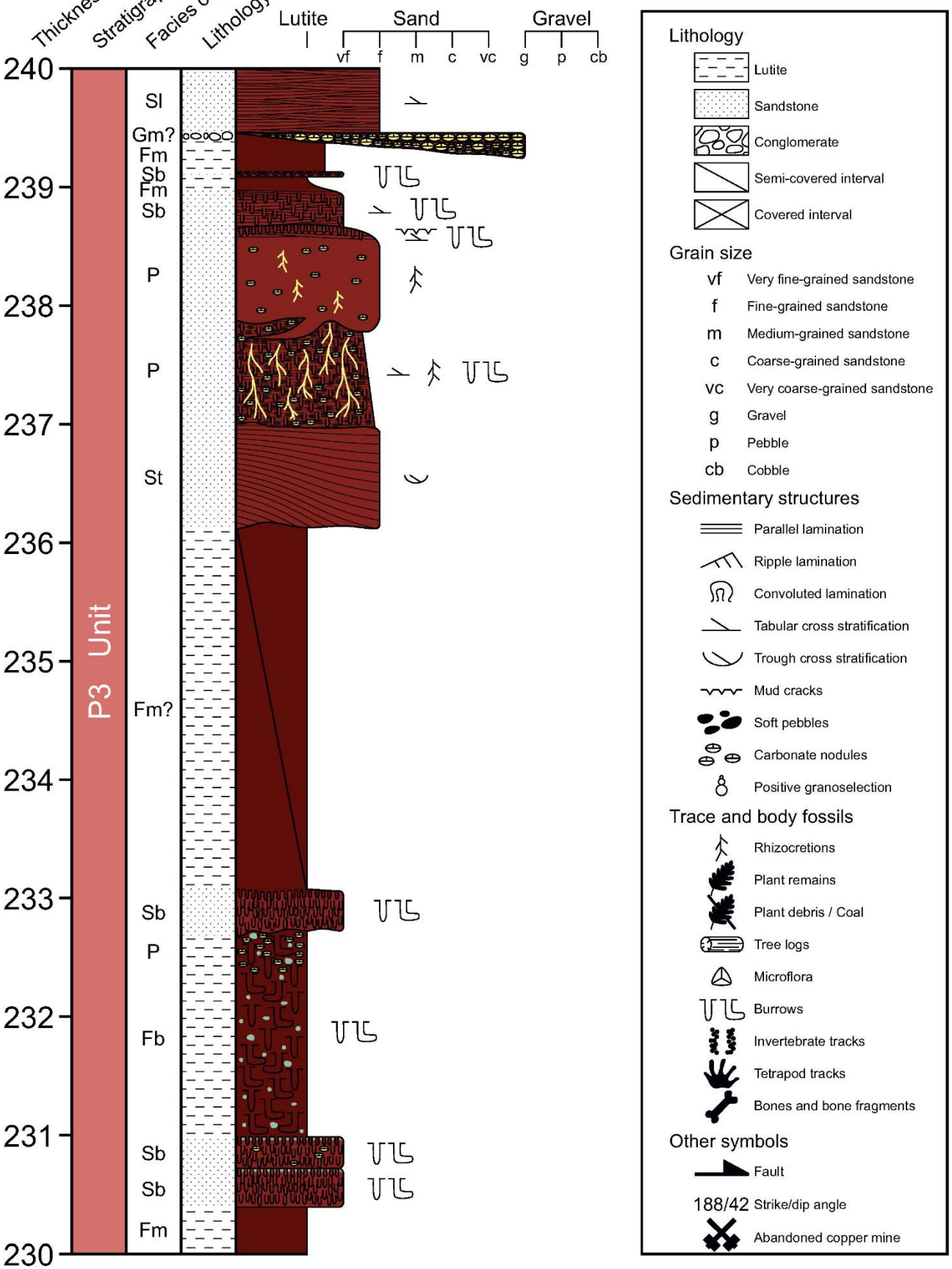

Log name: Cala del Pilar–Pla de Mar	Page 25/32
Location: Cala del Pilar–Muntanya Mala Section	

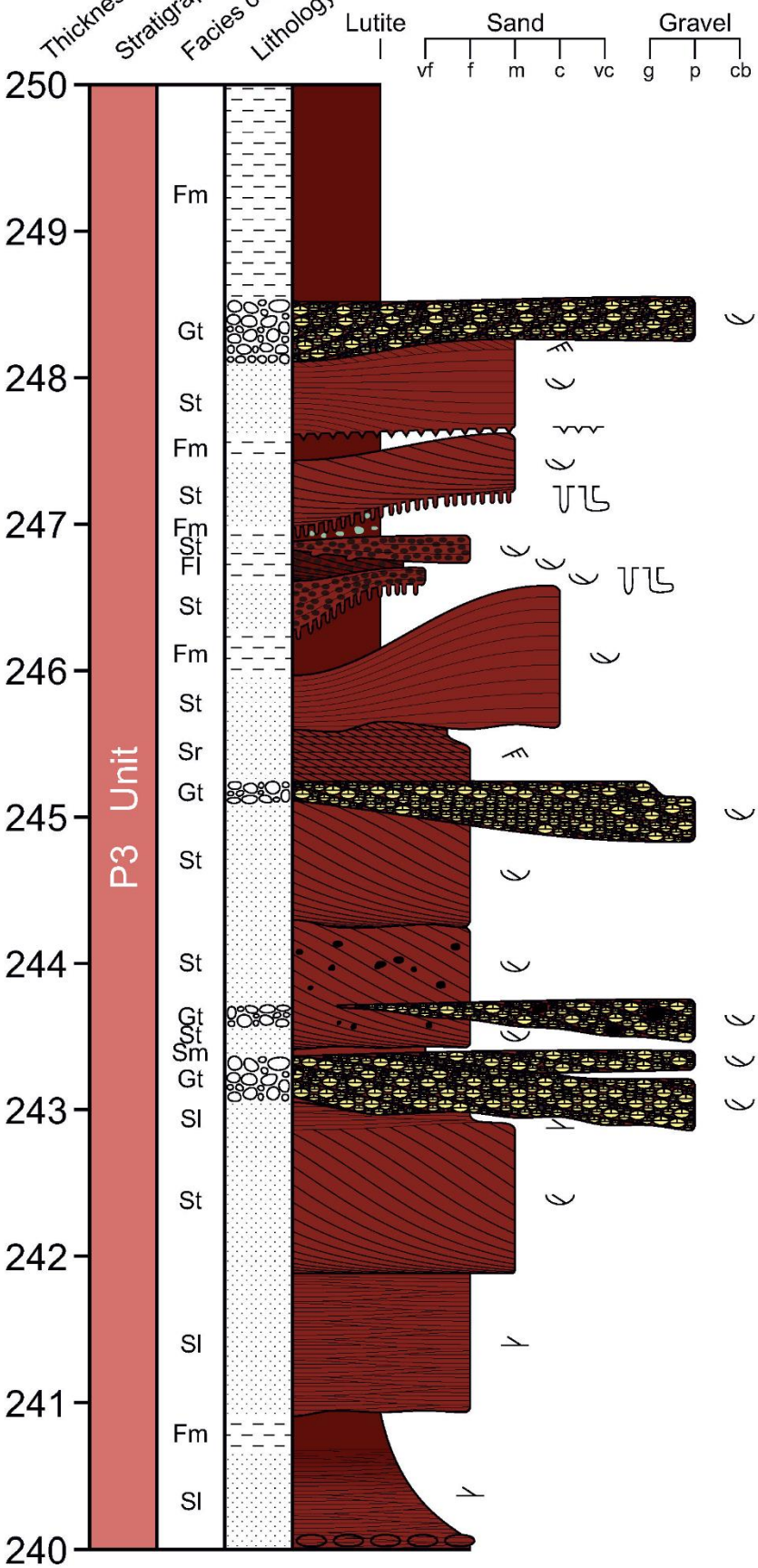

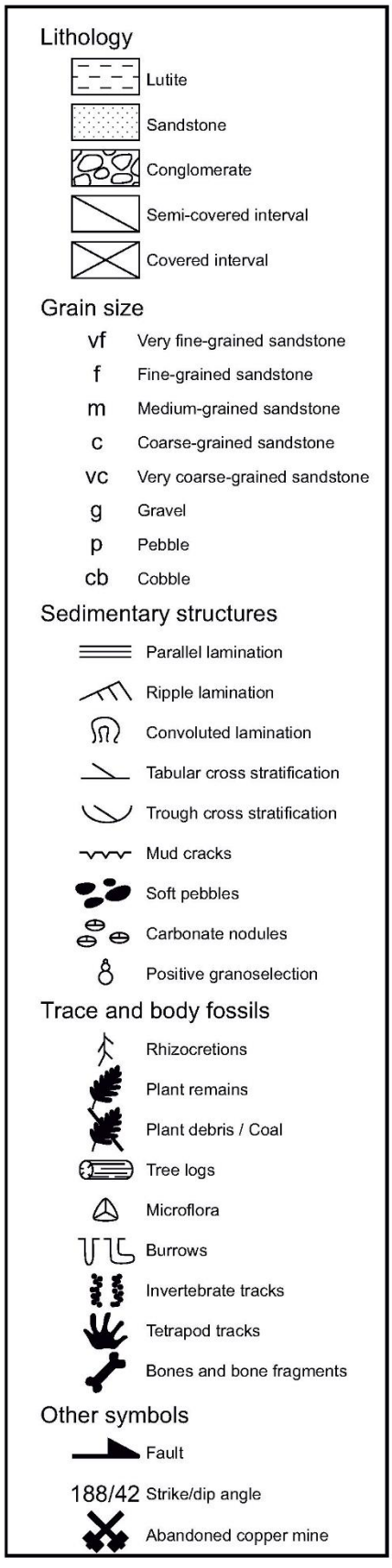

Log name: Cala del Pilar–Pla de Mar	Page 26/32
Location: Cala del Pilar–Muntanya Mala Section	

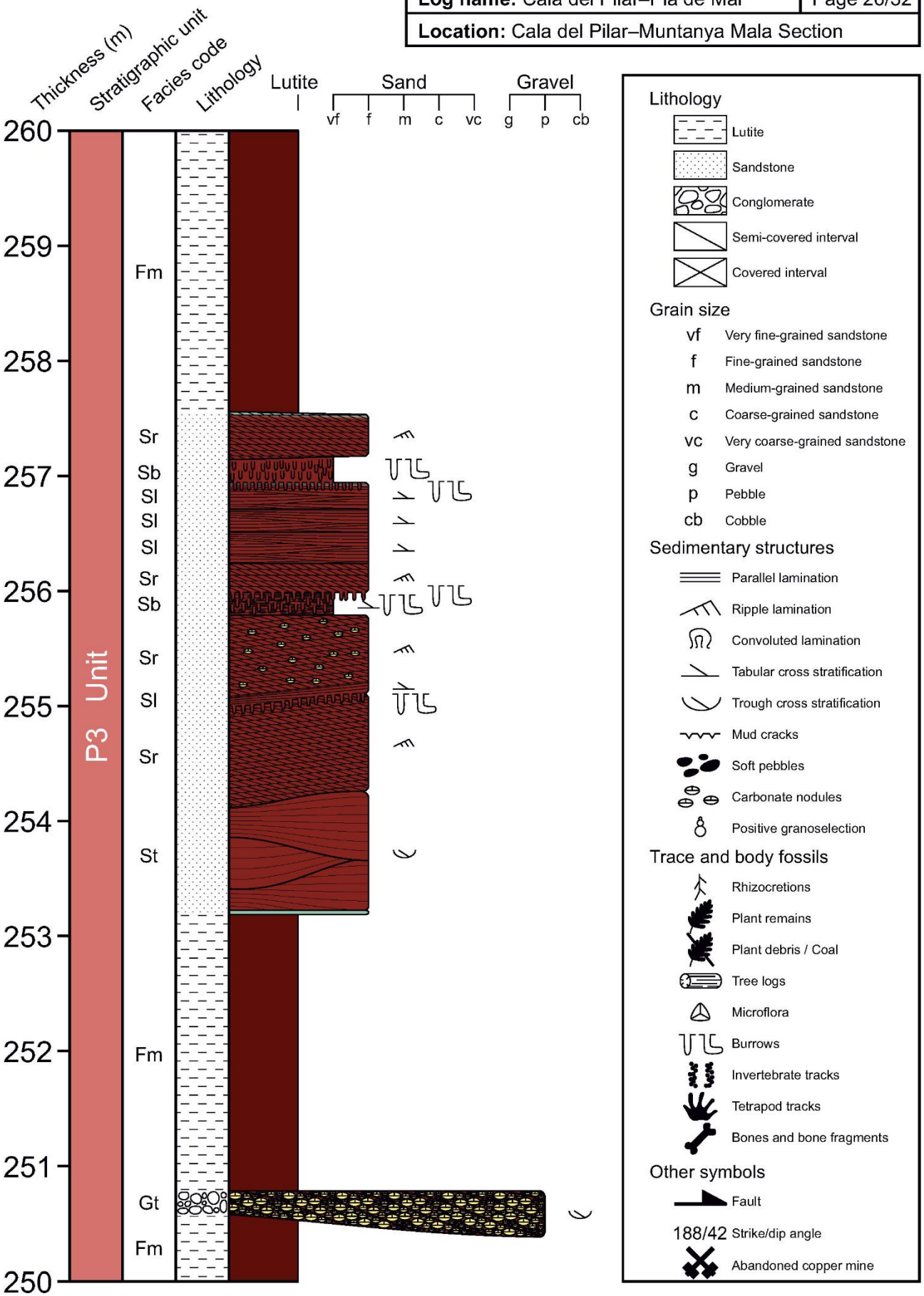

Log name: Cala del Pilar–Pla de Mar	Page 27/32
Location: Cala del Pilar–Muntanya Mala Section	

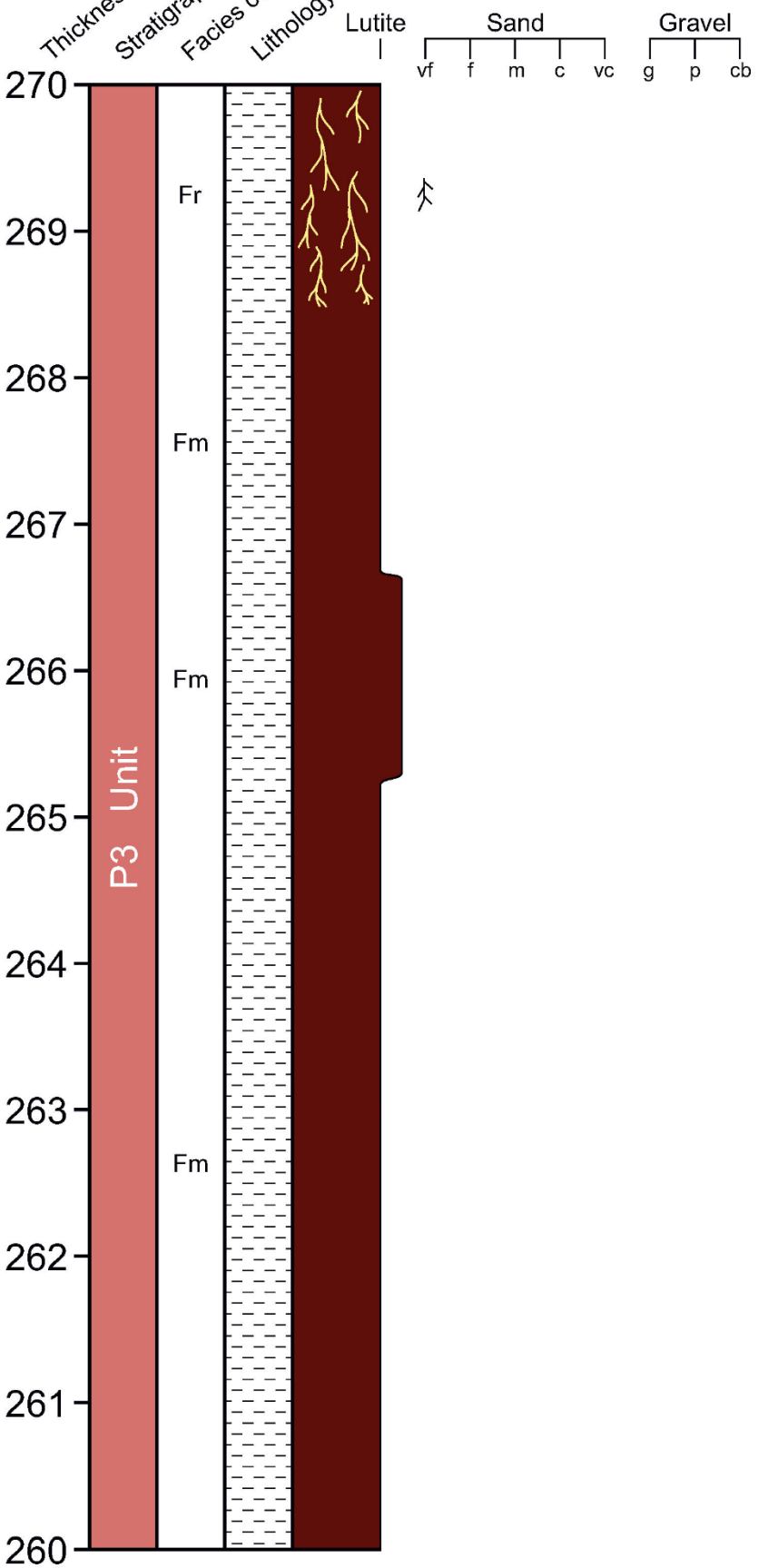

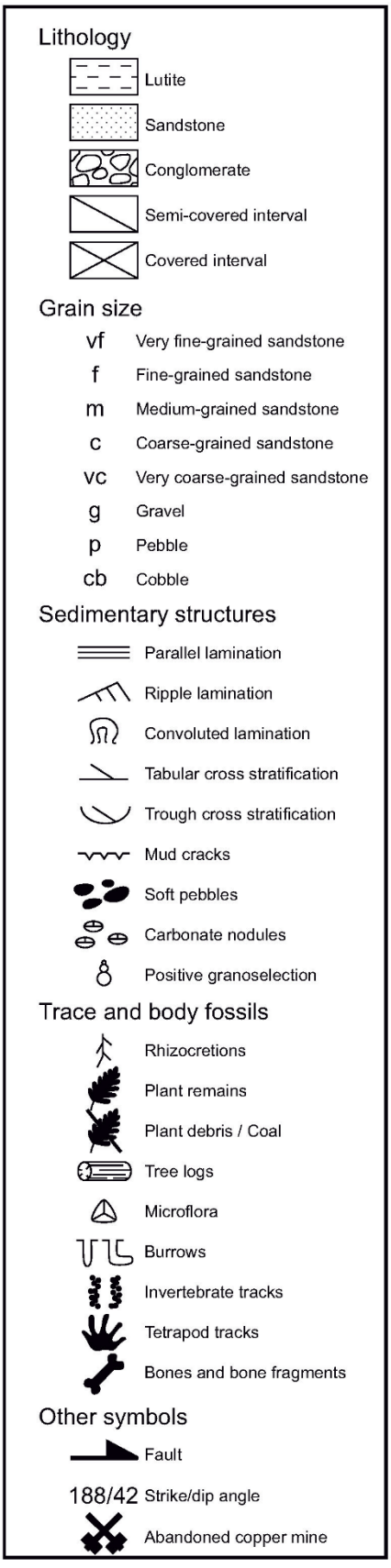

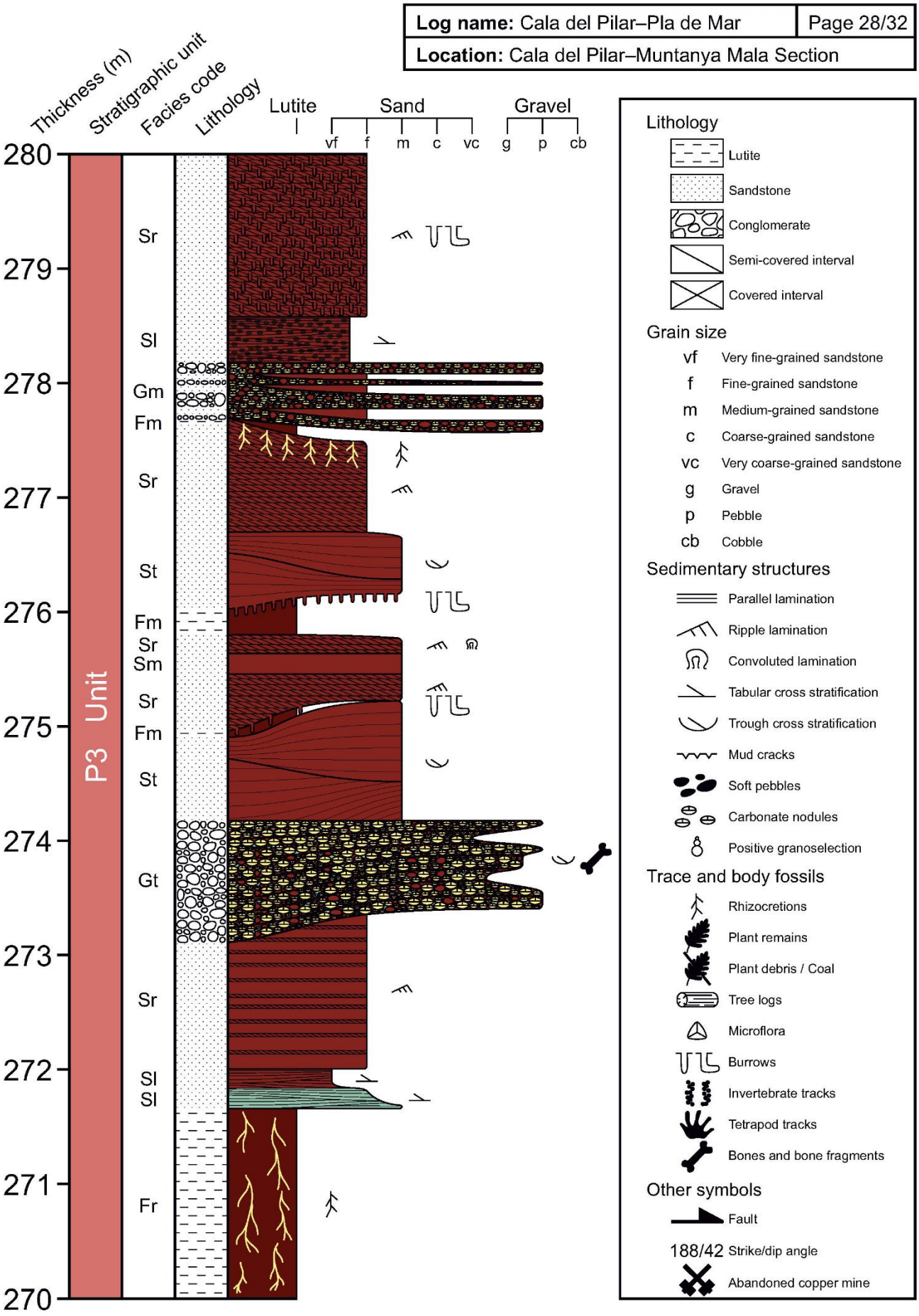
Log name: Cala del Pilar–Pla de Mar
Page 28/32
Location: Cala del Pilar–Muntanya Mala Section
Thickness (m)
Stratigraphic unit
Facies code
Lithology
Lutite
Sand
Gravel
vf f m c vc g p cb
280
279
278
277
276
275
274
273
272
271
270
P3 Unit
Sr
Sl
Gm
Fm
Sr
St
Fm
Sr
Sm
Sr
Fm
St
Gt
Sr
Sl
Sl
Fr
Lithology
Lutite
Sandstone
Conglomerate
Semi-covered interval
Covered interval
Grain size
vf Very fine-grained sandstone
f Fine-grained sandstone
m Medium-grained sandstone
c Coarse-grained sandstone
vc Very coarse-grained sandstone
g Gravel
p Pebble
cb Cobble
Sedimentary structures
Parallel lamination
Ripple lamination
Convoluted lamination
Tabular cross stratification
Trough cross stratification
Mud cracks
Soft pebbles
Carbonate nodules
Positive granoselection
Trace and body fossils
Rhizocretions
Plant remains
Plant debris / Coal
Tree logs
Microflora
Burrows
Invertebrate tracks
Tetrapod tracks
Bones and bone fragments
Other symbols
Fault
188/42 Strike/dip angle
Abandoned copper mine

Log name: Cala del Pilar–Pla de Mar	Page 29/32
Location: Cala del Pilar–Muntanya Mala Section	

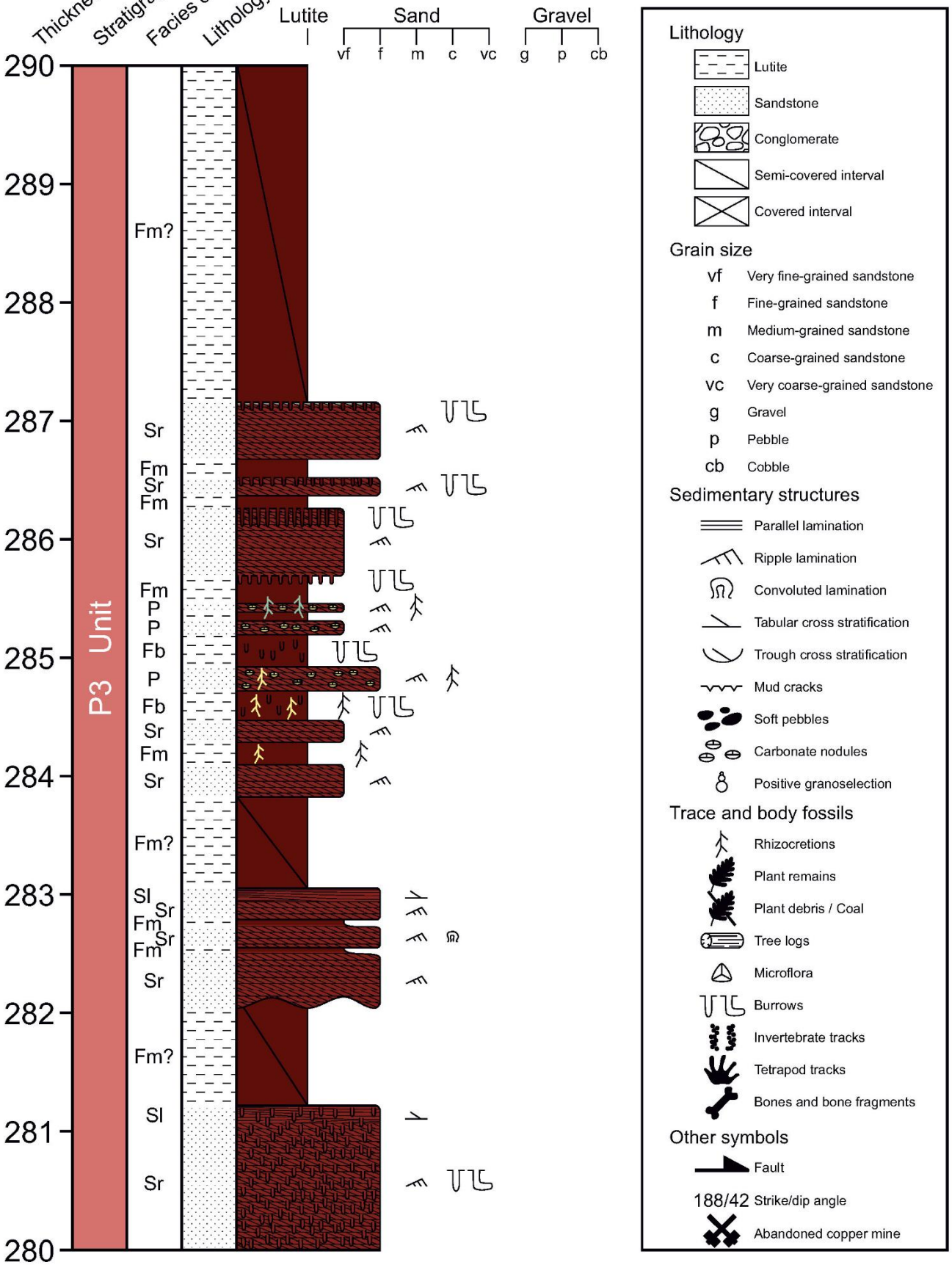

Log name: Cala del Pilar–Pla de Mar	Page 30/32
Location: Cala del Pilar–Muntanya Mala Section	

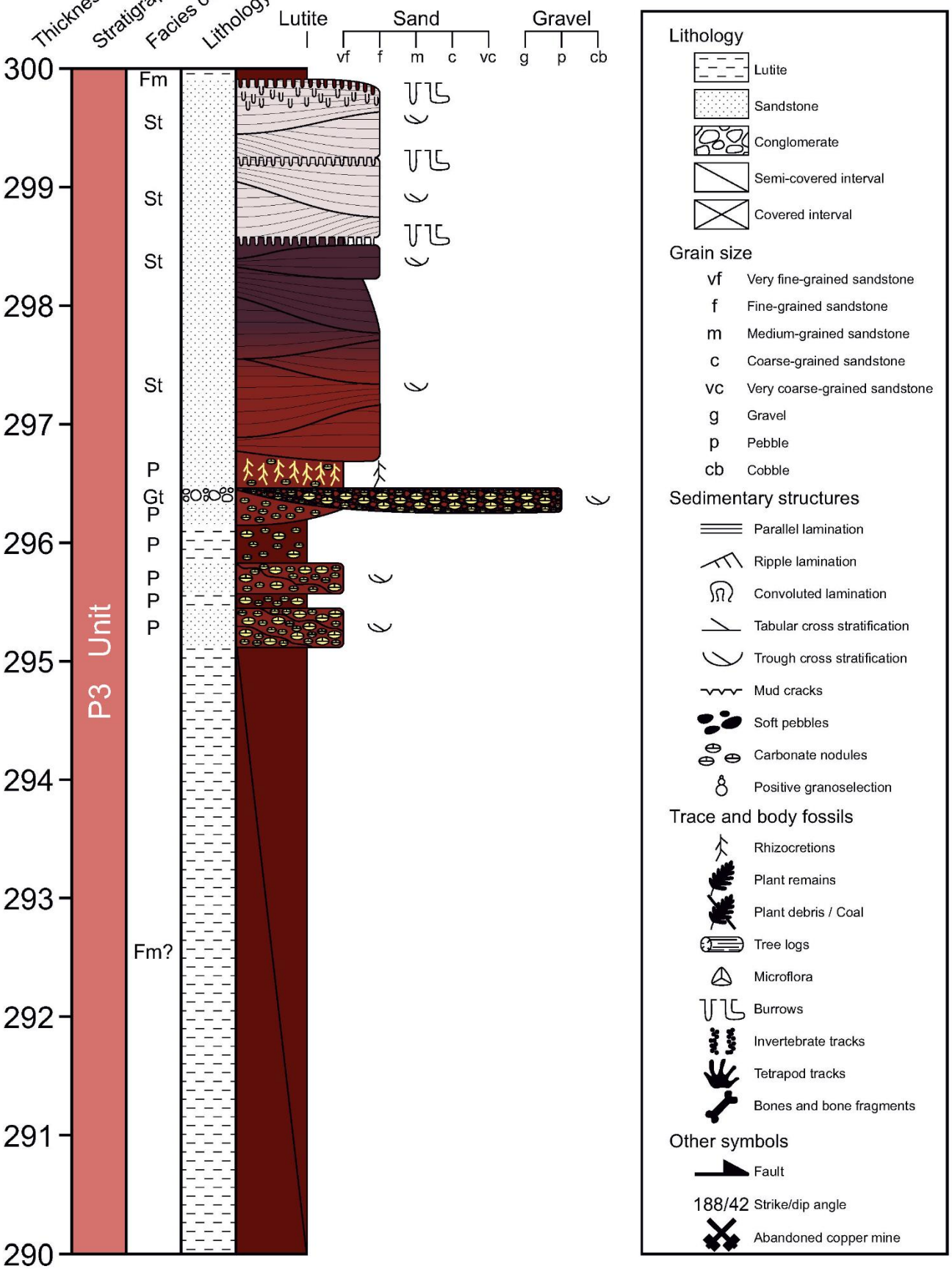

Log name: Cala del Pilar–Pla de Mar	Page 31/32
Location: Cala del Pilar–Muntanya Mala Section	

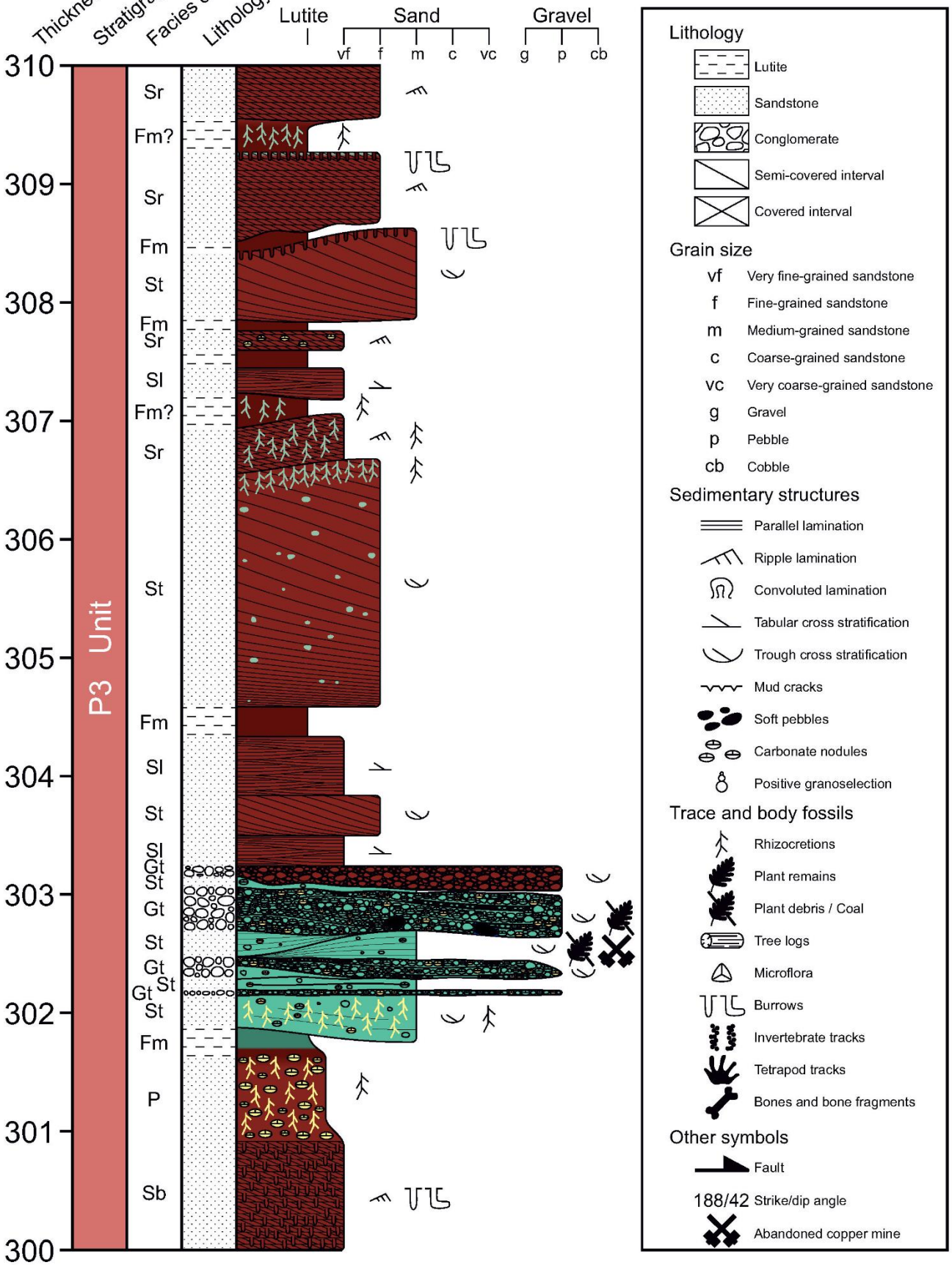

Log name: Cala del Pilar–Pla de Mar | Page 32/32

Location: Cala del Pilar–Muntanya Mala Section

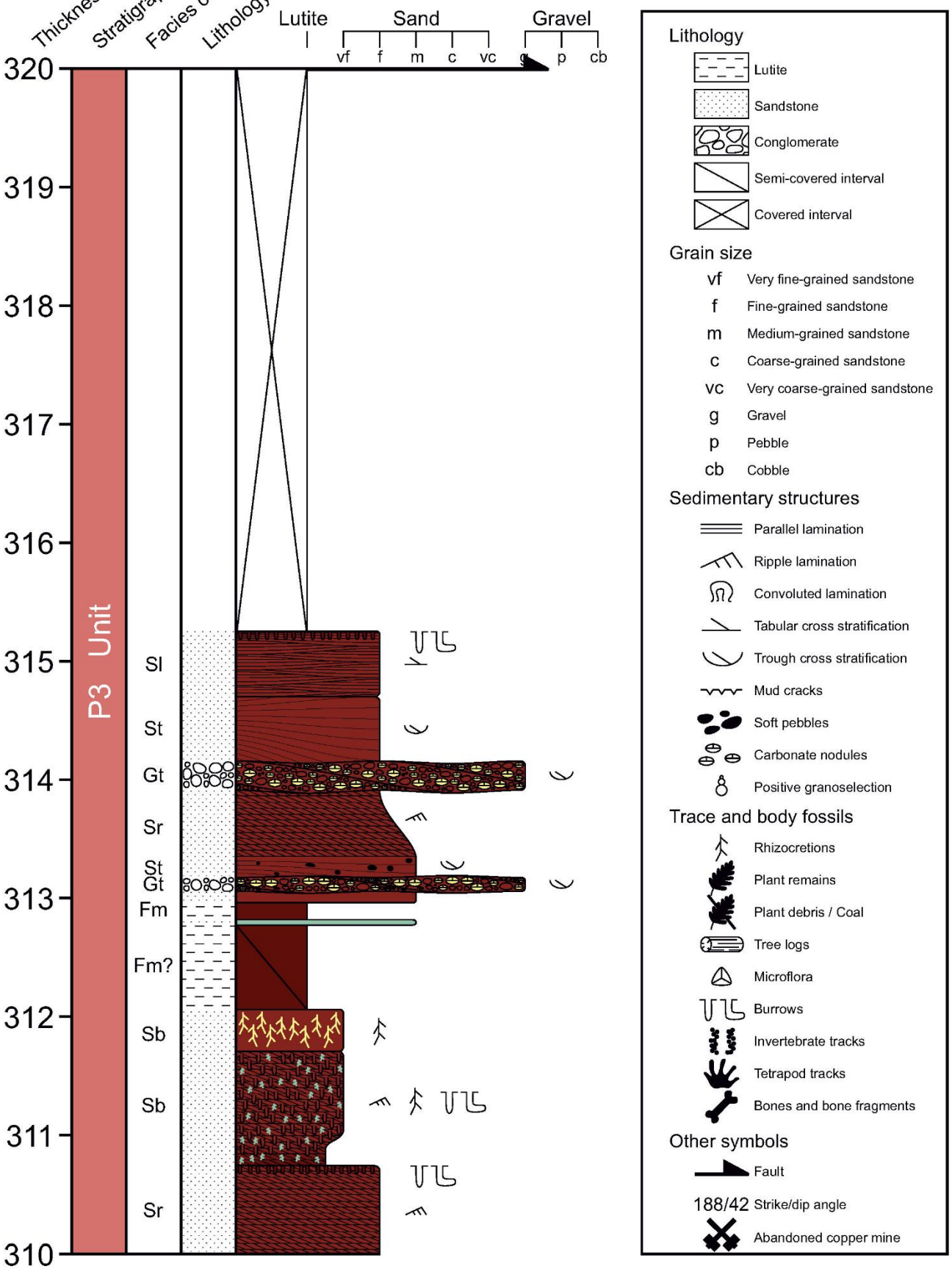

Character matrix

Protorothyris

000000000000000000000000000000000000000000000000000000000000000000000000000?000??0000

Paleothyris

000000000000000001000000100120000100000000000010?0000000000000???000001000110000

Thuringothyris

000001010000010011001010100010000000000000001000000000000??000????0000??101110?00

Euconcordia

010011000000011011001 10??0001000011000?000001010?000000?000000???0???????????000

Romeria prima

111101000000010000000110000 10?00011001?0??0?100000010?0?100000???0?1?1?1?1??0?00

Romeria texana

1111010000000??00100011000001?0001100100?00010?0?0?10?00100000???0???????????0???

Protocaptorhinus

111101000000011000001110?0011010001 01???1?0010?0??01000??00000???111??1111??0??0

Rhiodenticulatus

110101000000011011001101100 01???00101?101000100000?1?0001000001???1?10?111??0000

Saurorictus

?1111100000001?0010010011001 00???010????????1???????0???100???????????????????00

Labidosauriscus

111112000020011000001 0????1?10??????2110200121110??1????100011100???????????0010

Captorhinus laticeps

111111000020011000001101101011100010211020011101000100001100101001111101110000 10

Captorhinus aguti

111111101120111000001101101011100010211020011 1(0&1)1000100001100101002111101110000 10

Captorhinus magnus

111111000120011000001101101011100010211020 01?1010001000011001010?2111??111??0010

Captorhinus kierani

111111100?200110000011011010111000102100200111110001000 01?001?10?1???????????0010

Labidosaurus

111111010020010100111101101012101010211000011201001111101111111111111101110100 10

Labidosaurikos

111112213111210100111101111112111011211111111201101111102?11110111???????????1?21

Moradisaurus

1?110220311011?01??1??????2?11?1???111111111220111 1?110121111101112 1???1?10?1010

Rothianiscus

1?11031121112??1????1????12?12?1????1111?1212?01????????2?111????1211????1??1?10

Captorhinikos valensis

?????12121102?????????????????????????????000????????????2?????????21?????????01?

Gansurhinus

1??1?32121100?????????????????????????????????????1???????1?????????211???1????1??

Captorhinikos chozaensis

111111212010 11?00?0?0?????1?11?????????01001??0????1?11?201111???11?1111010?1010

Reiszorhinus

111101000000010000001100100011000110 1??????????????1000?10010?11?0??????????0?20

Opisthodontosaurus

??011300011001?????00110?01010???????0?0200010010??1????0100011010 1?0??110??0000

Kahneria

???????12110???????1??11101??1????????????2?1??????1?????11?010???2?1??1????????

Moradisaurinae indet. Mallorca

?????31?111?2???????0???

Balearosaurus bombardensis

?????31?1?1???

Appendix 13

Synthesis, Permian of Mallorca

Appendix 13 was published as:

Matamales-Andreu, R. (2022). Rèptils i avantpassats dels mamífers: registre fòssil del Permià de Mallorca. *In*: Pons, G.X.; del Valle, L.; McMinn, M.; Pinya, S. & Vicens, D. (Eds.). *Llibre de ponències i comunicacions de les VIII Jornades de Medi Ambient de les Illes Balears*. Societat d'Història Natural de les Balears, Universitat de les Illes Balears; Palma: 83–86. [in Catalan]

ISBN: 978-84-09-45184-5

DL: PM 00851-2022

In this work, R. Matamales-Andreu contributed in:

A. Integration and discussion of the previous data.
B. Writing of the original draft.
C. Preparation of all the figures (1).

Rèptils i avantpassats dels mamífers: registre fòssil del Permià de Mallorca

Reptiles and mammal ancestors: fossil record of the Permian of Mallorca

Rafel MATAMALES-ANDREU[1,2]

1 Museu Balear de Ciències Naturals, ctra. Palma-Port de Sóller km 30,5, 07100 Sóller, Mallorca, Illes Balears.
2 Institut Català de Paleontologia Miquel Crusafont, Universitat Autònoma de Barcelona, Edifici ICTA-ICP, c/ Columnes s/n, Campus de la UAB, 08193 Cerdanyola del Vallès, Barcelona, Catalunya. rafel.matamales@icp.cat

Resum: A l'illa de Mallorca (Illes Balears, Mediterrània occidental), les roques del Permià representen medis continentals de grans rius i planeres d'inundació. Corresponen a diferents ambients, des de canals fluvials meandriformes fins a basses que s'assecaven estacionalment. El cima era tropical i fortament estacional, amb períodes de sequera. Fins fa no gaire, les comunitats biològiques d'aquest període a Mallorca quasi no es coneixien en detall. Aquest treball sintetitza els resultats d'estudis recents sobre la flora i la fauna, proporcionant un llistat exhaustiu de les associacions fòssils i les seves implicacions. Això demostra la diversitat d'organismes que varen viure durant el Permià a Mallorca, i la seva utilitat en la interpretació paleoambiental, biostratigràfica, paleobiogeogràfica, tafonòmica, icnològica, morfofuncional i filogenètica. En general, aquests resultats indiquen que els jaciments de Mallorca són únics i d'importància internacional, per mor que són un dels pocs exemples de comunitats equatorials d'aquestes edats a Europa. Per això, el seu estudi continuat en el futur segurament permetrà d'aportar moltes noves dades de com eren els ecosistemes de la Terra abans de l'extinció massiva més greu que hi ha haguda mai.
Paraules clau: sauròpsids, sinàpsids, icnites, paleontologia, Illes Balears

Abstract: *On Mallorca (Balearic Islands, western Mediterranean), Permian rocks represent continental settings with large rivers and floodplains. They correspond to several kinds of depositional environments, from fluvial channels to seasonally transient waterholes. The climate was tropical and strongly seasonal, with dry spells. Until recently, the biological communities from this period in Mallorca were poorly known. The present work provides a synthesis of the recent works on the flora and fauna, providing an exhaustive account of fossil assemblages and their implications. This demonstrates the diversity of organisms that lived on Mallorca during the Permian, and their usefulness for palaeoenvironmental, biostratigraphic, palaeobiogeographical, taphonomical, ichnological, morphofunctional and phylogenetic interpretations. More broadly, these results indicate that the deposits of Mallorca are unique and of international importance, as they are among the few examples of Permian equatorial communities of Europe. Because of this, its continued study will allow us to provide many new data to shed light on the ecosystems of the Earth before the greatest mass extinction of all time.*
Key words: *sauropsids, synapsids, ichnites, palaeontology, Balearic Islands*

INTRODUCCIÓ

El Permià és un període clau a la història de la vida a la Terra, precedent a la extinció en massa més grossa que hi ha haguda mai (Benton, 2008). Durant el final del Carbonífer i el principi del Permià, el clima va passar progressivament d'unes condicions de casa de gel (*icehouse*) a unes condicions d'hivernacle (*greenhouse*) (Montañez *et al.*, 2007; Sun *et al.*, 2012). L'encalentiment del clima va començar a l'Artinskià (part mitjana-alta del Permià inferior), i aquesta tendència es va mantenir fins al final del període (Michel *et al.*, 2015). Aquestes condicions, juntament amb altres factors, varen contribuir a la determinació de les comunitats biològiques al llarg del temps. Pel que fa als tetràpodes terrestres, durant el Permià inferior abundaven els amfibis i els sinàpsids del grau dels "pelicosaures", coexistint amb diversos grups de rèptils (Ruta i Benton, 2008; Brocklehurst *et al.*, 2013). Aquesta situació va canviar cap a final del Permià inferior, quan els rèptils començaren a esser cada pic més abundants i els amfibis i els sinàpsids tornaren proporcionalment més escassos (Sahney i Benton, 2008; Benson i Upchurch, 2013). Aquesta dinàmica continuà durant tot el període, fins a l'extinció de la transició Permià–Triàsic, que consolidà el domini dels rèptils (dinosaures, rèptils voladors i rèptils marins) durant els 186 milions d'anys posteriors (Benton, 2008).

A Mallorca (Illes Balears, Mediterrània occidental) s'hi poden trobar roques d'origen continental corresponents al període Permià, recentment estudiades en detall (Matamales-Andreu *et al.*, 2021, 2022). Aquestes afloren intermitentment a la línia de costa dels municipis de Banyalbufar i Valldemossa, i es poden dividir en tres formacions litostratigràfiques, de base a sostre: Fm. Bec de s'Àguila, Fm. Port des Canonge i Fm. Pedra de s'Ase. Aquestes representen ambients terrestres de caràcter al·luvial, amb ventalls, rius meandriformes i planeres d'inundació que s'han datat dins el Permià mitjançant les icnofaunes de tetràpodes i les palinoassociacions (Matamales-Andreu *et al.*, 2022).

Concretament, la Fm. Port des Canonge s'ha datat com a Artinskià/Kungurià (Permià inferior), mentre que la Fm. Pedra de s'Ase s'ha datat com a Roadià/Wordià (Permià mitjà) (Matamales-Andreu *et al.*, 2022).

En aquestes unitats, especialment a la Fm. Port des Canonge, recentment s'hi ha trobat una elevada diversitat de fòssils, incloent-hi restes de plantes, invertebrats i vertebrats de diferents grups (Figura 1). L'objectiu d'aquesta comunicació és de proporcionar una relació actualitzada dels tàxons que s'hi han trobat i la seva significació. Per a una revisió exhaustiva dels antecedents anteriors a l'any 2021, es recomana de consultar Matamales-Andreu *et al.* (2021). Les dades de l'apartat següent es basen en Matamales-Andreu *et al.* (2022) i estudis en preparació.

EL REGISTRE FÒSSIL DEL PERMIÀ DE MALLORCA

Durant la deposició dels sediments que constituirien la Fm. Port des Canonge, Mallorca es trobava en una àrea on el clima era estacionalment sec, pel que les comunitats biològiques se solien concentrar a la vorera dels grans rius que travessaven la conca. Tot i que les comunitats vegetals devien esser relativament diverses, fins ara sols s'han trobat impressions de les tiges i fulles de les coníferes ?*Feysia* sp. i *Hermitia* sp., així com nombroses traces de rels i sistemes radiculars de diferents castes. Pel que fa als animals invertebrats, sols s'hi han observat traces fòssils de la seva activitat, en forma dels icnogèneres *Arenicolites* (produïts per possibles cucs o crustacis), *Cochlichnus* (produïts per cucs o larves d'insectes), *Cruziana* (produïts per tortuguetes, crustacis notostracis), *Palaeophycus* (produïts per diferents grups d'insectes), *Planolites* (produïts per cucs) i *Taenidium* (produïts per escarabats durant l'estivació). Aquests icnofòssils permeten de reconèixer tres icnofàcies diferentes: la icnofàcies d'*Skolithos*, pròpia d'ambients energètics com els lòbuls de desbordament, la icnofàcies d'*Scoyenia*, habitual en basses efímeres, i la icnofàcies de *Mermia*, típica de basses semipermanents. Aquestes dades reflecteixen un mosaic d'ambients a la vorera dels rius, amb zones inundades durant períodes de temps variables, en les que s'hi establien diferentes castes d'animals.

En aquests indrets, concretament als abeuradors temporals (*waterholes*), hi acudien representants de diferents grups de vertebrats. En la Fm. Port des Canonge, aquests s'han trobat en forma tant de traces de la seva activitat (potades) com de fòssils corporals (esquelets). Les potades corresponen als icnotàxons *Characichnos* isp. (arpades de natació de tetràpodes indeterminats), *Dimetropus leisnerianus* (produïts per sinàpsids "pelicosaures" indeterminats, de mida mitjancera), cf. *Dimetropus* isp. (produïts per sinàpsids "pelicosaures", possiblement caseids de mida mitjancera), *Dromopus* isp. (produïts per eurrèptils diàpsids araeoscelidis o varanòpids no varanodontins de mida petita), *Hyloidichnus bifurcatus* (produïts per eurrèptils captorrínids moradisaurins de dues mides diferentes, grossos i mitjancers), cf. *Pachypes ollieri* (produïts per pararrèptils pareiasauromorfs de mida grossa) i un vuitè morfotipus inèdit (produït per sinàpsids teràpsids de mida mitjancera), actualment en estudi. Pel que fa a les restes òssies, s'hi han identificat tres tàxons diferents, un eurrèptil captorrínid moradisaurí indeterminat de mida grossa, un conjunt de juvenils i subadults d'una altra espècie moradisaurí de mida mitjancera, i un sinàpsid teràpsid de mida mitjancera, actualment en estudi. Tots aquests evidencien unes comunitats biològiques diverses i complexes, probablement amb una estructura tròfica més semblant a l'actual (abundància d'herbívors i manco carnívors) que no a les del Carbonífer i Permià inferior (amb dominància de carnívors dependents del medi aquàtic). També és interessant el fet que s'han trobat potades i esquelets en nivells estratigràfics molt propers, que és una circumstància excepcional al registre fòssil. Aquestes potades s'han pogut correlacionar als seus possibles productors: *Hyloidichnus bifurcatus* de mida grossa al moradisaurí gros indeterminat, *Hyloidichnus bifurcatus* mitjancers al moradisaurí mitjancer, i potades de teràpsid al teràpsid actualment en estudi. Finalment, el conjunt de potades és, en general, característic del Permià inferior, tot i que és una època on fins ara mai no s'hi havien trobat fòssils de teràpsids.

La unitat suprajacent, la Fm. Pedra de s'Ase, conté una palinoassociació molt rica i variada, amb espores i pol·len atribuïble a algues (*Maculatasporites*), briòfits (*Reticulatisporites*), coes de cavall (*Calamospora*, *Verrucosisporites*), coníferes (*Chordasporites*, *Cordaitina*, *Gigantosporites*, *Illinites*, *Jugasporites*, *Limitisporites*, *Lueckisporites*, *Lunatisporites*, *Minutosaccus*, *Nuskoisporites*, *Potonieisporites*, *Sahnisporites*, *Triadispora*), falgueres (*Deltoidospora*, *Granulatisporites*, *Osmundacites*), licopodiòfits (*Densoisporites*, *Endosporites*, *Kraeuselisporites*, *Lundbladispora*, *Lycospora*, *Uvaesporites*), "pteridospermes" (*Alisporites*, *Crustaesporites*, *Falcisporites*, *Klausipollenites*, *Leiotriletes*, *Marsupipollenites*, *Paravesicaspora*, *Platysaccus*, *Protohaploxypinus*, *Stroter sporites*, *Vesicaspora*, *Vitreisporites*, *Vittatina*) i altres d'afinitat desconeguda (*Bascanisporites*, *Crucisaccites*, *Gardenasporites*, *Striatoabieites*). En general, correspon a un conjunt de plantes pròpies de climes secs, però amb elements lligats a ambients humits, que evidencien que hi havia masses d'aigua (rius) presents durant tot l'any, a la vorera dels que s'hi concentrava la vegetació. L'associació presenta un conjunt de palinospècies que permeten datar els estrats que els contenen dins el Permià mitjà–superior i, gràcies als estudis de paleomagnetisme, aquesta datació es pot precisar encara més dins la primera meitat del Permià mitjà. Pel que fa als invertebrats, s'ha trobat també qualque icnogènere comú amb la Fm. Port des Canonge, com *Arenicolites*, *Palaeophycus*, *Planolites* i *Taenidium*, amb les mateixes implicacions. De vertebrats s'hi han trobat els icnotàxons *Characichnos* isp. i *Hyloidichnus bifurctus* (de mida grossa), i ossos indeterminats. Aquest conjunt evidencia, al manco, la presència d'eurrèptils captorrínids moradisaurins de mida grossa també en aquesta formació.

FIGURA 1. *Dibuix esquemàtic amb els principals representants de la flora i la fauna del Permià de Mallorca. Amb coes de cavall, falgueres, "pteridospermes", coníferes, espores, pol·len, tortuguetes, diàpsids areoscelidis, eurrèptils captorrínids moradisaurins, sinàpsids "pelicosaures" i sinàpsids teràpsids. Algunes plantes, tortuguetes i alguns vertebrats inferits a partir de les espores, pol·len i traces de la seva activitat. Barra d'escala: 50 cm.*

CONCLUSIONS

Les roques del Permià de Mallorca presenten un registre fòssil excepcional a la Mediterrània occidental, amb abundants restes òssies de vertebrats associades a les potades fetes per aquestes mateixes espècies. A més, la seva datació dins el Permià inferior–mitjà la converteix en una de les millors localitats conegudes que representin les latituds paleoequatorials d'aquest període fora del continent americà. Per això, el seu estudi detallat és clau per aclarir com eren els ecosistemes de l'equador de Pangea, i com els organismes que hi vivien es vinculaven filogenèticament i paleogeogràfica amb altres comunitats biològiques ja documentades més a l'oest (Amèrica) i de latituds més elevades (Europa i Àfrica).

AGRAÏMENTS

Aquesta comunicació s'emmarca en el projecte "Mallorca abans dels dinosaures: estudi dels ecosistemes continentals del Permià i Triàsic amb especial èmfasi en les restes de vertebrats" (ref. 15 - 619/2020), concedit pel Departament de Cultura, Patrimoni i Política Lingüística (Consell Insular de Mallorca).

BIBLIOGRAFIA

Benton, M.J. 2008. *When life nearly died. The greatest mass extinction of all time*. Thames & Hudson, London, 336 p.

Benson, R.B. i Upchurch, P. 2013. Diversity trends in the establishment of terrestrial vertebrate ecosystems: interactions between spatial and temporal sampling biases. *Geology*, 41: 43-46.

Brocklehurst, N., Kammerer, C.F. i Fröbisch, J. 2013. The early evolution of synapsids, and the influence of sampling on their fossil record. *Paleobiology*, 39: 470-490.

Michel, L.A., Tabor, N.J., Montañez, I.P., Schmitz, M.D. i Davydov, V.I. 2015. Chronostratigraphy and paleoclimatology of the Lodève Basin, France: Evidence for a pan-tropical aridification event across the Carboniferous–Permian boundary. *Palaeogeography, Palaeoclimatology, Palaeoecology*, 430: 118-131.

Matamales-Andreu, R., Oms, O. i Fortuny, J. 2021. Paleoecosistemes del Permià i Triàsic continental de Mallorca (Illes Balears, Mediterrània occidental): síntesi i prespectives futures. In: Gómez-Pujol, Ll., Roig-Munar, F.X., Gelabert, B. i Martín, J.A. (Eds.). *De la terra a la mar i de la mar a la terra. Homenatge a Antonio Rodríguez-Perea.* Monografies de la Societat d'Història Natural de Balears, 34. Societat d'Història Natural de les Balears, Palma: 17-39.

Matamales-Andreu, R., Mujal, E., Dinarès-Turell, J., Kustatscher, E., Roghi, G., Oms, O., Galobart, À. i Fortuny, J. 2022. Early–middle Permian ecosystems of equatorial Pangaea: Integrated multi-stratigraphic and palaeontological review of the Permian of Mallorca (Balearic Islands, western Mediterranean). *Earth-Science Reviews*, 228: 103948.

Montañez, I.P., Tabor, N.J., Niemeier, D., DiMichele, W.A., Frank, T.D., Fielding, C.R., Isbell, J.L., Birgenheier, L.T. i Rygel, M. 2007. CO_2-forced climate and vegetation instability during Late Paleozoic glaciation. *Science*, 315: 87-91.

Ruta, M. i Benton, M.J. 2008. Calibrated diversity, tree topology and the mother of mass extinctions: the lesson of temnospondyls. *Palaeontology*, 51: 1261-1288.

Sahney, S. i Benton, M.J. 2008. Recovery from the most profound mass extinction of all time. *Proceedings of the Royal Society B*, 275: 759-765.

Sun, Y., Joachimski, M.M., Wignall, P.B., Yan, C., Chen, Y., Jiang, H., Wang, L. i Lai, X. 2012. Lethally hot temperatures during the Early Triassic greenhouse. *Science*, 338(6105): 366-370.

Appendix 14

Synthesis, continental Triassic of Mallorca

Appendix 14 was published as:

Matamales-Andreu, R. (2022). Rèptils i primers mosquits: registre fòssil del Triàsic continental de Mallorca. *In*: Pons, G.X.; del Valle, L.; McMinn, M.; Pinya, S. & Vicens, D. (Eds.). *Llibre de ponències i comunicacions de les VIII Jornades de Medi Ambient de les Illes Balears*. Societat d'Història Natural de les Balears, Universitat de les Illes Balears; Palma: 87–90. [in Catalan]

ISBN: 978-84-09-45184-5

DL: PM 00851-2022

In this work, R. Matamales-Andreu contributed in:

A. Integration and discussion of the previous data.
B. Writing of the original draft.
C. Preparation of all the figures (1).

VIII Jornades de Medi Ambient de les Illes Balears (2022-23) 87

Rèptils i primers mosquits: registre fòssil del Triàsic continental de Mallorca

Reptiles and earliest true flies: fossil record of the continental Triassic of Mallorca

Rafel MATAMALES-ANDREU[1,2]

1 Museu Balear de Ciències Naturals, ctra. Palma-Port de Sóller km 30,5, 07100 Sóller, Mallorca, Illes Balears.
2 Institut Català de Paleontologia Miquel Crusafont, Universitat Autònoma de Barcelona, Edifici ICTA-ICP, c/ Columnes s/n, Campus de la UAB, 08193 Cerdanyola del Vallès, Barcelona, Catalunya. rafel.matamales@icp.cat

Resum: A Mallorca (Illes Balears, Mediterrània occidental), s'hi poden trobar afloraments del Triàsic Inferior i Mitjà que representen medis continentals amb grans rius, llacs i planeres d'inundació. Aquests ambients es desenvoluparen en un clima tropical i estacional, amb intervals semi-àrids i d'altres de més plovers. No obstant això, històricament s'havia dedicat poca atenció a aquestes roques, amb mencions aïllades sobre la flora i la fauna. La present comunicació proporciona una síntesi dels resultats d'estudis recents sobre les comunitats biològiques d'aquestes edats, llistant exhaustivament els fòssils que s'hi han trobat i les seves implicacions. Això revela unes associacions amb una gran diversitat d'espècies de plantes i animals que varen viure a Mallorca durant el Triàsic Mitjà, les quals han permès de fer noves interpretacions paleoambientals, biostratigràfiques, paleobiogeogràfiques, tafonòmiques i icnològiques. Dins un context més ampli, aquests resultats destaquen els jaciments de Mallorca, de conservació excepcionalment bona, com un dels principals referents d'aquesta edat pel que fa a l'estudi dels insectes fòssils. Fins ara, sols s'ha estudiat una part de la biodiversitat real d'aquests paleoecosistemes, pel que s'haurà de completar amb futures investigacions que acabin de descriure aquestes comunitats ja recuperades després de l'extinció en massa més grossa que hi ha haguda mai.
Paraules clau: crustacis, insectes, sauròpsids, paleontologia, Illes Balears

Abstract: *On Mallorca (Balearic Islands, western Mediterranean), Lower–Middle Triassic outcrops represent continental palaeoenvironments with large rivers, lakes and floodplains. They developed under tropical and seasonal climates, with alternation of semi-arid and wet intervals. Historically, little attention had been paid to these rocks, with only isolated mentions to the flora and fauna they enclose. The present contribution provides a synthesis of the results of recent works on the biological communities of these ages, exhaustively listing the fossils that have been found and their implications. This reveals diverse assemblages of plants and animals that lived on Mallorca during the Middle Triassic, which have shed new light on palaeoenvironmental, biostratigraphic, palaeobiogeographical, taphonomical and ichnological interpretations. In a wider context, these results highlight the deposits from Mallorca, of exceptionally good preservation, as one of the most relevant examples to study fossil insects of that age. Only a part of the real biodiversity of these palaeoecosystems has so far been studied, which will have to be completed with future research on these communities, which had already recovered from the greatest mass extinction of all time.*
Key words: *crustaceans, insects, sauropsids, palaeontology, Balearic Islands*

INTRODUCCIÓ

El Triàsic és un període marcat per la recuperació dels ecosistemes després de la extinció en massa més grossa que hi ha haguda mai, conduint a l'origen de molts de grups moderns com els mamífers, les tortugues, els cocodrils i els dinosaures (Benton, 2008). Les condicions càlides i àrides del final del Permià es mantengueren durant el Triàsic Inferior i Mitjà, amb climes progressivament més estables (Sun *et al.*, 2012; Benton i Newell, 2014; Romano *et al.*, 2020). Durant aquestes èpoques, hi va haver una partida de renovacions faunístiques fruit de canvis climàtics intensos però breus. En el continent, els vertebrats més abundants durant el Triàsic Inferior pertanyien a grups d'amfibis temnospòndils i sinàpsids dicinodonts (Sahney i Benton, 2008; Benton i Newell, 2014), representant tàxons "de desastre", és a dir, grups que varen sobreviure a la extinció però que serien substituïts no gaire més tard. El Triàsic Mitjà va esser testimoni de l'inici de la gran radiació dels rèptils arcosauromorfs, que varen conviure amb nombrosos grups de sinàpsids cinodonts, la línia que donaria lloc als mamífers (Chen i Benton, 2014). Durant el Triàsic Superior, un grup d'arcosauromorfs, els dinosaures, va experimentar una gran radiació i diversificació, consolidant el seu domini durant els 186 milions d'anys posteriors.

A Mallorca (Illes Balears, Mediterrània occidental) s'hi poden trobar roques d'origen continental corresponents al període Triàsic, clàssicament atribuïdes a la fàcies de 'gresos bigarrats' (*Buntsandstein*), i que recentment s'han estudiat en detall (Matamales-Andreu *et al.*, 2021a, 2021b). Aquestes afloren únicament a vorera de mar entre la cala d'Estellencs i la punta de son Serralta, al municipi d'Estellencs, i es poden dividir en quatre formacions litostratigràfiques, de base a sostre: Fm. Punta Roja, Fm. Estellencs, Fm. Pedra Alta i Fm. Son Serralta (Matamales-

Andreu *et al.*, 2021b). Aquestes representen ambients terrestres de caràcter al·luvial, amb rius meandriformes, rius entrunyellats, planeres d'inundació i planeres mareals que s'han datat dins el Triàsic Inferior–Mitjà mitjançant les palinoassociacions i les faunes de "concostracis" (Matamales-Andreu *et al.*, 2021b, Scholze i Matamales-Andreu, 2021). Concretament, les Fms. Estellencs i Pedra Alta s'han datat com a Egeà (Anisià inferior, Triàsic Mitjà), i per tant s'ha inferit que la Fm. Punta Roja és de la part superior del Triàsic Inferior i la Fm. Son Serralta és de la part mitjana del Triàsic Mitjà (Matamales-Andreu *et al.*, 2021b).

En aquestes unitats, especialment a la Fm. Estellencs i en menor mesura a la Fm. Pedra Alta, clàssicament s'hi ha trobat una elevada diversitat de fòssils, remostrada recentment, que inclou abundants restes de plantes, invertebrats i vertebrats (Figura 1). L'objectiu d'aquesta comunicació és de proporcionar una relació actualitzada dels tàxons que s'hi han trobat i la seva significació. Per a una revisió exhaustiva dels antecedents anteriors a l'any 2021, es recomana de consultar Matamales-Andreu *et al.* (2021a). Les dades de l'apartat següent es basen en Matamales-Andreu *et al.* (2021b), Peñalver *et al.* (2022) i estudis en preparació.

EL REGISTRE FÒSSIL DEL TRIÀSIC CONTINENTAL DE MALLORCA

Les proves sedimentològiques i paleontològiques suggereixen que durant la deposició de les unitats del Triàsic continental de Mallorca, aquesta era a una conca situada a una latitud quasi equatorial, al marge oriental del supercontinent Pangea, amb un clima tropical estacional. En aquesta conca s'hi desenvolupaven ambients fluvials i lacustres, a la vorera dels quals s'hi concentrava la vegetació. Les plantes han deixat un registre abundant, reconeixent-hi coes de cavall (*Equisetites mougeotii*, *Neocalamites merianii* i *Schizoneura paradoxa*), possibles cicues (?*Cycadocarpidium* sp.), coníferes (*Aethophyllum stipulare*, *Albertia latifolia*, *Pelourdea vogesiaca*, *Voltzia heterophylla*, *Voltzia walchiaeformis*, *Willsiostrobus acuminatus*, *Willsiostrobus hexasacciphorus* i *Willsiostrobus rhomboidalis*) i falgueres (*Anomopteris mougeotii* i *Chiropteris digitata*). A través de l'estudi de les espores i el pol·len, a més, s'ha confirmat la presència de cicues (*Cycadopites*), coes de cavall (*Calamospora*, *Punctatisporites*, *Verrucosisporites*), coníferes (*Angustisulcites*, *Brachysaccus*, *Chordasporites*, *Cannanoropollis*, *Hexasaccites*, *Illinites*, *Limitisporites*, *Lunatisporites*, *Microcachryidites*, *Protodiploxypinus*, *Triadispora*, *Voltziaceaesporites*) i falgueres (*Convolutispora*), i també s'hi han reconegut acritarcs (*Baltisphaeridium*), algues (*Maculatasporites*), briòfits (*Porcellispora*), ginkgòfits (*Striatopodocarpites*), licopodiòfits (*Camarazonosporites*, *Densoisporites*, *Endosporites*, *Retusotriletes*), "pteridospermes" (*Alisporites*, *Falcisporites*, *Klausipollenites*, *Paravesicaspora*, *Platysaccus*, *Protohaploxypinus*) i altres formes d'afinitat desconeguda (*Aequitriadites*, *Cuneatisporites*, *Dictyotidium*, *Fuldaesporites*, *Heliosaccus*, *Palaeospongisporis*, *Striatoabieites*, *Sulcosaccispora*). En general, aquesta associació palinològica indica una edat dins el subestatge Egeà, corresponent a l'Anisià inferior, de la part baixa del Triàsic Mitjà. S'hi distingeixen dues comunitats principals, una de pròpia de les voreres de rius i basses, amb coes de cavall, coníferes no arborescents i qualque conífera arborescent, i una comunitat més pròpia d'ambients secs, amb qualque falguera i coníferes arbustives i arborescents.

S'ha reconegut, també, una fauna d'invertebrats i vertebrats moderadament diversa que capllevava els canals de petits torrentons que travessaven les planeres d'inundació i els estanyols formats als marges dels rius. Hi ha invertebrats que sols han romàs enregistrats en forma de traces fòssils de la seva activitat, en els icnogèneres *Gordia* (produïts per larves d'insectes), *Skolithos* (produïts per larves d'insectes), *Taenidium* (produïts per escabarats durant l'estivació) i *Rusophycus*, *Cruziana* i *Diplichnites* (produïts per tortuguetes, crustacis notostracis). Aquests icnogèneres corresponen a les icnofàcies d'*Skolithos*, típica d'ambients molt oxigenats i energètics, com per exemple lòbuls de desbordament, i d'*Scoyenia*, abundant en basses temporals. Dins els estanyols de les voreres dels rius s'hi han trobat fòssils excepcionalment ben conservats de crustacis "concostracis" (*Hornestheria* i cf. *Hornestheria*) i diversos insectes, com nimfes de mosquits d'aigua (efemèrids) (*Triassoephemera*, *Triassonurus*, cf. *Voltziaephemera* i un morfotip sedimentívor indeterminat), i diferentes castes de mosquits veritables, amb postes de moscardí (quironòmids) (*Clavapartus*) i pupes de la família extingida dels grauvogèl·lids (*Voltziapupa*). A les voreres d'aquests ambients hi vivien mosquits d'aigua adults (efemèrids) (*Hammephemera* i morfotip adult indeterminat), larves de mosquits de la fusta (anisopòdids) (*Protoanisolarva*), cuques molles (blatodeus) (possible *Voltziablatta*), gril·loblàtids (*Mallorcagryllus*) i insectes d'altres grups que encara no s'han estudiat en detall. Pel que fa als vertebrats, dins els estanyols s'hi ha documentat un petit peix osteïcti, i a les voreres dels canals dels torrentons s'hi han observat potades de petits arcosauromorfs, possiblement tanistrofèids, corresponents als icnogèneres *Prorotodactylus* i *Rhynchosauroides*. Dins aquest conjunt, en destaquen els "concostracis" del gènere *Hornestheria* i les potades de l'icnogènere *Prorotodactylus*, que confirmen l'edat d'aquestes unitats dins un Triàsic Mitjà molt antic, fregant l'Inferior. També són molt rellevants els fòssils de mosquits veritables (anisopòdids, quironòmids i grauvogèl·lids), per mor que són el registre més antic d'aquest grup (dípters) a nivell mundial, i de les nimfes sedimentívores de mosquits d'aigua (efemèrids), ja que són l'únic exemple d'aquest mode d'alimentació conegut en el registre fòssil d'insectes, present sols en un gènere actual nord-americà també d'efemèrids.

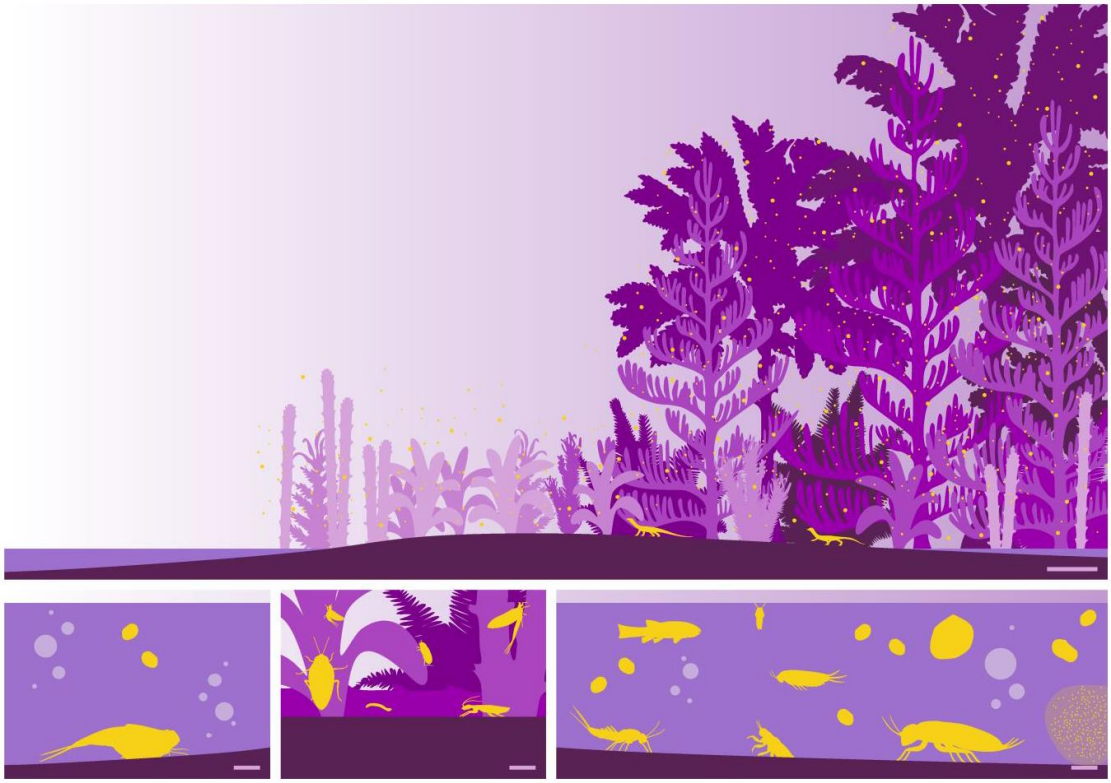

FIGURA 1. *Dibuix esquemàtic amb els principals representants de la flora i la fauna del Triàsic Mitjà continental de Mallorca. Dibuix superior amb coes de cavall, falgueres, "pteridospermes", coníferes, espores, pol·len i petits rèptils arcosauromorfs. Dibuix inferior esquerre amb "concostracis" i tortugueta. Dibuix inferior central: mosquits d'aigua adults, larva de mosquit de la fusta, cuca molla, escarabat i gril·loblàtid. Dibuix inferior dret amb "concostracis", nimfes de mosquit d'aigua, posta de moscardí i pupa de mosquit grauvogèl·lid. Algunes plantes, tortuguetes i vertebrats inferits a partir de les espores, pol·len i traces de la seva activitat. Barres d'escala: 50 cm per al dibuix superior i 5 mm per a les tres ampliacions inferiors.*

CONCLUSIONS

Les roques del Triàsic Inferior i Mitjà de Mallorca que representen ambients continentals contenen un registre fòssil molt important d'artròpodes excepcionalment ben conservats que inclou, entre d'altres, els mosquits veritables (dípters) més antics del món. També s'hi han trobat restes de diversos grups de plantes, i potades de petits rèptils. Aquesta associació ha permès de caracteritzar amb molt de detall l'ecosistema que va romandre enregistrat en aquestes roques, i comparar-lo amb altres de regions properes, especialment del Vosges (Europa). Per acabar de completar aquesta reconstrucció, seran necessàries futures campanyes de camp per localitzar els nivells que contenen les restes de la comunitat entomològica terrestre, que quasi no ha estada estudiada fins ara.

AGRAÏMENTS

Aquesta comunicació s'emmarca en el projecte "Mallorca abans dels dinosaures: estudi dels ecosistemes continentals del Permià i Triàsic amb especial èmfasi en les restes de vertebrats" (ref. 15 - 619/2020), concedit pel Departament de Cultura, Patrimoni i Política Lingüística (Consell Insular de Mallorca).

BIBLIOGRAFIA

Benton, M.J. 2008. *When life nearly died. The greatest mass extinction of all time*. Thames & Hudson, London, 336 p.

Benton M.J. i Newell, A.J. 2014. Impacts of global warming on Permo-Triassic terrestrial ecosystems. *Gondwana Research*, 25: 1308-1337.

Chen, Z.-Q. i Benton, M.J. 2012. The timing and pattern of biotic recovery following the end-Permian mass extinction. *Nature Geoscience*, 5(6): 375-383.

Matamales-Andreu, R., Oms, O. i Fortuny, J. 2021a. Paleoecosistemes del Permià i Triàsic continental de Mallorca (Illes Balears, Mediterrània occidental): síntesi i prespectives futures. In: Gómez-Pujol, Ll., Roig-Munar, F.X., Gelabert, B. i Martín, J.A. (Eds.). *De la terra a la mar i de la mar a la terra. Homenatge a Antonio Rodríguez-Perea*. Monografies de la Societat d'Història Natural de Balears, 34. Societat d'Història Natural de les Balears, Palma: 17-39.

Matamales-Andreu, R., Peñalver, E., Mujal, E., Oms, O., Scholze, F., Juárez, J., Galobart, À. i Fortuny, J. 2021b. Early–Middle Triassic fluvial ecosystems of Mallorca (Balearic Islands): biotic communities and environmental evolution in the equatorial western peri-Tethys. *Earth-Science Reviews*, 222: 103783.

Peñalver, E., Matamales-Andreu, R., Nel, A. & Pérez-de la Fuente, R. 2022. Early adaptations of true flies (Diptera) to moist and aquatic continental environments. *Papers in Palaeontology*, acceptat.

Romano, M., Bernardi, M., Petti, F.M., Rubidge, B., Hancox, J. i Benton, M.J. 2020. Early Triassic terrestrial tetrapod fauna: a review. *Earth-Science Reviews*, 210: 103331.

Sahney, S. i Benton, M.J. 2008. Recovery from the most profound mass extinction of all time. *Proceedings of the Royal Society B*, 275: 759-765.

Scholze, F. i Matamales-Andreu, R. 2021. Triassic clam shrimps ("Conchostraca"; Branchiopoda: Diplostraca) from Mallorca: Taxonomic description and interregional comparisons. *Zootaxa*, 4964(3): 471-496.

Sun, Y., Joachimski, M.M., Wignall, P.B., Yan, C., Chen, Y., Jiang, H., Wang, L. i Lai, X. 2012. Lethally hot temperatures during the Early Triassic greenhouse. *Science*, 338(6105): 366-370.

Appendix 15

Synthesis, marine Triassic of Mallorca

Appendix 15 was published as:

Matamales-Andreu, R. (2022). Mol·luscs, notosaures i ictiosaures: registre fòssil del Triàsic marí de Mallorca. *In*: Pons, G.X.; del Valle, L.; McMinn, M.; Pinya, S. & Vicens, D. (Eds.). *Llibre de ponències i comunicacions de les VIII Jornades de Medi Ambient de les Illes Balears*. Societat d'Història Natural de les Balears, Universitat de les Illes Balears; Palma: 91–94. [in Catalan]

ISBN: 978-84-09-45184-5

DL: PM 00851-2022

In this work, R. Matamales-Andreu contributed in:

A. Integration and discussion of the previous data.
B. Writing of the original draft.
C. Preparation of all the figures (1–2).

VIII Jornades de Medi Ambient de les Illes Balears (2022-23) 91

Mol·luscs, notosaures i ictiosaures: registre fòssil del Triàsic marí de Mallorca

Molluscs, nothosaurs and ichthyosaurs: fossil record of the marine Triassic of Mallorca

Rafel MATAMALES-ANDREU[1,2]

1 Museu Balear de Ciències Naturals, ctra. Palma-Port de Sóller km 30,5, 07100 Sóller, Mallorca, Illes Balears.
2 Institut Català de Paleontologia Miquel Crusafont, Universitat Autònoma de Barcelona, Edifici ICTA-ICP, c/ Columnes s/n, Campus de la UAB, 08193 Cerdanyola del Vallès, Barcelona.

Resum: A l'illa de Mallorca (Illes Balears, Mediterrània occidental), el Triàsic Mitjà (excepte la base) i Superior corresponen a medis marins de poca fondària i transicionals. Concretament, s'han interpretat com ambients mareals i llacunes evaporítiques costaneres, de vegades amb notable activitat volcànica. El clima era tropical i càlid, de cada vegada més suau, i segurament molt plover cap al final del període. Tot i que l'estudi dels fòssils d'aquestes unitats es remunta quasi a les primeres investigacions paleontològiques fetes a Mallorca, no s'han actualitzat en els darrers 50 anys. Aquest treball fa una primera passa cap a la revisió de tota la flora i fauna documentada fins avui. Això ressalta la importància de l'estudi d'aquests fòssils per resoldre qüestions de caire taxonòmic, paleobiogeogràfic, biostratigràfic, tafonòmic i paleoambiental. Aquestes dades demostren que les associacions de Mallorca s'assemblen a les d'altres indrets del peri-Tetis occidental, però amb particularitats que responen a la convergència de diferents províncies paleobiogeogràfiques. Per tant, la represa d'aquests estudis permetrà d'aclarir encara més aquests aspectes i valorar les afinitats de les faunes de Mallorca amb les de les conques centreeuropea, alpina, o altres de la península Ibèrica.
Paraules clau: bivalves, ammonoïdeus, sauròpsids, paleontologia, Illes Balears

Abstract: *On Mallorca (Balearic Islands, western Mediterranean), the Middle Triassic (except for its base) and the Upper Triassic correspond to shallow marine and transitional environments. Specifically, they have been interpreted as tidal settings and coastal evaporitic lagoons, sometimes with notable volcanic activity. The climate was warm and tropical, progressively milder, and probably rainier towards the end of the period. Even though the study of fossils from those units goes back to the first palaeontological works about Mallorca, they have not been updated in the last 50 years. The present contribution is a first step towards the revision of all the flora and fauna so far reported from those units. This highlights the importance of the study of these fossils to solve questions regarding taxonomy, palaeobiogeography, biostratigraphy, taphonomy and palaeoenvironments. These data show that the assemblages of Mallorca are similar to those of other sites in the western peri-Tethys, but with distinctive features that resulted from the convergence of different palaeobiogeographical provinces. Therefore, resuming the works on the Middle–Upper Triassic of Mallorca may clear these aspects even more, and gauge the affinity of the faunas of Mallorca to the faunas of basins of Central-Europe, Alps and the Iberian Peninsula.*
Key words: *bivalves, ammonoids, sauropsids, palaeontology, Balearic Islands*

INTRODUCCIÓ

Cap al Triàsic Mitjà, els ecosistemes de la Terra ja s'havien recuperat de la gran extinció en massa de la transició Permià–Triàsic (Irmis i Whiteside, 2011). Els climes eren de cada vegada més suaus i estables i, al peri-Tetis occidental, el nivell de la mar anava pujant progressivament, inundant moltes de les conques continentals que fins llavors havien estades ocupades per grans rius. Allà s'hi desenvoluparen grans plataformes carbonatades, en condicions climàtiques tropicals, on hi vivia una gran diversitat de mol·luscs, i els rèptils marins continuaven la seva diversificació. Al Triàsic Superior, el nivell de la mar va tornar a baixar en la major part de les conques. El clima continuava essent tropical, però poc després de l'inici del Triàsic Superior, hi va haver un interval de temps caracteritzat per esser molt més plover i humit, anomenat *esdeveniment plover del Carnià*. Durant aquest període és quan aparegueren o es diversificaren molts dels grups de vertebrats que serien emblemàtics durant la resta del Mesozoic, com les tortugues, els cocodrilomorfs, els fitosaures, els dinosaures i els mamífers (Benton *et al.*, 2014; Bernardi *et al.*, 2018; Dal Corso *et al.*, 2020). El Triàsic acabà amb una altra extinció massiva, que consolidà el domini dels dinosaures durant la resta del Mesozoic (Colbert, 1958).

A Mallorca (Illes Balears, Mediterrània occidental), les roques del Triàsic Mitjà i Superior que representen medis marins i transicionals són molt abundants, conformant una part important del relleu de les serres de Tramuntana i de Llevant. Es divideixen en cinc unitats principals, de base a sostre: M1, M2 i M3 (dins les fàcies *Muschelkalk*), fàcies *Keuper* i "formació Felanitx" (Matamales-Andreu *et al.*, 2021 i referències que s'hi esmenten). Representen diversos ambients marins (plataformes carbonatades i planeres mareals) i transicionals (llacunes costaneres i planeres fangoses),

sotmesos a una partida de cicles de pujada i baixada relativa de la mar. La unitat M3 s'ha datat dins el Ladinià (Triàsic Mitjà), reconeixent-hi la part alta del Ladinià inferior i la part baixa del Ladinià superior mitjançant les faunes d'ammonits i conodonts, mentre que la base de la "fm. Felanitx" s'ha datada dins el Norià superior (Triàsic Superior) en base a la palinoassociació (Matamales-Andreu *et al.*, 2021 i referències que s'hi esmenten). La datació de les altres unitats s'ha inferit en base a aquestes i a les formacions infra- i suprajacents.

Els fòssils són generalment molt escassos en aquestes unitats (Figures 1, 2), excepte en nivells determinats on els mol·luscs poden arribar a esser molt abundants. L'objectiu d'aquesta comunicació és de proporcionar una relació actualitzada dels tàxons que s'hi han trobat i la seva significació. Les dades de l'apartat següent es basen en Matamales-Andreu *et al.* (2021) i les referències que s'hi esmenten. També s'han tengut en compte altres estudis amb dades de flora i fauna, no llistades a l'article esmentat, com Hirsch (1972), Colom (1975, 1982), Boutet *et al.* (1982) i Barnolas (1991).

ELS REGISTRE FÒSSIL DEL TRIÀSIC MARÍ DE MALLORCA

Dins les fàcies *Muschelkalk*, els fòssils són sols abundants a la unitat M3; mai no s'han trobat fòssils a l'M2, i de l'M1 sols es coneixen artells de lliris de la mar indeterminats. De l'M3 en destaquen les bioturbacions d'invertebrats (de les quals *Planolites* n'és la més habitual), i els nivells de concentració de closques, amb abundants copinyes (*Bakevellia*, *Entolium*, *Gervillia*, *Leptochondria*, *Modiolus*, *Neoschizodus*, *Pleuromya*, *Pseudocorbula*, *Pseudoplacunopsis*, *Umbostrea* i *Unionites*) i qualque cornet (*Coelostylina* i *Loxonema*), nàutil (*Germanonautilus*), ofiura (*Aspidurella*), eriçó de la mar ("*Cidaris*"), lliri de la mar ("*Encrinus*"), serpúlid i, fins i tot, plantes del grup de les coes de cavall (*Equisetites*). Estratigràficament molt a prop, hi compareixen ammonits (*Gevanites*) que indiquen una edat dins la part alta del Ladinià inferior, en el Triàsic Mitjà. Un altre nivell de concentració conté copinyes (*Modiolus* i *Pseudocorbula*), cornets (*Cassianopsis*, *Loxonema* i *Naticopsis*), nàutils (*Germanonautilus*) i ammonits (*Anolcites*, *Iberites*, *Nannites*, *Protrachyceras* i *Thanamites*), que indiquen una edat dins la part baixa del Ladinià superior. D'altres llocs han proporcionat fòssils de manera aïllada, d'entre els quals en destaquen foraminífers (*Glomospira* i *Lingulina*), amebes testades (*Difflugia* i *Trigonopyxis*), copinyes (*Daonella*), conodonts (*Pseudofurnishius* i *Sephardiella*) i una vèrtebra caudal proximal d'un rèptil marí del grup dels ictiosauriformes basals (Ichthyosauriformes indet. aff. Grippidia). Aquest rèptil és especialment interessant perquè els altres ictiosauriformes basals coneguts són de la costa oest de nord-Amèrica i l'Àsia oriental, que corresponien als marges occidental i oriental de l'antic supercontinent Pangea, respectivament. El fet de trobar aquest exemplar a Mallorca suggereix que el peri-Tetis occidental era, a través d'Europa, el passadís que connectava aquests dos grups de poblacions.

Les fàcies *Keuper* han estades molt pobrament estudiades causa la seva gran deformació tectònica i la falta de bons afloraments. Sols s'hi han trobat un fragment d'un os llarg d'un rèptil (Reptilia indet.) i quatre vèrtebres, del coll, l'esquena i la coa, d'un rèptil marí sauropterigi (*Nothosaurus*), molt comú en altres conques d'Europa i el nord d'Àfrica. Dins nivells carbonatats a la base de les dolomies superiors ("fm. Felanitx") s'hi han trobades espores de licopodiòfits (*Anapiculatisporites*), pol·len de coníferes (*Corollina*, *Granuloperculatipollis*, *Ovalipollis*, *Tsugaepollenites* i *Triadispora*), i crustacis ostràcodes ("*Herpetocypris*"). La palinoassociació indica una edat de Norià superior, dins la part mitjana–alta del Triàsic Superior.

CONCLUSIONS

El Triàsic Mitjà marí de Mallorca conté un important registre de mol·luscs i altres invertebrats amb afinitats amb altres localitats del peri-Tetis occidental, amb espècies de les províncies germànica, alpina i sefardí. A més, també s'hi han trobat evidències de la presència d'un rèptil marí del grup dels ictiosauriformes, que suggereix que la zona que actualment correspon a Mallorca servia de passadís entre els marges occidental i oriental de Pantalassa, travessant Pangea. D'altra banda, el registre del Triàsic Superior és molt més escàs, amb fòssils de rèptils identificats com a notosaures, típics d'altres llocs del peri-Tetis occidental, i qualque resta vegetal.

AGRAÏMENTS

Aquesta comunicació s'emmarca en el projecte "Mallorca abans dels dinosaures: estudi dels ecosistemes continentals del Permià i Triàsic amb especial èmfasi en les restes de vertebrats" (ref. 15 - 619/2020), concedit pel Departament de Cultura, Patrimoni i Política Lingüística (Consell Insular de Mallorca).

FIGURA 1. *Dibuix esquemàtic amb els principals representants de la fauna del Triàsic Mitjà marí de Mallorca. Amb nàutils, ammonits, lliris de la mar i un ictiosauriforme basal. Barra d'escala: 50 cm.*

FIGURA 2. *Dibuix esquemàtic amb els principals representants de la flora i la fauna del Triàsic Superior de Mallorca. Amb coníferes, espores, pol·len i un notosaure. Plantes inferides a partir del pol·len. Barra d'escala: 50 cm.*

BIBLIOGRAFIA

Barnolas, A. (dir.) 1991. *Mapa Geológico de España. Escala 1:50.000. Sóller.* Segunda serie, primera edición. Instituto Tecnológico GeoMinero de España, Madrid, 62 p. + 1 mapa + 8 columnes estratigràfiques.

Bernardi, M., Gianolla, P., Massimo Petti, F., Mietto, P. i Benton, M.J. 2018. Dinosaur diversification linked with the Carnian Pluvial Episode. *Nature Communications*, 9: 1499.

Boutet, C., Rangheard, Y., Rosenthal, P., Visscher, H. i Durand-Delga, M. 1982. Découverte d'une microflore d'âge Norien dans la Sierra Norte de Majorque (Baléares, Espagne). *Comptes Rendus de l'Académie des Sciences de Paris, Série 2*, 294: 1267-1270.

Colbert, E.H. 1958. Tetrapod extinctions at the end of the Triassic period. *Proceedings of the National Academy of Sciences*, 44: 973-977.

Colom, G. 1975. *Geología de Mallorca I*. Gráficas Miramar, Diputación Provincial de Baleares, Palma, 297 p.

Colom, G. 1982. Notas paleontológicas y estratigráficas (referentes a Mallorca e Ibiza). *Bolletí de la Societat d'Història Natural de Balears*, 26: 195-206.

Dal Corso, J., Bernardi, M., Sun, Y., Song, H., Seyfullah, L.J., Preto, N., Gianolla, P., Ruffell, A., Kustatscher, E., Roghi, G., Merico, A., Hohn, S., Schmidt, A.R., Marzolli, A., Newton, R.J., Wignall, P.B. i Benton, M.J. 2020. Extinction and dawn of the modern world in the Carnian (Late Triassic). *Science Advances*, 6: eaba0099.

Hirsch, F. 1977. Essai de correlation biostratigraphique des niveaux Meso et Neotriasiques de facies «Muschelkalk» du domaine sepharade. *Cuadernos de Geología Ibérica*, 4: 511-526.

Irmis, R.B. i Whiteside, J.H. 2011. Delayed recovery of non-marine tetrapods after the end-Permian mass extinction tracks global carbon cycle. *Proceedings of the Royal Society B*, 279: 1310-1318.

Matamales-Andreu, R., Oms, O., Galobart, À. i Fortuny, J. 2021. Middle–Upper Triassic marine vertebrates of Mallorca (Balearic Islands, western Mediterranean). *Historical Biology*, 33(10): 2520-2533.

Picture and figure credits

Chapter covers

Rafel Matamales: Dissertation front and back covers, Table of contents cover, Abstract cover, Chapter 6 cover, Chapter 7 cover, Chapter 8 cover

Toni Pasqual: Chapter 1 cover

Henry S. Sharpe: Chapter 2 cover, Chapter 3 cover, Chapter 4 covers, Chapter 5 cover

Pictures in figures

Rafel Matamales: Figures 1.4A, 1.4C, 1.4D, 1.4E, 1.4F, 1.5A, 1.5B, 1.5C, 1.5D, 1.5F, 1.6B, 1.6C, 1.6D, 1.6E, 1.6F, 1.6G, 1.6H, 1.7B, 1.7C, 1.7D, 1.7E, 1.7F, 1.8A, 1.8B, 1.8C, 1.8E, 1.8F, 1.10D, 1.10E, 1.11B, 1.11C, 1.13A, 1.13C, 1.13d, 1.13E, 1.13G, 1.13I, 2.2A, 2.2B, 2.2C, 2.2D, 2.2E, 2.3A, 2.3B, 2.3C, 2.3D, 2.3E, 2.4A, 2.4B, 2.4C, 2.4D, 2.4E, 2.4F, 2.4G, 2.4H, 2.4I, 2.4J, 2.4K, 2.4L, 2.4M, 2.4N, 2.4O, 2.8A, 2.8B, 2.8C, 2.8D, 2.8E, 2.8F, 2.8G, 2.8H, 2.8I, 2.9A, 2.9B, 2.9C, 2.9D, 2.9E, 2.9F, 2.10A, 2.10B, 2.10C, 2.10D, 2.10E, 2.10F, 2.10G, 2.10H, 2.10I, 2.11A, 2.11B, 2.11C, 2.11D, 2.11E, 2.11F, 2.11G, 2.11H, 2.11I, 2.15C, 2.15D, 3.2A, 3.2B, 3.2C, 3.3A, 3.3B, 3.3C, 3.3D, 3.3E, 3.3F, 3.3G, 3.3H, 3.3I, 3.3J, 3.3K, 3.3L, 3.3M, 3.3N, 3.3O, 3.4A, 3.4B, 3.4C, 3.4D, 3.5A, 3.5B, 3.5D, 3.5E, 3.5F, 4.1B, 4.1C, 4.1D, 4.2A, 4.2B, 4.2C, 4.2D, 4.2E, 4.2F, 4.2G, 4.2H, 4.2I, 4.2J, 4.2K, 4.2L, 4.2M, 4.2N, 4.2O, 4.2P, 4.2Q, 4.2R, 4.2S, 4.2T, 4.2U, 4.2V, 4.2W, 4.2X, 4.2Y, 4.2Z, 4.2AA, 4.2BB, 4.2CC, 4.2DD, 4.4A, 4.4B, 4.4C, 4.4D, 4.4E, 4.4F, 5.2A, 5.2C, 5.2D, 5.2E, 5.3A, 5.3B, 5.3C, 5.3D, 5.3E, 5.3F, 5.5A, 5.5B, 5.5C, 5.5D, 5.5E, 5.5F, 5.5G, 5.5H, 5.5I, 5.5J, 5.5K, 5.5L, 5.5M, 5.5N, 5.5O, 5.5P, 5.5Q, 5.5R, 5.5S, 5.5T, 5.6A, 5.6B, 5.6C, 5.6D, 5.6E, 5.6F, 5.6G, 5.6H, 5.6I, 5.6J, 5.6K, 5.6L, 5.6M, 5.6N, 5.6O, 5.7A, 5.7B, 5.7C, 5.7D, 5.7E, 5.7F, 5.7G, 5.7H, 5.7I, 5.7J, 5.7K, 5.7L, A1.3A, A1.3B, A1.3C, A1.3D, A1.3E, A1.3F, A1.4A, A1.4B, A1.4C, A1.4D, A1.4E, A1.4F, A1.4H, A1.5A, A1.5B, A1.5C, A1.5D, A1.5E, A1.6A, A1.6B, A1.6C, A2.3G, A2.4, A3.1D, A3.1E, A3.2A, A3.2B, A3.2C, A3.2D, A3.2E, A3.3A, A3.3B, A4.2, A4.3B, A4.3D, A4.3F, A4.4A, A4.4C, A4.7B, A4.7D, A5.2A, A5.2B, A5.2C, A5.2D, A5.2E, A5.2F1, A5.2F2, A5.2F3, A5.2G, A5.2H, A5.2I, A5.2J, A5.2K, A5.2L, A5.2M, A5.2N, A5.2O, A5.2P, A5.2Q, A5.2R, A5.2S, A5.2T, A5.2U, A5.2V, A5.2W, A5.S2A, A5.S2B, A5.S2C, A5.S2D1, A5.S2D2, A5.S2D3, A5.S3A, A5.S3B, A5.S3C, A5.S3D, A5.S3E, A5.S4A, A5.S4B, A5.S4C, A5.S5A, A5.S5B, A5.S5C, A5.S5D, A5.S5E1, A5.S5E2, A5.S5E3, A5.S5E4, A5.S5E5, A5.S5E6, A5.S5F, A5.S5G, A5.S5H, A5.S6A1, A5.S6A2, A5.S6A3, A5.S6A4, A5.S6A5, A5.S6A6, A5.S6B, A5.S6C, A5.S6D, A5.S6E, A5.S6F1, A5.S6F2, A5.S6F3, A5.S6F4, A5.S6F5, A5.S6F6, A5.S6G, A5.S6H, A5.S6I, A5.S6J, A5.S6K1, A5.S6K2, A5.S6K3, A5.S6K4, A5.S6K5, A5.S6K6, A5.S6L, A5.S6M, A6.2, A6.3A, A6.3B, A6.3C, A6.3D, A6.4A, A6.4B, A6.5B, A6.5C, A7.1B, A8.1C, A8.1D, A8.1E, A8.1F, A10.1B, A10.1C, A10.1D

Chabier De Jaime: Figures 1.13H, 2.15A

Jaume Dinarès: Figures 1.4B, 1.6A, 1.10C, 1.10F

Àngel Galobart: Figure 1.11E

Josep Juárez: Figures 3.5C, 3.5G, A11.2A, A11.2B, A11.2C, A11.2D, A11.2E, A11.2F, A11.2G, A11.2H, A11.2I, A11.2J

Evelyn Kustatscher/Guido Roghi: Figures 2.7A, 2.7B, 2.7C, 2.7D, 2.7E, 2.7F, 2.7G, 2.7H, 2.7I, 2.7J, 2.7K, 2.7L, 2.7M, 2.7N, 2.7O, 2.7P

Borja López: Figure 3.5H

Sebastià Matamalas: Figures 1.7A, 1.10A, 1.10B, 1.11A, 1.11D, 1.11F, 1.11G, 1.11H, 1.11I, 1.13B, 1.13F, 3.2D, A1.4G

Eudald Mujal: Figures 1.8D

Enrique Peñalver: Figures 3.7A, 3.7B, 3.7C, 3.7D, 3.7E, 3.7F, 3.7G, 3.7H, 3.7I, 3.7J, 3.7K, 3.7L, 3.7M, 3.7N, 3.7O, 3.8A, 3.8B, 3.8C, 3.8D, 3.8E, 3.8F, 3.8G, 3.9A, 3.9B, 3.9C, 3.9D, A7.2A, A7.2B, A7.2C, A7.2D, A7.2E, A7.2F, A9.2, A9.3A, A9.3B, A9.4A, A9.4B, A9.4C, A9.6B, A9.6I, A9.6J, A9.6K, A9.6L, A9.6P, A9.6Q, A9.6R, A9.7A, A9.7B, A9.7C, A9.7D, A9.S1A, A9.S1B, A9.S1C, A10.1E, A10.3A, A10.3B, A10.3C, A10.3D, A10.3E, A10.3F, A10.3G, A10.4A, A10.4B, A10.4C, A10.4D, A10.5A, A10.5B, A10.5C, A10.5D, A10.S2A, A10.S2B, A10.S2C, A10.S2D, A10.S2E

Antoni Rodríguez/Feliu Calafat/Joan J. Fornós: Figures 2.15B, A2.3A, A2.3B, A2.3C, A2.3D, A2.3E, A2.3F, A2.3H, A2.3I, A2.3J, A2.3K, A2.3L, A7.1A

Francesc Xavier Roig: Figure 1.5E

Frank Scholze: Figures 3.6A, 3.6B, 3.6C, 3.6D, 3.6E, 3.6F, A8.2A, A8.2B, A8.2C, A8.2D, A8.2E, A8.3A, A8.3C, A8.3D, A8.3E, A8.4A, A8.4C, A8.5A, A8.5C, A8.5D, A8.6A, A8.6C, A8.6E, A8.7A, A8.7B, A8.8A, A8.8C, A8.8E, A8.9A, A8.9C, A8.9E, A8.10A, A8.10C, A8.10E, A8.11A, A8.11C, A8.11D, A8.12A, A8.12C, A8.12D, A8.12E, A8.12G

Figure design

Rafel Matamales: Figures 1.1, 1.2, 1.3, 1.4, 1.5, 1.6, 1.7, 1.8, 1.9, 1.10, 1.11, 1.12, 2.1, 2.2, 2.3, 2.4, 2.5 (adaptation), 2.6 (adaptation), 2.7 (adaptation), 2.8, 2.9, 2.10, 2.11, 2.12, 2.13, 2.14, 2.15, 2.17, 3.1, 3.2, 3.3, 3.4, 3.5, 3.6 (adaptation), 3.7 (adaptation), 3.8 (adaptation), 3.9 (adaptation), 3.10, 3.11, 4.1, 4.2, 4.3, 4.4, 4.5, 4.6, 5.1, 5.2, 5.3, 5.4, 5.5, 5.6, 5.7, 5.9, 6.1, 6.2, 6.3, 6.4, 6.5, 6.6, 6.7, A1.1, A1.2, A1.3, A1.4, A1.5, A1.6, A1.7, A2.1 (adaptation), A2.2 (adaptation), A2.3, A2.4, A3.1, A3.2, A3.3, A3.4, A3.5, A4.1, A4.2, A4.3, A4.4, A4.5, A4.6, A4.7 (adaptation), A5.1, A5.2 (adaptation), A5.3, A5.S1, A5.S2, A5.S3, A5.S4, A5.S5, A5.S6, A6.1, A7.1, A7.2 (adaptation), A8.1, A9.1, A11.1, A11.2, A13.1, A14.1, A15.1. Figures in tables 2.1, 2.2, 3.1, 3.2. Stratigraphic logs in Appendix 2 (148 pages), Appendix 6 (31 pages), Appendix 12 (32 pages)

Álex Serrano: Figure A4.S1

Jaume Dinarès: Figures 2.5 (original), 2.6 (original), A2.1 (original), A2.2 (original), A7.2 (original)

Enrique Peñalver: Figures 3.7 (original), 3.8 (original), 3.9 (original), A7.2 (original), A9.2, A9.3, A9.4, A9.5, A9.6, A9.7, A9.8, A9.S1, A9.S2, A9.S3, A10.1, A10.2, A10.3, A10.4, A10.5, A10.6, A10.S1, A10.S2

Eudald Mujal: Figures A4.7 (original), A5.2 (original), A6.2, A6.3, A6.4, A6.5, A6.6

Frank Scholze: Figures 3.6 (original), A8.2, A8.3, A8.4, A8.5, A8.6, A8.7, A8.8, A8.9, A8.10, A8.11, A8.12

Henry S. Sharpe: Figures 2.16, 3.12, 5.8, A4.8, A5.4